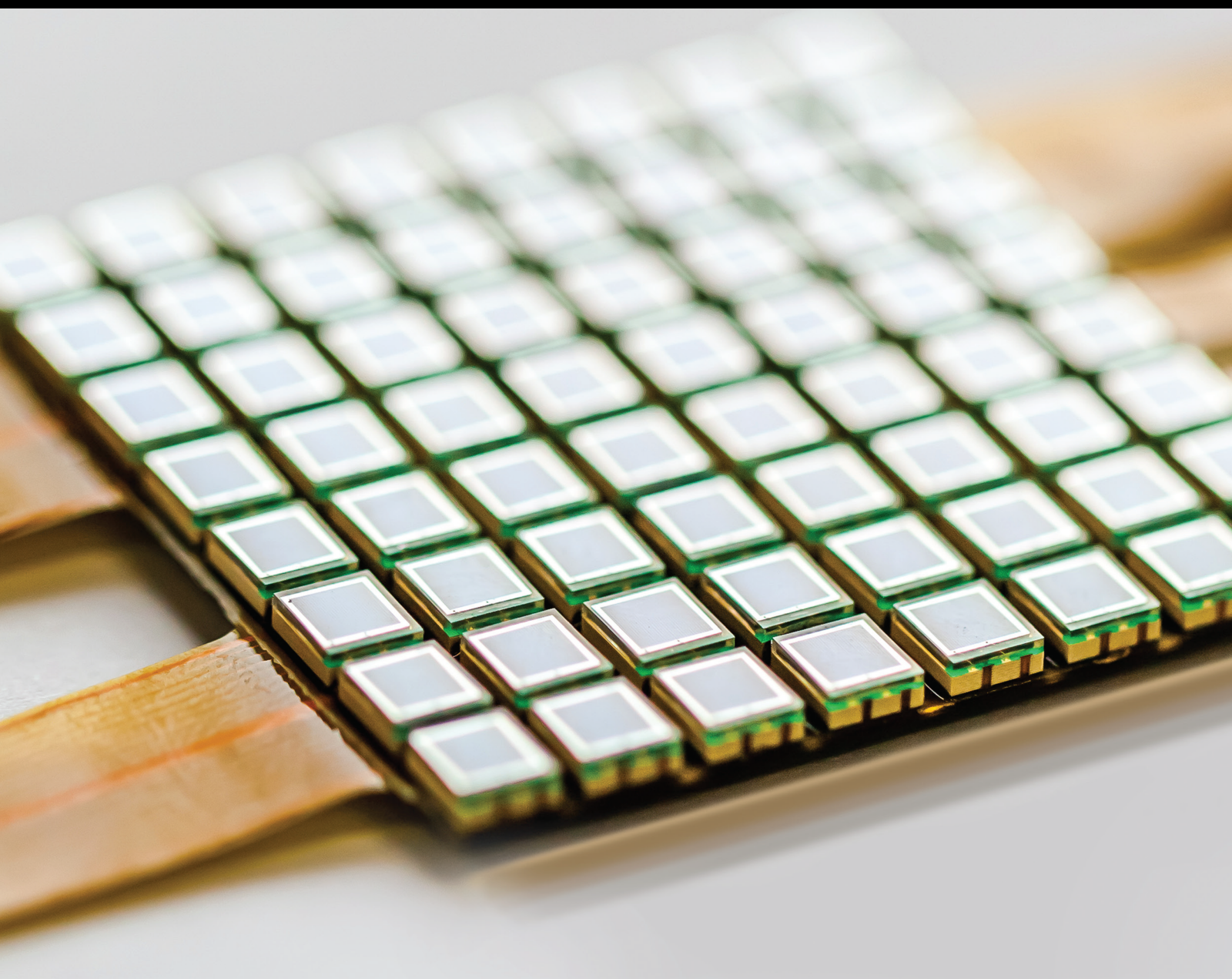


Advanced Machine Learning and Big Data Analytics with IoT Sensor Data

Lead Guest Editor: Sweta Bhattacharya

Guest Editors: Lalit Garg and Praveen Kumar Donta





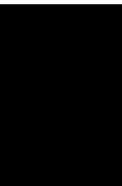
Advanced Machine Learning and Big Data Analytics with IoT Sensor Data

Journal of Sensors

Advanced Machine Learning and Big Data Analytics with IoT Sensor Data

Lead Guest Editor: Sweta Bhattacharya

Guest Editors: Lalit Garg and Praveen Kumar Donta






Copyright © 2024 Hindawi Limited. All rights reserved.

This is a special issue published in "Journal of Sensors." All articles are open access articles distributed under the Creative Commons Attribution License, which permits unrestricted use, distribution, and reproduction in any medium, provided the original work is properly cited.

Chief Editor

Harith Ahmad , Malaysia

Associate Editors

Duo Lin , China
Fanli Meng , China
Pietro Siciliano , Italy
Guiyun Tian, United Kingdom

Academic Editors

Ghufran Ahmed , Pakistan
Constantin Apetrei, Romania
Shonak Bansal , India
Fernando Benito-Lopez , Spain
Romeo Bernini , Italy
Shekhar Bhansali, USA
Matthew Brodie, Australia
Ravikumar CV, India
Belén Calvo, Spain
Stefania Campopiano , Italy
Binghua Cao , China
Domenico Caputo, Italy
Sara Casciati, Italy
Gabriele Cazzulani , Italy
Chi Chiu Chan, Singapore
Sushank Chaudhary , Thailand
Edmon Chehura , United Kingdom
Marvin H Cheng , USA
Lei Chu , USA
Mario Collotta , Italy
Marco Consales , Italy
Jesus Corres , Spain
Andrea Cusano, Italy
Egidio De Benedetto , Italy
Luca De Stefano , Italy
Manel Del Valle , Spain
Franz L. Dickert, Austria
Giovanni Diraco, Italy
Maria de Fátima Domingues , Portugal
Nicola Donato , Italy
Sheng Du , China
Amir Elzawwy, Egypt
Mauro Epifani , Italy
Congbin Fan , China
Lihang Feng, China
Vittorio Ferrari , Italy
Luca Francioso, Italy

Libo Gao , China
Carmine Granata , Italy
Pramod Kumar Gupta , USA
Mohammad Haider , USA
Agustin Herrera-May , Mexico
María del Carmen Horrillo, Spain
Evangelos Hristoforou , Greece
Grazia Iadarola , Italy
Syed K. Islam , USA
Stephen James , United Kingdom
Sana Ullah Jan, United Kingdom
Bruno C. Janegitz , Brazil
Hai-Feng Ji , USA
Shouyong Jiang, United Kingdom
Roshan Prakash Joseph, USA
Niravkumar Joshi, USA
Rajesh Kaluri , India
Sang Sub Kim , Republic of Korea
Dr. Rajkishor Kumar, India
Rahul Kumar , India
Nageswara Lalam , USA
Antonio Lazaro , Spain
Chengkuo Lee , Singapore
Chenzong Li , USA
Zhi Lian , Australia
Rosalba Liguori , Italy
Sangsoon Lim , Republic of Korea
Huan Liu , China
Jin Liu , China
Eduard Llobet , Spain
Jaime Lloret , Spain
Mohamed Louzazni, Morocco
Jesús Lozano , Spain
Oleg Lupan , Moldova
Leandro Maio , Italy
Pawel Malinowski , Poland
Carlos Marques , Portugal
Eugenio Martinelli , Italy
Antonio Martinez-Olmos , Spain
Giuseppe Maruccio , Italy
Yasuko Y. Maruo, Japan
Zahid Mehmood , Pakistan
Carlos Michel , Mexico
Stephen. J. Mihailov , Canada
Bikash Nakarmi, China

Ehsan Namaziandost , Iran
Heinz C. Neitzert , Italy
Sing Kiong Nguang , New Zealand
Calogero M. Oddo , Italy
Tinghui Ouyang, Japan
SANDEEP KUMAR PALANISWAMY ,
India
Alberto J. Palma , Spain
Davide Palumbo , Italy
Abinash Panda , India
Roberto Paolesse , Italy
Akhilesh Pathak , Thailand
Giovanni Pau , Italy
Giorgio Pennazza , Italy
Michele Penza , Italy
Sivakumar Poruran, India
Stelios Potirakis , Greece
Biswajeet Pradhan , Malaysia
Giuseppe Quero , Italy
Linesh Raja , India
Maheswar Rajagopal , India
Valerie Renaudin , France
Armando Ricciardi , Italy
Christos Riziotis , Greece
Ruthber Rodriguez Serrezuela , Colombia
Maria Luz Rodriguez-Mendez , Spain
Jerome Rossignol , France
Maheswaran S, India
Ylias Sabri , Australia
Sourabh Sahu , India
José P. Santos , Spain
Sina Sareh, United Kingdom
Isabel Sayago , Spain
Andreas Schütze , Germany
Praveen K. Sekhar , USA
Sandra Sendra, Spain
Sandeep Sharma, India
Sunil Kumar Singh Singh , India
Yadvendra Singh , USA
Afaque Manzoor Soomro , Pakistan
Vincenzo Spagnolo, Italy
Kathiravan Srinivasan , India
Sachin K. Srivastava , India
Stefano Stassi , Italy

Danfeng Sun, China
Ashok Sundramoorthy, India
Salvatore Surdo , Italy
Roshan Thotagamuge , Sri Lanka
Guiyun Tian , United Kingdom
Sri Ramulu Torati , USA
Abdellah Touhafi , Belgium
Hoang Vinh Tran , Vietnam
Aitor Urrutia , Spain
Hana Vaisocherova - Lislalova , Czech
Republic
Everardo Vargas-Rodriguez , Mexico
Xavier Vilanova , Spain
Stanislav Vitek , Czech Republic
Luca Vollero , Italy
Tomasz Wandowski , Poland
Bohui Wang, China
Qihao Weng, USA
Penghai Wu , China
Qiang Wu, United Kingdom
Yuedong Xie , China
Chen Yang , China
Jiachen Yang , China
Nitesh Yelve , India
Aijun Yin, China
Chouki Zerrouki , France

Contents

Retracted: A Smart Campus Implementation Architecture Based on Blockchain Technology

Journal of Sensors

Retraction (1 page), Article ID 9898640, Volume 2024 (2024)

Retracted: Next Generation IoT and Blockchain Integration

Journal of Sensors

Retraction (1 page), Article ID 9896189, Volume 2024 (2024)

Retracted: Wireless Sensor Network and AI Application for Educational Technology Course

Journal of Sensors

Retraction (1 page), Article ID 9875049, Volume 2024 (2024)

Retracted: Artificial Intelligence-Based Interactive Art Design under Neural Network Vision Valve

Journal of Sensors

Retraction (1 page), Article ID 9870968, Volume 2024 (2024)

Retracted: Mixed Linear Programming for Charging Vehicle Scheduling in Large-Scale Rechargeable WSNs

Journal of Sensors

Retraction (1 page), Article ID 9862861, Volume 2024 (2024)

Retracted: A 146-dB-Ohm Gain 14-pARMS Noise Patch-Clamp Amplifier for Whole-Cell Ion Current Detection

Journal of Sensors

Retraction (1 page), Article ID 9856934, Volume 2024 (2024)

Retracted: An Efficient Multispectral Image Classification and Optimization Using Remote Sensing Data

Journal of Sensors

Retraction (1 page), Article ID 9856102, Volume 2024 (2024)

Retracted: Construal Attacks on Wireless Data Storage Applications and Unraveling Using Machine Learning Algorithm

Journal of Sensors

Retraction (1 page), Article ID 9853625, Volume 2024 (2024)

Retracted: Architectural Interior Design and Space Layout Optimization Method Based on VR and 5G Technology

Journal of Sensors

Retraction (1 page), Article ID 9841087, Volume 2024 (2024)

Retracted: A 516 μ W, 121.2 dB-SNDR, and 125.1 dB-DR Discrete-Time Sigma-Delta Modulator with a 20 kHz BW

Journal of Sensors

Retraction (1 page), Article ID 9839150, Volume 2024 (2024)

Retracted: Exploration and Practice of Multidisciplinary Integration of Law Teaching under the Background of IOT and Wireless Communication

Journal of Sensors

Retraction (1 page), Article ID 9834804, Volume 2024 (2024)

Retracted: Enhance-Net: An Approach to Boost the Performance of Deep Learning Model Based on Real-Time Medical Images

Journal of Sensors

Retraction (1 page), Article ID 9832826, Volume 2024 (2024)

Retracted: Storage Method for Medical and Health Big Data Based on Distributed Sensor Network

Journal of Sensors

Retraction (1 page), Article ID 9831329, Volume 2024 (2024)

Retracted: A Mathematical Queuing Model Analysis Using Secure Data Authentication Framework for Modern Healthcare Applications

Journal of Sensors

Retraction (1 page), Article ID 9828646, Volume 2024 (2024)

Retracted: Data Acquisition through Mobile Sink for WSNs with Obstacles Using Support Vector Machine

Journal of Sensors

Retraction (1 page), Article ID 9827414, Volume 2024 (2024)

Retracted: Application and Analysis of RGB-D Salient Object Detection in Photographic Camera Vision Processing

Journal of Sensors

Retraction (1 page), Article ID 9818214, Volume 2024 (2024)

Retracted: Application of "TCM + Smart Elderly Care" in the Medical-Nursing Care Integration Service System

Journal of Sensors

Retraction (1 page), Article ID 9817023, Volume 2024 (2024)

Retracted: Improvement and Reduction of Self-Heating Effect in AlGaIn/GaN HEMT Devices

Journal of Sensors

Retraction (1 page), Article ID 9812862, Volume 2024 (2024)

Retracted: FMT Selector: Fourier-Mellin Transformer with High Speed Rotating in Ship Target Detection and Tracking Based on Internet of Things and Wireless Sensor Network

Journal of Sensors

Retraction (1 page), Article ID 9810638, Volume 2024 (2024)

Contents

Retracted: A Study of Language Use Impact in Radio Broadcasting: A Linguistic and Big Data Integration Approach

Journal of Sensors

Retraction (1 page), Article ID 9801803, Volume 2024 (2024)

Retracted: A Low Power ROIC with Extended Counting ADC Based on Circuit Noise Analysis for Sensor Arrays in IoT System

Journal of Sensors

Retraction (1 page), Article ID 9784532, Volume 2024 (2024)

Retracted: Difficulties and Countermeasures of Game Localization Translation Based on the IoT and Big Data

Journal of Sensors

Retraction (1 page), Article ID 9782351, Volume 2024 (2024)

Retracted: Monitoring of Single-Phase Induction Motor through IoT Using ESP32 Module

Journal of Sensors

Retraction (1 page), Article ID 9764305, Volume 2024 (2024)

Retracted: A Machine Learning in Binary and Multiclassification Results on Imbalanced Heart Disease Data Stream

Journal of Sensors

Retraction (1 page), Article ID 9762420, Volume 2024 (2024)

Retracted: Uncertainty Analysis of Key Influencing Factors on Stability of Tailings Dam Body

Journal of Sensors

Retraction (1 page), Article ID 9760423, Volume 2024 (2024)

Retracted: Innovative Application of Sensor Combined with Speech Recognition Technology in College English Education in the Context of Artificial Intelligence

Journal of Sensors

Retraction (1 page), Article ID 9870608, Volume 2023 (2023)

Retracted: Ethical Framework of Social Media Based on Text Analysis of Terms of Service of Six Major Platforms

Journal of Sensors

Retraction (1 page), Article ID 9846261, Volume 2023 (2023)

Retracted: Research on Localization Parameter Estimation and Algorithm in the Digital Television Terrestrial Broadcasting

Journal of Sensors

Retraction (1 page), Article ID 9846091, Volume 2023 (2023)

Retracted: GPS Receiver Position Estimation and DOP Analysis Using a New Form of the Observation Matrix Approximations

Journal of Sensors

Retraction (1 page), Article ID 9824593, Volume 2023 (2023)

Retracted: Selection of Optimum Internal Control Genes for RT-qPCR Analysis of Schisandra chinensis under Four Hormone Treatments

Journal of Sensors

Retraction (1 page), Article ID 9815293, Volume 2023 (2023)

Retracted: The Construction of Conceptual Framework of Enterprise Internal Control Evaluation Report

Journal of Sensors

Retraction (1 page), Article ID 9764359, Volume 2023 (2023)

Retracted: Logistics Supply Chain Management Mode of Chinese E-Commerce Enterprises under the Background of Big Data and Internet of Things

Journal of Sensors

Retraction (1 page), Article ID 9851864, Volume 2023 (2023)

Retracted: Analysis on the Educational Value of Winter Olympic Spirit in Track and Field Teaching Based on Data Mining under Artificial Intelligence

Journal of Sensors

Retraction (1 page), Article ID 9842703, Volume 2023 (2023)

Retracted: Construction and Development of Modern Brand Marketing Management Mode Based on Artificial Intelligence

Journal of Sensors

Retraction (1 page), Article ID 9758414, Volume 2023 (2023)

Retracted: The Application of Traditional Chinese Woodcut Printmaking Language in Digital Painting Based on Intelligent Computing

Journal of Sensors

Retraction (1 page), Article ID 9854518, Volume 2023 (2023)

Retracted: Preschool Education Based on Computer Information Technology Literacy and Big Data

Journal of Sensors

Retraction (1 page), Article ID 9832453, Volume 2023 (2023)

Retracted: Investigation on the Use of Virtual Reality in the Flipped Teaching of Martial Arts Taijiquan Based on Deep Learning and Big Data Analytics

Journal of Sensors

Retraction (1 page), Article ID 9823054, Volume 2023 (2023)

Retracted: Consumption Behavior Prediction Based on Multiobjective Evolutionary Algorithm

Journal of Sensors

Retraction (1 page), Article ID 9812637, Volume 2023 (2023)

Retracted: A Novel Multidose Dry Powder Inhaler and Its Application in Patients with Asthma and COPD

Journal of Sensors

Retraction (1 page), Article ID 9807538, Volume 2023 (2023)

Contents

Retracted: A BP Neural Network-Based Early Warning Model for Student Performance in the Context of Big Data

Journal of Sensors


Retraction (1 page), Article ID 9783572, Volume 2023 (2023)

[Retracted] Enhance-Net: An Approach to Boost the Performance of Deep Learning Model Based on Real-Time Medical Images

Vipul Narayan , Pawan Kumar Mall , Ahmed Alkhayyat , Kumar Abhishek , Sanjay Kumar , and Prakash Pandey 



Research Article (15 pages), Article ID 8276738, Volume 2023 (2023)

[Retracted] Uncertainty Analysis of Key Influencing Factors on Stability of Tailings Dam Body

Shanguang Qian and Kepeng Hou 


Research Article (11 pages), Article ID 7521356, Volume 2023 (2023)

[Retracted] FMT Selector: Fourier-Mellin Transformer with High Speed Rotating in Ship Target Detection and Tracking Based on Internet of Things and Wireless Sensor Network

Jiayi Xu , Changzhen Qiu , and Luping Wang


Research Article (8 pages), Article ID 2637529, Volume 2023 (2023)

[Retracted] Research on Localization Parameter Estimation and Algorithm in the Digital Television Terrestrial Broadcasting

Songjian Bao , Shouliang Yang, Hanwen Ou, and Jing Song


Research Article (12 pages), Article ID 1810507, Volume 2023 (2023)

[Retracted] Innovative Application of Sensor Combined with Speech Recognition Technology in College English Education in the Context of Artificial Intelligence

Juan Guo 


Research Article (11 pages), Article ID 9281914, Volume 2023 (2023)

[Retracted] Wireless Sensor Network and AI Application for Educational Technology Course

Xiaoyue Luo 

Research Article (11 pages), Article ID 2093354, Volume 2023 (2023)

[Retracted] Storage Method for Medical and Health Big Data Based on Distributed Sensor Network

Hui Chen , Zhao Song, and Feng Yang


Research Article (10 pages), Article ID 8506485, Volume 2023 (2023)

Techniques Based on Metaheuristics Combined with an Adaptive Neurofuzzy System and Seismic Sensors for the Prediction of Earthquakes

Anurag Rana , Gaurav Gupta , Pankaj Vaidya , Waleed Salehi , Shakila Basheer , and Madhulika Bhatia 

Research Article (14 pages), Article ID 5063981, Volume 2023 (2023)

Industrial Internet Sensor Node Construction and System Construction Based on Blockchain Technology

Jia Hong Zhou 

Research Article (13 pages), Article ID 6137395, Volume 2023 (2023)

Adaptive Fast Independent Component Analysis Methods for Mitigating Multipath Effects in GNSS Deformation Monitoring

Rong Yuan, Shengli Xie , Zhenni Li, and Zhaoshui He



Research Article (10 pages), Article ID 4604950, Volume 2022 (2022)





[Retracted] Monitoring of Single-Phase Induction Motor through IoT Using ESP32 Module

Abhinab Shukla , S. P. Shukla , S. T. Chacko , Md. Khaja Mohiddin , and Kinde Anlay Fante 

Research Article (8 pages), Article ID 8933442, Volume 2022 (2022)


An Efficient Multilevel Thresholding Scheme for Heart Image Segmentation Using a Hybrid Generalized Adversarial Network

A. Mallikarjuna Reddy , K. S. Reddy , M. Jayaram , N. Venkata Maha Lakshmi , Rajanikanth

Aluvalu , T. R. Mahesh , V. Vinoth Kumar , and D. Stalin Alex 


Research Article (11 pages), Article ID 4093658, Volume 2022 (2022)

[Retracted] Preschool Education Based on Computer Information Technology Literacy and Big Data

Lan Luo 






Research Article (10 pages), Article ID 4457811, Volume 2022 (2022)

[Retracted] Exploration and Practice of Multidisciplinary Integration of Law Teaching under the Background of IOT and Wireless Communication

Xiting Sun 

Research Article (8 pages), Article ID 3950001, Volume 2022 (2022)

Smart Home-Based Complex Interwoven Activities for Cognitive Health Assessment

Shtwai Alsubai , Abdullah Alqahtani , Mohemmed Sha , Sidra Abbas , Ahmad Almadhor , Vesely

Peter , and Huma Mughal 

Research Article (10 pages), Article ID 3792394, Volume 2022 (2022)





Evolution and Evaluation: Sarcasm Analysis for Twitter Data Using Sentiment Analysis

Monika Bhakuni, Karan Kumar , Sonia , Celestine Iwendi , and Avtar Singh 

Research Article (10 pages), Article ID 6287559, Volume 2022 (2022)

[Retracted] Application of "TCM + Smart Elderly Care" in the Medical-Nursing Care Integration Service System


Xuanxuan Wang, Huaiying Shi, Guo Lu, Zhiping Huang, Yichen Zhang, Yumei Lao, Guangjie Li, Xun

Gong , Ping Wang , Xing Wang , and Yidan Zhang 

Research Article (7 pages), Article ID 5154528, Volume 2022 (2022)






Contents

[Retracted] Architectural Interior Design and Space Layout Optimization Method Based on VR and 5G Technology

Yang Wu 



Research Article (10 pages), Article ID 7396816, Volume 2022 (2022)

[Retracted] An Efficient Multispectral Image Classification and Optimization Using Remote Sensing Data

S. Janarthanan , T. Ganesh Kumar , S. Janakiraman , Rajesh Kumar Dhanaraj , and Mohd Asif Shah 


Research Article (11 pages), Article ID 2004716, Volume 2022 (2022)

[Retracted] Analysis on the Educational Value of Winter Olympic Spirit in Track and Field Teaching Based on Data Mining under Artificial Intelligence

Ao Yu , Jianxing Wang, Yixin Zhou , Xiaoyu Qiao, Song Yan, Yufang Feng, Elvan Marcos, Lee Seok Jae, and Avera Fiaidhi

Research Article (8 pages), Article ID 9435846, Volume 2022 (2022)

Application of Heart Rate Combined with Acceleration Motion Sensor in Sports Dance Teaching

Lin Li, Yuanyuan Liu, Yue Gu , and Zhe Zhu


Research Article (11 pages), Article ID 6410339, Volume 2022 (2022)

[Retracted] Investigation on the Use of Virtual Reality in the Flipped Teaching of Martial Arts Taijiquan Based on Deep Learning and Big Data Analytics

Zhang HanLiang  and Zhang LiNa 


Research Article (14 pages), Article ID 3921842, Volume 2022 (2022)

Classification, Application, Challenge, and Future of Midair Gestures in Augmented Reality

Yi Lu , Xiaoye Wang, Jiangtao Gong, Lejia Zhou, and Sen Ge




Research Article (10 pages), Article ID 3208047, Volume 2022 (2022)

[Retracted] Difficulties and Countermeasures of Game Localization Translation Based on the IoT and Big Data

Qiaoke Sun 

Research Article (7 pages), Article ID 4651956, Volume 2022 (2022)

[Retracted] A Low Power ROIC with Extended Counting ADC Based on Circuit Noise Analysis for Sensor Arrays in IoT System

Ye Zhou , Wengao Lu , Shanzhe Yu, Dunshan Yu, Yacong Zhang, and Zhongjian Chen 




Research Article (12 pages), Article ID 5304613, Volume 2022 (2022)

Thermal and Wet Comfort of Clothing in Different Environments Based on Multidimensional Sensor Data Fusion and Intelligent Detection

Xia Hou 

Research Article (13 pages), Article ID 4163308, Volume 2022 (2022)

A Review of Security and Privacy Concerns in the Internet of Things (IoT)

Muhammad Aqeel, Fahad Ali, Muhammad Waseem Iqbal , Toqir A. Rana , Muhammad Arif, and Md. Rabiul Auwul 


Review Article (20 pages), Article ID 5724168, Volume 2022 (2022)

[Retracted] A BP Neural Network-Based Early Warning Model for Student Performance in the Context of Big Data

Chengxiang Shi  and Yun Tan


Research Article (10 pages), Article ID 2958261, Volume 2022 (2022)

[Retracted] Artificial Intelligence-Based Interactive Art Design under Neural Network Vision Valve

Yuqi Zhao 




Research Article (10 pages), Article ID 3628955, Volume 2022 (2022)

[Retracted] The Application of Traditional Chinese Woodcut Printmaking Language in Digital Painting Based on Intelligent Computing

Changhuan Chen 



Research Article (12 pages), Article ID 2223868, Volume 2022 (2022)

[Retracted] Selection of Optimum Internal Control Genes for RT-qPCR Analysis of *Schisandra chinensis* under Four Hormone Treatments

Xiuyan Liu , Lifan Zhang , and Shihai Yang 


Research Article (10 pages), Article ID 9299289, Volume 2022 (2022)

[Retracted] Consumption Behavior Prediction Based on Multiobjective Evolutionary Algorithm

Jun Li, Nor Siabbinti Jaharudin , and Yu Song 



Research Article (11 pages), Article ID 2525740, Volume 2022 (2022)

[Retracted] Application and Analysis of RGB-D Salient Object Detection in Photographic Camera Vision Processing

Qiang Fu 


Research Article (10 pages), Article ID 5125346, Volume 2022 (2022)

[Retracted] A Study of Language Use Impact in Radio Broadcasting: A Linguistic and Big Data Integration Approach

Young Praise Chukwunalu , Angela U. N. Nwankwere, Dereck A. Orji, and MohdAsif Shah 



Research Article (16 pages), Article ID 1440935, Volume 2022 (2022)

Robot Obstacle Avoidance Controller Based on Deep Reinforcement Learning

Yaokun Tang , Qingyu Chen, and Yuxin Wei

Research Article (10 pages), Article ID 4194747, Volume 2022 (2022)

[Retracted] A Smart Campus Implementation Architecture Based on Blockchain Technology

Jin Lu  and Bo Wu 

Research Article (14 pages), Article ID 2434277, Volume 2022 (2022)

Contents

[Retracted] Improvement and Reduction of Self-Heating Effect in AlGaIn/GaN HEMT Devices

Hui Chen , Naiyun Tang, and Zhipeng Zuo

Research Article (10 pages), Article ID 5378666, Volume 2022 (2022)

[Retracted] Construction and Development of Modern Brand Marketing Management Mode Based on Artificial Intelligence

Hailang Cui , Yuankun Nie, Zhanling Li, and Jun Zeng

Research Article (11 pages), Article ID 9246545, Volume 2022 (2022)

[Retracted] A Machine Learning in Binary and Multiclassification Results on Imbalanced Heart Disease Data Stream

Danish Hamid, Syed Sajid Ullah, Jawaid Iqbal, Saddam Hussain , Ch. Anwar ul Hassan , and Fazlullah Umar 


Research Article (13 pages), Article ID 8400622, Volume 2022 (2022)

[Retracted] GPS Receiver Position Estimation and DOP Analysis Using a New Form of the Observation Matrix Approximations

Ashok Kumar N , P. Sirish Kumar , Md. Khaja Mohiddin , Mulugeta Tegegn Gemedo , and Anup Mishra 


Research Article (12 pages), Article ID 6772077, Volume 2022 (2022)

[Retracted] The Construction of Conceptual Framework of Enterprise Internal Control Evaluation Report

Yushu Kuang, Zongkeng Li , and Changliang Pan



Research Article (11 pages), Article ID 2753001, Volume 2022 (2022)

[Retracted] Logistics Supply Chain Management Mode of Chinese E-Commerce Enterprises under the Background of Big Data and Internet of Things

Xiao Han  and Jingyi Wang



Research Article (7 pages), Article ID 7818944, Volume 2022 (2022)

[Retracted] Ethical Framework of Social Media Based on Text Analysis of Terms of Service of Six Major Platforms

Wanxi Mao  and Zhaoxin Wang 


Research Article (9 pages), Article ID 1136017, Volume 2022 (2022)

[Retracted] A Mathematical Queuing Model Analysis Using Secure Data Authentication Framework for Modern Healthcare Applications

A. Samson Arun Raj, R. Venkatesan, S. Malathi, V. D. Ambeth Kumar , E. Thenmozhi, Anbarasu Dhandapani , M. Ashok Kumar, and B. Chitra


Research Article (15 pages), Article ID 8397635, Volume 2022 (2022)

[Retracted] A 516 μ W, 121.2 dB-SNDR, and 125.1 dB-DR Discrete-Time Sigma-Delta Modulator with a 20 kHz BW

Lingwei Kong 






Research Article (9 pages), Article ID 9047631, Volume 2022 (2022)

[Retracted] A 146-dB-Ohm Gain 14-pARMS Noise Patch-Clamp Amplifier for Whole-Cell Ion Current Detection

Wenbin Pan 


Research Article (14 pages), Article ID 8469476, Volume 2022 (2022)

[Retracted] Mixed Linear Programming for Charging Vehicle Scheduling in Large-Scale Rechargeable WSNs

P. Suman Prakash , M. Janardhan , K. Sreenivasulu , Shaik Imam Saheb, Shaik Neeha , and M. Bhavsingh 

Research Article (13 pages), Article ID 8373343, Volume 2022 (2022)

Fuzzy Data Mining and Bioinformatics Analysis in Methylation Analysis of M6A Gene Promoter Region in Esophageal Cancer

Shuoming Wu, Xiangbao Yang, Xie Qiu, and Yinpeng Pan 




Research Article (12 pages), Article ID 4420717, Volume 2022 (2022)

[Retracted] A Novel Multidose Dry Powder Inhaler and Its Application in Patients with Asthma and COPD

Feng Shi , Chaoting Zhu , Tianqi Zhou , and Jianhui Liu 

Research Article (14 pages), Article ID 3051484, Volume 2022 (2022)

FogDedupe: A Fog-Centric Deduplication Approach Using Multi-Key Homomorphic Encryption Technique

Mohamed Sirajudeen Yoosuf, C. Muralidharan, S. Shitharth , Mohammed Alghamdi, Mohammed Maray , and Osama Bassam J. Rabie 

Research Article (16 pages), Article ID 6759875, Volume 2022 (2022)

[Retracted] Data Acquisition through Mobile Sink for WSNs with Obstacles Using Support Vector Machine

Guduri Sulakshana  and Govardhan Reddy Kamatam 

Research Article (20 pages), Article ID 4242740, Volume 2022 (2022)

[Retracted] Next Generation IoT and Blockchain Integration

Sarvesh Tanwar, Neelam Gupta, Celestine Iwendi , Karan Kumar , and Mamdouh Alenezi 

Review Article (14 pages), Article ID 9077348, Volume 2022 (2022)

[Retracted] Construal Attacks on Wireless Data Storage Applications and Unraveling Using Machine Learning Algorithm

Pravin R. Kshirsagar , Hariprasath Manoharan , Hassan A. Alterazi , Nawaf Alhebaishi , Osama Bassam J. Rabie , and S. Shitharth 

Research Article (13 pages), Article ID 9386989, Volume 2022 (2022)

Retraction

Retracted: A Smart Campus Implementation Architecture Based on Blockchain Technology

Journal of Sensors

Received 23 January 2024; Accepted 23 January 2024; Published 24 January 2024

Copyright © 2024 Journal of Sensors. This is an open access article distributed under the Creative Commons Attribution License, which permits unrestricted use, distribution, and reproduction in any medium, provided the original work is properly cited.

This article has been retracted by Hindawi following an investigation undertaken by the publisher [1]. This investigation has uncovered evidence of one or more of the following indicators of systematic manipulation of the publication process:

- (1) Discrepancies in scope
- (2) Discrepancies in the description of the research reported
- (3) Discrepancies between the availability of data and the research described
- (4) Inappropriate citations
- (5) Incoherent, meaningless and/or irrelevant content included in the article
- (6) Manipulated or compromised peer review

The presence of these indicators undermines our confidence in the integrity of the article's content and we cannot, therefore, vouch for its reliability. Please note that this notice is intended solely to alert readers that the content of this article is unreliable. We have not investigated whether authors were aware of or involved in the systematic manipulation of the publication process.

Wiley and Hindawi regrets that the usual quality checks did not identify these issues before publication and have since put additional measures in place to safeguard research integrity.

We wish to credit our own Research Integrity and Research Publishing teams and anonymous and named external researchers and research integrity experts for contributing to this investigation.

The corresponding author, as the representative of all authors, has been given the opportunity to register their agreement or disagreement to this retraction. We have kept a record of any response received.

References

- [1] J. Lu and B. Wu, "A Smart Campus Implementation Architecture Based on Blockchain Technology," *Journal of Sensors*, vol. 2022, Article ID 2434277, 14 pages, 2022.

Retraction

Retracted: Next Generation IoT and Blockchain Integration

Journal of Sensors

Received 23 January 2024; Accepted 23 January 2024; Published 24 January 2024

Copyright © 2024 Journal of Sensors. This is an open access article distributed under the Creative Commons Attribution License, which permits unrestricted use, distribution, and reproduction in any medium, provided the original work is properly cited.

This article has been retracted by Hindawi following an investigation undertaken by the publisher [1]. This investigation has uncovered evidence of one or more of the following indicators of systematic manipulation of the publication process:

- (1) Discrepancies in scope
- (2) Discrepancies in the description of the research reported
- (3) Discrepancies between the availability of data and the research described
- (4) Inappropriate citations
- (5) Incoherent, meaningless and/or irrelevant content included in the article
- (6) Manipulated or compromised peer review

The presence of these indicators undermines our confidence in the integrity of the article's content and we cannot, therefore, vouch for its reliability. Please note that this notice is intended solely to alert readers that the content of this article is unreliable. We have not investigated whether authors were aware of or involved in the systematic manipulation of the publication process.

Wiley and Hindawi regrets that the usual quality checks did not identify these issues before publication and have since put additional measures in place to safeguard research integrity.

We wish to credit our own Research Integrity and Research Publishing teams and anonymous and named external researchers and research integrity experts for contributing to this investigation.

The corresponding author, as the representative of all authors, has been given the opportunity to register their agreement or disagreement to this retraction. We have kept a record of any response received.

References

- [1] S. Tanwar, N. Gupta, C. Iwendi, K. Kumar, and M. Alenezi, "Next Generation IoT and Blockchain Integration," *Journal of Sensors*, vol. 2022, Article ID 9077348, 14 pages, 2022.

Retraction

Retracted: Wireless Sensor Network and AI Application for Educational Technology Course

Journal of Sensors

Received 23 January 2024; Accepted 23 January 2024; Published 24 January 2024

Copyright © 2024 Journal of Sensors. This is an open access article distributed under the Creative Commons Attribution License, which permits unrestricted use, distribution, and reproduction in any medium, provided the original work is properly cited.

This article has been retracted by Hindawi following an investigation undertaken by the publisher [1]. This investigation has uncovered evidence of one or more of the following indicators of systematic manipulation of the publication process:

- (1) Discrepancies in scope
- (2) Discrepancies in the description of the research reported
- (3) Discrepancies between the availability of data and the research described
- (4) Inappropriate citations
- (5) Incoherent, meaningless and/or irrelevant content included in the article
- (6) Manipulated or compromised peer review

The presence of these indicators undermines our confidence in the integrity of the article's content and we cannot, therefore, vouch for its reliability. Please note that this notice is intended solely to alert readers that the content of this article is unreliable. We have not investigated whether authors were aware of or involved in the systematic manipulation of the publication process.

Wiley and Hindawi regrets that the usual quality checks did not identify these issues before publication and have since put additional measures in place to safeguard research integrity.

We wish to credit our own Research Integrity and Research Publishing teams and anonymous and named external researchers and research integrity experts for contributing to this investigation.

The corresponding author, as the representative of all authors, has been given the opportunity to register their agreement or disagreement to this retraction. We have kept a record of any response received.

References

- [1] X. Luo, "Wireless Sensor Network and AI Application for Educational Technology Course," *Journal of Sensors*, vol. 2023, Article ID 2093354, 11 pages, 2023.

Retraction

Retracted: Artificial Intelligence-Based Interactive Art Design under Neural Network Vision Valve

Journal of Sensors

Received 23 January 2024; Accepted 23 January 2024; Published 24 January 2024

Copyright © 2024 Journal of Sensors. This is an open access article distributed under the Creative Commons Attribution License, which permits unrestricted use, distribution, and reproduction in any medium, provided the original work is properly cited.

This article has been retracted by Hindawi following an investigation undertaken by the publisher [1]. This investigation has uncovered evidence of one or more of the following indicators of systematic manipulation of the publication process:

- (1) Discrepancies in scope
- (2) Discrepancies in the description of the research reported
- (3) Discrepancies between the availability of data and the research described
- (4) Inappropriate citations
- (5) Incoherent, meaningless and/or irrelevant content included in the article
- (6) Manipulated or compromised peer review

The presence of these indicators undermines our confidence in the integrity of the article's content and we cannot, therefore, vouch for its reliability. Please note that this notice is intended solely to alert readers that the content of this article is unreliable. We have not investigated whether authors were aware of or involved in the systematic manipulation of the publication process.

Wiley and Hindawi regrets that the usual quality checks did not identify these issues before publication and have since put additional measures in place to safeguard research integrity.

We wish to credit our own Research Integrity and Research Publishing teams and anonymous and named external researchers and research integrity experts for contributing to this investigation.

The corresponding author, as the representative of all authors, has been given the opportunity to register their agreement or disagreement to this retraction. We have kept a record of any response received.

References

- [1] Y. Zhao, "Artificial Intelligence-Based Interactive Art Design under Neural Network Vision Valve," *Journal of Sensors*, vol. 2022, Article ID 3628955, 10 pages, 2022.

Retraction

Retracted: Mixed Linear Programming for Charging Vehicle Scheduling in Large-Scale Rechargeable WSNs

Journal of Sensors

Received 23 January 2024; Accepted 23 January 2024; Published 24 January 2024

Copyright © 2024 Journal of Sensors. This is an open access article distributed under the Creative Commons Attribution License, which permits unrestricted use, distribution, and reproduction in any medium, provided the original work is properly cited.

This article has been retracted by Hindawi following an investigation undertaken by the publisher [1]. This investigation has uncovered evidence of one or more of the following indicators of systematic manipulation of the publication process:

- (1) Discrepancies in scope
- (2) Discrepancies in the description of the research reported
- (3) Discrepancies between the availability of data and the research described
- (4) Inappropriate citations
- (5) Incoherent, meaningless and/or irrelevant content included in the article
- (6) Manipulated or compromised peer review

The presence of these indicators undermines our confidence in the integrity of the article's content and we cannot, therefore, vouch for its reliability. Please note that this notice is intended solely to alert readers that the content of this article is unreliable. We have not investigated whether authors were aware of or involved in the systematic manipulation of the publication process.

Wiley and Hindawi regrets that the usual quality checks did not identify these issues before publication and have since put additional measures in place to safeguard research integrity.

We wish to credit our own Research Integrity and Research Publishing teams and anonymous and named external researchers and research integrity experts for contributing to this investigation.

The corresponding author, as the representative of all authors, has been given the opportunity to register their agreement or disagreement to this retraction. We have kept a record of any response received.

References

- [1] P. S. Prakash, M. Janardhan, K. Sreenivasulu, S. I. Saheb, S. Neeha, and M. Bhavsingh, "Mixed Linear Programming for Charging Vehicle Scheduling in Large-Scale Rechargeable WSNs," *Journal of Sensors*, vol. 2022, Article ID 8373343, 13 pages, 2022.

Retraction

Retracted: A 146-dB-Ohm Gain 14-pARMS Noise Patch-Clamp Amplifier for Whole-Cell Ion Current Detection

Journal of Sensors

Received 23 January 2024; Accepted 23 January 2024; Published 24 January 2024

Copyright © 2024 Journal of Sensors. This is an open access article distributed under the Creative Commons Attribution License, which permits unrestricted use, distribution, and reproduction in any medium, provided the original work is properly cited.

This article has been retracted by Hindawi following an investigation undertaken by the publisher [1]. This investigation has uncovered evidence of one or more of the following indicators of systematic manipulation of the publication process:

- (1) Discrepancies in scope
- (2) Discrepancies in the description of the research reported
- (3) Discrepancies between the availability of data and the research described
- (4) Inappropriate citations
- (5) Incoherent, meaningless and/or irrelevant content included in the article
- (6) Manipulated or compromised peer review

The presence of these indicators undermines our confidence in the integrity of the article's content and we cannot, therefore, vouch for its reliability. Please note that this notice is intended solely to alert readers that the content of this article is unreliable. We have not investigated whether authors were aware of or involved in the systematic manipulation of the publication process.

Wiley and Hindawi regrets that the usual quality checks did not identify these issues before publication and have since put additional measures in place to safeguard research integrity.

We wish to credit our own Research Integrity and Research Publishing teams and anonymous and named external researchers and research integrity experts for contributing to this investigation.

The corresponding author, as the representative of all authors, has been given the opportunity to register their agreement or disagreement to this retraction. We have kept a record of any response received.

References

- [1] W. Pan, "A 146-dB-Ohm Gain 14-pARMS Noise Patch-Clamp Amplifier for Whole-Cell Ion Current Detection." *Journal of Sensors*, vol. 2022, Article ID 8469476, 14 pages, 2022.

Retraction

Retracted: An Efficient Multispectral Image Classification and Optimization Using Remote Sensing Data

Journal of Sensors

Received 23 January 2024; Accepted 23 January 2024; Published 24 January 2024

Copyright © 2024 Journal of Sensors. This is an open access article distributed under the Creative Commons Attribution License, which permits unrestricted use, distribution, and reproduction in any medium, provided the original work is properly cited.

This article has been retracted by Hindawi following an investigation undertaken by the publisher [1]. This investigation has uncovered evidence of one or more of the following indicators of systematic manipulation of the publication process:

- (1) Discrepancies in scope
- (2) Discrepancies in the description of the research reported
- (3) Discrepancies between the availability of data and the research described
- (4) Inappropriate citations
- (5) Incoherent, meaningless and/or irrelevant content included in the article
- (6) Manipulated or compromised peer review

The presence of these indicators undermines our confidence in the integrity of the article's content and we cannot, therefore, vouch for its reliability. Please note that this notice is intended solely to alert readers that the content of this article is unreliable. We have not investigated whether authors were aware of or involved in the systematic manipulation of the publication process.

Wiley and Hindawi regrets that the usual quality checks did not identify these issues before publication and have since put additional measures in place to safeguard research integrity.

We wish to credit our own Research Integrity and Research Publishing teams and anonymous and named external researchers and research integrity experts for contributing to this investigation.

The corresponding author, as the representative of all authors, has been given the opportunity to register their agreement or disagreement to this retraction. We have kept a record of any response received.

References

- [1] S. Janarthanan, T. Ganesh Kumar, S. Janakiraman, R. K. Dhanaraj, and M. A. Shah, "An Efficient Multispectral Image Classification and Optimization Using Remote Sensing Data," *Journal of Sensors*, vol. 2022, Article ID 2004716, 11 pages, 2022.

Retraction

Retracted: Construal Attacks on Wireless Data Storage Applications and Unraveling Using Machine Learning Algorithm

Journal of Sensors

Received 23 January 2024; Accepted 23 January 2024; Published 24 January 2024

Copyright © 2024 Journal of Sensors. This is an open access article distributed under the Creative Commons Attribution License, which permits unrestricted use, distribution, and reproduction in any medium, provided the original work is properly cited.

This article has been retracted by Hindawi following an investigation undertaken by the publisher [1]. This investigation has uncovered evidence of one or more of the following indicators of systematic manipulation of the publication process:

- (1) Discrepancies in scope
- (2) Discrepancies in the description of the research reported
- (3) Discrepancies between the availability of data and the research described
- (4) Inappropriate citations
- (5) Incoherent, meaningless and/or irrelevant content included in the article
- (6) Manipulated or compromised peer review

The presence of these indicators undermines our confidence in the integrity of the article's content and we cannot, therefore, vouch for its reliability. Please note that this notice is intended solely to alert readers that the content of this article is unreliable. We have not investigated whether authors were aware of or involved in the systematic manipulation of the publication process.

Wiley and Hindawi regrets that the usual quality checks did not identify these issues before publication and have since put additional measures in place to safeguard research integrity.

We wish to credit our own Research Integrity and Research Publishing teams and anonymous and named external researchers and research integrity experts for contributing to this investigation.

The corresponding author, as the representative of all authors, has been given the opportunity to register their agreement or disagreement to this retraction. We have kept a record of any response received.

References

- [1] P. R. Kshirsagar, H. Manoharan, H. A. Alterazi, N. Alhebaishi, O. B. J. Rabie, and S. Shitharth, "Construal Attacks on Wireless Data Storage Applications and Unraveling Using Machine Learning Algorithm," *Journal of Sensors*, vol. 2022, Article ID 9386989, 13 pages, 2022.

Retraction

Retracted: Architectural Interior Design and Space Layout Optimization Method Based on VR and 5G Technology

Journal of Sensors

Received 23 January 2024; Accepted 23 January 2024; Published 24 January 2024

Copyright © 2024 Journal of Sensors. This is an open access article distributed under the Creative Commons Attribution License, which permits unrestricted use, distribution, and reproduction in any medium, provided the original work is properly cited.

This article has been retracted by Hindawi following an investigation undertaken by the publisher [1]. This investigation has uncovered evidence of one or more of the following indicators of systematic manipulation of the publication process:

- (1) Discrepancies in scope
- (2) Discrepancies in the description of the research reported
- (3) Discrepancies between the availability of data and the research described
- (4) Inappropriate citations
- (5) Incoherent, meaningless and/or irrelevant content included in the article
- (6) Manipulated or compromised peer review

The presence of these indicators undermines our confidence in the integrity of the article's content and we cannot, therefore, vouch for its reliability. Please note that this notice is intended solely to alert readers that the content of this article is unreliable. We have not investigated whether authors were aware of or involved in the systematic manipulation of the publication process.

Wiley and Hindawi regrets that the usual quality checks did not identify these issues before publication and have since put additional measures in place to safeguard research integrity.

We wish to credit our own Research Integrity and Research Publishing teams and anonymous and named external researchers and research integrity experts for contributing to this investigation.

The corresponding author, as the representative of all authors, has been given the opportunity to register their agreement or disagreement to this retraction. We have kept a record of any response received.

References

- [1] Y. Wu, "Architectural Interior Design and Space Layout Optimization Method Based on VR and 5G Technology," *Journal of Sensors*, vol. 2022, Article ID 7396816, 10 pages, 2022.

Retraction

Retracted: A 516 μ W, 121.2 dB-SNDR, and 125.1 dB-DR Discrete-Time Sigma-Delta Modulator with a 20 kHz BW

Journal of Sensors

Received 23 January 2024; Accepted 23 January 2024; Published 24 January 2024

Copyright © 2024 Journal of Sensors. This is an open access article distributed under the Creative Commons Attribution License, which permits unrestricted use, distribution, and reproduction in any medium, provided the original work is properly cited.

This article has been retracted by Hindawi following an investigation undertaken by the publisher [1]. This investigation has uncovered evidence of one or more of the following indicators of systematic manipulation of the publication process:

- (1) Discrepancies in scope
- (2) Discrepancies in the description of the research reported
- (3) Discrepancies between the availability of data and the research described
- (4) Inappropriate citations
- (5) Incoherent, meaningless and/or irrelevant content included in the article
- (6) Manipulated or compromised peer review

The presence of these indicators undermines our confidence in the integrity of the article's content and we cannot, therefore, vouch for its reliability. Please note that this notice is intended solely to alert readers that the content of this article is unreliable. We have not investigated whether authors were aware of or involved in the systematic manipulation of the publication process.

Wiley and Hindawi regrets that the usual quality checks did not identify these issues before publication and have since put additional measures in place to safeguard research integrity.

We wish to credit our own Research Integrity and Research Publishing teams and anonymous and named external researchers and research integrity experts for contributing to this investigation.

The corresponding author, as the representative of all authors, has been given the opportunity to register their agreement or disagreement to this retraction. We have kept a record of any response received.

References

- [1] L. Kong, "A 516 μ W, 121.2 dB-SNDR, and 125.1 dB-DR Discrete-Time Sigma-Delta Modulator with a 20 kHz BW," *Journal of Sensors*, vol. 2022, Article ID 9047631, 9 pages, 2022.

Retraction

Retracted: Exploration and Practice of Multidisciplinary Integration of Law Teaching under the Background of IOT and Wireless Communication

Journal of Sensors

Received 23 January 2024; Accepted 23 January 2024; Published 24 January 2024

Copyright © 2024 Journal of Sensors. This is an open access article distributed under the Creative Commons Attribution License, which permits unrestricted use, distribution, and reproduction in any medium, provided the original work is properly cited.

This article has been retracted by Hindawi following an investigation undertaken by the publisher [1]. This investigation has uncovered evidence of one or more of the following indicators of systematic manipulation of the publication process:

- (1) Discrepancies in scope
- (2) Discrepancies in the description of the research reported
- (3) Discrepancies between the availability of data and the research described
- (4) Inappropriate citations
- (5) Incoherent, meaningless and/or irrelevant content included in the article
- (6) Manipulated or compromised peer review

The presence of these indicators undermines our confidence in the integrity of the article's content and we cannot, therefore, vouch for its reliability. Please note that this notice is intended solely to alert readers that the content of this article is unreliable. We have not investigated whether authors were aware of or involved in the systematic manipulation of the publication process.

In addition, our investigation has also shown that one or more of the following human-subject reporting requirements has not been met in this article: ethical approval by an Institutional Review Board (IRB) committee or equivalent, patient/participant consent to participate, and/or agreement to publish patient/participant details (where relevant).

Wiley and Hindawi regrets that the usual quality checks did not identify these issues before publication and have since put additional measures in place to safeguard research integrity.

We wish to credit our own Research Integrity and Research Publishing teams and anonymous and named external

researchers and research integrity experts for contributing to this investigation.

The corresponding author, as the representative of all authors, has been given the opportunity to register their agreement or disagreement to this retraction. We have kept a record of any response received.

References

- [1] X. Sun, "Exploration and Practice of Multidisciplinary Integration of Law Teaching under the Background of IOT and Wireless Communication," *Journal of Sensors*, vol. 2022, Article ID 3950001, 8 pages, 2022.

Retraction

Retracted: Enhance-Net: An Approach to Boost the Performance of Deep Learning Model Based on Real-Time Medical Images

Journal of Sensors

Received 23 January 2024; Accepted 23 January 2024; Published 24 January 2024

Copyright © 2024 Journal of Sensors. This is an open access article distributed under the Creative Commons Attribution License, which permits unrestricted use, distribution, and reproduction in any medium, provided the original work is properly cited.

This article has been retracted by Hindawi following an investigation undertaken by the publisher [1]. This investigation has uncovered evidence of one or more of the following indicators of systematic manipulation of the publication process:

- (1) Discrepancies in scope
- (2) Discrepancies in the description of the research reported
- (3) Discrepancies between the availability of data and the research described
- (4) Inappropriate citations
- (5) Incoherent, meaningless and/or irrelevant content included in the article
- (6) Manipulated or compromised peer review

The presence of these indicators undermines our confidence in the integrity of the article's content and we cannot, therefore, vouch for its reliability. Please note that this notice is intended solely to alert readers that the content of this article is unreliable. We have not investigated whether authors were aware of or involved in the systematic manipulation of the publication process.

Wiley and Hindawi regrets that the usual quality checks did not identify these issues before publication and have since put additional measures in place to safeguard research integrity.

We wish to credit our own Research Integrity and Research Publishing teams and anonymous and named external researchers and research integrity experts for contributing to this investigation.

The corresponding author, as the representative of all authors, has been given the opportunity to register their agreement or disagreement to this retraction. We have kept a record of any response received.

References

- [1] V. Narayan, P. K. Mall, A. Alkhayat, K. Abhishek, S. Kumar, and P. Pandey, "Enhance-Net: An Approach to Boost the Performance of Deep Learning Model Based on Real-Time Medical Images," *Journal of Sensors*, vol. 2023, Article ID 8276738, 15 pages, 2023.

Retraction

Retracted: Storage Method for Medical and Health Big Data Based on Distributed Sensor Network

Journal of Sensors

Received 23 January 2024; Accepted 23 January 2024; Published 24 January 2024

Copyright © 2024 Journal of Sensors. This is an open access article distributed under the Creative Commons Attribution License, which permits unrestricted use, distribution, and reproduction in any medium, provided the original work is properly cited.

This article has been retracted by Hindawi following an investigation undertaken by the publisher [1]. This investigation has uncovered evidence of one or more of the following indicators of systematic manipulation of the publication process:

- (1) Discrepancies in scope
- (2) Discrepancies in the description of the research reported
- (3) Discrepancies between the availability of data and the research described
- (4) Inappropriate citations
- (5) Incoherent, meaningless and/or irrelevant content included in the article
- (6) Manipulated or compromised peer review

The presence of these indicators undermines our confidence in the integrity of the article's content and we cannot, therefore, vouch for its reliability. Please note that this notice is intended solely to alert readers that the content of this article is unreliable. We have not investigated whether authors were aware of or involved in the systematic manipulation of the publication process.

Wiley and Hindawi regrets that the usual quality checks did not identify these issues before publication and have since put additional measures in place to safeguard research integrity.

We wish to credit our own Research Integrity and Research Publishing teams and anonymous and named external researchers and research integrity experts for contributing to this investigation.

The corresponding author, as the representative of all authors, has been given the opportunity to register their agreement or disagreement to this retraction. We have kept a record of any response received.

References

- [1] H. Chen, Z. Song, and F. Yang, "Storage Method for Medical and Health Big Data Based on Distributed Sensor Network," *Journal of Sensors*, vol. 2023, Article ID 8506485, 10 pages, 2023.

Retraction

Retracted: A Mathematical Queuing Model Analysis Using Secure Data Authentication Framework for Modern Healthcare Applications

Journal of Sensors

Received 23 January 2024; Accepted 23 January 2024; Published 24 January 2024

Copyright © 2024 Journal of Sensors. This is an open access article distributed under the Creative Commons Attribution License, which permits unrestricted use, distribution, and reproduction in any medium, provided the original work is properly cited.

This article has been retracted by Hindawi following an investigation undertaken by the publisher [1]. This investigation has uncovered evidence of one or more of the following indicators of systematic manipulation of the publication process:

- (1) Discrepancies in scope
- (2) Discrepancies in the description of the research reported
- (3) Discrepancies between the availability of data and the research described
- (4) Inappropriate citations
- (5) Incoherent, meaningless and/or irrelevant content included in the article
- (6) Manipulated or compromised peer review

The presence of these indicators undermines our confidence in the integrity of the article's content and we cannot, therefore, vouch for its reliability. Please note that this notice is intended solely to alert readers that the content of this article is unreliable. We have not investigated whether authors were aware of or involved in the systematic manipulation of the publication process.

Wiley and Hindawi regrets that the usual quality checks did not identify these issues before publication and have since put additional measures in place to safeguard research integrity.

We wish to credit our own Research Integrity and Research Publishing teams and anonymous and named external researchers and research integrity experts for contributing to this investigation.

The corresponding author, as the representative of all authors, has been given the opportunity to register their agreement or disagreement to this retraction. We have kept a record of any response received.

References

- [1] A. S. A. Raj, R. Venkatesan, S. Malathi et al., "A Mathematical Queuing Model Analysis Using Secure Data Authentication Framework for Modern Healthcare Applications," *Journal of Sensors*, vol. 2022, Article ID 8397635, 15 pages, 2022.

Retraction

Retracted: Data Acquisition through Mobile Sink for WSNs with Obstacles Using Support Vector Machine

Journal of Sensors

Received 23 January 2024; Accepted 23 January 2024; Published 24 January 2024

Copyright © 2024 Journal of Sensors. This is an open access article distributed under the Creative Commons Attribution License, which permits unrestricted use, distribution, and reproduction in any medium, provided the original work is properly cited.

This article has been retracted by Hindawi following an investigation undertaken by the publisher [1]. This investigation has uncovered evidence of one or more of the following indicators of systematic manipulation of the publication process:

- (1) Discrepancies in scope
- (2) Discrepancies in the description of the research reported
- (3) Discrepancies between the availability of data and the research described
- (4) Inappropriate citations
- (5) Incoherent, meaningless and/or irrelevant content included in the article
- (6) Manipulated or compromised peer review

The presence of these indicators undermines our confidence in the integrity of the article's content and we cannot, therefore, vouch for its reliability. Please note that this notice is intended solely to alert readers that the content of this article is unreliable. We have not investigated whether authors were aware of or involved in the systematic manipulation of the publication process.

Wiley and Hindawi regrets that the usual quality checks did not identify these issues before publication and have since put additional measures in place to safeguard research integrity.

We wish to credit our own Research Integrity and Research Publishing teams and anonymous and named external researchers and research integrity experts for contributing to this investigation.

The corresponding author, as the representative of all authors, has been given the opportunity to register their agreement or disagreement to this retraction. We have kept a record of any response received.

References

- [1] G. Sulakshana and G. R. Kamatam, "Data Acquisition through Mobile Sink for WSNs with Obstacles Using Support Vector Machine," *Journal of Sensors*, vol. 2022, Article ID 4242740, 20 pages, 2022.

Retraction

Retracted: Application and Analysis of RGB-D Salient Object Detection in Photographic Camera Vision Processing

Journal of Sensors

Received 23 January 2024; Accepted 23 January 2024; Published 24 January 2024

Copyright © 2024 Journal of Sensors. This is an open access article distributed under the Creative Commons Attribution License, which permits unrestricted use, distribution, and reproduction in any medium, provided the original work is properly cited.

This article has been retracted by Hindawi following an investigation undertaken by the publisher [1]. This investigation has uncovered evidence of one or more of the following indicators of systematic manipulation of the publication process:

- (1) Discrepancies in scope
- (2) Discrepancies in the description of the research reported
- (3) Discrepancies between the availability of data and the research described
- (4) Inappropriate citations
- (5) Incoherent, meaningless and/or irrelevant content included in the article
- (6) Manipulated or compromised peer review

The presence of these indicators undermines our confidence in the integrity of the article's content and we cannot, therefore, vouch for its reliability. Please note that this notice is intended solely to alert readers that the content of this article is unreliable. We have not investigated whether authors were aware of or involved in the systematic manipulation of the publication process.

Wiley and Hindawi regrets that the usual quality checks did not identify these issues before publication and have since put additional measures in place to safeguard research integrity.

We wish to credit our own Research Integrity and Research Publishing teams and anonymous and named external researchers and research integrity experts for contributing to this investigation.

The corresponding author, as the representative of all authors, has been given the opportunity to register their agreement or disagreement to this retraction. We have kept a record of any response received.

References

- [1] Q. Fu, "Application and Analysis of RGB-D Salient Object Detection in Photographic Camera Vision Processing," *Journal of Sensors*, vol. 2022, Article ID 5125346, 10 pages, 2022.

Retraction

Retracted: Application of “TCM + Smart Elderly Care” in the Medical-Nursing Care Integration Service System

Journal of Sensors

Received 23 January 2024; Accepted 23 January 2024; Published 24 January 2024

Copyright © 2024 Journal of Sensors. This is an open access article distributed under the Creative Commons Attribution License, which permits unrestricted use, distribution, and reproduction in any medium, provided the original work is properly cited.

This article has been retracted by Hindawi following an investigation undertaken by the publisher [1]. This investigation has uncovered evidence of one or more of the following indicators of systematic manipulation of the publication process:

- (1) Discrepancies in scope
- (2) Discrepancies in the description of the research reported
- (3) Discrepancies between the availability of data and the research described
- (4) Inappropriate citations
- (5) Incoherent, meaningless and/or irrelevant content included in the article
- (6) Manipulated or compromised peer review

The presence of these indicators undermines our confidence in the integrity of the article’s content and we cannot, therefore, vouch for its reliability. Please note that this notice is intended solely to alert readers that the content of this article is unreliable. We have not investigated whether authors were aware of or involved in the systematic manipulation of the publication process.

Wiley and Hindawi regrets that the usual quality checks did not identify these issues before publication and have since put additional measures in place to safeguard research integrity.

We wish to credit our own Research Integrity and Research Publishing teams and anonymous and named external researchers and research integrity experts for contributing to this investigation.

The corresponding author, as the representative of all authors, has been given the opportunity to register their agreement or disagreement to this retraction. We have kept a record of any response received.

References

- [1] X. Wang, H. Shi, G. Lu et al., “Application of “TCM + Smart Elderly Care” in the Medical-Nursing Care Integration Service System,” *Journal of Sensors*, vol. 2022, Article ID 5154528, 7 pages, 2022.

Retraction

Retracted: Improvement and Reduction of Self-Heating Effect in AlGaN/GaN HEMT Devices

Journal of Sensors

Received 23 January 2024; Accepted 23 January 2024; Published 24 January 2024

Copyright © 2024 Journal of Sensors. This is an open access article distributed under the Creative Commons Attribution License, which permits unrestricted use, distribution, and reproduction in any medium, provided the original work is properly cited.

This article has been retracted by Hindawi following an investigation undertaken by the publisher [1]. This investigation has uncovered evidence of one or more of the following indicators of systematic manipulation of the publication process:

- (1) Discrepancies in scope
- (2) Discrepancies in the description of the research reported
- (3) Discrepancies between the availability of data and the research described
- (4) Inappropriate citations
- (5) Incoherent, meaningless and/or irrelevant content included in the article
- (6) Manipulated or compromised peer review

The presence of these indicators undermines our confidence in the integrity of the article's content and we cannot, therefore, vouch for its reliability. Please note that this notice is intended solely to alert readers that the content of this article is unreliable. We have not investigated whether authors were aware of or involved in the systematic manipulation of the publication process.

Wiley and Hindawi regrets that the usual quality checks did not identify these issues before publication and have since put additional measures in place to safeguard research integrity.

We wish to credit our own Research Integrity and Research Publishing teams and anonymous and named external researchers and research integrity experts for contributing to this investigation.

The corresponding author, as the representative of all authors, has been given the opportunity to register their agreement or disagreement to this retraction. We have kept a record of any response received.

References

- [1] H. Chen, N. Tang, and Z. Zuo, "Improvement and Reduction of Self-Heating Effect in AlGaN/GaN HEMT Devices," *Journal of Sensors*, vol. 2022, Article ID 5378666, 10 pages, 2022.

Retraction

Retracted: FMT Selector: Fourier-Mellin Transformer with High Speed Rotating in Ship Target Detection and Tracking Based on Internet of Things and Wireless Sensor Network

Journal of Sensors

Received 23 January 2024; Accepted 23 January 2024; Published 24 January 2024

Copyright © 2024 Journal of Sensors. This is an open access article distributed under the Creative Commons Attribution License, which permits unrestricted use, distribution, and reproduction in any medium, provided the original work is properly cited.

This article has been retracted by Hindawi following an investigation undertaken by the publisher [1]. This investigation has uncovered evidence of one or more of the following indicators of systematic manipulation of the publication process:

- (1) Discrepancies in scope
- (2) Discrepancies in the description of the research reported
- (3) Discrepancies between the availability of data and the research described
- (4) Inappropriate citations
- (5) Incoherent, meaningless and/or irrelevant content included in the article
- (6) Manipulated or compromised peer review

The presence of these indicators undermines our confidence in the integrity of the article's content and we cannot, therefore, vouch for its reliability. Please note that this notice is intended solely to alert readers that the content of this article is unreliable. We have not investigated whether authors were aware of or involved in the systematic manipulation of the publication process.

Wiley and Hindawi regrets that the usual quality checks did not identify these issues before publication and have since put additional measures in place to safeguard research integrity.

We wish to credit our own Research Integrity and Research Publishing teams and anonymous and named external researchers and research integrity experts for contributing to this investigation.

The corresponding author, as the representative of all authors, has been given the opportunity to register their agreement or disagreement to this retraction. We have kept a record of any response received.

References

- [1] J. Xu, C. Qiu, and L. Wang, "FMT Selector: Fourier-Mellin Transformer with High Speed Rotating in Ship Target Detection and Tracking Based on Internet of Things and Wireless Sensor Network," *Journal of Sensors*, vol. 2023, Article ID 2637529, 8 pages, 2023.

Retraction

Retracted: A Study of Language Use Impact in Radio Broadcasting: A Linguistic and Big Data Integration Approach

Journal of Sensors

Received 23 January 2024; Accepted 23 January 2024; Published 24 January 2024

Copyright © 2024 Journal of Sensors. This is an open access article distributed under the Creative Commons Attribution License, which permits unrestricted use, distribution, and reproduction in any medium, provided the original work is properly cited.

This article has been retracted by Hindawi following an investigation undertaken by the publisher [1]. This investigation has uncovered evidence of one or more of the following indicators of systematic manipulation of the publication process:

- (1) Discrepancies in scope
- (2) Discrepancies in the description of the research reported
- (3) Discrepancies between the availability of data and the research described
- (4) Inappropriate citations
- (5) Incoherent, meaningless and/or irrelevant content included in the article
- (6) Manipulated or compromised peer review

The presence of these indicators undermines our confidence in the integrity of the article's content and we cannot, therefore, vouch for its reliability. Please note that this notice is intended solely to alert readers that the content of this article is unreliable. We have not investigated whether authors were aware of or involved in the systematic manipulation of the publication process.

In addition, our investigation has also shown that one or more of the following human-subject reporting requirements has not been met in this article: ethical approval by an Institutional Review Board (IRB) committee or equivalent, patient/participant consent to participate, and/or agreement to publish patient/participant details (where relevant).

Wiley and Hindawi regrets that the usual quality checks did not identify these issues before publication and have since put additional measures in place to safeguard research integrity.

We wish to credit our own Research Integrity and Research Publishing teams and anonymous and named external researchers and research integrity experts for contributing to this investigation.

The corresponding author, as the representative of all authors, has been given the opportunity to register their agreement or disagreement to this retraction. We have kept a record of any response received.

References

- [1] Y. Praise Chukwunalu, A. U. N. Nwankwere, D. A. Orji, and M. Shah, "A Study of Language Use Impact in Radio Broadcasting: A Linguistic and Big Data Integration Approach," *Journal of Sensors*, vol. 2022, Article ID 1440935, 16 pages, 2022.

Retraction

Retracted: A Low Power ROIC with Extended Counting ADC Based on Circuit Noise Analysis for Sensor Arrays in IoT System

Journal of Sensors

Received 23 January 2024; Accepted 23 January 2024; Published 24 January 2024

Copyright © 2024 Journal of Sensors. This is an open access article distributed under the Creative Commons Attribution License, which permits unrestricted use, distribution, and reproduction in any medium, provided the original work is properly cited.

This article has been retracted by Hindawi following an investigation undertaken by the publisher [1]. This investigation has uncovered evidence of one or more of the following indicators of systematic manipulation of the publication process:

- (1) Discrepancies in scope
- (2) Discrepancies in the description of the research reported
- (3) Discrepancies between the availability of data and the research described
- (4) Inappropriate citations
- (5) Incoherent, meaningless and/or irrelevant content included in the article
- (6) Manipulated or compromised peer review

The presence of these indicators undermines our confidence in the integrity of the article's content and we cannot, therefore, vouch for its reliability. Please note that this notice is intended solely to alert readers that the content of this article is unreliable. We have not investigated whether authors were aware of or involved in the systematic manipulation of the publication process.

Wiley and Hindawi regrets that the usual quality checks did not identify these issues before publication and have since put additional measures in place to safeguard research integrity.

We wish to credit our own Research Integrity and Research Publishing teams and anonymous and named external researchers and research integrity experts for contributing to this investigation.

The corresponding author, as the representative of all authors, has been given the opportunity to register their agreement or disagreement to this retraction. We have kept a record of any response received.

References

- [1] Y. Zhou, W. Lu, S. Yu, D. Yu, Y. Zhang, and Z. Chen, "A Low Power ROIC with Extended Counting ADC Based on Circuit Noise Analysis for Sensor Arrays in IoT System," *Journal of Sensors*, vol. 2022, Article ID 5304613, 12 pages, 2022.

Retraction

Retracted: Difficulties and Countermeasures of Game Localization Translation Based on the IoT and Big Data

Journal of Sensors

Received 23 January 2024; Accepted 23 January 2024; Published 24 January 2024

Copyright © 2024 Journal of Sensors. This is an open access article distributed under the Creative Commons Attribution License, which permits unrestricted use, distribution, and reproduction in any medium, provided the original work is properly cited.

This article has been retracted by Hindawi following an investigation undertaken by the publisher [1]. This investigation has uncovered evidence of one or more of the following indicators of systematic manipulation of the publication process:

- (1) Discrepancies in scope
- (2) Discrepancies in the description of the research reported
- (3) Discrepancies between the availability of data and the research described
- (4) Inappropriate citations
- (5) Incoherent, meaningless and/or irrelevant content included in the article
- (6) Manipulated or compromised peer review

The presence of these indicators undermines our confidence in the integrity of the article's content and we cannot, therefore, vouch for its reliability. Please note that this notice is intended solely to alert readers that the content of this article is unreliable. We have not investigated whether authors were aware of or involved in the systematic manipulation of the publication process.

In addition, our investigation has also shown that one or more of the following human-subject reporting requirements has not been met in this article: ethical approval by an Institutional Review Board (IRB) committee or equivalent, patient/participant consent to participate, and/or agreement to publish patient/participant details (where relevant).

Wiley and Hindawi regrets that the usual quality checks did not identify these issues before publication and have since put additional measures in place to safeguard research integrity.

We wish to credit our own Research Integrity and Research Publishing teams and anonymous and named external researchers and research integrity experts for contributing to this investigation.

The corresponding author, as the representative of all authors, has been given the opportunity to register their agreement or disagreement to this retraction. We have kept a record of any response received.

References

- [1] Q. Sun, "Difficulties and Countermeasures of Game Localization Translation Based on the IoT and Big Data," *Journal of Sensors*, vol. 2022, Article ID 4651956, 7 pages, 2022.

Retraction

Retracted: Monitoring of Single-Phase Induction Motor through IoT Using ESP32 Module

Journal of Sensors

Received 23 January 2024; Accepted 23 January 2024; Published 24 January 2024

Copyright © 2024 Journal of Sensors. This is an open access article distributed under the Creative Commons Attribution License, which permits unrestricted use, distribution, and reproduction in any medium, provided the original work is properly cited.

This article has been retracted by Hindawi following an investigation undertaken by the publisher [1]. This investigation has uncovered evidence of one or more of the following indicators of systematic manipulation of the publication process:

- (1) Discrepancies in scope
- (2) Discrepancies in the description of the research reported
- (3) Discrepancies between the availability of data and the research described
- (4) Inappropriate citations
- (5) Incoherent, meaningless and/or irrelevant content included in the article
- (6) Manipulated or compromised peer review

The presence of these indicators undermines our confidence in the integrity of the article's content and we cannot, therefore, vouch for its reliability. Please note that this notice is intended solely to alert readers that the content of this article is unreliable. We have not investigated whether authors were aware of or involved in the systematic manipulation of the publication process.

Wiley and Hindawi regrets that the usual quality checks did not identify these issues before publication and have since put additional measures in place to safeguard research integrity.

We wish to credit our own Research Integrity and Research Publishing teams and anonymous and named external researchers and research integrity experts for contributing to this investigation.

The corresponding author, as the representative of all authors, has been given the opportunity to register their agreement or disagreement to this retraction. We have kept a record of any response received.

References

- [1] A. Shukla, S. P. Shukla, S. T. Chacko, M. K. Mohiddin, and K. A. Fante, "Monitoring of Single-Phase Induction Motor through IoT Using ESP32 Module," *Journal of Sensors*, vol. 2022, Article ID 8933442, 8 pages, 2022.

Retraction

Retracted: A Machine Learning in Binary and Multiclassification Results on Imbalanced Heart Disease Data Stream

Journal of Sensors

Received 23 January 2024; Accepted 23 January 2024; Published 24 January 2024

Copyright © 2024 Journal of Sensors. This is an open access article distributed under the Creative Commons Attribution License, which permits unrestricted use, distribution, and reproduction in any medium, provided the original work is properly cited.

This article has been retracted by Hindawi following an investigation undertaken by the publisher [1]. This investigation has uncovered evidence of one or more of the following indicators of systematic manipulation of the publication process:

- (1) Discrepancies in scope
- (2) Discrepancies in the description of the research reported
- (3) Discrepancies between the availability of data and the research described
- (4) Inappropriate citations
- (5) Incoherent, meaningless and/or irrelevant content included in the article
- (6) Manipulated or compromised peer review

The presence of these indicators undermines our confidence in the integrity of the article's content and we cannot, therefore, vouch for its reliability. Please note that this notice is intended solely to alert readers that the content of this article is unreliable. We have not investigated whether authors were aware of or involved in the systematic manipulation of the publication process.

Wiley and Hindawi regrets that the usual quality checks did not identify these issues before publication and have since put additional measures in place to safeguard research integrity.

We wish to credit our own Research Integrity and Research Publishing teams and anonymous and named external researchers and research integrity experts for contributing to this investigation.

The corresponding author, as the representative of all authors, has been given the opportunity to register their agreement or disagreement to this retraction. We have kept a record of any response received.

References

- [1] D. Hamid, S. S. Ullah, J. Iqbal, S. Hussain, C. A. u. Hassan, and F. Umar, "A Machine Learning in Binary and Multiclassification Results on Imbalanced Heart Disease Data Stream," *Journal of Sensors*, vol. 2022, Article ID 8400622, 13 pages, 2022.

Retraction

Retracted: Uncertainty Analysis of Key Influencing Factors on Stability of Tailings Dam Body

Journal of Sensors

Received 23 January 2024; Accepted 23 January 2024; Published 24 January 2024

Copyright © 2024 Journal of Sensors. This is an open access article distributed under the Creative Commons Attribution License, which permits unrestricted use, distribution, and reproduction in any medium, provided the original work is properly cited.

This article has been retracted by Hindawi following an investigation undertaken by the publisher [1]. This investigation has uncovered evidence of one or more of the following indicators of systematic manipulation of the publication process:

- (1) Discrepancies in scope
- (2) Discrepancies in the description of the research reported
- (3) Discrepancies between the availability of data and the research described
- (4) Inappropriate citations
- (5) Incoherent, meaningless and/or irrelevant content included in the article
- (6) Manipulated or compromised peer review

The presence of these indicators undermines our confidence in the integrity of the article's content and we cannot, therefore, vouch for its reliability. Please note that this notice is intended solely to alert readers that the content of this article is unreliable. We have not investigated whether authors were aware of or involved in the systematic manipulation of the publication process.

Wiley and Hindawi regrets that the usual quality checks did not identify these issues before publication and have since put additional measures in place to safeguard research integrity.

We wish to credit our own Research Integrity and Research Publishing teams and anonymous and named external researchers and research integrity experts for contributing to this investigation.

The corresponding author, as the representative of all authors, has been given the opportunity to register their agreement or disagreement to this retraction. We have kept a record of any response received.

References

- [1] S. Qian and K. Hou, "Uncertainty Analysis of Key Influencing Factors on Stability of Tailings Dam Body," *Journal of Sensors*, vol. 2023, Article ID 7521356, 11 pages, 2023.

Retraction

Retracted: Innovative Application of Sensor Combined with Speech Recognition Technology in College English Education in the Context of Artificial Intelligence

Journal of Sensors

Received 19 December 2023; Accepted 19 December 2023; Published 20 December 2023

Copyright © 2023 Journal of Sensors. This is an open access article distributed under the Creative Commons Attribution License, which permits unrestricted use, distribution, and reproduction in any medium, provided the original work is properly cited.

This article has been retracted by Hindawi following an investigation undertaken by the publisher [1]. This investigation has uncovered evidence of one or more of the following indicators of systematic manipulation of the publication process:

- (1) Discrepancies in scope
- (2) Discrepancies in the description of the research reported
- (3) Discrepancies between the availability of data and the research described
- (4) Inappropriate citations
- (5) Incoherent, meaningless and/or irrelevant content included in the article
- (6) Manipulated or compromised peer review

The presence of these indicators undermines our confidence in the integrity of the article's content and we cannot, therefore, vouch for its reliability. Please note that this notice is intended solely to alert readers that the content of this article is unreliable. We have not investigated whether authors were aware of or involved in the systematic manipulation of the publication process.

Wiley and Hindawi regrets that the usual quality checks did not identify these issues before publication and have since put additional measures in place to safeguard research integrity.

We wish to credit our own Research Integrity and Research Publishing teams and anonymous and named external researchers and research integrity experts for contributing to this investigation.

The corresponding author, as the representative of all authors, has been given the opportunity to register their agreement or disagreement to this retraction. We have kept a record of any response received.

References

- [1] J. Guo, "Innovative Application of Sensor Combined with Speech Recognition Technology in College English Education in the Context of Artificial Intelligence," *Journal of Sensors*, vol. 2023, Article ID 9281914, 11 pages, 2023.

Retraction

Retracted: Ethical Framework of Social Media Based on Text Analysis of Terms of Service of Six Major Platforms

Journal of Sensors

Received 19 December 2023; Accepted 19 December 2023; Published 20 December 2023

Copyright © 2023 Journal of Sensors. This is an open access article distributed under the Creative Commons Attribution License, which permits unrestricted use, distribution, and reproduction in any medium, provided the original work is properly cited.

This article has been retracted by Hindawi following an investigation undertaken by the publisher [1]. This investigation has uncovered evidence of one or more of the following indicators of systematic manipulation of the publication process:

- (1) Discrepancies in scope
- (2) Discrepancies in the description of the research reported
- (3) Discrepancies between the availability of data and the research described
- (4) Inappropriate citations
- (5) Incoherent, meaningless and/or irrelevant content included in the article
- (6) Manipulated or compromised peer review

The presence of these indicators undermines our confidence in the integrity of the article's content and we cannot, therefore, vouch for its reliability. Please note that this notice is intended solely to alert readers that the content of this article is unreliable. We have not investigated whether authors were aware of or involved in the systematic manipulation of the publication process.

Wiley and Hindawi regrets that the usual quality checks did not identify these issues before publication and have since put additional measures in place to safeguard research integrity.

We wish to credit our own Research Integrity and Research Publishing teams and anonymous and named external researchers and research integrity experts for contributing to this investigation.

The corresponding author, as the representative of all authors, has been given the opportunity to register their agreement or disagreement to this retraction. We have kept a record of any response received.

References

- [1] W. Mao and Z. Wang, "Ethical Framework of Social Media Based on Text Analysis of Terms of Service of Six Major Platforms," *Journal of Sensors*, vol. 2022, Article ID 1136017, 9 pages, 2022.

Retraction

Retracted: Research on Localization Parameter Estimation and Algorithm in the Digital Television Terrestrial Broadcasting

Journal of Sensors

Received 19 December 2023; Accepted 19 December 2023; Published 20 December 2023

Copyright © 2023 Journal of Sensors. This is an open access article distributed under the Creative Commons Attribution License, which permits unrestricted use, distribution, and reproduction in any medium, provided the original work is properly cited.

This article has been retracted by Hindawi following an investigation undertaken by the publisher [1]. This investigation has uncovered evidence of one or more of the following indicators of systematic manipulation of the publication process:

- (1) Discrepancies in scope
- (2) Discrepancies in the description of the research reported
- (3) Discrepancies between the availability of data and the research described
- (4) Inappropriate citations
- (5) Incoherent, meaningless and/or irrelevant content included in the article
- (6) Manipulated or compromised peer review

The presence of these indicators undermines our confidence in the integrity of the article's content and we cannot, therefore, vouch for its reliability. Please note that this notice is intended solely to alert readers that the content of this article is unreliable. We have not investigated whether authors were aware of or involved in the systematic manipulation of the publication process.

Wiley and Hindawi regrets that the usual quality checks did not identify these issues before publication and have since put additional measures in place to safeguard research integrity.

We wish to credit our own Research Integrity and Research Publishing teams and anonymous and named external researchers and research integrity experts for contributing to this investigation.

The corresponding author, as the representative of all authors, has been given the opportunity to register their agreement or disagreement to this retraction. We have kept a record of any response received.

References

- [1] S. Bao, S. Yang, H. Ou, and J. Song, "Research on Localization Parameter Estimation and Algorithm in the Digital Television Terrestrial Broadcasting," *Journal of Sensors*, vol. 2023, Article ID 1810507, 12 pages, 2023.

Retraction

Retracted: GPS Receiver Position Estimation and DOP Analysis Using a New Form of the Observation Matrix Approximations

Journal of Sensors

Received 19 December 2023; Accepted 19 December 2023; Published 20 December 2023

Copyright © 2023 Journal of Sensors. This is an open access article distributed under the Creative Commons Attribution License, which permits unrestricted use, distribution, and reproduction in any medium, provided the original work is properly cited.

This article has been retracted by Hindawi following an investigation undertaken by the publisher [1]. This investigation has uncovered evidence of one or more of the following indicators of systematic manipulation of the publication process:

- (1) Discrepancies in scope
- (2) Discrepancies in the description of the research reported
- (3) Discrepancies between the availability of data and the research described
- (4) Inappropriate citations
- (5) Incoherent, meaningless and/or irrelevant content included in the article
- (6) Manipulated or compromised peer review

The presence of these indicators undermines our confidence in the integrity of the article's content and we cannot, therefore, vouch for its reliability. Please note that this notice is intended solely to alert readers that the content of this article is unreliable. We have not investigated whether authors were aware of or involved in the systematic manipulation of the publication process.

Wiley and Hindawi regrets that the usual quality checks did not identify these issues before publication and have since put additional measures in place to safeguard research integrity.

We wish to credit our own Research Integrity and Research Publishing teams and anonymous and named external researchers and research integrity experts for contributing to this investigation.

The corresponding author, as the representative of all authors, has been given the opportunity to register their agreement or disagreement to this retraction. We have kept a record of any response received.

References

- [1] A. K. N. P. S. Kumar, M. K. Mohiddin, M. T. Gameda, and A. Mishra, "GPS Receiver Position Estimation and DOP Analysis Using a New Form of the Observation Matrix Approximations," *Journal of Sensors*, vol. 2022, Article ID 6772077, 12 pages, 2022.

Retraction

Retracted: Selection of Optimum Internal Control Genes for RT-qPCR Analysis of *Schisandra chinensis* under Four Hormone Treatments

Journal of Sensors

Received 19 December 2023; Accepted 19 December 2023; Published 20 December 2023

Copyright © 2023 Journal of Sensors. This is an open access article distributed under the Creative Commons Attribution License, which permits unrestricted use, distribution, and reproduction in any medium, provided the original work is properly cited.

This article has been retracted by Hindawi following an investigation undertaken by the publisher [1]. This investigation has uncovered evidence of one or more of the following indicators of systematic manipulation of the publication process:

- (1) Discrepancies in scope
- (2) Discrepancies in the description of the research reported
- (3) Discrepancies between the availability of data and the research described
- (4) Inappropriate citations
- (5) Incoherent, meaningless and/or irrelevant content included in the article
- (6) Manipulated or compromised peer review

The presence of these indicators undermines our confidence in the integrity of the article's content and we cannot, therefore, vouch for its reliability. Please note that this notice is intended solely to alert readers that the content of this article is unreliable. We have not investigated whether authors were aware of or involved in the systematic manipulation of the publication process.

Wiley and Hindawi regrets that the usual quality checks did not identify these issues before publication and have since put additional measures in place to safeguard research integrity.

We wish to credit our own Research Integrity and Research Publishing teams and anonymous and named external researchers and research integrity experts for contributing to this investigation.

The corresponding author, as the representative of all authors, has been given the opportunity to register their agreement or disagreement to this retraction. We have kept a record of any response received.

References

- [1] X. Liu, L. Zhang, and S. Yang, "Selection of Optimum Internal Control Genes for RT-qPCR Analysis of *Schisandra chinensis* under Four Hormone Treatments," *Journal of Sensors*, vol. 2022, Article ID 9299289, 10 pages, 2022.

Retraction

Retracted: The Construction of Conceptual Framework of Enterprise Internal Control Evaluation Report

Journal of Sensors

Received 19 December 2023; Accepted 19 December 2023; Published 20 December 2023

Copyright © 2023 Journal of Sensors. This is an open access article distributed under the Creative Commons Attribution License, which permits unrestricted use, distribution, and reproduction in any medium, provided the original work is properly cited.

This article has been retracted by Hindawi following an investigation undertaken by the publisher [1]. This investigation has uncovered evidence of one or more of the following indicators of systematic manipulation of the publication process:

- (1) Discrepancies in scope
- (2) Discrepancies in the description of the research reported
- (3) Discrepancies between the availability of data and the research described
- (4) Inappropriate citations
- (5) Incoherent, meaningless and/or irrelevant content included in the article
- (6) Manipulated or compromised peer review

The presence of these indicators undermines our confidence in the integrity of the article's content and we cannot, therefore, vouch for its reliability. Please note that this notice is intended solely to alert readers that the content of this article is unreliable. We have not investigated whether authors were aware of or involved in the systematic manipulation of the publication process.

Wiley and Hindawi regrets that the usual quality checks did not identify these issues before publication and have since put additional measures in place to safeguard research integrity.

We wish to credit our own Research Integrity and Research Publishing teams and anonymous and named external researchers and research integrity experts for contributing to this investigation.

The corresponding author, as the representative of all authors, has been given the opportunity to register their agreement or disagreement to this retraction. We have kept a record of any response received.

References

- [1] Y. Kuang, Z. Li, and C. Pan, "The Construction of Conceptual Framework of Enterprise Internal Control Evaluation Report," *Journal of Sensors*, vol. 2022, Article ID 2753001, 11 pages, 2022.

Retraction

Retracted: Logistics Supply Chain Management Mode of Chinese E-Commerce Enterprises under the Background of Big Data and Internet of Things

Journal of Sensors

Received 17 October 2023; Accepted 17 October 2023; Published 18 October 2023

Copyright © 2023 Journal of Sensors. This is an open access article distributed under the Creative Commons Attribution License, which permits unrestricted use, distribution, and reproduction in any medium, provided the original work is properly cited.

This article has been retracted by Hindawi following an investigation undertaken by the publisher [1]. This investigation has uncovered evidence of one or more of the following indicators of systematic manipulation of the publication process:

- (1) Discrepancies in scope
- (2) Discrepancies in the description of the research reported
- (3) Discrepancies between the availability of data and the research described
- (4) Inappropriate citations
- (5) Incoherent, meaningless and/or irrelevant content included in the article
- (6) Peer-review manipulation

The presence of these indicators undermines our confidence in the integrity of the article's content and we cannot, therefore, vouch for its reliability. Please note that this notice is intended solely to alert readers that the content of this article is unreliable. We have not investigated whether authors were aware of or involved in the systematic manipulation of the publication process.

In addition, our investigation has also shown that one or more of the following human-subject reporting requirements has not been met in this article: ethical approval by an Institutional Review Board (IRB) committee or equivalent, patient/participant consent to participate, and/or agreement to publish patient/participant details (where relevant).

Wiley and Hindawi regrets that the usual quality checks did not identify these issues before publication and have since put additional measures in place to safeguard research integrity.

We wish to credit our own Research Integrity and Research Publishing teams and anonymous and named external

researchers and research integrity experts for contributing to this investigation.

The corresponding author, as the representative of all authors, has been given the opportunity to register their agreement or disagreement to this retraction. We have kept a record of any response received.

References

- [1] X. Han and J. Wang, "Logistics Supply Chain Management Mode of Chinese E-Commerce Enterprises under the Background of Big Data and Internet of Things," *Journal of Sensors*, vol. 2022, Article ID 7818944, 7 pages, 2022.

Retraction

Retracted: Analysis on the Educational Value of Winter Olympic Spirit in Track and Field Teaching Based on Data Mining under Artificial Intelligence

Journal of Sensors

Received 3 October 2023; Accepted 3 October 2023; Published 4 October 2023

Copyright © 2023 Journal of Sensors. This is an open access article distributed under the Creative Commons Attribution License, which permits unrestricted use, distribution, and reproduction in any medium, provided the original work is properly cited.

This article has been retracted by Hindawi following an investigation undertaken by the publisher [1]. This investigation has uncovered evidence of one or more of the following indicators of systematic manipulation of the publication process:

- (1) Discrepancies in scope
- (2) Discrepancies in the description of the research reported
- (3) Discrepancies between the availability of data and the research described
- (4) Inappropriate citations
- (5) Incoherent, meaningless and/or irrelevant content included in the article
- (6) Peer-review manipulation

The presence of these indicators undermines our confidence in the integrity of the article's content and we cannot, therefore, vouch for its reliability. Please note that this notice is intended solely to alert readers that the content of this article is unreliable. We have not investigated whether authors were aware of or involved in the systematic manipulation of the publication process.

In addition, our investigation has also shown that one or more of the following human-subject reporting requirements has not been met in this article: ethical approval by an Institutional Review Board (IRB) committee or equivalent, patient/participant consent to participate, and/or agreement to publish patient/participant details (where relevant).

Wiley and Hindawi regrets that the usual quality checks did not identify these issues before publication and have since put additional measures in place to safeguard research integrity.

We wish to credit our own Research Integrity and Research Publishing teams and anonymous and named external

researchers and research integrity experts for contributing to this investigation.

The corresponding author, as the representative of all authors, has been given the opportunity to register their agreement or disagreement to this retraction. We have kept a record of any response received.

References

- [1] A. Yu, J. Wang, Y. Zhou et al., "Analysis on the Educational Value of Winter Olympic Spirit in Track and Field Teaching Based on Data Mining under Artificial Intelligence," *Journal of Sensors*, vol. 2022, Article ID 9435846, 8 pages, 2022.

Retraction

Retracted: Construction and Development of Modern Brand Marketing Management Mode Based on Artificial Intelligence

Journal of Sensors

Received 3 October 2023; Accepted 3 October 2023; Published 4 October 2023

Copyright © 2023 Journal of Sensors. This is an open access article distributed under the Creative Commons Attribution License, which permits unrestricted use, distribution, and reproduction in any medium, provided the original work is properly cited.

This article has been retracted by Hindawi following an investigation undertaken by the publisher [1]. This investigation has uncovered evidence of one or more of the following indicators of systematic manipulation of the publication process:

- (1) Discrepancies in scope
- (2) Discrepancies in the description of the research reported
- (3) Discrepancies between the availability of data and the research described
- (4) Inappropriate citations
- (5) Incoherent, meaningless and/or irrelevant content included in the article
- (6) Peer-review manipulation

The presence of these indicators undermines our confidence in the integrity of the article's content and we cannot, therefore, vouch for its reliability. Please note that this notice is intended solely to alert readers that the content of this article is unreliable. We have not investigated whether authors were aware of or involved in the systematic manipulation of the publication process.

In addition, our investigation has also shown that one or more of the following human-subject reporting requirements has not been met in this article: ethical approval by an Institutional Review Board (IRB) committee or equivalent, patient/participant consent to participate, and/or agreement to publish patient/participant details (where relevant).

Wiley and Hindawi regrets that the usual quality checks did not identify these issues before publication and have since put additional measures in place to safeguard research integrity.

We wish to credit our own Research Integrity and Research Publishing teams and anonymous and named external researchers and research integrity experts for contributing to this investigation.

The corresponding author, as the representative of all authors, has been given the opportunity to register their agreement or disagreement to this retraction. We have kept a record of any response received.

References

- [1] H. Cui, Y. Nie, Z. Li, and J. Zeng, "Construction and Development of Modern Brand Marketing Management Mode Based on Artificial Intelligence," *Journal of Sensors*, vol. 2022, Article ID 9246545, 11 pages, 2022.

Retraction

Retracted: The Application of Traditional Chinese Woodcut Printmaking Language in Digital Painting Based on Intelligent Computing

Journal of Sensors

Received 22 August 2023; Accepted 22 August 2023; Published 23 August 2023

Copyright © 2023 Journal of Sensors. This is an open access article distributed under the Creative Commons Attribution License, which permits unrestricted use, distribution, and reproduction in any medium, provided the original work is properly cited.

This article has been retracted by Hindawi following an investigation undertaken by the publisher [1]. This investigation has uncovered evidence of one or more of the following indicators of systematic manipulation of the publication process:

- (1) Discrepancies in scope
- (2) Discrepancies in the description of the research reported
- (3) Discrepancies between the availability of data and the research described
- (4) Inappropriate citations
- (5) Incoherent, meaningless and/or irrelevant content included in the article
- (6) Peer-review manipulation

The presence of these indicators undermines our confidence in the integrity of the article's content and we cannot, therefore, vouch for its reliability. Please note that this notice is intended solely to alert readers that the content of this article is unreliable. We have not investigated whether authors were aware of or involved in the systematic manipulation of the publication process.

Wiley and Hindawi regrets that the usual quality checks did not identify these issues before publication and have since put additional measures in place to safeguard research integrity.

We wish to credit our own Research Integrity and Research Publishing teams and anonymous and named external researchers and research integrity experts for contributing to this investigation.

The corresponding author, as the representative of all authors, has been given the opportunity to register their agreement or disagreement to this retraction. We have kept a record of any response received.

References

- [1] C. Chen, "The Application of Traditional Chinese Woodcut Printmaking Language in Digital Painting Based on Intelligent Computing," *Journal of Sensors*, vol. 2022, Article ID 2223868, 12 pages, 2022.

Retraction

Retracted: Preschool Education Based on Computer Information Technology Literacy and Big Data

Journal of Sensors

Received 22 August 2023; Accepted 22 August 2023; Published 23 August 2023

Copyright © 2023 Journal of Sensors. This is an open access article distributed under the Creative Commons Attribution License, which permits unrestricted use, distribution, and reproduction in any medium, provided the original work is properly cited.

This article has been retracted by Hindawi following an investigation undertaken by the publisher [1]. This investigation has uncovered evidence of one or more of the following indicators of systematic manipulation of the publication process:

- (1) Discrepancies in scope
- (2) Discrepancies in the description of the research reported
- (3) Discrepancies between the availability of data and the research described
- (4) Inappropriate citations
- (5) Incoherent, meaningless and/or irrelevant content included in the article
- (6) Peer-review manipulation

The presence of these indicators undermines our confidence in the integrity of the article's content and we cannot, therefore, vouch for its reliability. Please note that this notice is intended solely to alert readers that the content of this article is unreliable. We have not investigated whether authors were aware of or involved in the systematic manipulation of the publication process.

In addition, our investigation has also shown that one or more of the following human-subject reporting requirements has not been met in this article: ethical approval by an Institutional Review Board (IRB) committee or equivalent, patient/participant consent to participate, and/or agreement to publish patient/participant details (where relevant).

Wiley and Hindawi regrets that the usual quality checks did not identify these issues before publication and have since put additional measures in place to safeguard research integrity.

We wish to credit our own Research Integrity and Research Publishing teams and anonymous and named external researchers and research integrity experts for contributing to this investigation.

The corresponding author, as the representative of all authors, has been given the opportunity to register their agreement or disagreement to this retraction. We have kept a record of any response received.

References

- [1] L. Luo, "Preschool Education Based on Computer Information Technology Literacy and Big Data," *Journal of Sensors*, vol. 2022, Article ID 4457811, 10 pages, 2022.

Retraction

Retracted: Investigation on the Use of Virtual Reality in the Flipped Teaching of Martial Arts Taijiquan Based on Deep Learning and Big Data Analytics

Journal of Sensors

Received 22 August 2023; Accepted 22 August 2023; Published 23 August 2023

Copyright © 2023 Journal of Sensors. This is an open access article distributed under the Creative Commons Attribution License, which permits unrestricted use, distribution, and reproduction in any medium, provided the original work is properly cited.

This article has been retracted by Hindawi following an investigation undertaken by the publisher [1]. This investigation has uncovered evidence of one or more of the following indicators of systematic manipulation of the publication process:

- (1) Discrepancies in scope
- (2) Discrepancies in the description of the research reported
- (3) Discrepancies between the availability of data and the research described
- (4) Inappropriate citations
- (5) Incoherent, meaningless and/or irrelevant content included in the article
- (6) Peer-review manipulation

The presence of these indicators undermines our confidence in the integrity of the article's content and we cannot, therefore, vouch for its reliability. Please note that this notice is intended solely to alert readers that the content of this article is unreliable. We have not investigated whether authors were aware of or involved in the systematic manipulation of the publication process.

In addition, our investigation has also shown that one or more of the following human-subject reporting requirements has not been met in this article: ethical approval by an Institutional Review Board (IRB) committee or equivalent, patient/participant consent to participate, and/or agreement to publish patient/participant details (where relevant).

Wiley and Hindawi regrets that the usual quality checks did not identify these issues before publication and have since put additional measures in place to safeguard research integrity.

We wish to credit our own Research Integrity and Research Publishing teams and anonymous and named external

researchers and research integrity experts for contributing to this investigation.

The corresponding author, as the representative of all authors, has been given the opportunity to register their agreement or disagreement to this retraction. We have kept a record of any response received.

References

- [1] Z. HanLiang and Z. LiNa, "Investigation on the Use of Virtual Reality in the Flipped Teaching of Martial Arts Taijiquan Based on Deep Learning and Big Data Analytics," *Journal of Sensors*, vol. 2022, Article ID 3921842, 14 pages, 2022.

Retraction

Retracted: Consumption Behavior Prediction Based on Multiobjective Evolutionary Algorithm

Journal of Sensors

Received 22 August 2023; Accepted 22 August 2023; Published 23 August 2023

Copyright © 2023 Journal of Sensors. This is an open access article distributed under the Creative Commons Attribution License, which permits unrestricted use, distribution, and reproduction in any medium, provided the original work is properly cited.

This article has been retracted by Hindawi following an investigation undertaken by the publisher [1]. This investigation has uncovered evidence of one or more of the following indicators of systematic manipulation of the publication process:

- (1) Discrepancies in scope
- (2) Discrepancies in the description of the research reported
- (3) Discrepancies between the availability of data and the research described
- (4) Inappropriate citations
- (5) Incoherent, meaningless and/or irrelevant content included in the article
- (6) Peer-review manipulation

The presence of these indicators undermines our confidence in the integrity of the article's content and we cannot, therefore, vouch for its reliability. Please note that this notice is intended solely to alert readers that the content of this article is unreliable. We have not investigated whether authors were aware of or involved in the systematic manipulation of the publication process.

Wiley and Hindawi regrets that the usual quality checks did not identify these issues before publication and have since put additional measures in place to safeguard research integrity.

We wish to credit our own Research Integrity and Research Publishing teams and anonymous and named external researchers and research integrity experts for contributing to this investigation.

The corresponding author, as the representative of all authors, has been given the opportunity to register their agreement or disagreement to this retraction. We have kept a record of any response received.

References

- [1] J. Li, N. S. Jaharudin, and Y. Song, "Consumption Behavior Prediction Based on Multiobjective Evolutionary Algorithm," *Journal of Sensors*, vol. 2022, Article ID 2525740, 11 pages, 2022.

Retraction

Retracted: A Novel Multidose Dry Powder Inhaler and Its Application in Patients with Asthma and COPD

Journal of Sensors

Received 22 August 2023; Accepted 22 August 2023; Published 23 August 2023

Copyright © 2023 Journal of Sensors. This is an open access article distributed under the Creative Commons Attribution License, which permits unrestricted use, distribution, and reproduction in any medium, provided the original work is properly cited.

This article has been retracted by Hindawi following an investigation undertaken by the publisher [1]. This investigation has uncovered evidence of one or more of the following indicators of systematic manipulation of the publication process:

- (1) Discrepancies in scope
- (2) Discrepancies in the description of the research reported
- (3) Discrepancies between the availability of data and the research described
- (4) Inappropriate citations
- (5) Incoherent, meaningless and/or irrelevant content included in the article
- (6) Peer-review manipulation

The presence of these indicators undermines our confidence in the integrity of the article's content and we cannot, therefore, vouch for its reliability. Please note that this notice is intended solely to alert readers that the content of this article is unreliable. We have not investigated whether authors were aware of or involved in the systematic manipulation of the publication process.

In addition, our investigation has also shown that one or more of the following human-subject reporting requirements has not been met in this article: ethical approval by an Institutional Review Board (IRB) committee or equivalent, patient/participant consent to participate, and/or agreement to publish patient/participant details (where relevant).

Wiley and Hindawi regrets that the usual quality checks did not identify these issues before publication and have since put additional measures in place to safeguard research integrity.

We wish to credit our own Research Integrity and Research Publishing teams and anonymous and named external researchers and research integrity experts for contributing to this investigation.

The corresponding author, as the representative of all authors, has been given the opportunity to register their agreement or disagreement to this retraction. We have kept a record of any response received.

References

- [1] F. Shi, C. Zhu, T. Zhou, and J. Liu, "A Novel Multidose Dry Powder Inhaler and Its Application in Patients with Asthma and COPD," *Journal of Sensors*, vol. 2022, Article ID 3051484, 14 pages, 2022.

Retraction

Retracted: A BP Neural Network-Based Early Warning Model for Student Performance in the Context of Big Data

Journal of Sensors

Received 22 August 2023; Accepted 22 August 2023; Published 23 August 2023

Copyright © 2023 Journal of Sensors. This is an open access article distributed under the Creative Commons Attribution License, which permits unrestricted use, distribution, and reproduction in any medium, provided the original work is properly cited.

This article has been retracted by Hindawi following an investigation undertaken by the publisher [1]. This investigation has uncovered evidence of one or more of the following indicators of systematic manipulation of the publication process:

- (1) Discrepancies in scope
- (2) Discrepancies in the description of the research reported
- (3) Discrepancies between the availability of data and the research described
- (4) Inappropriate citations
- (5) Incoherent, meaningless and/or irrelevant content included in the article
- (6) Peer-review manipulation

The presence of these indicators undermines our confidence in the integrity of the article's content and we cannot, therefore, vouch for its reliability. Please note that this notice is intended solely to alert readers that the content of this article is unreliable. We have not investigated whether authors were aware of or involved in the systematic manipulation of the publication process.

In addition, our investigation has also shown that one or more of the following human-subject reporting requirements has not been met in this article: ethical approval by an Institutional Review Board (IRB) committee or equivalent, patient/participant consent to participate, and/or agreement to publish patient/participant details (where relevant).

Wiley and Hindawi regrets that the usual quality checks did not identify these issues before publication and have since put additional measures in place to safeguard research integrity.

We wish to credit our own Research Integrity and Research Publishing teams and anonymous and named external researchers and research integrity experts for contributing to this investigation.

The corresponding author, as the representative of all authors, has been given the opportunity to register their agreement or disagreement to this retraction. We have kept a record of any response received.

References

- [1] C. Shi and Y. Tan, "A BP Neural Network-Based Early Warning Model for Student Performance in the Context of Big Data," *Journal of Sensors*, vol. 2022, Article ID 2958261, 10 pages, 2022.

Retraction

Retracted: Enhance-Net: An Approach to Boost the Performance of Deep Learning Model Based on Real-Time Medical Images

Journal of Sensors

Received 23 January 2024; Accepted 23 January 2024; Published 24 January 2024

Copyright © 2024 Journal of Sensors. This is an open access article distributed under the Creative Commons Attribution License, which permits unrestricted use, distribution, and reproduction in any medium, provided the original work is properly cited.

This article has been retracted by Hindawi following an investigation undertaken by the publisher [1]. This investigation has uncovered evidence of one or more of the following indicators of systematic manipulation of the publication process:

- (1) Discrepancies in scope
- (2) Discrepancies in the description of the research reported
- (3) Discrepancies between the availability of data and the research described
- (4) Inappropriate citations
- (5) Incoherent, meaningless and/or irrelevant content included in the article
- (6) Manipulated or compromised peer review

The presence of these indicators undermines our confidence in the integrity of the article's content and we cannot, therefore, vouch for its reliability. Please note that this notice is intended solely to alert readers that the content of this article is unreliable. We have not investigated whether authors were aware of or involved in the systematic manipulation of the publication process.

Wiley and Hindawi regrets that the usual quality checks did not identify these issues before publication and have since put additional measures in place to safeguard research integrity.

We wish to credit our own Research Integrity and Research Publishing teams and anonymous and named external researchers and research integrity experts for contributing to this investigation.

The corresponding author, as the representative of all authors, has been given the opportunity to register their agreement or disagreement to this retraction. We have kept a record of any response received.

References

- [1] V. Narayan, P. K. Mall, A. Alkhayat, K. Abhishek, S. Kumar, and P. Pandey, "Enhance-Net: An Approach to Boost the Performance of Deep Learning Model Based on Real-Time Medical Images," *Journal of Sensors*, vol. 2023, Article ID 8276738, 15 pages, 2023.

Research Article

Enhance-Net: An Approach to Boost the Performance of Deep Learning Model Based on Real-Time Medical Images

Vipul Narayan ¹, Pawan Kumar Mall ², Ahmed Alkhayyat ³, Kumar Abhishek ⁴,
Sanjay Kumar ⁵ and Prakash Pandey ⁶

¹Galgotias University, Greater Noida, India

²Lovely Professional University, India

³College of Technical Engineering, The Islamic University, Najaf, Iraq

⁴National Institute of Technology Patna, India

⁵Rajkiya Engineering College, Azamgarh, India

⁶Graduate School of Engineering, Mid-West University, Nepal

Correspondence should be addressed to Prakash Pandey; prakash.pandey@mu.edu.np

Received 17 August 2022; Revised 28 September 2022; Accepted 12 October 2022; Published 2 May 2023

Academic Editor: Sweta Bhattacharya

Copyright © 2023 Vipul Narayan et al. This is an open access article distributed under the Creative Commons Attribution License, which permits unrestricted use, distribution, and reproduction in any medium, provided the original work is properly cited.

Real-time medical image classification is a complex problem in the world. Using IoT technology in medical applications assures that the healthcare sectors improve the quality of treatment while lowering costs via automation and resource optimization. Deep learning is critical in categorizing medical images, which is accomplished by artificial intelligence. Deep learning algorithms allow radiologists and orthopaedic surgeons to make their life easier by providing them with quicker and more accurate findings in real time. Despite this, the classic deep learning technique has hit its performance limits. For these reasons, in this research, we examine alternative enhancement strategies to raise the performance of deep neural networks to provide an optimal solution known as Enhance-Net. It is possible to classify the experiment into six distinct stages. Champion-Net was chosen as a deep learning model from a pool of benchmark deep learning models (EfficientNet: B0, MobileNet, ResNet-18, and VGG-19). This stage helps choose the optimal model. In the second step, Champion-Net was tested with various resolutions. This stage helps conclude dataset resolution and improves Champion-Net performance. The next stage extracts green channel data. In the fourth step, Champion-Net combines with image enhancement algorithms CLAHE, HEF, and UM. This phase serves to improve Enhance-performance. The next stage compares the Enhance-Net findings to the lightness order error (LoE). In Enhance-Net models, the current study combines image enhancement and green channel with Champion-Net. In the final step, radiologists and orthopaedic surgeons use the trained model for real-time medical image prediction. The study effort uses the musculoskeletal radiograph-bone classification (MURA-BC) dataset. Classification accuracy of Enhance-Net was determined for the train and test datasets. These models obtained 98.02 percent, 94.79 percent, and 94.61 percent accuracy, respectively. The 96.74% accuracy was achieved during real-time testing with the unseen dataset.

1. Introduction

The IoT in medical imaging allows detection and remedial steps to be conducted in real time with the convenience of autoanalyzing imaging equipment characteristics. Numerous research has been conducted in medical imaging to investigate the use of various deep neural network- (DNN-) based models to categorize or diagnose illnesses. DNNs have been used to classify and diagnose diseases in the past.

Deep neural networks have been successfully applied to the classification and diagnosis of illnesses in various types of medical conditions [1–6]. In recent years, image classification, segmentation, and detection techniques have been coupled with an era in which diagnostic medical imaging is becoming increasingly popular and essential for medical diagnosis [7, 8]. A fundamental challenge with medical imaging, on the other hand, is the availability of big datasets with trustworthy ground truth analysis, which is difficult to

come by. Deep learning models (DLMs) have aided in the development of a number of advancements in the field of image classification [9–13].

According to a recent study [14], the depth of a network-oriented model is crucial for critical datasets. This demonstrates that a network-based model's depth is crucial for challenging datasets. The debate about shallow vs. deep nets has raged in DLMs for a long time. The issue of decreased feature reuse arises while training extremely deep learning models [15–17]. This makes the training procedure for these models difficult. In [18], to obtain higher accuracy and minimal error in training loss, create a deep learning model with the ideal resolution, depth, and breadth combination. Several approaches have been proposed throughout the literature to deal with raindrop detection problems. However, most of these do not consider the following system requirements: high detection rate, real-time constraint, and robustness under dynamic environments.

A DLM technique called Enhance-Net is proposed to enhance the overall performance of musculoskeletal radiographs and X-ray pictures in a clinical setting. The most interesting aspect of this study is the evaluation of the influence of three distinct image enhancement algorithms (CLAHE, UM, and HEF) on green channel grayscale medical musculoskeletal radiography X-ray images for DLMs. The following sections of the paper are divided into seven phases: in Section 3, we discussed the materials and processes that were utilized to create the proposed model, which was interesting. In Section 4, we have gone into further detail about the suggested model. In Section 5, we went through the simulation, the results, and the validation process in great depth. In Section 6, we have discussed about real-time verification and result outcome. The final segment of Section 7 was dedicated to the conclusion and future work.

2. Related Work

In [19], the study tested the model's efficiency by extending the depth (16-20 layers) on ImageNet Challenge held in 2014 on different datasets. The deep learning model's error rate reaches saturation at the 19th layer. The authors created a residual learning model to make training deeper networks easier [20]. On the ImageNet test dataset, the model has a 3.57 percent error rate [20]. The model designer may create the optimal size model constraint in the design [5, 21–23]. In [18], the study offers a scaling technique that uses a compound coefficient to scale evenly using three key parameters (width, depth, and resolution) simultaneously.

When IoT technology is used in healthcare applications, it helps improve the quality of care and lower costs through automation and better use of resources. IoT in medical imaging makes it easy to find out what is wrong and take steps to fix it in real time. This is made possible by the auto-analysis of the imaging equipment's parameters [24]. The Internet of things (IoT) lets people develop systems that use sensors, connected devices, and the Internet. In the ICU, monitoring patients is an essential thing to do. Even a slight delay in making decisions about how to treat a patient could cause permanent disability or even death. Most

ICU devices have sensors that can measure different health parameters, but it is still hard to keep an eye on them all the time. We are proposing a system based on the Internet of things (IoT), which can help speed up communication, find emergencies, and get in touch with medical staff. It can also help start quick, proactive treatment. This healthcare system makes it less likely that people will make mistakes or take too long to communicate, and it gives doctors more time to make decisions based on accurate observations [25]. Academic institutions and the commercial healthcare sector are devoting a significant amount of attention to the development of intelligent medical sensors, gadgets, cloud computing, and other technology related to healthcare. As a result of this, the Internet of things (IoT) has been identified as one of the most promising research subjects in the field of healthcare, namely, in the field of medical image processing. When conducting their analysis of medical photographs, researchers used a wide variety of machine learning and semisupervised learning, deep learning strategies, and artificial intelligence. These newly discovered methods are used in the process of illness detection, with the goal of assisting medical professionals in the early phases of disease diagnosis, as well as delivering findings that are accurate, consistent, efficient, and quick, and so lowering the mortality rate. In today's world, the coronavirus (COVID-19) has emerged as one of the most challenging and serious illnesses, and it is rapidly spreading around the globe [26]. The authors conducted an exhaustive study of the applications of WMSs as well as their advancements, and they compared the performance of WMSs to that of other platforms. The authors went through the benefits that these applications of these devices bring to the table when it comes to monitoring the health of people with illnesses such as cardiac arrest and Alzheimer's disease [27]. The Internet of things offers potential solutions that might reduce the load that is placed on healthcare institutions. For instance, RFID systems are used in medical institutions in order to both lower overall medical costs and improve the quality of treatment that is provided. Patients' cardiac impulses may be conveniently monitored by physicians thanks to healthcare monitoring schemes, which help physicians deliver an accurate diagnosis and improve patient care [28]. The authors [29] have shown a semisupervised learning model for the purpose of collecting the best possible collection of picture attributes. The primary focus of the ensemble learning model that has been provided is on the fact that the framework is taught to acquire various degrees of semantic representation of pictures in order to extract features of a better quality. In this way, the new set of features may be learnt with a bigger dataset via the process of constructing a more refined model. The expected fine-tuning CNN design makes use of a standard amount of medical picture attributes taken from a variety of modalities. Cloud computing (CC) is a model of distributed computing that makes it possible for companies and individual users to access virtualized computing, storage, and networking resources via the use of the Internet. At the moment, it is more economical, less difficult to manage, and more elastic to use these resources rather than a collection of local,

TABLE 1: Comparative analysis of recent work.

References	Study	Enhancement method	Modality	DNNs
[42]	Diabetic retinopathy	Green channel+CLAHE	Fundus images	U-Net
[43]	Retinal blood vessel segmentation	CLAHE	Fundus images	Encoder-decoder CNN
[44]	Tuberculosis detection	CLAHE, HEF, and UM	X-ray	EfficientNet-B4, ResNet-18, and ResNet-50
[45]	COVID-19	Pipeline for advanced contrast enhancement	Computed tomography (CT)	—
[46]	Medical images	UM	X-ray and CT	—
[47]	Pneumonia infection	CLAHE	X-ray	MobileNetV2 and EfficientNet: B0
[48]	COVID-19	AMF, NLMF, and CLAHE	X-ray	KL-MOB

TABLE 2: MURA-bone classification X-ray dataset.

Study of various parts	Training set	Testing set	Verification set
Elbow	2920	80	10
Finger	3130	79	13
Forearm	1160	62	8
Hand	4060	75	25
Humerus	670	61	9
Shoulder	4210	61	7
Wrist	5760	120	20
Total	21910	538	92

Complete dataset size: 22540.

physical ones. Cloud services are often kept in data centres, which typically consist of thousands upon thousands of individual computers [30]. In order to enhance the effectiveness of monitoring in IoT-based healthcare systems, a significant amount of research has been conducted. In this paper [31], the architecture that is employed in the Internet of things, particularly the cloud-integrated systems, is studied. In the Internet of things, accuracy and power consumption are two of the most essential concerns; as a result, this article discusses the research activities that are now underway to improve the functionality of healthcare systems that are based on the Internet of things. An expert application system has been developed [32] using the Internet of medical things (IoM). Collecting and analysing patients' physiological data are one of its primary functions to conduct a hands-on analysis of the medical sensor nodes that have been implanted into the body of the patient. In turn, it would detect the medical information of the patient utilising sophisticated portable gadgets. The security, protection, and privacy of medical data are becoming more complex issues for the Isle of Man as a result of the fact that patient information is very sensitive and should not be disclosed to anybody other than a medical expert. For this reason, a user authentication mechanism that is based on anonymity is recommended as the best solution to the problems with privacy preservation in the IoM.

The authors used transfer learning to train both DenseNet-161 and ResNet-50, deprived of using a fully

linked layer to get the desired results [33]. Their study used the Kimia Path24 dataset, which was available in grayscale and colour. A grayscale dataset was utilized using the DenseNet-161 algorithm, while the ResNet-50 algorithm used a colour dataset to obtain a classification accuracy of 98.87 percent. An updated ResNet model was presented [34]. Instead of global average pooling, authors added adaptive dropout. It achieved 87.71 percent classification accuracy in Montgomery County, 62.9 percent in NIH, and 81.8 percent in Shenzhen.

The STARE dataset was used in the research by the authors [35]. The dataset has been resized into three different datasets with resolutions of 31×35 pixels, 46×53 pixels, and 61×70 pixels and has been classified into 15 dissimilar eye diseases. The investigations found that the used datasets with sizes of 32×36 and 62×72 pixels had the maximum accuracy during training. In contrast, the input test dataset with sizes of 32×36 had the highest accuracy of 80.93 percent (for the input test dataset). Mahbod et al. [36] looked at dermoscopic picture collections with dimensions ranging from 64×64 pixels to 768×768 pixels. The author concludes that the classification performance of the small-sized dataset 64×64 pixels has been significantly reduced. In contrast, the classification performance of the large-sized dataset 128×128 pixels has shown significant improvement.

The X-ray picture has improved clarity and contrast as a result of the enhancement. Using the Gaussian high-pass filter as a starting point, this filter has been optimized to have

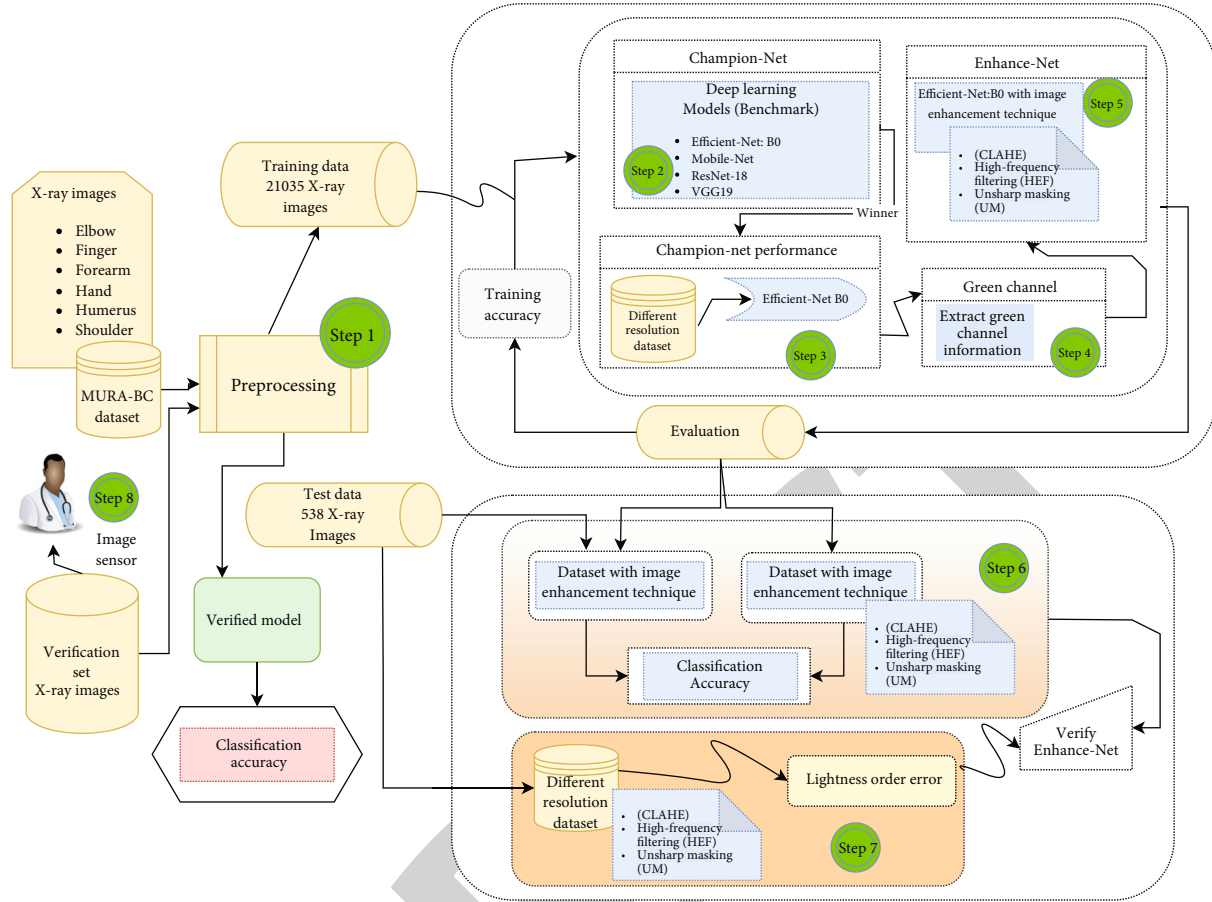


FIGURE 1: Block design of the proposed model.

TABLE 3: Parameters used for the enhancement techniques.

Enhancement model	Parameters
CLAHE	Clip limit: 40 Window size (W_s): 8×8
HEF	D_0 : 72
UM	Amount: 2 Radius: 5

offset = 0.5 and cutoff frequency = 0.05, respectively. In [37], the authors discussed a novel nonlinear UM enhancement model (NLUM) developed to increase the fine details in mammograms, aiding in diagnosing and treating breast cancer.

A new approach for determining CLAHE algorithm hyperparameters has been developed to generate images with improved contrast [38]. It prevents the intensity values of each tile histogram from exceeding the desired clip limit by setting a clip limit. According to [39], their research aims at examining and evaluating the accuracy of various picture quality improvement strategies. Another way of putting it is that the approaches of histogram equalization (HE), gamma correction (GC), and CLAHE preprocessing are being compared. According to the findings of this study, GC has the

highest sensitivity, whereas CLAHE has the highest accuracy in detecting GC. According to [40] research, the CLAHE and adaptive histogram equalization (AHE) methods are used to identify COVID-19 using the VGG19 model, with the goal of identifying COVID-19 [41] using the VGG19 model. Table 1 presents a comparative analysis of recent research findings.

3. Materials and Methods

In the musculoskeletal-based radiograph (MURA) (Rajpurkar et al., 2017), around 40500 X-ray images are gathered in one collection and used to diagnose musculoskeletal disorders. The dataset contains X-ray images that are 55.63 percent normal and 44.36 percent abnormal, respectively. The train and test datasets are organized into three sets (train, test, and verification). Every set includes seven subsets, one for each of the seven study joints: the shoulder (shoulder joint), elbow (elbow joint), humerus (humerus joint), finger (finger joint), wrist (wrist joint), and hand (hand joint). The MURA dataset was used to extract only normal X-rays, which were then used to create this dataset. Table 2 contains a detailed description of the X-ray dataset.

3.1. Various Image Enhancement Models. The representation of computation for various image enhancement approaches is discussed as follows:

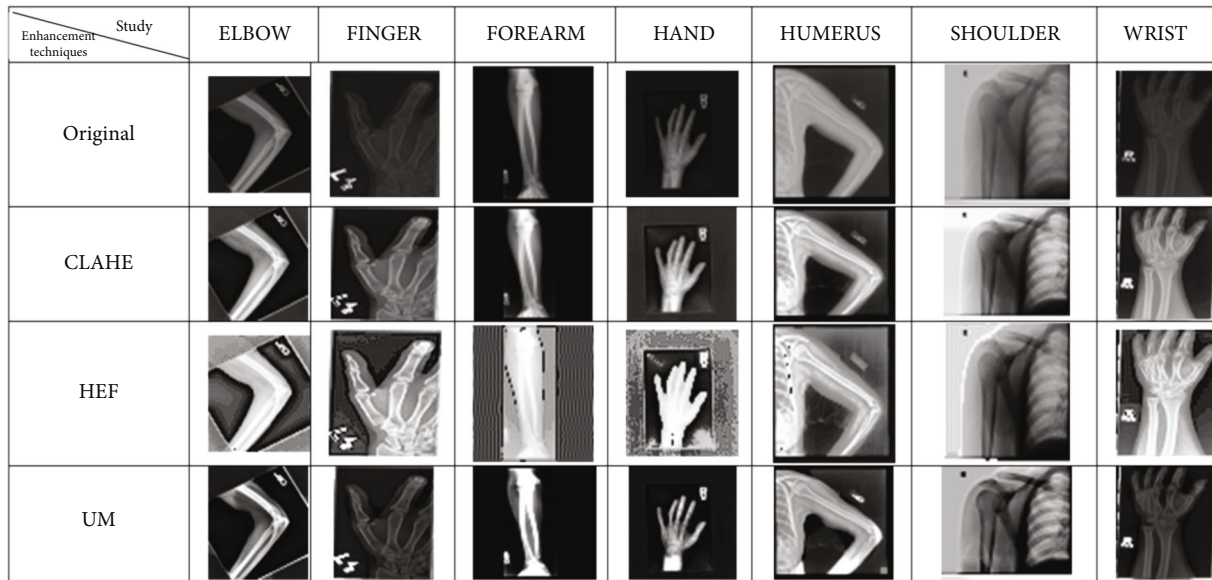


FIGURE 2: Outcomes of the enhancement techniques.

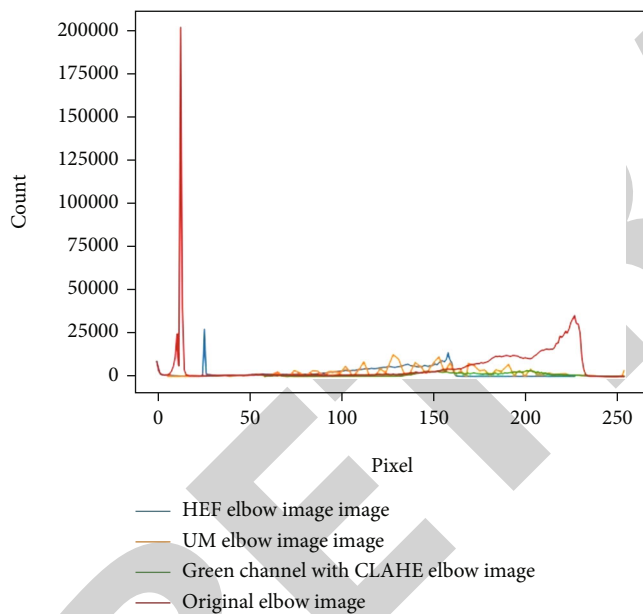


FIGURE 3: Histogram of MURA-BC-based random elbow image.

3.1.1. *CLAHE*. It is an image enhancement model [49] that has two important parameters: (1) Clip limit (C_{limit}), and (2) nonoverlapping regions ($Y_{contextual}$). The two parameters used in this model are responsible for controlling the enhanced quality of the image. X_{av} is the average amount of pixels in the grayscale computed as depicted in

$$X_{av} = \frac{X_{crX} \times X_{crY}}{X_g}, \quad (1)$$

where X_g is the gray level count in the $Y_{contextual}$, X_{crY} is the pixel count in the y dimensions $Y_{contextual}$, and X_{crX} is the

TABLE 4: Accuracy rate of various DLMs in the training phase.

Top five training accuracy					
Epoch	EfficientNet: B0	Epoch	ResNet-18	Epoch	VGG-19
20	92.12355	19	92.05999	20	91.96678
19	92.01339	20	92.05999	19	91.96578
17	91.84815	18	92.02763	18	90.844
16	91.67443	17	92.01863	17	90.53046
18	91.65749	16	92.01763	16	90.19998
Max %	92.12355	Max %	92.05999	Max %	91.96679

pixel count in the x dimensions of $Y_{contextual}$.

$$X_{acis} = \frac{X \sum c}{X_g}. \quad (2)$$

The distributed pixel is calculated and shown in

$$Pd = \frac{X_g}{X_{lp}}, \quad (3)$$

where X_{lp} is the remaining amount of clipped image pixels.

3.1.2. *HEF*. HEF is an image enhancement methodology based on a Gaussian filter to improve the sharpness of the edges in an image (Bundy and Wallen. 1984). The radius of the algorithm represents the sharpness intensity of the original image, which has been transformed and filtered using the filter function and Fourier transformation. A filtered image will be produced as a result of the inverse transformation. Second, the image's contrast is in sync with the histogram equalization setting on the computer. The Gaussian-based high-pass filter is computed in the manner

TABLE 5: Accuracy rate of testing of various deep learning-based models.

Epoch	EfficientNet: B0	Top five test accuracy		Epoch	VGG-19
		Epoch	ResNet-18		
19	91.30174	20	90.50178	20	88.1824
17	90.94181	19	90.40192	19	87.7625
16	90.16197	18	90.16197	18	89.802
9	89.0222	13	90.10198	17	88.0624
11	89.0222	12	89.86203	16	88.3623
Max %	91.30174	Max %	90.50178	Max %	89.802

TABLE 6: Error rate during the training phase of DLMs.

Epoch	EfficientNet-B0	Top five training error rate					
		Epoch	MobileNet	Epoch	ResNet18	Epoch	VGG19
19	0.241755	19	0.269972	19	0.242157	19	0.26715
20	0.244397	20	0.275724	20	0.242157	20	0.26815
18	0.259444	18	0.295539	18	0.249675	18	0.30285
17	0.260169	17	0.306982	17	0.249775	17	0.30717
16	0.262874	16	0.333399	16	0.249875	16	0.319
Min %	0.241755	Min %	0.269972	Min %	0.242157	Min %	0.26715

TABLE 7: Error rate during the testing phase of DLMs.

Epoch	EfficientNet: B0	Top five test error rate					
		Epoch	Mobile-net	Epoch	ResNet-18	Epoch	VGG-19
19	0.276527	12	0.291593	20	0.293466	18	0.32459
16	0.300061	16	0.296771	13	0.296771	16	0.37789
17	0.327415	19	0.298766	19	0.298766	20	0.38395
9	0.338509	10	0.303375	17	0.306369	17	0.40352
11	0.345888	15	0.317347	18	0.312	19	0.41603
Min %	0.276527	Min %	0.291593	Min %	0.293466	Min %	0.32459

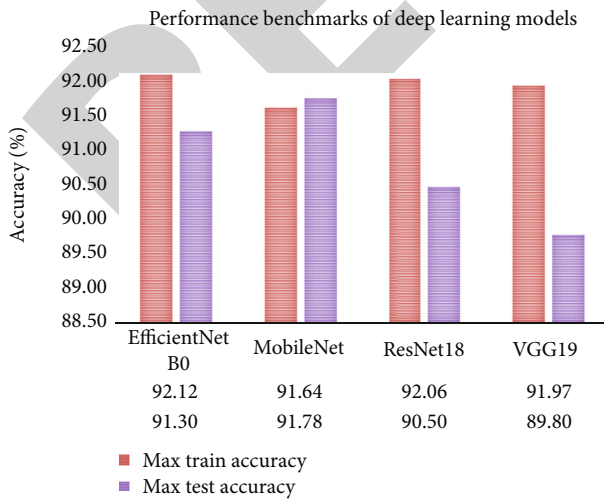


FIGURE 4: Training and testing accuracy of various DLMs.

shown in the diagram:

$$\text{Gau}_{\text{filter}(x,y)} = 1 - e^{-D^2(x,y)/2D_0^2}, \quad (4)$$

where D_0 is the cutoff distance. $F(i, j)$ is the Fourier transform computes as shown in

$$F(i, j) = \sum_{x=0}^{h-1} \sum_{y=0}^{w-1} f(x, y) e^{-j2\pi((ix/h)+(jy/w))}, \quad (5)$$

where i and $x = 0, 1, 2, \dots, h-1$ and j and $y = 0, 1, 2, \dots, w-1$. $F(x, y)$ is the inverse Fourier transformation computed as shown in

$$F(x, y) = \frac{1}{hw} \sum_{x=0}^{h-1} \sum_{y=0}^{w-1} f(i, j) e^{-j2\pi((ix/h)+(jy/w))}. \quad (6)$$

3.1.3. UM. UM is a kind of image enhancement method used to sharpen an image that has been captured (Polesel,

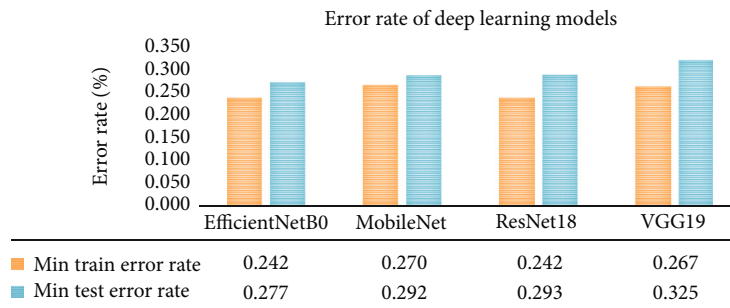


FIGURE 5: Training and testing error rate of various DLMs.

Ramponi and Mathews, 2000). The sharp details of the image are computed as a difference between the original image and the image with Gaussian blur applied to the original image. The input image is blurred using a Gaussian blur filter at the beginning of this technique. The radius of the blur and the amount of blur are the two key parameters for Gaussian blurry images (Ramponi, 1998). The radius has an effect on the size of the edge that needs to be enlarged. According to equation (7), the amount of darkness, lightness, and contrast is included in the edges of the images.

$$G(x, y) = \frac{1}{2\pi\sigma^2} e^{-((x^2+y^2)/(2\sigma^2))}, \quad (7)$$

where x, y is the horizontal and vertical distances from the source and σ is the Gaussian distribution. I_{enhanced} is the obtained image after enhancement as shown in

$$I_{\text{enhanced}} = (I_{\text{original}} + \text{contrast}_{\text{value}} * (I_{\text{blur}})), \quad (8)$$

where I_{original} is the original image and I_{blur} is the unsharp image.

4. Proposed Work

The proposed model is divided into four major phases: image preprocessing, a benchmark-based DLM training and validation from scratch, Champion-Net used with various resolution datasets, and the application of image enhancement models. The main features of the proposed model are the selection of the Champion-Net from the deep learning technique and the implementation of image enhancement models to improve the overall performance of the Champion-Net. The performance of Enhance-Net techniques is validated using the lightness order error (LoE). The block design of our proposed paradigm is depicted in Figure 1.

4.1. Research Environment. The virtual environment was used to conduct the research. The Ubuntu operating system has 12 GB of RAM, with six virtual CPU (Intel Xeon 2.2 GHz) processors in the server that are installed on the host virtual machine. The proposed experiment takes place in a CPU-based setting, and Python 3.0 is used for the simulation process.

4.1.1. Image Preprocessing Stage. In This stage, the preprocessing of X-ray images improves the raw image's important information. The dataset creation and transformation are two steps in the image preprocessing process.

4.1.2. Image Dataset Formation. In this stage, the MURA-BC-based X-ray data is used in different pixel computations for dataset formation such as 32×32 , 40×40 , 48×48 , 56×56 , 64×64 , 72×72 , 80×80 , and 88×88 pixels. The dataset is arranged in two packages: train and test. In the training package, around 21935 images are placed, and the test package contains 650 X-ray image samples from seven different groups.

4.1.3. Data Transformation. This step involves randomly cropping both the training and testing datasets with the four padding and flipping X-ray images in horizontal and flipping the training dataset. This strategy gives you an advantage over the rest of the dataset. The normalizing procedure is used to minimize signals that include undesired noise or distortion. Because of uneven staining and insufficient contrast, the X-ray picture acquired by the imaging modality system may be partial and lacking in important features, such as the patient's position.

4.2. Benchmark of Deep Learning-Based Model Training and Validation. This study started with a clean slate and trained the benchmark of deep learning-based models (EfficientNet: B0; MobileNet; ResNet18; and VGG19) from the ground up. This dataset of 3232 X-ray images from the MURA-BC experiment was used for train, validation, and testing.

4.3. Champion-Net Processed with Different Resolution Dataset. The performance of a DLM trained on datasets with different resolutions (4040, 4848, 5656, 6464, 7272, 8080, and 8888 pixels) was determined in this phase using different resolution datasets. This step will assist us in determining the best deep learning model from the deep learning models available.

4.4. Green Channel Extraction. The suggested model is designed to extract the green channel details and convert the image into a grayscale. In [50, 51], the authors have used only the green channel of the RGB colour image for conversion to a grayscale image. The green channel image keeps the most information. The green channel of fundus pictures is often utilized since several authors' findings have shown that

TABLE 8: Champion-Net performance based on various training datasets.

Epoch	EfficientNet: B0 32 × 32		EfficientNet: B0 40 × 40		EfficientNet: B0 48 × 48		EfficientNet: B0 56 × 56		EfficientNet: B0 64 × 64		EfficientNet: B0 72 × 72		EfficientNet: B0 80 × 80		EfficientNet: B0 88 × 88	
	Epoch	EfficientNet: B0 32 × 32	Epoch	EfficientNet: B0 40 × 40	Epoch	EfficientNet: B0 48 × 48	Epoch	EfficientNet: B0 56 × 56	Epoch	EfficientNet: B0 64 × 64	Epoch	EfficientNet: B0 72 × 72	Epoch	EfficientNet: B0 80 × 80	Epoch	EfficientNet: B0 88 × 88
20	16	92.12	19	93.07	20	92.54	20	92.55	20	93.1	12	93.89	19	94.64	18	94.86
19	19	92.01	17	92.94	18	92.33	16	92.3	16	93.03	15	93.86	18	94.55	19	94.5
17	20	91.84	20	92.74	19	92.33	12	92.3	12	93	14	93.77	17	94.53	16	94.47
16	18	91.67	14	92.65	16	92.29	19	92.18	19	92.94	18	93.71	12	94.39	13	94.45
18	13	91.65	18	92.63	17	91.99	18	92.14	18	92.89	20	93.7	13	94.39	11	94.44
Max %	Max %	92.12	Max %	93.07	Max %	92.54	Max %	92.55	Max %	93.1	Max %	93.89	Max %	94.64	Max %	94.86

TABLE 9: Champion-Net accuracy of various resolution test datasets.

Epoch	EfficientNet: B0 32 × 32		EfficientNet: B0 40 × 40		EfficientNet: B0 48 × 48		EfficientNet: B0 56 × 56		EfficientNet: B0 64 × 64		EfficientNet: B0 72 × 72		EfficientNet: B0 80 × 80		EfficientNet: B0 88 × 88	
	Epoch	%	Epoch	%	Epoch	%	Epoch	%	Epoch	%	Epoch	%	Epoch	%	Epoch	%
19	91.3	16	93.07	10	89.74	16	90.76	18	91.96	10	92.02	16	94.24	8	92.86	
17	90.94	19	92.94	7	89.68	14	90.46	17	91.3	14	91.9	20	93.46	4	92.38	
16	90.16	20	92.74	6	89.2	18	89.92	15	90.94	8	91.84	19	92.8	13	92.32	
9	89.02	18	92.65	14	89.08	20	89.92	11	90.58	13	91.78	17	92.68	19	92.14	
11	89.02	13	92.63	8	88.66	19	89.38	9	89.8	17	91.42	14	91.96	14	91.84	
Max %	91.3	Max %	93.07	Max %	89.74	Max %	90.76	Max %	91.96	Max %	92.02	Max %	94.24	Max %	92.86	

TABLE 10: Champion-Net training time for different resolution datasets.

Champion-Net with different image resolutions	Training time for 20 epochs
EfficientNet: B0 resolution 32×32	30 minutes
EfficientNet: B0 resolution 40×40	55 minutes
EfficientNet: B0 resolution 48×48	1 hour 50 minutes
EfficientNet: B0 resolution 56×56	2 hours 45 minutes
EfficientNet: B0 resolution 64×64	3 hours 20 minutes
EfficientNet: B0 resolution 72×72	5 hours
EfficientNet: B0 resolution 80×80	7 hours 50 minutes
EfficientNet: B0 resolution 88×88	Ours

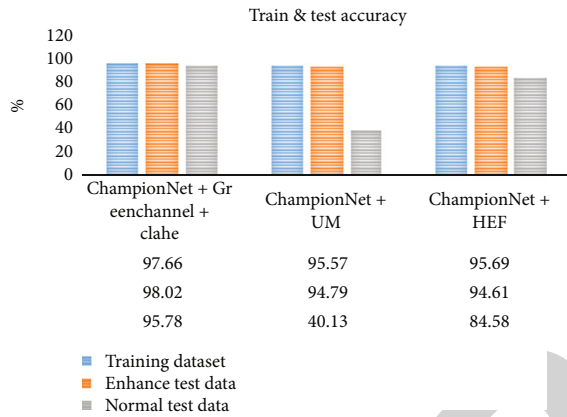


FIGURE 6: Dataset of training and testing accuracy (with and without enhancement).

the green channel of the RGB representation of retinal fundus images provides the most significant contrast. This is why the green channel of fundus images is so commonly used [52].

4.5. Image Enhancement Techniques. In total, three well-known enhancement techniques, (1) CLAHE, (2) HEF, and (3) UM, are developed in this paper. The parameters of enhancement techniques are listed in detail in Table 3 of this document. Figure 2 shows the results of enhancement techniques applied to a few of the input X-ray samples. In Figure 3, we showed a histogram chart representing the elbow bone images using MURA-BC data that were randomly selected.

5. Results and Its Validation

The proposed model's simulation is divided into three primary parts: (1) benchmark deep learning, (2) model training, and (3) validation. Champion-Net processing was done with various resolution datasets and application of image enhancing algorithms on Champion-Net. All three phases were simulated using Python 3.0.

The accuracy (Acc) and error rate (Er) of our model are used to assess its performance. Validation is carried out by using LoE.

5.1. Accuracy. The accuracy is the percentage of successfully categorized photos in the dataset (Mall, Singh, and Yadav, 2019) [53]. The parameter "accuracy" is computed as shown in (9) as follows:

$$A_{cc} = \frac{TP + TN}{\text{total number}}. \quad (9)$$

The total amount of the dataset for the images is computed as shown in (10) as follows:

$$\text{Total number} = (TN + TP + FP + FN), \quad (10)$$

where TN is the true negative, TP is the true positive, FP is the false positive, and FN is the false negative.

5.2. Order of Error. The naturalness of an image is critical for image enhancement approaches, yet the majority of these techniques are unable to adequately retain the naturalness of the image. Among the approaches (HEF, UM, and CLAHE) that have been examined, this IQA methodology delivers the most comprehensive answer. The difference between the original sample input picture I_{input} and the improved image $I_{enhanced}$ is used to calculate the level of entropy. Having a low LoE score suggests that you have found the greatest approach to keep the naturalness of your photographs. The LoE is calculated in the manner shown in

$$LoE = \frac{1}{h * w} \sum_{i=1}^h \sum_{j=1}^w RD(i, j). \quad (11)$$

$RD(x, y_{relative})$'s order difference may be expressed as h/w (height/width). The relative order difference between the original and enhanced images is determined in

$$RD(I, J) = \sum_{i=1}^h \sum_{j=1}^w (U(L(x, y), L(i, j)) \oplus (U(L_{enhance}(x, y), L_{enhance}(i, j)))). \quad (12)$$

For example, in (13) and (14), the unit step approach computes $L(x, y)$ lightness and $U(x, y)$ and the unit step

TABLE 11: Champion-Net training and testing accuracy of various enhancement techniques.

Champion-Net +green channel +CLAHE	Epoch	Champion- Net+HEF	Epoch	Champion- Net+UM	Epoch	Champion- Net +green channel +CLAHE	Epoch	Champion- Net+HEF	Epoch	Champion- Net+UM	Epoch	Champion- Net +green channel +CLAHE	Epoch	Champion- Net+HEF	Epoch	Champion- Net+UM	
20	97.66	20	95.57	20	95.69	17	98.02	20	94.79	16	94.61	18	95.78	13	40.13	18	84.58
19	96.02	18	95.27	17	95.27	15	96.63	19	93.77	18	94.39	16	94.02	12	35.93	7	77.2
17	94.87	19	95.06	16	95.26	14	94.64	16	92.93	14	93.53	20	91.6	10	35.75	9	76.72
18	94.45	17	94.99	19	95	18	97.45	17	91.2	19	93.41	15	93.06	9	34.55	3	76.66
15	94.79	16	94.74	18	94.98	12	96.42	18	90.9	20	93.11	13	91.32	18	28.49	12	75.52
Max %	97.66	Max %	95.57	Max %	95.69	Max %	98.02	Max %	94.79	Max %	94.61	Max %	95.78	Max %	40.13	Max %	84.58
Testing accuracy without enhancement on test datasets																	
Testing accuracy with enhancement on the test dataset																	
Accuracy testing with enhancement on the test dataset																	

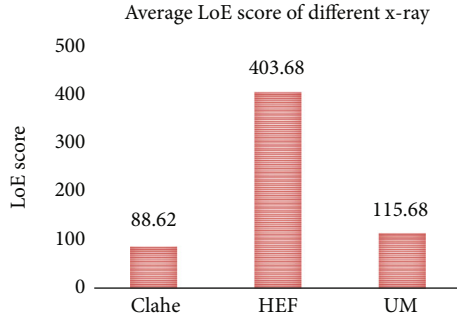


FIGURE 7: LoE score achieved in different image enhancement techniques.

TABLE 12: Different X-ray study datasets and their corresponding LoE score.

LoE_Score	CLAHE+green channel	HEF	UM
LoE_HUMERUS	85.29	585.7	104.1
LoE_SHOULDER	150.87	1.5	95.3
LoE_WRIST	53.35	403.6	83.8
Average_LoE_SCORE	88.62	402.6	115.6
LoE_ELBOW	106.87	407.9	138.8
LoE_FINGER	75.92	613.3	203.2
LoE_FOREARM	115.21	324.6	54.1
LoE_HAND	32.87	487.8	131.1

n = 92	Predicted yes	Predicted no
	Actual yes	42
Actual no	2	47

FIGURE 8: Confusion matrix.

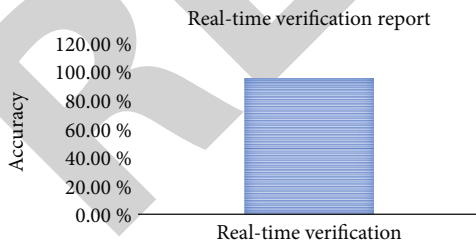


FIGURE 9: Real-time verification.

technique is depicted:

$$L(x, y) = \max_{c \in [r, g, b]} I^c(x, y), \quad (13)$$

$$U(x, y) = \begin{cases} 1, & x \geq y, \\ 0, & \text{else.} \end{cases} \quad (14)$$

5.3. *Experiment Result for Champion-Net Selection as Winner.* In order to conduct this experiment, we started with a clean slate and trained the deep benchmark learning algorithm from scratch on the MURA-BC 32 × 32 X-ray picture dataset. The model training was carried out for a total of 20 epochs. A detailed report on the training accuracy of DLMs is provided in Table 4 (EfficientNet: B0, MobileNet, ResNet-18, and VGG-19). In terms of maximum training accuracy, we achieved 92.12 percent, 91.64 percent, 92.05 percent, and 91.96 percent in the experiments.

The test accuracy of EfficientNet: B0, MobileNet, ResNet-18, and VGG-19 benchmark models is depicted in Table 5. The maximum test accuracy is calculated at 92.120%, 91.640%, 92.5%, and 91.960%.

A comparison of training error rates for the benchmark deep learning models EfficientNet: B0, MobileNet, ResNet-18, and VGG-19 is presented in Table 6. We acquire minimum training errors of 0.281, 0.4026, 0.2760, and 0.35249, for four different training scenarios.

The test accuracy of EfficientNet: B0, MobileNet, ResNet-18, and VGG-19 benchmark models is shown in Table 7. The minimum test error rate was obtained at 0.2765270, 0.2915930, 0.2934660, and 0.3245850.

As illustrated in Figures 4 and 5, the EfficientNet: B0 is selected as the Champion-Net based on the accuracy and error of training and testing. For training and testing, the highest accuracy (EfficientNet: B0) is 92.15 and 91.3, and the minimum training and testing of error rates are obtained at 0.24 and 0.27.

5.4. *Experimental Result for Champion-Net Computed with Different Resolution Datasets.* First and foremost, this experiment used the understanding of the link between DLM and various dataset resolutions. Second, estimate the amount of time it will take to train on various resolutions. The findings in Table 7 and Table 8 demonstrate the impact of various resolutions of X-ray image datasets on the organization using different resolution X-ray image datasets. Various resolution datasets are represented in Table 9 to help you estimate the training time. The performance of DLMs, on the other hand, improves as the resolution of the dataset increases. As the resolution of the dataset is increased, so is the amount of time spent training. As a result, it is clear from Tables 8–10 that the 64-64 pixel resolution dataset performs better in terms of accuracy and training time, while the 32-32 pixel resolution dataset performs the worst. As a result, we have chosen an image of a 64-64 pixel X-ray dataset.

5.5. *Experimental Result for Champion-Net with Different Image Enhancement Techniques.* The primary goal of this phase of research is to improve the overall performance of DLMs, which is now underway. We have processed the dataset that was finalized in the previous phase using several image enhancement algorithms, including HEF, CLAHE, and UM, to get the desired results. The findings in Table 10 and in Figure 6 demonstrate the organization and performance of Champion-Net along with the enhancement approaches on the datasets, in the presence and absence of

enhancement strategies, respectively. On the training dataset, the performance of all three image-enhancing algorithms is about the same in the range of 97.66 to 95.69 percent. The difference between the test datasets with and without enhancing methods was examined during the testing phase. It is evident that the green channel+CLAHE strategy surpasses both of the other two procedures, according to the results in Table 11. The green channel+CLAHE methodology obtained a 95.78 percent accuracy using enhancement techniques. HEF obtained an accuracy of 94.79 percent, while UM obtained an accuracy of 94.61 percent on the test dataset. Without the use of enhancement techniques, HEF obtained just 40.15 percent, and UM scored 84.5 percent on the test data, respectively.

5.6. Result Validation Using LoE. The low level of evidence (LoE) technique is used for result validation of the preceding phase of the experiment in the final step, as represented in Figure 7. Table 12 displays the LoE-based score of several bone X-ray scans. The lowest LoE score shows the optimal option [54], which keeps the naturalness of the photos even after they have been altered. It has a LoE of 88.62, which is the lowest of the three techniques tested. It is calculated that the HEF-based LoE score is around 403.6, whereas the UM LoE score value is around 115.6. The LoE of CLAHE verifies the outcome of the preceding phase.

6. Real-Time Verification

In this section, radiologists and orthopaedic surgeons perform real-time testing of the verified model using the trained model for real-time medical image prediction. They tested a total of 92 X-ray images. Figure 8 provides the details regarding the confusion matrix. The 96.74% accuracy is achieved during real-time testing, as shown in Figure 9. The suggested model produced the best result and improved classification performance during the experiments.

7. Conclusion

This paper has proposed a methodology for improving digital learning environments in the medical imaging field. The importance of the Internet of things in medical imaging technology is shown by how it is used in healthcare applications. We have also carried out a number of tests to enhance the overall accuracy of the proposed model and validate the findings through LoE techniques. The Champion-Net evaluation system was chosen from among the benchmark DLMs based on the accuracy and error rate of the data. Various resolutions are evaluated by the Champion-Net dataset in order to achieve the maximum possible Champion-Net performance. As part of the improvement phase, the green channel details are retrieved and retrained, and the best model is tested using image-enhancing techniques such as CLAHE, HEF, and UM.

This phase contributes to the production of Enhance-Net with improved performance. At the conclusion of the trial, we compare the findings of the Enhance-Net with the lightness order error (LoE). Using the suggested architecture

of Enhance-Net, the performance of the DLMs on the MURA-BC dataset is improved significantly. The Enhance-Net makes a significant contribution to IoT-based real-time prediction models on X-ray datasets in a dynamic manner. Results of the research include X-ray pictures that have been processed with green channel+CLAHE enhancement techniques in order to increase the performance of the DLM. In the future, The Enhance-Net can also be implemented for various other medical imaging problems. This approach offers medical practitioners an instant, comprehensive tool to help them through the treatment process in a variety of medical disciplines. Despite the fact that this study is confined to X-ray image modality, the same work may be expanded to include other medical acquisition methods in the future.

Data Availability

Dataset will be made available on request.

Ethical Approval

This paper does not contain any studies with human or animal subjects.

Conflicts of Interest

The authors declare that they have no conflicts of interest.

References

- [1] S. Balhara, N. Gupta, A. Alkhayyat et al., "A survey on deep reinforcement learning architectures, applications and emerging trends," *IET Communications*, vol. 16, no. 20, 2022.
- [2] B. Preveze, A. Alkhayyat, F. Abedi, A. M. Jawad, and A. S. Abosinnee, "SDN-driven Internet of health things: a novel adaptive switching technique for hospital healthcare monitoring system," *Wireless Communications and Mobile Computing*, vol. 2022, Article ID 3150756, 11 pages, 2022.
- [3] S. Srivastava and S. Sharma, "Analysis of cyber related issues by implementing data mining algorithm," in *2019 9th International Conference on Cloud Computing, Data Science & Engineering (Confluence)*, pp. 606–610, Noida, India, 2019.
- [4] D. S. Al-Dulaimi, A. G. Mahmoud, N. M. Hassan, A. Alkhayyat, and S. A. Majeed, "Development of pneumonia disease detection model based on deep learning algorithm," *Wireless Communications and Mobile Computing*, vol. 2022, Article ID 2951168, 10 pages, 2022.
- [5] V. Narayan and A. K. Daniel, "IOT based sensor monitoring system for smart complex and shopping malls," in *International Conference on Mobile Networks and Management*, pp. 344–354, Springer, 2021.
- [6] V. Narayan, A. K. Daniel, and A. K. Rai, "Energy efficient two tier cluster based protocol for wireless sensor network," in *2020 international conference on electrical and electronics engineering (ICE3)*, pp. 574–579, Gorakhpur, India, 2020.
- [7] N. M. Mamani, "Machine learning techniques and polygenic risk score application to prediction genetic diseases," *ADCAIJ: Advances in Distributed Computing and Artificial Intelligence Journal*, vol. 9, no. 1, pp. 5–14, 2020.

- [8] V. Narayan, R. K. Mehta, M. Rai et al., "To implement a web page using thread in Java," *International Journal of Current Engineering and Technology*, vol. 7, no. 3, pp. 926–934, 2017.
- [9] A. Kumar, K. Abhishek, C. Chakraborty, and N. Kryvinska, "Deep learning and Internet of things based lung ailment recognition through coughing spectrograms," *IEEE Access*, vol. 9, pp. 95938–95948, 2021.
- [10] A. Krizhevsky and G. Hinton, "Learning multiple layers of features from tiny images," University of Toronto, Toronto, Ontario, 2009.
- [11] A. Krizhevsky, I. Sutskever, and G. E. Hinton, "ImageNet classification with deep convolutional neural networks," *Advances in Neural Information Processing Systems*, vol. 25, pp. 1097–1105, 2012.
- [12] V. Ravi, H. Narasimhan, C. Chakraborty, and T. D. Pham, "Deep learning-based meta-classifier approach for COVID-19 classification using CT scan and chest X-ray images," *Multimedia Systems*, vol. 28, no. 4, pp. 1401–1415, 2022.
- [13] V. Narayan and A. K. Daniel, "A research protocol for detection and optimization of overlapping coverage in wireless sensor networks," *International Journal of Engineering and Advanced Technology*, vol. 8, Supplement 6, pp. 1–6, 2019.
- [14] K. Simonyan and A. Zisserman, "Very deep convolutional networks for large-scale image recognition," 2014, <https://arxiv.org/abs/1409.1556>.
- [15] S. Zagoruyko and N. Komodakis, "DiracNets: training very deep neural networks without skip-connections," 2017, <https://arxiv.org/abs/1706.00388>.
- [16] V. Narayan and A. K. Daniel, "Design consideration and issues in wireless sensor network deployment," *Invertis Journal of Science & Technology*, vol. 13, no. 3, p. 101, 2020.
- [17] D. Irfan, X. Tang, V. Narayan, P. K. Mall, S. Srivastava, and V. Saravanan, "Prediction of quality food sale in mart using the AI-based TOR method," *Journal of Food Quality*, vol. 2022, Article ID 6877520, 9 pages, 2022.
- [18] M. Tan and Q. Le, "EfficientNet: rethinking model scaling for convolutional neural networks," in *Proceedings of the 36th International Conference on Machine Learning*, pp. 6105–6114, Long Beach, California, 2019.
- [19] M. Jaderberg, K. Simonyan, A. Zisserman, and K. Kavukcuoglu, "Spatial transformer networks," 2015, <https://arxiv.org/abs/1506.02025>.
- [20] K. He, X. Zhang, S. Ren, and J. Sun, "Deep residual learning for image recognition," in *2016 IEEE Conference on Computer Vision and Pattern Recognition (CVPR)*, pp. 770–778, Las Vegas, NV, USA, 2016.
- [21] A. G. Howard, M. Zhu, B. Chen et al., "MobileNets: efficient convolutional neural networks for mobile vision applications," 2017, <https://arxiv.org/abs/1704.04861>.
- [22] V. Narayan and A. K. Daniel, "CHHP: coverage optimization and hole healing protocol using sleep and wake-up concept for wireless sensor network," *International Journal of Systems Assurance Engineering and Management*, vol. 13, Supplement 1, pp. 546–556, 2022.
- [23] V. Narayan and A. K. Daniel, "A novel approach for cluster head selection using trust function in WSN," *Scalable Computing: Practice and Experience*, vol. 22, no. 1, pp. 1–13, 2021.
- [24] A. Chandu, "A review on IoT based medical imaging technology for healthcare applications," *Journal of Innovative Image Processing*, vol. 1, no. 1, pp. 51–60, 2019.
- [25] B. Prajapati, S. Parikh, and J. Patel, "An intelligent real time IoT based system (IRTBS) for monitoring ICU patient," in *International Conference on Information and Communication Technology for Intelligent Systems*, pp. 390–396, Springer, 2017.
- [26] I. Ahmed, G. Jeon, and A. Chehri, "An IoT-enabled smart health care system for screening of COVID-19 with multi layers features fusion and selection," *Computing*, vol. 105, no. 4, pp. 743–760, 2023.
- [27] R. Miotto, F. Wang, S. Wang, X. Jiang, and J. T. Dudley, "Deep learning for healthcare: review, opportunities and challenges," *Briefings in Bioinformatics*, vol. 19, no. 6, pp. 1236–1246, 2018.
- [28] M. N. Birje and S. S. Hanji, "Internet of things based distributed healthcare systems: a review," *Journal of Data, Information and Management*, vol. 2, no. 3, pp. 149–165, 2020.
- [29] A. Kumar, J. Kim, D. Lyndon, M. Fulham, and D. Feng, "An ensemble of fine-tuned convolutional neural networks for medical image classification," *IEEE Journal of Biomedical and Health Informatics*, vol. 21, no. 1, pp. 31–40, 2017.
- [30] A. Darwish, A. E. Hassanien, M. Elhoseny, A. K. Sangaiah, and K. Muhammad, "The impact of the hybrid platform of Internet of things and cloud computing on healthcare systems: opportunities, challenges, and open problems," *Journal of Ambient Intelligence and Humanized Computing*, vol. 10, no. 10, pp. 4151–4166, 2019.
- [31] S. Selvaraj and S. Sundaravaradhan, "Challenges and opportunities in IoT healthcare systems: a systematic review," *SN Applied Sciences*, vol. 2, no. 1, 2020.
- [32] B. D. Deebak, F. Al-Turjman, M. Aloqaily, and O. Alfandi, "An authentic-based privacy preservation protocol for smart e-healthcare systems in IoT," *IEEE Access*, vol. 7, pp. 135632–135649, 2019.
- [33] M. Talo, "Automated classification of histopathology images using transfer learning," *Artificial Intelligence in Medicine*, vol. 101, article 101743, 2019.
- [34] Y. Zhang, X. Pan, C. Li, and T. Wu, "3D liver and tumor segmentation with CNNs based on region and distance metrics," *Applied Sciences*, vol. 10, no. 11, p. 3794, 2020.
- [35] B. K. Triwijoyo, B. S. Sabarguna, W. Budiharto, and E. Abdurachman, "Deep learning approach for classification of eye diseases based on color fundus images," in *Diabetes and Fundus OCT*, pp. 25–57, Elsevier, 2020.
- [36] A. Mahbod, G. Schaefer, C. Wang, R. Ecker, G. Dorffner, and I. Ellinger, "Investigating and exploiting image resolution for transfer learning-based skin lesion classification," 2020, <https://arxiv.org/abs/2006.14715>.
- [37] K. Panetta, Y. Zhou, S. Agaian, and H. Jia, "Nonlinear unsharp masking for mammogram enhancement," *IEEE Transactions on Information Technology in Biomedicine*, vol. 15, no. 6, pp. 918–928, 2011.
- [38] U. Kuran and E. C. Kuran, "Parameter selection for CLAHE using multi-objective cuckoo search algorithm for image contrast enhancement," *Intelligent Systems with Applications*, vol. 12, article 200051, 2021.
- [39] H. Raj and D. K. Vishwakarma, "Detection of COVID-19 in chest X-ray image using convolutional neural network," in *2021 2nd Global Conference for Advancement in Technology (GCAT)*, pp. 1–5, Bangalore, India, 2021.
- [40] B. K. Umri, E. Utami, and M. P. Kurniawan, "Comparative analysis of CLAHE and AHE on application of CNN algorithm in the detection of COVID-19 patients," in *2021 4th*

Retraction

Retracted: Uncertainty Analysis of Key Influencing Factors on Stability of Tailings Dam Body

Journal of Sensors

Received 23 January 2024; Accepted 23 January 2024; Published 24 January 2024

Copyright © 2024 Journal of Sensors. This is an open access article distributed under the Creative Commons Attribution License, which permits unrestricted use, distribution, and reproduction in any medium, provided the original work is properly cited.

This article has been retracted by Hindawi following an investigation undertaken by the publisher [1]. This investigation has uncovered evidence of one or more of the following indicators of systematic manipulation of the publication process:

- (1) Discrepancies in scope
- (2) Discrepancies in the description of the research reported
- (3) Discrepancies between the availability of data and the research described
- (4) Inappropriate citations
- (5) Incoherent, meaningless and/or irrelevant content included in the article
- (6) Manipulated or compromised peer review

The presence of these indicators undermines our confidence in the integrity of the article's content and we cannot, therefore, vouch for its reliability. Please note that this notice is intended solely to alert readers that the content of this article is unreliable. We have not investigated whether authors were aware of or involved in the systematic manipulation of the publication process.

Wiley and Hindawi regrets that the usual quality checks did not identify these issues before publication and have since put additional measures in place to safeguard research integrity.

We wish to credit our own Research Integrity and Research Publishing teams and anonymous and named external researchers and research integrity experts for contributing to this investigation.


The corresponding author, as the representative of all authors, has been given the opportunity to register their agreement or disagreement to this retraction. We have kept a record of any response received.

References

- [1] S. Qian and K. Hou, "Uncertainty Analysis of Key Influencing Factors on Stability of Tailings Dam Body," *Journal of Sensors*, vol. 2023, Article ID 7521356, 11 pages, 2023.

Research Article

Uncertainty Analysis of Key Influencing Factors on Stability of Tailings Dam Body

Shanguang Qian^{1,2} and Kepeng Hou¹ 

¹Faculty of Land Resources Engineering, Kunming University of Science and Technology, Kunming 650033, China

²Faculty of Architectural Engineering, Kunming Metallurgy College, Kunming 650033, China

Correspondence should be addressed to Kepeng Hou; qiansgqq@kust.edu.cn

Received 23 August 2022; Revised 11 September 2022; Accepted 27 September 2022; Published 20 April 2023

Academic Editor: Sweta Bhattacharya

Copyright © 2023 Shanguang Qian and Kepeng Hou. This is an open access article distributed under the Creative Commons Attribution License, which permits unrestricted use, distribution, and reproduction in any medium, provided the original work is properly cited.

With the continuous expansion of the mining scale of mineral resources, many tailings are produced. In order to avoid the impact of harmful substances in the tailings on the residents around the tailings pond, it is necessary to explain the stability improvement. The dam safety monitoring system is mainly composed of observation sensors, telemetry data acquisition module, industrial control network, and automatic monitoring system. Through the work of the computer, the dam observation data can be automatically collected, processed, analyzed, and calculated. This paper adopts the automated system that makes preliminary judgments and graded alarms on whether the dam's behavior is normal or not to provide early safety warning reports for monitoring objects. In this paper, combined with a specific example of a tailings reservoir dam body, the comprehensive uncertainty method is used to analyze factors such as the height of the tailings dam, the height of the wetting line, the cohesion of the tailings soil layer, and the internal friction angle, and the stability of the dam body is calculated. The results show that the sensitivity order of the dam stability safety factor K to each factor is as follows: internal friction angle of the tailing silt layer > the height of the wetting line > dam body height > the cohesion of the tailing silt layer. The most dangerous slip surface will jump at the 19-level subdam of the tailings pond. The remediation measures are of great significance for maintaining the ecology around the tailings pond and ensuring the personal safety of residents.

1. Introduction

China is a big mining country, but due to the continuous expansion of mining scale in recent years, the number of tailings discarded every year is increasing. Most of the tailings discarded every year are stored in tailings ponds, and only a small part is reused. With the continuous growth in the number of tailings ponds, there are great potential safety hazards in the process of tailings filling or comprehensive utilization and recovery [1]. If the tailings dam fails, it will not only cause damage to the ecological environment but also lead to casualties. According to incomplete statistics, up to now, only 70% of the total tailings ponds have been treated and utilized in the tailings ponds, and nearly one-third of the tailings ponds have not been treated, which is highly dangerous. Not only that, these tailings ponds are in

a very unfavorable situation due to their large storage [2] and old tailings pond facilities. Problems often occur in tailings ponds due to some force majeure. Therefore, the current operating efficiency of tailings ponds in China is low and the disaster risk is very high, which is needed to deal with urgently. Many experts and scholars at home and abroad have conducted in-depth research and discussion on the dam body stability of wet-draining tailings ponds, and their research focuses mainly on three aspects: seepage stability, dam body static stability, and dam body dynamic stability [3]. In the context of strengthening water conservancy construction, improving the safety of hydraulic structures, especially improving the level of dam safety monitoring, and ensuring the safety of reservoirs and dams are the top priorities related to national interests and social stability [4]. The establishment of an automatic monitoring

system for dam safety can shorten the data collection cycle, improve the work efficiency of dam observation, and reduce labor intensity [5]. And it can make full use of the reservoir's storage capacity to maximize its benefits in both flood control and water supply. At the same time, it can improve the management level of the reservoir, discover the hidden dangers of the dam in time, and provide a strong guarantee for the safe operation of the reservoir.

The dam safety monitoring system is a huge systematic project and has the characteristics of a large amount of information and a wide range of knowledge [6]. The static stability analysis of the dam body is based on the limit equilibrium theory. The dynamic stability of the dam body mainly considers the influence of the liquefaction of saturated sand, the change of pore water pressure, and the action of irregular waves on the stability of the dam body caused by the tailings dam under vibration conditions [7]. The research on the above three contents have its limitations, because the stability of the dam body is affected by various factors such as the dam body design, the internal friction angle φ of the deposited material, the cohesion, the tailings particle size, and the height of the wetting line, and the changes of each factor have different effects on the stability of the dam body. In engineering practice, it is often necessary to study the influence of the changes of various factors on the stability of the dam body and take preventive measures against the relevant influencing factors. The sensitivity analysis method in the uncertainty analysis method was originally used for financial evaluation. This paper studies and analyzes various factors and parameters that affect the stability of the dam body, selects the uncertain factors, sets their variation range, and analyzes their influence on the stability safety factor K of the tailings pond dam body. The tailings pond is a storage system specially used to store tailings [8]. Accurately evaluating the stability of tailings dams is the premise to prevent tailings pond instability and dam failure, threatening the safety of people's lives and properties, and to provide a basis for tailings pond disaster prevention and control. As we all know, the dam safety monitoring instrument is the eyes and ears of people to understand the operation state of the dam. It must be able to detect the small physical quantity changes of the dam stably and reliably for a long time in the harsh environment. Therefore, in some aspects (such as measurement accuracy and long-term stability), compared with other industrial monitoring industries, its requirements are higher and more difficult. The requirements include the static level, upright and inverted hammer, laser collimation from external observation to piezometer, subsidence meter, inclinometer, soil strain gauge, and earth pressure gauge for internal observation [9]. Its automated telemetry is based on highly reliable sensors. In recent years, with the increase of large-scale dam buildings and the application of high technology, dam safety monitoring is developing in the direction of integration, automation, digitization, and intelligence.

The safety supervision of dams has also gradually developed from manual inspections to intelligent, networked, and efficient directions. This requires the use of high-precision and high-stability sensors as the eyes and antennae of the

TABLE 1: The related work.

No.	Content
1	The dam safety monitoring
2	Factors affecting the stability of tailings dam body
3	Network of dam safety monitoring

intelligent monitoring system to monitor the dam in a wide range, continuously and in real time [10]. The dam safety monitoring mainly has the functions of checking the design, improving the construction, and evaluating the safety status of the dam, and monitoring the safety of the dam is the top priority. The significance of dam safety monitoring is mainly for people to accurately grasp the behavior of dams, better utilize engineering benefits, save engineering investment, and prevent major accidents. In this paper, a variety of observation sensors are used to monitor the tailings dam body in real time as shown in Table 1. By analyzing the factors related to the stability of the dam body, the functions such as rapid early warning can be realized to reduce the occurrence of hazards. In the field of dam safety monitoring, high-precision, high-stability, and high-reliability magnetostrictive liquid level sensors have been used in many aspects due to their unique working principles. In this paper, the displacement, cracks, and seepage of the dam are accurately monitored through the measurement of sensors, so as to better evaluate the safety status of the dam and avoid the occurrence of major accidents.

2. Materials and Methods

2.1. Sensor Layout of Tailings Pond. A tailings pond is a valley-type tailings pond. The designed total storage capacity of the tailings pond is $230 \times 104 \text{ m}^3$, the total dam height is 57 m, and the design level is the fourth-class pond. The amount of pulp discharged from the concentrator is $193.3 \text{ m}^3/\text{h}$, and the mine is drawn evenly in front of the tailings dam, and the distance between the draw openings is 6 m. The characteristics of tailings dam body and slurry are shown in Table 2. The surface water system in the reservoir area is distributed in a network, and the groundwater is directly recharged by atmospheric precipitation, and the recharge area is basically the same as that of the flowing area. The geomorphological conditions in the area are not conducive to the enrichment of groundwater. The main aquifer is limestone aquifer with low water content and simple hydrogeological conditions [11]. The rock stratum has complex structures, many faults, widely distributed joints, and the rock is very broken, which belongs to the medium-complex type of engineering geological conditions. The reservoir area has no adverse geological phenomena such as landslides, debris flows, and piping, the bank slope is stable, and the soil and water conservation is good.

The sensor layout is generally set on the straight section of the catchment ditch. The upstream and downstream ditch bottoms and slopes need to be protected by masonry to prevent water leakage. Special concrete or masonry water

TABLE 2: The characteristics of tailings dam.

<i>Initial dam</i>				
Dam bottom elevation	Dam height	Dam crest elevation	Dam crest width	Downstream slope ratio
611 m	19 m	830 m	3.2 m	1:2.2
<i>Late accumulation dam</i>				
Final dam height	Number of dams	Current dam height	Subdam height	Downstream slope ratio
668 m	20	656 m	1.6 m	1:2.8
Slurry composition	Slurry volume	Pulp concentration	The average particle size	Tailings dry bulk density
60%	192 m ³ /h	8%	0.07	1.9 t/m ³

diversion channels can be built. The water depth below the weir is designed to be lower than the mouth of the weir, resulting in free overflow at the mouth of the weir. In order to obtain accurate observation results, the weir wall should be perpendicular to the diversion channel and the direction of incoming water and be upright [12]. The weir plate is made of stainless steel, the surface should be flat and smooth, and the weir mouth is made at an angle of 45° from the downstream edge. The water gauge of the weir should be set upstream of the weir mouth, and the distance from the weir mouth should be 3 to 5 times the water head above the weir. The scale of the water gauge is changed to 0.1 mm. In order to stabilize the water flow upstream of the weir, a flow stabilization device can be installed upstream of the water gauge.

2.2. Structure of Tailings Dam Body

2.2.1. Initial Dam. The initial dam of the tailings pond was built on a slate foundation and was a rockfill permeable dam. The height of the dam is 40.5 m, the width of the dam crest is 4.0 m, the length of the dam crest is 115 m, the width of the dam bottom is 157.50 m, the downstream slope ratio is 1:2.0, and the upstream slope ratio is 1:1.7. The 2.0 m wide horse road is set at an elevation of 1156.5 m downstream, and there is a 0.7-1.0 m thick of sand and gravel filter layer upstream.

2.2.2. Late Accumulation Dam. The later accumulation dam is composed of various types of tailings. The upstream method is used to build the subdams step by step. The tailings discharge pipe is set at the top of the dam to disperse the ore, and the tailings are deposited in stages to form a sedimentary beach. In the later stage, the height of each stage of the accumulation dam is 3.0 m, the width of the step is 8.0-11.0 m, and the width of the top is 3.5 m.

2.3. Dam Safety Monitoring. The dam safety monitoring system is big data, which composed of a data acquisition and monitoring module, an expert analysis and prediction module, a risk analysis and evaluation module, and an early warning and forecast module, it can realize all-weather uninterrupted real-time online monitoring [13]. The effective monitoring of the dam body, surrounding banks and related facilities by the system, can provide operation data for the operation status of the dam and complete the stability analysis of the dam body and the dam slope. And through the

analysis of monitoring data, the evaluation results of the health status of the reservoir area are given, and the early warning and forecast of abnormal conditions are issued. The data results and their analysis results can be used as data support and decision-making basis for the daily management and emergency management of the reservoir area, thereby effectively improving the management level of the reservoir area. According to the analysis of business requirements, it is determined that the architecture of the dam safety monitoring system consists of five parts: acquisition layer, communication layer, network layer, data layer, and application layer. The system architecture is shown in Figure 1.

The safety factor of tailings comes from the monitoring data of sensors, including parameters such as wetting line and cohesion. The collected data is processed and evaluated, and an early warning result is finally obtained.

2.4. Analysis of Factors Affecting the Stability of Tailings Dam Body. According to Coulomb's law, the shear strength of sand can be known.

$$\tau = \sigma * \tan \varphi. \quad (1)$$

The shear strength of cohesive soil is as follows:

$$\tau = c + \sigma * \tan \varphi. \quad (2)$$

τ is the shear strength of the soil c is the cohesion of soil. φ is the angle of internal friction of soil. φ is the normal stress on the shear slip surface [14]. The internal friction is mainly caused by the surface friction between soil particles and the occlusal force between soil particles. The cohesion is mainly formed by the water film among soil particles subjected to the electric molecular attraction between adjacent soil particles and the cementation of compounds in the soil [15].

The grinding fineness of this tailings pond is less than 200 mesh (sieve size is 0.075 mm), and the mass of particles accounts for 60% of the total mass. It is tail silt, and the one deposited in the lower part is tail silt. The internal friction angle φ of tailing silt, which is generally between 28° and 36°. The void ratio is smaller, and the φ is larger. The cohesion c of tailing silt and tailing silt is generally small, about 10 kPa or less. For the dam body composed of cohesive soil, the dam body stability safety factor K is the ratio of the

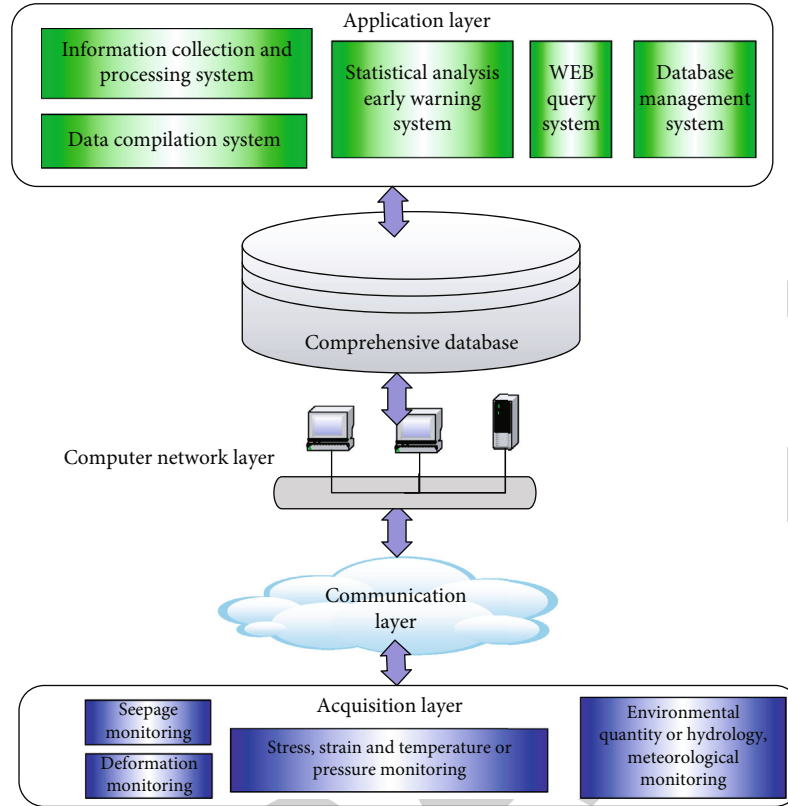


FIGURE 1: System architecture diagram.

stabilizing moment (equation (3)) to the sliding moment (equation (4)).

$$M_r = R * \left(\tan \varphi * \sum_{i=1}^N W_i * \cos a_i + c * \sum_{i=1}^N l_i \right), \quad (3)$$

$$M_s = R * \left(\sum_{i=1}^N W_i * \sin a_i + r * D \right), \quad (4)$$

$$K = \frac{M_r}{M_s}. \quad (5)$$

In the formula, α_i is the angle between the normal and the vertical line of the sliding surface of soil strip i . l_i is the arc length of the sliding surface of the strip i . c and φ are the cohesion and internal friction angle on the sliding surface. W_i is the soil bar weight, and the buoyancy of water should be considered for the part below the wetting line, and the buoyancy weight should be used. K is the resultant hydrodynamic force acting on the sliding soil body below the wetting line. r is the force arm of the dynamic hydration force D to the center O of the sliding surface. R is the sliding circle radius [16]. The stability of the dam body is affected by many factors, which are related to the particle composition, density, water content, mineral hydrophilicity, mineral colloid characteristics, water seepage state, thixotropy of cohesive soil, water level, and height of the dam body, and some factors are still related to each other and cannot be accurately determined. For the con-

venience of research and quantitative analysis, the single factor that can be measured experimentally is selected for analysis.

2.4.1. The Height H of the Accumulation Dam. The height of the accumulation dam increases year by year with the operation of the tailings pond, which is a variable. From equations (3)–(5), it can be seen that the safety factor K has nothing to do with the height H of the accumulation dam, which makes it easy to ignore the influence of the height of the accumulation dam. However, if there is a hard rock layer below the dam body and the burial is shallow, the arc surface of the slip crack can only be tangent to the hard rock layer, and the most dangerous slip surface is affected by the height factor H of the accumulation dam.

2.4.2. The Shear Strength Index of the Dam Sedimentary Layer. When the tailings are deposited, the coarse sand that is easy to settle settles and consolidates in front of the dam, and the silt settles sequentially in the clarification zone according to the particle size [17]. When the specific gravity, mass concentration, and particle size of the tailings entering the wet tailings pond do not change much, the tailings slurry volume, dry beach length, and clarification length are stable, and the tailings sand layer and the tailings soil layer are deposited in layers. Boundaries can be identified by engineering drilling. The particle characteristics of tailings, mineral hydrophilicity, mineral colloid characteristics, and thixotropy of cohesive soil are comprehensively reflected in two factors, internal friction angle φ and cohesion c , whose changes affect the dam body

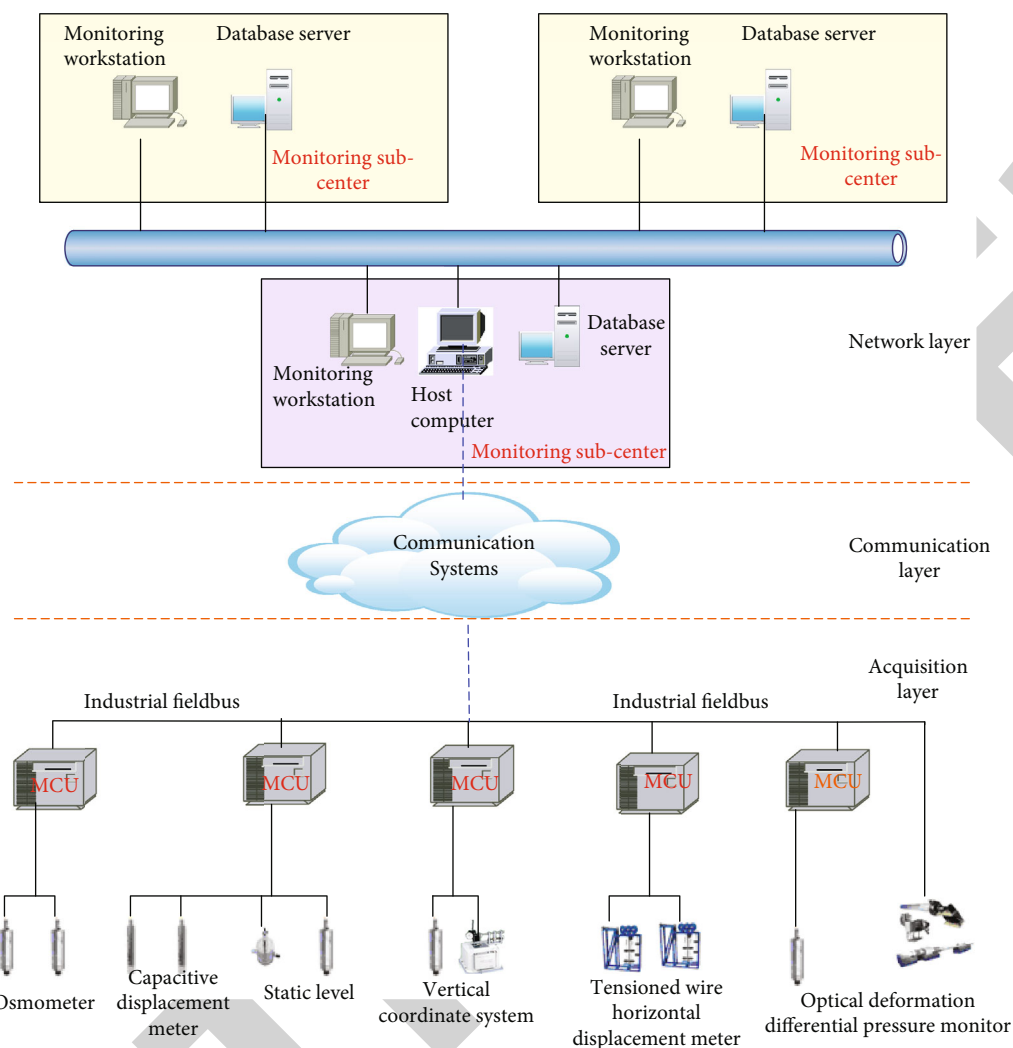


FIGURE 2: Network of dam safety monitoring system.

stability safety factor K . Because the tailing silt layer is deposited in the lower part and all below the infiltration line, it is the most prone to slipping surface. Therefore, the underwater internal friction angle and underwater cohesion of the tailing silt layer are studied in this paper.

2.4.3. The Height of the Wetting Line. The height of the wetting line is a variable, and the heights of the dry bulk and saturated sections of the soil strip have an impact on the stability of the dam body when calculated by the circular arc method. The growth of water content in the dam body will reduce the shear strength of the dam body, which is manifested as follows: first, the water flow takes away fine particles, which play a lubricating role between the coarser particles and reduce the internal friction force. The second is the thickening of the water film on the surface of the clay particles, which reduces the cohesion of the soil.

3. Result Analysis

3.1. System Composition. The dam safety monitoring system consists of an information acquisition system, a communica-

tion system, a network system, a comprehensive database system, and an application software system, including automatic acquisition or manual observation of sensors embedded in the dam body or installed (dam deformation, seepage, stress and strain, temperature, rainfall, water level, temperature and earthquake, etc.), measurement and control unit (MCU) host computer, monitoring center, and monitoring subcenter, and the system composition is shown in Figure 2. The system structure adopts a distributed architecture, and the data acquisition work is distributed to the measurement and control units close to more sensors to complete, and then the measured data is transmitted to the host computer. The measurement and control unit of each observation site of the system is a multifunctional intelligent instrument, which can control and measure various types of sensors.

The system selects sensors to mainly sense various physical quantities such as dam deformation, seepage, pressure, strain, temperature, environmental quantity, hydrology, and meteorology and inputs analog quantity, digital quantity, pulse quantity, state quantity, and other signals to the measurement and control unit. The measurement and control unit performs actual measurement, calculation, and

TABLE 3: Basic parameters of model calculation.

Item	Dry weight	Saturated weight	Cohesion	Internal friction angle	Underwater cohesion	Underwater internal friction angle
Tailings sand	17.7	19.8	7.6	34	7	32
Tailing silt	17.7	26.1	9.6	27.9	8.4	26.2
Initial dam	24	28.2	52	59	51	59
Bedrock	22	24	0	41	0	40

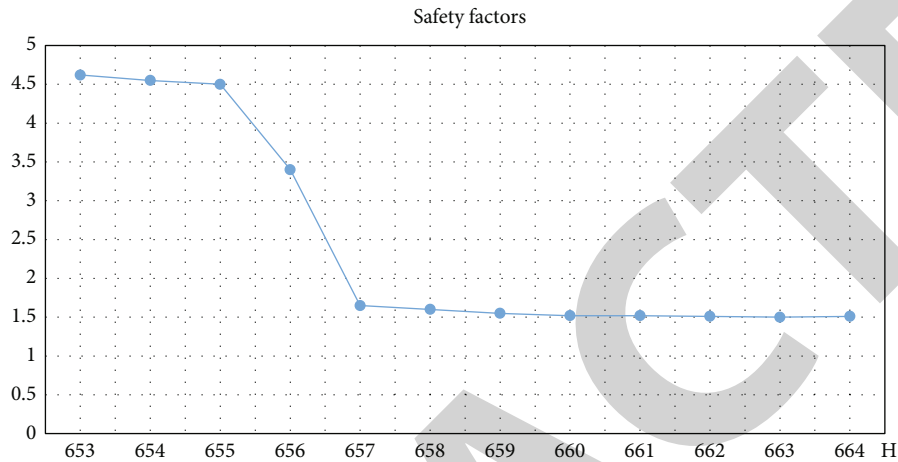


FIGURE 3: Sensitivity analysis of dam height of subdam.

storage according to the determined observation parameters, plans, and sequences and has self-checking, automatic diagnosis functions, and manual observation interfaces. According to the determined recording conditions, the observation results and error information are communicated with the designated monitoring center or other measurement and control units [18] Different measurement modules or boards can be selected to realize the signal acquisition of various types of sensors. The communication system adopts wired or wireless mode according to the site situation. And two communication modes can be used as backup channels for each other, and a communication system with dual channels as backup for each other can be established. The business application system is mainly a dam safety management software system; it can perform functions such as data reception, processing, storage, analysis, and early warning in the monitoring center and subcenter. The integrated database system can establish a unified data platform, unified data format, and standardize data standards for hydrological information and can effectively carry out data sharing and data analysis, providing a reliable foundation for business application systems. Interfaces can also be provided for data access to other related systems.

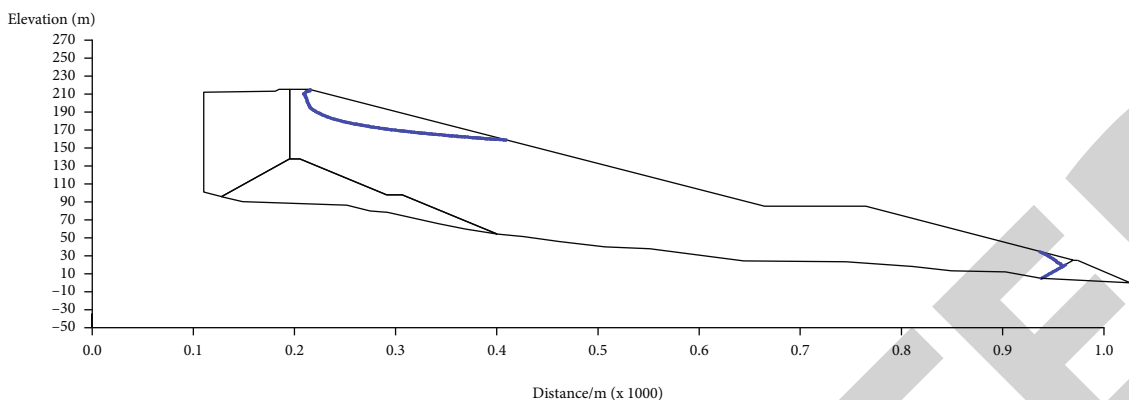
3.2. Stability Calculation Model of Tailings Dam Body. A mathematical model is established by taking the section of the central axis of the dam body, using the principle of the limit equilibrium method, and using the Swedish circular arc strip method to calculate the stability of the tailings pond dam body. This model also inputs the shape characteristic information of initial dam and accumulation dam (see

Table 2). The bedrock inclination angle is 7° , and the subdam is of grade 20, corresponding to a dam height of 658 m. The boundary line between the silt layer and the silt layer in the engineering detection is 22.4 m vertical depth below the slope. The average value of the infiltration line is 8 m, and the minimum length of the dry beach is 50 m, and a geometric model is established. The basic parameters of tailings sand, tailing silt, initial dam, and bedrock are shown in Table 3. For the level 4 tailings dam, the effective stress method is used for the hydraulic force, and the earthquake influence is not considered. In this paper, the geotechnical slope stability software is used to calculate the stability of complex soil slopes, and the width of the strip is 1 m. The arc stability calculation adopts automatic search for the most dangerous slip surface. The safety factor K of the dam body stability is 1.68, and the calculation result is as follows:

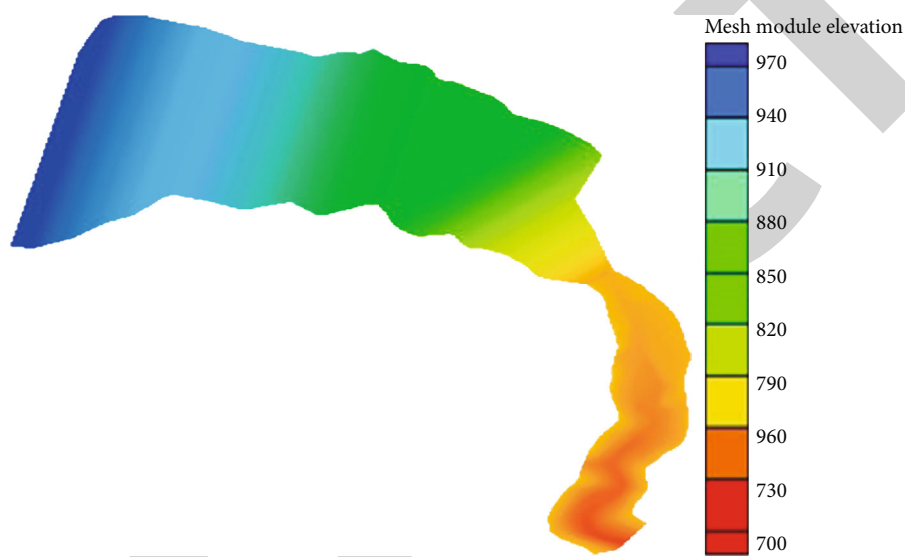
Four key influencing factors are selected, namely the dam height H , the wetting line height h , the underwater cohesion c of the tailing silt, and the underwater internal friction angle φ of the tailing silt, and the degree of their influence on the stability of the dam body is analyzed. Each factor varies by -15% , -10% , -5% , 5% , 10% , and 15% , respectively.

3.3. Sensitivity Analysis

3.3.1. Subdam Height. Figure 3 shows the influence of the height change of the subdam on the safety factor of the dam body stability. As the height of the subdam increases, the dam body stability safety factor K shows a downward trend. When the normal subdam increases by 2 m, the safety factor decreases by about 0.014.



(a) 2D graphics of tail dam



(b) Risk analysis of crack surface of primary dam



(c) Accumulation on sediment movement dam

FIGURE 4: Analysis of the risk of slippage of the tail dam crack.

For this dam body, when the level of subdams number is 18 (dam height + 655 m), the most dangerous slip crack arc surface appears on the initial dam (see Figure 2(a)), but the level of subdams number is 19 (when the dam height is +656.5 m, and the dam height is increased by 1.5 m), and the most dangerous slip crack arc surface appears on the accumulation dam, the posi-

tion jumps (see Figure 4), and the safety factor K also changes greatly.

The location of dangerous slip surface is a round toe or a round slope. It mainly depends on the depth of the hard layer, and the most prone to slip surface is always tangent to the top surface of the hard layer. For this dam body, this paper believes that the position abrupt change of the most

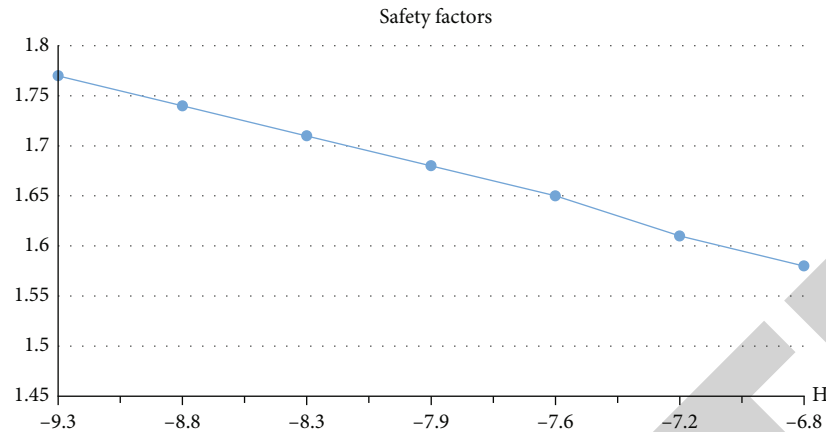


FIGURE 5: Sensitivity analysis of infiltrated line height.

dangerous slip crack arc surface with the dam height is related to the initial dam structure, the dip angle of the bedrock, and the characteristics of tailings deposition. In the initial stage of the dam, the dam was built with block stone concrete, filled with gravel, and the foundation was firm, which was equivalent to the retaining wall structure [19]. Part of the accumulation dam near the initial dam is subject to greater water pressure, and active earth pressure is applied to the initial dam [16], reaching the limit equilibrium state. When the subdam exceeds the critical height, the overall stability of the upper accumulation dam depends on the cohesion c of the tailings sediment layer and the internal friction angle φ .

3.3.2. Wetting Line Height. The dam body stability safety factor K changes inversely with the height of the wetting line, as shown in Figure 5. It can be seen from Figure 3 that the height of the infiltration line is higher, and the safety factor K of the dam body stability is smaller.

3.3.3. Cohesion. Figure 6 shows the influence of the change of the underwater cohesion of the tailing silt layer in the accumulation dam on the safety factor K of the stability of the dam body. It can be seen from Figure 6 that the influence of cohesion is small.

3.3.4. Internal Friction Angle. The variation of the underwater internal friction angle of the tailings in the accumulation dam has a great influence on the safety factor K of the dam body stability (Figure 5). It can be seen from Figure 7 that with the growth of the internal friction angle, the dam body stability safety factor K increases, and the dam body stability safety factor K is more sensitive to the change of the internal friction angle of the tailing silt layer.

Regardless of the sudden change of the height of the subdam on the dam body stability safety factor K , the sensitivity of each factor to the dam body stability safety factor K is ranked as follows: internal friction angle of tailing silt soil layer > wetting line height > dam height > tailing silt soil cohesion.

3.3.5. Case Analysis. The flow process of the breach is shown in Figure 8; the maximum flow of the breach is $469 \text{ m}^3/\text{s}$, and the flooding duration of the breach is 279 h. In order to simulate the propagation process of the levee-breaking flood in the protected area, the simulation time is 843 h, that is, during the period of $t = 252 \text{ h} \sim 877 \text{ h}$, the breaking flow is 0. The calculation is based on the two-dimensional shallow water equation, and the method proposed in this paper is used to establish a hydrodynamic model of flood evolution adapted to complex terrain in Figure 8. Take the embankment rupture on the right bank of a river as an example to calculate. The modeling area is 9568 km^2 , the grid side length is controlled by 250 m-400 m, the number of grids is 182860, and the average grid area is 0.049 km^2 .

Data-based evaluation of tailings dam safety is feasible and can reduce unnecessary investment in engineering construction. The combined analysis method of experiment and two-dimensional numerical model provides a quantitative analysis idea for tailings pond safety assessment, and provides a new research direction for future tailings pond management and safety assessment.

4. Discussion

According to the analysis of the above stability influencing factors, the stability improvement measures of the tailings dam body are expounded. First, the coarse-grained tailings should be selected when building the dam. The safety and stability of the mine is higher. The larger the size of the same tailings material, the larger the internal friction force and the agglomeration angle. Therefore, when building tailings dams, coarse tailings should be selected. In order to concentrate the coarse tailings into the dam body, it is necessary to discharge before the dam, so that the coarse tailings quickly settle in the dam area, and the fine tailings flow into the reservoir of the dam body [20]. A cyclone can also be used to sort the tailings particles, the coarse tailings are intercepted, and the fine tailings are directly discharged into the storage area.

The first point is to pay attention to the slope angle of the side slope of the mine dam when stacking the tailings dam. Therefore, it is necessary to check the inclination angle in

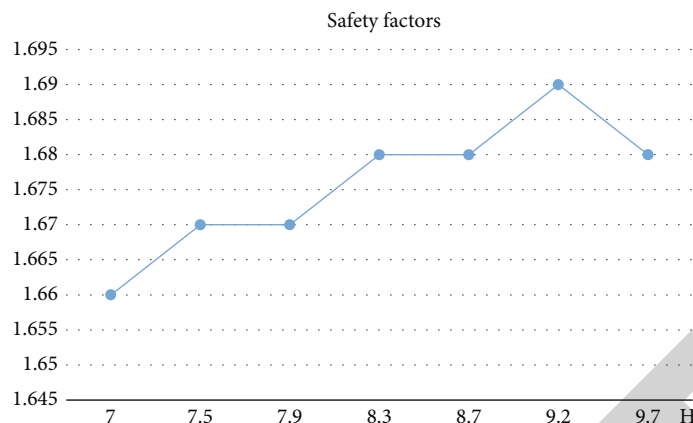


FIGURE 6: Sensitivity analysis of underwater cohesion of tailing silt.

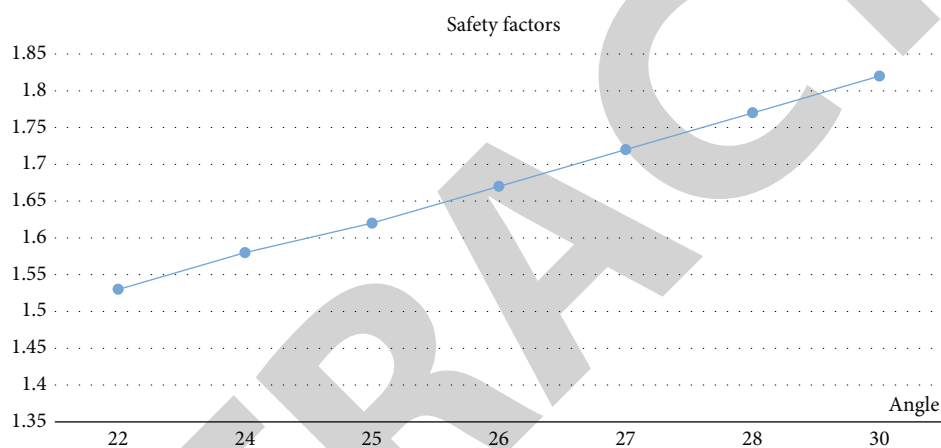


FIGURE 7: Sensitivity analysis of underwater internal friction angle of tailing silt.

advance and compare it according to the design scheme of the inclination angle. After the comparison, if the slope angle at this time meets the standard requirements, it can be stacked. If it does not meet the requirements, the dam slope angle needs to change in time [21]. If it is greater than the standard value, you can choose to slow down the stacking and reduce the slope angle. If it is lower than the standard value, slope pressing treatment is required to ensure that the inclination of the entire mine dam is within the design range.

The second point is to control the position of the entire mine dam on the river bank, which needs to calculate according to the wettability of the mine dam. First, the wettability determines the height of the entire mine dam, which is crucial to the stability [22]. At this time, the infiltration line exceeds the standard value, and corresponding measures should be taken immediately, that is, the water level around the dam can be reduced, the scope of the infiltration line can be reduced, the surrounding pressure can be reduced, and the length of the dry beach can be increased to ensure the stable position of the infiltration line. In addition, if the phenomenon of exceeding the water level occurs, it is necessary to discharge all the seepage water of the mine dam to avoid the collapse of the mine dam.

The third point is to control the position of the wetting line. Because the height of the infiltration line has a great influence on the stability of the dam slope, the highest position of the infiltration line corresponding to different dam heights should be given in the design [23]. The main measures to control the position of the infiltration line of the dam body are as follows: first, the water level reduced in the reservoir, a sufficient dry beach length maintained in front of the dam, and reduce the seepage pressure in the dam body, so as to reduce the position of the infiltration line of the dam body. The second is to take engineering measures for dam body seepage drainage, such as adding dam body seepage drainage facilities to remove seepage water inside the dam in time and reduce the infiltration line in the dam body.

In addition to the above measures, it is necessary to strengthen daily inspections and timely check whether the equipment parameters of the entire tailings pond meet the operating requirements. The first is to check the drainage performance of the tailings pond and dam. Water seepage avoids in tailings ponds, which leads to the collapse of the dam, second, plant green plants on the dam to avoid soil erosion on the surface of the dam. Third, the key indicators of the dam are complete and to avoid data errors. Fourth,

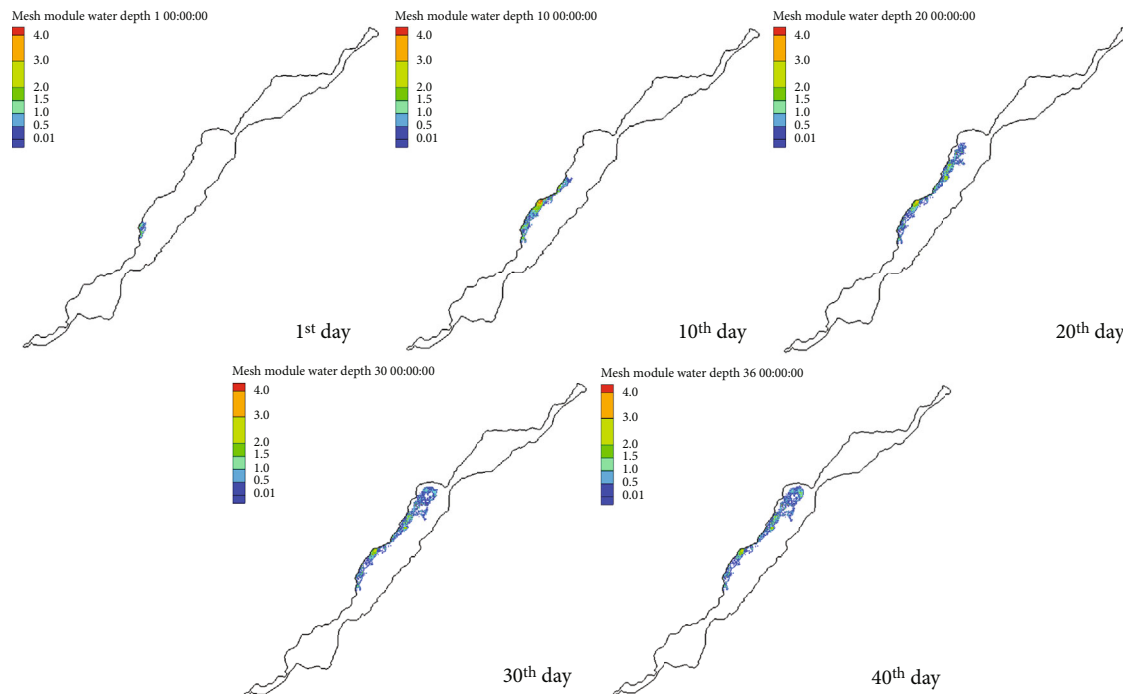


FIGURE 8: A real-time computing system for flood evolution of tailings.

during the maintenance of the dam, the accumulated tailings should be pretreated to avoid the reaction between the accumulated tailings and the air to produce toxic chemicals, which would endanger the ecological environment around the tailings pond.

In addition, the dam body should have monitored to check regularly and comprehensively whether there are abnormal conditions such as cracks, landslides, and leakage of infiltration lines. When abnormal conditions are found, they should be dealt with in time. When controlling the rising speed of the accumulation dam, prevent the rising speed from being too fast, so that the lower dam body cannot be consolidated in time and the strength is not enough, thus causing the deformation and cracks of the dam body.

5. Conclusion

The dam safety monitoring and management system software is an important part of the reservoir dam safety monitoring system. It has functions such as data acquisition, data processing, data management, data compilation, data analysis, and network management. By using the dam safety monitoring and management system software, reservoir managers and management leaders can keep abreast of the current state of the dam. The tailings dam can basically meet the requirements of the specification when operating under normal conditions. The safety factor calculated by each method is greater than 1.25. However, when the infiltration line exceeds 6.0 m, the dam body cannot meet the specification requirements under the dynamic state. The software of the dam safety monitoring system adopts the B/S structure. Except for the data collection service program that needs to be started on the server, as long as the computer user is

connected to the server through the network, it can be accessed through a browser to query monitoring data, graphics, security monitoring information, and evaluation conclusions. Therefore, in order to increase the safety reserve and improve the stability, it is necessary to strengthen the seepage drainage and reduce the height of the dam body infiltration line. (1) Subdam height, wetting line height, internal friction angle of tailing silt layer, and cohesion all affect the safety factor K of dam body stability. The friction angle of the tailing silt layer is deposited in the lower part, and the height reduction of the wetting line is the most effective way to improve the stability. (2) The height of the wetting line and the dam body stability safety factor K change in the opposite direction. The influence of the safety factor K of the body stability is more significant. (3) For this dam body, the most dangerous slip crack arc surface jumps at the height of the 19-level subdam, and the dam body stability safety factor K changes greatly. This paper considers that it is related to the initial dam structure, bedrock inclination, and tailings sedimentary characteristics. Further research is needed in the follow-up, and great attention should be paid to it in engineering practice.

Data Availability

The data used to support the findings of this study are available from the corresponding author upon request.

Conflicts of Interest

The author does not have any possible conflicts of interest.

Retraction

Retracted: FMT Selector: Fourier-Mellin Transformer with High Speed Rotating in Ship Target Detection and Tracking Based on Internet of Things and Wireless Sensor Network

Journal of Sensors

Received 23 January 2024; Accepted 23 January 2024; Published 24 January 2024

Copyright © 2024 Journal of Sensors. This is an open access article distributed under the Creative Commons Attribution License, which permits unrestricted use, distribution, and reproduction in any medium, provided the original work is properly cited.

This article has been retracted by Hindawi following an investigation undertaken by the publisher [1]. This investigation has uncovered evidence of one or more of the following indicators of systematic manipulation of the publication process:

- (1) Discrepancies in scope
- (2) Discrepancies in the description of the research reported
- (3) Discrepancies between the availability of data and the research described
- (4) Inappropriate citations
- (5) Incoherent, meaningless and/or irrelevant content included in the article
- (6) Manipulated or compromised peer review

The presence of these indicators undermines our confidence in the integrity of the article's content and we cannot, therefore, vouch for its reliability. Please note that this notice is intended solely to alert readers that the content of this article is unreliable. We have not investigated whether authors were aware of or involved in the systematic manipulation of the publication process.

Wiley and Hindawi regrets that the usual quality checks did not identify these issues before publication and have since put additional measures in place to safeguard research integrity.

We wish to credit our own Research Integrity and Research Publishing teams and anonymous and named external researchers and research integrity experts for contributing to this investigation.

The corresponding author, as the representative of all authors, has been given the opportunity to register their agreement or disagreement to this retraction. We have kept a record of any response received.

References

- [1] J. Xu, C. Qiu, and L. Wang, "FMT Selector: Fourier-Mellin Transformer with High Speed Rotating in Ship Target Detection and Tracking Based on Internet of Things and Wireless Sensor Network," *Journal of Sensors*, vol. 2023, Article ID 2637529, 8 pages, 2023.

Research Article

FMT Selector: Fourier-Mellin Transformer with High Speed Rotating in Ship Target Detection and Tracking Based on Internet of Things and Wireless Sensor Network

Jiayi Xu , Changzhen Qiu , and Luping Wang

Electronics and Communication Engineering, Sun Yat-sen University, Shenzhen, China

Correspondence should be addressed to Changzhen Qiu; qiuchzh@mail.sysu.edu.cn

Received 16 September 2022; Accepted 29 September 2022; Published 10 April 2023

Academic Editor: Sweta Bhattacharya

Copyright © 2023 Jiayi Xu et al. This is an open access article distributed under the Creative Commons Attribution License, which permits unrestricted use, distribution, and reproduction in any medium, provided the original work is properly cited.

The terminal guidance tracking always has high speed rotating and scale changing. It makes a large margin of error in current tracking algorithms, which can transmit wrong position in the wireless sensor networks of the Internet of Things. In this paper, we propose a selector based on Fourier-Mellin transformer, which can accurately track the target with high speed rotating. Firstly we use existing detector to get all proposal target per frame. Then, we use Fourier-Mellin matching to select the best target in the new frame. Our dataset is the ship video which is created by HRSC2016 in rotating. Experimental results show that the accuracy of this method is up to 89.8%. Compared with other traditional tracking algorithms, it has a leap forward. The FMT selector can be applied to the back end of the detector, and it can achieve a feasible effect in the field of terminal guidance tracking.

1. Introduction

Recently, object tracking is always applied in terminal guidance. The inner wall structure of the terminal guidance is not a smooth inner circle but a spiral shape of rifling. This structure ensures that the terminal guidance can spin at high speed. This structure is used because it reduces air drag, increases range, improves hit accuracy, and avoids terminal guidance drift. Due to the terminal-guided projectile rotates at high speed during flight, the image from the camera on the warhead should rotate at the same time. This makes target tracking difficult. In rotating target detection technology, one-stage detector [1, 2] and two-stage detector [3, 4] both have achieved good accuracy and speed. However, these mainstream target detectors can only detect all objects with corresponding features. They cannot carry out long-term detection for a specified target. In this case, tracking technology is needed.

The current tracking technology [5–8] has achieved good results in daily work. However, data such as location and angle detected by the IOT are characterized by hetero-

geneity and mass [9, 10]. At the same time, WSN will also be affected by their changes [11, 12]. The terminal guidance tracking is always accompanied by high speed rotation and scale changing. Sometimes it can rotate even more 45° per frame. Such the dramatic change must be destructive in daily tracker.

In view of this problem, many researchers usually use an external angle sensor to get the angle of rotation in practical engineering applications. They can make the image rotated back through matrix transformation by the computer, so as to achieve the purpose of antiangle rotation. But our method can accomplish tracking in the high speed rotating without the angle sensor and achieve the goal of accurate tracking each frame. We select the proposal target from front detector by Fourier-Mellin Transformer (FMT) selector we proposed. Specifically, our work makes the following contributions:

- (1) We propose a selector for tracking the object in high speed rotating based on FMT. It can overcome the rotation and scaling of objects. As we know, our first

method about FMT module was applied to rotating object tracking

- (2) We select a dataset of multiple target in HRSC2016 to test our FMT selector. We get their single image to rotate three different angle (18°, 30°, and 45°) per frame. Finally, we use a series of formulas to calculate the position and rotation of every frame's target. It used to be our ground truth to test the precision of our results

2. Related Work

2.1. Rotation Object Detectors. A traditional target detector uses horizontal bounding boxes to outline the target's contour. But ship target with large aspect ratio may have a lot of background redundancy in the boxes, which is not conducive to convergence during training. Therefore, a rotating target detector with angle information is proposed to accurately separate the background around the rotating target. On the basis of the rotation target detection, the two-stage method, one-stage method, and anchor-free method [13, 14] appear, respectively. They are very similar to the horizontal target detector. The two-stage method firstly generates a series of region proposal by RPN like R-CNN [15] and then filters, classifies, and fine-tune them by rotating detection head. This method can achieve good accuracy, but it is slightly slower to the first-stage detector. On the contrary, the first stage detector will sacrifice a little accuracy of detection to directly extract feature prediction object classification and position in a backbone network. They have more real-time detection performance. This kind of detector is still improved based on the series of YOLO [16], SSD [17], and Retina-Net [18]. The one-stage rotation detectors such as that in [1, 2] have achieved good performance. The last type is the anchor-free method that does not need specific anchor boxes. It can directly perform rotating boxes regression through key points such as corner points and center points. For example, the detector of [14] is also very fast and efficient.

2.2. Fourier-Mellin Transform Matching. Digital image is actually composed of 2D discrete signals, so it also has the ability to convert 2D discrete signals from spatial domain to frequency domain and also has some related characteristics in frequency domain. [19] have detailed statements about FMT. Firstly, the template image and the image with matching are both converted into spatial domain and frequency domain. Then, the template image is rotated and scaled which correctly relies on phase correlation technology. Finally, the adjusted template image is matched with

phase to obtain the translation amount. The terminal guidance image scene accompanied more and more jitter, rotation, and scale of the target. Matching in the spatial domain like MAD and NCC cannot cope with such scenes. In the frequency domain, the image rotation has no effect on the amplitude of the frequency domain, but the phase angle will change correspondingly. Therefore, we need to carry out polar coordinate transformation and logarithmic transformation for the amplitude spectrum of the frequency domain to convert the rotation factor and scale transformation factor into the translation relation in the polar coordinate system. Therefore, we can calculate the angle difference and scale scaling ratio between the template image and the image with matching to restore it. This method can be applied to many image processing. Earlier, O'Ruanaidh and Pun [20] use it to resistant to rotation and scaling in image watermarking; Yi et al. [21], Sellami and Ghorbel [22], and Ishiyama et al. [23] used FMT for 3D reconstruction, panorama construction, and fingerprint matching, respectively. As far as we know, no one has applied this module in rotation object detection, which is so sensitive to angle and scale information. Therefore, we add this module into the rotating target detection network based on deep learning. It can transform the information in the spatial domain into the frequency domain for analysis. It not only gets a good complete solution in theory but also has a good performance in accuracy.

2.3. Tracking by Detection. In fact, it is strongly related between tracking and detection. They are always combined in engineering and academic research. Earlier, the most representative algorithm is TLD [5], which uses LK trackers and introduces the detector to avoid the effect of target occlusion; the CSK algorithm [24] combines detection with correlation filtering tracking. Based on deep learning, such as Siamese series, match the target image with the deep network features to obtain the target position; recently, Huang et al. [25] try to add the tracking module into the general detector and get good results in the detection accuracy. In our work, we actually use frequency domain features to complete the matching work of the bounding box. We are going to finish a special task of selecting a particular target from among multiple candidates.

3. Method

Figure 1 shows the general framework of our method. In a FMT selector, we get an angle matcher and position matcher to get the final target. We will describe in detail the feature extraction and matching of FMT module.

$$F_2(u, v) = \frac{\exp(-j(ux_0 + vy_0))}{\sigma^2} F_1[\sigma^{-1}(u \cos \theta_0 + v \sin \theta_0), \sigma^{-1}(-u \cos \theta_0 + v \sin \theta_0)], \quad (1)$$

$$|F_2(u, v)| = |F_1[\sigma^{-1}(u \cos \theta_0 + v \sin \theta_0), \sigma^{-1}(-u \cos \theta_0 + v \sin \theta_0)]|. \quad (2)$$

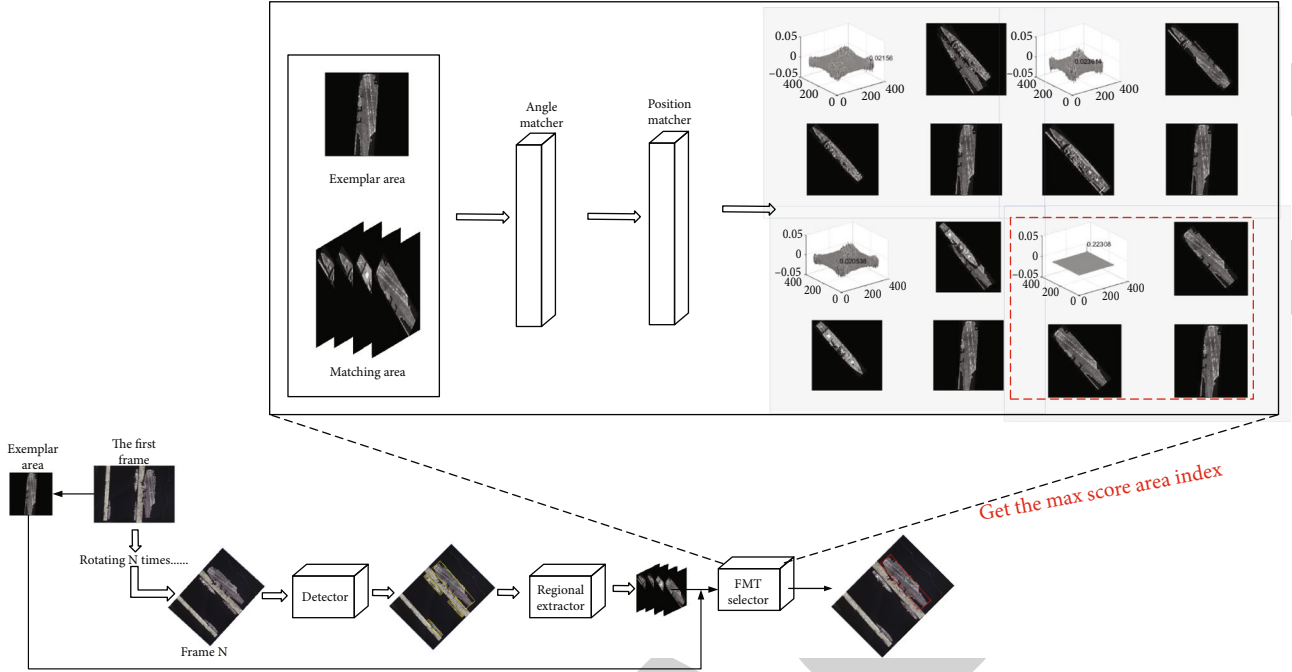


FIGURE 1: Overall framework of our method. We select the exemplar area in the first frame firstly. In the following N-frame rotation frame, the detector is sent to detect all targets and regional extractor extract them. The FMT selector is used to select the rotation frame with the highest score as the final target.

3.1. Angle Matching. In order to detect the scale ratio and angle difference between the target and exemplar, we need to transform the image after the Fourier transform to the polar coordinate domain in the FMT selector, because the polar coordinate transformation can solve the rotation and scaling problem, not including the translation relationship. Of course, we need to use Fourier properties to eliminate the translation factor as follows:

In Equation (1), F_1 is the Fourier transformation of I_{match} , and F_2 is the Fourier transformation of I_n , θ_0 and σ are their angle difference and scale ratio. Due to Fourier properties, we can eliminate the part of index and take the absolute value in Equation (1). We can get M_1 and M_2 as follows, which have no effect on position shift.

$$\begin{aligned} M_1(\rho \cos \theta, \rho \sin \theta) &= \frac{1}{K^2}, \\ M_2\left[\frac{\rho}{k} \cos(\theta - \Delta\theta), \frac{\rho}{k} \sin(\theta - \Delta\theta)\right]. \end{aligned} \quad (3)$$

Let $u = \rho \cos \theta$ and $v = \rho \sin \theta$ in Equation (3), and we can get the relation of two polar coordinate domain of amplitude-frequency Figure 2 as follows:

$$\begin{aligned} M_1(\theta, \log \rho) &= \frac{1}{K^2}, \\ M_2[\theta - \Delta\theta, \log \rho - \log k]. \end{aligned} \quad (4)$$

On the above equation, there is a translation relationship between the exemplar image and the matching area in the

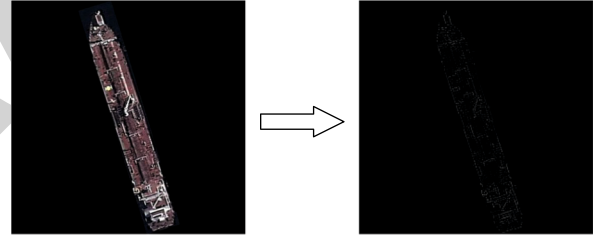


FIGURE 2: This is a high-pass filtering transform. To the right of the arrow is the original image, and to the left is the high-pass filtered image which can be found that it only save the key edge information of the target.

frequency domain. The translation factors are the scale ratio (represented by the ordinate difference) and the rotation (represented by the abscissas difference).

3.2. Position Matching. [26] previously worked with phase correlation for image matching. Phase correlation matching mainly calculates the translation difference between the signal $f_1(x, y)$ in the exemplar area and the signal $f_2(x, y)$ in the area to be detected. Assume $f_2(x, y)$ is obtained by translating $f_1(x, y)$ by (dx, dy) , i.e.,

$$f_2(x, y) = f_1(x - dx, y - dy). \quad (5)$$

Take the Fourier transform of formula and get this:

$$F_2(u, v) = F_1(u, v)e^{-2\pi j(udx+vdy)}. \quad (6)$$

Thus, the translation of f_1 and f_2 is the difference between the phase angle domains, which can be obtained

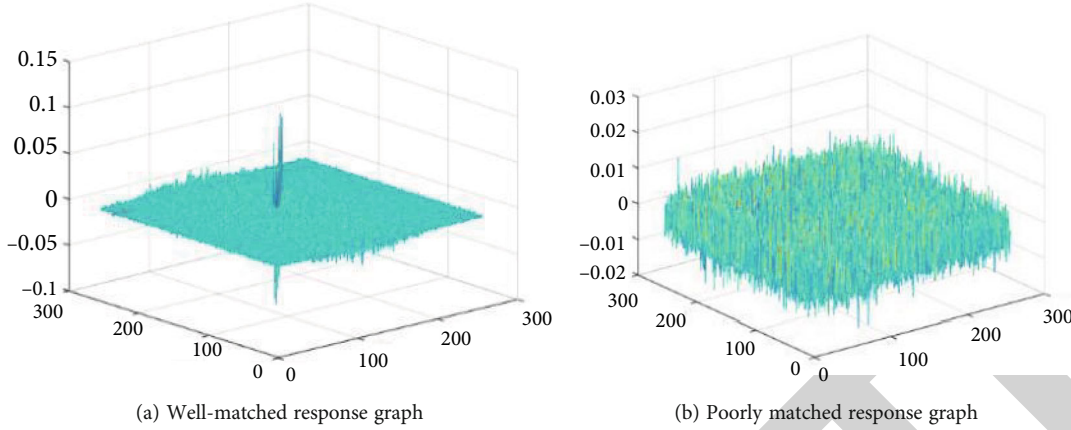


FIGURE 3: The response graph of matching. (a) The response of well-matched has a very clear peak, and the surrounding is relatively flat. (b) The poorly matched response graph has low peak value and strong side-peak interference around it.

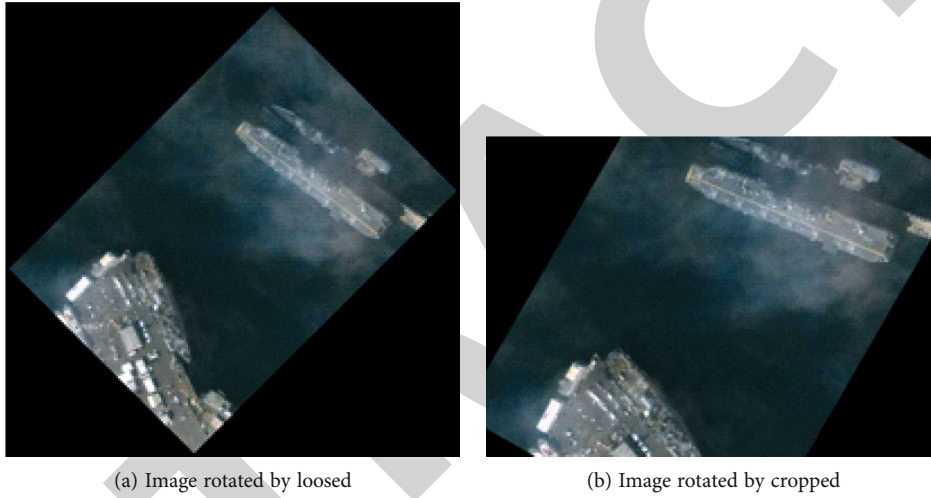


FIGURE 4: Two different rotations: (a) Large enough to contain the entire rotated image which is generally larger than original image; (b) make the same size as the original image, cropping the rotated image to fit.

by making the difference between the phase angle domains and then indexation:

$$e^{j(\Delta F_2(u,v) - \Delta F_1(u,v))} = e^{j(-2\pi(udx+vdv))}. \quad (7)$$

In the right equation of Equation (7), an impulse function can be obtained by the inverse Fourier transform, as shown in Figure 3. The translation of f_1 and f_2 can be found by looking for the coordinates of the peak values.

Come back to Equation (4); its angle factor and scale factor also have translation relationship. By subtracting the phase of $M_1(\theta, \log \rho)$ and $M_2(\theta, \log \rho)$, the optimal angle factor and scale factor can be found in the position of the peak value. There are two possible rotation angles that are 180° apart, so both should be matched by the phase correlation position with exemplar area. By comparing the peak, we can get the most suitable image matching.

By the same principle, if the matching image and the exemplar image are not the same object at all, the final result will be poor, and the peak of angle difference

between the two will be very low. We need to match all the areas of detection with the exemplar image in a frame of image, so their highest peak probability is the target box that we are interested in.

3.3. Implementation Details. Fourier-Mellin transform matching is poor for high-resolution images. The frequency of an image is an indicator of gray changes in the image, and it is the gradient of gray in the plane space. However, there is no one-to-one correspondence of the points between the spectrum map and the image. Therefore, high-resolution images are time-wasting in Fourier-Mellin transform matching, and many irrelevant details may affect the judgement. Therefore, for the high-resolution remote sensing target, we extracted all the ROI for the minimum peripheral square, and adjusted the image resolution to $256 * 256$. In addition, we may have two targets that are very close to each other, so that when one target is selected, another target will be added. It will affect the matching rate. Therefore, we mask the background around the target to exclude the possibility that it will be matched to the background target.

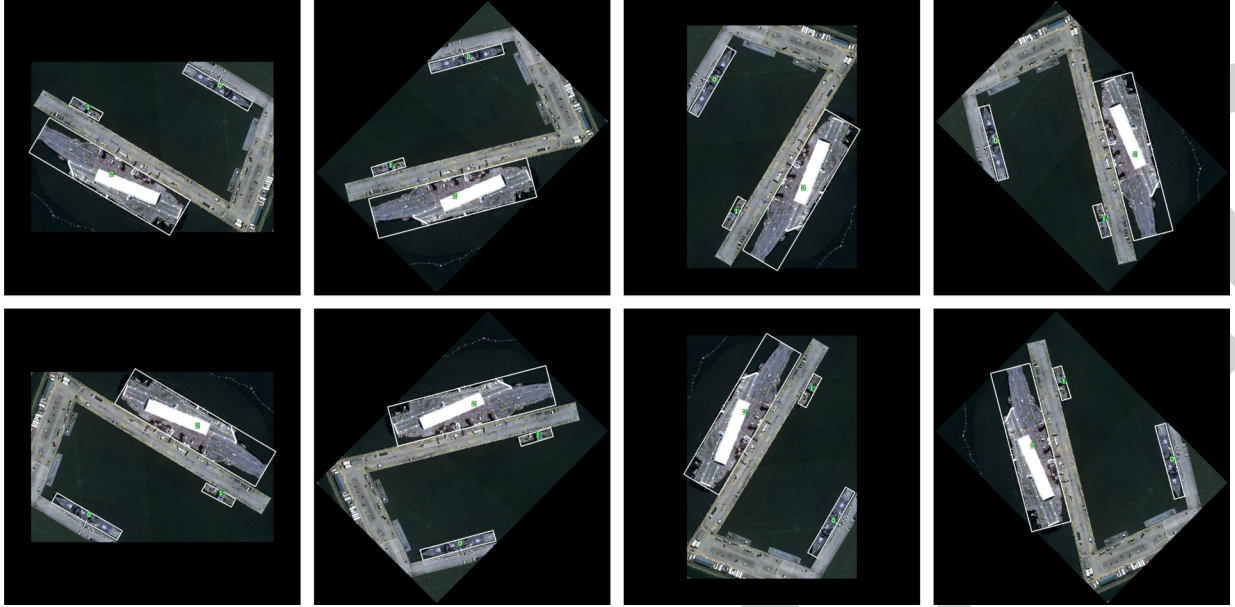


FIGURE 5: We selected the rotation labeling effect of 45° in each frame as an example. It can be seen that according to the original labeling of the first frame, the rotation frame positions and numbers of the following seven frames were accurate.

4. Experiments

4.1. Datasets. The proposed method is mainly for ship detection and tracking, so HRSC2016 dataset is the most suitable for testing the effect of our method. It is a dataset widely used for ship detection. Sizes range from 300×300 to 1500×900 , with a total of 2976 ship targets. We used 436 training set images and 181 verification set images to train the detection module we needed, and then, 453 test sets were used to detect the detection module and subsequent tracking.

The current target tracking datasets, such as VOT, OTB, and POT, have updated the representation of the rotating frame. But there are very few rotating objects in them. And all of them are slightly rotating. Hence, testing them cannot reflect the superiority of our rotating target frame in a specific high speed. Since there is no dataset to simulate the terminal guidance with high-speed rotating, we took the test set of HRSC2016 as the first frame of tracking video sequence and then rotated some angle for each frame (we made video sequences of rotation of 18° , 30° , and 45° for each frame, respectively) until returning to the angle position of the first frame. In order to make sure the edge of the image target's integrity, we will output all contents of the rotating image (as shown in Figure 4(a)) and not the fixed view image of the actual camera (as shown in Figure 4(b)).

Later, our work in the data set is mainly to mark the annotation of rotated frames. Because it is very time-consuming to mark frame by frame, we utilize the characteristics of rotation and the connection between rectangular coordinate system and polar coordinate system. The target position (x, y) , width (w) , height (h) , and angle (a) given by HRSC2016 dataset itself can be used to convert the related Information of each frame, i.e.,

TABLE 1: Performance scores (precision "Pr" of OP, success rate "Succ," and speed (fps)) for object tracking with the state-of-the-art on our own ship dataset modified by HRSC2016 with rotation 45° per frame.

Method	Pr	Succ	Speed
KCF [6]	0.12	0.17	68
TLD [5]	0	0	31
SiamRPN [7]	0.37	0.44	20
SiamMask [8]	0.12	0.24	18
Ours (Oriented_rcnn [27]+FMT)	0.83	0.86	5.7

$$\begin{cases} x_i = \sqrt{\left(x_0 - \frac{W_0}{2}\right)^2 + \left(y_0 - \frac{H_0}{2}\right)^2} \cos\left(\arctan \frac{y_0}{x_0} - \theta_i\right) + \frac{W_i}{2}, \\ y_i = \sqrt{\left(x_0 - \frac{W_0}{2}\right)^2 + \left(y_0 - \frac{H_0}{2}\right)^2} \sin\left(\arctan \frac{y_0}{x_0} - \theta_i\right) + \frac{H_i}{2}, \\ w_i = w_0, \\ h_i = h_0, \\ a_i = a_0 + \theta_i, \end{cases} \quad (8)$$

where (x_0, y_0) are the position of the initial frame and w_0 , h_0 , and a_0 are their width, height, and angle, respectively. W_0 and H_0 are the width and height of the picture. The corresponding parameters after the rotation of the i th frame are, respectively x_i , y_i , w_i , h_i , a_i , W_i , and H_i . θ_i represents the difference in rotation between the initial frame and the current frame.

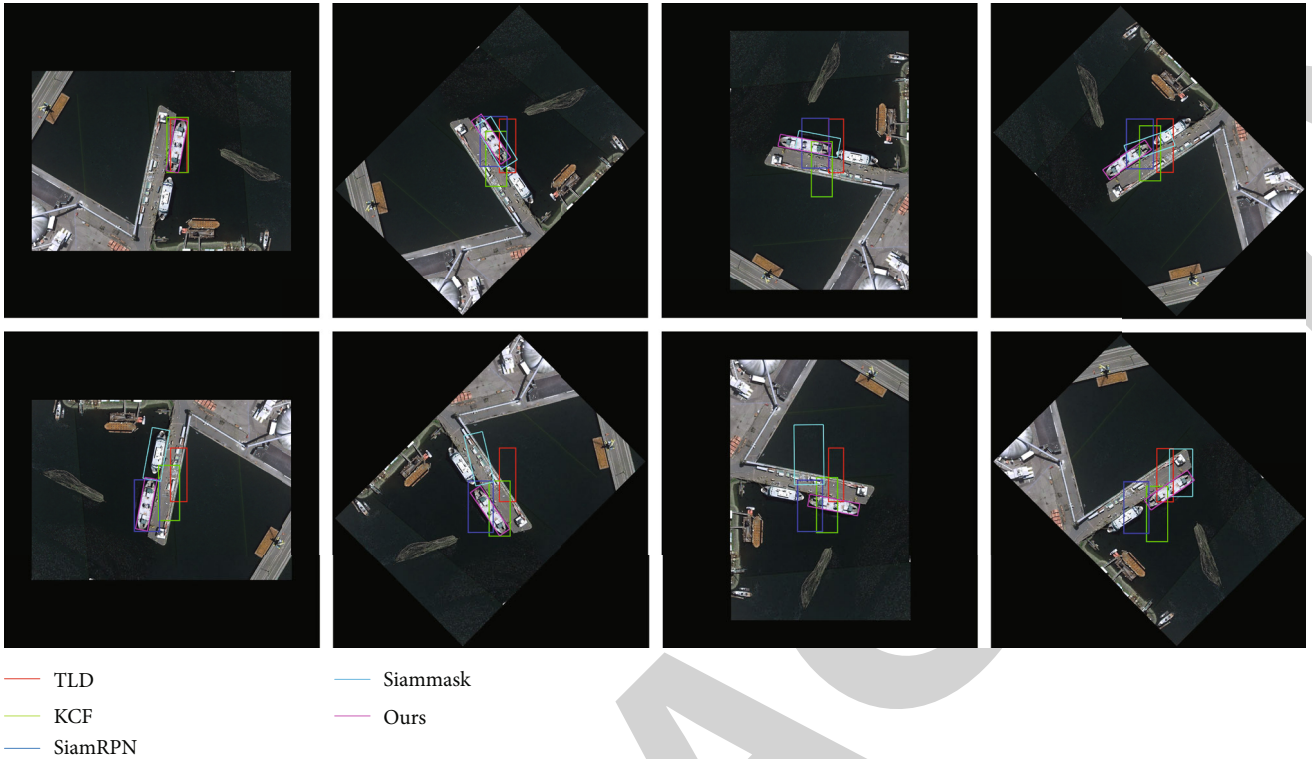


FIGURE 6: Example frames from one sequences of 45° rotation per frame. Our tracker got the best results.

We mark each object with a fixed number in the initial frame. As shown in Figure 5, the algorithm can accurately calculate the position of the rotated target, and the generated new target box can 100% include all the marked targets with no error.

4.2. Parameter Settings. We use a single RTX 2080Ti GPU for training under the setting of Batch size 2, which is the same as testing and inference. In the detecting stage, we use the MMRotate platform to generate the results of the initial frame. Our backbone is ResNet50 which will be pre-trained on ImageNet. We use the SGD algorithm for convergence fitting with the momentum of 0.9, and weight decay is 0.0001. In the HRSC2016 dataset, we kept the aspect ratio of the original image. Their longer edge was controlled within 1400 in the image input stage, while shorter edge was scaled in equal proportions. We perform 36 epochs during training. The initial learning rate was set to 0.005. In order not to miss any local minimum during near convergence and avoid gradient explosion, the learning rate was divided by 10 at the 24th and 33th epoch.

In the tracking stage, we used MATLAB 2016B to test and evaluate the subsequent experiments. The target that is extracted in the detecting stage is matched with the exemplar image. The highest scoring target is obtained as the tracking target of this frame. In order to improve the matching accuracy and running speed, we resize the target image to 256×256 .

TABLE 2: The results of different detector before the FMT selector. We tested together with the scenes of rotation changes of 18° , 30° , and 45° per frame (threshold of 0.5).

Method	Pr	Succ	Speed
R3det [28]+FMT	0.74	0.81	4.9
Redet [29]+FMT	0.83	0.90	1.5
Roi_trans [30]+FMT	0.82	0.84	5.5
Oriented_rcnn [27]+FMT	0.83	0.86	5.7

4.3. Evaluation. Now, we compare our algorithm with KCF [6], TLD [5], SiamRPN [7], and SiamMask [8], and the results obtained are shown in Table 1. According to the results, it is obvious that in the scene of such violent rotation, traditional and deep learning tracking methods have both achieved the terrible performance. The specific demonstration is shown in Figure 6. It can be seen that the traditional KCF and TLD algorithms based on machine learning have no solution to the rotation feature with such drastic changes in angle and position. The Siamese network, based on deep learning, can barely track a few frames but also lose targets later. However, our method detects the target in a whole image and selects the result with the best score as the current frame target. The FMT selector avoids the information error in adjacent frames due to the violent position change. Even if a frame fails to select a target, the tracking frame will not drift.

Pr is the precision from OTB2013 [28]. It uses Euclidean distance between the center point of the prediction box (x_1, y_1) and the center point of the ground truth box (x_2, y_2) as follows. We use the threshold of 20 pixels. If their distance is smaller than threshold, this frame will track successfully. Pr means the success rate of this rule.

$$\rho = \sqrt{(x_2 - x_1)^2 + (y_2 - y_1)^2}. \quad (9)$$

Succ is the success rate from OTB2013. It calculates the proportion of intersection and union (IOU) between bounding box and ground truth box. We use the threshold of 0.5. If their IOU is bigger than threshold, this frame will track successfully. Pr means the success rate of this rule.

In the current rotating object detection framework, the full image of the target detection will inevitably miss the target or detect wrong. And their accuracy of the detection frame is not enough. Therefore, we used our FMT selector in different performances of the rotating object detection framework. We evaluated the tracking accuracy, success rate, and speed of different modules combined with FMT, as shown Table 2. It can be seen that the performance of these detection frameworks is similar, mainly effected on the detection of itself. Our selector undertakes the task of correctly selecting the detection frame with the highest score.

In the representation of angle, due to every 360° is a period, our experiment wants to rotate it to its original position after many frames. 18° , 30° , and 45° will do just that. In addition, these three angles can reach different positions in each period of rotation. For example, about 30° rotation, the angle is 60° , 90° , 120° , 150° , 180° , 210° , 240° , 270° , 300° , 330° , and 360° ; about 45° rotation, the angle is 90° , 135° , 180° , 225° , 270° , 315° , and 360° . Although 30° and 45° have a common divisor, there will still be several different positions after the rotation.

5. Conclusion

In this paper, we propose an FMT selector to track the ship target based on Internet of Things and wireless sensor network. It can select the most suitable target in the high-speed rotating video, which is a common scenario in terminal guidance. None of the previous target tracking methods did a good job in this scenario. In the first place, we take the image to the detector to detect all object. Secondly, we use our FMT selector to pick the best target as the result of this frame. Fourier-Mellin Transformer has been used many image fields and achieved good results, so we think it can still perform well in target tracking. The experiments show that our method has absolute advantages over both machine learning-based and deep learning-based tracking method for our specially made rotating dataset in IOT and WSN. However, the scene we are facing is mainly aerial video, whose the tracking target is only possible of rotate and scale change (few targets are deformed). So this framework cannot be generalized to the general scene. And the processing speed is still relatively low. In a future work, we will carry out further research on these issues.

Data Availability

The datasets used and/or analyzed during the current study are available from the corresponding author on reasonable request.

Conflicts of Interest

The authors declared no potential conflicts of interest with respect to the research, authorship, and/or publication of this article.

References

- [1] M. H. Liao, B. G. Shi, and X. Bai, "TextBoxes++: a single-shot oriented scene text detector," *IEEE Transactions on Image Processing*, vol. 27, no. 8, pp. 3676–3690, 2018.
- [2] P. Sun, Y. Zheng, Z. Zhou, W. Xu, and Q. Ren, "R4Det: refined single-stage detector with feature recursion and refinement for rotating object detection in aerial images," *Image and Vision Computing*, vol. 35, no. 4, pp. 3163–3171, 2020.
- [3] J. Ma, W. Shao, H. Ye et al., "Arbitrary-oriented scene text detection via rotation proposals," *IEEE Transactions on Multimedia*, vol. 20, no. 11, pp. 3111–3122, 2018.
- [4] Q. Li, L. Mou, Q. Xu, Y. Zhang, and X. X. Zhu, "R3-Net: a deep network for multi-oriented vehicle detection in aerial images and videos," *IEEE Transactions on Geoscience and Remote Sensing*, vol. 57, no. 7, pp. 5028–5042, 2019.
- [5] Z. Kalal, K. Mikolajczyk, and J. Matas, "Tracking-learning-detection," *IEEE transactions on pattern analysis and machine intelligence*, vol. 34, no. 7, pp. 1409–1422, 2012.
- [6] J. F. Henriques, R. Caseiro, P. Martins, and J. Batista, "High-speed tracking with kernelized correlation filters," *IEEE transactions on Pattern Analysis and Machine Intelligence*, vol. 37, no. 3, pp. 583–596, 2015.
- [7] B. Li, J. Yan, W. Wu, Z. Zhu, and X. Hu, "High performance visual tracking with Siamese region proposal network," in *Proceeding of the 2018 IEEE Conference on Computer Vision and Pattern Recognition (CVPR 2018)*pp. 8971–8980, Salt Lake City, UT, USA, 18 June, 2018.
- [8] Q. Wang, L. Zhang, L. Bertinetto, W. Hu, and P. H. Torr, "Fast online object tracking and segmentation: a unifying approach," in *Proceeding of the 2019 IEEE/CVF Conference on Computer Vision and Pattern Recognition (CVPR 2019)*pp. 1328–1338, Long Beach, CA, USA, 15 June, 2019.
- [9] L. Molina-Espinosa, C. G. Aguilar-Madera, E. C. Herrera-Hernández, and C. Verde, "Numerical modeling of pseudo-homogeneous fluid flow in a pipe with leaks," *Computers & Mathematics with Applications*, vol. 74, no. 1, pp. 64–73, 2017.
- [10] M.-S. Pan, P.-L. Liu, and Y.-P. Lin, "Event data collection in ZigBee tree-based wireless sensor networks," *Computer Networks*, vol. 73, pp. 142–153, 2014.
- [11] L. Kong, M. Xia, X. Y. Liu et al., "Data loss and reconstruction in wireless sensor networks," *IEEE Transactions on Parallel and Distributed Systems*, vol. 25, no. 11, pp. 2818–2828, 2014.
- [12] H. Lu, J. Li, and M. Guizani, "Secure and efficient data transmission for cluster-based wireless sensor networks," *IEEE Transactions on Parallel and Distributed Systems*, vol. 25, no. 3, pp. 750–761, 2014.

Retraction

Retracted: Research on Localization Parameter Estimation and Algorithm in the Digital Television Terrestrial Broadcasting

Journal of Sensors

Received 19 December 2023; Accepted 19 December 2023; Published 20 December 2023

Copyright © 2023 Journal of Sensors. This is an open access article distributed under the Creative Commons Attribution License, which permits unrestricted use, distribution, and reproduction in any medium, provided the original work is properly cited.

This article has been retracted by Hindawi following an investigation undertaken by the publisher [1]. This investigation has uncovered evidence of one or more of the following indicators of systematic manipulation of the publication process:

- (1) Discrepancies in scope
- (2) Discrepancies in the description of the research reported
- (3) Discrepancies between the availability of data and the research described
- (4) Inappropriate citations
- (5) Incoherent, meaningless and/or irrelevant content included in the article
- (6) Manipulated or compromised peer review

The presence of these indicators undermines our confidence in the integrity of the article's content and we cannot, therefore, vouch for its reliability. Please note that this notice is intended solely to alert readers that the content of this article is unreliable. We have not investigated whether authors were aware of or involved in the systematic manipulation of the publication process.

Wiley and Hindawi regrets that the usual quality checks did not identify these issues before publication and have since put additional measures in place to safeguard research integrity.

We wish to credit our own Research Integrity and Research Publishing teams and anonymous and named external researchers and research integrity experts for contributing to this investigation.

The corresponding author, as the representative of all authors, has been given the opportunity to register their agreement or disagreement to this retraction. We have kept a record of any response received.

References

- [1] S. Bao, S. Yang, H. Ou, and J. Song, "Research on Localization Parameter Estimation and Algorithm in the Digital Television Terrestrial Broadcasting," *Journal of Sensors*, vol. 2023, Article ID 1810507, 12 pages, 2023.

Research Article

Research on Localization Parameter Estimation and Algorithm in the Digital Television Terrestrial Broadcasting

Songjian Bao ¹, Shouliang Yang,¹ Hanwen Ou,¹ and Jing Song²

¹School of Electronic Information and Electrical Engineering, Chongqing University of Arts and Sciences, Chongqing 402160, China

²Institute of Process Engineering, Chinese Academy of Sciences, Beijing 100190, China

Correspondence should be addressed to Songjian Bao; baosj@cqwu.edu.cn

Received 4 August 2022; Revised 21 September 2022; Accepted 26 September 2022; Published 30 March 2023

Academic Editor: Sweta Bhattacharya

Copyright © 2023 Songjian Bao et al. This is an open access article distributed under the Creative Commons Attribution License, which permits unrestricted use, distribution, and reproduction in any medium, provided the original work is properly cited.

This paper mainly studies the positioning based on time of arrival and time difference of arrival. The quantity to be obtained is mainly time. Time of arrival measurement value can be obtained directly through symbolic timing synchronization, and its effective information can be obtained at the same time. Symbolic timing synchronization in digital video broadcast-terrestrial system can be divided into two stages: rough estimation and fine estimation. Rough estimation is based on the maximum likelihood estimation algorithm. The main purpose of rough estimation is to estimate the starting position of orthogonal frequency division multiplexing symbols, so that the starting position falls within the cyclic prefix of orthogonal frequency division multiplexing symbols. The purpose of fine estimation is to determine exactly the starting position of the orthogonal frequency division multiplexing symbol. In this paper, the symbolic timing synchronization algorithm of digital video broadcast-terrestrial system is studied and analyzed, and simulation is carried out for different channel models. Simulation results show that the synchronization algorithm achieves the best performance in additive white Gaussian noise channel and has good estimation performance in slow fading Rayleigh channel.

1. Introduction

Noncooperative bistatic radar based on television signals announced by H.D. Griffiths and N.E.W. Long, University of London, UK. The experimental system uses crystal palace TV station as the transmitting signal, and a receiver is installed at the University of London, 11.8 km away. The receiver is composed of two channels, one of which only receives direct signals from TV stations. The antenna system is composed of 10 Yagi antenna elements. The other channel only receives the scattered signal of the target, and the antenna system consists of four subarrays, each consisting of 18 Yagi antenna elements. Dr. P.E. Holland in the United Kingdom has published another experimental system, working in the VHF/UHF television band. Different from the above-mentioned system, the two channels of the system are used to receive the scattered signals of the target, and the signal source with high stability is used to provide the reference signals for the two channels, so that the receiver

can extract the Doppler shift of the target signal. The receiver has no channel to receive direct signals [1].

Nanjing Institute of Electronic Technology also conducted a similar detection system research, using the broadcast AM signal as the detection signal, and did experiments, the results of which observed the aircraft target at a distance of 70 km. The system uses a technique called “orthogonal filtering” to extract weak scattered signals buried in broadcast AM signals [2].

To estimate the position of a mobile user, the location parameters to be estimated are distance, distance difference, and angle of arrival. The distance information can be obtained by measuring the field strength of the electric field or the arrival time of the signal. The distance difference information can be obtained by measuring the arrival time of the signal, and then subtraction, or directly measuring the time difference. The angle of arrival is obtained by processing the received signals from the array antenna of the base station. In various radio positioning systems, the basic

positioning methods and techniques are the same or approximate, and the positioning estimation of mobile stations is realized by measuring the characteristic measurements of certain signals as wireless positioning parameters [3]. The precise estimation of localization parameters is important to improve the accuracy of wireless localization. At present, the main parameters used for positioning are time of arrival (TOA), time difference of arrival (TDOA), angle of arrival (AOA), strength of arrival (SOA), etc.

The similarity of the time-based positioning in digital video broadcast-terrestrial (DVB-T) system and the time measurement ranging system in wireless positioning allows us to use the positioning model and algorithm of time-based measurement value in wireless positioning to realize the positioning of DVB-T signal [4]. For the measurement and estimation of time parameters, according to the different measurement methods, time-based positioning methods can be divided into the following three: the first is the uplink method. By measuring the arrival time of the uplink signal sent by the mobile station, at least three base stations are required to measure the TOA/TDOA, and then, the network calculates the position of the mobile station. The second method is downlink [5]. TOA/TDOA of downlink signals of at least three base stations is measured by mobile station, and then, positioning is achieved. It is a positioning technology based on mobile terminal. This method has been adopted by the GSM positioning standard. The third is the up-down-link hybrid method. This method is a combination of the above two methods and does not require the time reference of the base station. This paper mainly involves studying the estimation of temporal localization parameters, based on the localization of TDOA, so the focus is on explaining the estimation of temporal localization parameters [6]. Firstly, the estimation method of time measurement value and location model algorithm in wireless positioning are constructed. Then, a ranging location scheme based on DVB-T system symbol location synchronization is proposed. Finally, the simulation and performance analysis of the scheme are carried out. At present, the efficiency and accuracy of positioning based on the parameters of time of arrival (TOA), time difference of arrival (TDOA), angle of arrival (AOA), and field strength of arrival (SOA) are not ideal.

In order to further improve the localization efficiency and accuracy, this paper studies and analyzes the symbol timing synchronization algorithm based on TOA and TDOA in DVB-T system. The symbol timing synchronization is divided into two stages of symbol coarse estimation and symbol fine estimation, and the simulation is carried out according to different channel models. The simulation results show that the synchronization algorithm can achieve the best performance in AWGN channel and also has a good estimation performance in slow fading Rayleigh channel.

2. Influence of Synchronization Error on Data Demodulation

The input signal to a digital television terrestrial broadcast is a complex point on a constellation diagram. After the discrete inverse Fourier transform is applied to the N complex

numbers of the input, the last N_g sampling values of the output sequence are copied to the front of the sequence as cyclic prefixes. $N + N_g$ output data are through parallel serial transformation, and finally, these time domain data are through wireless channel transmission. If the length of the cyclic prefix is larger than the impact response of the channel, the intersymbol interference can be avoided. If the length of the cyclic prefix is greater than the impulse response of the channel, intersymbol interference can be avoided [7].

At the receiving end, considering the influence of channel fading and additive Gaussian noise, the received time domain signal can be expressed as

$$y_n = \frac{1}{\sqrt{N}} \sum_{k=0}^{N-1} X_k \cdot H_k \cdot e^{j2\pi n(k+\varepsilon)/N} + w_n, \quad (1)$$

where X_k represents the complex number of IDFT input, H_k represents the fading of the k subcarrier, ε represents the normalized carrier frequency offset, and w_n represents the IDFT output of additive Gaussian white noise. In additive White Gaussian noise channel, $|H_k| = 1$ is desirable. Before data demodulation, the cyclic prefix is removed first, and then, the remaining N data are demodulated through the discrete Fourier transform. If there are no synchronization errors and the SNR is high enough, we can demodulate the raw data correctly [8]. Different synchronization errors have different effects on data demodulation [9].

3. Advantages and Disadvantages of the Existing Algorithms

Linear least squares (LS) algorithm and its improved algorithm depend on mathematical principles and the advantages of simple structure, usually on the high signal to noise ratio in channel which is able to have a better estimation precision, and because the P^{-1} belong to the known data, the rest of the operation is completed after multiplication, and the attached is an addition operation; channel interpolation is also very convenient, which only needs to fill zero in hand line frequency domain transformation [10]. The disadvantage of this algorithm is that it needs at least twice the length of the guard interval as the longest multipath delay, the frequency band utilization is relatively low, and the accuracy will be greatly reduced in the case of low SNR because the influence of noise is not considered. At the same time, the estimation accuracy of LS and its improved algorithm will also be affected when the mutual interference between the frame body data and PN frame head data is relatively large.

PN loop correlation estimation algorithm is a widely used channel estimation algorithm for DVB-T at present, because it does not require large matrix inversion operation like LS and its improved algorithm, and the algorithm is relatively simple, and the channel estimation response is fast (it can be completed in a burst of data). However, this algorithm requires that the PN sequence has cyclic characteristics, and the frame header used for correlation operation should not be interfered by the OFDM symbols before and after [11]. In this way, similar to LS and its improved algorithm and PN frequency domain algorithm, when the

mutual interference between frame body data and frame head data in the received data is relatively large, in order to ensure the reliability of channel estimation, it is often required that the estimated multipath maximum delay should not exceed the cyclic guard interval of the hunting sequence [12].

In view of the defects of the above algorithm, the DTV system is sensitive to synchronization frequency offset and exists in the process of signal detection which detected signal peak position volatile and existence of pseudopeak misjudgment; this paper studies deeply the symbol synchronization algorithm, and the maximum likelihood estimation algorithm was improved, to reach the frame synchronization and to accurately get the start time of signal frames. Therefore, the algorithm has high timing accuracy.

4. Application of IoT, Big Data, and Machine Learning Techniques to Localization Parameter Estimation and Algorithms in Digital Television

The Internet of Things (IoT), big data analysis, and machine learning techniques are the troika of the intelligent era, which are of great significance for the intelligent development of science and technology. The IoT is an intelligent network that enables effective information interaction between people, people and things, and things and things through N information sensing devices. "Everything is perceived" and "everything is interactive" are the core values of the IoT. Big data analysis technology has been gradually applied commercially in recent years. With the rapid development of information technology, data has become the product of the operation of information system, which shows the characteristics of large scale, variety, irregularity, and fast speed. The value of big data analysis technology lies in mining the needed information from these data and providing reference for decision-makers. Machine learning technique is the core technology to realize artificial intelligence, which is widely applied in the field of intelligence. Machine learning technique refers to the ability of computers to learn and judge and to process data and to produce effective results without explicit instructions from humans [13].

The subsequent research of this paper applies IoT, big data analysis, and machine learning techniques to positioning parameter estimation and algorithm in digital TV and plans to design a positioning parameter estimation and algorithm system architecture in "smart +" digital TV based on big data analysis and machine learning in the IoT environment. The follow-up research will put forward the implementation ideas of intelligent positioning, intelligent prediction, intelligent operation, and maintenance of digital TV positioning system, so as to provide solutions for improving the accuracy and efficiency of digital TV positioning.

5. Maximum Likelihood Estimation Algorithm

5.1. Method Description. In the process of establishing synchronization, symbolic timing synchronization is usually carried out first. Only by determining the starting position

of OFDM symbol can correct FFT demodulation be carried out.

Maximum likelihood estimation (MLE) algorithm is implemented through the correlation operation of the sexual indulgence information carried by the time domain cyclic prefix [14].

The observation interval is shown in Figure 1. The number of OFDM symbols in the observation window is greater than the OFDM symbols of a complete $N + Ng$ sample value, so the size of the observation window is $2N + Ng$, the symbol of the $N + Ng$ sample value before the observation sample value is the $i - 1$ symbol, and the symbol of the current observation $N + Ng$ sample value is the i symbol. The symbol of the $N + Ng$ sample value after the observation sample value is the $i + 1$ symbol. Thus, $2N + Ng$ consecutive sample values are observed, which contains a complete OFDM symbol of $N + Ng$ sample values. However, the receiver does not know the starting position of this OFDM signal [15]. Here, we assume θ and define two sets:

$$\begin{aligned} I &= \{\theta - Ng + 1, \dots, \theta\}, \\ I' &= \{\theta + N - Ng + 1, \dots, \theta + N\}, \end{aligned} \quad (2)$$

where set I is the protection interval of the i -th multicarrier symbol cycle prefix and contains the same elements as set I' . $2N + Ng$ observation points are taken as a vector r , that is, $r = [r_1, r_2, \dots, r_{2N+Ng}]$.

It can be noted that the elements ($r(k), k \in I \cup I'$) in set I' and set I are corresponding to the same, so there are the following related characteristics [16].

$$E\{r(k)r^*(k+m)\} = \begin{cases} \sigma_s^2 + \sigma_n^2, & m = 0, \\ \sigma_s^2 e^{-j2\pi\Delta f}, & m = N, \forall k \in I, \\ 0, & \text{other,} \end{cases} \quad (3)$$

where $\sigma_s^2 = E[|s(k)|^2]$ is the energy of useful signal and additive white Gaussian noise, i.e., average power; $\sigma_n^2 = E[|n(k)|^2]$ is the variance of white Gaussian noise; and Δf is the normalized carrier frequency deviation.

The logarithmic likelihood function $\Lambda(\theta, \Delta f)$ is defined as the logarithm of probability density function $f(r|\theta, \Delta f)$, where $f(r|\theta, \Delta f)$ represents the joint conditional probability distribution of $2N + Ng$ sampling points given sign arrival time θ and frequency deviation Δf , namely,

$$\Lambda(\theta, \Delta f) = \lg f(r|\theta, \Delta f), \quad (4)$$

Among $2N + Ng$ sampling points, only the corresponding elements in set I and I' have correlation, and the other $2N$ sampling points can be regarded as independent [17]. For simplicity, $f(r(k))$ is directly used to represent the

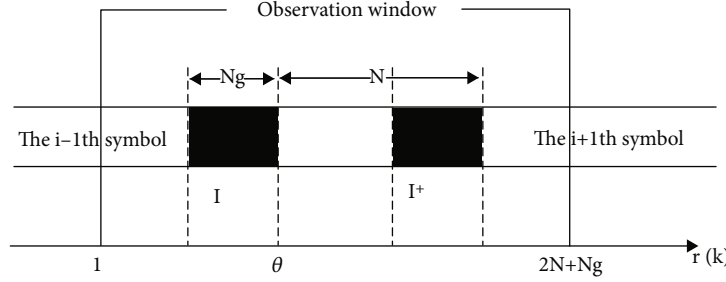


FIGURE 1: Schematic diagram of observation interval.

conditional probability $f(r|\theta, \Delta f)$. So this is the equation:

$$\begin{aligned} \Lambda(\theta, \Delta f) &= \lg \left(\prod_{k \in I} f(r(k), r(k+N)) \prod_{k \notin I \cup I'} f(r(k)) \right) \\ &= \lg \left(\prod_{k \in I} \frac{f(r(k), r(k+N))}{f(r(k))f(r(k+N))} \prod_k f(r(k)) \right). \end{aligned} \quad (5)$$

$f(*)$ is used to represent the (joint) probability density distribution function of a random variable. It can be noticed that both one-dimensional and two-dimensional probability density distribution functions are used in the equation. The product term $\prod_k f(r(k))$ is the product of $2N + \theta$ points, so the solution has nothing to do with the sign starting point θ [18]. Assuming that the information source is an independent equiprobability distribution, the real part and the imaginary step of $r(k)$ are independent of each other, so the value of $\prod_k f(r(k))$ has nothing to do with the frequency deviation Δf . Maximum likelihood estimation is required to estimate

the values of T and Δf that can maximize $\Lambda(\theta, \Delta f)$ [18]. Therefore, eliminating $\prod_k f(r(k))$ will not affect the maximum likelihood estimation of θ and Δf . Therefore, the equation can be simplified as

$$\Lambda(\theta, \Delta f) = \log \left[\prod_{k \in I} \frac{f(r(k), r(k+N))}{f(r(k))f(r(k+N))} \right]. \quad (6)$$

The above equation can also be written as

$$\Lambda(\theta, \Delta f) = \sum_{k=\theta}^{\theta+Ng-1} \log \left[\frac{f(r(k), r(k+N))}{f(r(k))f(r(k+N))} \right]. \quad (7)$$

Since $r(k)$ is a complex Gaussian random variable, $f(r(k), r(k+N))$ is a two-dimensional complex Gaussian distribution probability density function; by using the relevant characteristics in equation (6), the following equation can be obtained:

$$f[r(k), r(k+N)] = \frac{\exp \left\{ -(|r(k)|^2 - 2\rho \operatorname{Re} [e^{j2\pi\Delta f} r(k)r^*(k+N)] + |r(k+N)|^2) / ((\sigma_s^2 + \sigma_n^2)(1 - \rho^2)) \right\}}{\pi^2(\sigma_s^2 + \sigma_n^2)(1 - \rho^2)}, \quad (8)$$

where ρ is the amplitude of the correlation coefficient between $r(k)$ and $r(k+N)$; ρ can be expressed as the following equation:

$$\begin{aligned} \rho &= \left| \frac{E[r(k)r^*(k+N)]}{\sqrt{E[|r(k)|^2] \cdot E[|r^*(k+N)|^2]}} \right| = \left| \frac{\sigma_s^2 e^{-j2\pi\Delta f}}{\sigma_s^2 + \sigma_n^2} \right| = \frac{\sigma_s^2}{\sigma_s^2 + \sigma_n^2} \\ &= \frac{\text{SNR}}{\text{SNR} + 1}. \end{aligned} \quad (9)$$

$f[r(k)]$ is the probability density function of one-dimensional complex Gaussian distribution, which can be

obtained as

$$f[r(k)] = \frac{1}{\pi(\sigma_s^2 + \sigma_n^2)} \exp \left[-\frac{|r(k)|^2}{\sigma_s^2 + \sigma_n^2} \right]. \quad (10)$$

Put equations (8) and (9) into equation (7), and after relevant algebraic operations, the following equation can be obtained:

$$\begin{aligned} \Lambda(\theta, \Delta f) &= c_1 + c_2 \sum_{k=\theta}^{\theta+Ng-1} \left\{ \operatorname{Re} \left[e^{j2\pi\Delta f} r(k)r^*(k) \right] \right. \\ &\quad \left. - \frac{1}{2}\rho[|r(k)|^2 + |r(k+N)|^2] \right\} \\ &= c_1 + c_2 \{ |\alpha(\theta)| \cos(2\pi\Delta f + \angle\alpha(\theta)) - \rho\beta(\theta) \}, \end{aligned} \quad (11)$$

where $c_1 = -\log(1 - \rho^2)$, $c_2 = (2\rho/(\sigma_s^2 + \sigma_n^2)) \exp[-|r(k)|^2/(\sigma_s^2 + \sigma_n^2)]$ is constant, and $c_2 > 0$, so it has no influence on the maximum likelihood judgment, and the formula can be simplified as

$$\Lambda(\theta, \Delta f) = |\gamma(\theta)| \cos(2\pi\Delta f + \angle\gamma(\theta)) - \rho\Phi(\theta), \quad (12)$$

Among them,

$$\begin{aligned} \gamma(m) &= \sum_{k=m}^{m+Ng-1} r(k)r^*(k+N), \\ \Phi(m) &= \frac{1}{2} \sum (|r(k)|^2 + |r(k+N)|^2), \end{aligned} \quad (13)$$

where $\angle\gamma(\theta)$ represents the phase of complex number $\gamma(\theta)$ and $\gamma(m)$ is equal to the sum of the correlation values between two consecutive sample pairs of Ng length and N distance; namely, the first term of the formula is the weighted modulus of $\gamma(m)$, where the weighted modulus is determined by the frequency deviation; the second term of the equation is the energy term independent of the frequency deviation, which depends on the correlation coefficient ρ (SNR) [19].

The maximum likelihood algorithm estimates the symbol timing synchronization position and carrier frequency deviation at the same time, so the process of maximizing the logarithmic likelihood function above should be completed in two parts, namely,

$$\max_{(\theta, \Delta f)} \Lambda(\theta, \Delta f) = \max_{\theta} \max_{\Delta f} \Lambda(\theta, \Delta f) = \max_{\theta} \Lambda(\theta, \Delta f_{ML}(\theta)). \quad (14)$$

In terms of frequency deviation Δf , in order to maximize the formula, the cosine term should be first, namely,

$$2\pi\Delta f + \angle\gamma(\theta) = 2n\pi, \quad n \text{ as an integer.} \quad (15)$$

The maximum likelihood estimate of the frequency deviation Δf is obtained:

$$\hat{\Delta f}_{ML}(d) = -\frac{1}{2\pi} \angle\gamma(\theta) + n. \quad (16)$$

Considering the general situation, the carrier frequency deviation should be within a small range, taking $n = 0$, so there are

$$\hat{\Delta f}_{ML}(d) = -\frac{1}{2\pi} \angle\gamma(\theta). \quad (17)$$

Let $\cos = 1$; then, the maximum likelihood function of timing deviation θ is

$$\Lambda(\theta, \Delta f_{ML}(\theta)) = |\gamma(\theta)| - \rho\Phi(\theta). \quad (18)$$

Since the formula is only related to θ , the estimation of θ can be obtained by maximizing $\Lambda(\theta, \Delta f_{ML}(\theta))$, and then, the

estimation of timing deviation θ can be obtained by substituting θ into the formula. Therefore, the joint maximum likelihood estimation of θ and Δf becomes

$$\begin{aligned} \hat{\theta}_{ML} &= \arg \max_{\theta} \{|\gamma(\theta)| - \rho\Phi(\theta)\}, \\ \Delta f_{ML}(\theta) &= -\frac{1}{2\pi} \angle\gamma(\hat{\theta}_{ML}). \end{aligned} \quad (19)$$

For maximum likelihood symbol synchronization, $\gamma(\theta)$ and $\Phi(\theta)$ of $2N + Ng$ sampling points of received signals are calculated according to formula, respectively. Finally, estimation operation is performed according to formula. In this process, two factors affect the final result: one is the number of sample values of the cyclic prefix Ng , and the other is the correlation coefficient ρ determined by SNR. The former is known to the receiver, while the latter may also be fixed. $\gamma(\theta)$ basically provides an estimate of the sign timing θ and the frequency deviation Δf . When the modular value of $\gamma(\theta)$ is weighted with the energy term $\Phi(\theta)$, the peak value will appear at the moment of θ_{ML} , and the phase of $\gamma(\theta_{ML})$ is proportional to Δf .

In order to reduce the complexity of the algorithm, a new $\{c(k)\}$ sequence is generated by quantization of the receiving sequence. Then, perform relevant operations on the $\{c(k)\}$ sequence, as shown below, namely,

$$c_k = \Theta[r_k], \quad k = 1, 2, \dots, 2N + Ng, \quad (20)$$

where $\Theta[\cdot]$ is the complex quantizer:

$$\Theta[x] = \text{sign}(\text{Re}\{x\}) + j\text{sign}(\text{Im}\{x\}), \quad (21)$$

$$\text{where } \text{sign}(x) = \begin{cases} +1, & x \geq 0 \\ -1, & x < 0 \end{cases}.$$

5.2. Symbol Coarse Synchronization. In the actual multipath channel transmission, because OFDM symbols are diffused on the time axis, the cyclic prefix signal used for estimation operation has been interfered by the previous symbol, and the correlation performance is greatly reduced. The detected correlation peak position has a large fluctuation, and there is false peak misjudgment, which is worse when the SNR is low [20]. Therefore, the MLE algorithm is improved:

5.2.1. Truncate the Loop Prefix. The truncation length is jointly determined by the circulation length and channel dispersion length, as shown in Figure 2. If truncation is too small, multipath interference is not avoided. Too many cuts will reduce the accuracy of relevant judgment.

5.2.2. Threshold Judgment. Because of the influence of the noise and interference, the location of the maximum value is not stable and easy to cause the pseudo peak, so there is no correlation peak, but it reaches a certain threshold to determine the starting position of local maximum moment for symbols, so that it will have an estimated error and actual simulation, estimated to coarse symbol starting position in the center of the distribution of multipath [9]. However, as

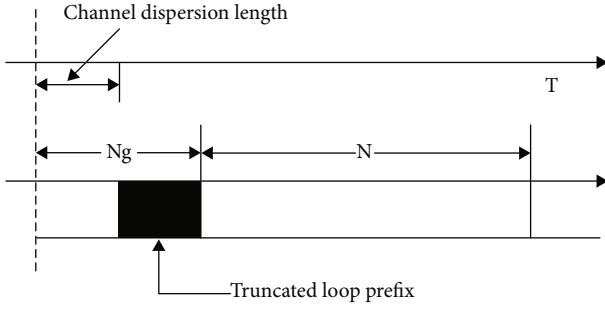


FIGURE 2: Multipath delay synchronization requirements.

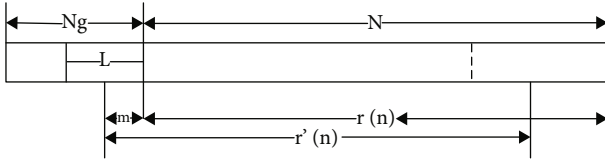


FIGURE 3: Coarse synchronization error falling into guard interval.

long as the coarse symbol synchronization position falls into the protection interval stably, its effect on the data signal is only phase deflection, and the introduced symbol timing synchronization error can be estimated and corrected by FFT postprecise symbol synchronization in the frequency domain [21]. The symbol starting position j_{est} is

$$j_{est} = \arg \max_{\theta} \left\{ \left| \sum_{k=\theta-L+1}^{\theta} r(k)r^*(k+N) \right| - \frac{1}{2} \sum_{k=\theta-L+1}^{\theta} (|r(k)|^2 + |r(k+N)|^2) \right\}. \quad (22)$$

As shown in Figure 3, when the synchronization position of the coarse symbol with the local maximum of the threshold value is judged, the estimation deviation of the synchronization position is m , and if $r(n)$ is a received N long data sequence $R(k) = FFT[r(n)]$, $r'(n) = r((n-m)_N)R_N(n)$, then the characteristics of the data within the cyclic prefix and FFT cyclic shift theorem can be obtained as follows [22]:

$$R'(K) = FFT[r'(n)] = R(k)e^{-j2\pi km/N}. \quad (23)$$

5.3. Symbol Fine Synchronization. The application environment of DVB-T is relatively complex, with large multipath delay and Doppler frequency shift. Therefore, there is no special training sequence in pilot pattern design, but continuous pilot and dispersed pilot are inserted into the data symbols, making the pilot density higher. Due to the large number and location of dispersed pilots, they can better reflect the characteristics of the channel, so using dispersed pilots as symbol synchronization fine estimation can achieve better performance [23].

After coarse symbol timing synchronization, FFT transformation is performed to obtain frequency domain data, and the delay characteristics of multipath channel are estimated based on the inserted dispersed pilot information to perform symbol fine synchronization [24].

Impulse response of time-varying multipath channel can be approximately expressed as

$$h(\tau, t) = \sum_{i=0}^l h_i \delta(\tau - \tau_i), \quad (24)$$

where τ_i is the time delay of path i , $h_i(t)$ is the time-varying fading of signal caused by propagation path and mobile reception of path i , and l is the total multipath number; then,

$$H(f, t) = \int_{-\infty}^{+\infty} h(\tau, t) e^{-j2\pi f \tau} d\tau = \sum_{i=0}^l h_i(t) e^{-j2\pi f \tau_i}. \quad (25)$$

Since $T_s = T + T_g$ is a symbol duration, sampling interval $T = T_u/N$, and the n subcarrier frequency of the discretized k symbol is $f_n = n/T$, then

$$H_k(n) = H(f_n, KT_s) = \sum_{i=0}^l h_i(KT_s) e^{-j2\pi(n\tau_i/T_u)}. \quad (26)$$

In the transmitter, $\{X_k(n) | n = 0 \dots N-1\}$ represents the signal of the n subcarrier of the k symbol. At the receiving end, the dispersion pilot signal inserted in the frequency domain is used to estimate the precise sign deviation. If the signal of the n subcarrier of the k symbol after correct synchronization is expressed as $Y_k(n) = X_k(n)H_k(n) + W_k(n)$, $W(n)$ is zero-mean complex Gaussian white noise. Then, the estimated channel frequency response is

$$\hat{H}_k(n) = \frac{Y_k(n)}{X_k(n)}, \quad n = 0 \dots N_p - 1. \quad (27)$$

Perform IFFT by adding N_p pilot frequencies to M (integer power of 2), and estimate the characteristics of $h(i)$:

$$\begin{aligned} \hat{h}(i) &= \frac{1}{M} \sum_{n=0}^{N_p-1} \hat{H}_k(n) e^{j2\pi(in/M)} \\ &= \frac{1}{M} \sum_{n=0}^{N_p-1} \frac{Y_k(n)}{X_k(n)} e^{j2\pi(in/M)}, \quad i = 0, 1, \dots, M-1. \end{aligned} \quad (28)$$

By averaging the channel impulse response function estimated by continuous N_{av} OFDM symbols, the channel delay power distribution \hat{S}_k can be obtained, which basically describes the delay characteristics of multipath channels:

$$\hat{S}_k = \frac{1}{N_{av}} \sum_{n=0}^{N_{av}-1} |\hat{h}_n(i)|^2. \quad (29)$$

The energy of each path needs to exceed a certain threshold Γ and is a local maximum. Therefore, the delay expression of the first path is estimated as follows:

$$\lambda = \frac{1}{2} \min \{k | \hat{S}_k > \Gamma, \hat{S}_k > \hat{S}_{k+1}, k = 0, 1, \dots, M-1\}. \quad (30)$$

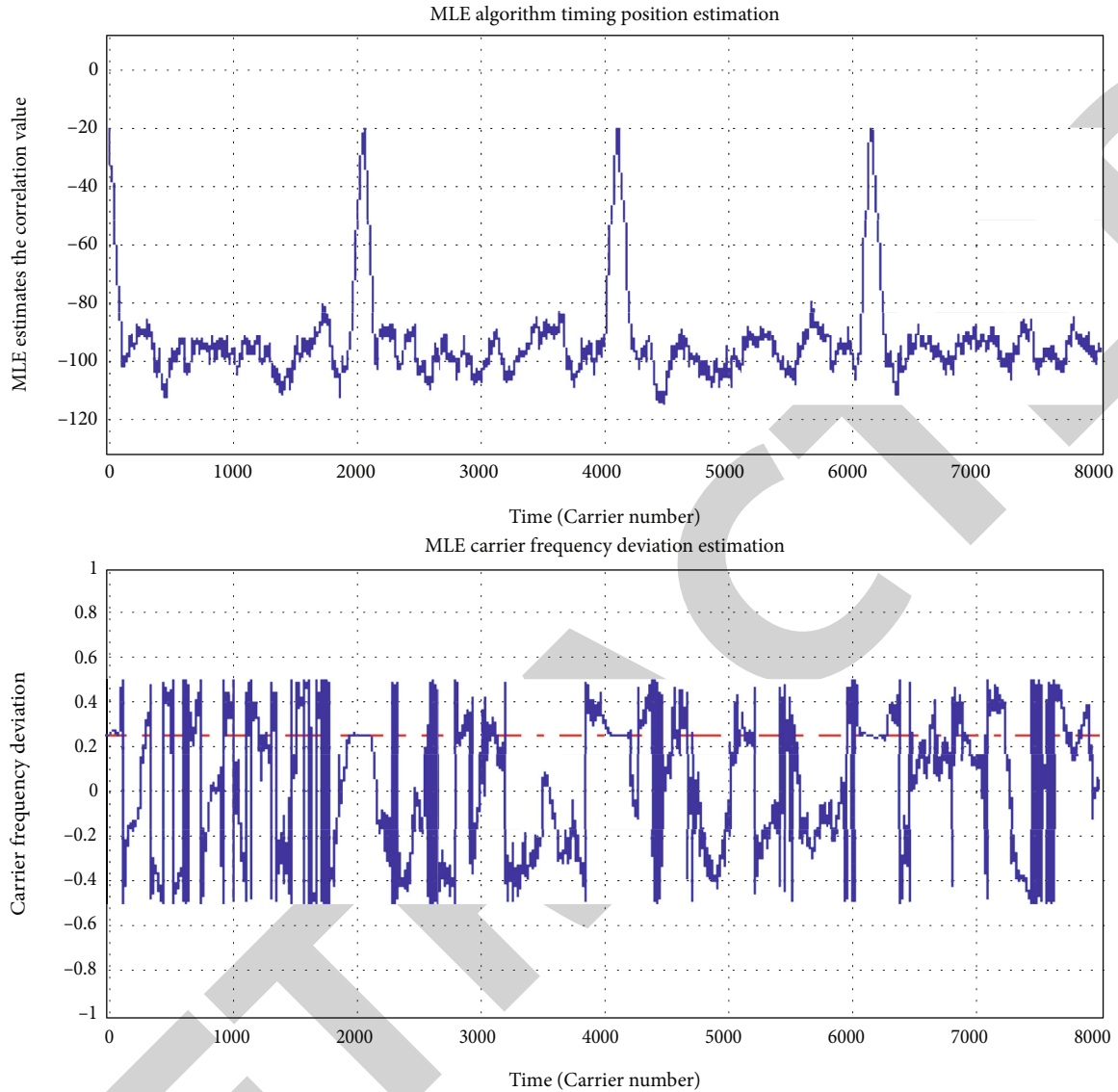


FIGURE 4: Simulation diagram of MLE algorithm.

Γ selection is a testing process, and its expression is

$$\Gamma = \max \{ \hat{\delta}_{\max} \times 10^{-\Gamma_1/10}, \hat{\delta}_{\min} \times 10^{\Gamma_2/10} \}, \quad (31)$$

where $\hat{\delta}_{\max}$ and $\hat{\delta}_{\min}$ are the maximum and minimum values in $\{\hat{\delta}_k, k=0, 1, \dots, M-1\}$. Corrected symbol starting position is

$$j'_{\text{est}} = j_{\text{est}} - \lambda. \quad (32)$$

6. Simulation and Performance Analysis

6.1. MLE Algorithm Simulation. In view of the above derivation process, its MATLAB simulation is given as follows: DVB-T 2k mode and 16QAM modulation, including $N =$

2048 subcarriers, protection interval length $Ng = 64$, $SNR = 15\text{dB}$, and carrier frequency deviation $\Delta f = 0.25$.

Figure 4, respectively, presents the simulation diagram of symbolic timing position estimation of MLE algorithm based on Gaussian channel environment and the simulation diagram of carrier frequency deviation estimation of MLE. As can be seen from the first figure, signal peaks appear near position 0, 2045, 4094, and 6142, respectively. In other words, the estimation operation carried out according to the formula can accurately obtain the position of θ_{ML} . The second figure is the maximum likelihood estimation of carrier frequency deviation Δf_{ML} obtained according to the formula based on the given position of the first figure. The dotted line in the figure is carrier frequency deviation.

Figure 5 simulates the change curve of correct symbolic timing probability of MLE algorithm with SNR in AWGN channel and Rayleigh channel. The system data used is the

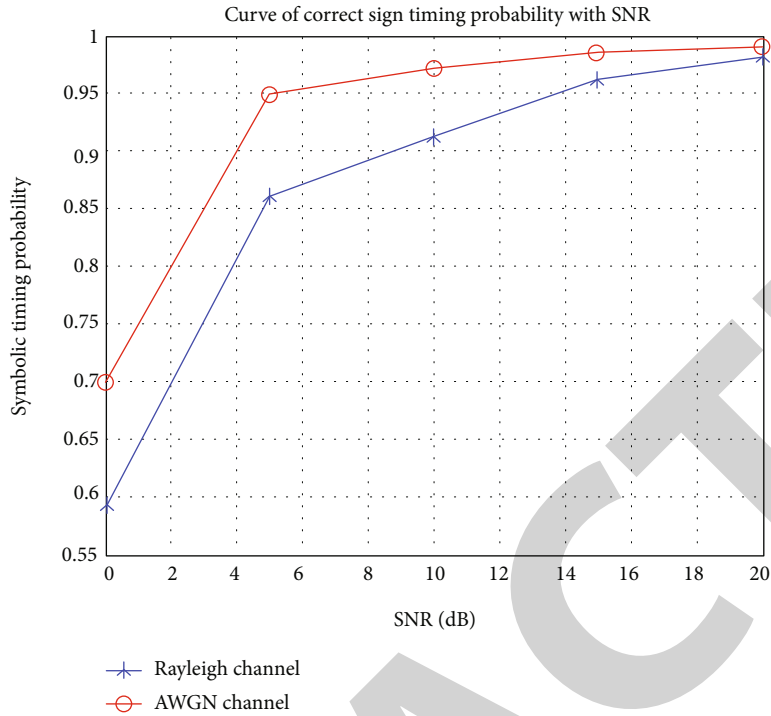


FIGURE 5: Curve of correct sign timing probability with SNR.

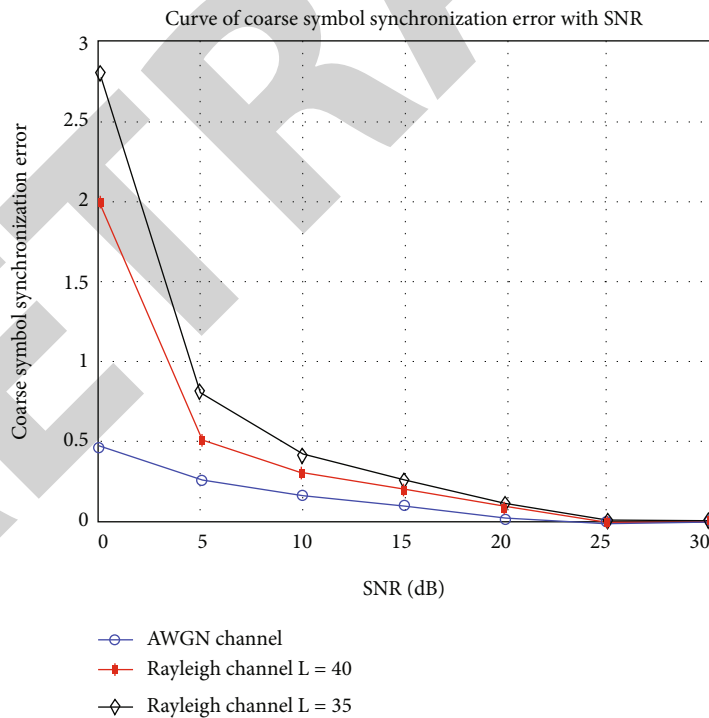


FIGURE 6: Curve of coarse sign synchronization error with SNR.

same as Figure 4, namely, DVB-T 2k mode and 16QAM modulation, including $N = 2048$ subcarriers and protection interval length $Ng = 64$; carrier frequency and sampling time are correctly synchronized. MATLAB is used for simulation.

According to the simulation figure, the correct symbol timing probability of the correlation algorithm in AWGN channel is better than that in Rayleigh channel, but the trend of both is that with the increase of SNR, the symbol

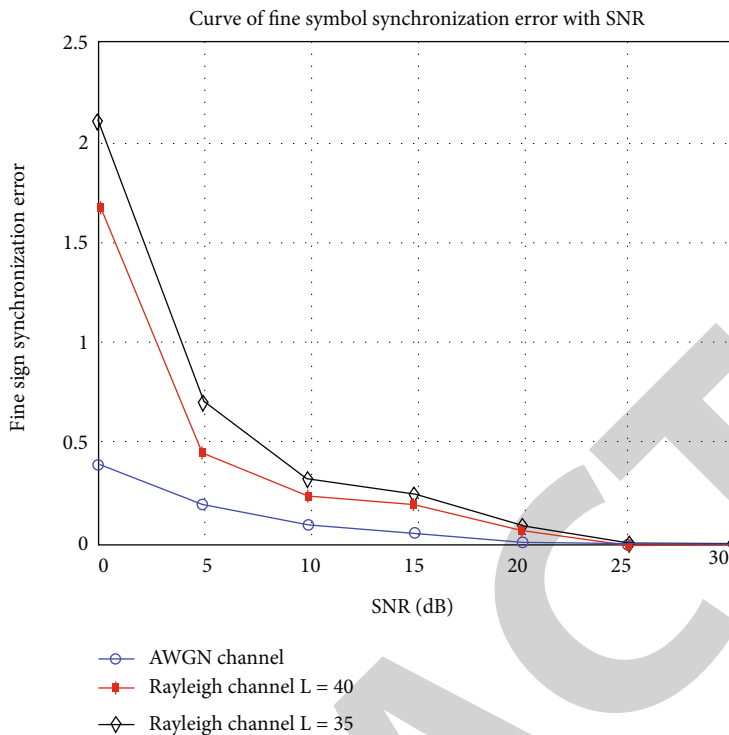


FIGURE 7: Curve of fine symbol synchronization error with SNR.

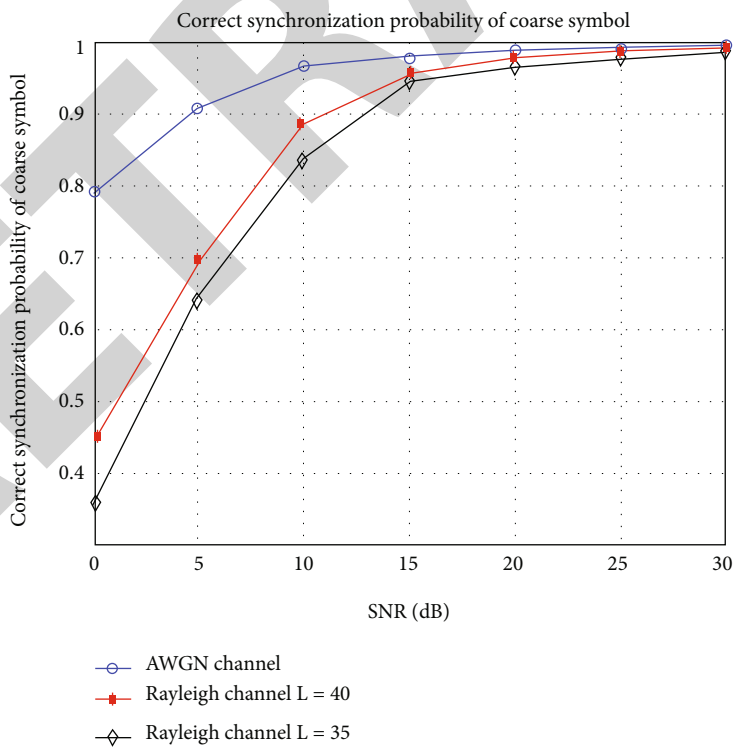


FIGURE 8: Correct synchronization probability of coarse symbol.

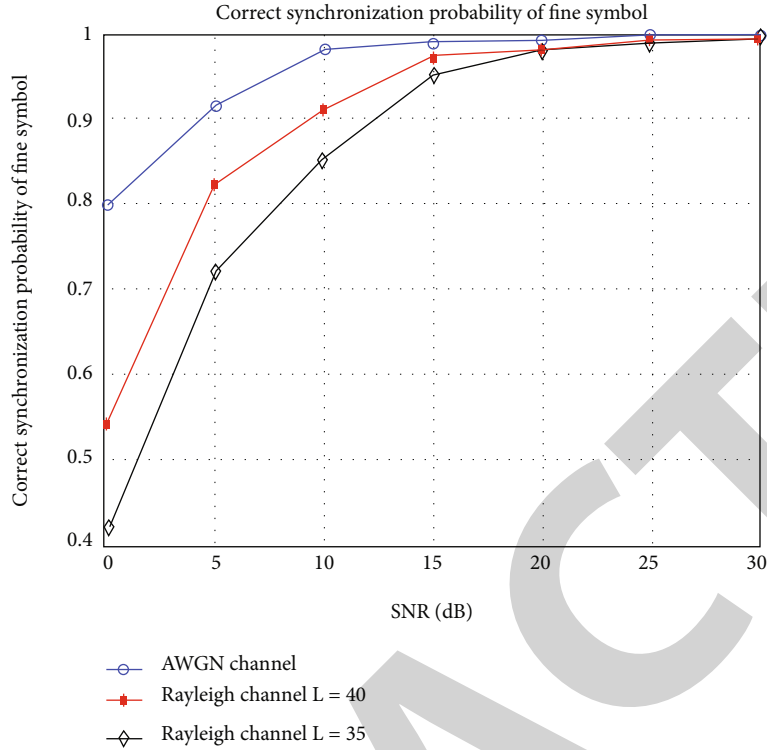


FIGURE 9: Correct synchronization probability of fine symbol.

synchronization probability is higher, especially when $\text{SNR} > 5$ dB, even in Rayleigh channel, the symbol synchronization probability is more than 85%, even in AWGN which is 95%. When $\text{SNR} > 10$ dB, both of them reach high probability, and sufficient precision is required for symbol synchronization, which verifies the effectiveness of MLE algorithm.

6.2. Simulation of Coarse and Fine Symbol Synchronization Algorithm. Rayleigh channel model consists of 20 paths without LOS. The maximum delay carrier number is 49, and the protection interval length meets the maximum delay condition of ISI. Rayleigh channel factor $K = 1/\sqrt{\sum_{i=1}^N \rho_i^2}$, where N is multipath number.

The algorithm is simulated under AWGN and Rayleigh channel model: $N = 2048$, $N_g = 64$, DVB-T system, and 16QAM modulation. Carrier frequency and sampling time are correctly synchronized. In Rayleigh channel, $N_{av} = 3$, $\Gamma_1 = 7$, and $\Gamma_2 = 15$.

Figure 6 shows the mean error of coarse symbol synchronization estimation for different SNR. In the figure, the synchronization error is less than half subcarriers in AWGN channel, and only 2 subcarriers ($L = 40$) are offset in Rayleigh channel, and the larger SNR is, the better the correlation is. The figure also compares the influence of different L on the synchronization error in Rayleigh channel, and it can be seen that the error at $L = 40$ is less than that at $L = 35$. This is because the multipath interference has been effectively avoided when $L = 40$, and reducing the cyclic prefix reduces the correlation of the prefix, so the error increases.

Figure 7 shows the change curve of symbolic synchronization position error with SNR after estimation and correction by symbolic synchronization algorithm. When the SNR is low, the error is significantly suppressed. When $\text{SNR} > 5$ dB, the performance of the algorithm is greatly improved, and the error is controlled within 1 sub-carrier. AWGN channel completely eliminates the error when $\text{SNR} > 20$ dB and completely eliminates the error when Rayleigh $\text{SNR} > 25$ dB. It can be seen that DVB-T system has a large number of subcarriers and strong antimultipath interference ability, so it can achieve high timing accuracy.

Figure 8 shows the synchronization probability of coarse symbols under different SNR conditions. It can be seen that the larger SNR is, the greater the probability of correct timing is. AWGN channel synchronization is the best; Rayleigh channel $L = 35$ is the worst.

Figure 9 shows the curve of the probability of fine symbol synchronization changing with SNR, and the synchronization accuracy is further improved. AWGN channel can be accurately synchronized when $\text{SNR} > 20$ dB, and the synchronization probability is up to 80% when $\text{SNR} = 0$. Rayleigh channel has high synchronization accuracy when $\text{SNR} > 5$ dB and accurate synchronization when $\text{SNR} > 25$ dB. This greatly improves the synchronization performance of MLE algorithm in multipath channels. In Rayleigh channel, the synchronization probability at $L = 40$ is higher than that at $L = 35$, which is consistent with theoretical analysis. Therefore, the length of the circular prefix should be selected according to the channel environment in practice.

7. Conclusion

The symbol timing synchronization algorithm of DVB-T system proposed in this paper is simulated in AWGN channel and Rayleigh channel model. Symbol timing synchronization algorithm can be carried out in both time domain and frequency domain, and this algorithm can get accurate θ_{ML} position and carrier frequency deviation Δf_{ML} . The correct symbol timing probability in AWGN channel is better than that in Rayleigh channel. With the increase of SNR, the symbol synchronization probability is higher, which verifies the effectiveness of the algorithm. In the case of different SNR, the average error of coarse symbol synchronization estimation is better correlated with the increase of SNR. After the symbol synchronization algorithm is estimated and corrected, the symbol synchronization position error is significantly suppressed at low SNR. This is because the DVB-T system has a large number of subcarriers, and its antimultipath interference ability is enhanced, so it can achieve high timing accuracy. In different SNR situations, the larger the SNR, the greater the probability of correct timing of coarse symbol synchronization, and then, the fine symbol synchronization, the synchronization accuracy is further improved. The simulation results show that the symbol timing synchronization algorithm can achieve the best performance in AWGN channel and also has a good estimation performance in the slow fading Rayleigh channel. Next, the further research works are how to choose the length of cyclic prefix intelligently according to the actual channel environment, because the length of cyclic prefix directly affects the precision of symbol timing synchronization and research of applies IoT, big data analysis, and machine learning techniques to positioning parameter estimation and algorithm in digital TV.

Data Availability

All data, models, and code generated or used during the study appear in the submitted article.

Disclosure

The views, conclusions, and data of the paper are open to the public.

Conflicts of Interest

The authors declare that they have no conflicts of interest.

Acknowledgments

This work was supported in part by research on Key Technology of Vehicle High Temperature Exhaust Gas Sensor in Chongqing University and Affiliated Institutes of Chinese Academy of Sciences (key project) (No. HZ2021013) and Exploration and Practice of New Engineering Upgrading Path of Telecommunication Major in the Vision of Professional Certification in Industry-School Cooperative Education Program of Ministry of Education (No. 201901107029).

References

- [1] R. F. Zhang, "Research on digital TV signal transmission technology," *Western Radio and Television*, vol. 28, pp. 234–236, 2022.
- [2] Y. J. Shuang, Q. Luo, J. J. Hu, and Y. Liu, "Research on digital cable TV transmission system," *Video Engineering*, vol. 46, pp. 5–7, 2022.
- [3] M. H. Qou, "Analysis of radio monitoring and positioning technology," *Electronic Test*, vol. 28, pp. 99–103, 2022.
- [4] Z. Z. Dou, Z. Yao, and M. Q. Lu, "Autonomous establishment of distributed spatial reference for radio area positioning system," *Acta Electronica Sinica*, vol. 50, pp. 841–848, 2022.
- [5] X. S. Wu, Z. J. Fang, T. H. Cheng, and X. Li, "A radio signal source location algorithm based on field intensity deviation function," *China Radio*, vol. 28, pp. 45–48, 2022.
- [6] C. Y. Kong, K. Zhou, K. B. Lu, G. Liao, and Q. Wei, "Analysis of the influencing factors of signal location using TDOA in radio sensor monitoring network," *China Radio*, vol. 27, pp. 63–66, 2021.
- [7] Q. Hu and M. S. Ge, "The invention relates to a new positioning technology based on digital television radio broadcast signal," *Guangdong Communication Technology*, vol. 2, pp. 50–54, 2009.
- [8] Z. H. Wang, "High precision positioning method based on digital TV broadcast signal," *Modern Business Trade Industry*, vol. 12, pp. 207–208, 2018.
- [9] T. Ma and S. Zhang, "Research on wireless location technology based on mobile broadcast network," *Information & Communications*, vol. 138, pp. 21–22, 2014.
- [10] H. Q. Guo and D. Z. Zhu, "Block iterative guided minimum variance algorithm and its application in line spectral object detection," *Journal of Harbin Engineering University*, vol. 43, pp. 55–61, 2022.
- [11] F. C. Yan, Y. F. Cheng, X. Y. Lu, and W. D. Cheng, "An improved algorithm for blind estimation of OFDM time parameters based on cyclic autocorrelation," *Journal of Signal Processing*, vol. 35, pp. 65–74, 2019.
- [12] H. Li, "Research on efficient algorithm for spectral density estimation of cyclic correlativity entropy," *Journal of Electronics & Information Technology*, vol. 43, pp. 310–318, 2021.
- [13] W. J. Liu and B. Q. Li, "Research on the application of Internet of Things, big data analytics and machine learning technology in disaster recovery," *Microelectronics & Computer*, vol. 35, pp. 55–58, 2018.
- [14] D. W. Bian, W. G. Guan, X. N. Tian, and F. F. Yue, "A TOA/TDOA wireless location algorithm based on mobile broadcast network," *Journal of Liaoning University of Technology (Natural Science Edition)*, vol. 33, pp. 8–11, 2013.
- [15] S. J. Bao, "A new algorithm for location parameter estimation in DTV ground broadcast network," *Journal of Physics: Conference Series, International Symposium on Artificial Intelligence and Intelligent Manufacturing, AIIIM*, vol. 2181, no. 1, pp. 012013–012059, 2022.
- [16] J. W. Wu, L. C. Liu, F. Wang, and X. Q. Lin, "Application of LoRa technology in differential satellite positioning system," *Information & Communications*, vol. 16, pp. 86–87, 2019.
- [17] G. Yang, M. Zhang, Q. Li, and S. Q. Yang, "Design of radio and television signal location monitoring system," *Radio and Television Technology*, vol. 42, pp. 135–137, 2015.

Retraction

Retracted: Innovative Application of Sensor Combined with Speech Recognition Technology in College English Education in the Context of Artificial Intelligence

Journal of Sensors

Received 19 December 2023; Accepted 19 December 2023; Published 20 December 2023

Copyright © 2023 Journal of Sensors. This is an open access article distributed under the Creative Commons Attribution License, which permits unrestricted use, distribution, and reproduction in any medium, provided the original work is properly cited.

This article has been retracted by Hindawi following an investigation undertaken by the publisher [1]. This investigation has uncovered evidence of one or more of the following indicators of systematic manipulation of the publication process:

- (1) Discrepancies in scope
- (2) Discrepancies in the description of the research reported
- (3) Discrepancies between the availability of data and the research described
- (4) Inappropriate citations
- (5) Incoherent, meaningless and/or irrelevant content included in the article
- (6) Manipulated or compromised peer review

The presence of these indicators undermines our confidence in the integrity of the article's content and we cannot, therefore, vouch for its reliability. Please note that this notice is intended solely to alert readers that the content of this article is unreliable. We have not investigated whether authors were aware of or involved in the systematic manipulation of the publication process.

Wiley and Hindawi regrets that the usual quality checks did not identify these issues before publication and have since put additional measures in place to safeguard research integrity.

We wish to credit our own Research Integrity and Research Publishing teams and anonymous and named external researchers and research integrity experts for contributing to this investigation.

The corresponding author, as the representative of all authors, has been given the opportunity to register their agreement or disagreement to this retraction. We have kept a record of any response received.

References

- [1] J. Guo, "Innovative Application of Sensor Combined with Speech Recognition Technology in College English Education in the Context of Artificial Intelligence," *Journal of Sensors*, vol. 2023, Article ID 9281914, 11 pages, 2023.

Research Article

Innovative Application of Sensor Combined with Speech Recognition Technology in College English Education in the Context of Artificial Intelligence

Juan Guo 

School of Foreign Languages, Hunan University of Science and Engineering, Yongzhou 425199, China

Correspondence should be addressed to Juan Guo; v21314025@stu.ahu.edu.cn

Received 23 August 2022; Revised 11 October 2022; Accepted 17 October 2022; Published 11 February 2023

Academic Editor: Sweta Bhattacharya

Copyright © 2023 Juan Guo. This is an open access article distributed under the Creative Commons Attribution License, which permits unrestricted use, distribution, and reproduction in any medium, provided the original work is properly cited.

English listening is an effective way to improve students' English expression ability and use oral communication. However, from the current situation of English teaching, the current English teaching methods are too single, and teachers do not focus on oral training in the classroom, resulting in low efficiency of classroom teaching. On the basis of following the principles of wholeness, interaction, balance, and sustainable development of educational ecology, by enhancing the synergy of ecological elements of English speaking classroom, promoting interactive dialogue among ecological subjects, and regulating classroom behaviors, it is conducive to giving full play to the advantageous role of information technology on English speaking teaching reform and promoting its sustainable development. This paper addresses the current situation of English listening teaching, especially the problem of reduced recognition rate of spoken language in noisy environment, and the principle of using dual-sensor speech recognition system proposed. We design the speech recognition method based on recurrent neural network by acquiring the weak vibration pressure speech signal of the jaw skin and the speech signal transmitted through the air during the vocalization process through the sensor. Deep machine learning algorithm is used for speech recognition in English teaching. A reasonable frame sampling frequency is set to obtain the English speech signal, then the feature parameters representing this speech signal are obtained by linear prediction coefficients, and the speech feature vector is generated, followed by the recurrent neural network algorithm to train the speech features. In the related experiments, by comparing with the commonly used speech recognition algorithms, it is proved that the proposed algorithm English teaching speech recognition has higher accuracy and faster convergence.

1. Introduction

With the rapid development of education and teaching, English listening training can no longer meet the diverse, comprehensive, and complex needs of the students. In such an environment, teachers must study the core literacy of the English curriculum in depth, grasp the learning situation and development trend of each stage, and plan and design classroom teaching according to students' cognitive, thinking, and learning rules to promote students' English learning and listening skills. Combined with teaching practice, we discuss how to cultivate the relationship between listening, speaking, reading, and writing in English teaching and teach from the creation of language environment, extracurricular

extension, and listening, speaking, reading, and writing in English. In terms of teaching content, the development of artificial intelligence and information technology provides rich learning resources for English speaking learning. Teachers should integrate learning resources according to actual teaching needs and feedback from students and focus on the integration of knowledge and ability as well as the integration of language and culture in teaching content, build a spider web-type knowledge structure, broaden the breadth and depth of language materials, and improve students' thinking and language use ability.

Many colleges are cutting back on college English teaching [1]. English classes in some colleges have been reduced from four to three hours a week. By the second semester of

grade two, there were only two classes per week. There are no college English courses for juniors and seniors. In addition, the teaching of spoken English is classified as a college English audio-visual instruction, and classes are only offered every three weeks. Colleges do not have any requirement for students' English speaking ability, nor do they offer any kind of English speaking test, or even include it in the scope of the college English syllabus. From the students' point of view, many colleges do not set a threshold line for English grades when admitting students, thus leading to a wide range of students' English proficiency. This also has a great impact on the teaching of spoken English in college. Learning motivation is the tendency to guide and maintain all kinds of learning activities and is a kind of internal motivation to directly promote students to study. Most of the students' English foundation is poor, coupled with the fact that high school English teaching is mainly focused on grammar learning, with the aim of getting high marks, and the classes are boring and tedious. This results in most students not being interested in English and students lacking the intrinsic motivation to learn to speak. From a pedagogical point of view, speaking instruction is mainly based on traditional classroom teaching. Students have fewer opportunities for oral input, and their oral output naturally becomes less [2].

The classroom ecological view emphasizes the creation of a harmonious and sustainable classroom ecological environment, which provides new ideas to solve the problems of imbalance and stagnant development of professional English speaking classroom ecology in the context of information technology. On the basis of following the principles of wholeness, interaction, balance, and sustainable development of educational ecology, enhancing the synergy of English speaking classroom ecological factors and promoting interactive dialogue among ecological subjects by using speech recognition will help give full play to the advantageous role of information technology in English speaking teaching reform, maintain the dynamic balance of English speaking classroom ecology, and promote its sustainable development.

Intelligent teaching method advocates use modern computer information technology to realize intelligent learning, improve students' advanced thinking ability and innovation training, and meet students' personalized development needs [3]. Instructional tools refer to the tools, media, or equipment used by teachers and students to transfer information in teaching and have undergone development from traditional means such as oral language, written text, and printed textbooks to modern means characterized by electronic audio-visual equipment, multimedia networks, and current applications of big data, virtual reality technology, and artificial intelligence technology. The modern teaching approach has changed the traditional teaching and learning methods, stimulated students' curiosity and desire for knowledge, and revitalized classroom teaching. The impact of technological breakthroughs and updates on teaching as an activity is far-reaching and extensive.

In terms of teaching philosophy, teachers should adhere to the "student-centered" basis, make reasonable use of the advantages of information technology, prevent information

technology from dominating the center of teaching or teachers from dominating classroom discourse, give students the opportunity to fully develop their potential, let students become the subject of designing learning activities, participate in the whole process of teaching, and be able to discuss, analyze, and formulate learning goals, learning plans, and learning strategies on their own and make full use of information technology tools and resources to promote the transformation of students' learning into open, personalized, and inquiry-based learning, helping students master language knowledge, improve their comprehensive language skills, and develop sustainable learning abilities in the process of learning to learn. In terms of teaching environment, as mentioned above, the overlimited teaching environment has become a limiting factor for English speaking classroom teaching. If the number of students in the class cannot be changed, teachers can adopt group teaching, change the classroom tables and chairs according to the actual teaching needs, create open and simulated communicative scenarios with the help of Internet resources, optimize the classroom ecological environment, and increase students' opportunities to use language. At the same time, teachers should make students fully aware of their main position in the classroom, maximize students' learning enthusiasm and autonomy, allow students to adjust their learning methods according to their own learning situation, and collect timely learning feedback to further improve teaching. In terms of teaching content, the development of modern information technology provides rich learning resources for oral English learning.

Teachers should integrate learning resources according to the actual teaching needs and feedback from students and pay attention to the integration of knowledge and ability as well as the integration of language and culture in the teaching content, build a cobweb-type knowledge structure, broaden the breadth and depth of language materials, and improve students' ability to think and use language. Finally, the evaluation subjects in the reform of English speaking informatics teaching include teachers and students, but the content of evaluation often revolves around the completion of students' language output tasks. To enable students to construct knowledge and improve their comprehensive literacy in a purposeful and targeted manner, the evaluation of students can also be extended to include their learning attitudes, potential, learning habits, and management. In addition, teachers and students can also evaluate teachers' teaching methods, teaching software, teaching content, and teaching environment to help teachers obtain feedback and improve their teaching in a more targeted and efficient way. Of course, the evaluation is not limited to simple score evaluation but can also be done in the form of interviews, questionnaires, and learning and resource usage data collection, in order to further optimize the teaching of spoken English. The communication and interaction between the subjects of the teaching ecology help transfer knowledge, information, emotion, and intellectual energy, which is the fundamental reason for the evolution of the English classroom ecology. Interaction in the ecological classroom includes group activities between teachers and students.

The ecological subjects of teaching should actively communicate with each other and coordinate with each other in dialogue and interaction to achieve common development. The application of information technology is a double-edged sword for the interaction between ecological subjects.

The popularity and high-speed development of the Internet help subjects to communicate with each other in real time through the network platform, but due to the advantages and disadvantages of the network environment, the subjective willingness of subjects to communicate, and the differences in ideas and goals, this kind of communication relying on electronic screens often has a certain lag and is not conducive to the emotional interaction between subjects. The emotional interaction between teachers and students is a catalyst for cognitive activities and an important condition for successful teaching. According to the ecological view of the classroom, teachers and students should communicate with each other in a timely manner and have equal dialogue with each other. Active, effective, and regular communication helps teachers and students achieve subjective construction and development of both teachers and students while transferring and exchanging knowledge. The teachers should abandon the indoctrination teaching method and emphasize the communication, sharing, and feedback between teachers and students as well as between students, so that students can explore, choose, and construct their own knowledge in an open and free atmosphere. In addition, teachers can guide students to gradually form “learning communities” through regular cooperative learning and communication. This not only helps students to reduce their discomfort and anxiety in the face of information-based teaching reform but also enables learning members with different knowledge structures, thinking styles, cognitive styles, and learning habits to complement each other. In addition, the “learning community” can help students understand the relationship between the individual and the group and between the parts and the whole and cultivate their sense of responsibility and team consciousness.

In recent years, artificial intelligence based on information technology and college English education have entered the stage of integration and innovation, which is rapidly overturning the educational ideas and methods accumulated for thousands of years and reconstructing the educational ecology. Intelligent speech technology, English language assessment system, language translation, intelligent oral practice, adaptive system, personalized learning center, and intelligent tutor system are widely used in college English teaching, bringing unprecedented opportunities for college English teaching. It provides a solution to the decades-old problems of insufficient teaching resources, difficulty in practicing “teaching to students according to their abilities,” and unscientific course evaluation in the field of college English teaching. It is obvious that the traditional teaching objectives, curriculum and teaching mode, and teachers’ expertise are not sufficient to cope with the needs of the new generation of AI technology. We must actively seek changes to find the right fit between AI and college English education.

The main contributions of this paper are the following: (1) the application and current situation of computer tech-

nology in English teaching are analyzed. (2) In order to overcome the backwardness and low accuracy of pronunciation evaluation methods, this paper applies deep learning in computer information technology to English speech recognition and constructs an LSTM-based speech recognition model to improve recognition accuracy. (3) Based on this, multiple parameters are considered to establish a reasonable and objective English speech recognition and pronunciation quality evaluation model.

2. Related Works

2.1. Current Research on College English Education in the Information Age. The practice of English speaking course reform has for a long time ignored the new characteristics arising from the encounter between information technology and professional English, thus triggering conflicts among the ecological elements within the teaching system and hindering the sustainable development of English speaking classroom ecology in the context of information technology. Teachers should conform to the development of the informatization era, grasp the advantageous role of information technology, and follow the principles of wholeness, interaction, balance, and sustainable development of the educational ecology to target and reconstruct the dynamic balance of the English speaking classroom ecology and promote the dual sustainable development of English speaking teaching and students’ speaking ability.

As students improve their knowledge structure and their critical thinking skills, their overall English skills improve significantly. In fact, however, only reading skills have improved significantly for most modern students. Other skills, especially spoken English, have been stagnant for a long time after entering school and have remained stagnant at the level of life-like expression [4]. There is a lack of connection between the teaching and learning of English in schools and the professional needs of modern students. Most students regard English courses, English majors, and personal ideas as separate entities that are difficult to create relationships and lack the ability to express professional knowledge content and personal understanding in English. In terms of output, after a period of learning English, students still have a variety of significant problems with their English speaking and writing skills, such as the living of content and the Chinese of language. Modern English language teaching requires students to learn the content of language knowledge from the shallow to the deep, while life-like language expressions are only stagnant at the bottom. If they stay at the level of life-like expressions for a long time, students will develop a kind of stereotype or fixed expression habit and then lack the desire and courage to break the fixed pattern at the psychological level.

In the past, English classes relied on a variety of auxiliary education tools, such as courseware, videos, and modern media. Even though they could strengthen the amount of educational information in a fixed time and improve the perceived effectiveness, they also restricted the initiative of teaching and learning to a certain extent. Second, teachers and students continue to use the classroom as the primary

formal site for teaching and learning. In the modern era of rapid development of artificial intelligence as well as the Internet, classroom formatting may lead to the loss of a wider scope of English education. Today, many schools in China are reducing the number of classrooms in their talent development programs. If you want to complete your school's English language education in listening, speaking, reading, writing, and general skills, it is difficult to do so with only a fixed number of hours, and some students will seek higher levels of English learning. Therefore, the formatting of the English curriculum has significantly constrained the development of English language teaching in terms of specific educational tools, educational content, and educational effectiveness [5].

Artificial intelligence is an interdisciplinary frontier discipline that is gradually transforming human thinking forms and traditional concepts and optimizing human knowledge and education. In the history of education development in our country, computer information technology provides great impetus for education reform, makes education work more efficient and effective, and makes education gradually fair and popular. In the era of artificial intelligence, these problems will be solved with the widespread application of catechism, adaptive learning systems, personal learning centers, intelligent tutors, etc., spawned by big data technology, computer vision, intelligent speech technology, and natural language processing technology [6]. The highly intelligent application of artificial intelligence in college English teaching is mainly reflected in the following aspects:

Intelligent teaching assistant system: there is a great lack of empirical research on robots supporting foreign language learning in China. For example, some learning systems create virtual interactive platforms for foreign language learners to provide interactive English listening and speaking courses [7, 8]. For example, Apple's Siri and Baidu's Xiaodu are intelligent machines based on big data. Machine translation systems can also be used to assist in teaching [9, 10]

Virtualized teaching: using holographic projection or VR technology, scenes from books, such as history and culture, can be presented in an immersive way to achieve true experiential immersion and improve student interest and learning [11]. "Second Life" is a free virtual 3D space developed by Linden Lab in 2003, which allows users to connect socially through speech and text. In addition to virtual social networking, "Second Life" can also be used for online teaching [12]. Teachers and students can conduct teaching activities in the various virtual spaces created by Second Life, simulating various scenarios in English listening and speaking instruction. This approach not only greatly enhances the fun of learning English for students but also increases the interactivity of learning

2.2. Status of Research on Speech Recognition Based on Deep Learning. Speech recognition is the research of how to convert speech information into text information. The areas of studies in speech can be subdivided into speech recognition, speech synthesis, and vocal recognition. It is involved in signal processing, natural language processing, etc. [13]. At the present stage, China's scientific and technological strength

has been greatly enhanced, and the old and relatively obsolete speech recognition technology is no longer able to meet the development speed of modern society. Although many intelligent terminal devices now have speech recognition function, which can complete the information exchange between human and machine, the accuracy and speed of speech recognition still need to be strengthened, and the current speech recognition algorithm and related technology are difficult to continue to develop. In this context, deep learning has become an important way to further develop speech recognition technology, which can perform pattern learning and information perception like human brain, and has a lot of theoretical research. However, deep learning is mostly in the theoretical stage and has not yet been widely applied to practical products. In order to solve this problem and promote the integration of theory and products, it is necessary to strengthen the research and development of key parts of speech recognition function, such as speech signal generation and propagation, so as to promote the better development of speech recognition technology.

In 2006, Ghasemi et al. proposed a deep belief network (DBN) with a greedy layer-by-layer unsupervised learning algorithm as its core [14]. The multilayer perceptron was pretrained by DBN and then fine-tuned by backpropagation algorithm. It provided an effective way to solve the problems of overfitting and gradient disappearance in deep network optimization. Novoa et al. contributed to the success of this practice. They used deep neural network (DNN) instead of GMM in the traditional Gaussian mixture model-Hidden Markov (GMM-HMM) system and proposed the DNN-HMM recognition method with phoneme states as the modeling unit, which significantly reduced the false recognition rate and brought it into the acceptable range for real users [15]. Compared to the GMM-HMM, the DNN replaces the GMM, and the states of the speech signal correspond to the observations using a deep neural network to build a simulated ensemble. The dimensionality of the output vector corresponds to the number of states of the HMM.

The use of convolutional neural networks (CNNs) for speech recognition mainly consists of stacking convolutional and pooling layers to obtain higher-level features. These layers are topped with a standard fully connected layer, representing the HMM state, which integrates the features trained in the network. It is better for speaker or mood changes. An increasing number of researchers have explored convolution on both the temporal and frequency axes [16].

These explorations and experiments show that the performance of CNN in DNN-HMM model is better than that of fully connected DBN. This is because DBN interprets input in any order, but in fact, the features of speech are closely related to frequency and time, and weight sharing enables CNN to capture these local correlations. Secondly, weight sharing and merging help CNN to capture equal variation differences and achieve better robustness and stability. For DBN, capturing such invariance at small frequency and time offsets requires a large number of parameters. Sainath et al. proved that CNN has better performance than DBN for large vocabulary tasks [17]. These experiments were carefully optimized by means of hyperparameter adjustment,

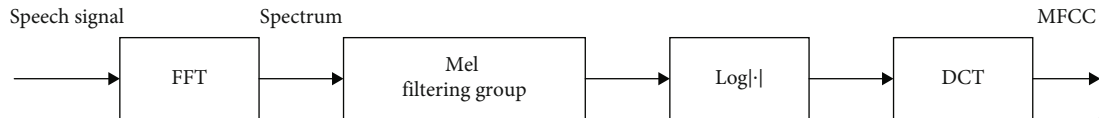


FIGURE 1: Extraction process of Mel frequency cepstrum coefficient.

limited weight assignment, and sequence training. Hsiao et al. studied the acoustic model of low resource language based on CNN and concluded that CNN could provide better robustness and generalization performance than DBN under the condition of low resource language [18].

Recurrent neural networks (RNN) can be used to process temporal signals. By adding feedback connections to the hidden layer, the input at the current moment is divided into two parts: (1) the input generated by the input sequence of the current moment, which is the same as the ordinary feed-forward neural network, and the transmitted neural network obtains the feature representation. (2) The second is the input generated by information retained in memory from the previous moment. Through this mechanism, the RNN can take advantage of the previous information [19, 20]. This acoustic model is further studied in literature [21]. Some progress has been made by using context-dependent speech units, using context-dependent states of LSTM output space, and using distributed training methods [22, 23]. Unlike the existing methods, the method proposed in this paper combines the Mel frequency cepstral coefficients and LSTM, while incorporating a multivariate model for evaluating the quality of English pronunciation.

3. Algorithm Design

3.1. English Speech Signal Data Enhancement. Before the speech signal is analyzed and processed, it needs to be enhanced with preprocessing, including preemphasis, windowing, endpoint detection, and noise filtering. This paper adds the noise in natural scenes to the existing Tibetan language data at different signal-to-noise ratios to achieve the effect of data enhancement and data expansion, respectively. In this study, the Mel frequency cepstrum coefficient (MFCC) feature parameter based on auditory characteristics is used to transform speech from the time domain to the cepstrum domain and extract speech features. The extraction process of MFCC is shown in Figure 1. The extraction process of Mel frequency cepstrum coefficients mainly includes the steps of FFT transformation, sister filtering, and logarithmic transformation. The noise and nonrelevant contents are filtered by nonlinear transformation.

The main extraction algorithms are fast Fourier transform (FFT), Mel filter, logarithmic operation, and discrete cosine transform (DCT). MFCC feature parameters will be used as input to the speech recognition model [24, 25]. The speech signal preprocessing is implemented by a first-order FIR high-pass digital filter in the MATLAB system digital filter toolbox. Adding windows to process the speech waveform is done using the Hamming windows, which are implemented by the window function normalized DTFT amplitude function in the MATLAB system speech toolbox.

The speech endpoint detection is implemented by Voicebox function in MATLAB system speech toolbox. The feature extraction process of speech signal based on Mel frequency cepstrum coefficient is implemented by MATLAB combined with speech toolbox programming.

3.2. LSTM-HMM-Based Model for Recognition of Spoken English. To improve the ability to fit the phoneme state distribution, LSTM is used instead of DNN and GMM. By training the LSTM, the posterior probabilities γ_t of different acoustic features can be represented, and the state S1 to S2 transfer probabilities are denoted by a_{s1s2} . The input feature of LSTM is MFCC. The number of nodes and hidden layers of the hidden layer can be determined according to the complexity of the task. The corresponding label data can be obtained through DNN model. The specific flow is shown in Figure 2.

The LSTM-HMM model first fuses contextual information through a multilayer LSTM, while the speech features are further extracted semantically through deep learning. If the input time series is long, it will inevitably exist the phenomenon of gradient disappearance; that is, the traditional RNN cannot model the long-term information very well. Because LSTM is commonly used in speech recognition research, the hidden layer neurons in a traditional RNN are replaced with LSTM memory blocks. The output of the hidden layer neurons of the LSTM is mainly completed by the LSTM memory block [26, 27]. The structure of the memory block is composed of four parts, which are memory cell, forget gate, input gate, and output gate. Among them, the memory block of LSTM mainly keeps the information that has influence on the present before the input sequence, and it is the core content of LSTM. The output of the memory cell of the previous moment together with the output of the hidden layer of the previous moment affects the memory and output of the memory block of the next moment. The function of the forget gate is to delete information in the memory block that has no effect on the present, and the function of the input gate is to keep the input useful information in the memory block. These two controls control the backward transmission of the memory delay time. The output gate controls how the output of the memory block is performed based on the current cell state.

The output of the input gate of the i th LSTM memory block in the hidden layer is

$$\hat{a}_i^t = \sum_j w_{ji} s_j^t + \sum_{k=1}^K \bar{w}_{ki} h_k^{t-1} \hat{w}_{ii} s_i^{t-1}, \quad (1)$$

$$\hat{b}_i^t = f(\hat{a}_i^t). \quad (2)$$

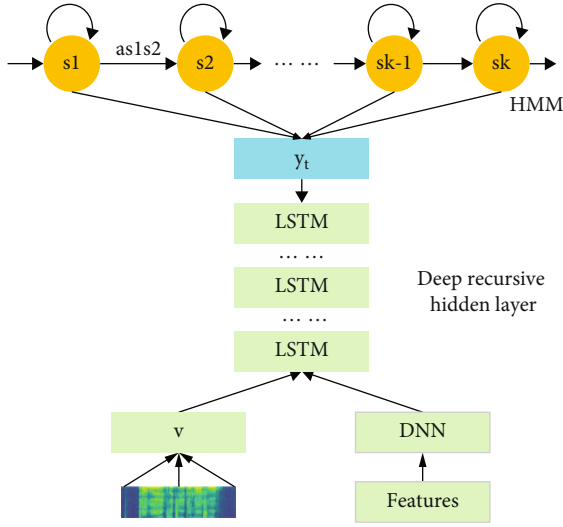


FIGURE 2: LSTM-HMM model.

Equation (1) gives the calculation process of the hidden layer of LSTM, and the result is brought into Equation (2) to get the output. The output of the forgetting gate of the i th LSTM memory block in the hidden layer is

$$\tilde{a}_i^t = \sum_j w_{ji} x_j^t + \sum_{k=1}^K \tilde{w}_{ki} h_k^{t-1} + \tilde{w}_{ii} s_i^{t-1}, \quad (3)$$

$$\tilde{b}_i^t = f(\tilde{a}_i^t). \quad (4)$$

That is, the outputs of both gates are determined by the current input x_j^t , the output h_k^{t-1} of each memory block at the previous moment, and the output s_i^{t-1} of this memory block at the previous moment, using Sigmoid as the activation function, and the outputs of the memory blocks are shown below:

$$s_i^t = \tilde{b}_i^t g(a_i^t) + \tilde{b}_i^t s_i^{t-1}. \quad (5)$$

3.3. A Multi-Covariate Model for Evaluating the Quality of English Pronunciation. The block diagram of the multiparameter English pronunciation quality evaluation model is shown in Figure 3. In this study, the correlation coefficient between the MFCC feature parameters of standard utterances and the MFCC features output from the speech recognition model is used as the quantitative index of pronunciation accuracy to judge whether the pronunciation is clear and accurate. The speech rate evaluation is quantified using the ratio of the standard utterance duration to the test utterance duration. The rhythm evaluation uses the pairwise variability index (PVI) proposed by Low of Nanyang Technological University, Singapore, to calculate the respective rhythmic correlation between the standard utterance and the input utterance.

It is worth noting that according to the durational variability feature of English speech unit durations, this paper uses the improved dPVI parameter calculation formula to

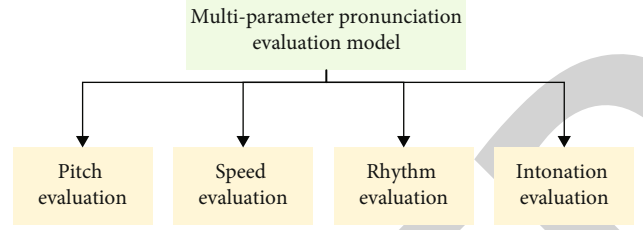


FIGURE 3: Multiparameter English pronunciation quality evaluation model.

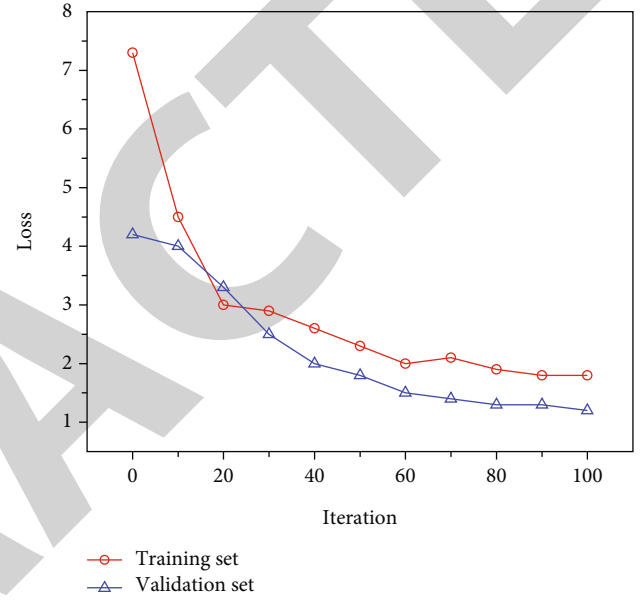


FIGURE 4: Loss variation during training.

compare and calculate the syllable unit segment durations of standard and test utterances separately, and the converted parameters are used as the basis for systematic evaluation, as shown in

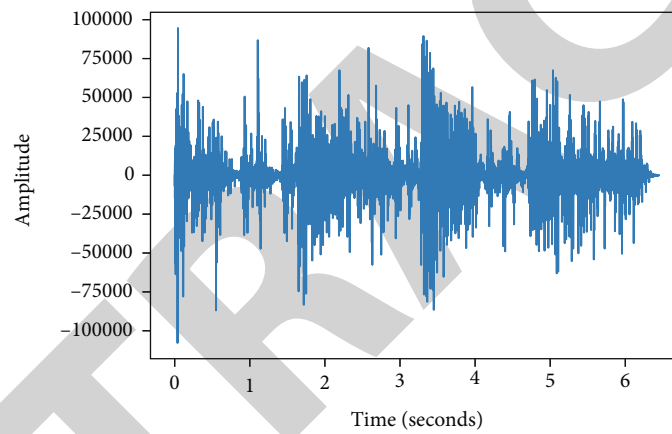
$$\text{dPVI} = 100 \times \frac{\sum_{k=1}^{m-1} |d1_k - d2_k| + |d1_t - d2_t|}{\text{Len}}, \quad (6)$$

where d is the length of the speech unit segment of the sentence division (e.g., d_k is the length of the k th speech unit segment), m is min (Std. units, test units), and Len is the length of the standard utterance. Since the test utterance length has been regularized to be comparable to the standard utterance length before the PVI operation, only Len can be used as the calculation unit.

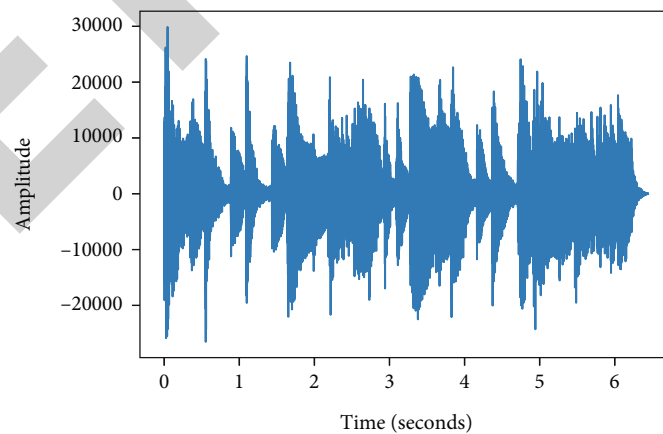
3.4. Sensor Control System. The sensor control system mainly includes the following functions: the voice acquisition and recognition unit is responsible for the conversion of external sound from analog signal to digital signal and digital signal to control command. The voice remote extension processing unit is used to process the remote voice information incoming through Wi-Fi and access the information to the voice acquisition and recognition unit for



FIGURE 5: Performance variation during training.



(a) Original speech



(b) Enhanced speech

FIGURE 6: Comparison before and after enhancement.

processing and subsequently return the feedback information of the voice processing result to the voice remote extension unit. For better interactive experience, this system implements a traditional interface interaction terminal based

on voice interaction, which is responsible for information display and system configuration. The control and feedback unit uses a network composed of ZigBee wireless sensors to control all terminal devices online, while receiving their

TABLE 1: Effect of data enhancement on speech recognition models.

Dataset	Error rate (%)	
	Without enhancement	Enhancement
Training set	35.49	30.58
Validation set	34.92	28.72
Test set	31.03	25.96

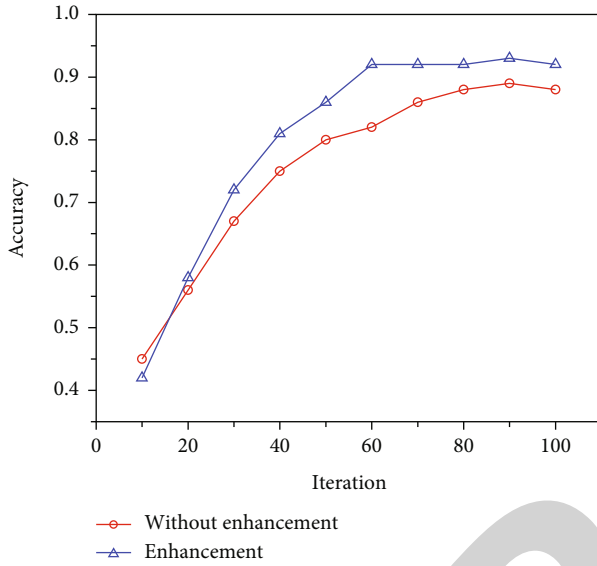


FIGURE 7: Accuracy curves on the validation set with and without enhancement.

TABLE 2: Comparison with commonly used methods on the test set.

Dataset	Error rate (%)	
	Without enhancement	Enhancement
GMM-HMM	33.69	31.24
DNN-HMM	30.58	29.48
CNN-HMM	29.73	27.85
Methodology of this paper	31.03	25.96

feedback information and making corresponding processing work.

4. Experiments

4.1. Experiment Preparation. In this paper, an English speech database constructed by retrieval on the web is used. The data were mainly obtained from websites related to English language education. The dataset is the pronunciation of specific English utterances after the extraction of the 13th-order MFCC feature parameters. It includes a total of 8800 speech data (88 persons pronouncing 10 utterances, each utterance repeated 10 times), with 44 men and 44 women between the ages of 18 and 26. Before MFCC feature parameter extraction, the sampling rate is set to 16 kHz, 16-bit coding is used,

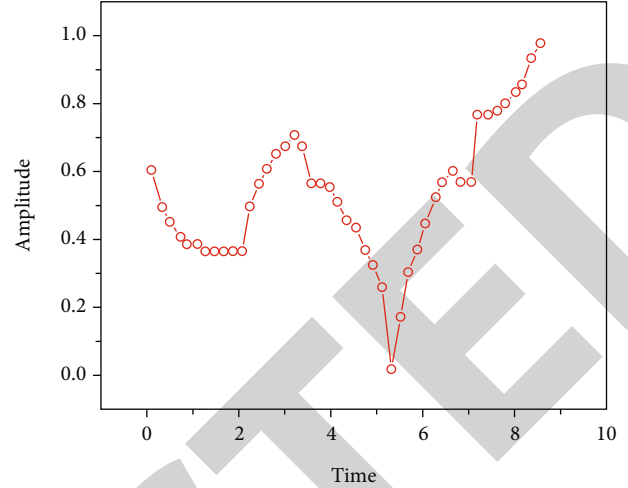


FIGURE 8: Intonation curves of standard speech.

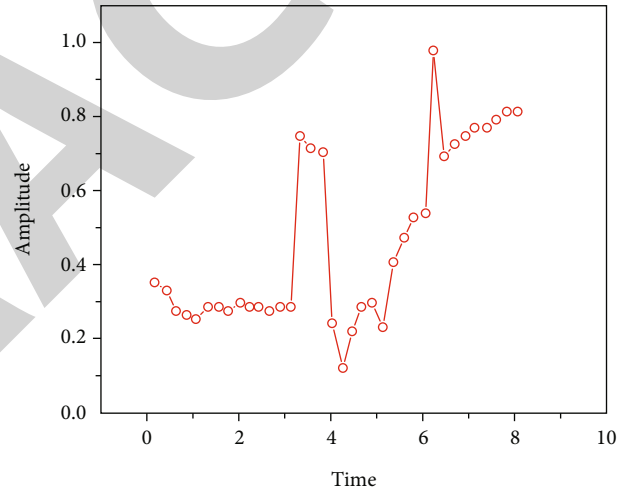


FIGURE 9: Intonation curves of test speech.

TABLE 3: Analysis of pronunciation evaluation effect (%).

Indicators	Evaluation Diversity		
	Agreement rate	Adjacent agreement rate	Pearson
Pitch	86.25	99.58	0.8
Speech	82.08	100.00	0.493
Rhythm	85.00	98.75	0.543
Intonation	80.00	98.33	0.627

and the Hamming window plus window function is used with a preemphasis filter function of $1 - 0.97Z^{-1}$. The dataset is divided into training set : validation set : test set = 60 % : 15% : 25%. The experimental environment is RAM 128 GB and Nvidia 3090 GPU; operating system and software platform are Ubuntu 20.04, TensorFlow 1.14, and Python 3.7. and Python 3.5.

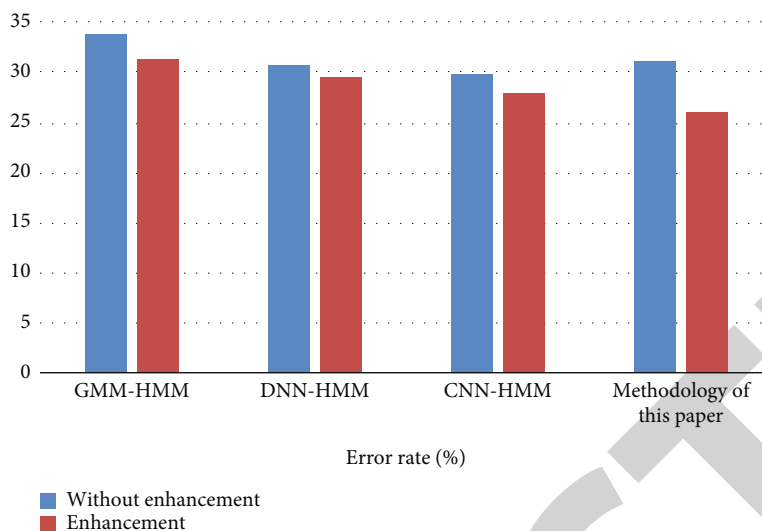


FIGURE 10: Analysis of pronunciation evaluation effect (%).

LSTM uses gate structure and memory cells to control the information flow of the input model, which enables the information to be propagated over a longer period of time and has better modeling capability for contextual information. The LSTM-HMM model structure built in this paper contains three hidden layers; each layer consists of 256 memory cells. All the hidden layers in the model are connected with ReLU number with an initial learning rate of 0.008, and the output layer uses softmax function for classification with an initial learning rate of 0.001. A total of 100 iterations of Epoch are used for model training, and the loss curves and performance improvement on the training and validation sets are shown in Figures 4 and 5. As can be seen in Figures 4 and 5, the model is trained for 100 rounds, and the model performance reaches the optimum at around 80 rounds while the loss converges.

4.2. Analysis of the Effect of Data Enhancement Processing.

In this paper, the “babble” noise in natural scenes is used to enhance the data by the method of additive noise. The waveforms of the speech data are shown in Figure 6. The original spoken training data is relatively clean, as shown in Figure 6(a), and can be regarded as the data in an ideal environment. In contrast, there are various kinds of noise in natural scenes, which have a greater impact on the speech data. Therefore, this paper performs data enhancement by adding noise as shown in Figure 6(b), and it can be seen that the speech after adding noise is closer to the data in real scenes.

Table 1 shows the effect of the model after training the model using the original training data and the augmented training data, where the word recognition error rates on the training set, validation set, and test set are shown. It can be seen that training with the augmented data can significantly improve the performance of the model and make the speech recognition model more robust in its representation of utterances. Figure 7 shows the change in accuracy on the validation set with and without enhancement during

training. With enhancement, not only the accuracy of the model is improved but the speed of fitting is also improved.

4.3. Analysis of the Effect of Spoken English Recognition.

Table 2 shows that with the data enhancement, the end-to-end model has a recognition word error rate of 25.96%, and the error rate is reduced by 5.07%. The performance of the proposed model in this paper exceeds other models.

4.4. Analysis of the Effect of English Pronunciation Evaluation.

Speed rate and pitch are relatively easy to evaluate. Intonation evaluation is more difficult. Intonation evaluation is designed to automatically judge whether the intonation of the pronunciation is standard by means of computation and indicate the difference between it and standard pronunciation. In intonation studies, pitch is the most basic and important constituent of intonation. Figures 8 and 9 show the articulatory intonation curves of standard and test speech extracted by the autocorrelation function method. The phonetic material form of pitch is expressed as the fundamental frequency variation of the vocal folds. From the change of fundamental frequency, different patterns of intonation height rise and fall changes can be determined; i.e., pitch can determine different patterns of intonation rise and fall. Therefore, the key to intonation evaluation is to extract the pitch corresponding to each frame of speech signal in a sentence.

For college student groups with different English speaking levels and with the suggestions of relevant English speech experts, various grades were set separately for different evaluation indicators (pitch, speed, rhythm, and intonation) as well as for the overall evaluation. Given that the subjectivity of the teachers in the manual evaluation process may have an influential impact on the evaluation results, the coefficient was used in this paper to test the reliability of the manual evaluation results. Moreover, the evaluation results of the two teachers were averaged (rounded off) to obtain each evaluation index and the overall score of different

sentences for different students as the final manual evaluation results. The experimental results are shown in Table 3 and Figure 10. The higher the indexes in the table, the better the model proves to be. The adjacent agreement rate of all four indexes can be close to 100%, among which the evaluation validity of pitch is the most accurate.

5. Conclusions

With the fast improvement of computer information technology capabilities in the Internet era, the appearance of application algorithm platforms such as Baidu, Tencent, and Xunfei has continued to promote the deep deployment of AI applications. Intelligent applications have gradually emerged on an exploding scale and serve all levels of university English teaching. Today's smart classrooms, smart translators, smart human-computer dialogue software, and smart writing correction software are just the beginning of language learning intelligence. In the age of information technology, school education should update its teaching concept to achieve personalized, intelligent, and interactive learning by virtue of advances in artificial intelligence technology. This paper explores the problems in the evaluation of college English voice recognition and pronunciation qualities. In the aspect of spoken English learning, some computer-assisted language study systems at home and abroad mainly focus on the learning of words and grammar, with only one or two evaluation indexes as the basis of evaluation, which have certain functional defects and can only give learners an aggregate score for their pronunciation. In terms of English speaking evaluation, English speaking test is still based on manual scoring with strong subjective will, different standards, and slow speed, which is more subjective and less repeatable and stable. To address these problems, this paper proposes an LSTM-HMM-based English speaking recognition method and considers multiparametric evaluation index method. The speech recognition model proposed in this paper has been experimentally verified to have a high accuracy rate. The adopted evaluation methods are credible and can give learners timely, accurate, and objective evaluation and feedback guidance to help learners find out the differences between their own pronunciation and the standard pronunciation, thus improving the efficiency of learning spoken English. In the future, we plan to conduct research on the integration of computer information technology and university English education using knowledge graph and graph convolution based.

Data Availability

The datasets used during the current study are available from the corresponding author on reasonable request.

Conflicts of Interest

The author declares that he has no conflict of interest.

Acknowledgments

This work was supported by the Teaching Reform in Hunan Province (HNJG-2021-0957): Research and practice of blended teaching mode of college English reading and writing course under the background of "gold course."

References

- [1] Z. Zhijie, "Analysis of college English teaching strategies in the context of globalization," *Agro Food Industry Hi-Tech*, vol. 28, no. 1, pp. 968–972, 2017.
- [2] Z. Wu, H. Li, X. Zhang, Z. Wu, and S. Cao, "Teaching quality assessment of college English department based on factor analysis," *International Journal of Emerging Technologies in Learning*, vol. 16, no. 23, pp. 158–170, 2021.
- [3] Y. Dan-Ping, "College English interactive teaching mode under an information technology environment," *Agro Food Industry Hi-Tech*, vol. 28, no. 1, pp. 534–537, 2017.
- [4] P. Zhou, X. Wu, H. Xu, and G. Wang, "The college students' oral English education strategy using human-computer interaction simulation system from the perspective of educational psychology," *Frontiers in Psychology*, vol. 12, 2021.
- [5] M. Liu, "Research on college English teaching reform under "Internet plus applied talent" training mode," *Agro Food Industry Hi-Tech*, vol. 28, no. 3, pp. 3363–3365, 2017.
- [6] L. Hu and W. Yao, "Design and implementation of college English multimedia aided teaching resources," *The International Journal of Electrical Engineering & Education*, vol. 2021, article 002072092098351, 2021.
- [7] J. Li and H. Chen, "Construction of case-based oral English mobile teaching platform based on mobile virtual technology," *International Journal of Continuing Engineering Education and Life Long Learning*, vol. 31, no. 1, pp. 87–103, 2021.
- [8] P. Wang and S. Qiao, "Emerging applications of blockchain technology on a virtual platform for English teaching and learning," *Wireless Communications and Mobile Computing*, vol. 2020, Article ID 6623466, 10 pages, 2020.
- [9] M. Yamada, "The impact of Google neural machine translation on post-editing by student translators," *The Journal of Specialised Translation*, vol. 31, pp. 87–106, 2019.
- [10] S. Xie, Y. Xia, L. Wu, Y. Huang, Y. Fan, and T. Qin, "End-to-end entity-aware neural machine translation," *Machine Learning*, vol. 111, no. 3, pp. 1181–1203, 2022.
- [11] M. Holly, J. Pirker, S. Resch, S. Brettschuh, and C. Gütl, "Designing VR experiences—expectations for teaching and learning in VR," *Educational Technology & Society*, vol. 24, no. 2, pp. 107–119, 2021.
- [12] S. C. Baker, R. K. Wentz, and M. M. Woods, "Using virtual worlds in education: Second Life® as an educational tool," *Teaching of Psychology*, vol. 36, no. 1, pp. 59–64, 2009.
- [13] O. Z. Mamyrbayev, K. Alimhan, B. Amirgaliyev, B. Zhumazhanov, D. Mussayeva, and F. Gusmanova, "Multimodal systems for speech recognition," *International Journal of Mobile Communications*, vol. 18, no. 3, pp. 314–326, 2020.
- [14] F. Ghasemi, A. Mehrdehnavi, A. Fassihi, and H. Pérez-Sánchez, "Deep neural network in QSAR studies using deep belief network," *Applied Soft Computing*, vol. 62, pp. 251–258, 2018.
- [15] J. Novoa, J. Fredes, V. Poblete, and N. B. Yoma, "Uncertainty weighting and propagation in DNN-HMM-based speech

Retraction

Retracted: Wireless Sensor Network and AI Application for Educational Technology Course

Journal of Sensors

Received 23 January 2024; Accepted 23 January 2024; Published 24 January 2024

Copyright © 2024 Journal of Sensors. This is an open access article distributed under the Creative Commons Attribution License, which permits unrestricted use, distribution, and reproduction in any medium, provided the original work is properly cited.

This article has been retracted by Hindawi following an investigation undertaken by the publisher [1]. This investigation has uncovered evidence of one or more of the following indicators of systematic manipulation of the publication process:

- (1) Discrepancies in scope
- (2) Discrepancies in the description of the research reported
- (3) Discrepancies between the availability of data and the research described
- (4) Inappropriate citations
- (5) Incoherent, meaningless and/or irrelevant content included in the article
- (6) Manipulated or compromised peer review

The presence of these indicators undermines our confidence in the integrity of the article's content and we cannot, therefore, vouch for its reliability. Please note that this notice is intended solely to alert readers that the content of this article is unreliable. We have not investigated whether authors were aware of or involved in the systematic manipulation of the publication process.

Wiley and Hindawi regrets that the usual quality checks did not identify these issues before publication and have since put additional measures in place to safeguard research integrity.

We wish to credit our own Research Integrity and Research Publishing teams and anonymous and named external researchers and research integrity experts for contributing to this investigation.

The corresponding author, as the representative of all authors, has been given the opportunity to register their agreement or disagreement to this retraction. We have kept a record of any response received.

References

- [1] X. Luo, "Wireless Sensor Network and AI Application for Educational Technology Course," *Journal of Sensors*, vol. 2023, Article ID 2093354, 11 pages, 2023.

Research Article

Wireless Sensor Network and AI Application for Educational Technology Course

Xiaoyue Luo 

Chongqing College of Electronic Engineering, Chongqing 401331, China

Correspondence should be addressed to Xiaoyue Luo; 200820025@cqcet.edu.cn

Received 26 August 2022; Revised 1 October 2022; Accepted 25 November 2022; Published 10 February 2023

Academic Editor: Sweta Bhattacharya

Copyright © 2023 Xiaoyue Luo. This is an open access article distributed under the Creative Commons Attribution License, which permits unrestricted use, distribution, and reproduction in any medium, provided the original work is properly cited.

Over the course of its long development, the modern educational technology curriculum has undergone several changes and amassed a lot of information. Theoretically speaking, the state places a strong priority on the use of IT in schools. Students majoring in education should take educational technology courses so that they can learn the characteristics and application techniques of core current information-based teaching media and incorporate them into their own lesson plans and classroom activities. This will help them meet the information needs of today's classrooms as they evolve with the advent of educational modernization and availability of educational information. Thus, this research employs a wireless sensor network (WSN) to gather and send data on ed tech classes and then employs AI to assess those classes' quality and guide real-time changes to how they are taught and complete the following tasks: (1) The development status of educational technology courses and WSN at home and abroad is introduced. (2) The application of WSN in teaching is introduced, the basic principle of GRU neural network and related optimization algorithms is expounded, and the quality evaluation system of educational technology courses is constructed. (3) The IPSO-Adam-GRU evaluation model improves the GRU neural network's hyperparameters with the help of the improved PSO approach and Adam gradient descent. The model is fed test data for evaluation, and the findings are compared to those from an expert's evaluation to determine how well the model performs. The results demonstrate that the model established for this article is superior to others since it provides a more accurate assessment.

1. Introduction

The 21st century is a century of high technology and a century of education. The competition between economy and technology is, in the final analysis, the competition of talents and education. The modernization of a country requires the modernization of talents. Only by realizing the modernization of the quality of talents can our education be in an invincible position in the competition [1]. The modernization of talent quality is largely dependent on education, and education reform often focuses on cultivating talents with a broad range of abilities. Currently, my nation is working hard to adopt high standards of education for its citizens. An emphasis on all-round, all-inclusive education is defined by cultivating creative abilities with inventive spirit and practical competence as its primary focus. High-quality education is a contemporary educational philosophy and way of thinking that aims to develop individuals into high-quality

talents capable of blending in with today's society [2]. The core of implementing quality education is curriculum reform. How to reform the educational technology curriculum in higher normal schools on the basis of quality education is the key to ensuring the quality of educational technology personnel training. Only through courses can the primary issues with developing educational technology courses and analyzing cutting-edge educational and teaching concepts be turned into real educational power [3]. A mediator between teaching and learning is the curriculum. The curriculum is taught in order to achieve the educational concepts, facts, and knowledge that teachers wish to impart. The quality of instruction is directly impacted by the concepts of curriculum setting, scientific curriculum design, and the efficacy of curriculum in teaching [4]. Books about instructional technology now come in numerous forms and editions. The contents of various editions of textbooks are various and complete. From teaching theory to educational technology

ability and from teaching resource production to teaching software operation, all include hardware operation and teaching software use. The basic knowledge of content, theory, and practice covers a wide range. With so many teaching contents, targeted learning is difficult for learners. Consequently, the creation of focused resources is a pressing issue in present education, and tailored instruction is difficult to accomplish with the existing material [5].

The traditional education systems have its own advantages but have associated issues like lack of flexibility, narrow scope of programs, lack of accessibility, cost issues, and monotonous learning experience. The rapid growth of Internet and advanced technologies has ignited the need of achieving quality education anywhere, anytime online considering the choice and pace of the students. The online education system requires data transfer, which also have associated issues in terms of availability of speed and optimized network communication to ensure students can access the resources seamlessly and conveniently. There are also issues relevant to inappropriate usage of data, insecure data transfer, and breaches performed by malicious third party vendor organizations.

Even in the research of educational software, the creation of courseware is fairly involved, and it is challenging for students to comprehend so many different teaching resources. The majority of the current textbooks on instructional technology are merely a collection of data points. The main problem with textbooks is the wide range of topics they cover and the variety of material they include. The learner base is relatively inconsistent, but in modern educational technology, teaching students of all majors is assumed to have the same level of learning. Despite this, learners from a variety of professional backgrounds are less likely to be consistent when it comes to their learning. Consequently, when instructing, we must accurately assess the abilities of our students, carefully craft our lesson plans to include both theoretical and practical information, and make necessary adjustments based on these considerations in order to avoid the failure of the lesson and the subsequent abandonment of the learning process halfway through [6]. Thus, achieving educational objectives requires logically organizing and adjusting the instructional content. It is crucial to adapt the curriculum and procedures when teaching with modern educational technology, finish the students' work in accordance with that level, and assess their level of proficiency. Under typical conditions, the course's teaching material should be integrated in accordance with the learner's overall capacity for practical application and professional caliber. Otherwise, the teaching content is out of the scope of the learner's ability level, and the teaching of the course will lose the value of knowledge imparting itself [7].

The content of modern educational technology courses is rich and complex, involving teaching theory, hardware installation and operation, software use, selection and personalized processing of teaching materials, and production of teaching courseware. This means that the entire teaching process must consider the range of learners' abilities to be more targeted and differentiated. The application of theory, the operation of software, and the production and process-

ing of courseware should all be matched in content. This course uses contemporary instructional technology. It is determined by Zhao et al.'s [8] properties and operations. Wireless sensor networks (WSNs) combine computer, network, and wireless communication technologies. Tiny sensors are placed throughout the monitoring area to collect data. This self-organizing wireless multihop network may be a good alternative when wired access cannot be used to transmit data at a high enough standard [9]. This paper uses the WSN to collect and transmit the data of educational technology courses and then uses AI to evaluate the quality of educational technology courses and adjust the teaching strategies of modern educational technology courses in time.

The unique contributions of the paper include the following:

- (i) Exploration of the development status of education technology courses and WSN at home and abroad
- (ii) Implementation of WSN, GRU neural network, and related optimization algorithm in teaching
- (iii) Development of IPSO-Adam-GRU evaluation model for achieved enhanced classification results

The organization of the paper is as follows: Section 2 discusses the review of related studies followed by the methodology adopted in Section 3. Section 4 presents the experimentation results and analysis and the conclusions are discussed in Section 5.

2. Related Work

To date, there are a total of 19 MOOC-related courses on major learning platforms that are part of a network resource course of contemporary educational technology courses. Students' understanding of the course's material is directly tied to the teaching content [10]. Massive open online courses (MOOCs) are free online courses available for any individual to enroll, thereby providing flexible and affordable means to learn new skills and technologies to progress in the professional career. The MOOCs are closely related to the needs of the industry, and it helps individual to learn skills that meet the demands of the industry following an extremely cost-effective process of learning. The courses are offered in diversified areas by professors from eminent universities. Internet connection is one of major requirements to avail such courses and could be a barrier in remote areas where connectivity is relatively low. Technical and theoretical knowledge points are the foundation of all current educational technology resource courses. When it comes to developing students' abilities and knowledge, most courses require students to create teaching scenarios using multimedia technology, apply conventional instructional methods, collect online educational resources, create personalized teaching resources, operate and apply software, evaluate information technology, and integrate curriculum and case studies [11]. Courses that cover the installation, debugging, and installation and configuring of satellite data receiving cards, the receipt and use of IP resources, and other

technical skills are also available. Knowledge of educational technology theory, teaching communication methods and theories, basic principles for selecting and implementing educational media, and fundamental principles for instructional design are all included in theoretical knowledge [12]. With the gradual promotion of educational informatization, teachers' educational technical ability needs to closely follow the lectures of educational informatization; a growing number of academic institutions and researchers have started to place greater emphasis on the development of teachers' educational technical skills. Normal students' capacity to use educational technology is taught in the contemporary educational technology course. Many academics use this course as a research entry point to improve the educational technology capability for normal students, according to the course's current teaching conditions. The key areas of curriculum innovation, teaching mode change, and teaching assessment are covered by research on modern educational technology [13]. Reference [14] redesigned the course by combining the concepts and methods of Intel's future education and training program in the modern educational technology course and developed a problem-solving and project-based learning methodology built on cutting-edge educational technologies. Reference [15] investigates and addresses the two basic difficulties of current educational technology public courses: content setting and experimental course creation. Reference [16] examines the use of task-driven teaching approaches in order to improve the quality and efficiency of present educational technology public classes. The ultimate objective is to provide all children access to cutting-edge instructional technologies. According to reference [17], the TPACK idea was included into the design of current educational technology public courses in order to give students with a fresh viewpoint on technology integration, therefore fostering their growth of educational technology application skills. Reference [18] constructed the "FLIPPR" flipped teaching model based on the modern educational technology courses and teaching characteristics of colleges and universities, applied it in teaching practice through experimental research, and finally verified the effectiveness of the "FLIPPR" flipped teaching model constructed. Modern educational technology public courses are now being taught using a "mixed and integrated" teaching model, according to reference [19]. The actual teaching of the course on current educational technologies was then conducted using this teaching methodology. The long-used teaching method can be used to teach modern educational technology in an efficient manner. Reference [20] examines and highlights issues with present teaching practices in the sector and offers solutions by contrasting the instructional strategies used by teachers of modern educational technology courses. As a new generation of sensor network, WSN has been given a high priority by all governments. It has been used in a wide range of industries in the United States, Japan, and other nations via constant research and development [21]. Intel Corporation and the University of California, Berkeley, lead research work on "dusting" technology. They succeeded in creating a fully functional sensor the size of a bottle cap that can perform functions such as

computation, detection, and communication. In 2002, Intel Research Labs researchers connected 32 sensors the size of prescription medicine bottles to the Internet to read the climate on Maine's "Big Duck Island" to assess the conditions of a petrel's nest [22]. In addition, Mitsubishi Electric Corporation has also successfully developed a small, low-power wireless module envisaged for WSNs, which can build a peer-to-peer network using specific low-power wireless [23]. My nation almost started researching WSNs and their modern uses at the same time as other industrialised nations. It initially made an official appearance in the information and automation field research report of the Chinese Academy of Sciences' "Knowledge Innovation Project Pilot Field Direction Research" in 1999. As one of the five major projects in terms of civilian use, WSNs involve urban public safety, public health, safety production, intelligent transportation, environmental monitoring, and other fields [24]. The study in [25] emphasized on improving remote music education using 5G networks. The network speed was identified to have the most significant impact on students' online classes. The framework implemented convolutional neural networks (CNNs) to train the intelligent system and also deliver remote music education to the students in the presence of 5G networks. The proposed system outperformed the traditional system and yielded an accuracy of 99.13 percent. The study in [26] used big data to upgrade the traditional system, promote coconstruction, and share digital resources and information. The study presented the concept of smart campus which focused on four spectrums, namely, student curriculum management module, information release and communication module, teaching support module, and daily office management module. The higher education management system used the WSN technology to seamlessly perform activities and ensure proper communication in the smart campus system. The study in [27] used the concept of flipped classroom in music teaching with the support of two technologies, namely, artificial intelligence and wireless networking. The teachers and students were able to interact with each other using interactive devices supported by intelligent networking technologies. The CNN module was implemented to ensure the system is smart and able to provide automatic classification of the course materials. The proposed model yielded an accuracy of 98.25% when compared with the traditional KNN system.

3. Method

3.1. Teaching Method Based on Wireless Sensor Network. The application in teaching needs to be based on the characteristics of the WSN. For example, code additions and improvements to wireless network protocols are performed. The application process includes the following: (1) analyze the course and find out the difficulties and key points that need to be used in the WSN experiment, for example, the antenna part involved in the foundation of wireless communication. Since this part of the content is very abstract and has strong theoretical knowledge, different types of antennas and performance parameters can be set through the platform in the classroom. Comparing the performance of different

types of antennas enables students to intuitively understand the impact of antenna design parameters on performance. In introducing the hidden terminal and exposed terminal of the carrier sense multiple access/collision avoidance (CSMA/CA) protocol, the influence of different parameters on the performance of the protocol is reasonably designed, and then, the simulation results are analyzed by using the chart tool. CSMA/CA is a protocol that is used for carrier transmission in the 802.11 networks. It was developed with an objective to minimize the potential of collision likely to occur when multiple stations send their signals over a data link layer. The CSMA first checks the state of the medium in each station before a transmission is started. This enables averting the potential collisions by listening to the broadcasting nodes and then guiding the devices to transmit the signal if the channel is free. Hence, when a node receives a packet, it ensures the channel is clear and no other node transmits at the same time. In case the channel is not clear, the node waits for a randomly chosen time frame and then rechecks the clearance of the channel which is called the backoff factor. The channel thus remains idle while the backoff counter reaches zero and the node transmits the packet. If the channel is not free, the backoff factor is reset and the process is repeated. (2) Design the corresponding network model according to the difficulty of the course. During the simulation, the network model is established according to the main purpose to be simulated. Sensor network, sensor network communication, and sensor network service make up the three key components of WSN design. Periodic experimental data, network topology data, and other basic data types can be used to categories the sensor nodes in the system. Along with the real data of these fundamental data kinds, the data to be conveyed in the sensor network should be able to discriminate between the data of these fundamental data types. This requires adding an identification header to the header of each data packet to be transmitted to indicate which data type the data packet to be transmitted belongs to. (3) Simulate and collect data through the network model. Once the network model is built, it is necessary to collect the simulation performance and statistics of the network protocol, such as the network delay performance of a certain protocol, packet loss rate, and extra service load. Statistics can be collected on a single object in a network model, or global statistics can be collected on the entire network. For example, if you want to know whether a site is a hidden terminal, you need to collect the relevant network performance of the site, such as packet loss rate and channel collision probability. Finally, the application framework of educational technology courses based on WSNs and AI constructed in this paper is shown in Figure 1.

3.2. Gated Recurrent Unit. Recurrent neural networks (RNNs) are a class of neural networks that are good at dealing with sequences of nonlinear features. An LSTM and a gated recurrent unit (GRU) are the most common RNNs. LSTM, a gated RNN that can successfully tackle the gradient vanishing issue of RNN, has gained a lot of interest following GRU. Based on the LSTM neural network, GRU has been enhanced and its gating mechanism is simpler than LSTM.

This greatly expedites the training process. The major advantage of using LSTM lies in its ability to address the vanishing gradient problem. The vanishing gradient problem makes network training difficult for long sequence of words or integers. The gradients are used for updating the RNN parameters, and in case of long sequence of words or integers, the gradients become smaller to an extent that no network training is possible to be performed. The LSTM networks help to eliminate such problems and enables capturing of long-term dependencies between keywords or integers in a sequence which is separated by large distance. The Hadamard product operation and sigmoid function are the GRU neural network's fundamental operations. The Hadamard product of two vectors is similar to the concept of matrix addition. The elements corresponding to the same row and column of the given vectors or matrices are multiplied together in order to form a new vector or matrix. It is a binary operation that considers two matrices of similar dimensions and produces another matrix similar to the dimension of the operands. In the sense, each element i, j is the product of the elements i, j of the two original matrices. The network is capable of forgetting and storing data in the range between zero and one when employing the sigmoid function. The structure diagram of GRU neural network is shown in Figure 2.

The GRU's reset gate, denoted in Figure 2 by the sign r_t , regulates how much of the past information is forgotten at once. The status of the buried layer is affected by the reduction in r_t because more information from the previous instant is lost. To regulate how much of the preceding moment's memory is kept in sync with the current state, z_t acts as the GRU neural network's update gate. The input and forgetting gates in LSTM are identical to the z_t , and the bigger the z_t , the more information is preserved at the present instant. Therefore, GRU neural network has higher training efficiency and less memory than LSTM.

Both the reset gate r_t and the update gate z_t are obtained by combining the input at the current moment with the state of the hidden layer at the previous moment. The reset gate output value r_t and the update gate output value z_t are shown in

$$r_t = \sigma(w_r x_t + u_r h_{t-1}), \quad (1)$$

$$z_t = \sigma(w_z x_t + u_z h_{t-1}). \quad (2)$$

The output of the hidden layer at the previous moment is to add the reset gate output to the current input x_t and put it into the Tanh activation function to get the current activation state \tilde{h}_t . The output n_z of the hidden layer at the previous moment and the activation state \tilde{h}_t of the current hidden layer are shown in

$$n_z = w x_t + u(r_t \otimes h_{t-1}), \quad (3)$$

$$\tilde{h}_t = \text{Tanh}(n_z), \quad (4)$$

where \otimes is the Hadamard product operation, W is the neural network weight of the hidden layer state at the previous

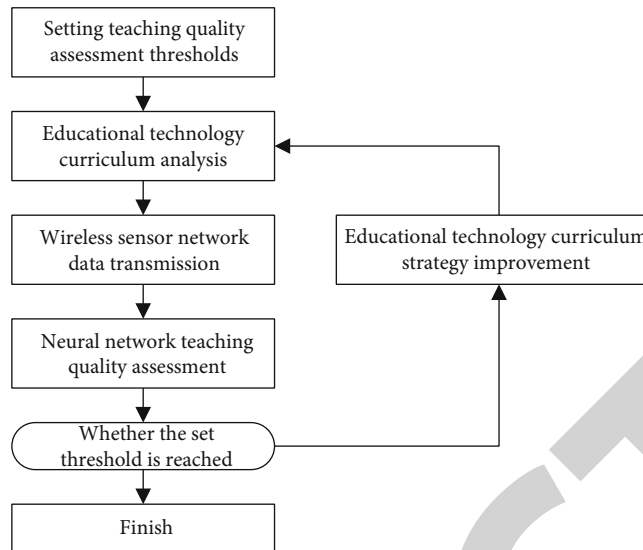


FIGURE 1: Framework of educational technology courses based on WSN and AI.

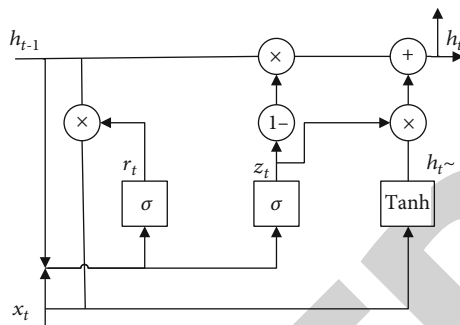


FIGURE 2: GRU neural network structure diagram.

moment, and u is the neural network weight when the state is input at the current moment.

The advantages of GRU over LSTM are as follows: z_t and $1 - z_t$ can process current and historical information at the same time, thus not only improving training speed but also saving running space. The hidden layer state h at the current moment is obtained under the combined action of the hidden layer state at the previous moment and the current hidden layer activation state, and the hidden layer state function h_t at time t is shown in

$$h_t = (1 - z_t)h_{t-1} + z_t\tilde{h}_t. \quad (5)$$

It can be seen from equations (1) to (5) that the GRU neural network does not increase over time and forget past information. The preceding data is instead effectively forgotten and preserved to the following GRU unit, establishing a dependence relationship between the prior moment and the present moment and preventing the gradient from dissipating.

3.3. Optimization Algorithm

3.3.1. Particle Swarm Optimization. Particle swarm optimization (PSO) was first proposed by American academics in 1995. The PSO method is carefully examined, and the inertia

weight is added to the particle speed. The PSO algorithm, also known as the standard PSO method, is improved overall by this improvement. The PSO has multiple advantages over the other traditional optimization methods. The primary advantage is its simple concept, easier implementation, robustness in the control of the parameters, and enhanced computational efficiency. The PSO yields faster and cheaper outcomes in comparison to other methods and it can also be parallelized. PSO does not use the gradient of the problem which is being optimized and it does not require problem to be differentiable. PSO may be thought of as the behavioral mechanism involved in flock foraging in birds. The area where the problem is solved is analogous to the flight space of a flock of birds, and each bird is regarded as a particle without volume and mass to represent a candidate solution to the problem. In flying space, each particle has two components of velocity and position. Firstly, the particle swarm is initialized, and the particle finds the individual extreme value by dynamically updating its own speed and position globally. At the same time, iterative search is carried out in the solution space, and the particle continuously updates the speed and position of the particle according to the optimal solution pbest found by itself and the optimal solution gbest found by the group. When two optimal solutions are found, the particle update individual velocity and position are shown in

$$v_{ij}(t+1) = v_{ij}(t) + c_1r_1[p_{ij} - x_{ij}(t)] + c_2r_2[p_{gj} - x_{ij}(t)], \quad (6)$$

$$x_{ij}(t+1) = x_{ij}(t) + v_{ij}(t+1), \quad (7)$$

where i is the number of particles in the particle swarm, $i = 1, 2, \dots, n$. j is the dimension of the target space, $j = 1, 2, \dots, d$. v_i is the particle velocity, $v_i \in [-v_{\max}, v_{\max}]$, and the size of the velocity v depends on the properties of the objective function. c_1 and c_2 are learning factors, also known as acceleration factors, usually $c_1 = c_2 = 2$. r_1 and r_2 are uniform and

mutually independent random numbers, and the value range is $[0, 1]$.

The PSO algorithm's local search capability is significantly diminished when the particle cannot effectively control its own flight speed since it is difficult for the particle to discover the ideal solution. In order to effectively control the speed of particles, the inertia weight w is introduced. The velocity and position of the improved particles are shown in

$$v_{ij}(t+1) = wv_{ij}(t) + c_1r_1[p_{ij} - x_{ij}(t)] + c_2r_2[p_{gj} - x_{ij}(t)], \quad (8)$$

$$x_{ij}(t+1) = x_{ij}(t) + v_{ij}(t+1). \quad (9)$$

Equation (8) demonstrates that the inertia weight w has a significant impact on the particle swarm's velocity. When w is greater, the particle step size is also greater, causing the flight speed to be faster and resulting in an overall rough search. Smaller values of w result in smaller particle step sizes, slower speeds, and finer local searches. The current position of the particle swarm is determined by the position at the previous moment and the current speed and is also indirectly affected by the inertia weight w , so the inertia weight w plays an important role in PSO.

Various studies have implemented PSO in education. As an example, PSO technique was implemented in association with back propagation algorithm for feed forward neural networks. The optimization of neural network parameters was done considering parameters such as hidden neurons, learning rate, and activation function. The model was implemented on education dataset focusing on the increase in the number of private universities every year. The dataset consisted of 380 educational institutes which participated in the accreditation program of National Assessment and Accreditation Council. The hybrid of PSO and back propagation yielded promising accuracy and fitness function in comparison to the traditional state-of-the-art approaches. One study designed an optimal neural network architecture using PSO technique on the higher education data. The study used PSO technique in association with recurrent neural network LSTM to find the optimal solution for the feed forward neural network. The dataset of 500 educational institutes collected from the NAAC official site was used for the study. The hybrid model involving PSO and LSTM yielded promising results considering the RMSE and accuracy metrics.

3.3.2. Adam Algorithm. Adaptive moment estimation (Adam) was proposed by scholars at the ICLR conference in 2014. There is a big difference between the Adam algorithm and the stochastic gradient descent (SGD). The SGD algorithm has only one learning rate, and the alpha function is used to generally update the learning rate in the algorithm. It is possible to change the Adam algorithm's learning rate by adjusting the first- and second-order moment estimations of the gradient. The Adam algorithm utilizes a momentum factor and an adaptive learning rate to improve the speed of conver-

gence. The Adam optimization algorithm has several advantages over other traditional approaches. It is easier to implement and requires lesser memory space making it computationally efficient. The algorithm works more efficiently in case of sparse gradients, nonstationary objectives, and larger datasets with larger parameters. The current time step V_t and weight θ_t are shown in

$$V_t = \gamma V_{t-1} + \eta \nabla \theta f(\theta_t), \quad (10)$$

$$\theta_t = \theta_{t-1} - V_t. \quad (11)$$

Adaptive adjustment is carried out in combination with different learning rates of weights, where $\gamma = 0.9$ and $\eta = 0.001$ by default, and the adaptive learning rates are shown in

$$E[g^2]_t = 0.9E[g^2]_{t-1} + 0.1g_t^2, \quad (12)$$

$$\theta_{t+1} = \theta_t - \frac{\eta}{\sqrt{E[g^2]_t + \varepsilon}} \cdot g_t, \quad (13)$$

where $E[g^2]_t$ is the exponentially decaying mean of the squared gradient, g_t is the gradient at the current moment, and ε is a very small parameter, in order to avoid a denominator of 0.

3.4. The Principle of the Improved Particle Swarm Algorithm. PSO continuously iteratively updates the solution until it finds and decides the global optimal solution. The PSO method's iterative optimization procedure is susceptible to the problem of falling into a local optimum though. As a result, this issue must be addressed; this paper optimizes the PSO algorithm by selecting an appropriate learning factor and combining the improved inertia weight and the introduced variation factor, thereby improving the convergence speed of the PSO algorithm. The improved part of the PSO algorithm is as follows:

3.4.1. Improve Inertia Weights. In this paper, a nonlinear inertia weight is used to improve the shortcomings of the standard particle swarm optimization algorithm. The improved nonlinear weight $w_i(k)$ is shown in

$$w_i(k) = w_{\max} - (w_{\max} - w_{\min}) \tan\left(\frac{k}{T_{\max}}\right) \times \frac{\pi}{6}. \quad (14)$$

The inertia weight $w_i(k)$ improved in this paper is a nonlinear function. When the iteration number k gradually increases, the value of the inertia weight $w_i(k)$ gradually decreases. However, when the number of iterations k tends to infinity, the inertia weight $w_i(k)$ will approach a fixed value, so $w_i(k)$ first increases and then decreases to meet the global and local search requirements of the PSO algorithm. The fitness f of the particle is shown in

$$f = \frac{1}{N} \sum_{i=1}^N (y_i - \hat{y}_i)^2, \quad (15)$$

where N is the number of samples, y_i is the predicted data, and \hat{y}_i is the measured data.

3.4.2. Introduce a Variation Factor. This work enhances the PSO algorithm by incorporating a mutation component, which is based on the genetic algorithm's principle of mutation. The adaptive mutation factor quickly and randomly initializes the particle with a certain mutation rate after each update of the particle's speed and position. This increases the particle's local search range over time, preventing the PSO algorithm from entering the local optimum. In order to accurately judge whether the PSO algorithm has fallen into the local optimal solution, the fitness variance is used as the index to judge the aggregation density during particle search. The variance is shown in

$$\sigma^2 = \sum_{i=1}^N \left(\frac{f_i - \bar{f}}{F} \right)^2, \quad (16)$$

$$F = \max(1, |f_i - \bar{f}|), \quad (17)$$

where \bar{f} is the average fitness value, f_i is the fitness value of the i th particle, and F is the normalized calibration factor.

The link between particle fitness, individual ideal fitness, global optimal fitness, and permitted error determines whether or not to mutate. The local optimum position is where the particle is trapped if it satisfies the mutation requirement. In order to make the particle jump out of this position, the position needs to be mutated and updated, so that the search range of the particle is expanded and the position mutates.

3.5. Educational Technology Course Quality Evaluation System. According to the theory of quality education and the principles of curriculum setting generally followed in the world, the quality assessment of educational technology courses should follow the following principles.

3.5.1. The Principle of Pertinence. It means that the content of the course must be clearly targeted, that is, the target teaching object. Computer professional courses make up a significant component of the curriculum system in terms of the number of class hours. The application-oriented courses, which are closely related to the major of educational technology and include computer-aided teaching, application of multimedia technology, development of multimedia courseware, and application of network education, not only have a single course category and a small proportion of class hours, but the majority of the content also focuses on the elaboration of fundamental concepts and theories. According to the training goal of educational technology major, we need to solve the shortage of students' information technology ability. Strengthening the development of computer courseware and hardware maintenance and the cultivation of applied talents in network education, the application-oriented talents of teaching window technology are urgently needed in the current society, which means that the future educational technology will be dominated by systematic methods and information technology.

TABLE 1: Educational technology course quality evaluation system.

Index	Label
Teachers are passionate about teaching	V1
Teachers are full of energy and energy when teaching this course	V2
Teachers can keep students interested in the classroom	V3
The teacher clearly explains the course content	V4
Teachers will illustrate course content with examples	V5
Teachers encourage students to ask questions	V6
Teacher encourages students to participate in class discussions	V7
Actively communicate with students and create a relaxed atmosphere	V8
Teachers treat each student kindly	V9
Continuously update knowledge and master the frontiers of disciplines	V10
Students develop a positive learning attitude	V11
Looking forward to learning new knowledge and skills	V12
Actively communicate with teachers	V13
Learned basic principles, general concepts, and theories	V14
The ability to analyze and solve problems is improved	V15

3.5.2. The Principle of Application. Learning is for application, and curriculum setting's fundamental tenet is fit for students' real-world application. A person's value is revealed not just by the quantity of knowledge he has mastered but also by the quantity of accomplishments and advantages he reaps by using that knowledge. Practicality is shown in curriculum design. First, it is necessary to help students find the link between theory and practice. The second is to help students improve their ability to deal with and solve practical problems, so as to improve their personal value.

3.5.3. Developmental Principle. Paying attention to the future development of students is the basic principle of quality education. Two opposing teaching philosophies can be seen in the purposes of knowledge transmission and human growth. The former is focused on encouraging people's knowledge structures, while the latter is focused on learning. We highlight that students should be able to pursue their own independent research in the field after completing a course, allowing them to understand the teaching and learning strategies used in educational technology disciplines. Curriculum should be conducive to the cultivation of students' various abilities, such as the ability to retrieve, process, utilize information, create thinking, learn independently, and realize self-monitoring. The courses offered by educational technology should be appropriately expanded horizontally and vertically, looking at the overall situation of educational reform and development and broadening students' thinking.

3.5.4. Scientific Principle. First of all, the setting of the curriculum must conform to the students' cognitive regulations. In any case, the reform must respect the laws of students' cognitive habits and psychological acceptance. Secondly, the curriculum reform should be guided by the curriculum

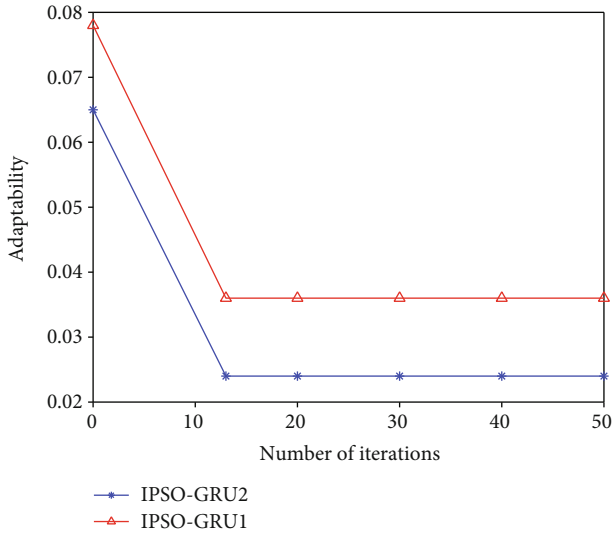


FIGURE 3: Adaptability comparison of IPSO-GRU1 and IPSO-GRU2.

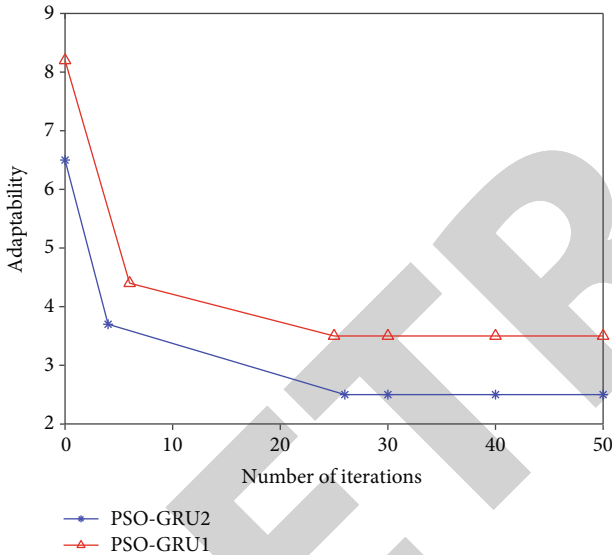


FIGURE 4: Adaptability comparison of PSO-GRU1 and PSO-GRU2.

theory, in line with the evolution and development principles of the educational technology curriculum itself.

According to the above principles, the quality evaluation system of educational technology courses is constructed as shown in Table 1.

4. Experiment and Analysis

4.1. *Experimental Data and Preprocessing.* This work builds an experimental dataset of 635 sets of data in accordance with the educational technology course quality evaluation system. In order to make the trained prediction model more accurate and ensure that the unit indicators of different types of data are in the same order of magnitude, this paper uses a normalization method to process the experimental data, the

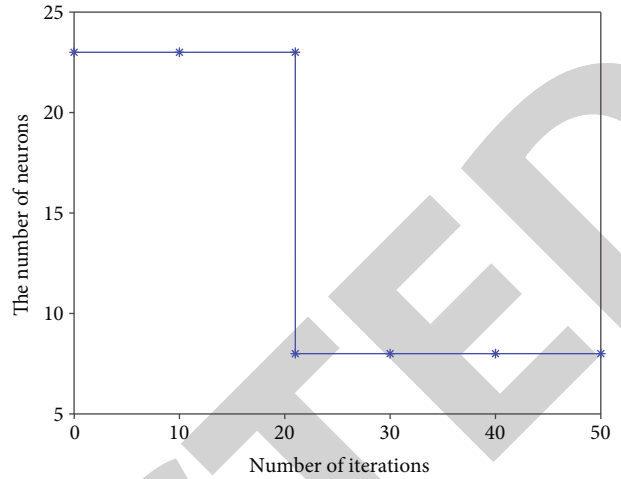


FIGURE 5: Optimization of the number of neurons in the first hidden layer.

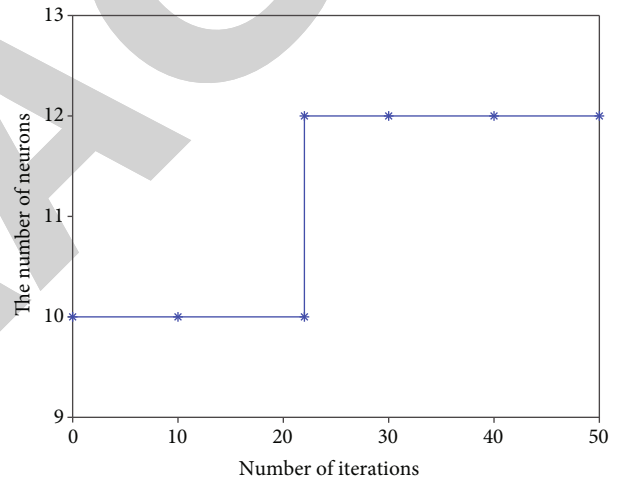


FIGURE 6: Optimization of the number of neurons in the second hidden layer.

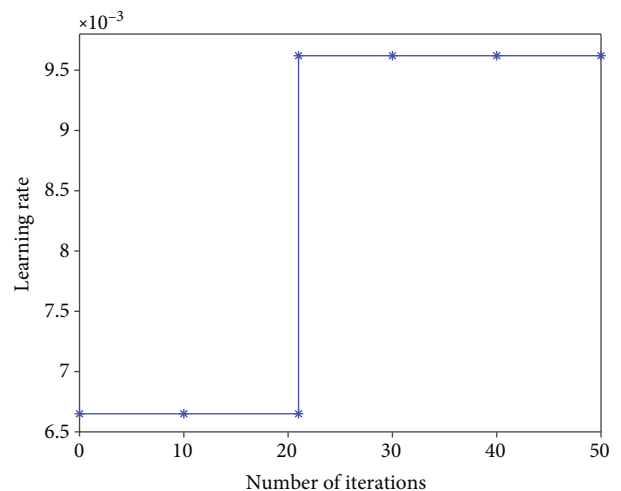


FIGURE 7: Learning rate optimization.

TABLE 2: Comparison of model output results with expert evaluation results.

Number	1	2	3	4	5	6	7	8
Model output	0.756	0.819	0.885	0.912	0.627	0.675	0.733	0.849
Expert results	0.749	0.818	0.885	0.908	0.628	0.674	0.731	0.850

purpose of which is to map the experimental data to the [0, 1] interval. Normalization is shown in

$$y = \frac{x - x_{\min}}{x_{\max} - x_{\min}}. \quad (18)$$

4.2. IPSO-Adam-GRU Prediction Model Parameter Settings.

The biggest disadvantage of GRU neural network is that it is difficult to reasonably determine the hyperparameters, which is easy to cause overfitting, which reduces the accuracy of prediction. In view of the above shortcomings, this paper uses the IPSO algorithm for global optimization and reduces the training range to the neighborhood of the global optimal solution, thereby shortening the running time and improving the training accuracy. Since the hyperparameters may be determined adaptively during the training process thanks to the local optimization carried out by the Adam algorithm, there is less chance that the model's prediction accuracy will suffer from inappropriate hyperparameter selection. The hyperparameters optimized in this paper include the number of hidden layers, the number of neurons in each hidden layer, and the learning rate.

4.2.1. The Choice of the Number of Hidden Layers. Reasonable selection of the number of hidden layers of GRU neural network is the first step in optimizing GRU neural network. IPSO optimizes one hidden layer of GRU, and IPSO optimizes two hidden layers of GRU as IPSO-GRU1 and IPSO-GRU2, respectively. Similarly, the optimization of one hidden layer of GRU by PSO and the optimization of two hidden layers of GRU by PSO are expressed as PSO-GRU1 and PSO-GRU2, respectively. Comparing the fitness of the above four models, the fitness comparison between IPSO-GRU1 and IPSO-GRU2 is shown in Figure 3. The fitness comparison between PSO-GRU1 and PSO-GRU2 is shown in Figure 4.

It can be seen from the horizontal comparison of Figures 3 and 4 that the fitness values of IPSO-GRU1 and IPSO-GRU2 are much lower than those of PSO-GRU1 and PSO-GRU2. That is to say, regardless of whether the hidden layer is one layer or two layers, the optimization accuracy of IPSO-GRU is much higher than that of PSO-GRU. It has been confirmed that IPSO, which was suggested in Chapter 3, has a higher optimization accuracy than PSO. As the number of iterations rises, PSO-GRU optimizes twice before the fitness tends to a fixed value. However, IPSO-GRU is chosen since it can attempt optimization more quickly and avoid hitting the local optimum. The fitness of IPSO-GRU1 and IPSO-GRU2 can be compared longitudinally in Figure 3, which demonstrates that when the GRU neural network has two hidden layers, the optimization accuracy is higher than that of only one hidden layer. Although the

accuracy is not much improved, considering that GRU belongs to deep learning, it is generally a multilayer hidden layer, and because the data predicted in this paper is nonlinear. In order to achieve high prediction accuracy of the model, this paper selects two hidden layers.

4.2.2. Selection of the Number of Neurons in the Hidden Layer of Each Layer. GRU neural networks with two hidden layers and IPSO and Adam gradient descent algorithms tuned and chosen for hyperparameters have a greater optimization accuracy than those with only one hidden layer. The number of neurons in the first hidden layer, the number of neurons in the second hidden layer, and the learning rate are all tuned hyperparameters. The number of iterations has been adjusted to 50 to make tracking easier. As illustrated in Figures 5 and 6, the first hidden layer optimization and second hidden layer optimization are both displayed in the same figure.

As can be seen in Figure 5, there are increasingly less neurons in the first hidden layer, and this number remains an integer throughout the optimization process. When there are between 0 and 20 iterations, the first hidden layer can have up to 23 neurons. The number of neurons is optimized more quickly as the number of iterations rises. Hyperparameter optimization is shown to be faster and more efficient using IPSO. To get the appropriate number of neurons in the first hidden layer, we may iterate up to 22 times, which is what we call a constant value. Because of this, the first hidden layer has 8 neurons.

Figure 6 shows that the number of neurons in the second hidden layer is increasing during the optimization process, and that number is an integer. There must be at least 10 neurons in the second hidden layer when the number of iterations is between zero and twenty. As the number of iterations increases, the number of neurons gets optimized more quickly. The local optimum is avoided in IPSO as the number of neurons increases. The number of neurons in the second hidden layer tends to stabilize at 12, which is a constant amount, when the number of repeats approaches 22. As a result, there are now just 12 neurons in the second hidden layer.

4.2.3. Learning Rate Optimization. The learning rate is an important hyperparameter in the GRU neural network. The learning rate is mainly used to adjust the network weight by adjusting the gradient length in the Adam gradient descent algorithm. The smaller the learning rate used, the higher the optimization accuracy and the easier it is to converge to a local minimum. The higher the learning rate, the lower the local optimization accuracy and easy to miss local minima. The learning rate optimization is shown in Figure 7.

It can be seen from Figure 7 that the whole process of learning rate optimization is on the rise, but the learning rate value range is constant. When the number of iterations is in [0, 20], the learning rate is the smallest and kept at 0.665×10^{-2} . As the number of iterations increases, the learning rate optimization speed increases rapidly. When the number of iterations increases to 21, the learning rate optimization tends to a constant value, which is 0.962×10^{-2} .

4.3. Optimal Model Performance Detection. The model is initialized with the experiment's best parameters, and after being trained with the training set of data, the best model is discovered. The model is then fed the data from the test set, and the output is compared to the output from the experts. The final experimental results are shown in Table 2. It can be seen that the model proposed in this paper is very close to the expert evaluation results, which proves the performance superiority of the model.

5. Conclusion

In order to develop teachers who can master contemporary educational theories, flexibly use a variety of contemporary teaching media and means to integrate teaching resources, and support the efficient growth of educational informatization, higher education institutions offer a public course on educational technology. Its curriculum content is broad, applicable, and practical and is made up of various academic fields like education, computer science, psychology, learning, and science. As for the educational technology public course materials currently on the market, from the perspective of teaching content, it consists of three parts: basic education theory, basic information technology, and cases of information technology and curriculum integration. From the syllabus of the course, generally 30% of the class time is used to teach teaching concepts, 30% of the class time is used to teach modern teaching techniques, and 30% of the class time is used to conduct case analysis. To sum up, the educational technology course includes the knowledge, practice, activity content structure, and practice space for the smooth development of innovative education, and such a comprehensive course is very conducive to the development of innovative education. Modern information technology is used by teachers to virtualize actual teaching situations, create an immersive learning environment, pique students' interest in learning, pique their cognitive conflict, and develop students' problem-solving skills. Encourage children to learn on their own, to see the connections between what they are learning and their peers, teachers, and the world at large, and to finally understand how to apply and transfer what they have learned. Therefore, this paper uses the wireless sensor network to collect and transmit the data of educational technology courses and then uses artificial intelligence to evaluate the quality of educational technology courses, adjust the teaching strategies of modern educational technology courses in time, and complete the following tasks: (1) The development status of educational technology courses and WSN at home and abroad is introduced. (2) The application of WSN in teaching is introduced, the basic

principle of GRU neural network and related optimization algorithms is expounded, and the quality evaluation system of educational technology courses is constructed. (3) The improved PSO algorithm and Adam gradient descent are used to optimize the hyperparameters of the GRU neural network, thereby constructing the IPSO-Adam-GRU evaluation model. The test data is input into the model for performance testing, and the output results are compared with the expert evaluation results. The results show that the evaluation accuracy of the model in this paper is very high, which further prove the superiority of the proposed model. The study model could be further evaluated on larger dataset and compared with the traditional state-of-the-art algorithm considering additional metrics of evaluation. This could be considered for implementation as part of the future research work.

Data Availability

The datasets used during the current study are available from the corresponding author on reasonable request.

Conflicts of Interest

The author declares that he has no conflict of interest.

Acknowledgments

The research is supported by the Chongqing Social Science Planning Youth Project: Research on the path of high-quality training of rural teachers under the background of the construction of Chengdu Chongqing double City Economic Circle (2021ndqn82).

References

- [1] B. Lepori, M. Seeber, and A. Bonaccorsi, "Competition for talent. Country and organizational-level effects in the internationalization of European higher education institutions," *Research Policy*, vol. 44, no. 3, pp. 789–802, 2015.
- [2] R. Florida, "The flight of the creative class: the new global competition for talent," *Liberal Education*, vol. 92, no. 3, pp. 22–29, 2006.
- [3] B. C. Bruce and J. A. Levin, "Educational technology: media for inquiry, communication, construction, and expression," *Journal of Educational Computing Research*, vol. 17, no. 1, pp. 79–102, 1997.
- [4] M. Wang and X. Zheng, "Embodied cognition and curriculum construction," *Educational Philosophy and Theory*, vol. 50, no. 3, pp. 217–228, 2018.
- [5] S. Lazar, "The importance of educational technology in teaching," *International Journal of Cognitive Research in Science, Engineering and Education*, vol. 3, no. 1, pp. 111–114, 2015.
- [6] A. R. J. Yeaman, "Deconstructing modern educational technology," *Educational Technology*, vol. 34, no. 2, pp. 15–24, 1994.
- [7] Y. Ying, "Application of flipped classroom teaching mode based on MOOC in modern educational technology teaching," *Journal of Computational and Theoretical Nanoscience*, vol. 14, no. 2, pp. 1075–1078, 2017.

Retraction

Retracted: Storage Method for Medical and Health Big Data Based on Distributed Sensor Network

Journal of Sensors

Received 23 January 2024; Accepted 23 January 2024; Published 24 January 2024

Copyright © 2024 Journal of Sensors. This is an open access article distributed under the Creative Commons Attribution License, which permits unrestricted use, distribution, and reproduction in any medium, provided the original work is properly cited.

This article has been retracted by Hindawi following an investigation undertaken by the publisher [1]. This investigation has uncovered evidence of one or more of the following indicators of systematic manipulation of the publication process:

- (1) Discrepancies in scope
- (2) Discrepancies in the description of the research reported
- (3) Discrepancies between the availability of data and the research described
- (4) Inappropriate citations
- (5) Incoherent, meaningless and/or irrelevant content included in the article
- (6) Manipulated or compromised peer review

The presence of these indicators undermines our confidence in the integrity of the article's content and we cannot, therefore, vouch for its reliability. Please note that this notice is intended solely to alert readers that the content of this article is unreliable. We have not investigated whether authors were aware of or involved in the systematic manipulation of the publication process.

Wiley and Hindawi regrets that the usual quality checks did not identify these issues before publication and have since put additional measures in place to safeguard research integrity.

We wish to credit our own Research Integrity and Research Publishing teams and anonymous and named external researchers and research integrity experts for contributing to this investigation.

The corresponding author, as the representative of all authors, has been given the opportunity to register their agreement or disagreement to this retraction. We have kept a record of any response received.

References

- [1] H. Chen, Z. Song, and F. Yang, "Storage Method for Medical and Health Big Data Based on Distributed Sensor Network," *Journal of Sensors*, vol. 2023, Article ID 8506485, 10 pages, 2023.

Research Article

Storage Method for Medical and Health Big Data Based on Distributed Sensor Network

Hui Chen ¹, Zhao Song,² and Feng Yang¹

¹College of Social Development and Public Administration, Northwest Normal University, Lanzhou 730070, China

²Academic Administration Office, Lanzhou Jiaotong University, Lanzhou 730070, China

Correspondence should be addressed to Hui Chen; chenhui7911@nwnu.edu.cn

Received 9 August 2022; Revised 3 October 2022; Accepted 13 October 2022; Published 3 February 2023

Academic Editor: Sweta Bhattacharya

Copyright © 2023 Hui Chen et al. This is an open access article distributed under the Creative Commons Attribution License, which permits unrestricted use, distribution, and reproduction in any medium, provided the original work is properly cited.

Monitoring and collecting medical data using embedded medical diagnostic devices with multiple sensors and sending these actual measured data to the corresponding health monitoring centers using multipurpose wireless networks to take necessary measures to coordinate with family medical service centers and regional medical service departments is a popular medical big data architecture. However, healthcare big data is characterized by large data volume, fast growth, multimodality, high value and privacy, etc. How to organize and manage it in a unified and efficient way is an important research direction at present. In response to the problems of low balance and poor security in the storage of data collected by distributed sensor networks in healthcare systems, we propose a distributed storage algorithm for big data in healthcare systems. The platform adopts Hadoop distributed file system and distributed file storage framework as the healthcare big data storage solution, and implements data integration, multidimensional data query and analysis mining components based on Spark-SQL data query tool, Spark machine learning algorithm library and its mining and analysis pipeline development, respectively. The distributed storage model of big data and three data storage levels are constructed using cloud storage architecture, and the data storage intensity as well as levels are calculated by high data access in the upper level, data connection in the middle level, and data archiving in the lower level according to the set known data granularity, odds, and elasticity to realize big data storage. It is experimentally verified that the above algorithm has high distribution balance and low load balance in the storage process.

1. Introduction

In recent years, with the rapid development of information technology, the field of medical health and medical research is entering the era of big data, and the daily growth of medical health data has reached the terabyte level. The huge amount of medical and health data contains great value. Building a medical and health data storage platform to realize unified storage and retrieval of data is conducive to sharing data among different medical and health institutions [1–3]. Moreover, the addition of data analysis service function on the platform is conducive to the development of auxiliary diagnosis and treatment and disease prediction technology. Medical and health data is big data, which is characterized by complex data sources, diverse structures, huge scale, rapid growth, and multimodality. Among them, multimodality includes two-dimensional data, images,

videos, text documents, etc. However, in the current healthcare service business, the real-time availability of data acquisition, the reliability of storage devices, and the accuracy of data analysis are still the three major problems that need to be solved.

Traditional relational databases cannot store unstructured data and are limited by the performance of a single machine, which cannot meet the demand of data storage. Distributed technology is widely used in the field of storage with its advantages of low cost, high reliability, and large capacity, which provides a new idea for storing massive medical and health data. The technology stores, manages, and processes massive data in a distributed manner by connecting multiple common devices and supports the storage of unstructured data [4–7]. As a result, healthcare big data is usually stored in distributed file systems or nonrelational (NoSQL) databases, and the distributed parallel computing

model improves the system data analysis to further optimize the query performance of the storage system. The advantages and disadvantages of the existing distributed medical data storage system are shown in Figure 1.

Experts have conducted a lot of research and improvements for the business requirements of healthcare data storage system and the limitations of Hadoop system and summarized the improvement methods of Hadoop-based healthcare data storage system as follows. HDFS uses data blocks as data reading and writing units and stores metadata in the memory of NameNode, but since healthcare data contains a large amount of HDFS uses data blocks as data read and write units, and stores metadata in the memory of NameNode. In addition, the Hadoop replica storage policy makes it easy for nodes with frequent read and write operations to reach the load threshold and trigger the load balancing operation of the system several times. Therefore, by optimizing the small file processing strategy and improving the copy selection strategy of Hadoop, the performance optimization of the Hadoop-based medical health data storage system can be achieved [8–10]. The Hadoop distributed system has the advantages of low cost, high scalability, and high reliability, and is suitable for storing time-sensitive medical health data but cannot meet the demand of real-time storage. HDFS aims to achieve high throughput at the cost of high latency; HDFS aims to achieve high throughput at the cost of high latency and is not suitable for low latency read requests, but medical health data has more read and fetch operations, and the long response time will affect the user experience. How to combine MapReduce, Spark, and other big data analysis technologies for parallel processing of data sets is the key to analyze the value of data. There have been many healthcare data storage solutions based on improved Hadoop storage systems, and good research results have been achieved in system storage performance optimization, efficient retrieval, and data analysis [11].

Since the reform and opening, medical and health care construction in China has gradually emerged, and its construction is divided by geography. As the concept of medical and health care is built based on medical and health care services, medical and health care services are continuously carried out under the promotion of the government, and medical and health care construction provides convenience for residents' lives and greatly improves their quality of life.

In recent years, the social service function of medical and health care in major cities is high, the construction of infrastructure has achieved leapfrog development, and a medical and health care service system covering 4 levels of city, district, street, and residence have been established. At present, the research on the probabilistic characteristics modeling of big data distributed storage for the regional distribution of medical and health density can be divided into two major aspects: the probabilistic density model of big data distributed storage with the characteristic probability distribution function simulating the regional distribution of medical and health density, and the fitting estimation model driven by the historical data of regional distribution of medical and health density. The former lacks accuracy and universality due to the disadvantages of many factors affecting the

distributed storage of big data with health care density area distribution and large differences in spatial and temporal distribution, which makes it difficult to form a generalized application; while the latter uses the historical operational data of health care density area distribution as the sample base and builds the model of probabilistic characteristics of big data distributed storage with health care density area distribution by data-driven. The latter model is based on the historical data of health care density area distribution, and has better generalizability. Beta distribution is used to fit the prediction error of big data distributed storage with health care density area distribution, and then the distribution of prediction error of big data distributed storage with health care density area distribution is used to determine the size of energy storage capacity [12–15]. The *t*-distribution with shift factor and scaling factor is used to describe the big data distributed storage with regional distribution of medical health density, and then the model parameters are estimated using historical data samples. A third order Gaussian distribution function was used to fit the probability distribution of the longitudinal moments of the big data distributed storage of the regional distribution of health care density, and good results were achieved.

The prediction errors of the big data distributed storage of health care health density regional distribution were modeled using exponential distribution and normal distribution functions, respectively, and then the parameters of the distribution functions were estimated using the great likelihood estimation and least squares method. However, the above-mentioned modeling of probabilistic properties of big data distributed storage of health care health density area distribution have the commonality of using a priori distribution models to simulate the probability density of big data distributed storage of health care health density area distribution, so there are two drawbacks: the effect of parameter estimation on sample data relies on the a priori definition set by human subjectivity, and it is difficult to guarantee if the assumptions of the a priori model are biased [16–18]. The convergence of the fitted model is difficult to guarantee if the assumptions of the prior model are biased; the differences in the spatial-temporal distribution of the distributed storage of big data with regional distribution of healthcare density make it necessary to use different probability density distributions for different regions, which does not meet the requirement of universal adaptation of modeling.

Although the Hadoop-based approach for medical and health data storage system has an extremely practical value, it is not applicable to some specific application scenarios because the density region distribution of medical and health resources and patient groups are not considered. The optimal extraction of density region distribution in big data environment can effectively improve the data quality in big data environment. The optimal extraction of density region distribution needs to get the density value near each data quality sample, give the region where the samples are aggregated, and complete the optimal extraction of density region distribution. The traditional method first forms the original transaction data set and gives the distribution rules of the

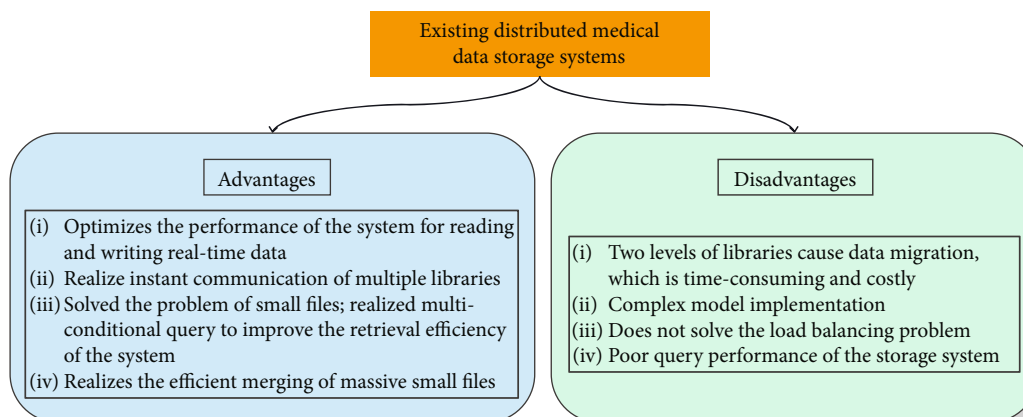


FIGURE 1: Strengths and weaknesses of existing distributed medical data storage systems.

data, but neglects to give the region where the data samples are aggregated, resulting in low extraction accuracy.

Time series-based method for optimal extraction of density region distribution in big data environment. The method first uses the time series model to identify the time series of each data state volume, classifies the density region distribution in the time series, uses the high-density clustering method to get the density value near each data quality sample, gives the region where the samples are aggregated, and introduces the label movement speed into the sliding window adaptive adjustment process to complete the optimal extraction of the density region distribution in the big data environment. Therefore, this paper proposes the big data distributed storage algorithm for medical and health system, constructs the big data distributed storage algorithm through cloud storage architecture, and considers the density region distribution through density estimation algorithm to achieve the balance between storage system and actual demand, guarantees the antiattack of stored data, and realizes the big data distributed encrypted storage.

2. Related Work

2.1. Traditional Medical Health Data Storage System. Currently, the construction of mature hospital systems mainly includes HIS (Hospital Information System), EMRS (Electronic Medical Record System), RIS (Radiology Information Management System), and PACS (Image Archiving and Communication System). The schematic diagram of the construction of in-hospital medical and health storage system is shown in Figure 2. Traditional healthcare data storage systems mostly use relational databases, such as MySQL and SQLServer, which organize data through a relational model and store each record in a two-dimensional table in the form of rows, but relational databases need to satisfy a predefined relational model and each record has a fixed data length [19, 20]. As the in-hospital system is only for a single business or a single data type of the hospital, the amount of data stored and managed is relatively small, so the relational database can meet the demand.

With the continuous development of network and information technology, the scale and complexity of medical and

health data are getting larger and larger, which leads to the following limitations of using relational database for the storage of large-scale medical and health data: (1) medical and health data contain more unstructured data; however, the structure of relational database is relatively fixed and cannot be applied to the storage of unstructured data. (2) Relational database is limited by the storage capacity of single machine and cannot be applied to the storage scenario of medical and health care big data. Although the relational database supports distributed expansion, the installation and maintenance costs are high due to the complex rules of distributed relational database partitioning. (3) The scalability of relational database is poor, and it is difficult to realize data sharing among different medical and health institutions. (4) The read and write of relational database must go through SQL parsing, and the performance of concurrent read and write on large-scale data is weak. (5) The volume of data is too large, which makes it difficult for data analysis software to analyze data effectively and accurately. In summary, the traditional relational database can no longer meet the storage needs of terabytes and petabytes of medical and health data in the era of big data [21, 22].

2.2. Distributed Medical and Health Data Storage System. After a long development, the data storage system has gradually evolved from a stand-alone storage system to a storage system that supports distributed expansion. Subsequently, distributed solutions for relational databases and NoSQL databases that natively support distributed storage have emerged. This section introduces Hadoop distributed storage system and NoSQL database, respectively. Hadoop is a mainstream distributed system supporting massive data storage and processing, including Hadoop File System (HDFS), MapReduce, Hadoop Data Base (HBase), and other important components [23, 24]. Among them, HDFS is the data storage and management center of Hadoop system, with high fault tolerance, efficient writing, and other characteristics. The NameNode is responsible for managing the metadata and DataNode nodes of the file system, and the DataNode is the actual working node of the file system, which is responsible for storing and retrieving data and sending the stored block information to the NameNode

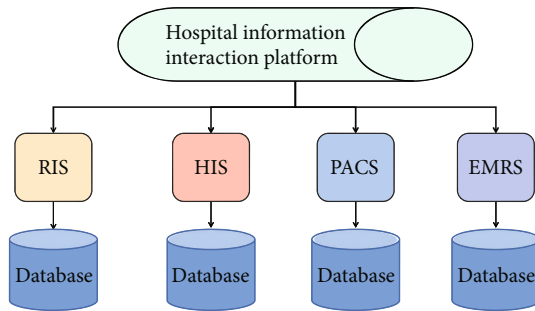


FIGURE 2: Schematic diagram of medical institution storage system construction.

periodically. The HDFS architecture diagram is shown in Figure 3.

MapReduce is a model for processing and generating large-scale datasets, which achieves parallel processing of massive datasets in a highly reliable and fault-tolerant way. MapReduce improves the cluster's ability to handle massive data by decomposing tasks to be processed by multiple Hadoop runtime nodes when processing large datasets. For applications that require random reads, the data is stored in HBase, a column-oriented nonrelational database whose underlying data is stored in HDFS to ensure data reliability, and its integration with MapReduce ensures the efficiency of the system when analyzing large amounts of data.

As shown in Figure 3, HBase is composed of HMaster, HRegionServer, HRegion, and Zookeeper components. Among them, HMaster is the master server of HBase cluster and is responsible for allocating HRegionServer for HRegion; HRegionServer is responsible for providing data writing, deleting, and searching services for clients; HRegion is a subtable divided by row key, which is the smallest unit of storage and processing in HBase; ZooKeeper NoSQL database stores data without fixed structure, simple data organization, good scalability, and suitable for storing large amount of data. The database can be divided into columnar database, document database, and key-value database [25–27]. Among them, the document database represented by MongoDB supports storing a variety of structural data, and has powerful query function and indexing ability, which is suitable for the massive data application scenario with frequent reading and fetching operations.

Distributed technology can realize the unified storage and query of medical and health data, but there are still some problems in the current research. For example, medical health data contains a large amount of patient privacy information, and none of the current storage solutions consider data privacy protection. Due to the high sensitivity of healthcare data, organizations usually use a centralized approach to manage the data; however, the management approach is not transparent enough, which can easily lead to data tampering and privacy leakage. These problems directly threaten data security and user privacy in healthcare, making it difficult to share data among organizations at all levels and unable to fully utilize the value of healthcare data. In recent years, with the continuous development of blockchain technology, it has become an effective means to secure

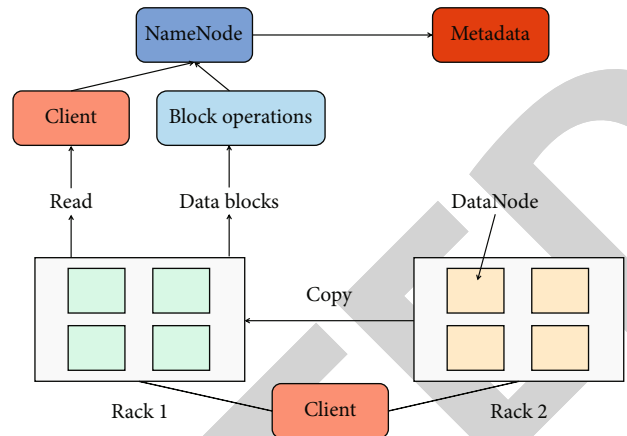


FIGURE 3: HDFS architecture diagram.

data sharing. Using cryptographic knowledge, data can be secured from tampering, unforgeable, and decentralized transmission access. However, as an emerging technology, blockchain still lacks theoretical support for distributed system architecture and experimental testing for high concurrent read and write operations. Future research can focus on blockchain technology based on distributed architecture to realize a distributed medical and health care big data storage model based on privacy protection [28, 29].

To make better use of medical and health information resources to make scientific decisions, it is necessary to dig deeper into the value of medical and health data. Current healthcare big data analysis technologies are focused on statistical analysis and decision-making, especially MongoDB-based healthcare data storage systems, with less research related to data analysis. Knowledge graph has emerged in the field of natural language processing and has become an effective organization form for presenting data knowledge. Using this technology to organize healthcare data helps to extract healthcare knowledge and realize healthcare knowledge reasoning, remote consultation, recommended medication, disease prediction, and other auxiliary diagnosis and treatment services.

2.3. Research Status of Density Region Distribution. For mining out high-density regions in data sources, the essence is the process of dividing a data object into subregions (or subsets) of different sizes. The objects in each subregion are highly like each other in terms of information, while not similar to the information of the objects in other subregions. And in the field of data mining, there are many density-based data mining algorithms that can be borrowed for mining out high-density data regions in data sources, such as the classical DBSCAN algorithm. However, the traditional density-based data clustering algorithms, when facing the data set with uneven density distribution, are often not good for the data set to region the data set according to the density distribution of the data. In addition, the traditional algorithm has redundant operations in object domain query, which requires domain query judgment for each sample point, yet it is not necessary to perform query judgment

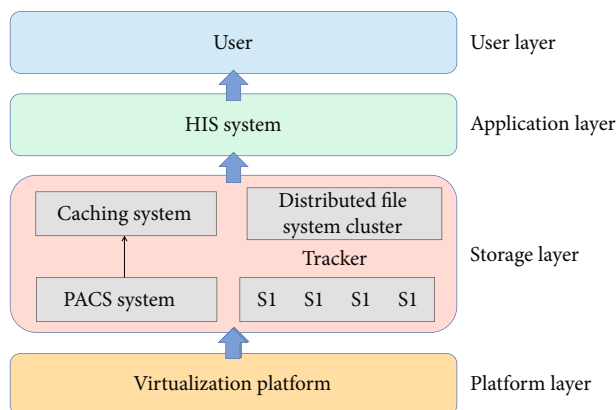


FIGURE 4: Model structure.

operations for all object domains in a determined high-density subset.

Although the above method is of great practical value, it is not applicable to some specific application scenarios. For example, in exploring the changes of animal habits by collecting migration data of North American hoofed animals, the data is obtained by radio telemetry means with large positioning errors and sampling intervals, and large errors are introduced when extracting metadata features such as speed and curvature, resulting in extremely unreliable classification results. In addition, the trajectory data obtained by means of radar scanning, Wi-Fi indoor positioning, cellular positioning, Flickr photo location data, etc. have similar statistical characteristics. For this kind of data, if the trajectory data of different categories overlap severely in space, it is generally considered that its separability is not strong; on the contrary, if there is a certain degree of separation of trajectories in space, their location-related features can be fully explored [30].

The two-dimensional space where the two-dimensional trajectory segments are located is divided, and the minimum description length (MDL) is used as the criterion for selecting the granularity of the division, and the rectangular homogeneous region containing only one type of trajectory is extracted as the feature. Compared with the trajectory pattern feature method, this method not only improves the classification accuracy of trajectories, but also enhances the training efficiency of the classifier. However, this method assumes that the significant regions are approximately rectangular in distribution, which is not always applicable in practice. In addition, to reduce the search complexity of the optimal classification, the method uses the projection to x - and y -axis to select the division points of each axis alternately, which is a limitation in the division of the trajectory cluster distribution. To solve this limitation, a strategy of spatial region merging is proposed to extract homogeneous regions; however, this method does not eliminate the limitation of rectangular region shape and still has strong limitations. In addition, Gaussian mixture model (GMM) is proposed to fit the distribution of trajectory segments in space, which eliminates the defects of region division method and extends the application to the problem of classifying trajectory data in 3D or even higher dimensions.

However, the drawback of GMM method is that it introduces the number of Gaussian components K . Different values of K will affect the classification results: smaller values of K are not enough to describe the complex trajectory region distribution, and larger values of K may lead to training failure due to the complexity of the model. To more accurately portray the density distribution of the dataset, the region is divided according to the density distribution, and the concept of region and region area is introduced in the traditional density-based clustering algorithm, and the algorithm is improved to portray the density distribution of the dataset with the number of points per unit area.

3. Methods

3.1. Model Structure. The distributed storage of medical and health care big data proposed in this paper is shown in Figure 4. This architecture consists of application layer, storage layer, and platform layer. The application layer consists of clients of HIS system and PACS system, which are responsible for providing users with operation interface, information management, image viewing, and other functions. The storage layer is a two-level storage model of local side and cloud side, the local side consists of HIS server and PACS server, which can be built on the local server side and is responsible for storing and managing.

The local side consists of HIS server and PACS server, which can be built on the local server side and is responsible for storing and managing the structured information data and recent image data of the hospital; the cloud side is built by FastDFS large-scale distributed cluster, which is responsible for the permanent storage of long-term files. The platform layer is a virtual platform built on top of the infrastructure by virtualization technology, which facilitates the provision of cloud services through the rational and efficient use of server resources.

3.2. Distributed Sensor Network. Distributed sensor network-based medical health monitoring system is a networked physiological monitoring physiotherapy system for collecting users' body status data, which should have the functions of automatic recording, continuous monitoring, warning notification, intelligent judgment, self-correction, and standard transmission. Noninvasive physiological signal monitoring system is an important part of the monitoring system, which consists of multiple sensors that measure medical data including important vital signs such as blood pressure, blood glucose, heart rate, blood oxygen concentration, and arterial oxygen pressure saturation. For example, a noninvasive wristwatch blood pressure monitor allows users to wear it around like a watch, monitor blood pressure, and record pulse rate 24/7 without discomfort for long periods of time. Over the Internet, medical monitoring data based on a distributed sensor network is transmitted by multiple complementary wireless networks to a specific health monitoring center, where it is integrated into the permanent electronic medical record of the designated user. As a result, the medical staff at the health monitoring center can monitor various vital signs of the user at any appropriate time, and if any

TABLE 1: NameNode server parameters.

NameNode server	CPU	Memo	Disk	Bandwidth
NameNode1	FT1500	32GDDR4	240GSSD	1G
NameNode2	ARM	32GDDR4	240GSSD*2	1G
NameNode3	ARM*2	32GDDR4*2	240GSSD*4	1G
NameNode4	E52620V4*4	32GDDR4*2	240GSSD*4	1G
NameNode5	E52620V4*4	32GDDR4*4	240GSSD*8	1G

abnormal physical signs are detected, the medical staff will give appropriate medical instructions before the condition deteriorates, and then take steps to treat the condition. The health monitoring center specialists can also accurately locate the user, consult with his or her home monitoring center doctor, and coordinate with local medical services using the fastest delivery method to take timely medical assistance. The goal of the health monitoring system is to monitor the health status of the user at anytime and anywhere. Therefore, the following two typical situations are illustrated: when the user is at home or near his residence, and when the user is far from home or in another city. Considering these two situations, the author proposes that the distributed health monitoring system, health monitoring center will be distributed to each region. In case 1, the user's medical monitoring data will be sent to the home health monitoring center; in case 2, the medical monitoring data will be sent to the corresponding visiting health monitoring center.

3.3. Distributed Storage Algorithm. When data storage requirements are acquired by storage nodes, the distributed data storage continuously sends preservation requests. Therefore, through the storage capacity analysis and data storage hierarchy designed in this paper, if the demand of Equation (7) can be achieved after computing, the data is preserved, and if not, Equations (1)–(7) are repeatedly executed. At the same time, the data storage process is adjusted into three levels, firstly, the upper level completes data height access, the lower level realizes data archiving, and the middle level mainly takes over the connection between the upper and lower levels. Among them, the upper layer of the data storage process is mainly represented by the following Equations (1)–(7). If the adoption probability of distributed data is expressed through $P(x)$, the inverse relationship appears in the expectation of its adoption probability as $EP(x)$ as well as the elastic expectation as $E[T(x)]$, so the elastic expectation of distributed data is calculated through

$$E[P(x)] = \frac{\lambda - \lambda^2 E[T(x)]^2 - E[T(x)]}{E[T(x)]}. \quad (1)$$

In Equation (1), the degree of obedience of the distributed data is described by A . If the result obtained from Equation (1) is negative, it is known that the blocked state is inversely proportional to the smooth state when the data is stored, and at this time, the distributed data storage is continued to be completed. If the result obtained is positive, it

is necessary to control the preservation capacity during data storage and achieve continuous data storage by modifying the data granularity. Since the result obtained from Equation (1) will make the data storage smoothly affected and the calculated value is negative, if the data granularity is small, the result obtained from the calculation of Equation (1) may appear positive. Therefore, manipulating the data elasticity $T(x)$ by the granularity rate p can improve the congestion of data storage and reduce the degree of storage space being occupied. Since a negative correlation exists between $T(x)$ and p , it is known, based on this conclusion, that $T(x)$ can maintain its original value by means of Equation (2).

$$T(x) \Rightarrow p. \quad (2)$$

The expected value of $E[T(x) \Rightarrow p]$ can reach the time function, therefore, is described by Equation (3) as:

$$E[T(x) \Rightarrow p] = \int E[T(x)]. \quad (3)$$

Therefore, based on Equation (3), if at this stage we still set p to be the data preservation access granularity rate, i.e., the next moment $T(x)$ can be completed by the following

$$T(x) = \int E[T(x)] + E[T(x) \Rightarrow p]. \quad (4)$$

Since the distributed storage has a limited bandwidth during the big data storage, $T(x)$ can be completely covered by the storage hierarchy, while the confirmed coverage association Δt corresponding to the random moment can be expressed by

$$\Delta T(x) = p \int_{\Delta}^{\Delta t} \sqrt{\Delta^2 - T(x)^2}. \quad (5)$$

Based on Equation (5), the big data distributed storage intensity index $\Delta\lambda$ is described by

$$\Delta\lambda = \frac{E[T(x)] - \lambda}{1 - \lambda^2 E[T(x)]^2 - E[T(x)]}. \quad (6)$$

Based on the calculation of Equation (6), the calculation of data elasticity $T(x)$ and big data distributed storage

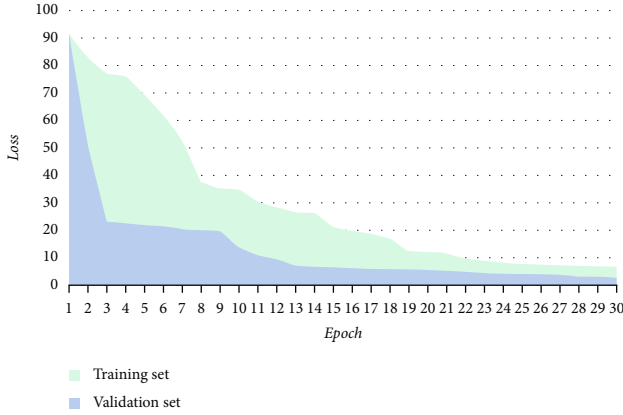


FIGURE 5: Training set and test set loss convergence during training.

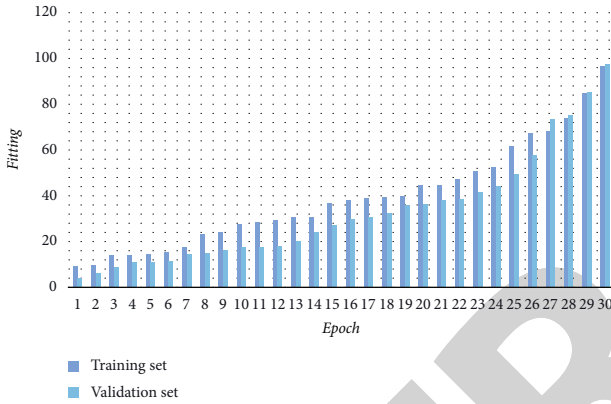


FIGURE 6: Training set and test set performance improvement during training.

TABLE 2: Different algorithms to store the time spent.

Amount of data/ Mb	This article algorithm	Huge amount of spatial data cloud storage and query algorithms	Hadoop-based big data storage algorithm
2000	26	67	58
4000	34	72	64
6000	39	79	78
8000	47	85	88
10000	49	88	92
12000	53	94	98
14000	57	107	114
16000	59	132	126
18000	65	144	139
20,000	72	156	141

gradient Δ can be completed by

$$T(x) = \Delta(1 - \Delta)(\sqrt{1 - \Delta\lambda}). \quad (7)$$

With Equation (7), the process of distributed storage of data can be reached. Meanwhile, the final distributed storage

of big data is described in the form $\Delta(X)$ via

$$\Delta(X) = E_{\text{sent}}(c) \cdot c \cdot P(x) \cdot \Delta\lambda \cdot T(x). \quad (8)$$

In the Equation (8), it is the result of the calculated preservation of the distributed storage of big data.

3.4. Density Area Distribution. In the big data environment, most of the original state data time series contain multiple feature data, so in the process of optimizing the extraction of feature data in the big data environment, it is necessary to use the time series model to divide all the collected data states into multivariate continuous time series, give the high-quality data state volume amplitude change law, extract the feature data state characteristics, and calculate the feature data on the time. The effect of the feature data on the time series fitting is calculated, and the residuals of the time series fitting of each data distribution state are obtained. The specific steps are detailed as follows: suppose, by α'_{dfyy} represents the number of each data state set in the big data environment, and X_{th} represents the value of the data state volume l at the moment h . Using Equation (9), all the collected data states are divided into a multivariate continuous time series

$$rt'_{ghpp} = \frac{\alpha'_{dfyy} * X_{th}}{p'_{fgg}}, \quad (9)$$

where p'_{fgg} represents the autoregressive moving average function. Suppose y'_{dfujj} represents the high-quality data state change law, ω' represents the type of change law, o'_{fgij} represents the time interval in which different data state quantities are periodically changed, and m'_{fg} represents the observation point of each data state quantity existing on the time series, using equation (10) to give the high quality data state quantity amplitude law.

$$t'_{df} = \frac{m'_{fg} \times o'_{fgij}}{\omega' \mp p'_{dfpp}} \times y'_{dfujj} \mp \kappa'_{fg} \quad (10)$$

where p'_{dfpp} represents the impulse function and κ'_{fg} represents the delay operator. Suppose by g'_{vbhjk} represents the time series of high-quality data, the distribution of g'_{vbhjk} obeys the autoregressive moving average function represented by p'_{fggg} , and rr'_{dfgg} represents the influence factor of the characteristic data, the characteristic data state characteristics are extracted using

$$p'_{opll} = \frac{p'_{fggg} \mp rr'_{dfgg}}{g'_{vbhjk}} \mp t'_{df}. \quad (11)$$

In an observed time series, different time points are affected by different feature data. Suppose by Z'_t and $v_j(B)$ represent the type of feature data, respectively, and $k'_{z,v_j(B)}$

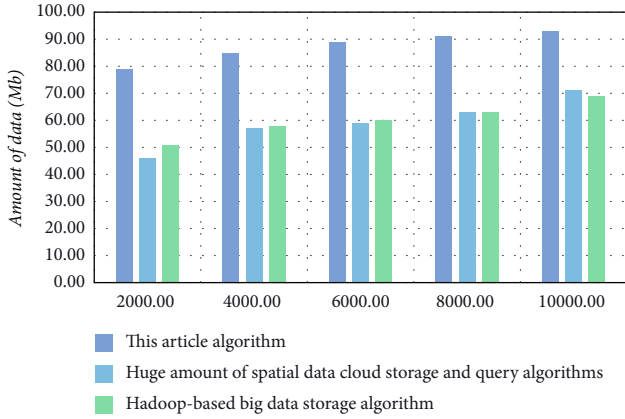


FIGURE 7: Comparison of read rates of different algorithms (Mb/s).

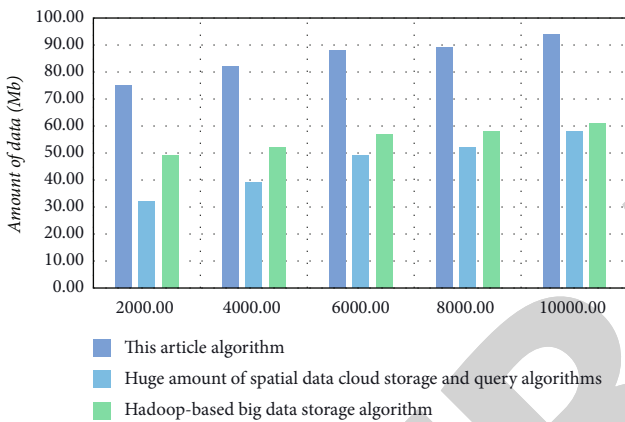


FIGURE 8: Comparison of write rate of different algorithms (Mb/s).

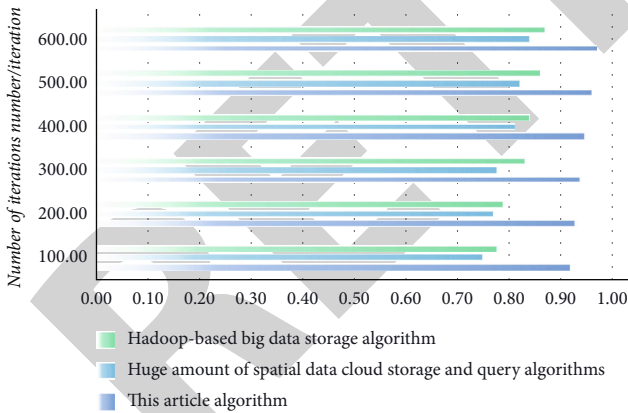


FIGURE 9: Density regional distribution utilization.

represents the number of feature data, the effect of feature data on the time fit is obtained using

$$E'_{sdpp} = \frac{k_{z_i, v_j(B)} \times \{v_j(B) \pm Z'_t\}}{p'_{opll} \times u'_{jkk}} \mp rt'_{ghpp}, \quad (12)$$

where u'_{jkk} represents the moment of feature data generation.

3.5. Data Processing. Because the total amount of collected data is huge and diverse, the platform needs to clean, transform, classify, integrate, and process the data and then store them in a distributed database. The built healthcare big data platform uses the distributed database SequoiaDB to store data, and the SequoiaDB distributed database contains data nodes, cataloging nodes, and coordination nodes. When an application sends an access request to the coordinating node, the coordinating node first calculates the optimal data node by communicating with the cataloging node and distributes the query task, and finally returns the query results of each data node to the application after aggregation.

The data computing platform uses the Spark computing framework, which supports a variety of data storage models and can be combined with Hadoop to share storage resources and computation in a Hadoop cluster, and Spark can compute data that is accessed frequently and centrally and store such data in memory to improve access efficiency. Users submit data requests on the healthcare platform, and the platform analyzes the user input and presents the data. In addition to direct data list display, the data presentation method also provides data graphical display, coding the platform statistical classification of data into graphics, using the mainstream visualization technology html5, the introduction of chart drawing tool library chart.js, the data will be presented in the form of statistical chart reports.

4. Experiments and Results

4.1. Experiment Setup. A simulation experiment is needed to verify the overall effectiveness of the distributed storage method for health care big data based on density area distribution. The experimental data comes from the internal data of multiple cities in a province in China. Experimental environment: 5 machines are used to correspond to the data stored in each cell. The configuration of each machine is: CPU is i5-2400, 3.1GHz; OS is Win10Ulti-mate, 10 T of available disk space, and 8 physical cores of the processor. A Hadoop 2.6.5 system was built in the cluster to provide HDFS file system for distributed storage of files, and YARN was used to manage the cluster. Meanwhile, Hive 2.1.1 was built on HDFS as the temporal data organization and query engine. Spark 2.1.1 platform was built on YARN, and Python 3.6 was used to develop system functions. All experiments were done by running Spark programs. Table 1 describes the specific configuration information of the five NameNodes.

The experimental metrics are the network node survival period after data fusion and the network energy consumption during the fusion process. Among them, the network node survival period: after distributed data fusion, it will be divided into different types of data nodes, and with the extension of time, there will be a large amount of data influx into each node, and the current data fusion node will be scattered, and the time between the current data fusion node is established and scattered is the network node survival period.

We plot the training set and test set loss convergence and performance improvement during training in Figures 5 and 6.

4.2. Experimental Results. When raw big data is stored, if there is an unbalanced distribution, it is easy to generate local hotspots, which makes larger loads appear in some nodes and makes empty loads appear continuously in some nodes at the same time. Therefore, based on the original big data distribution balance degree, the original big data distribution balance state of different algorithms is analyzed. The time required to store big data at different quantities for different algorithms is analyzed, and the analysis results are shown in Table 2. According to Table 2, with the growth of data quantity, the storage spending time of three algorithms gradually increases, and when the data quantity is 2000 Mb, the storage spending time of massive spatial data cloud storage and query algorithm is the highest, reaching 67 s, and when the data quantity is 20000, the storage spending time of this algorithm remains the highest among three algorithms, 156 s, higher than the Hadoop-based big data. The storage algorithm 15 s, higher than the algorithm of this paper 84 s, the algorithm of this paper storage spending time is at least 26 s, so using the algorithm of this paper, can effectively reduce the big data storage spending time.

The analysis of the ability to read/write data can effectively determine the real-time nature of the storage algorithm, and the analysis results are shown in Figures 7 and 8 by comparing different algorithms through data reading and writing operations in the case of different data volumes. According to Figures 7 and 8, the read data rates of the three algorithms are 79 Mb s^{-1} , 46 Mb s^{-1} , and 51 Mb s^{-1} when the data volume is 2000 Mb, and the read/write rates of the three algorithms are improved when the data volume is increasing, but when the data volume reaches 10000 Mb, the read data rate of the Hadoop-based big data storage algorithm remains the lowest among the three algorithms. The algorithm in this paper has the lowest read and write data rates of 93 Mb s^{-1} and 94 Mb s^{-1} , respectively, at this data volume, which keeps the highest among the three algorithms, and the algorithm in this paper still keeps the highest read and write data rates at other data volumes, therefore, it shows that the algorithm in this paper has high read and write data rates and can realize faster distributed storage of big data.

The utilization rate of density area distribution under different iterations is analyzed, and the utilization rate of density area distribution of different algorithms is derived by comparing three algorithms, and the analysis results are shown in Figure 9. According to Figure 9, with the increase of iteration number, the utilization rate of data density area distribution of three algorithms increases, and the utilization rate of data density area distribution of this algorithm always remains above 90% between 100 and 600 iterations, which indicates that the utilization rate of data density area distribution of this algorithm is high.

5. Conclusion

In the era of big data, the scale of medical and health data expands dramatically, and the data presents multimodal characteristics. The traditional relational database can no longer guarantee the efficient storage and fast response of massive data, and for this reason distributed storage technol-

ogy provides a new idea for storing massive medical and health data. Based on the advantages of HDFS, HBase, and MapReduce, the Hadoop-based healthcare data storage system further optimizes the storage and query performance to realize a smart healthcare storage system that integrates high throughput, fast location, and efficient analysis. The distributed database based medical health data storage system can meet the demand for unified storage and fast response of multimodal medical health data and provides a platform support for subsequent multimodal data analysis and medical health data mining.

In this paper, we study the distributed storage algorithm of medical and health care big data considering density area distribution, design the process of big data distributed storage through cloud storage architecture, and use the density area distribution algorithm to complete the distribution and decryption of the stored big data, so that the stored big data can play the maximum efficiency, and verify the storage capability of the algorithm in this paper through experiments. The load balance is lower, and the encryption is more resistant to attack. In the future research phase, we can continuously optimize the big data distributed storage algorithm so that it can be applied to various fields. In the future, we plan to conduct research on distributed medical and health data storage schemes for privacy data protection and medical and health knowledge inference.

Data Availability

The datasets used during the current study are available from the corresponding author on reasonable request.

Conflicts of Interest

Declares that they have no conflict of interest.

References

- [1] J. Mittendorfer and M. Niederreiter, "Striking complexity of the photon field in medical devices with heterogeneous density distribution and challenges for industrial irradiators," *Radiation Physics and Chemistry*, vol. 190, p. 109778, 2022.
- [2] R. A. Jordan, G. Sydney, and E. Andrea, "Relevance of spatial and temporal trends in nymphal tick density and infection prevalence for public health and surveillance practice in long-term endemic areas: a case study in Monmouth County, NJ [J]," *Journal of Medical Entomology*, vol. 4, p. 4, 2022.
- [3] G. He, Z. Ma, X. Wang, Z. Xiao, and J. Dong, "Does the improvement of regional eco-efficiency improve the residents' health conditions: empirical analysis from China's provincial data," *Ecological Indicators*, vol. 124, article 107387, 2021.
- [4] E. C. Emond, A. Bousse, L. Brusaferrri, B. F. Hutton, and K. Thielemans, "Improved PET/CT respiratory motion compensation by incorporating changes in lung density," *IEEE Transactions on Radiation and Plasma Medical Sciences*, vol. 99, pp. 1–1, 2020.
- [5] L. F. Knudsen, A. J. Terkelsen, P. D. Drummond, and F. Bircklein, "Complex regional pain syndrome: a focus on the autonomic nervous system," *Clinical Autonomic Research*, vol. 29, no. 4, pp. 457–467, 2019.

Research Article

Techniques Based on Metaheuristics Combined with an Adaptive Neurofuzzy System and Seismic Sensors for the Prediction of Earthquakes

Anurag Rana ¹, Gaurav Gupta ¹, Pankaj Vaidya ¹, Waleed Salehi ^{1,2},
Shakila Basheer ³, and Madhulika Bhatia ⁴

¹Yogananda School of AI Computers and Data Sciences, Shoolini University, Bajhol, Solan 173229, India

²Rana University, Kabul, Afghanistan

³Department of Information Systems, College of Computer and Information Science, Princess Nourah bint Abdulrahman University, P.O. Box 84428, Riyadh 11671, Saudi Arabia

⁴Amity University, Noida, India

Correspondence should be addressed to Waleed Salehi; ahmadwaleed.sedqi18@gmail.com

Received 14 September 2022; Revised 23 September 2022; Accepted 12 October 2022; Published 2 February 2023

Academic Editor: Sweta Bhattacharya

Copyright © 2023 Anurag Rana et al. This is an open access article distributed under the Creative Commons Attribution License, which permits unrestricted use, distribution, and reproduction in any medium, provided the original work is properly cited.

This research looked into the viability of using metaheuristic algorithms in conjunction with an adaptive neurofuzzy system to predict seismicity and earthquakes. Different metaheuristic algorithms have been combined with an artificial intelligence (AI) algorithm. Subjected to seismicity is a promising factor. The new sensors have many advantages over the older, more impressive-looking ones, including (a) a generally linear relationship between the measured values and real ground motion (described above), (b) the ability to measure three orthogonal components of ground movement in a single unit, (c) sensitivity to a very broad range of frequencies, and (d) high dynamic range, which allows for the detection of both very small and fairly large tremors. To accept the acquired results as a hybrid model of an adaptive neurofuzzy inference system with particle swarm optimization (PSO), genetic algorithm (GA), and extreme machine learning (ELM) (ANFIS-PSO-GA-ELM) implemented. According to the dataset, all approaches produce excellent and realistic predictions of seismic loads; however, the method ANFIS-PSO produces better results. All the strategies demonstrated a high level of predictability. Finally, this research urges researchers to investigate the performance of triple hybrid MT algorithms using a variety of hybrid metaheuristic methodologies, rather than the existing double hybrid MT algorithms.

1. Introduction

An earthquake is the shaking of the earth's surface which causes seismic waves is suddenly release of energy in the lithosphere. The area's seismicity defines the frequency, kind, and size of earthquakes experienced throughout time. The creation of positive electrical charges in the ground as a result of plate movement driven by rock compression could explain for odd electromagnetic signals before an earthquake. Time, epicenter distance, and peak ground acceleration are the three most essential input variables in

determining earthquake magnitude. The seismometer tool measured the magnitudes of the earthquakes using the most common scale, the moment magnitudes. Many research groups are working hard to keep an eye on the risk of an earthquake, but earthquake forecasting and prediction are difficult. Earthquakes have been more common in recent years, causing unrelenting fear in people's lives and economy. Geoscientists and structure engineers have attempted to protect from the earthquake devastation, but the only solution is to precisely and timely estimate the magnitude of the earthquake. With the help of technical advancements,

recent advancements in seismology have given prominence to the crucial information concerning earthquakes. Fuzzy logic (FL) and neural networks (NN) are the expert systems having the ability of human reasoning and produce a technical approach. Earthquake forecasting and prediction is a subfield of seismology related with the magnitude, time, and area of future earthquakes [1]. Soft computing literature demonstrates that soft computing offers a superior solution to uncertainty concerns [2]. Fuzzy logic deals with uncertainty by offering a human-oriented knowledge representation and artificial neural networks (ANN) for self-learning and rule generalization [3]. NN and FL are integrated to create the neurofuzzy system (NFS), which includes learning and reasoning abilities, respectively, which are merged in ANFIS to provide superior prediction capabilities. [4]. The NN used to address many complicated issues in a variety of disciplines. [5–10] used neural networks to investigate the item and image. Artificial neural networks incorporating swarm algorithms, such as the fruit fly optimization algorithm (FOA), have proven to an effective method for determining the best classifier. For earthquake data, NN RBF is employed as a classifier [11]. The classification challenges are solved with ANN, support vector machines (SVM), and classification trees (CT) [12]. The classification problem-solving approaches include logistic regression Bayesian network, discriminative analysis, fuzzy logic, linear regression, k -mean clustering methodology, and evolutionary algorithms. Hybrid techniques, such as neurofuzzy-based classification, fuzzy probabilistic neural networks, and recursive partitioning of the majority class algorithm, have been used. Using neural nets and aFOA, the creation of classifier for the categorization [13]. ANN and ANFIS show how earthquake occurrence can be used in a variety of ways in Iran [14]. Their research looked at the temporal-spatial variations in the parameters of seismicity in Iran's neurofuzzy-based classification. In Iran earthquake, the principal component analysis standardizes the data to predict the magnitude of earthquake by ANFIS. An ANFIS system was used to explain grid partition; future earthquake predictions, subtractive clustering, and fuzzy C -means are among the algorithms used in ANFIS modeling for earthquake prediction using data from Iran earthquakes [15]. In the Indian Himalayan Region, the prediction of peak ground acceleration was compared using input as region of earthquake and output as moment of the earthquake by two models ANN and ANFIS [16]. Several researchers have used soft computing techniques to evaluate characteristics of earthquake-related research, and researchers have reported the mapping of damage before happening of earthquake using remote sensing in conjunction with a soft computing strategy [17]. In comparison to neural systems, a critical advantage of neurofuzzy systems is their ability to reason about a specific condition. The researcher presents a comparison in this study in order to forecast the magnitude of the earthquake. As a result, a comparison of methodologies will aid in the magnitude prediction of future earthquakes. In light of the aforementioned research activities, this work presents a comparison of ANFIS with alternative approaches for predicting earthquake acceleration and proposed the triple hybrid model.

2. Literature Review

In this research study [18], Kamath and Kamat proposed the ANFIS techniques in the Andaman Nicobar to forecasting the magnitude of earthquake. A synergistic effect was generated by combining ANN and FIS systems. The European-Mediterranean Seismological Centre provided a 956-earthquake dataset from October 1, 2004 to February 20, 2016. Major variables are depth, previous seismic events magnitude, latitude, and longitude used to calculate the magnitude of incoming earthquakes in the study. ANFIS is a model that combines ANN for learning capacity with fuzzy system to compute numerical language grade estimations. For model training, the ANFIS architecture consists fuzzy nodes of subtractive clustering (accept ratio: 0.5, range of influence: 0.2, reject ratio: 0.15, and squash factor: 1.25) and a hybrid algorithm with eight fuzzy rules. The model of ANFIS produces accurate results faster on the inputted dataset, and the model's performance is tested using root mean squared error (RMSE). This research concludes that using ANFIS, an intelligent approach for earthquake magnitude prediction may be built. In this research [19], Nguyen et al. used PSO to optimize an ANN to solve problem of ground response. This study looks to compute the deflection of building in horizontal manner after considerable seismic loading by using the hybrid PSO-based ANN approach (e.g., the input data taken from Chi-Chi earthquake database). To execute the series of finite element (FE), the training and testing were done by PSO-ANN. The FEM simulation accounting for 80% and 20% on the total dataset, the dataset had 2081 and 8324 testing training testing datasets, respectively. The inputs include Chi-Chi earthquake soil elastic modulus (E), dynamic time (s), dilation angle (λ), friction angle (ϕ), bending stiffness (EI), structure axial stiffness (EA), unit weight (γ), and Poisson's ratio (ν), with output as horizontal deflection (U_x). The results explained the reliability of PSO-ANN is more in assessing ground response and horizontal displacement in short structures following an earthquake. The study [20] by Hasanipanah et al. used the conjunction of particle swarm optimization with ANFIS to illustrate forecasting rock fragmentation. In this model, the values of rock fragmentation, burden, spacing, specific charge, maximum charge, and stemming used per delay were measured on the 72 blast events. Research work focused on the two hybrid techniques [21]; for forecasting peak ground acceleration (PGA), parameters are investigated. The accuracy of the ANFIS approach has been improved with the implementation PSO and GA with ANFIS. The developed hybrid model was implemented on the Pacific Earthquake Engineering Research (PEER) center data. In this hybrid model, the magnitude, source to site distance, faulting mechanisms, and average S-wave velocity of earthquake were used. In comparison to the ANFIS and a few soft computing techniques, the generated model PSO-ANFIS-PSO and GA-ANFIS-GA performed well. The developed model estimate the PGA parameter based on the acquired results, but the PSO-ANFIS-PSO model gives more effective and better results. ANFIS with PSO and GA [22] were used in this study to develop hybrid models for ground

vibration forecasting. The data samples 86 was created from two quarries in Iran to develop prediction models. The input parameters are burden, spacing, stemming, distance from the blast locations, powder factor, and max charge per delay (MCD) whereas peak particle velocity (PPV) is the output value. As per the results of sensitivity analysis, the MCD was discovered to be the most efficient PPV parameter. To assess the models' applicability and efficiency, the determination coefficient (R^2) and root mean square error (RMSE). The model ANFIS-GA and ANFIS-PSO results demonstrated the capability of accurately forecasting the vibration of ground. In comparison with model ANFIS, ANFIS-GA exhibited a 61% (percent) reduction in RMSE and increase ten percent in R^2 , while the model ANFIS-PSO explained a 53% (percent) reduction in RMSE and a nine-percent increase in R^2 . With the GA and PSO, the ANFIS performance has been improved.

3. Analytical Techniques Performed

The analytical techniques were presented, and their architecture was displayed for better understanding.

3.1. Seismic Devices/Sensors. The frequency and severity of earthquakes are on the rise around the globe. Global geological scientists have verified that the Himalayas are due for a devastating earthquake. Important structures should be equipped with seismic sensors and SHM sensors (for measuring things like 3D deflection, vibration, stress, and strain). Figure 1 demonstrates the working of seismic sensors and SHM. Scientists can evaluate the damage from even moderate earthquakes with the aid of seismic monitoring equipment and devices. Then, by utilizing mathematical models, we can extrapolate and foretell the extent to which buildings can be damaged by major earthquakes. The seismic activity of an earthquake can be recorded by seismographs. They are part of a global seismographic network and are deployed underground in locations all over the planet. The seismograph records the ground motion just where the instrument is placed. A seismometer consists primarily of four parts: the seismic sensors themselves, a data gathering and storage unit, a power system, and telemetry for transmitting data in real time to data centers. The latter two systems are typically constructed using off-the-shelf parts, such as batteries, chargers, and solar panels for the energy system, and internet service hardware, cell modems, radios, and/or microwave links for the telemetry. Typically referred to as "data loggers," these devices are equipped with a digitizer, a time stamping mechanism, and software for transmitting data in a uniform format over a telemetry network. The seismic sensors represent the station's highest level of specialization. What if the sensor is affixed to the ground, how would you detect any ground motion? The inertia of a mass is exploited by two types of measuring instruments known by distinct names: seismometers and accelerometers. The basic idea is to use a spring or pendulum to swing a heavy object back and forth. In spite of the fact that the ground is shifting, the mass has not yet budged, not until the spring or pendulum has been extended far enough. In order to keep track of

the instrument's readings, we will need to secure a writing implement to the mass and some sort of paper to the ground. The seismometers and accelerometers available today are far superior to their predecessors. To prevent the mass from shifting with respect to the ground, they employ feedback loops. In order to store and telemeter the data, they use magnets and capacitors to generate voltages and currents that can be easily monitored by digitizers. We can utilize physics to precisely match the measured values to what the ground actually did because the seismometer's or accelerometer's mechanical system never really leaves its "rest position." The addition of the word "meter" to the name of these instruments reflects the fact that they are, in fact, a meter, a device that measures and displays values over time, rather than a pen and paper. The new sensors have many advantages over the older, more impressive-looking ones, including (a) a generally linear relationship between the measured values and real ground motion (described above), (b) the ability to measure three orthogonal components of ground movement in a single unit, (c) sensitivity to a very broad range of frequencies, and (d) high dynamic range, which allows for the detection of both very small and fairly large tremors. Think about how old recording paper was: maybe 1 ft (30 cm) in height. From the smallest to the greatest ground motions, a current sensor would need a sheet of paper roughly 3 miles (5 km) tall to record everything. That is not really useful. The data logger is an important advance because it makes the data digitally available, enables them to be transmitted via contemporary telemetry options, and enables them to be immediately processed in computers to provide earthquake information rapidly and even earthquake early warnings. Excellent in both sound and appearance, these instruments are a real find. Both seismometers and accelerometers suffer from a single major flaw. The gap between a little earthquake (M_0) and the greatest quakes we have ever recorded ($M_{9.5}$) is on the order of 3,000,000,000, while the smallest to largest signal any of them can measure is on the order of 10,000,000 (10 million) (3 billion). Therefore, we set up both locations jointly. An earthquake between magnitudes M_{-1} and M_{-4} can be recorded accurately by the seismometer in the vicinity. All the way from magnitude three (M_3) to magnitude eight and a half ($M_{8.5}$) can be detected by an accelerometer. When the earthquake is large enough and far enough away from the station, both sensors will pick it up. To capture the full picture of what is going on, we set up seismometers and accelerometers wherever possible.

3.2. ANFIS: Adaptive Neurofuzzy Inference System. Neurofuzzy inference system, also known as an ANFIS (adaptive network-based fuzzy inference system) a type of ANN [23–25]. The ANFIS is a neurofuzzy technique fused together with neural network and the fuzzy inference system. In terms of functionality, the ANFIS model is similar to the radial basis function network (RBFN) [26]. In driven of data techniques for integration of ANFIS nets, the clustering of a training set of data samples of function is approximated. Rule-based management process, pattern recognition, classification tasks, and various other challenges

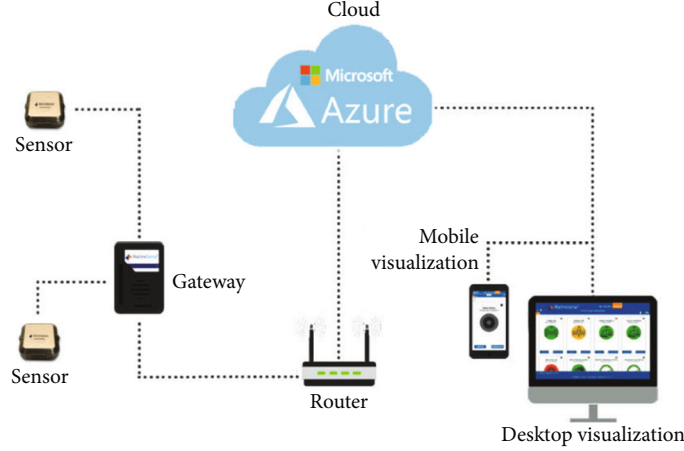


FIGURE 1: Working model of sensors (source: ResearchGate).

have all been effectively solved using ANFIS networks. The FIS combines Takagi-Sugeno-Kang's fuzzy model [27, 28] to define systematic way to produce fuzzy rules on an input data and output data. A rule-based system whose antecedent is composed of linguistic variables and the consequent is represented by a function of the input variables was made. Its inference method is based on a set of fuzzy rules (IF-THEN) with the capacity to approximate nonlinear functions through learning. The following step of the algorithm that is developed for generating the TSK fuzzy model. The algorithm starts iteratively by fuzzy clustering the data. In each iteration, the input and output data clustered with an increased number of clusters. The steps are structure identification and parameter identification.

3.3. ANFIS Architecture. Let us suppose the FIS has two input variables (m and n) and a single output (o). The fuzzy rules of Takagi and Sugeno [29] are included in the rule base:

$$\text{If } m \text{ is } X \text{ and } n \text{ is } Y \text{ then } o \text{ is } f(m, n). \quad (1)$$

In the antecedents, X and Y are set of fuzzy, and in the consequent, $o = f(m, n)$ is a crisp function. m and n are input variables, and $f(m, n)$ is polynomial.

When $f(m, n)$ is constant, a Sugeno fuzzy model for zero-order emerges, which can be as Mamdani FIS special example [30], where the each rule of consequence given through fuzzy singleton. If $f(a, b)$ is first-order polynomial, the Sugeno is first order.

A first-order Takagi-Sugeno fuzzy approach is as follows:

$$\text{Rule 1 : If } m \text{ is } X_1 \text{ and } n \text{ is } Y_1, \text{ then } f_1 = p_1 m + q_1 n + r_1,$$

$$\text{Rule 2 : If } m \text{ is } X_2 \text{ and } n \text{ is } Y_2, \text{ then } f_2 = p_2 m + q_2 n + r_2,$$

(2)

$$\begin{aligned} f_1 &= p_1 m + q_1 n + r_1, \\ \Rightarrow f &= \frac{w_1 f_1 + w_2 f_2}{w_1 + w_2} = w_1 f_1 + w_2 f_2, \\ f_2 &= p_2 m + q_2 n + r_2. \end{aligned} \quad (3)$$

For Takagi-Sugeno model, reasoning approaches are given in Figure 2, and Figure 3 explained the ANFIS model architecture, for comparisons with similar layer nodes to performing same functions.

Layer-1: every node i has function node that is adaptable:

$$O_i^1 = \mu_{X_i}(m). \quad (4)$$

If i input for node m , X_i is linguistic variable linked with function node, and X 's membership function is μ_{X_i} . $\mu_{X_i}(m)$ is usually selected as

$$\begin{aligned} \mu_{X_i}(m) &= \frac{1}{1 + [(m - b_i)^2] l_i} \\ \text{or } \mu_{X_i}(m) &= \exp \left\{ - \left(\frac{m - b_i}{l_i} \right)^2 \right\} \end{aligned} \quad (5)$$

where $\{a_i, b_i, c_i\}$ is the parameter set of premise and a is the input.

Layer-2: each fixed node computes strength of firing ω_i . The product of all input signals has an output node, which is provided as follows:

$$O_i^2 = \omega_i = \mu_{X_i}(m) * \mu_{Y_i}(n), \quad i = 1, 2 \quad (6)$$

The node function can be T -norm operator which performs fuzzy AND in general.

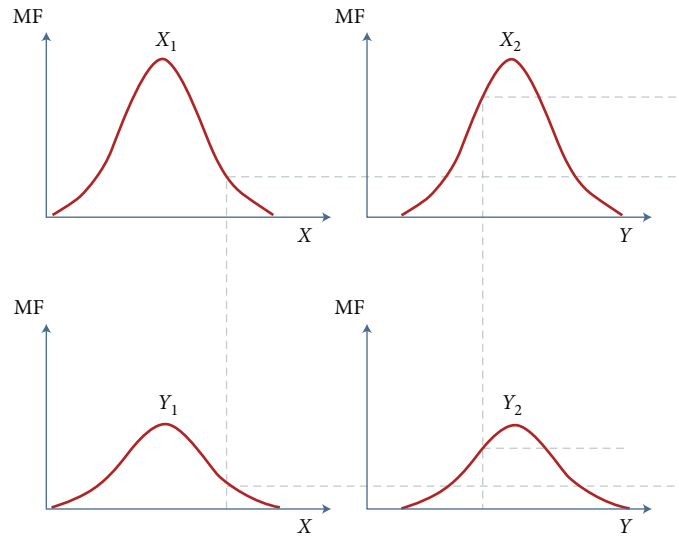


FIGURE 2: A first order with two inputs with two rules, Takagi-Sugeno fuzzy model reasoning (source: ResearchGate).

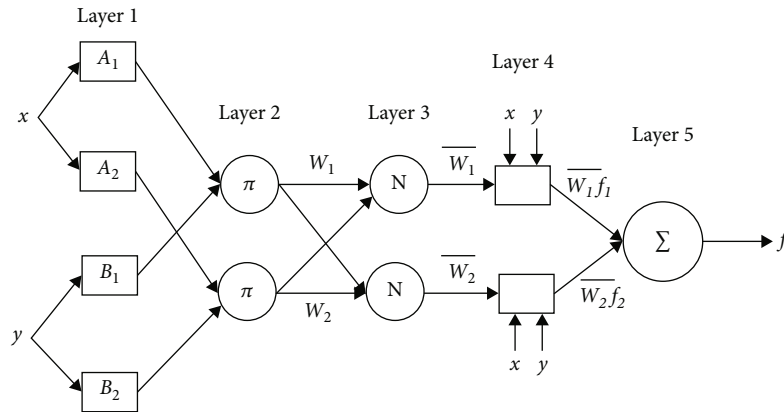


FIGURE 3: Type-3's counterpart architecture of the ANFIS (source: <http://slideplayer.com>).

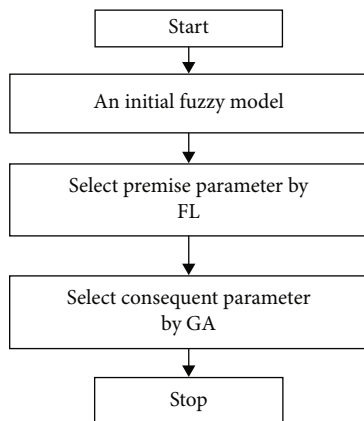


FIGURE 4: Flowchart of a fuzzy system based on GA (source: <http://researchgate.net>).

Layer-3: there is only fixed nodes. The ratio of i^{th} strength of firing rules to the sum of every firing strengths which calculated each i^{th} nodes. The normalized firing

strength has i^{th} node's output, which is given by

$$O_i^3 = \bar{\omega}_i = \frac{\omega_i}{\omega_1 + \omega_2}, i = 1, 2. \tag{7}$$

For convenience, outputs are referred to normalize firing strengths in this layer.

Layer-4: adaptive node with function node defined by

$$O_i^4 = w_i f_i = w_i(p_i m + q_i + r_i), i = 1, 2, \tag{8}$$

where the firing strength is normalized in ANFIS, the third layer output is I , and resultant set of parameters is $\{p_i, q_i, r_i\}$.

The parameters refer in this layer as subsequent parameter.

Layer-5: the fixed node is one, which gives overall output as sum of all the input signal, i.e.,

$$O_i^5 = \sum_i w_i f_i = \frac{\sum_i w_i f_i}{\sum_i w_i}. \tag{9}$$

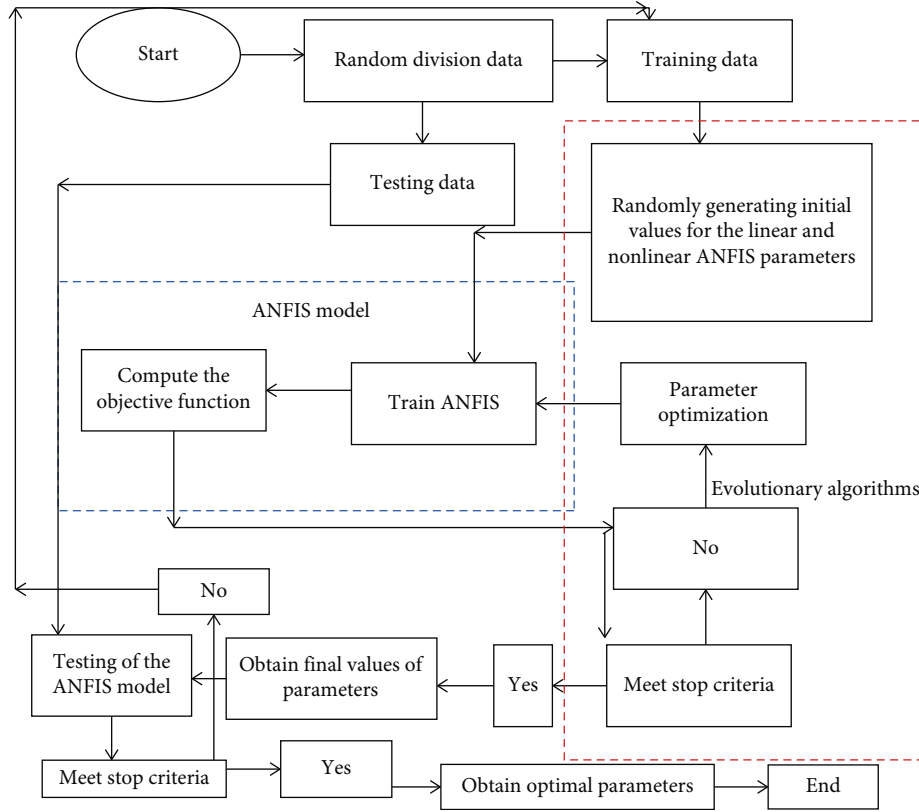


FIGURE 5: ANFIS-GA model procedure (source: <http://google.com>).

As a result, we have develop an adaptive network which functions similarly to Sugeno fuzzy.

The premise parameters values can be taken as linear combination of subsequent parameters in ANFIS architecture.

The following is an example of the output f :

$$\begin{aligned}
 f &= \frac{w_1}{w_1 + w_2} f_1 + \frac{w_2}{w_1 + w_2} f_2 \\
 &= \bar{w}_1 f_1 + \bar{w}_2 f_2 \\
 &= (\bar{w}_1 x) p_1 + (\bar{w}_1 y) q_1 + (\bar{w}_1) r_1 + (\bar{w}_2 x) p_2 + (\bar{w}_2 y) q_2 + (\bar{w}_2) r_2,
 \end{aligned} \tag{10}$$

in the following parameters $p_1, q_1, r_1, p_2, q_2,$ and r_2 , the f is linear fun.

Least square identifies subsequent parameters in forward-pass of learning process, and error signals derive the squared-error to output at every nodes in backward pass, where the output layer to input layer propagate backward. In a step of backward propagation, the parameters of premise were updated by gradient descent approach [31].

3.4. ANFIS with Particle Swarm Optimization Algorithm. Kennedy and Eberhart invented PSO, an intelligent evolutionary, stochastic optimization approach, that replicates social behaviors of flocking birds (1997). Every solution in PSO is a “bird” in space search that is referred as “particle” [32]. Optimization, multiobjective programming, combinatorial optimization, clustering, min-max disadvantages, clas-

sification, prediction, and more other applications of engineering should all be solved using the PSO application [33]. PSO has been effectively used in many engineering issues to solve [34–36] due to the fast convergence rate of comparisons with other algorithms. ANFIS-PSO is global minimization which deals with flaws and returns at point or in n -dimensional space. The concept on which it is based is random population generation and modeling and simulation of mass movement of fish. Particles in the same communication group accelerate towards particles with higher competence over time. Despite each method’s excellent performance on the challenges, continuous optimization problems are solved with tremendous success. ANFIS-PSO is better at solving prediction and forecasting problems.

Algorithms proceed iteratively, updating the velocities and locations as follows:

$$v_{id} = wv_{id} + c_1 r_1 (P_{id} - X_{id}) + c_2 r_2 (P_{gd} - X_{id}), \tag{11}$$

$$X_{id} = X_{id} + v_{id}, \tag{12}$$

where d is the nos. of dimensions $(1, 2, \dots, O)$.

The population size is i $(1, 2, \dots, N)$.

The inertia weight is w .

c_1 and c_2 are two positive constants.

r_1 and r_2 are random values in the range $[0, 1]$.

The i^{th} particle is new velocity calculated using the first Equation (11), which takes into account three terms:

- (i) Prior velocity of particle
- (ii) The difference between the particle's prior and present best positions
- (iii) The distance between the swarm's best particles

Equation (12) calculated the new position of a particle.

3.5. ANFIS with Genetic Algorithm. To derive the initial fuzzy model, the evolutionary algorithm is paired with a fuzzy logic system, similar to the ANFIS model. As the initial model of fuzzy was established, algorithm of genetic utilized through update generated fuzzy rules subsequent parameters to develop the ANFIS-GA system [37]. Evolutionary algorithm was used to fine tune model of fuzzy by updating subsequent parameters produced by the first fuzzy model. The evolutionary algorithm looks for best fit of fuzzy model's subsequent parameter over full solution space. The lateral load output findings are more dependable in the ANFIS-GA approach, and for the first output, there was no difference between results of both phases of test and train. Figure 4 shows a GA-based fuzzy model flow chart for prediction and seismic data. In Figure 5, the technique of the ANFIS-GA model explains how the training and testing datasets are processed and ANFIS-GA model results located in the network.

3.6. Extreme Learning Machine Structure (ELM). ELM is ANN learning approach. Machine learning for unique layer direct feed NN structure was supplied by ELMs, which employ the random projection concept and model of early perceptron to problem-solving approaches. ELM, or with only single hidden layer feedforward nets, is a feedforward ANN with a single layer of hidden neurons. To improve performance and avoid a time-consuming iterative training process, ELM [38, 39] uses a single layer or many layers as a machine learning system. ELM is a direct feedforward approach for clustering, sparse approximation, regression, compression, classification, and learning of features that does not tweak hidden node settings and uses them to interpret other findings, making it an authentic algorithm. Figure 6 shows the ELM model's structure, which is partitioned into input, output, and hidden layer. ELM learning approach was developed alleviate the drawbacks of feedforward ANN, particularly in terms of learning speed.

4. Development of Computation Models

4.1. ANFIS-PSO-GA-ELM Model. The earthquake's peak ground acceleration was calculated in terms of magnitude, focal depth, hypocenter, and S-wave (avg) velocity. Evolutionary algorithms have ANFIS, PSO, and GA techniques are developed using a filtered database with 18964 records. The training data was chosen from the 18964 data points, with 15171 (80%) serving as the training dataset and rest of 3793 serving as the testing dataset to assess model's performance. The ANFIS-PSO, ANFIS-GA, and ELM are used to estimate the peak ground acceleration parameter once the datasets have been arranged. Tables 1 and 2 show the

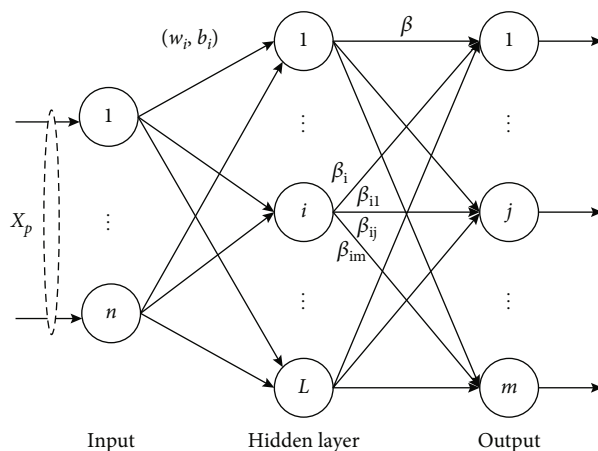


FIGURE 6: The ELM model's structure.

TABLE 1: ANFIS-PSO parameter.

Parameter(s)	Value(s)
Population size	75
Number of epochs (maximum)	15000
Weight (inertia)	1
Learning coefficient (local)	1
Learning coefficient (global)	2

TABLE 2: ANFIS-GA parameter.

Parameter(s)	Value (s)
Population size	75
Number of epochs (maximum)	15000
Percentage of crossover	0.45
Percentage of mutation	0.75
Selection	0.8

parameters of the PSO and GA algorithms, respectively, where the number of epochs is stopping criteria. The ANFIS-PSO and ANFIS-GA parameters listed in the table were selected as trial-and-error procedures. In addition, Figure 7 depicts the RMSE values evolution for hybrid approaches for number of epochs in PGA estimation.

This work will employ the ANFIS-PSO-GA method to optimize the parameters of hidden layer and weights of input layer as shown in Figure 8. The hidden layer produced offsets in random way using ELM. Also, to enhance ELM's stability and accuracy, the used weights which are optimal and offset were taken as hidden layer bias and input weights. The ELM network structure is unstable; this research improves the ELM algorithm with using the ANFIS-PSO-GA algorithm to optimize the N sets of randomly generated input weights and bias b of the hidden layer, using the optimal and bias as ELM improving the network's stability and algorithm's accuracy. Create N as input weight set and b bias for hidden layer at random. The position vector of particle is

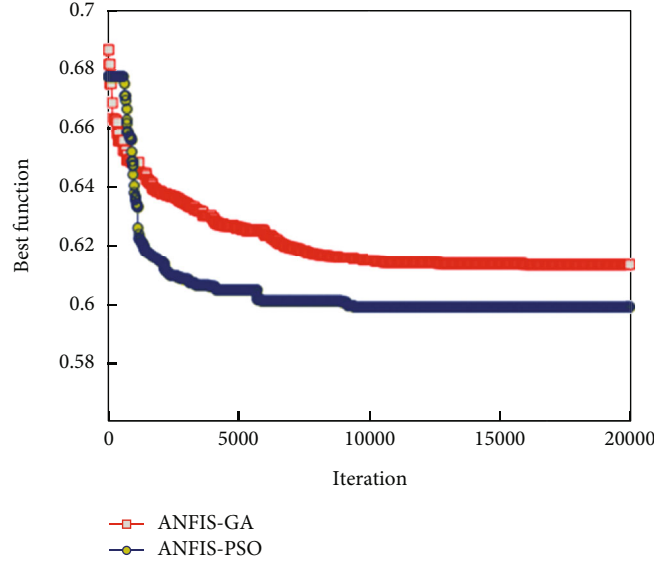


FIGURE 7: In order to estimate peak ground acceleration, the number of epochs multiplied by itself [39].

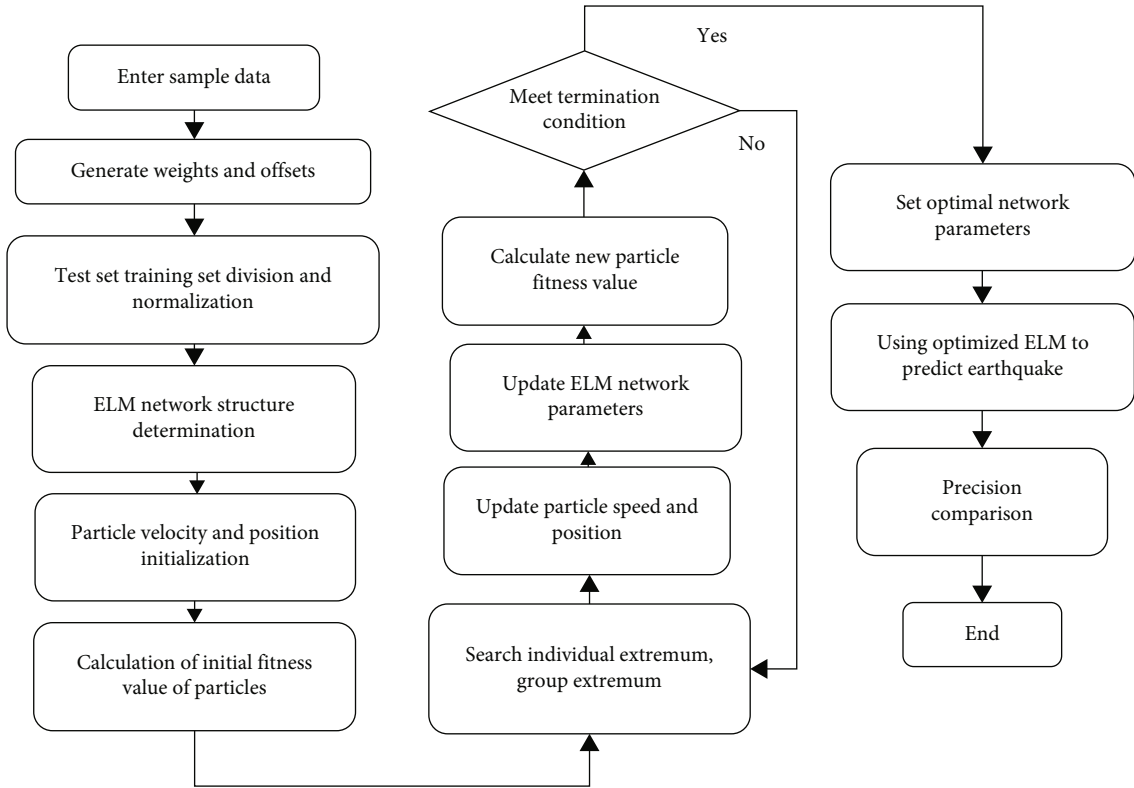


FIGURE 8: ANFIS-PCO-GA-ELM algorithm based on machine learning.

set in particle swarm, specifically $x_{ij} = [\omega, b]$ ($i = 1, 2, \dots, N$, $j = 1, 2, \dots, M$, S is the sum of dimensions ω and b). It finds each particle came nearer to the best place and best particles in group via an iterative technique, resulting in the optimal solution of, b being found. The position and speed of particles are updated at each iteration:

$$\begin{aligned}
 v_{pS}^{E+1} &= \bar{\omega} \cdot v_{pS}^E + c_1 r_1 (a_{pS}^E - x_{pS}^E) + c_2 r_2 (a_{pS}^E - x_{pS}^E), \\
 x_{pS}^{E+1} &= x_{pS}^E + v_{pS}^{E+1}, \\
 \bar{\omega} &= \bar{\omega}_{\max} - \frac{\bar{\omega}_{\max} - \bar{\omega}_{\min}}{E_{\max}} * E.
 \end{aligned} \tag{13}$$

TABLE 3: Previous earthquake datasets (sample).

S.no.	File name	Magnitude	Focal depth	Hypocenter	Avg. S wave	Max acc. (PGA)
1.	AIC0010104032357	5.1	33	131.8186	145.7944	6.377672
2.	AIC0010109271814	4.3	15	59.85619	145.7944	8.008801
3.	AIC0010410050833	4.8	12	79.20026	145.7944	9.106972
4.	AIC0010501091859	4.7	13	15.81847	145.7944	32.98061
5.	AIC0010506201404	4.6	9	52.73296	145.7944	5.124961
6.	AIC0010612191833	4.4	15	48.65247	145.7944	6.80512
7.	AIC0010704151219	5.4	16	66.45873	145.7944	12.42596
8.	AIC0019804222032	5.4	10	24.22194	145.7944	53.17925
9.	AIC0019903161643	4.9	12	75.45403	145.7944	9.272437
10.	AIC0020104032357	5.1	33	117.903	316.9376	7.210437
11.	AIC0020109271814	4.3	15	53.06409	316.9376	7.350292
12.	AIC0020410050833	4.8	12	86.59592	316.9376	5.520461

TABLE 4: Testing and training stages' performance of ANFIS-PSO-GA-ELM.

Model	Stage	Mean_absolute error	Root_mean_square error	R
ANFIS-PSO-GA-ELM	Training	0.34	0.48	0.85
	Testing	0.39	0.52	0.85

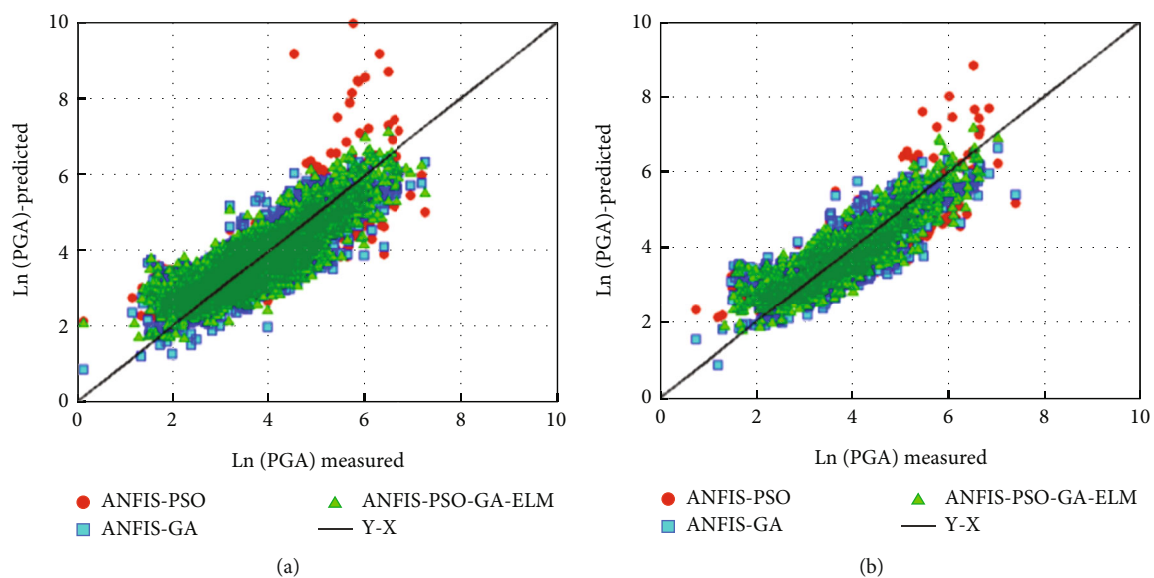


FIGURE 9: Scattered plot showing projected and observed peak ground acceleration for (a) training and (b) testing.

The $v_{ps} = [v_{p1}, v_{p2}, \dots, v_{ps}]$ is particle p flying speed, the value range $[v_{max,s}, v_{min,s}]$, the particle velocity set and $[-1, 1]$ range; c_1 and c_2 is learning factors, and the random numbers are r_1 and r_2 between the $[0, 1]$ interval. The position range $x_{ps} : [x_{min,s}, x_{max,s}]$; optimal position a_{ps} is found the particles; optimal position g_{ps} is found by the whole swarm particle; ω is inertial weight, and the maximum-minimum weight ω_{max} and ω_{min} with values 0.7 and 0.3. E

is the total number of epoch, and E_{max} is the max number of epoch.

4.2. Application of Model. The data of this paper belong from the recorded data of Himalayan range of Himachal Pradesh. The sample of data shown in Table 3.

Assuming input $x_i = \{\text{magnitude, focal depth, earthquake hypocenter, avg. shear wave velocity}\}$ and output

TABLE 5: Performance of other models.

Model	Stage	Mean_absolute error	Root_mean_square error	R
ANFIS-PSO-GA-ELM	Training	0.34	0.48	0.85
	Testing	0.39	0.52	0.85
ANFIS-PSO [41]	Training	0.44	0.56	0.85
	Testing	0.46	0.60	0.85
ANFIS-GA [41]	Training	0.48	0.60	0.83
	Testing	0.48	0.61	0.84
ANFIS-ELM	Training	0.51	0.64	0.81
	Testing	0.52	0.63	0.82
ANN-SA [42]	Training	0.53	0.67	0.81
	Testing	0.53	0.68	0.81
GP [42]	Training	0.53	0.67	0.79
	Testing	0.53	0.68	0.80
GP-SA [42]	Training	0.55	0.69	0.81
	Testing	0.55	0.70	0.81

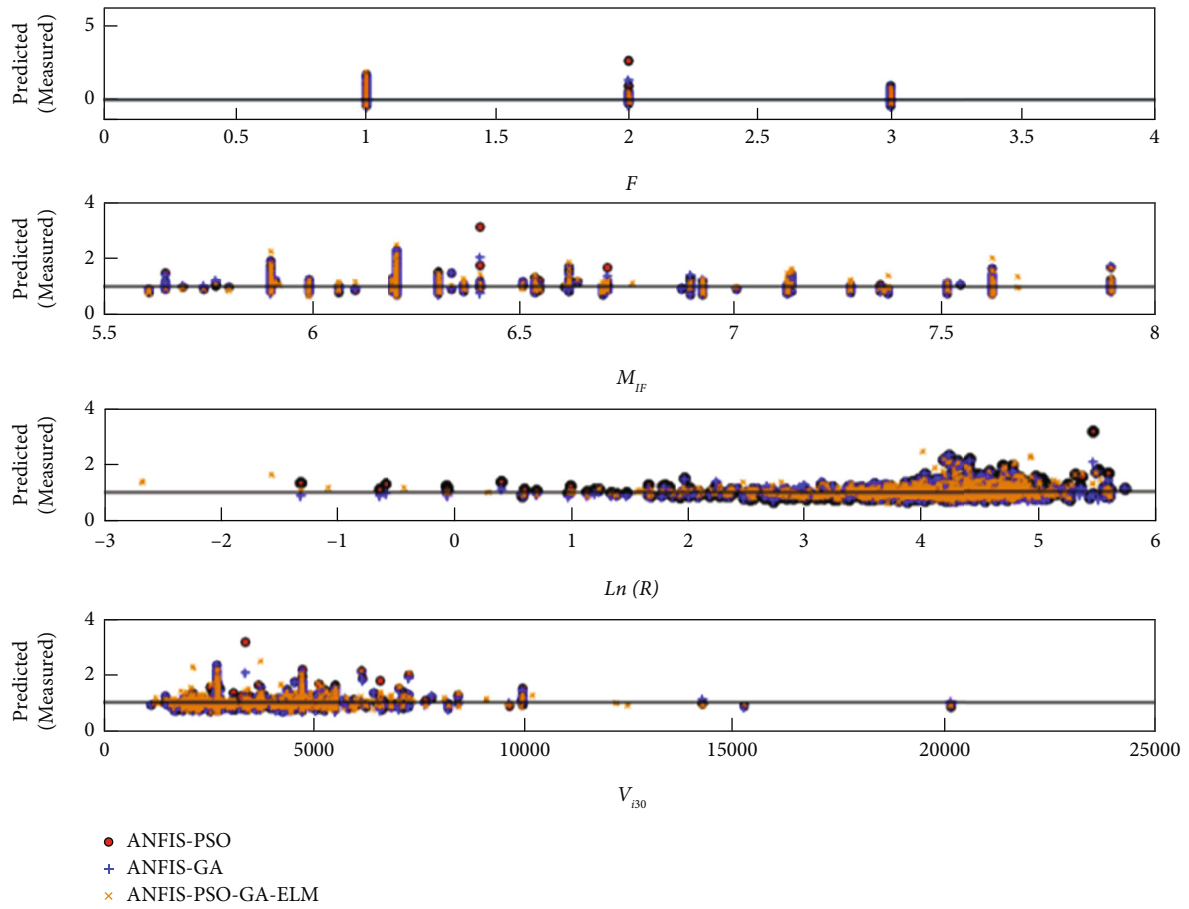


FIGURE 10: In terms of input variables, the ratio between expected and observed peak ground acceleration.

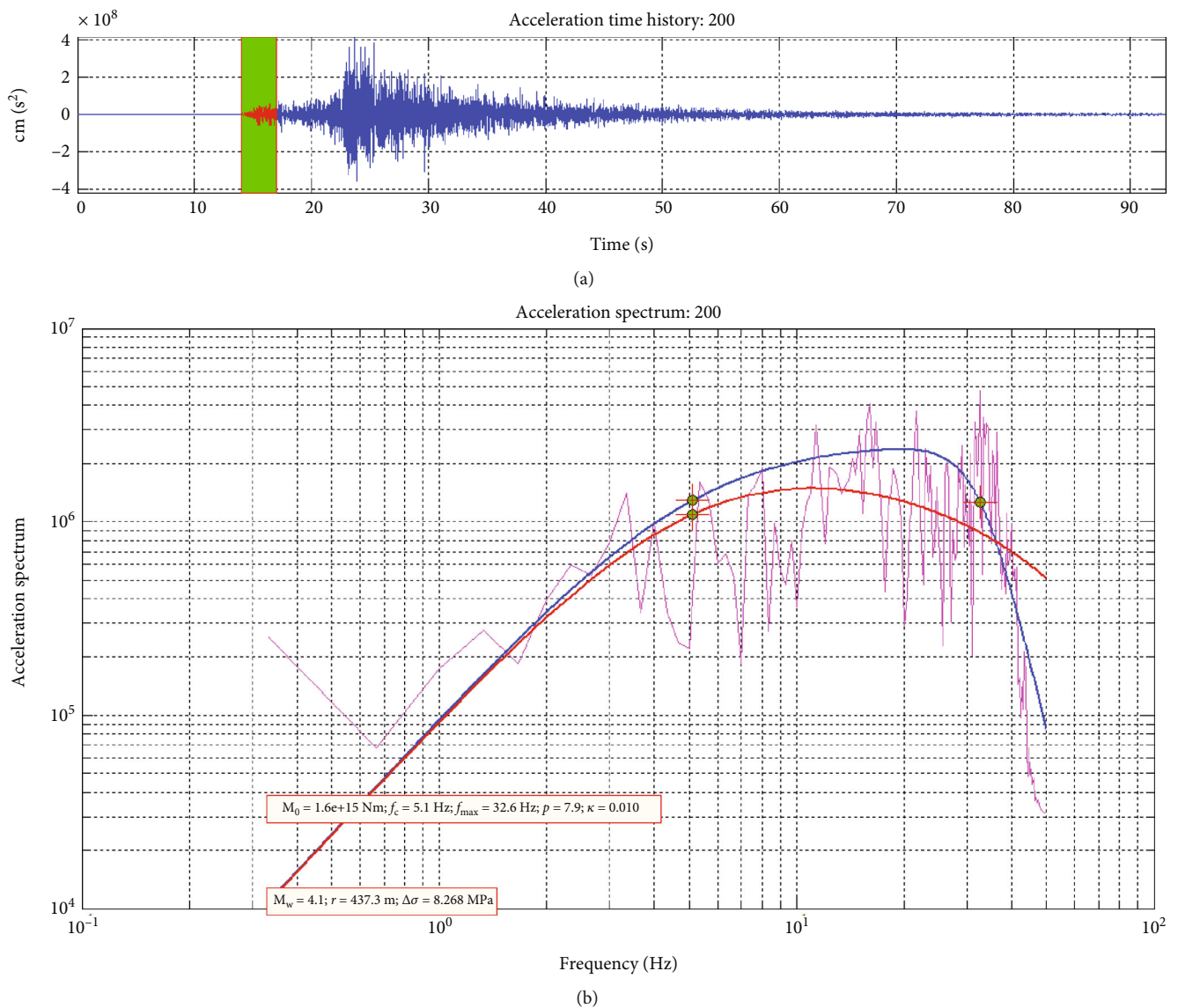


FIGURE 11: (a) Accelerated time history at 2 sec time data. (b) Acceleration spectrum at 2 sec with respect to frequency.

$y = \{\text{Acceleration (max)}\}$, for earthquake prediction the experimental steps based on approaches of ANFIS-PSO-GA-ELM as follows:

- (i) Step-1: determination the sample train, test data, and dataset for prediction. The maintenance technique will be used to train the ANFIS-PSO-GA-ELM network in this study
- (ii) Step-2: to increase the APSO-ELM algorithm's rate of convergence, normalize the sample set
- (iii) Step-3: using the Python programming libraries, create a three-layer ANFIS-PSO-GA-ELM network structure, then in each layer, determine the excitation function and numbers of neuron, choose Sigmoid as excitation function
- (iv) Step-4: optimize ELM parameters is used in the ANFIS-PSO-GA to obtain optimal parameter values of network, such as the input layer's optimal value of hidden layer linked with weight (w). With weight and bias, the output layer was connected with hidden layer
- (v) Step-5: the training effect of ANFIS-PSO-GA-ELM compared with other approaches, data is trained using the classic backpropagation neural network and ELM model, and then, the training accuracy of ANFIS-PSO-GA-ELM, ELM model, and backpropagation NN is compared
- (vi) Step-6: for earthquake prediction models ANFIS-PSO-GA-ELM, ELM was used for inputting the data and for comparing backpropagation NN accuracy

5. Discussion and Result

In the stages of training and testing, the correlation coefficient (R), error indicator analyses, root mean square error (RMSE), and mean absolute error (MAE) can be defined in this fashion [39].

$$\begin{aligned} \text{MAE} &= \frac{\sum_{i=1}^N |J_i - K_i|}{N}, \\ \text{RMSE} &= \sqrt{\frac{1}{N} \sum_{i=1}^N (J_i - K_i)^2}, \\ R &= \frac{\sum_{i=1}^N (J_i - J_m)(K_i - K_m)}{\sqrt{(\sum_{i=1}^N (J_i - J_m)^2) \sqrt{(\sum_{i=1}^N (K_i - K_m)^2)}}, \end{aligned} \quad (14)$$

where the measured value was represented as K_i , the prediction values were represented as J_i , the data points number represented as N , observation mean value was represented as K_m , and predictions mean value was represented as J_m [40–43]. Table 4 shows the results of ANFIS-PSO-GA-ELM, ANFIS-GA, and ANFIS-PSO during the stages of training and testing. When compared to the other generated models, the ANFIS-PSO-GA-ELM model gave higher performance with accuracy ($R = 0.85$, $\text{RMSE} = 0.48$, and $\text{MAE} = 0.34$) during training stages. In comparison to other created models, the ANFIS-PSO network predicts the peak ground acceleration parameter with better accuracy ($R = 0.85$, $\text{RMSE} = 0.52$, and $\text{MAE} = 0.39$) during testing stages. Observed and predicted values of PGA showed in scatter plots for both phases of train and test using constructed models shown in Figures 9(a) and 9(b), for greater illustration. The ANFIS-PSO-GA-ELM model has reduced observed and predicted PGA scatter values than other developed model demonstrated. It is worth noting that the developed ANFIS-PSO, ANFIS-GA, and ANFIS-ELM models are extremely accurate. However, the ANFIS-PSO-GA-ELM triple hybrid model performs better than the hybrid model.

The generated models' performance is also compared to that of certain well-known soft computing-based models, such as the ANFIS-PSO, ANFIS-GA, ANFIS-ELM, ANN-SA, GP, and GP-SA algorithms. Table 5 explains the findings of statistical error parameters for the given approaches as well as the constructed models.

To have strong prediction ability, the error of predictive model is independent to input factors. As a result, Figure 10 shows the ratios of projected PGA parameter to observed values for several created models for magnitude, focal depth, and Avg S-wave velocity. The accuracy of the model will deteriorate as the scattering in this figure grows. The ANFIS-PSO-GA-ELM model's predictions are accurate in relation to the input parameters, as can be seen in these graphs.

As a result, it is shown in Figures 11(a) and 11(b), calculated using Brune model implementation on ANFIS-PSO-GA-ELM model optimized data. That result also helps to calculate the estimation of source parameter of earthquake.

6. Conclusion

It is quite difficult to make accurate predictions about the most important components of seismic loading. In this study, a soft computing method was employed to overcome the prediction problem by deleting a few unneeded parameters of input. Specifically, the parameters included in the study were the following: The ANFIS approach that was used to pick the relevant features for the purpose of predicting the components that were the most important in seismic loading. However, the ANFIS-PSO-GA-ELM method generates the most accurate and reliable forecasts of seismic loads among all of the approaches that were utilized in this work. All of the ways that were utilized produced outstanding and realistic predictions of seismic loads. In addition, the ELM nets have shown the best results when it comes to the prediction of the b value as a parameter. As a consequence of this, both the ANFIS-GA and ANFIS-PSO methods have been judged to be effective; however, the experimental findings in this earthquake prediction show that the extreme learning machine (ELM) method combined with the ANFIS-PSO-GA method yields superior results. As a result, it is recommended that the ELM method be used in neural networks in order to achieve the best possible outcomes. The predictions made by the ANFIS-PSO-GA-ELM model are accurate, with a trend that is less noticeable in relation to the parameters that were input. In the future, research should concentrate on the performance of algorithms that make use of hybrid metaheuristic techniques. Particular attention should be paid to triple hybrid approaches.

Data Availability

The numerical data collected from various stations are used for fact findings of this study.

Conflicts of Interest

The authors declare that they have no conflicts of interest.

Acknowledgments

This research is supported by the Princess Nourah Bint Abdulrahman University Researcher Supporting Project number PNURSP2023R195, Princess Nourah Bint Abdulrahman University, Riyadh, Saudi Arabia.

References

- [1] R. K. Kamat and R. S. Kamath, "Visualization of earthquake clusters over space: K-means approach," *Journal of Chemical and Pharmaceutical Sciences (JCHPS)*, vol. 10, no. 1, pp. 250–253, 2017.
- [2] R. S. Kamath, "Design and development of soft computing model for teaching staff performance evaluation," *International Journal of Engineering Sciences & Research Technology (IJESRT)*, vol. 3, no. 4, pp. 3088–3094, 2014.
- [3] H. Demuth and M. Beale, *Neural Network Toolbox for Use with MATLAB*, MathWorks, Inc, 2015.

- [4] D. Bystrov and J. Westin, *Practice*, Neuro-fuzzy logic systems Matlab Toolbox GUI, 2016.
- [5] H. Adeli and S. L. Hung, "A concurrent adaptive conjugate gradient learning algorithm on MIMD shared-memory machines," *The International Journal of Supercomputing Applications*, vol. 7, no. 2, pp. 155–166, 1993.
- [6] S. Hung and H. Adeli, "An adaptive conjugate gradient learning algorithm for effective training of multilayer neural networks," *Applied Mathematics and Computation*, vol. 62, no. 1, pp. 81–102, 1994.
- [7] N. Bourbakis, P. Kakumanu, S. Makrogiannis, R. Bryll, and S. Panchanathan, "Neural network approach for image chromatic adaptation for skin color detection," *International Journal of Neural Systems*, vol. 17, no. 1, pp. 1–12, 2007.
- [8] P. Gopych, "Biologically plausible BSDT recognition of complex images: the case of human faces," *International Journal of Neural Systems*, vol. 18, no. 6, pp. 527–545, 2008.
- [9] M. Vatsa, R. Singh, and A. Noore, "Integrating image quality in 2v-SVM biometric match score fusion," *International Journal of Neural Systems*, vol. 17, no. 5, pp. 343–351, 2007.
- [10] A. Khashman and B. Sekeroglu, "Document image binarisation using a supervised neural network," *International Journal of Neural Systems*, vol. 18, no. 5, pp. 405–418, 2008.
- [11] A. Rana, A. Kumar, and A. Sharma, "Neural network radial basis function classifier for earthquake data using aFOA," *International Journal of Advanced Research*, vol. 4, no. 8, pp. 537–540, 2016.
- [12] A. Rana, P. Vaidya, and G. Gupta, "A comparative study of quantum support vector machine algorithm for handwritten recognition with support vector machine algorithm," *Materials Today: Proceedings*, vol. 56, pp. 2025–2030, 2022.
- [13] A. Rana and A. Sharma, "Optimization of radial basis neural network by mean of amended fruit fly optimization algorithm," *Journal of Computer and Mathematical Sciences*, vol. 5, no. 3, pp. 262–272, 2014.
- [14] A. Zamani, M. Reza, and A. Safavi, "application of neural network and ANFIS model for earthquake occurrence in Iran," *Earth Science Informatics*, vol. 6, no. 2, pp. 71–85, 2013.
- [15] M. Mirrashid, "Earthquake magnitude prediction by adaptive neuro-fuzzy inference system (ANFIS) based on fuzzy C-means algorithm," *Natural Hazards*, vol. 74, no. 3, pp. 1577–1593, 2014.
- [16] A. Mittal, S. Sharma, and D. P. Kanungo, "A comparison of ANFIS and ANN for the prediction of peak ground acceleration in Indian Himalayan Region," in *Proceedings of the International Conference on Soft Computing for Problem Solving (SocProS 2011)*, pp. 457–468, Roorkee India, 2011.
- [17] B. Mansouri and Y. Hamednia, "A soft computing method for damage mapping using VHR optical satellite imagery," *IEEE Journal of Selected Topics in Applied Earth Observations And Remote Sensing*, vol. 8, no. 10, pp. 4935–4941, 2015.
- [18] R. S. Kamath and R. K. Kamat, "Earthquake magnitude prediction for Andaman-Nicobar Islands: adaptive neuro fuzzy modeling with fuzzy subtractive clustering approach," *Journal of Chemical and Pharmaceutical Sciences*, vol. 10, pp. 1228–1233, 2017.
- [19] H. Nguyen, H. Moayedi, L. K. Foong et al., "Optimizing ANN models with PSO for predicting short building seismic response," *Engineering with Computers*, vol. 36, no. 3, pp. 823–837, 2020.
- [20] M. Hasanipanah, H. B. Amnieh, H. Arab, and M. S. Zamzam, "Feasibility of PSO-ANFIS model to estimate rock fragmentation produced by mine blasting," *Neural Computing and Applications*, vol. 30, no. 4, pp. 1015–1024, 2018.
- [21] A. Kaveh, S. M. Hamze-Ziabari, and T. Bakhshpoori, "Feasibility of PSO-ANFIS-PSO and GA-ANFIS-GA models in prediction of peak ground acceleration," *International Journal of Optimization in Civil Engineering*, vol. 8, no. 1, pp. 1–14, 2018.
- [22] H. Yang, M. Hasanipanah, M. M. Tahir, and D. T. Bui, "Intelligent prediction of blasting-induced ground vibration using ANFIS optimized by GA and PSO," *Natural Resources Research*, vol. 29, no. 2, pp. 739–750, 2020.
- [23] J. S. R. Jang, C. T. Sun, and E. Mizutani, "Neuro-fuzzy and soft computing: a computational approach to learning and machine intelligence," *IEEE Transactions on Automatic Control*, vol. 42, no. 10, pp. 1482–1484, 1997.
- [24] J. S. R. Jang and C. T. Sun, "Neuro-fuzzy modeling and control," *Proceedings of the IEEE*, vol. 83, no. 3, pp. 378–406, 1995.
- [25] J. S. R. Jang, "ANFIS: adaptive-network-based fuzzy inference system," *IEEE Transactions on Systems, Man, and Cybernetics*, vol. 23, no. 3, pp. 665–685, 1993.
- [26] J. S. R. Jang and C. T. Sun, "Functional equivalence between radial basis function networks and fuzzy inference systems," *IEEE Transactions on Neural Networks*, vol. 4, no. 1, pp. 156–159, 1993.
- [27] M. Sugeno and G. T. Kang, "Structure identification of fuzzy model," *Fuzzy Sets and Systems*, vol. 28, no. 1, pp. 15–33, 1988.
- [28] T. Takagi and M. Sugeno, "Fuzzy identification of systems and its applications to modeling and control," *IEEE Transactions on Systems, Man, and Cybernetics*, vol. SMC-15, no. 1, pp. 116–132, 1985.
- [29] T. Takagi and M. Sugeno, "Derivation of fuzzy control rules from human operator's control actions," *IFAC Proceedings Volumes*, vol. 16, no. 13, pp. 55–60, 1983.
- [30] E. H. Mamdani and S. Assilian, "An experiment in linguistic synthesis with a fuzzy logic controller," *Int. J. Man-Machine Studies*, vol. 7, no. 1, pp. 1–13, 1975.
- [31] S. Haykin, *Neural Networks - a Comprehensive Foundation*, Pearson Education (Singapore) Pvt. Ltd., Indian Branch, 4th edition, 2003.
- [32] A. Rana and D. Sharma, "Mobile ad-hoc clustering using inclusive particle swarm optimization algorithm," *International Journal of Electronics and Information Engineering*, vol. 8, no. 1, pp. 1–8, 2018.
- [33] K. Khan and A. Ahai, "A comparison of BA, GA, PSO, BP and LM for training feed forward neural networks in e-learning context," *International Journal of Intelligent Systems and Applications*, vol. 4, no. 7, pp. 23–29, 2012.
- [34] Y. Bao, T. Xiong, and Z. Hu, "PSO-MISMO modeling strategy for multistep-ahead time series prediction," *IEEE Transactions on Cybernetics*, vol. 44, no. 5, pp. 655–668, 2014.
- [35] M. Hasanipanah, M. Noorian-Bidgoli, D. J. Armaghani, and H. Khamesi, "Feasibility of PSO-ANN model for predicting surface settlement caused by tunneling," *Engineering Computations*, vol. 32, no. 4, pp. 705–715, 2016.
- [36] E. T. Mohamad, D. J. Armaghani, E. Momeni, A. H. Yazdavar, and M. Ebrahimi, "Rock strength estimation: a PSO-based BP approach," *Neural Computing and Applications*, vol. 30, no. 5, pp. 1635–1646, 2018.

- [37] I. P. Panapakidis and A. S. Dagoumas, "Day-ahead natural gas demand forecasting based on the combination of wavelet transform and ANFIS/genetic algorithm/neural network model," *Energy*, vol. 118, pp. 231–245, 2017.
- [38] P. Jagtap and G. N. Pillai, "Comparison of extreme-ANFIS and ANFIS networks for regression problems," in *2014 IEEE International Advance Computing Conference (IACC)*, pp. 1190–1194, Gurgaon, India, 2014.
- [39] A. Kaveh, S. M. Hamze-Ziabari, and T. Bakhshpoori, "M5' algorithm for shear strength prediction of HSC slender beams without web reinforcement," *International Journal of Modeling and Optimization*, vol. 7, no. 1, pp. 48–53, 2017.
- [40] A. Kaveh, S. M. Hamze-Ziabari, and T. Bakhshpoori, "Patient rule-induction method for liquefaction potential assessment based on CPT data," *Bulletin of Engineering Geology and the Environment*, vol. 77, no. 2, pp. 849–865, 2018.
- [41] X. Huang, M. Luo, and H. Jin, "Application of improved ELM algorithm in the prediction of earthquake casualties," *PLoS One*, vol. 15, no. 6, article e0235236, 2020.
- [42] A. H. Alavi and A. H. Gandomi, "Prediction of principal ground-motion parameters using a hybrid method coupling artificial neural networks and simulated annealing," *Computers and Structures*, vol. 89, no. 23-24, pp. 2176–2194, 2011.
- [43] A. K. Mohammadnejad, A. K. Mousavi, S. M. Torabi, M. Mousavi, and A. H. Alavi, "Robust attenuation relations for peak time-domain parameters of strong ground motions," *Environment and Earth Science*, vol. 67, no. 1, pp. 53–70, 2012.

Research Article

Industrial Internet Sensor Node Construction and System Construction Based on Blockchain Technology

Jia Hong Zhou 

Information Engineering Department, Eastern Liaoning University, Dandong, 118000 Liaoning, China

Correspondence should be addressed to Jia Hong Zhou; zhoujiahong@elnu.edu.cn

Received 29 August 2022; Revised 1 October 2022; Accepted 25 November 2022; Published 30 January 2023

Academic Editor: Sweta Bhattacharya

Copyright © 2023 Jia Hong Zhou. This is an open access article distributed under the Creative Commons Attribution License, which permits unrestricted use, distribution, and reproduction in any medium, provided the original work is properly cited.

The present industrial Internet platform (IIP) is subjected to numerous complex security issues, and thus technologies that focus on achieving data security of the IIP has become top priority. The data security crisis of IIP gets mainly reflected in the malicious deletion and theft of data, the random access of terminal devices, and the low security of traditional security authentication methods. Blockchain technology adopts distributed network architecture, wherein through asymmetric encryption mechanism, it helps to solve problems associated with single point of downtime and privacy data leakage of central management of industrial Internet. In addition, considering the accept of random access and deletion of industrial interconnection terminal equipment, this paper uses the role access control mechanism based on Hyperledger, thereby regulating user access according to the user's role in the platform and management of terminal equipment through chain code. The paper includes the following contributions: (1) firstly, it expounds the research background and significance of the IIP and introduces the research status of the industrial Internet and blockchain at home and abroad. (2) Secondly, the IIP architecture is designed based on blockchain technology and implements a sensor node management and monitoring system. (3) Thirdly, the paper uses the gateway to preprocess the collected data, thereby reducing the data transmission delay and improving the real-time and effectiveness of the data. The paper finally implements neural network to evaluate the construction quality of industrial Internet sensor nodes and obtains promising test results.

1. Introduction

With the rapid development and update of information technology, it has become the current development trend to connect sensors and hardware devices to the network for management, and the IoT has also become a research hotspot at home and abroad. The IoT has changed the original concept in the continuous development and is no longer limited to sensing technologies such as radio frequency identification, and the coverage has been expanded. It breaks the limitation that the network is only connected by terminal devices such as computers and realizes the interconnection and information exchange between people, people and things, and things and things [1, 2]. The various sensing devices connected to the IoT become the eyes and ears of humans to perceive the

surrounding environment and objects, thereby realizing intelligent management, remote control, real-time positioning, and environmental monitoring of various things connected to the IoT. Further, due to the improvement of people's requirements for quality of life and the needs of social development, large-scale IoT applications such as smart cities, smart homes, and smart transportation are also popular [3, 4]. In recent years, with the emergence and rise of 5G technology, it has provided new opportunities for the development of the IoT. In this context, all walks of life have joined the ranks of information and industry integration. At the same time, it has also accelerated the revolution of industrial Internet technology and has gradually formed an automated and information-based architecture system. Industrial Internet services take advantage of IoT communications and cover a wide range of

applications including heavy industry, medical industry, aerospace, transportation, and other key national industries that have played an important role [5, 6]. In order to promote the development of industrial intelligence and build an enabling platform for efficient data collection and function management, the industrial Internet architecture is proposed. At the same time, with the continuous rise of new technologies such as AI, cloud computing, edge computing, 5G, and blockchain, integration with new technologies has become one of the current development directions. According to the main application scenarios and actual needs of the industrial Internet, the future will develop in the direction of intelligent management, optimization of production processes, flexible production, and industrial upgrading [7]. At the same time, the scale of the industry is expanding, and the upgrading of the industry also needs to be carried out simultaneously. Among them, it is inevitable to use large-scale sensors to collect a large amount of data, and data communication technology to implement effective real-time monitoring and management of production. Due to the alternation of new and old equipment in industrial production, the factory area is generally large, which leads to complex and scattered types of production equipment and sensor nodes connected to the industrial Internet [8]. At the same time, in order to ensure efficient and stable production, the number of monitoring nodes set up has also greatly increased, which has brought great pressure to equipment management and data transmission. In addition, compared with general IoT devices, the industrial production process is rapid and large scale; the production environment is complex, and the network environment is poor, which affects the transmission of data. In this way, the staff cannot obtain effective data for the first time to effectively monitor and manage the production process and industrial equipment. If the problem is not detected in time, it will lead to production delays and economic losses, so there are higher requirements for the real time and stability of data [9]. The traditional supervision platform is centralized in the cloud, and there are many factors affected by data transmission, and there is no good way to deal with the huge data. Therefore, traditional factory management methods have been unable to keep up with the speed and demand of the development of emerging industries at this stage. Therefore, enterprises urgently need a set of efficient and intelligent equipment management and control system to supervise and control their production equipment scientifically and efficiently [10]. The industrial Internet needs to adapt to various protocol devices to aggregate, collect, and transmit data of various types and formats. Gateways serve a crucial role in connecting one generation of technology to the next by bridging the gap between different types of networks and data transfer [11]. On top of standard gateway hardware, the industrial Internet gateway provides data management, filtering, analysis, monitoring, and administration capabilities to more broadly address the issue of data management [12]. Some security features of blockchain technology provide possible solutions to the security problems faced by the industrial Internet. The so-called blockchain is a multiparty participation and maintenance, and the data information on the chain supports anyone through the theory of data structure and

cryptography, distributed ledger technology that cannot be modified. The blockchain has the characteristics of decentralized management, the entire network maintenance of the ledger data, the data information cannot be tampered with by anyone, and the data information security encryption. Each data block in the blockchain ledger is subject to multiple valid transaction confirmations by other nodes in the entire network. The consensus mechanism is used to maintain the consistency of all node information in the entire network, and cryptography is used to ensure the data security and unforgeability of the distributed ledger [13]. All of the nodes in a distributed network work together to update the blockchain ledger. The data in the global ledger is backed up locally on each node, where it is verified and managed. In addition, the identity access concept of blockchain technology may guarantee that only the data's rightful owner can access the data. At the same time, blockchain enables the decentralized trading and storing of digital assets. The usage of smart contracts in a blockchain environment guarantees that agreed-upon conditions will be met [14]. A smart contract is a piece of code written in a computer language, which is a protocol that is run by nodes in a blockchain for automation [15]. This research designs and implements a set of industrial Internet sensor node management and monitoring system based on blockchain. According to the results of actual data collection through multiple tests, there is a big difference between the actual required valid data and the collected complete data. Invalid data will lead to slow system processing progress and increase response time, so this paper uses gateway to preprocess the collected data, thereby reducing the data transmission delay and improving the real-time and validity of the data. At the same time, a new sensor node identification method is designed, which is easy to manage, and each piece of data can be quickly traced back to the source to improve management efficiency. This paper also uses smart contracts to manage configuration files in an Industrial Internet environment. After completing the above work, this paper uses neural network to evaluate the construction quality of industrial Internet sensor nodes.

The unique contributions of the paper include the following:

- (i) Development of an IIP architecture considering blockchain technology to implement sensor node management and system
- (ii) Use of gateway for processing the collected data, reducing the data transmission delay thereby improving the real-time and effectiveness of the data

The organization of the paper is as follows. Section 2 discusses the related study. Section 3 presents the methods followed by experimental results and analysis in Section 4. Section 5 presents the conclusion.

2. Related Work

The Internet of Things (IoT) is a chance to construct an intelligent environment made possible by the integration of

the physical and network worlds, which emerged as a result of the steady progress of science and technology in modern civilization. The Industrial Internet is a branch of the IoT, focusing more on the interaction and information transfer between devices and people, and has very broad development and application prospects. With the rapid rise of a new round of scientific and technological innovation revolution around the world, it not only promotes the sustainable development of the manufacturing industry, but at the same time, its transformation to digitalization and intelligence has also been further promoted to the national strategic height [16, 17]. The IIP is an important part of the industrial Internet. It is mainly supported by new-generation innovative technologies such as big data, cloud computing, machine learning, and AI as well as smart devices. It is an application of “Internet +” deep integration in the industrial field. The IIP contains several main goals: to effectively allocate industrial production resources and comprehensively improve production and management efficiency [18]. In addition, it also has a positive impact on the digital and intelligent transformation of the manufacturing industry, completing the upgrading of industrial intelligent production and management, and is also conducive to the upgrading of industrial production and flexible customization. From a global analysis, the industrial Internet has gradually formed its own technical system, and the R&D of related companies has begun to take shape, and the applicable scenarios are increasingly enriched [19]. There are some typical examples of IIP, mainly including HiaCloud platform as an equipment and automation enterprise; the research and development focus on scenarios such as reconstructing the production and maintenance operations of enterprises in the digital environment. Siemens’ MindSphere platform uses the cloud platform to realize the fault early warning function. In addition, the Haier-COSMOplat platform is also a relatively mature IIP at this stage [20]. As a big manufacturing country, although China is still in its infancy in the construction of an IIP, its technological infrastructure and comprehensive capabilities are relatively weak, and the platform covering the entire industry has not yet been completed. However, the platforms for certain industries and fields have begun to take effect and are gradually expanding their influence. The relatively mature IIP in my country at this stage include Yonyou IIP, Aerospace Cloud INDICS Platform, Inspur IIP, etc. [21]. Reference [22] proposes a cloud-based IIP that combines “device management” and “application enablement”. The use of microservice technology reduces the coupling between management platforms, supports flexible access to multiple applications, is easy to expand and develop, and breaks the current status quo of fragmented development and low utilization in the current industrial Internet industry. Integrate partners on the entire industry line to provide a safe and efficient “one-stop” service platform. This solution mainly solves the problem of multiple application multiplexing and access. It does not flexibly use the gateway as the core device in the industrial Internet and does not provide a good solution at the data level. Reference [23] designed and developed a blockchain-based industrial IoT service platform. In order to adapt to large-

scale equipment access, the article selected the Logchain blockchain system. Based on M2M IoT standards and blockchain hybrid applications, a blockchain-enabled IoT service layer platform is built to provide IoT users the option of using either centralized or decentralized databases to keep track of their data. As an interconnection device of a complex network, the gateway plays an indispensable role in the network system and is used to realize the interconnection and intercommunication of different networks and perform protocol conversion. Reference [24] proposed a smart home system platform based on Raspberry-PI gateway and cloud service for interoperability between various traditional home appliances and different communication technologies and protocols. It provides the functions of controlling home appliances and analyzing data, but the application scenarios are relatively limited, and there is no better way to deal with the real time and effectiveness of data transmission. It is not suitable for complex scenarios such as industrial environments. Reference [25] designed an IoT gateway monitoring system based on edge computing. In view of the diversity of IoT device communication protocols and the lack of cloud computing power, edge computing technology was used. Based on EdgeX Foundry framework, a set of temperature and humidity alarm system using Modbus protocol is constructed, which has high application value. However, it is mainly aimed at the early warning function, and there are still deficiencies in the functions of monitoring and management. At the same time, the expansion performance and maintainability of the system are poor. Reference [26] proposes a dual-deposit escrow transaction protocol that combines bilateral payment deposits with simple cryptographic primitives, implemented using blockchain-based smart contracts. The security argument of the protocol is carried out by means of a game, which proves that the complete Nash’s equilibrium of the subgame of the game is a game in which buyers and sellers cooperate and are honest and trustworthy. Reference [27] proposed to use the characteristics of blockchain technology to solve the problems of information asymmetry in the current instrument leasing platform. Combining blockchain technology in the leasing platform allows lessor and lessee nodes to build a decentralized blockchain network and install a smart contract in it to complete the leasing process, so that the transaction information generated during leasing and the data generated when the instrument is used can be uploaded to the blockchain, and then a consensus is reached to form a block record in the network. Reference [28] proposes a general framework for authentication and authorization in a restricted environment. Access to terminal devices requires authentication and authorization to ensure the security of the platform. Addresses a major limitation of the datagram transport layer security protocol by protecting application-layer paid payloads. Reference [29] also proposed the distributed ledger management technology through blockchain to realize the sharing of IoT data and solve the problem of trust in traditional centralized institutions. The monitoring and management of terminal equipment is very important to the security of the IIP, which ensures the continuous, efficient and trouble-free operation of industrial equipment. Reference

[30] mainly measures and tracks the state of the network. They provide different levels of management through plugins and extensions. One method of network monitoring is to use probes to measure network indicators to actively monitor terminal device status. By configuring pairs of network devices, a certain amount of traffic is introduced into the network to monitor key indicators and ensure the quality of device operation. Reference [31] developed a food anti-counterfeiting traceability system using Blockchain and the Internet of Things. The framework used decentralized storage technology and Blockchain to store traceability related data for food during the process of food production; sale and transportation to ensure uniqueness of the food are retained. The IoT technology helps in maintaining authenticity and reliability of the data stored in the Blockchain. Reference [32] a layered architecture using Blockchain and machine learning is proposed. The study includes using industrial internet-of-things for smart manufacturing applications. The architecture consisted of five layers, namely, sensing, network layer, transport layer in association with Blockchain, applications, and advanced services. The Blockchain technology helped in gathering access control information, and machine learning helped to detect various forms of attacks, namely, Denial of Service (DoS), Distributed Denial of Service (DDoS), injection, man in the middle (MitM), brutforce, cross-site scripting, and scanning attacks. The framework was evaluated against the state of the art models considering accuracy, precision, sensitivity, and the Matthews correlation coefficient.

3. Method

3.1. Design of Industrial Internet Security Platform Based on Blockchain

3.1.1. Requirements' Analysis. In recent years, while the IIP has brought convenience, intelligence, and full-factor connection, the security problems faced by the IIP have become increasingly serious. Infrastructure as a service (IaaS) technology has gained quite some momentum having shorter life cycle. The developers of platform as a service have enough knowledge to understand the various industrial aspects and implement professional technologies. The research and development of PaaS have not been able to bridge the gap between manufacturing and consumption. Thus, the development of IaaS on the existing cloud platforms leads to increased investment in cost and poor usability. There are also issues relevant to transmission of complex unstructured data that are diversified and also has variability. With the continuous development of information technology, the security of sensitive data on the IIP has become an increasingly serious problem, restricting the further development of the IIP. In the new strategic system for the development of the global industrial Internet, how to protect the security of platform data has become the research focus of the outlines of various countries. Since most of the traditional IIP use a centralized network architecture, when the central server encounters an external hacker attack, the platform will not only face the consequences of paralysis but also face

the serious situation of data theft or malicious modification. Businesses will face irreparable losses. In addition, in terms of terminal equipment management, the management of underlying terminal equipment by traditional IIP is rather chaotic. The data stored in the database is greatly polluted, resulting in the embarrassing situation of being unable to convert data into value in the face of massive data information. In terms of permissions to the platform, the central server will have a super administrator who controls the permissions of the entire platform. He can manipulate any data information on the platform, making the platform data lack of credibility and reliability, and also causing the problem of self-stealing within the personnel. Therefore, based on the above security issues, it is very necessary to develop a blockchain-based decentralized secure Internet platform, and it is also an imminent practical need. Hyperledger Fabric is an open source Blockchain permission which was initiated in 2015. It is a modular general-purpose framework that provides unique identity management and also renders access control features suitable to be implemented in various industrial applications. The framework includes a unique organization of members that interact with each other on the network. The transaction flow is initiated when a client application sends transaction proposal to the peers in each organization for endorsement. The peers authenticate the identity of the submitting clients and authority for submitting the transaction. The outcome of the proposed transaction is simulated, and if it matched the expected result, an endorsement signature is sent back to the client. The client collects the endorsements from the peers, and when defined numbers of endorsements are received, the transaction is sent to the ordering service. The ordering service checks if the required numbers of endorsements are received; then, the approved transactions are packaged into blocks, and the blocks are sent to peer nodes in each organization. The peer node validates the transactions and then adds a new block to the ledger, and the status of the ledger gets updated making new transaction committed. Based on the Hyperledger blockchain development platform and using a series of development tools for the Hyperledger ecosystem, this paper builds a blockchain-based industrial Internet security platform. Through the role-based access mechanism, it is ensured that the data in the platform can only be operated by specific personnel, and the terminal data is encrypted, packaged, and uploaded to a traceable and nontamperable blockchain network. At the same time, it manages specific terminal equipment based on role-based permissions to achieve the effect that a specific person is responsible for the specific equipment. At the same time, the faulty equipment can be quickly held accountable, repaired and operated quickly. The specific functions are as follows.

- (1) *User Role Management.* Different management rights are given based on the roles assigned by users; each role has its own key, and the key can be used as user authentication and rights management rights. The platform has different user rights to define the terminal equipment that the user can operate and the database information content that can be

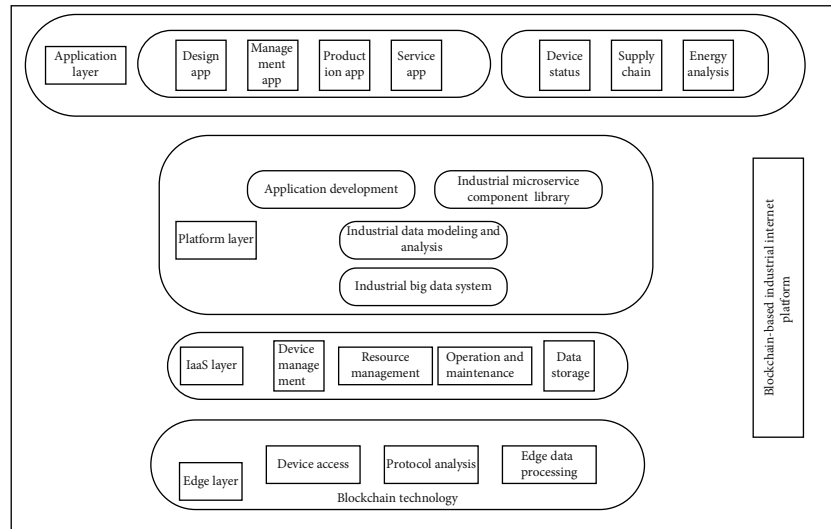


FIGURE 1: Blockchain-based industrial Internet platform architecture.

operated. In this way, the effect of data isolation can be achieved according to different roles of users

- (2) *Data Query Function.* According to the user's role level in the platform, the user's operation authority is determined, such as data reading, data uploading, etc. For some sensitive data, the platform sets that only roles with specific permissions can view it, preventing the possibility of unrelated personnel from leaking data within the enterprise. At the same time, users can also choose the data information on the chain according to their own needs. Users can also view the running status of the entire blockchain network and quickly repair faulty nodes
- (3) *Device Management Function.* It can collect and process terminal device data and use the device's own key to package and upload it to the blockchain network. The configuration file of the device can be viewed, updated, and replaced through the blockchain network
- (4) *Chaincode Management Function.* Administrators can deploy new chaincodes according to business needs and can also update and replace old chaincodes
- (5) *Blockchain Network Management Function.* Administrators can deploy network nodes, establish secure channels, add or delete platform organizations, and authorize and revoke certificates

3.1.2. Platform Design Principles. Business requirements are the source of platform design. This is the beginning of designing a platform. The first criterion for evaluating the quality of a platform is suitability. The data security of the Industrial Internet is one of the main reasons that restrict its development, and the blockchain technology is unique in its data structure and storage method which can ensure the security of data and information and can perfectly solve the pain points of the current industrial Internet. With the

continuous change of industrial Internet requirements and the sharp increase in the amount of data, this platform can quickly add new services on the original basis through a modular mechanism to meet changing business needs. The reliability of this platform includes two aspects; one is to effectively ensure the safety and reliability of platform data. Instead, it can ensure the long-term safe and stable operation of the platform. The spatial data and attribute data of this platform can be organically combined and interacted, and the data information between each module can be transmitted to each other to achieve smooth interaction. This platform adopts visual page design and process-style structured design. After simple business training, users can take up jobs quickly, saving enterprise training costs, saving time, and improving personnel efficiency. This platform adopts a role-based data access and management method. For nonprivate data, it can realize data sharing and improve the closeness of collaboration between various departments. For private data, the data is encrypted on the chain through asymmetric encryption, and only those with the private key can access and view the data. Compared with other traditional platform development solutions, it can greatly reduce development time and platform development costs.

3.1.3. Platform Architecture Design. Through the analysis of the requirements mentioned above, the overall architecture of the blockchain-based feature design platform is shown in Figure 1.

The blockchain network is added to the architecture of the traditional IIP, and the blockchain technology is used to manage terminal equipment, data resources, and access rules. The main change is reflected in the addition of the blockchain platform to the IaaS layer, connecting the edge layer and the platform layer through the blockchain network. IaaS is a cloud service that provides access to completely provisioned on-demand computing infrastructure that is possible to be managed over the internet. The IaaS model enables companies to access all the benefits of computing resource without facing overhead issues in the

deployment, maintenance, and operation of in-house infrastructure. IaaS also provides scalability and resource management enabling consumers to work on a “pay and use” model wherein they can pay rent and use additional computational resources when enhanced performance is required. The use of IaaS in blockchain helps organizations unlock inexhaustible pool of computing, network, and storage resources in order to develop the best possible infrastructure for their business. The management of terminal devices at the edge layer is mainly controlled by the chain code. The chain code runs in the blockchain network, and the terminal device can obtain updated configuration information from the chain code in real time. At the platform layer, data management is mainly carried out through asymmetric encryption technology, and the data is packaged, encrypted, and stored in a distributed database to ensure the security of data resources. Users use their own digital certificates to authenticate through the client and then enter the blockchain network. Users can do the following operations according to their operating permissions. (1) Users can access information and data within their own authority. Some of the data on the blockchain are privately encrypted data, and only users with a specific key can view this part of the data. The other part is the public dataset which can be viewed and audited by all users on the blockchain. (2) Users can perform specific operations on devices within their authority, such as viewing or updating device configuration files. Of course, the records of these operations of the user will be written into the blockchain, and if the equipment is abnormal, it can be quickly repaired and the responsibility can be determined. The data generated by the terminal device is encrypted by the device’s own unique Mac address to form a unique pair of public and private keys. In this way, information with sensitive data can be encrypted with its own public key and uploaded to the blockchain network. Then, only operators who have the private key of the device can decrypt the terminal data and view the private data. Once the data is on the chain, the data cannot only be traced back but also cannot be tampered with, which not only increases the credibility of the enterprise but also ensures the integrity and credibility of the data.

3.2. Permission Management

3.2.1. User Rights Division. The model file includes definitions for all users who interact with the platform, including administrators who create access control rules and other authenticated users who need access to restricted resources. In this scenario, each participant is identified by a unique ID, and their characteristics are also tracked. Users with different identities have different attributes and operation permissions. Ordinary users act as requesters of information access and obtain data information through the authority assigned by the organization manager. Compared with ordinary users, organization administrators have the authority to manage ordinary users, user certificate security authentication, and channel management. Organization administrators ensure the safe operation of the entire platform. In this article’s application, there is one transaction for granting access and another for revoking user access. Addition-

ally, there is a transaction that delegates permissions to other users, who will then be able to transfer the access they have been granted to other users.

3.2.2. User Permission Operation. This article defines the access control policy when implementing user rights access control. Below is a list of the rules considered in the application in this article. These rules include the following. (1) A specific role can only access the resources specified by the permission. (2) Users with specific roles can send transactions. (3) Access rights for different modules of the platform. (4) Members of certain groups will be granted access to the archive. The five sets that make up an access policy are the actors, the resources, the circumstances, the behaviors, and the actions. The access control model in this study is a role-based access control model because, in the base model, users have access to resources based on the roles established in the platform. This article provides many classes of actors to represent various organizational responsibilities within the context of the access control architecture presented here. They may also have automatic access to some resources, depending on their jobs and circumstances. While initial ACP module definitions are static, an authorized user may submit a transaction to dynamically modify a user’s access control. Events are an important part of the platform when used with platform queries. The event module is used to query the log of transaction information. The log entry indicates that the result of the event was fired from the transaction function. Also, they can call external applications. This article considers the case of persisting access requests and denying requests after several consecutive efforts. As a result, triggers for external applications will be triggered in response to necessary security considerations such as triggering intrusion alarms to prevent unauthorized access.

3.2.3. Role-Based Permission Control Process. Access control and authorization is extremely important in hyperledger composing wherein the security architecture of business networks shared by organization members in the Blockchain. Hyperledger composer enables admin control on the resources or data; a participant is entitled to access in a business network. Hyperledger fabric uses access control lists to manage access to the resources by associating policies with the resources. The role access control mechanism based on ACP policy is implemented through chain code, which can be regarded as a smart contract in Hyperledger. The main task of chaincode is to define the logic of each transaction and the conditions that need to be met. Once these logics and rules are written into the chain code, they will be automatically executed and will not change unless the new chain code is used to replace the rules on the old chain code. When the corresponding transaction is committed, the corresponding transaction handler function is automatically called. The above figure shows the access control process based on ACP. First, the user submits the access rights transaction, and the platform first checks the user’s rights according to the ACP access rights policy. If the transaction submitted by the user does not have permission to access, the platform will send an error message and return. If the user passes the ACP mechanism, the platform

will call the prewritten authorization rules of the chain code on the blockchain for rejudgment. If the authorization rule is passed, the authorization API will be called for authorization, otherwise an error message will be sent and returned. In the permission access process, it is necessary to pass two permission checks because, if each permission check directly calls the chain code on the blockchain for judgment, the efficiency is very low. If some unauthorized transaction accesses are filtered through the ACP policy first, the efficiency of the platform will be greatly improved, and the smooth operation of the platform will be ensured.

3.3. Terminal Device Management

3.3.1. Network Management Protocol. The supervision and management of the enterprise network is very important, and it is the basic issue to ensure the network service. Changes in network node configuration may be made automatically based on observations of network behavior, which can be gathered via a variety of methods of monitoring the status of network nodes and measuring their performance. In order to have a full picture of the state of a network, it is necessary to monitor not only the performance and traffic but also the status of each device and interface. Syslog is a widely used standard protocol for logging and transmitting networked notification messages about state transitions. While simple network management protocol (SNMP) is a specific protocol for monitoring and basic administration of network devices, syslog is routinely used to track changes on any PC, server, or device. In the IIP, there are many ways to manage network devices. Most of the IIP are directly managed through the command line interface, but this method also requires the most manual labor. Therefore, it is not economical and cannot scale equipment efficiently, and the management network of increasing scale and complexity requires more platform based and automated solutions. The SNMPv3 protocol adds configuration rules for remote devices. However, the SNMP protocol is still mainly used for monitoring, because the support of this protocol for modifying device properties is very limited, and it needs to rely on the technical support of the manufacturer. NETCONF, on the other hand, focuses on device configuration through an open application programming interface using an extensible markup language-based device behavior model.

3.3.2. Device Management Process. The sequence flow of blockchain-based terminal device management is as follows. To begin, digital certificates are used by legitimate network administrators to prove their identity. Following this, users may make changes to the blockchain-recorded configuration of devices, so long as they have permission to do so for that device or set of devices. Hyperledger describes a blockchain-based architecture that may be used to maintain authentication certificates. To prevent adding unintentional human mistake into the configuration stored in the blockchain, it is important to perform syntax checking on device configuration files that have been updated. Moreover, new configurations may be signed with the administrator's certificate for

operational identification and attribution. Time stamp, administrator ID, device ID, and encrypted device configuration are the components of a transaction. When a transaction is recorded in a newly added block to the blockchain, that block's peers get a copy of the transaction. When a new block is introduced to the blockchain, an event will be sent to alert all managed devices to incorporate the new block into the blockchain. This will allow the device ID to determine whether the change changes the device's settings. The device then uses its private key to decrypt the blockchain-stored configuration and apply the updated settings locally. The blockchain keeps a record of every modification that can be checked by audit and security teams. The specific sequence of the process of changing the configuration file of the terminal device is as follows. (1) The administrator obtains the old configuration file of a specific device or device group from the blockchain network and decrypts the new configuration file through his own private key. (2) The administrator modifies the old configuration file and (3) performs semantic verification on the modified configuration file, so that the modified configuration file conforms to the grammar rules. (4) The semantically verified configuration file is encrypted and written into a new block, and the block is added to the blockchain after being sorted by the sorting node. (5) The administrator receives a notification that the configuration file has been successfully distributed into the blockchain network. (6) The device goes to the blockchain network to query the configuration file information if it is selected to download the configuration file and decrypt the configuration file with its own private key for loading. (7) After the device loads the application, the new block information, including whether the new configuration file has been successfully applied, the hash value of the configuration file, and the download and application timestamps are packaged and written into the block for security auditing.

3.3.3. Chain Code Design. In the Fabric architecture system, chain code is equivalent to the implementation of smart contracts in the blockchain network. There are two types of chain codes: user-level chain codes and platform-level chain codes. The platform-level chain codes are responsible for the processing of the Fabric node's own platform configuration, endorsement, and verification. User-level chaincode is designed by developers according to their own development needs. It provides state processing logic based on blockchain distributed ledger, and a variety of complex applications can be developed based on it. After the chaincode is deployed, it automatically runs in the blockchain network of Fabric and runs in the isolation sandbox. Nodes can interact with the chain code according to the protocol and operate the distributed ledger data. After starting the Fabric network, users can operate the chaincode in various ways to check whether the network is running well. The fundamental rule of creating a chaincode is that it must not include any secret information. All mandatory data is sent in the form of parameters, and authentication is handled by means of a key-pair consisting of a username and a password. When attempting to utilize any of the CRUD functions in chaincode, an administrator

must first input the appropriate credentials. CRUD function is an acronym used in computer programming that includes four functions that are implemented for performing storage related applications. These functions are create, read, update, and delete. If the right login and incorrect key are given, the read, update, and delete operations will fail. This article refers to this process as the key verification method since the chaincode will attempt to decrypt the configuration file as a security precaution, and if this decryption fails, the whole request will fail. When performing the create operation, the configuration file is encrypted with the specified key since it does not yet exist, and there is no way to check that the key is legitimate. Forged requests still need an attacker to change the network device's settings in order to cause it to download the configuration file and retrieve the device ID. If they have, this security issue is beyond the control of this article. Therefore, the worst case is that any configuration file located in the blockchain is set, or the database is never accessed by the network device.

3.4. Data Safe Storage

3.4.1. Data Upload Process. Data security is the core of an enterprise. Ensuring the integrity, privacy, and availability of data is the basic requirement of an IIP and the basis of network security. The collection and storage of data is mainly manifested in the edge layer and the IaaS layer in the blockchain-based platform architecture, and the terminal data is uploaded to the chain through six links. They are data collection, network isolation and data caching, signature packaging, edge data processing, sorting consensus, and distributed database storage.

3.4.2. Data Collection and Signature. The packaged blockchain has its own unique identity rights management function. Through the security authentication of the terminal device, a unique public and private key is generated for each terminal device. The public and private keys correspond to the unique IP of the terminal device itself, so that a list corresponding to the public and private keys of the terminal device is formed. Through the function of identity authentication authority, on the one hand, the random access and malicious destruction of terminal devices are prevented, and the security of data is protected. On the other hand, blockchain adopts a distributed network architecture. Compared with the centralized data collection for high-frequency data collection in the production process of industrial equipment, the load pressure of data collection and storage on the platform can be greatly reduced. Through the industrial gatekeeper technology, network isolation and data caching are performed on the data collected from the terminal equipment. Then, by calling the SDK interface function of the blockchain platform, the public key of the terminal device is used to encrypt and package its own data. The encrypted data will have a unique data identity, so if the encrypted data is specifically tampered and deleted, the data identity will not match the original one. In this way, when the edge data is processed, it can be deleted, or an alarm can be notified to the administrator for subsequent processing. When the PaaS

layer needs to process data, the encrypted data can be decrypted through the public-private key correspondence table. Platform as a Service (PaaS) focuses on the developers and the programmers enabling them to create, run, and manage their applications without botheration of developing and maintaining complex hardware infrastructures. The components that are required for developing and maintaining software applications are performed by the cloud provider ensuring that the developers have enough time to focus on code and new feature development. If it cannot be decrypted effectively, the data is an invalid data that has been tampered with or deleted, and it can be deleted and isolated or discarded. In this way, data tampering and leakage can be effectively prevented by packaging the signature of the data.

3.4.3. Network Node Consensus and Distributed Storage. The consensus mechanism is the security barrier for the blockchain to ensure the consistency of distributed ledgers, and the consensus mechanism is also the main factor restricting the efficiency of data on chain. The frequency of data collection by the IIP is generally at the HZ level, so it is very important to choose a consensus mechanism suitable for the IIP. At present, the mainstream consensus is PoW, POS, and other consensus mechanisms that use incentive measures. This type of consensus mechanism ensures the safe and smooth operation of the blockchain network, but it is inefficient and cannot meet industrial-level data requirements. Hyperledger Fabric adopts PBFT and Kafka sorting consensus, which can greatly reduce the time required for consensus and effectively relieve the load pressure of the data uploading process. Different from the centralized data storage method used by traditional IIP, blockchain technology uses distributed data storage. There is no central node in the server nodes; they are all equal, and each node must back up the complete data storage. In this way, even if a node is attacked and cannot work, other nodes can still run, ensuring the normal operation of the platform and not causing the entire platform to stop serving due to a single point of downtime. Blockchain technology also uses cryptography for data storage, which ensures that data cannot be tampered with integrity and authenticity and fundamentally ensures the security of data in the industrial Internet platform.

3.5. BP Neural Network Theory

3.5.1. BP Neural Network Idea and Network Structure. In terms of multilayer feedforward neural networks, the BPNN is a classic model. To ensure that each layer is error-free at all times. Both signal forward propagation and error reverse propagation are included in the BPNN's learning process. Each hidden layer and connection weight processes and calculates the input signal, which is then output in the complete forward direction by the input layer. This is the end outcome of the propagation process itself. Back propagation of errors is a process that uses an error function to determine the difference between a target anticipated value and the final output. If the error reaches the desired error level, the learning process finishes; otherwise, the mistake will propagate

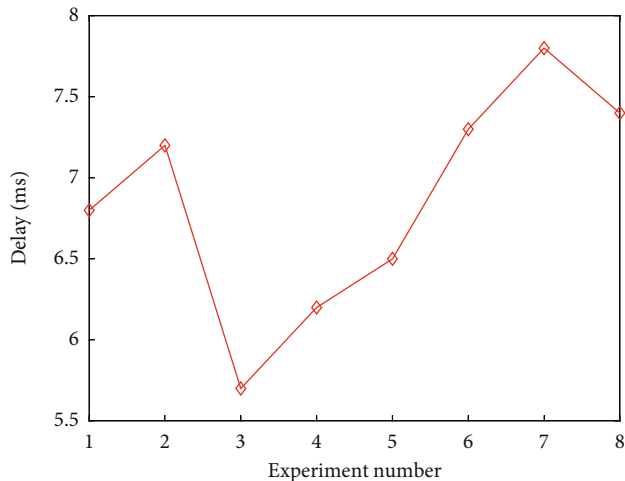


FIGURE 2: System delay test.

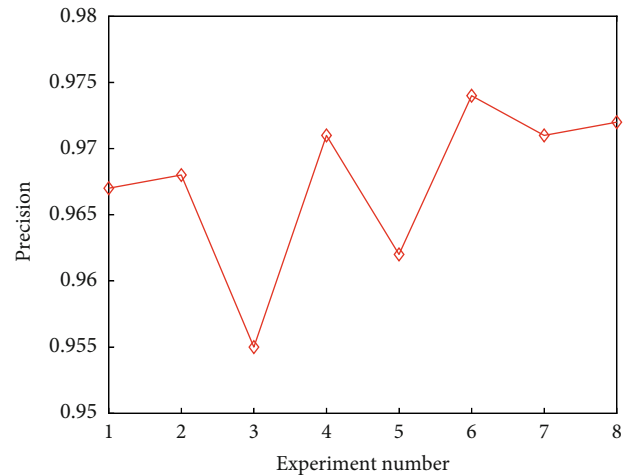


FIGURE 4: System precision test.

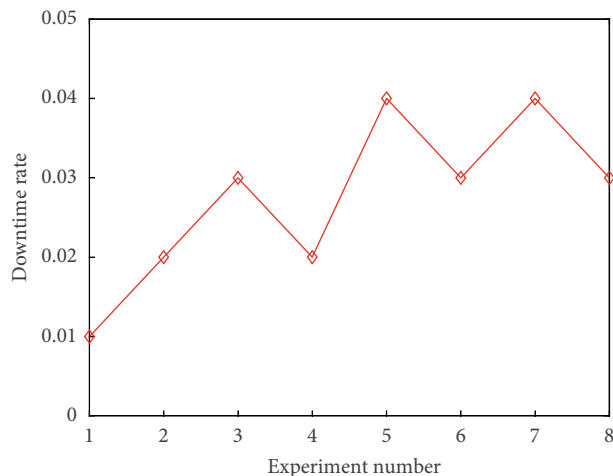


FIGURE 3: Downtime rate test.

backwards through all hidden levels to the input layer in some form. When the final error value achieves the network's goal error requirement or the number of iterations specified by the network is reached, the learning process comes to a conclusion, and the network's error value is assigned to each layer. For nonlinear processing, the three-layer BPNN with one hidden layer is extensively utilized.

3.5.2. BP Neural Network Learning Process. What happens when there are three layers of neurons (input, hidden, and output) with data samples that are all equal in number? The process of learning is as follows. Network target expects the output feature vector t to be x , which is the input feature vector of the input layer. x is an in-layer feature vector. Neuron thresholds in each of these layers are based on these weights and these thresholds, which are used to connect each layer together (w_{ij} , w_{jk} , p_j , and p_k). The activation function is a sigmoid function. These are the steps in the BPNN learning process as a result of this.

- (1) Establish a connection to the network and begin working. Weights and thresholds of the network are given random integers between 0.5 and 0.5, and the network's target accuracy, the maximum number of repetitions M , and the error function are established
- (2) In the data collection, choose sample n , input vector $x(n)$, and the anticipated output value t by random selection (n)
- (3) Using the sample data $x(n)$, the connection weight w_{ij} and the hidden layer's threshold p_j determine the input value hi and the output value ho for each neuron in the hidden layer

$$hi_j(k) = \sum_{i=1}^n w_{ij}x_i(k) - p_j, \quad (1)$$

$$ho_j(k) = f(hi_j(k)) \quad (2)$$

- (4) Calculate each neuron's input and output values yi and yo based on the hidden layer's output, connection weight, and output layer threshold

$$yi_k(n) = \sum_{i=1}^m w_{jk}ho_j(n) - p_k, \quad (3)$$

$$yo_k(n) = (yi_k(n)) \quad (4)$$

A forward propagation technique is used in the BPNN's learning process. There are several layers of transmission of data from the input to the output; this section discusses the error back propagation process, which is used to remedy forward propagation mistakes.

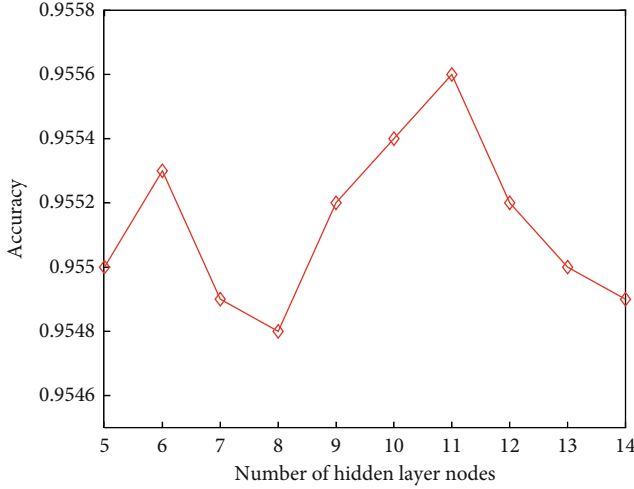


FIGURE 5: The influence of the number of hidden layer nodes on the training effect.

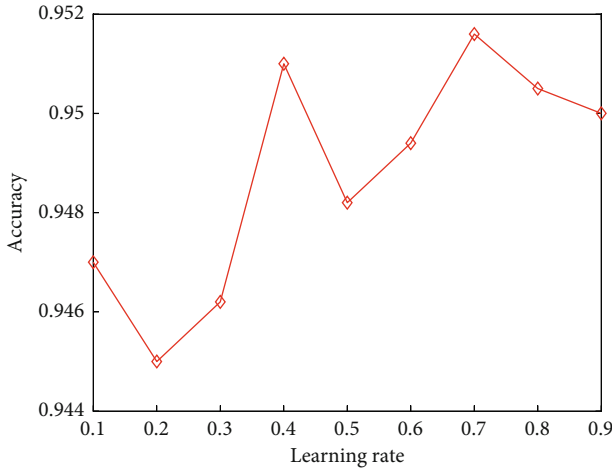


FIGURE 6: The influence of the learning rate on the training effect.

- (5) Calculate the error between the actual output $yo(n)$ and the predicted goal output $k(n)$ using the error function, and then apply the partial derivative to each output layer neuron

$$\delta_k(n) = yo(n)(1 - yo(n))(k(n) - yo(n)) \quad (5)$$

- (6) Use the output of hidden layer neurons and the partial derivatives of neurons in the output layer to change connection weights and thresholds between hidden and output layers. n is the value before correction, while $n + 1$ is the value after correction. The correction formula is as follows:

$$w_{jk}^{n+1} = w_{jk}^n + \mu \delta_k(n) h o_j(n), \quad (6)$$

$$b_k^{n+1}(n) = b_k^n(n) + \mu \delta_k(n) \quad (7)$$

- (7) In order to get a partial derivative of neurons in the hidden layer, you must take into account their connection weight, partial derivative of output layer error, and their hidden-layer output. As a result, the weight and threshold of each neuron in the input layer may be adjusted to match those of neurons in the hidden layer

- (8) Calculate the global total error as E

$$E = \frac{1}{2m} \sum_{n=1}^m \sum_{k=1}^q (k_k(n) - y_k(n))^2 \quad (8)$$

- (9) Judge whether the network error satisfies $E < \varepsilon$; if so, the BPNN learning process ends. Otherwise, randomly select the next sample and turn to step (3) to continue learning and training the sample until the error meets the requirements or the number of iterations reaches the maximum number of iterations and the training ends

3.5.3. Limitations of BP Neural Networks. According to mathematical theory, BPNN can handle issues involving intricate internal systems and can do any sophisticated nonlinear mapping. There are certain restrictions to the capacity of the BPNN to perform nonlinear mappings. (1) The network structure is difficult to decipher. The fundamental reason for this is the absence of adequate theoretical advice for determining the number of hidden layers and the number of neurons in each hidden layer. (2) During the learning phase, the error convergence speed is sluggish. This happens because the gradient descent approach of BPNN convergence means that the number of iterations of network training rises, while the error drops slowly or even stay the same. (3) The learning process is easy to fall into the minimum value. In practical applications, the BPNN may not find the desired solution and fall into a local minimum during the training process, resulting in the failure of the network structure error to converge well. (4) The learning step size affects the network convergence speed. If the learning step size of BPNN is too large, the network will be unstable, and if it is too small, it will affect the convergence speed and cause long training time. (5) The training and learning of the network is unstable. There is no fixed method to find the best weights and thresholds for the initial selection of weights and thresholds between the connection layers. When the samples change, the trained network model has to retrain the network. For nonlinear systems, the initial value has a lot to do with whether the learning can reach the minimum value and whether the result converges. The BPNN has its limitations wherein the actual performance of the model is dependent on the input data. Also the model

TABLE 1: Experimental comparison between model output and expert evaluation results.

Number	1	2	3	4	5	6	7	8
Model output	0.759	0.817	0.744	0.621	0.887	0.715	0.912	0.833
Expert results	0.760	0.816	0.745	0.620	0.886	0.715	0.914	0.835

tends to be extremely sensitive towards noisy data, and hence, matrix-based approach is considered preferable instead of using minibatches.

4. Experiment and Analysis

4.1. Data Source and Preprocessing. In this paper, a dataset is constructed for experiments based on the data collected by the gateway industrial Internet sensor nodes. The dataset includes 1800 sets of data.

The sample data is normalized and preprocessed since the network's input data has distinct dimensions and physical meanings; the input features have different numerical ranges, and the numerical ranges between different features vary substantially. To make weight adjustment easier given the high fluctuation in the input value, the data is normalized and then transformed to (0, 1) or (-1, 1). However, the BPNN has a sigmoid excitation function with a derivative that varies between (0, 1) and (-1, 1) across a wider range of values. In order to improve the BPNN's computational efficiency, normalizing sample data aids the network in reaching a quick convergence. In this study, we choose to normalize our data using the following procedure.

$$z_i = \frac{x_i - x_{\min}}{x_{\max} - x_{\min}}. \quad (9)$$

4.2. System Function Test. Each test is more than 1500 times; the average value is taken after the test, and the results of 8 tests are obtained in total.

- (1) *System Delay.* This indicator is also a very important indicator in the system. The final result of the experiment is shown in Figure 2. It can be seen that the delay of the system is very small, which proves the efficiency of the system to transmit data
- (2) *System Downtime Rate.* This indicator is one of the most important indicators of the information system, which is related to whether the system can complete the basic functions efficiently and accurately. The same 8 experiments were performed on the system to verify its downtime times, and the results obtained are shown in Figure 3. As can be seen from the figure, the downtime rate of the system is very low, which can prove that the system is very stable
- (3) *System Accuracy Rate.* The system accuracy rate is one of the important indicators to ensure the accu-

rate transmission of system data. If the accuracy rate is too low, it will affect the user experience and reduce trust. The same method of taking the average of 8 experiments is adopted, and the results obtained are shown in Figure 4. It can be seen that the accuracy of the system is very high and can meet the needs of users

4.3. Model Parameter Analysis. We utilize the method to get a ballpark estimate of how many neurons should be in the hidden layer of the model network structure, and then we use experimentation to hone down on the best value. 15 neurons are present in the input layer, but only 1 is present in the output layer. Training data is used to build a reliable model, whereas test data is used to double check the model's accuracy. Figure 5 depicts the prediction accuracy change curve when the number of neurons in the hidden layer of the model is varied. As can be observed in the picture, the prediction accuracy of the model peaks at 11 neurons in the hidden layer, which is optimal for gauging the quality of IIP creation. Therefore, it is preferable to choose 11 neurons for the hidden layer in the subsequent tests, taking into account the total performance metrics. Since the learning rate might affect the experiment's precision, we choose several learning rates and plot their effects in Figure 6. It is clear that the optimal performance is reached with a learning rate of 0.7.

4.4. Model Evaluation Accuracy Experiment. In order to verify the validity of the model proposed in this chapter in evaluating the construction quality of industrial Internet sensor nodes. The test data of each dataset is fed into the model, and the obtained results are compared with the expert results, as shown in Table 1. From the experimental results in the table, the output of the model proposed in this paper is very close to the expert evaluation results, and the error is very small. Therefore, it can be proved that the model proposed in this paper has good performance in evaluating the construction quality of industrial Internet sensor nodes.

5. Conclusion

Aiming at the problems such as the difficulty in guaranteeing the data security of the IIP, the confusion of terminal equipment management, and the unclear division of roles and permissions, this paper designs a secure industrial Internet architecture based on the Hyperledger fabric framework in combination with the security features of the blockchain. This paper has completed the following work: (1) this paper firstly expounds the research background and significance of the IIP and introduces the research status of the industrial Internet and blockchain at home and abroad. (2) Design

an IIP architecture based on blockchain technology, and implement a sensor node management and monitoring system. 3) According to the results of actual data collection through multiple tests, there is a big difference between the actual required valid data and the collected complete data. Invalid data will lead to slow system processing progress and increase response time, so this paper uses gateway to preprocess the collected data, thereby reducing the data transmission delay and improving the real time and validity of the data. At the same time, a new sensor node identification method is designed, which is easy to manage, and each piece of data can be quickly traced back to the source to improve management efficiency. This paper also uses smart contracts to manage configuration files in an Industrial Internet environment. After completing the above work, this paper uses neural network to evaluate the construction quality of industrial Internet sensor nodes.

Data Availability

The datasets used during the current study are available from the corresponding author on reasonable request.

Conflicts of Interest

The author declares that he has no conflict of interest.


References

- [1] H. Chegini, R. K. Naha, A. Mahanti, and P. Thulasiraman, "Process automation in an IoT-fog-cloud ecosystem: a survey and taxonomy," *Internet of Things*, vol. 2, no. 1, pp. 92–118, 2021.
- [2] K. Shafique, B. A. Khawaja, F. Sabir, S. Qazi, and M. Mustaqim, "Internet of things (IoT) for next-generation smart systems: a review of current challenges, future trends and prospects for emerging 5G-IoT scenarios," *IEEE Access*, vol. 8, pp. 23022–23040, 2020.
- [3] S. M. A. A. Abir, S. N. Islam, A. Anwar, A. N. Mahmood, and A. M. T. Oo, "Building resilience against COVID-19 pandemic using artificial intelligence, machine learning, and IoT: a survey of recent progress," *Internet of Things*, vol. 1, no. 2, pp. 506–528, 2020.
- [4] I. Lee and K. Lee, "The Internet of things (IoT): applications, investments, and challenges for enterprises," *Business Horizons*, vol. 58, no. 4, pp. 431–440, 2015.
- [5] J. Q. Li, F. R. Yu, G. Deng, C. Luo, Z. Ming, and Q. Yan, "Industrial Internet: a survey on the enabling technologies, applications, and challenges," *IEEE Communications Surveys & Tutorials*, vol. 19, no. 3, pp. 1504–1526, 2017.
- [6] W. Qin, S. Chen, and M. Peng, "Recent advances in industrial Internet: insights and challenges," *Digital Communications and Networks*, vol. 6, no. 1, pp. 1–13, 2020.
- [7] I. F. Siddiqui, S. U. J. Lee, A. Abbas, and A. K. Bashir, "Optimizing lifespan and energy consumption by smart meters in green-cloud-based smart grids," *IEEE Access*, vol. 5, pp. 20934–20945, 2017.
- [8] E. Sisinni, A. Saifullah, S. Han, U. Jennehag, and M. Gidlund, "Industrial Internet of things: challenges, opportunities, and directions," *IEEE Transactions on Industrial Informatics*, vol. 14, no. 11, pp. 4724–4734, 2018.
- [9] P. K. Malik, R. Sharma, R. Singh et al., "Industrial Internet of things and its applications in industry 4.0: state of the art," *Computer Communications*, vol. 166, pp. 125–139, 2021.
- [10] H. Boyes, B. Hallaq, J. Cunningham, and T. Watson, "The industrial Internet of things (IIoT): an analysis framework," *Computers in Industry*, vol. 101, pp. 1–12, 2018.
- [11] W. Z. Khan, M. H. Rehman, H. M. Zangoti, M. K. Afzal, N. Armi, and K. Salah, "Industrial Internet of things: recent advances, enabling technologies and open challenges," *Computers & Electrical Engineering*, vol. 81, article 106522, 2020.
- [12] J. Wan, S. Tang, Z. Shu et al., "Software-defined industrial Internet of things in the context of industry 4.0," *IEEE Sensors Journal*, vol. 16, no. 20, pp. 7373–7380, 2016.
- [13] J. Yli-Huumo, D. Ko, S. Choi, S. Park, and K. Smolander, "Where is current research on blockchain technology? A systematic review," *PLoS One*, vol. 11, no. 10, article e0163477, 2016.
- [14] M. Andoni, V. Robu, D. Flynn et al., "Blockchain technology in the energy sector: a systematic review of challenges and opportunities," *Renewable and Sustainable Energy Reviews*, vol. 100, pp. 143–174, 2019.
- [15] D. Macrinici, C. Cartoceanu, and S. Gao, "Smart contract applications within blockchain technology: a systematic mapping study," *Telematics and Informatics*, vol. 35, no. 8, pp. 2337–2354, 2018.
- [16] Q. Wang, X. Zhu, Y. Ni, L. Gu, and H. Zhu, "Blockchain for the IoT and industrial IoT: a review," *Internet of Things*, vol. 10, article 100081, 2020.
- [17] R. Sanchez-Iborra and M. D. Cano, "State of the art in LP-WAN solutions for industrial IoT services," *Sensors*, vol. 16, no. 5, p. 708, 2016.
- [18] M. M. Iivari, P. Ahokangas, M. Komi, M. Tihinen, and K. Valtanen, "Toward ecosystemic business models in the context of industrial Internet," *Journal of Business Models*, vol. 4, no. 2, 2016.
- [19] J. Wang, C. Xu, J. Zhang, J. Bao, and R. Zhong, "A collaborative architecture of the industrial Internet platform for manufacturing systems," *Robotics and Computer-Integrated Manufacturing*, vol. 61, article 101854, 2020.
- [20] R. A. Potyrailo, "Multivariable sensors for ubiquitous monitoring of gases in the era of Internet of things and industrial Internet," *Chemical Reviews*, vol. 116, no. 19, pp. 11877–11923, 2016.
- [21] X. Lin, J. Wu, A. K. Bashir, J. Li, W. Yang, and J. Piran, "Blockchain-based incentive energy-knowledge trading in IoT: joint power transfer and AI design," *IEEE Internet of Things Journal*, vol. 9, no. 16, 2020.
- [22] X. Zhang and X. Ming, "A comprehensive industrial practice for industrial Internet platform (IIP): general model, reference architecture, and industrial verification," *Computers & Industrial Engineering*, vol. 158, article 107426, 2021.
- [23] J. Li, J. J. Qiu, Y. Zhou, S. Wen, K. Q. Dou, and Q. Li, "Study on the reference architecture and assessment framework of industrial Internet platform," *IEEE Access*, vol. 8, pp. 164950–164971, 2020.
- [24] Y. Wang, Y. Zhang, F. Tao, T. Chen, Y. Cheng, and S. Yang, "Logistics-aware manufacturing service collaboration optimization towards industrial internet platform," *International Journal of Production Research*, vol. 57, no. 12, pp. 4007–4026, 2019.

- [25] C. Wang, L. Song, and S. Li, "The industrial Internet platform: trend and challenges," *Strategic Study of Chinese Academy of Engineering*, vol. 20, no. 2, pp. 15–19, 2018.
- [26] I. Karamitsos, M. Papadaki, and N. B. Al Barghuthi, "Design of the blockchain smart contract: a use case for real estate," *Journal of Information Security*, vol. 9, no. 3, pp. 177–190, 2018.
- [27] A. Khatoon, "A blockchain-based smart contract system for healthcare management," *Electronics*, vol. 9, no. 1, p. 94, 2020.
- [28] R. Yuan, Y. B. Xia, H. B. Chen, B. Y. Zang, and J. Xie, "Shadow: private smart contract on public blockchain," *Journal of Computer Science and Technology*, vol. 33, no. 3, pp. 542–556, 2018.
- [29] A. Bahga and V. K. Madiseti, "Blockchain platform for industrial Internet of things," *Journal of Software Engineering and Applications*, vol. 9, no. 10, pp. 533–546, 2016.
- [30] Y. Zhang, P. Zhang, F. Tao, Y. Liu, and Y. Zuo, "Consensus aware manufacturing service collaboration optimization under blockchain based industrial Internet platform," *Computers & Industrial Engineering*, vol. 135, pp. 1025–1035, 2019.
- [31] Y. Lu, P. Li, and X. He, "A food anti-counterfeiting traceability system based on blockchain and Internet of things," *Procedia Computer Science*, vol. 199, pp. 629–636, 2022.
- [32] H. Mrabet, A. Alhomoud, A. Jemai, and D. Trentesaux, "A secured industrial Internet-of-things architecture based on blockchain technology and machine learning for sensor access control systems in smart manufacturing," *Applied Sciences*, vol. 12, no. 9, p. 4641, 2022.

Research Article

Adaptive Fast Independent Component Analysis Methods for Mitigating Multipath Effects in GNSS Deformation Monitoring

Rong Yuan,¹ Shengli Xie²,, Zhenni Li,³ and Zhaoshui He⁴

¹School of Automation, Guangdong University of Technology and Guangdong Key Laboratory of IoT Information Technology, Guangzhou 510006, China

²Key Laboratory of Intelligent Information Processing and System Integration of IoT (GDUT) and Key Laboratory of Intelligent Detection and The Internet of Things in Manufacturing (GDUT), Ministry of Education, Guangzhou 510006, China

³School of Automation, Guangdong University of Technology and 111 Center for Intelligent Batch Manufacturing Based on IoT Technology (GDUT), Guangzhou 510006, China

⁴School of Automation, Guangdong, Guangdong University of Technology and Guangdong-HongKong-Macao Joint Laboratory for Smart Discrete Manufacturing (GDUT), Guangzhou 510006, China

Correspondence should be addressed to Shengli Xie; shlxie@gdut.edu.cn

Received 1 September 2022; Revised 29 September 2022; Accepted 3 October 2022; Published 9 November 2022

Academic Editor: Sweta Bhattacharya

Copyright © 2022 Rong Yuan et al. This is an open access article distributed under the Creative Commons Attribution License, which permits unrestricted use, distribution, and reproduction in any medium, provided the original work is properly cited.

Carrier-phase multipath is the main problem of GNSS deformation monitoring. Traditional methods usually adopt sidereal day filtering to mitigate the multipath. However, the necessity of presetting the session duration of the static baseline solution reduces the timeliness of the methods in real engineering. Moreover, these methods are not suitable for the systems that contain different types of GNSS satellites (e.g., BDS). To address the problems, this paper proposes an Adaptive Fast Independent Component Analysis (AF-ICA) method for mitigating multipath effects in GNSS deformation monitoring, which can effectively process the multi-GNSS data and separate several multipath signals. In the experimental study, compared with Sidereal Filtering in Observation Domain (SF-OD) method, AF-ICA method can improve both the positioning accuracy and peak-to-peak value. In GNSS deformation monitoring positioning accuracy, AF-ICA method can achieve the root-mean-square (RMS) of 1 mm horizon-tally and 2 mm vertically. Compared with the MSF method, the positioning accuracy of the AF-ICA method in the direction of ENU is improved by 44%, 14%, and 31%, respectively, and the corresponding peak-to-peak values increased by 36%, 17%, and 29%, respectively. Our proposed method can automatically get the monitoring information without estimating the orbit period in advance to realize automatic deformation monitoring. Through the automatic monitoring solution, the AF-ICA method in this paper can be applied to the natural disaster monitoring in the Internet of Things and provides real-time data monitoring information for disaster early warning.

1. Introduction

GNSS has been one of the leading high-precision positioning technologies and is widely used in dynamic deformation monitoring of engineering constructions [1, 2], such as dams, bridges, high-rise buildings, and railway roadbeds [3–7]. In short-baseline GNSS measurements for deformation monitoring, differential GNSS techniques can largely eliminate common-mode errors between the reference and the rover GNSS stations resulting from ionospheric and tropospheric refraction and delays, satellite and receiver

clock biases, and orbital errors. However, carrier-phase multipath effects cannot be removed with this approach and still have significant effects on GNSS position estimates [8]. Due to the reflection or diffraction caused by nearby obstacles, GNSS multipath phenomenon occurs when signals travel from a satellite to a receiver via several paths. Multipath is mainly decided by the satellite constellation, receiver environment, and reflector positions. In deformation monitoring, the operation of the satellites directly affects the multipath since the receiver and reflector positions are relatively stable. Thus, multipath features can be extracted and used to reduce

positioning errors by analyzing the operation of the satellites. For example, as the satellite operating cycles are usually stable, the corresponding multipath also has a similar periodic variation. By using the previous observation measurements to model different satellites separately, Sidereal Filtering (SF) was employed to mitigate the multipath [9–12]. But it is necessary to preset the session duration of the static baseline solution in classic deformation monitoring, which reduces the timeliness of the method. Dong et al. [13] constructed a single-difference observation equation based on a single receiver with multiple antennas and proposed to establish a multipath hemispherical map (MHM) with satellite altitude and azimuth as independent variables. However, when these methods are used to mitigate the multi-GNSS multipath, the multipath model will have a very large matrix, which makes it impossible to achieve lightweight calculation. Moreover, an increase in the number of satellite and signal frequency types [14] by using multi-GNSS observation could make the multipath more complicated [15].

In order to mitigate the multi-GNSS multipath result from different types of GNSS satellites, a novel filtering method called AF-ICA is proposed to mitigate multipath in this paper, which can improve the timeliness of dynamic deformation monitoring by combining signal processing technologies and the principle of SF. In the AF-ICA method, the multi-GNSS single epoch solution is input as a signal with multipath to be processed, and the desired output signal is used as the multipath model. First, mean smoothing filter (MSF) method is used to denoise by calculating the mean value of a window. Then, the Fast Independent Component Analysis (FastICA) is adopted to separate the multipath signal generated by different types of satellites from the source signals by combining prior engineering information. Next, to improve the timeliness of the method, first-order Fourier fitting formula is used to get the signal period. We can recover the complete multipath signal by the linear fitting formula according to the period of the separated signal. Finally, we can obtain the final deformation monitoring results by removing the multipath signal. Contributions of this paper can be summarized as follows:

Considering the complicated multipath signal generated by different types of satellites in the GNSS deformation monitoring, we propose to use FastICA to separate the multipath signal from the source signals. In order to improve the timeliness, we design the AF-ICA method: obtain the prior period range of the separated signal (i.e., multipath signal) according to the actual engineering experience, and then use the prior period information as the basis to judge whether FastICA can separate the signal, so as to determine the smallest MSF window. Our method mitigates the multipath in the coordinate domain and can automatically get the session duration of mean filtering by extracting multiple multipath signal periods corresponding to the BDS orbit through the ICA algorithm without estimating the orbit period in advance like classical SF-OD method.

Our proposed method can automatically get the session duration of mean filtering by extracting multiple multipath signal periods corresponding to the BDS orbit through the ICA algorithm without estimating the orbit period in

advance to realize automatic deformation monitoring and improve engineering efficiency. Through the automated monitoring solution, the AF-ICA method in this paper can be applied to the natural disaster monitoring in the Internet of Things and provides real-time data monitoring information for disaster early warning.

2. Methodology

Considering the complicated multipath signal generated by different types of satellites and the timeliness of traditional SF methods, the AF-ICA method is presented to address the problems in this paper. In our case, the multi-GNSS single epoch solution is input as a signal with multipath to be processed, and the desired output signal is used as the multipath model. First, the multipath signal is weak in the source signals. Thus, the MSF method needs to be first used for denoising to get the multipath signal with enough strength. Then, FastICA is adopted to separate the multipath signal generated by different types of satellites from the source signals by combining prior engineering information. The environmental information includes two aspects: one is that the observation data contains GPS satellites whose orbital period is close to a sidereal day, another is that three multipath signals need to be separated because BDS satellite has three types of orbits. Next, to improve the timeliness of the system, first-order Fourier fitting formula is used to get the signal period. We can recover the complete multipath signal by the linear fitting formula according to the period of the separated signal. Finally, we can obtain the final deformation monitoring results by removing the multipath signal. As shown in Figure 1, AF-ICA method contains two parts: first is the MSF using the single epoch GNSS static positioning solution to wipe off the influence of Gaussian white noise, and second is the FastICA method for extracting multiple multipath signal periods. After removing the high frequency signal with MSF method, the remaining low frequency signal is the multipath signal to be separated.

2.1. MSF for Denoising. Classic GNSS deformation monitoring algorithm uses the static baseline solution method to obtain the positioning accuracy of millimeter level. The static baseline solution needs to set the session duration in advance, and then use the static postprocessing method to solve the baseline. In this paper, the method of single epoch solution combined with MSF is used to obtain millimeter positioning accuracy. The main purpose of MSF is to provide clean multipath signals for subsequent ICA methods. There is no need to preset the session duration, and the duration is automatically controlled by the AF-ICA method. Meanwhile, the final result of MSF algorithm is equivalent to the static postprocessing baseline solution. MSF algorithm using the single epoch solution is described as follows.

Normal equation of fixed solution in the static postprocessing baseline solution can be written as

$$\left(\sum_i^n H_i^T P_i H_i \right) X = \left(\sum_i^n H_i^T P_i Z_i \right), \quad (1)$$

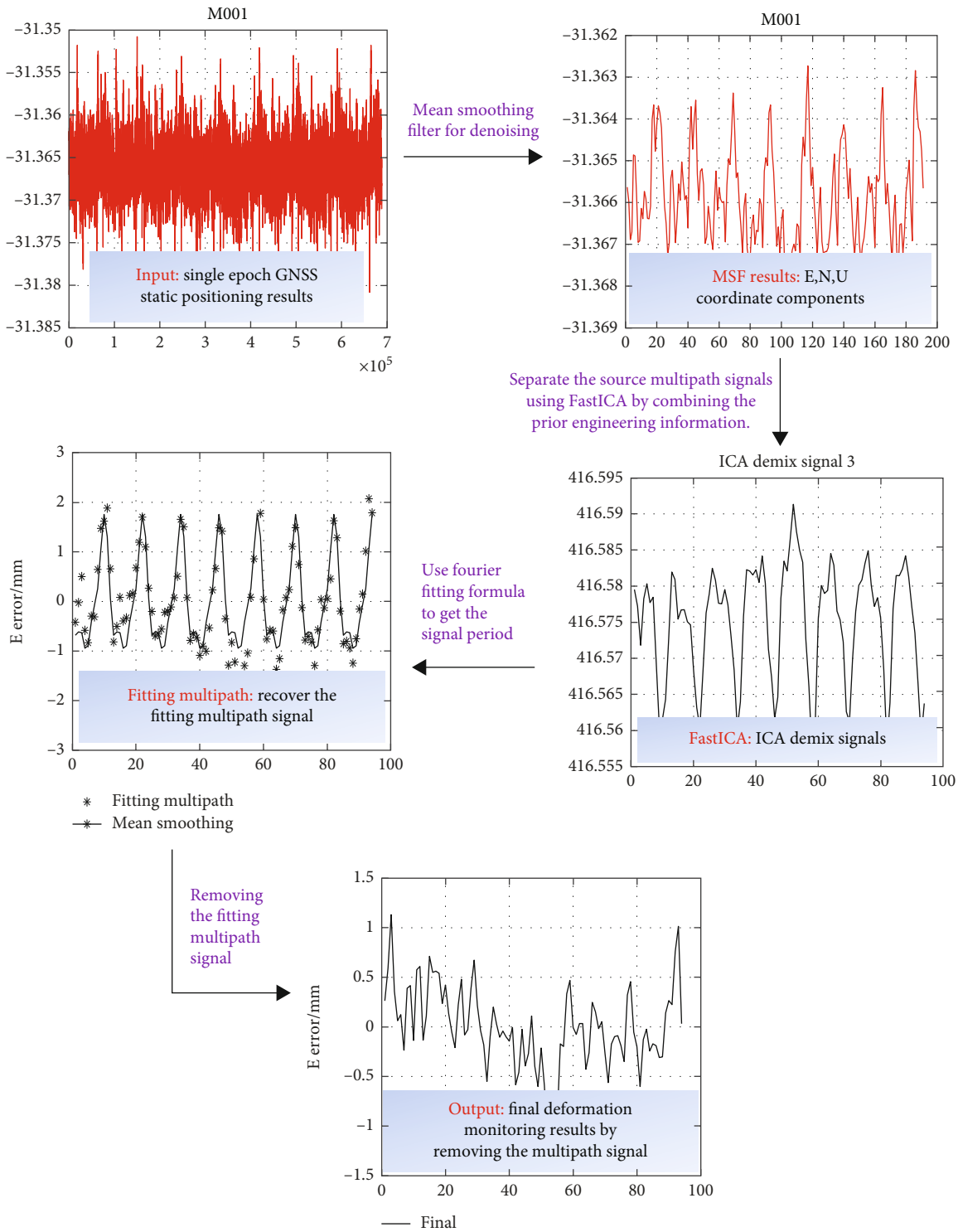


FIGURE 1: Flowchart for the AF-ICA method ((1) input: static single epoch results; (2) MSF: weaken the influence aroused by noise; (3) FastICA: separate the multipath signal; (4) first-order Fourier fitting formula: get multipath signal period; (5) recover the fitting multipath signal; and (6) output: deformation monitoring result by removing the fitting multipath signal).

where $X = [\delta X \ \delta Y \ \delta Z]^T$ is regarded as the baseline component of the fixed solution to be estimated, H_i is the coefficient matrix of the i -th epoch which can be calculated from the satellite position and the receiver position, P_i is the observation

equation weight matrix of the i -th epoch which can be calculated by satellite altitude angle or floating solution residual, and Z_i is the estimated residual of the observation. Each session duration collects n epochs observation data.

Least-square method can be used to calculate the fixed solution X in (1)

$$X = \left(\sum_i^n H_i^T P_i H_i \right)^{-1} \left(\sum_i^n H_i^T P_i Z_i \right), \quad (2)$$

where X can be calculated by n epoch iterations. The n -th iteration could be written as

$$\begin{aligned} X^{(n)} &= X, \\ &= \left(\sum_i^n H_i^T P_i H_i \right)^{-1} \left(\sum_i^n H_i^T P_i Z_i \right), \\ &= \mu \cdot (H_1^T P_1 Z_1 + \dots + H_{n-1}^T P_{n-1} Z_{n-1}) + \mu \cdot (H_n^T P_n Z_n), \end{aligned} \quad (3)$$

where $X^{(n)}$ represents the result of the n -th iteration; $X_n = (H_n^T P_n H_n)^{-1} \cdot (H_n^T P_n Z_n)$ represents the least-squares result of the n -th epoch; and $\mu = (H_1^T P_1 H_1 + \dots + H_n^T P_n H_n)^{-1}$ represents the inverse of the coefficient matrix in normal equation.

Iterative formula can be obtained by further decomposing (3):

$$X^{(n)} = \alpha \cdot X^{(n-1)} + \beta \cdot X_n, \quad (4)$$

where α, β is regarded as the smoothing coefficient and can be expressed as

$$\begin{aligned} \alpha &= \left(I + (H_1^T P_1 H_1 + \dots + H_{n-1}^T P_{n-1} H_{n-1})^{-1} \cdot H_n^T P_n H_n \right)^{-1}, \\ \beta &= \left(I + (H_n^T P_n H_n)^{-1} \cdot (H_1^T P_1 H_1 + \dots + H_{n-1}^T P_{n-1} H_{n-1}) \right)^{-1}, \end{aligned} \quad (5)$$

where I is a unit matrix.

2.2. AF-ICA for Mitigating Multipath Effects. In the static baseline solution, the duration of the session needs to be set in advance. While the AF-ICA is proposed in this paper can automatically analyze the session duration by using the single epoch solution. Before introducing the AF-ICA method, let us first introduce the FastICA method.

FastICA is a signal processing method for transforming an observed multidimensional random vector into components that are statistically as independent from each other as possible [16]. The standard ICA model could be written as

$$\begin{aligned} x &= As, \\ &= \sum_{i=1}^n a_i s_i, \end{aligned} \quad (6)$$

where $x = [x_1, x_2, \dots, x_m]^T$ is regarded as the observed mixtures, $s = [s_1, s_2, \dots, s_n]^T$ represents the unknown sources, and $A = [a_1, a_2, \dots, a_m]^T$ is the unknown mixing matrix of size

$m \times n$. With the assumption that $m \geq n$ and that sources s are mutually independent, the ICA could optimally estimate a demixing matrix, say B , to separate the original signals s based on some rules of optimization (such as the least squares). Then the best approximation vector of s can be derived from

$$y = Bx, \quad (7)$$

where $y = [y_1, y_2, \dots, y_n]^T$, which is the best approximation vector of s . Generally, the process of the ICA algorithm can be divided into three steps: first, center x , i.e., subtract its mean vector $m = E\{x\}$ so as to make x a zero-mean variable; second, whiten the observed mixtures to get the whitening signals $z = Vx$, where V is the whitening matrix, and $E\{zz^T\} = I$ (I is a unit matrix); third, get a rotation matrix W , such that $y = Wz$, by the specific independence optimization rule. In the ICA algorithm, the sources s consist of one Gaussian source at most, but the separated components y are uncertain in amplitude and order.

FastICA is based on a fixed-point iteration for finding a maximum of the non-Gaussianity of y . To begin with, we first show the one-unit version of FastICA [17]. Denote the derivative of the nonquadratic functions are

$$\begin{aligned} g_1(u) &= \tanh(a_1 u), \\ g_2(u) &= u \exp(-u^2/2), \end{aligned} \quad (8)$$

where $1 \leq a_1 \leq 2$ is a suitable constant, often taken as $a_1 = 1$.

Object of GNSS deformation monitoring can be expressed by the baseline solution results in three components E, N, and U of the topocentric coordinate system. When using FastICA for multipath signal separation (here we think that the source signal is a multipath signal), we regard the three coordinate components of ENU as mixed signals x , $m = 3$. According to engineering experience and GNSS satellite orbital period [18], we can obtain three kinds of prior information:

- (a) Source signal contains a multipath signal with a period of a sidereal day
- (b) Maximum period of the signal in the source signal would not exceed one sidereal day
- (c) Total number of source signals meets the requirements: $n \leq 3$

3. Results and Discussion

In this section, a comprehensive experimental study has been conducted to inspect the performance of our proposed method. The content consists of three parts: the experimental setup, comparative experiments using the MSF, the SFOD, and the AF-ICA methods, and the discussion.

3.1. Experimental Setup. To test our proposed methods, data from an experiment with a railway roadbed deformation monitoring project were used. This experiment was

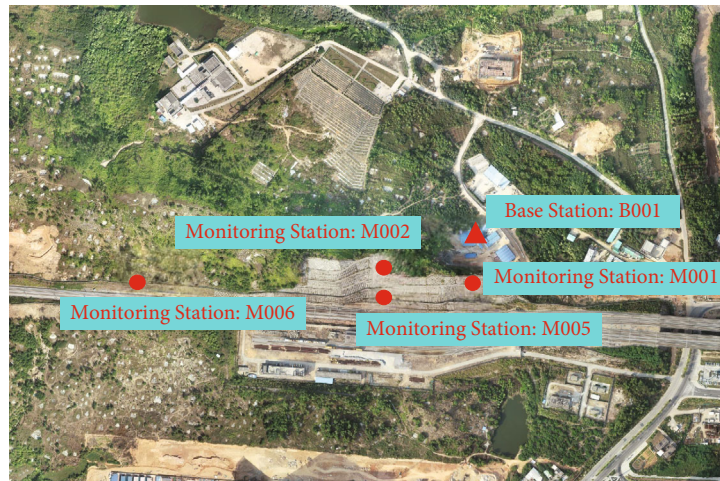


FIGURE 2: Distribution of each monitoring station.

TABLE 1: MSF accuracy under different kinds of session duration (Unit: mm).

Session duration	E	N	U	Session duration	E	N	U
1 s	7.6	7.6	10.6	45 min	3.3	3.2	4.4
15 s	7.1	7.1	9.9	1 hour	3.0	2.9	4.1
30 s	6.9	6.9	9.6	2 hours	2.5	2.3	3.2
60 s	6.7	6.6	9.3	3 hours	2.2	2.0	2.7
3 min	6.0	5.9	8.2	4 hours	1.9	1.8	2.4
5 min	5.6	5.5	7.6	6 hours	1.7	1.6	2.2
15 min	4.5	4.3	5.9	12 hours	0.7	0.7	0.8
30 min	3.7	3.6	5.0	24 hours	0.5	0.6	0.6

conducted on the Guangshan railway. It monitored the impact on the completed roadbed during construction and used GNSS receivers to monitor the deformation. In the monitoring area, we selected a firm position that is not easy to deform at the top of the mountain as the reference point, marked as B001. Four monitoring points noted as M001, M002, M005, and M006 were arranged along the railway in the monitoring area. The distribution of each observation station is shown in Figure 2.

The location was chosen because it was clearly subject to multipath effects from the smooth reflective surfaces of the railway roadbed. ComNav GNSS L1/L2 dual-frequency K506 receivers with Harxon HX-CSX601A survey antennas were used in the base and monitoring stations. The baselines between the base station and monitoring station were about 100-500 m. Due to this short baseline, satellite clock errors, receiver clock errors, satellite orbit error, ionospheric delay, tropospheric delay, and other common errors are removed by double differencing. The test began on March 3, 2020, and lasted for 8 days. The detailed data processing strategy is first analyze the positioning accuracy after MSF denoising, then use the classic SF-OD method to analyze the positioning accuracy after removing the multipath, and finally, use the AF-ICA method to analyze the positioning accuracy after the multipath is removed.

3.2. Experiment with MSF. Position accuracy obtained from the relative positioning of GNSS single epoch (i.e., interval = 1 s) is cm level, which cannot meet the mm level accuracy requirements of deformation monitoring, and MSF processing is required. In order to analyze the relationship between positioning accuracy and session duration in MSF, we designed 16 kinds of session duration: 1 s, 15 s, 30 s, 60 s, 3 min, 5 min, 15 min, 30 min, 45 min, 1 hour, 2 hours, 3 hours, 4 hours, 6 hours, 12 hours, and 24 hours and then used MSF algorithm for processing. The average positioning accuracy of the four monitoring stations' baseline results after MSF was counted in the ENU geographical coordinate system.

In this test, the 3-sigma principle (99.7% confidence probability) is used to count the positioning accuracy. The statistical results are shown in Table 1, and the relationship between positioning accuracy and session duration is shown in Figure 3.

As can be seen from Table 1 and Figure 3:

the longer the session duration, the higher the positioning accuracy. After more than 12 hours, the positioning accuracy is better than 1 mm, and then increasing the duration has little improvement on the positioning accuracy. When the session duration is within 0-1 hour, the effect of increasing duration on the positioning accuracy is very obvious, and it enters a turning point near 1 hour. After the

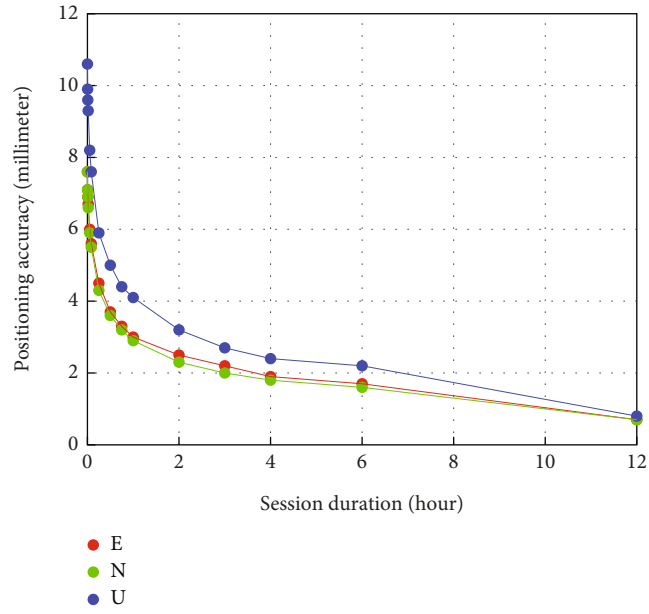


FIGURE 3: Relationship between positioning accuracy and session duration.

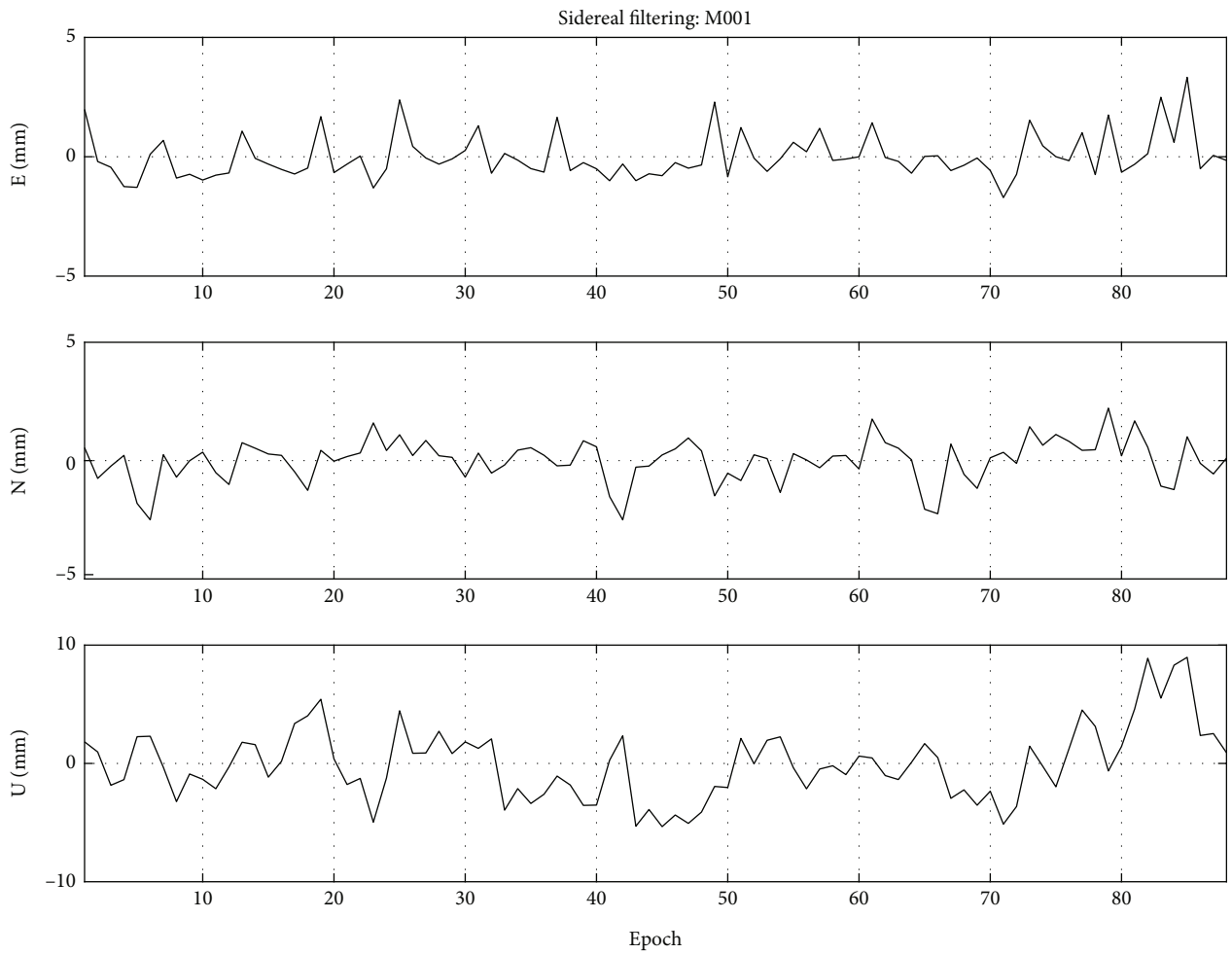


FIGURE 4: ENU error of M001 station after SF-OD.

TABLE 2: Positioning accuracy using 2 hours of MSF and SF-OD methods.

Monitoring station	Positioning accuracy (RMS)/mm						Peak-to-peak value (maximum minus minimum)/mm					
	E		N		U	E		N		U		
	MSF	SF-OD	MSF	SF-OD		MSF	SF-OD	MSF	SF-OD	MSF	SF-OD	
M001	1.0	0.9	0.7	0.9	3.4	3.0	4.2	5.0	3.8	4.7	16.1	14.3
M002	0.5	0.8	0.7	0.5	1.6	2.2	2.4	3.2	3.2	2.7	7.7	12.0
M005	0.8	0.6	0.6	0.6	1.6	1.5	3.5	3.6	2.8	3.3	7.2	10.1
M006	0.8	0.9	0.5	0.7	2.4	1.7	3.4	4.7	2.7	3.9	12.2	9.8

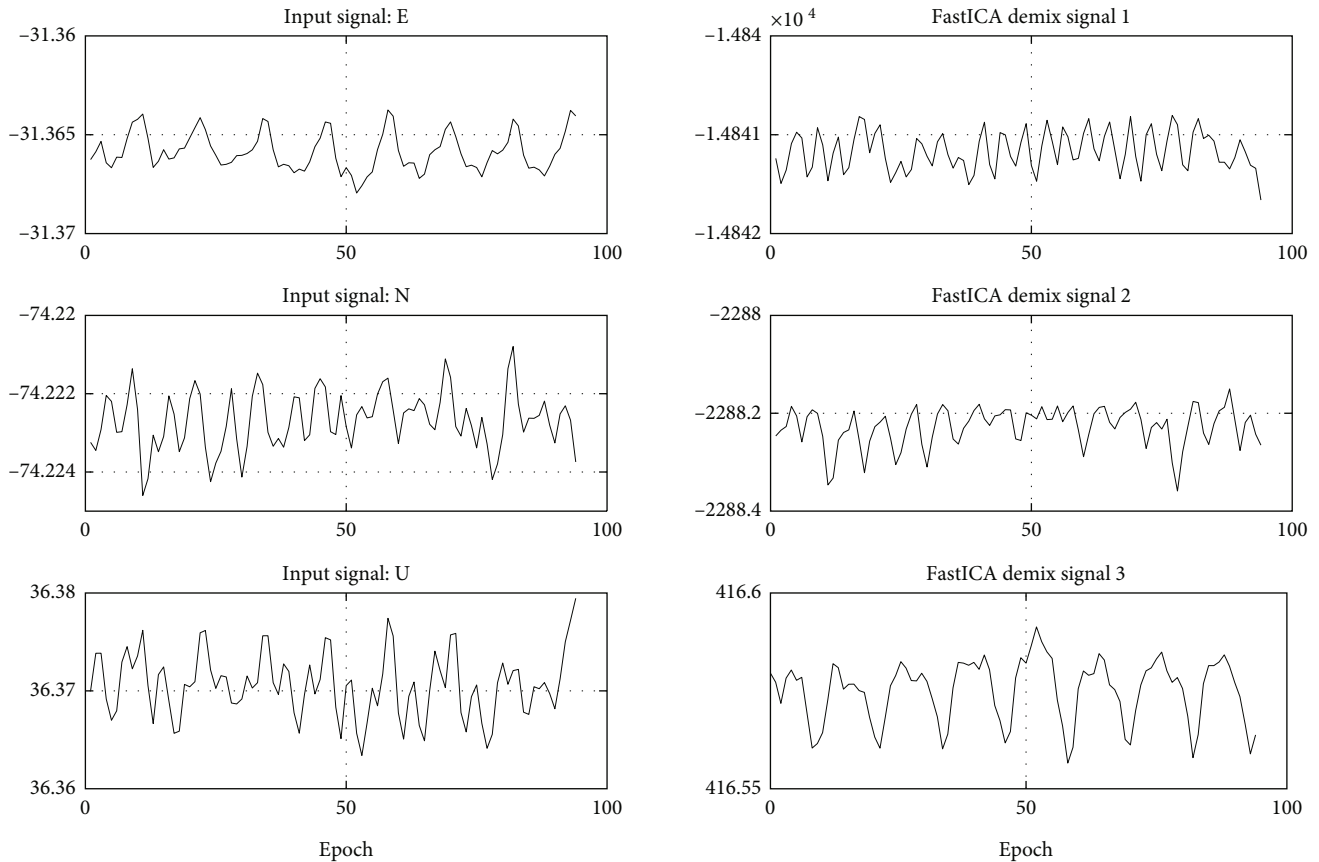


FIGURE 5: Period and graph of multipath signal of M001 by FastICA (three figures on the left are the time series of ENU coordinates, and the three pictures on the right are the multipath signals separated by FastICA).

duration exceeds 1 hour, the horizontal positioning accuracy is better than 3 mm and the altitude positioning accuracy is better than 4 mm.

In summary, we suggest that in GNSS deformation monitoring using MSF method, it is more appropriate to select 1-12 hours for the duration, which can not only obtain mm level positioning accuracy but also ensure a fast deformation monitoring result.

3.3. Experiment with SF-OD. We use the SF-OD method to eliminate multipath signals and analyze the positioning accuracy after removing multipath. The data processing strategy of SF-OD is first collect data for one sidereal day, then get the difference between second sidereal day with

the first sidereal day in observation domain, and finally, obtain the deformation of the second sidereal day relative to the first sidereal day. The SF-OD method uses a 2 hours interval for processing. The first day as a reference and calculate the single difference residuals. The positioning solution is carried out after removing the single difference residuals in the same period of the next day. Due to the adoption of the sidereal day period, we only process the GPS dual-frequency data. Figure 4 shows the ENU positioning error of M001 station after removing the multipath signal, Table 2 lists the positioning accuracy statistics using 2 hours of MSF and SF-OD methods.

Compared with MSF, the positioning accuracy of SF-OD increases by -9%, -10%, and 2% in the three directions of

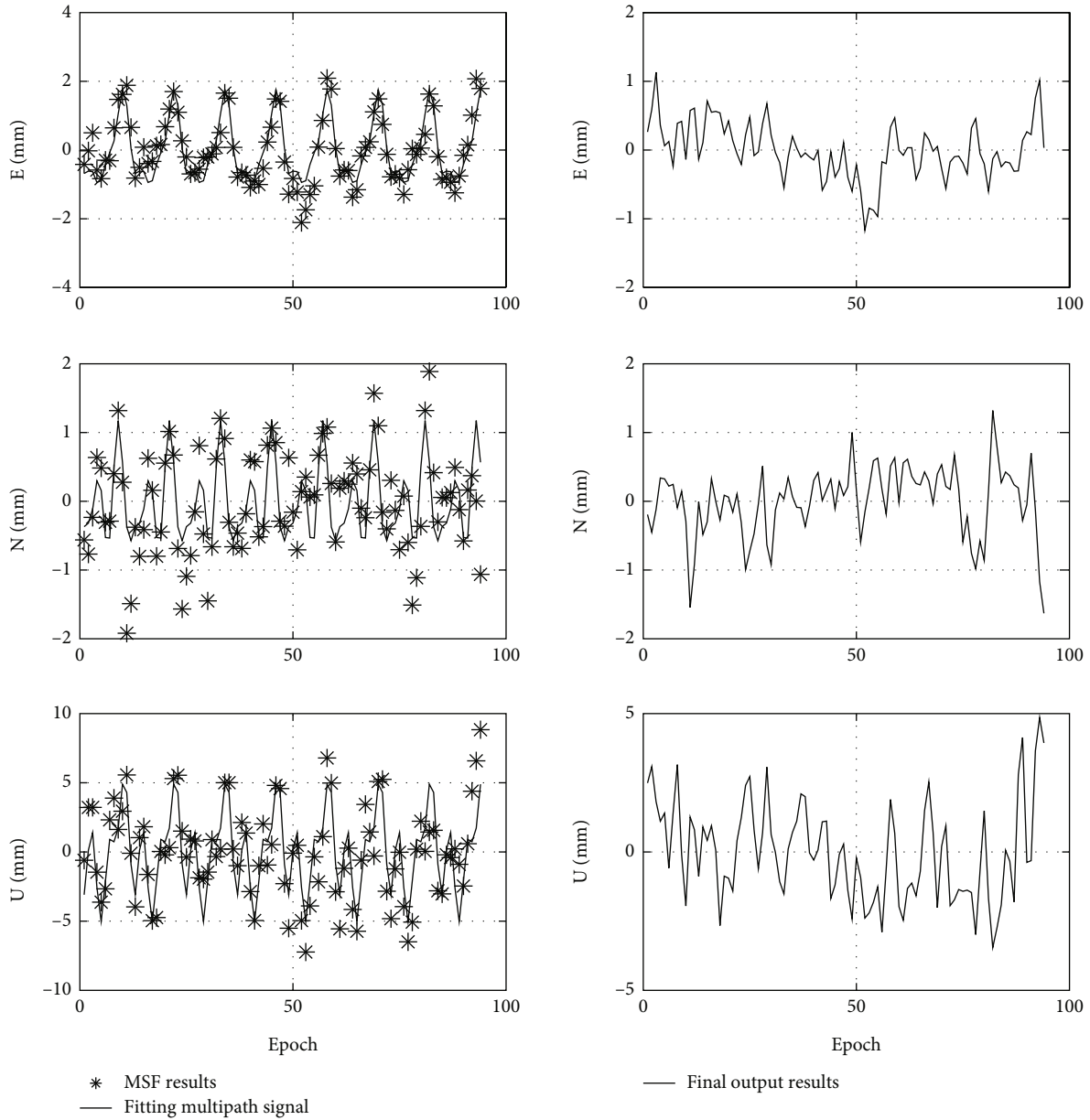


FIGURE 6: ENU error of M001 station after AF-ICA (asterisk points and line on the left figures, respectively, represent the MSF results and fitting multipath signal of ENU coordinates. Line on the right pictures are the ENU positioning results after AF-ICA).

ENU. The corresponding peak-to-peak value increases are -23%, -17%, and -16%. It can be seen that although SF-OD can effectively deal with the influence of sidereal day multipath signals, the positioning accuracy and peak-to-peak value are worse than those of the MSF method. The possible reason is that SF-OD only processes GPS data, while MSF processes GPS+BDS data which contains more satellites.

3.4. Experiment with AF-ICA. According to the data results of the MSF test, the session duration range of MSF is controlled within 1-12 hours. Firstly, four monitoring stations are tested through a priori information in AF-ICA, and it is concluded that the minimum session duration that can separate multipath signals is 2 hours. Subsequent AF-ICA analysis is processed based on the MSF results of 2 hours.

Figure 5 shows the period and graph of separating the multipath signal of M001 station by FastICA method. The input signal is the E, N, and U coordinate components after MSF, and the output signal is the separated three independent multipath signals. Through the first-order Fourier fitting formula, the periods of the three multipath signals are 8 hours, 12 hours, and 24 hours, respectively. It can be seen that compared with the sidereal day period in GPS data, the GPS+BDS data used in this test adds two multipath signals with smaller cycles, which may be mainly due to the use of multiple orbit types of satellites in GNSS relative positioning.

After the multipath signal is separated by the FastICA method, the complete multipath signal is generated by the linear fitting formula. Figure 6 plots the positioning error of M001 station before and after multipath signal removal

TABLE 3: Accuracy after removing multipath signals by AF-ICA compared with MSF.

Monitoring station	Positioning accuracy (RMS)/mm						Peak-to-peak value (maximum minus minimum)/mm					
	E		N		U		E		N		U	
	MSF	AF-ICA	MSF	AF-ICA	MSF	AF-ICA	MSF	AF-ICA	MSF	AF-ICA	MSF	AF-ICA
M001	1.0	0.4	0.7	0.5	3.4	1.8	4.2	2.3	3.8	3.0	16.1	8.3
M002	0.5	0.3	0.7	0.5	1.6	1.4	2.4	1.7	3.2	2.0	7.7	7.4
M005	0.8	0.4	0.6	0.6	1.6	1.0	3.5	1.9	2.8	3.0	7.2	4.5
M006	0.8	0.6	0.5	0.5	2.4	1.8	3.4	2.6	2.7	2.3	12.2	8.8

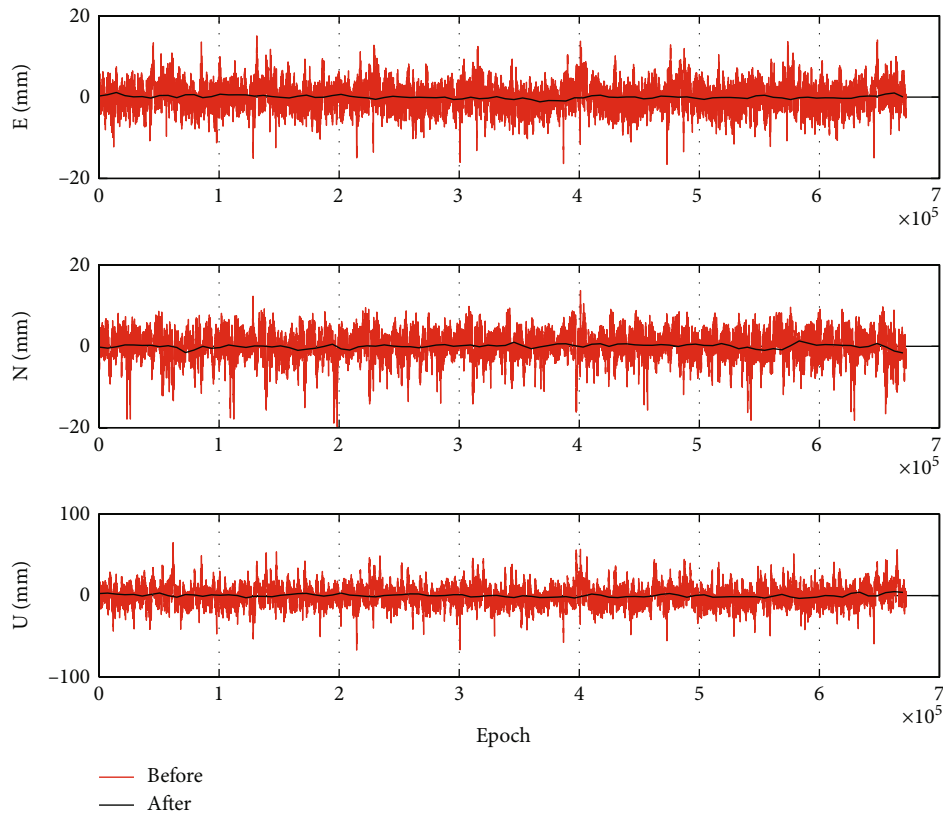


FIGURE 7: ENU error of M001 station before and after multipath signal removal by AF-ICA for 8 days.

by FastICA method. In Figure 6, the results after MSF are represented by asterisk points, fitting multipath represents the complete multipath signal, and finally represents the positioning error after multipath signal removal. Table 3 lists the accuracy statistics after removing multipath signals by AF-ICA compared with MSF. Figure 7 plots the positioning error of M001 station before and after multipath signal removal by AF-ICA.

Compared with MSF, the positioning accuracy of the AF-ICA method is improved by 44%, 14%, and 31% in the three directions of ENU. The corresponding peak-to-peak value increases were 36%, 17%, and 29%. It can be seen that the AF-ICA method can effectively deal with the influence of multipath signals during multi-GNSS fusion positioning, and the positioning accuracy is significantly improved compared with the simple MSF method.

3.5. Discussion. In the above experiments, we use two different methods to mitigate the multipath in deformation monitoring. To compare the MSF method and sidereal day filtering method, we use the SF-OD method to process GPS dual-frequency data. Although SF-OD effectively processes the influence of sidereal day multipath on the positioning accuracy, peak-to-peak values are worse than those of the MSF method. On the other hand, through the analysis of 8-day static test results by the AF-ICA method, according to a priori information of multipath signal, we determined that the minimum session duration meeting the multipath signal separation is 2 h, and successfully separated the multipath signals of four stations. Compared with the simple MSF method, the positioning accuracy of the AF-ICA method is improved by 44%, 14%, and 31% in the three directions of ENU. The corresponding peak-to-peak value increases were

36%, 17%, and 29%. The AF-ICA method can effectively solve the problem of multiperiod multipath signals caused by multiple satellite orbits of GNSS. The AF-ICA can automatically identify the session duration, to realize automatic deformation monitoring.

4. Conclusion

In this study, we proposed a novel method called the AF-ICA method to address the complicated multipath in the deformation monitoring of the GNSS that contains multiple types of satellites and improve the timeliness. The experimental results show that our method can achieve mm level positioning accuracy and meet the requirements of GNSS deformation monitoring. At the same time, by analyzing the value range of session duration, it is found that the session duration of 1-12 hours is more appropriate, which can not only obtain ideal positioning accuracy but also ensure fast deformation monitoring. Compared with the simple MSF method and the SF-OD method, the proposed AF-ICA method is able to improve both the positioning accuracy and peak-to-peak values. In a word, our method is more appropriate for mitigating multipath than the traditional sidereal filtering method, especially in multi-GNSS fusion positioning.

Data Availability

The datasets generated during and/or analyzed during the current study are available from the corresponding author for academic purposes.

Conflicts of Interest

The authors declared no potential conflicts of interest with respect to the research, authorship, and/or publication of this article.

Acknowledgments

The authors acknowledge the National Natural Science Foundation of China under Grant 62273106 and the Key Research and Development Program of Guangdong Province under Grant 2019B010141001.

References

- [1] Y. Yang, J. L. Li, A. B. Wang et al., "Preliminary assessment of the navigation and positioning performance of BeiDou regional navigation satellite system," *Science China Earth Sciences*, vol. 57, no. 1, pp. 144–152, 2014.
- [2] C. Liu, P. Lin, X. Zhao, and J. Gao, "Reducing GPS carrier phase errors in the measurement and position domains for short-distance static relative positioning," *Acta Geodaetica et Geophysica*, vol. 51, no. 1, pp. 81–93, 2015.
- [3] J. W. Lovse, W. F. Teskey, G. Lachapelle, and M. E. Cannon, "Dynamic deformation monitoring of tall structure using GPS technology," *Journal of Surveying Engineering*, vol. 121, no. 1, pp. 35–40, 1995.
- [4] S. Nakamura, "GPS measurement of wind-induced suspension bridge girder displacements," *Journal of Structural Engineering*, vol. 126, no. 12, pp. 1413–1419, 2000.
- [5] X. Meng, G. W. Roberts, A. H. Dodson, E. Cossier, J. Barnes, and C. Rizos, "Impact of GPS satellite and pseudolite geometry on structural deformation monitoring: analytical and empirical studies," *Journal of Geodesy*, vol. 77, no. 12, pp. 809–822, 2004.
- [6] W. S. Chan, Y. L. Xu, X. L. Ding, and W. J. Dai, "An integrated GPS accelerometer data processing technique for structural deformation monitoring," *Journal of Geodesy*, vol. 80, no. 12, pp. 705–719, 2006.
- [7] P. Psimoulis, S. Pytharouli, D. Karambalis, and S. Stiros, "Potential of global positioning system (GPS) to measure frequencies of oscillations of engineering structures," *Journal of Sound and Vibration*, vol. 318, no. 3, pp. 606–623, 2008.
- [8] P. Elósegui, J. L. Davis, R. T. K. Jaldehag, J. M. Johansson, A. E. Niell, and I. I. Shapiro, "Geodesy using the global positioning system: the effects of signal scattering on estimates of site position," *Journal of Geophysical Research*, vol. 100, no. B6, pp. 9921–9934, 1995.
- [9] K. Choi, A. Bilich, K. M. Larson, and P. Axelrad, "Modified sidereal filtering: implications for high-rate GPS positioning," *Geophysical Research Letters*, vol. 31, no. 22, 2004.
- [10] A. E. Ragheb, P. J. Clarke, and S. J. Edwards, "GPS sidereal filtering: coordinate- and carrier-phase-level strategies," *Journal of Geodesy*, vol. 81, no. 5, pp. 325–335, 2006.
- [11] A. E. Ragheb, P. J. Clarke, and S. J. Edwards, "Coordinate-space and observation-space filtering methods for sidereally repeating errors in GPS: performance and filter lifetime," in *Proceedings of the 2007 National Technical Meeting of The Institute of Navigation*, pp. 480–485, San Diego, CA, 2007.
- [12] K. M. Larson, A. Bilich, and P. Axelrad, "Improving the precision of high-rate GPS," *Journal of Geophysical Research*, vol. 112, no. B5, 2007.
- [13] D. Dong, M. Wang, W. Chen et al., "Mitigation of multipath effect in GNSS short baseline positioning by the multipath hemispherical map," *Journal of Geodesy*, vol. 90, no. 3, pp. 255–262, 2016.
- [14] W. Gao, X. Meng, C. Gao, S. Pan, Z. Zhu, and Y. Xia, "Analysis of the carrier-phase multipath in GNSS triple-frequency observation combinations," *Advances in Space Research*, vol. 63, no. 9, pp. 2735–2744, 2019.
- [15] X. Tang, G. W. Roberts, C. M. Hancock, and J. Yu, "GPS/BDS relative positioning assessment by zero baseline observation," *Measurement*, vol. 116, pp. 464–472, 2018.
- [16] W. J. Dai, D. W. Huang, and C. S. Cai, "Multipath mitigation via component analysis methods for GPS dynamic deformation monitoring," *GPS Solutions*, vol. 18, no. 3, pp. 417–428, 2014.
- [17] A. Hyvarinen and E. Oja, "Independent component analysis: algorithms and applications," *Neural Networks*, vol. 13, no. 4-5, pp. 411–430, 2000.
- [18] Q. Zhang, W. Yang, S. Zhang, and X. Liu, "Characteristics of BeiDou navigation satellite system multipath and its mitigation method based on Kalman filter and Rauch-Tung-Striebel smoother," *Sensors*, vol. 18, no. 2, p. 198, 2018.

Retraction

Retracted: Monitoring of Single-Phase Induction Motor through IoT Using ESP32 Module

Journal of Sensors

Received 23 January 2024; Accepted 23 January 2024; Published 24 January 2024

Copyright © 2024 Journal of Sensors. This is an open access article distributed under the Creative Commons Attribution License, which permits unrestricted use, distribution, and reproduction in any medium, provided the original work is properly cited.

This article has been retracted by Hindawi following an investigation undertaken by the publisher [1]. This investigation has uncovered evidence of one or more of the following indicators of systematic manipulation of the publication process:

- (1) Discrepancies in scope
- (2) Discrepancies in the description of the research reported
- (3) Discrepancies between the availability of data and the research described
- (4) Inappropriate citations
- (5) Incoherent, meaningless and/or irrelevant content included in the article
- (6) Manipulated or compromised peer review

The presence of these indicators undermines our confidence in the integrity of the article's content and we cannot, therefore, vouch for its reliability. Please note that this notice is intended solely to alert readers that the content of this article is unreliable. We have not investigated whether authors were aware of or involved in the systematic manipulation of the publication process.

Wiley and Hindawi regrets that the usual quality checks did not identify these issues before publication and have since put additional measures in place to safeguard research integrity.

We wish to credit our own Research Integrity and Research Publishing teams and anonymous and named external researchers and research integrity experts for contributing to this investigation.

The corresponding author, as the representative of all authors, has been given the opportunity to register their agreement or disagreement to this retraction. We have kept a record of any response received.

References

- [1] A. Shukla, S. P. Shukla, S. T. Chacko, M. K. Mohiddin, and K. A. Fante, "Monitoring of Single-Phase Induction Motor through IoT Using ESP32 Module," *Journal of Sensors*, vol. 2022, Article ID 8933442, 8 pages, 2022.

Research Article

Monitoring of Single-Phase Induction Motor through IoT Using ESP32 Module

Abhinab Shukla ¹, S. P. Shukla ², S. T. Chacko ³, Md. Khaja Mohiddin ⁴,
and Kinde Anlay Fante ⁵

¹Research Scholar, Department of Electrical Engineering, Bhilai Institute of Technology, Durg, Chhattisgarh, India

²Faculty, Department of Electrical Engineering, Bhilai Institute of Technology, Durg, Chhattisgarh, India

³Faculty, Department of Electrical Engineering, UPU Govt. Polytechnic, Durg, Chhattisgarh, India

⁴Faculty, Department of Electronics & Telecommunication, Bhilai Institute of Technology, Raipur, Chhattisgarh, India

⁵Faculty of Electrical and Computer Engineering, Jimma Institute of Technology, Jimma University, Jimma, Ethiopia

Correspondence should be addressed to Abhinab Shukla; abhinab.shukla@gmail.com
and Kinde Anlay Fante; kinde.anlay@ju.edu.et

Received 1 September 2022; Accepted 5 October 2022; Published 9 November 2022

Academic Editor: Sweta Bhattacharya

Copyright © 2022 Abhinab Shukla et al. This is an open access article distributed under the Creative Commons Attribution License, which permits unrestricted use, distribution, and reproduction in any medium, provided the original work is properly cited.

The condition monitoring of rotating machines for critical applications plays an important role in reducing downtime. With Industry 4.0, the role of IoT in online condition monitoring of electrical machines has gained considerable significance. The main aim of the paper is the use of IoT for online monitoring of motor parameters like current, temperature, vibration, and humidity and observing its online trending using a web server. Data can be accessed in form of graphs and widgets by visiting the web page. The advantage of this project is the real-time monitoring of the motor from any remote area and in case of any abnormality operating personnel can take necessary steps for preventing complete breakdown. The proposed work can help industry people in online monitoring of motors and in the future work can be extended for fault prediction and classification.

1. Introduction

Condition monitoring of motors is very important, and a maintenance schedule is always implemented for every electrical machine. In the proposed work with the use of IoT technology motor parameters like temperature, current, voltage, and vibration can be accessed wirelessly. All these parameters can be analyzed by operator from anywhere and in case of any fault condition alert can be raised. IoT based condition monitoring when joined with machine learning can help in classification and prediction of faults. Electrical motors are work horse for any industry [1, 2]. Electrical motors have to be maintained and monitored on regular basis. Breakdown or faults in such rotating machines can hamper the industry in various ways. Proposed method of monitoring motors can be used for real time parameter

monitoring of motors and to generate regular notification in case any parameter shoots up from its regular value [3, 4].

2. Related Work

In reference to various research papers, IoT technology is already being used for data collection and fault prediction of electrical motors. In this method, development boards like Arduino, Nodemcu, and Raspberry-pi are used as processor, and various sensors are interfaced with them for data collection. With the use of Wi-Fi modules, all the parameters can be stored in cloud [1, 5–8]. In reference paper [4], Nodemcu has been used for acquiring motor parameters for traction drive and upload it in cloud.

Other work done in this field is condition monitoring of motors using GSM modules and radio frequency

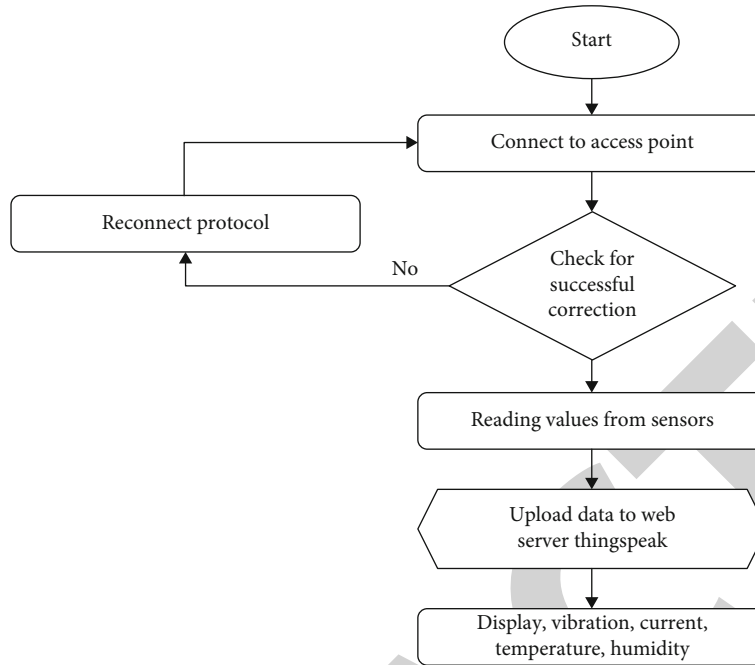


FIGURE 1: Flowchart showing entire process.

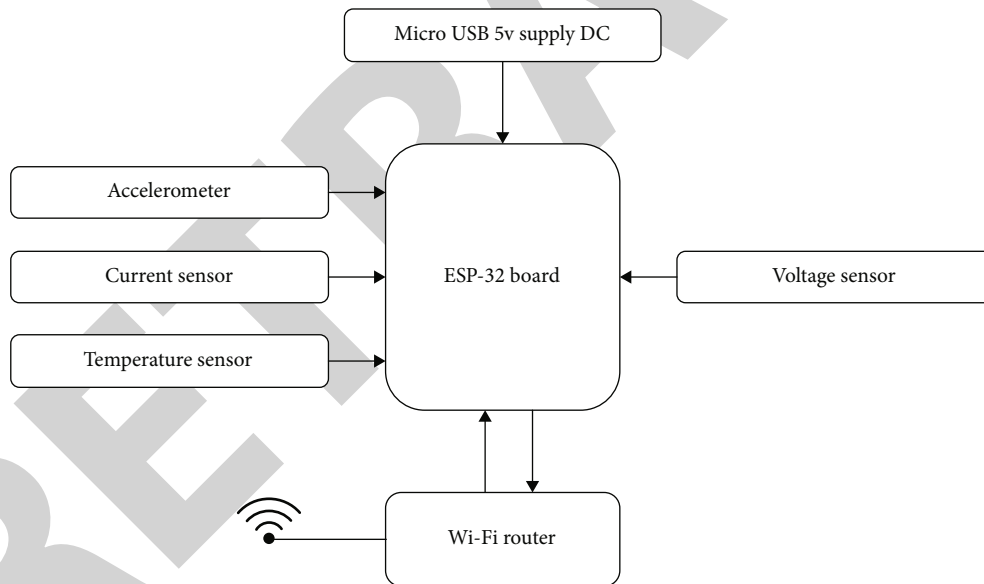


FIGURE 2: Block diagram of hardware.

TABLE 1: Motor rating.

Name	Power	Speed	Voltage	Frequency
1PH induction motor	320 W	1350 RPM	220 V	50 Hz

waves [9, 10]. Hardware module consists of printed circuit board, and along with these, sensors, ICs, and processors are mounted. Data collected is sent to control and monitoring room. Hence, operator can go through all the real time data and can take decisions as per requirement [2, 3].

In most of the previous work done, sensors that have been used for parameter collection are ADXL 345, ACS 7212, and LM 35 as acceleration, current, and temperature sensors, respectively [8, 11]. In contrast to it in reference paper [9], piezoelectric transducer is used to collect vibration data for motors and storing it in cloud using Nodemcu.

In reference paper [10], it can be analyzed that after data acquisition, various fault detection methods can be adopted, and it has been concluded that MCSA method is best for fault detection in electrical motors [12, 13]. Motor current signature analysis is a popular predictive maintenance tool

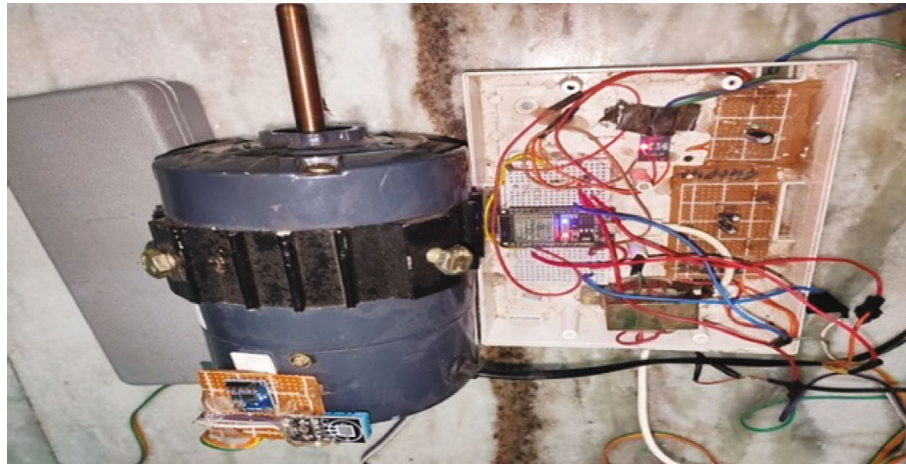


FIGURE 3: Experimental setup.

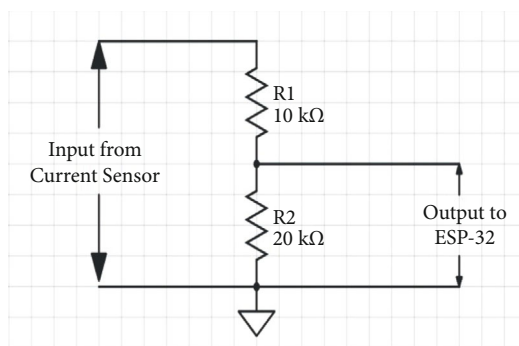


FIGURE 4: Signal conditioning circuit for 5-volt reference to 3.3 volt.

for electrical motors, and it mainly uses current spectrum for analysis [14, 15].

3. Proposed Work

In the proposed work, ESP32 board is used as processor. Sensors used for collecting parameters are DHT 11, ACS 712, and ADXL 345. Data collected from various sensors are uploaded to cloud using THINGSPEAK platform. All the live data of parameters can be seen using IoT platform inform of graphs and widgets [16, 17]. Assembled hardware has been used with a single-phase induction motor, and results were discussed for it. Figure 1 explains the flowchart for entire process in the proposed work. When the supply is given to ESP32 board, it connects with the access point [18, 19]. The sensors connected to motors start delivering signals to GPIO pins of ESP32 board. As real time data gets uploaded to cloud operator in the field can monitor current, vibration, temperature, and humidity of motor from any part of world with only requirement of internet in laptop or smart phone [20, 21].

Operating personnel working on the motor can monitor the data in real time. In case, any of the parameter magnitude crosses the limit [22, 23]. Operator can start the shutdown process which will prevent the machine from having

complete breakdown. With things, speak cloud platform limits can be set for each field [24]. If in any abnormal condition the parameter value of motor increases and breaches the set limit then an alert or notification can be sent to operator. Such protocol can play very important role for protection of motors [25, 26].

Prediction of faults and its classification of industrial machines can also be possible. The real time data from motors can be given to trained artificial neural network, and the output of the ANN model will be the prediction of fault and its type [27]. If the fault is of incipient stage, machine can be scheduled for maintenance. In future, the proposed work can be expanded for having fault prediction and its classification for various motors.

4. Block Diagram of Hardware

Figure 2 shows the block diagram which explains the interconnections between the sensors and processor. Block diagram also elaborates the type of sensor and data which has to be collected from motor. The ESP32 module is powered with a 5V 2A adapter.

4.1. Development Boards and Sensors

4.1.1. ESP32. ESP32 is a series of low-cost, low-power system on a chip microcontroller with integrated Wi-Fi and dual-mode Bluetooth [28]. The ESP32 board has 15 ADC pins, and each pin has 12-bit resolution with range from 0 to 4095.

4.1.2. Current Sensor. A hall effect current sensor called the ACS712 is used to measure current. It is both cost-effective and provides a precise solution for AC and DC current detection. Its output sensitivity ranges from 66 to 185 mV/A. A hall effect current sensor called the ACS712 is used to measure current [29]. It is both cost-effective and provides a precise solution for AC and DC current detection. Its output sensitivity ranges from 66 to 185 mV/A.

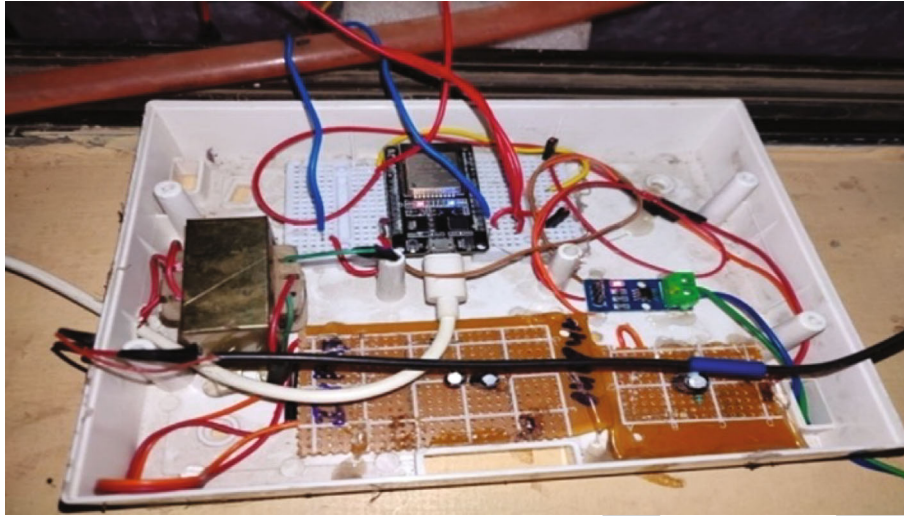


FIGURE 5: Assembled circuit.

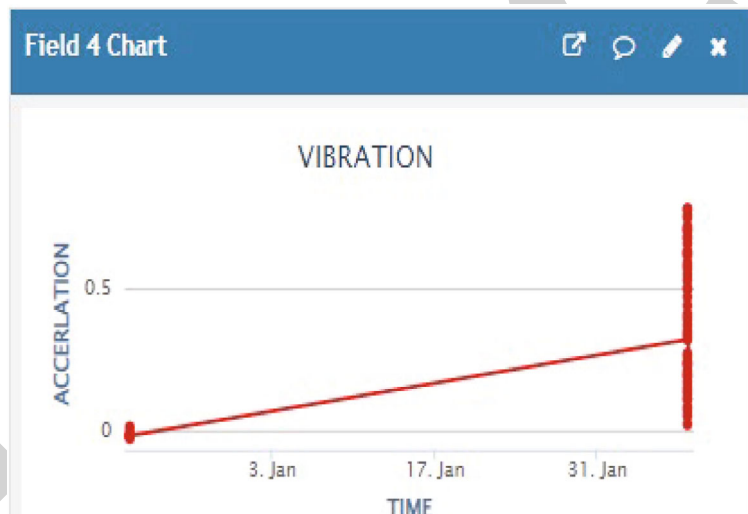


FIGURE 6: Vibration graph of motor.

4.1.3. Vibration Sensor. The vibration sensor or accelerometer utilized is the ADXL 335, a tiny, thin, low-power, three-axis accelerometer with signal-conditioned voltage outputs. It has a 3 g range and measures full scale acceleration. Both static and dynamic accelerations are measured. This is where the dynamic acceleration caused by motion, shock, or vibrations is monitored. Different bandwidths for three axes can be chosen depending on the application [30]. The X and Y axes have bandwidths ranging from 0.5 Hz to 1600 Hz, while the Z axis has bandwidths ranging from 0.5 Hz to 550 Hz. It displays three values for each of the three axes that represent motor vibrations. Vibrations are measured based on the values acquired in three axes.

4.1.4. Voltage Sensor. A voltage sensing circuit measures the voltage and creates an output voltage that meets the Wi-Fi board's requirements. A 230 V/12 V potential transformer is employed, and the output is converted to DC via a rectifier when needed. The rectifier output is rippled out using a

capacitor [31]. The output remains high enough to be transmitted to the microcontroller. As a result, a potential divider circuit is utilized to obtain the requisite voltage of 5 V, which is then fed into the ESP32.

4.1.5. Temperature Sensor. The DHT11 is a temperature and humidity sensor that is widely used. The sensor includes a dedicated NTC for temperature measurement and an 8-bit microprocessor for serial data output of temperature and humidity values.

4.1.6. Single Phase Induction Motor. A single-phase squirrel cage induction motor for testing purposes and its rating is shown in Table 1.

4.2. Technology Used. In this research, the Internet of Things technology (IoT) is used to monitor an induction motor. In IoT (Internet of Things), the Internet of Things (IoT) is a network of smart devices and things that are equipped with

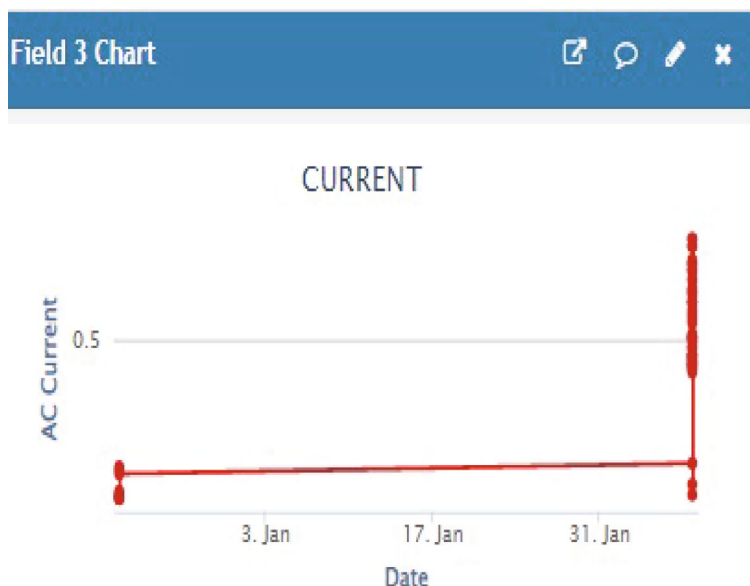


FIGURE 7: Current intake graph of motor.

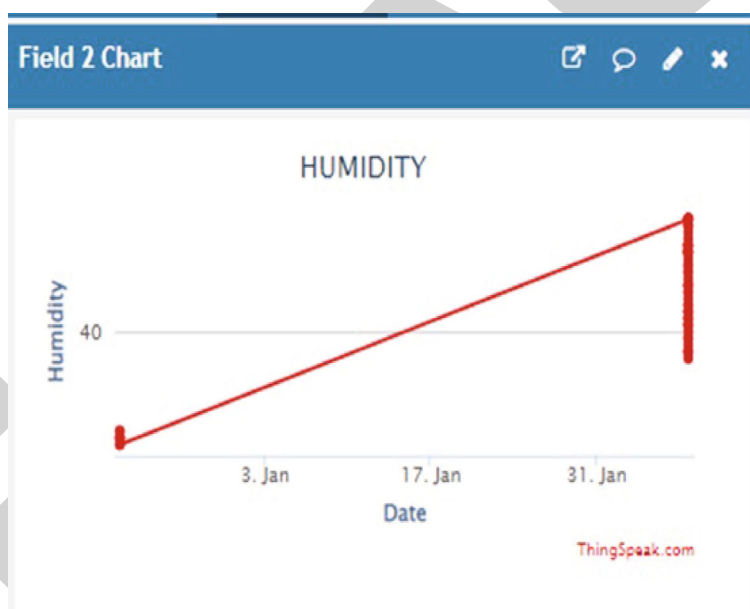


FIGURE 8: Humidity graph of motor.

various sensors and network to gather and transmit data. In IoT/cloud platform, the IoT platform is the heart of the Internet of Things architecture, as it connects the physical and virtual worlds, allowing items to communicate with one another [32]. Thing speak is a cloud platform by Math Works. It has been used as the IoT platform in this research. It generates graphical displays for data uploaded to the platform by devices in real time. Thing speak is frequently used for prototyping and proof of concept IoT applications.

5. Experimental Setup and Assembly

Figure 3 shows the experimental set up developed in this research work. The goal of real time monitoring of 1-pH

induction motor is done by continuously monitoring the parameters with the use of different sensors [25]. Current sensor ACS 712, ADXL acceleration sensor, DHT 11 temperature sensor, and voltage sensor circuit are used to sense parameters RMS current, vibration, temperature, and voltage, respectively. All the data sensed will be in accordance with the instruction coded to ESP32 module.

The ESP32 module has fifteen ADC pins, and it can sense voltage between 0 volt to 3.3 volt. Corresponding to this range value can be assigned between zero to 4095. The analog input has 12-bit resolution. The data collected can be analyzed and stored in cloud using ESP32 module [17]. There are various general purpose input output pins in ESP32 module which can be used for reading and writing

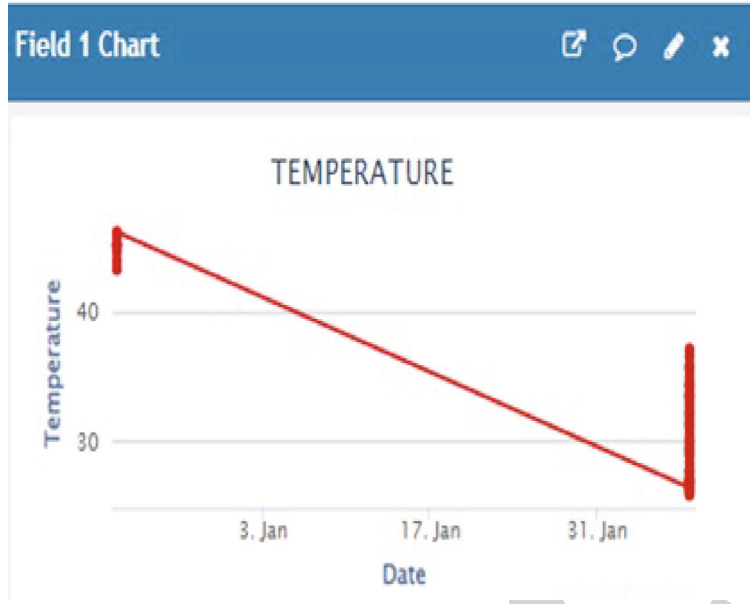


FIGURE 9: Temperature graph of motor body.

data. For storing the data in things speak platform account is to be created, and a new channel is generated. Number of fields has to be chosen proportional to the number of parameters under monitoring. Each field is being given with its own parameter and then it can be visualized using various graphical forms. In this work, parameters of healthy motor and abnormal motor have been shown and compared. User with this system can visit things speak website and can monitor the motor anytime from anywhere [18, 19]. In case of any abnormal operation, emergency protocol can be implemented and motor can be turned off [22]. Hence, such systems can improve the longevity and reliability of rotating machines.

6. Formula Used for Data Sampling

6.1. Sampling of AC Current Data. AC current withdrawn from induction motor is sensed using hall effect current sensor. The output voltage coming from sensor is converted to voltage under 3.3 volts. Signal conditioning circuit for the reference voltage conversion is shown in Figure 4. This is done because the reference voltage for ESP32 for reading analog values is 3.3 volt only. As mentioned, ESP32 is a 12-bit ADC hence scale for resolution is kept from 0 to 4095. ACS 712 05B module has sensitivity of around 185 mV. The formula used for calculation of RMS current is mentioned below.

$$I_{\text{RMS}} = \sqrt{\frac{(I_{\text{SUM}}/\text{Measurement Count})}{4095 \times (3.3/0.185)}} \text{ Amps.} \quad (1)$$

6.2. Sampling of Vibration Data. ADXL 335 GY-61 sensor is used to detect vibration in motor. Initially, the sensor is calibrated, and the error is subtracted from the expression of main equation. The GY-61 sensor used in this work has a

sensitivity of 330 mV per G. The formula used for calculation of acceleration is given below.

$$\text{Acceleration} = \left\{ \frac{((\text{sensor output} \times 3.23)/4095 - 1.47)}{0.33} \right\} \text{ M/S}^2. \quad (2)$$

6.3. Sampling of Temperature and Humidity Data. The instruction code uploaded to ESP32 uses DHT 11 library for getting data values and for updating it in regular intervals. DHT-11 sensor provides temperature and humidity data using its data output pin [11]. The single wire two-way communications are used for data retrieval process.

6.4. Sampling of Voltage Data. The output of voltage sensor circuit is given to ESP32 module. The ESP32 module reads the output from sensor within the scale of resolution from 0 to 4095, and the reference voltage is 3.3 volt. The transformer converts 240 V to 12 V, and the secondary is connected to arrangement of rectifier with zener diode. Five-volt logic across zener diode is reduced to proportional 3.3 V, and the logic is given to ESP32 module ADC pin [9]. As the single-phase supply varies, the logic level to ESP32 module also changes in reference to 3.3 V. As per the formula given in the code single phase voltage gets recorded and stored in cloud IoT platform.

7. Experimental Results

Figures 3 and 5 show the entire assembled circuit set up. The developed code is uploaded to module. Sensors are interfaced to ESP32 board. Once the module is powered up, it gets connected to internet, and sensors start accumulating the data. All the data is sent to things speak IoT platform and user can monitor the parameters with the help of graphs and widgets. From Figures 4–8, various graphs are shown

below, and the parameters that can be monitored are current, temperature, humidity, vibration, and power. From the graphs, it can be assessed that x axis comprises of date, and y axis comprises of the magnitude of the parameter. When the system turns on, the dark red dotted points on the graph show present value of the parameter. The straight-line which traces with in the various dates shows the changes by comparing the present-day status with the last period when system was turned on. Hence, it should not be concluded that graphs are linear in nature. The present value of parameter can be seen by tracing the latest entry of red dark dot and by double clicking with in it the graphical display becomes more dynamic as it shows minute by minute entry of data from the sensors.

With all these parameters, any threshold limit can be set and if the set limit for any required parameter is crossed then notification or alert can be sent to the operator using IoT platform. Therefore, it can be assessed that such systems can be used for real time monitoring of various electrical machines.

ADXL sensor is used for retrieving vibration data from motor. Sensor is placed on top of the motor body and as soon as motor starts values from the sensor can be seen on graph. ADXL sensor measures acceleration in x , y , and z -axis in g unit. From the graph Figure 6, motor had present vibration value of $0.71M/S^2$.

Single phase induction motor current data is retrieved from current sensor ACS 712. From the graph Figure 7, current magnitude is approximately one ampere. The ACS 712 sensor has an output error percentage of around $\pm 1.5\%$.

Temperature and humidity data are taken from DHT 11 sensor which has been mounted on motor body. As the motor started temperature value started increasing, this happens as winding of the motors starts heating up with the safety insulation point. After a certain point temperature of the motor body reaches a saturation value of around thirty-nine-degree Celsius (Figure 9), DHT 11 humidity sensor can measure from twenty percent to eighty percent range with accuracy of five percent.

8. Conclusion

In this paper, a single-phase induction motor has been monitored in real time environment. All the important parameters can be visualized using things peak platform. Any deviation of parameter can be seen by operating personnel, and necessary action can be taken for improving longevity of motor. In future, such methods can be used for data acquisition from industrial motors, and at the same time, all the data set can be given to ANN model for fault prediction and classification. Processor such as raspberry pi can be used for data collection and running ANN algorithm. ANN is used for achieving fault prediction and classification. The proposed research mainly contributes in collection of important motor parameters and provides means of its monitoring through cloud platforms. The proposed research also contributes in planning effective maintenance schedule of motors. The developed IoT based method is very effective in having real time monitoring of motors.

Acronyms

IoT: Internet of Things
 MCSA: Motor Current Signature Analysis
 ANN: Artificial neural network
 RMS: Root mean square
 DHT: Digital temperature and humidity sensor.

Data Availability

All data used to support the findings of this study are included in the article.

Conflicts of Interest









The authors declare that they have no conflicts of interest.

References

- [1] R. Iyer and A. Sharma, "IoT based home automation system with pattern recognition," *International Journal of Recent Technology and Engineering*, vol. 8, no. 2, p. 3925, 2019.
- [2] F. P. Mahdi, M. Habib, M. Ahad et al., "Face recognition-based real-time system for surveillance," *Intelligent Decision Technologies*, vol. 11, no. 1, pp. 79–92, 2017.
- [3] K. Phasinam, T. Kassanuk, P. P. Shinde et al., "Application of IoT and cloud computing in automation of agriculture irrigation," *Journal of Food Quality*, vol. 2022, Article ID 8285969, 8 pages, 2022.
- [4] M. K. Mohiddin and V. B. S. S. Indira Dutt, "An optimum energy consumption hybrid algorithm for XLN strategic design in WSN'S," *International Journal of Computer Networks and Communications (IJCNC)*, vol. 11, no. 4, pp. 61–80, 2019.
- [5] R. Pooshkar, R. Raj, and M. Chandra, *Email based remote access and surveillance system for smart home infrastructure*, Elsevier, 2016.
- [6] P. Agarwal, D. K. Sharma, V. L. Varun et al., "A survey on the scope of cloud computing," *Materials Today: Proceedings*, vol. 51, pp. 1–4, 2021.
- [7] M. Mohiddin and V. B. S. Dutt, "Minimization of energy consumption using X-layer network transformation model for IEEE 802.15.4-based MWSNs," in *Proceedings of the 5th International Conference on Frontiers in Intelligent Computing: Theory and Applications*, S. Satapathy, V. Bhateja, S. Udgata, and P. Pattnaik, Eds., vol. 515 of *Advances in Intelligent Systems and Computing*, pp. 741–751, Springer, Singapore, 2017.
- [8] V. Jain, A. Al Ayub Ahmed, V. Chaudhary, D. Saxena, M. Subramanian, and M. Mohiddin, "Role of data mining in detecting theft and making effective impact on performance management," in *Proceedings of Second International Conference in Mechanical and Energy Technology*, S. Yadav, A. Haleem, P. K. Arora, and H. Kumar, Eds., vol. 290 of *Smart Innovation, Systems and Technologies*, pp. 425–433, Springer, Singapore, 2023.
- [9] M. Mohiddin, R. Kohli, V. B. S. Dutt, P. Dixit, and G. Michal, "Energy-efficient enhancement for the prediction-based scheduling algorithm for the improvement of network lifetime in WSNs," *Wireless Communications and Mobile Computing*, vol. 2021, Article ID 9601078, 12 pages, 2021.
- [10] P. K. R. Maddikunta, Q.-V. Pham, D. C. Nguyen et al., "Incentive techniques for the internet of things: a survey," *Journal of*

Research Article

An Efficient Multilevel Thresholding Scheme for Heart Image Segmentation Using a Hybrid Generalized Adversarial Network

A. Mallikarjuna Reddy ¹, K. S. Reddy ², M. Jayaram ³, N. Venkata Maha Lakshmi ⁴,
Rajanikanth Aluvalu ⁵, T. R. Mahesh ⁶, V. Vinoth Kumar ⁶ and D. Stalin Alex ⁷

¹Department of Computer Science & Engineering, Anurag University, Hyderabad, India

²Department of Information Technology, Anurag University, Hyderabad, India

³Department of CSE (Data Science), Sreyas Institute of Engineering & Technology, Hyderabad, India

⁴Department of CSE, PSCMR College of Engineering & Technology, Vijayawada, India

⁵Department of Information Technology, Chaitanya Bharathi Institute of Technology, Hyderabad, India

⁶Department of Computer Science and Engineering, Jain (Deemed-to-be University), Bengaluru, India

⁷Department of Computer Science and Engineering (Data Science), State University of Bangladesh, Dhaka, Bangladesh

Correspondence should be addressed to D. Stalin Alex; drstalinalex.cse@sub.edu.bd

Received 24 August 2022; Revised 21 September 2022; Accepted 30 September 2022; Published 8 November 2022

Academic Editor: Sweta Bhattacharya

Copyright © 2022 A. Mallikarjuna Reddy et al. This is an open access article distributed under the Creative Commons Attribution License, which permits unrestricted use, distribution, and reproduction in any medium, provided the original work is properly cited.

Most people worldwide, irrespective of their age, are suffering from massive cardiac arrest. To detect heart attacks early, many researchers worked on the clinical datasets collected from different open-source datasets like PubMed and UCI repository. However, most of these datasets have collected nearly 13 to 147 raw attributes in textual format and implemented traditional data mining approaches. Traditional machine learning approaches just analyze the data extracted from the images, but the extraction mechanism is inefficient and it requires more number of resources. The authors of this research article proposed a system that is aimed at predicting heart attacks by integrating the techniques of computer vision and deep learning approaches on the heart images collected from the clinical labs, which are publicly available in the KAGGLE repository. The authors collected live images of the heart by scanning the images through IoT sensors. The primary focus is to enhance the quality and quantity of the heart images by passing through two popular components of GAN. GAN introduces noise in the images and tries to replicate the real-time scenarios. Subsequently, the available and newly created images are segmented by applying a multilevel threshold operation to find the region of interest. This step helps the system to predict the accurate attack rate by considering various factors. Earlier researchers have obtained sound accuracy by generating similar heart images and found the ROI parts of the 2D echo images. The proposed methodology has achieved an accuracy of 97.33% and a 90.97% true-positive rate. The reason for selecting the computed tomography (CT-SCAN) images is due to the gray scale images giving more reliable information at a low computational cost.

1. Introduction

Using the CNN, the entire image is processed which requires lot of resources and needs high-end GPU which makes the deployment of the model expensive. Image segmentation

can find the region of interest by clustering the pixels with homogenous labels. Since working with only fewer parts of the images reduces the resources, it is more efficient than the CNN. This process also enhances the granularity of the images by focusing only on the characteristics that are

associated with the boundaries of the images. The recognition of different class labels in the MRI or CT scan images is known as “image stratification.”

Image stratification is a basic method of picture interpretation that allows the utilization of satellite pictures as a geographical frame of reference is image stratification. To regionalize the patterns of emergence associated with particular human activities, to focus subsequent efforts on qualitative evaluation and the collection of field or airborne data, and to reduce the differences with quantitative estimates of particular landscape parameters associated with human activities, stratification is used in human dimension studies. With this technique, a detailed image can be divided into a number of straightforward spatial structure scenes.

Each image pixel is associated with a class description, such as a human, a flora, or an automobile. The system did follow by semantic fragmentation that deals with many items of the same category. On the contrary, instances of the same class have been treated as different isolated examples in instance segmentation [1]. The most widely used techniques for image fragmentation include the thresholding approach, methods used for border identification, regional methodologies, strategies used for categorization, methods dependent on the shade, tactics depending on the selective differential approximation, and processes relying on the ANN. In general, threshold segmentation is done based on a single value throughout the image where the resultant contains binary classification, i.e., whose values are greater than the threshold and are considered as objects and values less than the threshold are considered as the background. This approach is not appropriate for the CT scans, so the proposed model has implemented a multithreshold concept which categorizes the regions into complex objects, simple backgrounds, complex backgrounds, and others. Multitiered thresholding is a technique that divides a grey image into numerous areas. For the image and the fragments of the image in specified areas, which correlate to one background and additional subjects, this approach calculates more than one boundary.

One of the notorious innovative approaches used in the image stratification process is GAN. GANs are employed in reinforcement learning, fully supervised learning, and semisupervised learning. With practice, this method can create new data with the same metrics as the training dataset. GANs are typically measured using the inception score, which assesses how varied the generator’s results are (as determined by an image classification, often Inception-v3) or Frechet inception distance (FID). GANs have been suggested as a fast and precise way to predict the generation of high-energy jets [2]. A generator and a discriminator are present in GANs. The generator attempts to trick the discriminator by creating fraudulent samples of data (such as an image and audio) whereas the discriminator attempts to differentiate between genuine and bogus samples. Both the generator and the discriminator are neural networks, and throughout the training phase, they compete with one another. The procedures are repeated multiple times, and each time, the generator and discriminator become better at what they are doing. Mainly, GANs are classified into 5

types. They are Vanilla GAN, LAPGAN, CGAN, SRGAN, and DCGAN.

GANs are the algorithms that use two neural models that play against each other (the “adversarial”) to create new synthesis situations for transmitting actual statistics. These were frequently utilized in the production of images, videos, and speech. In a couple of years, there has been a stunning progress in using the GANs. The elevated realistic photo generation has significantly increased image preservation. Not every GAN produces images. For example, GANs were also employed by researchers to create synthetic text input voice. For illustration, GAN may be used for comics and cartoons to generate facial representation automatically. A specific data collection, such as anime character models, trains the generative networks. By evaluating the dataset of supplied photos, the GAN produces new actors.

2. Literature Survey

According to Dorgham et al. [3], the advancements in image segmentation in medicine have shown tremendous results. The need to attain the effectiveness of this segmentation was crucial. A multi-iterative approach is needed to explore the search space to solve any medical-related image segmentation issues. For this, the developers here have introduced an MBO framework that computes based on several threshold points. This method was developed as a comparative study with the previously known brute-force methodology and two other multiple iterative frameworks, namely, DPSO and fractional-related DPSO. A similarity index grid and higher disturbance-to-signal rates were utilized to calculate the effectiveness of the fragmented derived images. The authors claim that their developed framework has increased the efficiency in segmenting the images with incredible speed

Abualigah et al. [4] explain the importance of multilevel thresholding and its drawbacks of difficulty in computation as the number of threshold values increases. This paper proposes a development-based DAOA algorithm that uses the standard differential mathematical operations to solve the problem to solve these issues. In the context of a multilevel threshold challenge, the described approach is used to assess Kapur across class deviation measures. Leveraging eight reference photos from two separate groups, environmental and CT COVID-19 images, the proposed DAOA will be employed for evaluation. The standard assessment measures used to verify the exactness of divided images are PSNR and SSIM. In comparison with various thresholding approaches, the suggested technique performance is assessed. There are a variety of different threshold levels of 2–6 shown in the results. The recommended strategy is superior and provides better alternatives than other comparison approaches, as per experimental data

Sun et al. [5] explain the importance of early-stage predictions in diagnosing brain tumors that could lead to cancer using a more profound understanding of medical image analysis. According to the authors, MRI imaging has shown advanced trends in identifying any injury in the brain and could easily explain its anatomy. This study extensively discusses the different modern approaches to brain tumor

fragmentation [6–8]. The statistical research and the effectiveness evaluation of current methods are carried out. The article showed that several image segmentation algorithms are extensively addressed. One of the best optimal fragmentation approaches of the brain MRI tumor may be used to deliver practical responsiveness findings, accuracy, and DICE. This survey report gives complete knowledge about the different categorization strategies, including their advantages and disqualifications. Quality criteria indicate the performance of the approaches

From the authors' point of view in [9], diverse image diagnostics have various problems, such as inhomogeneity of intensity, distortion, small comparison, and undefined borders. The developers proposed a novel, utterly mechanized technique for categorizing clinical images that uses the benefits of thresholds and a dynamic contour concept to address these problems. In the present work, the optimizer of Harris Hawks is utilized to determine the best target value for the first classification contour [10–12]. A substantially different Gaussian filter is used to improve the acquired shape of the dynamic contour prototype additionally. This framework is said to experiment over the two datasets. One contains many attributes that define several challenging aspects, and the other has a collection of many ranges of normal hearts, diseases, and issues. The evaluation was carried out with a DICE score which showed better differentiation in the skin with 0.90 and cardiac with a 0.93 DICE scores.

Because of several reasons [13], particularly air contamination, there are a significant growth in the number of chest-related illnesses and an alarming increase in the number of such victims. The developers here have used a machine training technique in this investigation to identify several chest-related disorders with the CNN on the chest X-ray collection. The method is oriented towards standard image differentiation algorithms, incorporating cutoff, k -mean grouping, and boundary identification. The CNN cannot detect and interpret the overall piece simultaneously, repetitively examining the tiny pixel areas until the complete image is captured. Spatial adjustment levels and VGG19 have been utilized to retrieve functions, and ReLU stimulation was implemented as an accelerator because of its underlying minimal complexity and great computational speed [14–16]. The significant contribution of the current technique is that the image's fundamental, predictive characteristics remain, coupled with a substantial drop in dimensions.

Ramos-Soto et al. [17] automated fragmentation of retinal blood vessels is an alarming issue, and the drawbacks of meeting the problems in fragmentation with the standard measures are explained in detail. This paper is aimed at overcoming those by experimenting with two datasets. The approach presented has three parts, pretreatment, primary treatment, and posttreatment. The initial phase is applying image softening techniques [18–20]. The preliminary handling phase will be separated into two combinations: the new optimized top hat, homomorphic screening, and medium screen, the first to split the dense vessels. Then, the intermediate configuration is utilized to separate narrow

vessels using the MCET-HHO multilayer method, which is optimized using a high-hat system, homomorphic processing, paired and segmented. In the later stage, morphological image modifications are also performed. The efficiencies achieved from the first dataset are 0.98, 0.75, and 0.96. The values from the second dataset are 0.98, 0.74, and 0.95 for the second dataset

According to the investigators of [21], one of several primary factors of mortality is cardiovascular disease. Immediate treatment increases the quality of therapy and decreases the fatality rate. Investigators have been drawn to create a certified insightful wellness decision assistance platform by using ECG signals for wellness diagnosis. In this investigation, the ECG data for sufferers with AI methods are analyzed to provide a sophisticated, early intervention system for three prevalent cardiac illnesses, apnea, AF, and HF. This system is used to develop three distinct approaches to AI-ANN, SVM, and KNN. ECG impulses from PhysioNet are examined, information from the researchers is gathered, and four characteristics are retrieved and utilized as a categorization system source. The conclusions demonstrate that the recommended AI approaches have significant advantages, which can save lives of cardiomyopathies [22, 23]. The recognition rate with KNN is 92.4%, with $k = 1$. The ANN delivers 95.7% efficiency at 33 stages, whereas the most excellent reliability in categorization is achieved with a cluster efficiency of SVM of 97.8%.

The authors [24] present an algorithm for two phases in this work. The primary step involves ECG separation relying on NN with the conservative principle of the convoluted BSTM. The further action is based on the CNN applied to ECG beats collected across multiple periods from the preceding phase. ECG pulses are converted into 2D images through limited-time Fourier transform to authenticate normal ECGs and forecast premature cardiac demise from heart damage, such as arrhythmias or severe cardiac inability. The exactness of various timeframes was examined [1, 25–27]. With 4 min ECG, we have diagnosed heart failure spontaneously at 100 percent, arrhythmia at 97.9 percent, and abrupt cardiac arrest at 100 percent [28–31].

Table 1 represents the merits and demerits that occurred during the segmentation of heart images performed by different researchers. Further research can focus on the significant limitations identified in this article.

3. Proposed System

In the proposed system, first, the model tries to preprocess the CT images collected from the Kaggle repository [32]. The sample images of the dataset are shown in Figure 1.

3.1. Multilevel Threshold Segmentation. Multilevel thresholding parts a grayscale into several distinct zones. This segmentation method chooses multiple thresholds and splits the target picture into several brightness zones, with each zone representing a different background and various items. In accordance with the image pixel distribution around the mean, the peak pixel values are coarser in a wider interval.

TABLE 1: Comparative study on the heart image segmentation process.

S. no.	Authors	Algorithms used	Merits	Demerits/future work
(1)	Dorgham et al.	MBO	The framework is more reliable and effective, applying multistage threshold values for image fragmentation	An effective balance for searching at local and global points needs to be addressed
(2)	Abualigah et al.	DATA	Improved local search among the tested standard methodologies	In the future, this methodology can be applied to many industrial and text processing techniques
(3)	Sun et al.	DeepMedic+CRF, Ensemble+CRF	Provided a complete study about the previously used algorithms and did a contrast survey that could guide beginners to research this topic	In the future, an efficient hybrid method could be used for optimal differentiation
(4)	Tamoor et al.	Gaussian-based spatially varied contour	A broad penalty term and distance validation terms were incorporated for smooth evolution	It could be experimented with in applying to other types of issues as well
(5)	Sapna Juneja	CNN, ReLU	Least dimensionality issue	DL techniques could apply by choosing more data attributes and computing a whole lot of information
(6)	Ramos-Soto et al.	MCET-HHO multilayer method	The developed framework is claimed to outperform the standard procedure and shows an incredible analysis of visuals in detail	In the future, reinforcement algorithms could be applied
(7)	Bataineh et al.	KNN, ANN, and SVM	Increased accuracy	The ANN approach might have been driven under overriding. In the future, the developers plan to extend the research by intaking more features and working on larger-scale data
(8)	Haleem et al.	Bi-LSTM	The states that the developed method reduced work for domain experts with calculating necessary data with a simultaneous approach	100% accuracy may show a machine overriding issue and ignorance in dimensionality

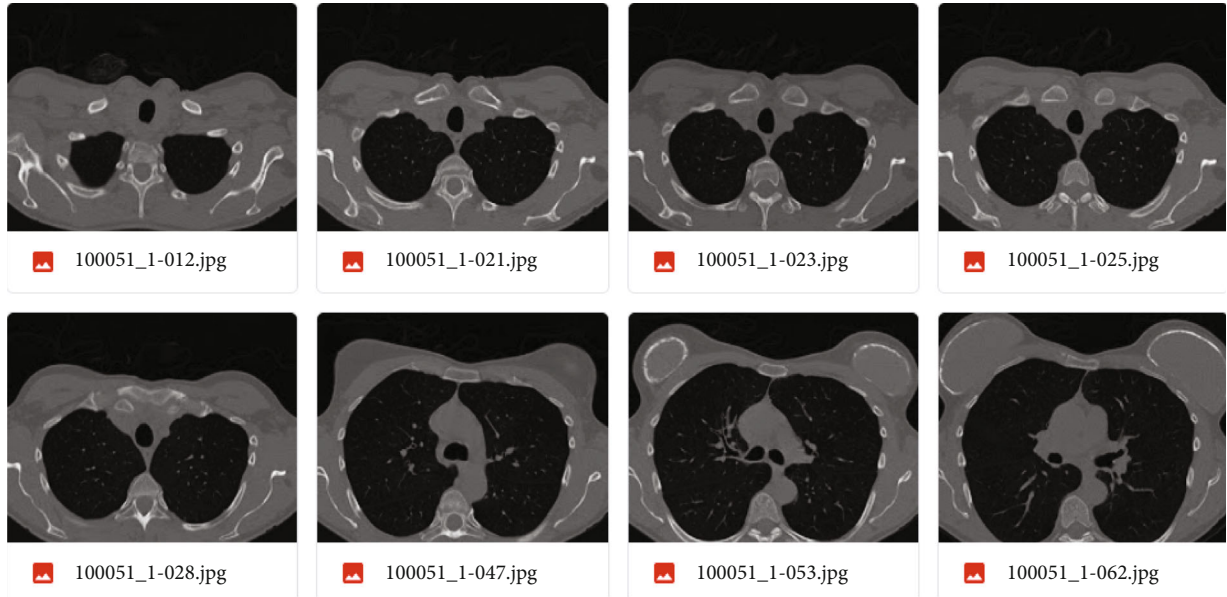


FIGURE 1: Sample CT images of the heart collected from clinical dataset.

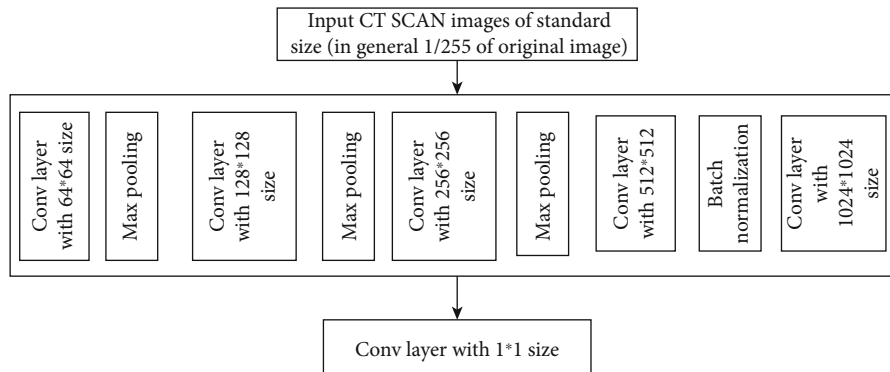


FIGURE 2: Neural network architecture of the encoder component in U-Net.

When used on objects with colorful or intricate backgrounds, the method works far better than bilevel thresholding. Pixels above and below the threshold are categorized as belonging to the white and black classes, respectively, based on an initial estimate of the threshold (for example, mean picture intensity). Effective segmentation of the entire image is performed using several thresholds discovered at each stage utilizing metrics like mean and standard deviation.

3.2. U-NET Integration. In this model, the images are pre-processed using a widespread neural network known as “U-Net,” which consists of encoding and decoding parts. This model prioritizes the class labels assigned to each pixel based on the localization parameters, which play their role in the segmentation of the images. U-Net is integrated with GANs to color the infected parts in the images because with the black and white images, it is difficult to recognize the level of infection. The infected parts of the image are passed as the input to the “autoencoder” for extracting the high-level details from the infection.

3.3. Encoding Mechanism. With the failure of common compression techniques like JPEG, the encoder portion of the network is utilized for encoding and occasionally even for compression algorithm purposes. The network’s encoder component, which has a smaller number of concealed units in each layer, performs the encoding. The decoder, which predicts the presence of class labels through queries, allows for better use of spatial data than global average pooling. The ML-Decoder is extremely effective and scales well to hundreds of classes thanks to a redesign of the decoder architecture and the use of a novel group-decoding approach. ML-Decoder consistently offers a superior speed-accuracy tradeoff than employing a larger backbone.

The encoder part consists of 4 downsampling layers from size 64×64 to 1024×1024 , which are associated with the ReLU activation function, which is defined as shown as follows:

$$\text{ReLU}(x) = \text{maximum}(0, \text{input_pixel}), \quad (1)$$

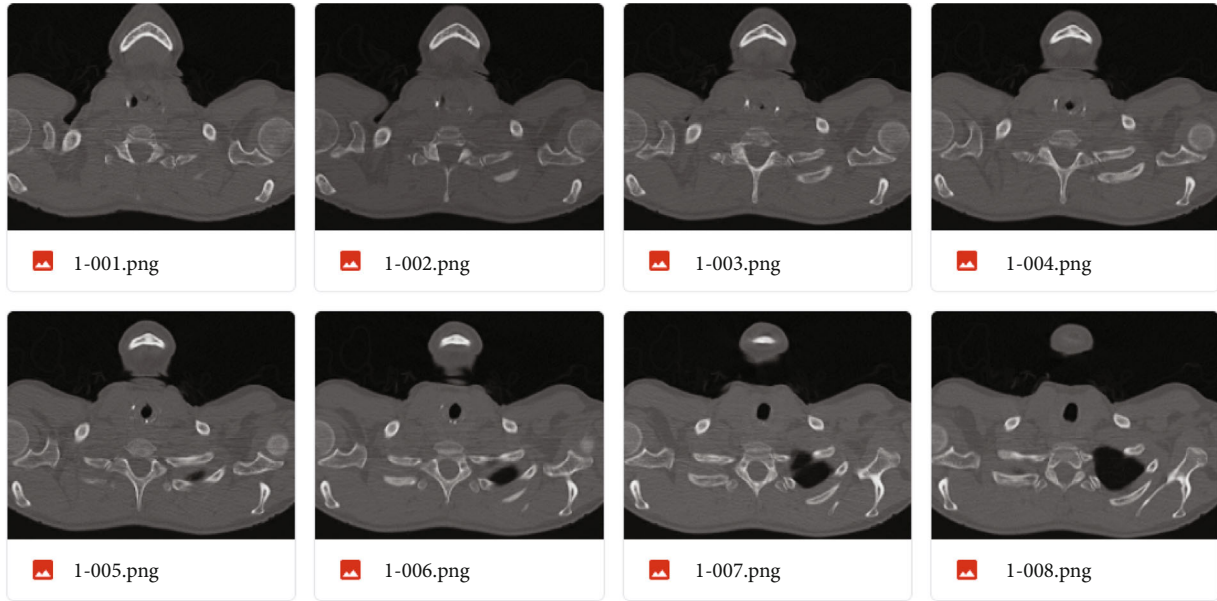


FIGURE 3: Preprocessed CT scan heart images.

```

Input: Load the Heart CT_Scan Images, HCTSCAN
Output: Segmentation of the images based on the threshold values
Begin:
1. Define the hyper parameters like learning rate, batch size, and number of epochs
2. Define callbacks with the following estimators
i. model checkpoint to store the best model after compilation
  ii. set the CSV logger to save the best scores acquired by the model
  iii. define the Tensor Flow board with an early stopping mechanism to reduce the validation loss
3. Fit and compile the training dataset by shuffling the records
4. i. if threshold value<= length(masked_image) then
   Create a predicted mask to have a segmented image
  ii. else expand the image to concatenate with previous ROI bounds
5. store the images in the necessary directory
End

```

PSEUDOCODE 1: Pseudocode for segmentation.

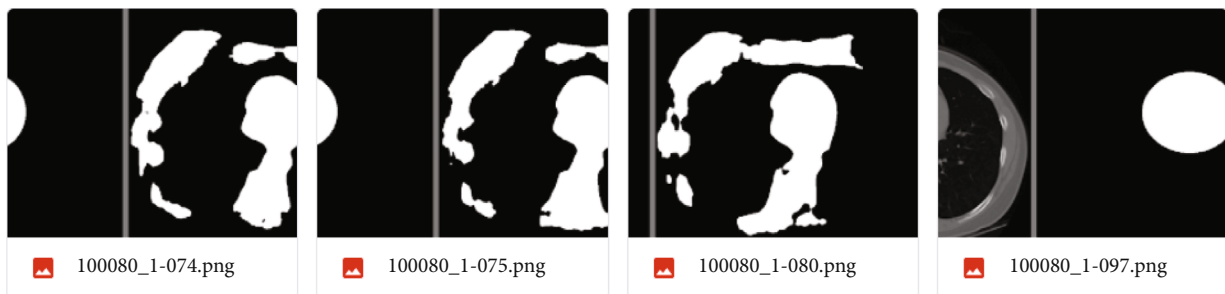


FIGURE 4: Segmentation output of CT scan heart images.

where `input_pixel` denotes the vector representation of the features in terms of pixels.

The architecture of the encoder neural network is shown in Figure 2. The encoder with four layers also contains three max-pooling layers to extract low- and high-level features from the images.

The decoder part of the U-Net works precisely opposite to the encoder, with four upsampling layers and three max-pooling layers. The output of the preprocessed images is shown in Figure 3.

To create annotated images, the model takes the help of GAN architecture and creates a segmented image, as represented as follows.

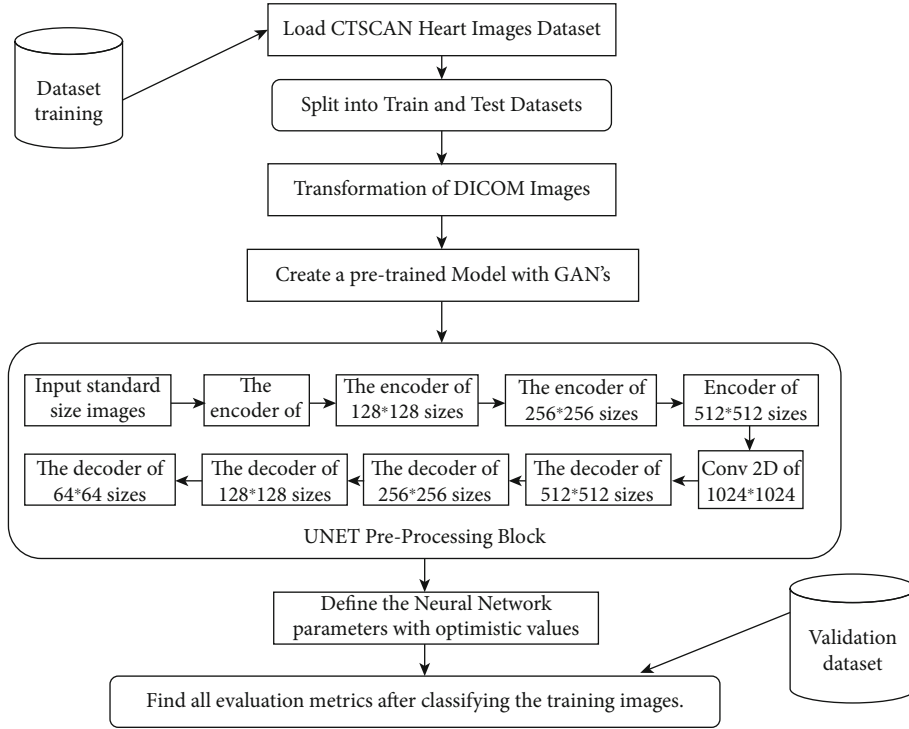


FIGURE 5: Architecture of the classification process of heart CT scan images.

Applying the Pseudocode 1 creates segmented images, as shown in Figure 4.

Figure 5 represents the overall architecture of the proposed model. In this architecture, the first principal component is splitting the dataset and creating a validation dataset to evaluate the model's performance. The second component is enhanced by creating new images using data augmentation and GANs. The novelty of this research is the creation of new images based on the augmented operation. The augmentation process involves the following steps:

- (1) Perform horizontal and vertical flips with a scale value of 1
- (2) Rotate images at 45 degrees with actual data on the x -axis and with masked data on the y -axis
- (3) Apply a color transformation on the DICOM images to transform them into RGB images to create .jpg images

The third component of the model is cleaning the images by applying the U-Net operation as a preprocessing step. The fourth component is to segment the cleaned noisy images based on the threshold images. This decision-making step either creates masked images that are ready for prediction or creates concatenated images for further operations. Finally, the images are evaluated based on two types of metrics. One involves machine learning metrics like accuracy and others. The second one requires image processing metrics based on epochs like DICE coefficient and others.

TABLE 2: All metric values for each epoch.

Epoch	DICE_COEF	IOU	Loss	Precision	Recall
0	0.26	0.18	0.73	0.22	0.81
1	0.38	0.30	0.61	0.42	0.84
2	0.44	0.37	0.55	0.49	0.85
3	0.46	0.40	0.53	0.52	0.85
4	0.48	0.43	0.51	0.56	0.87

4. Results and Discussion

The convolution neural network is defined for five epochs, and all the results for each epoch are tabulated in Table 2.

In Figures 6(a) and 6(b), the x -axis represents the epoch number and the y -axis represents the percentage values of all the possible metrics. Figure 6(a) shows that all-important metrics have increased gradually and reached optimistic values. Figure 6(b) shows that the loss evaluation has progressively decreased, which is the essential characteristic of any accurate model.

The DICE coefficient is the ratio of the overlapped area multiplied by two intersections and the total area covered by the images. The result does illustrate as shown in equation (2), and it is also known as the "F1-score."

$$\text{DICE coefficient } (I_1, I_2) = \frac{2 * \text{overlapped area}}{\text{combined image area}}, \quad (2)$$

where the overlapped area presents the number of pixels which belongs to more than one cluster. Combined image

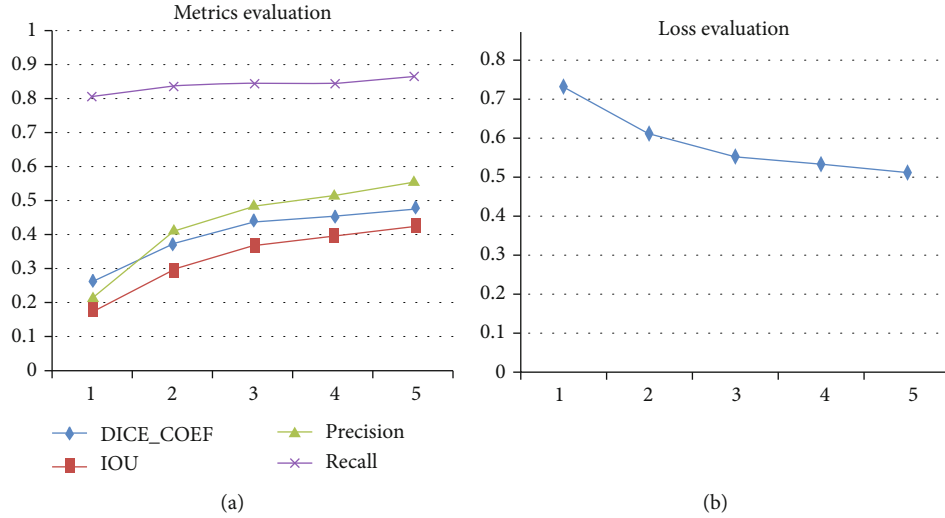


FIGURE 6: (a, b) Evaluation metrics for different epochs during the training phase.

TABLE 3: Evaluation metrics of different images available in the dataset.

S. no.	Image	Accuracy	F1	Recall	Precision
0	100051_1-026	0.99	0	1	0
1	100051_1-030	0.99	0	1	0
2	100051_1-044	0.92	0	1	0
3	100051_1-045	0.93	0	1	0
4	100051_1-049	0.93	0	1	0
5	100051_1-050	0.94	0	1	0
6	100051_1-052	0.95	0	1	0
7	100051_1-057	0.96	0.73	0.85	0.64
8	100051_1-068	0.99	0.93	0.95	0.90
9	100051_1-070	0.99	0.92	0.94	0.90
10	100051_1-071	0.99	0.93	0.95	0.91
11	100051_1-074	0.98	0.88	0.95	0.81
12	100051_1-077	0.97	0.85	0.98	0.75
13	100051_1-094	0.98	0.92	0.87	0.97
14	100051_1-097	0.95	0.82	0.89	0.76
15	100051_1-101	0.96	0.81	0.87	0.76

areas represent the intersection of the region of different images, whose boundaries are shared.

The intersection over the union, otherwise known to be the Jaccard index for binary classification, is computed as the ratio of the intersection area and union area and is shown as follows:

$$\text{IOU}(I_1, I_2) = \frac{\text{area of intersection}}{\text{area of the union}}. \quad (3)$$

Recall and precision are generally similar in definitions but not so. The memory is the retrieval ratio and relevant values among all the retrieved values.

Precision is the ratio of retrieval and relevant values among all appropriate values. These are illustrated in equations (4) and based on the components of the confusion matrix.

$$\begin{aligned} \text{Recall}_{\text{Classification}} &= \frac{\text{correctly classified images}}{\text{correctly classified images} + \text{incorrectly classified images by model}}, \\ \text{Precision}_{\text{Classification}} &= \frac{\text{correctly classified images}}{\text{correctly classified images} + \text{incorrectly classified images by dataset}}. \end{aligned} \quad (4)$$

In Table 3, this research article has published a few critical image metrics like accuracy, recall, precision, and F1-score, to portray the quality of the images during the training phase.

The proposed model has considered the test dataset with a 20% validation rate, and in Table 3 as a sample, it has exhibited the metrics related to learning algorithms. The table represents that the recall value for most of the images is 1, which means that the misclassification rate is 0. It also shows cases that the accuracy of all the images are above 93%; this proves that the system can easily pass the deployment test and predicts the test images passed by the user during the real-time scenario with an average of 95%. Initially, the model has suffered with 0% precision but it gradually recovered with the increase of epochs and randomly selecting the images. Since the F1-score is the weighted average of recall and precision, its performance also gradually increased in proportion to the precision. The overall accuracy, precision, and recall of the proposed system are shown in Figure 7.

Table 4 compares the proposed algorithm and previous researchers' work. It is proven that the proposed model has the highest accuracy and improved by +0.6% than Bi-LSTM.

Figure 8 has proved that the accuracy has gradually increased and the proposed system has reached the highest accuracy than model "BiLSTM." Most of the deep learning

```

recall_value = recall_score(y, y_pred, labels=[0, 1], average="binary", zero_division=1)
precision_value = precision_score(y, y_pred, labels=[0, 1], average="binary", zero_division=1)
SCORE.append([name, acc_value, f1_value, recall_value, precision_value])

""" Metrics values """
score = [s[1:] for s in SCORE]
score = np.mean(score, axis=0)
print(f"Accuracy: {score[0]:0.5f}")
print(f"F1: {score[1]:0.5f}")
print(f"Recall: {score[2]:0.5f}")
print(f"Precision: {score[3]:0.5f}")

df = pd.DataFrame(SCORE, columns=["Image", "Accuracy", "F1", "Recall", "Precision"])
df.to_csv("/content/drive/MyDrive/CT_HEART_DATASET/files/score.csv")

Test: 334 / 334
100% ██████████ 334/334 [07:32<00:00, 1.36s/it] Accuracy: 0.97336
F1: 0.48986
Recall: 0.90972
Precision: 0.51285
    
```

FIGURE 7: Evaluation metrics of the proposed model after all epochs of training and validation.

TABLE 4: Analysis of previous works and the proposed work.

S. no.	Author	Algorithms used	Accuracy
(1)	Dorgham	MBO	75
(2)	Abualigah	DATA	82.39
(3)	Sun	DeepMedic+CRF, Ensemble+CRF	89.5
(4)	Tamoor	Gaussian-based spatially varied contour	93
(5)	SapnaJuneja	CNN, ReLU	93.7
(6)	Ramos-Soto	MCET-HHO multilayer method	95
(7)	Bataineh	KNN, ANN, and SVM	96.8
(8)	Haleem	Bi-LSTM	96.9
(9)	Proposed	MLTH-GAN	97.3

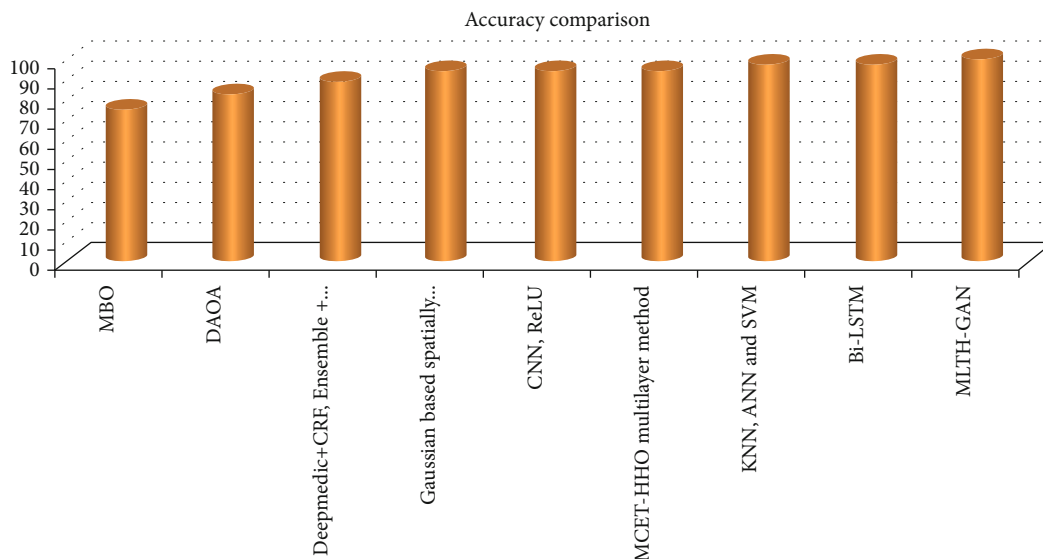


FIGURE 8: Efficiency of the proposed system.

models have above 93%, but in the traditional approaches, it is just in the range of 75% to 80%.

5. Conclusion

From the results and discussion, it is observed that the proposed model has obtained more efficient accuracy than the previous researchers' work. It is also observed that rather than working on textual parameters or inputs taken from the patients by querying their depression levels, it is better to work on 2D-echo to better predict the heart attack levels. Most researchers think that working with GANs will increase the complexity of the model. However, these proposed systems can prove that GANs, even though they increase the complexity, provide more qualitative data, which helps not improve the accuracy, recall, and precision. This system also helps in reducing the loss of the model during the validation phase. In a future work, the researchers can work on transfer learning to pretrain the models. It is also essential to modify the fully connected layers as per the requirement of the applications. The proposed research has shown an improvement of nearly +0.6% when compared to the base model, which is considered as "Bi-LSTM." In the future work, the model can retrain the weights by using latest network models of transfer learning with the help of the swarm intelligence algorithm.

Data Availability

The dataset will be shared by the corresponding author upon reasonable request.

Conflicts of Interest

The authors declare that there is no conflict of interest regarding the publication of this paper.

References

- [1] P. Grandhe, "A novel method for content based 3D medical image retrieval system using dual tree M-band wavelets transform and multiclass support vector machine," *Journal of Advanced Research in Dynamical and Control Systems*, vol. 12, no. 3, pp. 279–286, 2020.
- [2] S. SilpaPadmanabhuni and P. Gera, "Synthetic data augmentation of tomato plant leaf using meta intelligent generative adversarial network: milgan," *International Journal of Advanced Computer Science and Applications (IJACSA)*, vol. 13, no. 6, 2022.
- [3] O. M. Dorgham, M. Alweshah, M. H. Ryalat, J. Alshaer, M. Khader, and S. Alkhalaleh, "Monarch butterfly optimization algorithm for computed tomography image segmentation," *Multimedia Tools and Applications*, vol. 80, no. 20, pp. 30057–30090, 2021.
- [4] L. Abualigah, A. Diabat, P. Sumari, and A. H. Gandomi, "A novel evolutionary arithmetic optimization algorithm for multilevel thresholding segmentation of COVID-19 CT images," *PRO*, vol. 9, no. 7, p. 1155, 2021.
- [5] L. Sun, R. K. Gupta, and A. Sharma, "Review and potential for artificial intelligence in healthcare," *International Journal of System Assurance Engineering and Management*, vol. 13, no. S1, pp. 54–62, 2022.
- [6] P. Chaitanya Reddy, R. M. S. Chandra, P. Vadiraj, M. Ayyappa Reddy, T. R. Mahesh, and G. Sindhu Madhuri, "Detection of plant leaf-based diseases using machine learning approach," *2021 IEEE International Conference on Computation System and Information Technology for Sustainable Solutions (CSITSS)*, pp. 1–4, 2021.
- [7] N. A. Siddique, S. Paheding, C. P. Elkin, and V. K. Devabhaktuni, "U-Net and its variants for medical image segmentation: a review of theory and applications," *IEEE Access*, vol. 9, pp. 82031–82057, 2021.
- [8] S. Niyas, S. Pawan, M. A. Kumar, and J. Rajan, "Medical image segmentation using 3D convolutional neural networks: a," 2021, <https://arxiv.org/abs/2108.08467>.
- [9] M. Tamoor and I. Younas, "Automatic segmentation of medical images using a novel Harris Hawk optimization method and an active contour model," *Journal of X-Ray Science and Technology*, vol. 29, no. 4, pp. 721–739, 2021.
- [10] J. Ma, H. Xu, J. Jiang, X. Mei, and X.-P. Zhang, "DDcGAN: a dual-discriminator conditional generative adversarial network for multi-resolution image fusion," *IEEE Transactions on Image Processing*, vol. 29, pp. 4980–4995, 2020.
- [11] Z. Wang, Y. Zou, and P. X. Liu, "Hybrid dilation and attention residual U-Net for medical image segmentation," *Computers in Biology and Medicine*, vol. 134, article 104449, 2021.
- [12] D. Yang, T. Xiong, D. Xu, and S. K. Zhou, "Segmentation using adversarial image-to-image networks," in *Handbook of Medical Image Computing and Computer Assisted Intervention*, pp. 165–182, Elsevier, 2020.
- [13] S. Juneja, A. Juneja, G. Dhiman, S. Behl, and S. Kautish, "An approach for thoracic syndrome classification with convolutional neural networks," *Computational and Mathematical Methods in Medicine*, vol. 2021, Article ID 3900254, 10 pages, 2021.
- [14] T. Tuncer, S. Dogan, and A. Subasi, "EEG-based driving fatigue detection using multilevel feature extraction and iterative hybrid feature selection," *Biomedical Signal Processing and Control*, vol. 68, article 102591, 2021.
- [15] S. P. Singh, L. Wang, S. Gupta, H. Goli, P. Padmanabhan, and B. Gulyás, "3D deep learning on medical images: a review," *Sensors*, vol. 20, no. 18, p. 5097, 2020.
- [16] S. Shojaedini, M. Zarvani, S. Saberi, and R. Azmi, "Residual learning: a new paradigm to improve deep learning-based segmentation of the left ventricle in magnetic resonance imaging cardiac images," *Journal of Medical Signals & Sensors*, vol. 11, no. 3, pp. 159–168, 2021.
- [17] O. Ramos-Soto, E. Rodríguez-Esparza, S. E. Balderas-Mata et al., "An efficient retinal blood vessel segmentation in eye fundus images by using optimized top-hat and homomorphic filtering," *Computer Methods and Programs in Biomedicine*, vol. 201, article 105949, 2021.
- [18] A. Mallikarjuna Reddy, G. RupaKinnera, T. Chandrasekhara Reddy, and G. Vishnu Murthy, "Generating cancelable fingerprint template using triangular structures," *Journal of Computational and Theoretical Nanoscience*, vol. 16, no. 5, pp. 1951–1955, 2019.
- [19] G. Sirisha and A. M. Reddy, "Smart healthcare analysis and therapy for voice disorder using cloud and edge computing," in *2018 4th international conference on applied and theoretical computing and communication technology (iCATcct)*, pp. 103–106, Mangalore, India, 2018.

- [20] A. M. Reddy, S. Yarlagadda, and H. Akkinen, "An extensive analytical approach on human resources using random forest algorithm," *International Journal of Engineering Trends and Technology*, vol. 69, no. 5, pp. 119–127, 2021.
- [21] A. Bataineh, W. Batayneh, T. Harahsheh et al., "Early detection of cardiac diseases from electrocardiogram using artificial intelligence techniques," *International Review on Modelling and Simulations (IREMOS)*, vol. 14, no. 2, p. 128, 2021.
- [22] G. S. Gowramma, T. R. Mahesh, and G. Gowda, "An automatic system for IVF data classification by utilizing multilayer perceptron algorithm," *ICCTEST-2017*, vol. 2, pp. 667–672, 2017.
- [23] I. Kavati, A. M. Reddy, E. S. Babu, K. S. Reddy, and R. S. Cheruku, "Design of a fingerprint template protection scheme using elliptical structures," *ICT Express*, vol. 7, no. 4, pp. 497–500, 2021.
- [24] M. S. Haleem, R. Castaldo, S. M. Pagliara et al., "Time adaptive ECG driven cardiovascular disease detector," *Biomedical Signal Processing and Control*, vol. 70, article 102968, 2021.
- [25] T. R. Gadekallu, D. S. Rajput, M. Reddy et al., "A novel PCA-whale optimization-based deep neural network model for classification of tomato plant diseases using GPU," *Journal of Real-Time Image Processing*, vol. 18, no. 4, pp. 1383–1396, 2021.
- [26] T. R. Gadekallu, N. Khare, S. Bhattacharya et al., "Early detection of diabetic retinopathy using PCA-firefly based deep learning model," *Electronics*, vol. 9, no. 2, p. 274, 2020.
- [27] C. Venkatesh, L. Dr Ramana, S. Yamini, E. A. Nasr, A. K. Kamrani, and M. K. Aboudaif, "A neural network and optimization based lung cancer detection system in CT images," *Public Health*, vol. 10, p. 188, 2022.
- [28] K. Ramana, M. R. Kumar, K. Sreenivasulu et al., "Early prediction of lung cancers using deep saliency capsule and pre-trained deep learning frameworks," *Frontiers in Oncology*, vol. 12, 2022.
- [29] K. Ramana, M. R. RajanikanthAluvala, and G. N. Kumar, "Leaf disease classification in smart agriculture using deep neural network architecture and IoT," *Journal of Circuits, Systems and Computers*, vol. 31, no. 15, 2022.
- [30] M. A. Reddy, S. K. Reddy, S. C. N. Kumar, and S. K. Reddy, "Leveraging bio-maximum inverse rank method for iris and palm recognition," *International Journal of Biometrics*, vol. 14, no. 3-4, pp. 421–438, 2022.
- [31] M. R. Sarveshvar, A. Gogoi, A. K. Chaubey, S. Rohit, and T. R. Mahesh, "Performance of different machine learning techniques for the prediction of heart diseases," *2021 International Conference on Forensics, Analytics, Big Data, Security (FABS)*, vol. 1, pp. 1–4, 2021.
- [32] <https://www.kaggle.com/dataset/f41e0bab640002775b00e050b81a1144786324951b0576f5d71fd820d6ef13dc>.

Retraction

Retracted: Preschool Education Based on Computer Information Technology Literacy and Big Data

Journal of Sensors

Received 22 August 2023; Accepted 22 August 2023; Published 23 August 2023

Copyright © 2023 Journal of Sensors. This is an open access article distributed under the Creative Commons Attribution License, which permits unrestricted use, distribution, and reproduction in any medium, provided the original work is properly cited.

This article has been retracted by Hindawi following an investigation undertaken by the publisher [1]. This investigation has uncovered evidence of one or more of the following indicators of systematic manipulation of the publication process:

- (1) Discrepancies in scope
- (2) Discrepancies in the description of the research reported
- (3) Discrepancies between the availability of data and the research described
- (4) Inappropriate citations
- (5) Incoherent, meaningless and/or irrelevant content included in the article
- (6) Peer-review manipulation

The presence of these indicators undermines our confidence in the integrity of the article's content and we cannot, therefore, vouch for its reliability. Please note that this notice is intended solely to alert readers that the content of this article is unreliable. We have not investigated whether authors were aware of or involved in the systematic manipulation of the publication process.

In addition, our investigation has also shown that one or more of the following human-subject reporting requirements has not been met in this article: ethical approval by an Institutional Review Board (IRB) committee or equivalent, patient/participant consent to participate, and/or agreement to publish patient/participant details (where relevant).

Wiley and Hindawi regrets that the usual quality checks did not identify these issues before publication and have since put additional measures in place to safeguard research integrity.

We wish to credit our own Research Integrity and Research Publishing teams and anonymous and named external researchers and research integrity experts for contributing to this investigation.

The corresponding author, as the representative of all authors, has been given the opportunity to register their agreement or disagreement to this retraction. We have kept a record of any response received.

References

- [1] L. Luo, "Preschool Education Based on Computer Information Technology Literacy and Big Data," *Journal of Sensors*, vol. 2022, Article ID 4457811, 10 pages, 2022.

Research Article

Preschool Education Based on Computer Information Technology Literacy and Big Data

Lan Luo 

JiuJiang university, Jiangxi, Jiujiang 332005, China

Correspondence should be addressed to Lan Luo; 1703300074@e.gzhu.edu.cn

Received 5 August 2022; Revised 24 August 2022; Accepted 2 September 2022; Published 12 October 2022

Academic Editor: Sweta Bhattacharya

Copyright © 2022 Lan Luo. This is an open access article distributed under the Creative Commons Attribution License, which permits unrestricted use, distribution, and reproduction in any medium, provided the original work is properly cited.

In this practical framework, the preschool teacher is reinforced to utilize a more significant teaching model, like forming real-time-based contextual issues, to help participants to identify a deep learning-based learning model. Numerous studies have been released as a result of the popularity of the use of CIT in preschool education as a research subject. Due to the fact that it broadens teaching resources, provides learning time flexibility, and strengthens teacher-student relationships, this teaching method has received a lot of attention in academia. Teaching strategies in preschool classrooms combine elements of both direct instruction and free play. Among these, CIT stands out as a powerful tool for boosting students' motivation and engagement in the classroom. Integrate new technology and science into the classroom setting, as well as implement pedagogical changes that make use of IT. Preschool education informatization is now deploying new technology in a variety of preschools, yet there are still flaws. In this paper, a theoretical and problematic-based classifier model, a deep learning-based methodology that was reinforced by utilising a Python-based model to create the comprehensive among preschool students and high-phase semantic parameters, and to enhance computer-based teaching through estimation and text design that can detect high-frequency-based knowledge samples, are used. In this practical model, teachers are insisted to utilize significant frameworks like contextual issues to provide skills to students. The results show that this integrated CIT teaching method is suitable for students and able to raise their aptitude and enthusiasm for studying. By offering new theoretical and practical results about preschool education, the study helps to reform preschool education.

1. Introduction

Internationalization is currently undergoing rapid development for English proficiency [1]. English classes make it difficult to ensure instructional effectiveness. The number of classrooms is rapidly increasing in tandem with the shift in educational paradigms. The teacher must teach numerous students throughout the real teaching process, and it is tough. Researchers discovered that when the static image target detection model is used, the results are unsatisfactory [2]. As a result, researchers integrate the video's temporal and context information to conduct target detection [3]. The detection is first completed by a single frame of photos in the postprocessing stage.

However, because this method is usually multistage, the findings are influenced by the results, and correcting errors in the prior stage might be difficult. There are unresolved

issues in the video caused by object motion [4]. To improve the identification accuracy, recently researchers employed Long Short-Term Memory (LSTM) to combine video time to maximize the features of fuzzy frames [5]. In addition, the feature propagation is achieved via optical flow-related technologies. In video target detection, recurrent neural networks (RNN) are interleaved with feature extractors [6]. There are numerous flaws in the current research's accuracy when compared to prior studies [7]. Its performance will be affected by the detecting target and will have a certain gap. The complex situations and model design are all areas where it could be improved [8]. The SSD base network has been adequately replaced. To improve computational efficiency, the network's characteristics are employed to tune the network parameters. The deep feature map's data is blended upward improving the accuracy of tiny target calibration. Finally, experiments involving student behavior are

examined. It shows that small target recognition accuracy may be enhanced without affecting the computation speed of standard algorithms. These are important for improving the efficiency of English classroom teaching since they assist teachers to understand the student's learning status [9].

Language teaching professionals must adapt concepts and roles, as well as systematize the disorganized techniques of language training [10]. Teachers should be able to formulate the process of learning using network resources and manage every student's capability. Artificial intelligence is used extensively in the development of intelligent computer-assisted education systems [11]. The final goal of the study is to assume relevant educational and teaching tasks, i.e., to equip the computer system for optimal instruction [12]. The significance of current system education broadens the preschool learning. Individuals are acquiring a growing number of network teaching platforms. Due to the network education environment's increasing complexity and temporal and spatial isolation, management and teachers are having difficulty assembling dynamic learning [13]. This leads to a straightforward reproduction and a one-sided pursuit in current teaching [14]. With such a large number of online learners, determining a reliable method for collecting learning status has become crucial [15].

Time is a critical issue that must be addressed immediately with the advancement of multimedia and network technologies [16]. Individuals have been constantly exploring and attempting to apply new technology [17]. Simultaneously, we attempt to teach children according to their aptitudes and to provide individualized education based on pupils' diverse learning foundations, skills, and other characteristics [18]. It is difficult to educate because of a lack of teacher resources and instructional efficiency standards. Modern education eliminates the geographical constraints associated with conventional schooling [19]. It is critical for optimizing the resource benefits of varied existing educational systems while maintaining an acceptable resource allocation. Additionally, it presents a workable solution to the problem [20].

To tackle the issues of the current network system, this study builds and creates a model of a network teaching system. Computer-assisted instruction is progressing toward intelligent instruction. It is a style of instruction that utilizes a computer to simulate the instructional thinking process of professionals, with the students at the center and the computer serving as the channel [21]. Intelligent teaching is founded on contemporary educational theory and utilizes the latest breakthroughs in artificial intelligence to enable students to acquire knowledge in order to accomplish the objective of truly personalized instruction [22]. The majority of the research effort has been directed to ad hoc research institutes, the majority of which are research and demonstration systems, and just a few have been thoroughly explored [23]. It will contribute positively to China's education reform through computer-assisted systems.

In the past, theorists and researchers debated whether or not young children should use computers in school [24]. One viewpoint argues that technology is inappropriate for young children because they require concrete items to solid-

ify their information. Additionally, excessive screen time can overwhelm a young child's senses, resulting in concentration issues and difficulty focusing. Similarly, excessive use of technology may increase the risk of muscular-skeletal injuries in young children. Additional potential negative implications of early technology use include diminished reading abilities and a loss of imagination. The opposing perspective asserts that developmentally appropriate technology use can aid in the learning of young children, particularly in the area of emergent reading abilities. The usage of technology by younger children has been associated with greater motivation and student-centered learning practices [25].

The argument in early childhood settings has recently changed from whether or not to use technology to how to utilize it and how it affects children's learning and development [26]. Determining the proper level of technology integration into pedagogical practice and curriculum design is a challenge for educators and policymakers in early childhood settings. Several scholars have suggested that practitioners take a deliberate approach to technology use, assessing the technology's design to see if it supports creativity, curiosity, and play, encourages kid engagement, and provides an authentic learning experience. Researchers invented the phrase "developmentally appropriate technology use" to describe learning that is led by children and encourages collaborative problem-solving [27]. The goal of this research was to perform a thorough review of the literature to identify the impact of digital technology in education settings.

Researchers highlight a range of ways that children might be involved in global contexts when describing the textual landscape [28]. While there has been a rise in calls and an expansion of children's experiences of this environment in their literacy teaching over the last decade, there are still differences over the function of new technologies in childhood settings. Others worry that young children will be exposed to unsuitable content, put their safety in danger through Internet contacts, or interpret data without critical thinking [29].

At the same time, examinations have revealed a backlog in efficiency and proficiency among new technologies, as seen in Figure 1. Following an examination of the role those new technologies appear to play in the practices under investigation, researchers [30] work to elicit technologies that might be influencing these practices, as well as how a shift in the researcher's perspective might reveal other important aspects of children's interactions with new technologies. It has been argued that some preschools expose children to academic pressure at an inappropriate age. In the context of educational initiatives, this is a particularly pressing issue. Frustration and a loss of interest in learning are the results of attempting to master reading, writing, and arithmetic before one is developmentally ready.

Hence in this paper, the research on preschool education based on computer information technology literacy and big data was described. The further part of this article is categorized as follows: part II provides the related works; part III explains the proposed method; part IV explains the results and discussion; part V explains the conclusion.

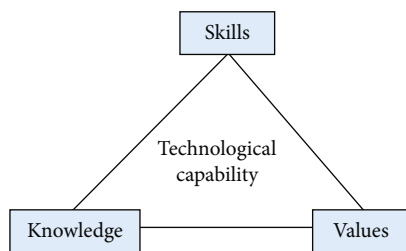


FIGURE 1: Link between technical capability factors.

2. Related Works

Language teachers in a networked environment must analyze existing communication channels from the practice end of the teaching, as well as modify ideas and roles [31]. By researching the teaching network using the UML framework language, Reference [32] offers a methodology and pattern design to swiftly produce reliable performance. The modern system-based teaching learns from the literature [33], including learning fillings, and each platform concentrates primarily on nurturing students' capabilities of listening, speaking, reading, and writing. Traditional language-learning methods are combined literature. Teachers should be able to create the learning process using network resources and attain every capability of students to steer the system [34]. The student method is significantly at personalized education, according to the literature, and it is responsible for the systematic depiction of students' knowledge level and other data [35]. The primary goal is of features and attitudes while also providing a framework for content creation and instructional tactics. Educational goals should encompass cognitive ability and emotion, with cognitive ability targets separated into six tiers based on the difficulty of intellectual activity [36].

The framework was designed following an extensive investigation. The student model is built on the interaction and response history of the students, and it is updated as the students' learning changes. The technology can then personalize lessons based on the student model. This study creates a DL based on past research and the current state of the Chinese language network education system. It also categorizes students' learning and offers various teaching tactics and materials depending on those characteristics. By developing a learning environment based on the characteristics of pupils in real time, the technique enables true customized teaching [37].

Deep learning is a crucial topic in education, despite the reality that the research themes are so different. This information has come from text and voice recognition, as well as certain specialist tournaments. Deep learning is an educational strategy that encourages pupils to think outside the box while also modifying their learning patterns in order to improve learning quality. Multimedia education has gained in popularity in schools during the 1990s, with a growing number of people considering problem-solving as an important part of the learning process. Teachers should emphasize the vital role of students' learning and assist them through autonomous thinking, according to the study.

CNKI published 7177 papers on the topic of "deep learning" between 2005 and 2019. There was just one result for "deep learning" and "teaching ideology and politics," whereas deep learning is defined as the development of new ideas based on a deep understanding of the subject [38].

Students' ability to critically examine, reflect on, and express what they have learned is emphasized in deep learning. I defined the properties of deep learning and said that higher-order thinking is the most essential part of deep learning in the study. They also mentioned that heuristic theory can assist students to improve their higher-order thinking abilities, which is an important part of deep learning [39].

Meanwhile, many academics distinguish between deep and shallow learning in various ways. Surface learning differs from deep learning. Similarly, the methodology examines the current status of deep learning research and, based on that assessment, offers some current research fields. Learning on a more in-depth level due to China's late entry into deep learning research, research on the underlying theory of deep learning [40].

Researchers [41] look at how high school students might learn more deeply about philosophy by relating it to their personal lives and taking action. Students should be taught in a way that takes into account their long-term development guides students' thinking through the use of a real-life problem situation and inspires them to study deeply [42]. In this way, students will be able to learn about philosophy and politics while simultaneously strengthening their core reading. In the political theory class, the strategy is built on a system that recommends what students enjoy and three machine learning models that can figure out what individuals like.

These algorithms are used by this platform. Machine learning and deep systems were used to investigate an online teaching system for ideological and political education. This was done in order to have a better understanding of how deep learning and machine learning are used in institutions [43]. Deep learning has recently sparked a lot of interest in education, and there is a rising corpus of literature on the topic each year. Although there is a handful, there are few studies that integrate deep learning research into the teaching of specific courses, such as high school philosophy and politics. The majority of the literature focuses on how to help students learn more profoundly from their passions, as well as teaching philosophies and methodology improvements [44]. The majority of it emphasizes the importance of "problems" in assisting students in learning more deeply, but there is almost no literature on how to design countermeasures.

3. Methodology

3.1. Data Collection. The main contexts for preschool instruction are, as already said, kindergartens and preprimary schools. We focused on Level 1 (K1; 3- to 4-year-olds), Level 2 (K2; 4- to 5-year-olds), and Level 3 when it comes to kindergarten (K3; 5- to 6-year-olds). Children between the ages of 3 and 6 may also enroll in kindergarten in a mixed-age setting. 13 kindergartens were randomly selected

from Shanghai's urban and suburban areas. All kids in the districts among the ages of 3 and 6 had access to these kindergartens. Data were gathered through the use of random sampling. The original sample of 710 participants included more than 700 children, aged 36 to 72 months, from 45 K2 and seven mixed-age classrooms. The sample size was reduced to 681 after children older than 71 months or less than 48 months were excluded. The control group (341 students) and a study group were separated into two groups (340 students). A study group is a group in which children's education is combined with computer-based instruction, as opposed to a control group, which is a group in which children get a traditional education. 88% of courses had lead teachers, and 18% had assistant teachers. According to the survey, all observed teachers (98%) held an early childhood education (ECE) teaching certificate, 77% had an associate degree or above in ECE, and 75% had majored in ECE. In comparison to Guizhou, Shanghai's classes had fewer students and better teacher-to-child ratios, which led to more qualified teachers. Urban classrooms in Shanghai and Guizhou frequently had longer preschool hours, better teacher-to-child ratios, and a larger percentage of teachers with an associate degree than schools in suburban or rural areas. Compared to children in Guizhou, children in Shanghai had a longer history of preschool attendance and came from families with higher levels of parental education and wealth [45]. Tables 1 and 2 provide the dataset description in detail.

3.2. Theoretical Basis of Intelligent Technology Literacy (ITL). This method of utilizing deep learning (DL) framework for researching on preschool teaching is significantly obtained from the research on neural networks. A multilayer-based perceptron uses various hidden layers as a structure. It uses the mechanism of the human brain to intercept the data like sounds, images, and texts. DL-based models can produce various pattern-based methodologies. In view of certain research analysis, it primarily focuses on three different methods: convolution neural network, multilayer neuron-based self-encoding, and deep confidence network. This form of neural network has the capability of learning itself; the primary characteristics of training the data can be obtained, so it has a higher rate of fault tolerance and ability of memory association. Incorporating neural and ITL can significantly enhance the network's intelligence, speed of response, and adaptability. ITL is a unique methodology that realizes the evolution of preschool mode, as it can entirely explore the behavior of participants and can guide students in forming their ability and intelligence. System based on expert analysis, student and teacher method, and machine-man interface are four vital parameters of typical ITL. The primary structure of ITL is depicted in Figure 2.

The key component of the activity is significant how to sort out the instructing content or how to educate. The intelligent point of interaction fills in as the framework's and clients' intuitive connection point, giving intelligent interactive media information input, and client data and conducting procurement and information yield for other modules. Regular language handling, information base upkeep, understudy model introduction, instructor model versatile

change, and different capacities are all essential for the ITL. Understudy model is an information structure addressing students' mental state, and it is the premise of ITL instruction. The dynamic design of the understudy model shows the development and association of the four parts of the ITL in the learning system, as well as their jobs in instructing choice. It tends to be seen that the understudy method is a significant function, which learns understudies' learning exercises. By analyzing understudies' learning ways of behaving, it records and changes the data depicting understudies' customized characteristics, for example, their insight structure, learning capacity, furthermore, learning propensities, to draw new education methodologies.

In light of the possibility of savvy education, the design of a shrewd network showing framework is planned as a three-level B/S formation: client cooperation layer, showing application layer, what is more, dataset server layer. The client connection layer incorporates the connection points of interaction of understudies, instructors, and framework overseers and understands the association between the framework and clients through programs. The understudy association connection point is the modified showing content and learning interface given by the framework to various students.

3.3. Formation of Intelligent Technology Literacy. Understudies sign in to the framework first and afterward partake in the preevaluation test intentionally, with the goal that the framework can get a starter comprehension of understudies' information level, mental capacity, learning style, most loved learning procedures, etc. In the subsequent review, the framework will choose the participants in the showing information base that are appropriate for understudies' qualities and real level as per the understudies' learning literature, cooperation with the framework, and execution in the framework indicative test; what is more, powerfully put together understudies' learning by the educating systems in the instructing model. At the time of the process, the framework progressively creates the education system as indicated by the understudy model. Understudies can pick, judge, and manage a huge sum of information involving a canny thinking system in the canny showing collaborator framework, which shows the learning strategy designated and works on the learning impact. The groundwork of all improvement is framework investigation, which is a significant phase of computer programming. In the phase of framework investigation, an exact comprehension of the framework prerequisites and the inward working system of the framework is useful in precisely getting a handle on the framework prerequisites, with the goal that the particular substance of programming development can still up in the air, to see completely the clients' prerequisites for the framework.

After learning an information point, understudies first consolidate their insight through relating works out and afterward survey their mental capacity using tests. The test inquiries of every information point incorporate three sorts: single-decision on participant's questions, questions based on judgment, and survey questions. Each question can test no less than one of the over six mental capacities. The steps

TABLE 1: Classroom characteristics.

	Total M (SD)	Rural Guizhou range	Urban Guizhou M (SD)	Suburban Shanghai	Urban Shanghai	Total
Preschool hours	8.22 (0.79)	5.18–9.6	7.67 (1.41)	8.87 (0.54)	8.03 (0.48)	8.39 (0.18)
Number of children led by one teacher	14.97 (5.69)	3–34	17.91 (7.51)	18.80 (4.81)	13.08 (2.59)	11.29 (3.31)
Teacher has an ECE background	0.71 (0.47)	0–2	0.68 (0.48)	0.76 (0.44)	0.68 (0.48)	0.75 (0.46)
Teacher has an associate degree or higher	0.76 (0.44)	0–3	0.67 (0.49)	0.78 (0.43)	0.73 (0.46)	0.85 (0.38)
Public preschool	0.80 (0.42)	0–2	0.88 (0.35)	0.78 (0.44)	0.87 (0.36)	0.68 (0.48)
Quality measures						
MELE: LA	26.02 (4.46)	17–35	23.02 (4.70)	25.33 (4)	27.17 (4.30)	27.92 (3.91)
MELE: CIAL	33.49 (5.31)	24–45	30.64 (3.11)	30.49 (4.89)	33.72 (4.54)	38.31 (4.34)
MELE: CASM	18.71 (3.14)	9–26	16.25 (4.70)	18.46 (2.34)	19.89 (2.07)	19.78 (1.18)
MELE: FS	22.61 (1.97)	16–25	21.20 (3.07)	23 (1.50)	23.44 (0.62)	23.41 (0.98)
MELE: total	100.80 (11.92)	68–121	91.08 (13.89)	96.25 (8.28)	104.20 (7.92)	109.40 (8.02)

TABLE 2: Child development and child characteristics.

	Total M (SD)/n (%)	Range	Rural Guizhou M (SD)	Urban Guizhou	Suburban Shanghai	Urban Shanghai
EAP-ECDS	70.35 (13.90)	34–99	57.24 (12.32)	65.7 (10.64)	75.48 (10.83)	80.09 (9.53)
Age in month	57.96 (4.4)	48.07–71.4	57.4 (4.8)	55.03 (3.52)	59.09 (3.59)	59.75 (3.89)
Boys	360 (52.86)	—	83 (52.91)	82 (54.37)	105 (51.24)	94 (53.46)
Preschool exposure (month)						
0–4	12 (1.85)	—	11 (7.64)	2 (0.76)	0	0
4–7	36 (5.85)	—	20 (14.6)	5 (2.99)	5.63 (4.50)	2 (1.29)
8–13	49 (8.02)	—	26 (20.62)	11 (7.47)	9 (8.88)	3 (1.93)
14–19	246 (41.8)	—	48 (35.89)	64 (47.02)	69 (39.77)	66 (43.32)
20–25	156 (25.89)	—	18 (12.99)	29 (20.8)	61 (33.72)	50 (33.06)
26–31	56 (10.19)	—	6 (3.83)	19 (13.44)	17 (8.98)	16 (10.27)
32–37	33 (5.35)	—	4 (2.30)	9 (5.98)	7 (3.94)	15 (8.98)
>38	19 (3.02)	—	5 (2.31)	3 (1.49)	9 (4.498)	5 (3.22)

involved in the processing of text flow are depicted in Figure 3.

When you the test based on the preschool students, their answer is based on the cognitive capability of more parameters individually. After the preschool students finalize a certain type of question, they can estimate every capability of cognitive in this question type as below.

$$f_i = \frac{m_{ji}(1)}{m_{ji}(1) + m_{ji}(-1)}, j = 1, 2, \dots, 4. \quad (1)$$

Most of them are desirable, $1 \leq i \leq m$; here, m is the total question of test of this j^{th} capability correctly responded in

this type of test. $m_{ji}(-1)$ is the total answer which is wrongly answered to the ability of the cognitive interface.

Suppose the type of question for every knowledge space consists of various choices, false or true answers. Based on equation (1), the capabilities of every question are estimated to formulate the evaluation ability of every question type. The proposed framework is illustrated below:

$$G = \begin{bmatrix} g_{11} & g_{12} & g_{16} \\ g_{21} & g_{22} & g_{26} \\ g_{31} & g_{32} & g_{36} \end{bmatrix}. \quad (2)$$

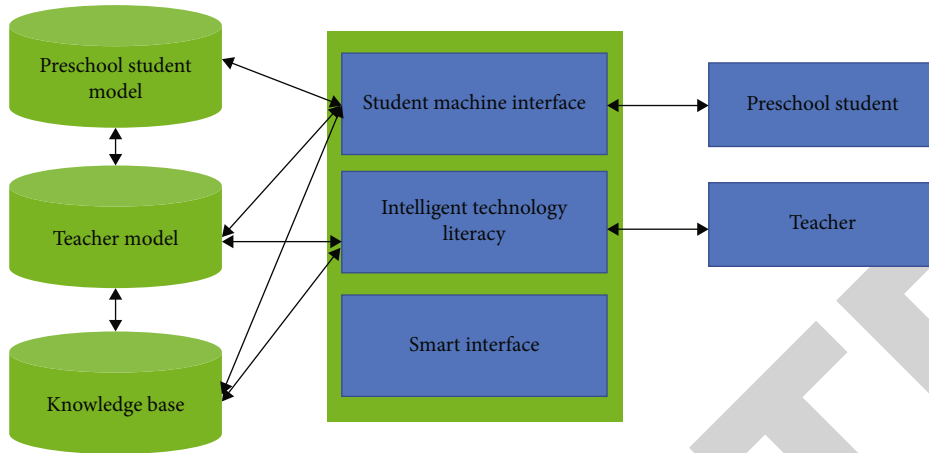


FIGURE 2: Primary structure of ITL.

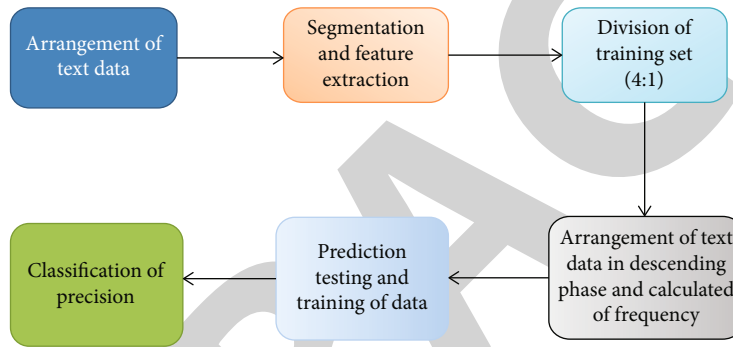


FIGURE 3: Processing of text flow.

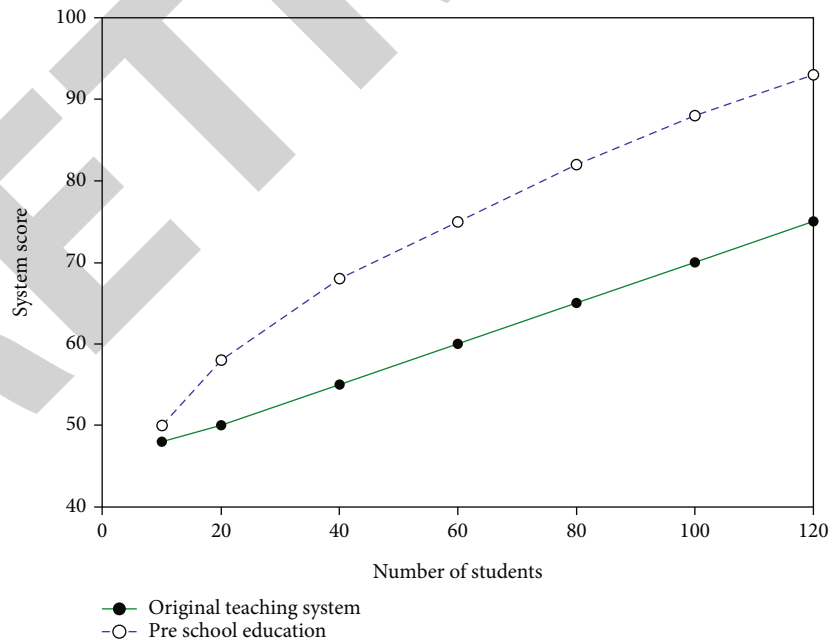


FIGURE 4: Original system teaching score and preschool teaching score.

Based on them, $g_{11} \sim g_{16}$ illustrates the estimation range of the six abilities of single questions. $g_{31} \sim g_{36}$ illustrates the estimation range of six abilities of the survey questions.

Knowledge range is a vital parameter of brilliant assistant-based teaching. The entire processing of a neural network is a measurable procedure for the participation of students

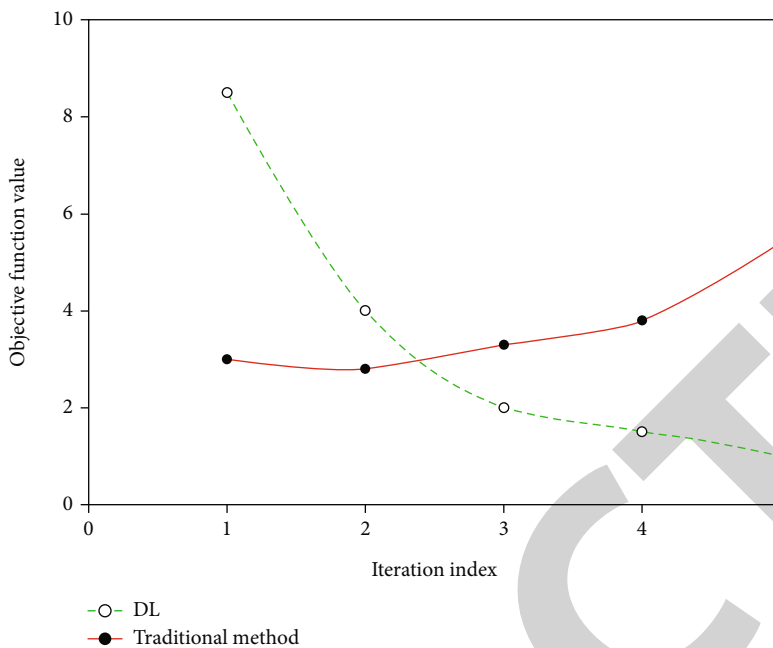


FIGURE 5: Iteration times of the target value.

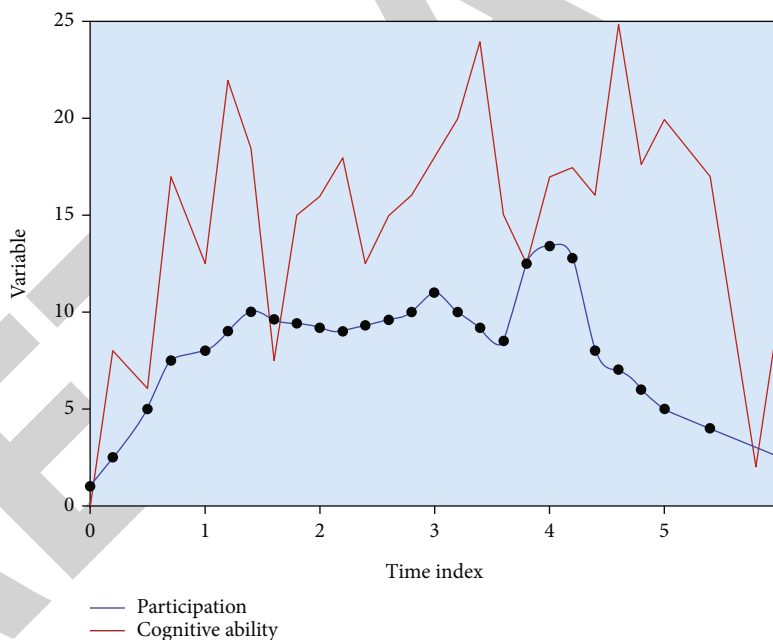


FIGURE 6: Preschool method-based line graph.

in a system. The procedure segregates the participant degree into three various phases. The students' participants in the department are identified as the output axis, which eventually finalizes the mapping from various space dimensional to another dimensional space.

$$\begin{aligned}
 D_{bp} : A &\longrightarrow B, \\
 A &= \{A_1, A_2, A_3, A_4 \dots \dots, A_m\}, \\
 B &= \{B\}.
 \end{aligned}
 \tag{3}$$

The component of master choice-making component can be viewed as the surmising motor in the smart showing colleague framework. For the most part, it embraces the technique for consolidating two degrees of thinking, that is, thinking in light of semantic organization and thinking in view of creation rules. Among them, thinking in view of the semantic organization is utilized to decide the instructing content, while thinking in view of creation rules is utilized to determine the educating technique. Not quite the same as rule-based thinking, case-based thinking is viewed

as thinking in light of past experience. Therefore, in some shrewd showing partner frameworks, case-based thinking is taken on.

The estimation to solve the quantitative estimation of problem and dimension of capability. Based to the various methods of estimation to estimate the student's ability, describe the different weights of question types $V = (V_1, V_2, V_3)$. The weight-based question is illustrated:

$$V_1 = \frac{V_1}{(V_1, V_2, V_3)}. \quad (4)$$

The weight of the question based on true or false is as follows:

$$V_2 = \frac{V_2}{(V_1, V_2, V_3)}. \quad (5)$$

The weight of questions based on fill in the blanks is as follows:

$$V_3 = \frac{V_3}{(V_1, V_2, V_3)}, \quad (6)$$

$$V_1, V_2, V_3 = 1.$$

Based on them, V_1, V_2, V_3 are, individually, the estimation range of the answer on average of every question type of students after considered test. Utilizing equation (2) and weight V to estimate the final calculation analysis of different abilities,

$$T = G * V = (T_1, T_2, T_3, T_4, T_5, T_6). \quad (7)$$

Estimate the cognitive capability of preschool students after learning this point of knowledge

$$H = \sum_{j=1}^6 T_1 \times M_j. \quad (8)$$

4. Result and Discussion

The proposed cognitive-based methodology is a key element of the preschool. Individuals have been concentrating on the human mental process for a long time. Albeit some advancement has been made, in light of the fact that the human mental interaction is such a compound issue, laying out an ideal understudy mental methodology at this phase is just perfect. We should initially tackle the issue of how to address mental capacity to decide on understudies' mental capacity. Understudies have an assortment of inclinations. Two inclinations are considered in this plan: information instructing and information show. The showing strategy for information alludes to the ropes understudies like to be taught, and the introduction of information alludes to the media wherein learning capability is introduced. We can utilize illustrations to exclusively address the information in the

model. Figure 4 illustrates the comparative analysis of teaching score for the original and preschool teaching system.

The teaching methodology is utilized to manage the content of teaching based on the student's model in the teaching methodology. This strategy function has developed three primary strategies. (1) Maintain the learning process using knowledge points. (2) Utilized prerequisite-based knowledge NN alters the association loads of the organization structure through versatile calculation, so the organization approaches the normal information yield relationship, can consequently change the boundaries as per the changes of info information, and can advance the framework to better mirror the learning attributes of understudies. The number of information level hubs is 5. The yield layer is planned as per the understudies' learning state and attributes to be communicated. As of now, the set result incorporates the dominance of specific learning content, learning strategies, and learning propensities. The number of stowed away layers is set on a case-by-case basis. The model understands the communication between the clients and the framework, and it is the point of interaction of two-way exercises of educating and picking up, including understudy association interface, instructor communication connection point, and head interaction interface; simultaneously, it incorporates the plan of interfaces among the models. The model primarily utilizes web to express and convey the substance.

Preschoolers often make mistakes in their learning because they are not mature enough to understand the depths of the methods they are using. This particular system will iterate based on the student's examination in the learning process. After a period of time, students get emotion, by which the network can enhance the learning process of the students by utilizing psychological parameters. Figure 5 illustrates the deviation in the target score with a total of repetitions. As of now, the set result incorporates the dominance of specific content on learning, learning strategies, and learning propensities. The total of stowed away sheets is set on a case-by-case basis. The model understands the cooperation between the clients and the framework, and it is the connection point of two-way exercises of instructing and getting the hang of, including the understudy collaboration interface, educator association point of interaction, and head interaction interface; simultaneously, it incorporates the plan of interfaces based on the framework. The model utilizes the web to infer and impart the substance.

Although some advancement has been made, in light of the fact that human mental interaction is like significant issue, laying out an ideal understudy mental stage model is just ideal. We should initially settle the issue of how to address mental capacity to decide understudies' mental capacity. Understudies have an assortment of inclinations. Two inclinations are considered in this plan: information instructing and information presentation. The showing strategy for information alludes to the ropes understudies like to be taught, and the introduction of information alludes to the media wherein learning content is introduced. Figure 6 illustrates the variable score of ability based on preschool methodology.

5. Conclusion

The machine learning-based methodology of the unique course contents of the preschool teaching framework was formed utilizing Python language, using text-based validation, and training from the questionnaires; this proposed framework is utilized to learn the knowledge frequencies of the participants and interrelated details. This framework can be utilized to manage classroom learning of very basic science online and can enhance the significance and reliability of preschool learning. In this practical model, teachers are insisted to utilize significant frameworks like contextual issues to provide skills to students. Moreover, the results showed the original system teaching score and preschool teaching score, iteration times of the target value, and the preschool method-based line graph. The future enhancement of intelligent technology literacy is analyzed and is framed out that this area with an attractive methodology view is significant for future design and methodology. Future research needs to assess the effectiveness of information technology included in the model of learning with the model without technology.

Data Availability

The data used to support the findings of this study are available from the corresponding author upon request.

Conflicts of Interest

The author declares that there are no known competing financial interests or personal relationships that could have appeared to influence the work reported in this paper.

References

- [1] H. I. Holi, S. S. S. Scatolini, and Q. S. Al Washahi, *The Role of EMI in the Internationalization of Omani Higher Education Institutions (HEIs)*, English-Medium Instruction in Higher Education in the Middle East and North Africa: Policy, Research, and Pedagogy, 2022.
- [2] S. Bahri, H. Fitrah, S. Wahyudin, and A. Juhaidi, "New model of student development strategy to strengthening educational quality: an causal perspective from Indonesia Islamic educational institutions approach," *Journal of Positive School Psychology*, vol. 21, pp. 1417–1426, 2022.
- [3] T. L. P. Nguyen, "Teachers' strategies in teaching reading comprehension," *International Journal of Language Instruction*, vol. 1, no. 1, pp. 19–28, 2022.
- [4] A. Mondal, "Supervised machine learning approaches for moving object tracking: a survey," *SN Computer Science*, vol. 3, no. 2, pp. 1–21, 2022.
- [5] N. Lu, W. Yidan, L. Feng, and J. Song, "Deep learning for fall detection: three-dimensional CNN combined with LSTM on video kinematic data," *IEEE Journal of Biomedical and Health Informatics*, vol. 23, no. 1, pp. 314–323, 2019.
- [6] A. M. Obeso, J. Benois-Pineau, M. S. G. Vázquez, and A. Á. R. Acosta, "Visual vs internal attention mechanisms in deep neural networks for image classification and object detection," *Pattern Recognition*, vol. 123, article 108411, 2022.
- [7] Y. Yang, H. Song, S. Sun, Y. Chen, X. Tang, and Q. Shi, "A feature temporal attention based interleaved network for fast video object detection," *Journal of Ambient Intelligence and Humanized Computing*, pp. 1–13, 2021.
- [8] Z.-Q. Zhao, P. Zheng, X. Shou-tao, and W. Xindong, "Object detection with deep learning: a review," *IEEE transactions on neural networks and learning systems*, vol. 30, no. 11, pp. 3212–3232, 2019.
- [9] Y.-C. Kuo, H.-C. Chu, and M.-C. Tsai, "Effects of an integrated physiological signal-based attention-promoting and English listening system on students' learning performance and behavioral patterns," *Computers in Human Behavior*, vol. 75, pp. 218–227, 2017.
- [10] R.-J. Simons, J. van der Linden, and T. Duffy, "New learning: three ways to learn in a new balance," in *New Learning*, pp. 1–20, Springer, Dordrecht, 2000.
- [11] M. Xu, D. Liu, and Y. Zhang, "Design of interactive teaching system of physical training based on artificial intelligence," *Journal of Information & Knowledge Management*, vol. 21, no. Supp02, p. 2240021, 2022.
- [12] H. Lahza, H. Khosravi, G. Demartini, and D. Gasevic, "March. Effects of technological interventions for self-regulation: a control experiment in learnersourcing," *LAK22: 12th International Learning Analytics and Knowledge Conference*, pp. 542–548, 2022.
- [13] L. A. Jesacher-Roessler and E. Agostini, "Responsive leadership within professional learning networks for sustainable professional learning," *Professional Development in Education*, vol. 48, no. 3, pp. 364–378, 2022.
- [14] F. Callard, "Replication and reproduction: crises in psychology and academic labour," *Review of General Psychology*, vol. 26, no. 2, pp. 199–211, 2022.
- [15] C. B. Hodges, S. Moore, B. B. Lockee, T. Trust, and M. A. Bond, *The Difference between Emergency Remote Teaching and Online Learning*, 2020.
- [16] I. Ali, I. Ahmedy, A. Gani, M. U. Munir, and M. H. Anisi, "Data collection in studies on Internet of things (IoT), wireless sensor networks (WSNs), and sensor cloud (SC): similarities and differences," *IEEE Access*, vol. 10, pp. 33909–33931, 2022.
- [17] S. O. S. B. Hadeeba and W. F. W. Yusoff, "Proposed framework for the usage of information technology tools to enhance knowledge management process of organizations," *The Journal of Organizational Management Studies*, vol. 2022, pp. 1–7, 2022.
- [18] M. H. Koomen, S. Kahn, and T. Shume, "Including all learners through science teacher education," in *Handbook of Research on Science Teacher Education*, pp. 363–375, Routledge, 2022.
- [19] C. Y. Fung, S. I. Su, E. J. Perry, and M. B. Garcia, "Development of a socioeconomic inclusive assessment framework for online learning in higher education," in *Socioeconomic Inclusion during an Era of Online Education*, pp. 23–46, IGI Global, 2022.
- [20] K. Yadav, J. S. Alshudukhi, G. Dhiman, and W. Viriyasitavat, "ITSA: an improved tunicate swarm algorithm for defensive resource assignment problem," *Soft Computing*, vol. 26, no. 10, pp. 4929–4937, 2022.
- [21] R. Kaliisa, B. Rienties, A. I. Mørch, and A. Kluge, *Social Learning Analytics in Computer-Supported Collaborative Learning Environments: A Systematic Review of Empirical Studies*, vol. 3, Computers and Education Open, 2022.
- [22] M. A. Chaudhry, M. Cukurova, and R. Luckin, "A transparency index framework for AI in education," 2022, <https://arxiv.org/abs/2206.03220>.

Retraction

Retracted: Exploration and Practice of Multidisciplinary Integration of Law Teaching under the Background of IOT and Wireless Communication

Journal of Sensors

Received 23 January 2024; Accepted 23 January 2024; Published 24 January 2024

Copyright © 2024 Journal of Sensors. This is an open access article distributed under the Creative Commons Attribution License, which permits unrestricted use, distribution, and reproduction in any medium, provided the original work is properly cited.

This article has been retracted by Hindawi following an investigation undertaken by the publisher [1]. This investigation has uncovered evidence of one or more of the following indicators of systematic manipulation of the publication process:

- (1) Discrepancies in scope
- (2) Discrepancies in the description of the research reported
- (3) Discrepancies between the availability of data and the research described
- (4) Inappropriate citations
- (5) Incoherent, meaningless and/or irrelevant content included in the article
- (6) Manipulated or compromised peer review

The presence of these indicators undermines our confidence in the integrity of the article's content and we cannot, therefore, vouch for its reliability. Please note that this notice is intended solely to alert readers that the content of this article is unreliable. We have not investigated whether authors were aware of or involved in the systematic manipulation of the publication process.

In addition, our investigation has also shown that one or more of the following human-subject reporting requirements has not been met in this article: ethical approval by an Institutional Review Board (IRB) committee or equivalent, patient/participant consent to participate, and/or agreement to publish patient/participant details (where relevant).

Wiley and Hindawi regrets that the usual quality checks did not identify these issues before publication and have since put additional measures in place to safeguard research integrity.

We wish to credit our own Research Integrity and Research Publishing teams and anonymous and named external

researchers and research integrity experts for contributing to this investigation.

The corresponding author, as the representative of all authors, has been given the opportunity to register their agreement or disagreement to this retraction. We have kept a record of any response received.

References

- [1] X. Sun, "Exploration and Practice of Multidisciplinary Integration of Law Teaching under the Background of IOT and Wireless Communication," *Journal of Sensors*, vol. 2022, Article ID 3950001, 8 pages, 2022.

Research Article

Exploration and Practice of Multidisciplinary Integration of Law Teaching under the Background of IOT and Wireless Communication

Xiting Sun 

Fujian Vocational College of Agriculture, Fuzhou 350009, China

Correspondence should be addressed to Xiting Sun; sunxiting188@outlook.com

Received 22 August 2022; Revised 14 September 2022; Accepted 20 September 2022; Published 12 October 2022

Academic Editor: Sweta Bhattacharya

Copyright © 2022 Xiting Sun. This is an open access article distributed under the Creative Commons Attribution License, which permits unrestricted use, distribution, and reproduction in any medium, provided the original work is properly cited.

The exploration and practice of multidisciplinary integration of legal teaching under the background of wireless communication are still at the primary level, facing the situation of low degree of multidisciplinary integration of legal teaching and low contribution of wireless communication technology and Internet of Things technology to multidisciplinary integration of legal teaching. To solve these problems, it is necessary to take wireless communication technology and Internet of Things technology as the internal driving force to promote the development of multidisciplinary integration of legal teaching, so that wireless communication technology and Internet of Things technology depend on the strategy of legal and multidisciplinary integration teaching, hide in the teaching link, and use wireless communication technology to solve the pain points in the multidisciplinary integration of legal teaching, so as to serve teaching.

1. Introduction

The multidisciplinary integration of law teaching in western developed countries is better than that in eastern countries [1]. Economic development promotes the reform of the form and structure of education. Due to its strong economic strength, western developed countries are also ahead of eastern countries in the development of education [2]. As early as the middle of the nineteenth century, western countries put forward the concept of multidisciplinary integration teaching. In the 1980s, Liu Zhonglin proposed the value of multidisciplinary integration teaching. After hundreds of years of precipitation, western developed countries have made some achievements in the multidisciplinary integration of legal teaching. The multidisciplinary integration of law teaching in China has just started. Although the degree of development of multidisciplinary integration between the East and the West is different, they have the same development goals, development concepts, and development principles for the development of multidisciplinary integration of legal teaching [3].

The promotion of wireless communication technology. The wave of industrial technology has pushed the development trend of talents towards the construction of comprehensive and compound talents [4]. The transformation of talent demand must promote the transformation of education mode, and it is urgent to promote the integrated development of disciplines to build new compound talents. In the field of legal education, through the deep integration of law and multidisciplinary, the independent knowledge system of various disciplines is integrated into a whole, so as to cultivate new comprehensive, compound, high-level, and high-quality talents [5]. The Internet of Things uses various information sensors to realize information exchange and remote control management between people, things and things, and people and things. Internet of Things technology is widely used in many fields with its superior information transmission ability and control ability. The Internet of Things technology has also been widely used in the multidisciplinary field of law teaching, such as the information transmission of online virtual classrooms and the construction of virtual classroom scenes. The Internet of Things is a core

technology for the development of multidisciplinary integration of legal education, which plays a great role in promoting the multidisciplinary integration of legal education.

The changing trend of law teaching. Human resources are an important part of social resources and an important driving force for social development. Education is the source of human resources [6]. At present, college teachers tend to instill knowledge directly to students, and ignore the students' grasp of the overall knowledge. And in the teaching process, the independence of each subject teaching is strong, and subject interaction is low, resulting in students' knowledge system confusion. In order to change this situation, China successively put forward the concept of multidisciplinary integration development in 2007 and promulgated the "10-year development plan of education informatization" to promote the development of multidisciplinary integration education in China. At present, the development of multidisciplinary in-depth integration education system has become the development trend of Chinese education. However, it still faces problems such as late start, slow development, and backward system [7].

2. Current Situation of Multidisciplinary Integration of Law Teaching under the Background of Wireless Communication

2.1. Development Status of Exploration and Practice of Multidisciplinary Integration of Legal Teaching. The connotation of multidisciplinary integration and development of legal teaching is to meet the needs of high-level, applied, and high-quality talents in society. Through scientific and reasonable design of courses, the heads of various disciplines in colleges and universities should not only teach undergraduate courses but also speak out the contents of interdisciplinary courses, so as to make the teaching of law more attractive and persuasive, and cultivate students' ability to flexibly use subject knowledge. The development of multidisciplinary integration of legal education is to meet the needs of social development, the expansion of legal disciplines, and the promotion of subject value and students' professional value [8].

The integration model of law and some subjects is difficult to establish effectively [9]. The integration of law and science and engineering is difficult both to establish the integration mode of basic knowledge within the discipline and to establish the guarantee mechanism of external wireless communication technology. The recipient of subject integration is college students. The knowledge system of law students and science and engineering students is very different. The establishment of internal integration mechanism is related to the cultivation of students' comprehensive quality after subject integration [10]. The establishment of interdisciplinary integration model needs to break through the boundaries of disciplines, consider the development of social economy, consider the links and contradictions between disciplines, and develop a high level of interdisciplinary integration model with the joint efforts of educators and researchers. Discipline integration needs not only internal integration

but also external support of wireless communication technology [10].

The integration of law and some subjects brings new impact. On the one hand, teachers are not familiar with the new integrated subjects and teaching level is not enough [11]. Before the multidisciplinary integration of legal education is not implemented, some university teachers may only need to be familiar with the knowledge in the undergraduate course of law [12]. However, after the implementation of multidisciplinary integration of legal education, these university teachers should also teach subjects they are not familiar with. On the other hand, the development of multidisciplinary integration model of law is not mature, and there is no reference precedent. Law and multidisciplinary integration does not find their own position, no clear direction of development, will make these disciplines face a variety of shocks, challenges [13].

The overall degree of multidisciplinary integration of law teaching is not high. The overall low degree of multidisciplinary integration of legal education is the reason why it is difficult to establish an effective model for multidisciplinary integration of legal education and faces various shocks [14]. The Chinese government formally began to implement the concept of multidisciplinary development in 2007, and the multidisciplinary integration of law started later. Therefore, the development of multidisciplinary integration of law is facing the dilemma of late start, slow development, lack of precedent, and low overall development level [6, 7, 11, 15].

2.2. Application of IOT and Wireless Communication Technology in Multidisciplinary Integration of Legal Teaching. With the continuous development of Internet of Things and wireless communication technology, people are eager to show the charm of wireless communication technology in different applications. The application of things and Internet of Things and wireless communication technology in the exploration and practice of multidisciplinary integration of law education has an obvious effect on promoting law to expand the scope of disciplines, adapt to social development, and enhance the value of disciplines. But there are still some deficiencies [16].

Things and Internet of Things and wireless communication technology has a low degree of application and a small range of applications in law teaching. The development of things and Internet of Things and wireless communication technology has been very mature to meet the needs of social development. However, the multidisciplinary integration of legal education is a new field of things and Internet of Things and wireless communication technology, which is faced with immature development model, imperfect core technology, and incomplete application scope. Nowadays, relevant researchers have not solved the core problems in the field of multidisciplinary integration of legal education, and the development of multidisciplinary integration of legal education is still a long way to go [17].

The application area of things and Internet of Things and wireless communication technology in law teaching is not balanced. Due to the regional imbalance of educational development, there is also regional imbalance in the

application of things and Internet of Things and wireless communication technology in the multidisciplinary integration of legal teaching. Specifically, the integration degree of developed eastern regions is strong, while that of underdeveloped western regions is weak. Because of its strong economic strength, the investment in education in the eastern region is much higher than that in the western region, and things and Internet of Things and wireless communication technology in the eastern region is also more developed than that in the western region, so the multidisciplinary integration of things and Internet of Things and wireless communication technology in legal teaching in the eastern region is significantly better than that in the western region [18].

There is no normative system for things and Internet of Things and wireless communication technology to promote the multidisciplinary integration of legal teaching. Exploring the multidisciplinary integration of legal teaching based on wireless communication technology has not yet established a unified normative system in the industry, resulting in uneven levels of the entire industry. When developing the multidisciplinary integration model of legal teaching, various problems are often exposed, which are ignored because there is no unified industry norm. However, these problems often appear again in the process of practical application, which will cause a lot of waste of manpower and material resources, which is one of the reasons why the multidisciplinary integration of legal teaching based on things and Internet of Things and wireless communication technology in the industry has not been widely developed. Establishing a normative system of things and Internet of Things and wireless communication technology to promote the multidisciplinary integration of legal teaching is an important step in the development of things and Internet of Things and wireless communication technology in the multidisciplinary integration of legal teaching [19].

3. Questionnaire Survey

3.1. Investigation Process

3.1.1. Investigation Purpose. Investigation on Discipline Integration of Law Schools in Colleges and Universities

3.1.2. Investigation Objects. A questionnaire survey was conducted among 400 law students randomly selected from different regions nationwide.

Determination of the number of respondents:

$$n = \frac{M \times Z^2 \times \sigma^2}{(M - 1) \times \Delta^2 + Z^2 \sigma^2}. \quad (1)$$

As in formula (1), in this formula, M represents the total number; in this survey, it refers to the number of legal students in national universities, and σ^2 refers to the overall variance. After calculation, $n=402.16$, so the number of subjects in this experiment was 400.

3.1.3. Investigation Methods. Sampling method: first by stratified sampling to determine the number of people in various

regions, and then by simple random sampling method to extract students for investigation.

Survey method: questionnaire survey method.

3.1.4. Survey Content. First, through the understanding of law students' learning situation, estimate the legal teaching situation.

Second, through the understanding of the law students' classroom learning form, estimate the law classroom situation.

Third, through the multidisciplinary integration of college courses, to estimate the degree of multidisciplinary integration of legal teaching in Chinese universities.

Fourth, through the understanding of students' opinions on college courses, to further understand the degree of multidisciplinary integration of legal teaching in colleges and universities in China.

Fifth, by understanding the development of multidisciplinary integration of Internet of Things and wireless communication technology in legal teaching, the development trend of multidisciplinary integration of legal teaching under the background of wireless communication network is speculated.

3.1.5. Reliability Analysis of Investigation Process

(1) First, Validity Analysis. As shown in Table 1, the validity analysis results of the data generated by the survey results are as follows. The four factors of characteristic root value (before rotation) are greater than 1, the four factors of cumulative variance explanation rate % (after rotation) are greater than 50%, the KMO value is 0.610, and the Barthes spherical value is 0.0000. From the above results, it can be seen that the validity results are good, the correctness of the questionnaire data is high, and the validity is high.

(2) Second, Reliability Analysis. Reliability analysis is a common method to test the reliability of the survey results. Specifically, the questionnaire is used to repeatedly measure the subjects, and the consistency of the results is obtained.

Reliability analysis of Cronbach's alpha coefficient in the experiment

$$\alpha = \frac{H}{H - 1} \left(1 - \frac{\sum p_i^2}{p_x^2} \right). \quad (2)$$

Formula (2) shows the value of α in this survey, and the results are shown in Table 2. In accordance with the provisions of Cronbach's alpha coefficient, it is acceptable when $\alpha > 0.7$, so the results of this survey have high reliability.

3.2. Investigation Significance. It has been more than ten years since the promulgation of the ten-year development plan of educational informatization in China. However, we have not achieved good results in the development of multidisciplinary integration of legal education. The investigation of the subject integration of college law schools and the problems existing in the integration of the subjects demonstrated by the results of the investigation can give us a systematic understanding of the multidisciplinary integration of legal education in colleges and universities across the

TABLE 1: Validity analysis.

Project	Factor 1	Factor 2	Factor 3	Factor 4	Commonality
Are law classes boring?	0.76	-0.31	0.2	0.15	0.738
How many disciplines of law in your school's law school?	0.71	0.07	-0.08	-0.2	0.56
Are you having trouble accepting yourself after surgery?	-0.51	0.47	-0.07	0.02	0.491
How many interdisciplinary disciplines in your school?	-0.52	0.09	0.63	0.09	0.494
Will the teacher teach other subjects in class?	-0.52	-0.15	-0.09	-0.24	0.36
Do you use Internet of Things and Wireless Communication Technology tools in class?	-0.21	0.48	0.14	-0.05	0.299
Please rate your usual grades.	-0.11	-0.14	0.17	0.77	0.648
Do you think the teacher's class is wonderful?	-0.1	-0.66	0.07	0.11	0.467
Do you interested in it?	0.25	0.44	0.14	0.37	0.411
Are you interested in the intersection with law?	0	0.14	0.5	0.02	0.267
Can you accept the "one subject and two divisions" model?	0.22	-0.31	0.57	0.01	0.418
Internet of Things and Wireless Communication Technology is very helpful for you	0.22	-0.02	-0.41	0.53	0.497
Eigenvalues (before rotation)	2.11	1.28	1.19	1.08	—
Variance explanation rate (before rotation)	17.61%	10.63%	9.89%	8.96%	—
Cumulative variance interpretation rate (before rotation)	17.61%	28.24%	38.13%	47.08%	—
Eigenvalues (after rotation)	1.88	1.35	1.26	1.15	—
Variance explained rate % (after rotation)	35.67%	31.29%	30.53%	29.60%	—
Cumulative variance explained rate % (after rotation)	55.67%	56.96%	67.48%	57.08%	—
"KMO" value		0.61			—
Barth's spherical value		0			—
df		66			—
P value		—			—

TABLE 2: Reliability analysis.

Sample size	Number of entry	Cronbach's α coefficient
400	13	0.904

country. The rapid development of Internet of Things and wireless communication technology has brought new opportunities for development. It is of great significance to propose targeted solutions according to the problems to improve the degree of multidisciplinary integration of law in colleges and universities across the country.

3.3. Display of Survey Results

3.3.1. Views on Multidisciplinary Integration of Law Teaching.

As shown in Figure 1, students' opinions on legal investigation mainly focus on enriching the form of class and increasing the integration of subjects, which is consistent with the current situation of multidisciplinary integration of legal teaching in China. Notification realizes the internal mode and external guarantee of multidisciplinary integration mode of legal teaching through Internet of Things and wireless communication technology and promotes the development of multidisciplinary integration of legal teaching.

3.3.2. Correlation Analysis between Students' Usual Scores and Class Wonderful Degree.

The results of variance analysis

of students' usual scores and class wonderful degree are shown in Table 3, which shows that the P -value is less than 0.05. According to statistical knowledge, the original hypothesis is rejected, that is, there is a certain correlation between students' usual scores and class wonderful degree.

The study shows that there is a close relationship between students' usual scores and class wonderful degree, that is to say, the form of college teachers' lectures will affect the enthusiasm of students to listen to the class and then affect the usual results. The teaching of college teachers after multidisciplinary integration of law teaching should not only pay attention to the diversity of teaching contents but also pay attention to the quality level of teaching contents, and the most important is the acceptability of students. Internet of Things and wireless communication technology provides external guarantee for the integration of legal disciplines, participates in the classroom, and makes the explanation of college teachers more vivid and persuasive.

3.3.3. Comparison of Multidisciplinary Integration of Legal Teaching in Different Schools.

Figure 2 shows that there is a big difference in the multidisciplinary integration of legal teaching in different schools. The number of legal teaching integration disciplines in 5-10 schools is more, indicating that different schools attach different importance to the practice and exploration of multidisciplinary integration of legal teaching. As an applied discipline, law has its application fields in sociology, economics, psychology, medicine,

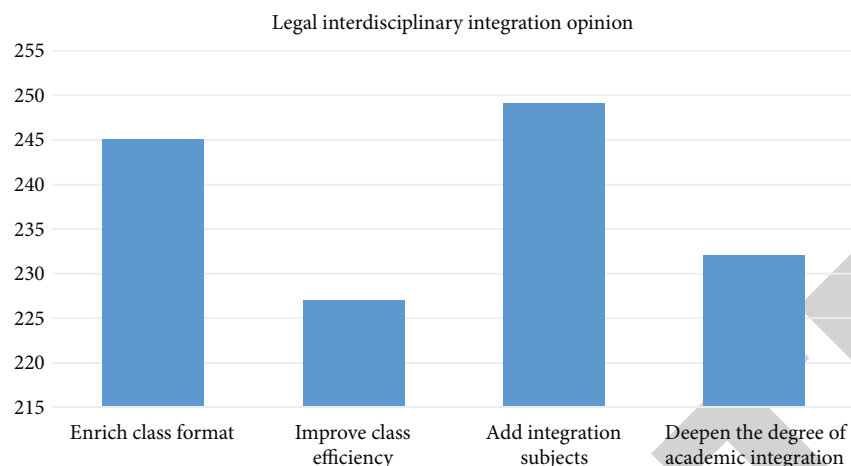


FIGURE 1: Multidisciplinary integration of legal teaching.

TABLE 3: Variance analysis of students' normal scores and class wonderfulness.

(a) Summary

Group	Number of observations	Sum	Average	Variance
Column 1	4	78	19.5	171
Column 2	4	242	60.5	1753.667
Column 3	4	284	71	2423.333
Column 4	4	172	43	824.6667
Column 5	3	24	8	13
Column 6	4	800	200	18418.67

(b) Variance analysis

Source of difference	SS	df	MS	F	P-value	F crit
Between groups	92609.65	5	18521.93	4.447356	0.008977	2.809996
Within group	70800	17	4164.706			
Total	163409.7	22				

and so on. The multidisciplinary integration of law teaching can enhance the competitiveness of law itself and increase the professional value of legal workers.

4. Solutions to Multidisciplinary Integration of Law Teaching Based on Internet of Things and Wireless Communication Technology

4.1. Things and Wireless Communication Technology Depends on the Integration of Law and Multidisciplinary Teaching Strategy, Hidden in the Teaching Link. Internet of Things technology and wireless communication technology are the internal driving force to promote the development of multidisciplinary integration of legal teaching. In recent years, with the rapid development of wireless communication technology, especially since the birth of 5G communication technology, wireless communication technology has had an important impact on various fields. In terms of discipline integration, the opportunities for legal teaching and

more discipline integration play a great role in promoting social development and enhancing the development value of law discipline. The combination of Internet of Things technology and information technology can build a digital learning development model and interactive video courseware design to promote the diversity of college teachers' classes. The combination of Internet of Things technology and other related technologies to build a management platform for the multidisciplinary integration mode of campus information-based intelligent law education can guarantee the multidisciplinary integration mode of law in the internal and become an important guarantee for the practice and exploration of law in the external. At the same time, it is also a guarantee for the smooth progress of teaching after the multidisciplinary integration of law teaching. As a technical support, the Internet of Things technology plays an important role in promoting the multidisciplinary integration of law teaching.

4.2. IOT and Wireless Communication Technology Depends on the Integration of Law and Multidisciplinary Teaching

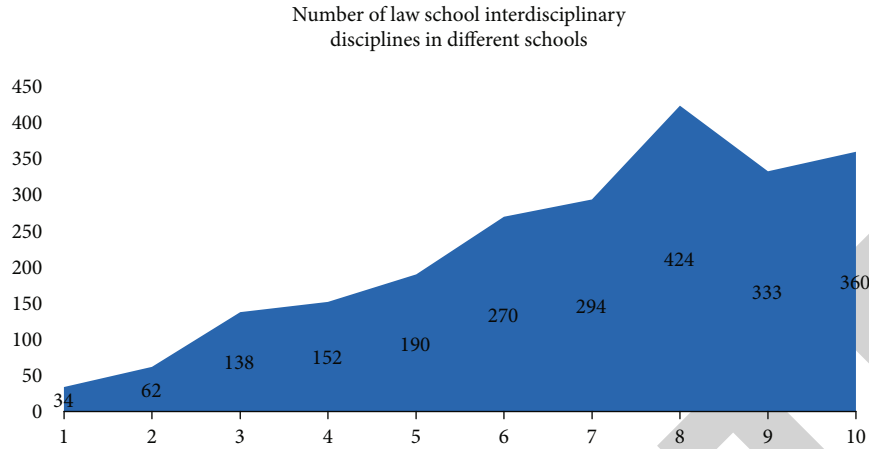


FIGURE 2: Number of multidisciplinary integration of legal teaching in different schools.

TABLE 4: Willingness to accept the two-teacher model in lesson one.

Usually using electronic products	Acceptance willingness of one lesson and two teachers		Total
	Unwilling	Willing	
Would not	48	100	148
Will	85	167	252
Total	133	267	400

Strategy, Hidden in the Teaching Link. Technical personnel apply IOT and wireless communication technology to solve various problems in law and multidisciplinary integration teaching. As shown in Table 4, most law schools will use things and wireless communication technology in their daily learning. [9] Internet of Things and wireless communication technology can improve the efficiency of students' access to information after class, and the daily learning and communication of French students will be very convenient. Things and wireless communication technology in class will make the multidisciplinary teaching mode of law teaching more efficient and convenient, reduce the burden of preparing lessons for college teachers, and also make the classroom more lively and interesting, and improve the learning efficiency of students. As shown in Table 4, most law school students are willing to accept the "one lesson, two teachers" teaching model.

The teaching mode of "one lesson and two teachers" mainly refers to the legal subject teachers as the main lecturer, and the interdisciplinary teachers use things and wireless communication technology equipment to supplement the explanation of college teachers in the main lecturer [14].

This "one lesson, two teachers" lecture mode is mainly established because the integration time of some disciplines is relatively short, and the teachers who examine law may not have a comprehensive understanding of other disciplines, which cannot bring students more convincing explanations. The lecture mode of "one lesson and two teachers" is based on the fifth generation of communication technol-

ogy, which plays an important role in promoting the multidisciplinary integration of legal teaching [17].

4.3. Internet of Things and Wireless Communication Technology Focuses on Solving the Pain Points in the Multidisciplinary Integration of Legal Teaching, So as to Serve Teaching. The development of multidisciplinary integration of legal education is difficult. Figure 3 shows that the main problems faced by the development of multidisciplinary integration of law teaching are the single form of class, students do not adapt to the operation mode of multidisciplinary integration of law teaching, the superficial lack of in-depth teaching content, and the uneven distribution of subject resources [8]. The application of things and wireless communication technology combined with information technology can realize the operation mode management of law teaching after multidisciplinary integration. By optimizing the teaching form, it can make the course content more colorful, solve the problems of boring course and obscure content, and solve the problem of uneven distribution of discipline resources at night. Things and wireless communication technology focuses on solving the pain points in the multidisciplinary integration of legal teaching, promoting the practice and exploration of the multidisciplinary integration of legal teaching, so as to serve teaching [14].

4.4. Internet of Things and Wireless Communication Technology as the Driving Force to Promote the Development of Multidisciplinary Integration of Law Teaching. Internet of Things technology and wireless communication technology are the internal driving force to promote the development of multidisciplinary integration of legal teaching. In recent years, with the rapid development of wireless communication technology, especially since the birth of 5G communication technology, wireless communication technology has had an important impact on various fields [8]. In terms of discipline integration, the opportunities for legal teaching and more discipline integration play a great role in promoting social development and enhancing the development value of law discipline [14]. The combination of Internet of Things technology and information technology can build a digital learning

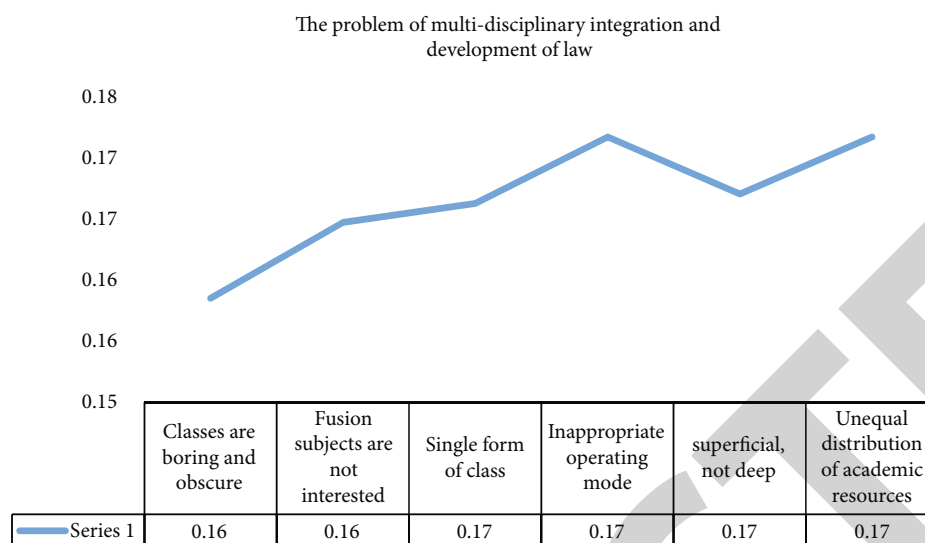


FIGURE 3: The problem of multidisciplinary integration development of law teaching.

development model and interactive video courseware design to promote the diversity of college teachers' classes [20]. The combination of Internet of Things technology and other related technologies to build a management platform for the multidisciplinary integration mode of campus information-based intelligent law education can guarantee the multidisciplinary integration mode of law in the internal and become an important guarantee for the practice and exploration of law in the external. At the same time, it is also a guarantee for the smooth progress of teaching after the multidisciplinary integration of law teaching. As a technical support, the Internet of Things technology plays an important role in promoting the multidisciplinary integration of law teaching [21].

5. Conclusion

In order to meet the needs of society for high-level, applied, and high-quality talents, it is necessary to realize the multidisciplinary integration of legal teaching. At present, the exploration and practice of multidisciplinary integration of legal teaching under the background of things and wireless communication technology still at the primary level, facing the situation that the degree of multidisciplinary integration of legal teaching is not high, the contribution of things and wireless communication technology to the multidisciplinary integration of legal teaching is low, and the degree of multidisciplinary integration of legal teaching shows regional differences. To solve these problems, it is necessary to use things and wireless communication technology as an internal driving force for the development of multidisciplinary integration of legal teaching. Internet of Things and things and wireless communication technology is dependent on the strategy of law and multidisciplinary integration teaching, hidden in the teaching link, and the teaching mode of "one lesson, two teachers" is established. At the same time, Internet of Things and things and wireless communication technology is used to solve the pain points in the multidisciplinary integration of law teaching, so as to serve the teaching.

Data Availability

The datasets used and/or analyzed during the current study are available from the corresponding author on reasonable request.

Conflicts of Interest








The author declared no potential conflicts of interest with respect to the research, authorship, and/or publication of this article.

References

- [1] C. Xia, "Development and prospect of modern internet of things and wireless communication technology," *Electronic Testing*, vol. 18, pp. 119-120, 2020.
- [2] N. Hanqi, S. Yunqi, and H. Jie, "Cognitive wireless network optimization strategy based on machine learning," *Computer technology and development*, vol. 30, no. 5, pp. 125-131, 2020.
- [3] C. Zenan and Q. Wang, "Exploration on the curriculum development of music in lower grades of primary schools based on multidisciplinary integration —taking a rural primary school in Zhangjiakou City, Hebei Province as an example," *Art Review*, vol. 4, 2021.
- [4] C. Lei, "Strategies for pre-service training of multidisciplinary integration ability of general teachers in rural primary schools," *Forest Teaching*, vol. 12, 2021.
- [5] Z. Tong, "The significance of interdisciplinary integration of labor education," *Education*, vol. 43, 2021.
- [6] D. Junjun, "Practice path of thematic interdisciplinary integration," *Sichuan education*, vol. 24, 2021.
- [7] Q. Wang, "On the basic principles and strategies of interdisciplinary integration of labor education," *Education*, vol. 43, 2021.
- [8] C. Ping, "The security problems and preventive measures of Internet of Things and Wireless Communication technology," *Wireless interconnection technology*, vol. 18, no. 17, 2021.

Research Article

Smart Home-Based Complex Interwoven Activities for Cognitive Health Assessment

Shtwai Alsubai ¹, Abdullah Alqahtani ¹, Mohemmed Sha ¹, Sidra Abbas ²,
Ahmad Almadhor ³, Vesely Peter ⁴, and Huma Mughal ⁵

¹College of Computer Engineering and Sciences, Prince Sattam bin Abdulaziz University, Al-Kharj, Saudi Arabia

²Department of Computer Science, COMSATS University, Islamabad, Pakistan

³Department of Computer Engineering and Networks, College of Computer and Information Sciences, Jouf University, Sakaka 72388, Saudi Arabia

⁴Information Systems Department, Faculty of Management, Comenius University in Bratislava, Odbojárov 10, 82005 Bratislava 25, Slovakia

⁵Department of Computer Science, Kinnaird College for Women, Lahore 54000, Pakistan

Correspondence should be addressed to Mohemmed Sha; ms.mohamed@psau.edu.sa and Vesely Peter; peter.vesely@fm.uniba.sk

Received 23 September 2022; Revised 30 September 2022; Accepted 6 October 2022; Published 12 October 2022

Academic Editor: Sweta Bhattacharya

Copyright © 2022 Shtwai Alsubai et al. This is an open access article distributed under the Creative Commons Attribution License, which permits unrestricted use, distribution, and reproduction in any medium, provided the original work is properly cited.

With the prevalence of cognitive diseases, the health industry is facing newer challenges since cognitive health deteriorates gradually over time, and clear signs and symptoms appear when it is too late. Smart homes and the IoT (Internet of Things) have given hope to the health industry to monitor and manage the elderly and the less-abled in the comfort of their homes. Smart homes have been most influential in detecting and managing cognitive diseases like dementia. They can give a comprehensive view of the ADL (Activities of Daily Living) of dementia patients. ADLs are categorized as activities of daily life and complex interwoven activities. First signs of cognitive decline appear when a cognitively impaired individual tries to perform complex activities involving planning, analyzing, calculating, and decision making. Therefore, we analyze individuals' performance while performing complex activities as opposed to Simple ADL. Artificial Intelligence has been one of healthcare's most promising techniques for prediction and diagnosis. When applied to ADL data, machine learning and deep learning algorithms can conveniently and accurately analyze activity patterns and predict the first signs of cognitive decline. Our proposed work uses machine and deep learning classifiers to classify dementia and healthy individuals by analyzing complex interwoven activity data. We use the subset of the CASAS (Centre of Advanced Studies in Adaptive Systems) dataset for eight complex activities performed by 179 individuals in a smart home setting. decision tree, Naive Bayes, support vector, multilayer perceptron classifiers, and deep neural networks have been used for classification. Their results and performances are compared to determine the best classifier. It is observed that deep neural networks and multilayer perceptron show the best results for classifying dementia vs. healthy individuals when evaluating their complex interwoven activities.

1. Introduction

There has been a rapid increase in mental disorders and the people suffering from them in the last few years. Over 1 billion people suffer from one mental disease, addiction, dementia, or schizophrenia [1] [2]. WHO (World Health Organization) has concluded that the investment in mental health has not matched the awareness scale of mental health problems. In 2010 reduced productivity and poor health

owing to poor mental health resulted in a \$2.5 trillion loss worldwide. This figure is expected to rise to \$6 trillion by 2030 at the current rate [2, 3]. Early intervention can reduce the healthcare system's burden globally and eventually reduce the associated mortality rate [4, 5]. At present cognitive health is analyzed in the clinic using a cognitive function test like MMSE (Mini-Mental State Examination) and MoCA (Montreal Cognitive Assessment) and other neurological exams like CDR (Clinical Dementia Rating) and

assessment of ADL. The information regarding a patient's ADLs is gathered via a questionnaire filled by the patient himself or his/her guardian, hence making the entire assessment process subjective [6, 7]. This can result in an inaccurate assessment. It has been observed that very subtle signs and symptoms first appear in the daily activities of individuals suffering from cognitive decline, which clinicians can easily miss in a physical exam. For the said reason, HAR (Human Activity Recognition) is emerging as an effective method to monitor an individual's movements and activities and has gained special focus in the field of research to improve healthcare systems. [8, 9]. Smart homes with multiple sensors are a promising tool for HAR to gather data regarding ADL. Smart homes have multiple networks of sensors that can gather an overview of residents' activity patterns in terms of their health, security, safety, independent activities, and their social lives [10, 11] as can be seen in Figure 1.

The ADLs gathered via sensors in a smart home are divided into simple and complex activities. Simple activities are the activities performed to manage an individual's basic needs, like grooming, dressing, toileting, and eating. The complex activities include activities that enable an individual to live independently in the community. This would be planning a bus route, managing medication, finances, etc. Complex activities are interrelated activities that require a degree of decision-making and calculations. While simple activities are recorded based on a single sensor event, recording complex activities is not as easy and requires input from multiple sensors [10, 12].

ML(Machine Learning) and DL(Deep Learning) tools are commonly used to perform an in-depth analysis of all activities [13]. Several researchers have analyzed ADLs, compared outcomes, and identified patterns to differentiate cognitively impaired from healthy individuals. The proposed work aims to compare and contrast the efficacy of different ML and DL algorithms to analyze a publicly available dataset CASAS for complex activities obtained by different sensor readings in a smart home setting. The dataset includes a combination of both simple and complex activities.

The biggest challenge for a patient suffering from cognitive impairment is leading an independent lifestyle. Living an independent life requires not just the ability to perform daily life functional activities but also the individual to perform several complex daily activities that are dependent on other activities but require a degree of calculation and decision making [14]. Complex activities, also known as IADL (Instrumental Activities of Daily Living), are a deciding factor in diagnosing a cognitive disease. Presently, the gold standard for assessment is an in-clinic exam that can be subjective. Our primary motivation is to analyze the complex activities in the daily lives of individuals to detect the earliest signs of cognitive decline. Hence we aim to accurately and timely predict the presence of cognitive impairment or dementia by analyzing the complex activities done in daily life. We use different ML and DL techniques to find the most accurate prediction model and then compare and contrast each model's results to determine the efficacy and determine which model is best for classification. This paper aims to contribute to research in the following aspects:

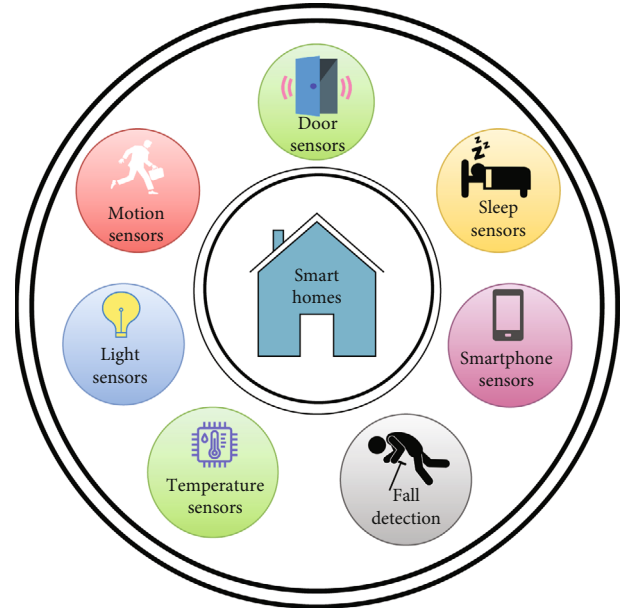


FIGURE 1: Sensors in a smart home environment for cognitive health assessment.

- (i) Proposes an approach to classify dementia individuals by analyzing complex activities performed in a smart home setting to detect the earliest signs of dementia using machine learning and deep learning
- (ii) Present a comparison between machine learning and deep learning algorithms to evaluate the best model and provide a baseline study
- (iii) Deep learning algorithm enhances dementia individuals' detection rate compared to a machine learning algorithm and overperforms the baseline paper detection rate

The rest of the paper is structured as follows: Section 2 is a literature review of the previous work in the early detection of dementia via examining ADL data. Section 3 gives a detailed overview of the proposed approach. Experimental analysis and results are presented in Section 4, where all the different techniques employed for classification are discussed. Section 5 provides the discussion on experimental analysis. The results of all the classifiers are compared and contrasted. Finally, Section 5 concludes the paper by sharing the best model and performance.

2. Literature Review

Smart homes have been the solution of choice for the aging population and those with disabilities. Researchers have gathered ADL to analyze, diagnose, and predict cognitive health problems.

In one such research [4], the author has used the DL technique to detect the early symptoms of MCI (Mild Cognitive Impairment). Using the time-series prediction technique, he has further handled the issue of missing sensor signals, which often arise in real-time data gathering due to

sensor failure. Furthermore, the author proposes an autoencoder-based technique to reduce the dimension of the data so that deviation in human behavior can be detected using an RNN-based approach. A persisting abnormal behavior indicates a problem and alerts of MCI. In [15], a robot-enabled activity support system has been proposed and is evaluated in a smart home testbed. The robot is useful in monitoring the activities of the residents and can assist in daily activities where needed.

The possibility of detecting changes in psychological, cognitive, and behavioral symptoms of Alzheimer's disease by using unobtrusively collected smart home behavior data and machine learning techniques was evaluated in [16]. The authors have analyzed the publicly available CASAS dataset and have tried to handle imbalanced data using the Weka tool. Four models, Support Vector Regression, Linear Regression, Support Vector Regression with a Radial Basis Function kernel, and k-nearest neighbors algorithms, were used to predict mobility, cognitive, and mood-related symptoms from gathered in-home behavior data.

In another research paper [17], the author uses unobtrusively collected smart home behavioral data to diagnose functional health decline. Activity data from the CASAS dataset was obtained from 38 smart homes, and the functional health assessment of participants was conducted using the IADL-C questionnaire. This data was then analyzed using different ML algorithms. [8] uses a multisensor approach to recognize complex activities using a CNN (Convolutional Neural Network) and an LSTM (Long Short Term Memory) model and compare the performance of both models. In [18], the authors use a machine learning model to assess the quality of activity in smart homes and classify the activities as simple and complex compared to a neurologist's assessment. The author also uses a machine learning approach to assess the accuracy of predicting cognitive health conditions like dementia, MCI, and Alzheimer's disease.

3. Proposed Approach

The proposed work aims to predict healthy vs. dementia patients based upon the analysis of ADL data about complex activities as shown in Figure 2. The responses of individuals towards complex activities will help classify individuals and enable early detection of the onset of dementia. The proposed approach is divided into five steps: data selection, pre-processing, features extraction, and ML and DL classifiers to classify healthy individuals and those with dementia.

3.1. Data Selection. Choosing the most suitable dataset and determining the right instrument for data collection is of utmost importance in an experimental setup. Therefore, after a careful selection process, we selected a subset of the CASAS dataset. The dataset has been made publicly available by "The Centre for advanced studies in adaptive systems," a department at Washington State University in the School of Electrical Engineering and Computer Science. It aims to research the use of smart home technology to test real data. The dataset comprises a mix of simple and complex activities that were used to perform our analysis.

Our dataset contains 179 individuals, 145 of whom are healthy, 32 suffering from MCI, and two being diagnosed with dementia. The dataset contains 24 daily life activities, where the first eight activities are simple tasks, and last eight activities are complex tasks. Tasks from 9-16 are unlabeled and not classified as simple or complex hence they have been excluded from our current research. Each participant was evaluated on the eight complex activities that were part of daily life activities like selecting a magazine from the coffee table to read it during a commute on the bus, heating a heating pad for 3 minutes using the microwave to take along, before leaving for the bus take medicine for motion sickness, calculating the bus route and estimating the time to leave for the bus and the total journey from the map, and then the individual was expected to calculate the bus fare and gather the correct change needed. The individual was also assessed on the complex activity of finding a recipe from the recipe book for spaghetti sauce and gathering all the ingredients for making it. The picnic basket activity involved making a basket by gathering all necessary things from the cupboard and putting them in the basket. Lastly, the individual was expected to exit towards the door with the picnic basket. These were the eight complex activities that the individuals were evaluated.

Multiple sensors in a smart home setting were utilized to gather the activity data. A combination of motion sensors, door sensors, burner sensor, temperature sensors, etc. has been used to evaluate a complex task.

3.2. Data Preprocessing. The ability to extract information from data is directly linked to data quality. The quality of data depends on how clean and meaningful the data is. In order to make our data suitable for evaluation, we preprocessed the data.

3.2.1. Checking for Missing Values. All attributes were checked for missing values. Missing values, i.e., sensor values with no readings, were replaced with zeros.

3.2.2. Categorizing into Numeric Values. All nonnumeric attributes were assigned categorical values. The attribute diagnosis had two values, healthy and dementia. '1' was assigned to healthy while '0' was assigned to dementia.

3.2.3. Scaling All Quantities. Values of all sensors were then normalized within a range using a min-max scaler. This scales the sensor readings between 0 and 1 without changing the distribution's shape and retaining the data's original properties. ML and DL results improve considerably if the data is scaled.

3.3. Feature Extraction. In any given dataset, certain features are irrelevant to specific research or include details that do not contribute anything significant to the research process. In order to eliminate unnecessary processing, extracting the relevant features from the dataset is essential. The redundant sensor readings were eliminated by performing the Pearson correlation. The threshold was identified at 90%. All attributes greater than 90% were eliminated because they were highly correlated. Almost 58 sensors were highly correlated.

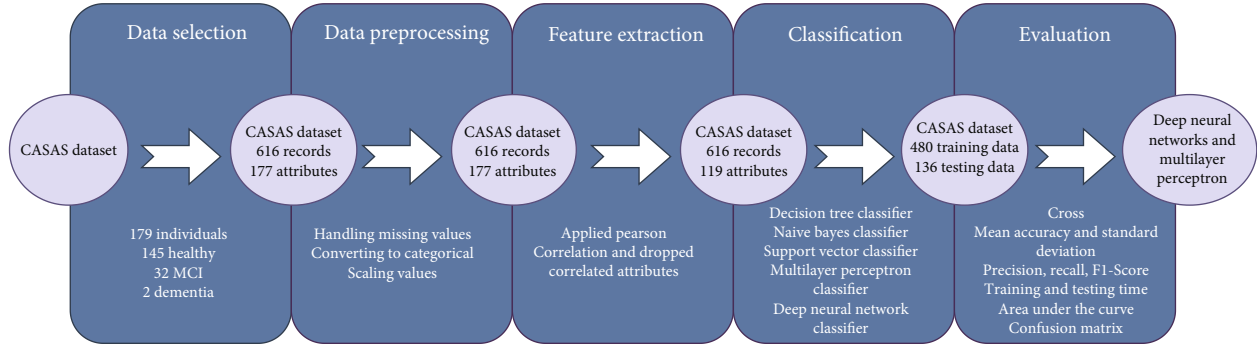


FIGURE 2: Proposed methodology.

Hence, they were eliminated. The classification was applied to the readings from the remaining sensors.

3.4. Classification Models. Artificial Intelligence techniques can be accurately used in healthcare for the prediction and diagnosis of disease in an objective manner. ML and DL are the most commonly used AI techniques for disease prediction. We applied four ML models on to our dataset comprising complex activity data. They were DTC (decision tree classifier), NB (Naive Bayes), SVC (support vector classifier), and MLP (Multilayer perceptron) classifier. We also used a deep neural network comprising four dense layers to classify our data.

3.5. Evaluation Metric. For each of the models implemented, several evaluation metric tools were used to evaluate the performance of each model and to compare which model yields the best output. We compare and contrast the following:

3.5.1. Cross-Validation Scores of the Training Data. Since K-fold cross-validation (CV) is an effective measure in model selection, we performed a 10-fold CV on our training dataset for each model [19]. Then we computed the mean accuracy after the validations process for all ten iterations and the means' standard deviation to ensure the data's homogeneity.

3.5.2. The Mean Accuracy and the Standard Deviation of Accuracy of the Training Data. When performing the CV, it is important to calculate the average of all ten results to get an overview of the model performance and also to include a measure of the variance of all ten outcomes in order to rule out any unusual outcomes in the form of outliers [20].

3.5.3. The Time Each Model Took to Train. How many seconds it took for the ML model to calculate the accuracy? Training time is usually more than testing time since training data is a bigger proportion of the dataset.

3.5.4. The Accuracy of the Testing Data. The models are then applied to the testing data, and their accuracy is computed.

3.5.5. The Time Each Model Took on the Testing Data. Testing the model of test data extracted from the dataset.

3.5.6. Precision. It is defined as the

$$\frac{\text{TruePositive}}{\text{TruePositive} + \text{FalsePositive}} \quad (1)$$

Precision is useful in determining how accurately the model predicted the real positive outcomes out of all the positive outcomes predicted.

3.5.7. Recall. It is defined by the formula:

$$\frac{\text{TruePositive}}{\text{TruePositive} + \text{FalseNegative}} \quad (2)$$

Recall helps identify the accurate positive predictions in proportion to the actual positive values in the dataset.

3.5.8. F1-Score. It is defined by the formula:

$$2 * \frac{\text{Precision} * \text{Recall}}{\text{Precision} + \text{Recall}} \quad (3)$$

Since Precision and Recall are not accurate in determining the true picture of the model performance, F1-score is used to determine the combined effect of Precision and Recall by calculating their harmonic mean.

3.5.9. Support. This is simply the number of instances/records fed to a model for training or testing.

3.5.10. Confusion Matrix. Gives a summary of the no. of instances: True Positive, False Positive, False Negative, and True Negative.

3.5.11. Area under the Curve (AUC). It is a graphical representation of how well a model can distinguish between two classes. The higher the area, the better the performance of the model.

4. Experimental Analysis and Results

The proposed approach aims to diagnose dementia using complex activity data from a publicly available dataset. We train different classifiers with the given data and analyze the outcome to obtain the model that gives the most accurate results. The experimental analysis was performed over

TABLE 1: Summary of findings for decision tree classifier.

CV mean accuracy	0.967
CV standard deviation	0.028
Accuracy of prediction	0.97
Training time	0.215 seconds
Prediction time	0.03 seconds

TABLE 2: Results of decision tree classifier for dementia detection.

	Precision	Recall	F1-score	Support
Dementia	0.97	0.97	0.97	59
Healthy	0.97	0.97	0.97	77
Accuracy	—	—	0.97	137
Macro avg.	0.97	0.97	0.97	137
Weighted avg.	0.97	0.97	0.97	137

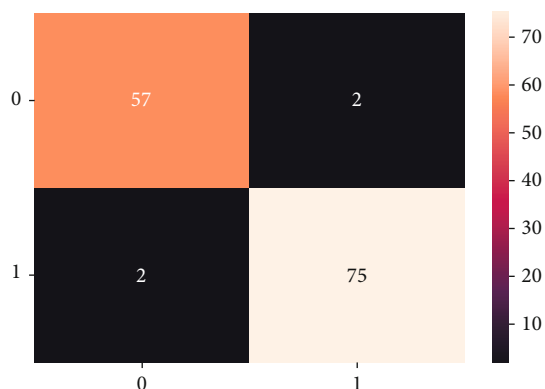


FIGURE 3: Decision tree confusion matrix.

the famous web-based IDE notebook—Google Colab, and implementation was done using Python 3.6. The first task before data preprocessing was to split the data into train and test samples. We used a 78:22 ratio for train and test, respectively. Of the 616 records available, 480 were used for training and 136 for testing.

4.1. Decision Tree Classifier. Decision tree algorithms are supervised ML classifiers. They operate by splitting the dataset into categories based on a criterion. The data is iteratively split till a homogeneous subset containing records with the same class labels is obtained. Gini Index, Information gain, and Gain ratio are commonly used indices to perform the split [21]. Our DTC uses the default “Gini Index” to perform the classification.

Table 1 shows that the mean accuracy obtained from the ten iterations of 10-fold cross-validation yielded 97% accuracy with a minimal standard deviation of 0.0208, indicating that all iterations gave somewhat similar results. The training time was 0.215 seconds, whereas the prediction was very fast and took only 0.03 seconds.

Table 2 is an overview of the performance of our decision tree classifier model. It can be observed that the precision-recall and F1-score all give a score of 97%. Out

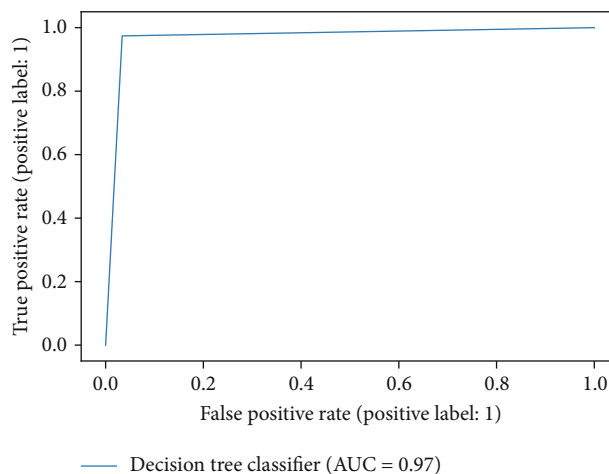


FIGURE 4: Area under the curve for decision tree classifier.

TABLE 3: Naive Bayes classifier.

CV mean accuracy	0.831
CV standard deviation	0.053
Accuracy of prediction	0.85
Training time	0.263 seconds
Prediction time	0.012 seconds

TABLE 4: Results of Naive Bayes classifier for dementia detection.

	Precision	Recall	F1-score	Support
Dementia	0.74	1.00	0.85	59
Healthy	1.00	0.73	0.84	77
Accuracy	—	—	0.85	136
Macro avg.	0.87	0.86	0.85	136
Weighted avg.	0.89	0.89	0.85	136

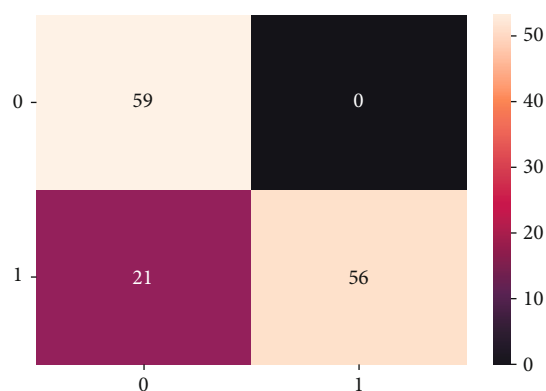


FIGURE 5: Naive Bayes confusion matrix.

of the total participants in the test data, 59 dementia patients and 77 healthy individuals are in our test dataset. Figure 3 is a confusion matrix of the model. It gives a summary of predicted vs. actual outcomes. Our model accurately predicted 57 out of 59 dementia patients and 75 out of 77 healthy individuals via the decision tree classifier. There were only four

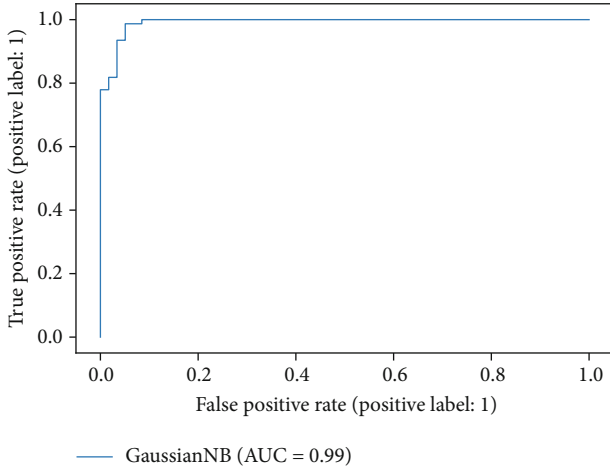


FIGURE 6: Area under the curve for Naive Bayes classifier.

misclassifications. Figure 4 is the ROC curve for our decision tree classifier. The model effectively differentiated between dementia and healthy individuals with 97% accuracy. It can be seen in the graph that the True Positive rate rapidly increased to 0.97 while the False Positive rate was fairly low, and after reaching 0.97, the graph becomes flat, and the rate becomes almost constant.

4.2. Naive Bayes Classifier. The NB classifier is a probabilistic classifier based on the Bayes theorem. By using conditional and prior probabilities, we can ascertain the probability of a class. These complex calculations are important to determine class probability since prior, and conditional probabilities can be easily obtained from the given dataset. NB Classifier fundamentally operates on the probabilistic principle as defined by

$$P(c|x) = \frac{P(x|c)P(c)}{P(x)}, \quad (4)$$

where $P(c|x)$ is the posterior probability, $P(x|c)$ is the likelihood, $P(c)$ is the class prior probability, and $P(x)$ is the prediction probability.

Table 3 shows that the mean accuracy obtained after a 10-fold CV for the NB classifier is 0.831 with a standard deviation of 0.053. The training and prediction time for the NB classifier is much less than the decision tree classifier because the NB classifier is a relatively simple and easy classifier, which is an advantage in processing time but is a significant drawback owing to its Naive nature. The overall prediction accuracy achieved was 0.85.

Table 4 summarizes important findings from the model implementation. The precision value for dementia is 0.74, recall is one, and the F1-score is 0.85%, whereas the precision for healthy individuals is 1.00, recall 0.73, and the F1-score is 0.84. The overall accuracy of test data was 0.85.

Figure 5 is the confusion matrix of the actual vs. predicted outcomes. The model was able to classify all dementia patients correctly but misclassified 21 healthy individuals, thus decreasing the accuracy of the model. Only 56 healthy

TABLE 5: Summary of findings for support vector classifier.

CV mean accuracy	0.967
CV standard deviation	0.025
Accuracy of prediction	0.85
Training time	0.12 seconds
Prediction time	0.005 seconds

TABLE 6: Results of support vector classifier for dementia detection.

	Precision	Recall	F1-score	Support
Dementia	0.97	0.98	0.97	59
Healthy	0.99	0.97	0.98	77
Accuracy	—	—	0.98	136
Macro avg.	0.98	0.98	0.98	136
Weighted avg.	0.98	0.98	0.98	136

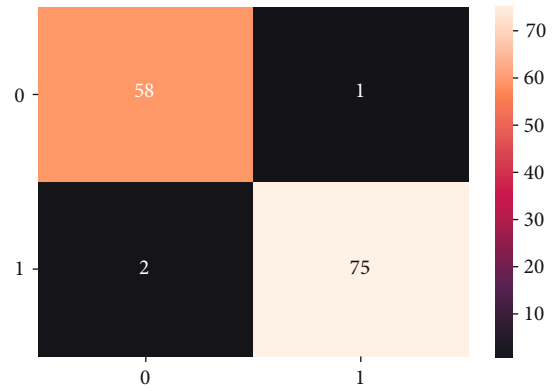


FIGURE 7: Support vector classifier confusion matrix.

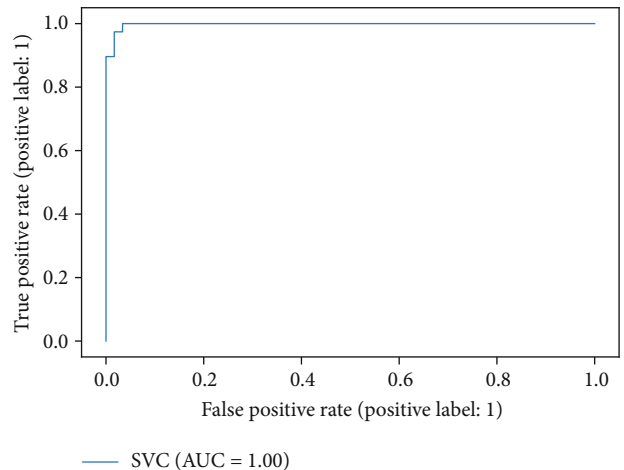


FIGURE 8: Area under the curve for support vector classifier.

individuals could be predicted from the test data set. The ROC curve in Figure 6 shows an area under the curve equal to 0.99.

4.3. Support Vector Classifier. SVC is a supervised ML algorithm that can be used for classification or regression

TABLE 7: Summary of findings for MLP classifier.

CV mean accuracy	0.971
CV standard deviation	0.0298
Accuracy of prediction	0.99
Training time	11.95 seconds
Prediction time	0.011 seconds

TABLE 8: Results of MLP classifier for dementia detection.

	Precision	Recall	F1-score	Support
Dementia	1.00	0.98	0.99	59
Healthy	0.99	1.00	0.99	77
Accuracy	—	—	0.99	136
Macro avg.	0.99	0.99	0.99	136
Weighted avg.	0.99	0.99	0.99	136

challenges. The proposed work uses SVC to classify dementia and healthy individuals by analyzing data of complex daily activities in a smart home environment. Each data point is mapped onto an n-dimensional plane, where each class is then separated using a hyperplane [22]. The objective is to find a hyperplane with maximum distance from the points closest to the line, also known as the support vectors.

Table 5 shows that the mean accuracy obtained after applying 10-fold CV is 0.967, and the standard deviation was nominal, i.e., 0.025. Table 6 shows that the precision, recall, and F1-score range from 0.97-0.99 for dementia and healthy values, indicating that our algorithm gives quite accurate results. Training and prediction time for SVC are less than for DTC and NB.

Figure 7 is a confusion matrix for the SVC. The matrix shows that the algorithm can successfully classify 58 instances of dementia and 75 instances of healthy individuals with only three misclassifications. The ROC curve in Figure 8 shows an area under the curve equal to 1.00, which shows the excellent performance of the algorithm.

4.4. Multilayer Perceptron Classifier. An MLP neural network is a neural network where each neuron imitates the way a human brain works and learns results using mathematical operations. The input layer consists of neurons that receive the data; after processing at each neuron, the data is passed to one or more hidden layer that performs mathematical operations and passes it to the output layer that predicts output [23]. Backpropagation is used whereby the neural network learns through the errors that occur. The error is computed between predicted and actual output, and adjustments are made, allowing the model to learn. Table 7 shows the performance of our MLP classifier for predicting dementia vs. healthy patients from complex activity data. The mean accuracy obtained from a 10-fold CV was 0.971, and the standard deviation was only 0.0298 between the ten iterations. The MLP classifier achieved about 99% prediction accuracy by training the neural network in 11.95 seconds and obtaining the predictions using the test data in 0.011 seconds. Although

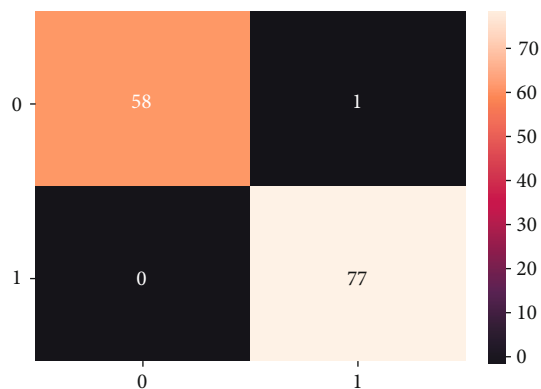


FIGURE 9: Multilayer perceptron confusion matrix.

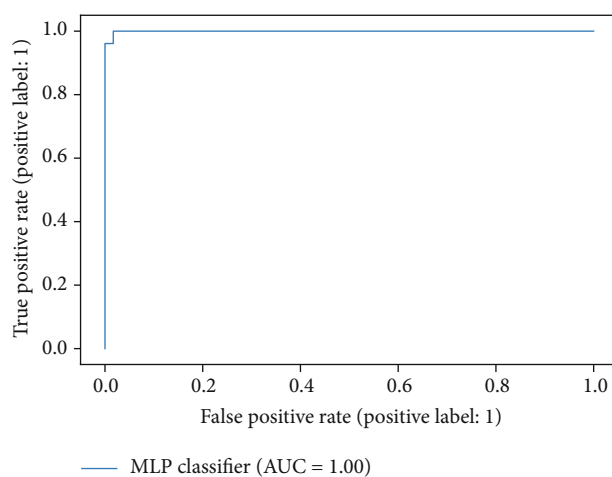


FIGURE 10: Area under the curve for multilayer perceptron classifier.

the training time for MLP is quite a lot because of the complex computations involved, it has been observed that they can achieve high accuracies. Table 8 is the classification report of the MLP classifier and indicates that precision, recall, and F1-score for both classes are between 0.99 and 1, which is close to 100%.

Figure 9 is a confusion matrix for our MLP classifier, and as can be seen, our algorithm successfully classified all the healthy individuals and only misclassified dementia patients. The ROC curve in Figure 10 also indicates a 100% accuracy with the area under the curve equal to 1.

4.5. Deep Neural Networks. A DNN (Deep Neural Network) is a type of Neural Network that has multiple hidden layers that are densely connected. The capability of a DNN to extract features from raw sensor data and give a meaningful output using complex mathematical operations makes DNN the state-of-the-art Artificial Intelligence technique. DNNs have been successfully used in healthcare, where they have exceeded human accuracy by far. Using complex activity data, the proposed work employed DNNs to predict healthy vs. people living with dementia. A DNN model was constructed using 4 dense layers.

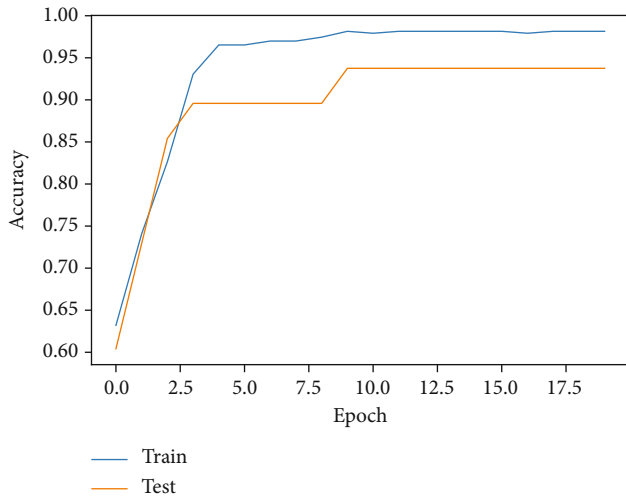


FIGURE 11: Deep neural networks accuracy per epoch curve.

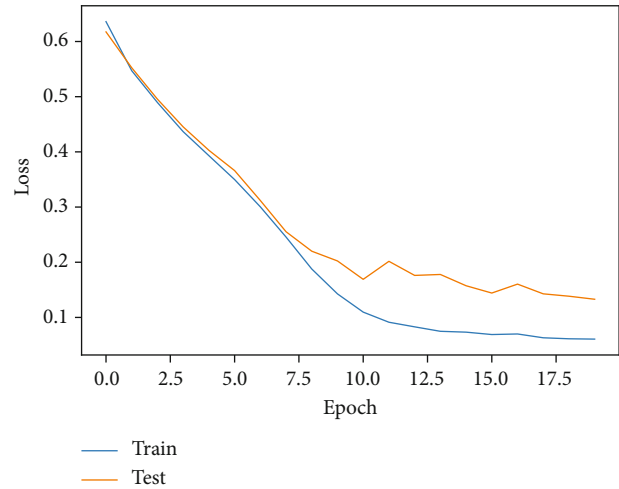


FIGURE 13: Deep neural networks loss per epoch curve.

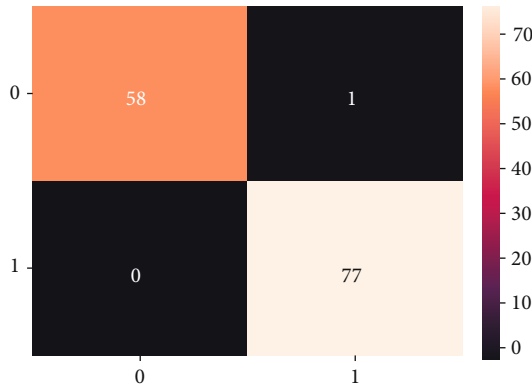


FIGURE 12: Deep neural networks confusion matrix.

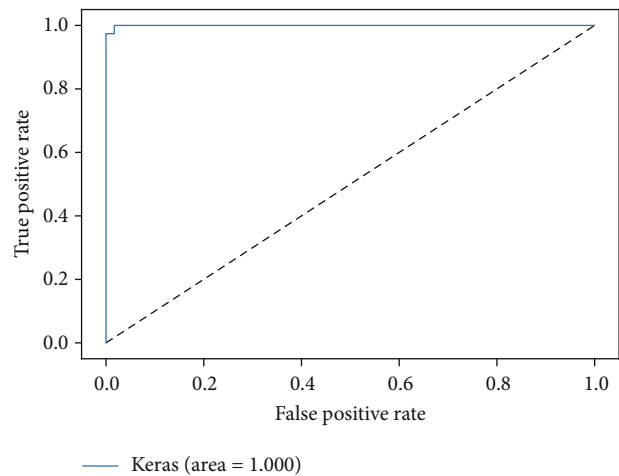


FIGURE 14: Deep neural network area under the curve.

A ReLU activation function was used in the first three layers, and a sigmoid function was used in the fourth layer that yields the output predicting whether the individual is a healthy or dementia patient. Twenty epochs were used to train our model with a batch size of 16. The training accuracy quickly jumped from 0.57 after the first epoch to 0.78 after the second. The accuracy gradually increased from 0.78 to 0.986 in 20 epochs. Similarly, the prediction accuracy jumped from 0.75 after the first epoch to 0.85 after the second epoch and rose to 0.96 after 20 epochs. As shown in Figure 11, the accuracy for train and test rapidly increased during the first three epochs and then became steady after three epochs. Figure 12 is the confusion matrix of our classification using the DNN model. Only one dementia patient was misclassified; the rest of the healthy individuals and the dementia patients have been correctly classified, indicating excellent accuracy.

Figure 13 illustrates the loss/error of train and test data behavior per epoch. It is observed that the training error was very high after the first epoch, i.e., 0.64, and the testing error was 0.62. For training and test data, the loss steadily decreased per epoch. The decrease slowed after ten epochs when the curve became less steep and flatter. The final loss after 20 epochs for training data was 0.061, and for test data,

it was reduced to 0.13. The ROC curve also indicates an AUC of 1, indicating an excellent classification of both classes in Figure 14.

5. Discussion

We tested five different ML classifiers on the publicly available dataset comprising data of 179 individuals, 145 of which were healthy individuals, 32 were suffering from MCI, and two were diagnosed with dementia. Data collected from sensors in a smart home setting were gathered against eight complex tasks. The resulting data were then classified using the DTC, the NB classifier, the SVC, the MLP classifier, and a DNN model. The results obtained are summarized in Table 9.

The DNN and MLP classifier yielded the best accuracy and area under the ROC curve. The NB and SVC returned less accuracy in predicting dementia vs. healthy individuals. While the MLP classifier gives accurate results, it takes the longest training time; therefore, it is not the most efficient

TABLE 9: Summary of results obtained from different classifiers.

	Accuracy	Training time	Prediction time	AUROC
Decision tree	0.97	0.215 s	0.03 s	0.97
Naive Bayes	0.85	0.263 s	0.012 s	0.99
Support vector	0.85	0.12 s	0.005 s	1.00
Multilayer perceptron	0.99	11.95 s	0.011 s	1.00
Deep neural network	0.99	4.401 s	4.401 s	1.00

in processing and takes longer due to its complex algorithm. DNNs have also yielded excellent accuracy but require a longer processing time than DTC, NB, and SVC. For SVC, although it takes the least processing time, it yields poor accuracy. So it can be concluded that in terms of Accuracy and ROC, MLP and DNN are the best classifiers for predicting dementia using complex activities data, given that training time is not of much relevance.

6. Conclusion

The proposed work attempts to compare and contrast the performance of the different classifiers for the prediction of dementia using ML techniques on complex activity data. We observed that most classifiers successfully classified dementia and healthy from the given data with a slight variation in accuracy. Deep neural networks and multilayer perceptron performed very well in classifying our classes. We conclude that AI techniques are very effective in the early diagnosis and prediction of dementia. Using smart homes, we can conveniently diagnose dementia patients by observing their behavior in their complex daily activities. Multilayer perceptron and deep neural networks have been deemed the best classifiers for this classification task since they can achieve accuracies as high as 99%. One of the earliest signs of dementia appears when individual attempts to perform complex daily activities that involve cognitive brain functions like planning, analyzing, and calculating. Our proposed work can detect these behavioral changes very early in individuals, thus helping medical professionals detect dementia earlier and accurately. The sooner the diagnosis is made, the easier it is to manage the disease.

Data Availability

The [Complex Interwoven Activities] data used to support the findings of this study are included within the article.

Conflicts of Interest

The authors declare that they have no conflicts of interest.

References

- [1] J. Rehm and K. D. Shield, "Global burden of disease and the impact of mental and addictive disorders," *Current Psychiatry Reports*, vol. 21, no. 2, pp. 1–7, 2019.
- [2] The Lancet Global Health, "Mental health matters," *The Lancet. Global Health*, vol. 8, no. 11, article e1352, 2020.
- [3] A. Mubashar, K. Asghar, A. R. Javed et al., "Storage and proximity management for centralized personal health records using an IPFS-based optimization algorithm," *Journal of Circuits, Systems and Computers*, vol. 31, no. 1, p. 2250010, 2022.
- [4] S. Sharma and A. Ghose, "Unobtrusive and pervasive monitoring of geriatric subjects for early screening of mild cognitive impairment," in *2018 IEEE International Conference on Pervasive Computing and Communications Workshops (PerCom Workshops)*, pp. 179–184, IEEE, Athens, Greece, 2018.
- [5] M. U. Sarwar and A. R. Javed, "Collaborative health care plan through crowdsource data using ambient application," in *In 2019 22nd International Multitopic Conference (INMIC)*, Islamabad, Pakistan, 2019IEEE.
- [6] L.-N. Kwon, D.-H. Yang, M.-G. Hwang et al., "Automated classification of normal control and early-stage dementia based on activities of daily living (adl) data acquired from smart home environment," *International Journal of Environmental Research and Public Health*, vol. 18, no. 24, p. 13235, 2021.
- [7] A. R. Javed, M. U. Sarwar, H. U. Khan, Y. D. Al-Otaibi, and W. S. Alnumay, "PP-SPA: privacy preserved smartphone-based personal assistant to improve routine life functioning of cognitive impaired individuals," *Neural Processing Letters*, 2021.
- [8] K. Woodward, E. Kanjo, K. Taylor, and J. A. Hunt, "A multi-sensor deep learning approach for complex daily living activity recognition," in *Proceedings of the 2022 Workshop on Emerging Devices for Digital Biomarkers*, pp. 13–17, New York, NY, USA, 2022.
- [9] A. R. Javed, R. Faheem, M. Asim, T. Baker, and M. O. Beg, "A smartphone sensors-based personalized human activity recognition system for sustainable smart cities," *Sustainable Cities and Society*, vol. 71, article 102970, 2021.
- [10] A. R. Javed, "Automated cognitive health assessment in smart homes using machine learning," *Sustainable Cities and Society*, vol. 65, article 102572, 2021.
- [11] V. Kumar, G. S. Lalotra, and R. K. Kumar, "Improving performance of classifiers for diagnosis of critical diseases to prevent COVID risk," *Computers and Electrical Engineering*, vol. 102, article 108236, 2022.
- [12] P. F. Edemekong, D. L. Bomgaars, S. Sukumaran, and S. B. Levy, "Activities of daily living," in *In StatPearls*, StatPearls Publishing, 2021.
- [13] M. U. Sarwar, A. R. Javed, F. Kulsoom, S. Khan, U. Tariq, and A. Kashif Bashir, "PARCIV: recognizing physical activities having complex interclass variations using semantic data of smartphone," *Software: Practice and Experience*, vol. 51, no. 3, pp. 532–549, 2021.

- [14] L. C. Jacqueline Wesson, J. D. Crawford, N. A. Kochan, H. Brodaty, and S. Reppermund, "Measurement of functional cognition and complex everyday activities in older adults with mild cognitive impairment and mild dementia: validity of the large Allen's Cognitive Level Screen," *The American Journal of Geriatric Psychiatry*, vol. 25, no. 5, pp. 471–482, 2017.
- [15] G. Wilson, C. Pereyda, N. Raghunath et al., "Robot-enabled support of daily activities in smart home environments," *Cognitive Systems Research*, vol. 54, pp. 258–272, 2019.
- [16] A. Alberdi, A. Weakley, M. Schmitter-Edgecombe et al., "Smart home-based prediction of multidomain symptoms related to Alzheimer's disease," *IEEE Journal of Biomedical and Health Informatics*, vol. 22, no. 6, pp. 1720–1731, 2018.
- [17] A. A. Aramendi, A. Weakley, A. A. Goenaga, M. Schmitter-Edgecombe, and D. J. Cook, "Automatic assessment of functional health decline in older adults based on smart home data," *Journal of Biomedical Informatics*, vol. 81, pp. 119–130, 2018.
- [18] P. N. Dawadi, D. J. Cook, and M. Schmitter-Edgecombe, "Automated cognitive health assessment using smart home monitoring of complex tasks," *IEEE Transactions on Systems, Man, and Cybernetics: Systems*, vol. 43, no. 6, pp. 1302–1313, 2013.
- [19] Y. Jung, "Multiple predicting K-fold cross-validation for model selection," *Journal of Nonparametric Statistics*, vol. 30, no. 1, pp. 197–215, 2018.
- [20] M. Rafał, "Cross validation methods: analysis based on diagnostics of thyroid cancer metastasis," *ICT Express*, vol. 8, no. 2, pp. 183–188, 2022.
- [21] S. Tangirala, "Evaluating the impact of Gini index and information gain on classification using decision tree classifier algorithm," *International Journal of Advanced Computer Science and Applications*, vol. 11, no. 2, pp. 612–619, 2020.
- [22] D. A. Pisner and D. M. Schnyer, "Support vector machine," in *Machine Learning*, pp. 101–121, Elsevier, 2020.
- [23] M. Desai and M. Shah, "An anatomization on breast cancer detection and diagnosis employing multi-layer perceptron neural network (MLP) and convolutional neural network (CNN)," *Clinical eHealth*, vol. 4, pp. 1–11, 2021.

Research Article

Evolution and Evaluation: Sarcasm Analysis for Twitter Data Using Sentiment Analysis

Monika Bhakuni,¹ Karan Kumar ,² Sonia ,¹ Celestine Iwendi ,³ and Avtar Singh ⁴

¹Yogananda School of Artificial Intelligence, Computer and Data Science, Shoolini University, Solan, India

²Electronics and Communication Engineering Department, Maharishi Markandeshwar Engineering College, Maharishi Markandeshwar (Deemed to be University), Mullana, Ambala-133207, India

³School of Creative Technologies, University of Bolton, Bolton BL3 5AB, UK

⁴Department of Electronics and Communication Engineering, Adama University of Science and Technology, Adama, Ethiopia

Correspondence should be addressed to Karan Kumar; karan.170987@gmail.com, Sonia; soniacsit@yahoo.com, and Avtar Singh; avtarsingh@astu.edu.et

Received 28 July 2022; Accepted 29 August 2022; Published 11 October 2022

Academic Editor: Sweta Bhattacharya

Copyright © 2022 Monika Bhakuni et al. This is an open access article distributed under the Creative Commons Attribution License, which permits unrestricted use, distribution, and reproduction in any medium, provided the original work is properly cited.

This paper addresses the evolution and evaluation of sarcasm in textual form. The growing popularity of social networking sites is well known, and every individual generates a whole new set of opinions in form of blogs, microposts, etc. Sentiment analysis is one of the fastest evolving aspects of artificial intelligence categorizing opinions under positive, negative, or neutral sentiments. One such part of sentiment analysis is sarcasm. Sarcasm is becoming a common phenomenon in networking sites where expressing murky feelings wrapped by positive words for conveying contempt is highly used, making it difficult to understand the actual meaning of a statement. When reading customer reviews or complaints, it might be helpful to understand the consumers' genuine intentions in order to enhance the efficiency of customer support or after-sales services. In this paper, different classifiers—decision tree, Naïve Bayes, k-nearest, and support vector machine are used to predict a statement under the category sarcastic or nonsarcastic using tweeter data; the following proposed methodology is used for the experimental evaluation concluding that the given classifiers SVM gains the highest accuracy of 93%, whereas Naïve Bayes and decision tree are performing well with an accuracy of 83% and 86%, respectively, along with the lowest of 51% attained by KNN.

1. Introduction

One of the leading aspects of artificial intelligence is natural language processing (NLP); as easy to say, it is otherwise to interpret currently the most enduring and apprehensive study worldwide in understanding opinions, particularly sentiments of an individual. Specific nouns used to elaborate opinions depending on the case scenarios are one of the major research areas. In recent years, the world has encountered a lot of recurrent changes, wherein the process of being upfront on words is well justify by social networking sites. Unlike the traditional anonymous survey or questionnaire, online posts, interactions, reviews, and media offer, it is more efficient and accurate insight into the minds of people around the world [1]. The growing popularity of Twitter,

Facebook, and Instagram has deluded the era with a lot of opinions saying positive, negative, and neutral statements. Just as artificial intelligence is becoming more sophisticated and the internet more accessible, so too is the ability to observe human behavior [1].

Over the recent years, ML and AI are the new hot topics of this era; the formulated approaches are a part of a whole new categorizing of products and appliances [2]. Machine learning algorithms can be classified in four types: supervised, semisupervised, reinforcement, and unsupervised learning. Supervised learning is a kind of machine learning that has the capability to construct a function from a labeled set. Because of the presence of the labeled output value, supervised learning can construct a decent model. This can be happening because the expected results which need to

be processed by the model are already provided in the training dataset [3].

Sentiments are defined as an opinion held or expressed by different people at the same time about a particular topic or otherwise. Sentiment analysis can be said as a process of collecting and analyzing data based on human feeling, reviews, or thoughts [4]. The applications for the following can be stated as monitoring the social media, product analytics, customer analysis, business analytics, etc. Sentiment analysis in the real world is becoming increasingly pivotal, specifying that it is domain-centred, i.e., results of one domain cannot be applied to another domain [4]. Another synonym that can be used is opinion mining, where a speaker speaks about a particular entity and discusses its feedback. The growth of information available in social media makes sentiment analysis more crucial [5]. There are a few key challenges faced by sentiment analysis such as entity-named recognition, anaphora recognition, parsing, sarcasm detection, and many others. From the commercial perspective, sentiment analysis can provide online advice and recommendations for both the customers and merchants [5].

Sarcasm is defined as a mode of paradoxical wit depending on its effect on bitter and often ironic language that is usually directed towards an individual. In this era, people are directing their common way of speaking towards sarcasm, and a lot of sarcasm is stated in order to subjectify a particular topic. In essence, sarcasm can be said to as the new way of expressing an opinion. It can be expressed via speech, text, etc. Understanding sarcasm in speech, it becomes interpretable because a lot of gestures are associated with sarcasm, use of a facial expression, tone, and gestures can be used to identify sarcasm. In textual form, it is marginally difficult to interpret sarcasm; dealing with just a set of words becomes slightly difficult to interpret. Detection of sarcasm is one of the leading areas of research, understanding the true opinion of a person under sarcastic statements. The application of the following can be stated as marketing research, opinion mining, and information categorizing, also benefiting areas of interest in NLP.

What makes the task of detecting sarcasm hard is that it is hard to understand human emotion, sometimes without prior knowledge of the topic. Sarcasm resembles lying in some context, making it a more problematic and a hard task [6]. To understand one's intent in the text, we need to classify sarcasm, and it is important to devise a system that could generate a good and reliable training set for the classifier, a labeled bag of words, and an algorithm that could detect sarcasm [7]. There are, however, various other challenges that are posed by streaming data from social media itself. [8]. Sarcasm detection plays a vital role in the company's feedback where they can analyze customers' true intentions about their product.

The following work is proposed in this paper: sentiment analysis utilising natural language processing, followed by sarcasm detection. The paper addresses the concurrent need for sarcasm detection making it useful for knowing the intent of people. Understanding the intents and actual ideas of customers while reading their reviews or complaints also

aids in improving the effectiveness of after-sales service or consumer assistance. The existing system is based on four classifiers for prediction; the classifiers are supervised categorical classification, which results in the detection of a statement under the categories sarcastic and nonsarcastic. The data are processed under the specification needed for the classifier to analyze efficiently. The data preprocessing is done using different libraries from the natural language tool kit (nlTK), summarizing the results useful for the prediction and further analysis. The classifiers, Naïve Bayes, decision tree, SVC, and KNN are trained and tested for twitter data, which is scraped using twint library, and the detection of sarcasm is hence proposed.

The main points of the initial research are basically as follows:

- (i) The current system uses the several supervised classifiers stated above to train and evaluate a model for the prediction of sarcastic and nonsarcastic comments
- (ii) Twint, a Twitter scraping tool, is used to start gathering data and collect 10,000 tweets in total for analysis

2. Literature Survey

Dharmavarapu and Bayana [9] proposed a methodology for constructing reliable and effective algorithms for sarcasm detection on Twitter. The output divides the given list of tweets into sarcastic and nonsarcastic tweets and using sentiment analysis to organize the tweets into positive, negative, or neutral tweets by the probabilities. Naïve Bayes algorithm is used for the classification of tweets, wherein AdaBoost is used to determine the polarity of the same. The use of only two classifiers is done to predict the same making it vulnerable for counter classifiers interpretation.

An eminent researcher in the field [10] define sarcasm's effects on sentiment analysis; the effect of sarcasm scope on the polarity of the tweets is classified in their study and also mentions the rules that can be used for sentiment analysis incorporated with sarcasm performing with higher accuracy. GATE is their developed hashtag for tokenizing, so that sentiment and sarcasm found within hashtags can be detected more easily. The following are their result for their classification; the hashtag tokenization achieves a precision of 98%, while the sarcasm detection achieved 91% precision. The study was published in 2014, and since then, many recurring changes have been seen in terms of sarcasm covenants, necessitating the urgent need for a new, generalized approach.

"Sentiment Analysis for Sarcasm Detection on streaming short text data" by Prasad et al. [8], has presented the counter problem with social media dataset, known as short text data, i.e., use of short forms and slang along with usage of sarcasm. The paper compares different classification algorithms for the detection of sarcastic tweets, use of random forest, gradient boosting, decision tree, adaptive boost, logistic regression, and Gaussian Naïve Bayes for the twitter

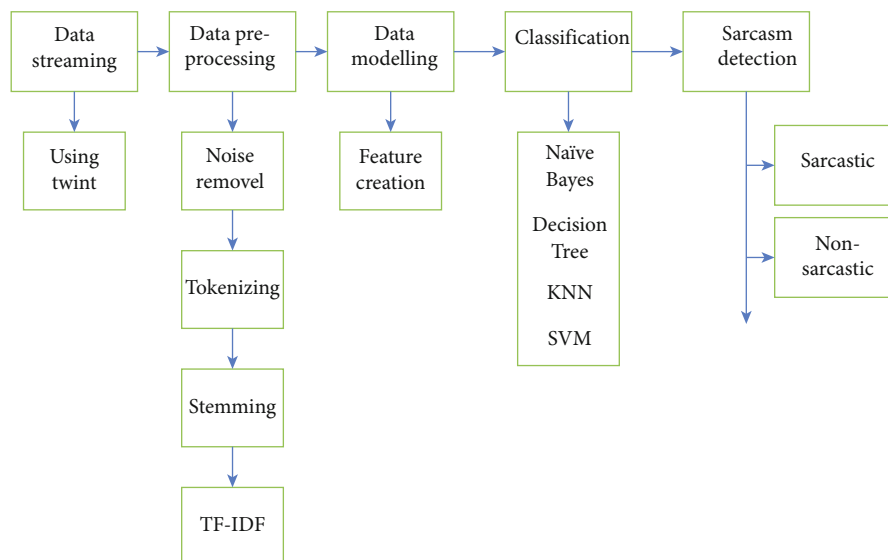


FIGURE 1: Flowchart representing the proposed methodology.

TABLE 1: Feature creation.

Fields	Data type	Range
Tweets	Object	
Polarity	Float	-1 to +1
Subjectivity	Float	0 to 1

streaming API with the highest accuracy of 81.82% of gradient boost for results of testing for a split of 60:40. Their paper finally concludes with a way of improving the existent sarcasm detection algorithm. Validation on only a 2000 tweet dataset that includes general tweets with sarcastic or nonsarcastic labels serves as the dataset provided for the proposed approach.

“Opinion Mining in Twitter–Sarcasm Detection” [6] by Parveen et al. has made a presentation that the work of impact created by the presence of sarcasm using different components of the tweet. With the use of two datasets, i.e., before adding sarcastic tweets and after adding sarcastic tweets, they have incorporated three different classifiers: Naïve Bayes, maximum entropy, and support vector machine for the impact evaluation of sarcasm-related features on sentiment classification. The results concluded an enhancement after the involvement of sarcasm related features, signifying that the polarity of a tweet was misread due to the presence of sarcasm. The state-of-the-art approaches to sentiment analysis, however, perform less well in Twitter than they do when they are applied to larger texts because of the character limit (140 characters per tweet) and the usage of informal language.

Sindhu and Vadivu’s “A Comprehensive Study on Sarcasm Detection Technique in Sentiment Analysis” [7] has covered numerous methodologies and procedures used in sentiment analysis to identify sarcasm in text; data used in the following work are Amazon product reviews. The biggest numbers of model implementations are obtained through

Twitter API. Detection of sarcasm is done using classifiers and rule-based methods. Using the SVM, an accuracy of 54.1% achieved.

“A pattern-based Approach for Sarcasm Detection on Twitter” [11] by Bouazizi and Ohtsuki presents the work of a pattern-based approach for the detection of sarcasm and also finds the effectiveness of the model created for sarcasm detection. Data are retrieved from Twitter API. Four sets of feature extraction are used which include as a witticism, a whimper, a form of evasion, and sarcasm. Sentiment-related features, punctuation-related features, lexical and syntactic features, and pattern-related features are employed to classify texts, and their suggested strategy achieves an accuracy of 83.1%.

Several researchers [12] use the concept of a supervised machine learning-based approach to defining sarcasm detection on Facebook, concentrating on both post contents (such as text or images) and Facebook users’ interactions with those posts. Data collection was done using Facebook graph API. Public 10 pages were selected for the collection of the sarcastic post. Machine learning classifiers were used for the analysis, where random forest and SVM performed better than the rest.

Khare et al. [13] proposed a methodology for analysis of sentiment for government bodies in their paper “Sentiment Analysis And Sarcasm Detection Of Indian General Election Tweets”. Analysis is done on Twitter data of duration 2019 where a collection of tweets is done for Lok Sabha election. The textual information contained in tweets is handled using an SVM classifier. The authors have written about a subject where some users tweet in jest. They have achieved an accuracy of 84 percent when comparing their model outcome to the results of the election, which is sufficient for transfer learning. Moreover, the dataset used for the following methodology is from the data science website Kaggle; the full dataset of tweets linked to the election is accessible.

Ashwitha et al. [14] later studied sarcasm detection using natural language processing, covering the striking properties

```

c = twint.Config()
c.Store_object = True
c.Pandas = True
c.Search = "sarcasm"
c.Limit = 10000

twint.run.Search(c)

1524110655720239105 2022-05-10 19:34:31 +0000 <HasbaraBoblin> @iFahadz20 @coaxialcreature @r_kleinsmith @GothamKnights Wel
1524110647176445953 2022-05-10 19:34:29 +0000 <SarcasmWinnipeg> @_BABACAR @SagED_UP programming!!!
1524110634245365761 2022-05-10 19:34:26 +0000 <buckplace271> @welllllpp @DraftExpress yes let me get my sarcasm in: I'm su
1524110632399867905 2022-05-10 19:34:26 +0000 <CSurvivor9> @gggreeneyes1975 Correct.
1524110632110460931 2022-05-10 19:34:25 +0000 <OlderGamer74> @Orangulent @WomensHealthMag @HilaryDuff And it's called sarc
1524110625638879232 2022-05-10 19:34:24 +0000 <SarcasticRofl> Red Fort is Shani Mandir ▶▶
1524110621851234306 2022-05-10 19:34:23 +0000 <XcuseMySarcasm> Lol I told these kids not to run down this hill, but nooo t
1524110616679653377 2022-05-10 19:34:22 +0000 <CSurvivor9> @enoch5040 Correct.
1524110589089521664 2022-05-10 19:34:15 +0000 <CSurvivor9> @DOW280TEN 🙄
1524110568508260352 2022-05-10 19:34:10 +0000 <Lokesh77198654> बहुत दिनों से बायकॉट का ट्रेड नहीं चला है लगता है साउथ इंडियन फिल्मों व
1524110568306757633 2022-05-10 19:34:10 +0000 <aaron_abbah> To think that I love sarcasm, on a whole different level, it's
1524110553827917824 2022-05-10 19:34:07 +0000 <thatswhatTYSaid> My sarcasm and my bitterness are both cold brewed.
1524110547112927232 2022-05-10 19:34:05 +0000 <CSurvivor9> @Polterbyte Correct.
1524110536245342209 2022-05-10 19:34:03 +0000 <zooystationaz> @GOPLleader It's a good thing the oil companies have even more

```

FIGURE 2: Scrapping Twitter data.

of satire that affects the social and personal relationship; the authors proposed that sarcasm evaluation bridges the gap between mutual communication of machines and humans. The work is based on four approaches lexicon, pattern, machine learning, and context-based. The project's goal is to demonstrate how current technology may be used to tackle social issues and barriers to free speech. The accuracy gained by their work is 96%. The key difference can be stated as utilising a hyperbolic feature set.

3. Materials and Methods

In this proposed work as in Figure 1, there are four categories that implement in accordance with the desired result: (a) collection of data; (b) preprocessing of the data; (c) feature creation; (d) sarcasm detection. Feature Creation are mentioned here with in Table 1.

3.1. Data Collection. Prior to any analysis, the collection of valid data is one of the prominent tasks in the evaluation of any subject. Validity of the data affects the whole process of analysis, and the collection of unbiased data that is wholly transparent and builds a bridge in understanding the sentiments in this case.

Twitter intelligence tool or twint is an advanced Twitter scraping tool in python that is used for scraping tweets from Twitter without Twitter API being used. The work in the following uses the following tool in order to collect data from Twitter with the keyword "sarcasm". A total of 10,000 tweets are collected using twint, and the processing on the following is done.

Figure 2 shows the full description of how data are gathered using twint in the following research. The code used

can be further generalized for any keyword, wherein here, it is specified for "sarcasm". The comparison of present work with other eminent researchers in this field has been summarized in Table 2.

10013 entries; 0 to 10012.

Data columns (total 38 columns).

3.2. Data Preprocessing. Data preprocessing is a technique used in data mining to change data into information that is more suitable for work. In the data preprocessing, the input data is first taken, and hashtags are located. These hashtags are eliminated from the data entry [9, 15]. The following module includes field selection, data cleaning including noise removal, tokenization, and stemming. The processing of the data gathered is done in the following way.

3.2.1. Desired Column Selection. Column selection is one of the major steps in processing the data. A greater impact is made only when the primary column that needs to be processed is used other than subjectify the whole dataset. Since the data collected comes with fields that may not necessarily be used in the processing, and hence it becomes vital for selecting a major column for the study.

Dataset here contains 38 columns mentioning id, tweets, hashtags, cashtags, usr_id, usr_id_name, etc. Before beginning the classification stage, several of the fields in this collection of Twitter data need to be processed. Work completed is specifically bound within the language parameter, i.e., English. Before processing the data, only those tweets are considered with specified language English, making the dataset specific to over 8000 rows. The area of concern is tweets, and hence all the other fields are dropped in

TABLE 2: Comparison with other work.

Authors	Sarcasm dataset	Classifiers used						Accuracy gained	
		LR	SVM	RF	KNN	DT	NB		AB
[8]	Twitter	•		•		•	•	•	DT: 71.05 NB: 75.18 RF: 77.94 AB: 76.06 LR: 32.03
[13]	Twitter: general election		•						SVM: 80
[19]	Twitter	•		•			•		NB: 57 LR: 80 RF: 80.5
[12]	Facebook		•				•		NB: 73.66 SVM: 88.3
[1]	Twitter	•	•						SVM: 79 LR: 80
[20]	Twitter		•	•	•				SVM: 77.9 KNN: 58 RF: 81

LR: Logistic regression, SVM: Support vector machine, RF: Random forest, KNN: K-nearest neighbor, DT: Decision tree, NB: Naïve Bayes, AB: AdaBoost.

```

+ Code + Text
[ ] df = pd.read_csv('tweets_sarcastic.csv')
df.head()

```

Unnamed: 0	id	conversation_id	created_at	date	timezone	place
0	15243833381466664961	15243833381466664961	1.652276e+12	2022-05-11 13:38:14	0	NaN
1	1524383334180306944	1524383334180306944	1.652276e+12	2022-05-11 13:38:03	0	NaN
2	1524383319588282369	1524383319588282369	1.652276e+12	2022-05-11 13:37:59	0	NaN

FIGURE 3: Data frame of Twitter data.

```

[2] df = pd.read_csv('tweets_en.csv')
data = df[['tweet']]
data.head()

```

tweet
0 #shoppingstar https://t.co/D42vV9R2
1 @GOP if you all want to take away MY Woman's r...
2 @loah_ @TaylenBader This is sarcasm right y'a...
3 @O_sasi @OfficialPDPNig @PeterObi Surely, the ...
4 @ChrisBertram33 @LincolnsBible Above I think w...

FIGURE 4: Data frame with language specification.

TABLE 3: Results obtained by different classifiers.

Classifier	Precision		Recall		F1-score	
	0	1	0	1	0	1
Decision tree	0.83	0.90	0.90	0.83	0.86	0.86
Naïve Bayes	0.78	0.90	0.90	0.77	0.84	0.83
KNN	0.49	0.98	1.0	0.07	0.66	0.14
SVM	0.89	0.98	0.98	0.89	0.93	0.93

TABLE 4: Accuracy for different classifiers.

Classifier	Accuracy
Decision tree	0.86
Naïve Bayes	0.83
KNN	0.51
SVM	0.93

the table, and a new data frame is made with just the column recognized as “tweets”.

Figures 3 and 4 describe the words stated above, where the only concerned data field, i.e., tweets are considered, and a new dataframe is made which will commence the further processing. Further Table 3 and Table 4 are summarizing the results and accuracy level obtained through different classifiers.

8174 entries; 0 to 8173.

Data columns (total 1 column).

3.2.2. Data Cleaning. Data cleaning is a process of removing incompetent data and making the data considerably informative for the desired study. Removing all the unilluminating data from the dataset for the desired output is the major concern of data cleaning. Since the data contains a lot of special symbols, removal of all the same is required. One common library in python that supports the cleaning of data is related to regular expression, named as “re”. Following is an example of data cleaning in the study.

```
Uncleansed Text:Hey-Can I ask some of my
fans on #twitter to #subscribe to my
#YouTube channel? Where I got none!
#podcast #socialmedia #sarcasm #NFL
```

```
Clean Text : Hey- Can I ask some of my
fans on twitter to subscribe to my
YouTube channel? Where I got none!
Podcast socialmediasarcasmNFL.
```

(1) *Noise Removal.* One of the factors for text analysis is noise removal. In text classification, it is vital to make data apprehensively beneficial in favour of the study. In order to achieve maximum output, processes are applied to data for the utmost results. A process for removing characters’ digits, URLs, stop words, punctuation, piece of text, etc., from the text is noise removal. The cleansed data is further used for the next phase.

In the work commenced, following Figure 5 is the example of noise removal, where the unwanted information depending on the goal of the project is done. Table 5 further describes the Accuracy Test for it.

```
Uncleansed text:@jackpuckering93
@ramsfanryan @Boro Surely suggesting
someone `enjoys a FFP charge` is
sarcasm, not irony. Anyway, Jack,
enjoy the Champo.
```

```
Cleansed text: Surely suggesting someone
enjoys a FFP charge is sarcasm not
irony Anyway Jack enjoy the Champo
```

(2) *Stop Words Removal.* Stop words can be defined as words that are commonly used in the English language. These words are removed as they are classified as non-useful words and take up space in database; therefore removal of these words is preferred for analysis.

```
Some common stopwords are ['i', 'me', 'my',
'myself', 'we', 'our', 'ours', 'ourselves',
'you', "you're", "you've", "you'll", "you'd",
'your', 'yours', 'yourself', 'yourselves',
'he', 'him', 'his'] etc.
```

In preprocessing, stop words are removed for the flexibility for the processed analysis; here is the output gained after removing these stop words from the column “tweets” to insure better classification.

```
Un-cleansed Data: Our brain is at smooth
it cant even detect sarcasm

Cleansed Data:brain smooth cant even
detect sarcasm
```

(3) *Tokenization.* One of the aspects of text processing is tokenization, dividing the text into smaller sections known as tokens with the use of delimiters. It is one of the main features of lexically analyzing the text [16]. Tokenization is performed on tweets to break them down into perfect meaningful modules from a sentence [8]. These tokens are further used as vocabulary in traditional NLP using count vectorize and TF-IDF. The division of data is further used in the analysis.

The following example stated below shows how data is tokenized done for in the tweets, considering the tweets, and following Figure 3 shows the code used to tokenize to make



FIGURE 5: Data after noise removal.

TABLE 5: Accuracy test.

Statement	Prediction using SVM
Trying some holiday at the office!	1
I am not busy but ttyl!	1
Ttyl	0

the sentence more meaningful in accordance with the analysis.

```
Uncleansed Data: life peronal pleasure
every moment day life suffering love
matter uncomfotable fear self
indulgence weakness character become
hate.

Cleansed Data:['life', 'personal',
'pleasure', 'every', 'moment', 'day',
'life', 'suffering', 'love',
'matter', 'uncomfotable', 'fear',
'self',
```

(4) *Stemming*. Stemming is another important aspect of natural language understanding, reducing the word to its stem making it viable in reducing the vocabulary and summarizing different words to their roots for input making it easier for the analysis. The main aim of this is to reduce the repetition of words by dropping the suffix of the word to arrive at the basic form of the word [16].

Utilization of stemming is done in the commenced work by reducing the word to its stem so that the vocabulary is reduced.

Figure 6 shows the words stemmed to their root and the data further ready for analysis.

(5) *Term Frequency Inverse Document Frequency*. The significance of a word (term) to a document within the corpus is quantified by the TF-IDF statistic [17]. In text summarization and classification software, TF-IDF is frequently used to end filtering words. Additionally, it is employed to

enhance a word’s frequency in a document proportionally. Inverse term frequency-document frequency (TF-IDF) is a part of information retrieval [16].

A numeric static concluding the importance of a word in the collection, further it is used in the work to detect the word occurrence and its importance. The following image as shown in Figure 7 shows the length of frequency. The code of the following is also mentioned in the same.

3.3. *Feature Creation*. After the data is fully cleansed, feature creation for further analysis is done. New features promoting the analysis are created. This feature helps in developing a data frame with useful fields that is feasible for further analysis.

Polarity classification, a fundamental component of sentiment analysis, examines whether an opinion on a certain trait or facet of a target is expressed in a document or a sentence. [5]. The new fields added are polarity and subjectivity in the respective study, whereas another research direction is subjectivity or objectivity identification [5]. Positive, negative, and neutral feelings are the three categories used to categorize sentiment analysis. Now that it is wise to know the polarity of a particular statement, different interpretations can be made in reference to the polarity, and moving forward is subjectivity; it defines whether a statement is under any subject. With the use of the text blob, polarity and subjectivity are classified.

Range Index: 8174 entries; 0 to 8173.

Data columns (total 3 columns):

3.4. *Sarcasm Detection*. Sarcasm and humor are key human characteristics and one of the largest gaps that artificial intelligence must bridge as they try to become more humanlike in intuition and behavior [1]. Although there are several algorithms in machine learning that are meant to accomplish precisely that, categorizing text based on its sentiment presents many particular difficulties. These can be summed up in the following query: “What kinds of features do we use? [18].”

The sarcasm detection in the proposed model is classified using different supervised categorical machine

	tweet	cleantweet
0	#shoppingstar https://t.co/Di42bVs6f2	shoppingstar
1	@GOP if you all want to take away MY Woman's r...	want take away woman right want take gun right...
2	@toah_ @TaylenBader This is sarcasm right y'a...	sarcasm right gotta start use tone indic shit ...
3	@O_ssai @OfficialPDPNig @PeterObi Surely, the ...	sure sarcasm confirm lol
4	@ChrisBertram33 @LincolnsBible Above I think w...	think sarcasm mayb someday rage amp bp rise move
5	Me: "I don't get affected if someone ignores m...	dont get affect someon ignor also someone doesn...
6	@scacewater Round up and tell the student he g...	round tell student got lucki way end semest lu...
7	Got a lot of laughs from this thread. It was f...	got lot laugh thread fun interact moron didnt ...
8	You are wrong. We all want trump on Twitter. W...	wrong want trump twitter love truth blunt sarc...

✓ 0s completed at 7:40 PM

FIGURE 6: Clean data after stop words, tokenizing, and stemming removal.

```

from sklearn.feature_extraction.text import TfidfVectorizer
# create the transform
tf_idf_vectorizer = TfidfVectorizer()
# tokenize and build vocab
T = tf_idf_vectorizer.fit(data.cleantweet)
print(len(T.vocabulary_))

```

10450

FIGURE 7: Length of vocabulary after vectorizing.

classification: decision tree, Naïve Bayes, KNN, and support vector machine. Decision tree classifier poses a series of carefully crafted questions about the features that are supplied to the algorithm [8]. Naïve Bayes is a log-linear model; that is, in both cases the probability of a document belonging to a class is proportional.

The model is trained and tested with a ratio of 80:20 split of the 8000 tweets collected. Accuracies are gained from different classifiers, and the prediction of a particular statement is done on the bases of the highest accuracy among the four classifiers.

4. Results

4.1. Dataset. Data generation in this era is immense. Data is gathered from different social networking sites. This data can be both informative and noninformative, purely based on the needs. In this work, data are gathered from one such networking site, Twitter, where millions of tweets are generated on a single day moreover a single topic. Since the work is to check whether a statement is sarcastic or nonsarcastic, the use of sarcastic tweets is done to train the model, using

the keyword “sarcasm”, and data is scrapped out of Twitter and classified as sarcastic or nonsarcastic on the basis of subjectivity after the cleaning of data. A total of 8000 tweets are gathered, with the preferred language English. Classification of sarcastic and nonsarcastic is done using 0 and 1, respectively.

4.1.1. Comparison Table

(1) *Experimental Evaluation.* The following Figure 8 shows the word cloud that is processed in the work. The use of the python library WordCloud is done for the formation of the figure. As the figure suggests, these are the following words that are majorly encountered in the tweets, specifying that the tweets related to sarcasm revolve around these words, making it efficient for the machine to learn and interpret for sarcasm detection.

The classifier model is trained using the dataset, and this paper authenticates the use of supervised classifiers for natural language processing; the result obtained is mentioned below in the table giving the precision, recall, and F1-score for each classifier. It can be clearly stated that the highest

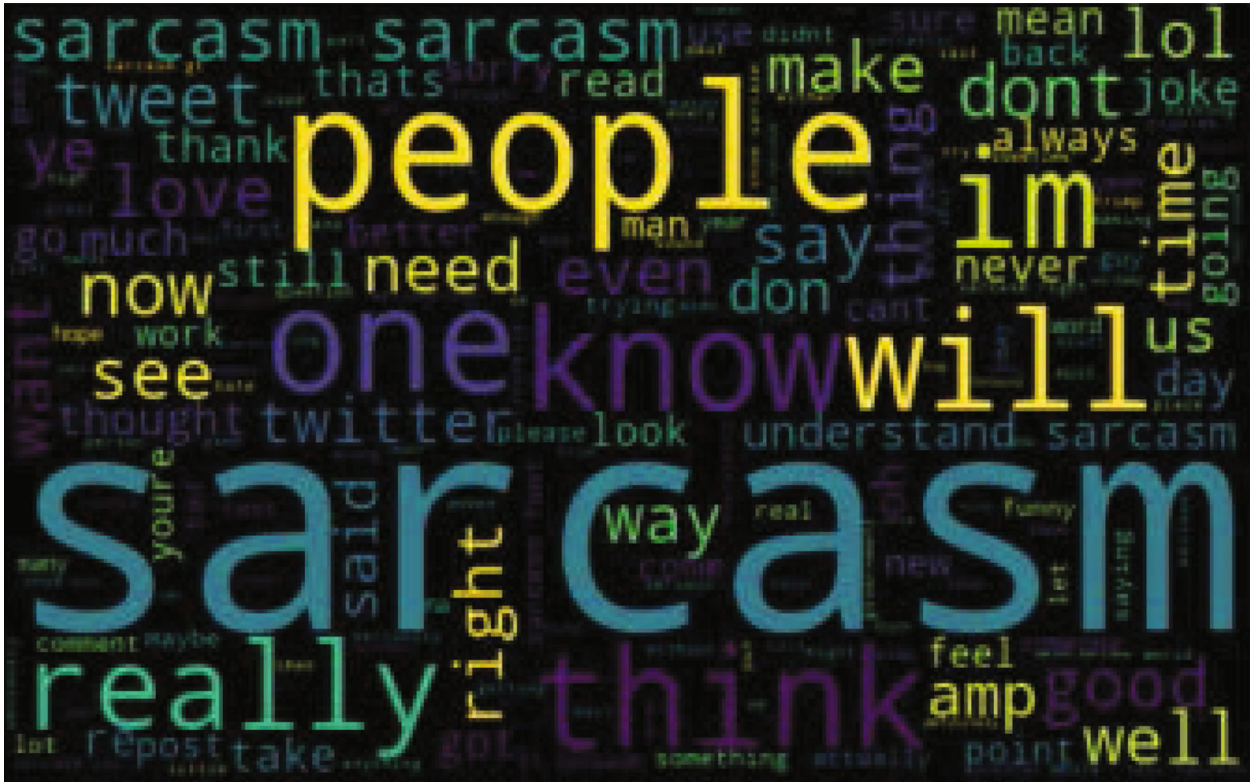


FIGURE 8: Word cloud.

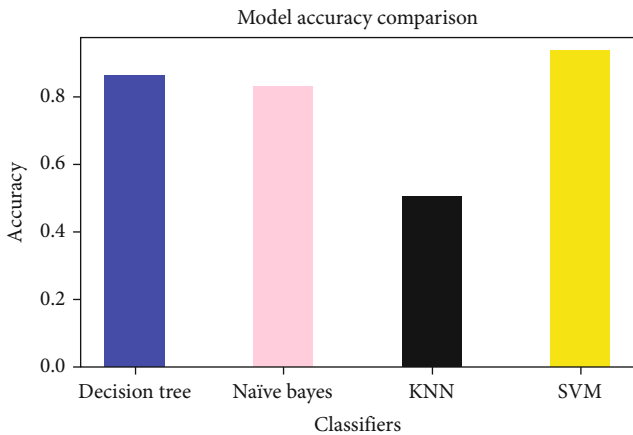


FIGURE 9: Model accuracy comparison.

accuracy is gained by SVM with 93% wherein the lowest is by KNN. Decision tree is performing greater than that of KNN; similarly, Naïve Bayes with an accuracy of 83% is also a good representative of the data.

4.2. *Evaluation Metrics.* For this study, the evaluation metrics of recall, precision, F1-score, and accuracy are used. The mathematical definition of these indices are expressed as follows:[21],where TP: true positive, FP: false positive, FN: false negative, and TN: true negative.

$$\text{Recall} = \frac{TP}{TP + FN}, \tag{1}$$

$$\text{Precision} = \frac{TN}{TN + FN}, \tag{2}$$

$$F1 - \text{score} = \frac{2TP}{2TN + FP + FN}, \tag{3}$$

$$\text{Accuracy} = \frac{TP + TN}{TP + FN + TN + FP}. \tag{4}$$

The Figure 9 shows the comparison of model accuracy gained by the different classifiers.

4.3. *Analysis.* The basic redemption of this work can be classified as the prediction of a statement; all the models are used although known that the highest accuracy is of SVM, testing was done by feeding different statements and evaluating whether the statement was sarcastic or not, using 0 and 1, respectively.

5. Conclusion and Future Work

By now, it is well known to us the diverse nature of data considering sarcasm; well it is not bound to any specification, and thus it becomes a challenge for a machine to interpret the sentiments of an individual, moreover, sarcasm. For a machine to adapt to these recurrent challenges, algorithms need to be processed time and again. Analyzing the sentiment of tweets gives an interesting insight to the opinions of the public about a certain event [6].Therefore; this work is purely based on the aspect of detection of sarcasm using Twitter data, which changes

itself repeatedly. By comprehending the intents and true thoughts of customers when reading their feedback or complaints, it also helps to improve the effectiveness of after-sales services or consumer assistance.

This paper aims the classification of sentiments categorized under positive, negative, and neutral sentiments, extending to sarcasm detection. The data collection is done through Twitter, which needs to be preprocessed before any conclusion. Different classifiers are involved in the preceding of our aim. It can be clearly stated that the different supervised algorithms are fit and reliable for the detection of sarcasm.

Future work with traditional machine learning and natural language processing can be used for classifying sarcastic tweets are positive sarcasm and negative sarcasm; this area of research can bring more clarity for a machine to understand sarcasm.

Further, there are an extended versions of sarcasm stated as satire, pun, banter, humor, etc., which can also be classified using the same technique, making machine to understand better and achieve the desired conclusion.

Data Availability

Real-time data has been taken from Twitter and can be available from the author upon request.

Conflicts of Interest

The authors declare that there is no conflict of interest regarding the publication of this paper.

References

- [1] L. I. Novic, "A machine learning approach to text-based sarcasm detection," 2022, https://academicworks.cuny.edu/gc_etds/4856Discoveradditionalworksat:https://academicworks.cuny.edu.
- [2] M. Razno, "Machine learning text classification model with NLP approach," *Computational Linguistics and Intelligent Systems*, vol. 2, pp. 71–73, 2019.
- [3] S. G. Wicana, T. Y. Ibisoglu, and U. Yavanoglu, "A review on sarcasm detection from machine-learning perspective," in *Proceedings - IEEE 11th International Conference on Semantic Computing, ICSC 2017*, pp. 469–476, San Diego, CA, USA, 2017.
- [4] P. Garg and V. Bassi, *Sentiment Analysis of Twitter Data Using NLTK in Python*, 2016.
- [5] L. Yue, W. Chen, X. Li, W. Zuo, and M. Yin, "A survey of sentiment analysis in social media," *Knowledge and Information Systems*, vol. 60, no. 2, pp. 617–663, 2019.
- [6] S. Parveen and S. N. Deshmukh, "Opinion mining in Twitter-sarcasm detection," *Politics*, vol. 1200, p. 125, 2017.
- [7] C. Sindhu and G. Vadivu, "Sentiment analysis and opinion summarization of product feedback," *International Journal of Recent Technology and Engineering*, vol. 8, no. 2S4, pp. 59–64, 2019.
- [8] A. G. Prasad, S. Sanjana, S. M. Bhat, and B. S. Harish, "Sentiment analysis for sarcasm detection on streaming short text data," in *2017 2nd International Conference on Knowledge Engineering and Applications (ICKEA)*, pp. 1–5, London, UK, 2017.
- [9] B. D. Dharmavarapu and J. Bayana, "Sarcasm detection in Twitter using sentiment analysis," *International Journal of Recent Technology and Engineering (IJRTE)*, vol. 8, no. 1, 2018.
- [10] A. Alsharef, K. Aggarwal, D. Koundal, H. Alyami, and D. Amedy, "An automated toxicity classification on social media using LSTM and word embedding," *Computational Intelligence and Neuroscience*, vol. 2022, Article ID 8467349, p. 8, 2022.
- [11] M. Bouazizi and T. O. Ohtsuki, "A pattern-based approach for sarcasm detection on Twitter," *IEEE Access*, vol. 4, pp. 5477–5488, 2016.
- [12] A. Alsharef, K. Aggarwal, M. Kumar, and A. Mishra, "Review of ML and AutoML solutions to forecast time-series data," *Archives of Computational Methods in Engineering*, pp. 1–15, 2022.
- [13] A. Khare, A. Gangwar, S. Singh, and S. Prakash, "Sentiment analysis and sarcasm detection of Indian general election tweets," 2022, <https://arxiv.org/abs/2201.02127>.
- [14] A. Aswitha, G. Shruthi, H. R. Shruthi, M. Upadhyaya, A. P. Ray, and T. C. Manjunath, "Sarcasm detection in natural language processing," *Materials Today: Proceedings*, vol. 37, Part 2, pp. 3324–3331, 2021.
- [15] J. Sharma, M. Arora, Sonia, and A. Alsharef, "An illustrative study on Multi Criteria Decision Making Approach: Analytical Hierarchy Process," in *2022 2nd International Conference on Advance Computing and Innovative Technologies in Engineering (ICACITE)*, pp. 2000–2005, 2022.
- [16] P. Dharwal, T. Choudhury, R. Mittal, and P. Kumar, "Automatic sarcasm detection using feature selection," in *2017 3rd International Conference on Applied and Theoretical Computing and Communication Technology (ICATccT)*, pp. 29–34, Tumkur, India, 2017.
- [17] S. M. Sarsam, H. Al-Samarraie, A. I. Alzahrani, and B. Wright, "Sarcasm detection using machine learning algorithms in Twitter: a systematic review," *International Journal of Market Research*, vol. 62, no. 5, pp. 578–598, 2020.
- [18] Y. Mejova, V. Shirsat, and R. S. Jagdale, *Sentiment Analysis: An Overview Comprehensive Exam Paper*, 2009.
- [19] T. Jain, N. Agrawal, G. Goyal, and N. Aggrawal, "Sarcasm detection of tweets: a comparative study," in *2017 Tenth International Conference on Contemporary Computing (IC3)*, pp. 1–6, Noida, India, 2017.
- [20] N. Pawar and S. Bhingarkar, "Machine learning based sarcasm detection on Twitter data," in *2020 5th International Conference on Communication and Electronics Systems (ICCES)*, pp. 957–961, Coimbatore, India, 2020.
- [21] A. Y. Muaad, H. JayappaDavanagere, J. V. B. Benifa et al., "Artificial intelligence-based approach for misogyny and sarcasm detection from Arabic texts," *Computational Intelligence and Neuroscience*, vol. 2022, Article ID 7937667, 9 pages, 2022.

Retraction

Retracted: Application of “TCM + Smart Elderly Care” in the Medical-Nursing Care Integration Service System

Journal of Sensors

Received 23 January 2024; Accepted 23 January 2024; Published 24 January 2024

Copyright © 2024 Journal of Sensors. This is an open access article distributed under the Creative Commons Attribution License, which permits unrestricted use, distribution, and reproduction in any medium, provided the original work is properly cited.

This article has been retracted by Hindawi following an investigation undertaken by the publisher [1]. This investigation has uncovered evidence of one or more of the following indicators of systematic manipulation of the publication process:

- (1) Discrepancies in scope
- (2) Discrepancies in the description of the research reported
- (3) Discrepancies between the availability of data and the research described
- (4) Inappropriate citations
- (5) Incoherent, meaningless and/or irrelevant content included in the article
- (6) Manipulated or compromised peer review

The presence of these indicators undermines our confidence in the integrity of the article’s content and we cannot, therefore, vouch for its reliability. Please note that this notice is intended solely to alert readers that the content of this article is unreliable. We have not investigated whether authors were aware of or involved in the systematic manipulation of the publication process.

Wiley and Hindawi regrets that the usual quality checks did not identify these issues before publication and have since put additional measures in place to safeguard research integrity.

We wish to credit our own Research Integrity and Research Publishing teams and anonymous and named external researchers and research integrity experts for contributing to this investigation.

The corresponding author, as the representative of all authors, has been given the opportunity to register their agreement or disagreement to this retraction. We have kept a record of any response received.

References

- [1] X. Wang, H. Shi, G. Lu et al., “Application of “TCM + Smart Elderly Care” in the Medical-Nursing Care Integration Service System,” *Journal of Sensors*, vol. 2022, Article ID 5154528, 7 pages, 2022.

Research Article

Application of “TCM+ Smart Elderly Care” in the Medical-Nursing Care Integration Service System

Xuanxuan Wang,^{1,2} Huaiying Shi,³ Guo Lu,⁴ Zhiping Huang,³ Yichen Zhang,⁵ Yumei Lao,³ Guangjie Li,³ Xun Gong⁶, Ping Wang², Xing Wang⁷, and Yidan Zhang⁴

¹Department of Integrated Traditional Chinese and Western Medicine, Hubei Cancer Hospital, Tongji Medical College, Huazhong University of Science and Technology, Wuhan, China

²Clinical College of Hubei University of Chinese Medicine, Wuhan, China

³Medical Administration Division of Cadre Sanatorium of Hainan & Geriatric Hospital of Hainan (CSH), Haikou, China

⁴College of Traditional Chinese Medicine, Hainan Medical University, Haikou, China

⁵Department of Biology, Shenzhen MSU-BIT University, Shenzhen, China

⁶Xi'an Innovation College of Yan'an University, Xi'an, China

⁷Xi'an University of Architecture and Technology, Xi'an, China

Correspondence should be addressed to Ping Wang; pwang54@163.com, Xing Wang; wx15829061908@163.com, and Yidan Zhang; bingdun0898@163.com

Received 21 July 2022; Revised 16 August 2022; Accepted 22 August 2022; Published 11 October 2022

Academic Editor: Sweta Bhattacharya

Copyright © 2022 Xuanxuan Wang et al. This is an open access article distributed under the Creative Commons Attribution License, which permits unrestricted use, distribution, and reproduction in any medium, provided the original work is properly cited.

As a country with the fastest population aging rate in the world, China's existing elderly care and medical resources are not enough to meet the growing and complex needs of elderly care and health services. The Chinese government is actively promoting the integrated development of medical and elderly care institutions, but it has yet to give full play to the inexpensive and existing advantages of traditional Chinese medicine in the treatment of diseases and rehabilitation of the elderly, by sorting out the advantages of “TCM + intelligent pension” in medical expenses, pension costs, disease prevention, intelligent pension services, and so on. In view of the current problems existing in China's pension, this paper mainly proposes to solve the pension dilemma in China from several aspects: improving the supervision and evaluation system, increasing capital investment, building a unified digital medical and pension service platform, and strengthening the talent training in the field of traditional Chinese medicine integration. The application of the “TCM + smart elderly care” system into the medical and elderly care service system is promoted to effectively improve the operation efficiency of the whole medical and elderly care service system and the satisfaction of elderly families.

1. Introduction

With the aging of China's society, people's health awareness has also been greatly improved. The development of the current healthy aging strategy must solve the problems of elderly care and medical care, which is also the key to the implementation of the current strategy. The normalization of chronic diseases in the elderly and the increase of the average life expectancy of the population are also the threshold of the current pension construction. China has the largest elderly population in the world and is one of the fastest

population aging countries in the world. The existing elderly care and medical resources are not enough to meet the growing and complex needs of elderly care and health services. On one hand, there is a relative lack of medical and health professionals in the existing institutions providing elderly care services, and the cost of medical services is high. On the other hand, the integrated development of existing medical and elderly care service institutions has not been realized, which is not only reflected in the lack of legal support in the policies and regulations of medical and elderly care service institutions, but in the allocation of medical and

elderly care service resources as well. In China, traditional Chinese medicine has a thousand-year-long cultural foundation and robust mass recognition, and it also has a unique role and advantages in elderly care. Life quality of the elderly can be improved utilising the unique advantages in medical treatment, elderly care, and disease prevention, especially in the treatment of chronic disease treatment. Thus, development of medical-nursing care integration and further development of elderly care could be realized. With the development of modern Internet technology and big data analysis, a proposal that Chinese governments at all levels and relevant departments promote the advantages of traditional Chinese medicine, apply “TCM + Smart Elderly Care” system into the medical and elderly care service system, and improve the work efficiency and satisfaction of the elderly is proposed. Therefore, the development of medical and nursing services can effectively solve the problems of high cost of elderly care services and low TCM nursing ability. It is also proposed to promote the application of “TCM + intelligent pension” in medical care from four aspects: improving the supervision and evaluation system, increasing capital investment, building a unified digital medical and pension service platform, and strengthening the talent training of TCM integration of elderly care.

2. The Obvious Population Aging Trend in China

By the end of 2021, there were 267.36 million people aged 60 or above in China, accounting for 18.90% of the total population, with 20.56 million people aged 65 or above, accounting for 14.2% of the total population. It is estimated that by 2050, the elderly population in China will reach a peak of 487 million, accounting for 34.9% of the total population [1]. For the first time in China, the number of people aged 60 and above surpasses that of those aged 0-15. According to the prediction of the United Nations, the period from 2000 to 2050 will be the stage of rapid aging of the population structure in China, which can be roughly divided into three stages: in the first stage, the proportion of the population aged 65 and above will rise from 6.97% in 2000 to 11.7% in 2020, a rise of only 4.63% in 20 years. The second stage is the period of rapid aging from 2020 to 2040, when the proportion of the population aged 65 and above will rise from 11.7% in 2020 to 21.8% in 2040, an increase of 10.1% in 20 years. The third stage is the peak plateau period from 2040 to 2050. This stage will be the serious stage of China's population aging, but the rate of population aging will begin to decline, and there will be only 1% increase in 10 years in the proportion of elderly population. China Elderly Care Financial Development Report (2016) pointed out that it is estimated that by 2030, the population over 65 years old in China will reach 280 million, accounting for 20.2% of the total population. In 2055, the elderly population will reach its historical peak, exceeding 400 million with a proportion rising to 27.2%. During this period, the aging rate before 2040 is the highest with the proportion increasing by 0.5% per year on average [2].

3. Current Status of Elderly Care in China

Developed countries in Europe and the United States become aging society when their per capita GDP is 5000-10000 USD, while China becomes aging society with a per capita GDP of 1000 USD [3-5]. According to the results of the seventh Chinese national census, there are over 260 million people aged 60 and above in China, accounting for 18.70% of the total population. More than 90% of the elderly are taken care of at home. However, the home-based elderly care service is still in its infancy in China. According to the survey conducted by Qiao Xiaochun, professor of Population Institute of Peking University, the proportion of home-based elderly care in Beijing is over 98% [6, 7]. Home and community elderly care systems at all levels in China are in the process of construction, but the system design requires to be perfected, and there is a lack in professional elderly care service institutions and nursing personnel.

In sharp contrast to China's huge elderly population, China's social elderly care service supply is seriously insufficient. Either the elderly care service institutions and facilities or professional medical and nursing service practitioners and management personnel are insufficient to meet the realistic needs in China. Nowadays, China's elderly care service personnel training is insufficient, high-quality medical care management personnel is in shortage, seriously restricting the development of China's social elderly care service. At present, China's county-level nursing homes are generally small in scale, with few beds, incomplete functions, and limited service capacity. The size of common elderly care service institutions is generally small, most of which are rebuilt from other facilities, with low professional service level and lack of professional service personnel. Some also have hazard in fire and food safety.

At present, China's elderly care system is based on the “9073” model, which is based on home care, supported by community care and supplemented by institutional care. That is, 90% of the elderly are taken care of at home, 7% are supported by community elderly care services, and 3% are taken care of in elderly care institutions.

According to the 2021 Blue Book on Pension Risks for the Middle Class in Large and Medium-sized Cities, jointly released by AIA and the World Social Security Research Centre of the Chinese Academy of Social Sciences, among the survey samples of more than 5,000 urban residents with annual incomes of 100,000 yuan or more in 10 cities, 70% of them have not participated in any annuity or commercial insurance plan, and the replacement rate of social pension income is only about 35% [8, 9]. Different from developed countries in Europe and the United States, China faces the dilemma of “the higher the income, the lower the pension replacement rate.” The second and third pillars did not compensate well, and the participation rate of this survey sample was only 20%.

According to the Report of High Quality Development of Yangtze River Delta Elderly Care Finance, jointly released by Changjiang Endowment and First Finance and Economics, by the end of 2019, as the first pillar of elderly care finance, the basic endowment insurance fund and the

national social security fund took up a proportion of 71.7%, enterprise annuity and occupational pension combined as the second pillar accounted for 22.4%, while in the third pillar, the income of commercial pension insurance and institutional individual tax deferred commercial pension insurance only accounted for 5.9%, far lower than the United States (the proportion of the third pillar reached 31.3% in 2019) and other developed countries [10].

4. Advantages of “TCM + Smart Elderly Care” in Medical-Nursing Care Integration

4.1. Advantages in Medical Expense. According to statistics from the National Health Commission, stroke, hypertension, diabetes, chronic obstructive pulmonary disease, and other chronic diseases have become the main health problems of Chinese residents [11, 12]. The elderly with gradual degradation of body function and imbalance of Yin and Yang and five elements is a group with high incidence of chronic disease. The unique advantages of the overall concept of TCM and balance of Yin and Yang and five elements can be utilised in treatment. The pathogenesis of diseases in the elderly can be understood through diagnosis methods of TCM. The use of internal and external treatment, acupuncture, massage, cupping therapy, and other TCM therapies can achieve the balance of Yin and Yang, replenish Qi, increase blood, delay aging, and play an obvious role in the treatment of chronic diseases of the elderly.

4.2. Advantages in Elderly Care Expense. TCM plays a unique role in chronic disease therapy and health care for the elderly. As Su Wen: Shang Gu Tian Zhen Lun said, “Understand the law of Yin and Yang. Follow the correct method of preserving health. Eat meals regularly. Do your exercise properly.” Self-health care can be achieved by develop a reasonable diet habit, standardize the daily life work and rest schedule, and adjust personal mood properly [13]. Regarded as the achievement of Chinese people’s wisdom, TCM after thousands of years of development formed the Chinese herbal medicine therapy of both internal and external medication, ointment, fumigation, pesticide, and other nondrug therapy such as seasonal diet, exercise, acupuncture, and massage. In such way, meridians can be activated, Qi and blood regulated, body strengthened, physical fitness of the elderly improved and is essential for elderly health care. The effect of TCM therapy is basically the same as that of aromatherapy widely used in European and American countries in the prevention and rehabilitation of diseases for the elderly. The elderly health care method of TCM is the inheritance and development of the concept of keeping healthy in China for two thousand years. It contains excellent Chinese traditional culture spirit and has obvious advantages in technology and cost in the elderly care service.

4.3. Advantages in Disease Prevention. The elderly is a group with high incidence of chronic diseases. Effective disease prevention methods can reduce the occurrence of chronic diseases and play a great role in improving the quality of life of the elderly. As is said in Huang Di Nei Jing, “the sage does

not cure disease but prevent disease, does not cure disorder but prevent disorder.” The concept of “prevent” in TCM runs through the whole cycle of disease cure from disease prevention to recurrence prevention after recovery [14, 15]. The concept of “prevent” is based on the diagnosis method of “look, listen, question and feel the pulse” of TCM to effectively intervene in people’s physical health, and at the same time, with the help of the principle of emotion regulation of TCM, to carry out psychological counselling and disease decompression training for the elderly, so as to maintain a good state of mind and mood. Also, with the help of emotion regulation, reasonable diet, regular sleep, and Ba Duan Jin and Tai Chi exercise, it is realized to prevent diseases before occurrence, play an important role in the treatment of chronic diseases, improve the quality of life of the elderly, and meet the elderly care demand of preventing diseases and pursuing health better.

4.4. Technical Advantages of Smart Elderly Care. “Internet + TCM + Smart Elderly Care” can effectively integrate online and offline resources and expand the application of information technology in the field of elderly care services. The data collected by a unified comprehensive information platform for elderly care can be shared and exchanged between the national medical care integrated information system and the “Healthy Fujian” platform and promote information sharing, in-depth development, and rational utilization of health information and elderly care service information of the elderly. The elderly can obtain personal health and disease diagnosis information through various terminals. Government elderly care service regulation departments can achieve supervision of the whole process of services, including the latest epidemic situation, institution rating, service quality, beds subsidy, combined punishment, and elderly care service personnel management. Information regarding the elderly can be shared among government elderly care and health service departments and elderly care service and supervision can be promoted.

5. SWOT Analysis of the “Traditional Chinese Medicine + Intelligent Pension” Mode

SWOT analysis is also known as situation analysis, in which “SWOT” represents advantage (strength), disadvantage (weakness), opportunity (opportunity), and threat (threat), respectively. This part conducts a systematic evaluation of four aspects of TCM AI development through SWOT analysis (Table 1).

5.1. Advantage. Artificial intelligence has two obvious advantages of assisting clinical medical activities and realizing dynamic health management. Experts point out that TCM intelligence cannot replace doctors, but it can be used as the assistant to doctors, and the preview function helps doctors and patients save time and assist the clinical diagnosis of TCM; experts also believe that TCM intelligence can realize dynamic health management, disease warning, especially in remote mountainous areas and other health stations and backward medical suburbs.

TABLE 1: SWOT analyzes the four aspects of the development of “Traditional Chinese medicine + intelligent pension”.

Superiority-S	Weakness-W	Opportunity-O	Challenge-T
Assist in clinical medical activities; realize dynamic health management	The algorithm design and model construction are unreasonable; lack of professional personnel; lack of humanistic care	The introduction of relevant policies; progress in computer technology; market demand is wide	Technical standards are difficult to be unified; poor equipment use experience; database establishment faces a bottleneck

5.1.1. Assisted Clinical Medical Activities. Through comprehensive and objective data collection, mining, and in-depth analysis, TCM AI forms patients’ electronic medical records to help clinicians to understand patients’ current disease status and past diagnosis and treatment history, provides an objective reference basis for clinical diagnosis, and reduces the probability of misdiagnosis and missed diagnosis. At the same time, the prediagnosis and pre-examination function of TCM artificial intelligence can help patients to understand the development of their own disease in advance, help patients to choose the right way to seek medical treatment, and save patients’ time and money costs.

5.1.2. Realization of Dynamic Health Management. Traditional wearable health management devices stay at the level of data collection and prediction. Users can only obtain their own health status, but they cannot obtain correct and reasonable health management measures. However, in dealing with subhealth states, crude data analysis and prediction will no longer be used. Therefore, the analysis and mining of massive big data have become the breakthrough point to solve this problem. Intelligent wearable devices can use big data analysis technology to help users to identify their physical fitness and provide appropriate health management solutions. However, the government and health service agencies can derive the diseases and health characteristics of people in different regions, generate disease profiles, timely identify high-risk groups, and carry out effective intervention measures.

5.2. Disadvantages. At present, the “TCM + intelligent pension” mode still has the following problems: the development of TCM AI has disadvantages such as unreasonable algorithm design and model construction, lack of TCM AI composite talents, and lack of humanistic care.

5.2.1. Algorithm Design and Model Construction Are Unreasonable. At present, many AI devices excessively isolate the relationship between diagnosis and diagnosis. In the face of diseases with a single condition and a clear diagnosis, AI devices can still provide better diagnosis plans, but in the face of more complex cases, the lack of diagnostic flexibility and flexibility will be highlighted. Moreover, many devices lack the ability of independent learning and cannot carry out independent learning and judgment based on probability theory. As the collected data continues to accumulate, the work of improving the later optimization and upgrading still needs to be completed manually, which increases the maintenance cost of intelligent devices.

5.2.2. Lack of TCM AI Talents. According to the Global AI Talent Report, there are only over 50,000 AI talents in China, with only one-tenth of those working in the medical sector, while even fewer talents in TCM. At present, most of the scientific research units in the development of TCM AI equipment are TCM universities, and there is a relatively long-term gap between compound talents in the two fields of TCM and artificial intelligence.

5.2.3. Lack of Humanistic Care. Although the diagnosis and treatment of artificial intelligence brings great convenience to medical activities, it cannot give humanistic care to patients. In addition to enduring the physical pain caused by the diagnosis and treatment process, patients are also under huge psychological pressure. Doctors need to give humanistic care to patients, not just as “machines waiting for repair.” In addition, patients are often unable to accurately describe their condition due to great psychological stress and lack of expertise, or to illness limitations. Because to this ambiguous or distorted information, AI instrument applicability will be severely challenged.

5.3. Opportunities. In recent years, TCM AI has welcomed many opportunities. First, the introduction of relevant policies can provide a more appropriate environment for the development of AI; second, the progress of computer technology can promote the improvement of TCM AI algorithm; and third, the market demand is extensive, so that TCM AI can alleviate the uneven distribution of medical resources in China.

5.3.1. Introduction of Relevant Policies. With the rapid development of artificial intelligence and people’s growing demand for health, the Chinese government and relevant departments also attach great importance to the combination of artificial intelligence and medical and health care and have successively issued a number of policies to encourage and guide the development of intelligent medical care. The opinions on promoting the development of “Internet + Medical and Health” issued in 2018 also introduced AI technology into the field of TCM, emphasizing the development and application of the intelligent auxiliary system for TCM syndrome differentiation and treatment and creating a new environment for the development of TCM AI.

5.3.2. Progress in Computer Technology. Basic computer technologies such as computing power, algorithm model, data resources, and microsensors are becoming increasingly mature and perfect, which provides the possibility to fill the algorithm loopholes of TCM intelligent devices.

5.3.3. Extensive Market Demand. In 2018, China made more than 8.3 billion visits to medical treatment, with 6.0 visits per person, compared with 2.59 doctors per 1,000 people. In addition, the distribution of medical resources in China is uneven in China. High-quality medical resources are mainly concentrated in economically developed cities such as Beijing, Shanghai, and Guangzhou, while TCM resources in rural and remote areas with underdeveloped economy and inconvenient transportation are lacking. The imbalance has led to large numbers of patients flocking to big hospitals in big cities and overloading local healthcare workers. Therefore, the development of auxiliary diagnosis and treatment and pre-examination system can effectively relieve the pressure of outpatient and emergency hospitals and also promote the implementation of three-level diagnosis and treatment.

5.4. Challenge. At present, TCM AI faces two challenges. First, the establishment of a TCM large database faces a bottleneck. In the interview process, experts pointed out that most of the databases used by intelligent devices are collected independently by the development units, which is difficult to realize data interaction and establish a big data network with a wide range of application. Second, the current utilization rate of TCM intelligent equipment is not high, and the experience sense is not strong.

5.4.1. The Establishment of a TCM Large Database Faces a Bottleneck. There is no unified standard for the establishment of TCM database, which is the main difficulty in establishing a consistent TCM database. According to the interview experts, due to the different understanding of diseases and diagnosis and treatment methods, the language description is also controversial, which makes a large number of incomplete data and missing data in the TCM database, leading to a bias in the analysis and utilization. However, the state has not issued personal privacy security and other issues in the process of data collection without relevant laws and regulations. In the process of data collection, it is a key problem to clarify the ownership of the rights and responsibilities of information collection, storage, management, sharing, and use.

5.4.2. Poor Equipment Use Experience. At present, the utilization rate of TCM intelligent equipment is not high, and the experience sense is not strong. There are three reasons for this phenomenon: first, the current use experience of TCM artificial intelligence, the intelligent equipment cannot cope with the complex and changeable conditions, and the operation is complicated and inefficient; second, the quality of TCM medical staff is generally inefficient; third, TCM intelligent equipment maintenance and update, equipment upgrading, and data maintenance, the high cost affects the popularization of TCM intelligent equipment at the grassroots.

6. Existing Problems

6.1. Multiple Government Department Management and Imperfect Supervision Evaluation System. The Chinese government has introduced many policies to benefit the people in order to support the development of the TCM model of

combining medical care with elderly care. But this model involves the human resources and social security department, health department, civil administration department, TCM management department, medical insurance management department, finance department, big data management department, and other concerning departments. As a result, department functions and responsibilities are still unclear, for instance, health and elderly care resource integration lags behind caused by multiple management of medical insurance expense reimbursement, effective cohesion, and deep integration is absent, resulting in the fragmentation of elderly care funds, due to the imperfection, ineffective implementation, or unstable implementation of the supervision and evaluation system, elderly care service level of various medical, and nursing institutions varies.

6.2. High Elderly Care Expense and Imperfect Medical Insurance Policies. To establish the TCM medical and elderly care service system requires a large amount of money to introduce professional medical personnel and increase infrastructure. As investment costs increase, elder care expense will also increase, and full payment will bring burden to most families. At present, the market of medical and elderly care service system is not mature, the market access mechanism is not perfect, and the high risk of social investment leads to low investment enthusiasm. In addition, the old-age medical insurance system is not perfect, and the TCM diagnosis and treatment, nursing, massage, and other expenses of medical and nursing institutions are either not all included in the medical insurance reimbursement policy or the reimbursement ratio is low, which will become a key factor affecting the development of TCM medical and elderly care service system.

6.3. Serious Shortage of Medical and Elderly Care Service System Professionals and Insufficient TCM Elderly Care Capacity. The insufficiency of TCM elderly care professionals seriously affects the development of TCM medical and elderly care service system. At present, there is not enough attention to the elderly care service in the TCM education system. There are few universities and professional training and education institutions offering TCM elderly care specialty, and the professional supply obviously lags behind the elderly care demand. At the same time, factors such as high intensity of elderly care work in TCM institutions, low payment, and difficulty in promotion make relevant professionals reluctant to work in elderly care institutions. Most of the medical service staff are retired people or domestic service staff with junior and senior high school degrees, while few of them are highly educated and have certificates.

6.4. Lack of High-Level TCM Talents. At present, China has not yet established a sound and perfect TCM medicine and health service system, especially the lack of relevant professional and technical personnel, pension institutions are often at a disadvantage compared with hospitals, and talents have become the bottleneck of the sustainable development of pension institutions. In addition, due to the limited development space provided by pension institutions, those high-

quality talents are unwilling to be limited by the limited development space and difficult to guarantee the salary, which further hinders the implementation of the combination of medical care and nursing care in pension institutions. Second, most traditional Chinese medicine doctors have been working in western medicine in social health centers for a long time, and the concept of traditional Chinese medicine has gradually weakened. Therefore, it is necessary to strengthen the training of TCM talents, such as organizing TCM skill training courses, signing TCM technical support agreements with superior TCM hospitals, and increasing the introduction of TCM talents.

6.5. Lack of Standardization of Resource Allocation. The existing nursing institutions have little allocation of TCM resources, and many nursing institutions do not even have TCM nursing services. Without the management and guidance of standardized documents, community health service centers and elderly care institutions cannot reasonably plan the allocation of TCM resources, which is bound to not give a place to TCM nursing. Related elderly care institutions are more powerless in promoting the combination of TCM nursing and elderly care services. Although TCM nursing services have a large demand and involve a wide range of areas, if good planning cannot be carried out and corresponding standards are formulated before the implementation, the implementation plan may not be systematic, and it will face many difficulties in the process of promotion, which ultimately makes it difficult to carry out various TCM nursing projects smoothly.

7. Recommended Solutions

7.1. Continue to Strengthen Government Guidance and Improve the Supervision and Evaluation System. First of all, it is of vital importance to define the government department responsibility, establish the interdepartment coordination mechanism, break departmental administrative barriers, sort out department responsibilities, gradually straighten out policies to promote the development of medical and elderly care service system, and ensure the effective interdepartment connection and collaboration of policy. Full use of Internet technology system and the urban cloud platform should be made. Additionally, it is effective to utilise the special advantage of TCM in medical and elderly care service system. A sound cooperation mechanism should be established between TCM and recuperation institutions; more medical and nursing resources should be provided to rural areas, communities, and families; and deep integration of medical resources, elderly care institutions resources, and TCM resources should be promoted. Second, the government should strengthen the evaluation, supervision, and management of TCM elderly care service institutions; improve the information monitoring system; establish the elderly care demand assessment system; ensure policy effective implementation; and form a long-term and stable TCM “medical and elderly care integration” elderly care model. Third, the comprehensive security system for long-term care should be thoroughly studied; policy support for the handi-

capped elderly and their families should be increased; and the effective supply of quality elderly care services should be taken seriously.

7.2. Increase Capital Input and Give Full Play to the Role of Medical Insurance. Due to the high construction cost of TCM medical and elderly care service institutions, government should set up special funds to increase financial support, lower the threshold of social access, relax policy support restrictions, and encourage social capital to actively participate in the construction of TCM medical and elderly care service institutions. At the same time, government should formulate medical insurance policies that accord with the characteristics of TCM, promote eligible elderly care services of TCM and TCM materials into the scope of medical insurance coverage, increase the old-age service reimbursement ratio, and promote multi-cooperation to fully utilise medical insurance so as to ease pressure of the high cost of elderly care services, provide affordable medical and elderly care services to the elderly, and promote better benefits to people of TCM.

7.3. Build a Unified Digital Medical and Elderly Care Service Platform and Utilise the Efficacy of Big Data. Digital platforms should be established to link government service with market service and to provide convenient services of elderly care policies, public service, and public welfare services for all users. It should be aimed to realize that in one platform can elderly care service supply be provided, with one set of data can elderly care service resources be controlled, on one mobile phone can elderly care services be handled, on one map can elderly care service situation be shown, with one set of algorithms can elderly care intelligence decision be assisted. Big data, IoT, and blockchain should be utilised to strengthen the support of science and technology, make elderly care services more convenient, and make government subsidies more targeted. Health care consortium should be utilised in mechanism integration and resource integration to provide high-quality health care services for the elderly.

7.4. Strengthen Personnel Training in the Field of TCM Integration in Medical and Elderly Care. Strengthening the training of TCM professionals is the key driving force to promote the development of TCM medical and elderly care system. To start with, TCM elderly rehabilitation, TCM elderly nursing, and other relevant majors could be set up in colleges and universities. Professionals can be introduced to TCM elderly care institutions through special training and specialised training. In addition, personnel training system should be improved according to the service demand; training of TCM theory, knowledge, and skills should be strengthened; assessment criteria should be standardized; qualification access should be set up; and personnel vocational level of TCM in the medical and elderly care service industry should be improved constantly. Last but not the least, an evaluation and incentive system should be established and perfected, salary and compensation system should be optimised, basic salary of nursing staff should be

Retraction

Retracted: Architectural Interior Design and Space Layout Optimization Method Based on VR and 5G Technology

Journal of Sensors

Received 23 January 2024; Accepted 23 January 2024; Published 24 January 2024

Copyright © 2024 Journal of Sensors. This is an open access article distributed under the Creative Commons Attribution License, which permits unrestricted use, distribution, and reproduction in any medium, provided the original work is properly cited.

This article has been retracted by Hindawi following an investigation undertaken by the publisher [1]. This investigation has uncovered evidence of one or more of the following indicators of systematic manipulation of the publication process:

- (1) Discrepancies in scope
- (2) Discrepancies in the description of the research reported
- (3) Discrepancies between the availability of data and the research described
- (4) Inappropriate citations
- (5) Incoherent, meaningless and/or irrelevant content included in the article
- (6) Manipulated or compromised peer review

The presence of these indicators undermines our confidence in the integrity of the article's content and we cannot, therefore, vouch for its reliability. Please note that this notice is intended solely to alert readers that the content of this article is unreliable. We have not investigated whether authors were aware of or involved in the systematic manipulation of the publication process.

Wiley and Hindawi regrets that the usual quality checks did not identify these issues before publication and have since put additional measures in place to safeguard research integrity.

We wish to credit our own Research Integrity and Research Publishing teams and anonymous and named external researchers and research integrity experts for contributing to this investigation.

The corresponding author, as the representative of all authors, has been given the opportunity to register their agreement or disagreement to this retraction. We have kept a record of any response received.

References

- [1] Y. Wu, "Architectural Interior Design and Space Layout Optimization Method Based on VR and 5G Technology," *Journal of Sensors*, vol. 2022, Article ID 7396816, 10 pages, 2022.

Research Article

Architectural Interior Design and Space Layout Optimization Method Based on VR and 5G Technology

Yang Wu 

Academy of Fine Arts, Nanjing Xiaozhuang University, Nanjing, 210000 Jiangsu, China

Correspondence should be addressed to Yang Wu; wuyang@njxzc.edu.cn

Received 11 August 2022; Revised 12 September 2022; Accepted 22 September 2022; Published 8 October 2022

Academic Editor: Sweta Bhattacharya

Copyright © 2022 Yang Wu. This is an open access article distributed under the Creative Commons Attribution License, which permits unrestricted use, distribution, and reproduction in any medium, provided the original work is properly cited.

With the continuous optimization of the living environment, people's requirements for its comfort and cultural taste are also constantly improving, and their understanding and requirements for the appearance and style of the building and the layout of the building space have been further deepened, thus forming a situation of diversification and diversification of the style and form of the architectural appearance and interior design. There are a lot of layout problems in modern engineering and real life, and the indoor space layout is a very important branch. The indoor space layout focuses on the indoor scenes that people rely on for production and life. At the same time, indoor scene models are gradually applied to more and more fields. The urgent need for indoor scene modeling has also led to relevant research on indoor space layout. Because of its wide application prospects and great commercial value, indoor space layout has become an important research topic in the field of computer graphics and computer vision. As the computer-aided design is widely used in the field of intelligent design, indoor space layout has also become an important research field. Focusing on the automatic design and optimization of indoor space layout, this paper proposes an optimization method based on design constraints for the automatic generation of a layout plan based on the given layout boundary or layout space. The room units in the interior space layout are represented by polygons composed of multiple rectangles, and the constraints and rules in the layout design are transformed into constraints on related rectangles. Experimental results show that our scene redirection method is effective. Comparing with the results of uniform scaling further proves the effectiveness of our redirection algorithm.

1. Introduction

Generally speaking, layout design is about the reasonable arrangement and proper placement of objects. There are a lot of layout design problems in modern engineering and real life, such as the layout of VLSI, the container shipping of freight terminals, and the architectural layout design of the construction field. Because layout design has a wide range of application prospects and great commercial value, layout design problems everywhere make layout research have universal and profound practical significance [1]. Space layout design is the main content of layout design because most layout design problems are closely related to space, such as the cutting of one-dimensional space, the indoor layout plan design of two-dimensional space, and the cockpit layout of three-dimensional space. The so-called spatial layout design refers to dividing a given space into

a combination of small spaces or reasonably arranging some objects to be laid out in the space under the constraint framework of some objective and subjective layout conventions and design criteria [2]. The research on spatial layout design stems from the fact that traditional methods cannot meet the current needs of efficient design. Traditional layout design is often designed manually by designers or aided by interactive modeling software. Due to the limitation of designers' professional ability and knowledge level, traditional layout design is mainly based on repeated trial and error and requires a lot of professional knowledge, design experience, and creative intuition [3]. The key points of interior design space layout are shown in Figure 1.

Because the traditional design mode mainly depends on manpower, the design process often consumes a lot of manpower and energy. Therefore, changing the traditional layout

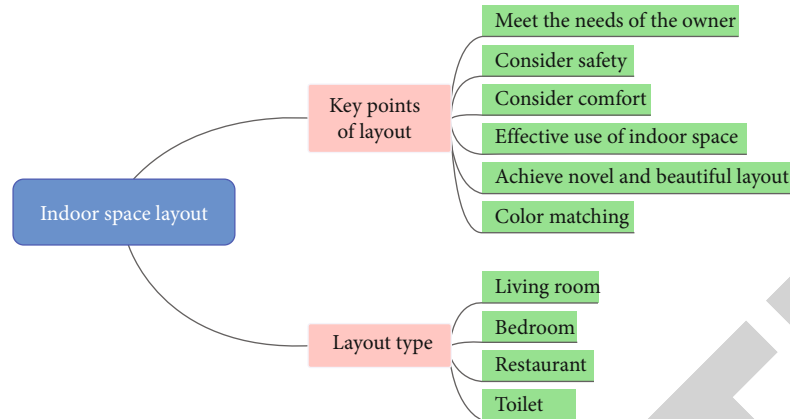


FIGURE 1: The key points of interior design space layout.

design mode and realizing the automatic design of spatial layout have become an urgent research problem in the current industry and academia. Since the 1960s, computer-aided design has been widely used in the field of intelligent design, and computer-aided layout design has gradually formed [4]. This field involves mathematical modeling, modern optimization, artificial intelligence, graphic interaction, and other related technologies. With the development of computer-aided design and the rise of artificial intelligence, as an important research field of intelligent design, the application and research of spatial layout design have also entered a new stage. Indoor space layout focuses on indoor layout, which is not only an important research problem in interior design but also an important research direction in layout design [5]. Compared with other types of layout problems, indoor space layout has more research value. Indoor space layout is widely used in interior design, computer games, virtual reality, and other fields. Among them, in the field of architecture, indoor space layout includes the design of a layout plan and the layout optimization of indoor scenes. The traditional indoor space layout mode often costs a lot of manpower because it widely relies on labor. In the field of games, in order to reduce the cost, the scene design of large-scale computer games often reduces the indoor scene model as much as possible or reuses the existing scene model, which will weaken the diversity and authenticity of the game scene and seriously affect the user's game experience. In the field of virtual reality, indoor scenes are one of the most used scenes of VR or AR technology [6]. However, indoor scenes in virtual reality are often carefully designed by professional designers and need to adapt to the real physical environment where users live. Such strict design requirements make indoor space layouts more and more important in the field of virtual reality. The automatic design and optimization of indoor space layout can be applied to these fields: assist indoor scene modeling by automatically designing the layout plan of the indoor scene and optimizing the home layout of the indoor scene [7]. Through the automatic design of indoor space layout to achieve the efficient creation of large-scale indoor scenes in computer games and through the optimization of indoor space layout, virtual roaming can be realized in the actual

physical space of various scales. With the increasing demand for indoor scene modeling, indoor space layout has aroused widespread interest in academia and has gradually become a research hotspot in the field of computer-aided design.

The automatic design and optimization of indoor space layout have important research significance. On the one hand, due to the important application background of indoor space layout in many fields; on the other hand, the traditional layout design relies heavily on labor and is inefficient [8]. The existing layout design methods are simple and immature, and there are a series of problems such as unsatisfactory effects and complex human interaction. The automatic design and optimization of indoor space layout can greatly reduce the workload of designers, and even directly serve users. The ultimate goal of automatic design and optimization of indoor space layout is to follow and simulate the designer's design thinking in the design process and strive to achieve automatic or intelligent design [9]. This can greatly reduce the workload of designers to improve the efficiency and quality of layout design, and even directly reduce the threshold of layout design, serve the majority of users, and let more ordinary users become designers. Focusing on the automatic design and optimization of indoor space layout, this paper proposes an optimization method based on design constraints for the automatic generation of a layout plan based on the given layout boundary or layout space. The room units in the interior space layout are represented by polygons composed of multiple rectangles, and the constraints and rules in the layout design are transformed into constraints on related rectangles.

2. Related Work

2.1. Research Status of VR Technology. VR technology is virtual reality technology, which enables real people to experience the same things and things as the real world in the virtual information world created by computers. It has the basic characteristics of multi-perception, immersion, interaction, and imagination. This virtual technology integrates many kinds of science and technology, such as computer graphics and image technology, reality simulation technology, and multimedia technology [10]. However, due to the

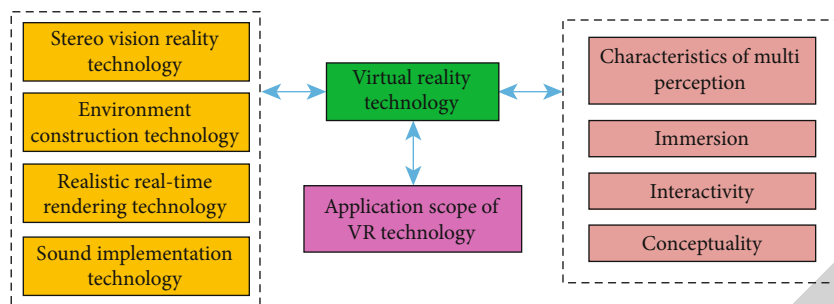


FIGURE 2: The introduction of virtual reality technology.

limitations of current technology and sensing technology, it can only simulate ordinary perception systems. Immersion, also known as immersion or telepresence, existence, etc., specifically refers to the real experience of people in the virtual world in the first person. Of course, the current technology has not reached the optimal level [11]. Conceivability, that is, in the virtual world, presents the things that the objects you want to do in the virtual world, what effect can be achieved by doing so, and even the things and things that cannot exist in the real world can be conceived in the virtual world. [12]. The information obtained by humans through vision is the most one of all human senses, so stereo display technology plays an indispensable role in virtual reality technology. The introduction of virtual reality technology is shown in Figure 2.

The integration of digital technology into environmental space design can improve the humanization and appeal of the environment, so as to enhance people's participation in the environment and effectively improve the interaction between the environment and people. Although digital technology relies on the combination of science and technology and artistic elements, we need to recognize that digital technology is a way of expressing design, and the designer's thinking and design of the site is the basis for the implementation of the design scheme. One of the significant advantages of digital design compared with previous modeling design is its telepresence [13]. The key to creating telepresence is an immersive experience, and the immersive effect of VR digital technology depends on people's perception of it. When people perceive the visual, olfactory, gustatory, tactile, and other stimuli brought by the virtual world, the brain will receive the positive feedback of this information, forming psychological immersion, just like entering the real world and personally feeling the whole site. Digital design can also play an important role in the selection of design styles [14]. When designing a large-scale environmental space, the designer will integrate environmental psychology and the knowledge of various professional disciplines, and carry out the design according to the location conditions obtained from the analysis in the early stage of the design, combined with the historical and cultural background around the design area. The purpose of environmental space design is to coordinate the contradiction between the design coordinator and the site [15]. If the designer does not consider the surrounding environment, it is tantamount to designing an island in the city. In order to avoid this phe-

nomenon, designers can choose a design style that is more suitable for the site through VR technology, so as to avoid the design being out of tune with the surrounding environment in urban planning.

This digital furniture has realistic lighting and shadows, which are coordinated with the surrounding real environment [16]. At the same time, users can also save the designed room image and share it with others. With the continuous development of modern environmental space design, the expression of design is gradually diversified, and the combination with technology is also increasingly close. VR technology is developing rapidly, which has changed the way people communicate with the digital world to a certain extent [17]. People expect to get a stronger sense of immersion, and VR will realize people's wishes and change the way people work, play, and communicate. At the same time, the characteristics of VR itself will bring changes in performance technology to environmental space design and help designers better display design blueprints. Display space technology is generally three-dimensional. Now with the development of urbanization and modernization, many display space technologies have shown a strong universality. On the basis of good three-dimensional embodiment, we have now developed many kinds of embodiment methods. On this basis, we choose to improve technology to ensure the efficiency of innovative technology and its affinity to the people to a certain extent. On this basis, we show that the application analysis of VR technology in space design is particularly critical.

2.2. Architectural Style and Spatial Layout. In the history of architectural development, people's design and aesthetics of architectural style are constantly changing. The design of building appearance is mainly dependent on the construction of the load-bearing structure. Generally speaking, it is the covering of the additional structural system [18]. It is closely related to the structure because the appearance design cannot exist independently beyond the structure. When it comes to the idea of architectural appearance design, it should be clear that the graphic design mainly depends on the overall idea, requiring that the design function, area, and environment can be combined with each other according to the shape and quantity of the geometric plane [19]. The design style of the outer eaves of the building should fully reflect the profound cultural heritage consistent with the local culture, the superior natural landscape

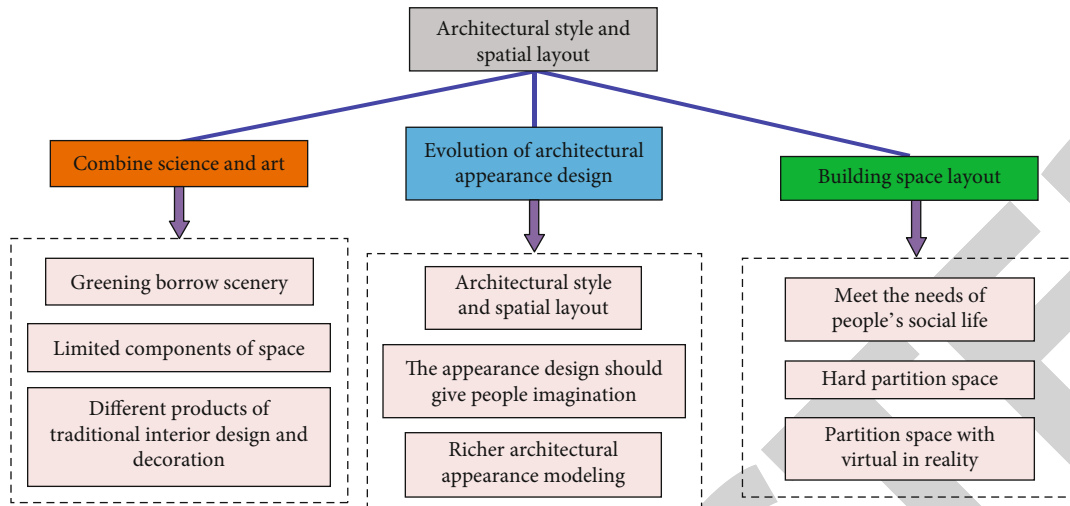


FIGURE 3: The architectural style and spatial layout.

conditions, and the modernization of the new century. In the design and management of the building eaves, we should adhere to the first-class standard, reflect the urban positioning, highlight local characteristics, show the style of the times, and reflect the atmospheric, fresh, and beautiful architectural style. The design that highlights those flat shapes mostly uses the integrity of the plane as the main facade and pursues some changes of lines and doors and windows on its basis, so that the whole building can become bright in front of the eyes, giving people a simple and light feeling, and create a unique artistic conception [20]. Therefore, if the shape of the building is lively, there are no restrictions, which requires the designer not only to have rigorous ideas but also to have creative thinking, and constantly improve their own level while designing a richer architectural appearance shape.

When foreign-designed buildings appear around us, they not only change our thinking but also change our own living standards. There are great differences between different cultures in Europe and us. Now we are used to accepting these differences and ignoring the innovation and development of our traditional architectural design, which is worth thinking about [21]. If we want to change this mode, we must leave space for people to imagine the appearance design, so that each of us can feel the charm of the building. When it comes to the purpose of interior design, it is to adapt to the needs of people in today's rapidly changing modern society through a reasonable indoor and outdoor environment. Therefore, interior designers must put the needs of the objects to be served for spatial functions first [22]. Always adhere to the harmony and unity of architectural interior design and human life, which requires the use of knowledge of disciplines such as ergonomics, aesthetic psychology, and environmental science. With these, we can better understand and analyze the different feelings of human physiology, psychology, and vision, so as to make an interior design that meets the needs of different people. Designers naturally introduce the outdoors into the interior through design. This design technique is called the outdoors of interior design

[23]. Through the hole in the wall or the transparent large glass curtain wall, the vivid outdoor natural scenery is directly introduced into the interior, so as to integrate the indoor and outdoor environment. This flowing open space allows users to directly feel the sun, fresh air, or lush plants so that they can experience the breath of nature and cultural artistic conception. The architectural style and spatial layout are shown in Figure 3.

Nowadays, when creating a reasonable indoor space, interior design should attach great importance to the combination of science and art. From the perspective of the development of architectural appearance design and indoor environment design, the rise of those innovative styles must correspond to the social productivity at that time. Among them, the application of science and technology is the fundamental requirement. There is no correct thinking in creation [24]. In principle, its unity with thought is a major problem. Therefore, interior design is a comprehensive balance between science and art, people's physiological and psychological needs, and spiritual and material. In the architectural style and spatial layout design, we should pay attention to the coordination between details to make the architectural style consistent with the layout design. The design should consider the comprehensive aesthetic, psychological, and other elements [25]. Architectural style and spatial layout are related to people's quality of life, safety, health, comfort, and other issues. In the face of rapid development today, we should divergently think and create an architectural style suitable for the development of the times.

2.3. Application of 5G Technology in Smart Building. In the process of smart building construction in China, driven by 5G technology, it can have a good development space. Therefore, in practical work, it is necessary to collect the status and equipment operation data of smart buildings according to 5G technology, integrate different functional modules, and comprehensively improve the implementation effect of 5G technology, so that smart buildings can achieve vigorous development in the new era and show modern innovative

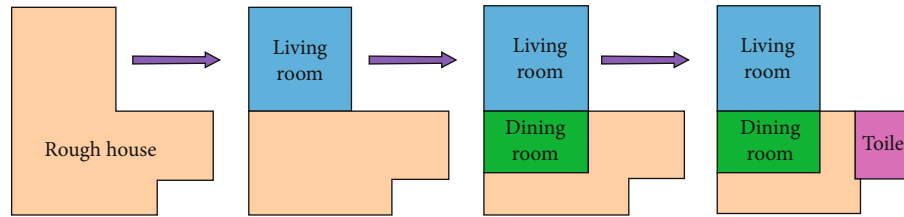


FIGURE 4: The process of indoor layout.

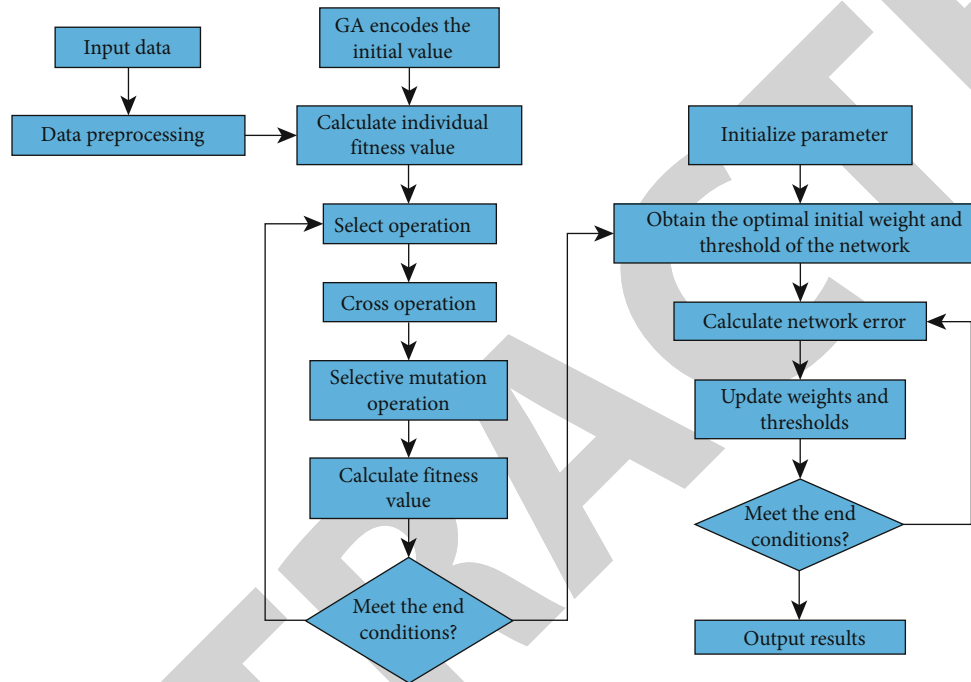


FIGURE 5: The flow chart of the multi-objective genetic algorithm.

ideas [26]. In the process of specific application, the technology mainly completes the data transmission at high speed, which has the advantages of reducing delay and saving energy consumption and effectively improves the overall construction effect [27]. At the same time, it also improves the carrying capacity of the network, meets the standards and requirements of different technical solutions, and also expands the technical support of vertical industries. In terms of technical composition, it optimizes the network slicing function through the service mode of automation architecture, so that the feasibility can be fully revealed.

In smart buildings, users' demand for information and communication is gradually increasing. For example, users' requirements for communication systems include network coverage and communication quality [28]. Therefore, according to the development status of smart buildings, we should optimize the current technical mode and solve the instability of signal acquisition in the past. During the implementation of 5G technology, it can provide users with a more stable and reliable communication experience and reduce the delay problem in the connection process. Therefore, the smart building industry needs to keep up with the development direction of the times and constantly expand

the current development ideas [29]. In terms of the establishment of available reference signals, we should integrate the positioning function into the smart building, set the corresponding information reference signals according to the channel state of the smart building, and synchronize the corresponding information platform to transmit information in the form of wireless signals, and then cooperate with the positioning technology to provide reliable information, quickly find the source of the signal, and propose an effective smart building intelligent management scheme, and reduce the probability of unexpected problems in smart buildings [30]. In terms of the establishment of the actual system, it is necessary to provide multi-path information transmission channels after reducing the interference source of the signal according to the corresponding zero power and non-zero power according to the scientific setting of the communication frequency. This way can enrich people's experience in smart buildings and highlight the application advantages of mobile communication technology itself [31]. In the process of technology implementation, we should realize the mutual integration of different smart building systems and constantly expand the current business development platform.

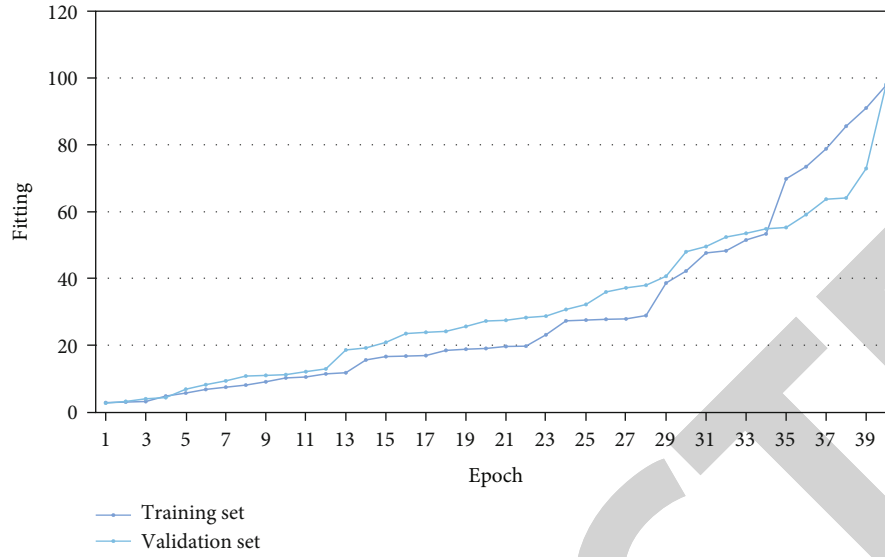


FIGURE 6: Schematic diagram of training process performance improvement.

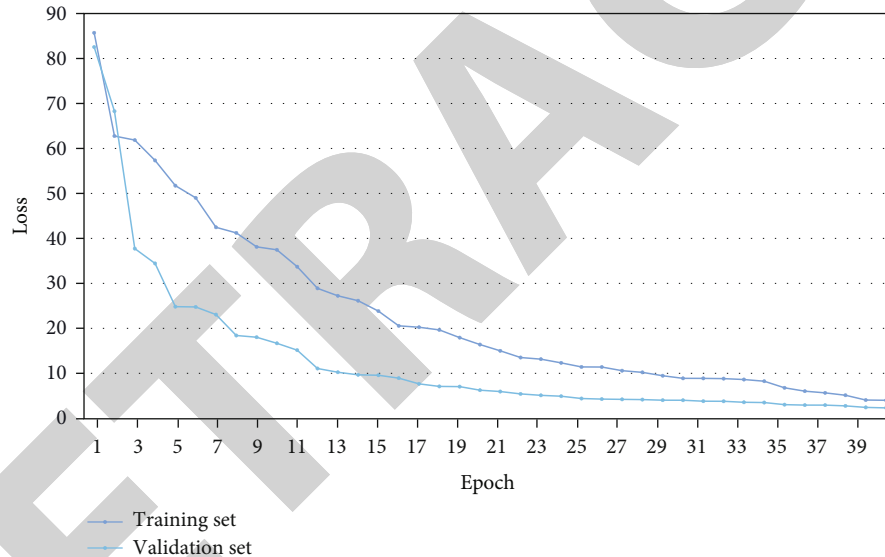


FIGURE 7: The training process loss convergence schematic.

3. Design of Application Model

3.1. Basis of Interior Space Layout. Compared with flexible curves, geometric forms show more rational beauty, and different polygons and their combinations in different indoor space layouts will have different expression effects and psychological effects on users. Therefore, people should pay attention to the role of geometric form in indoor space layout, carefully appreciate the value of space layout shown by the combination of geometric form and other attributes, and let geometric form always appear as the protagonist in indoor space layout. For example, residential buildings can be regarded as the spatial division of fixed areas according to specific design constraints and conditions, forming different functional areas and rooms. Creating real and rich indoor scenes is an important part of 3D modeling technology, and indoor scenes are also the basis of some important

TABLE 1: Optimized layout parameter results of the same furniture.

Number	Furniture name	Length	Width	Layout optimization results	
				X	Y
1	Bed-1	2000	900	450	1000
2	Bed-2	2000	900	2550	1000
3	Bed-3	2000	900	450	3800

applications. Indoor space layout design is the core content of indoor scene modeling and the basis of indoor scene generation. Focusing on the automatic design and optimization of indoor space layout, this section mainly introduces some basic concepts related to indoor space layout.

TABLE 2: Optimized layout parameter results of the different.

Number	Furniture name	Length	Width	Layout optimization results	
				X	Y
1	Bookcase	1650	600	150	500
2	Bed	600	500	600	500
3	Desk	500	850	450	1500

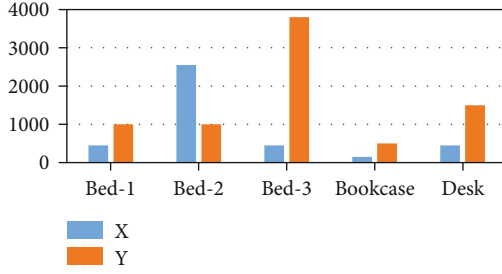


FIGURE 8: Histogram of optimization results.

Indoor scenes cannot be simply regarded as a collection of three-dimensional models. A high-quality indoor scene needs to fully reflect the semantic functions and layout structure of three-dimensional scenes. Therefore, indoor space layout design is the core of indoor scene modeling, and it is also the basis of indoor scene modeling. Indoor space layout includes space, furniture, and their interrelationships and requirements. These relationships and requirements are the constraints of the layout. The convenience of personnel activities and environmental comfort should be comprehensively considered from the perspectives of furniture configuration, furniture placement, and personnel psychological needs. There is no interference between dormitory furniture, and the greater the distance between them, the better. It is expressed by the following objective function.

$$F_1(x) = \sum_{i=1}^n \sum_{j=1}^n (x_i - x_j)^2. \quad (1)$$

When the area, number, and size of furniture are certain, the area occupied by furniture and activity area is certain. In order to maximize the utilization of the central area of personnel activities in the design, this paper uses the following function to describe the distance of this activity.

$$F_2(x) = \sum_{i=1}^n w_i (x_i - x_a)^2. \quad (2)$$

In this paper, the design variable is defined as the position parameter of furniture, and the mathematical expression is as follows.

$$X = \{X_1, X_2, \dots, X_n\} = \{(x_1, y_1), (x_2, y_2), \dots, (x_n, y_n)\}. \quad (3)$$

The constraints of the optimal layout of dormitory interior space mainly involve the following three categories. Furniture layout is mainly constrained by the dormitory space, which cannot exceed the boundary of the dormitory, but also meet the positional relationship between adjacent furniture with distance requirements. Its mathematical expression is as follows.

$$\begin{aligned} \frac{s_i}{2} &\leq x_i \leq L - \frac{s_i}{2}, \\ \frac{q_i}{2} &\leq y_i \leq W - \frac{q_i}{2}, \end{aligned} \quad (4)$$

$$|x_i - x_j| = d_{xij},$$

$$|y_i - y_j| = d_{yij}.$$

Secondly, the furniture in the dormitory does not interfere with each other and cannot be staggered. Its mathematical expression is as follows.

$$|x_i - x_j| \geq \frac{s_i + s_j}{2}, \quad (5)$$

$$|y_i - y_j| \geq \frac{q_i + q_j}{2}.$$

To ensure that all furniture will not affect personnel access, the mathematical expression of this constraint is as follows.

$$|x_i - x_d| \geq \frac{s_i + L_d}{2}, \quad (6)$$

$$|y_i - y_d| \geq \frac{q_i + W_d}{2}.$$

The above optimization design model of indoor space layout aims to maximize the utilization of indoor effective activity space while considering the convenience of personnel activities, environmental comfort, and facility support, combined with appropriate optimization algorithms, the optimization design of indoor space layout can be carried out. The process of indoor layout is shown in Figure 4.

The interior space consists of a living space and a balcony. The living space is the main activity area of members, and the space layout is flexible, while the balcony is mostly used to stack sundries and dry clothes, which is a living auxiliary space and less responsible for personnel activities. In the interior space layout design, space division belongs to a higher level of layout design. The result of space division is

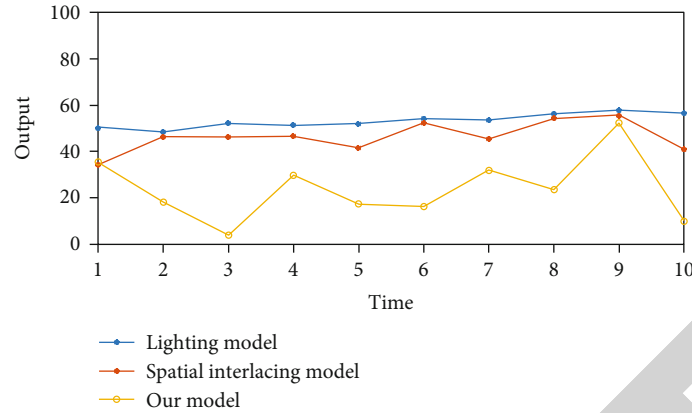


FIGURE 9: The test results of the consumption coefficient.

usually the planning blueprint in the construction industry, which can reflect the construction and space allocation of buildings in three-dimensional space. The layout plan is usually used as the representation method, and the layout plan also provides guidance for the generation of indoor scenes, which is convenient for the design and modeling of indoor scenes. Space division is mainly used in the early stage of design. On the basis of the above space division, the furniture in each room unit is arranged in the room unit according to specific layout rules and functional requirements.

3.2. Improve the Optimization Layout Method. A home layout is a low-level layout design in indoor space layout design, and the result of a home layout is usually the indoor environment that people rely on for production and life. For newly designed houses, the layout of rooms may be an important factor affecting the floor area and facade appearance. Therefore, there is no given contour to follow. The reconstruction of the existing building does not allow the interior architect to have such freedom and takes the floor area, some columns, and walls as fixed geometric constraints. In view of the fuzziness and polymorphism of the evaluation indicators of the spatial layout itself, the current evaluation of the spatial layout scheme mainly depends on the field investigation, the experience of designers, and the feedback of residents. At the same time, combined with the characteristics of the space environment, it adopts a multi-objective genetic algorithm to optimize the indoor space layout and solve it. This method can provide theoretical support for the research of space layout and space utilization design. The flow chart of the multi-objective genetic algorithm is shown in Figure 5.

On the basis of the above space division, the furniture in each room unit is arranged in the room unit according to specific layout rules and functional requirements. The home layout is a low-level layout design in indoor space layout design. For the design work, a reasonable and objective evaluation standard is very important. However, for our research work, because there is no reasonable evaluation standard, in most cases, we can only obtain the evaluation of the method by comparing it with other design methods, or by means of user research.

4. Experiments and Results

An excellent interior space layout design algorithm should be able to extract constraints from the existing layout and reconstruct similar results, so we hope to evaluate our algorithm through reconstruction. We only extract dimensional constraints and adjacent constraints from a given design. Apply our algorithm to the defined area of the layout, take the generated layout as a division of sub-areas, and then continue to generate new layouts on each sub-area. The experiments in this paper were conducted on a Dell T7920 workstation with an NVIDIA RTX1080TI graphics card and 32G RAM. In the experiments, the Adam optimization method is used as the optimizer, the initial value of the learning rate is 0.001, and the training period is 120. Our art image data is downloaded from Artlib world art appreciation library and other websites, and professional art students are invited to clean and screen the data. The training process performance enhancement and loss convergence are shown in Figures 6 and 7.

Given the layout area and design constraints, we apply the hierarchical algorithm framework to generate the indoor space layout, and the polygon layout area can be generated in a course to fine way. In the MATLAB environment, based on the improved multi-objective genetic algorithm, the indoor space layout of the dormitory is optimized, and the results are shown in Tables 1 and 2 and Figure 8.

In the space layout optimization scheme, beds and desks are arranged along the dormitory wall and placed at the four corners of the room, which reduces the interference of the external environment on the sleeping space and learning space, and ensures the relative independence of personal activity space. Among them, sleep space has the strongest demand for privacy, so the combination of going to bed and off the table can provide users with a better privacy environment. In order to verify the performance of the indoor environment spatial layout optimization system of the algorithm, the energy consumption coefficient day of indoor environment spatial layout optimization is introduced. The test results of the consumption coefficient are shown in Figure 9.

The communication space is the shared activity space of dormitory members. The optimization plan will set it centrally in the indoor central area to facilitate the daily access of personnel and the development of communication activities. The dormitory furniture adopts the combination of going to bed and getting off the table, which can reduce the floor area of the furniture, and is placed in the four corners of the room, ensuring the centralization and maximization of the indoor effective activity space. A personal wardrobe and bookcase are set under the bed for convenient use.

5. Conclusion

Traditional layout plan design usually requires interior designers to go through repeated experiments and explorations, and requires a lot of professional knowledge and design experience, so layout plan design is a very time-consuming process. The purpose of our research is to automate this design process and design a reasonable indoor space layout for residential buildings automatically and efficiently. Focusing on the automatic design and optimization of indoor space layout, this paper proposes an optimization method based on design constraints for the automatic generation of a layout plan based on the given layout boundary or layout space. The room units in the interior space layout are represented by polygons composed of multiple rectangles, and the constraints and rules in the layout design are transformed into constraints on related rectangles. Experimental results show that our scene redirection method is effective. Comparing with the results of uniform scaling further proves the effectiveness of our redirection algorithm.

For the problem of text research, we can do further in-depth mining from the following aspects. For layout design, we need to consider as many design constraints as possible to meet the diversified and personalized needs of users. Therefore, whether there is a better method or mathematical model so that more design constraints and criteria can be considered a problem worthy of consideration in the future. We hope to apply these methods and ideas to the home layout design of indoor scenes, which will be a very promising research work. In addition, our research work mainly focuses on the indoor space layout design of residential buildings. How to extend our method to other layout design problems is also a director of research value. In the future, we plan to carry out the method of architectural interior design and space layout optimization based on recurrent neural network technology.

Data Availability

The datasets used during the current study are available from the corresponding author on reasonable request.

Conflicts of Interest

The author declares that he has no conflict of interest.

References

- [1] G. Pintore, E. Almansa, M. Agus, and E. Gobetti, "Deep3-DLayout," *ACM Transactions on Graphics*, vol. 40, no. 6, pp. 1–12, 2021.
- [2] W. Choi, Y. W. Chao, C. Pantofaru, and S. Savarese, "Indoor scene understanding with geometric and semantic contexts," *International Journal of Computer Vision*, vol. 112, no. 2, pp. 204–220, 2015.
- [3] S. Asadi, M. Fakhari, R. Fayaz, and A. Mahdavi-parsa, "The effect of solar chimney layout on ventilation rate in buildings," *Energy and Buildings*, vol. 123, pp. 71–78, 2016.
- [4] S. S. Kumar and J. C. P. Cheng, "A BIM-based automated site layout planning framework for congested construction sites," *Automation in Construction*, vol. 59, pp. 24–37, 2015.
- [5] S. M. Mousavi, T. H. Khan, and Y. W. Lim, "Impact of furniture layout on indoor daylighting performance in existing residential buildings in Malaysia," *Journal of Daylighting*, vol. 5, no. 1, pp. 1–14, 2018.
- [6] M. Hayat, S. H. Khan, M. Bennamoun, and S. An, "A spatial layout and scale invariant feature representation for indoor scene classification," *IEEE Transactions on Image Processing*, vol. 25, no. 10, pp. 4829–4841, 2016.
- [7] G. Lacanna, C. Wagenaar, T. Avermaete, and V. Swami, "Evaluating the psychosocial impact of indoor public spaces in complex healthcare settings," *HERD: Health Environments Research & Design Journal*, vol. 12, no. 3, pp. 11–30, 2019.
- [8] H. Liu, X. Wang, Y. Chen, D. Kong, and P. Xia, "Optimization lighting layout based on gene density improved genetic algorithm for indoor visible light communications," *Optics Communications*, vol. 390, pp. 76–81, 2017.
- [9] X. Tong, K. Liu, X. Tian, L. Fu, and X. Wang, "FineLoc: a fine-grained self-calibrating wireless indoor localization system," *IEEE Transactions on Mobile Computing*, vol. 18, no. 9, pp. 2077–2090, 2019.
- [10] D. Kim and Y. J. Ko, "The impact of virtual reality (VR) technology on sport spectators' flow experience and satisfaction," *Computers in Human Behavior*, vol. 93, pp. 346–356, 2019.
- [11] P. Shan and W. Sun, "Auxiliary use and detail optimization of computer VR technology in landscape design," *Arabian Journal of Geosciences*, vol. 14, no. 9, pp. 1–14, 2021.
- [12] A. Kostis and P. Ritala, "Digital artifacts in industrial co-creation: how to use VR technology to bridge the provider-customer boundary," *California Management Review*, vol. 62, no. 4, pp. 125–147, 2020.
- [13] N. Kato, T. Tanaka, S. Sugihara, and K. Shimizu, "Development and evaluation of a new telerehabilitation system based on VR technology using multisensory feedback for patients with stroke," *Journal of Physical Therapy Science*, vol. 27, no. 10, pp. 3185–3190, 2015.
- [14] M. Holly, J. Pirker, S. Resch, S. Brettschuh, and C. Gütl, "Designing VR experiences—expectations for teaching and learning in VR," *Educational Technology & Society*, vol. 24, no. 2, pp. 107–119, 2021.
- [15] M. Javaid and I. H. Khan, "Virtual reality (VR) applications in cardiology: a review," *Journal of Industrial Integration and Management*, vol. 7, no. 2, pp. 183–202, 2022.
- [16] S. Mun, M. Whang, S. Park et al., "Overview of VR media technology and methods to reduce cybersickness," *Journal of Broadcast Engineering*, vol. 23, no. 6, pp. 800–812, 2018.

Retraction

Retracted: An Efficient Multispectral Image Classification and Optimization Using Remote Sensing Data

Journal of Sensors

Received 23 January 2024; Accepted 23 January 2024; Published 24 January 2024

Copyright © 2024 Journal of Sensors. This is an open access article distributed under the Creative Commons Attribution License, which permits unrestricted use, distribution, and reproduction in any medium, provided the original work is properly cited.

This article has been retracted by Hindawi following an investigation undertaken by the publisher [1]. This investigation has uncovered evidence of one or more of the following indicators of systematic manipulation of the publication process:

- (1) Discrepancies in scope
- (2) Discrepancies in the description of the research reported
- (3) Discrepancies between the availability of data and the research described
- (4) Inappropriate citations
- (5) Incoherent, meaningless and/or irrelevant content included in the article
- (6) Manipulated or compromised peer review

The presence of these indicators undermines our confidence in the integrity of the article's content and we cannot, therefore, vouch for its reliability. Please note that this notice is intended solely to alert readers that the content of this article is unreliable. We have not investigated whether authors were aware of or involved in the systematic manipulation of the publication process.

Wiley and Hindawi regrets that the usual quality checks did not identify these issues before publication and have since put additional measures in place to safeguard research integrity.

We wish to credit our own Research Integrity and Research Publishing teams and anonymous and named external researchers and research integrity experts for contributing to this investigation.

The corresponding author, as the representative of all authors, has been given the opportunity to register their agreement or disagreement to this retraction. We have kept a record of any response received.

References

- [1] S. Janarthanan, T. Ganesh Kumar, S. Janakiraman, R. K. Dhanaraj, and M. A. Shah, "An Efficient Multispectral Image Classification and Optimization Using Remote Sensing Data," *Journal of Sensors*, vol. 2022, Article ID 2004716, 11 pages, 2022.

Research Article

An Efficient Multispectral Image Classification and Optimization Using Remote Sensing Data

S. Janarthanan ¹, T. Ganesh Kumar ¹, S. Janakiraman ², Rajesh Kumar Dhanaraj ¹,
and Mohd Asif Shah ³

¹School of Computing Science and Engineering, Galgotias University, India

²Pondicherry University, Puducherry, India

³Kebri Dehar University, Ethiopia

Correspondence should be addressed to Mohd Asif Shah; ayanlehasen@kdu.edu.et

Received 22 August 2022; Revised 1 September 2022; Accepted 15 September 2022; Published 8 October 2022

Academic Editor: Sweta Bhattacharya

Copyright © 2022 S. Janarthanan et al. This is an open access article distributed under the Creative Commons Attribution License, which permits unrestricted use, distribution, and reproduction in any medium, provided the original work is properly cited.

A significant amount of effort and cost is required to collect training samples for remote sensing image classifications. The study of remote sensing and how to read multispectral images is becoming more important. High-dimensional multispectral images are created by the various bands that show how materials behave. The need for more information about things and the improvement of sensor resolutions have led to the creation of multispectral data with a higher size. In recent years, it has been shown that the high dimensionality of these data makes it hard to preprocess them in multiple ways. Recent research has demonstrated that one of the most crucial methods to address this issue is by adopting a variety of learning strategies. But as the data gets more complicated, these methodologies are not adequate to support. The proposed methodology shows that the classification experiment using remote sensing images indicates the maximum likelihood classifier with different deep learning models; weight vector (WV) AdaBoost and ADAM can greatly limit overfitting, and it obtains high classification accuracy. Proposed VGG16 and Inception v3 increase classification accuracy along with optimization process produce 96.08%.

1. Introduction

Multispectral sensors now capture the earth's surface reflectance in hundreds of frequency bands because of the advancement in sensor technology. As a result, multispectral pictures may be used for a wide range of activities, from categorization to environmental monitoring. For example, classification accuracy is reduced when dimensionality grows and training samples are restricted, according to the Hughes phenomenon. Multispectral images may contain strong correlations between [1] neighboring and nonadjacent bands, which lowers the quantity of data that may be used for further analysis, including categorization. Accurate categorization is dependent on the extraction of certain characteristics. Band Correlation Clustering (BCC) is a new unsupervised feature extraction [2, 3] approach introduced in this paper. There are three key processes in the suggested technique, which are the bands' correlation coefficient is cal-

culated, the bands are clustered according to the correlation coefficient matrix, and the means of each cluster are calculated with a new methodology for feature extraction. Classification accuracy and time consumption are used to assess the support vector machine approach. [4] The resulting features are supplied into nonparametric Support Vector Machine (SVM) and parametric Machine Learning (ML), two supervised classifications, for the assessment process. [5] Comparable results are obtained using [6] unsupervised feature extraction via clustering. An evaluation of the findings demonstrates that the suggested BCC performs well in terms of computing expenses to increase the accuracy in classification steps.

Object-Based Image Classification (OBIC) [7] is used to classify Very-High-Resolution (VHR) pictures. Most OBIC [8] classification algorithms use 1D features hand-crafted from picture objects (superpixels). This letter introduces a deep OBIC framework utilizing [9, 10] Convolutional

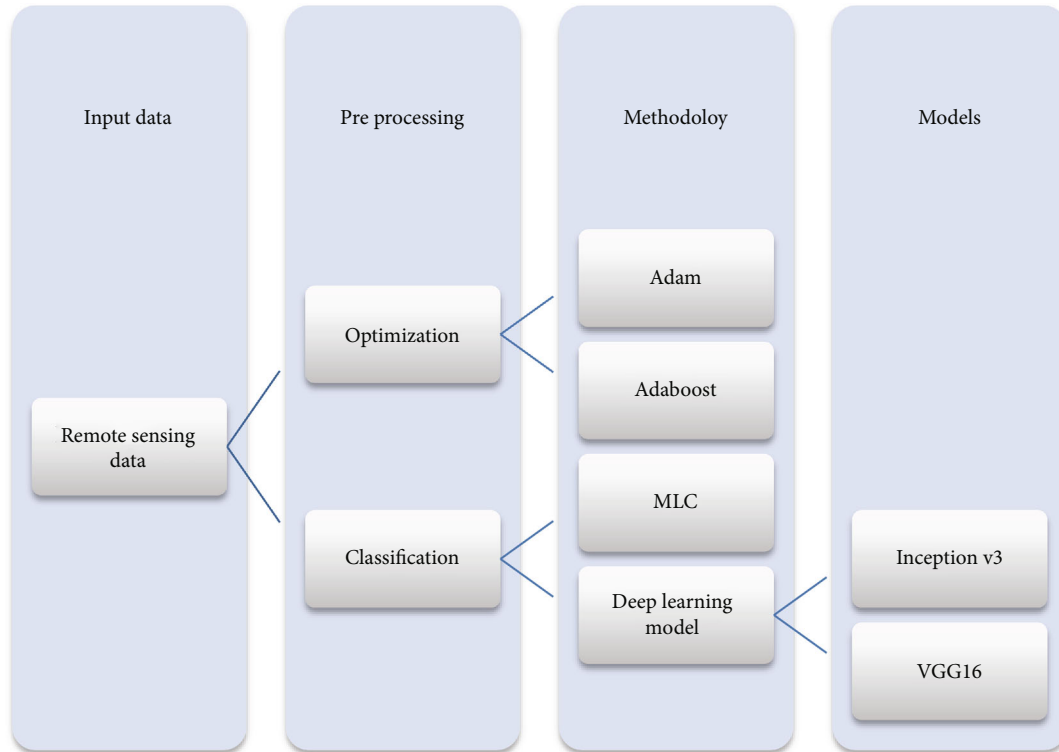


FIGURE 1: Classification and optimization processing steps.

Neural Networks (CNNs) to extract 2D deep superpixel features [11]. Before designing the network [12], studied superpixel mask regulations before experiments, the proposed framework for better overall accuracy, coefficient, and F-measure is delivered by our DiCNN-4 (Double-input CNN) [13] model. [14] On picture dataset than standard OBIC approaches. AdaBoost is a fantastic ensemble learning technique that combines several weak classifiers to create a strong classifier, eventually increasing the classification accuracy. [15] However, the AdaBoost combination overlooks the performance of basic classifiers at the per-class level and concentrates on their total performance. AdaBoost's ability to enhance classification accuracy is hampered by this, [16] which makes overfitting a concern in subsequent rounds. In this paper, an enhanced [17, 18] AdaBoost algorithm with Weight Vector (WV AdaBoost) is suggested to reduce these drawbacks and preserve the advantages of AdaBoost. Each class is assigned a weight to indicate the recognition [16, 19] ability of the base classifiers using weight vectors. AdaBoost and WV AdaBoost base classifiers are trained using an Artificial Neural Network (ANN), Naive Bayes, and a decision tree [20]. The classification experiment using Remote Sensing (RS) data demonstrates that WV AdaBoost beats AdaBoost by producing much greater classification accuracy. It can greatly reduce overfitting, within a limited number of repetitions, and WV AdaBoost may increase classification accuracy to the greatest possible level.

Labeling samples from each image is frequently a necessary step in the processing of multitemporal remotely sensed data, but it is a laborious and time-consuming operation. [21] The ground items frequently do not change consider-

ably over time, thus, certain labels can be reused with the proper consistency checks. Using just one labeled picture, a new framework for weakly supervised transfer learning [22] is described in this process to categorize multitemporal remote sensing images. [23] Our system can categorize all the other multitemporal images chronologically without any labeling effort by exploiting the consistency of time-series images and a domain adaption mechanism. [24] Our system obtains a classification accuracy that is comparable to what would be obtained with [25] supervised learning. [26] With the training samples for one temporal dataset, our system is still able to handle multitemporal remote sensing images, as mentioned Figure 1 with input data, preprocessing and methodology applied, and inception v3 and VGG16 model for image classification and accuracy.

1.1. The Motivation for the Proposed Work. The main motivation for multispectral image classification and receiving better accuracy as a result compared with multistage techniques and predefined models applied to improvise the accuracy of the remote sensing data set with inception v3 and VGG16, primary goal and motivation required to analyze and improvise the accuracy with optimization techniques to increase the accuracy and computation cost reduced.

2. Related Work

2.1. Methodology. By utilizing the Adam optimizer and comparing it to VGG16 [27] and Inception v3, the suggested technique produce the result with excellent accuracy while

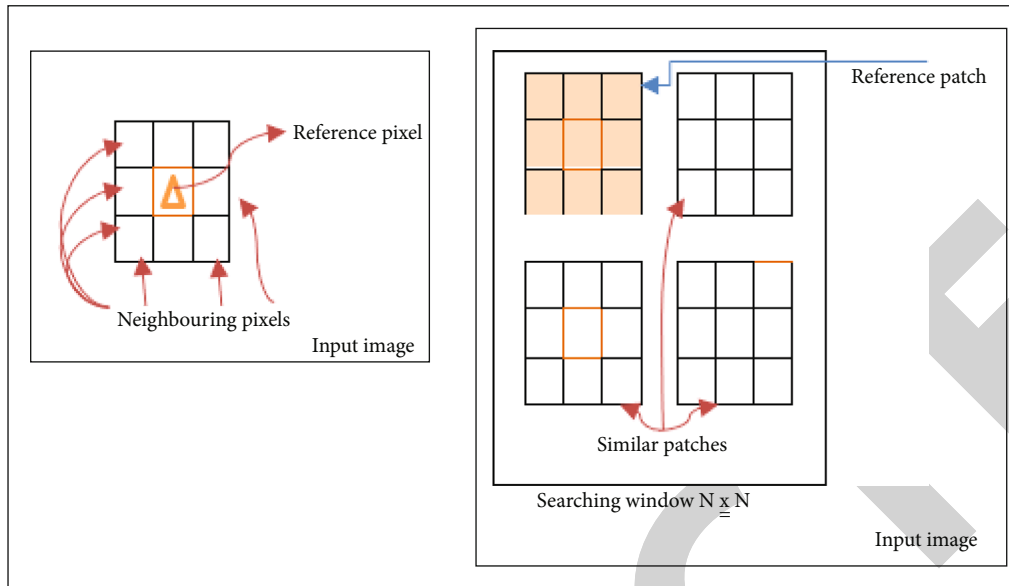


FIGURE 2: Patch extraction process.

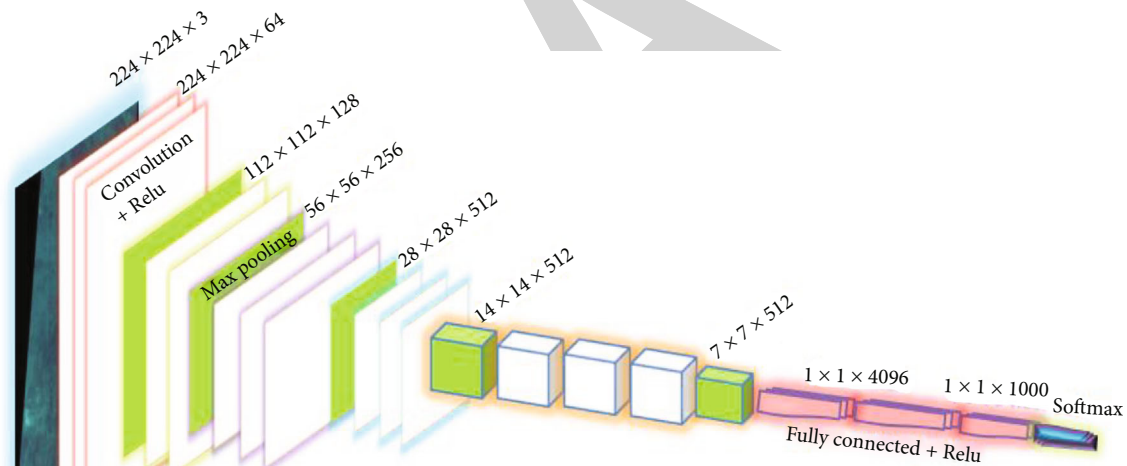


FIGURE 3: VGG 16 model process flow architecture.

requiring minimal computing time. The following model is described in detail to train a deep learning network.

2.1.1. Normalization. This article analyzes remote sensing data using single-layer and deep convolutional networks. Given the enormous input data dimensionality and little labeled data, direct application of supervised (shallow or deep) convolutional networks to multi- and [28] hyperspectral imaging is problematic. The recommend combining unsupervised learning [29] of sparse features with greedy layer-wise unsupervised pretraining. [30] The technique uses sparse representations to enforce population and lifetime sparsity and to compute the logarithm of every pixel using data normalization.

$$a = \frac{((b - \min) * 255)}{(\max - \min)}, \tag{1}$$

where b represent the grayscale value of the original image, and a represent the grayscale value after normalized image. \min and \max were the grayscale level of the sample image with minimum and maximum range were 0 to 255.

2.1.2. Patch Extraction. The training image set consists of image patches from the stacked covariance matrix. [31] The approach group image patches into k clusters. Random mini-batches are retrieved with 50% overlap (stride 8) and resolution determines patch sizes. High resolution requires

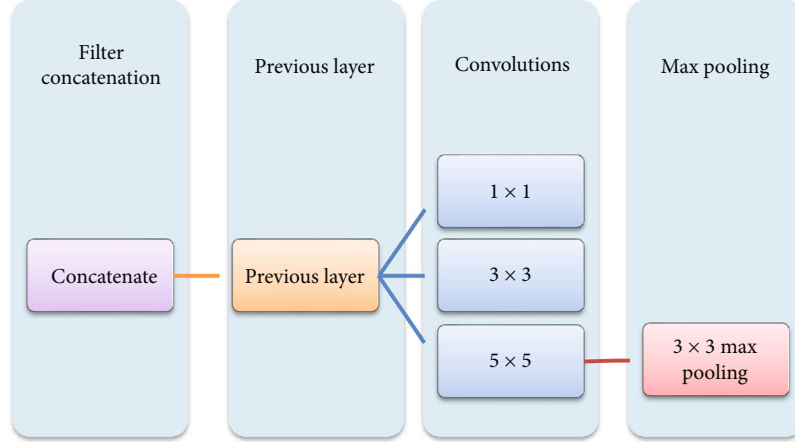


FIGURE 4: Inception operation with reduced dimensions.

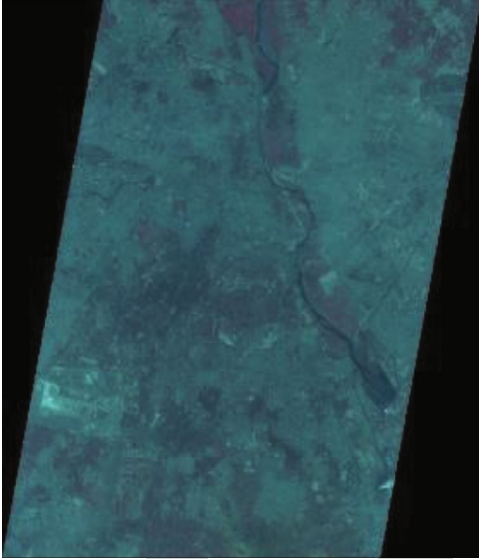


FIGURE 5: Combined 3 band tiff image.

tiny patches with the testing image set has 16×16 nonoverlapping picture patches. [32] These pure patches are labeled using the posterior probability computation. In Figure 2, input image with reference pixel and neighboring pixels with similar patches are explained.

2.1.3. Model Training. Batch normalization and VGG16 feature extraction are used. The classification [33] layer is fully linked, batch normalized, and ReLU. The Xavier approach [34] initializes the fully connected layer's weights. Adam uses a 0.001 learning rate and 0.00001 weight decay. This model clusters remote sensing data (GDC-SAR). In Figure 3, input image and convolution plus ReLU and max pooling resolution are reduced from $224 \times 224 \times 3$ with $1 \times 1 \times 1000$ with fully connected ReLU and softmax with VGG16 architecture.

2.1.4. Maximum Likelihood Classifier. One of the most often used techniques for categorization in remote sensing is the maximum likelihood classifier, which places a pixel into

the class that it most closely resembles. The posterior probability of a pixel belonging to class k is used to define the likelihood L_k .

$$L_K = P\left(\frac{k}{K}\right) = P(k) * \frac{P(X/k)}{\sum P(i) * P(X/i)}, \quad (2)$$

where, $P(k)$ is the prior probability of class k , and $P(X/k)$ is the probability density function or conditional probability to witness X from class k .

$\sum P(i) * P((X/i))$ is likewise shared by all classes, and $P(k)$ is typically believed to be equal to each other as well. As a result, $P(X/k)$, or the probability density function, determines L_k . The probability density function is based on the multivariate normal distribution for mathematical reasons. The probability in the case of normal distributions may be stated as follows:

$$L_k(X) = \frac{1}{((2\pi)^n)/(2|\Sigma_k|(1/2))} \exp\left[-\frac{1}{2}(X - \mu_k) \sum_k^{-1} (X - \mu_k)t\right], \quad (3)$$

where, n the number of bands, X image data of bands n , and $L_k(X)$ belongs to the class k . μ_k is the average class k vector, Σ_k is the covariance matrices and class k variance, and $|\Sigma_k|$ is an indicator of Σ_k . The likelihood is the same as the Euclidean distance when the variance-covariance matrix is symmetric, and it is the same as the Mahalanobis distances when the determinants are equal.

2.1.5. Inception v3. A module for Google Net, Inception v3 is a convolutional neural network that aids in object recognition and image analysis. The Google Inception Convolutional Neural Network, which was first shown at the ImageNet Recognition Challenge, is in its third iteration. In Figure 4 represents the filter concatenation operation along with previous layer and convolutions layer 1×1 , 3×3 and 5×5 with max pooling of 3×3 .

TABLE 1: Parameters of IRS P-6 LISS IV Satellite.

Parameter	Description
Parameter	LISS IV data
Sensor	L4MX
Sat-ID	IRS-P6
Product ID	142866521
Sensor orientation	Delhi
SAR band	3 band
Angle range	Latitude 28.615513 Longitude 77.216714
Image format	GEOTIFF
Range resolution	5.8 m

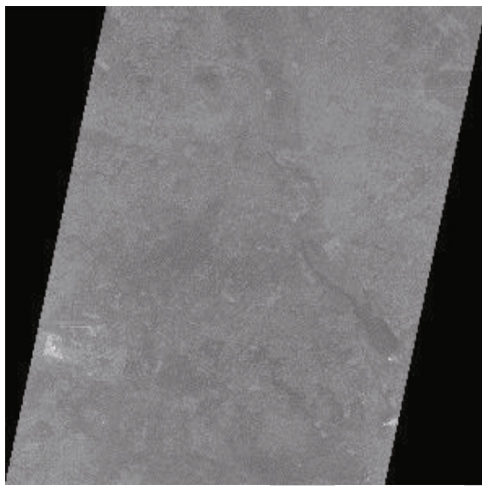


FIGURE 6: Band 2 tiff image.

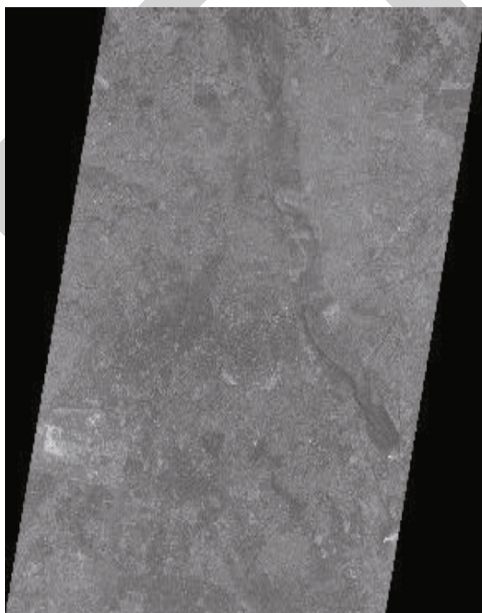


FIGURE 7: Band 3 tiff image.

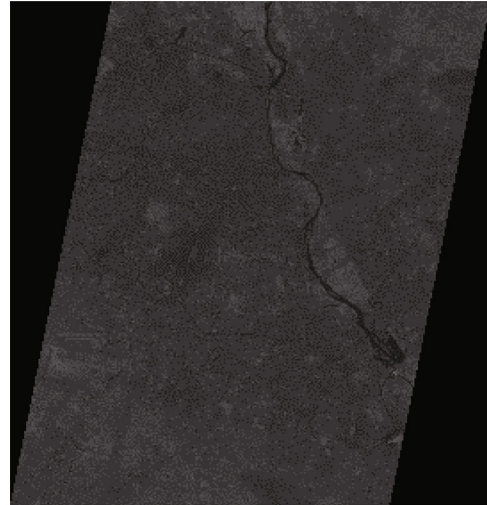


FIGURE 8: Band 4 tiff image.

2.1.6. Adam Optimization Process. The Adam optimization algorithm's primary goal is quicker computing [35] with a limited number of tuning parameters such as epochs, learning rate, batch size, learning rate, optimizer, and a number of neurons. Additionally, adjust the number of layers for beta 2 second moment estimations of 0.999 and near to 1.0 and beta 1 decay rates of 0.9.

First, the gradient (g) with time (t) step.

$$g(t) = f'(X(t-1)). \quad (4)$$

Second, to calculate moments, moving average (m) with hyperparameter beta 1.

$$m(t) = \text{beta1} * m(t-1) + (1 - \text{beta1}) * g(t). \quad (5)$$

Then update the moments with moving average (v) with a second in beta 2.

$$v(t) = \text{beta2} * v(t-1) + (1 - \text{beta2}) * g(t). \quad (6)$$

Next, bias adjusted with correction for the 1st moment

$$\text{mhat}(t) = \frac{m(t)}{(1 - \text{beta1}(t))}. \quad (7)$$

And then 2nd moment

$$\text{vhat}(t) = \frac{v(t)}{(1 - \text{beta2}(t))}. \quad (8)$$

A static decay schedule is required to be applied.

$$\begin{aligned} \text{beta1}(t) &= \text{beta1}^t, \\ \text{beta2}(t) &= \text{beta2}^t. \end{aligned} \quad (9)$$

Read: Input data (stored in the folder)
Decode: Convert it into JPEG to RGB grid pixels with channels
 Convert it into a floating point
Input: Neural network
 Rescale the pixel:
Range: Between (0 : 255) to the [0,1]
 Output: Preprocessed tensors.

ALGORITHM 1: Algorithm Procedure: Preprocessing.

Source image labeled: $Y_s = \{(a_i^s, b_i^s)\}_{i=1}^{n^s}$

Target image unlabeled: $Y_t = \{(a_j^t)\}_{j=1}^{n^t}$

Class labels, $Y_t = \{(b_j^t)\}_{j=1}^{n^t}$

Assign parameters:

Epoch value = 100;

Min-batch size: Bs = 32;

Learning rate $\alpha = 2.0 \times 10^{-4}$,

1st and 2nd decay rate exponential

With $\beta_1 = 0.9$, $\beta_2 = 0.999$ and

Epsilon: 1.0×10^{-8}

Initially use VGG16 and inception v3 model trained with dataset and pre-training with CNN to initialize feature generation G and classified images C1, C2, C3 and C4 alone

for **epoch = 1 : num_epoch do**

Shuffle the random source and target image data set and organize it into N_b

Groups each size m

for $k = 1 : N_b$ do

Select mini-batches: Y_{sk}, Y_{tk} from Y_s and Y_t

Need to train the G, C1, C2, C3 AND C4 on Y_{sk} by optimizing (1) to (10) using Adam same is required to be done for C1 to C4 (11)

End for

End for

Classify the different class target domain $\{(a_j^t)\}_{j=1}^{n^t}$ using source and target

Return $\{(b_j^t)\}_{j=1}^{n^t}$

ALGORITHM 2: Proposed Inception v3 and VGG 16 algorithm.

Finally, calculate the value of the iteration of the parameter.

$$x(t) = x(t-1) - \alpha * \frac{mhat(t)}{\sqrt{vhat(t) + \epsilon}}, \quad (10)$$

where alpha is step size and eps are small value (epsilon) and sqrt () is the square root function.

2.1.7. AdaBoost Process. Adaboost first chooses a training subset at random. By choosing the training set depending on the precision of the previous training, it iteratively trains the AdaBoost machine learning model. It gives incorrectly categorized observations at a [15] larger weight so that they will have a higher chance of being correctly classified in the upcoming round. Additionally, based on the trained classi-

fier's accuracy, weight is assigned to it in each iteration. [36] The more accurate classifier will be given more weight. This method iterates until the entire training set fits perfectly, or until the stated maximum number of estimators has been reached [37] to categorize the voting algorithm created for the selection.

3. Data Processing

3.1. Data Set. We used information from IRS P6 LISS IV remote sensing from ISRO for dataset analysis, refer to <https://directory.eoportal.org/web/eoportal/satellite-missions/i/irs-p6>. The area being studied is only the Delhi region of India, which is centered at latitude 0.00000 and longitude 75.00000 and scene center at latitude 28.615513 and longitude 77.216714, respectively. Figure 5 shows combined bands of RGB and Table 1 gives a brief description of the IRS P6 LISS IV data we used in our work. Figure 6

TABLE 2: Comparison between parameters existing techniques with the accuracy level.

Classification techniques used	Data set used	Software used	Accuracy assessment	Overall accuracy	Reference
Maximum likelihood technique	Landsat 8 satellite image	ERDAS imagine	Kappa statistic	82.5%	N. A. Mahmon, et al., 2015
RNN	LISS IV image	MAT lab	Kappa coefficient	87.69%	T. Vignesh, et al., 2021
SVM (support vector machines) and CNN	Google earth Landsat-8	MATLAB R2017a	Overall accuracy	70.89% 73.79%	M. Kim et al.2018
CNN	South Korea region – Google earth	MATLAB R2017a	Overall accuracy	95.7%	M. Kim et al.2018
VGG16 with Adam	Google earth and Bing maps	Python	Average accuracy	78.72	W. Teng et al., [26]
Proposed inception v3 with Adam	LISS IV	Python	Accuracy		

TABLE 3: Comparison between new parameters with proposed Scheme.

Delhi region	SVM	MLC	K-means clustering	Adam optimization	VGG 16 model	Inception v3 model
Band 2	75.68	89.52	76.72	92.21	90.80	95.50
Band 3	76.51	88.72	77.65	93.75	91.00	95.80
Band 4	68.25	90.21	76.62	94.52	92.40	96.40
Combined	95.6	90.52	78.33	96.72	93.20	96.60
Average	79.01	89.74	77.33	94.3	91.85	96.08

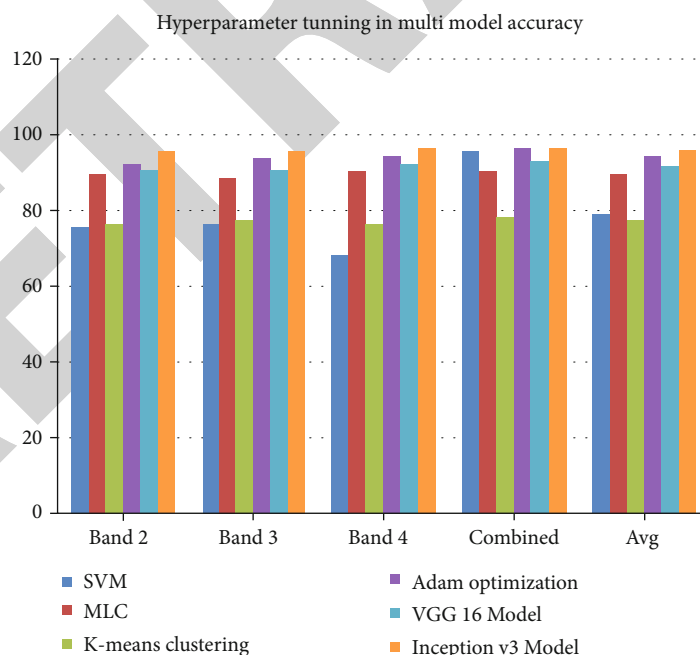


FIGURE 9: Comparison between existing vs. proposed multimodel accuracy.

represents band 2 tiff image, Figure 7 represents band 3 tiff image, and Figure 8 represents band 4 tiff image.

In Table 1, it mentions about Indian remote sensing p-6 LISS IV data set description in detail.

3.1.1. Data Preprocessing. The data is first level-0 preprocessed to improve quality for a more effective picture enhancement and analysis procedure. [38] Through preprocessing, binary conversion of two complex elements and

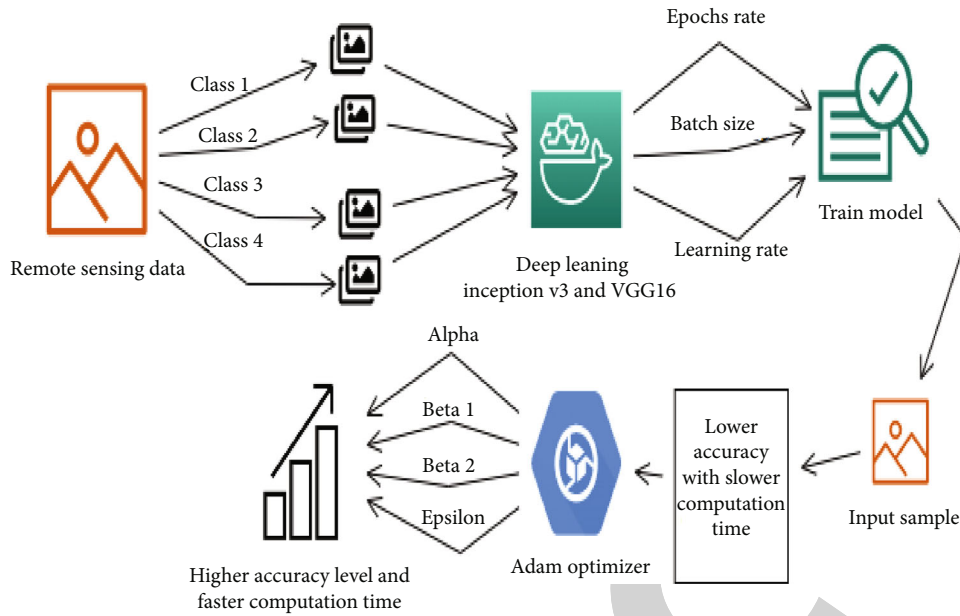


FIGURE 10: Proposed manual workflow architecture with Inception v3 and VGG16 model.

TABLE 4: User Accuracy level with sample data.

Class	Accuracy	Samples data
Class 1	1.00	1
Class 2	1.00	1
Class 3	1.00	1

these with image file formats of (.tiff extension), such that image matrix is used for patch construction and analysis, distortions are reduced and image qualities are increased. (Figures 6, 7, and 8) (Band 2, 3, and 4).

4. Results and Discussion

The three classes were used to train the model. The outcomes are also evaluated in comparison with the earlier models such as the SVM, K-means, maximum likelihood (MLC), and adaptive movement estimation. Table 2 shows the effective stochastic optimization approach with accuracy levels per class expressed as percentages.

The ultimate accuracy of a data set was assessed by averaging all of its patches. In Table 3, the range of the proposed fields of examination was advantageous. It might be challenging to distinguish mixed-class urban settlements from other urban regions. This is because there aren't many significant urban centers in these locations. The bulk of them are mixed communities, as seen in Figures 5, 6, 7, and 8. A patch may have several classes while creating the ground truth, but after categorization, it only gets one label that corresponds to the largest class. This leads to decreased accuracy along with a resolution discrepancy between SAR pictures and remote sensing data. In the above table, Ada-boost is analyzed as a combined result of each band.

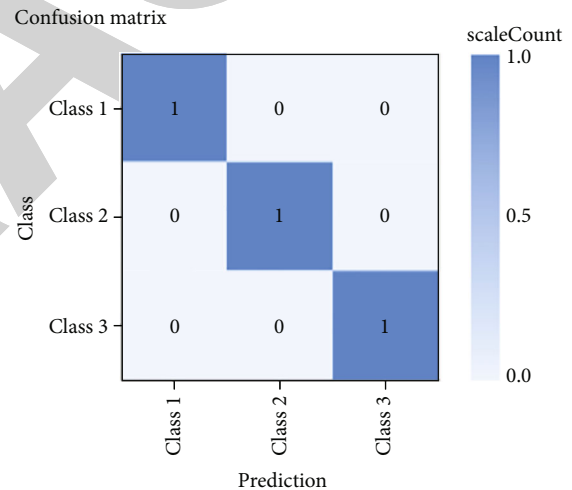


FIGURE 11: Confusion matrix.

Each model and machine learning algorithm gives the best accuracy level when compared with the new deep learning model in the python environment with ImageNet and Google Net model like VGG16 and Inception v3 model produces high accuracy level of finding the above table number. In Table 3, with the accuracy level of each band being analyzed with sample image data set for the classification accuracy train and test set prepared for the analysis of work and the manual operational categorization of sample class, the following hyperparameter tuning is used: Epochs 10, Batch size 16, learning rate 0.001, and input sample accuracy level 96.08. In Figure 9, it represents the proposed model.

The below-mentioned test results analyze with the Google AI web application with classes 1, 2, and 3, and combined bands are being analyzed with <https://teachablemachine.withgoogle.com/>. In Figure 10, it represents the proposed

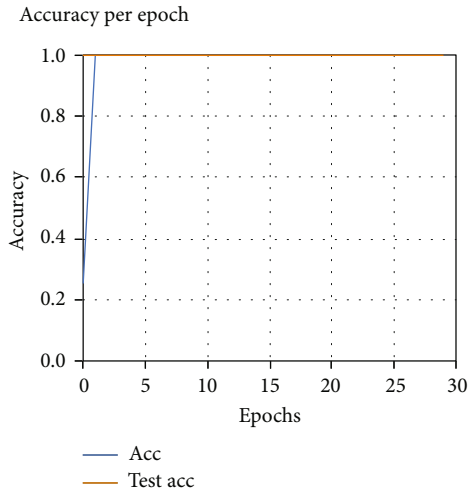


FIGURE 12: Accuracy per Epoch class 2.

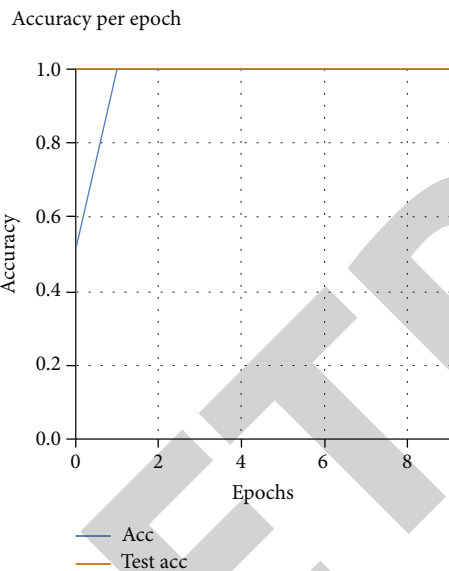


FIGURE 13: Accuracy per Epoch class 3.

workflow with deep learning model and optimization function process clearly.

In Table 4, it represents the sample data along with various labeled sample classes were imported for the training and different hyperparameter tuning of values like batch size, epoch rate, and learning rate 0.0001 being trained with inception v3 and VGG16 model, by importing the input sample accuracy level and confusion matrix class and prediction rates shown in Figure 11.

In Figure 12, it represents the accuracy per epoch with testing accuracy comparison level of class 2 sample data. Figure 13 shows the accuracy per epoch class 3 sample data, and Figure 14 shows the combined data set range level showing in the graphical.

In Figure 15, it represents the loss per epoch combined test loss and loss range level showing in the graph.

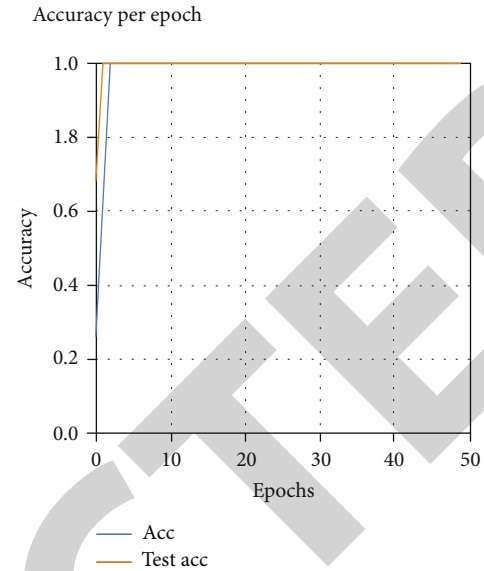


FIGURE 14: Accuracy per Epoch class combined.

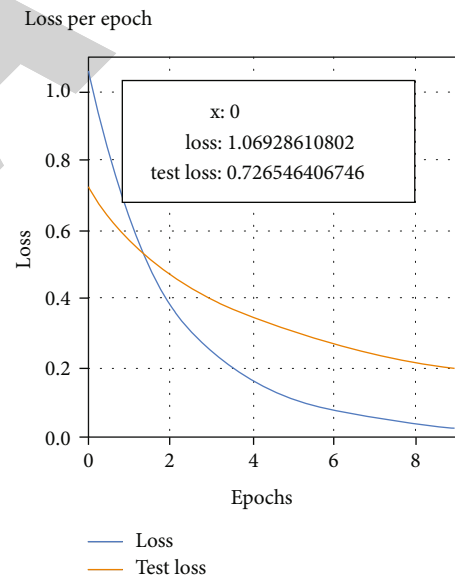


FIGURE 15: Loss per Epoch combined.

5. Conclusion and Future Scope

Deep learning is used to categorize land cover via stochastic optimization. The proposed model has a 96.08 percent accuracy rate using overlapping remote sensing picture patches. The trial findings show that the algorithm performs in line with the best practices. Hence, a general model is created, and it can be used for a variety of image data sets. Likewise, we will be able to divide the more specific classes like volume more accurately. In this research primary finding merge two deep learning model inception v3 and VGG16 with Adam optimization produce better accuracy level compare to the existing models stated in Table 2, and in the future scope

the segregation of mixed-class groups, it has not yet been investigated along with the deep learning model, and it can be considered for future research directions.

Data Availability

The data that support the findings of this study are available upon reasonable request.

Conflicts of Interest

The authors declare that they have no competing interests.

Authors' Contributions

The individual contributions of authors to the manuscript should be specified in this section. The first author analyzed and wrote the introduction, methodology, results, and the second author guided the preparation of the document with the corresponding format and support for the data set reception work area. The third and fourth authors concluded with a comparison and corresponding authors to ensure the completeness and verification procedure.

References

- [1] A. Ghorbanian and A. Mohammadzadeh, "An unsupervised feature extraction method based on band correlation clustering for hyperspectral image classification using limited training samples," *Remote Sensing Letters*, vol. 9, no. 10, pp. 982–991, 2018.
- [2] J. Song, S. Gao, Y. Zhu, and C. Ma, "A survey of remote sensing image classification based on CNNs," *Big Earth Data*, vol. 3, no. 3, pp. 232–254, 2019.
- [3] Y. Wei, X. Luo, L. Hu, Y. Peng, and J. Feng, "An improved unsupervised representation learning generative adversarial network for remote sensing image scene classification," *Remote Sensing Letters*, vol. 11, no. 6, pp. 598–607, 2020.
- [4] M. Cong, Z. Wang, Y. Tao, J. Xi, C. Ren, and M. Xu, "Unsupervised self-adaptive deep learning classification network based on the optic nerve microsaccade mechanism for unmanned aerial vehicle remote sensing image classification," *Geocarto International*, vol. 36, no. 18, pp. 2065–2084, 2021.
- [5] K. A. Adepoju and S. A. Adelabu, "Improving accuracy of Landsat-8 OLI classification using image composite and multisource data with Google Earth Engine," *Remote Sensing Letters*, vol. 11, no. 2, pp. 107–116, 2020.
- [6] A. Chatterjee, J. Saha, J. Mukherjee, S. Aikat, and A. Misra, "Unsupervised land cover classification of hybrid and dual-polarized images using deep convolutional neural network," *IEEE Geoscience and Remote Sensing Letters*, vol. 18, no. 6, pp. 969–973, 2021.
- [7] Y. Wu, P. Zhang, J. Wu, and C. Li, "Object-oriented and deep-learning-based high-resolution mapping from large remote sensing imagery," *Canadian Journal of Remote Sensing*, vol. 47, no. 3, pp. 396–412, 2021.
- [8] X. Zhang, X. Tan, G. Chen, K. Zhu, P. Liao, and T. Wang, "Object-based classification framework of remote sensing images with graph convolutional networks," *IEEE Geoscience and Remote Sensing Letters*, vol. 19, pp. 1–5, 2022.
- [9] X. Zhang, Q. Wang, G. Chen et al., "An object-based supervised classification framework for very-high-resolution remote sensing images using convolutional neural networks," *Remote Sensing Letters*, vol. 9, no. 4, pp. 373–382, 2018.
- [10] S. Shi, Y. Zhong, J. Zhao, P. Lv, Y. Liu, and L. Zhang, "Land-use/land-cover change detection based on class-prior object-oriented conditional random field framework for high spatial resolution remote sensing imagery," *IEEE Transactions on Geoscience and Remote Sensing*, vol. 60, pp. 1–16, 2022.
- [11] X. He and Y. Chen, "Optimized input for CNN-based hyperspectral image classification using spatial transformer network," *IEEE Geoscience and Remote Sensing Letters*, vol. 16, no. 12, pp. 1884–1888, 2019.
- [12] R. K. Dhanaraj, V. Ramakrishnan, M. Poongodi et al., "Random forest bagging and X-means clustered antipattern detection from SQL query log for accessing secure mobiledata," *Wireless Communications and Mobile Computing*, vol. 2021, Article ID 2730246, 9 pages, 2021.
- [13] X. Yu, J. Fan, J. Chen, P. Zhang, Y. Zhou, and L. Han, "Nest-Net: a multiscale convolutional neural network for remote sensing image change detection," *International Journal of Remote Sensing*, vol. 42, no. 13, pp. 4898–4921, 2021.
- [14] A. E. Maxwell, T. A. Warner, and F. Fang, "Implementation of machine-learning classification in remote sensing: an applied review," *International Journal of Remote Sensing*, vol. 39, no. 9, pp. 2784–2817, 2018.
- [15] P. Dou and Y. Chen, "Remote sensing imagery classification using AdaBoost with a weight vector (WV AdaBoost)," *Remote Sensing Letters*, vol. 8, no. 8, pp. 733–742, 2017.
- [16] S. Janarthanan and K. Rajan, "Secure efficient geometric range queries on encrypted spatial data," 2017.
- [17] S. Bera and V. K. Shrivastava, "Analysis of various optimizers on deep convolutional neural network model in the application of hyperspectral remote sensing image classification," *International Journal of Remote Sensing*, vol. 41, no. 7, pp. 2664–2683, 2020.
- [18] T. R. Gadekallu, G. Srivastava, M. Liyanage et al., "Hand gesture recognition based on a Harris Hawks optimized convolutional neural network," *Computers and Electrical Engineering*, vol. 100, article 107836, 2022.
- [19] C. L. Chowdhary, M. Alazab, A. Chaudhary, S. Hakak, and T. R. Gadekallu, *Computer Vision and Recognition Systems Using Machine and Deep Learning Approaches: Fundamentals, Technologies and Applications*, Institution of Engineering and Technology, 2021.
- [20] T. K.-A. Williams, T. Wei, and X. Zhu, "Mapping urban slum settlements using very high-resolution imagery and land boundary data," *IEEE Journal of Selected Topics in Applied Earth Observations and Remote Sensing*, vol. 13, pp. 166–177, 2020.
- [21] W. Liu, R. Qin, and F. Su, "Weakly supervised classification of time-series of very high resolution remote sensing images by transfer learning," *Remote Sensing Letters*, vol. 10, no. 7, pp. 689–698, 2019.
- [22] S. Krishnamoorthi, P. Jayapaul, R. K. Dhanaraj, V. Rajasekar, B. Balusamy, and S. K. Islam, "Design of pseudo-random number generator from turbulence padded chaotic map," *Nonlinear Dynamics*, vol. 104, no. 2, pp. 1627–1643, 2021.
- [23] C. Guobin, Z. Sun, and L. Zhang, "Road identification algorithm for remote sensing images based on wavelet transform and recursive operator," *IEEE Access*, vol. 8, pp. 141824–141837, 2020.

Retraction

Retracted: Analysis on the Educational Value of Winter Olympic Spirit in Track and Field Teaching Based on Data Mining under Artificial Intelligence

Journal of Sensors

Received 3 October 2023; Accepted 3 October 2023; Published 4 October 2023

Copyright © 2023 Journal of Sensors. This is an open access article distributed under the Creative Commons Attribution License, which permits unrestricted use, distribution, and reproduction in any medium, provided the original work is properly cited.

This article has been retracted by Hindawi following an investigation undertaken by the publisher [1]. This investigation has uncovered evidence of one or more of the following indicators of systematic manipulation of the publication process:

- (1) Discrepancies in scope
- (2) Discrepancies in the description of the research reported
- (3) Discrepancies between the availability of data and the research described
- (4) Inappropriate citations
- (5) Incoherent, meaningless and/or irrelevant content included in the article
- (6) Peer-review manipulation

The presence of these indicators undermines our confidence in the integrity of the article's content and we cannot, therefore, vouch for its reliability. Please note that this notice is intended solely to alert readers that the content of this article is unreliable. We have not investigated whether authors were aware of or involved in the systematic manipulation of the publication process.

In addition, our investigation has also shown that one or more of the following human-subject reporting requirements has not been met in this article: ethical approval by an Institutional Review Board (IRB) committee or equivalent, patient/participant consent to participate, and/or agreement to publish patient/participant details (where relevant).

Wiley and Hindawi regrets that the usual quality checks did not identify these issues before publication and have since put additional measures in place to safeguard research integrity.

We wish to credit our own Research Integrity and Research Publishing teams and anonymous and named external

researchers and research integrity experts for contributing to this investigation.

The corresponding author, as the representative of all authors, has been given the opportunity to register their agreement or disagreement to this retraction. We have kept a record of any response received.

References

- [1] A. Yu, J. Wang, Y. Zhou et al., "Analysis on the Educational Value of Winter Olympic Spirit in Track and Field Teaching Based on Data Mining under Artificial Intelligence," *Journal of Sensors*, vol. 2022, Article ID 9435846, 8 pages, 2022.

Research Article

Analysis on the Educational Value of Winter Olympic Spirit in Track and Field Teaching Based on Data Mining under Artificial Intelligence

Ao Yu ¹, Jianxing Wang,² Yixin Zhou ³, Xiaoyu Qiao,⁴ Song Yan,⁵ Yufang Feng,⁶ Elvan Marcos,⁷ Lee Seok Jae,⁸ and Avera Fiaidhi⁹

¹College of Physical Education, Woosuk University, Jeonju55338, Jeollabuk-do, Republic of Korea

²Information Science and Engineering, Chongqing Jiaotong University, 400074 Chongqing, China

³Shanghai Business School, Shanghai 201400, China

⁴School of Education, Woosuk University, Jeonju 55338, Jeollabuk-do, Republic of Korea

⁵Sport Medicine, Beijing Sport University, Beijing 100000, China

⁶Computer Graphics, Shandong University of Technology, 255049 Shandong, China

⁷Iloilo Science and Technology University, Iloilo, Philippines

⁸Kookmin University, Seoul, Republic of Korea

⁹Lakehead University, Lakehead, Canada

Correspondence should be addressed to Ao Yu; 631418070113@mails.cqjtu.edu.cn

Received 31 August 2022; Revised 13 September 2022; Accepted 20 September 2022; Published 7 October 2022

Academic Editor: Sweta Bhattacharya

Copyright © 2022 Ao Yu et al. This is an open access article distributed under the Creative Commons Attribution License, which permits unrestricted use, distribution, and reproduction in any medium, provided the original work is properly cited.

School sports is the basis for the development of mass sports and competitive sports. It goes without saying that the key to the development of school physical education is school physical education, and the teaching of track and field (TAF) courses occupies an irreplaceable position in students' growth education. The stepping stone for the cultivation of sports awareness plays a pivotal role in the better healthy growth of students and the improvement of the physical quality of all citizens. As a major gold medalist in the Olympic Games, TAF is welcomed, valued, and popularized by many countries. Especially in colleges and universities, TAF can cultivate the will of college students and the spirit of continuous improvement. The Winter Olympics (WO), adhering to the spiritual concept of overcoming challenges and facing difficulties, embodies the strength of unity and collective. Based on the current situation of TAF teaching in a university, this paper uses data mining technology to analyze the students' favorite TAF events and their mastery of the WO knowledge and then combines the educational value of the WO spirit to conduct research to explore the teaching significance of the WO spirit to the TAF curriculum.

1. Introduction

TAF is the mother of sports and occupies an important position in all sports. It has the characteristics of various types, rich contents, and various forms of exercise. Actively developing TAF sports can meet the development needs of students of different ages in the core literacy of sports. Track and field venues and equipment generally include standard track and field venues, 400 m standard runways, starters, relay batons, hurdle frames, jumping viaducts, high jump crossbars, high jump pole controllers, springboards, and

shot put. TAF sports are based on walking, running, jumping, and throwing and are an important means to promote students' basic athletic ability. In the process of participating in the TAF games, the students gradually formed a fair and just competition awareness and good moral behavior, and in the process of sports, they could constantly hone their willpower and cultivate their spirit of bravery and struggle. This is the embodiment of the spirit of the Winter Olympics. In the preliminary group, the athletes with good results should be equally allocated to different groups as far as possible. In the subsequent rounds, the grouping is based on the

results of the athletes in the previous round. If possible, athletes from the same country or region should be separated.

Excellent achievements have been made in the research on the educational value of the WO spirit in TAF teaching. For example, a scholar proposed that the spiritual education of the WO is not only a social phenomenon but also school education at all levels. WO spiritual education has a positive effect on allowing people all over the world to participate in sports activities and improve their sports level. The surface structure of track and field track has developed from the soil layer to the mixed layer of cinder, lime, and clay. Experience shows that it is suitable for most 400 m semicircular runways to be built with a curve radius of 35 m to 38 m. IAAF proposes to build a runway with a radius of 36.50 m as far as possible. WO spiritual education inspires people, especially students, to participate in TAF sports, understand the connotation and spirit of TAF sports, and understand cooperation and competition [1]. In addition, a scholar expounded his views from different perspectives. He believed that the spirit of the WO not only emphasizes the essential content of sports competitions but also includes social culture, knowledge education, and other content, which are important factors in promoting human progress and maintaining world peace. The Olympic Games is a world-class sports event that combines sportsmanship, national spirit, and internationalism and symbolizes world peace, friendship, and unity. This is the embodiment of the Olympic spirit. It is also a valuable spiritual wealth and intangible cultural heritage of mankind. Human beings should inherit and carry forward the spirit of the WO, transmit positive energy to human beings, and make full use of the spirit of participation, enterprising spirit, solidarity, and dedication in social practice, so as to promote the continuous progress of mankind [2]. A scholar believes that the spirit of the WO in TAF is reflected in the fact that students can work hard in the process of TAF competition, maximizing their potential in physical, mental, technical, and intellectual to win the competition. Olympic is a competitive spirit, an attitude to life, a philosophy of life, and a harmonious, free, healthy, and positive modern ethics, and the Olympic movement is a common heritage of human civilization. It is noted that the Olympic Games integrate sports, culture, and education; bring about perfect harmony between people's body and mind, spirit, and quality; and fully develop human potential and virtue. It is the best and most perfect philosophy of human life so far. At the same time, in an equal, friendly, fair, and just competition environment, we will promote the peaceful development of mankind through mutual respect [3]. Although many scholars believe that the spirit of the WO has a very important educational value, there is an extremely lack of research on the integration of the spiritual education of the WO into daily physical education in China and the introduction of the experience of the integration of the spiritual education of the WO into school sports abroad. The ethical value in the Olympic spirit is the greatest respect and advocacy for human potential and free creation, human civilization and good order, and the inheritance and development of all good moral values and ethical norms of mankind. It guides people to pursue the most optimized eth-

ical concept of survival and development, which is the guarantee for the harmonious coexistence of human beings and the environment and the coordinated development of individuals and society.

This paper first analyzes the concept of data mining and proposes data mining methods in the field of education. Then, through field inspections and interviews, we understand the current situation of WO spiritual education in TAF teaching in a university. Through the current situation, we can reflect whether the school is in TAF teaching. The education of the WO spirit should be promoted. From the experimental point of view, most students and teachers agree with the WO spirit. Finally, this paper puts forward the teaching significance of the WO spirit to the TAF and hopes that schools can popularize the WO spirit to students in the TAF teaching.

2. Data Mining

2.1. The Technical Meaning of Data Mining. Data mining is the process of extracting potential and useful information from a large amount of noisy practical application data [4]. Data mining is usually related to computer science, and it achieves the above goals through many methods such as statistics, online analysis and processing, information retrieval, machine learning, expert systems (relying on past empirical rules), and pattern recognition. Applying data mining to process educational affairs data can discover the laws it contains, and applying these laws to education and teaching management will contribute to the reform of education and teaching and improve the level of running schools and management [5]. Data mining mainly includes three steps: data preparation, rule finding, and rule representation. Data preparation is to select the required data from the relevant data sources and integrate them into a data set for data mining. Rule finding is to find out the rules contained in the data set by some method. Rule representation is to express the found rules in a way that users can understand as much as possible.

Applying association rules in data mining, text mining, and other technologies to the field of education can present useful knowledge and information discovered to educators and, at the same time, push learning suggestions according to the learning situation of learners. It plays a significant role in realizing teacher and learning improvement in learning [6]. The process of data mining in teaching practice is shown in Figure 1, which will eventually form teaching knowledge. In recent years, data mining has attracted great attention in the information industry. The main reason is that there are a large number of data that can be widely used, and there is an urgent need to convert these data into useful information and knowledge. The acquired information and knowledge can be widely used in various applications, including business management, production control, and market analysis.

2.2. Educational Data Mining Methods. Prediction: prediction is the use of historical data to find out the development law of things and build models to predict the characteristics of future data. Data mining uses ideas from the following

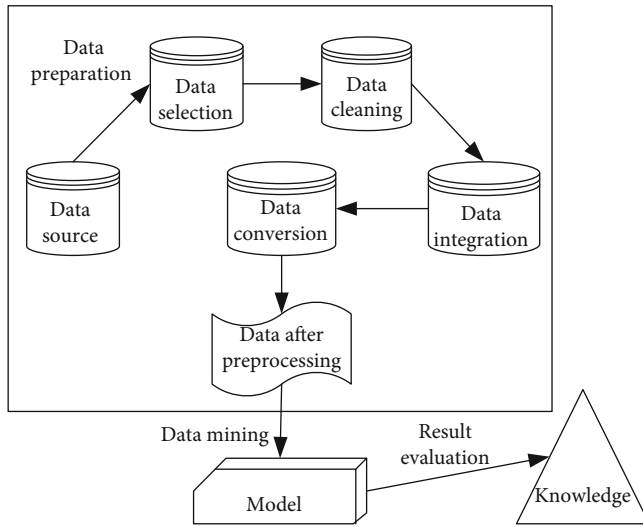


FIGURE 1: Data mining process.

fields: sampling, estimation, and hypothesis testing of statistics; search algorithm, modeling technology and learning theory of artificial intelligence, pattern recognition, and machine learning.

Clustering: according to the characteristics of different data with different characteristics, we can divide a complete set of data into several different subsets. For example, researchers divide learners into different groups according to their different learning ability levels and then provide appropriate learning resources and organize appropriate learning activities for different groups [7, 8]. The difference between clustering and classification is that the classification required by clustering is unknown. Clustering makes the objects in the same cluster have great similarity, while the objects in different clusters have great differences.

Relational mining: relational mining is about finding meaningful connections between large amounts of data in order to provide the necessary support for certain decisions. It is an important and difficult-to-dig knowledge point in the database and is widely used in opinion decision-making systems [9]. The type of data can be structured, semistructured, or even heterogeneous. The methods of discovering knowledge can be mathematical, nonmathematical, or inductive. The knowledge finally found can be used for information management, query optimization, decision support, and data maintenance. For example, by analyzing the courses selected by students, we can understand which aspects of course learning students are more inclined to learn, so as to provide reference for course development [10]. Rule mining technology refers to extracting hidden, potential, previously unknown, and useful knowledge and rules from databases. This involves association rule mining. Association rules reflect the interdependence between transactions in the form of $X \implies Y$ [11]. The formulas for the support and confidence of an association rule are as follows:

$$S = F \left[\frac{X \& Y}{N} \right], \quad (1)$$

$$C = \frac{F(X \& B)}{F(X)}. \quad (2)$$

Among them, S represents the support degree, F represents the probability function, and N represents the number of times.

3. Analysis of the Current Situation of Experimental Research and Teaching

3.1. Study Preparation

(1) Research purpose

My country's TAF events have always been at a disadvantage. In the final analysis, it is the disconnection of the reserve force training system, and the training of TAF athletes by school physical education has become the mainstay of transporting TAF reserve forces. Therefore, the development of TAF sports is the general trend and the inevitability of social development. However, in the process of TAF teaching, teachers must convey the spirit of the WO to students and make students believe in the Olympic concept in TAF training and competitions, in order to promote the rapid development of sports. Therefore, this paper actively explores and studies the educational significance of the spirit of the WO to the TAF teaching and strives to incorporate it into the TAF teaching.

(2) Research methods

This paper conducts a field trip to a university to investigate the current situation of the school's TAF teaching and the current situation of the WO spiritual education and through interviews with 250 students and 47 physical education teachers to understand their cognition and attitude towards the WO spiritual education in TAF teaching. The interview method collects information through direct face-to-face conversation between researchers and respondents, which is flexible and adaptable. Interviews are widely used in education investigation, job search, consultation, etc. They include both fact investigation and opinion consultation and are more used for personality and individual research.

3.2. Current Situation of TAF Teaching and WO Spiritual Education

(1) Current situation of TAF teaching

The TAF teaching projects that the school have implemented include relay running, obstacle running, sprint, long jump, high jump, softball, and long-distance running. As shown in Table 1, a survey is conducted on the types of TAF events that the students of the school like. The top three are relay running, obstacle running, and sprint running, accounting for more than 50% of the population; long-distance running, which is also a track race, ranks first from the bottom, indicating that students like intense and interesting projects, while long-distance running is

TABLE 1: Students' favorite athletics.

	Number of people	Proportion (%)	Sort
Relay run	152	60.8	1
Obstacle course	137	54.8	2
Sprint	128	51.2	3
Long-distance running	26	10.4	8
Long jump	123	49.2	4
High jump	119	47.6	5
Softball	86	34.4	6
Shot put	72	28.8	7

relatively boring. It is difficult to arouse students' interest in participating. In the field events, about 50% of the students like the long jump and high jump; 34.4% of the students like the softball project, and relatively few students like the shot put project, accounting for 28.8%. On the whole, there is little difference in the students' liking for running and jumping items, and the liking for throwing items is slightly lower. Differences among students in various aspects lead to different needs for the types of TAF events, which requires teachers to pay attention to the needs of students in teaching, fully implement the content of TAF teaching, and promote the all-round development of all students.

(2) Students' mastery of WO knowledge

In order to understand the students' mastery of WO knowledge, 5 questions related to Olympic and WO knowledge were designed, and the correct rate of students' answers on these questions was obtained, as shown in Figure 2. The Olympic ideological system is an organic combination of quality education, which mainly includes Olympic education, the consistency of objectives, the practical concept of quality education, and the integration of promoting quality education. It mainly includes three aspects: First, the cognition of the Olympic motto, the correct rate is 69.6%. The second is the understanding of the Olympic spirit. The correct answer rate is only 27.2%, indicating that students have less understanding of the Olympic spirit of "unity, friendship, and fair competition." The third is the understanding of the history and events of the WO. The correct answer rates for the WO events and the Summer Olympics events are relatively high, showing 58% and 60.8%, respectively. But knowledge of the location of the first WO showed a correct answer rate of 15.6%.

The survey results show that the students have a certain understanding of the basic knowledge and history of the WO, but they still lack the awareness of the Olympic spirit. The content of the rules and regulations is more concerned, but the content of the Olympic history, spirit, and educational core is insufficient.

3.3. The Current Situation of WO Education in TAF Teaching

(1) The form of spiritual education of the WO

The implementation of Winter Olympic education is based on rich, diverse, and creative educational activities, and through these well-designed educational activities, the goal of Olympic educational value is realized. According to the survey, the school's activities related to Winter Olympic education are mainly inactive courses, with lectures (24.3%), knowledge contests (12.7%), WO handwritten newspapers (16.2%), and dryland projects (15.1%) mainly. With the promotion of the school's dryland project, dryland ice and snow sports have shown certain advantages, and dryland sports have also become one of the main methods of the school's WO education activities. As can be seen from Figure 3, the activities of WO education are rich and diverse, with different forms. At the same time, according to the actual situation of the school, localized educational activities are produced according to local conditions. Compared with traditional curling, dry land curling can only be performed on ice, with high requirements for entry technology and long learning cycle. Dry land curling has the characteristics of small footprint, easy learning, and mastery, and not affected by seasons. As long as the ground is flat and smooth, indoor and outdoor learning, training, and competitions can be held at any time. However, there are also problems of insufficient design, weak integration, simple design of activity content, and insufficient innovation. The existence of these problems will directly affect students' understanding of the spirit of the WO and limit the actual effect of Olympic education.

(2) The cognition of the spiritual education value of the WO in the TAF teaching

Students believe that the value of WO spiritual education in TAF teaching is mainly reflected in the following: (1) strengthening the spirit of unity, accounting for 26.4%; (2) established a tenacious spirit that is not afraid of setbacks, accounting for 20.8%; (3) cultivate the spirit of fair competition, accounting for 16.8%; (4) enhance self-confidence, accounting for 14.8%; and (5) strengthen moral cultivation, accounting for 9.6%. Table 2 and Figure 4 are surveys of students' cognition of the value of WO spiritual education in TAF teaching. It can be seen that most students believe that WO spiritual education can bring certain value to themselves, mainly reflected in knowledge and cultural value and life. In terms of value, outstanding value and collective value, students fully realized the value of the WO spirit to individuals. But the awareness of the social value, competitive value, moral value, and emotional value of Olympic education is low. The Olympic spirit is a self-challenging spirit of "faster, stronger, and higher". At the same time, it is also a fair, just, equal, and free spirit of sports competition. The spirit of self-challenge and fair competition contained in the Olympic Games constitute the cornerstone of contemporary human self-improvement and social interaction. The presentation of this result is inseparable from the design of my country's WO spiritual education activities. The simplicity and unity of the WO spiritual education practice and the inability of the content of educational practice to fully reflect

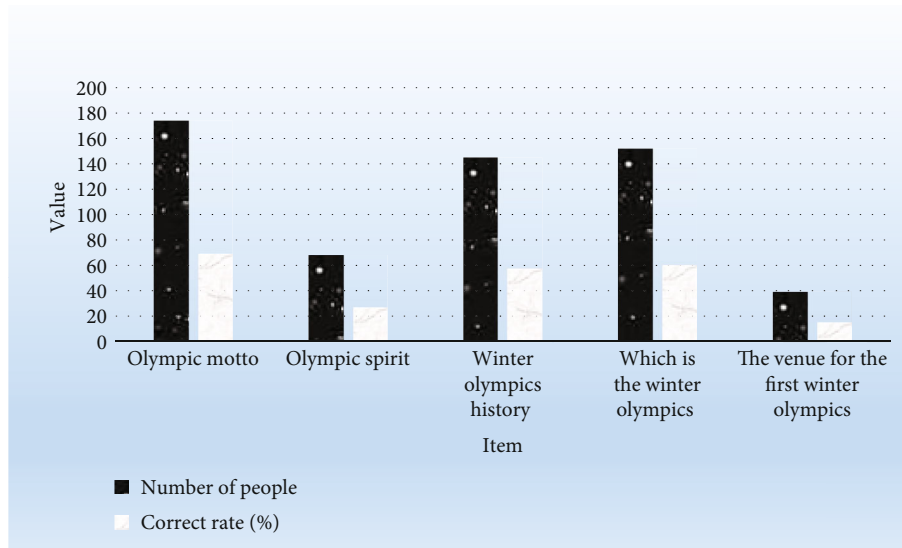


FIGURE 2: Students' mastery of WO knowledge.

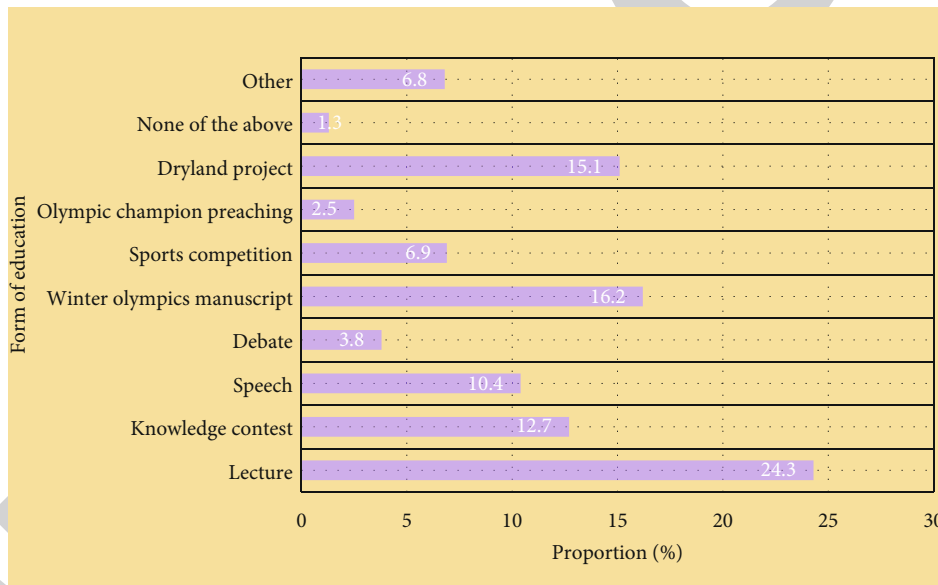


FIGURE 3: The form of WO spiritual education.

TABLE 2: Students' cognition of the value of WO spiritual education in TAF teaching.

	Number of people	Proportion (%)
Optimistic attitude to life	18	7.2
Boost self-confidence	37	14.8
Build a tenacious spirit	52	20.8
Increase solidarity	66	26.4
Strengthen moral cultivation	24	9.6
Cultivate the spirit of fair competition	42	16.8
Other	11	4.4

various aspects of educational value have led to students' lack of awareness of TAF. The cognitive level of the educational value that needs to go deep into the spirit of the WO in teaching is relatively shallow.

Physical education teachers are dominant in the course of TAF teaching. The degree of importance that physical education teachers place on TAF classes determines the effect of TAF teaching and is an important guarantee for the smooth development of TAF classes and their long-term development. As shown in Table 3, in a survey of the school's physical education teachers' cognitive attitudes on whether the WO spirit should be popularized in TAF teaching, it was found that 45 people believed that it was necessary or very necessary to popularize the WO spirit in TAF classes, accounting for 95.74% of the total number of

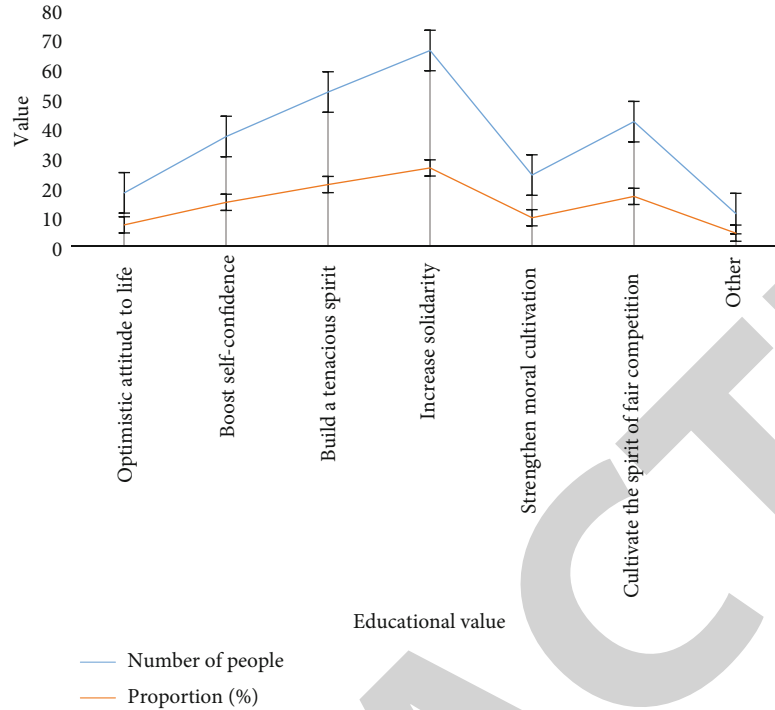


FIGURE 4: Statistics on the cognitive value of spiritual education in the WO.

TABLE 3: Attitudes of physical education teachers to popularizing the spirit of the WO in TAF classes.

	Very necessary	Needed	It does not matter	No need
Number of people	8	37	2	0
Proportion (%)	17.02	78.72	4.26	0

physical education teachers, and only 2 people believed that it was indifferent or unnecessary to popularize the spirit of the WO. The above data clearly shows that the popularization of the spirit of the WO in the TAF class is essential, which is conducive to the long-term development of the school's TAF teaching and to the students. Spiritual education has a positive effect.

3.4. Analysis of the Value and Practical Problems of WO Spiritual Education in TAF Teaching

- (1) Insufficient understanding of the value of WO spiritual education

The effective development of WO spiritual education needs to be based on a deep understanding of the value of WO spiritual education. Only on the basis of recognizing and understanding the connotation and significance of the value of WO spiritual education can the implementers and participants of WO spiritual education consciously take the initiative to participate in and create Olympic practical activities [12, 13]. However, through this practical interview on the school's WO spiritual education in TAF teaching, it

can be seen that the school and teachers do not fully understand the spiritual value of the WO. In the investigation of the current situation of TAF teaching, the school's heavy workload and the school's opposition to the WO spiritual education have become obstacles to the development of TAF teaching.

- (2) The value of WO spiritual education is out of touch with practice

The value and practice of WO spiritual education are complementary and inseparable. The spiritual education value of the WO provides the theoretical basis and action guide for specific practical activities, and the spiritual education value of the WO continuously enriches the theory in practice. The two are mutually dependent and complementary [14]. Judging from this research and survey, the value and practice of WO spiritual education are somewhat separated and need to be integrated. The specific manifestations are as follows.

One is the lack of coupling between the globalized WO spiritual education value and the localized WO spiritual education practice. In order to ensure the practical effect of Winter Olympics spiritual education, it needs to be combined with localized educational concepts and cultural values. The value of WO spiritual education has a common guiding significance for all students, but in the process of WO spiritual education practice, it is necessary to combine the characteristics of students and the situation of school education, realize localized creation, combine with each other, and achieve organic unity. Judging from the current Olympic education practice, there have indeed been some localized practical activities for the WO, but the degree of

coupling with the spiritual education value of the WO is not high enough, and the degree of conformity is not enough. In the process of localization, the Olympic Games cannot be fully realized and penetrated and value concept.

The second is the separation of theoretical knowledge and practice of WO spiritual education. The instillation of the WO spiritual education theory should be integrated into the track and field teaching practice process. Judging from the actual situation of the current WO spiritual education, the WO spiritual education for students is relatively simple, and there is no comprehensive education model [15]. Students' understanding of the spirit of the WO mainly comes from inactive courses, including the mastery of Olympic sports knowledge, the study of history and culture, and the experience of Olympic values mainly through sports participation and the mastery of sports skills. The theory and practice of Olympic education should be better integrated, combining active and inactive courses to achieve students' comprehensive understanding of Olympic values.

Third, in the process of local practice of WO spiritual education, the form of educational activities focuses on team value and social value in the cultivation of values and does not pay enough attention to the development of students themselves. Athletics teaching did not play a dominant role in the practice of WO spiritual education, resulting in low participation of students in track and field sports and insufficient understanding of the value of WO spiritual education [16].

4. An Analysis of the Value of Conducting Winter Olympics Spiritual Education in Track and Field Teaching

(1) Establish a good sports outlook on life and values

Athletics is an important part of college students' study and life, and the purpose, thought, and spirit of the WO can give college students a healthy and optimistic attitude towards life. In the fierce confrontation and competition in TAF competitions, teammates must trust each other and cooperate tacitly. If there is no spirit of unity and cooperation, it will be difficult to go higher and farther. Students follow the WO spirit in the process of participating in TAF sports, which can enhance mutual understanding, understanding and trust, suggest friendship, consciously form team spirit, and attach importance to solidarity and mutual assistance. At the same time, the spirit of the WO also provides rich cultural resources for the construction of a harmonious campus and provides an important guarantee for students to establish lofty ideals and beliefs, improve their cultural awareness, and establish a sense of social morality and responsibility.

(2) Cultivate independent personality and sense of competition

WO spiritual education is a kind of personality education that respects individual differences and focuses on indi-

vidual development. In TAF sports, students are constantly cultivated to develop comprehensively the personality of self-determination, self-discipline, self-esteem, self-love, self-respect, and self-respect. College students can improve their self-awareness and their own health through TAF sports. The spirit of the WO advocates that students must have a fair competition, abide by the rules of the game, and have an upright sports spirit. Under the guidance of the spirit of the WO, cultivate a fair and just competition spirit, improve competition awareness and sense of order, and develop an independent personality.

(3) Cultivate the quality of sports will


Because in the relationship between the educational value of the WO, people and society are the main body and are in the active position. The WO are objects and are in a position to be served. Therefore, people's choice of practice, cognition, comprehension, evaluation, and absorption of the spirit of the WO and its meaning all contain various intentional thinking of the subject. It is difficult for a person with weak will to obtain a long-term survival qualification in a highly competitive society and even more difficult to gain a foothold in his career. Now, some students have the characteristics of strong self-awareness, poor restraint ability, quick acceptance of new things, and weak will quality. Therefore, it is particularly important to pay attention to the cultivation of students' will and quality. The quality of will determines the survivability and competitiveness of contemporary students in the future. The spirit of the WO has a positive effect and value on the formation of a good will and a sense of competition among students.

5. Conclusion

WO spiritual education has a very important impact on the healthy growth of students and the formation of personal and social values. Through the investigation and analysis of the value and practice of Winter Olympic education for college students, this paper understands the current situation of WO spiritual education in college TAF teaching under the background of the WO through investigation and research and analyzes the school's TAF teaching. The status quo of cognition of the educational value of Olympic spirit and teachers' attitude towards popularizing the Winter Olympic spirit in TAF teaching. The experiment shows that students believe that the educational value of the Winter Olympic spirit in TAF teaching is mainly reflected in the ability to enhance the spirit of solidarity, tenacity, and fair competition. And 95.74% of teachers believe that the WO spirit needs to be popularized in TAF teaching, indicating that both students and teachers recognize the educational significance of the WO spirit in TAF teaching. To this end, the article finally discusses the educational value of WO spiritual education in TAF teaching, which is mainly to cultivate students' spiritual will and promote their healthy personality development. The key to improving IoT technology is to combine RFID technology, sensor network, M2M system

Research Article

Application of Heart Rate Combined with Acceleration Motion Sensor in Sports Dance Teaching

Lin Li,^{1,2} Yuanyuan Liu,^{2,3} Yue Gu ,^{1,2} and Zhe Zhu²

¹School of Physical Education, Hunan International Economics University, Changsha, 410205 Hunan, China

²School of Graduate, Adamson University, Hermita, 1000 Manila, Philippines

³Humanities College, Wuhan University of Engineering Science, Wuhan, 430000 Hubei, China

Correspondence should be addressed to Yue Gu; yue.gu@adamson.edu.ph

Received 11 July 2022; Revised 24 August 2022; Accepted 30 August 2022; Published 6 October 2022

Academic Editor: Sweta Bhattacharya

Copyright © 2022 Lin Li et al. This is an open access article distributed under the Creative Commons Attribution License, which permits unrestricted use, distribution, and reproduction in any medium, provided the original work is properly cited.

Because of the large amount of exercise, sports dance has the characteristics of good viewing and strong movement, and has gradually entered the campus in recent years. However, sports dance is not only difficult, but also has a wide variety of categories except modern dance and Latin dance. In addition to these two categories, there are 10 kinds of dances in total. Therefore, in teaching, schools have no choice, and students cannot understand which dance styles are most effective for students' physical exercise. In order to solve the problem that there are many kinds of sports dance and the effect of students' exercise is unclear, this paper studied sports dance teaching based on heart rate combined with acceleration motion sensor, and obtained the energy consumption in sports dance teaching by using this measurement method. After comparing the effects, four kinds of dance activities, namely quickstep, waltz, rumba, and samba, which are more conducive to physical exercise, were screened out for students in the complex sports dance. In addition, in order to confirm the experimental results of the article, after the teacher improved the physical dance teaching according to the content of the article, it was found that before the experiment, the average scores of the two groups of subjects were 17.5 points and 16.75 points. After the experiment, the scores of the two groups increased by 3.5 points and 2.8 points, respectively. Through the experimental results and data, it can be shown that the research in this paper has played a good role in the improvement of sports dance teaching.

1. Introduction

Nowadays, physical education is more and more valued in schools. According to the "Opinions on Strengthening Youth Sports and Enhancing Youth Physical Fitness" issued by the State Council, in China, the Ministry of Education stipulates that the frequency of physical education is once a day and ensures that 50% of the class time is medium to high-intensity physical activity. In order to meet the country's requirements for students' physical exercise, the types and scope of physical activities have been expanded, and sports dance has also been incorporated into the elective physical education curriculum of many schools. As a relatively novel sports activity, sports dance is different from traditional running and jumping, various ball games or swimming, etc. It is also different from the ease of use of traditional dances. Because of its certain degree of difficulty, a

large part of the introduction of sports dance is aimed at exercising students' physical fitness and cultivating students' professional dance skills as a secondary purpose. However, there is currently no objectively measured data on whether physical dance teaching achieves any purpose. Therefore, the objective measurement of physical activity in sports dance has a very important reference value for the specialization reform of physical education classes in the future. There are many methods for measuring physical activity, but they all have certain limitations. The physical activity questionnaire is in the form of recall and self-report, which is greatly influenced by subjectivity, and has low reliability and validity in children and adolescents. The double-labeled water method is expensive, the test cycle is long, and only the total energy consumption can be obtained. Indirect calorimetry equipment has poor portability and high operating requirements, and is often used as a

calibration standard for other methods. In order to test whether physical dance teaching really plays a role in students, it is of practical significance to study the physical energy consumption of physical dance.

Because of the difficulty of physical dance coordination and the long-term nature of physical education, physical education teaching has always been a hot research topic among researchers. On the basis of factor analysis, Osadtsiv T et al. established a physical fitness level evaluation system for sports dance teaching for young dancers [1]. His research can promote the improvement of sports dance teaching, but more practical verification is still needed. Liu Y scientifically analyzed the influence of sports dance on the dynamic characteristics of the foot movement of college students. The effects of sports dance on the pressure intensity and gait characteristics of college students' insole were studied through experimental tests. His research was of great significance for guiding the force of the foot in sports dance [2]. Nonetheless, his research on foot injuries in dance was lacking. Granados D et al. introduced machine assistance, proposing a combined cognitive and physical performance feedback for assisting the dance sports learning process [3]. His research has revolutionized the teaching method of sports dance, but the teaching efficiency needs to be improved. In order to improve the effect of physical dance teaching, Wang Y studied the teaching design and application of high school dance courses based on 3D holographic technology, and designed a dance teaching process based on 3D holographic technology [4]. His research can well break down the main points and show them repeatedly in front of students, so that students can master the skills and content of dance movements. Weng X et al. conducted a research on the aesthetic training in the teaching of sports dance for college students [5]. His research has promoted the aesthetic diversity of sports dance, but the practical content is too complicated and needs to be further simplified.

In various sports or physical education, motion sensors provide assistance for our movement methods. Valero E et al. proposed a novel visual-inertial localization method, which can be directly integrated into the heart rate combined acceleration motion sensor for simulation and training [6]. Although his research was relatively novel and effective, the equipment involved was relatively expensive. Hutchinson M et al. proposed a motion sensor data collection strategy. His research was initially used to identify interference sources and avoid danger, and then also used in sports dance teaching. First, the parameters of the release source were estimated using the Markov chain Monte Carlo sampling method, and then the most informative operation was selected from a set of possible choices using the concept of maximum entropy sampling [7]. His research has demonstrated at the numerical simulation level that the performance is greatly improved compared to traditional methods, but the accuracy needs to be improved. Shin SH et al. proposed a sensor with multifunctional flexible motion [8]. His research can further expand the sensing limit, accuracy, and functionality of motion sensors, but also has the problem of being too expensive to implement. Gaidhani A et al. designed a heart rate combined acceleration motion

sensor that can be used to monitor respiration during exercise, which was subsequently used in sports dance teaching [9]. His research has broadened the applicability of motion sensors, but the effect still needs long-term testing in practice.

Based on the heart rate combined with the acceleration motion sensor, this paper studied the energy consumption in sports dance teaching, drew the results, and compared them, so as to screen out the sports dance that has a good effect on students' exercise. The innovation of this article was that in addition to using Actiheart heart rate combined with acceleration motion sensor, Comsed K4b2 equipment was also used to measure the energy consumption of sports dance, which made the experimental results more accurate.

2. Method of Heart Rate Combined with Acceleration Motion Sensor

2.1. Physical Dance Teaching Mode. As an emerging sport, sports dance has quickly set off a learning boom in the campus and society with its distinctive features of social entertainment and performance competition. In order to adapt to the development of the times, many colleges and universities have successively added sports dance majors. Sports dance is a comprehensive sports event that integrates sports, art, dance, and music, and is scored in terms of basic techniques, dance styles, musical performance, choreography, field effects, and on-the-spot performance [10]. It is also a difficult and beautiful sport that is scored in six aspects: basic technique, dance style, musical expression, choreography, field effect, and on-the-spot performance. In order to achieve the best results in sports dance competitions, one can pursue superb techniques, more creative choreography, best field effects, and highly infectious expressiveness [11]. This also means that the education of sports dance in schools is very difficult. The introduction of different types of sports dance is shown in Figure 1.

As shown in Figure 1, sports dance is mainly divided into two categories: modern dance and Latin dance. There are many different dance styles under these two categories. The modern dance items include foxtrot, tango, quickstep, waltz, and Vienna waltz. Latin dance groups include rumba, cha cha, cowboy, samba, and bullfight. There are different styles of dance, each with its own characteristics. To sum up, the artistic expression of different dances has its own unique form of expression and aesthetic connotation in each art field. Due to the differences in the types of art, the cultivation of artistic expression has its own characteristics. Even so, there are commonalities in artistic expression in all fields, that is, they all pursue the harmony and unity of spiritual emotions and external skills, and have reached an emotional resonance of artistic conception.

Because of the diversity of sports dance types and the complexity and time-consuming of learning, even professional dance schools have to go through years of training to learn all types roughly. Most students will only choose one of them for intensive study. Because there are many types of dance sports, schools have limited funds for hiring teachers. It is impossible to recruit teachers to teach every

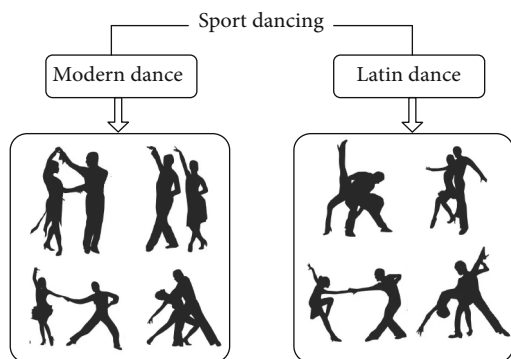


FIGURE 1: Schematic diagram of different types of sports dance.

type of dance, so sports dance is selective for students, both in terms of teaching and students' learning [12]. This article cannot cover all categories in the teaching of sports dance. Taking rumba as an example to make a basic explanation, rumba dance is characterized by romantic style and charming dancing posture. Both men and women pay attention to body posture. The dance is soft and graceful, and the footwork is graceful. It is more about the feeling of the body and it is relatively difficult for Cha Cha, but Cha Cha has other characteristics. Among the ten dance types, dancers have to learn different content for different dance methods [13].

2.2. Physical Fitness Measurement Methods in Sports Dance Teaching. In sports dance, the heart rate monitoring method is easily affected by factors such as emotions, body temperature, and environment, and the heart rate has a lag in response. The pedometer method cannot distinguish exercise intensity, and the accuracy is greatly affected by exercise intensity and activity type. The accelerometer is a widely used objective measurement method. The three-axis accelerometer ActiGraph GT3X+ is a commonly used accelerometer, but its accuracy is not high in the measurement of static and low-intensity physical activity. Therefore, this paper used Actiheart heart rate combined with acceleration motion sensor to study sports dance in teaching. Actiheart heart rate combined with accelerometer motion sensor (Cambridge Neurotechnology, Cambridge, UK) is currently the only measurement tool in the world that combines heart rate and accelerometer [14]. Studies have shown that Actiheart is a good predictor of physical activity in a laboratory setting. Previous studies have been conducted in the laboratory, and there has been no validation of field physical activity items in the free-moving state. The activity environment of sports dance is similar to the laboratory environment, so it is more effective to use Actiheart to objectively and accurately measure the physical activity level of sports dance.

Actiheart is currently the only heart rate combined acceleration motion sensor that can simultaneously collect heart rate and vertical axis activity counts. By converting the electronic signal into the energy consumption index, the energy consumption is estimated by using the prediction formula built in the device. Actiheart measures a wide range of physical activity of varying intensities (heart rate 31-250). It can

store the collected data in the device at the end of the test. Usually, the data can be saved for 1-3 weeks. It is downloaded and exported to an Excel file via a docking station and dedicated software, which includes data such as activity counts, energy expenditure, and heart rate. In actual use, Actiheart is fixed on the corresponding test site of the chest through 3 M electrode pads. Figure 2 is the structure and measurement diagram of the Actiheart sensor.

As shown in Figure 2, Actiheart (Cambridge Neurotechnology, Cambridge, UK) is a combined heart rate and acceleration motion sensor. In actual measurement, Actiheart weighs about 8 grams and is 188 mm long, and can measure ACC, HR, HRV, and 15 s, 30 s, and 60 s of ECG. The memory capacity is 128 kb, which can store 60s of records for 11 days. Heartbeat interval and ECG waveform data can be recorded for about 24 hours and 13 minutes, respectively. Acceleration is measured by a piezoelectric element in the Actiheart, reacted by a frequency of 1-7 Hz (3 dB) and stored as counts, and counts are linearly related to acceleration by a factor of 0.003 m/s per count per minute [15]. Actiheart is tested by fixing two 3 M pads to the corresponding test site on the chest, and the two pads are placed in the lower part between leads V1 and V2 and at the position of V4 or V5.

The way to improve the accuracy of physical activity measurement is to collect a variety of activity data indicators for analysis and conversion (such as heart rate, activity count, etc.). The effect of measuring physical activity by heart rate alone is not very satisfactory, and the combination of acceleration and heart rate in the teaching of sports dance by the Actiheart motion sensor can greatly improve the accuracy of prediction of energy consumption, which is very important for the measurement of sports dance in this paper. Because in sports dance teaching, some scholars have found that the ACC+HR is more accurate than the ACC or HR alone, and the prediction ability of the ACC+HR is better. Therefore, this paper believes that Actiheart can better predict physical activity energy expenditure by effectively combining acceleration and heart rate compared to using either indicator alone (using acceleration or heart rate indicator alone) [16].

In sports dance, in order to detect the effectiveness and intensity of the activity, in addition to the Actiheart heart rate combined with the acceleration motion sensor used to measure the heart rate, oxygen consumption is also another important parameter to be measured. Therefore, this paper uses Comsed K4b2 (Comsed, Rome, Italy) gas metabolism analyzer with Actiheart sensor to measure sports dance activities in teaching. It uses the principle of indirect calorimetry to measure the oxygen consumption under various exercise intensities by analyzing the content of oxygen and carbon dioxide in each breath and calculating the energy consumption per unit time. Comsed K4b2 can measure the oxygen consumption under different sports, and is often used as the gold standard to verify the validity and reliability of the energy consumption measurement methods of other instruments. Figure 3 is the measurement principle diagram of the K4b2 equipment.

As shown in Figure 3, K4b2 can be used in combination with Actiheart in the teaching of sports dance because of its

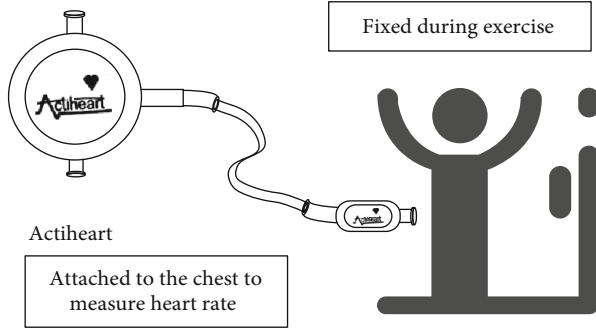


FIGURE 2: Actiheart sensor measurement structure diagram.

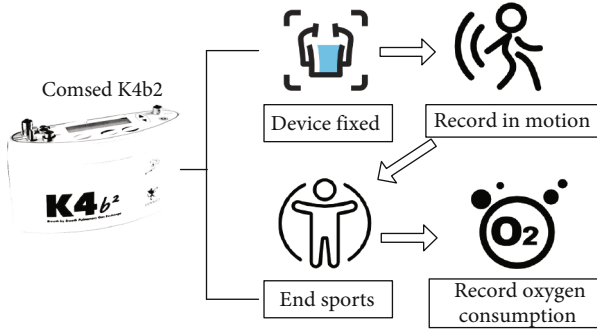


FIGURE 3: Measurement principle diagram of K4b2 device.

accurate measurement of oxygen consumption. The calculation of K4b2 energy consumption (Energy Expenditure, EE) adopts Weir formula:

$$EE(Kcal/min) = 3.9 \times (VO_2) + 1.1 \times (VCO_2). \quad (1)$$

Among them, EE stands for Energy Expenditure, that is, energy consumption. Kcal is the calorie consumption per minute of sports dancing. After each part of the K4b2 test, the data is exported to Excle on the computer through the built-in software of the device. The sampling interval of Actiheart is set to 60s, so the data of K4b2 is processed by JMP10.0 and converted into a time interval of 60s corresponding to Actiheart time synchronization [17]. Actiheart can derive 3 predictions with its own software, namely ACC (accelerometry), HR (heart rate), and ACC+HR to record the data per minute:

$$ACC = a * \left(\sqrt{A_x^2 + A_y^2} \right)^{p1} + b * A_z^{p2}, \quad (2)$$

$$HR = \left| A_z * \frac{p1}{p2} \right| (A_x + A_y), \quad (3)$$

$$accelerometry + heart rate = A_z^p + A_x A_y. \quad (4)$$

In the formula, a, b, p1, and p2, respectively, represent coefficients related to individual characteristics (height, weight, etc.), and the data should conform to normal distribution and homogeneity of variance. The comparison between the measured value of K4b2 and the predicted value

of the three Actiheart predictions can use the paired sample T test. $P < 0.05$ means the difference is statistically significant.

For the data processing of Actiheart, Matlab7.0 programming is used for calculation. The calculation formula of net energy consumption per unit time and unit weight during exercise is $AEE = (E_{gross} - E_{rest})/M$ (unit : cal/kg/min). AEE is the English abbreviation of Active energy expenditure, E_{gross} is the English abbreviation of Gross energy expenditure, and E_{rest} is the English abbreviation of Rest energy expenditure. The unit of acceleration integral value is per minute. The sum of acceleration integral value is defined as counts/min, which is the average value over a period of time [18]. In signal processing, the second-order cutoff frequency 17Hz butterworth low-pass filter is used to filter the original signal. The integral value of the acceleration raw signal is often used to calculate the average acceleration. For the convenience of calculation, the following calculation formula is used to calculate the root mean square value of acceleration in the vertical direction:

$$aRMS = \sqrt{\frac{1}{T} \int_{t=0}^T (x(t) - \bar{x})^2 dt}. \quad (5)$$

The formula is also often written:

$$aRMS = \sqrt{\frac{1}{N} \sum_{n=1}^N (x_n - \bar{x})^2}. \quad (6)$$

The root mean square (RMS) of the acceleration in the horizontal direction is:

$$aRMS = \sqrt{\frac{1}{N} \sum_{n=1}^N (x_n)^2}. \quad (7)$$

After the acceleration in the horizontal or vertical direction is detrended, the integral calculation formula is:

$$I_a = \frac{1}{T} \int_{t=0}^T (x(t) - \bar{x}) dt, \quad (8)$$

$$\bar{w} = \frac{U_{ij}}{\sum_{i=1}^n U_{ij}} (i, j = 1, 2, \dots, n), \quad (9)$$

$$W_i = \frac{\bar{w}_i}{\sum_{j=1}^n \bar{w}_j} (i, j = 1, 2 \dots n). \quad (10)$$

The acceleration integral calculation formula is:

$$I_a = \frac{1}{T} \int_{t=0}^T x(t) dt. \quad (11)$$

In the formula, the parameter representation method of acceleration root mean square and integral value is: zRMS is the root mean square acceleration of the vertical direction after detrending (minus the mean). xRMS is the root mean

square of the horizontal acceleration after detrending. xRMS is the root mean square value of the original horizontal acceleration. Iaz is the integral value per minute after the vertical acceleration detrend. Iax is the integral value per minute after the horizontal acceleration is detrended. IA_{tot} is (IA_{tot} = Iaz + Iax) the sum of the acceleration integral per minute in the horizontal direction and the acceleration integral per minute in the vertical direction. Iaz is the integral value per minute after the acceleration in the vertical direction minus the acceleration of gravity (g).

The formula for calculating the root mean square error is:

$$\text{RMSE} = \sqrt{\frac{1}{n} \sum_{i=1}^n (X_{\text{measure}} - X_{\text{presume}})^2}. \quad (12)$$

Among them, X measurement refers to the actual measured value, and X estimate is the estimated value using a regression.

The formula for calculating relative error is:

$$\text{RE} = \frac{1}{n} \sum_{i=1}^n |X_{\text{measure}} - X_{\text{presume}}|. \quad (13)$$

Among them, X_{measure} is the actual measured value, and X_{presume} is the data estimated by the regression. The calculation of energy consumption during exercise is the calculation formula of net energy consumption per unit time and unit weight:

$$E_{\text{net}} = (E_{\text{gross}} - E_{\text{rest}}) / \text{Mass}, \quad (14)$$

$$\text{AW} = \lambda \max W. \quad (15)$$

Among them, E_{net} represents the energy consumption caused by exercise, E_{gross} represents the total energy consumption during exercise, and E_{rest} represents the most basic energy consumption consumed by the human body in a quiet state. Units in the formula: the unit of energy consumption is cal/kg/min and the unit of body weight is kg. In the AW calculation formula, $\lambda \max$ is the maximum eigenvalue of A , W is the corresponding eigenvector, W is normalized as a weight vector, and the maximum and minimum eigenvalues can be calculated from the weight vector. The specific formula is as follows:

$$\lambda \max = \frac{1}{n} \sum_{i=1}^n \frac{(AW)_i}{W_i}, \quad (16)$$

$$\lambda \min = W_i \left| \frac{n}{AW} * (i + AW) \right|. \quad (17)$$

In Actiheart's motion sensor data processing, because of the i element of (Aw) in the calculation formula of maximum and minimum eigenvalue $\lambda_{\max\&\min}$, it is difficult for the results in the same judgment matrix to show strict consistency. If there is complete consistency, $\lambda_{\max} = n$, and except for $\lambda_{\max} = n$, other eigenvalues are 0. In addition,

the energy consumption index of sports dance activities is a single-level ranking, and it also needs to pass the consistency test, which means that the allowable range of inconsistency is determined for A . The formula for calculating the consistency and testing is as follows:

$$\text{CI} = \frac{\lambda_{\max} - n}{n - 1}, \quad (18)$$

$$\text{CR} = \frac{\text{CI}}{\text{RI}}. \quad (19)$$

After the calculation of the formula, the method and data sorting method of the Actiheart heart rate combined with acceleration motion sensor and Cosmed K4b2 in sports dance activities can be summarized. Figure 4 is the technical roadmap of K4b2 with Actiheart heart rate combined acceleration motion sensor.

3. Experimental Design and Data of Sports Dance Teaching

This section will describe the simultaneous measurement of 8 common sports dance teaching activities for middle school students aged 11-17 using Cosmed K4b2 gas metabolism analyzer and Actiheart, based on the reference value measured by K4b2 indirect calorimetry. At the same time, Actiheart's three energy consumption predictions were used to estimate the energy consumption value, and the validity of Actiheart's ACC+HR, ACC and HR for predicting the energy consumption of common sports dance in adolescents was verified [19].

3.1. Objects. This study selected 65 middle school students aged 11-17 from some middle schools in Shanghai, including 24 boys and 41 girls, who were healthy and had no exercise taboos. All tests are signed by the parents and me. Table 1 is the basic information of the tested personnel.

3.2. Design. Because sports dance mainly includes two major categories, modern dance and Latin dance. The two categories of modern and Latin include many different categories, such as tango, quickstep, waltz, cha-cha, rumba, samba, etc. [20]. The elective syllabus of sports dance in most schools only stipulates the major category of sports dance, and does not specify any subcategories. Therefore, the calculation of sports dance in this paper will be compared with several common items selected by most schools. Among them, there are four types of Latin dance: Cha Cha, Rumba, Samba, and Bullfighting. Table 2 shows the content of the test dances and the specific test time. Figure 5 shows the specific flow of the experiment.

As shown in Figure 5, both parts of the test were completed in the dance studio. The tested students wear the Actiheart, and the test process is kept synchronized with the recording time of the K4b2 gas metabolism analyzer. There is a time interval between each dance activity. The heart rate returns to the resting heart rate level and then the next physical activity test is performed. Rest Energy Expenditure (REE) was measured by lying down. After the

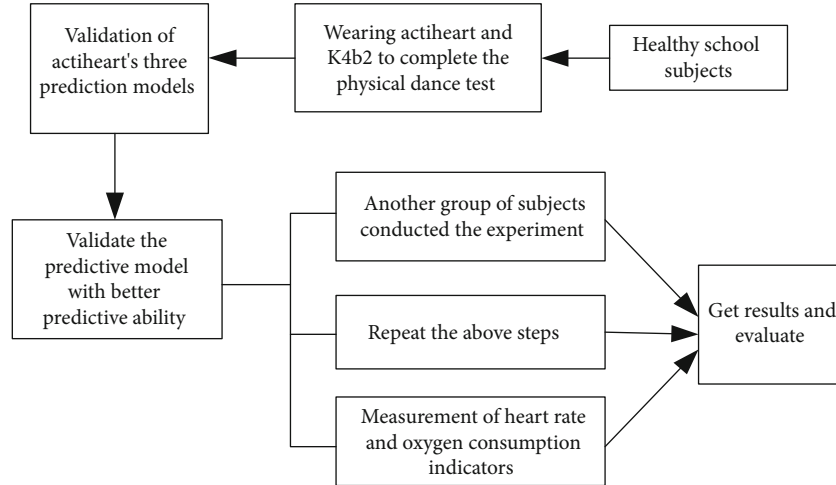


FIGURE 4: Technology roadmap.

TABLE 1: Basic information of the tested personnel.

Age	Height(cm)	Weight(kg)	BMI	Resting heart rate(bpm)
9($n = 24$)	137.46 ± 7.67	32.58 ± 9.1	13.96 ± 0.88	90.32 ± 9.01
10($n = 22$)	144.68 ± 11.5	40.56 ± 10.89	16.45 ± 0.99	90.53 ± 9.64
11($n = 24$)	149.71 ± 5.89	42.58 ± 9.45	21.33 ± 2.75	85.11 ± 10.34
Total ($n = 65$)	142.35 ± 8.29	37.45 ± 9.89	17.51 ± 2.9	88.32 ± 9.01

TABLE 2: Test dance content and test time.

Classification	Dance category	Time(min)
Modern	Quickstep dance	4
	Tango	5
	Waltz	8
	Vienna waltz	9
Latin	Cha cha dance	6
	Rumba	7
	Samba	5
	Bullfight dance	6

dance experiment of all students is completed, the results are summarized.

4. Results and Discussion

4.1. Comparison of Energy Consumption of Modern Dance in Sports Dance

4.1.1. Comparison of Energy Consumption between Tango and Quickstep. This section starts with the modern dance in sports dance for comparison. Two dances with different dance styles but similar dance methods are used for experiments. Then, the Actiheart heart rate combined with the acceleration motion sensor and the K4b2 device are used for calculation to test whether the ordinary sports dance teaching is effective. After the results are counted, the sports

dance that is more beneficial to the students is screened and decided, and the space for the teacher to improve the sports dance movement is provided. Figure 6 shows the energy consumption comparison results of Tango and Quickstep measured by the Actiheart motion sensor.

As shown in Figure 6, in the Tango test project, with K4b2 indirect calorimetry as the standard, the energy consumption of Tango measured by K4b2 indirect calorimetry is 2.66 ± 0.34 Kcal/min. The energy consumption of Tango measured by ACC+HR prediction is 1.3 ± 1.4 Kcal/min, the energy consumption of Tango measured by ACC prediction is 1.1 ± 1.2 Kcal/min, and the energy consumption value of Tango measured by HR prediction is 1.24 ± 1.29 Kcal/min. In the quick step dance test item, the energy consumption value of quick step dance measured by ACC+HR prediction is 2.33 ± 1.26 Kcal/min, and the energy consumption value of quick step dance measured by ACC prediction is 2.70 ± 1.58 Kcal/min, and the energy consumption of trot measured by HR prediction is 1.70 ± 1.23 Kcal/min. Taking K4b2 indirect calorimetry as the standard, the energy consumption of fast-step dance measured by K4b2 indirect calorimetry was 2.54 ± 1.22 Kcal/min. Through the comparison in Figure 6, it can be concluded that quickstep dance is more energy-intensive than tango, and it is easier to exercise students' physical fitness in the teaching of sports dance.

4.1.2. Comparison of Energy Consumption between Waltz and Vienna Waltz. Next, the modern dance types in another group of sports dances is measured, namely the waltz and the Vienna waltz. Although these two groups of dances look

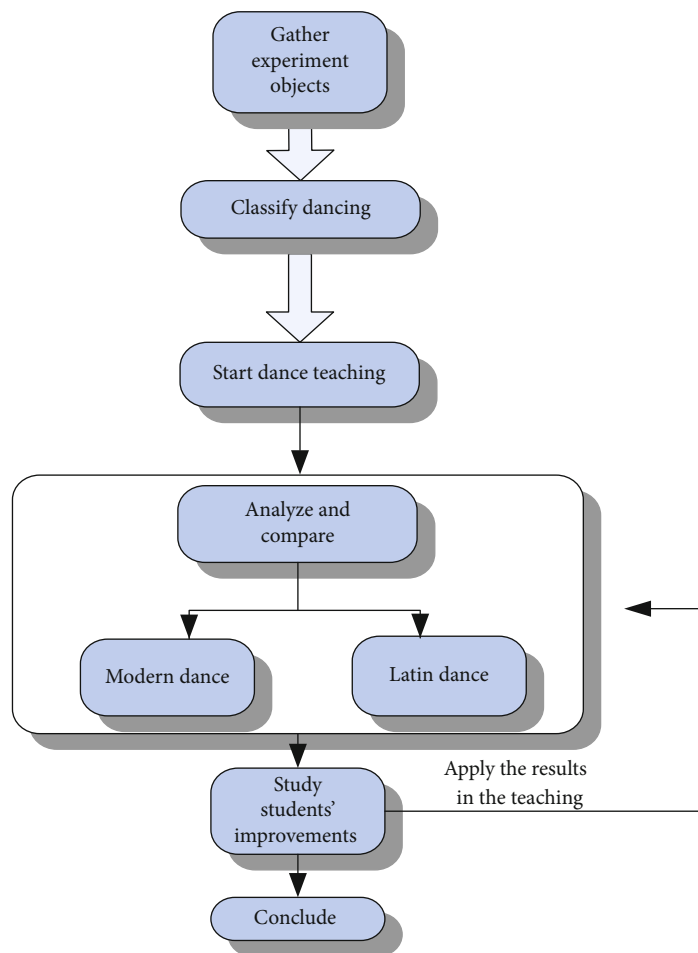


FIGURE 5: Experimental process.

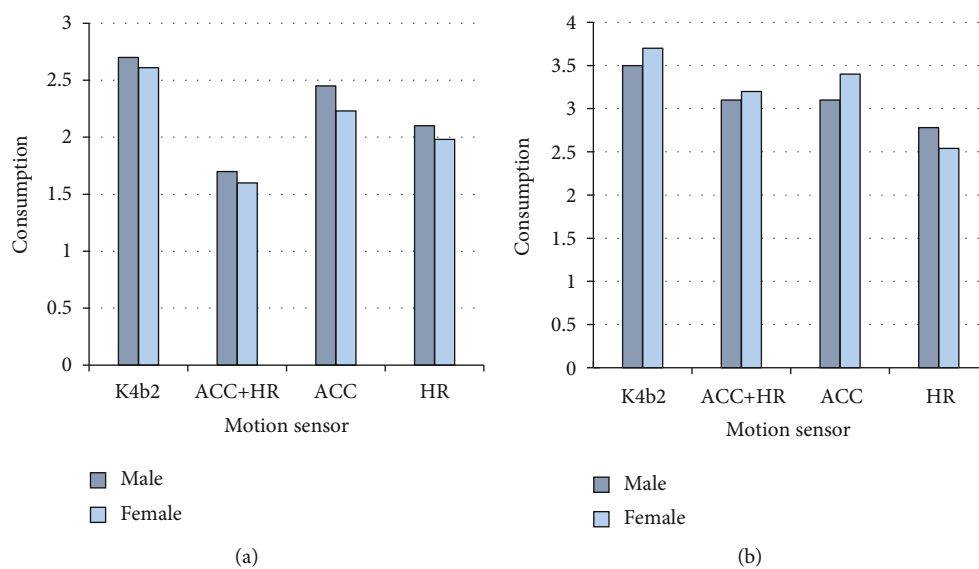


FIGURE 6: Comparison of energy consumption between (a) Tango and (b) Quickstep.

similar, there are differences in many movement details in the teaching. Figure 7 shows the energy consumption comparison results of the waltz and the Vienna waltz measured by the Actiheart motion sensor.

As shown in Figure 7, in the waltz test project, the K4b2 indirect calorimetry was used as the standard, and the K4b2 indirect calorimetry measured the energy consumption of the waltz was 1.85 ± 0.36 Kcal/min. The energy consumption

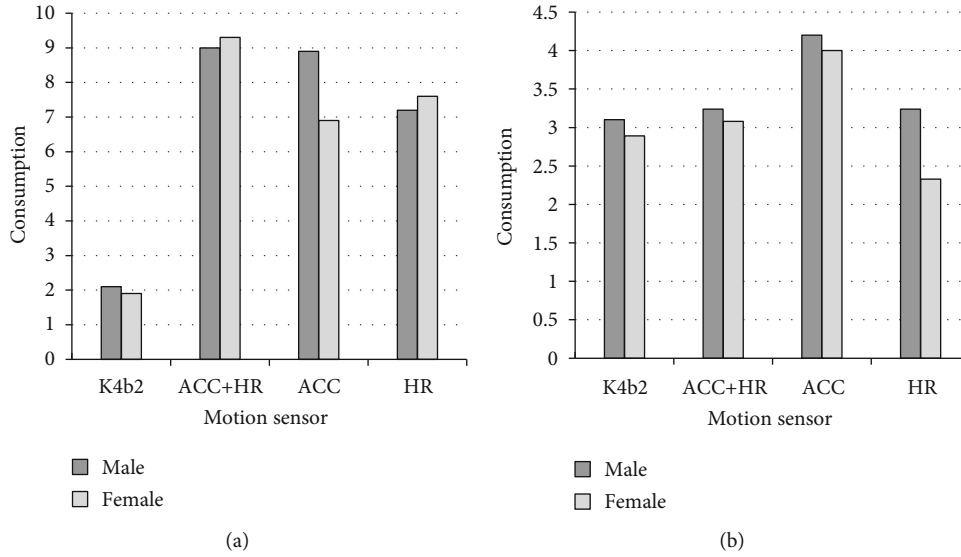


FIGURE 7: Comparison of energy consumption between (a) Waltz and (b) Vienna waltz.

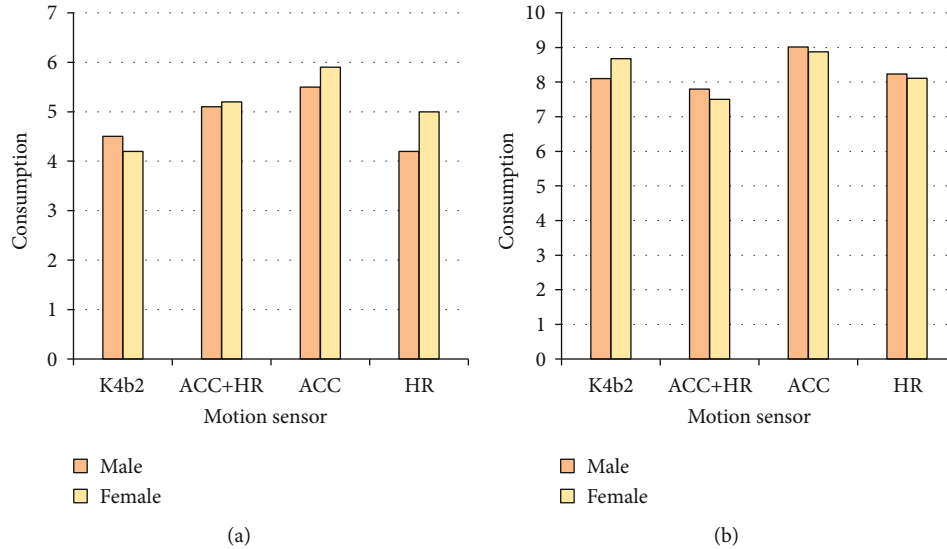


FIGURE 8: Comparison of energy consumption between (a) Cha Cha and (b) Rumba.

of the waltz measured by the ACC+HR prediction is 7.24 ± 2.90 Kcal/min, the energy consumption of the waltz measured by the ACC prediction is 7.80 ± 3.15 Kcal/min, and the energy consumption of the waltz measured by the HR prediction is 4.02 ± 3.80 Kcal/min. In the test project of the Vienna waltz, the K4b2 indirect calorimetry was used as the standard, and the K4b2 indirect calorimetry measured the energy consumption of the Vienna waltz to 2.57 ± 0.55 Kcal/min. The energy consumption of the Vienna waltz measured by the ACC+HR prediction is 2.79 ± 0.53 Kcal/min, the energy consumption value of Vienna waltz measured by ACC prediction is 3.75 ± 0.86 Kcal/min, and the energy consumption value of Vienna waltz measured by HR prediction is 2.08 ± 1.14 Kcal/min. According to the comparison of the calculation results, it can be seen that in the comparison of modern dance of sports dance, the waltz has a more energy-consuming effect

than the Vienna waltz, which can play a good role in promoting the teacher in dance teaching [21].

4.2. Energy Consumption Comparison of Latin Dance in Sports Dance

4.2.1. Comparison of Energy Consumption between Cha Cha and Rumba. After the calculation of the modern dance types in sports dance, the next thing to compare is the Latin dance type in sports dance. As a common popular dance category, Latin dance is very popular in current school education. Figure 8 is the comparison result of energy consumption between Cha Cha and Rumba in Latin dance measured by Actiheart motion sensor.

As shown in Figure 8, in the test item of Qiaqia, the K4b2 indirect calorimetry method is used as the standard,

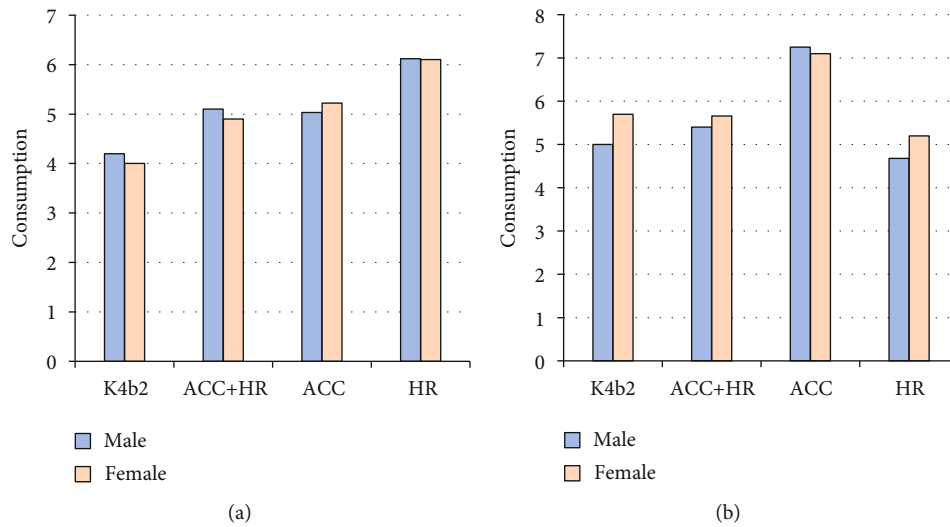


FIGURE 9: Comparison of energy consumption between (a) Samba dance and (b) Bullfight dance.

TABLE 3: Results of the physical dance skills assessment.

Variable	Test group	Control group	Test group (after test)	Control group (after test)
Variable	4.7 ± 0.1	4.65 ± 0.06	5.1 ± 0.2	4.88 ± 0.36
Action completion	5.15 ± 0.06	5.04 ± 0.84	6.3 ± 0.07	5.97 ± 0.84
Accuracy of music rhythm	4.3 ± 0.88	4.3 ± 0.35	5.4 ± 0.91	4.45 ± 0.45
Body posture and line aesthetics	5.6 ± 0.1	5.0 ± 0.83	5.8 ± 0.2	6.0 ± 0.91
Total	17.5 ± 0.28	16.75 ± 2.26	21 ± 0.31	19.55 ± 3.15

and the energy consumption value of Qiachai measured by the K4b2 indirect calorimetry method is 3.73 ± 0.99 Kcal/min. The energy consumption of Cha Cha measured by the ACC+HR prediction is 4.00 ± 1.25 Kcal/min, the energy consumption of Cha Cha dance measured by ACC prediction is 4.58 ± 1.35 Kcal/min, and the energy consumption value of Cha Cha dance measured by HR prediction is 3.34 ± 1.65 Kcal/min. In the Lombard test project, the energy consumption value of Lombard measured by K4b2 indirect calorimetry is 7.14 ± 2.00 Kcal/min, the energy consumption of rumba measured by the ACC+HR prediction is 7.19 ± 1.95 Kcal/min, the energy consumption of rumba measured by the ACC prediction is 8.05 ± 2.51 Kcal/min, and the energy consumption value of Lombard measured by HR prediction is 5.73 ± 3.48 Kcal/min. It can be seen that Cha Cha and Rumba are not only more energy-intensive than modern dance, but also more energy-intensive in sports dance teaching.

4.2.2. Comparison of Energy Consumption between Samba Dance and Bullfight Dance. Finally, the energy consumption of samba dance and bullfighting dance in Latin dance is compared. Although samba and bullfighting sounds relatively small, they are very common in some sports dance teaching today because of their exotic movements. Figure 9 shows the samba and bullfight dances measured by Actiheart motion sensors energy consumption comparison results.

According to Figure 9, in the test project of Samba, the energy consumption value of Samba measured by K4b2 indirect calorimetry is 4.00 ± 0.86 Kcal/min, and the energy consumption value of Samba measured by ACC+HR prediction is 4.15 ± 1.00 Kcal/min, the energy consumption value of Samba measured by ACC prediction is 4.65 ± 1.43 Kcal/min, and the energy consumption value of Samba measured by HR prediction is 4.27 ± 2.15 Kcal/min. The average energy consumption of bullfighting dance was analyzed, the overall energy consumption value measured by K4b2 indirect calorimetry was 3.86 ± 2.67 Kcal/min, the energy consumption value of Samba measured by ACC+HR prediction was 3.75 ± 2.70 Kcal/min, the energy consumption value of Samba measured by ACC prediction was 4.27 ± 3.01 Kcal/min, and the energy consumption value of Samba measured by HR prediction was 2.86 ± 2.68 Kcal/min. Therefore, it can be concluded that samba dance is more energy-intensive in sports dance teaching. The energy consumption experiment results of the four groups of sports dances can show that the quickstep, waltz, rumba, and samba are more energy-intensive.

4.3. Evaluation of Physical Dance Teaching for Improved Energy Consumption Results. Through comparison and summarization, it can be concluded that quickstep, waltz, rumba, and samba are more suitable for students to train in sports dance. After experimenting on the energy consumption in sports dance through the Actiheart heart rate

acceleration motion sensor, the teacher will then inform the teacher of the experimental results. The basic situation of dance sports skills and interest level in sports dance learning was analyzed [22].

Before the experiment, the teacher divided the experimental group into two groups according to their dance level, and conducted an assessment of the physical dance skills of the two groups of respondents. The survey results are shown in Table 3.

From the table, it can be found that before the experiment, the average score of the respondents in the experimental group was 17.5 points, while the average score of the respondents in the control group was 16.75 points. After the experiment, the scores of the two groups increased by 3.5 points and 2.8 points, respectively. Through the data, it can be found that the experiments in this paper have also played a role in the improvement and application of sports dance in schools.

5. Conclusion

Based on heart rate combined with acceleration motion sensor, this paper studied sports dance teaching. Heart rate combined with acceleration motion sensor has a great role in each exercise, which was reflected in the measurement of heart rate and energy consumption. By using this measurement method to obtain the effect of energy consumption in sports dance teaching, it can screen more targeted and more conducive dance activities for physical exercise for students in complex sports dance. The Actiheart heart rate combined with acceleration motion sensor used in this paper was the only measurement tool in the world that combined heart rate and accelerometer. At the same time, the Comsed K4b2 gas metabolism analyzer was combined with the motion sensor to conduct experiments on the energy consumption of the measured dance activities. The test results of the article showed that quickstep, waltz, rumba, and samba are more suitable for students to train in sports dance. Therefore, these four dances should be more promoted in the physical dance teaching activities in schools. Due to the limited length of the article, it is impossible to elaborate on the method in more detail, and the experiment is not comprehensive enough. It is expected that this topic can be studied in a more comprehensive way in the future.

Data Availability

All the data used to support the findings of the study are included within the work.

Conflicts of Interest

There are no potential competing interests in our work.

Acknowledgments

This work was supported by the Scientific Research Project of Hunan Provincial Department of Education. (Lin Li Research on the impact of sunshine line dance on college students'

physical and mental health in the context of healthy China, Scientific Research Project of Hunan Provincial Department of Education. (21C0851) under development).

References

- [1] T. Osadtsiv, V. Sosina, and O. Lykhanenko, "Control in the physical preparation of athletes aged 8-9 years in sport dancing," *Journal of Kinesiology and Exercise Sciences*, vol. 27, no. 80, pp. 21–25, 2017.
- [2] Y. Liu, "Impact of sport dancing on the dynamics characteristic of foot movement of college students," *Leather and Footwear Journal*, vol. 18, no. 2, pp. 109–116, 2018.
- [3] D. F. P. Granados, B. A. Yamamoto, H. Kamide, J. Kinugawa, and K. Kosuge, "Dance teaching by a robot: combining cognitive and physical human-robot interaction for supporting the skill learning process," *IEEE Robotics and Automation Letters*, vol. 2, no. 3, pp. 1452–1459, 2017.
- [4] Y. Wang, "Development and application of 3D holographic technology in dance teaching," *IPPTA: Quarterly Journal of Indian Pulp and Paper Technical Association*, vol. 30, no. 8, pp. 488–492, 2018.
- [5] X. Weng, Q. Zheng, X. Wu, B. Wang, and L. Gong, "Research on aesthetic training of university students in Dancesport teaching," *Open Access Library Journal*, vol. 8, no. 6, pp. 1–4, 2021.
- [6] E. Valero, A. Sivanathan, F. Bosché, and M. Abdel-Wahab, "Analysis of construction trade worker body motions using a wearable and wireless motion sensor network," *Automation in Construction*, vol. 83, pp. 48–55, 2017.
- [7] M. Hutchinson, H. Oh, and W. H. Chen, "Adaptive Bayesian sensor motion planning for hazardous source term reconstruction," *IFAC-PapersOnline*, vol. 50, no. 1, pp. 2812–2817, 2017.
- [8] S. H. Shin, D. H. Park, J. Y. Jung, M. H. Lee, and J. Nah, "Ferroelectric zinc oxide nanowire embedded flexible sensor for motion and temperature sensing," *ACS Applied Materials & Interfaces*, vol. 9, no. 11, pp. 9233–9238, 2017.
- [9] A. Gaidhani, K. Moon, Y. Ozturk, S. Lee, and W. Youm, "Extraction and analysis of respiratory motion using wearable inertial sensor system during trunk motion," *Sensors*, vol. 17, no. 12, p. 2932, 2017.
- [10] X. L. Wang and J. Liu, "The exploration of the "trinity" teaching mode of sports dance in university," *Journal of Guangzhou Sport University*, vol. 41, no. 5, pp. 125–128, 2021.
- [11] Y. C. He and G. S. Du, "Research on the aesthetic characteristics of dance sport," *Journal of Physical Education*, vol. 22, no. 1, pp. 58–61, 2015.
- [12] S. Hu and X. H. Xie, "Analysis on the teaching mode of sport dance in colleges and universities," *Bulletin of Sport Science & Technology*, vol. 29, no. 2, pp. 92–93, 2021.
- [13] J. H. Chen, "Research on the innovation and development of sports dance teaching in universities," *Theory and Practice of Education*, vol. 40, no. 21, pp. 62–64, 2020.
- [14] X. F. Li and J. H. Xu, "Research progress of sports dance at home and abroad: based on visualization of scientific knowledge map," *Journal of Beijing Sport University*, vol. 41, no. 4, pp. 89–96, 2018.
- [15] S. Afaq, M. Loh, J. Kooner, and J. Chambers, "Evaluation of three accelerometer devices for physical activity measurement amongst south Asians and Europeans," *Physical Activity and Health*, vol. 4, no. 1, pp. 1–10, 2020.

- [16] M. Klass, V. Faoro, and A. Carpentier, "Assessment of energy expenditure during high intensity cycling and running using a heart rate and activity monitor in young active adults," *PLoS One*, vol. 14, no. 11, article e0224948, 2019.
- [17] A. Yurtman and B. Barshan, "Novel non-iterative orientation estimation for wearable motion sensor units acquiring accelerometer, gyroscope, and magnetometer measurements," *IEEE Transactions on Instrumentation and Measurement*, vol. 69, no. 6, pp. 3206–3215, 2020.
- [18] C. Lian, X. Ren, Y. Zhao et al., "Towards a virtual keyboard scheme based on wearing one motion sensor ring on each hand," *IEEE Sensors Journal*, vol. 21, no. 3, pp. 3379–3387, 2021.
- [19] A. Zanchini and M. Malaguti, "Energy requirements in top-level Dancesport athletes," *Journal of Human Sport and Exercise*, vol. 9, no. 1, pp. 148–156, 2014.
- [20] R. Bai, D. W. Lin, M. Cui, and K. Wang, "Practical thinking on process of sports dance Sinicization," *Journal of Shenyang Sport University*, vol. 40, no. 4, pp. 138–144, 2021.
- [21] S. D. Ottavio, L. Lunetta, and M. Angioi, "Energy requirement in top-level dance sport athletes," *Journal of Dance Medicine & Science*, vol. 20, no. 4, pp. 168–173, 2016.
- [22] R. X. Ma, "On the specific physical training functions and ways based on dance sports features," *Journal of Anshan Normal University*, vol. 21, no. 6, pp. 55–58, 2019.

Retraction

Retracted: Investigation on the Use of Virtual Reality in the Flipped Teaching of Martial Arts Taijiquan Based on Deep Learning and Big Data Analytics

Journal of Sensors

Received 22 August 2023; Accepted 22 August 2023; Published 23 August 2023

Copyright © 2023 Journal of Sensors. This is an open access article distributed under the Creative Commons Attribution License, which permits unrestricted use, distribution, and reproduction in any medium, provided the original work is properly cited.

This article has been retracted by Hindawi following an investigation undertaken by the publisher [1]. This investigation has uncovered evidence of one or more of the following indicators of systematic manipulation of the publication process:

- (1) Discrepancies in scope
- (2) Discrepancies in the description of the research reported
- (3) Discrepancies between the availability of data and the research described
- (4) Inappropriate citations
- (5) Incoherent, meaningless and/or irrelevant content included in the article
- (6) Peer-review manipulation

The presence of these indicators undermines our confidence in the integrity of the article's content and we cannot, therefore, vouch for its reliability. Please note that this notice is intended solely to alert readers that the content of this article is unreliable. We have not investigated whether authors were aware of or involved in the systematic manipulation of the publication process.

In addition, our investigation has also shown that one or more of the following human-subject reporting requirements has not been met in this article: ethical approval by an Institutional Review Board (IRB) committee or equivalent, patient/participant consent to participate, and/or agreement to publish patient/participant details (where relevant).

Wiley and Hindawi regrets that the usual quality checks did not identify these issues before publication and have since put additional measures in place to safeguard research integrity.

We wish to credit our own Research Integrity and Research Publishing teams and anonymous and named external

researchers and research integrity experts for contributing to this investigation.

The corresponding author, as the representative of all authors, has been given the opportunity to register their agreement or disagreement to this retraction. We have kept a record of any response received.

References

- [1] Z. HanLiang and Z. LiNa, "Investigation on the Use of Virtual Reality in the Flipped Teaching of Martial Arts Taijiquan Based on Deep Learning and Big Data Analytics," *Journal of Sensors*, vol. 2022, Article ID 3921842, 14 pages, 2022.

Research Article

Investigation on the Use of Virtual Reality in the Flipped Teaching of Martial Arts Taijiquan Based on Deep Learning and Big Data Analytics

Zhang HanLiang ^{1,2} and Zhang LiNa ³

¹Department of Sport and Health, Tianshui Normal University, China

²The National University of Malaysia, Malaysia

³China Gansu International Economic and Technical Cooperation Co., Ltd., China

Correspondence should be addressed to Zhang HanLiang; 1703300060@e.gzhu.edu.cn

Received 5 August 2022; Revised 22 August 2022; Accepted 5 September 2022; Published 6 October 2022

Academic Editor: Sweta Bhattacharya

Copyright © 2022 Zhang HanLiang and Zhang LiNa. This is an open access article distributed under the Creative Commons Attribution License, which permits unrestricted use, distribution, and reproduction in any medium, provided the original work is properly cited.

Flipping classroom teaching of martial arts “Taijiquan” is a contemporary teaching method that primarily uses information technology tools to accomplish the natural fusion of information technology and education and teaching. Digital teaching materials influence the conventional classroom. The conventional teaching approach of teacher instruction and student learning is no longer satisfactory to students. Virtual reality (VR) technology and physical education integration and development have currently emerged as a new trend, but research on its application to martial arts is still in its theoretical stages and lacks concrete application countermeasures and schemes, necessitating further investigation and study. This paper intends to investigate the use of virtual reality technology in martial arts education. The architecture of virtual reality based on the deep learning algorithm is suggested. The student dataset is collected, and they are split into two groups: control and study groups. Traditional teaching is provided to the control group, and deep learning-based VR-assisted teaching is provided to the study group using the Deep Binary Hashed Convolutional Neural Network (DBH-CNN). Statistical analysis is done using Student’s *t*-test, logistic regression analysis, and analysis of variance (ANOVA). According to the study findings, the majority of students see virtual reality technology-assisted martial arts education favorably, and their passion for studying martial arts has greatly increased.

1. Introduction

Convenience and impact offered by information technology coexist in the rapidly evolving, ever-changing 21st century. The flipped classroom model has attracted the attention of researchers in the field of education both at home and abroad in recent years. Because of the advent of the flipped classroom, the conventional method of instruction has been turned on its head. Compared to other fields of study, physical education stands out as a very practical subject. The flipped classroom is a new kind of classroom that has emerged as a result of the information society and offers promising new approaches to advancing education reform in the United States. Studies in various fields have shown

that the flipped classroom model is more effective than standard lecture-style instruction [1]. Taijiquan is a kind of Chinese martial art that emphasizes health, self-defense, and the avoidance of illness via a combination of physical training and mental concentration, drawing on the knowledge and spirit of China’s long history of social production. Taijiquan instruction has progressed over the years, but it has run across challenges along the way. These challenges include the monotony of a single teaching topic, the inflexibility of a single teaching approach, and the lack of consistency in technical action speaking. To master Taijiquan, one must have a firm knowledge of its technical rules. This allows for a deeper comprehension of its meaning, which in turn has a beneficial effect on one’s physical well-being, cultural

achievements, and sense of self. By developing students' individualized learning, the pedagogical practice of flipping classrooms takes into account students' physical and mental characteristics, personality hobbies, and other factors, allowing for more time for teachers and students to interact and thereby increasing students' engagement in class. The flipped classroom paradigm is based on the idea that teachers should be students first. This approach to education emphasizes student autonomy, collaboration, and customization. Supportive better education may help pupils develop their creative skills. The drab and boring techniques often used to teach physical education are ineffective in getting pupils excited about learning. This is why it is crucial to revamp the way that universities and colleges teach physical education. Taijiquan carries with it a wealth of historical and cultural significance. Through the use of media technologies, students are more likely to engage in the teaching methods of interaction, sharing, and group discussion to build the learning theme of body sensation from boxing theory [2]. Wan [3] states that in a self-study setting, students share their goals for the class and discuss challenges they have had speaking with professors to better prepare for class and get more practice with classroom teaching abilities. To successfully address students' concerns about failing to keep up with class material, the flipping classroom model has been developed. To maximize classroom efficiency, teachers often use particular strategies to get students engaged. Stop the passive learning that has plagued classroom instruction for so long. By coordinating their preclass activities based on their independent study, students are better prepared to make the most of their classroom time, and instructors are less likely to feel overwhelmed by their students' demands for individual attention during class. The relative or ambiguous nature of technical norms is, of course, also a hallmark of traditional Chinese culture. To achieve "normative mastery" of Taijiquan's technical motions, one must have a firm grip on the "degree" of the standard at which it is held [4]. Inverting the conventional classroom structure and fusing the martial arts education model is also proposed. College martial arts programs use a grading system to help students build self-esteem, learn to put their health and martial arts first, become more proficient in these areas, become more engaged in class, and learn to train themselves. With its distinctive cultural meaning and action attractiveness, as well as its liveliness, the martial arts grade system is liked by students and provides them with an excellent basis for a lifetime of physical activity. To a certain extent, the pedagogical strategy of "flipping the classroom" [5], which is aimed at increasing students' motivation and engagement in a class by introducing them to new ideas and concepts, parallels the overall objective of collegiate martial arts instructors. By infusing a martial arts curriculum and inverting the traditional classroom structure, we can better serve our students. Three key facets illustrate how the flip classroom pedagogical approach and the martial arts segment teaching activity are integrated: preclass, in-class, and after-school modules, and they are all interconnected. Because martial arts are often taught in a classroom setting, instructors must be well prepared for each lesson. The promotion of martial

arts courses is quite light at universities. Many people who train in martial arts are not fully informed about what is expected of them. Many college students, like many adults, have not trained consistently or undertaken standardized exercise training. Their martial arts techniques, however, are not conventional. Standardized behavior, martial arts expertise, and power control are all emphasized in the various belts of martial education. This means that the instructor has to provide thorough explanations and demonstrations of each martial arts technique being taught. Enhance not just pupils' technical martial arts skills but also their mental and spiritual flexibility. According to Zhang [6], the shift away from conventional teacher evaluation's focus on results at the expense of the process would help move China's physical education system in a more positive direction, especially for students with less of a background in sports. Participation in the love of sports may promote students' physical health and foster their intellectual development. A "flip classroom" strategy for teaching is shown in Figure 1.

As a result, the following learning goals are established for the martial arts section: First, the spirit of martial arts, give students homework so they may learn about the history and culture of martial arts; second, the action basics of martial arts show students how to perform basic techniques and drills; and third, let students compete in tournaments. Play the instructional video, break down the movement in slow motion and explain the evaluation criteria for the martial arts grading system, then go through the basics of the action in front of your class, and have a conversation about it. By doing so, trainees may learn the foundational techniques of martial arts more thoroughly [7]. For educators' prioritization of class time for lesson planning, create useful instructional movies and instruct students by having them enjoy the video, analyze it, dissect its essential elements, and then replicate its presentation on their own. Make a picture plan and a decomposition plan for the three views (front, left, and top) to see how they break down. For preclass work that students should be doing, allow students to see Bruce Lee's seminal martial arts film, "Jingwumen," as well as the martial arts component of the exam, "2016 Taijiquan Competition," during a flip teaching lesson to help them grasp the martial arts ethos. Allow students to see the film to better comprehend the nature of martial arts, the significance of martial arts, and the criteria for martial arts systems. The educator arranges small and large group opportunities for pupils to talk, do, and get feedback. Using the flipped classroom model, students first view the necessary videos for the martial arts component of the exam section to grasp the concept of movement imitation. A classroom-flipping system that uses martial arts grades is examined. Teacher assessment, student self-evaluation, and peer and community evaluation are the common constituents [8]. Students are dissatisfied with the traditional teaching model of teacher instruction and student learning. Virtual reality (VR) technology and physical education integration and development are a new trend, but research on its application to martial arts is yet in its theoretical phases and lacks real application countermeasures and plans, requiring an additional study. The purpose of this paper is to look at the possibility of using

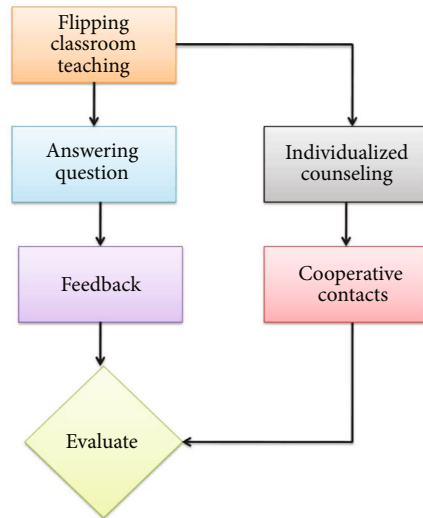


FIGURE 1: Flip teach model flow.

VR for teaching martial arts. It is proposed that a deep learning algorithm forms the basis of VR's underlying architecture. DBH-CNN approaches for effective image retrieval are designed to train hash functions that map-related images to binary codes in the Hamming space that are semantically associated while maintaining similarity. A deep CNN can automatically learn fundamental filters and hierarchically combine them to allow the description of latent ideas for pattern recognition.

1.1. Contributions of the Study. The following are the contributions of the study:

- (i) After collecting the student dataset, we next randomly assigned half to the control group and half to the research group
- (ii) Comparatively, the control group receives traditional teaching, while the experimental group is given virtual reality (VR) teaching based on deep learning and the use of a Deep Binary Hashed Convolutional Neural Network (DBH-CNN)
- (iii) Student's *t*-tests, regression analyses, and analyses of variance (ANOVA) are used for statistical analysis

The remaining work is divided into the following sections: Section 2, which includes the literature review and problem statement; Section 3, which includes the proposed methodology; Section 4, which includes the result and discussion; and Section 5, which includes the conclusion.

2. Literature Review

Virtual reality (VR) has been the subject of much research by academics interested in its potential in the classroom Table 1. The martial arts served an indispensable function in the classroom because of their position as a transmitter of national cultural patrimony via sport. They discussed the challenges and innovative methods for successful martial

arts education in higher education from many perspectives. For the first time, there was a theoretical foundation for how best to teach martial arts in academic settings [9]. To better educate, Zhang et al. [10] presented their system's architecture and execution. The sentence to be change as a "The VR technology was incorporated into the system to improve student engagement and classroom efficiency. The findings demonstrate that virtual reality technology has the potential to alter the standard method of instruction, pique students' curiosity in schoolwork, and enhance the standard of education in Korea [11]. The study's findings paved the way for more VR technology use in the classroom. In their presentation of a calculus course in "virtual reality," Bos et al. [12] detail how lectures might be adapted for use in VR and AR hardware systems. The primary goal of Pu and Yang [13] was to integrate VR technology into courses on political and ideological theory in higher education. In the study, students served as participants and were split into two groups: the experimental and the control. Groups A1 and B2 engaged in VR classroom learning reported 8.2% and 8.1% increases in political theory class interest, correspondingly [14]. The implications of this cutting-edge technology have not been adequately explored or explained [15]. Studying the psychological and social aspects of working together in a virtual environment was the subject of this empirical study. We piloted the use of a collaborative immersive virtual environment (CIVE) for instruction in two hypsography-related situations, the creation of which was the product of a multidisciplinary team. Using convolutional neural networks (CNNs), Kamel et al. [16] present a system called Tai Chi for teaching Tai Chi based on position estimation. Because of the limitations of conventional teaching techniques like one-to-many tutorials and video viewing, we designed our solution to address this issue. The VR-supported hybrid flipped classroom paradigm introduced and studied by Xiao and Hong [17] may provide a three-dimensional virtual learning scenario that mimics a user's physical presence in a virtual or fictional setting, providing a novel cognitive experience. University professors' and students' perspectives on the notion of flipped learning and the realization of autonomous learning via flipped learning are presented by Antonova and Mernkov [18]. Survey findings indicate that student adaptation to flipped learning is challenging. The kids cannot learn on their own. To quantify the benefits of flipped classes in higher education, Salihu and Zayyanu [19] systematically reviewed 43 empirical studies of students' cognitive, emotional, and interpersonal outcomes. In higher education, the flipped classroom model promotes a long-term, collaborative, and learner-centered classroom [20]. The implementation of flipped learning in a 14-week undergraduate biology course uses virtual worlds as self-learning medium and then explores how students responded to this method[21]. In the essay, a flipped learning experiment on preservice teacher preparation using remote learning is described [22]. To statistically examine 20 domestic and foreign experimental investigations of flipped classrooms, the meta-analysis approach was used [23]. To look at the outcomes of students' academic

TABLE 1

S. no.	Reference	Methods	Drawbacks
1	Goehle [9]	With an explanation of how the lecture was implemented in both virtual reality and an augmented reality hardware system, it gives a lesson for a typical Calculus subject that is based on “virtual reality.”	The foundation of traditional education is interpersonal relationships and direct human communication. The connections between pupils and general human communication may suffer as a result.
2	Zhang et al. [10]	The primary intention of this essay is to integrate virtual reality technology into college and university courses on political and ideological philosophy.	Due to the small sample size and lack of expertise, the VR classroom suggested in this article could have certain disadvantages.
4	Bos et al. [12]	The use of VR technology, programs, and material as a teaching and learning tool for geography is discussed.	There are several restrictions when trainers display motions since martial arts routines are complicated. Virtual reality technology and physical education integration and development have emerged as a new trend, but research in the area of martial arts is still in the theoretical stage and lacks concrete application countermeasures and plans, necessitating additional investigation and study.
5	Pu and Yang [13]	To investigate the use of virtual reality in teaching martial arts.	
6	Šašinka et al. [15]	Their multidisciplinary team created a special application for establishing a collaborative immersive virtual environment (CIVE) as a software solution for educational purposes.	Fostering team cohesiveness while members of the team work remotely is one of the main difficulties of managing virtual teams.
7	Kamel et al. [16]	Convolutional neural networks (CNNs) are the basis of the iTai-Chi, Tai Chi training system. Their methodology attempts to address the drawbacks of conventional teaching techniques like one-to-one tutorials and video viewing that result from a lack of enough precise feedback.	Since there is inadequate data in the third dimension, many researchers struggle to estimate 3D VR in a single shot.
8	Xiao and Hong [17]	A VR-supported hybrid flipped classroom model was developed, and its characteristics were examined. This model might provide a three-dimensional virtual learning environment that would imitate a user’s actual presence in an imagined or virtual setting, which would be a novel cognitive experience.	There were challenges in education, such as the necessity for instructors and pupils to adapt to their new duties.
9	Antonova and Mernkov [18]	It outlines students’ attitudes regarding the notion of autonomous learning achieved via flipped learning as well as university lecturers’ perspectives of the concept.	The research found several issues with the flipped learning model’s adoption in higher education.
10	Jang and Kim [20]	The 43 empirical studies of students’ cognitive, emotional, and interpersonal outcomes to quantify the impact of flipped classes in higher education.	The flipped classroom is not a magic bullet, and how well students use the preclass time is a major factor in how beneficial it is.
11	Yano [21]	The deployment of flipped learning in a 14-week undergraduate biology course employs virtual environments as self-learning media and then discusses how students responded to this strategy.	Students may find it difficult to study independently utilizing these mediums, especially if the topic is new to them or contains abstract ideas.
12	Prokhorova et al. [22]	In the essay, a flipped learning experiment on preservice teacher preparation using remote learning is described.	The lack of efficient teaching techniques in distant learning led to instructor uncertainty and forced them to change their lesson plans, instructional strategies, and communication instruments.
13	Zhang et al. [23]	To statistically examine 20 domestic and foreign experimental investigations of flipped classrooms, the meta-analysis approach was used.	When a class is flipped, more preparation and effort must be spent on content development than in a conventional setting. This is especially true when course material or certain classroom activities are moved online.
14	Pardimin et al. [24]	To look at the outcomes of students’ academic performance and reactions to flipped classes.	The unconventional setting might be difficult for students who have never experienced flipped learning.
15	Jin [25]	They develop a system that can publish English test papers, generate and administer a personal library of test papers, track students’ practice progress, and evaluate students’ performance. This system consists of a teacher, a student, and an administrator.	These early studies have certain relative limitations in that they solely cover technology and explore little of the interaction between knowledge engineering and applied linguistics theory.

performance and reactions to flipped classes, Pardimin et al. [24] develop a system that can publish English test papers, generate and administer a personal library of test papers, track students' practice progress, and evaluate students' performance. This system consists of a teacher, a student, and an administrator [25].

Research into the topic shows that although many academics study the impact of education on students, very few investigate the effects of flipping the classroom while teaching martial arts. Some of the data preprocessing that machine learning generally involve is eliminated. These algorithms are capable of processing text and visual data that is unstructured. When compared to previous techniques, DBH-CNN's major benefit is its ability to automatically and unassisted identify key characteristics.

2.1. Problem Statement. There are several issues with real classroom instruction right now. Consequently, it is still important to maintain a commitment to pedagogical innovation and correction and to actively adopt a variety of methods to guarantee the steady development of the pedagogical process. A more effective kind of education than the standard lecture format is one that emphasizes the development of students' bodies and interests. To apply the flipped classroom method, it is recommended that college Taijiquan teachers use the Internet and other multimedia carriers. Ability building should focus on helping students improve their learning, thinking, and doing skills. By flipping their classrooms, educators may better grasp their students' situations.

3. Proposed Methodology

The deep learning algorithm is used to suggest how virtual reality should be built. The students are put into two groups: the control group and the study group. Traditional teaching is given to the control group, while Deep Binary Hashed Convolutional Neural Network-based VR-assisted deep learning teaching is given to the study group (DBH-CNN). Statistical analysis is performed using Student's *t*-tests, regression analysis, and analysis of variance. Figure 2 shows the proposed methodology.

3.1. Student Dataset. "Student datasets are collected from Nankai University, Tianjin, China. As a basis of the university's clearance of this research, students in grades one through four were registered via online study platforms and groups recently formed for the new semester's remote learning to participate in the study from 10 am February 15 to 10 am February 17, 2020. Table 2 depicts the data description."

3.2. Splitting of Groups. Here, the gathered data are separated into 2 teams, namely, the control group and the study group. The traditional education is provided to the students in the control group, which included 3522 participants, while the study group makes use of a Deep Binary Hashed Convolutional Neural Network (DBH-CNN) to get deep learning-based VR-based teaching which included 3700 participants.

3.2.1. Traditional Teaching. Typically, in a traditional classroom setting, students strive to take notes as quickly as the instructor speaks. They are too busy attempting to write down the teacher's words to stop and consider the lesson, which means they may miss some key aspects. By contrast, when students use video and other prepared material, they are in charge of their learning; they may pause, rewind, and skip through content at their convenience. Anyone who is learning English as a second language might benefit from taking the courses many times. Collaborative learning projects may also promote students' socialization, collaboration, and cultural diversity, which in turn facilitates students' ability to assist one another in learning and to work together regardless of their degrees of expertise. In-class activities including experiential exercises, team projects, problem sets, and assignments that were formerly given as individual homework allow teachers to spend more time focusing on fostering synthesis and exploring application.

3.2.2. Application of Virtual Reality Technology. Virtual reality (VR) is a relatively new technology that merges many established ones, including computer graphics, sensor technology, and artificial intelligence technology. The computer simulation system creates a dynamic three-dimensional scene for the user to interact with, and this scene has innate interactive, interactive, and theoretical qualities due to the user's reliance. It is possible to get multimodal input in the form of sight, sound, and touch. As a result of the deep learning algorithm being used in the creation of interactive teaching activities, not only can the demands of differentiated instruction be met, but also instructors' ability to carry out their work effectively is enhanced. Learning activities in a virtual reality-based interactive classroom may be broken down into two categories: those that take place during class time and those that take place outside of class time, according to the classroom's specific features. Through the application of VR technology, our real-world settings may be transformed into 3D immersive learning spaces that seamlessly merge the physical and digital realms. Flipped classrooms provide instructors the freedom to include interactive learning activities both within and outside of the traditional classroom while still delivering the course material. By analyzing the data collections of various learners and further extracting valuable learning patterns, smart learning environments could create new and more effective learning models that they could then use to make suggestions and recommendations to learners over time, possibly even during their future careers.

3.3. Deep Binary Hashed Convolutional Neural Network (DBH-CNN). In this part, we provide the overall architecture for binary hashing, and then, we discuss the DBH-CNN approach we suggest for binary hashing. It is posed as a classification issue with a strict binary restriction. Finally, we show how the back-propagation method may be used to train the network to minimize a loss function.

3.3.1. Binary Hashing. The goal of hashing methods is to find small binary code portrayals of data that are different enough from each other to be able to tell them apart. There have been

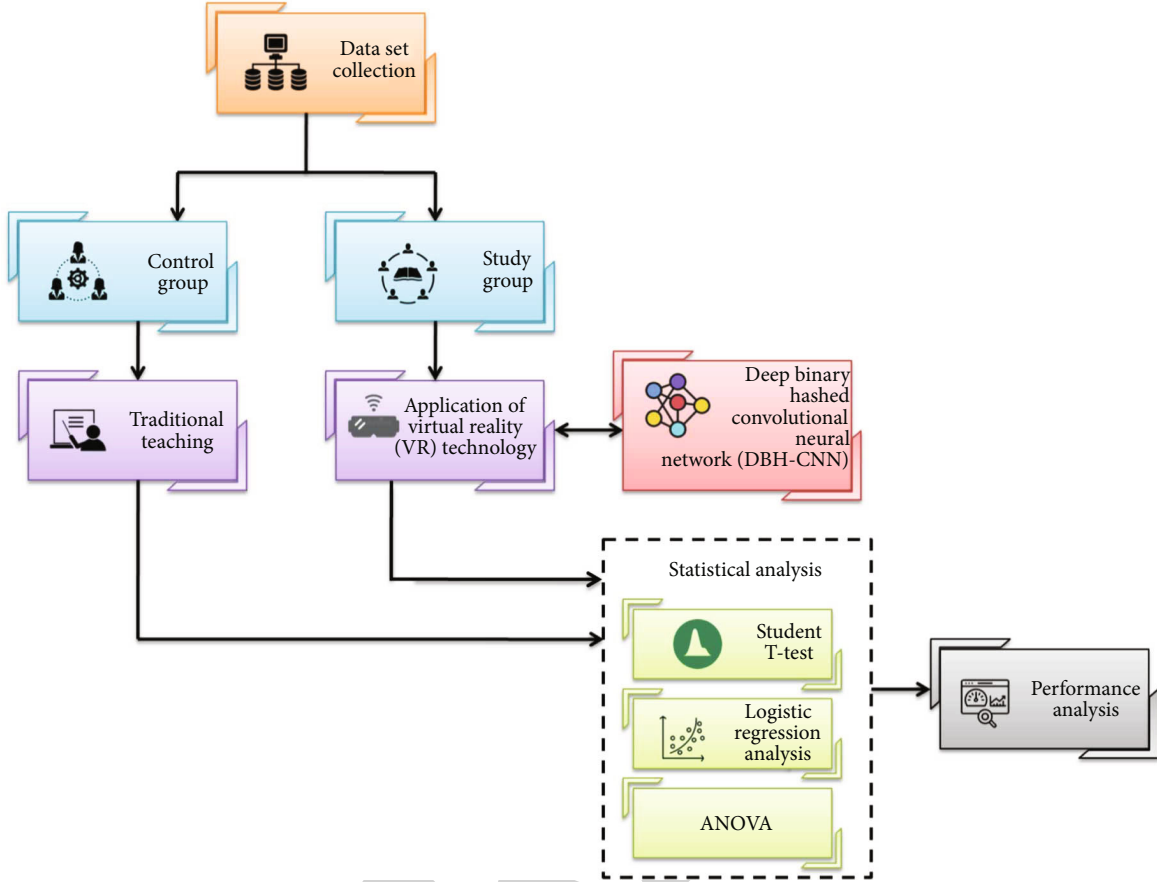


FIGURE 2: Proposed methodology.

TABLE 2: Data description [26].

Total quantity	Men	Women
7222	2908	4314

different ideas for how to use hashing to figure out the projection matrix. Most of the older methods were limited by similar tools, nonlinear depictions that could not be scaled, or hand-crafted features that were not very good. It has recently been suggested to learn both nonlinear representations of pictures and basic binary codes simultaneously using hashing algorithms based on deep learning. Specifically, we propose a CNN-based hashing technique that incorporates a binary representation layer between the fully connected and classification layers. To ensure that the learned binary representations of the data maintain semantic similarity, we “point-by-point” train the network using a collection of pictures and the labels that correspond with them. Discrete value systems that are useful for classification have been included in the loss function to push the binary layer closer to them. This is because the network would be trained to provide consistent binary representations for identically tagged input.

3.3.2. DBH-CNN. The proposed DBH-CNN is composed of the following layers: convolution, max-pooling, nonlinear transformations, fully connected layers, an LBE, and a classi-

fication layer. We forward propagate over the network and then quantize the output of the LBE layer to get the binary representations for X in the RGB space. As with regular layers, the output of one hidden layer is sent into the next. For this reason, we derive the l -th layer’s output in this way:

$$R^l = h(q^l R^{l-1} + g^l). \quad (1)$$

The l -th layer is learned projection matrix and bias. The proposed network’s LBE layer also generates the following results:

$$R^{L-1} = h(q^{L-1} R^{L-2} g^{L-1}). \quad (2)$$

3.3.3. Relaxation. Since the CNN is trained on considerably smaller batches of data, it is debatable whether or not the optimality of binary codes generated by the CNN using the same method is warranted if the whole training set is used to optimize the binary codes directly. By using the back-propagation technique and stochastic gradient descent (SGD), the network may be trained and improved. We modify its loss function and include a quantization requirement to aid it in learning more accurate binary representations. With our approach, a deep CNN simultaneously learns the feature representation and the binary coding. A complete

optimization issue is tackled by using the back-propagation technique.

3.3.4. Backpropagation. All through the training process, the functional form gradients concerning a system's variables must be calculated. It is necessary to calculate partial derivatives to determine gradients $\partial E_{x_n} / \partial q_{ji}^{L_j}$ and $\partial E_{x_n} / \partial g_{ji}^{L_j}$ for a single training example x_n and then recover the overall gradients by averaging over all the training examples. So, to calculate the loss function's gradient relative to the output layer's parameters, we do the following:

$$\begin{aligned} \frac{\partial E_{x_n}}{\partial q_{ji}^{L_j}} &= \frac{\partial E_{\zeta}}{\partial a^{L_j}} \frac{\partial a^{L_j}}{\partial q_{ji}^{L_j}} = b_i \delta_j^L, \\ \frac{\partial E_{x_n}}{\partial g_{ji}^{L_j}} &= \frac{\partial E_{\zeta}}{\partial g^{L_j}} \frac{\partial g^{L_j}}{\partial g_{ji}^{L_j}} = \delta_j^L. \end{aligned} \quad (3)$$

For the nonlinear function h , the derivatives are denoted by $h'(\cdot)$. With the use of the basic function of variables, we can calculate the error as

$$\delta_j^L = \hat{f} - f. \quad (4)$$

When expressed as a vector, we get

$$\delta^L = \hat{y} - y. \quad (5)$$

Afterward, we determine the goal function's gradients relative to the LBE layer's settings as follows:

$$\begin{aligned} \frac{\partial E_{x_n}}{\partial q_{ji}^{L-1}} &= \frac{\partial E_{\zeta}}{\partial a_j^{L-1}} \frac{\partial a_j^{L-1}}{\partial q_{ji}^{L-1}} + \frac{\gamma}{2} \frac{\partial E_Q}{\partial a_j^{L-1}} \frac{\partial a_j^{L-1}}{\partial q_{ji}^{L-1}}, \\ &= R_i^{L-2} \left(\vartheta_j^{L-1} + \frac{\gamma}{2} Q_j \right) = R_i^{L-2} \delta_j^{L-1}, \\ \frac{\partial E_{x_n}}{\partial c_{ji}^{L-1}} &= \frac{\partial E_{\zeta}}{\partial a_j^{L-1}} \frac{\partial a_j^{L-1}}{\partial c_{ji}^{L-1}} + \frac{\gamma}{2} \frac{\partial E_q}{\partial a_j^{L-1}} \frac{\partial a_j^{L-1}}{\partial c_{ji}^{L-1}}, \\ &= \vartheta_j^{L-1} + \frac{\gamma}{2} Q_j = \delta_j^{L-1}, \end{aligned} \quad (6)$$

where δ_j^{L-1} is categorization loss (j) and quantification loss (percent) make up the mistake at the j th neuron of the LBE layer. The vector representation of the loss stored procedure elements is calculated with the help of the basic function of derivatives.

$$\begin{aligned} \vartheta^{L-1} &= \left((q) \delta^L \right) \odot (1 - \tan h^2(a^{L-1})), \\ Q &= -2(b - R^{L-1}) \odot (1 - \tan h^2(a^{L-1})), \end{aligned} \quad (7)$$

where ϑ^{L-1} denotes the Hadamard product. To calculate the gradient for the remaining layers, we may use the same method as before:

$$\begin{aligned} \frac{\partial E_{x_n}}{\partial w_{ji}^{L_j}} &= z_i^{L-1} \delta_j^L, \\ \frac{\partial E_{x_n}}{\partial c_{ji}^{L_j}} &= \delta_j^L. \end{aligned} \quad (8)$$

where δ_j^L is to get the j^{th} part of the l^{th} layer's error vector; you would do something like:

$$\delta^l = \left((q^l)^T \delta^l \right) \odot h' (a^l). \quad (9)$$

Gradient descent is then used to update the parameters for each training sample in minibatches (Mb) as follows:

$$q_{ji}^l = q_{ji}^l - \alpha \sum_{n=1}^{M_b} \frac{\partial E_{x_n}}{\partial q_{ji}^l}, \quad (10)$$

$$g_{ji}^l = g_{ji}^l - \alpha \sum_{n=1}^{M_b} \frac{\partial E_{x_n}}{\partial g_{ji}^l}. \quad (11)$$

Algorithm 1 proposes a complete learning algorithm for the proposed DBH-CNN which paces knowledge acquisition.

3.4. Statistical Analysis. "Student's t -test, analysis of variance (ANOVA), and logistic regression analysis are the three methods that are used in statistical analysis".

3.4.1. Student's t -Test. Student's t -test is used to prove the hypothesis that there is no variance between the 3 groups. It is used for several circumstances, including the following.

To get to a conclusion whether a test indicates (as an estimate of a group mean) differs significantly from a certain group mean.

$$T = \frac{W - p}{LI}, \quad (12)$$

where W is the sample mean, p is the population mean, and LI is the standard error of the mean

$$S = \frac{W_1 - W_2}{LI_{Y_1 - W_2}}, \quad (13)$$

wherein $W_1 - W_2$ signifies the distinction.

It is determined to predict the data shown from the two variable samples differ considerably. Whenever variables are measured on the same participants during a drug, a paired t -test is commonly used.

The paired t -test equation is

$$n = \frac{m}{LI_m}, \quad (14)$$

where m stands for the overall mean and LI stands for the standard error of the variance. To evaluate component


```

Input: Training examples  $\{x_n\}$  with their corresponding
labels  $\{y_n\}$ , mini-batch size ( $M_b$ ) of training examples, learning rate  $\alpha$ ,
several iterations  $T$ , parameter  $\gamma$ .

Output:  $\{W^l, c^l\}_{l=1}^L$ 
  for  $t=1,2,\dots,T$  do
    for each training example,  $x_n$  in  $M_b$  do
      Set  $z^0 = x_n$ 
      For  $l=1,2,3,\dots,L$  do
        Perform feedforward computation for  $z^l$  using
        (1) for other layers, and (2) and
         $b_n = \tanh(a^{l-1})$  for LBE layer.
      end
      for  $l=L,L-1,\dots,1$  do
        Compute the gradients according to ((3))- (9).
      end
      for  $l=L,L-1,\dots,1$  do
        Update the weights and biases according to (10) and (11)
      end
    end
  end

Return:  $\{w^l, c^l\}_{l=1}^L$ 

```

ALGORITHM 1: DBH-CNN algorithm.

variations, the t -test can be utilized. The t -test employs the proportion of deviations.

3.4.2. *Logistic Regression Model.* The proportional odds (PO) framework, which is the most widely employed logistic design, has been developed.

The groups could be sorted naturally whereas if response parameter Y was ordinal, like “fitness condition good/moderate/bad.” The polytomous logistic regression model could be used, but it does not employ the sorting data. The use of cumulative possibilities, cumulative odds, and cumulative logits becomes a technique to compensate for the sorting. Those numbers have been specified in $(g + 1)$ -sorted groups.

$$Q(B \leq i) = q_1 + \dots + q_i, \quad (15)$$

$$(B \leq i) = \frac{Q(B \leq i)}{1 - Q(B \leq i)} = \frac{q_1 + \dots + q_i}{q_{i+1} + \dots + q_{g+1}}, \quad (16)$$

$$(B \leq i) = \ln \left(\frac{Q(B \leq i)}{1 - Q(B \leq i)} \right), \quad i = 1, \dots, g. \quad (17)$$

Regarding ordinal response information, the cumulative logistic representation is specified as

$$\text{logit}(B \leq i) = \alpha_i + \beta_1 A_1 + \dots + \beta_{ik} A_k, \quad i = 1, \dots, g. \quad (18)$$

We get multiple model equations (g) and one logistic variable (β) for every group/covariate pair.

As a result, the generalized cumulative logistic regression method has a lot of variables. In other circumstances, though, a parsimonious method becomes feasible. If the logistic parameters are independent of i , every covariate

has only a single common variable. As a result, the cumulative odds were calculated as follows:

$$\text{odds}(B \leq i) = \exp(\alpha_i) \exp(\beta_1 A_1 + \dots + \beta_k A_k), \quad i = 1, \dots, g. \quad (19)$$

Such that, the m odds for every cut-off group i vary exclusively in terms of the intercepts, implying that the odds were proportionate.

When the ordinal result B gets associated with an underpinning underlying continuous variable, for instance, whenever B is indeed a categorized continuous variable like age ranges or cash economic classes, the somewhat strict proportional odds hypothesis could be particularly fitting. Ordinal variables that have been evaluated by an investigator, on the other hand, are another essential sort of ordinal variable. Regarding biomedical analysis, these factors are common.

3.4.3. *ANOVA Test.* Analysis of variance (ANOVA) is a statistical technique used to break down aggregate reports of variability into more manageable subsets for use in follow-up analyses. When there are three or more data sets, a one-way ANOVA is performed to determine the correlation between the variables. The traditional analysis of variance (ANOVA) F -statistic is the percentage of the null model with the anthropic principle average sums of squares to the whole model. The parameters are calculated using the least-squares approach, with all variances being identical. This may be expressed as

$$M = \frac{NS_{\text{between}}}{NS_{\text{error}}}, \quad (20)$$

where

$$NS_{\text{between}} = \frac{\sum_{i=1}^j o_i (\bar{B}_i - \bar{B})^2}{j-1} m \quad (21)$$

$$NS_{\text{error}} = \frac{\sum_{i=1}^j \sum_{k=1}^{o_i} (B_{ik} - \bar{B}_i)^2}{h-j}. \quad (22)$$

The Welch-test-statistic is defined as

$$X = \frac{\sum_{i=1}^j x_i \left[(\bar{B}_i - \bar{B})^2 / (j-1) \right]}{1 + ((2(j-2))/(j^2-1)) \sum_{i=1}^j [(1-x_i/v)^2 / (h_i-1)]}, \quad (23)$$

where $X_j = n/t_1^2$, $v = \sum_{i=1}^j X_i$, and $B = 1/v \sum_{i=1}^j X_i Y_i$ is defined as

$$m = \frac{j^2 - 1}{3 \sum_{i=1}^j \left[(1-x_j/v)^2 / (h_i-1) \right]}. \quad (24)$$

The Brown-Forsythe-test-statistic is defined as

$$M^* = \frac{\sum_{i=1}^o h_i (\bar{B}_i - B)^2}{\sum_{i=1}^o (1-h_i/h) S_i^2}, \quad (25)$$

when L_o is factual, the allocation of M^* is appropriate by a central M distribution with degrees of freedom $o-1$ and m , where m is defined as

$$\frac{1}{m} = \frac{\sum_{i=1}^o d_i^2}{h_i - 1}, d_i = \frac{(1-h_i/h) S_i^2}{\sum_{i=1}^o (1-h_i/h) S_i^2}. \quad (26)$$

To calculate the generalized p value, the generalized p value is now computed as $p = 1-l$, where r is the sample size.

$$l = H \left(I_{o-1, h-o} \left(\frac{h-o}{o-1} \hat{t}_c \left(\frac{h_1 t_1^2}{C_1 C_2, \dots, C_{o-1}}, \frac{h_2 t_2^2}{C_1 C_2, \dots, C_{o-1}}, \frac{h_3 t_3^2}{(1-C_2) C_3, \dots, C_{o-1}}, \dots, \frac{h_1 t_o^2}{(1-C_{o-1})} \right) \right) \right). \quad (27)$$

The prediction is calculated concerning the separate Beta stochastic process in an F -distribution having $I_{o-1, h-o}$.

$$C_k \sim \text{beta} \left(\sum_{i=1}^k \frac{(h_i-1)}{2}, \frac{h_{k+1}-1}{2} \right), \quad k = 1, 2, \dots, o-1. \quad (28)$$

The p value is calculated by numerically integrating the anticipated value in the p value formula about the beta random variables.

4. Result and Discussion

Experiments are done to further confirm its effectiveness in real implementation. For experiment's validity, use the attribute information about the virtual reality classroom account gathered from the network. In this study, the parameters are used accuracy, learning efficiency, achievement improvement rate, physical quality of the students, affection and attitude indicators, VR technology cognition, and application. The findings were compared to those obtained using existing approaches. The existing methods like "Recursive Neural Network (RNN), Graph Neural Network (GNN), Back propagation-Neural Network (BP-NN), and Multilayer Neural network (ML-NN)" are compared with the proposed method to attain the greatest performance in this work.

The term "learning efficiency" refers to the correlation between a learner's PME and an outcome measure of performance, such as a test score or the time it takes to complete a task properly. Teaching and learning strategies that encourage students to take an active role in their education and growth are what we mean when we talk about "effective learning." Consider it a step beyond rote memorization and imitation of classroom practices to educate students well on how to learn independently. The quantitative judgment and statistical analysis of a teacher's performance in an interactive classroom are carried out via the lens of a teaching benefit and a novel assessment method. Figure 3 depicts the comparison of learning efficiency for existing and proposed methodologies.

When compared to the existing method, the proposed method has greater learning efficiency. RNN has a 75%, GNN has a 65%, BP-NN has an 84%, ML-NN has a 58%, and the proposed DPH-CNN has 96% learning efficiency.

In the analysis stage, accuracy is the percentage of times a classifier correctly predicted the actual value of a label. It may also be stated as a ratio of the number of correct evaluations to the overall number of tests. The accuracy is calculated using the equation:

$$\text{Accuracy} = \frac{(A+B)}{(A+B+C+D)}, \quad (29)$$

where A is the true negative, B is the true positive, C is the false positive, and D is the false negative.

Figure 4 shows the comparison of accuracy for existing and proposed methodologies. When compared to the existing method, the proposed method has greater accuracy. RNN has a 55%, GNN has an 88%, BP-NN has a 66%, ML-NN has a 70%, and the proposed DPH-CNN has 98% accuracy.

A design approach is used as a pedagogical platform to investigate the viability of a deep learning-based, augmented reality-based, interactive classroom. After using this strategy, the virtual reality interactive classroom is much more stable. The primary reason is that a deep learning algorithm is utilized to examine the VR-interactive classroom throughout the creation phase of this methodology.

Figure 5 shows the comparison of achievement improvement rates for existing and proposed methodologies. When

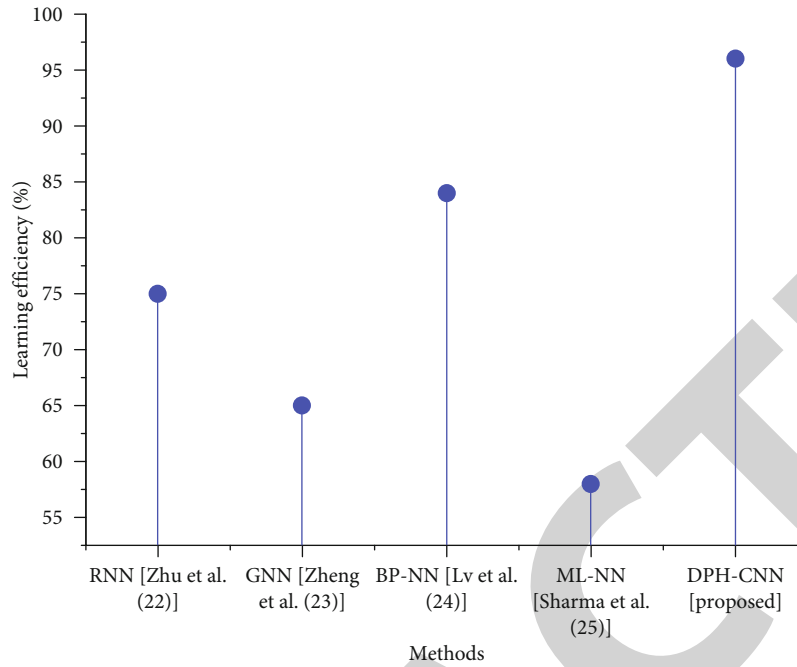


FIGURE 3: Comparison of learning efficiency for existing and proposed methodologies.

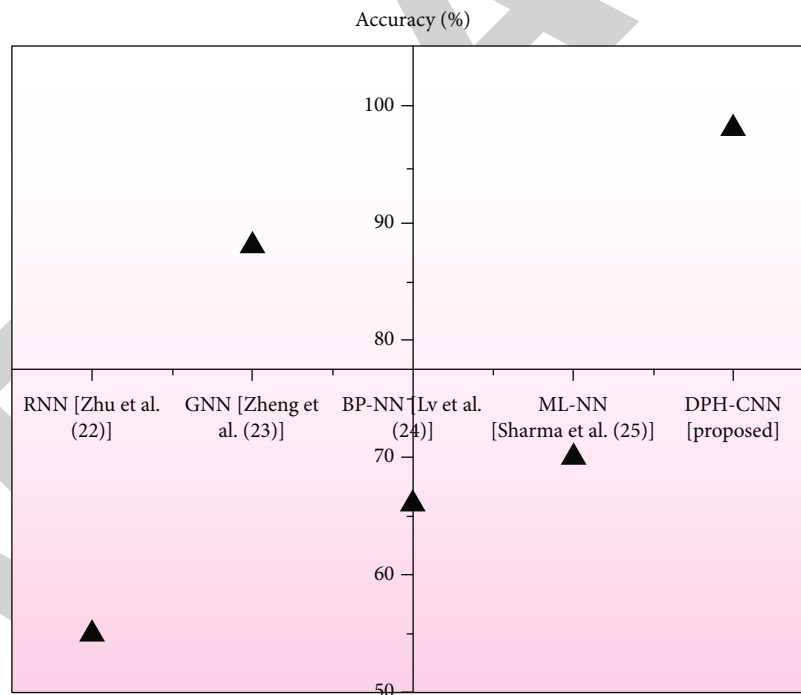


FIGURE 4: Comparison of accuracy for existing and proposed methodologies.

compared to the existing method, the proposed method has a greater achievement improvement rate. RNN has an 85%, GNN has a 66%, BP-NN has a 75%, ML-NN has a 55%, and the proposed DPH-CNN has a 94% achievement improvement rate.

The students in the experimental group and the control group are compared based on their physical appearance and general health in this research. Figure 6 displays the out-

comes of the tests. Therefore, this article indicates that both conventional instruction and instruction aided by virtual reality technology both contribute to the general enhancement of students' physical well-being. Students may get a psychological high from using VR technology to study before or after class, but this has little impact on their motivation. It does not promise that pupils will be able to push over their laziness and keep training. The author hypothesizes that

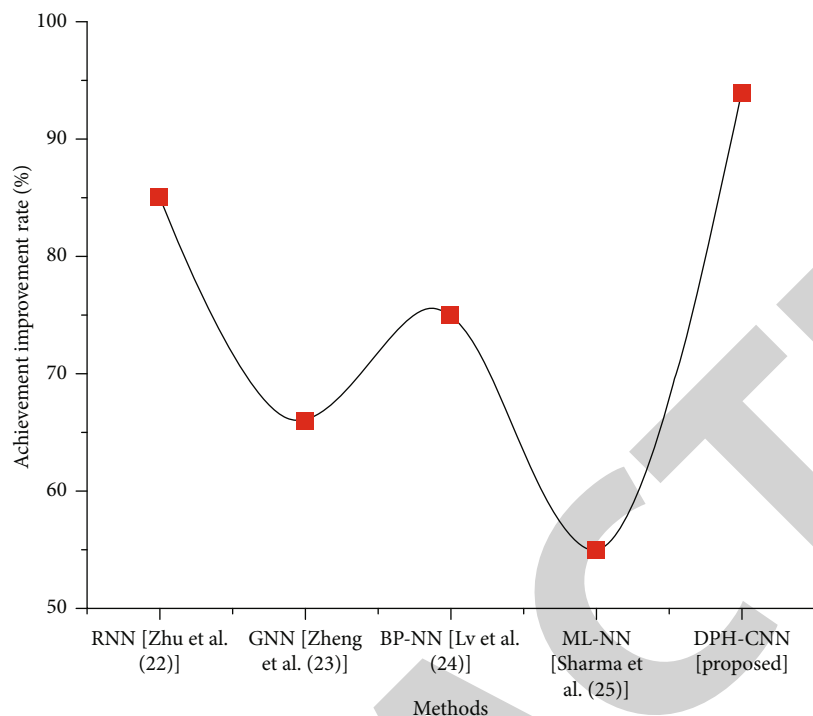


FIGURE 5: Comparison of achievement improvement rate for existing and proposed methodologies.

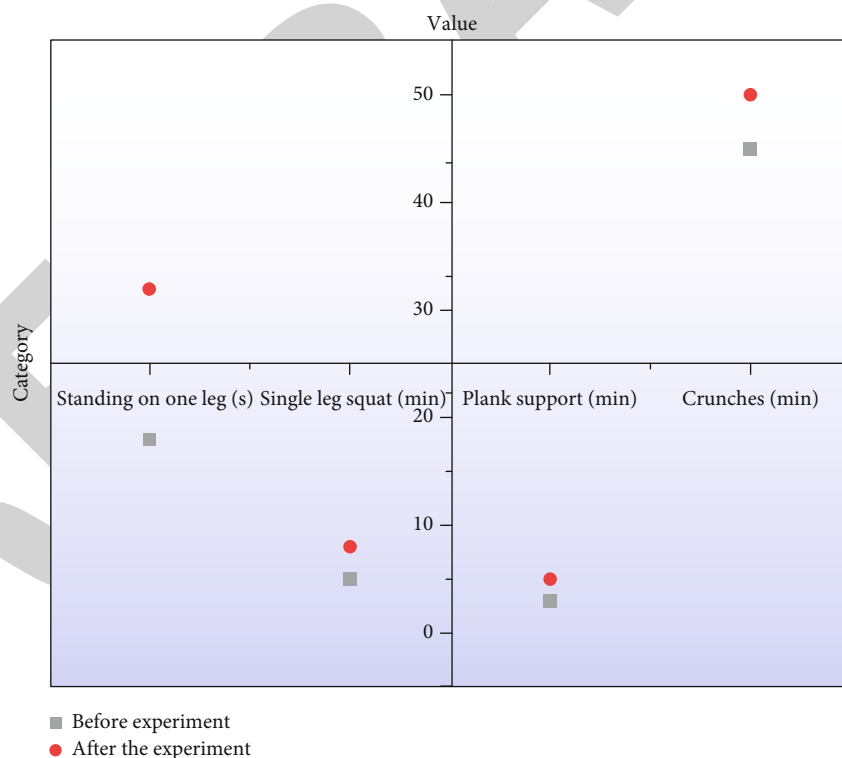


FIGURE 6: Comparison of basic physical quality of the students in the experimental group and the control group.

the experimental group’s slightly better test value of basic physical fitness compared to the control group is due to the increased excitement of the students to study martial arts made possible by the use of virtual reality technology.

Interaction with the material and a desire to learn are examples of students’ learning interests and sentimental openness to instruction, only by storing up knowledge and abilities unless they are sufficiently motivated to do so.

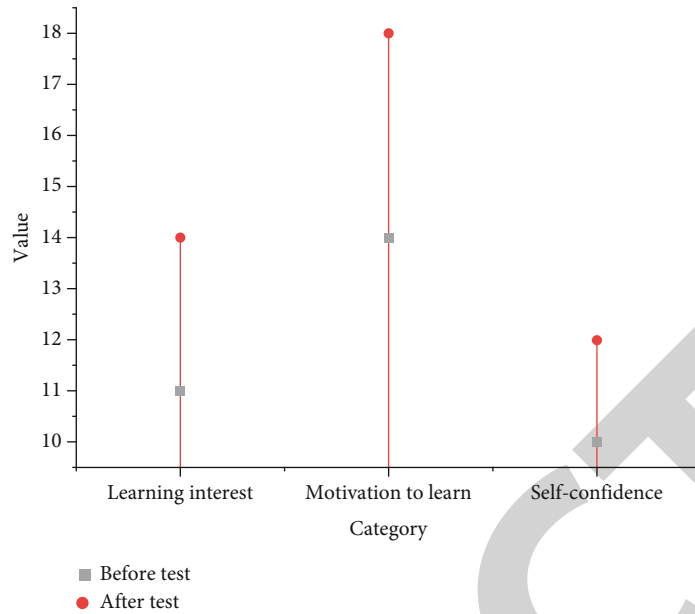


FIGURE 7: Comparative analysis of two groups of students' affection and attitude indicators after the experiment and before the experiment.

Self-confidence refers to a person's belief in his or her abilities to accomplish a task while learning motivation describes the inner drive to encourage, inspire, and direct kids toward academic success. Figure 7 shows the results of a preliminary statistical analysis of emotional disposition test markers of the groups of students during learning.

Students in the experimental group demonstrated more enthusiasm, desire, and confidence in their ability to study martial arts than those in the control group did. Since students in the experimental group wore VR headsets before class, they benefited from a new immersive learning experience, and the physical motions of martial arts were more clearly conveyed in front of their eyes thanks to the situational substitution teaching approach. The system may track the evolution of martial arts moves from a variety of perspectives.

As seen in Figure 8, there are five possible degrees of agreement (strongly agree, agree, slightly agree, unsure, and disagree) represented by the letters A, B, C, D, and E, respectively. According to the poll, using VR to teach martial arts has been well received by pupils, and many report a renewed interest in the subject as a result. The primary reason is that the stereoscopic rotation of the gadget allows for seeing the movie from any angle and in any direction. In addition to providing students with a more engaging learning environment, VR may improve their capacity to watch and analyze movements and aid them in more thoroughly correcting incorrect movements based on accurate comprehension and recognition. It raises the bar for what is considered "normal" in martial arts. On the other hand, it is a useful supplementary resource for students' education. It transforms kids' learning strategies while fostering more independence and curiosity in the classroom. However, not all pupils are comfortable with this methodology.

4.1. Discussion. The usage of RNNs in disciplines including pattern recognition, image processing, intelligent control,

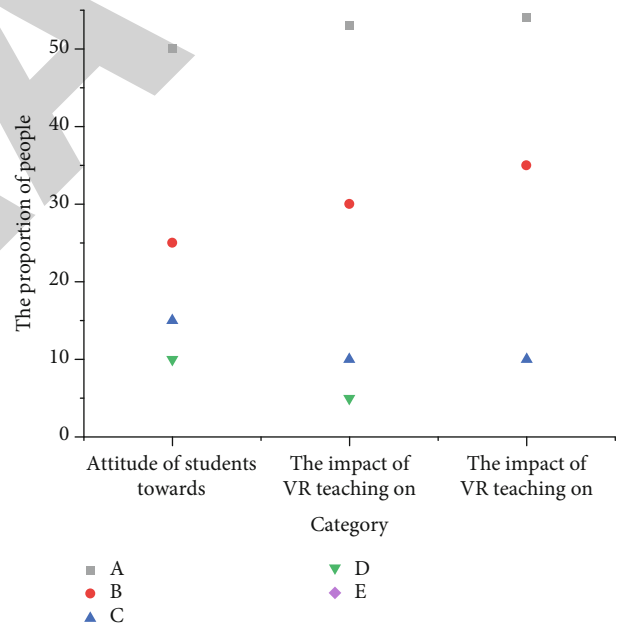


FIGURE 8: VR technology cognition and application.

signal processing optimization calculations, and others have made them large-scale nonlinear dynamic systems with feedback loops. The issue of vanishing gradients, which affects RNNs [27], makes it difficult for these networks to learn from extended data sequences. Gradients are a vital part of the RNN variable update, and as they decrease in magnitude, the learning gains from these updates diminish to zero. Most fundamental GNN restrictions [6] are works of GNN confined to a set number of points. Time and space complexity are greater. We can reduce the time spent on edge processing graphs by classifying them into fewer categories. Based on big data technologies and GNN, it creates

an interactive teaching system for Tai Chi that is ideological and political. Each expert is only used for a small number of input instances in BP-NN [28]. As new situations emerge, the Mixture of Experts is unable to swiftly adjust its parsing. Existing Mixtures of Experts cannot be modified to include additional types of expertise if such types are suddenly needed. The BP-NN adjusts to the speed of learning. The learning step length selection, difficulty defining the size and direction of the weights, and difficulty controlling the learning rate are all improved in the method for the conventional BP neural network. Most notably, ML-NN [29] has the drawbacks of losing neighborhood information, having additional parameters to optimize, and not being translation invariant. This implies that neural networks may typically be tried against a problem with an unknown form even if other kinds of machine learning algorithms have already failed; ML-NN flexibility is used in solving issues with nonlinear geometries. So in this work, we propose an architecture of virtual reality based on the deep learning algorithm of the Deep Binary Hashed Convolutional Neural Network (DBH-CNN).

5. Conclusion

It is clear that there are problems with the way we have always done things in the classroom, but it does not mean conventional techniques are without value. Advances in science and technology have a subtle but discernible impact on educational reform and pedagogical experimentation. The key to advancing the reform of pedagogical practices is figuring out how to more effectively use cutting-edge scientific and technological tools in the classroom. In the video presentation, the activity is shown in a more three-dimensional, intuitive, and multiangle way. The film is enhanced with action explanations and music, and students utilize virtual reality (VR) technology to simulate realistic training scenarios, all to better their ability to grasp and recall martial arts techniques. It performs multidirectional observation and gains an immersed learning opportunity, which in turn increases the quality of students' martial arts movements by their attention and delight, and gradually improves the quality of motions over time. When compared to other existing approaches like RNN, GNN, BP-NN, and ML-NN, the DBH-CNN has 98% accuracy. However, research in the field of martial arts is still at the theoretical stage and lacks practical application countermeasures and plans, demanding more inquiry and study. Virtual reality technology has developed as a new trend. This suggests that there is merit and potential in using VR technology to train martial artists. There are, of course, issues with using VR technology to teach martial arts, and we should do everything we can to address them. To gain the respect and appreciation of students, it must also do more research on the benefits of using virtual reality technology in its professional context. It seems clear that the use of VR technology to aid martial arts is practical. There is still little research on the use of VR and its real effects on instruction and student learning. Future research will involve detailed quantitative validation of the

results, including comparisons of their efficacy to conventional methods like GIS.

Data Availability

The data used to support the findings of this study are available from the corresponding author upon request.

Conflicts of Interest

The authors declare that they have no known competing financial interests or personal relationships that could have appeared to influence the work reported in this paper.

References

- [1] L. Tong, *Research on the Application of Flipping Classroom in Taijiquan Teaching in Colleges and Universities*, MDPI, Basel, Switzerland, 2019.
- [2] R. N. Mody and A. R. Bhoosreddy, "Multiple odontogenic keratocysts: a case report," *Annals of Dentistry*, vol. 54, no. 1-2, pp. 41-43, 1995.
- [3] H. Wan, *Research on Teaching Reform Practice of the Course of Wushu Duan System in Colleges and Universities-Based on the Application of the Theory of "Flip Classroom"*, Francis Academic Press, 2018.
- [4] Z. Yuqing, C. Mingliang, Z. Haoyang, and Z. Yong, "VR technology and application in martial arts," in *2021 IEEE 7th International Conference on Virtual Reality (ICVR)*, pp. 240-245, Foshan, China, 2021.
- [5] H. Garg, "Digital twin technology: revolutionary to improve personalized healthcare," *Science Progress and Research (SPR)*, vol. 1, no. 1, 2020.
- [6] L. Zheng, "Analysis of tai chi ideological and political course in university based on big data and graph neural networks," *Scientific Programming*, vol. 2021, Article ID 9914908, 9 pages, 2021.
- [7] A. Yap and C. Goto-Jones, "Loyalty, deference, and exploitation in traditional and mixed martial arts," in *The Philosophy of Mixed Martial Arts*, pp. 30-42, Routledge, 2021.
- [8] B. Ahmed and A. Ali, "Usage of traditional Chinese medicine, Western medicine and integrated Chinese Western medicine for the treatment of allergic rhinitis," *Official Journal of the Zhende Research Group*, vol. 1, no. 1, pp. 1-9, 2020.
- [9] G. Goehle, "Teaching with virtual reality: crafting a lesson and student response," *International Journal for Technology in Mathematics Education*, vol. 25, no. 1, 2018.
- [10] N. Zhang, X. Chen, and H. Yin, "Significance and possibility of VR technology embedded in the teaching of ideological and political theory course in colleges and universities," *IEEE Access*, vol. 8, pp. 209835-209843, 2020.
- [11] A. Shahabaz and M. Afzal, "Implementation of high dose rate brachytherapy in cancer treatment," *SPR*, vol. 1, no. 3, pp. 77-106, 2021.
- [12] D. Bos, S. Miller, and E. Bull, "Using virtual reality (VR) for teaching and learning in geography: fieldwork, analytical skills, and employability," *Journal of Geography in Higher Education*, vol. 46, no. 3, pp. 479-488, 2022.
- [13] Y. Pu and Y. Yang, "Application of virtual reality technology in martial arts situational teaching," *Mobile Information Systems*, vol. 2022, Article ID 6497310, 13 pages, 2022.

Research Article

Classification, Application, Challenge, and Future of Midair Gestures in Augmented Reality

Yi Lu ¹, Xiaoye Wang,¹ Jiangtao Gong,² Lejia Zhou,¹ and Sen Ge¹

¹Beijing University of Technology, Beijing, China

²Institute for AI Industry Research (AIR), Tsinghua University, Beijing, China

Correspondence should be addressed to Yi Lu; luyi@bjut.edu.cn

Received 31 August 2022; Accepted 22 September 2022; Published 5 October 2022

Academic Editor: Sweta Bhattacharya

Copyright © 2022 Yi Lu et al. This is an open access article distributed under the Creative Commons Attribution License, which permits unrestricted use, distribution, and reproduction in any medium, provided the original work is properly cited.

Augmented Reality (AR) technology provides many opportunities to enhance people's experience in interacting with data. Midair gesture, a natural interaction mode in AR, interacts with virtual elements without any auxiliary devices. It has become a hot topic of interest for researchers with the development of gesture recognition technology. From the perspective of user experience, the types of midair gesture, gesture recognition technology, applications were discussed. The challenges of air gesture interaction from two aspects of user experience and technology were analyzed, and the importance of collaborative gesture and low-cost user experience in the future were emphasized. Finally, the application prospect of air gesture interaction distance education, medical health, industry, office, and so on is discussed.

1. Introduction

Augmented reality (AR) allows users to perform tasks in both real and virtual environments by overlapping virtual content in the real world [1]. AR is featured by real-time interaction, where gesture, voice, body posture, and even eye movements can be interaction mode. Gesture with wide application in human-computer interaction (HCI) can be used as input media for various media, including mobile phones, computers, televisions, large screen displays, etc. Its interaction can be direct touch, using physical devices (e.g., pens, remote controls, and handles) and body posture or their combinations. Gestures not using any physical medium are called midair gestures. Compared with using handle and touch, midair gesture realizes nonphysical contact with computer and manipulates objects in virtual environment with less constraints. In AR, natural midair gestures provide an intuitive interactive method to connect the virtual and real worlds. More natural and flexible than handle and buttons, midair gesture interaction can intuitively demonstrate information and express intention, which reduces the user's learning cost, and greatly enhances immersive interaction [2, 3].

There are a variety of midair gestures, and the gesture type may vary with the application environments. According to different time, use environment and functions, the classification methods of gestures are also different. This paper will explain the different classifications from the perspective of user experience. The change of gesture classification is also closely related to the development of gesture recognition technology. Gesture recognition is the key to midair gesture interaction. It is a technology to operate the device by capturing human's limb movements and converting them into corresponding commands [4]. Currently, gesture based systems such as Microsoft Kinect and Leap Motion, which support hand and whole body tracking, have become ubiquitous. Midair gesture has become a popular interaction mode with the emergence of more and more systems such as Microsoft HoloLens and Magic Leap [5]. In the design of midair gestures, the core is to provide a comfortable user experience. Gesture type and gesture recognition technology are important factors that affect the user experience, and also determine the application of midair gesture. Therefore, midair gesture interaction in AR has important research value. The future user experience design of midair gesture will be benefited from the understanding of its current design,

application, and technical development. To this end, the recent development of midair gesture in AR is combed and analyzed, and the future development trend of midair gesture is discussed, with the focus on the following aspects: (1) different classification methods of midair gestures; (2) typical application fields of midair gestures; (3) challenges and future development of midair gesture interaction.

2. Classification and Elicitation Study of Midair Gestures

2.1. Classification of Midair Gestures

2.1.1. Classification in HCI. Gesture is often used for assisting verbal communication, and the research on midair gesture also originates from the observation of daily interpersonal communication. Therefore, the earliest classification of midair gestures was also based on speech [6–8]. The midair gesture based on the language environment provides a basis for the classification of gestures in HCI in the future. The interface combining gesture and voice is explored through human to human communication. Researchers have also done a lot of work on the interface of simple midair gesture control. It has always been a hot issue in HCI. Karam and Schraefel created a wide range of taxonomies and proposed a model of deictic, schematic, manipulation, signal, and sign language gestures. In this model, gestures are also equivalent to symbolic or descriptive gestures, which are used to describe body shape and the form indicated by speech [9]; Aigner et al. extended their model, and found that pointing, pantomime, direct manipulation, signal gesture, and icon gesture are the most popular gestures by analyzing 5500 gestures [10]. Moreover, gestures were further divided into static gestures and dynamic gestures according to their temporal state, and signal gestures were further divided into Semaphoric Static, Semaphoric Dynamic, and Semaphoric Stroke. Icon gestures were divided into Iconic Static and Iconic Dynamic. Point gesture is used to indicate the object and direction. Semaphoric-Static and Semaphoric-Dynamic are related to the social culture we are familiar with. For example, in daily life, we thumb up to mean “OK”. Unlike Semaphoric-Static and Semaphoric-Dynamic, Semaphoric-Stroke has special meanings in some cases, especially in controlling multimedia, such as palm waving to switch to the next page. Pantomimic gesture is a more vivid performance action or continuous action. Icon-Static and Icon-Dynamic are related to images and icons, performing specific tasks with a shape (circle, triangle, etc.) made by hand. Manipulation gesture is also an abstract gesture used to manipulate objects, such as zoom in and out.

2.1.2. Classification Based on Time. According to the dimension of time, midair gestures can be classified into static gestures and dynamic gestures. Static gesture is the specific state of the hand including the posture, position, and direction of the hand. Dynamic gesture is a time series of hand states, which means that the posture, position, and direction of dynamic gesture will change with time. Because dynamic gesture has a higher degree of freedom and more operable actions, it is more difficult to recognize in gesture recogni-

tion. Nevertheless, dynamic gesture can be recognized more easily with the maturity of gesture recognition technology.

2.1.3. Classification Based on Definition Mode. Midair gestures are classified into predefined and user-defined gestures from the perspective of technology and experience. Predefined gestures mean that system engineers have designed gestures according to one’s usage habits for the use of systems or some applications before we use some system devices, and users have to learn to use these gestures. User-defined gestures are usually gesture types defined by users according to their own preferences, which requires more complex gesture recognition technology. For example, Wang et al. have created a gesture AR authoring system, in which users completes freehand interaction using a visual programming interface to match gestures with the response of AR virtual content. It improves the flexibility and independence of freehand interaction [11]. However, more researchers are inclined to study user-defined gestures with the continuous development and maturity of gesture recognition technology. This method has many advantages. Users do not have to learn before using the system, and the interaction is more natural. Moreover, it is also consistent with the user-centered design principle in HCI.

2.1.4. Classification Based on Task Type. The classification of gestures is closely related to their purpose and use environment. Communicative gestures are often suitable for performing some “abstract” tasks, such as controlling menus, turning on/off devices, media control tasks, especially signal gestures. According to Groenewald et al., midair gestures are mainly used for selection, navigation, and operation tasks. Manipulation gesture is also suitable for “physics based interaction” operation tasks in addition to navigation tasks. It can be interpreted as operating virtual objects like real objects, providing users an immersive experience that they are directly operating something, like playing a virtual basketball with tapping gestures, throwing a paper plane with kneading actions, etc. Generally, a more immersive user experience can be created with the combination of “physics-based interaction” and sensory effects such as vision and hearing in the AR environment with the combination of virtuality and reality. Therefore, midair gestures can be divided into abstract gestures and gestures based on physical operations according to their current application in AR. Abstract gestures are used to perform operations like menu selection, mode switching, switching, and object adjustment. Such gestures are also related to culture and habits. Of course, they also convey some special semantics. For example, swinging the palm indicates the state of fish swimming. Gestures based on physical operations are closely related to daily life, including grasping, kneading, tapping, etc.

At present, the exploration of gesture applications is also constantly innovated based on a variety of gesture recognition technologies, shifting from leisure AR applications to deeper areas. Abstract gestures are often ambiguous, and it is a challenge for users to learn specific actions. To this end, some studies have focused on how to use simple gestures to operate a variety of tasks, thus reducing users’ learning burden while enhancing the user experience. Designers









	Forward	Backward	Start	Stop
Close shot				
Long shot				

FIGURE 1: The gesture set determined by Samimi et al. according to the evaluation results.



FIGURE 2: Usage scenario of midair gesture (Samimi et al.).

from Leap Motion are exploring a one-hand operation scheme suitable for AR, using simple kneading gestures to execute a variety of quick commands. Besides, they designed three gesture modes, i.e. throwing mode, slingshot mode, and time mode to test the kneading gesture scheme. They hope to create more one-hand control modes, and enable each hand to perform a variety of tasks by combining with two-hand gestures.

2.2. Elicitation Study. As gesture recognition technology has become mature with diversified applications, relevant gestures are also in large number. Therefore, later studies have also focused more on evaluating different sets of midair gestures to know the effective gestures for specific operation tasks.

Researchers need to evaluate the most comfortable gestures for users, so as to explore the gestures with user preference in AR. The most common method is gesture elicitation study. Gesture elicitation is a technology widely used to recognize self-discoverable gesture words in HCI [12]. Usually, the participants are shown the reference (effect), and then they are asked to propose a more matching (easy and intuitive) gesture. Researchers classify a large number of data after collecting a large number of gestures, so as to obtain the gestures with user preference. However, such research is limited to hand and finger movements using specific technologies (e.g., public displays, TV, AR, and VR) [12], such as using midair gestures to control TV media. Figure 1 shows the set of midair gestures determined by Samimi et al. for TV presenters through elicitation study. The gesture set consists of five gestures from two camera shots (long shot and close shot). The results of the evaluation study show that the derived set of gestures will not consume too much phys-

ical strength and attention of the host. The host using these gestures are enabled to control the AR content in the TV and tell stories in a modern way with more power of expression. Figure 2 shows the usage scenario [13].

Wobbrock et al. developed a set of user-defined gestures according to the degree of consensus among participants, and classified the induced gesture vocabulary. This classification method aims to expand the gesture design space in the desktop environment [14]. Lee conducted a Wizard of Oz study on the AR multimodal interface, aiming to explore the types of gestures people want to use in the tasks of virtual object manipulation. The experimental results showed that the most popular gesture types are pointing, translation, and rotation gestures [15]. Piumsombon et al. explored the types of natural gestures in AR through experiments and determined the gesture sets corresponding to the four basic tasks of select all, open, close, and select horizontal menu. They got 800 user-defined gestures in 40 tasks, and finally got 44 user-defined gesture “consensus sets”, providing an important reference for designers of user experience. This gesture set represents the gesture preferences of users in AR tasks [16]. Moran-Ledesma et al. utilized heuristic research methods to determine the gesture set in which physical props are used to control VR and carried out necessary construction on the basis of previous work, so as to include the selection of both gestures and physical objects used together [12].

3. Interactive Application of Midair Gesture for AR

3.1. Midair Gesture in Multimedia. Many researches focus on gesture control of various types of media, such as video, virtual content playback, and so on. The interaction with

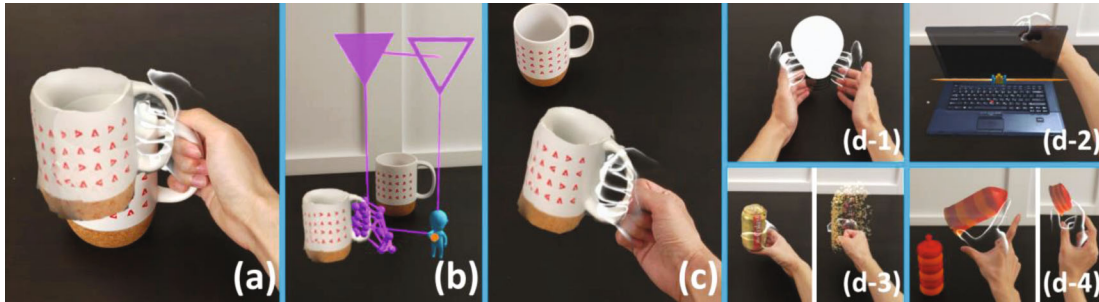


FIGURE 3: GesturAR: an authoring system for creating freehand interactive augmented reality applications (Wang et al.).

users in applications is not limited to mobile electronic devices. In the AR vehicle interaction system, the displayed content can be switched through midair gestures. Outdoor AR advertisements trigger the playback of virtual content through the waving and staying of gestures. Rovelo Ruiz et al. [17] introduced a set of gestures for controlling panoramic videos. In addition, Siddhpuria et al. [18] explored the use of discrete micro gestures with smart watches to control remote media. And several studies used midair gesture interaction to improve the user experience of smart TV, especially multimode technology and interaction [19, 20]. Rateau et al. [21] proposed user-defined gestures to define virtual interaction space in a universal environment.

3.2. Embodied AR Presentation. Midair gesture interaction has shown many advantages in experimental dynamic simulation, three-dimensional object display, and other aspects. Most systems predefine the virtual content triggered by each gesture—create mapping relationships. Besides, users need to learn these gestures in advance, and the execution of predefined gestures will trigger predefined actions. For example, Chalktalk VR/AR is a simulation tool for creating drawings in face-to-face brainstorming. Users can call vivid and intelligent virtual elements through aerial drawing to explain scientific knowledge online. All triggers need to be preprogrammed [22]. In the Post-Post-it system, researchers designed a series of natural and near-realistic midair gestures to move, copy, delete, and virtual post, and it is used for brainstorming in online classes [23]. Wang et al. created the GesturAR on HoloLens2 using Unity3D. Users can complete freehand interaction by using the visual programming interface to match gestures with the response of AR virtual content [11]. Unlike other works, users design gestures to interact with virtual elements completely on their own in GesturAR, which improves the flexibility and independence of freehand interaction (Figure 3).

3.3. Midair Gesture in Teaching Presentation. Midair gesture interaction based on AR demonstration can intuitively display information, so it has great potential in performance, speech, and teaching. Vision based real-time gesture recognition has the advantages of low learning cost, noncontact control, richer, and more natural interactive actions. Therefore, gestures often replace the keyboard and mouse to complete the basic virtual interaction function in the teaching scene [2]. For example, predefined gestures are mapped to

virtual interactive commands, and the multimedia platform is operated with midair gestures such as confirm, return, select, grab, and release. Users do not need other auxiliary tools by combining the demonstration, entertainment, and teaching of multimedia technology with gesture recognition technology, and a natural direct and humanized HCI experience is achieved with the use of gestures.

Saqib et al. proposed a dynamic demonstration tool that directly operates the virtual interface using the Leap Motion. Users can call virtual graphic elements in real time through body posture, so as to use daily actions to enhance the ability of communication with the audience [24] (Figure 4).

At present, many AR education use HMDs and holographic projection to create teaching environments, but Gong et al. created HoloBoard base on pseudo holographics. They designed and implemented a rich set of novel interaction technologies, including body posture interaction, gesture and handle interaction, and tactile feedback, so that teachers and users can achieve naked eye augmented reality teaching experience through immersive demonstration, role-playing, and behind the scenes lectures [25].

Another typical application is the midair gesture operation AR experiment. With the help of multimedia, simulation, AR, and other technologies, the relevant software and hardware operating environment that can assist the operation links of traditional experiments is created on the computer, and the experimenter can complete various experiments as in the real environment. An example is the immersive chemical experiment system with head-mounted displays and Leap Motion gesture input devices. Learners are free to grab, drag, and drop experimental instruments according to the actual operation mode to complete the experimental operation. In addition, Geping et al. discussed the impact of experiments based on gesture interaction technology on learners' experience, and found that virtual experiments based on gesture interaction technology can effectively enhance learners' immersive experience, thereby increasing their learning motivation [26].

The application of midair gesture in teaching is not limited to virtual experiments, but can also realize the 6DOF tracking effect with good stability and high accuracy with the help of AR glasses and monocular and multicamera. It can complete the operations of two hand linkage, midair triggering, dragging, and moving, and realize the natural and flexible interactive experience of midair gesture.

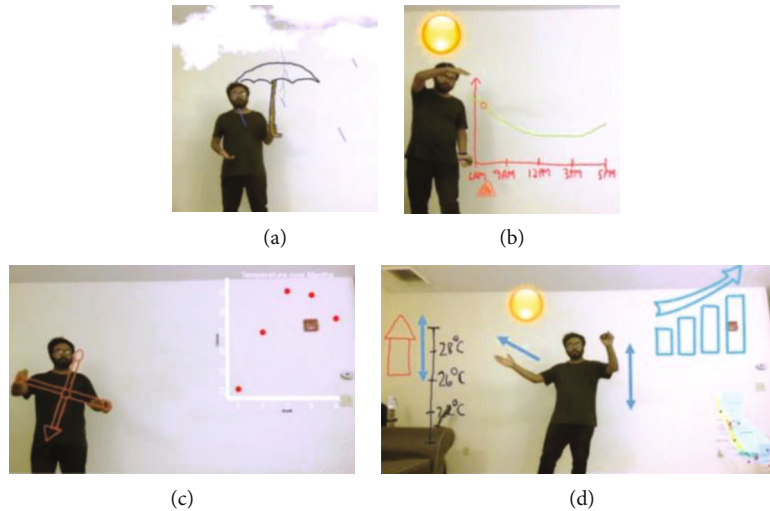


FIGURE 4: Interactive body driven graphics based on AR video (Saquib et al.).

In the field of education, midair gesture interaction has changed the traditional teaching method, made the teaching content expressed in a more wonderful way, and enhanced the interactivity and entertainment in the teaching process. Different from the application in other fields, teaching demonstration is not only personal experience but also expression and communication. Therefore, when using head mounted display, the personal experience effect is good, but the communication effect may be poor. So technically, using Leap Motion and Kinect for tracking and recognition will be more suitable for use in teaching situations, because it can help teachers avoid additional physical burden and will not restrict communication. The application of midair gesture in the field of education and teaching is of great value. The reason is that the AR teaching environment itself has several particularities:

- (1) *Environmental Diversity*. The environment configuration of online and offline classes is different. In offline classes, teachers move near the podium, but because their body posture often shifts between facing the blackboard and facing the students, and the radial rotation is omnidirectional. In this process, it is easy to cause false recognition due to occlusion. It is necessary to consider how to use gesture recognition equipment to accurately track midair gestures. In remote classes, the interaction range is limited, and it is also required to consider the way of gesture recognition and how to configure the camera so that gestures can display a full range of presentation contents in a limited range. In addition, the interaction between teachers and students in the online classes has also become difficult, which will also affect the user's interactive experience
- (2) *Multiplicity of Interactive Content*. Blackboard writing and speech contain rich contextual information. Different from pure single user interaction, teachers are constantly interacting with students through

teaching content while interacting with AR space. It is necessary to consider equally individual user experience and demonstrating and imparting knowledge to others. This makes the task of gesture interaction more complex. How to improve user experience and teaching efficiency will be the key research content of the application of midair gesture interaction in teaching presentation

- (3) *High-Frequency Use of Gestures and Large Number of Meaningless Actions*. Most teachers have accumulated a considerable number of unconscious gestures in their long-term teaching work. These gestures vary from person to person and often only express the feelings of teachers when expressing knowledge, with little relevance with the knowledge itself. These gestures are likely to be recognized by the system as primitives with the ability to activate interactive tasks. Such feature of users like teacher imposes higher requirements for interaction design. Because the midair gesture belongs to the user interface that is always in the "on" state, the system needs to distinguish between user actions that drive interaction tasks and those that are only unconscious operations. It is necessary to prevent the situation in which users can do nothing about the equipment by making full use of the situational information in the teaching state

Midair gesture interaction has broad prospects in teaching. Especially because the epidemic control and prevention become normalized, more students have to take online classes. Compared with the traditional boring video online classes, AR allows teachers to interact with students while demonstrating through midair gestures. In addition, it realizes the demonstration of the surgical process by multiperson remote cooperation in the surgical training teaching. In some skills training, engineers can also demonstrate mechanical assembly through midair gestures. Through the

remote auxiliary function, learners get remote virtual guidance.

4. Challenges of Midair Gesture Interaction

4.1. Gesture Recognition. Midair gesture interaction depends on gesture recognition. For midair gestures, the mainstream recognition method is gesture recognition based on computer vision. Gesture recognition is a perceptual computing user interface, which enables the computer to capture and interpret gestures and execute commands according to the understanding of a gesture [27]. Gesture recognition usually includes the following steps: first, acquire the gesture frame, then, track the gesture, extract the features (finger state, thumb state, skin color, alignment, finger, and palm position) [27], and finally, classify to get the output gesture. As shown in Figure 5.

Gesture acquisition is to capture human gesture images by computer [28], which can be achieved with vision based recognition. Webcams or depth cameras can be used in the absence of needs for special equipment. In addition, special tools can also be used, such as motion sensing and input devices that capture hand gestures and motion (Microsoft Kinect, Leap motion, etc.) [29]. Researchers use a portable device, Leap Motion to achieve a full hand skeleton and perform object operations with higher accuracy [30]. In the study of gesture interaction only, researchers have explored a variety of methods to carry out the best gesture recognition for specific gestures. Lee et al. [31] designed gloves with conductive fabric on fingertips and palms for gesture recognition, using vibrating motors for tactile feedback and marks around the wrist for tracking gloves and also designed some gestures for selection, grasping, cutting, and copying. Lee and Hollerer created HandyAR, a system enabling freehand interaction with standard webcams. Its gestures supported are limited to the open/closed hand for object selection and hand rotation for object inspection [32]. Their subsequent work allowed the relocation of objects using unmarked tracking [33]. Fernandes and Fernandez used hand images to train statistical models to allow freehand detection [34]. And FingARtips [35] enabled users to knead and move virtual contents by detecting benchmarks on their fingertips. The 3D geometry of hand is retrieved for collision detection of hand virtual objects with the development of RGB-D and stereo camera [36, 37]. Although the air gesture interaction based on computer vision, which does not require additional equipment, is more natural, the accuracy of recognition is still limited by many factors. So most previous work mapped the specified gestures to limited operations, namely selection, translation, or rotation, without considering their easy and natural operation. In other words, gesture detection is only used as a substitute function of the mouse to operate 3D content, and the flexibility of the hand has not been brought into full play. Therefore, when performing gesture interaction, we need to consider the needs of specific interaction scenarios and tasks, so as to improve the user interaction experience.

Gesture recognition is still developing. Of course, there are difficulties and challenges, and more experiments are still needed for exploration and testing. For example:

- (1) *Accurate Dynamic Gesture Recognition.* Hand gesture and motion acquisition technology is still an important technology that restricts free gesture interaction. Especially for the recognition and acquisition of dynamic gestures, the accuracy of interactive gesture motion capture and recognition should be improved
- (2) *Gesture Detection Under Different Light, Color and Other Complex Backgrounds.* The gesture background is simple in most of the existing gesture detection processes, but the actual background in practical applications is more complex. We can work in any complex environment, such as a teacher's teaching scenario. Therefore, it will be an important topic in the future to study how to improve the accuracy of gesture recognition in complex background
- (3) *Delay in Gesture Recognition.* As gesture recognition requires a complex process, different technologies are required at different stages to complete it, and problems in any step will affect the whole gesture recognition process. Therefore, a perfect gesture recognition architecture is particularly important

4.2. User Experience. Researchers have been trying to improve user experience while carrying out technological innovation. However, there are still problems to be improved and solved.

- (1) *Gesture Learning.* Different gesture effects should be achieved in different task scenarios. Some gestures require users' additional learning and memorizing. Too many or too complex gestures will increase the burden of users' memory
- (2) *Transformation from Traditional Interaction Form to Midair Gesture Interaction.* It is a gradual process of the transition from traditional mouse and keyboard to midair gesture. Although it tends to be difficult for users to get rid of their previous usage habits, midair gesture interaction is not completely divorced from the original form of interaction. Designers need to find a balance between the two to improve user satisfaction
- (3) *Midair Gesture and Multimodal Interaction.* In multimodal interaction scenarios, each interaction mode has its own unique role. There is no agreement on which part of the interface functions are more suitable for gesture manipulation or the combination of gesture and speech, which is particularly important for improving the user experience
- (4) *Perception of Interactive Information.* The research of AR interaction focuses on how users interact with virtual objects. Therefore, the problems to be solved in gesture interface design are how users perceive such interaction, which information can be or cannot be interacted with, which information needs gesture interaction, and how to give users correct judgment



FIGURE 5: Basic process of gesture recognition.



FIGURE 6: Examples of the application of AR in medical and industrial training (Source: Microsoft official website).

- (5) *Definition of Free Midair Gesture.* Researchers of user experience are pursuing a common goal: to achieve free midair gesture interaction. However, a consensus is to be reached on what kind of gesture can be called free gesture interaction

5. Future of Midair Gesture Interaction

5.1. Prospect of Midair Gesture in Education, Health Care, Industry, and Other Professional Fields. The application field of midair gesture interaction is expanding. Depending on continuous breakthrough, AR interaction technology will produce more practice value regarding its application in education, health care, industry, office, and other scenarios. For example, in medical, surgeons use make gestures in front of the camera using computer vision technology to achieve operations such as zooming, rotating, image clipping, and switching slides, which avoids repeated disinfection when doctors use other equipment. In addition, the application also covers surgical training, psychotherapy, etc. The reform of medical education will occur with immersive learning tools built for medical students and nursing professionals. Various 2D and 3D data (such as X-ray, ultrasound, and human structure) are displayed in AR to help surgeons practice the surgical process. Gesture recognition could also create a better life for some disabled patients. Some researchers are also exploring how to transform the sign language of deaf mutes into written language by gesture recognition, for communicating with others in an environment combining virtuality and reality.

In addition, the way of education has also experienced great changes under the influence of normalized COVID-19 control and prevention. And distance teaching is also a great challenge for teachers. In addition to AR experiments, the directions of future exploration are drawing demonstrations, teaching demonstrations in STEM education, and Gamification course content presentations. At present, the exploration of midair gestures in education is still in the development stage. Also, there are many pain points of interactive experience: poor user experience of the technology and lack of real feedback and emotional interaction, resulting

in unsatisfactory educational results. Therefore, an important aspect of realizing natural gesture interaction will be designing a more natural way of gesture interaction, so that the boring and profound knowledge can be conveyed to students in a more vivid form without affecting the teacher's experience or causing fatigue. As shown in Figure 6.

5.2. Cooperative Gestures to Improve Work Efficiency. In many jobs, communication, cooperation, and sharing between people are essential. A more immersive interactive experience will be brought by multiple users operating virtual content through gestures and working together to share virtual space. Most of the current application research of midair gesture only tracks a single framework and supports the experience of a single user. The interactive effect of collaborative presentation can be enriched with the merging of multiple users. For example, Saquib et al. [24] thought that the sense of experience and interest of interaction with the audience can be enhanced, and more diverse cooperative actions can be created, if they can track multiple skeletons and realize the performance of multiperson cooperation.

Remote collaboration and remote communication are the future ways to improve work efficiency; no matter it is in study, office, or industrial production. Especially in the face of normalized COVID-19 control and prevention, AR makes remote work more efficient and convenient. In the workspace of remote collaboration, collaborative interaction has become an essential part. Also, collaborative gestures will play a greater role to help improve work efficiency. AR is shifting towards a social model, and collaborative gestures are also worth exploring in the future.

The metaverse world will also be a world of interoperability and social integration. The future metaverse space will cover a variety of devices, and gesture interaction will be an important part to improve the sense of interactive experience in such virtual experience layer based on physical space. Currently, speech communication still dominates in the metaverse space, and it is difficult to realize the simulation of sensory and body language. Besides, it does not have the sense of social space and cannot provide a fully immersive

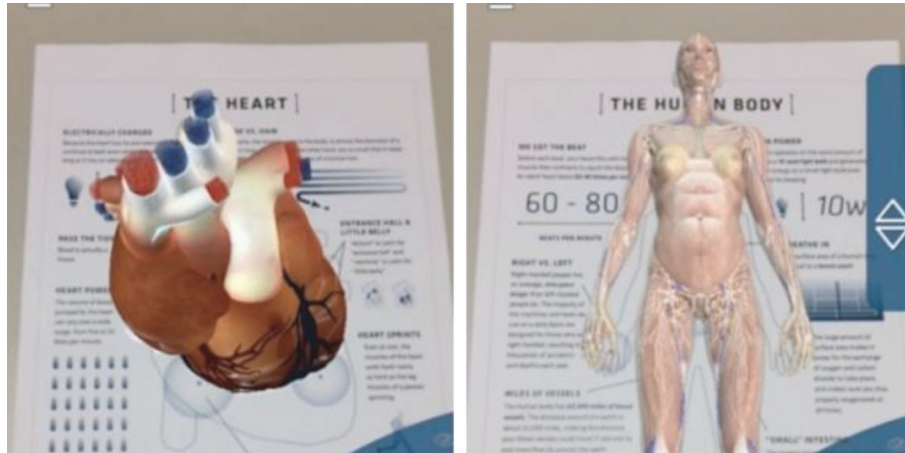


FIGURE 7: Application of traditional mobile AR in medical teaching.



FIGURE 8: Photo wake up: 3D character animation from a single photo (Weng et al.).

experience. But, all this will be the direction of future efforts. Metaverse space is making natural and immersive AR interaction experience a reality with the continuous innovation of technology.

5.3. Low-Threshold and Low-Cost User Experience. The experience of augmented reality nowadays still depends on high-cost hardware devices, such as AR glasses, which often discourages many users and also limits the diversified development of gesture interaction. Therefore, more low-threshold and low-cost entrances (e.g. smart phones) should be opened up to the world integrating virtuality and reality. According to the third report of the long-term survey of «AR Usage and Consumer Attitudes Report of ARtillery» in 2020, it is expected that the penetration rate of mobile AR users will almost coincide with that of Internet users by 2023, which means that all Internet users may be mobile AR users. With smart phones as the entrance, gestures are undoubtedly the fastest way of interaction. Mobile phone users can achieve very interesting results by painting and placing mobile AR objects with midair gestures anytime and anywhere. Especially in the field of teaching, the previous mobile AR is more about the enhancement of visual effects, and the transformation of 2D plane effects into 3D stereo vision [38] (Figure 7). If one can also interact with it with midair gestures, a more immersive experience will be

produced, with the advantages of saving time and cost. Figure 8 shows the design and implementation case of AR midair gestures interaction of art works in art exhibition by Weng et al. [39].

At present, mobile AR is facing many problems. In mobile AR, users have to raise their arms for a long time, with one hand for gesture interaction. In consequence, inaccurate AR positioning and gesture recognition will occur, resulting in poor AR experience and shortened user experience time. Therefore, it is necessary to consider enhancing user utilization by both enhancing the user experience and improving technology. It is believed that accurate midair gesture interaction with virtual objects can be realized on mobile phones with the development of technology.

6. Summary and Discussion

With a focus the midair gesture interaction in AR, the literature and main results in the field of midair gesture interaction were systemically studied by the literature research method. From the perspective of user experience, the gesture types in midair gesture interaction and the typical applications of midair gesture in AR as well as the challenges and future of midair gesture interaction were analyzed. The aim is to give reference and interactive experience design suggestions to designers in gesture interaction research.

Midair gesture interaction is a more natural and flexible interaction method, and will be an important interaction method in AR. In terms of the application of midair gestures, a detailed analysis was carried out on the application and potential research value of midair gestures in the field of education. In the field of education, air gesture interaction for teaching has important research value because of the particularity of experience environment, user type, and interaction purpose. The user experience of gesture interaction needs to be considered from the educational attribute, functional attribute, and interactive attribute. In addition, the combination of gestures and multisense and multichannel can also meet the user needs for immersive experience.

There are still challenges in gesture recognition technology and user experience. The earliest gesture classification comes from communication, while the classification of midair gestures in AR will be detailed to specific task types and lay more emphasis on user experience. In most of the existing research results, the evaluation of gestures is implemented in the laboratory environment. Because of the diversity of gestures and the universality of task types, it is difficult to form a general gesture set, which requires researchers to design corresponding gesture types for different task needs and carry out multiple experiments in real scenes, rather than just laboratory research. For a wider application, more field evaluations are needed to understand what gestures are effective for what tasks, so as to provide a better user experience. Midair gesture interaction is a free input method, but for the user experience, it is not only necessary to consider the freedom of the hand, but also to consider the overall comfort from the perspective of ergonomics. At present, most gesture output devices in AR are still head mounted displays, which are not suitable for long-term wearing. Therefore, the hardware design also needs to be fully evaluated. In addition, from the application cases of midair gestures, we can see that the use types of gestures are not complex, such as rotation, translation, and switching, which are related to two factors; one is limited by gesture recognition technology. Gesture recognition is a complex process. To achieve accurate gesture recognition, a perfect technical framework is required. Therefore, midair gestures are not suitable for overly accurate interactive tasks; on the other hand, simple gestures can reduce the burden of users' learning and memory, which is more suitable for user experience. It can be said that it is a trend of interaction that simple gestures control diverse content.

In a word, designers need to consider all aspects of technology, experience, and innovative applications to enhance user stickiness and personalized experience. With the continuous development of AI, hybrid reality and gesture recognition technology, midair gesture interaction will be more natural and comfortable, and its application field will be more extensive.

Data Availability

The datasets used and/or analyzed during the current study are available from the corresponding author on reasonable request.

Conflicts of Interest

The authors declared no potential conflicts of interest with respect to the research, authorship, and/or publication of this article.

References

- [1] R. Azuma, "A survey of augmented reality," *Presence: teleoperators & virtual environments*, vol. 6, no. 4, pp. 355–385, 1997.
- [2] Y. Wu, X. Zhang, and P. W. Fu, *Human Computer Interaction Technology and Application*, China Machine Press, 2020.
- [3] T. Vuletic, A. Duffy, L. Hay, C. McTeague, G. Campbell, and M. Grealy, "Systematic literature review of hand gestures used in human computer interaction interfaces," *International Journal of Human-Computer Studies*, vol. 129, pp. 74–94, 2019.
- [4] Z. Wei, L. Zeyi, C. Jian, K. Mingyu, D. Xiaoming, and W. Hong'an, "Overview of dynamic gesture understanding and interaction," *Journal of software*, vol. 32, no. 10, pp. 3051–3067, 2021.
- [5] C. Groenewald, C. Anslow, J. Islam, C. Rooney, P. J. Passmore, and B. L. Wong, "Understanding 3D mid-air hand gestures with interactive surfaces and displays: a systematic literature review," in *Proceedings of the 30th International BCS Human Computer Interaction Conference (HCI)*, Poole, United Kingdom, 2016.
- [6] A. Kendon, "How gestures can become like words," in *This Paper Is a Revision of a Paper Presented to the American Anthropological Association, Chicago, Dec 1983*, Hogrefe & Huber Publishers, 1988.
- [7] C. Cadoz, *Les Réalités Virtuelles*, Flammarion, Paris, 1994.
- [8] D. McNeill, *Hand and Mind: What Gestures Reveal about Thought*, The University of Chicago Press, Chicago, London, 1995.
- [9] M. Karam and M. C. Schraefel, *A taxonomy of gestures in human computer interactions. Technical report ECSTR-IAM05-009, electronics and computer science*, University of Southampton, 2005.
- [10] R. Aigner, D. Wigdor, H. Benko et al., "Understanding mid-air hand gestures: a study of human preferences in usage of gesture types for hci," vol. 2, Microsoft Research Tech Report MSR-TR-2012-111, 2012.
- [11] T. Wang, X. Qian, F. He, X. Hu, Y. Cao, and K. Ramani, "GesturAR: an authoring system for creating freehand interactive augmented reality applications," in *The 34th Annual ACM Symposium on User Interface Software and Technology*, pp. 552–567, Virtual Event, USA, 2021.
- [12] M. Moran-Ledesma, O. Schneider, and M. Hancock, "User-defined gestures with physical props in virtual reality," *Proceedings of the ACM on Human-Computer Interaction*, vol. 5, no. ISS, pp. 1–23, 2021.
- [13] N. Samimi, S. von der Au, F. Weidner, and W. Broll, "AR in TV: design and evaluation of mid-air gestures for moderators to control augmented reality applications in TV," in *20th International Conference on Mobile and Ubiquitous Multimedia*, pp. 137–147, Leuven, Belgium, 2021.
- [14] J. O. Wobbrock, M. R. Morris, and A. D. Wilson, "User-defined gestures for surface computing," in *Proceedings of the 27th international conference on Human factors in computing*

- systems - *CHI 09. Volume 8*, p. 1083, New York, New York, USA, 2009.
- [15] M. Lee, "Multimodal speech-gesture interaction with 3D objects in augmented reality environments (2010)," in *Department of Computer Science and Software Engineering*, University of Canterbury, Christchurch, 2010.
- [16] T. Piumsomboon, A. Clark, M. Billingham, and A. Cockburn, "User-defined gestures for augmented reality," in *IFIP Conference on Human-Computer Interaction*, pp. 282–299, Springer, Berlin, Heidelberg, 2013.
- [17] G. A. Rovelo Ruiz, D. Vanacken, K. Luyten, F. Abad, and E. Camahort, "Multi-viewer gesture-based interaction for omni-directional video," in *Proceedings of the SIGCHI Conference on Human Factors in Computing Systems*, pp. 4077–4086, Toronto, ON, Canada, May 2014.
- [18] S. Siddhpuria, K. Katsuragawa, J. R. Wallace, and E. Lank, "Exploring at-your-side gestural interaction for ubiquitous environments," in *Proceedings of the 2017 Conference on Designing Interactive Systems*, pp. 1111–1122, Edinburgh, UK, June 2017.
- [19] I. A. Zaiți, Ş. G. Pentiuc, and R. D. Vatavu, "On free-hand TV control: experimental results on user-elicited gestures with leap motion," *Personal and Ubiquitous Computing*, vol. 19, no. 5-6, pp. 821–838, 2015.
- [20] N. K. Dim, C. Silpasuwanchai, S. Sarcar, and X. Ren, "Designing mid-air TV gestures for blind people using user- and choice-based elicitation approaches," in *Proceedings of the 2016 ACM Conference on Designing Interactive Systems*, pp. 204–214, Brisbane, Australia, June 2016.
- [21] H. Rateau, L. Grisoni, and B. De Araujo, "Mimetic interaction ipaces: controlling distant displays in pervasive environments," in *Proceedings of the 19th International Conference on Intelligent User Interfaces*, pp. 89–94, Haifa, Israel, February 2014.
- [22] K. Perlin, Z. He, and F. Zhu, "Chalktalk VR/AR," *Artificial Intelligence Meets Virtual And Augmented Worlds*, 2010, No 2017/2 (2017): Proceedings of the 10th International Workshop on Semantic Ambient Media Experiences (SAME 2017): Artificial Intelligence MEETS Virtual and Augmented Worlds (AIVR) - in conjunction with SIGGRAPH Asia.
- [23] J. H. Lee, D. Ma, H. Cho, and S. H. Bae, "Post-post-it: a spatial ideation system in VR for overcoming limitations of physical post-it notes," in *2021 CHI Conference on Human Factors in Computing Systems*, pp. 1–7, Yokohama, Japan, 2021.
- [24] N. Saquib, R. H. Kazi, L. Y. Wei, and W. Li, "Interactive body-driven graphics for augmented video performance," in *Proceedings of the 2019 CHI Conference on Human Factors in Computing Systems*, pp. 1–12, Glasgow, Scotland UK, 2019.
- [25] J. Gong, T. Han, S. Guo et al., "Holo board: a large-format immersive teaching board based on pseudo holo graphics," in *The 34th Annual ACM Symposium on User Interface Software and Technology*, pp. 441–456, Virtual Event, USA, 2021.
- [26] L. Geping and N. Gao, "The influence mechanism of gesture interactive virtual experiment on learning experience," *Research on Modern Distance Education*, vol. 33, no. 2, pp. 22–32, 2021.
- [27] P. Meenakshi and S. M. Pawan, "Hand gesture recognition for human computer interaction," in *2011 International Conference on Image Information Processing*, pp. 1–7, Shimla, India, 2011.
- [28] C. Ananya, T. Anjan Kumar, and K. S. Kandarpa, *A Review on Vision-Based Hand Gesture Recognition and Applications*, vol. 11, IGI Global, 2015.
- [29] M. Yasen and S. Jusoh, "A systematic review on hand gesture recognition techniques, challenges and applications," *Peer J Computer Science*, vol. 5, article e218, 2019.
- [30] N. S. Safiee and A. W. Ismail, "AR home deco: virtual object manipulation technique using hand gesture in augmented reality," *Innovations in Computing Technology and Applications*, vol. 3, 2018.
- [31] J. Y. Lee, G. W. Rhee, and D. W. Seo, "Hand gesture-based tangible interactions for manipulating virtual objects in a mixed reality environment," *International Journal of Advanced Manufacturing Technology*, vol. 51, no. 9-12, pp. 1069–1082, 2010.
- [32] T. Lee and T. Hollerer, "Handy AR: markerless inspection of augmented reality objects using fingertip tracking," in *11th IEEE International Symposium on Wearable Computers, ISWC 2007*, pp. 83–90, Boston, MA, USA, October 2007.
- [33] T. Lee and T. Hollerer, "Multithreaded hybrid feature tracking for markerless augmented reality," *IEEE Transactions on Visualization and Computer Graphics*, vol. 15, no. 3, pp. 355–368, 2009.
- [34] B. Fernandes and J. Fernandez, "Bare hand interaction in tabletop augmented reality," in *SIGGRAPH 2009: Posters*, Association for Computing Machinery, 2009.
- [35] V. Buchmann, S. Violich, M. Billingham, and A. Cockburn, "Fing ARTips: gesture based direct manipulation in augmented reality," in *Proceedings of the 2nd international conference on Computer graphics and interactive techniques in Australasia and South East Asia*, pp. 212–221, Singapore, 2004.
- [36] H. Benko, R. Jota, and A. Wilson, "Miratable: freehand interaction on a projected augmented reality tabletop," in *Proceedings of the SIGCHI conference on human factors in computing systems*, pp. 199–208, Austin Texas, USA, 2012.
- [37] O. Hilliges, D. Kim, S. Izadi, M. Weiss, and A. Wilson, "Holo desk: direct 3d interactions with a situated see-through display," in *Proceedings of the SIGCHI Conference on Human Factors in Computing Systems*, Austin Texas, USA, 2012.
- [38] M. C. Hsieh and J. J. Lee, "Preliminary study of VR and AR applications in medical and healthcare education," *Journal of Nursing and Health Studies*, vol. 3, no. 1, p. 1, 2018.
- [39] C. Y. Weng, B. Curless, and I. Kemelmacher-Shlizerman, "Photo wake-up: 3d character animation from a single photo," in *Proceedings of the IEEE/CVF Conference on Computer Vision and Pattern Recognition*, pp. 5908–5917, Long Beach, CA, USA, 2019.

Retraction

Retracted: Difficulties and Countermeasures of Game Localization Translation Based on the IoT and Big Data

Journal of Sensors

Received 23 January 2024; Accepted 23 January 2024; Published 24 January 2024

Copyright © 2024 Journal of Sensors. This is an open access article distributed under the Creative Commons Attribution License, which permits unrestricted use, distribution, and reproduction in any medium, provided the original work is properly cited.

This article has been retracted by Hindawi following an investigation undertaken by the publisher [1]. This investigation has uncovered evidence of one or more of the following indicators of systematic manipulation of the publication process:

- (1) Discrepancies in scope
- (2) Discrepancies in the description of the research reported
- (3) Discrepancies between the availability of data and the research described
- (4) Inappropriate citations
- (5) Incoherent, meaningless and/or irrelevant content included in the article
- (6) Manipulated or compromised peer review

The presence of these indicators undermines our confidence in the integrity of the article's content and we cannot, therefore, vouch for its reliability. Please note that this notice is intended solely to alert readers that the content of this article is unreliable. We have not investigated whether authors were aware of or involved in the systematic manipulation of the publication process.

In addition, our investigation has also shown that one or more of the following human-subject reporting requirements has not been met in this article: ethical approval by an Institutional Review Board (IRB) committee or equivalent, patient/participant consent to participate, and/or agreement to publish patient/participant details (where relevant).

Wiley and Hindawi regrets that the usual quality checks did not identify these issues before publication and have since put additional measures in place to safeguard research integrity.

We wish to credit our own Research Integrity and Research Publishing teams and anonymous and named external researchers and research integrity experts for contributing to this investigation.

The corresponding author, as the representative of all authors, has been given the opportunity to register their agreement or disagreement to this retraction. We have kept a record of any response received.

References

- [1] Q. Sun, "Difficulties and Countermeasures of Game Localization Translation Based on the IoT and Big Data," *Journal of Sensors*, vol. 2022, Article ID 4651956, 7 pages, 2022.

Research Article

Difficulties and Countermeasures of Game Localization Translation Based on the IoT and Big Data

Qiaoke Sun 

Graduate School, Xi'an International Studies University, Xi'an 710128, China

Correspondence should be addressed to Qiaoke Sun; sunqiaoke188@outlook.com

Received 19 August 2022; Revised 8 September 2022; Accepted 15 September 2022; Published 4 October 2022

Academic Editor: Sweta Bhattacharya

Copyright © 2022 Qiaoke Sun. This is an open access article distributed under the Creative Commons Attribution License, which permits unrestricted use, distribution, and reproduction in any medium, provided the original work is properly cited.

With the development of international social facilitation brought about by the technological progress of various social media, games are spread internationally as a key application for entertainment and social interaction. At present, my country has introduced more than tens of thousands of games from abroad. There are cultural differences and grammatical differences between different countries. The introduced game dubbing and NPC subtitles are not completely the same as the meaning of the country of origin of the game. The result of the incomprehensible words usually makes the game player unable to understand part of the game in the game, while affecting the game experience; it also hinders international cultural exchanges and curbs the strategic expansion of game companies. Big data technology is an inevitable product of the rapid development of data science. It uses various data collection, data storage, and data analysis tools to provide data-based decision support for users in need. The data plane provides tool support for translation. IoT technology relies on various sensors and microdevices to collect status information of different things. IoT devices all have a central server. Currently, game companies translate overseas games through teamwork. Using IoT devices, teams can translate status and progress information, stored in the server to support the progress control of game localization translation. This paper firstly conducts a survey on the questionnaires issued by the translation team leaders of multinational game companies, conducts statistical processing on the collected data, analyzes and summarizes the difficulties existing in the current game localization translation, and finally designs a corresponding game based on big data and Internet of Things technology. In localization translation strategy, through follow-up investigations on companies that have adopted the strategy, it is found that the dilemma of game localization translation has been solved.

1. Introduction

Electronic technology originated in 1998, and the concept of e-sports was first proposed in 2003. In 2009, the video game League of Legends was officially launched. Under normal circumstances, the glory period of online games is three to five years. As a MOBA game that has been in operation for ten years, "League of Legends" not only continues to grow in popularity, quickly breaks the rules, and attracts a large number of game users and fans, but also with the continuous improvement of operating capabilities, the game continues to evolve and develop through international competition, middle and lower three complete, and closed industrial chains [1].

How to quickly enter the local market is one of the problems that various industries need to overcome to develop economic interests and develop international markets. This article takes the hero lines in League of Legends as an example to discuss the problems and strategies of localization translation in the game industry, in order to provide a reference for the future localization translation of the game industry and the development of the international market of domestic games. Loanwords have become a very common phenomenon in commercial games. Not only business games, foreign words can be seen everywhere in daily life. This is because globalization is going on, and our country has close exchanges with other countries in the world, which will inevitably lead to exchanges and conflicts. Games from

other countries are produced in such an environment and are gradually used by everyone. League of Legends, a 20-30-minute MOBA (team strategy game) game, has not only successfully gained a large number of users and fans during its 10-year operation but also targeted the market and made a lot of money [2–4]. It has also developed an infinitely possible industrial chain, exuding greater market potential. Localization plays an important role in developing domestic market and adjusting operation strategy. Through the research on the translation strategy of League of Legends, we can sort out several factors that affect the e-sports industry represented by the translation strategy of League of Legends. Studying the application of the localization translation strategy of League of Legends from the perspective of economics can reveal the benefits of language transfer in terms of product benefits and provide new research ideas and directions for economic development.

2. Theories Related to Game Localization Translation

2.1. Four Value Criteria. Information value is the most basic criterion. If the translator does not understand the content of the game, first, translate it literally according to the English title, and the translated title will deviate from the original content. This is the most serious error in the localization translation of the game. In order to better convey the content of the game, the translated title needs to faithfully convey the information related to the original game content, so as to realize the unified title form of the translation and the original game content. For cultural value, the translation of game titles is not only a conversion between two languages but also an exchange between two cultures. This is one of the most important tasks of the game title. The translation reflects cultural values and promotes cultural exchange. For cultural background [5, 6], the source language is different from the target language, so the translator should fully understand and accurately convey the cultural information and emotion carried by the original title. For aesthetic value, the translation of the game emphasizes getting rid of the shackles of the original words, grasping the ideological and aesthetic content of the work, and carrying out new artistic creations. To realize the aesthetic value, we must first pay attention to the refining of words. William Somerset Maugham said: “Speech has power, sound and shape; only by taking these into account can we write striking sentences.” Therefore, when choosing words, we must strive to have both sound and beauty. For significance, compare the Chinese translations of the following three groups of English titles: it is not difficult to find that the second translation method can give full play to its Chinese characteristics and conform to the theme and artistic conception of the original work. For commercial value, game is an art that combines culture and business. Commercial considerations should be taken into account when translating titles. To achieve commercial value, translators are required to fully grasp cultural characteristics and aesthetic tastes and create titles that audiences like to see and like.

2.2. Three Methods. Transliteration is a method of translation that uses one language to read and write the pronunciation of words or phrases in another language. It is rarely used for game translation, but it is indispensable. The names of people and places referred to in the title of the game, if any, should be transliterated to be familiar to the audience or of significant historical and cultural significance. This transliteration preserves the rhythm of the original title, attracting exotic audiences with rich content. Literal translation is to preserve the content and form of the original title as much as possible according to the characteristics of the source language and the target language [7]. This is the easiest and most efficient method when the source and target languages perform the same function. In free translation, due to cultural differences between China and foreign countries, overemphasis on form will lead to lack of connotation. In order to let game consumers thoroughly understand the deep meaning of the equivalence of the original title and to achieve the equivalence of the original title and the target title, free translation must be used in terms of information and aesthetics.

2.2.1. Investigation and Analysis of Factors Affecting Game Localization Translation. In order to investigate the current situation of game localization translation, the author distributed corresponding online questionnaires to different game companies and game consumers and collected 2,000 valid questionnaires. Through analysis of the questionnaires, it was found that there are four main factors affecting game localization translation and direction.

2.2.2. Linguistic Factors. Linguistic factors have a direct and critical impact on the translation process. Linguistic factors include phonetic factors, lexical factors, and sentence pattern factors.

English is a language of intonation, and there are many kinds of rhymes in English poetry: alliteration, interline rhyme, line ending rhyme, etc. There are many ways to rhyme. There are vowel-consonant rhyme and full rhyme and half rhyme (depending on the number of syllables that rhyme). Chinese is a tonal language. Chinese ancient poetry can be flat or oblique. Also, distinguish between ascending rhyme, descending rhyme, and advancing rhyme [8, 9].

Generally speaking, different tones are not allowed to rhyme. Since many of the characters in the game have gods or legends in their backstories, it is inevitable that certain lines from the Bible will be translated, taking into account linguistic elements in different languages, as follows:

- (1) “An eye for an eye”—The Righteous (Kyle)

Machine translation: one eye for the other. National costume translation: an eye for an eye, a tooth for a tooth! This sentence comes from the Bible—Exodus: Old Testament, and also in Matthew’s gospel: an eye for an eye, a leg for a leg. In order to avoid excessive retribution, the role of Judge Angel Kyle in the background story is God’s judge; she believes that as God’s judge, good and evil should be her principle, and this idiom evolved into an inseparable

Chinese idiom that often goes together appear. This is an eye for an eye, an eye for an eye, not simply an eye for an eye, and it satisfies the rhyme requirement of a heavier pronunciation of the whole sentence; each half seems to emphasize the other, more like a decree or a sentence. Godly majesty. Two sentences, or two parts of a sentence, which appear to each say two things, actually respond to each other, expound on each other, complement each other, and say one thing. Express the meaning of a complete sentence in a staggered, penetrating, complementary manner. This figure of speech is called intertextuality in Chinese.

- (2) “Ashes return to ashes, and earth returns to earth”—Evelyn Outside the Window

MT: ash for ashes, dirt for dirt. Translation of national clothes: dust, dust returns to earth.

Evelyn’s quote from Genesis 3.19 is ashes to ashes and ashes to ashes. In the sure and sure hope of resurrection to eternal life. You are you and you will go back to where you came from [10]. In the game, in order to realize the simplicity of the characters’ lines in the characters and at the same time to reflect Evelyn, a woman who is tough and does not speak much because of her background as an assassin, the Chinese Bible version is directly used here, ashes to ashes, ashes to ashes, original translation: the dust returns to the dust, the earth returns to the earth. The reference materials for the game localization process are shown in Table 1.

2.2.3. Environmental Factors. Language and culture are inseparable, and social and cultural background knowledge determines the deep semantics of language. Cultural context refers to the cultural, historical, and social context of the source and target languages. Due to different historical development processes, different geographical locations, and different social development stages in the same period, different national and cultural backgrounds lead to different perceptions of people’s perceptions of things. Therefore, with their values, customs, traditions, literature, and religious beliefs, words with different cultural meanings were produced. The translation of words and sentences depends on its own language and cultural environment, including geographical environment, customs, social history, literary allusions, religious beliefs, and many other factors. Translation skills can hardly compensate for cultural complexity [11, 12]. Therefore, it is necessary to have a comprehensive and thorough understanding of the source language and target language culture. The questionnaire data of vocabulary translation and cultural fit are shown in Table 2.

2.2.4. Globalization. Reconstructing translation-triggered contexts from a local perspective can stimulate the potential of the target culture to foreign knowledge systems. The localization of translation comparison and optimization strategy is to express the meaning of other languages as much as possible, without giving up the mother tongue when expressing power, and only the correct translation can reflect the potential of the mother tongue [13]. In order to avoid the spread of mixed culture, the localization translation strategy should

TABLE 1: Reference materials for the game localization process.

Game type	Material reference
League of Legends	0.26
PUBG	0.38
CrossFire	0.36

take the cultural value orientation as a reference, rewrite the source language text through cultural participation, and reduce the disgusting cultural phenomenon in the source language text. In the right circumstances, such subtle cultural changes can facilitate localized reconstruction and facilitate global and local interactions, primarily through negotiation and reconciliation of cultural differences and by deescalating cultural tensions, through their own national globalization, making its own contribution. The use of new technologies in translation is shown in Table 3.

2.2.5. Personal Factors. The complexity of translation and the particularity of the translator determine the uncertainty of the translation process. At the same time, the translation team is also very important. The current translation team collaboration rate is shown in Table 4.

A translator is a real, emotional, productive, and creative being. Therefore, an individual’s knowledge reserve, translation strategy selection, and understanding of source and target languages are translated into a variety of individual translation styles. The translation strategies in League of Legends’ character lines are applied. The accuracy of vocabulary translation is shown in Table 5.

3. Problems Existing in Game Localization Translation

3.1. The Problem of Vocabulary Translation. Vocabulary is the basic unit of game language and contains rich cultural connotations. In game localization translation, the use of game vocabulary must pay attention to the context. Without paying attention to the context, the translation or substitution of words will make it difficult for the public to understand.

In the process of game localization translation, there will be some obscure words. The translation is long, rigid, and difficult to understand. Not all game consumers can understand it, which is obviously contrary to the original intention of game localization translation and is not conducive to causing game consumer interest.

The translation of game localization often lacks a beautiful feeling, and the accuracy of the original expression is lacking. The imprint of translation is relatively heavy, and it is very common to mechanically directly quote the original language in game localization translation, which makes the expression of the translation a bit too far-fetched and lacks the feeling of beauty. There is a huge commercial interest in game translation [14–16]. Therefore, the translation of the game should be elegant and gorgeous, and the accuracy of the original expression should be the same, which will

TABLE 2: Vocabulary translation and cultural fit.

Game type	Vocabulary translation and cultural fit
League of Legends	0.28
PUBG	0.35
CrossFire	0.37

TABLE 3: Use of new technologies in translation.

Game type	New technology in translation
League of Legends	Simultaneous interpretation equipment
PUBG	Human translation
CrossFire	Google Translate

TABLE 4: Team translation collaboration efficiency.

Team	Translation collaboration efficiency
A	0.29
B	0.48
C	0.23

TABLE 5: Vocabulary translation accuracy.

Game type	Translation accuracy
League of Legends	0.31
PUBG	0.33
CrossFire	0.36

enhance the communication effect of the game. The translation of the game translation is equally good and bad.

3.2. The Problem of Cultural Differences. In the sequence of historical development, culture first appeared, and then, language emerged. Because different countries have different cultures, this requires translators to have strong cultural communication skills. Translators should be aware of the cultural differences between their own country and other countries to avoid disagreements and misunderstandings. In the process of localization of translation games, because both countries have a long history, the two countries have regions with customs and historical allusions [17].

Different historical backgrounds have led to some incomprehensible expressions in the translation process of the two game languages. This is especially true of customs, which affect and restrict the accuracy of game localization translation.

3.3. There Is No Reference Material. Since the translation of traditional games does not have high value, the current game localization translations are often new types of game translations, and the understanding and translation of new things often have higher requirements for translators.

Moreover, even if the translator has high professional quality, the translation accuracy rate is not high, because the translation is an innovative operation, and it may be pos-

sible to translate without reference documents or guidance programs [18].

There will be many translation errors, and the novelty of the game industry itself also determines the particularity of its translation. The current multinational game companies also lack corresponding technological tools to achieve localized game translation. Solve the problem of no reference material.

3.4. Inefficient Teamwork. Translating large-scale games often requires the cooperation of multiple roles to complete the task. Game translation involves subtitles, roles, dubbing, code comment processing, and other content. Only with the cooperation of multiple directions can the complete translation of the game be completed.

Some multinational game companies arrange teams to process game translation in sequence, and some multinational game companies start the entire translation team at the same time for translation. However, there are various team problems in the current translation, such as the mismatch between characters and dubbing translations and some game characters. The background is cute, but the feeling of dubbing and translation is other types. Excessive contrast between these will affect the game consumers' sense of game experience, reduce the translation progress of the translation team, and lengthen the time for the game to go online. Usually, games have a heat period, and if the heat ends during the translation period, it will be a big loss for multinational game companies.

4. Countermeasures for Game Localization Translation Based on Big Data and Internet of Things Technology

4.1. Game Localization Vocabulary Translation Strategy Based on Big Data Technology. The purpose of game localization is to attract the attention of consumers. The use of easy-to-understand language in the translation of game localization can help consumers understand the products promoted by the game, shorten the distance between consumers and game owners, and arouse consumers and products. Empathy in turn helps to increase product sales and increase the revenue of game developers. The data collection-related tools in big data technology can collect the dictionary of the country of origin of the game and at the same time crawl the latest usage data of the vocabulary in the game localization translation in social media and understand the vocabulary in the game localization translation after comprehensive analysis. Different meanings represented in different scenarios. Combined with its dictionary and network meaning, a comprehensive analysis of the meaning of the vocabulary will more accurately describe the vocabulary of the NPC in the game, allowing game consumers to experience the best game experience. In response to the translation problem caused by cultural differences, game companies can recruit big data technology professionals and have a good understanding of the country of origin of the game. The big data formula algorithms involved in

this questionnaire are shown in (1a)–(1d).

$$\text{Translate} = \frac{\sum (T_i - \bar{X})(Y_i - \bar{Y})}{\sqrt{\sum (\text{BigData}_i - \text{IOT})^2 \sum (\text{BIGDATA}_i - \bar{Y})^2}}, \quad (1a)$$

$$\text{var} \left(\sum_{i=1}^n \text{Translate}_i \right) = \sum_{i=1}^n \text{var}(V_i) + 2 \sum_{i,j:i < j} \text{cov}(\text{BigData}_i, \text{IOT}_j), \quad (1b)$$

$$\mathfrak{R}(\text{Trans}) = \frac{E(t_i = t_i, \text{Game} = \text{staff}_j)r}{E(Q = q_j)j}, \quad (1c)$$

$$\text{Game Trans} = \sum (E_i - \bar{y})^2 = \hat{\beta}^T \mathbf{X}^T \mathbf{y} - \frac{1}{n} (E^T \mathbf{u} \mathbf{u}^T \mathbf{y}). \quad (1d)$$

Among them, T , X , and Y represent different types of games; var represents functional variables; cov represents variance; E represents expectation; Game Trans represents the result of localized translation of the game; and u and y involved represent the translation of the game, respectively, engagement and team participation rates.

The historical development and cultural development are analyzed, and the relationship between the localization translation of the game and the historical culture is obtained, so that the cultural data of the country of origin of the game and the cultural data of the local country can be accurately translated. Through interviews with the heads of related companies in multinational game cooperation, it is found that the accuracy of the vocabulary and cultural matching of game localization translation has been greatly improved after combining with big data technology. The specific situation is shown in Figure 1.

The purpose of the game is to attract the attention of consumers, make them interested in the product, and successfully make consumers buy the product. Therefore, for example, in the translation process of Russian game language, we must pay attention to the simplicity of the language. If you use words that are too difficult to understand, consumers will lose interest in the game, resulting in consumers not buying this product, so that the income of the game owner will not increase. Therefore, the translation of game localization cannot use words that are too difficult to understand and must pay attention to the simplicity of vocabulary. This is mainly manifested in the method of using abbreviated words and easy-to-understand words.

Big data technology can traverse the dictionaries of both the country of origin of the game and the country of demand for game localization, analyze the best translation method for each sentence, realize the simplest translation of vocabulary, use abbreviated and short vocabulary, and finally improve the game.

Through interviews with the heads of related enterprises in multinational game cooperation, it is found that the combination of big data technology can greatly improve the suc-

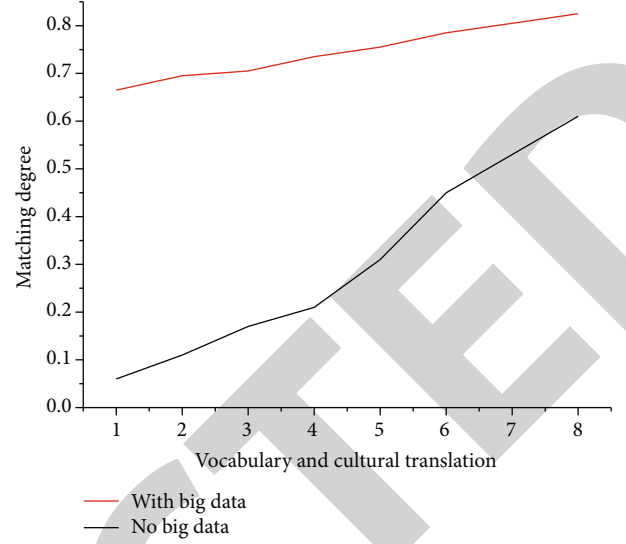


FIGURE 1: Changes in the matching degree of vocabulary and cultural translation.

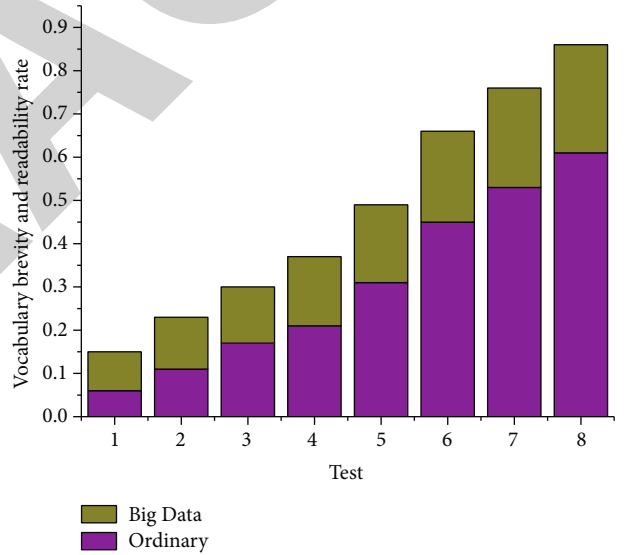


FIGURE 2: Vocabulary brevity and readability changes.

cinctness and readability of their game localization translation vocabulary. The specific situation is shown in Figure 2.

4.2. Strategy for Collecting Reference Materials for Game Localization Translation Based on Big Data Technology. In view of the fact that there are few translation reference materials in the current game localization translation process, big data technology can collect a large amount of game type data, store the data before and after the localization translation in the database, and then use the answer data.

The two databases are compared and analyzed, and the rules before and after localization translation are found, and the rules are spelled together, and the fragmented translation skill materials are provided to translators who do not

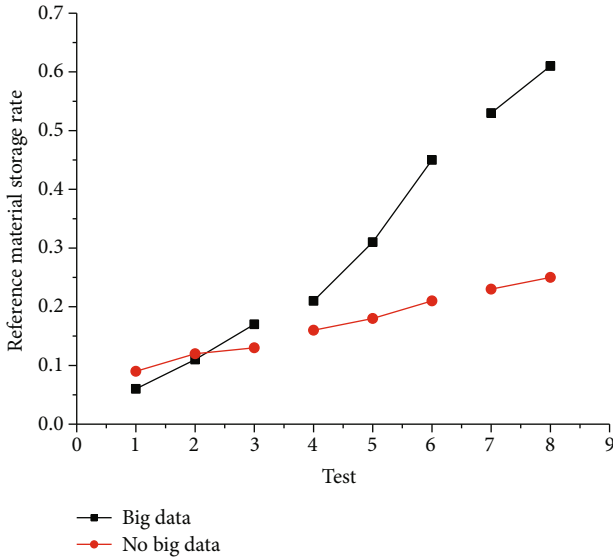


FIGURE 3: Reference material storage rate changes.

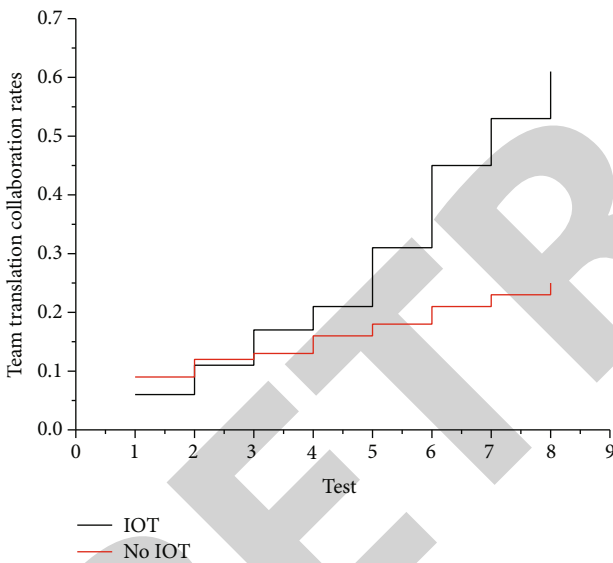


FIGURE 4: Changes in team translation collaboration rates.

have translation materials to refer to, so as to realize the splicing of similar game clips existing in history. Thus, the best translation combination can be obtained.

Through interviews with the heads of relevant enterprises in multinational game cooperation, it is found that the storage rate of reference materials for localized translation of their games has been greatly improved after combining with big data technology. The specific situation is shown in Figure 3.

4.3. Translation Strategy of Game Localization Team Based on IoT Technology. There are various sensor devices and RFID tags in the Internet of Things technology. For the communication and cooperation problems in the translation process, the Internet of Things provides sensor devices that

can be carried around. With these sensor devices, team members can quickly exchange game information.

Players can also use the information collected by the device to correct some translation errors in the process of game localization translation. Through the cooperation investigation and analysis, it is found that after combining the Internet of Things technology, the change of the cooperation rate of the game localization translation team is shown in Figure 4.

The division of labor between dubbing translation and character information translation can use IoT sensor information to distinguish the situation of each other, correct the correctness of the relevant translation in time, and ensure the matching degree of character information and dubbing. Through interviews with the heads of relevant enterprises in multinational game cooperation, it is found that the combination of Internet of Things technology has greatly improved the game consumer experience.

5. Conclusion

The accurate translation of game localization is a key element in promoting game products. In the global environment, game internationalization plays an extremely important social role. As an important part of game internationalization, game localization translation has obvious cultural characteristics. The use of vocabulary in the game reflects the national customs, cultural background, customs, etc. of the country of origin of the game. Due to the accelerated development of economic globalization, my country has introduced a large number of foreign game products under the new system of open economy supported by the government, and domestic products have also flowed into overseas markets in large quantities. International games have shown a trend of diversified development. Games of foreign origin often appear in people's lives, so the localized translation of games can help multinational game companies go abroad to develop international markets and can also reduce the social distance between Chinese citizens and international netizens. Only successful local translation of games will capture the psychology of game consumers, allow game consumers to purchase corresponding game products, and increase the sales of game products, and game companies will benefit. In order to achieve this goal, translators need to abide by the translation principles of game localization, use translation skills based on big data and Internet of Things technology, and pay attention to the problems that arise in the process of game localization translation. Only in this way, game localization translation can help enterprises and make enterprises stand firm in the international game business.

The game itself has a limited lifespan, generally no more than five years, but League of Legends has been around for 10 years, and not only the official organization, the game planning team works well, not to mention the translation team of game fusion into the local culture and atmosphere. From the history of League of Legends, we can learn not only about localization strategies but also how different types of products should be translated. League of Legends may not

Retraction

Retracted: A Low Power ROIC with Extended Counting ADC Based on Circuit Noise Analysis for Sensor Arrays in IoT System

Journal of Sensors

Received 23 January 2024; Accepted 23 January 2024; Published 24 January 2024

Copyright © 2024 Journal of Sensors. This is an open access article distributed under the Creative Commons Attribution License, which permits unrestricted use, distribution, and reproduction in any medium, provided the original work is properly cited.

This article has been retracted by Hindawi following an investigation undertaken by the publisher [1]. This investigation has uncovered evidence of one or more of the following indicators of systematic manipulation of the publication process:

- (1) Discrepancies in scope
- (2) Discrepancies in the description of the research reported
- (3) Discrepancies between the availability of data and the research described
- (4) Inappropriate citations
- (5) Incoherent, meaningless and/or irrelevant content included in the article
- (6) Manipulated or compromised peer review

The presence of these indicators undermines our confidence in the integrity of the article's content and we cannot, therefore, vouch for its reliability. Please note that this notice is intended solely to alert readers that the content of this article is unreliable. We have not investigated whether authors were aware of or involved in the systematic manipulation of the publication process.

Wiley and Hindawi regrets that the usual quality checks did not identify these issues before publication and have since put additional measures in place to safeguard research integrity.

We wish to credit our own Research Integrity and Research Publishing teams and anonymous and named external researchers and research integrity experts for contributing to this investigation.

The corresponding author, as the representative of all authors, has been given the opportunity to register their agreement or disagreement to this retraction. We have kept a record of any response received.

References

- [1] Y. Zhou, W. Lu, S. Yu, D. Yu, Y. Zhang, and Z. Chen, "A Low Power ROIC with Extended Counting ADC Based on Circuit Noise Analysis for Sensor Arrays in IoT System," *Journal of Sensors*, vol. 2022, Article ID 5304613, 12 pages, 2022.

Research Article

A Low Power ROIC with Extended Counting ADC Based on Circuit Noise Analysis for Sensor Arrays in IoT System

Ye Zhou , Wengao Lu , Shanzhe Yu, Dunshan Yu, Yacong Zhang, and Zhongjian Chen 

School of Integrated Circuits, Peking University, Beijing 100871, China

Correspondence should be addressed to Wengao Lu; wglu@pku.edu.cn

Received 9 September 2022; Accepted 23 September 2022; Published 3 October 2022

Academic Editor: Sweta Bhattacharya

Copyright © 2022 Ye Zhou et al. This is an open access article distributed under the Creative Commons Attribution License, which permits unrestricted use, distribution, and reproduction in any medium, provided the original work is properly cited.

As the Internet of Things (IoT) is rapidly integrated into our daily life, the demand for high performance readout integrated circuit (ROIC) design for sensor arrays is boosting. This paper presents a low power, low noise ROIC with 14-bit column-parallel extended counting (EC) ADCs for sensor arrays targeting the IoT applications. The proposed EC-ADC adopts a pseudodifferential architecture to cancel even-order nonlinearity. The analog front-end is a G_m stage, which employs a current-reuse topology to boost the transconductance and reduce noise without increasing current consumption. The upper 9-bit conversion is implemented during integration, and the residual voltage is converted by a 5-bit single-slope (SS) ADC, where the comparator is reused. A ping-pong integrator is proposed to reduce the reset time and improve linearity, eliminating the power-hungry CTIA structure. The ROIC is designed in 0.18 μm 1P5M CMOS process for a 640×480 sensor array. Power consumption of the ROIC is 33 mW, and each column ADC consumes 40.1 μW . Simulation results show an input-referred noise of 0.89 LSB (1.74 μV_{rms}), an integral nonlinearity of +0.92/-0.70 LSB, an ENOB of 12.87 bits, and a FoM of 131.1 fJ/step.

1. Introduction

The growing interest in the field of smart sensors has set new limits on realizing different sensors that are capable to capture myriad types of signals. These applications are often size constrained, while requiring high energy efficiency and stability [1–4]. With the advantages of low cost, small size, and good uniformity, uncooled infrared focal plane arrays (IRFPA) can be applied in IoT applications, such as composition analysis, smart monitoring, and spectral analysis [5–12].

Currently, the mainstream IRFPAs adopt vanadium oxide (VO_x) [5, 6] or amorphous silicon ($\alpha\text{-Si}$) microbolometers [7, 8], or silicon diodes as the thermosensitive sensors [9, 10]. Compared with $\text{VO}_x/\alpha\text{-Si}$ microbolometers, silicon diodes are fabricated with monocrystalline silicon and have the advantages of CMOS process compatibility, low noise, high uniformity, and huge potential for pixel size reduction [11]. However, the temperature sensitivity of silicon diodes is lower than that of $\text{VO}_x/\alpha\text{-Si}$ microbolometers, which leads to smaller signal voltage [12]. Therefore, the noise of the readout integrated circuit (ROIC) will have more severe impact and need to be reduced to achieve high

SNR. Increasing power consumption is a common way to lower noise. But the sensors of the IRFPA are sensitive to substrate temperature, which means decreasing power consumption of the ROIC is important to minimize the temperature drift. Besides, the miniaturized and portable development tendency also poses strict requirements on power dissipation. In addition, the ROIC needs to attain reasonable linearity to reduce fixed background noise [13]. In summary, the ROIC for silicon diode IRFPA needs to achieve low noise and good linearity under high power efficiency.

To meet these requirements, the integrated analog-to-digital converter (ADC) plays a key role. In recent years, the extended counting (EC) ADC has been developed as an excellent candidate among various kinds of the ADC solutions for large-scale sensor array ROICs [14–18]. Compared with other ADC types such as successive approximate register (SAR) ADC, delta-sigma ($\Delta\text{-}\Sigma$) ADC, and SS-ADC, EC-ADC achieves a good balance between bit-depth, conversion speed, and area. EC-ADCs implement coarse A/D conversion through multiple reset operation with a 1/1.5-bit feedback digital-to-analog converter (DAC) during the

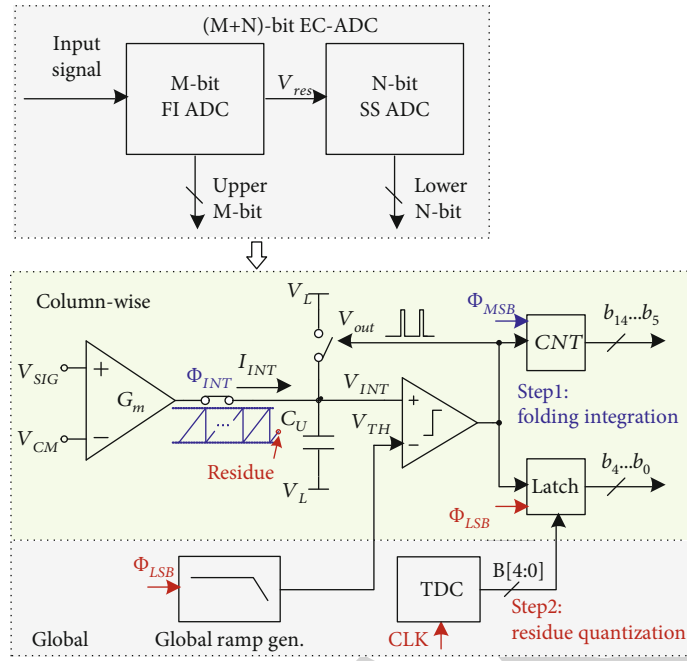


FIGURE 1: Conceptual block diagram of the proposed ROIC.

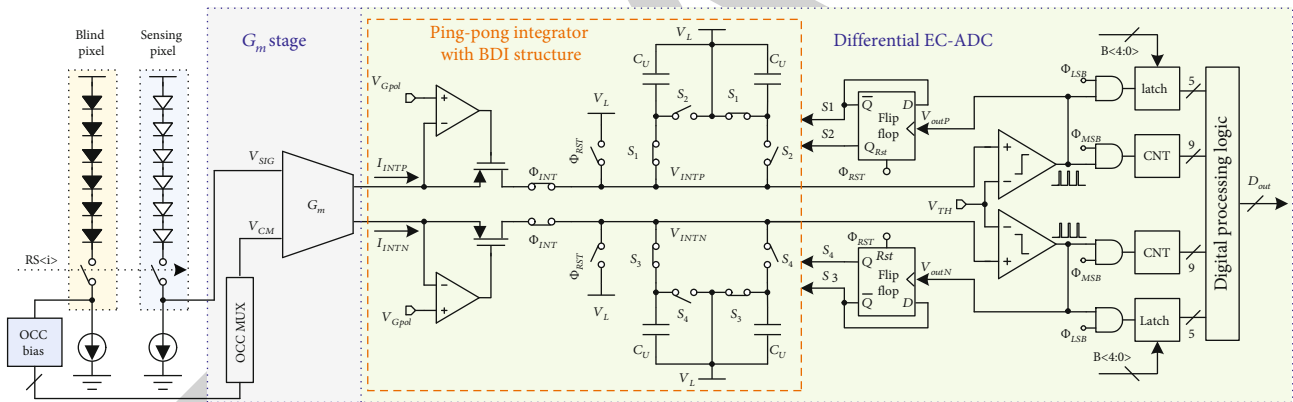


FIGURE 2: Circuit diagram of the proposed ROIC and its signal flow in one column.

folding integration (FI) period. And the analog residue is then quantified during the EC period. This combination can maximize the integration time, thereby reducing noise while enhancing bit-depth with better power efficiency. However, to improve linearity and provide source-and-sink integration current during the integration period, a capacitive transimpedance amplifier (CTIA) is often needed in the integrator. The CTIA block is power-hungry to achieve high slew rate and bandwidth. In [15], a folded cascode operational amplifier (op-amp) with gain boosting is adopted to improve the linearity of the CTIA, while the power consumption is too high for large-scale sensor array application. In [16], a current compensation technique is proposed to provide compensation current during the FI period, thus easing the power budget. But an extra high frequency clock is introduced which will generate jitter noise and increase design complexity and digital crosstalk. Some

CTIA-less architectures have also been reported. In [17], a passive integrator which included a capacitor and an injection transistor is used to replace the power-hungry CTIA structure. Yet the input signal range is unidirectional, which impairs input signal swing and signal-to-noise ratio (SNR). Moreover, there is reset time caused by the reset operation during integration, which will further degrade the accuracy and linearity [18].

In this paper, a low power ROIC with 14-bit column-wise EC-ADCs targeting a 640×480 silicon diode uncooled IRFPA under 50 Hz frame rate is proposed. A FI ADC and a single-slope (SS) ADC are combined for the upper 9-bit and lower 5-bit conversions, respectively. As the analog front-end, the G_m stage is the main power consumption and noise source. We adopt a pseudodifferential current-reuse structure to boost the transconductance and lower noise without increasing current consumption. A passive ping-pong

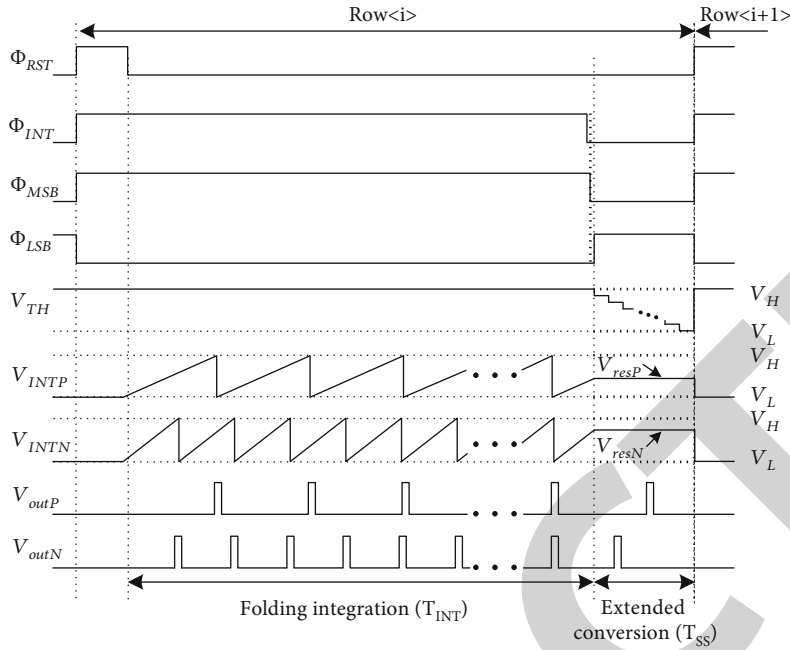


FIGURE 3: Timing diagram of the proposed ROIC.

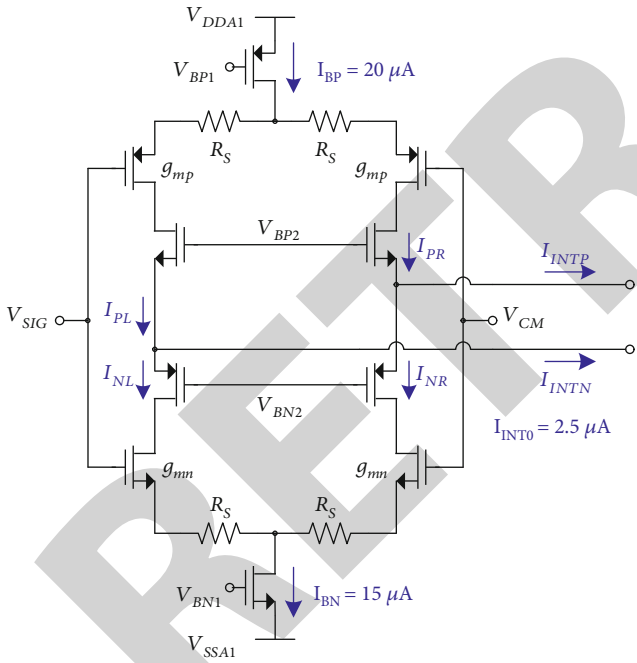


FIGURE 4: Proposed circuit schematic of the current-reuse G_m stage, incorporating the outside current source to increase the transconductance.

integrator architecture comprising two switched capacitors with buffered direct injection (BDI) structure is proposed to replace the power-hungry CTIA, saving energy while keeping high linearity. The comparator with positive feedback (PFB) technique is shared between the FI and the SS-ADC to reduce power dissipation and circuit complexity. The proposed ROIC achieves a good balance between power efficiency, resolution, and noise performance. The remaining

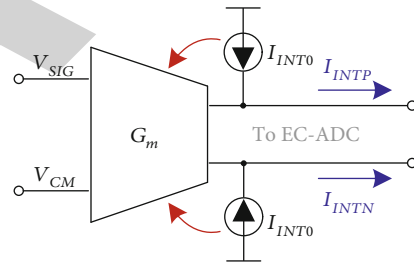


FIGURE 5: Traditional G_m stage with extra biasing current source.

of this paper is organized as follows. The ROIC system architecture including system overview, circuit diagram, and its operation principle is described in Section 2. The detailed circuit design, noise, and linearity analysis are presented in Section 3. Chip layout and postsimulation results are given in Section 4. Section 5 concludes this paper.

2. Proposed EC-ADC-Based ROIC Architecture

2.1. ROIC Structure Overview. Figure 1 shows a conceptual block diagram of the proposed ROIC. Each column-wise ADC consists of a 10-bit (including one redundant bit) FI ADC and a 5-bit SS-ADC. In step 1, the FI ADC converts the differential voltage into current and implements coarse A/D conversion through charging-and-resetting process during the FI period. The reset or folding times are proportional to the integrating current and recorded in the counter. In step 2, integration stops, V_{TH} starts to ramp down, and the residue voltage is further quantified by the SS-ADC. The upper 10-bit and lower 5-bit are then sent out serially to generate the final conversion results.

The circuit diagram of the proposed EC-ADC-based ROIC and its signal flow are shown in Figure 2. This circuit is a pseudodifferential implementation of Figure 1. In this

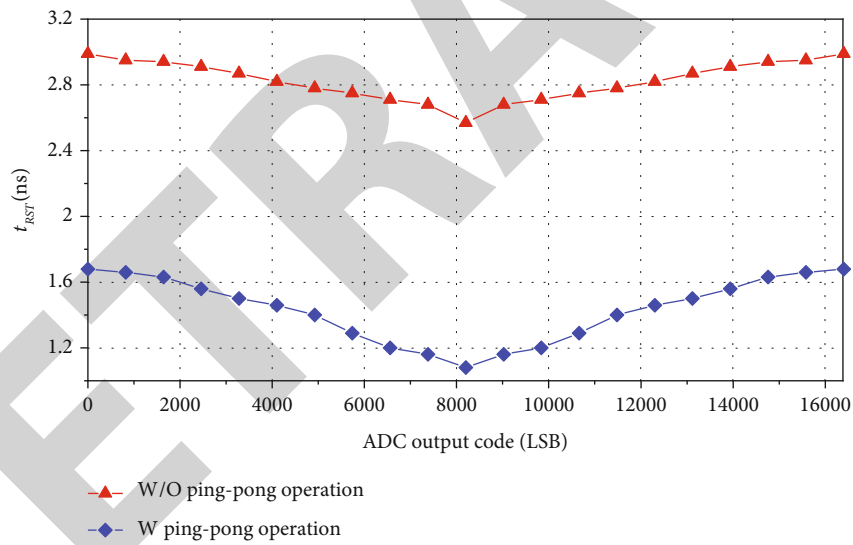
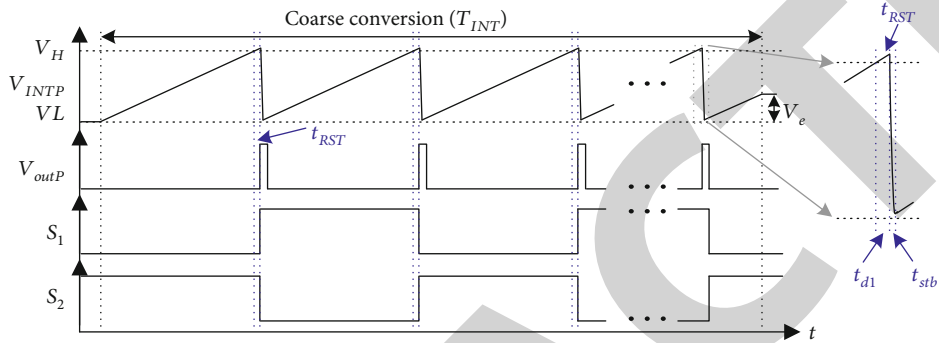
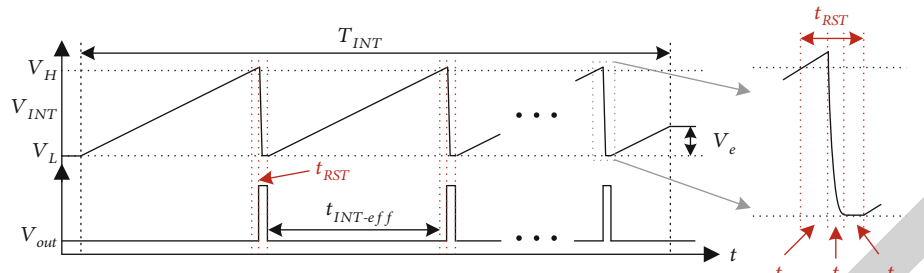


FIGURE 6: Continued.

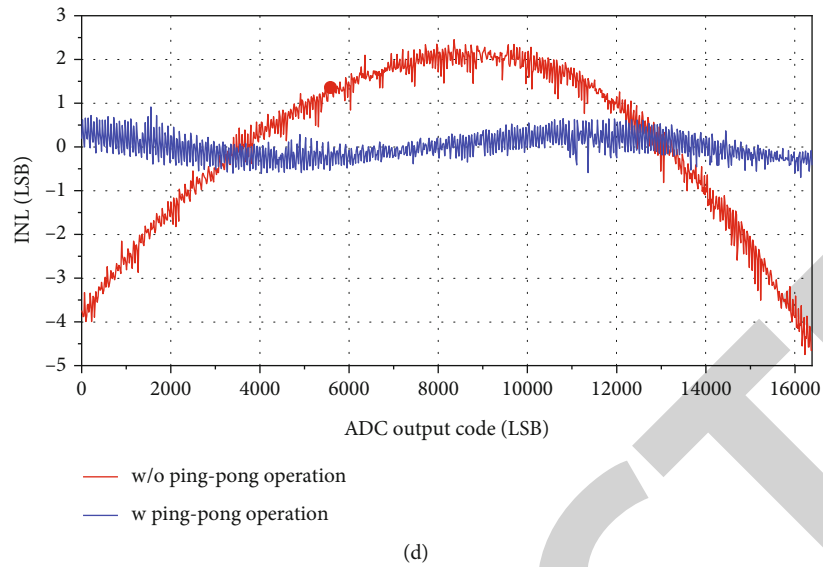


FIGURE 6: Illustration of the timing diagram of (a) the conventional reset operation and (b) the proposed ping-pong reset operation. Comparison of (c) the reset time and (d) INL performance between proposed ping-pong structure and conventional structure under the same power consumption.

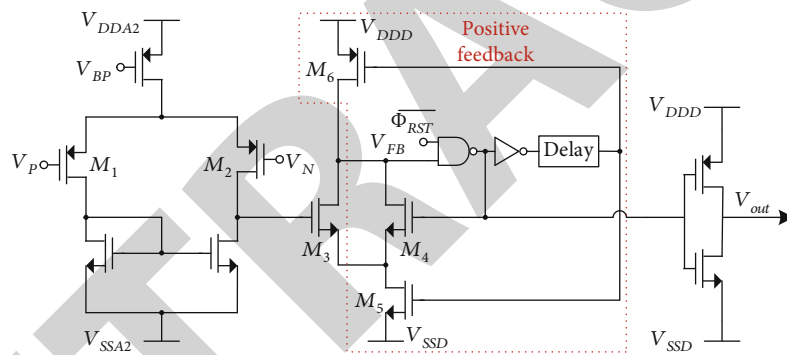


FIGURE 7: Comparator structure with positive feedback circuit.

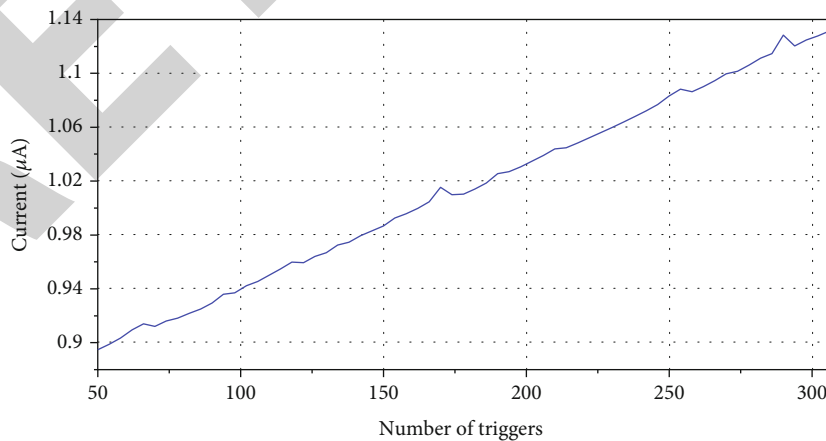


FIGURE 8: Variation of the comparator current of different number of triggers.

scheme, six silicon diodes biased at constant current are connected in series as the thermosensitive sensors, and the diode voltages change with temperature. When radiation arrives, the temperature of the sensitive pixel changes while the tem-

perature of the blind pixel is unaffected. As a result, the differential voltages are measured and quantified row by row. To minimize the spatial nonuniformity of the diodes, on-chip calibration (OCC) is adopted to provide calibrated

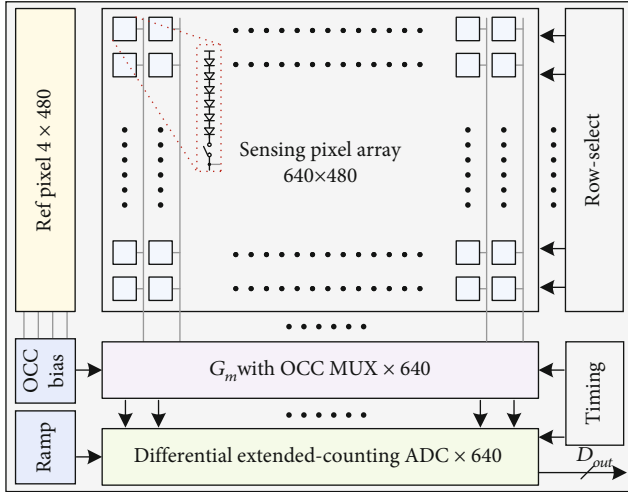


FIGURE 9: Block diagram of the chip core.

common-mode voltage V_{CM} to the G_m stage. The OCC block is a low noise 6-bit DAC, where the noise is less than $1 \mu V_{rms}$ (0.5 LSB). The proposed ROIC adopts pseudodifferential topology, which can reduce the relative quantization step size, cancel common-mode disturbances such as substrate temperature variation, and improve linearity by subtracting even-order distortion. Each column readout circuit includes a G_m stage and a differential EC-ADC. The EC-ADC uses ping-pong integrator instead of CTIA structure to reduce power dissipation while maintaining good linearity. A BDI structure, which is composed of a PMOS transistor and a feedback amplifier, is employed to offer higher current injection efficiency and stabilize the voltage at the output of G_m stage.

Figure 3 shows the timing diagram of the proposed ROIC. In the i -th row period, after autozero operation, the voltage difference between the sensing and blind pixels is converted into differential integration currents. $V_{INTP(N)}$ starts to ramp up during integration, in which the integrator adopted ping-pong structure. When one capacitor is connected to the comparator for integration, the other is reset to V_L . Each time $V_{INTP(N)}$ reaches the threshold voltage V_H , the comparators are triggered to switch $S_{1(3)}$ and $S_{2(4)}$. Such switching between integration and reset can reduce reset time and improve linearity, which will be further explained in Section 3.3. When Φ_{INT} and Φ_{MSB} are turned off, integration stops, and there is a residue voltage $V_{resP(N)}$. Then, Φ_{LSB} is turned on, V_{TH} starts to ramp down from V_H to V_L , and the comparator flips when V_{TH} reaches $V_{resP(N)}$. Note that Φ_{INT} , Φ_{MSB} , and Φ_{LSB} have different operation time to avoid false trigger and reduce the effects of charge injection. Finally, the MSBs and LSBs are combined and read out serially through the registers.

In this design, a differential G_m stage is directly connected to diodes to provide high input impedance to sense the voltage signals, which can eliminate preamplifier for better hardware efficiency. The FI ADC has one redundant bit and performs conversion while integration, which can increase the integration time to achieve better noise performance

compared with conversion-after-integration method. The ramp voltage for fine conversion is generated by a global ramp generator which is shared by the whole arrays. The comparator is also shared between the FI and the SS-ADC to further save energy and decrease system complexity.

2.2. Circuit Noise Analysis. This section focuses on noise analysis and optimization of the column readout circuit. Since the column ADC is directly connected to the diode sensors, it is most convenient to calculate the total noise as input-referred noise. To minimize the influence of the circuit noise on the whole image system, it is essential to reduce the circuit noise to a low level, for example, less than 1 LSB root-mean-square (RMS) noise under 14-bit resolution. The circuit noise contribution comes from the G_m stage (including thermal and flicker noise), the reset (kTC) noise and the comparator (V_{CMP}^2), and need to be integrated over a bandwidth of $1/2T_{INT}$ [19]. The input-referred noise contributed by G_m can be expressed as

$$\overline{V_{n,Gm}^2} = \int_{f_1}^{1/2T_{INT}} \left(\frac{8kT}{3G_m} + \frac{K}{C_{ox}W_{G_m}L_{G_m}f} \right) df, \quad (1)$$

where f_1 is chosen to avoid divergence at $f = 0$ and is equal to $1/4nt_{frame}$, where n is the number of frames being sampled [20]. The noise charge accumulated on the integrators from kTC and comparator is $NkTC_U$ and $\overline{V_{CMP}^2}C_U^2/2T_{INT}$, respectively, where N is the number of triggers during the folding integration period (T_{INT}). And this noise charge divided by T_{INT} equals to noise current. Then, the input-referred noise from kTC and comparator is given by

$$\begin{aligned} \overline{V_{n,kTC,CMP}^2} &= \frac{1}{G_m^2} \left(NkTC_U + V_{CMP}^2 C_U^2 \frac{1}{2T_{INT}} \right) \frac{1}{T_{INT}^2} \\ &= \frac{1}{G_m^2 T_{INT}^2 / C_U^2} \left(N \frac{kT}{C_U} + \overline{V_{CMP}^2} \frac{1}{2T_{INT}} \right), \end{aligned} \quad (2)$$

where k is Boltzmann's constant and T is the circuit absolute temperature. In this design, T_{INT}/C_U is in the order of tens of megohm, and G_m is with the order of hundreds of siemens. In general, the $G_m^2 T_{INT}^2 / C_U^2$ term is rather large, which means (2) is much smaller than (1) and the G_m stage is the main noise source of the circuit. According to (1) and (2), increasing G_m is of great importance for decreasing the overall circuit noise.

3. Circuit Design

3.1. Pseudodifferential G_m Stage. To achieve higher noise efficiency of the G_m stage, a current-reuse topology is adopted, which is also known as the inverter-based structure, as shown in Figure 4. PMOS and NMOS input-pairs are stacked to double the transconductance without increasing power consumption. Instead of adding extra current sources at the output ports as shown in Figure 5, the proposed design incorporates the biasing source into the G_m stage, which further increases the G_m . Therefore, the thermal noise

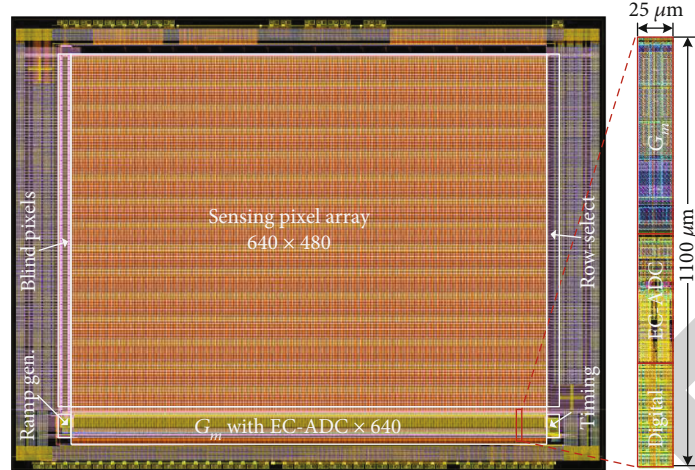


FIGURE 10: Chip layout.

of the G_m stage is reduced and the noise in (2) is also suppressed. The area of input-pairs is doubled compared with traditional structure, which further restrain the flicker noise according to (1). The source resistors R_S are utilized to improve linearity through negative feedback.

In Figure 4, $I_{BP} = 20 \mu A$, $I_{BN} = 15 \mu A$, and $I_{INT0} = 2.5 \mu A$. The PMOS and NMOS transistors of the input pairs are sized $2.56 \text{ mm}/0.5 \mu\text{m}$ and $2.56 \text{ mm}/1 \mu\text{m}$, respectively. The resistance of R_S is $4 \text{ k}\Omega$. The integration current ($I_{INTP(N)}$) is the difference between $I_{PR(L)}$ and $I_{NR(L)}$. The direction of $I_{INTP(N)}$ is continuously flowing out during integration. In this pseudodifferential design, for a 16 mV_P (32 mV_{PP}) signal of V_{SIG} , $I_{INTP(N)}$ has a swing of $\pm 1.75 \mu A$ under $2.5 \mu A$ common-mode current, which is translated into $\pm 70\%$ frequency swing range by the following EC-ADC.

3.2. Ping-Pong Integrator and Nonlinearity Analysis. During the coarse conversion period, the integration current is converted into frequency signal and recorded in the counter. Each time the node $V_{INTP(N)}$ reaches the threshold voltage V_H , the comparator will activate, and $V_{INTP(N)}$ is reset to V_L . In this charging-and-resetting process, the amount of charge Q_{INT} accumulated on the integration capacitor during one conversion period is expressed as below:

$$Q_{INT} = I_{INT} T_{INT} = N \times (C_U V_R + I_{INT} t_{RST}) + C_U V_{res}, \quad (3)$$

where N is the number of triggers, t_{RST} is reset time, and V_R is equal to $(V_H - V_L)$. Ideally, the charge packet $C_U V_R$ is used to quantify the signal charge Q_{INT} , in which the correlation between signal charge and counting number is written as $Q_{INT} = N_{ideal} C_U V_R$, where N_{ideal} is the ideal resetting times if there is no reset time and residual voltage. However, as shown in Figure 5(b), the existence of t_{RST} and V_{res} causes nonlinearity. During the FI period, the nonlinearity of quantization number ΔN can be calculated as follows:

$$N = \frac{I_{INT} T_{INT} - C_U V_{res}}{C_U V_R + I_{INT} t_{RST}} \approx \frac{I_{INT} T_{INT}}{C_U V_R + I_{INT} t_{RST}}, \quad (4)$$

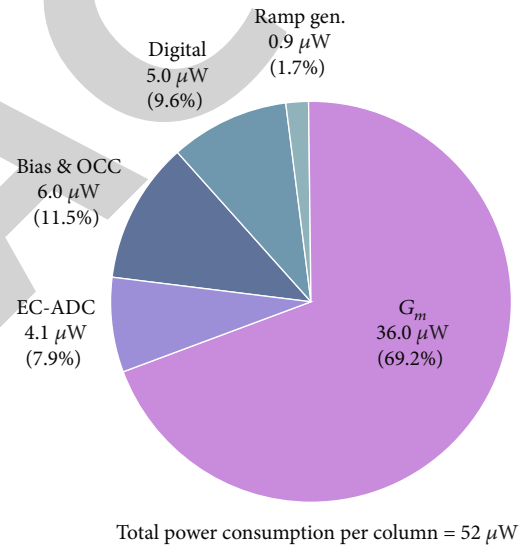


FIGURE 11: Power consumption breakdown average to per column.

$$\begin{aligned} \Delta N &= N_{ideal} - N = \frac{I_{INT} T_{INT}}{C_U V_R} - \frac{I_{INT} T_{INT}}{C_U V_R + I_{INT} t_{RST}} \\ &= \frac{I_{INT} T_{INT}}{C_U V_R} \times \frac{1}{1 + C_U V_R / (I_{INT} t_{RST})}. \end{aligned} \quad (5)$$

An approximation is made in (4) because $I_{INT} T_{INT}$ is normally much larger than $C_U V_{res}$ and V_{res} is further processed by the SS-ADC in this work. For a 50 Hz 640×480 array, T_{INT} is set as $40 \mu s$. The charge packet $C_U V_R$ is decided by the input range and ADC resolution and is set to be about 0.52 pC in this design. According to (5), ΔN is positively related to I_{INT} and t_{RST} , which means that the nonlinearity will increase with integration current and reset time.

In conventional reset operation as shown in Figure 6(a), the reset time t_{RST} is composed of three parts: the time between when V_{INT} reaches V_H and turning on the reset switch (t_{d1}), charging time of C_U (t_{CH}), and the time

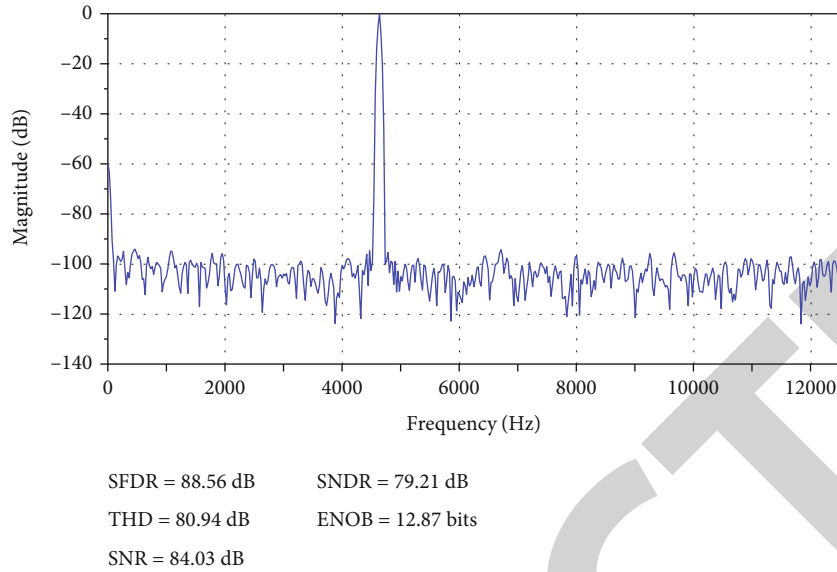


FIGURE 12: FFT spectrum in postsimulation.

between the end of the charging and turning off the reset switch (t_{d2}). V_{INT} will not start rising until another period ($t_{CH} + t_{d2}$) passed, and this period increases with the increasing of signal current [18]. Decreasing the propagation delay of the comparator can shorten the reset time, but this requires higher power consumption. Moreover, in conventional reset operation, t_{d1} and t_{CH} are necessary periods allowing V_{INT} to reset fully and must maintain a reasonable length.

To solve the above problems, a ping-pong architecture is adopted to reduce the reset time without increasing power consumption. Different from conventional structure, $S_{1(3)}$ and $S_{2(4)}$ will turn on alternatively when $V_{INTP(N)}$ reaches the threshold voltage V_H . Because reset operation of the capacitor is completed before connecting to the comparator, charging time t_{CH} and the restart delay t_{d2} due to turning off the reset switch in conventional structure is eliminated, as shown in Figure 6(b). The time for the node $V_{INTP(N)}$ to stabilize (t_{stb}) is less than 200 ps, which is much smaller than $t_{CH} + t_{d2}$ in conventional structure. Moreover, as there is not charging time limitation in the proposed ping-pong architecture, t_{d1} can also be further decreased. As a result, the total reset time t_{RST} is much reduced. Figure 6(c) shows the comparison of t_{RST} between the proposed and conventional structure in the case of the same power dissipation. It can be observed that t_{RST} is much reduced with the proposed ping-pong operation, leading to higher linearity. Figure 6(d) shows linearity comparison. The integral nonlinearity (INL) is reduced from +2.45/-4.75 LSB to +0.92/-0.70 LSB, which further proves the effectiveness of this design.

The integration capacitor C_U is implemented with 645-fF MIM capacitor, which is sized as $2 \times 4 \mu\text{m}/30 \mu\text{m}$. The switches $S_1 \sim S_4$ are sized to minimum values to minimize unwanted charge injection. Using a CTIA structure can also achieve high linearity, but the power consumption will

increase to tens of μW because CTIA needs to provide integration current. In this design, each feedback amplifier consumes only 100 nA. In general, the proposed ping-pong integrator greatly reduces power consumption while keeping high linearity.

Although the mismatch between the two capacitors in the proposed ping-pong integrator may introduce extra nonlinearity, this nonlinearity is quite limited. When considering mismatch, the capacitance is C_{u1} and C_{u2} , respectively. And the injected charge of every two reset operations is $(C_{U1}V_R + C_{U2}V_R)$, which is independent of the mismatch. Only the last reset operation introduces nonlinearity, and the three sigma of capacitance mismatch is 0.5% according to the statistical model provided by foundry. This 0.5% mismatch leads to $0.5\% \times 32 = 0.16$ LSB nonlinearity in the proposed upper 9-bit and lower 5-bit EC-ADC. Monte-Carlo simulation results are also given in Section 4 for verification.

3.3. Comparator with PFB Technique. To reduce the propagation delay (t_{d1}) during the ping-pong reset operation, the comparator is required to response quickly when V_{INT} reaches the threshold voltage. Figure 7 illustrates the proposed comparator with positive feedback (PFB) circuit. When Φ_{RST} drops down and integration starts, V_P is lower than V_N , V_{FB} is charged to V_{DD} , and M_5 is turned on while M_6 and M_3 are turned off, which diminish the leakage current of the second stage. When V_P rises and reaches V_N , M_3 is turned on, and the race between M_3 and M_6 is avoided; thus, V_{FB} drops faster. The feedback path of M_4 and the AND gate also accelerates dropping of V_{FB} . As a result, the delay of the comparator is reduced. When V_{FB} drops to zero, V_{out} turns high, and V_P is reset to V_L by the ping-pong integrator. Note that when V_{FB} is low, M_6 will turn on through the delay path (after V_P is reset to V_L), and V_{FB} will be pulled back to V_{DD} . After precharging V_{FB} , M_6 will be turned off again through the delay path, and

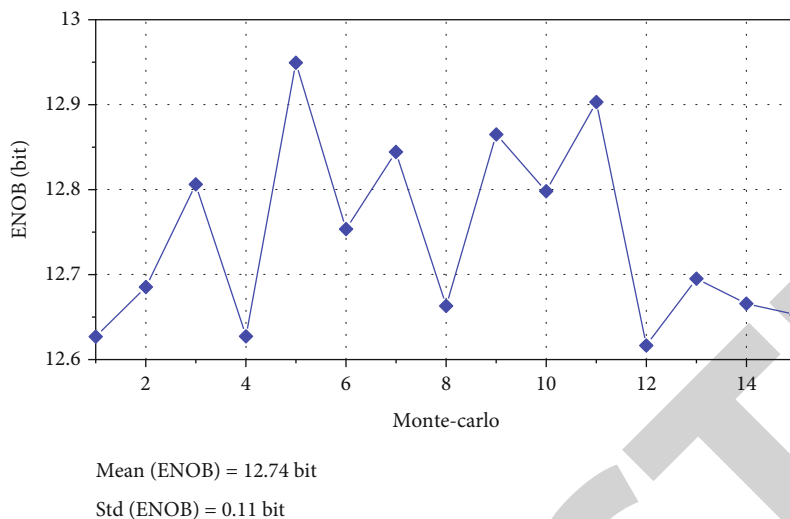


FIGURE 13: The ENOB performance in Monte-Carlo postsimulation.

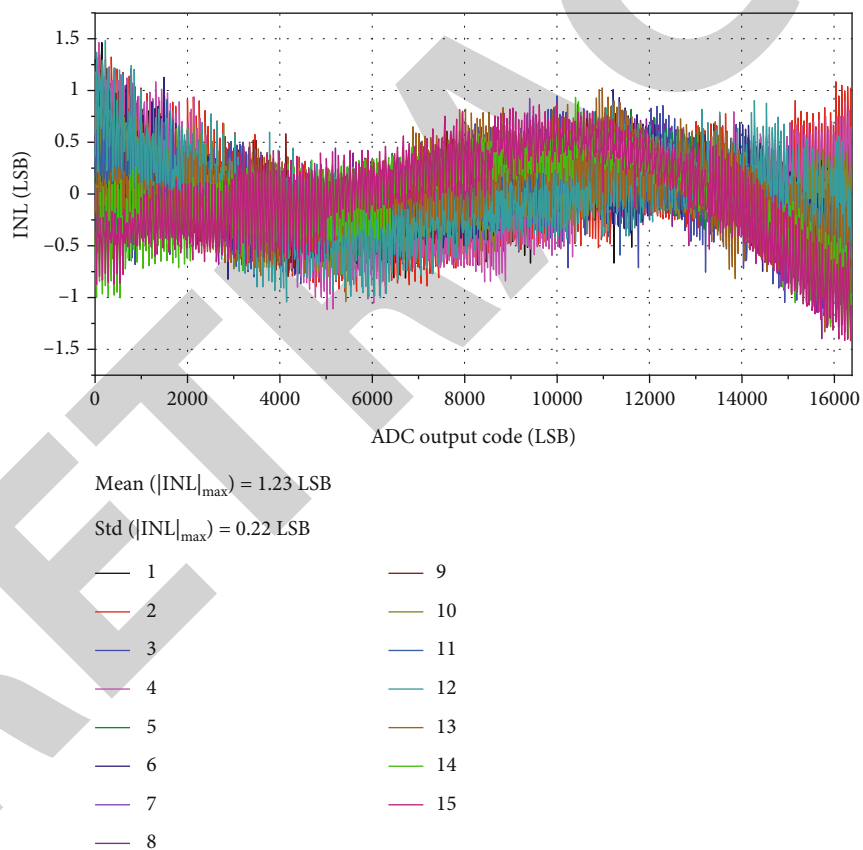


FIGURE 14: The INL performance in Monte-Carlo postsimulation.

an operating cycle is completed. The proposed PFB circuit can reduce the delay and the static power of the comparator. In this design, the ground of the comparators is separated into V_{SSA2} and V_{SSD} to reduce the ground crosstalk. As shown in Figure 8, the maximum current consumption is less than $1.14 \mu A$. And the comparator consumes less power when the number of triggers is lower.

4. Postlayout Simulation Results

Figures 9 and 10 show the block diagram and layout of the 640×480 silicon diode uncooled IRFPA chip, respectively. The proposed ROIC is designed in $0.18 \mu m$ 1P5M CMOS process. The chip size is $1.95 \text{ mm} \times 1.50 \text{ mm}$. The blind pixels and the ramp generator are placed on the left side

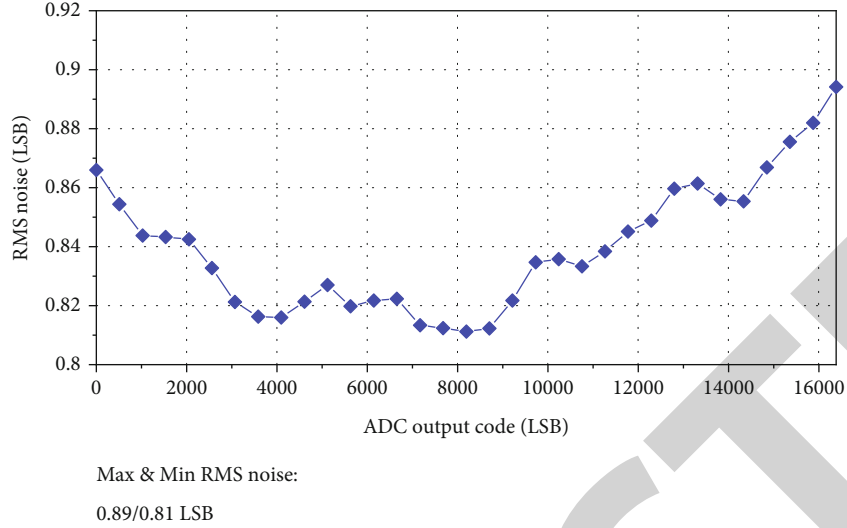


FIGURE 15: Input-referred noise performance in postsimulation.

TABLE 1: ROIC performance summary.

Parameter	Value
Process	0.18 μm
Power supply	1.8 V
Array size	640 \times 480
Frame rate	50 Hz
Pixel rate	15.36 Mp/s
Sensor material	Silicon diodes
Pixel pitch	25 μm
ROIC input range	± 16 mV
ADC resolution	14 bits
INL	+0.92/-0.70 LSB
Input-referred RMS noise	1.74 μV_{rms} /0.89 LSB
ROIC power consumption	33 mW
Power consumption of the G_m stage per column	36 μW
Power consumption of the EC-ADC per column	4.1 μW

while the row selector and timing control circuit being at the right side to reduce the digital crosstalk. Part of the input-pairs (not labeled) of G_m stage has been placed in the pixels, which shortens the analog path. Figure 11 shows the power consumption breakdown, total power consumption of the proposed ROIC is 33 mW, and each column ADC consumes 40.1 μW (including G_m and EC-ADC). As the front end, G_m takes up a significant portion of the overall power budget to reduce the total noise. The power consumption of the G_m stage can be reduced at the cost of degraded noise and linearity performance. Figure 12 shows the FFT spectrum with a 4.639 kHz 32 mV_{pp} sinusoid input signal under 25 kS/s sampling rate. The SFDR, SNR, SNDR, and ENOB are 88.56 dB, 84.03 dB, 79.21 dB, and 12.87 bits, respectively. Figure 13 shows the Monte-Carlo analysis of ENOB. The minimum and average ENOB are 12.61 bits and 12.74 bits. INL of the proposed ROIC in 15-run Monte-Carlo simulation is presented in Figure 14. All curves are within +1.49/-1.41

LSB, and the typical INL is +0.92/-0.70 LSB. The average and standard deviation of maximum |INL| is 1.23/0.22 LSB, which indicates the impact of mismatch is limited. Figure 15 shows the input-referred RMS noise under different ADC output code; each point is calculated as the standard deviation of 128 samples taken in transient noise simulation. The reset (kTC) noise increases with number of triggers, while the main noise source is the G_m stage. Benefited from low noise design of the G_m stage, the RMS noise is kept within 1.74 μV (0.89 LSB).

The performance of the proposed ROIC is summarized in Table 1. The total power consumption is 33 mW, including the column ADC and ADC peripheral circuit. Table 2 presents the performance comparison with previous works. Various figures of merits (FoM) are calculated for a fair performance comparison in circuit energy efficiency. FoM₁ and FoM₂ are used for evaluating the performance of the ROIC, and FoM₃ is used for representing the performance of

TABLE 2: Comparison with previous works.

Parameter	[21]	[22]	[23] ^a	[16] ^a	[24]	This work ^a
Process (nm)	130	90	180	180	90	180
Array size	580 × 450	1920 × 1440	—	1024 × 768	960 × 720	640 × 480
Frame rate (Hz)	60	50	—	30	35	50
ROIC power (mW) ^b	50	64	—	104	28	33
ADC type	PWM- $\Delta\Sigma$	SAR	TS-SS	EC	TS-SS	EC
Resolution (bit)	12	10	12	14	12	14
Conversion time (μ s)	37	13.8	10	43.4	39.7	40
ADC power per column (μ W)	71.2	27.3	72	15	6.35	40.1
INL (LSB)	5.91/-2.28	0.81/-0.50	1.06/-0.84	+3.69/-9.83	5.73/-7.3	0.92/-0.70
ENOB (bits)	9.44	10.5	11.25	10.7 ^c	9.13 ^c	12.87
FoM ₁ (fj/step) ^d	779.5	452.1	—	269.0	282.6	131.1
FoM ₂ (nJ) ^e	3.19	0.463	—	4.39	1.16	2.15
FoM ₃ (fj/step) ^f	3792.8	261.9	295.6	391.3	449.9	214.3

^aSimulation results. ^bROIC power = (column ADC power) × (the number of columns) + ADC peripheral circuit power. ^cENOB is calculated as $\log_2(2^{\text{ADC resolution}/\epsilon})$, where ϵ is the maximum between |INL| and input-referred RMS noise. ^dFoM₁ = (ROIC power)/(array size × frame rate × $2^{\text{ADC resolution}}$). ^eFoM₂ = (ROIC power)/(array size × frame rate). ^fFoM₃ = (column ADC power × conversion time)/ 2^{ENOB} .

column ADC. For various FoMs, this work shows state-of-art level performance: FoM₁ of 131.1 fj/step, FoM₂ of 2.15 nJ, and FoM₃ of 214.3 fj/step. Regarding FoM₁, FoM₃, INL, and ENOB, this work shows competitive performance compared to other works. It can be seen that the proposed ROIC is more power efficient while maintaining high linearity and noise performance.

5. Conclusion

In order to meet the energy efficiency and image quality of the infrared imagers applied in IoT system, this paper presents a low-power ROIC with column-level EC-ADCs. The proposed circuit can be applied to digital readout application for large-scale sensor arrays, such as uncooled IRFPA and CMOS image sensors. Based on circuit noise analysis, a current-reuse topology has been used as the G_m stage to boost the transconductance and improve power-noise efficiency. The EC-ADC adopts a pseudodifferential architecture to reduce distortion. According to the nonlinearity analysis, a passive ping-pong integrator architecture is proposed to improve the linearity through reducing the reset time. Moreover, the comparator is shared between the coarse and fine conversion to reduce circuit complexity and power consumption. The comparator employs a positive feedback circuit to improve speed while reducing static power dissipation. To perform a fair performance comparison with previous works, different kinds of FoM were calculated to evaluate the ROIC power efficiency. According to the postsimulation results, the proposed ROIC achieves an ENOB of 12.87 bits, an input-referred noise of $1.74 \mu V_{\text{rms}}$ (0.89 LSB), a FoM₁ of 131.1 fj/step, a FoM₂ of 2.15 nJ, and a FoM₃ of 214.3 fj/step, which meets the low noise, high accuracy, and power-efficiency requirements in IoT sensor readout applications.

Data Availability

The datasets used and/or analyzed during the current study are available from the corresponding authors on reasonable request.

Conflicts of Interest

The authors declare that they have no conflicts of interest.

Acknowledgments

This work was supported by the National Natural Science Foundation of China (No. 61973008 and No. 61976009) and National Key Research and Development Program of China (No. 2018YFB2002403).

References

- [1] A. Rezvanitabar, G. Jung, Y. S. Yaras, F. L. Degertekin, and M. Ghovanloo, "A power-efficient bridge readout circuit for implantable, wearable, and IoT applications," *IEEE Sensors Journal*, vol. 20, no. 17, pp. 9955–9962, 2020.
- [2] Z. Chen, X. Liu, H. Yang et al., "Processing near sensor architecture in mixed-signal domain with CMOS image sensor of convolutional-kernel-readout method," *IEEE Transactions on Circuits and Systems I: Regular Papers*, vol. 67, no. 2, pp. 389–400, 2020.
- [3] M. Nazhamaiti, X. Han, Z. Liu et al., "NS-MD: near-sensor motion detection with energy harvesting image sensor for always-on visual perception," *IEEE Transactions on Circuits and Systems II: Express Briefs*, vol. 68, no. 9, pp. 3078–3082, 2021.
- [4] K. D. Choo, L. Xu, Y. Kim et al., "Energy-efficient motion-triggered IoT CMOS image sensor with capacitor array-assisted charge-injection SAR ADC," *IEEE Journal of Solid-State Circuits*, vol. 54, no. 11, pp. 2921–2931, 2019.

Research Article

Thermal and Wet Comfort of Clothing in Different Environments Based on Multidimensional Sensor Data Fusion and Intelligent Detection

Xia Hou 

School of New Materials and Shoes & Clothing Engineering, Liming Vocational University, Quanzhou, 362000 Fujian, China

Correspondence should be addressed to Xia Hou; houxia@stu.cpu.edu.cn

Received 19 August 2022; Revised 6 September 2022; Accepted 8 September 2022; Published 29 September 2022

Academic Editor: Sweta Bhattacharya

Copyright © 2022 Xia Hou. This is an open access article distributed under the Creative Commons Attribution License, which permits unrestricted use, distribution, and reproduction in any medium, provided the original work is properly cited.

With the improvement of quality of life, people pay more and more attention to the comfort performance of clothing, of which thermal and wet comfort is an important part of evaluating the comfort of clothing, referring to the performance of keeping the human body in a reasonable thermal and wet state. When the human body sweats a lot or is in a highly humid environment, the clothing fabric will be soaked to make people feel wet, which seriously affects the comfort performance of clothing wear, and with the rapid development of sensing technology, the comfort of human clothing can be comprehensively evaluated by a variety of sensing data (clothing pressure, temperature, humidity, and heart rate). Therefore, how to analyze and process these data and establish an objective and accurate evaluation criterion for clothing comfort is a difficult problem and has attracted the attention of many researchers. In this paper, an improved kernel function fuzzy kernel c-means clustering algorithm is used to analyze the pressure at specific points in human activities. Unsupervised clustering analysis was performed for five clustering metrics (mean, pressure range, temperature range, humidity range, and heart rate variability). The clustered samples were learned and discriminated by a support vector machine to determine the comfort level of the clothing. The method can be applied to multi-indicator and multiclassification problems, providing smart clothing researchers with an intelligent, objective, and accurate method for evaluating clothing comfort. Experiments show that the method designed in this paper has good performance experience in terms of mean value, pressure range, temperature range, humidity range, and heart rate variability.

1. Introduction

With the progress of the times, people's living standards continue to improve, and people's requirements for clothing are not only a gorgeous appearance, but also pay more attention to the comfort of wearing clothing feeling. And in a survey, questionnaire shows that 78.5% of consumers' survey results on clothing comfort requirements are much higher than the style, workmanship, and price of clothing [1, 2]. And in this case, it requires clothing with good moisture wicking and other functions to ensure that clothing has good thermal and wet comfort performance, so that the human body is in a comfortable state.

At present, consumers pay more and more attention to the comfort of clothing. Especially, after decades of development, the comfort of clothing is subdivided into hot and

humid comfort, contact comfort, fit (sport) comfort and visual comfort. The comfort of clothing mainly includes thermal and wet comfort, contact comfort, body (sports) comfort, and visual comfort [3, 4]. Research shows that in the heat and humidity comfort, contact comfort, and body (sports) comfort on the human dressing comfort contribution ratio of 61.5%, 11.5%, and 9%, respectively [5], it can be seen that the clothing heat and humidity comfort is a more important part of the clothing comfort [6].

As an important part of clothing comfort, it is the most widely researched field at home and abroad, which analyzes the heat and moisture exchange law between the integrated human body, clothing, and the environment from a deeper level and a broader perspective. Therefore, many scholars have done relevant research on it, for example, from the perspective of fibers on the composition, structure, and performance of

fibers [7]; from the perspective of yarns on the performance of yarns, twist, hairiness, etc. [8]; and from the perspective of fabrics on the performance of fabrics and structure and other aspects [9]; there are also more and more scholars and experts on different types of clothing research and development [10, 11]. These studies have also improved the comfort of people wearing clothing to varying degrees, but there are still many issues that need to be studied and explored by subsequent scholars.

Smart clothing is an extension and expansion of clothing, but it is still a type of clothing, so the comfort of the human body when wearing it must be considered. The comfort of clothing means that with the development of clothing, people pay more and more attention to the comfortable feeling when wearing clothing to meet their physiological and psychological needs [12, 13]. Therefore, in the design and production process of clothing, it is necessary to consider the comfort feeling produced by the human body when wearing. Nowadays, many consumers take the comfort of clothing as the main reference standard for clothing selection [14]. And more researchers of clothing materials and clothing styles take clothing comfort as a key research topic. Smart clothing is also a combination of clothing and information technology, where miniaturized and flexible electronic components are implanted into advanced textile materials and textile technology to make it have information perception, computational analysis, communication, and other functions [15, 16]. It can provide intelligent analysis, decision support, and feedback to the user based on the changes in the surroundings of the person currently working in a particular environment.

In order to achieve the functions of smart clothing, it is necessary to combine key technologies such as textile, communication, computer, and microelectronics. Since smart garments need to be sufficiently portable, low energy consumption and durable in production and application, flexible sensors and functional textiles, flexible power generation and energy storage devices, flexible display devices, low-power chips and circuit boards, flexible stretchable wires, flexible device processing and packaging technologies, new testing instruments, and information security are essential key technologies in smart garments.

These studies have also improved the comfort of people wearing clothing to varying degrees, but there are still many problems that need to be studied and explored by subsequent scholars [17, 18]. The samples after clustering are learned and discriminated by support vector machine to determine the comfort of clothing. This method can be applied to multi-index multiclassification problems and provides an intelligent, objective, and accurate clothing comfort evaluation method for smart clothing researchers. Experiments show that the method designed in this paper has excellent performance experience in average value, pressure range, temperature range, humidity range, and heart rate variability.

2. Multifunctional Clothing Design System and Evaluation System

Currently, knitted garments are the most closely integrated textile category between smart wearable devices and garments, and its flexibility and weavability are more in line

with the current development trend [19]; therefore, knitted garments are mainly considered in the combination approach, and most smart wearable devices are sensor-based components [19]. With the development of sensor miniaturization and regionalization, the layout of wearable devices is no longer limited to parts but to the whole-body domain network of human garments. In addition to interacting and communicating with human body information, it can monitor, collect, and transmit interaction data from the surrounding environment.

Therefore, this paper investigates the combination of smart wearable devices and target consumers' clothing from several aspects to meet the needs of target consumers for functional clothing in specific environments (or specific safety situations) in terms of safety, comfort, and design aesthetics. Based on an in-depth understanding of the needs of target consumers, we select suitable smart wearable devices (matching the characteristics of the target information) and explore the form of combination with functional clothing to conclude a design process that can balance function and aesthetics. Figure 1 shows the basic process of the study of combining smart wearable devices with target consumers' clothing.

With the popularity of mobile terminals such as smartphones and iPads, most wearable smart devices rely on mobile terminals to receive and analyze data. Currently, wearable devices and mobile terminals mainly transmit data through short-range wireless transmission, such as Bluetooth (Bluetooth), Zigbee, Wifi, and light fidelity (LiFi) technologies [20, 21]. The interaction between wearable devices and mobile terminals is mostly one-way, i.e., the interaction between wearable devices and terminals is relatively single, and the degree of data sharing is low, which affects the functional effect of the products. Therefore, in order to achieve high service efficiency of information processing between wearable devices and terminals, it is necessary to study the data information transmission and interaction between wearable devices and between wearable devices and mobile terminals, i.e., multi-interaction.

The multi-interaction framework of smart wearable device data transmission is shown in Figure 2.

For the multiple interaction methods between smart wearable devices and mobile terminals, this paper divides the information interaction methods into two categories: one is the information interaction triggered by human behavior, such as touch and click and behavior recognition; the other is the precise monitoring and interpretation of behavior language through wireless data transmission technology, which is still immature.

In this paper, we establish a single connection between smart wearable devices and mobile terminals through the current relatively mature near-field communication technology (e.g., FC technology), Bluetooth technology, and iBeacon technology [22, 23]. A diversified and full-coverage interaction mode between multiple smart wearable devices and mobile terminals is established, and a low-consumption and multifunctional optimized connection scheme is concluded.

This paper proposes a multifunctional apparel evaluation system for the apparel production process based on the research methods of related literature. First, the design

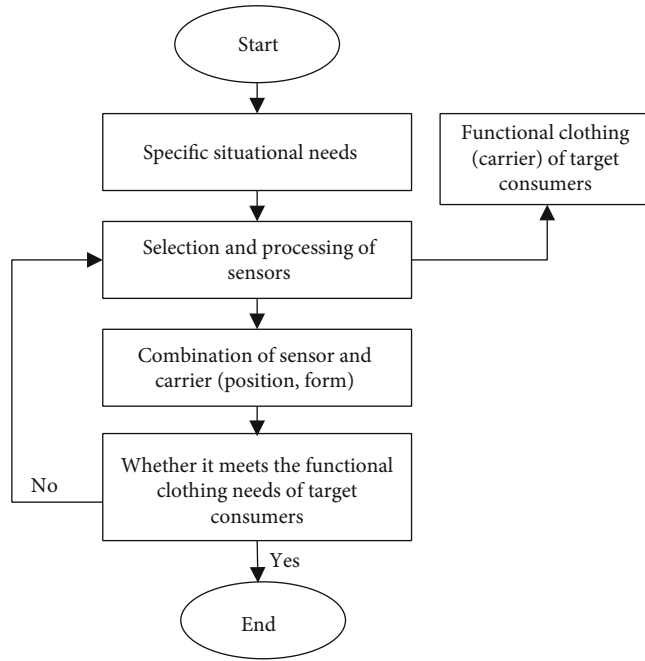


FIGURE 1: Basic process of research on the combination of intelligent wearable devices and clothing of target consumers.

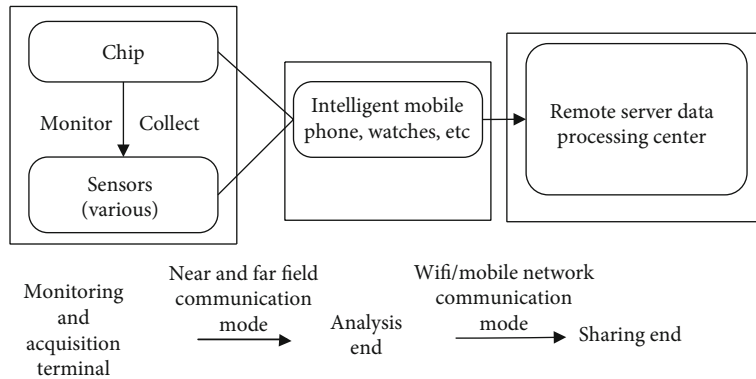


FIGURE 2: Intelligent wearable device data transmission multi-interaction mode framework.

aesthetics of the garment, such as style, color, and fabric, are evaluated using the principle of formal beauty; then its functions are comprehensively tested, including physical testing, wearable (interactive) technology testing, considering comfort, safety, economy, and other factors, safety testing, and structural continuity testing, to make it industrially valuable. The multifunctional garment design evaluation system is shown in Figure 3.

3. Kernel-Based Fuzzy C-Means Clustering Algorithm

An improved fuzzy kernel clustering algorithm, called fuzzy ISODATA, is a clustering algorithm that uses affiliation to determine the degree to which each data point belongs to a particular cluster. In many complex practical applications,

it is necessary to replace the kernel function in linear space with a more expressive high-dimensional space. The nonlinear problem is transformed into a linear problem by constructing new feature vectors and finally clustering in the high-dimensional feature space.

In the feature space F , the objective function expression of the improved FKCM clustering algorithm is

$$J_m(U, V) = \sum_{i=1}^c \sum_{k=1}^n u_{ik}^m \|\phi(x_k) - \phi(v_i)\|^2, \quad (1)$$

where $m \in [1, +\infty)$ is a fuzzy index, also known as a weighted index; an integer $c (2 \leq c \leq n)$ is the number of cluster categories; u_{ik}^m is the membership degree of the k th sample belonging to the first class; x_k is the k th sample; $\phi(x_k)$ and $\phi(v_i)$,

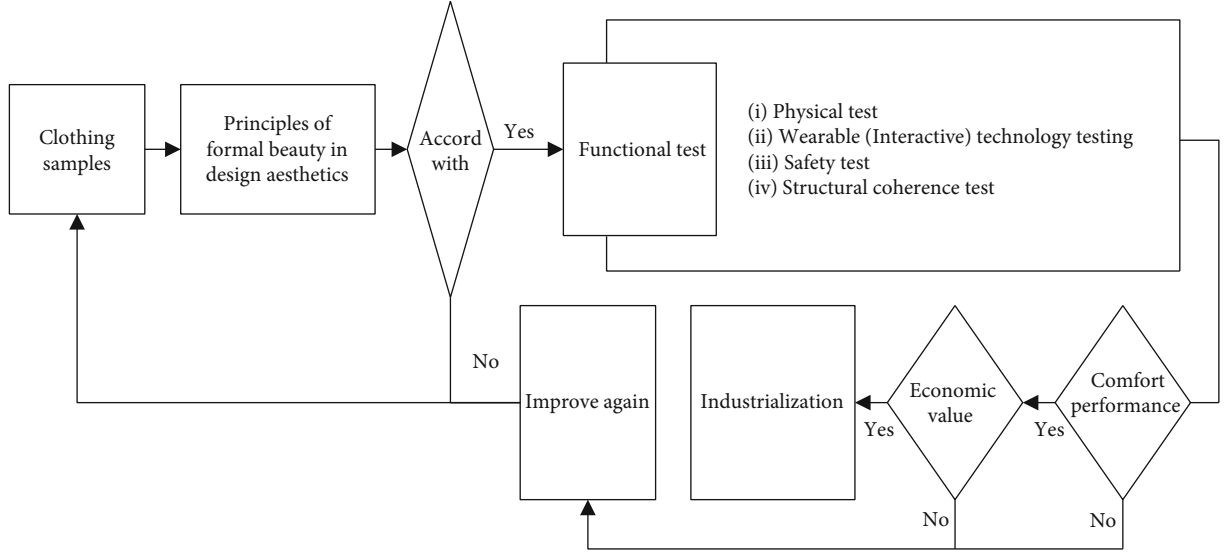


FIGURE 3: Multifunction clothing design evaluation system.

respectively, represent the images of samples and cluster centers in the feature space F , so $\|\phi(x_k) - \phi(v_i)\|^2$ is the distance from the j th sample to the i th cluster center in the kernel space.

$\|\phi(x_k) - \phi(v_i)\|^2$ It can also be expressed as

$$\|\phi(x_k) - \phi(v_i)\|^2 = K(x_k, x_k) + K(v_i, v_i) - 2K(x_k, v_i), \quad (2)$$

$$K(x_i, y_i) = \exp\left(-\frac{\|x_i - y_i\|^2}{2\sigma^2}\right), \quad (3)$$

where σ^2 is a constant. Substituting Equation (3) into Equation (2), we get

$$\|\phi(x_k) - \phi(v_i)\|^2 = 2 - 2K(x_k, v_i). \quad (4)$$

Substitute Equation (4) into Equation (1) to get

$$J_m(U, V) = 2 \sum_{i=1}^c \sum_{k=1}^n u_{ik}^m (1 - K(x_k, v_i)). \quad (5)$$

The minimum value of Equation (5) is the optimization condition, and the corresponding sample membership function and cluster center expression can be obtained as

$$u_{ik} = \frac{(1 - K(x_k, v_i))^{-1/(m-1)}}{\sum_{j=1}^c (1 - K(x_k, v_j))^{1/(m-1)}}, \quad (6)$$

$$v_i = \frac{\sum_{k=1}^n u_{ik}^m K(x_k, v_i) x_k}{\sum_{k=1}^n u_{ik}^m K(x_k, v_i)}. \quad (7)$$

Introducing the index weight coefficient into the kernel function of the FKCM clustering algorithm can improve the accuracy of the FKCM clustering algorithm. Therefore,

in the cluster analysis of clothing comfort indicators, the Gaussian kernel function in the algorithm is modified to

$$K(x_i, x_j) = \exp\left(-\frac{\sum_{i=1}^c (\omega_i (x_i - y_i))^2}{2\sigma^2}\right). \quad (8)$$

Among them ω is the weight coefficient.

Since each index has different degrees of importance to the judgment of clothing comfort, it is necessary to determine the weight corresponding to each index. Among them, the subjective weighting method is divided into layers and the Delphi method. This method is mature and easy to use. Therefore, this paper uses the Delphi method to determine the corresponding indicators weight value.

In summary, the basic steps of the improved FKCM algorithm are as follows:

- (1) Data preprocessing determine the number of clusters c , the fuzzy coefficient m , and the scale parameter to σ^2 and the function, and initialize the membership matrix u_{ik} , and set the iteration precision
- (2) Update membership matrix u_{ik} according to Equation (6)
- (3) Calculate the kernel function
- (4) If $\|U_{i+1} - U_i\| < \varepsilon$, stop the iteration, get the cluster center v_i , and the membership matrix u_{ik} ; otherwise, return to step (2).

4. Principle of Data Classification Based on Support Vector Machine

The multi-index sample set establishes a corresponding model between clustering categories and clothing comfort levels through certain rules. In this process, the relationship

between a single index and the wearing comfort of the subjects and its importance to the overall comfort can be considered at the same time. The construction of this model provides a quantitative criterion for the evaluation of clothing comfort, which makes the evaluation of clothing comfort more objective. This paper uses SVM to classify the clustered results.

Assume that the given separable data sample is (x_i, y_i) , $i = 1, 2, \dots, l$ where $x_i \in R^n, y_i \in [-1, +1]$. The linear discriminant in the dimensional space is

$$f(x) = (m^* x_i) + n. \quad (9)$$

The classification hyperplane equation is

$$(m^* x_i) + n = 0. \quad (10)$$

Among them m is the weight vector; n is the bias vector.

The distance from the 2-type sample to the hyperplane is $1/\|m\|$, and when $\|m\|^2$ is the smallest, the interval distance is the largest.

$$\phi(m) = \min \frac{1}{2} \times \|m\|^2. \quad (11)$$

Introducing Lagrange multipliers yields

$$L = \frac{1}{2} \times \|m\|^2 - \sum_i a_i (v(m \times x_i + n) - 1). \quad (12)$$

Among them, $a_i \geq 0$ is the Lagrange multiplier; $m = \sum_{i=1}^l a_i y_i x_i$.

Combined with Equation (12), the optimized dual equation and optimal classification function are obtained as

$$\max = \sum_{i=1}^l a_i - \frac{1}{2} \sum_{i=1}^l \sum_{j=1}^l a_i a_j y_i y_j (x_i \times x_j), \quad (13)$$

$$f(x) = \text{sgn} \left\{ \left(\sum_{i=1}^l a_i y_i (x_i \times x) \right) + n \right\}. \quad (14)$$

The clothing comfort classification problem in this paper is a linear inseparable problem. Therefore, the decision function needs to be replaced by the kernel function, and the optimal hyperplane classification function is obtained as

$$f(x) = \text{sgn} \left\{ \left(\sum_{i=1}^l a_i y_i k(x_i, x) \right) + n \right\}. \quad (15)$$

In this paper, the clustered samples are divided into two parts; one part is used for learning, and the discriminant rules of clothing comfort are established. The remaining samples are judged by the established discriminant rules, and their types are determined, so as to discriminate the comfort level of clothing.

5. Comfort Experiment and Analysis

In order to ensure the accuracy of the experimental results, 30 volunteers were selected to wear the same tight-fitting clothing and perform the same actions as the subjects in Chapter 3, and collect four quantitative indicators of pressure, temperature, humidity, and human heart rate between the human body and the clothing, and ask the subjects' subjective feelings during the experiment; 1 represents discomfort, and 2 represents comfort. After simple processing of the data collected by the system, the clothing comfort analysis is carried out. In this paper, five parameters are selected as the clothing evaluation index. Among them, the pressure average and range at points C, E, I, J , and L are used as two pressure indicators; it is expressed by pressure, and the unit is pa; the temperature range value at point p is used as the temperature index, and the unit is °C; the humidity extreme difference value at point O is used as humidity, and the unit of degree index is %; the heart rate change rate during the human experiment is used as the heart rate discrimination index, and the unit is 4%.

The physical parameters of the selected 30 subjects and the subjective evaluation of clothing comfort during the experiment are shown in Table 1:

After the experiment, the specific values of the five comfort evaluation indicators of the 30 subjects are shown in Table 2:

Based on the improved FKCM clustering based on the MATLAB platform. Determine the fuzzy coefficient $m = 2$, the scale parameter $\sigma^2 = 0.4$, and the iteration accuracy 0.00001. Use the Del Pei method to determine the corresponding weight coefficient $\omega = (0.3, 0.3, 0.15, 0.15, 0.1)$ of the clothing comfort index set. The KF clustering effectiveness index of the improved FKCM clustering analysis results is used to determine the optimal number of classifications as shown in Table 3. It can be seen that the KF index value shows that the sample data set is divided into two categories, that is, the number of clustering categories $c = 2$.

The cluster center matrix when clothing comfort is divided into two categories is

$$V = \begin{bmatrix} 5958.88 & 5131.41 & 31.72 & 52.81 & 15.9 \\ 2837.23 & 3364.46 & 29.93 & 32.32 & 4.46 \end{bmatrix}. \quad (16)$$

Since the relationship between the indicators is nonlinear, the ordinary linear classification is no longer suitable for the evaluation of clothing comfort. In this paper, the LIBSVM software developed by Professor Chih-Jen Lin of National Taiwan University is used for multiclassification and discriminative model [24]. The SVM type is selected as C-SVC, the Gaussian kernel function is selected for nonlinear transformation, the loss function P is 01, and the termination criterion is 0.001. 15 groups of test samples are selected from two types of objects, including 8 samples in the first category and 7 samples in the second category. The identification results are shown in Table 4. It can be seen that the judgment model has accurately identified the classes of the samples.

TABLE 1: Subjective evaluation of clothing comfort in the course of 30 subjects body parameters and experiment.

Subjects	Height	Weight	Shoulder width	Bust	The waist	Hipline	Subjective evaluation
1	177	72	44	92	83	102	1
2	178	71	45	93	82	102	1
3	178	72	45	96	85	99	1
4	176	71	43	95	82	96	1
5	177	72	44	96	84	97	1
6	183	75	43	93	97	88	1
7	182	74	42	96	99	89	1
8	181	72	45	95	98	87	1
9	179	73	42	94	102	85	1
10	177	72	41	92	104	84	1
11	178	71	42	93	102	79	1
12	172	68	43	92	89	97	1
13	174	72	45	95	85	94	1
14	173	72	43	95	87	96	1
15	175	71	42	91	78	98	1
16	181	75	44	99	78	96	1
17	167	61	42	85	71	95	2
18	169	59	42	85	72	89	2
19	179	68	42	92	81	97	1
20	178	63	42	93	74	94	2
21	164	55	42	95	84	97	1
22	178	56	43	78	77	84	2
23	174	55	42	78	74	85	2
24	176	64	41	86	82	94	2
25	164	55	41	88	82	97	2
26	172	71	43	95	82	98	2
27	177	61	42	85	77	94	2
28	175	57	40	75	74	85	2
29	168	55	41	87	74	87	2
30	170	52	41	75	74	83	2

In this paper, the clustering algorithm based on the improved FKCM is applied, and after clustering the comfort index samples of 30 subjects for many times, two categories are determined as the optimal number of clusters. And use the support vector machine to learn some of the samples, establish a discriminant rule, and use this rule to discriminate the comfort of the remaining samples, so as to identify the accuracy of the discriminant rule. Experiments show that a clothing comfort evaluation method based on the combination of improved FKCM clustering and support vector machine proposed in this paper can intelligently classify and identify clothing comfort and avoid the judgment of subjects and subjective factors in the evaluation process impact on results. It provides a reference and evaluation method for comfort discrimination for the production researchers of smart clothing and also provides a research idea for the next multilevel comfort evaluation.

6. Fabrics under Different Moisture Content

In order to obtain the variation of thermal insulation properties of fabrics at different moisture contents, this section will start from the following two aspects.

6.1. Changes of Thermal Conductivity of Fabrics with Different Water Content. The sportswear fabrics provided by T Apparel were chosen as the experimental materials for testing, mainly 10 kinds of woven and knitted fabrics. These 10 fabrics were placed in a constant temperature and humidity chamber (ambient temperature: $20 \pm 2^\circ\text{C}$; ambient humidity $65 \pm 5\%$) for 12 hours, and the basic parameters of the fabrics were tested. The results are shown in Table 5.

The above 10 kinds of fabrics were uniformly treated with moisture, and the prepared fabrics were placed in deionized water to make them completely wet, and then they were taken out and placed in a constant temperature and

TABLE 2: Comfort measurement parameters of 30 subjects.

Subjects	Pressure/pa		Temperature $p/^\circ\text{C}$	Humidity 0/%	Heart rate/%
	Average value	Range	Range	Range	Rate of change
1	5754	4192	0.7	44	29
2	5887	2432	1.2	43.5	22
3	5193.7	5008	1.4	37.9	25
4	6245	7544	1.7	42.5	26
5	9333.8	6423	1.5	36.4	18
6	6113.27	4551	1.7	42.5	22
7	6641.7	4975	1.5	43.5	15
8	5888.6	2872	1.4	34.5	16
9	4933	6728	1.4	31.5	14
10	5076.2	7335	2.2	38	9
11	7196.55	7336	2.1	39	8
12	5855.35	3934	2.8	34.8	9
13	4905.75	4687	1.8	35.8	17
14	6591.75	6369	1.6	39.4	11
15	4923.25	3996	0.9	31.5	13
16	5415	5869	1.6	36.62	11
17	3089.25	4905	0.6	24.5	10
18	2826	5432	0.3	14.2	7
19	4748.75	5126	1.4	18.1	12
20	3599	4006	1.2	16.4	5
21	5527.25	5297	1	15.4	5
22	2882.25	3851	0.8	12.3	4
23	2587.25	3732	1.4	12.7	0
24	3113.75	3731	1.4	12.8	1
25	4233	2114	0.5	7.5	8
26	2425.25	2906	0.4	21.4	3
27	2588	4378	0.8	12.9	8
28	1859.5	1574	0.4	15.5	4
29	1598	5	1541	0.3	13.3
30	1241.25	2927	0.1	9.6	2

TABLE 3: Actual clustering numbers and value of KF.

Preset classification number	2	3	4
Actual classification number	2	3	3
KF value	31.0948	22.7665	Nan

humidity room, until the fabric moisture content reached the moisture content to be measured. Test it after rate requirement. According to different fabric types, the moisture content of woven fabrics is set to 5%, 10%, 15%, and 18%, and the moisture content of knitted fabrics is set to 10%, 20%, 30%, 40%, 50%, and 60%.

The whole process of the experiment was completed in a constant temperature and humidity room. The thermal conductivity of 10 kinds of fabrics and the heat preservation rate of the fabrics were tested by using the KESF-7 precise instantaneous thermal property tester. The test process was com-

pleted according to the requirements of the experimental instrument. This experiment was carried out to obtain the test results of the thermal conductivity and the thermal insulation rate of the fabric under different moisture contents and draw them into a line graph, and the change rule is as follows.

6.2. *Influence of Different Moisture Contents on the Thermal Conductivity of Fabrics.* Read the test results of thermal conductivity of fabrics with different moisture contents on the KESF-7 precision instantaneous thermal property tester C.

The following will take the average of the 5 test results of each fabric, import the data results into the origin software, and draw a line graph of the change of thermal conductivity with moisture content of woven fabrics and knitted fabrics, as shown in Figure 4, and the abscissa in the broken-line graph represents the moisture content of the woven fabric and the knitted fabric, the ordinate represents the thermal conductivity of the fabric, and the broken line in the figure

TABLE 4: Discriminant result.

Judgment category	First kind	Class II
Sample number	1, 2, 5, 7, 8, 9, 10, 12, 14, 19	15, 17, 24, 25, 28, 30

represents the change of the thermal conductivity of the fabric with the increase of the moisture content.

By observing Figure 4, it can be found that after the fabric is treated with moisture, the thermal conductivity of the fabric increases with the increase of moisture content. This is because with the increase of water content in the fabric, the content of still air contained in the fabric decreases, the thermal conductivity of the fabric increases, the thermal performance of the fabric decreases. Generally, the heat transfer performance of fabrics is related to the structure, density, thickness, moisture content, and other factors of the material. For different fabrics, the thermal conductivity of fabrics is affected by moisture content to different degrees.

- (1) Variation law of thermal conductivity of woven fabrics affected by moisture content

It can be seen from Figure 4 that the thermal conductivity of woven 1#-woven 5# fabrics increases with the increase of moisture content, and the thermal conductivity of woven fabrics increases with the increase of moisture content. The trend is gradually slowing down.

- (2) Variation law of thermal conductivity of knitted fabrics affected by moisture content

It can be seen from Figure 4 that the thermal conductivity of knitted 6#-knitted 10# fabrics shows a continuous increasing trend with the increase of moisture content. When the moisture content is less than 40%, the thermal conductivity of different knitted fabrics, the increasing trend of thermal conductivity of different knitted fabrics is different, and when the moisture content is greater than 40%, the increasing trend of thermal conductivity of different knitted fabrics is close to the same. This is mainly due to the different forms of moisture in the fabric, which may be because when the moisture content is less than 40%, the moisture in the fabric mainly exists in the state of bound water and intermediate water.

Among them, when the moisture content of the knitted 8# fabric reaches 20%, the thermal conductivity of the fabric increases significantly, which is almost 2.3 times that of the fabric when the moisture content is 10%. This is mainly because when the moisture content of the fabric is 10%, the surface of the fabric has almost no wet feeling and is similar to the nonmoist state. When the moisture content is 20%, the fabric begins to feel wet, and because the knitted 8# fabric is larger, and when the moisture in the fabric increases, the air content in the fabric decreases significantly, resulting in an increase in the thermal conductivity of the fabric and a significant decrease in the thermal conductivity of the fabric.

When the moisture content of knitted 10# fabric is less than 40%, the heat transfer rate of the fabric changes slowly with the increase of the moisture content, which may be because the cotton fiber has hygroscopic expansion after blending with cotton and polyester, and the thickness of the fabric increases after moisture content.

6.3. *Influence of Different Moisture Content on the Thermal Insulation Rate of Fabrics.* The KESF-7 precision instantaneous thermal property tester was used to test the heat preservation rate of the fabric under different moisture contents, and the change of the heat preservation rate of the fabric under different moisture contents was obtained through the calculation equation of the heat preservation rate, such as

$$\delta = \frac{w_0 - W_1^*}{W_0} 100\%. \quad (17)$$

In the equation, W_0 is the thermal power of the empty plate, and W_1 is the thermal power when the fabric is covered.

The following will take the average of the five test results of each fabric, import the data into the origin software, draw a line graph of the change of the thermal insulation rate of the fabric with the moisture content, and analyze the woven fabrics and knitted fabrics, respectively. As shown in Figure 5, the abscissa in the broken line graph represents the moisture content of the woven fabric and the knitted fabric, the ordinate represents the thermal insulation rate of the fabric, and the broken line in the figure represents the change of the thermal insulation rate of the fabric with the increase of the moisture content happening.

By observing Figure 5, it can be found that with the increase of the moisture content, the change trend of the thermal insulation rate of the two fabrics is roughly the same, that is, the thermal insulation rate of the fabrics shows a decreasing trend with the increase of the moisture content. The specific change law of the thermal insulation rate of woven fabrics and knitted fabrics affected by moisture content is as follows.

- (1) The variation law of the thermal insulation rate of woven fabrics affected by the moisture content

It can be seen from Figure 5(a) that the thermal insulation rate of woven 1# and woven 5# fabric shows a continuous decreasing trend with the increase of moisture content, but the decreasing trend of thermal insulation rate is different between different woven fabrics. When the moisture content reaches 18%, the thermal insulation rate of woven 1#, woven 2#, and woven 5# fabrics tends to be stable.

TABLE 5: Basic parameters of fabric.

Fabric number	Fabric classification	Thickness mm	Square meter gram weight g/m ²	Volume weight g/cm ³	Thermal conductivity/w/m . °C	Heat preservation rate/%	Permeability	Moisture permeability/g/m ² × 24 h
Woven 1#	Woven	0.112	72.58	0.661	0.05	19%	6.88	1710.3
Woven 2#	Woven	0.105	72.59	0.689	0.03	22%	4.69	1734.5
Woven 3#	Woven	0.117	71.85	0.605	0.04	25%	7.40	1703.2
Woven 4#	Woven	0.118	79.16	0.672	0.04	25%	3.54	1705.5
Woven5#	Woven	0.145	97.41	0.677	0.05	20%	5.06	1732.8
Woven 6#	Knitting	1.021	250.74	0.245	0.07	32%	211.93	1869.7
Woven 7#	Knitting	1.251	251.94	0.203	0.06	31%	589.52	2016.5
Woven 8#	Knitting	2.420	357.44	0.149	0.04	42%	544.22	2031.7
Woven 9#	Knitting	0.493	141.51	0.288	0.05	29%	286.71	1773.9
Woven 10#	Knitting	1.243	308.64	0.245	0.06	27%	192.73	1984.1

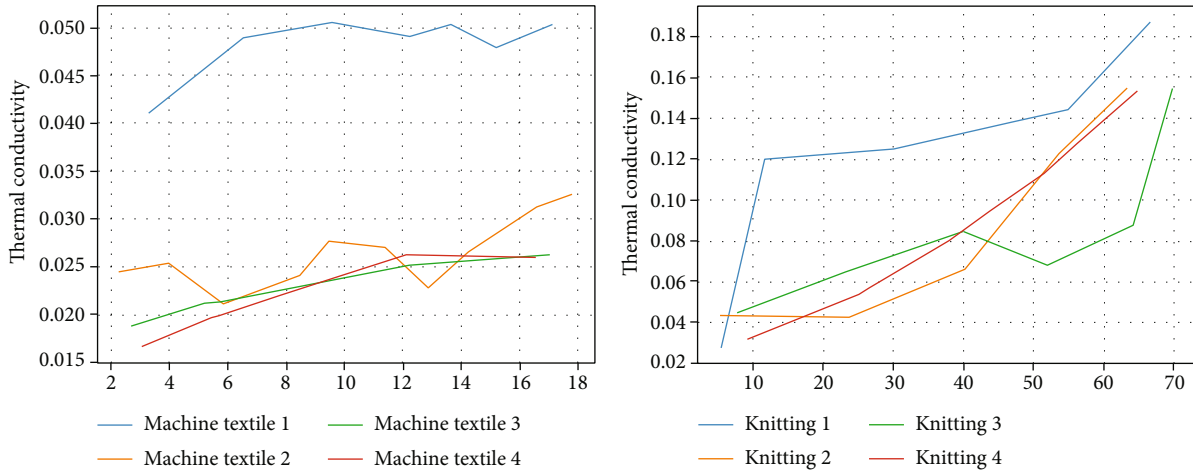


FIGURE 4: Line chart of the change of thermal conductivity of two kinds of fabrics with moisture content.

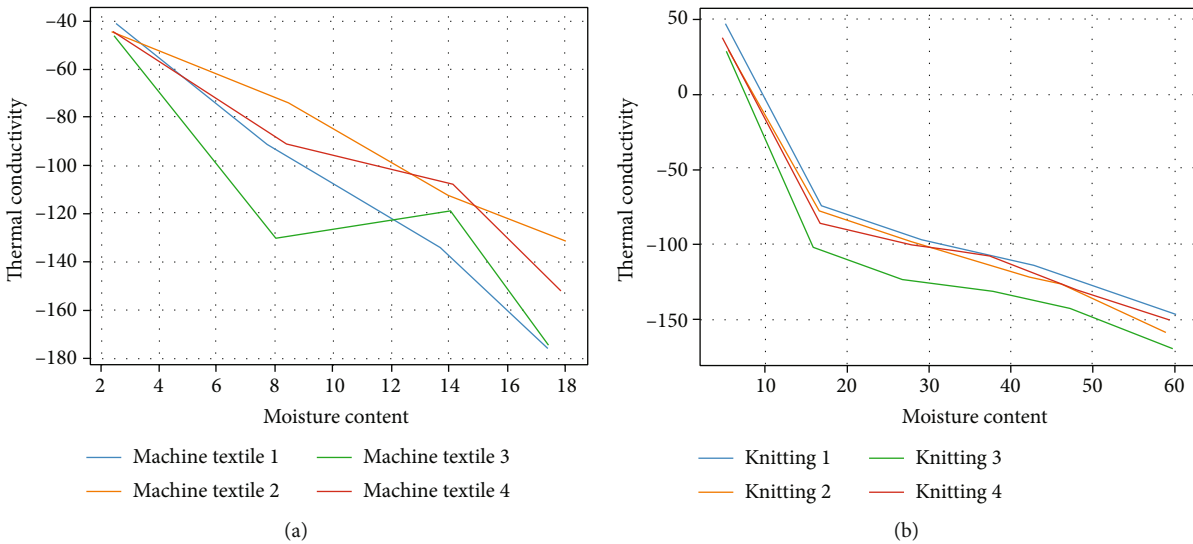


FIGURE 5: The line graph of the change of moisture content.

(2) The variation law of the thermal insulation rate of knitted fabrics affected by the moisture content

It can be seen from Figure 5(b) that the thermal insulation rate of knitted 6# and knitted 10# fabrics shows a continuous decreasing trend with the increase of moisture content. When the moisture content is between 10% and 20%, the decreasing trend of the thermal insulation rate of the fabric is the most obvious. This is mainly because when the moisture content is 10%, the surface of the fabric has almost no moisture feeling similar to the state without moisture and has a certain thermal insulation performance, while when the moisture content is 20%, the surface of the fabric feels wet, and the thermal insulation performance of the fabric changes significantly different.

6.4. Significant Analysis of the Influence of Different Moisture Contents on the Thermal Insulation Performance of Fabrics.

In order to accurately judge the significance of the influence of different moisture contents on the thermal insulation performance of fabrics, the analysis of variance was carried out on the test results for further exploration.

ANOVA is usually divided into one-factor, two-factor, and multifactor experimental data analysis of variance according to the number of experimental factors studied. It is an important method for analyzing experimental data in experimental research. It can analyze the respective functions of various factors and make quantitative estimates. Since the factors that affect the thermal performance of fabrics in this experiment include different fabrics and different moisture content, the analysis of variance method of the results of the two-factor independent observation value test is selected.

The experimental results of the thermal conductivity of fabrics under different moisture contents and the thermal insulation rate of fabrics under different moisture contents

TABLE 6: Variance analysis of woven fabric thermal conductivity.

Source	Type 3 sum of squares	df	Mean square	<i>F</i>	Sig
Calibration model	.001a	7	.000	57.488	.000
Intercept	.027	1	.027	8506.917	.000
Moisture content	.000	3	5.109E-5	16.295	.000
Textile	.001	4	.000	88.384	.000
Error	.3.763E-5	12	3.135E-6		
Total	.028	20			
Total corrected	.001	19			

a. *R*square = 971 (adjust *R*square = 954).

TABLE 7: Variance analysis of thermal conductivity of knitted fabrics.

Source	Type 3 sum of squares	df	Mean square	<i>F</i>	Mean square
Calibration model	.038a	9	.004	26.185	.000
Intercept	.360	1	.360	2232.307	.000
Moisture content	.034	5	.007	42.705	.000
Textile	.004	4	.001	5.536	.004
Error	.003	20	.000		
Total	.401	30			
Total corrected	.041				

a. *R* = .922 (adjust *R* = .887).

were processed and analyzed by SPSS software, and the following results were obtained.

The statistical results of variance analysis of the effect of different moisture content on the thermal conductivity of woven fabrics are shown in Table 6, where factor *A* is the moisture content of the fabric, which is divided into 4 levels, and factor *B* is different woven fabrics, which is divided into 5 levels.

In the table, the sum of squares and sig of the moisture content of different factors are 0.0003, 5.109E-5, 16.293, and 0.0003, respectively. The sum of squares, degrees of freedom, mean square, *F* of different woven fabrics, and sig value are 0.001, 4, 0.000, 88.383, and 0.000, respectively. The sig value represents the result of the significance test. When it is less than 0.05, the null hypothesis is rejected, and the factor is considered to have a significant impact on the result; when it is greater than 0.05, the null hypothesis is accepted, and the factor is considered to have no significant result on the result, and the higher the *F* value, the more significant the result. Larger values indicate more significant differences.

In Table 6, the sum of squares and sig of the moisture content of different factors are 0.0003, 5.109E-5, 16.293, and 0.0003, respectively. The sum of squares, degrees of freedom, mean square, *F* of different woven fabrics, and sig value are 0.001, 4, 0.000, 88.383, and 0.000, respectively. The sig value represents the result of the significance test. When it is less than 0.05, the null hypothesis is rejected, and the factor is considered to have a significant impact on the result; when it is greater than 0.05, the null hypothesis is accepted, and the factor is considered to have no significant result on the result, and the higher the *F* value, the

more significant the result. Larger values indicate more significant differences.

It can be seen from Table 7 that the sig<0.001 of the factors with different moisture contents indicates that there is a significant difference in the thermal conductivity of the fabrics under different moisture contents; the sig.<0.001 of the woven fabrics with different factors indicates the thermal conductivity between different woven fabrics. There is a significant difference in the thermal conductivity of woven fabrics, which indicates that moisture content has a significant effect on the thermal conductivity of woven fabrics.

The statistical results of variance analysis of the effect of different moisture content on the thermal conductivity of knitted fabrics are shown in Table 7, where factor *A* is the moisture content of the fabric, which is divided into 6 levels, and factor *B* is different knitted fabrics, which is divided into 5 levels.

In the table, the sig of knitted fabrics with different moisture content and different factors are 0.000 and 0.004, respectively. The factors with different moisture content sig<0.001 indicate that there are significant differences in thermal conductivity of fabrics under different moisture content; sig<0.001 for different knitted fabrics indicates that there are significant differences in thermal conductivity between different knitted fabrics. Therefore, the moisture content has a significant effect on the thermal conductivity of knitted fabrics.

7. Conclusion

Fabric is the material basis of clothing production, playing an indispensable carrier role, fabric and clothing interdependent, closely related. Usually the heat and moisture transfer

performance of fabric affects the heat and moisture comfort performance of human wearing clothes, and the two have a close correlation. In this paper, the comfort performance of clothes is studied by different algorithms. Firstly, the thermal and moisture comfort performance of clothes under different wet environments is evaluated by real person wearing experiments, and the thermal and moisture transfer performance of fabrics under different moisture content rates is tested by physics testing methods. Then a suitable clustering method was selected to cluster and analyze the known classified data to establish a suitable data classification model. Finally, the clustered data are divided into two parts to learn by vector machine or discriminant analysis method to determine the classification rule and then use the rule to discriminate the data in the remaining part to determine its type, so as to determine the accuracy of the discriminant rule. The sig of woven fabrics with different moisture contents and factors are 0000 and 0.148, respectively. Sig<0.001 for factors with different moisture contents indicates that there is a significant difference in the insulation rate of fabrics with different moisture contents, while sig.>0001 for woven fabrics with different factors indicates that there is no significant difference in the insulation rate of different woven fabrics.

Data Availability

The experimental data used to support the findings of this study are available from the corresponding author upon request.

Conflicts of Interest

The authors declared that they have no conflicts of interest regarding this work.

Acknowledgments

This study is supported by the Research on Friction Comfort of New Clothing Fabrics Based on Long-Distance Running (No. jz180909).

References

- [1] Q. Li, G. Chen, Y. Cui et al., "Highly thermal-wet comfortable and conformal silk-based electrodes for on-skin sensors with sweat tolerance," *ACS Nano*, vol. 15, no. 6, pp. 9955–9966, 2021.
- [2] T. Mansoor, L. Hes, and V. Bajzik, "A new approach for thermal resistance prediction of different composition plain socks in wet state (part 2)," *Autex Research Journal*, vol. 21, no. 2, pp. 238–247, 2021.
- [3] Y. Zhong, F. Zhang, M. Wang et al., "Reversible humidity sensitive clothing for personal thermoregulation," *Scientific Reports*, vol. 7, no. 1, pp. 1–8, 2017.
- [4] W. Yang, W. Gong, C. Hou et al., "All-fiber tribo-ferroelectric synergistic electronics with high thermal-moisture stability and comfortability," *Nature Communications*, vol. 10, no. 1, pp. 1–10, 2019.
- [5] S. Nagasawa, T. Sakoi, and A. K. Melikov, "Add-on local sweating simulation system for a dry thermal manikin," *Science and Technology for the Built Environment*, vol. 27, no. 7, pp. 971–985, 2021.
- [6] W. Chen, X. Li, X. Chen, and Y. Xiong, "Research on influence mechanism of running clothing fatigue based on BP neural network," *Journal of Intelligent & Fuzzy Systems*, vol. 40, no. 4, pp. 7577–7587, 2021.
- [7] P. Roelofsen, "A computer model for the assessment of employee performance loss as a function of thermal discomfort or degree of heat stress," *Intelligent Buildings International*, vol. 8, no. 4, pp. 195–214, 2016.
- [8] M. I. Iqbal, F. Sun, B. Fei, Q. Xia, X. Wang, and J. Hu, "Knit architecture for water-actuating woolen knitwear and its personalized thermal management," *ACS Applied Materials & Interfaces*, vol. 13, no. 5, pp. 6298–6308, 2021.
- [9] A. Angelucci, M. Cavicchioli, I. A. Cintorri et al., "Smart textiles and sensorized garments for physiological monitoring: a review of available solutions and techniques," *Sensors*, vol. 21, no. 3, p. 814, 2021.
- [10] L. Peng, B. Su, A. Yu, and X. Jiang, "Review of clothing for thermal management with advanced materials," *Cellulose*, vol. 26, no. 11, pp. 6415–6448, 2019.
- [11] Z. E. Kanat and N. Özdil, "Application of artificial neural network (ANN) for the prediction of thermal resistance of knitted fabrics at different moisture content," *The Journal of the Textile Institute*, vol. 109, no. 9, pp. 1247–1253, 2018.
- [12] M. Guan, S. Annaheim, M. Camenzind et al., "Moisture transfer of the clothing–human body system during continuous sweating under radiant heat," *Textile Research Journal*, vol. 89, no. 21–22, pp. 4537–4553, 2019.
- [13] D. Pani, A. Dessi, J. F. Saenz-Cogollo, G. Barabino, B. Fraboni, and A. Bonfiglio, "Fully textile, PEDOT: PSS based electrodes for wearable ECG monitoring systems," *IEEE Transactions on Biomedical Engineering*, vol. 63, no. 3, pp. 540–549, 2016.
- [14] A. P. Chan, Y. P. Guo, F. K. Wong, Y. Li, S. Sun, and X. Han, "The development of anti-heat stress clothing for construction workers in hot and humid weather," *Ergonomics*, vol. 59, no. 4, pp. 479–495, 2016.
- [15] Q. Zhao, Z. Lian, and D. Lai, "Thermal comfort models and their developments: a review," *Energy and Built Environment*, vol. 2, no. 1, pp. 21–33, 2021.
- [16] M. Młynarczyk, G. Havenith, J. Léonard, R. Martins, and S. Hodder, "Inter-laboratory proficiency tests in measuring thermal insulation and evaporative resistance of clothing using the Newton-type thermal manikin," *Textile Research Journal*, vol. 88, no. 4, pp. 453–466, 2018.
- [17] P. Cheng, J. Wang, X. Zeng, P. Bruniaux, and X. Tao, "Motion comfort analysis of tight-fitting sportswear from multi-dimensions using intelligence systems," *Textile Research Journal*, vol. 92, no. 11–12, pp. 1843–1866, 2022.
- [18] G. B. Tseghai, B. Malengier, K. A. Fante, and L. Van Langenhove, "The status of textile-based dry EEG electrodes," *Autex Research Journal*, vol. 21, no. 1, pp. 63–70, 2021.
- [19] J. Shi, S. Liu, L. Zhang et al., "Smart textile-integrated micro-electronic systems for wearable applications," *Advanced Materials*, vol. 32, no. 5, article 1901958, 2020.
- [20] N. Ma, Y. Lu, J. He, and H. Dai, "Application of shape memory materials in protective clothing: a review," *The Journal of the Textile Institute*, vol. 110, no. 6, pp. 950–958, 2019.
- [21] W. El Hachem, J. Khoury, and R. Harik, "Combining several thermal indices to generate a unique heat comfort assessment

- methodology,” *Journal of Industrial Engineering and Management*, vol. 8, no. 5, pp. 1491–1511, 2015.
- [22] P. Cheng, D. Chen, and J. Wang, “Research on prediction model of thermal and moisture comfort of underwear based on principal component analysis and Genetic Algorithm–Back Propagation neural network,” *International Journal of Nonlinear Sciences and Numerical Simulation*, vol. 22, no. 6, pp. 607–619, 2021.
- [23] Y. Lu, F. Wang, and H. Peng, “Effect of two sweating simulation methods on clothing evaporative resistance in a so-called isothermal condition,” *International Journal of Biometeorology*, vol. 60, no. 7, pp. 1041–1049, 2016.
- [24] A. Soroudi, N. Hernández, J. Wipenmyr, and V. Nierstrasz, “Surface modification of textile electrodes to improve electrocardiography signals in wearable smart garment,” *Journal of Materials Science: Materials in Electronics*, vol. 30, no. 17, pp. 16666–16675, 2019.

Review Article

A Review of Security and Privacy Concerns in the Internet of Things (IoT)

Muhammad Aqeel,¹ Fahad Ali,² Muhammad Waseem Iqbal ,¹ Toqir A. Rana ,^{3,4} Muhammad Arif,⁵ and Md. Rabiul Auwul ⁶

¹Department of Software Engineering, The Superior University, Lahore, Pakistan

²Department of Information Technology, The Superior University, Lahore, Pakistan

³Department of Computer Science and IT, The University of Lahore, Lahore, Pakistan

⁴School of Computer Sciences, Universiti Sains Malaysia, Penang, Malaysia

⁵Department of Computer Science, The Superior University, Lahore, Pakistan

⁶Faculty of Science and Technology, Department of Mathematics, American International University-Bangladesh, Dhaka, Bangladesh

Correspondence should be addressed to Md. Rabiul Auwul; rabiulauwul@gmail.com

Received 29 July 2022; Revised 26 August 2022; Accepted 8 September 2022; Published 29 September 2022

Academic Editor: Sweta Bhattacharya

Copyright © 2022 Muhammad Aqeel et al. This is an open access article distributed under the Creative Commons Attribution License, which permits unrestricted use, distribution, and reproduction in any medium, provided the original work is properly cited.

The recent two decades have witnessed tremendous growth in Internet of things (IoT) applications. There are more than 50 billion devices connected globally. IoT applications' connectivity with the Internet persistently victimized them with a divergent range of traditional threats, including viruses, worms, malware, spyware, Trojans, malicious code injections, and backdoor attacks. Traditional threats provide essential services such as authentication, authorization, and accountability. Authentication and authorization are the process of verifying that a subject is bound to an object. Traditional authentication and authorization mechanisms use three different factors to identify a subject to verify if the subject has the right capability to access the object. Further, it is defined that a computer virus is a type of malware. Malware includes computer viruses, worms, Trojan horses, spyware, and ransomware. There is a high probability that IoT systems can get infected with a more sophisticated form of malware and high-frequency electromagnetic waves. Purpose oriented with distinct nature IoT devices is developed to work in a constrained environment. So there is a dire need to address these security issues because relying on existing traditional techniques is not good. Manufacturers and researchers must think about resolving these security and privacy issues. Most importantly, this study identifies the knowledge and research gap in this area. The primary objective of this systematic literature review is to discuss the divergent types of threats that target IoT systems. Most importantly, the goal is to understand the mode of action of these threats and develop the recovery mechanism to cover the damage. In this study, more than 170 research articles are systematically studied to understand security and privacy issues. Further, security threats and attacks are categorized on a single platform and provide an analysis to explain how and to what extent they damage the targeted IoT systems. This review paper encapsulates IoT security threats and categorizes and analyses them by implementing a comparative study. Moreover, the research work concludes to expand advanced technologies, e.g., blockchain, machine learning, and artificial intelligence, to guarantee security, privacy, and IoT systems.

1. Introduction

Current trends of technology “connect the unconnected,” which means every object that can be connected will be connected in the upcoming years. The IoT is the network of physical objects containing sensors and processing powers

embedded in devices to connect the end-users to wide-area networks for transmission [1]. It can be seen everywhere around us, including automobiles, public lights, domestic appliances, health-care systems, and personal digital assistants like Google Home. For example, IoT gateways allow fast and easy access to the IoT world, and they are

compatible with IoT servers (Microsoft Azure, Amazon AWS, IBM Cloud, Google Cloud, etc.) and customized servers that support MQTT. Globally, IoT devices are attached to the Internet and communicate information through embedded sensors and software [2]. These devices minimize the human effort to create easiness in life and maximize resource utilization. These devices help humans to make better decisions for upgrading the standard of a user's life [3]. The idea of connecting the unconnected devices is almost 188 years old. It was introduced in 1832 when the first electromagnetic telegraph was invented. At that time, the idea was translated into the terms "Embedded Internet" or "Pervasive Computing," and the first-ever connected device was Coca-Cola vending machine [4].

Today's term "The Internet of Things (IoT)" was first introduced by Kelvin Ashton in 1999 to advance communication and facilitate human interaction in a virtual environment. According to a survey, the number of connected devices touches the figure of 50 billion by the end of 2020 and will grow to 14.7 billion by 2023 [5]. Nowadays, IoT technology is primarily seen in industries and commercial sectors. The interconnected divergent kinds of intelligent gadgets vary from simple wearable and household devices to large machines. These objects contain chips that are used to inspect and pursue the facts. It is predicted that the IoT market will touch the figure of 5.8 billion by the end of 2020, which is 21% higher than in 2019. This technology is used in intelligent projects, i.e., smart cities, smart farming, smart homes, and health-care systems. According to Grand View Research, the small patient market generates around \$1.8 billion by the end of 2026 [6].

The significance and contribution of this research on IoT security and privacy are the well-being of humanity according to people's likes, needs, wishes, and desires without any explicit instruction to IoT devices. These devices also serve the community by aiding in surgery, weather forecasting, animal identification, and automobile tracking.

The rapid growth of intelligent devices made IoT a growing technology, so it is essential to understand the privacy and security challenges. It is necessary to understand and address these issues for human sake. Humans can get benefit to handle these security and privacy threats in IoT. This systematic literature review (SLR) provides significant guidelines for IoT security and privacy issues. In this study, 170 research articles have been used as a reference to conduct the survey for security and privacy issues in IoT.

2. Literature Review

Tremendous work and effort have been made recently to cope with safety and confidential problems in IoT. Many reports and surveys are published to address IoT security-related issues and challenges. Yang et al.'s survey presents the safety and personal issues with solutions directly related to low-end systems [7]. Different authors briefly discuss the IoT security-based issues and challenges for networks, devices, and systems [2]. Weber and Gopi and Rao's surveys discuss the challenges and issues concerned with security in four steps such as (1) limitations of IoT devices like battery life extension, (2) lightweight com-

putation, (3) classification of security attacks, and (4) control access mechanisms and architecture [8, 9]. The discussion is also available on different IoT architecture layers (presentation, network, transport, and application).

Weber's survey discusses security and privacy challenges, and researchers also present a security framework for IoT-based devices [8]. The IoT devices are getting fame globally that involve other innovating technologies widely used in the whole world to transport goods from region to region. This technology is visibly becoming familiar. The low-ended devices contain different sensing gadgets and also have the capacity to interconnect with other similar gadgets and can transmit facts or information. The main challenge of IoT devices is related to privacy and security. The administration of that extensive data to process reliably and securely in machines is a real problem. These IoT also present challenges for individuals' protection, safety, and confidentiality. In this research article, the authors discuss the growing requirement of this technology for appropriate regulatory and technicalities to heal the gap between automated surveillance by IoT-based devices and the official rights of people unaware of their safety and confidentiality risk. Aleisa and Renaud identify the issues and challenges related to IoT privacy, its principles, threats, and proposed solutions [10].

Tewari and Gupta presented another survey for security-related problems in IoT devices. This article analyzes IoT devices' layered architecture and highlights new security issues. They discussed the crosslayer heterogeneous integration problems and provided tools and techniques for research in IoT [11]. The comparison of different studies in various aspects (simulation tools, mechanisms, IoT devices security, and privacy) was made by Noor and Hassan in 2019. It explores the current IoT security mechanisms such as authentication, security encryption, trust management, and emerging technologies to secure IoT devices [12].

Further, a study is presented on personal and safety-related problems identified by the experts in IoT devices and highlights how privacy is different from the other fields. It contains facts belonging to IoT specialists who tried to perceive safety and confidential problems and proposed new security protocols for efficient security and privacy mechanisms (SPMs) [13]. Most all connected devices have high risks and threats and can be hacked.

The objective behind this malicious act may differ depending upon the intruder's intention. There are mainly two types of threats, i.e., natural threats and human threats. The data can be protected from natural hazards, but devices may be physically damaged and not be restored. Moreover, many researchers have made tremendous efforts to protect IoT devices from human-generated threats and attacks. Table 1 shows the comparison of different types of attacks in IoT.

Cybersecurity threats can be categorized into two main types based on their objectives. The intruder intends to knock out the targeted device in the first type completely. In the second type, the attacker aims to get the privileges of admin or unauthorized access privileges to targeted devices. Divergent methods are utilized to gain unauthorized access, i.e., malware, denial of service, SQL injection, and cybercriminal. With the advancement of technologies, these

TABLE 1: Comparison of security and privacy attacks in IoT.

Reference paper	Attack type	Citation	Year	Objectives
Sybil attacks and their defenses in the IoT [14].	Sybil attacks	131	2014	Sybil attacks and defenses scheme research issues for Sybil defense in IoT.
Deceptive attack and defense game in honeypot-enabled networks for the IoT [15].	Deceptive attack	38	2016	Designed and extended a game-theoretic model.
Secure Location of Things (SLOT): mitigating, localization, and spoofing attacks in the IoT [16].	Spoofing	04	2017	The maximum likelihood estimator (MLE) for the tag's location is essential to protect IoT devices from malicious attacks.
Securing the SDN infrastructure of IoT-fog networks from MitM attacks [17].	Man in the middle attack	12	2017	The security issues of open flow channels like MitM attacks.
A security design for detecting buffer overflow attacks in IoT devices [18].	Buffer overflow attack	02	2018	They suggest lightweight design methodologies and architectural techniques to solve IoT devices' security problems.
Side-channel security analysis of our signature for cloud-based IoT [19].	Side-channel security	04	2018	Proposed an algorithm to secure UOV and related signatures from side-channel attacks.
IoT application protection against power analysis attack [20].	Power analysis attack	11	2018	Different attack scenarios of SPA introduced a branchless countermeasure approach.
Security in fog computing: a novel technique to tackle an impersonation attack [21].	Impersonation attack	12	2018	Q-learning algorithm detects the impersonation attack more accurately in fog computing-based networks.
Routing attacks and mitigation methods for RPL-based IoT [22].	Routing attacks	18	2018	Discussed RPL comprehensively. Study and present the RPL standard, mitigation methods, and published attacks in detail.
DDoS attack detection and mitigation with software-defined IoT framework [23].	Distributed DoS	44	2018	Introduced a framework for software-defined Internet of Things (SD-IoT).
Extensive validation of a SIR epidemic model to study the propagation of jamming attacks against IoT wireless networks [24].	Jamming attacks	01	2019	Proposed the SIR epidemiological model for jamming attacks in physical and MAC layers in IoT wireless networks.
A mobile code-driven trust mechanism for detecting internal attacks in sensor node-powered IoT [25].	Internal attacks	03	2019	Introduced the energy-efficient mobile code-driven trust mechanism (MCTM) to identify and handle malicious forwarding attacks, like a black and grey hole.
Analytical model for Sybil attack phases in the IoT [26].	Sybil attacks	03	2019	Sybil attacks from the IoT perspective comprehensively. Introduced and implemented an algorithm based on K -means clustering.
RAV: relay aided vectorised secure transmission in physical layer security for the IoT under active attacks [27].	Active attacks	05	2019	Introduced a transmission scheme for IoT networks to secure downlink communication.
An efficient collision power attack on AES encryption in edge computing [28].	Power analysis attack	04	2019	Discussed three AES implementations in edge computing. Introduced a new type of collision attack for masked linear layers and masked S -boxes.
IoT-FBAC: function-based access control scheme using identity-based encryption in IoT [29].	Access control	06	2019	They have proposed a new scheme to control access to IoT devices. They named it the function-based access control scheme.
A real-time intrusion detection system for wormhole attacks in the RPL-based IoT [30].	Wormhole attack	09	2019	Proposed a system to detect wormhole attacks. This intrusion detection system runs on Contiki OS and Cooja simulator.
Detection of multiple-mix-attack malicious nodes using perceptron-based trust in IoT networks [31].	Malicious node	03	2019	We mainly discussed three attacks: replay, tamper, and drop. Suggest an approach of perceptron detection (PD) to identify malicious nodes.
Averaged dependence estimators for DoS attack detection in IoT networks [32].	DoS attacks	06	2020	They have proposed a framework for DoS detection. Experimentally tested this framework with an actual IoT attack.
Deep recurrent neural network for IoT intrusion detection system [33].	Intrusion detection System	03	2020	Proposed an automatic intrusion detection system to implement fog computing security against cyberattacks.

cyberattacks are also getting advanced. Cyberattacks pull the attention of researchers [2, 7, 9, 13, 18, 30] to address these issues, but still, these issues are needed to be addressed.

With the growth of connected devices, problems and challenges are also increasing rigorously. Many new and emerging technologies are integrated with IoT to overcome these issues, i.e., fog computing, artificial intelligence, and blockchain. These advanced technologies are also used in collaboration with IoT to solve security and privacy issues. These technologies, especially blockchain, are gaining the attention of researchers and playing the role of a trusted third party. The blockchain can protect IoT devices, security, and safety-critical data. Integrating blockchain with IoT technology can provide an effective solution for security- and privacy-related issues and the challenges of IoT gadgets. Many researchers [3, 8, 15, 20, 28, 34, 37, 39, 43] also address the collaboration of these technologies and provide a robust solution. Table 2 presents some work done by researchers in recent years to address IoT security threats and attacks.

IoT applications are used globally to facilitate users, but there are still issues with security and privacy. Many researchers have discussed significant guidelines and solutions to cater to these issues. Table 3 shows the comparison of cyberattacks in IoT applications.

Another study is conducted by Sengupta et al. about the industrial IoT issues. It classifies the security and privacy attacks on their destructibility that explains to provide a blockchain-based solution [74]. Further, Wang et al. and Weber have discussed blockchain technology and explored some features such as access management, decentralization, asymmetric encryption, and smart contracts [75, 76]. Khan and Salah discussed the layered architecture networking, management, and communication protocols [77]. Another study conducted by Qian et al. explores layer-based architecture security and privacy problems for IoT [78]. The proposed security mechanisms eliminate the need for a third party to protect IoT terminal devices [79]. The security mechanism using blockchain technology's decentralization feature in two conditions has been discussed in the remote cloud, network terminal, and devices [80, 81]. Bitcoin currency is a modern and visibly growing blockchain-based technology [82, 83]. IoT devices are progressively inclined to assault and cannot ensure themselves [84]. Besides that, it cannot be handled after the execution of the blockchain [85]. The solution for blockchain to eliminate safety is to use confidential transmission of the facts and figures [86–88].

3. Review Methodology

The study is grounded in an SLR on IoT security and privacy issues by analyzing a significant data stream of substantial literature. There are three classified phases: planning, conducting, and reporting the review. Figure 1 describes the classified phases for this study.

3.1. Phase 1: Planning the Review. To conduct SLR on security and privacy issues in IoT, we followed the methodology proposed by Kitchenham [89]. The main work is divided

TABLE 2: IoT security threats and attacks.

Focus area	References
Insecure nearest node discovery	[22, 34, 35]
Replay attack	[6, 36, 37]
Sleep deprivation attack	[38–40]
Buffer overflow attack	[6]
Jamming attacks	[41–43]
DoS attacks	[6, 44]
Spoofing attacks	[45–47]
Insecure initialization and configuration	[41–43, 45, 48]
Routing attack	[49–51]
Sinkhole and wormhole attacks	[52–54]
Sybil attacks	[14, 55–57]
Authentication and secure communication	[52, 53, 56–60]
End-to-end security	[61, 62]
Session hijacking	[63–65]
Deprivation attack	[66, 67]
Insecure interfaces	[68]

into three steps: planning, conducting, and reporting the reviews.

3.1.1. Study Selection. This step describes the criteria to select material by studying the abstract, introduction, and conclusion sections of different research papers. Only those research articles are selected that fulfill the following requirements:

- (i) Written in the English language
- (ii) Describe the security challenges of IoT devices
- (iii) Discuss the emerging technology-based solutions to IoT devices' security and privacy issues
- (iv) Provide information about IoT devices
- (v) Provide information about IoT threats
- (vi) Present techniques to solve the problems of IoT devices
- (vii) Published between 2003 and March 2021

Further, some absolute principles are excluded:

- (i) Papers are not written in the English language
- (ii) Papers related to IoT devices and applications were issued before 2003
- (iii) Papers do not relate to IoT devices
- (iv) Papers with less than four pages
- (v) Papers that do not report any empirical study and solution
- (vi) Papers without significant opinions and viewpoints
- (vii) Irrelevant theses

TABLE 3: Comparison of cyberattacks in IoT applications.

Reference paper	Cited by	Year	Objectives
Cyberentity security in the IoT [69].	111	2013	The cyberentity domains in the U2IoT. Cybersecurity requirements, security attacks, and system vulnerabilities in the context of the cyberentities in the U2IoT.
Cybersecurity and the IoT: vulnerabilities, threats, intruders, and attacks [70].	221	2015	Cybersecurity attacks. Identification and vulnerabilities of threats. Malicious attacks.
Defense against black holes and selective forwarding attacks for medical WSNs in the IoT [71].	43	2016	Issues in wireless routing. Cyberattacks on IoT devices, especially black holes, and selective forwarding (SF) attacks.
Intrusion detection system to detect sinkhole attack on RPL protocol in the IoT [72].	76	2017	Identify the sinkhole attack in the network. Introduced an intrusion detection system (IDS) based on RPL as a routing protocol.
Cybersecurity threats to IoT applications and service domains [73].	30	2017	Discussed IoT applications and also presented significant cybersecurity challenges and issues.

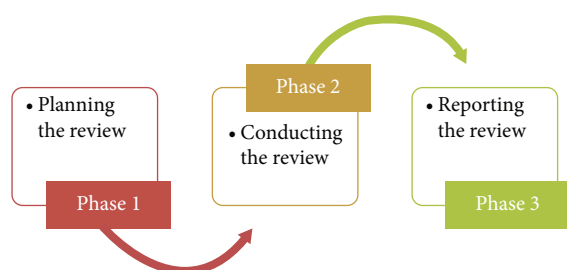


FIGURE 1: Systematic literature review (SLR) planning phases.

3.1.2. Data Extraction and Quality Assessment. To perform the quality assessment of this article, both qualitative and quantitative methods are used. There is no restriction in terms of experimental design. A quality assessment study checklist ensures the data extraction fulfills the quality criteria. Table 4 shows a list of general questions to measure the quality of selected papers by using two scales for the quality assessment checklist: yes = 1 and no = 0.

3.1.3. Identification of the Need for Review. The main objective of this study is to closely analyze the existing literature on IoT security, privacy, and threats to IoT systems. The study highlights significant research findings in the field of IoT security. The other purpose of this study is to emphasize utilizing emerging technologies for better solutions.

3.1.4. Inclusion/Exclusion Criteria. The criteria of inclusion and exclusion of papers are decided based on the significance of the literature. Initially, 500 papers were downloaded in IoT security and privacy. After the slight screening, 345 articles were filtered according to their duplication and irrelevance. The best 245 articles were identified in the next round by carefully reading their titles, abstracts, and introductions. Finally, we read full papers to further categorize them according to work needs, and 176 were selected to answer the questions related to our research problem. Figure 2 shows the inclusion and exclusion criteria for the selection of papers.

3.1.5. Specifying the Research Questions. The research questions are made based on the existing research studies. The

significant articles and in-depth knowledge motivate us to create questions.

The research questions for this study are described below.

RQ1: How has IoT evolved drastically in the modern era?

RQ2: What types of challenges and issues of IoT systems are essential to be addressed?

RQ3: Why do IoT security and privacy challenges need to be reported?

RQ4: How the security and privacy challenges are classified?

RQ5: How do emergent technologies can resolve these issues in IoT applications?

3.1.6. Bibliographic Database. We use some digital libraries to search for the required material: Academia, Science Direct, Google Scholar, Google Search, Springer, IEEE Xplore, and Research Gate to conduct this survey. These automated libraries comprise literature linked to the discipline of security and IoT. In this research article, the studies are limited to research journals and conference papers published between 2003 and 2021. Figure 3 describes the detailed information of the digital libraries used for this article.

We classified the papers based on the discussed attacks. Only 1% of the articles addressed access-level attacks, 16% described cryptanalysis attacks, and 10% discussed network-based security issues. The percentage of other attacks is presented in Figure 4.

3.2. Phase 2: Conducting the Review. Figure 5 shows the three subphases for the review: (i) study selection, (ii) data extraction and quality assessment, and (iii) data extraction and synthesis.

The umbrella terms such as security, privacy, low-ended devices, and small automatic and fully automated devices are identified to determine the search engine. In the end, the Boolean operators “OR” and “AND” combine the various keywords and create different combinations for searching terms related to research questions. Some examples of keywords and operators to extract data are given:

- (i) Security “OR” privacy issues “OR” security “OR” privacy challenges “OR” problems

TABLE 4: Quality assessment of the survey.

No	Item	Yes	No
Q1	Are the aims and objectives of the research clearly stated?	1	
Q2	Does the author review previous studies?	1	
Q3	Is current and relevant research used?	1	
Q4	Does work seem helpful for this research?	1	
Q5	Does the author appear to have any biases (gender, race, class, or politics)?		0
Q6	Is the writing clear and easy to follow?		0
Q7	Are visuals such as tables, charts, maps, and figures helpful?	1	
Q8	Are visuals such as tables, charts, maps, and figures confusing or hard to read?		0
Q9	Is there any need to conduct more research on this subject?	1	
Q10	Is the article relevant to this domain of research?	1	
Q11	Have the researcher(s) adequately carried out the data collection process?	1	
Q12	Have the researcher(s) used enough data to support their results and analysis?		0
Q13	Is there a detailed comparison of other techniques in the experiment?		0



FIGURE 2: Flow diagram for the inclusion and exclusion criteria.

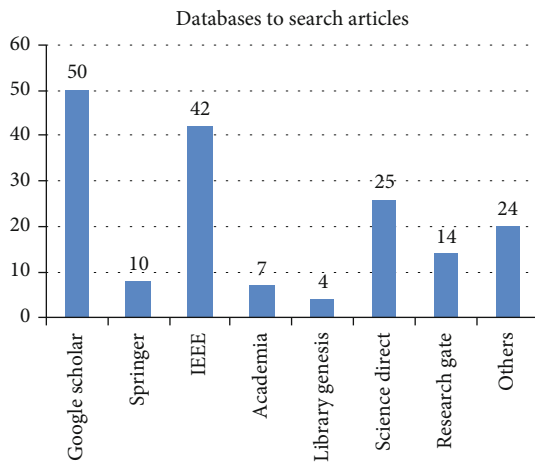


FIGURE 3: Databases used to search research papers.

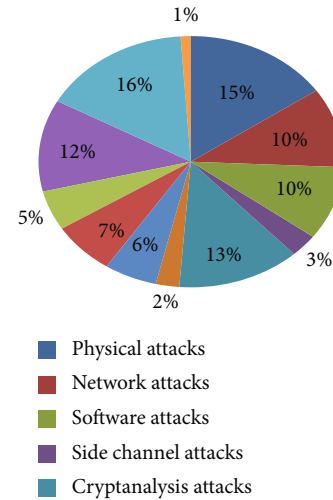


FIGURE 4: Databases used to search research papers.

- (ii) IoT “OR” low ended “OR” small “OR” handheld “OR” consumer connected “OR” smart “OR” automated “OR” mobile devices
- (iii) Security “OR” privacy issues “OR” challenges in IoT devices “AND” security problems in smart devices “AND” security challenges in mobile devices

3.3. Phase 3: Reporting the Review. In this phase, the discussed research questions are answered by keeping in mind the significance of the study.

3.3.1. RQ1: How Has IoT evolved Drastically in the Modern Era? IoT technology is growing faster day by day and dominating globally. According to a survey conducted in 2019 by

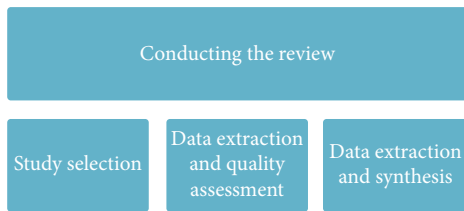


FIGURE 5: Phases for conducting the review.

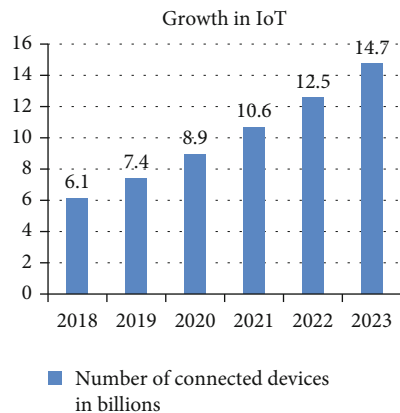


FIGURE 6: Growth in IoT devices during 2018-2023 [6].

Gartner, it is predicted that the IoT market will touch the figure of 5.8 billion by the end of 2020, which is 21% higher than in 2019 [6]. According to a current report for the year 2018-2023 that Cisco IBSG conducts, the number of connected devices was 6.1 billion in 2018 and will grow to 14.7 billion by 2023. The growth of IoT devices is shown in Figure 6.

3.3.2. RQ2: What Types of Challenges and Issues of IoT Systems Are Essential to be Addressed? Nowadays, the rapid growth of intelligent devices made IoT a growing technology. It is essential to understand all challenges and deal with issues related to these devices; the advancement and maintainability of IoT devices make these systems complex to manage. The system cannot prevail due to these IoT issues such as outdated software and hardware, compatibility issues, security issues, cloud attacks, modifications, difficulties related to passwords, low-ended worms, facts related to security, and confidential provocations. Further, IoT discrepancies may also occur due to untrustworthy communication, problem finding the device's effectiveness, automation systems for data management, limited IoT device management, low power network support, IoT operating systems, and processor-related issues [77, 90].

3.3.3. RQ3: Why Do IoT Security and Privacy Challenges Need to Be Reported? Advancements in technology can be seen in recent years, introducing variant types of IoT devices. These devices are connected to many networks and each other, making them vulnerable and easy to attack. To mitigate the vulnerabilities of the devices that share sensitive information/data, it is essential to identify all possible attacks to make countermeasures or defense strategies. Figure 7 shows the different issues and challenges in IoT devices.

3.3.4. RQ4: How the Security and Privacy Challenges Are Classified? The security threats in IoT are classified into various types like physical attacks, network attacks, software-based attacks, data attacks, side-channel attacks, cryptanalysis attacks, access-level attacks, and strategy-level attacks. Figure 8 shows the classification of IoT security attacks.

(1) Physical Attack. In physical attacks, direct physical access to the devices is required. Physical attacks utilize the hardware components of IoT devices [70, 91]. Based on interaction with the targeted systems, the physical attack is classified into three categories, i.e., invasive attacks, noninvasive attacks, and semi-invasive attacks [92, 93].

Invasive attacks: the category of attacks in which the attacker needs to approach the chips or detach the targeted devices physically is known as invasive attacks. High skills and specialized tools are required to launch invasive physical attacks depending on what type of attack is to be established and IoT device [92].

Noninvasive attacks: in this category of physical attacks, the attacker approaches the targeted devices using the device's input interface. These attacks harm the targeted IoT devices without physical damage.

Semi-invasive attacks: in this category of physical attacks, the attacker approaches the targeted IoT devices without interacting with internal structures and wires.

Jamming attacks: these attacks are designed to block IoT network wireless communication channels by employing malicious nodes that generate noise signals [94]. Other categories known as reactive jamming attacks generate the interfering signals only when the transmission channels communicate [95].

Object replication: this type of attack intruder injects a duplicate node into the IoT network to alter its function. The objective of object replication attacks is to steal the information and authentication credentials by introducing a replicated malicious node [96, 97].

Malicious node injection attacks: in malicious node injection attacks, attackers physically inject a malicious node between two or additional existing nodes of an IoT network. The term "man in the middle attacks" can also be referred to as "malicious node injection attacks" [91, 98].

Sleep denial attack: these attacks affect the sleep mode and keep the device awake to increase the battery consumption and affect IoT devices. In some cases, these attacks transfer unauthenticated packets; the decoding of these transmitted packets causes wastage of battery. The intruder observes the IoT networks to determine when to reseal the packet [99, 100].

Tampering attacks: the main objective behind node tampering attacks is to access the IoT device to alter other communication layers' functions or steal the data like cryptographic keys [101, 102].

Permanent denial of service (PDoS): permanent denial-of-service attacks (PDoS), also known as plashing, is an attack that damages the device so severely that it requires replacement or reinstallation of hardware. BrickerBot, coded to exploit hard-coded passwords in IoT devices and cause a permanent denial of service, is one such example of malware

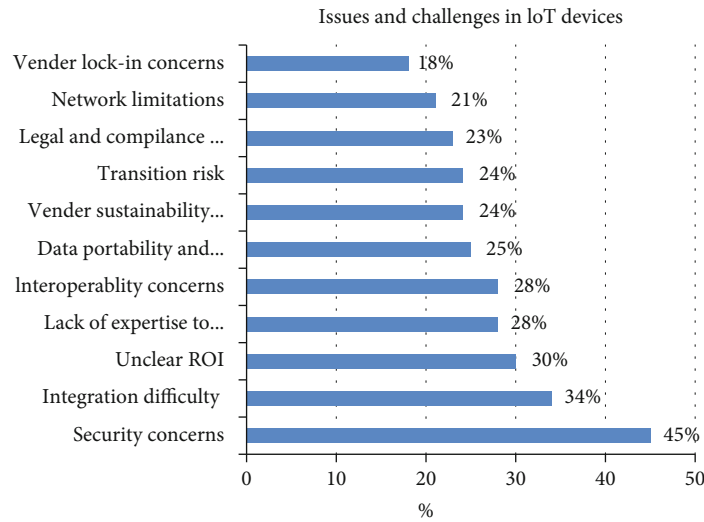


FIGURE 7: Comparison of issues and challenges of IoT [6, 9].

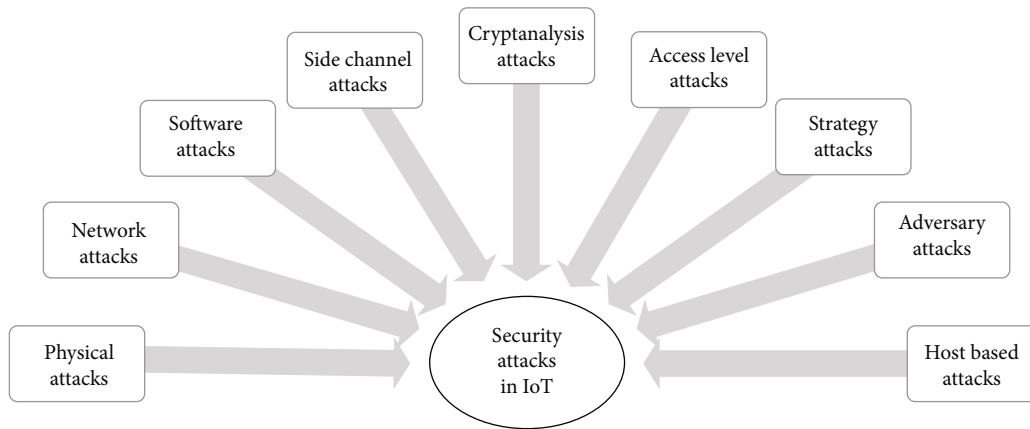


FIGURE 8: Classification of IoT security attacks.

that could be used to disable critical equipment on a factory floor wastewater treatment plant or an electrical substation [103].

Fake node injection: fake node injection attacks are one of the most damaging attacks for IoT devices in which attackers insert a malicious node or generate a false identity with the help of a fake node to access the IoT network and flow the incorrect information hits all the nodes in the network [104]. These attacks also lead to poor performance by consuming whole IoT system resources. In worse cases, false node injection attacks can destroy the entire IoT network or help the attacker take complete control of the IoT network [105].

Hardware Trojan: in HT, attackers physically insert a malicious circuit or modify an existing circuit in IoT devices to alter the circuit’s operation. The primary purpose behind Trojan attacks is to bypass the authentication and access control mechanisms, steal information, or seriously damage the chips [106]. In HT, attackers physically insert a malicious circuit or modify an existing circuit in IoT devices to alter the circuit’s operation [107].

Outage attack: outage attacks prevent remote IoT devices from completing their routine task. In worse cases, these attacks turn off IoT devices. Outage attacks may launch a sleep denial attack and drain the battery to shut down the remote IoT device [108]. An example of these attacks is Stuxnet, inserted in Iran’s nuclear process control program. Due to the Stuxnet attack, the system cannot detect emergency conditions. Therefore, it does not turn off [109].

Tag cloning: the tag cloning attacks scan the RFID tags from the targeted device into the attacker’s defined RFID tag, providing access to confidential information about individuals. The tag cloning attacks can cause financial loss and damage the manufacturer’s image in the market [110]. Tag cloning attacks are launched to access highly confidential data such as information account bank accounts [111].

Radio frequency interference attacks: in RF interference attacks, powerful radio frequency signals are utilized to disrupt RFID communication between IoT devices. Attackers use radio frequency signals to generate solid interfering signals, known as radio jamming attacks [96, 112].

TABLE 5: Comparison of physical attacks in IoT.

Sr. #	Security issue	Reference	Affected layer	IoT level	Category	Attack type
1	Jamming	[28, 95]	Physical layer	Low level	Physical attack	Active
2	Object replication	[97, 104]	Network layer	Low level	Physical attack	Active
3	Malicious node injection	[91, 98]	Network layer, perception layer	High level	Physical attack	Active
4	Sleep denial attack	[99, 100]	MAC layer, physical layer	Low level	Physical attack	Active
5	Tampering	[101, 102]	Physical layer	Low level	Physical attack	Active
6	Permanent denial of service (PDoS)	[6]	MAC layer	High level	Physical attack	Active
7	Fake node injection	[36, 105]	Network layer	High level	Physical attack	Active
8	Hardware Trojan	[39, 108]	Application layer	Low level	Physical attack	Active
9	Outage attack	[109]	Network layer	Low level	Physical attack	Passive
10	Tag cloning	[111]	Perception layer	Intermediate level	Physical attack	Active, internal
11	Radio frequency interference attacks	[96, 112]	Application layer, physical layer	Intermediate level	Physical attack	Active

A detailed comparison of physical attacks in IoT devices has been summarized in Table 5.

(2) *Network Attacks*. The network attacks are classified into the following subtypes.

Sinkhole attack: to launch sinkhole attacks, intruders inject a malicious node that presents itself to other IoT network nodes as the best shortest channel for communication. This malicious node collects and “sinks” all of the information packets which flow on the targeted IoT network. Therefore, this malicious node is called a “sinkhole,” and these attacks are named “sinkhole attacks” [113]. These attacks reduce the performance of targeted networks because the whole traffic of the IoT network flows towards the sinkhole. Still, this malicious node does not drop even a single message packet; they also harm the other performance-related attributes like efficiency and reliability of communication and disrupt the network protocols, especially the RPL protocol of IoT networks [114, 115].

Wormhole attack: in wormhole attacks, the attackers generate private channels between two or more nodes of an IoT network by controlling these nodes or injecting malicious code into the network to alter the transmission path, and attackers receive the transmitted information and send only the selective packet to the destination. Wormhole attacks are launched to damage network topologies and disturb network traffic [116–118].

Sybil attack: in Sybil attacks, attackers generate multiple fake identities by injecting a malicious node that pretends as multiple ordinary users. They are single user or attacker who launches divergent identities by utilizing a single platform. Fake profiles on social media sites like Twitter, Facebook, or Instagram also fall into Sybil attacks [119]. They also can be launched to attack routing algorithms [14].

Selective forwarding: in selective forwarding attacks, the attacker launches a malicious node placed on the route between the source and a destination node, which acts like

a black hole that receives all the message packets flowing on the IoT network, but in this case of selective forwarding, the malicious node sends only the particular message packets to the destination and drops the remaining message packets. Selective forwarding attacks can filter all types of traffic [120, 121].

Traffic analysis attack: in traffic analysis attacks, the attackers launch a malicious node to notify the daily traffic routines to collect the routing information. The encryption of message packets is not enough to protect the IoT network from traffic analysis attacks. The distance from the root node and the less information is collected [122].

Man in the middle attack: man in the middle attacks attackers launch a malicious node between two nodes to intercept the two nodes’ communication without their permission. The concept of man in the middle attacks is similar to the middle person who intercepts the communication between two persons by opening the letters before handing them over to the original recipient. IoT devices can launch these attacks by implementing various SSS hijacking, session hijackings, DSN spoofing, or side jacking [111, 123].

Routing information attack: routing information attacks are launched to redirect, spoof, misdirect, and drop the information packets. These attacks are projected to alter the way of message routing [104]. The altering attacks also fall in this category, launched to modify the routing information. Network partitioning, routing loop, rushing, and replay routing information are also subtypes of routing information attacks [120].

RFID spoofing: in RFID unauthorized access, attackers read the information of RFID tags without user permission. RFID systems do not have robust mechanisms to protect IoT devices because RFID tags are readable to everyone [124].

RFID unauthorized access: in RFID unauthorized access, attackers read the information of RFID tags without user permission. RFID systems do not have robust mechanisms to protect IoT devices because RFID tags are readable to everyone [124].

TABLE 6: Comparison of network attacks in IoT.

Sr. #	Security issue	Reference	Affected layer	IoT level	Category	Attack type
1	Sinkhole	[114, 115]	Network layer	Intermediate level	Network attacks	Active
2	Wormhole	[116, 117]	Network layer	Intermediate level	Network attacks	Active
3	Sybil	[14]	Network layer	Intermediate level	Network attacks	Active, internal
4	Selective forwarding	[120, 121]	Network layer	Low to intermediate	Routing attacks	Active, internal
5	Traffic analysis attack	[122]	Network layer	Low level	Network attacks	Passive
6	Man in the middle attack	[111, 123]	Network layer	Low to intermediate level	Network attacks	Active
7	Routing information attack	[120]	IPv6Network layer	Intermediate level	Network attacks	Active
8	RFID spoofing	[127–129]	Physical layer, network layer	Low level	Network attacks	Active
9	Unauthorized access	[124]	Perception layer	Intermediate level	Network attacks	Active
10	Replay attack	[126]	6LoWPAN adaptation layer and network layer	Intermediate level	Network attacks	Active
11	DoS/DDoS attack	[104]	Perceptions layer, network layer	High level	Network attacks	Active

Replay attack: in replay attacks, an attacker receives, stores, intercepts the message packet, replays or resends it, and presents it as its packet. Intruders gain the trust of the targeted IoT node by sending a message packet. Once attackers develop confidence, they access specific information such as packets received by the sensors or message packets sent to a cloud-based server [125]. The replay attacks are deceptive attacks that decrease network performance because they utilize network resources like bandwidth and are launched against protocols used for authentication [126].

DoS/DDoS attack: DoS attacks also affect network communication. DoS attacks are launched to affect data transmission between nodes by jamming the radio signals or injecting the fake malicious node on the IoT network [104].

A detailed comparison of network attacks in IoT devices has been summarized in Table 6.

(3) *Software Attacks.* Software attacks are malicious programs or codes that are put down purposefully to damage, harm, or gain unauthorized access to someone's device.

Operating system attacks: operating systems have to run many services and many open ports; by using these open ports, attackers installed malicious programs to alter the functions and steal the data or information.

Viruses: it is a computer program that can make copies by replicating itself and can infect other devices by transmitting via transferring infected files through wire or wireless networks, USBs, or different such types of portable devices. Due to limited memory and storage space and lack of update mechanisms, it is challenging to secure IoT gadgets from viruses, so they quickly become victims of attackers. Mirai, SILEX, Stuxnet, and BrickerBot are some types of viruses created to attack IoT devices [112]. CIH is a virus that attacks BIOS, and due to the CIH Virus attack, IoT devices are unable to boot [130].

Worms: a worm is a virus that can replicate itself but cannot alter the system's files or functions. Worms continuously repeat themselves to create copies and fill the entire

disk and memory space, so worms slow down or crash IoT devices. UbootKit is a worm that infects divergent types of IoT devices and affects the bootloader of IoT gadgets. This worm can transfer from one device to another and fully control these devices [130]. Linux bricking worm can disable the infected IoT device [131]. Silex is another worm that overwrites IoT devices' storage disks [132]. BrickerBot is a worm that destroys or bricks the infected IoT devices [133].

Trojan horse: Trojans are malicious programs that seem harmless to the user and are downloaded and installed into the device by tricking them. After activation, it harms the user's devices by stealing data, deleting user files, or spreading viruses, worms, or other malicious applications. Hackers can control IoT devices through Trojan attacks or capture username, passwords, screenshots, bank details, and account information [134]. Hackers use Zeus Game over Trojan to attack IoT devices to access bank account details [135].

Phishing attacks: in phishing attacks, the malicious program is usually intruded on by a fraud communication that appears to come from reliable sources. Phishing attacks' objective is to steal information like the device's password or username or activate a malicious application into an IoT device [91, 136].

Backdoor attacks: back door is a malicious and complex code that can bypass authentication processes to remotely access system resources. The operating systems for IoT devices like RTOS or Contiki have back doors that can be used to gain unauthorized access [137]. This type of attack has been designed to hack an IoT system by breaking its security mechanisms such as cryptography and authentication using different techniques.

Brute force search attacks: brute force search attacks are programs that use divergent techniques to hack and break IoT applications' security mechanisms [138].

A detailed comparison of operating system attacks in IoT devices has been summarized in Table 7.

(4) *Web Attacks.* IoT web applications have numerous weaknesses due to poor coding. Hackers use these weaknesses to

TABLE 7: Comparison of operating system attacks in IoT.

Sr. #	Security issue	Reference	Affected layer	IoT level	Category	Attack type
1	Viruses	[2, 130]	Application layer	Intermediate level	Software attacks	Active
2	Worms	[5, 130, 133]	Application layer	Intermediate level	Software attacks	Active
3	Trojan horse	[7, 135]	Application layer	Intermediate level	Software attacks	Active
4	Phishing attacks	[91, 136]	Application layer	Low level	Software attacks	Passive
5	Backdoor attacks	[137]	Data processing layer	Low level	Software attacks	Active
6	Brute force search attacks	[12]	Transport layer, network layer	Low level	Software attacks	Active

access these IoT web applications' databases or servers containing sensitive personal or financial information. In some cases, the IoT web applications are linked with other infected applications, due to which these software applications become vulnerable to divergent attacks [112]. The standard web applications attacks are the following.

DDoS attacks: in DDoS attacks, hackers block the system or network resources. A most common example of a DDoS attack in IoT is access denial to a resource by flooding it with too many requests [23, 139].

Explication of a misconfiguration: security misconfiguration is improper configuration settings or mistakes in the configuration which cause misuse of data, privileges, and passwords. The poorly configured IoT applications lead to security- and privacy-related issues. In many IoT devices, the poor configuration, default settings, or technical issues of databases, operating systems, and other such components arise many security problems.

Malicious code injection: malicious code injection is when attackers attempt to control IoT devices or IoT networks by physically introducing malicious code into the device or IoT network nodes. The main goal of injecting this code is to steal data and bypass the access controls [91, 112, 140].

SQL injection attacks: SQL injection attacks are the subcategory of injection attacks. In these SQL injection attacks, attackers inject malicious SQL queries to access a database server to retrieve the information inaccessible to attackers [141].

Path-based DoS attacks: in these types, attackers attack multiple hop paths end-to-end communication by flooding data packets. The path-based DoS attacks can quickly have launched and affect or destroy a very large portion of IoT networks, usually wireless sensor-based networks. The path-based DoS attacks harm the IoT networks by sending too many legitimate packets and engaging the whole network resources to the desired device [142, 143].

Malware is an abbreviation of malicious software intentionally designed to damage computers and IoT devices to steal personal data, bypass access controls, and harm computers and IoT devices without the user's permission. IoT malware such as Aidra, Mirai, and Bashlite are IoT malware families that scan the machine to look for open ports to gain access [144].

Spyware: malicious hackers attack IoT devices by using spyware. Spywares are malicious software applications that collect information about users' activities without their knowledge instead of physically damaging IoT devices. Some IoT Spywares like Duqu are designed to monitor users' web

browsing habits [145]. IoT spyware can record videos and send them to intruders through emails. sKy Wiper is another example of spyware. This spyware can record microphone signals or communication and send them to intruders through a Bluetooth connection [134].

Reprogram attack: in reprogramming attacks, intruders attack the IoT devices by using weakly protected programming codes; attackers modify or reprogram the code to control IoT devices or in some cases; they hijack the code to contain the entire IoT network. IoT devices can easily be reprogrammed remotely by modifying network programming systems [146].

A detailed comparison of web application attacks in IoT devices has been summarized in Table 8.

(5) *Firmware Attacks.* New vulnerabilities are designed to attack the Internet every day, so installing new security patches and updating the firmware in IoT devices are very important. The diverse variety of IoT devices cannot update their systems regularly.

Control hijacking: in this type of attack, intruders made modifications in coding to hijack the IoT systems' control and affect the control flow. These attacks are format string vulnerability, buffer overflow attacks, and integer overflow attacks [147].

Reverse engineering: in reverse engineering attacks, intruders damaged the embedded IoT devices and generated serious issues by analyzing IoT software applications such as firmwares. Attackers look for input parsing errors in the program's code, and then, the attacker advertised his skills to resolve the issue and get access to the device's sensitive data [148, 149].

Eavesdropping: eavesdropping attacks are passive attacks in which attackers take advantage of poorly secured network transmission and steal information during transmission from IoT devices. We can say that intruders hear or read the victim's conversation secretly. The eavesdropping attacks are hardly detected because they do not affect the IoT network's normal working [70, 150].

A detailed comparison of firmware attacks in IoT devices has been summarized in Table 9.

(6) *Side-Channel Attacks.* The side-channel attacks are the most hardware-based severe IoT attacks. IoT devices are more vulnerable to these attacks due to limited resources like battery power, storage and processing power, open doors for

TABLE 8: Comparison of web application attacks in IoT.

Sr. #	Security issue	Reference	Affected layer	IoT level	Category	Attack type
1	DDoS attacks	[23, 139]	Application layer, network layer	High level	Software attacks	Active
2	Explication of a misconfiguration	[112]	Network layer, application layer	Low level	Routing	Active
3	Malicious code injection	[91, 112, 140]	Application layer	High level	Software attacks	Active, external
4	SQL injection attacks	[141]	Application layer	Low level	Software attacks	Active
5	Path-based DoS attacks	[142, 143]	Application layer	High level	Software attacks	Active
6	Malware	[144]	Application layer, data processing layer	Low level	Software attacks	Passive
7	Spyware	[134, 145]	Application layer	Low level	Software attacks	Passive
8	Reprogram attack	[146]	Application layer	Low level	Software attacks	Active

TABLE 9: Comparison of firmware attacks in IoT.

Sr. #	Security issue	Reference	Affected layer	IoT level	Category	Attack type
1	Control hijacking	[147]	Transport layer	Low level	Software attacks	Active
2	Reverse engineering	[148, 149]	Application layer	Intermediate level	Software attacks	Active
3	Eavesdropping	[70, 150]	Physical layer	Low level to intermediate level	Software attacks	Passive
4	Malware	[144]	Data processing layer	Low level	Software attacks	Passive

side-channel attacks, and the problematic detection of these malicious programs [151, 152].

Timing attacks: timing attacks are launched by implementing timing variations such as overclocking, which is frequently utilized to inject malicious nodes or other IoT gadgets' faults to leak sensitive information [107]. These attacks can measure the time an application takes to finish specific tasks and then utilize it to steal sensitive data like bank account numbers, PIN codes, passwords, and cryptographic keys. The purpose behind side-channel timing attacks is to extract the key of encryption algorithms [93, 153].

Power analysis attacks: in power analysis, attackers closely measure the power consumed by various cryptographic hardware components of IoT devices and then analyze electric current change to extract the confidential information stored in devices. The power analysis attacks are further classified into three subcategories, i.e., simple power analysis attacks (SPA), differential power analysis attacks (DPA), and correlation power analysis attacks (CPA), which are described below [20, 93, 107, 154].

Fault analysis attacks: in fault analysis attacks, the attacker introduced a crypto node with fault and then analyzed the difference between correct and faulty text to extract the cryptographic key value. To launch this attack, intruder required special knowledge about the design of hardware devices. To inject the fault, attackers use various techniques like voltage glitching, tampering with clock pin, EM disturbances, and laser glitching [65, 154, 155].

Electromagnetic attacks: attackers capture and analyze electromagnetic radiations to extract sensitive personal information from IoT devices' hardware components like display screens. In some cases, attackers place a microan-

tenna closer to the integrated circuit (IC) to capture electromagnetic signals. These electromagnetic attacks are used in military operations [93, 107, 156].

Cryptanalysis attacks: the ciphertext-only attacks are launched to access encrypted information or ciphertext only; these attacks cannot let the attacker get the corresponding plaintext. The main challenge in these attacks is to convert the ciphertext into plaintext which determines these attacks' success in IoT systems [157].

Known-plaintext attacks: in known plaintext attacks, the attacker's main challenge is to extract the plaintext from the crypto text with some known plaintext, which is a small portion of this crypto text. To guess the remaining part of the crypto text, attackers may implement various methods like detecting the encryption key, or divergent shortcut techniques can also be applied [157].

Chosen-plaintext: in chosen-plaintext attacks, attackers access the encryption devices to extract the algorithm that encrypted the plaintext. The attacker then utilized this encryption algorithm to determine the encryption key by converting various time-divergent chosen-plaintext into crypto text and then analyzing and comparing the resultant crypto text through which the attacker generates the encryption key of an IoT-based cryptosystem [157, 158].

Chosen-ciphertext attacks: in chosen-ciphertext attacks, attackers attempt to get temporary access to the decryption mechanisms by converting the chosen-ciphertext into plaintext and then this plaintext to describe the subsequent ciphertext. Chosen-ciphertext attacks are related to decryption mechanisms in IoT systems [158].

(7) *Access-Level Attacks.* The IoT system contains limited resources and infrastructure, making them more vulnerable

to various attacks. In IoT systems based on access level, the security attacks are categorized into two types.

Active attacks: in active attacks, attackers read and attempt to modify the IoT-based system's message packets or hardware. The vigorous attacks affect the working of IoT networks. They can disrupt routing protocols by altering routing information [159]. The primary purpose is to insert errors or noise signals in message transmission [113, 160].

Masquerade attacks: in masquerade attacks, the attacker presents itself as another authenticated or real user and transmits data on the IoT network by using this fake identity [159].

Modification of message: in modification attacks, attackers tamper the message packets; they modify data, change the sequence of message packets, or cause delays in the delivery of the targeted message packets [159].

Repudiation: in repudiation attacks, attackers successfully send or, in some cases, receive the message, and after sending or receiving, he denies that he has received or sent any such type of message [159].

Replay: in replay attacks, intruders read, modify, and send it to the original recipient without their knowledge [126].

Denial of service attacks: in denial of service attacks, attackers made too many requests for resources to decrease IoT networks' performance [104].

(8) *Passive Attacks.* In passive attacks, the attacker accesses the message or steals the information stored in an IoT system and utilizes this data, but he does not modify the steered content. These attacks do not damage the targeted IoT systems but affect confidentiality. The main objective behind passive attacks is to steal secret sensitive information like bank account numbers, PIN codes, and passwords. In passive attacks, intruders observe circumstances and can switch from passive to active attacks [113, 160, 161].

Traffic analysis attacks: in a traffic analysis, the attacker secretly observes and stores the information about the IoT network. They record the various transmitted message packets like length, size, or sequence of message packets, which may help the attacker guess the conversation's nature [122].

Privacy attacks: in this type of attack, the intruder observes and records confidential, sensitive information and publically leaks this information later. These attacks are known as the "release of message content" [162].

(9) *Strategy Attacks.* To target IoT devices, attackers utilize divergent techniques that extract confidential information for an attacker. These techniques implement various strategies to inject malicious code, malicious nodes, or errors in IoT devices. Some systems require physical interaction and damage the hardware devices, while others can implement remotely.

Logical attacks: in logical attacks, attackers remotely access the IoT devices to launch the bug without physically damaging the device. In other words, the attacks in which attackers logically access the IoT devices by utilizing communication channels are named "logical attacks" [163].

Physical attacks: to launch physical attacks, attackers need to physically approach the targeted IoT device. These attacks also severely damage and modify the settings and configuration of the target IoT device. Tempering attacks and malicious node injection are examples of physical attacks [164, 165].

(10) *Adversary-/Location-Based Attacks.* An attacker can be an insider who understands the targeted IoT system or reside inside the boundary of the targeted IoT network, or it can be an outsider without any knowledge about the system or launch the attack from anywhere; therefore, based on adversary location, IoT attacks are classified into two main types, i.e., internal attacks or external attacks.

Internal attacks: an insider who has access to the device injects the malicious code or nodes in the IoT network. In these attacks, attackers belong to the same IoT network; they have deep knowledge about the implemented software technology, hardware devices, and complete IoT infrastructure [166]. These attacks are divided into four categories, i.e., unintentional actors, technology perception actors, compromised actors, and emotional attackers. These attacks affect the network layer and physical layer [167].

External attacks: an outsider remotely accesses the IoT network to inject an error or bug in external attacks. Attackers launch these attacks from anywhere or can utilize any other public network. Attackers have almost zero or very little knowledge about implemented technology and architecture of the targeted IoT system [168, 169].

(11) *Host-Based Attacks.* In host-based attacks, attackers target IoT devices' operating systems to extract cryptographic keys and other confidential information. Host-based attacks are launched by attacking host systems of IoT devices. These attacks are classified into three types, i.e., user-compromised attacks, software-compromised attacks, and hardware-compromised attacks.

User-compromised attacks: user-compromised attacks are launched to extract confidential data from IoT devices such as passwords, keys, and bank account details. In some cases, attackers launch these attacks to read or even hear their conversation [119].

Software-compromised attacks: software-compromised attacks are launched to exhaust IoT systems by overflowing the resource buffers. One example of software-compromised attacks suddenly runs out of the battery of IoT battery-operated devices [168].

Hardware-compromised attacks: IoT systems' attacker tamper hardware devices to steal data or inject bugs and malicious nodes in hardware-compromised attacks. To launch these attacks, attackers need to physically access the IoT devices [119].

3.3.5. *RQ5: How the Advanced Technologies Resolve These Security and Privacy Issues?* Undoubtedly, putting all the things on IoT gives us many intelligent devices to enhance digitalization. But still, there are many security and privacy

issues in the IoT that can be solved by integrating some advanced technologies to become more secure.

The blockchain technique can ensure the security of IoT that got compromised. A blockchain is a decentralized approach that makes an immutable database. The following features make it more trustworthy while discussing security. The miners do timestamp a chain of blocks and perform validation. Blockchain uses a powerful hashing technique, SHA-256, to authenticate and integrate data. Digital signatures were implemented for the verification. All the changes are made by verifying other blocks, i.e., having the valid node address. Putting in or retrieving data from a partnership does not involve any third that gains global trust. The connectivity of IoT with so many other devices makes it easy to attack. Blockchain is considered to get IoT out of vulnerability.

Especially in IoT, it becomes difficult to detect any countermeasures with the growing threats and their complexity level when numerous devices are attached [170]. Artificial intelligence (AI) could play a valuable role here, and the concept works as a system/machine is trained by giving some data. The given data makes a cognitive memory, and the system becomes artificial intelligence for the desired scenarios [171].

Artificial intelligence is followed by machine learning and deep learning algorithms that make machines artificially intelligent and efficient to make intelligent decisions [172, 173]. While discussing the IoT, an artificially intelligent system that uses an algorithm and machine/deep learning for processing the data can be trained to detect any threat and perform specific actions [174, 175].

3.4. Future Research Directions. Future directions provide the door for researchers to continue research in this significant area.

- (1) There is a need to develop a standard platform to share IoT-based research datasets
- (2) Keeping in mind the limited resources of IoT devices is the cost-efficient way to resolve IoT systems' security issues
- (3) There is a need to develop a cost-efficient blockchain-based solution to resolve IoT systems' security issues
- (4) There is a need to develop the most efficient artificial intelligence-based solution to resolve IoT systems' security issues
- (5) Secure the data stored in a remotely located publically accessible IoT system under the control of attackers
- (6) Implementing emerging technologies can resolve maximum security issues of IoT systems

4. Conclusion

This study emphasizes IoT systems' major security concerns to let the users know about the risks associated with these gadgets. To better understand, the classification of IoT threats into divergent categories has been made. Further, a detailed comparison of each class is provided.

The attacks launched by injecting malicious nodes to steal information packets and reduce the network's performance are classified as network attacks. To target both security and privacy simultaneously, attackers float side-channel attacks. In cryptanalysis attacks, the attacker accesses the decryption key to convert cipher text into plaintext. In access-level attacks, attackers take advantage of the limited resources to steal or alter the information. In active attacks, attackers read and modify the message packets, while in passive attacks, attackers can read the message but do not make any modifications. In strategy-level attacks, attackers implement various strategies to inject malicious code into the IoT devices. Some attacks require physical interaction and damage the hardware devices, so they are called physical attacks, while others can implement them remotely; therefore, they are called logical attacks. An attacker can be an insider who understands the targeted IoT system or can be an outsider without any knowledge about the system; therefore, IoT attacks are classified into internal or external attacks based on adversary location. In hardware-compromised attacks, the attacker tampers hardware to steal data. Software attacks are the injection of malicious programs purposefully to gain unauthorized access to the device. Due to poor coding, hackers access these IoT web applications, databases, or servers. Attacks launched due to a lack of firmware updates are called firmware attacks.

Further, we have classified these categories into subcategories. More than 75 IoT security threats are discussed in this systematic literature review to help manufacturers to secure IoT systems. In this modern era, new emerging technologies like blockchain, artificial intelligence, machine learning, and other advanced technologies (fog and cloud computing) are integrated with IoT technology to resolve security and privacy challenges. These emerging technologies, especially blockchain technology, can provide a better and more cost-efficient solution for IoT security issues. In the end, we sum up this review paper by suggesting some future research ideas in IoT security, which still need researchers' attention.

Data Availability

The data used in this research will be available upon request from the corresponding author.

Conflicts of Interest

The authors declare that they have no conflicts of interest.

Acknowledgments

The authors would like to thank the support of all coauthors.

References

- [1] N. C. Winget, A. R. Sadeghi, and Y. Jin, "Invited: can IoT be secured: emerging challenges in connecting the unconnected," in *Proceedings of the 53rd Annual Design Automation Conference*, pp. 1–6, New York, USA, 2016.

- [2] G. S. Hukkeri and R. H. Goudar, "IoT: issues, challenges, tools, security, solutions and best practices," *International Journal of Pure and Applied Mathematics*, vol. 120, no. 6, pp. 12099–12109, 2019.
- [3] S. G. H. Soumyalatha, "Study of IoT: understanding IoT architecture, applications, issues and challenges," *International Journal of Advanced Networking & Applications*, vol. 478, 2016.
- [4] A. S. Genadiarto, A. Noertjahyana, and V. Kabzar, "Introduction of Internet of Thing technology based on prototype," *Jurnal Informatika*, vol. 14, no. 1, pp. 47–52, 2018.
- [5] N. Sharma, M. Shamkuwar, and I. Singh, "The history, present and future with IoT," in *Internet of Things and Big Data Analytics for Smart Generation*, pp. 27–51, Springer, 2019.
- [6] K. Hamid, M. W. Iqbal, A. U. R. Virk et al., "K-Banhatti Sombor invariants of certain computer networks," *Computers Materials & Continua*, vol. 73, no. 1, pp. 15–31, 2022.
- [7] Y. Yang, L. Wu, G. Yin, L. Li, and H. Zhao, "A survey on security and privacy issues in Internet-of-Things," *IEEE Internet of Things Journal*, vol. 4, no. 5, pp. 1250–1258, 2017.
- [8] R. H. Weber, "Internet of things: privacy issues revisited," *Computer Law and Security Review*, vol. 31, no. 5, pp. 618–627, 2015.
- [9] A. Gopi and M. K. Rao, "Survey of privacy and security issues in IoT," *International Journal of Engineering & Technology*, vol. 7, no. 2.7, p. 293, 2018.
- [10] N. Aleisa and K. Renaud, "Privacy of the Internet of Things: a systematic literature review," in *Proceedings of the 50th Hawaii International Conference on System Sciences*, pp. 1–10, Hilton Waikoloa Village, Hawaii, 2017.
- [11] A. Tewari and B. B. Gupta, "Security, privacy and trust of different layers in Internet-of-Things (IoTs) framework," *Future Generation Computer Systems*, vol. 108, pp. 909–920, 2020.
- [12] M. B. M. Noor and W. H. Hassan, "Current research on Internet of Things (IoT) security: a survey," *Computer Networks*, vol. 148, pp. 283–294, 2019.
- [13] O. O. Bamasag and K. Youcef-Toumi, "Towards continuous authentication in Internet of Things based on secret sharing scheme," in *Proceedings of the WESS'15: Workshop on Embedded Systems Security*, pp. 1–8, Amsterdam, Netherlands, 2015.
- [14] K. Zhang, X. Liang, R. Lu, and X. Shen, "Sybil attacks and their defenses in the Internet of Things," *IEEE Internet of Things Journal*, vol. 1, no. 5, pp. 372–383, 2014.
- [15] Q. D. La, T. Q. S. Quek, J. Lee, S. Jin, and H. Zhu, "Deceptive attack and defense game in honeypot-enabled networks for the Internet of Things," *IEEE Internet of Things Journal*, vol. 3, no. 6, pp. 1025–1035, 2016.
- [16] P. Zhang, S. G. Nagarajan, and I. Nevat, "Secure Location of Things (SLOT): mitigating localization spoofing attacks in the Internet of Things," *IEEE Internet of Things Journal*, vol. 4, no. 6, pp. 2199–2206, 2017.
- [17] C. Li, Z. Qin, E. Novak, and Q. Li, "Securing SDN infrastructure of IoT–fog networks from MitM attacks," *IEEE Internet of Things Journal*, vol. 4, no. 5, pp. 1156–1164, 2017.
- [18] B. Xu, W. Wang, Q. Hao et al., "A security design for the detecting of buffer overflow attacks in IoT device," *IEEE Access*, vol. 6, pp. 72862–72869, 2018.
- [19] H. Yi and Z. Nie, "Side-channel security analysis of UOV signature for cloud-based Internet of Things," *Future Generation Computer Systems*, vol. 86, pp. 704–708, 2018.
- [20] J. Moon, I. Y. Jung, and J. H. Park, "IoT application protection against power analysis attack," *Computers and Electrical Engineering*, vol. 67, pp. 566–578, 2018.
- [21] S. Tu, M. Waqas, S. U. Rehman et al., "Security in fog computing: a novel technique to tackle an impersonation attack," *IEEE Access*, vol. 6, pp. 74993–75001, 2018.
- [22] A. Raouf, A. Matrawy, and C.-H. Lung, "Routing attacks and mitigation methods for RPL-based Internet of Things," *IEEE Communications Surveys & Tutorials*, vol. 21, no. 2, pp. 1582–1606, 2019.
- [23] D. Yin, L. Zhang, and K. Yang, "A DDoS attack detection and mitigation with software-defined Internet of Things framework," *IEEE Access*, vol. 6, pp. 24694–24705, 2018.
- [24] M. López, A. Peinado, and A. Ortiz, "An extensive validation of a SIR epidemic model to study the propagation of jamming attacks against IoT wireless networks," *Computer Networks*, vol. 165, article 106945, 2019.
- [25] N. Tariq, M. Asim, Z. Maamar, M. Z. Farooqi, N. Faci, and T. Baker, "A mobile code-driven trust mechanism for detecting internal attacks in sensor node-powered IoT," *Journal of Parallel and Distributed Computing*, vol. 134, pp. 198–206, 2019.
- [26] A. K. Mishra, A. K. Tripathy, D. Puthal, and L. T. Yang, "Analytical model for sybil attack phases in Internet of Things," *IEEE Internet of Things Journal*, vol. 6, no. 1, pp. 379–387, 2019.
- [27] N. Zhang, R. Wu, S. Yuan, C. Yuan, and D. Chen, "RAV: relay aided vectorized secure transmission in physical layer security for Internet of Things under active attacks," *IEEE Internet of Things Journal*, vol. 6, no. 5, pp. 8496–8506, 2019.
- [28] Y. Niu, J. Zhang, A. Wang, and C. Chen, "An efficient collision power attack on AES encryption in edge computing," *IEEE Access*, vol. 7, pp. 18734–18748, 2019.
- [29] H. Yan, Y. Wang, C. Jia, J. Li, Y. Xiang, and W. Pedrycz, "IoT-FBAC: function-based access control scheme using identity-based encryption in IoT," *Future Generation Computer Systems*, vol. 95, pp. 344–353, 2019.
- [30] S. Deshmukh-Bhosale and S. S. Sonavane, "A real-time intrusion detection system for wormhole attack in the RPL based Internet of Things," *Procedia Manufacturing*, vol. 32, pp. 840–847, 2019.
- [31] L. Liu, Z. Ma, and W. Meng, "Detection of multiple-mix-attack malicious nodes using perceptron-based trust in IoT networks," *Future Generation Computer Systems*, vol. 101, pp. 865–879, 2019.
- [32] Z. A. Baig, S. Sanguanpong, S. N. Firdous, V. N. Vo, T. G. Nguyen, and C. So-In, "Averaged dependence estimators for DoS attack detection in IoT networks," *Future Generation Computer Systems*, vol. 102, pp. 198–209, 2020.
- [33] M. Almiani, A. Abu Ghazleh, A. Al-Rahayfeh, S. Atiewi, and A. Razaque, "Deep recurrent neural network for IoT intrusion detection system," *Simulation Modelling Practice and Theory*, vol. 101, article 102031, 2020.
- [34] M. Malik, Kamaldeep, and M. Dutta, "Defending DDoS in the insecure Internet of Things: a survey," in *Advances in Intelligent Systems and Computing*, pp. 223–233, Springer, Singapore, 2018.
- [35] R. Doshi, N. Apthorpe, and N. Feamster, "Machine learning DDoS detection for consumer Internet of Things devices," in *2018 IEEE Security and Privacy Workshops*, pp. 29–35, San Francisco, CA, USA, 2018.

- [36] J. Pacheco, S. Hariri, and S. Hariri, "Anomaly behavior analysis for IoT sensors," *Transactions on Emerging Telecommunications Technologies*, vol. 29, no. 4, article e3188, 2018.
- [37] P. Gope, R. Amin, S. K. Hafizul Islam, N. Kumar, and V. K. Bhalla, "Lightweight and privacy-preserving RFID authentication scheme for distributed IoT infrastructure with secure localization services for smart city environment," *Future Generation Computer Systems*, vol. 83, pp. 629–637, 2018.
- [38] J. Sherry, C. Lan, R. A. Popa, and S. Ratnasamy, "Blind box: deep packet inspection over encrypted traffic," in *Proceedings of the 2015 ACM Conference on Special Interest Group on Data Communication*, pp. 213–226, London, UK, 2015.
- [39] M. R. Naqvi, M. W. Iqbal, S. K. Shahzad et al., "A concurrence study on interoperability issues in IoT and decision making based model on data and services being used during interoperability," *Lahore Garrison University Research Journal of Computer Science and Information Technology*, vol. 4, no. 4, pp. 73–85, 2020.
- [40] O. Brun, Y. Yin, E. Gelenbe, Y. M. Kadioglu, J. Augusto-Gonzalez, and M. Ramos, "Deep learning with dense random neural networks for detecting attacks against IoT-connected home environments," in *International ISCIS Security Workshop*, pp. 79–89, Springer, London, UK, 2018.
- [41] Y. Li, L. Shi, P. Cheng, J. Chen, and D. E. Quevedo, "Jamming attacks on remote state estimation in cyber-physical systems: a game-theoretic approach," *IEEE Transactions on Automatic Control*, vol. 60, no. 10, pp. 2831–2836, 2015.
- [42] S. Vadlamani, B. Eksioglu, H. Medal, and A. Nandi, "Jamming attacks on wireless networks: a taxonomic survey," *International Journal of Production Economics*, vol. 172, pp. 76–94, 2016.
- [43] Y. Guan and X. Ge, "Distributed attack detection and secure estimation of networked cyber-physical systems against false data injection attacks and jamming attacks," *IEEE Transactions on Signal and Information Processing Over Networks*, vol. 4, no. 1, pp. 48–59, 2018.
- [44] B. Park, "Threats and security analysis for enhanced secure neighbor discovery protocol (SEND) of IPv6 NDP security," *International Journal of Control and Automation*, vol. 4, no. 4, 2011.
- [45] Y. W. P. Hong, P. C. Lan, and C. C. J. Kuo, "Enhancing physical-layer secrecy in multiantenna wireless systems: an overview of signal processing approaches," *IEEE Signal Processing Magazine*, vol. 30, no. 5, pp. 29–40, 2013.
- [46] L. Xiao, L. J. Greenstein, N. B. Mandayam, and W. Trappe, "Channel-based detection of sybil attacks in wireless networks," *IEEE Transactions on Information Forensics and Security*, vol. 4, no. 3, pp. 492–503, 2009.
- [47] B. Cheng, D. Zhu, S. Zhao, and J. Chen, "Situation-aware IoT service coordination using the event-driven SOA paradigm," *IEEE Transactions on Network and Service Management*, vol. 13, no. 2, pp. 349–361, 2016.
- [48] S. H. Chae, W. Choi, J. H. Lee, and T. Q. S. Quek, "Enhanced secrecy in stochastic wireless networks: artificial noise with secrecy protected zone," *IEEE Transactions on Information Forensics and Security*, vol. 9, no. 10, pp. 1617–1628, 2014.
- [49] A. Dvir and L. Buttyan, "VeRA-version number and rank authentication in RPL," in *2011 IEEE Eighth International Conference on Mobile Ad-Hoc and Sensor Systems*, pp. 709–714, Valencia, Spain, 2011.
- [50] C. Pu and S. Hajjar, "Mitigating forwarding misbehaviors in RPL-based low power and lossy networks," in *2018 15th IEEE Annual Consumer Communications & Networking Conference*, pp. 1–6, Las Vegas, NV, USA, 2018.
- [51] A. Le, J. Loo, A. Lasebae, A. Vinel, Y. Chen, and M. Chai, "The impact of rank attack on network topology of routing protocol for low-power and lossy networks," *IEEE Sensors Journal*, vol. 13, no. 10, pp. 3685–3692, 2013.
- [52] K. Weekly and K. Pister, "Evaluating sinkhole defense techniques in RPL networks," in *2012 20th IEEE International Conference on Network Protocols*, pp. 1–6, Austin, TX, USA, 2012.
- [53] F. Ahmed and Y. Ko, "Mitigation of black hole attacks in routing protocol for low power and lossy networks," *Security and Communication Networks*, vol. 9, no. 18, pp. 5143–5154, 2016.
- [54] H. H. Pajouh, R. Javidan, R. Khayami, A. Dehghantaha, and K.-K. R. Choo, "A two-layer dimension reduction and two-tier classification model for anomaly-based intrusion detection in IoT backbone networks," *IEEE Transactions on Emerging Topics in Computing*, vol. 7, no. 2, pp. 314–323, 2019.
- [55] S. Sivaraju and G. Umamaheswari, "Detection of sinkhole attack in wireless sensor networks using message digest algorithms," in *2011 International Conference on Process Automation, Control and Computing*, pp. 1–6, Coimbatore, India, 2011.
- [56] Q. Cao and X. Yang, "Sybil fence: improving social-graph-based sybil defenses with user negative feedback," <http://arxiv.org/abs/1304.3819>.
- [57] N. Maheshwari and H. Dagale, "Secure communication and firewall architecture for IoT applications," in *2018 10th International Conference on Communication Systems Networks*, pp. 328–335, Bengaluru, India, 2018.
- [58] L. Alvisi, A. Clement, A. Epasto, S. Lattanzi, and A. Panconesi, "SoK: the evolution of sybil defense via social networks," in *2013 IEEE Symposium on Security and Privacy*, pp. 382–396, Berkeley, CA, USA, 2013.
- [59] A. Mohaisen, N. Hopper, and Y. Kim, "Keep your friends close: incorporating trust into social network-based sybil defenses," in *2011 Proceedings IEEE INFOCOM*, pp. 1943–1951, Shanghai, China, 2011.
- [60] M. Wazid, A. K. Das, S. Kumari, and M. K. Khan, "Design of sinkhole node detection mechanism for hierarchical wireless sensor networks - Wazid -2016- Security and Communication Networks," *Security and Communication Networks*, vol. 9, 4614 pages, 2016.
- [61] S. Raza, T. Chung, S. Duquennoy, D. Yazar, T. Voigt, and U. Roedig, *Securing Internet of Things with lightweight ipsec*, Swedish Institute of Computer Science, Kista, Sweden, 2010.
- [62] S. Raza, S. Duquennoy, J. Höglund, U. Roedig, and T. Voigt, "Secure communication for the Internet of Things—a comparison of link-layer security and IPsec for 6LoWPAN," *Security and Communication Networks*, vol. 7, 2668 pages, 2014.
- [63] J. Granjal, E. Monteiro, and J. S. Silva, "Application-layer security for the wot: extending coap to support end-to-end message security for Internet-integrated sensing applications," in *Wired/Wireless Internet Communication*, pp. 140–153, Springer, Berlin, Heidelberg, 2013.
- [64] L. Barreto, A. Celesti, M. Villari, M. Fazio, and A. Puliafito, "An authentication model for IoT clouds," in *2015 IEEE/*

- ACM International Conference on Advances in Social Networks Analysis and Mining*, pp. 1032–1035, Paris, France, 2015.
- [65] M. H. Ibrahim, “Octopus: an edge-fog mutual authentication scheme,” *IJ Network Security*, vol. 18, no. 6, pp. 1089–1101, 2016.
- [66] H. Xie, Z. Yan, Z. Yao, and M. Atiquzzaman, “Data collection for security measurement in wireless sensor networks: a survey,” *IEEE Internet of Things Journal*, vol. 6, no. 2, pp. 2205–2224, 2019.
- [67] O. A. Osanaiye, A. S. Alfa, and G. P. Hancke, “Denial of service defence for resource availability in wireless sensor networks,” *IEEE Access*, vol. 6, pp. 6975–7004, 2018.
- [68] L. A. Tawalbeh, F. Muheidat, M. Tawalbeh, and M. Quwaider, “IoT privacy and security: challenges and solutions,” *Applied Sciences*, vol. 10, no. 12, p. 4102, 2020.
- [69] H. Ning, H. Liu, and L. T. Yang, “Cyberentity security in the Internet of Things,” *Computer*, vol. 46, no. 4, pp. 46–53, 2013.
- [70] M. Abomhara and G. M. K. Ien, “Cyber security and the Internet of Things: vulnerabilities, threats, intruders and attacks,” *Journal of Cyber Security and Mobility*, vol. 4, no. 1, pp. 65–88, 2015.
- [71] A. Mathur, T. Newe, and M. Rao, “Defence against black hole and selective forwarding attacks for medical WSNs in the IoT,” *Sensors*, vol. 16, no. 1, 2016.
- [72] R. Stephen and D. L. Arockiam, “Intrusion detection system to detect sinkhole attack on rpl protocol in Internet of Things,” *International Journal of Electrical Electronics and Computer Science*, vol. 4, no. 4, 2016.
- [73] K. Skouby, R. Tadayoni, and S. Tweneboah-Koduah, “Cyber security threats to IoT applications and service domains,” *Wireless Personal Communications*, vol. 95, no. 1, pp. 169–185, 2017.
- [74] J. Sengupta, S. Ruj, and S. Das Bit, “A comprehensive survey on attacks, security issues and blockchain solutions for IoT and IIoT,” *Journal of Network and Computer Applications*, vol. 149, article 102481, 2020.
- [75] Q. Wang, X. Zhu, Y. Ni, L. Gu, and H. Zhu, “Blockchain for the IoT and industrial IoT: a review,” *Internet of Things*, vol. 10, article 100081, 2019.
- [76] R. H. Weber, “Internet of Things – new security and privacy challenges,” *Computer Law & Security Review*, vol. 26, no. 1, pp. 23–30, 2010.
- [77] M. A. Khan and K. Salah, “IoT security: review, blockchain solutions, and open challenges,” *Future Generation Computer Systems*, vol. 82, pp. 395–411, 2018.
- [78] Y. Qian, Y. Jiang, J. Chen et al., “Towards decentralized IoT security enhancement: a blockchain approach,” *Computers and Electrical Engineering*, vol. 72, pp. 266–273, 2018.
- [79] A. Sultan, M. A. Mushtaq, and M. Abubakar, “IoT security issues via blockchain: a review paper,” in *Proceedings of the 2019 International Conference on Blockchain Technology*, pp. 60–65, Espoo, Finland, 2019.
- [80] A. Dorri, S. S. Kanhere, R. Jurdak, and P. Gauravaram, “Blockchain for IoT security and privacy: the case study of a smart home,” in *2017 IEEE International Conference on Pervasive Computing and Communications Workshops*, pp. 618–623, Kona, HI, USA, 2017.
- [81] M. R. Naqvi, M. W. Iqbal, M. U. Ashraf et al., “Ontology driven testing strategies for IoT applications,” *Materials & Continua*, vol. 70, no. 3, pp. 5855–5869, 2022.
- [82] M. I. Sarwar, M. W. Iqbal, T. Alyas et al., “Data vaults for blockchain-empowered accounting information systems,” *IEEE Access*, vol. 9, no. 2021, pp. 117306–117324, 2021.
- [83] M. Akram, M. W. Iqbal, S. A. Ali, M. U. Ashraf, K. Alsubhi, and H. M. Aljahdali, “Triple key security algorithm against single key attack on multiple rounds,” *Materials & Continua*, vol. 72, no. 3, pp. 6061–6077, 2022.
- [84] D. Minoli and B. Occhiogrosso, “Blockchain mechanisms for IoT security,” *Internet of Things*, vol. 1–2, pp. 1–13, 2018.
- [85] F. K. Gondal, S. K. Shahzad, M. W. Iqbal, M. Aqeel, and M. R. Naqvi, “Business process model for IoT based systems operations,” *LGU, Research Journal for Computer Science and IT*, vol. 5, no. 4, pp. 1–10, 2021.
- [86] K. M. Sadique, R. Rahmani, and P. Johannesson, “Towards security on Internet of Things: applications and challenges in technology,” *Procedia Computer Science*, vol. 141, pp. 199–206, 2018.
- [87] S. K. Shahzad, M. W. Iqbal, and N. Ahmad, “Privacy agents for IoT cloud communication,” in *IoT BDS-2nd International Conference on Internet of Things, Big Data and Security*, pp. 239–245, Prague, Czech Republic, 2017.
- [88] K. Fan, S. Wang, Y. Ren et al., “Blockchain-based secure time protection scheme in IoT,” *IEEE Internet of Things Journal*, vol. 6, no. 3, pp. 4671–4679, 2019.
- [89] B. Kitchenham, *Procedures for Performing Systematic Reviews*, Keele University, Keele, UK, 2004.
- [90] T. Xu, J. B. Wendt, and M. Potkonjak, “Security of IoT systems: design challenges and opportunities,” in *2014 IEEE/ACM International Conference on Computer-Aided Design*, pp. 417–423, San Jose, CA, USA, 2014.
- [91] J. Deogirikar and A. Vidhate, “Security attacks in IoT: a survey,” in *2017 International Conference on I-SMAC*, pp. 32–37, Palladam, India, 2017.
- [92] S. Bhunia and M. Tehranipoor, Eds., “Physical Attacks and Countermeasures,” in *Hardware Security*, pp. 245–290, Morgan Kaufmann, 2019.
- [93] M. Hutle and M. Kammerstetter, “Resilience against physical attacks,” in *Smart Grid Security*, pp. 79–112, Syngress, Boston, USA, 2015.
- [94] A. Fadele, M. Othman, I. Hashem, I. Yaqoob, M. Imran, and M. Shoaib, “A novel countermeasure technique for reactive jamming attack in Internet of Things,” *Multimedia Tools and Applications*, vol. 78, 2019.
- [95] A. Mpitziopoulos, D. Gavalas, C. Konstantopoulos, and G. Pantziou, “A survey on jamming attacks and countermeasures in WSNs,” *IEEE Communications Surveys & Tutorials*, vol. 11, no. 4, pp. 42–56, 2009.
- [96] H. Li, Y. Chen, and Z. He, “The survey of RFID attacks and defenses,” in *2012 8th International Conference on Wireless Communications, Networking and Mobile Computing*, pp. 1–4, Shanghai, China, 2012.
- [97] S. Hameed, F. I. Khan, and B. Hameed, “Understanding security requirements and challenges in Internet of Things (IoT): a review,” *Journal of Computer Networks and Communications*, vol. 2019, Article ID 9629381, 14 pages, 2019.
- [98] F. Kandah, Y. Singh, W. Zhang, and C. Wang, “Mitigating colluding injected attack using monitoring verification in mobile ad-hoc networks,” *Security and Communication Networks*, vol. 6, no. 4, pp. 539–547, 2013.
- [99] M. Pirretti, S. Zhu, N. Vijaykrishnan, P. McDaniel, M. Kandemir, and R. Brooks, “The sleep deprivation attack

- in sensor networks: analysis and methods of defense,” *International Journal of Distributed Sensor Networks*, vol. 2, 287 pages, 2006.
- [100] A. Gallais, T.-H. Hedli, V. Loscri, and N. Mitton, “Denial-of-sleep attacks against IoT networks,” in *2019 6th International Conference on Control, Decision and Information Technologies*, pp. 1025–1030, Paris, France, 2019.
- [101] S. Alam and D. De, “Analysis of security threats in wireless sensor network,” *International Journal of Wireless & Mobile Networks*, vol. 6, no. 2, pp. 35–46, 2014.
- [102] M.-L. Messai, *Classification of Attacks in Wireless Sensor Networks*, 2014, arXiv:1406.4516.
- [103] C. Koliass, G. Kambourakis, A. Stavrou, and J. Voas, “DDoS in the IoT: Mirai and other botnets,” *Computer*, vol. 50, no. 7, pp. 80–84, 2017.
- [104] M. El-hajj, A. Fadlallah, M. Chamoun, and A. Serhrouchni, “A survey of Internet of Things (IoT) authentication schemes,” *Sensors*, vol. 19, no. 5, 2019.
- [105] P. Ganapathi and D. Shanmugapriya, “A survey of attacks, security mechanisms and challenges in wireless sensor networks,” *International Journal of Computer Science and Information Security*, vol. 4, 2009.
- [106] S. Bhunia, M. S. Hsiao, M. Banga, and S. Narasimhan, “Hardware trojan attacks: threat analysis and countermeasures,” *Proceedings of the IEEE*, vol. 102, no. 8, pp. 1229–1247, 2014.
- [107] S. Sidhu, B. J. Mohd, and T. Hayajneh, “Hardware security in IoT devices with emphasis on hardware trojans,” *Journal of Sensor and Actuator Networks*, vol. 8, no. 3, 2019.
- [108] M. Tehranipoor and F. Koushanfar, “A survey of hardware trojan taxonomy and detection,” *IEEE Design & Test Of Computers*, vol. 27, no. 1, pp. 10–25, 2010.
- [109] A. Matrosov, E. Rodionov, D. Harley, and J. Malcho, “Stuxnet under the microscope,” *ESET LLC*, 2010.
- [110] M. Lehtonen, D. Ostojic, A. Ilic, and F. Michahelles, “Securing RFID systems by detecting tag cloning,” in *Lecture Notes in Computer Science*, vol. 5538, pp. 291–308, Springer, Berlin, Heidelberg, 2009.
- [111] M. Obaidat, S. Obeidat, J. Holst, A. al Hayajneh, and J. Brown, “A comprehensive and systematic survey on the Internet of Things: security and privacy challenges, security frameworks, enabling technologies, threats, vulnerabilities and countermeasures,” *Computers*, vol. 9, p. 44, 2020.
- [112] H. Akram, D. Konstantas, and M. Mahyoub, “A comprehensive IoT attacks survey based on a building-blocked reference model,” *International Journal of Advanced Computer Science and Applications*, vol. 9, no. 3, 2018.
- [113] I. Butun, P. Österberg, and H. Song, “Security of the Internet of Things: vulnerabilities, attacks, and countermeasures,” *IEEE Communications Surveys & Tutorials*, vol. 22, no. 1, pp. 616–644, 2020.
- [114] S. Pundir, M. Wazid, D. P. Singh, A. K. Das, J. J. P. C. Rodrigues, and Y. Park, “Designing efficient sinkhole attack detection mechanism in edge-based IoT deployment,” *Sensors*, vol. 20, no. 5, 2020.
- [115] S. Tahir, S. T. Bakhsh, and R. A. Alsemmeari, “An intrusion detection system for the prevention of an active sinkhole routing attack in Internet of Things,” *International Journal of Distributed Sensor Networks*, vol. 15, Article ID 155014771988990, 2019.
- [116] Y.-C. Hu, A. Perrig, and D. B. Johnson, “Packet leases: a defense against wormhole attacks in wireless networks,” in *IEEE INFOCOM 2003. Twenty-second Annual Joint Conference of the IEEE Computer and Communications Societies*, pp. 1976–1986, San Francisco, CA, USA, 2003.
- [117] A. Mosenia and N. K. Jha, “A comprehensive study of security of Internet-of-Things,” *IEEE Transactions on Emerging Topics in Computing*, vol. 5, no. 4, pp. 586–602, 2017.
- [118] B. Mustafa, M. W. Iqbal, M. Saeed, A. R. Shafqat, H. Sajjad, and M. R. Naqvi, “IOT based low-cost smart home automation system,” in *2021 3rd International Congress on Human-Computer Interaction, Optimization and Robotic Applications*, pp. 1–6, Ankara, Turkey, 2021.
- [119] M. Nawir, A. Amir, N. Yaakob, and O. B. Lynn, “Internet of Things (IoT): taxonomy of security attacks,” in *2016 3rd international conference on electronic design*, pp. 321–326, Phuket, Thailand, 2016.
- [120] D. Sisodia, *On the State of Internet of Things Security: Vulnerabilities, Attacks, and Recent Countermeasures*, University of Oregon, 2020.
- [121] L. Bysani and A. Turuk, “A survey on selective forwarding attack in wireless sensor networks,” in *2011 International Conference on Devices and Communications*, pp. 1–5, Mesra, India, 2011.
- [122] A. Mayzaud, R. Badonnel, and I. Chrisment, “A taxonomy of attacks in RPL-based Internet of Things,” *International Journal Of Network Security*, vol. 18, no. 3, pp. 459–473, 2016.
- [123] Z. Cekerevac, Z. Dvorak, L. Prigoda, and P. Cekerevac, “Internet of things and the man-in-the-middle attacks—security and economic risks,” *MEST Journal*, vol. 5, no. 2, pp. 15–25, 2017.
- [124] M. M. Ahemd, M. A. Shah, and A. Wahid, “IoT security: a layered approach for attacks defenses,” in *2017 International Conference on Communication Technologies*, pp. 104–110, Rawalpindi, Pakistan, 2017.
- [125] K. Zhao and L. Ge, “A survey on the Internet of Things security,” in *2013 Ninth International Conference on Computational Intelligence and Security*, pp. 663–667, Emeishan, China, 2013.
- [126] D. He, S. Chan, and M. Guizani, “Security in the Internet of Things supported by mobile edge computing,” *IEEE Communications Magazine*, vol. 56, no. 8, pp. 56–61, 2018.
- [127] I. Andrea, C. Chrysostomou, and G. Hadjichristofi, “Internet of Things: security vulnerabilities and challenges,” in *2015 IEEE Symposium on Computers and Communication*, pp. 180–187, Larnaca, Cyprus, 2015.
- [128] A. Kamble and S. Bhutad, “Survey on Internet of Things (IoT) security issues solutions,” in *2018 2nd International Conference on Inventive Systems and Control*, pp. 307–312, Coimbatore, India, 2018.
- [129] A. Mitrokotsa, M. R. Rieback, and A. S. Tanenbaum, “Classifying RFID attacks and defenses,” *Information Systems Frontiers*, vol. 12, no. 5, pp. 491–505, 2010.
- [130] E. Ronen, A. Shamir, A. O. Weingarten, and C. O’Flynn, “IoT goes nuclear: creating a zig bee chain reaction,” in *2017 IEEE symposium on security and privacy*, pp. 195–212, San Jose, CA, USA, 2017.
- [131] E. Bertino and N. Islam, “Botnets and Internet of Things security,” *Computer*, vol. 50, no. 2, pp. 76–79, 2017.
- [132] S. Edwards and I. Profetis, “Hajime: analysis of a decentralized Internet worm for IoT devices,” *Rapidity Networks*, vol. 16, pp. 1–18, 2016.
- [133] H. Takase, R. Kobayashi, M. Kato, and R. Ohmura, “A prototype implementation and evaluation of the malware detection

- mechanism for IoT devices using the processor information,” *International Journal of Information Security*, vol. 19, no. 1, pp. 71–81, 2020.
- [134] M. M. Ogonji, G. Okeyo, and J. M. Wafula, “A survey on privacy and security of Internet of Things,” *Computer Science Review*, vol. 38, article 100312, 2020.
- [135] C. Dong, G. He, X. Liu, Y. Yang, and W. Guo, “A multi-layer hardware trojan protection framework for IoT chips,” *IEEE Access*, vol. 7, pp. 23628–23639, 2019.
- [136] A. Tsow, “Phishing with consumer electronics-malicious home routers,” *MTW*, vol. 190, 2006.
- [137] L. Sha, F. Xiao, W. Chen, and J. Sun, “IIoT-SIDefender: detecting and defense against the sensitive information leakage in industry IoT,” *World Wide Web*, vol. 21, no. 1, pp. 59–88, 2018.
- [138] S. Boddy and J. Shattuck, *The Hunt for IoT: The Rise of Thingsbots*, F5 Labs, Seattle WA, USA, 2017.
- [139] J. Mirkovic and P. Reiher, “A taxonomy of DDoS attack and DDoS defense mechanisms,” *ACM SIGCOMM Computer Communication Review*, vol. 34, no. 2, pp. 39–53, 2004.
- [140] M. Farooq, M. Waseem, A. Khairi, and P. Mazhar, “A critical analysis on the security concerns of Internet of Things (IoT),” *International Journal of Computers and Applications*, vol. 111, no. 7, pp. 1–6, 2015.
- [141] L. Qian, Z. Zhu, J. Hu, and S. Liu, “Research of SQL injection attack and prevention technology,” in *2015 International Conference on Estimation, Detection and Information Fusion*, pp. 303–306, Harbin, China, 2015.
- [142] D. Martins and H. Guyennet, “Wireless sensor network attacks and security mechanisms: a short survey,” in *2010 13th international conference on network-based information systems*, pp. 313–320, Takayama, Japan, 2010.
- [143] M. L. Mahajan, D. Verma, and Aropolis technical Campus Indore, “Review of prevention techniques for denial of service attacks in wireless sensor network,” *International Journal of Engineering Research*, vol. V4, no. 5, article IJERT-V4IS051191, 2015.
- [144] Q. D. Ngo, H. T. Nguyen, V. H. Le, and D. H. Nguyen, “A survey of IoT malware and detection methods based on static features,” *ICT Express*, vol. 6, no. 4, pp. 280–286, 2020.
- [145] B. Bencsáth, G. Pék, L. Buttyán, and M. Félegyházi, *Duqu: analysis, detection, and lessons learned*, ACM European Workshop on System Security, Bern, Switzerland, 2012.
- [146] U. Sabeel and S. Maqbool, “Categorized security threats in the wireless sensor networks: countermeasures and security management schemes,” *International Journal of Computers and Applications*, vol. 64, no. 16, pp. 19–28, 2013.
- [147] A. Mohanty, I. Obaidat, F. Yilmaz, and M. Sridhar, “Control-hijacking vulnerabilities in IoT firmware: a brief survey,” in *Proceedings of the 1st International Workshop on Security and Privacy for the Internet-of-Things (IoTSec), and attack taxonomy*, New York, USA, 2015.
- [148] M. R. Naqvi, M. Aslam, M. W. Iqbal, S. K. Shahzad, M. Malik, and M. U. Tahir, “Study of block chain and its impact on Internet of Health Things (IoHT): challenges and opportunities,” in *2020 international congress on human-computer interaction, optimization and robotic applications*, pp. 1–6, Ankara, Turkey, 2020.
- [149] M. Ghasemi, M. Saadaat, and O. Ghollasi, “Threats of social engineering attacks against security of Internet of Things (IoT): the selected papers of the first international conference on fundamental research in electrical engineering,” in *Lecture Notes in Electrical Engineering*, pp. 957–968, Springer, Singapore, 2019.
- [150] I. Naumann and G. Hogben, “Privacy features of European eID card specifications,” *Network Security*, vol. 2008, no. 8, pp. 9–13, 2008.
- [151] H. D. Tsague and B. Twala, “Practical techniques for securing the Internet of Things (IoT) against side channel attacks,” in *Internet of things and big data analytics toward next-generation intelligence*, pp. 439–481, Springer, 2018.
- [152] H. Y. Ghafoor, A. Jaffar, R. Jahangir, M. W. Iqbal, and M. Z. Abbas, “Fake news identification on social media using machine learning techniques,” in *Lecture Notes in Networks and Systems*, pp. 87–98, Springer, Singapore, 2022.
- [153] A. A. Pammu, K.-S. Chong, W.-G. Ho, and B.-H. Gwee, “Interceptive side channel attack on AES-128 wireless communications for IoT applications,” in *2016 IEEE Asia Pacific Conference on Circuits and Systems*, pp. 650–653, Jeju, Korea, 2016.
- [154] S. Bhunia and M. Tehranipoor, Eds., “Side-channel attacks,” in *Hardware Security*, pp. 193–218, Morgan Kaufmann, 2019.
- [155] F. K. Gondal, S. K. Shahzad, A. Jaffar, and M. W. Iqbal, “A process oriented integration model for smart health services,” *Intelligent Automation & Soft Computing*, vol. 35, no. 2, pp. 1369–1386, 2023.
- [156] A. Sayakkara, N. A. Le-Khac, and M. Scanlon, “Leveraging electromagnetic side-channel analysis for the investigation of IoT devices,” *Digital Investigation*, vol. 29, pp. S94–S103, 2019.
- [157] D. Shree and S. Ahlawat, “A review on cryptography, attacks and cyber security,” *International Journal of Advanced Research in Computer Science*, vol. 8, no. 5, 2017.
- [158] S. S. Kulkarni, H. M. Rai, and S. Singla, “Design of an effective substitution cipher algorithm for information security using fuzzy logic,” *International Journal of Innovations in Engineering and Technology*, vol. 1, no. 2, 2012.
- [159] R. Datta and N. Marchang, “Chapter 7-security for mobile ad hoc networks,” in *Handbook on Securing Cyber-Physical Critical Infrastructure*, pp. 147–190, Morgan Kaufmann, Boston, USA, 2012.
- [160] C. Li, “Security of wireless sensor networks: current status and key issues,” *Smart Wireless Sensor Networks*, vol. 14, pp. 299–313, 2010.
- [161] J. Grover and S. Sharma, “Security issues in wireless sensor network — a review,” in *2016 5th International Conference on Reliability, Infocom Technologies and Optimization*, pp. 397–404, Noida, India, 2016.
- [162] K. Somasundaram and K. Selvam, “IOT – attacks and challenges,” *International Journal of Engineering and Technical Research*, vol. 8, no. 9, 2018.
- [163] I. Stelliou, P. Kotzanikolaou, M. Psarakis, C. Alcaraz, and J. Lopez, “A survey of IoT-enabled cyberattacks: assessing attack paths to critical infrastructures and services,” *IEEE Communications Surveys & Tutorials*, vol. 20, no. 4, pp. 3453–3495, 2018.
- [164] M. N. Aman, K. C. Chua, and B. Sikdar, “Mutual authentication in IoT systems using physical unclonable functions,” *IEEE Internet of Things Journal*, vol. 4, no. 5, pp. 1327–1340, 2017.
- [165] S. Babar, A. Stango, N. Prasad, J. Sen, and R. Prasad, “Proposed embedded security framework for Internet of Things

- (IoT),” in *2011 2nd International Conference on Wireless Communication, Vehicular Technology, Information Theory and Aerospace Electronic Systems Technology*, pp. 1–5, Chennai, India, 2011.
- [166] D. Stiawan, M. Y. Idris, R. F. Malik, S. Nurmaini, N. Alsharif, and R. Budiarto, “Investigating brute force attack patterns in IoT network,” *Journal of Electrical and Computer Engineering*, vol. 2019, Article ID 4568368, 13 pages, 2019.
- [167] T. Wang, G. Zhang, A. Liu, M. Z. A. Bhuiyan, and Q. Jin, “A secure IoT service architecture with an efficient balance dynamics based on cloud and edge computing,” *IEEE Internet of Things Journal*, vol. 6, no. 3, pp. 4831–4843, 2019.
- [168] M. D. M. Hossain, M. Fotouhi, and R. Hasan, “Towards an analysis of security issues, challenges, and open problems in the Internet of Things,” in *2015 IEEE World Congress on Services*, pp. 21–28, New York, NY, USA, 2015.
- [169] S. Alanazi, J. Al-Muhtadi, A. Derhab et al., “On resilience of wireless mesh routing protocol against DoS attacks in IoT-based ambient assisted living applications,” in *2015 17th International Conference on E-health Networking, Application Services*, pp. 205–210, Boston, MA, USA, 2015.
- [170] P. Kumar, G. P. Gupta, and R. Tripathi, “Toward design of an intelligent cyber attack detection system using hybrid feature reduced approach for IoT networks,” *Arabian Journal for Science and Engineering*, vol. 46, pp. 1–30, 2021.
- [171] S. Lee, A. Abdullah, N. Jhanjhi, and S. Kok, “Classification of botnet attacks in IoT smart factory using honeypot combined with machine learning,” *Peer J Computer Science*, vol. 7, article e350, 2021.
- [172] S. B. Gopal, C. Poongodi, D. Nanthiya, R. S. Priya, G. Saran, and M. S. Priya, “Mitigating DoS attacks in IoT using supervised and unsupervised algorithms—a survey,” *IOP Conference Series: Materials Science and Engineering*, vol. 1055, no. 1, article 012072, 2021.
- [173] J. Manhas and S. Kotwal, “Implementation of intrusion detection system for Internet of Things using machine learning techniques,” in *Multimedia Security*, pp. 217–237, Springer, Singapore, 2021.
- [174] A. Churcher, R. Ullah, J. Ahmad et al., “An experimental analysis of attack classification using machine learning in IoT networks,” *Sensors*, vol. 21, no. 2, p. 446, 2021.
- [175] S. Sahmim and H. Gharsellaoui, “Privacy and security in Internet-based computing: cloud computing, Internet of Things, cloud of things: a review,” *Procedia Computer Science*, vol. 112, pp. 1516–1522, 2017.

Retraction

Retracted: A BP Neural Network-Based Early Warning Model for Student Performance in the Context of Big Data

Journal of Sensors

Received 22 August 2023; Accepted 22 August 2023; Published 23 August 2023

Copyright © 2023 Journal of Sensors. This is an open access article distributed under the Creative Commons Attribution License, which permits unrestricted use, distribution, and reproduction in any medium, provided the original work is properly cited.

This article has been retracted by Hindawi following an investigation undertaken by the publisher [1]. This investigation has uncovered evidence of one or more of the following indicators of systematic manipulation of the publication process:

- (1) Discrepancies in scope
- (2) Discrepancies in the description of the research reported
- (3) Discrepancies between the availability of data and the research described
- (4) Inappropriate citations
- (5) Incoherent, meaningless and/or irrelevant content included in the article
- (6) Peer-review manipulation

The presence of these indicators undermines our confidence in the integrity of the article's content and we cannot, therefore, vouch for its reliability. Please note that this notice is intended solely to alert readers that the content of this article is unreliable. We have not investigated whether authors were aware of or involved in the systematic manipulation of the publication process.

In addition, our investigation has also shown that one or more of the following human-subject reporting requirements has not been met in this article: ethical approval by an Institutional Review Board (IRB) committee or equivalent, patient/participant consent to participate, and/or agreement to publish patient/participant details (where relevant).

Wiley and Hindawi regrets that the usual quality checks did not identify these issues before publication and have since put additional measures in place to safeguard research integrity.

We wish to credit our own Research Integrity and Research Publishing teams and anonymous and named external researchers and research integrity experts for contributing to this investigation.

The corresponding author, as the representative of all authors, has been given the opportunity to register their agreement or disagreement to this retraction. We have kept a record of any response received.

References

- [1] C. Shi and Y. Tan, "A BP Neural Network-Based Early Warning Model for Student Performance in the Context of Big Data," *Journal of Sensors*, vol. 2022, Article ID 2958261, 10 pages, 2022.

Research Article

A BP Neural Network-Based Early Warning Model for Student Performance in the Context of Big Data

Chengxiang Shi  and Yun Tan

Department of Mathematics and Information Engineering, Chongqing University of Education, Chongqing, China

Correspondence should be addressed to Chengxiang Shi; shicx@cque.edu.cn

Received 19 July 2022; Revised 24 August 2022; Accepted 3 September 2022; Published 28 September 2022

Academic Editor: Sweta Bhattacharya

Copyright © 2022 Chengxiang Shi and Yun Tan. This is an open access article distributed under the Creative Commons Attribution License, which permits unrestricted use, distribution, and reproduction in any medium, provided the original work is properly cited.

Nowadays, educational data mining technology has received more and more attention from scholars in China, and the application of correlation between student behavior data and student achievement to teaching management has become a hot research topic. Starting from the study of the potential association between book borrowing and student achievement in the big data environment, the paper analyzes the correlation between book borrowing and student achievement based on the Apriori algorithm and concludes that there is a strong correlation rule between book borrowing and student achievement. Based on BP neural network prediction algorithm, the paper constructs an early warning model for student performance by predicting book borrowing through course performance. The absolute value of the error between the predicted value of book borrowing and the real value of borrowing is used as a basis to make early warning for students' performance, so as to realize the monitoring of students' learning situation, thereby providing theoretical suggestions for teachers' teaching and promoting the school's management of students.

1. Introduction

Under the background of big data, people will generate a large amount of behavioral data every day. With the development of database technology, many potential correlations can always be mined from people's behavioral data. The development of a country's education is related to the country's future; therefore, how to link data mining technology with education has become an important hot spot at present. This paper aims to analyze students' book borrowing behavior through big data mining technology, realize early warning of students' academic performance, so as to optimize student management, improve teachers' work efficiency, and better serve students.

Traditional student learning behavior analysis is mostly carried out through questionnaire surveys, manual evaluation, and other methods. This not only is time cost high and errors are large but also there are many non-objective factors that make the results often not objective enough. With the development of computer networks and the Internet, scholars at home and abroad have begun to use educa-

tional data mining technology to analyze students' behaviors; for example, foreign scholar Professor Andrew Kyngdon [1] established an automatic scoring model based on a new neural network model in his research. Compared with traditional research methods, this research result is more scientific and improves the accuracy of the results. In the research on student behavior based on big data, there are also many studies on the correlation between library borrowing data and students' learning behavior; for example, Chinese scholars Yang Xinya [2], Wu Xudong [3], and others conducted research on the correlation between book borrowing and students' grades through SPSS and neural network algorithms and found that there was a greater correlation between student borrowing and student performance. Although studies have shown that there is a large correlation between student borrowing behavior and student performance, there are relatively few applied studies on this association.

Machine learning has been a popular choice in analyzing students' performances. As an example, the study in [4, 5] used two datasets for the classification and analysis of

students' performance using five machine learning algorithms. As part of the study, eighteen experiments were conducted which helped in predicting the performance of the students. The study in [6] presented a prediction model to predict students' performance in secondary education. As part of the study, five classification algorithms were used, namely, Logistic Regression, *K*-Nearest Neighbor (KNN), Support Vector Machine (SVM), XGBoost, and Naïve Bayes, considering dataset from two Portuguese school reports and surveys. The imbalanced dataset was pre-processed using *K*-Means SMOT (Synthetic Minority Oversampling Technique) before the actual classification was performed. The study also used an interpretable LIME (Local Interpretable Model-Agnostic Explanation) model for all the classifiers used in the study.

Therefore, the paper collected desensitized book borrowing information for five professional students from a school and a college in the past four years from 2016/01 to 2020/09 through communication with the school library management center and the academic affairs office, and the performance information of all students in the 2016 grade. Firstly, the collected data is processed, and then the Apriori algorithm is used to study the association rules between book borrowing and students' grades, and it is found that there is a strong correlation between book borrowing and students' grades. Finally, on the basis of the mining results of association rules, the BP neural network algorithm [7] is used to construct a student performance early warning model to monitor the performance of students in various majors. By comparing the early warning status of student performance of different majors, it provides a valuable reference for the talent training direction of the school.

The unique contribution of the paper includes:

- (i) Implementation of Apriori algorithm to study the association between book borrowing and students' grades
- (ii) Implementation of BP neural network algorithm to develop early warning model pertaining to students' performance in order to monitor the performance of students in various majors

2. Data Sources and Data Processing

2.1. Data Sources. With the support of the school library management center and the Academic Affairs Office, the paper collected desensitized library borrowing information of students in a college of a university and the grade information of all students in the class of 2016 in a subordinate secondary college in the last four years during 2016/01-2020/09. Among them, library borrowing data information contains book barcode, processing time, request number, and other field information. And student performance data information contains course name, course nature, course grade, and other field information.

2.2. Data Pre-Processing. In order to facilitate later studies, the raw data need to be cleaned to retain the data of research value. The paper mainly uses SPSS statistical analysis soft-

ware to conduct preliminary data processing. The specific treatment method is as follows: Because the system may malfunction during the students' borrowing process, resulting in errors such as missing information and garbled code in the borrowed book information entry. Therefore, before analyzing the data, the paper uses SPSS to filter out the problematic data using book call number and book name as keywords. For example, for the column of book call number, clear data types obviously have abnormal data. Considering that there are students who change departments midway, take a break from school, serve in the military, and retake courses after being discharged from the military resulting in grade data that is not meaningful to study, this paper uses students' names as keywords to count the total number of courses taken by students in their four years of study, and if a student does not have the same number of courses as other students in the same major, the student is considered to be in the above situation and then clear the information of this part of students. The book borrowing information through data cleaning retains the book borrowing information data of students in a certain college of a university for the past four years from 2016 to September 2020, with a total of 18091 items, and the grade data retains the grade information data of all students in the 2016 class of the college, with a total of 33758 items. For the following research, the paper uses SPSS to classify the data of book borrowing after preliminary processing, and summarizes the book borrowing information of students of the same major in a table, and then uses the COUNTIF function to check the book borrowing information. Statistically, the COUNTIF function helps to count data that meets a particular criterion. This helped to calculate the total amount of books borrowed by each student in the past four years. For the preliminary processed score data, the paper uses SPSS to classify the data and summarize the scores of students of the same major in a table. Finally, the book borrowing data and grade data are integrated according to different majors and different students. The integrated data is as follows in Table 1 (due to too much data, the text only shows the data of some students in a certain major):

2.3. Data Conversion. The data type of the Apriori algorithm requires category data, so the book loan data and the grade data need to be converted before implementing the algorithm.

2.3.1. Conversion of Book Loan Data. The library's book circulation information necessarily reflects some behavioral characteristics of students. The paper uses the indicator of the total number of books borrowed in the book lending information to reflect students' enjoyment of reading. It is understood that in order to promote reading, the university requires students to read at least 30 books during their four years of college for completing the reading block for credit. According to this requirement, the paper classifies students' preferences for reading into three categories, and the classification rules and data conversion results are as follows in Table 2 (due to too much data, only some students' data are shown in the article):

TABLE 1: Integration data (partial) table.

Course title	Credits	Whether degree course	Name	
			Bao*dong	Bu*jin
course1	2.00		61.00	67.00
course2	3.00		72.00	73.00
course3	1.00		81.00	76.00
course4	2.00		63.00	66.00
course5	4.00	Y	68.00	76.00
course6	4.00	Y	75.00	80.00
course7	3.50		74.00	82.00
course8	3.50	Y	73.00	81.00
course9	3.50	Y	78.00	74.00
course10	3.50		79.00	65.00
course11	4.00		73.00	80.00
course12	4.50		77.00	78.00
course13	5.50	Y	92.00	65.00
course14	2.50	Y	82.00	90.00
course15	2.50	Y	71.00	72.00
course16	2.50	Y	60.00	78.00
course17	4.00	Y	89.00	68.00
course18	4.00	Y	70.00	81.00
course19	4.00		76.00	81.00
course20	4.00		76.00	76.00
course21	4.00		76.00	83.00
Total number of books borrowed			36	45

TABLE 2: Borrowing level classification rules.

Total number of books borrowed	Corresponding borrowing level
[50, +∞)	A
[30, 50)	B
[0, 30)	C

As Table 3 shows, for example, if Zhang *Yao, a student of Computer Science and Technology Major (School Enterprise Class), borrows books for a total of 60 times, then his corresponding reading level is A.

2.3.2. Conversion of Grade Data. The paper uses the professional composite score to describe the good or bad professional performance of students, where the professional composite score is calculated as:

$$\text{professional composite score} = \frac{\sum \text{Score in each major course} \times \text{Corresponding professional course credits}}{\sum \text{Credits in each major course}} \quad (1)$$

The composite score is considered as combining the items representing a variable to create a score or data point pertaining to the same variable. The score forms reliable

and authentic measures of latent and theoretical constructs. In academics, the composite score is also considered the sum of passing scores.

The overall professional grades of each student were calculated, and the students' overall professional grades of the five majors were clustered into three categories by SPSS, and the clustering results are shown in Table 4:

As shown in the above table, the paper classifies student performance into three categories: excellent, good, and poor, where category 1 indicates that student performance is poor, category 2 indicates that student performance is good, and category 3 indicates that student performance is excellent. The achievement data were transformed according to the clustering results, and the transformed data (partial data) are shown in Table 5:

As the above table shows, for example, Ai*Ling of Internet of Things Engineering (School Enterprise Class) has a comprehensive professional score of 91.42, which corresponds to a performance level of Category 3.

3. Study of the Correlation between Book Borrowing and Student Achievement

3.1. Principle of Association Rule Apriori Algorithm. Association rules are a type of data mining function used to mine hidden connections between data from a dataset, denoted as $X \rightarrow Y$, where the set of items X is called the

TABLE 3: Table dividing the degree of students' preference for reading (partial data).

Name	Specialty	Total number of borrowings	Borrowing level
Zhang*Yao	Computer Science and Technology Major (School Enterprise Class)	60	A
Feng*Ya	Computer Science and Technology Major (General Admission Class)	61	A
Tan*qin	Mathematics and Applied Mathematics Major	38	B
Ran*Le	Mathematics and Applied Mathematics Major	31	B
Zhang*Wei	Mathematics and Applied Mathematics Major	24	C
Hao*Fei	Internet of Things Engineering Major (School Enterprise Class)	18	C

TABLE 4: Clustering center for student achievement by category.

Clustering center	Achievement level		
	1	2	3
	70.03	76.65	84.15

precondition and Y is the association result corresponding to X . Apriori algorithm is the most classical mining association rule in association analysis. Apriori algorithm is used to understand the way in which two or more objects are related to each other leading to the creation of association rules between the objects. This algorithm is also known as frequent pattern mining algorithm and is implemented on dataset consisting of huge number of transactions. In essence, it calculates the support, confidence, and lift of all permutations of the item set one by one, and finds frequent item sets that satisfy minimum support, minimum confidence, and lift greater than 1. In the paper, the Support, Confidence, and Lift are calculated as follows:

$$\begin{aligned}
 Sup(X) &= \frac{\text{Number of occurrences of item set } X \text{ in the transaction set}}{\text{Total number of transactions in the transaction set}}, \\
 Con(X \rightarrow Y) &= \frac{Sup(X, Y)}{Sup(X)}, \\
 Lift(X \rightarrow Y) &= \frac{Con(X \rightarrow Y)}{Sup(Y)}.
 \end{aligned} \tag{2}$$

Using the Apriori algorithm to mine the association rules between book borrowing and student performance, compared with other association rule algorithms, this algorithm has the advantage of using an iterative method of layer-by-layer search to mine data. The algorithm is easy to implement. And it can mine the connotative, unknown but actual data relationship.

3.2. Model of Correlation between Book Borrowing and Student Achievement

3.2.1. Model Assumption. There must be some connection between students' use of library resources and student achievement. For the association between library borrowing information and student achievement, the paper makes the following hypothesis: there is some connection between student achievement and the total number of books borrowed, and students with better achievement tend to enjoy reading.

3.2.2. Model Building and Solving. The paper implements Apriori algorithm by Python, and the minimum support and minimum confidence in the algorithm are set to 10% and 60%, respectively, and the results obtained are as follows in Figure 1:

From the analysis results, it can be obtained that the lift of both obtained association rules is greater than 1, indicating that the obtained association rules are meaningful. With a minimum support of 10%, the following association exists between students' enjoyment of reading and student achievement: 60.28% of the students who liked reading more had a good overall score and 60.64% of the students who had a poor overall score did not like reading.

4. Research on Performance Alert Model Based on BP Neural Network

4.1. Theory Related to BP Neural Network Algorithm. Neural networks are divided into biological neural networks and artificial neural networks. Artificial neural networks have the ability of parallel processing of information, self-learning ability, and inference ability, and are widely used in multiple fields such as pattern recognition intelligent robots, automatic control, and prediction estimation. BP (back propagation) neural network is the most traditional neural network, which was proposed in 1986 by a research group led by Rumelhart and McClland. The BP neural network model topology includes an input layer, a hidden layer, an output layer, and at least one hidden layer. Between the input and hidden layers are the weights of the network, indicating the strength of the connection between the two neurons. Any neuron in the hidden layer or output layer integrates the information from the neuron in the previous layer, simulating the principle in biology that a neuron must be stimulated to be triggered, and outputs the integrated information as the neuron in that layer. The algorithm steps are as follows:

Step 1: A sample is taken from the training sample set and its input information is fed into the network.

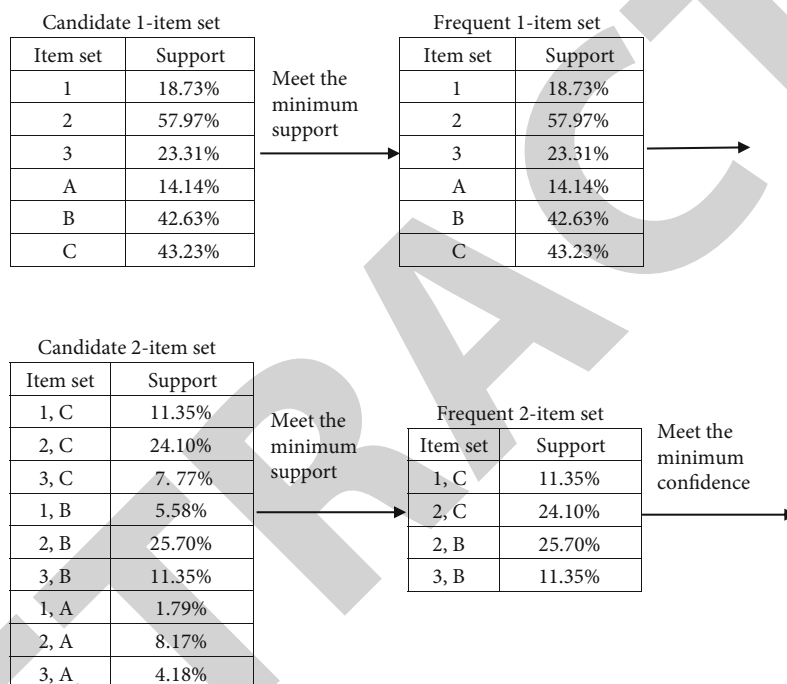
Step 2: The output of each layer node is calculated from the network forward.

Step 3: Calculate the error between the actual output and the desired output of the network.

Step 4: Starting from the output layer and working backwards to the first hidden layer, the individual connection weights of the entire network are adjusted in the direction of error reduction according to certain principles.

TABLE 5: Transformed data.

Name	Specialty	Professional composite score	Achievement level
Ai*Ling	Internet of Things Engineering Major (School Enterprise Class)	91.42	3
Pai*	Mathematics and Applied Mathematics Major	73.09	1
Bu*jin	Internet of Things Engineering Major (General Admission Class)	75.90	2
Cao*	Computer Science and Technology Major (School Enterprise Class)	77.20	2
Cao*Wei	Computer Science and Technology Major (General Admission Class)	89.45	3
Chen*Li	Mathematics and Applied Mathematics Major	76.47	2
Chen*Ha	Internet of Things Engineering Major (General Admission Class)	89.52	3
Du*you	Mathematics and Applied Mathematics Major	77.60	2



Rules for correlating reading levels with student achievement

Rule	Support	Confidence	Lift
B→2	25.70%	60.28%	1.04
1→C	11.35%	60.64%	1.40

FIGURE 1: Results of association rule analysis.

Step 5: The above steps are repeated for each sample in the training sample set until the required error is achieved for the entire network training sample set.

The BP neural network independently trains the input and output data according to the error back propagation algorithm, finds a reasonable connection between the input and output data, and realizes the prediction of the result. Compared with prediction methods such as least squares regression and grey model. It has strong nonlinear modeling ability, so the prediction of nonlinear data is more accurate. Therefore, this paper chooses to use BP neural network algorithm to predict students' grades.

4.2. Performance Alert Model Modeling. From the correlation analysis between student grade data and total student book circulation data in the previous chapter, it is known that the following correlations exist between grades and total book circulation: Students who enjoy reading more tend to have good overall scores, and those with poor overall scores tend to dislike reading. Based on the above study, this chapter uses BP neural networks to establish an early warning model of student performance. The model takes students' major course grades as input and the total number of books borrowed as output and is trained by BP neural network to predict the total number of books borrowed by students.

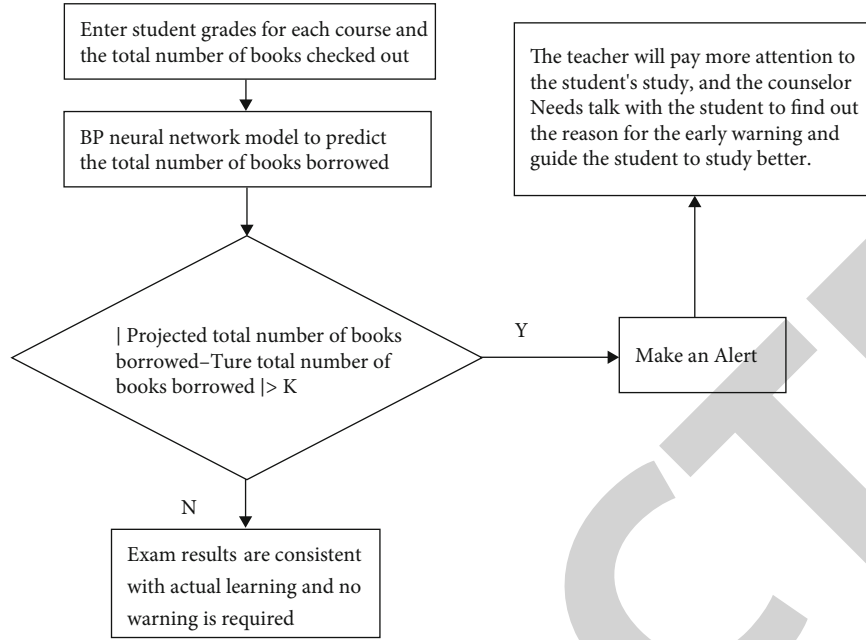


FIGURE 2: The flow of the performance alert model.

Set the threshold K for making the achievement warning, where K is calculated by the formula:

$$K = |\text{Projected total number of books borrowed} - \text{True total number of books borrowed}|. \quad (3)$$

If the error between the predicted result and the true value is greater than a certain threshold K , a grade warning is made for the student, indicating that there is a gap between the actual learning situation of the student and the result of the test score feedback, or that there is a suspicion of falsification of the student's book borrowing, which requires the teacher of the class to pay more attention to this part of the students in class and the counselor to strengthen the guidance of this part of the students' learning and life. The flow of the performance alert model is shown in Figure 2:

4.3. Implementation of Performance Alert Model

4.3.1. Discussion of the Achievement Warning Model Threshold K . Since the four majors, namely, Mathematics and Applied Mathematics Major, Internet of Things Engineering Major (General Admission Class), Computer Science and Technology Major (School Enterprise Class), and Computer Science and Technology Major (General Admission Class), include further 21 major courses, the paper uses the grade data of the students in the above four majors and the data of the total number of books borrowed to determine the threshold K . This helped in triggering the warning through model training. Students' grade data and students' total book borrowing data are imported into MATLAB, with the grade data package as input and the total book borrowing data as target, into the BP neural network toolbox, wherein the model is tuned to test data, validation data,

and training data ratios by the distribution of errors between the predicted and true values of book borrowing. Set the hidden layer of BP neural network as 10 layers, 25% of the data as test data, 15% of the data as validation data, and 60% of the data as training data, and the least squares optimization algorithm was selected to train the data to get the most desirable results, the results are as follows in Figure 3:

The error plot shows that the prediction accuracy of the model test set and validation values is high, indicating that the use of the model can achieve the purpose of predicting the total number of books borrowed through the professional course grades. The poor prediction accuracy of the training set indicates that there is a discrepancy between some students' learning performance and their actual learning situation.

After investigation, it is learned that approximately 20% of the students in the college will receive an academic warning from the school's academic affairs office in their senior year, on the eve of graduation. Combined with the error histogram in Figure 4, more than 78% of the students' book borrowing total volume predicted value and the true value of the error absolute value is within 25. Thus, in the paper, the threshold K for the achievement warning model to trigger achievement warning is set to 25. If $K > 25$, achievement warning is made, and if K is within the interval of $[0, 25]$, achievement warning is not made.

4.3.2. Model Implementation and Results Analysis. The professional course grades and the total number of books borrowed of the students of the college are imported into MATLAB, the grade data package is used as input, the total number of books borrowed is used as target, the hidden layer of BP neural network is defined as 10 layers, 25% of the data is used as test data, 15% of the data is used as validation data, 60% of the data is used as training data, and the least squares

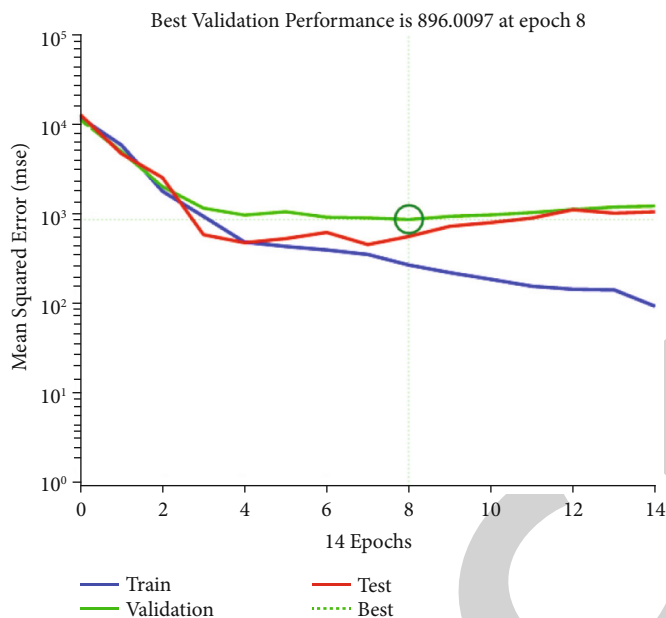


FIGURE 3: Error diagram.

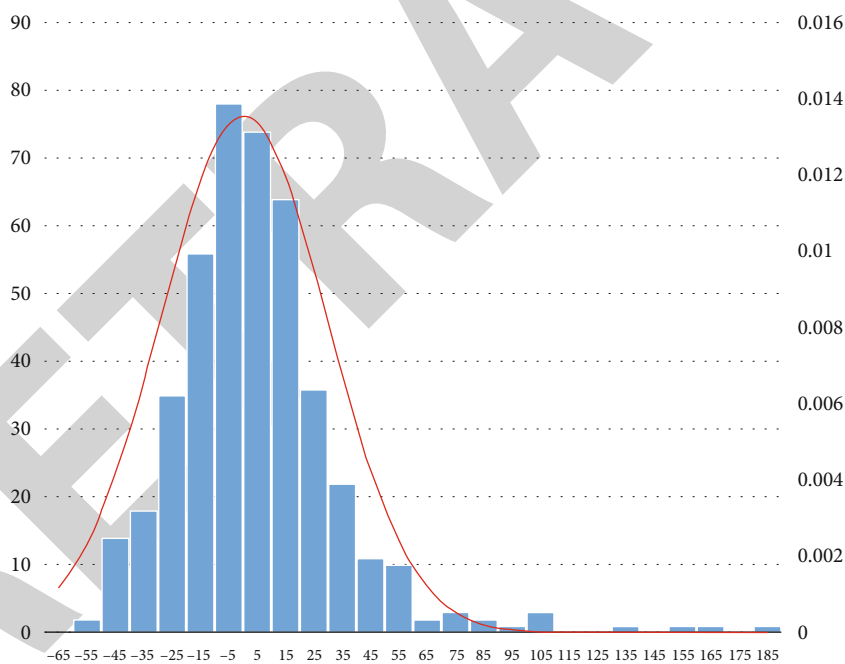


FIGURE 4: Error histogram.

optimization algorithm is selected to train the data. After running the data using MATLAB, the predicted and true values of the total number of books borrowed are obtained as follows in Figure 5:

A summary of the percentage of students who made performance warnings for each major is obtained as follows in Table 6:

Comparing the percentage of students who made achievement alerts in the five majors, the following results can be obtained: The most students in the Internet of Things

Engineering Major (General Admission Class) had the highest number of performance warnings, followed by the following in descending order: Mathematics and Applied Mathematics Major, Computer Science and Technology major (School Enterprise Class), Computer Science and Technology Major (General Admission Class), and Internet of Things Engineering Major (School Enterprise Class). Through understanding with the professional counselors, comparing the proportion of the number of academic warnings made by the Academic Affairs Office of the students of

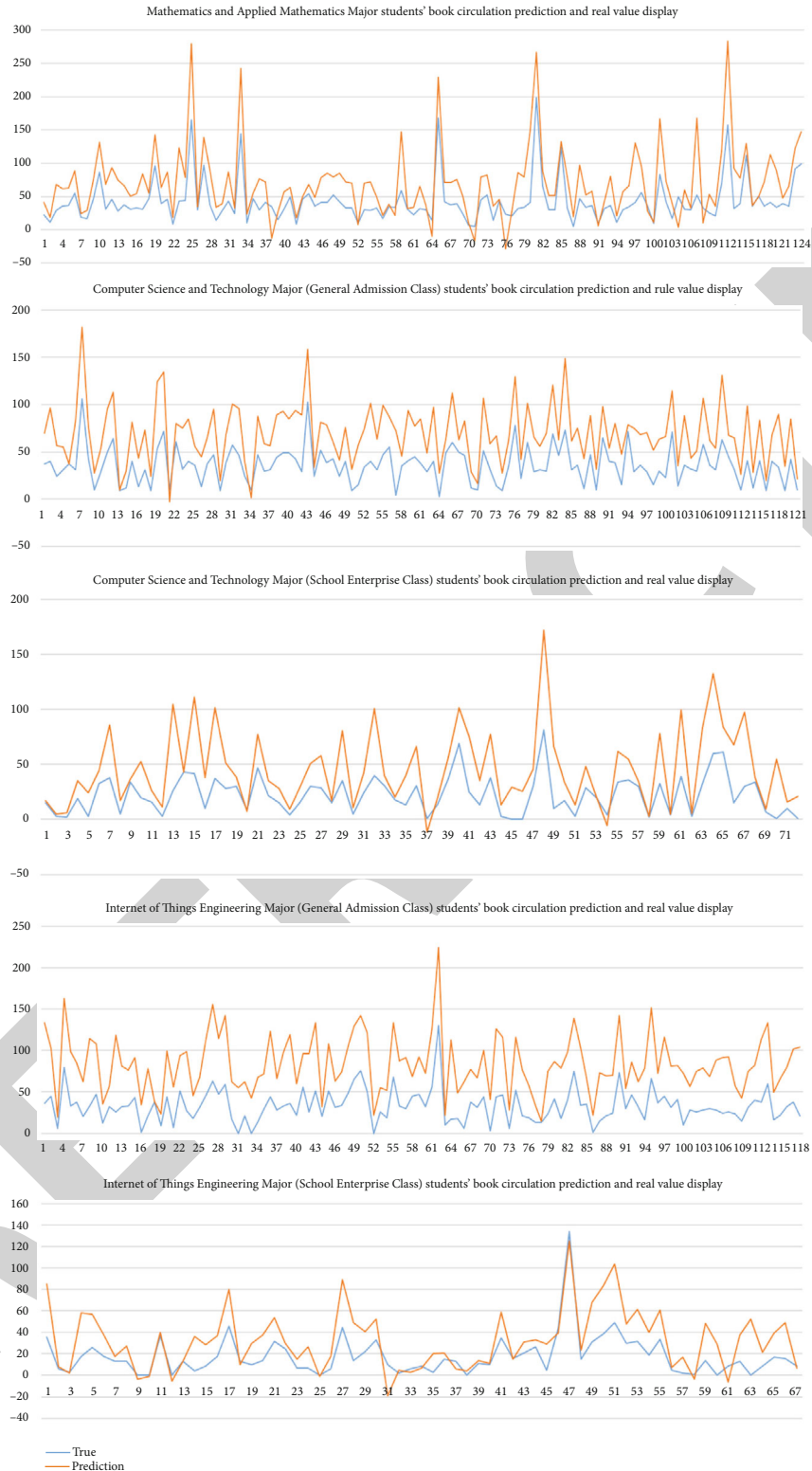


FIGURE 5: Students' book circulation prediction and real value display.

each major before graduation and the proportion of the number of early warnings analyzed by the results of the model, it is found that the difference between the two is within 5%. This shows that the model has a high early warning on student performance and has a certain reference value.

Comparing the proportion of students with grade warnings in the general admission class and the school enterprise class in Table 7, it can be found that the performance warning of the school enterprise class is significantly better than that of the general admission class.

TABLE 6: Summary of the percentage of students making performance warnings.

Major	Percentage of students making alerts
Mathematics and Applied Mathematics Major	33.06%
Computer Science and Technology Major (General Admission Class)	13.22%
Computer Science and Technology Major (School Enterprise Class)	22.22%
Internet of Things Engineering Major (General Admission Class)	35.60%
Internet of Things Engineering Major (School Enterprise Class)	10.45%

TABLE 7: Proportion of early warning students for different school-running nature.

The nature of running a school	Percentage of students making alerts
General admission class	27.27%
School enterprise class	16.51%

This result is consistent with last year's results of the school's national-level subject assessment.

In previous research, although some scholars have applied the BP neural network algorithm to the student performance early warning model, the research object is often a student of a certain major, and the error of the model is about 10%. This paper studies the early warning situation of students' performance in different school-running nature and majors, and the number and type of research objects are more than in previous studies. From the two dimensions of the nature of running a school and the major, by comparing with the actual situation, it is verified that the error of the model is within 5%, which improves the accuracy of the model.

5. Conclusion

This article mainly uses the four-year university grade data and book borrowing data of a certain school as the research object. First, using the Python programming language, the Apriori algorithm is used to mine the association rules of the book borrowing and student score data. It is found that there is a certain positive correlation between student grades and the total amount of books borrowed. Students who like to read will not have bad grades, and students with better grades also prefer to read. Then, based on the conclusion that there is a strong association rule between student performance and the total amount of book borrowing, using the BP neural network algorithm and taking student performance as input and the total amount of student book borrowing as the target, after neural network training, predict the total number of student books borrowed and use the absolute value of the difference between the predicted result and the true value to reasonably set the threshold K , thereby constructing the early warning model of student performance. This model realizes the monitoring of student performance and is widely used in the management of students' learning behavior. Using this model to give early warnings to students of five different majors in a certain uni-

versity, compare the warnings of students in different majors, and learn that in university study, more attention should be paid to cultivating students' practical ability, combining theoretical knowledge with practice, and encouraging students to go out of campus and go to internships in enterprises corresponding to their majors.

However, this article still has the following shortcomings: One is that the data samples in this article are not large enough, which leads to the unsatisfactory promotion value of the association rules. In the follow-up research, it is necessary to increase the data samples to improve the promotion of the association rules. The second is the insufficient use of book borrowing information. It only uses the information of the total amount of borrowed books of students and does not use the data of the book category. However, by reading the literature, it can be found that the category information of borrowed books is very important for studying student performance. The significance of the research requires further exploration and analysis. The third is that this article does not make better improvements to the algorithms involved, and further study and research are needed for three issues in the future.

Data Availability

The data used to support the findings of this study are included within the article.

Conflicts of Interest

The authors declare that they have no conflicts of interest.

Acknowledgments

This research was partly financially supported through grants from the Chongqing Higher Education Teaching Reform Research Key Project (No. 222166), the Chongqing Science and Technology Bureau Technology Innovation and Application Development Key Project (No. cstc2020jcsx-dxwtBX0044), the Chongqing Science and Technology Bureau Technology Innovation and Application Development General Project (No. cstc2020jcsx-msxmX0152), and the Scientific Research Project of Chongqing University of Education (No. KY202107B).

References

- [1] S. Dan, L. Dongbo, and F. Xia, "Research on course grade prediction and course early warning based on multi-source data

Retraction

Retracted: Artificial Intelligence-Based Interactive Art Design under Neural Network Vision Valve

Journal of Sensors

Received 23 January 2024; Accepted 23 January 2024; Published 24 January 2024

Copyright © 2024 Journal of Sensors. This is an open access article distributed under the Creative Commons Attribution License, which permits unrestricted use, distribution, and reproduction in any medium, provided the original work is properly cited.

This article has been retracted by Hindawi following an investigation undertaken by the publisher [1]. This investigation has uncovered evidence of one or more of the following indicators of systematic manipulation of the publication process:

- (1) Discrepancies in scope
- (2) Discrepancies in the description of the research reported
- (3) Discrepancies between the availability of data and the research described
- (4) Inappropriate citations
- (5) Incoherent, meaningless and/or irrelevant content included in the article
- (6) Manipulated or compromised peer review

The presence of these indicators undermines our confidence in the integrity of the article's content and we cannot, therefore, vouch for its reliability. Please note that this notice is intended solely to alert readers that the content of this article is unreliable. We have not investigated whether authors were aware of or involved in the systematic manipulation of the publication process.

Wiley and Hindawi regrets that the usual quality checks did not identify these issues before publication and have since put additional measures in place to safeguard research integrity.

We wish to credit our own Research Integrity and Research Publishing teams and anonymous and named external researchers and research integrity experts for contributing to this investigation.

The corresponding author, as the representative of all authors, has been given the opportunity to register their agreement or disagreement to this retraction. We have kept a record of any response received.

References

- [1] Y. Zhao, "Artificial Intelligence-Based Interactive Art Design under Neural Network Vision Valve," *Journal of Sensors*, vol. 2022, Article ID 3628955, 10 pages, 2022.

Research Article

Artificial Intelligence-Based Interactive Art Design under Neural Network Vision Valve

Yuqi Zhao 

Graduate School of Advanced Imaging Science, Multimedia & Film in Chung-Ang University, Seoul 156-756, Republic of Korea

Correspondence should be addressed to Yuqi Zhao; 3321010317@stu.cpu.edu.cn

Received 20 July 2022; Revised 23 August 2022; Accepted 3 September 2022; Published 25 September 2022

Academic Editor: Sweta Bhattacharya

Copyright © 2022 Yuqi Zhao. This is an open access article distributed under the Creative Commons Attribution License, which permits unrestricted use, distribution, and reproduction in any medium, provided the original work is properly cited.

Interactive art design (IAD) is an organic integration of art and technology. From the perspective of the development of AI machines from ancient times to the present, it has gone through the stages of command interface, graphical interface, and multimedia interface. The development of interactive art has been around for some years. As an art form, it not only brings optimization and enjoyment to people's quality of life but also meets the needs of human-computer interaction, improves the efficiency of art design, and realizes human-human interaction. The purpose is to bring different feelings and experiences to the works and people's psychology. In particular, the application of AI in IAD has not only brought great changes to designers. It also derives the interaction of behavioral limbs, which brings a greater experience and interaction to the audience, thereby creating a better interactive effect. Therefore, this paper completes the following work: (1) the research progress of AI in IAD at home and abroad is introduced. (2) The combination of AI and IAD is proposed, and the basic principle of RBF neural network and intelligent optimization algorithm are introduced, and the evaluation index of IAD is constructed. (3) Using the constructed dataset to test two intelligent optimization algorithms, the results show that the PSO-RBF model is more excellent in evaluating the quality of IAD. The trained model is used for experiments, and the output of the model is compared with the expert evaluation results, and the error is very small. Comparing the quality indicators of IAD before and after the integration of AI, the results show that AI has an excellent improvement effect on IAD.

1. Introduction

The evolution of manufacturing equipment and production procedures has played a significant role in human civilization's growth throughout thousands of years. Future technological advances in the form of the fourth industrial revolution will be another major step forward in human civilization's progress toward a more intelligent society. Now is the moment for new generation information technology, new energy, and new transportation technology to take center stage in human civilizational evolution and change [1–3]. Intelligent technology will lead to productivity improvements and breakthroughs in a wide range of sectors, including IAD, as it develops in a steady and consistent manner. The popularity of artificial intelligence (AI) has risen to an all-time high, and many multinational corporations, both at home and abroad, are ready to spend significant sums of money to acquire top personnel to investigate different applications of AI. As far as big data is concerned,

China is a major nation on the Internet that generates a lot of data every day, which makes it a better place to train AI algorithms than other countries [4, 5]. AI is now being researched to differing degrees in several domains, and the field of art design is an essential foundation for the use of AI technology, particularly in IAD [6, 7]. Google released the intelligent voice home assistant Google Home and announced that future development will be dominated by AI. Alibaba's AI design platform "Luban" completed the design of 400 million posters on "Double Eleven", reaching 8,000 designs per second. In 2017, during the "two sessions" in China, government departments wrote AI for the first time in their work reports, and research on AI has become a strategic policy of the country. During China's "two sessions" in 2018, AI was mentioned again, which fully shows that AI has been valued and supported by the country today [8, 9]. In today's advocating people-oriented and paying attention to humanistic care, the intervention of intelligent technology in IAD is undoubtedly a key factor for human

beings to move towards humanistic care. The center of interaction is to create meaningful experience, and its essence is the interaction and communication between people and works. To effectively integrate AI with IAD, we must pay greater attention to the humanization of the interactive experience. Combining AI with IAD is precisely the research of today's trending themes. The use of AI to IAD may affect not just the appearance of IAD but also whether it will be replaced by robots. The unknown is a psychological hazard [10–12]. For instance, many individuals fear that AI may replace their occupations. In actuality, the intervention of AI is a postintelligent period of art and design in which people and computers coevolve. The fast growth of AI has become an inescapable obstacle on the path to the advancement of human science and technology in the digital era. From smart city to smart home to smart design, artificial intelligence is advancing in every aspect of our lives [13, 14]. With the continuous pursuit of personal feelings and personalization, the efforts of artists and designers are not enough. It is also necessary to use technology to support the continuous development of personalized needs. AI is on the verge of a revolution in intelligence. With the fast advancement of technology, there are an increasing number of AI applications in IAD. With the fast advancement of computer technology and the Internet [15], the interactive characteristics of creative design have grown more pronounced and unique. In an unprecedented manner, the computer as a control device governs the interaction process. On the basis of the present intelligent technology used in IAD, AI has also started to emerge in our everyday lives. Intelligent IAD may adapt to the recipient's behaviour, posture, voice, expression, temperature, remote control, and climatic change through robotics, computers, sensors, intelligent programmes, intelligent materials, and other intelligent technologies [16, 17]. Combining IAD with AI extends the conventional creative form. Intelligent technology's participation has brought forth new issues, but it has also provided us with a fresh viewpoint from which to reconsider art. This paper uses the research hotspot of AI to cut into the IAD and conducts research on the developing intelligent IAD. The neural network is then utilised to assess the quality of the interface design after the incorporation of artificial intelligence, providing a strong academic theoretical foundation for AI in the area of IAD.

The unique contribution of the paper includes the following:

- (i) Implementation of AI in interactive art design
- (ii) Development of a framework using RBF algorithm and PSO for optimization
- (iii) Evaluation of the PSO-RBF model in comparison to the state-of-the-art approaches

2. Related Work

Domestic research on AI art design has only started in recent years, and a systematic research method has not yet been formed. It mainly tends to study the art form of a specific field of AI. Reference [18] begins with a detailed discussion of what is singularity technology and singularity art

and the relationship between technology and art in the context of the development of singularity technology. It systematically introduces the changes brought by intelligent technology and intelligent materials to traditional art design. This paper discusses in detail how the current artists use AI technologies such as intelligent robots, intelligent interaction, and virtual reality to realize art design creation and the impact of the development of intelligent materials on art design in the future. It boldly speculates and reasonably deduces the transformation of future art under the impact of singularity. With the fast development of AI technology, reference [19] describes in detail how virtual reality technology might be artistically merged with art design. It examines the link between science, art, and aesthetics, as well as the ideas and practises associated with mixing virtual reality technology with art design. Based on virtual reality technology and under the guidance of virtual art design, the author builds the primary content of virtual reality art design research in collaboration. By taking virtual reality art design as an entry point, we can grasp the research paradigm of digital art design macroscopically. According to reference [20], modern art design and virtual reality technology may now be integrated in a new way. The research is carried out from the research objects, research tasks, realization means and artistic characteristics of virtual reality art design, etc., respectively. It is concluded that virtual reality technology will have a big influence on art design in the future because of the development of AI. Reference [21] discusses the impact of the development of AI technology on art design and redefines the new relationship between art and technology from the perspective of AI development and discusses the potential of AI art in terms of the value of artists and works of art. Reference [22] believes that art is a creative activity carried out by human beings through free will, and AI only plays a role in sharing part of human labor in this process. There is a fundamental difference between this kind of labor and the creative activities of human beings in artistic creation, that is, whether there is free will or not, and all creations performed before AI has free will cannot be called artistic design. Reference [23] systematically discusses the relationship between art and science, as well as the research content of virtual reality art design. Reference [24] briefly introduces the impact of AI, virtual reality, and other high-tech technologies on the traditional interactive mode of art design and expounds the influence of subjective and objective factors on the development of IAD from the aspects of sensory, media, and aesthetic characteristics. Reference [25] gave a detailed introduction to the penetration of AI, virtual reality, holographic projection, robots, and other high-tech technologies into art design by means of exhibition cases. Reference [26] systematically discusses virtual reality art design. The author describes the immersive artistic aesthetic experience and virtual and real space of virtual reality art design in the way of works appreciation. The western research on AI art design is earlier than China, and the research on AI art design has made certain achievements. Western scholars' research on AI art is mainly carried out from two aspects: theory and art design practice. The growth of IAD, intelligent art design, and creative

philosophy from 1964 to 2011 is detailed in reference [27]. Predicting how art design will evolve and how intelligent elements will influence it is also important. Reference [28] compares the design of contemporary new media art with those of historic virtual art from the viewpoints of artistic aesthetics and creative expression. There is a comparison between conventional and virtual reality art in reference [29]. Virtual art design has progressed from fantasy to immersive experience, as described in this piece. References [30, 31] discuss in detail the relationship between art design and AI through GAN, an art group obvious composed of three artists in Paris. Reference [32] imitates many works of art masters by reconstructing ANNs and using AI recognition technology. An impressive amount of work has been done by reference [33] in the area of artificial intelligence art design, particularly in the area of combining robots and humans and then controlling the creative production of human behaviour. Reference [34] uses AI pattern recognition technology to study the visual information recognition and image generation art of intelligent robots.

3. Method

3.1. Application of AI in IAD

(1) IAD of intelligent platform: the first stage of development is IAD with intelligent platform as the main part. Taichung conducts human-computer interactive art creation. At this stage, AI already has certain natural language, machine vision, etc. By simulating works designed by human intelligence, technology is used to collect, analyze, model, and sort out massive data. When the designers need to create a certain work, the relevant data or information can be extracted from the database at the first stage. Then, the work can be deconstructed by the designer, and the required relevant work generated can be created with the help of a single click. For example, Alibaba's Luban can design 8,000 posters in one second. Designing intelligent design platforms has become easier because of the advances in science and technology. In addition to Luban, there are also intelligent platforms related to design, which can implement automatic color matching through various matching methods, coloring, correction, and other functions, so as to provide more and more designers with convenient services. Among them, in terms of text matching text IAD, intelligent color matching is first collected, analyzed, and refined in the database. Then, the pixels on the image are captured, a reasonable algorithm is selected within the system, and different pixels are fed back in the form of text, and the final color matching model is formed for different color distribution areas to complete the work. Another example is the IAD of text matching images, the main principle of which is to automatically generate design proposals through design suggestions. According to different needs, AI can judge the excellent design works by collating massive data

and comparing the data of the works of excellent designers

- (2) IAD of intelligent machines: the second stage of development of artificial intelligence ushered in the intelligent machine-oriented mode and intelligent machines can complete the works required by users through simulation and cloning. Compared with the first stage, this stage is more artistic and expressive. In August 2015, German research experts announced the results of AI research, the main content of which is that the AI system is carrying out deep learning on the painting style of the world's famous painters. Through the multilevel network structure, different levels of information in the image are extracted. For example, when learning a painting, AI will first select large color blocks with large color differences and then gradually deepen the color, pay attention to more painting details, and use the polyline to achieve the application purpose of the visual recognition function. At the same time, in the actual process of extracting various kinds of fine information, the AI machine will also filter unnecessary factors through its own software. Especially in IAD, AI machines have the best performance in painting design. The principle of its painting design is realized through neural network, image experience, and related main functions
- (3) IAD of human-machine collaboration in intelligent technology: the third stage of AI development has ushered in the human-machine collaborative creation model. IAD with the help of human-machine collaboration mode allows users to get a whole-hearted immersive experience or create works together with designers. This form is also a mainstream way in the future. The essence of immersive synaesthesia experience is the art produced by the interaction of people, equipment, and space. It is a spatial interaction of people, machines, and interfaces. The word synaesthesia is derived from the wide variety of experiments conducted by artists who have explored the impact and cooperation of senses, namely, seeing and hearing. Synaesthesia is found in all forms of arts, namely, visual music, music visualization, audiovisual art, abstract film, and intermedia. Thus, a new artistic logic is formed, which can mobilize the various senses of the participants, help them better understand the information of the works, and give timely feedback. However, in this field with a common structure of space, the participants and the works can create a very strong sense of immersion through interaction. Virtual reality technology is such a product, and the difference between it and the real world is gradually narrowing with the advancement of technology, and the boundaries between the two are gradually overlapping, and it is even difficult to distinguish and define in some cases. The emergence of virtual

reality technology not only has a great impact on people's way of life but also gradually subverts the original way of human cognition. The continuous development of strong intelligent IAD has higher and higher requirements for designers. Intelligent interactive art is the art of responding to changes in the recipient's behavior, posture, and voice through intelligent tools such as intelligent robots. Through such advanced technical equipment, designers can use language, expressions, etc. to create a variety of interactive artworks

3.2. The Structure and Characteristics of RBF Neural Network. RBFs have just one independent variable: their distance from the origin. The monotonic function of the Euclidean distance from any point in the space to the midway is sometimes referred to as the midpoint distance. For the RBF neural network, the hidden layer neurons are excited by radial basis functions, the input vector is transformed once, and the low-dimensional mode is converted to the high-dimensional mode before the output of the hidden layer neurons is weighted and summed. The cover theorem ensures the RBF neural network's mathematical logic. For example, a nonlinear pattern classification issue is more linearly separable in high-dimensional space than in low-dimensional space, according to the theorem. Only one hidden layer exists in RBF neural networks, unlike other forward neural networks, which have several hidden layers. For example, there is no processing done by neurons in the input layer before transmitting data to the hidden layer neurons. This is a direct link. Radial basis functions, which may be characterized as nonlinear, nonnegative, radially symmetric decay functions, are used in the activation function of the hidden layer. The hidden layer is connected to the output layer through a linear weighted link. As a result, there is no connectivity between neurons inside a single layer of an RBF neural network. There are no local minima in an RBF neural network since it has an extremely basic topology. The output function of the RBF neural network can generally be expressed as

$$F(x) = \sum_{i=1}^n w_i \varphi(\|x - c_i\|), \quad (1)$$

where c represents the center of the basis function, w_i represents the weight, and $\varphi(\|x - c_i\|)$ is a set of radial basis functions, so $F(x)$ is expressed as a set of radial basis functions for linearity fit.

The commonly used radial basis functions are as follows:

(1) Gaussian function:

$$\varnothing(x, c) = \exp\left(-\frac{(x-c)^2}{2\sigma^2}\right) \quad (2)$$

(2) Anomalous sigmoid function:

$$\varnothing(x, c) = \frac{1}{1 + \exp\left(\frac{(x-c)^2}{\sigma^2}\right)} \quad (3)$$

(3) Fit the quadratic function:

$$\varnothing(x, c) = \frac{1}{1 + \sqrt{(x-c)^2 + \sigma^2}} \quad (4)$$

wherein σ represents the width of the radial basis function. The smaller the σ , the smaller is the width of the radial basis function and the greater the selectivity of the radial basis function

The Gaussian function is the most often used, and it offers the following benefits: the depiction is straightforward. When it is the same, the selectivity is greatest and the breadth is least. Because the general function may be represented as a linear combination of a number of basis functions, it has high smoothness and can take any derivative. RBF consists of two layers of processing wherein the first input is mapped into each RBF in the hidden layer. The function which is used normally is the Gaussian function, and its value depends on the distance to the center of the input space, similar to the concept of Euclidean distance. The weighted connection between the neurons in the hidden layer and the neurons in the output layer produces a linear combination according to the approximation principle of the RBF neural network. The RBF neural network has only one hidden layer which is also known as the feature vector. The RBF neural network features the following: in the RBF neural network, there is just one hidden layer and a basic structure. Only output data is sent to hidden layer neurons in the RBF neural network's input layer. There is no further processing. The radial basis function, a local function, activates the buried layer neurons in the RBF neural network. Only if the input data is in a small region will the function produce a meaningful response; i.e., the output will be nonzero. Transform the global optimal problem into a linear summation of local optima. The main advantage of using RBF is that it uses only one hidden layer and radial basis function is used as activation function which help in approximation. The model is easily designable and has good generalization and strong tolerance towards input noise and online learning ability.

3.3. Comparison of RBF Neural Network and BP Neural Network. Both RBFNN and BPNN are nonlinear multilayer feedforward neural networks, and they are both general-purpose approximators. From a certain point of view, the two are the same, because for any BPNN, an RBF neural network can be found to replace it and vice versa. But there are many differences between the two, as follows:

(1) RBFNN only uses weighted connections between the hidden layer and output layer, direct connections between the input layer and the hidden layer, and weighted connections between all the layers of BPNN, from a network structure viewpoint. A nonlinear excitation function is used by the hidden layer

neurons of the BPNN in comparison to a Gaussian excitation function by the hidden layer neurons of the RBF neural network. The number of hidden layers and neurons in the hidden layer of the BPNN are unknown. The number of hidden layers and the number of neurons in the hidden layer cannot be modified after the network model has been established. When a certain issue requires more or fewer neurons in a hidden layer, an RBF neural network has just one hidden layer

- (2) From the perspective of the training algorithm, the BPNN adopts the gradient descent method, that is, starting from a certain starting point, training samples in the direction of error reduction, so that the error reaches the minimum value. However, for practical problems in reality, the network is more complex, and the error function is a curved surface in a multidimensional space. The error is easy to fall into a local minimum value of the curved surface. Therefore, the movement of the point in all directions will lead to an increase in the error, so that the error will fall into local minima rather than global minima. Because it is hidden inside an infinite range of space, this function is always nonzero in the input space used by the BPNN hidden layer. As a global approximation neural network, the weights of the whole network must be adjusted during each training session. The rate of training is rather sluggish. A small subset of the input space is used by the RBF neural network's hidden layer, which employs radial basis functions with nonzero values. It is a local approximation neural network, so it does not get trapped in local minima, and the RBF neural network converges fast
- (3) From the perspective of approximation ability, theoretically, both RBF neural network and BPNN can approximate any nonlinear system with arbitrary precision. Due to the different excitation functions used, the approximation performance is also different. The convergence speed of RBF neural network is faster than that of BPNN, and the topology of RBF neural network is clear. It has good approximation ability for nonlinear systems, and RBF neural network has become the main model in many fields because of its stronger vitality

3.4. Intelligent Optimization Algorithm

3.4.1. *Genetic Algorithms.* Genetic algorithm (GA) can be mainly divided into the following processes:

- (1) Coding: the parameters of the issue space cannot be directly dealt with by the GA. In order for it to be used, it must be transformed into a genetic code string based on a certain coding technique, which is an individual. This conversion process is called coding. The problem to be solved by coding is to express the candidate solutions in the population with a simple and practical genetic code string. The encoding method also affects

the performance of the genetic algorithm. There are two commonly used encoding methods. The binary encoding method converts the parameters to be solved in the original problem into binary form; that is, the encoded symbols are only represented by binary symbols 0 and 1. The binary coding method conforms to the structure of chromosomes, the operations of crossover and mutation are simple, and there are many algorithm modes. However, since the gene length needs to be determined first in the solution process, the precision of the parameters is also limited, and the precision cannot be changed during the solution process. And the individual length of the binary coding method is long, so the solution efficiency is low. It is possible to encode an individual's genetic information using a floating-point encoding approach, which implies that each gene is represented by the original value of the parameter, which is an integer number in a certain range. Solution accuracy and efficiency are both enhanced by using floating-point encoding

- (2) Generating a population: the first step in generating a population is to define the number of individuals, that is, the population size. When the population size is large, it is easy to find the optimal solution, but the calculation time of the algorithm will be prolonged. Reducing the population size can shorten the calculation time, but it is prone to premature maturation. The second step is to randomly generate gene strings for each chromosome
- (3) The fitness function, which is used in the genetic algorithm to represent the quality of the individual's location: when a person has a higher fitness level, they are closer to finding the best answer, increasing the likelihood that their traits will be passed down to future generations. As a result, those who are less fit will have a decreased chance of passing on their traits to the next generation, in keeping with the idea of survival of the fittest. Fitness function construction has two requirements: the fitness function's value cannot be zero, and the fitness function's rise must be compatible with the optimization of the objective function, which means it must increase in a direction consistent with that function's optimization
- (4) The selection operation is to select suitable individuals to reproduce offspring on the basis of the fitness evaluation of individuals in the population. People who are more physically fit are more likely to be chosen, whereas those who are less physically fit are less likely to be chosen. The most commonly used selection method is the wheel selection method, which takes the sum of the fitness of all individuals as a roulette wheel. The fitness of each individual corresponds to a part of the area in the roulette, and the greater the fitness, the larger the area occupied by the individual. When the wheel is rotated, the position of the pointer is the selected individual

TABLE 1: AI IAD evaluation index system.

Index	Label
Product structural strength	L1
Environmentally friendly interior materials	L2
Link part safety	L3
Efficient packaging	L4
Beautiful surface decoration	L5
Good visual experience	L6
Sanitary details are in place	L7
Safe for extreme use	L8
Potential hazard control	L9
Reasonable function	L10
Easy to transport	L11
Reasonable roundness of shape	L12
Smooth interaction	L13
Comfortable interface design	L14
High scalability	L15
Material seams smooth	L16
Environmentally friendly packaging materials	L17
High functional innovation	L18

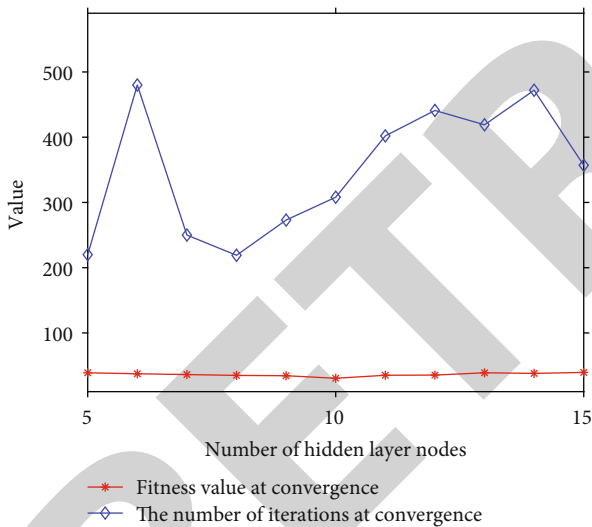


FIGURE 1: Convergence of genetic algorithm with different number of hidden layer nodes.

- (5) Crossover operation, that is, the main parts of the two parent individuals are exchanged in a certain way, thereby forming two new individuals: crossover operation is the main feature that distinguishes the genetic algorithm from other algorithms, and the crossover operation affects the global search ability of the entire genetic algorithm. There are different crossover algorithms for different encoding methods
- (6) Mutation operation, that is, to change some gene positions of some individuals in the population: according to the different coding methods, it is divided into

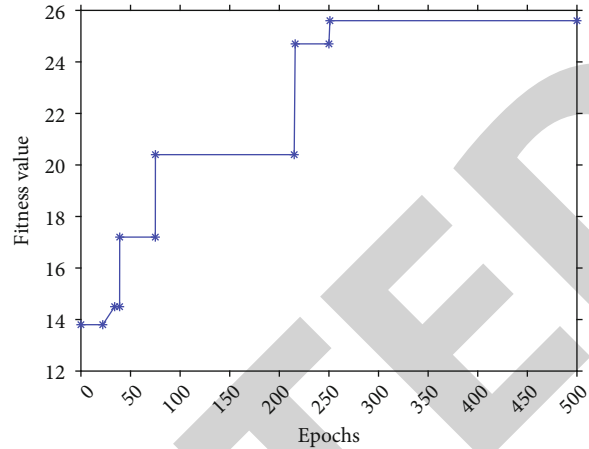


FIGURE 2: The optimal individual fitness curve of the genetic algorithm population.

real-valued variation and binary variation. The mutation operation generally has two processes. The first process is to judge whether the individual needs to be mutated according to the preset mutation probability. The second process is to select random locations for mutation of individuals that need to be mutated. It is possible to boost the global search capabilities of the algorithm by incorporating mutation in the early stages of an iteration in order to assure the multidirectionality of population members and avoid premature phenomena. Secondly, we want to improve the algorithm's capacity to quickly find the ideal solution for each person in the latter stages of the iteration. Obviously, in the early stage of iteration, a small mutation probability cannot guarantee the multidirectionality of the population. In the later stage of iteration, individuals are concentrated in the neighborhood of the optimal solution, and a large mutation probability will destroy the optimal solution gene. As a result, the mutation probability should be higher in the early stages of iteration and lower in the latter stages, as explained above

3.4.2. The Principle of Particle Swarm Optimization Algorithm.

From the modelling of birds' social systems, the development of PSO (particle swarm optimization) was born. Consider a scenario in which a flock of birds is out foraging in an area where there is only one food source and no one in the flock knows where it is. Knowing the distance to the food, the easiest technique to locate the food is to approach the bird closest to the meal and scan the area surrounding that bird. A flock of birds is the starting point for PSO's social simulation, and each of the birds is referred to as a particle. Using the objective function, each particle has a fitness value that is based on its present location and the best place it has previously looked for. An iteration of this process occurs in which the particle flies at a predetermined speed, which is determined by a fitness function value and the particle's flying direction and distance. Particle speed is governed by "two extreme values": the "individual extreme value" or pBest, which is the particle's best possible location in the iterative process. Iteratively searching for the

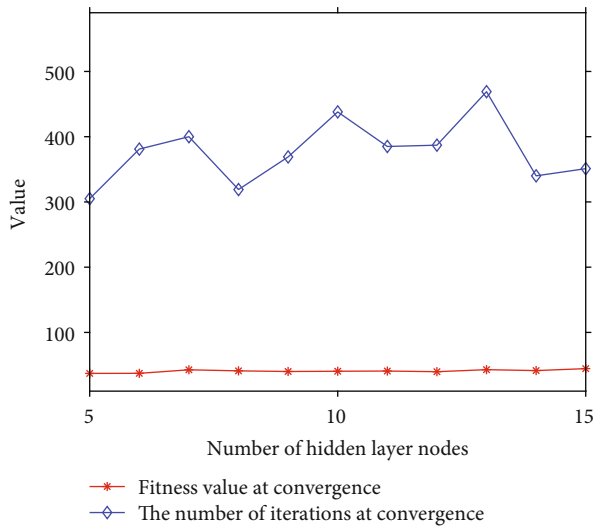


FIGURE 3: Convergence of PSO with different numbers of hidden layer nodes.

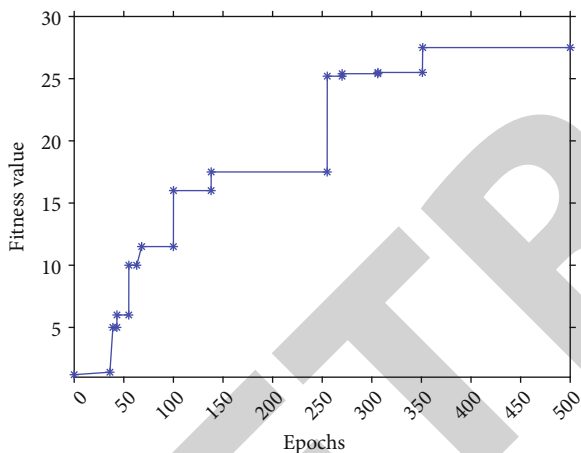


FIGURE 4: The optimal individual fitness curve of the PSO population.

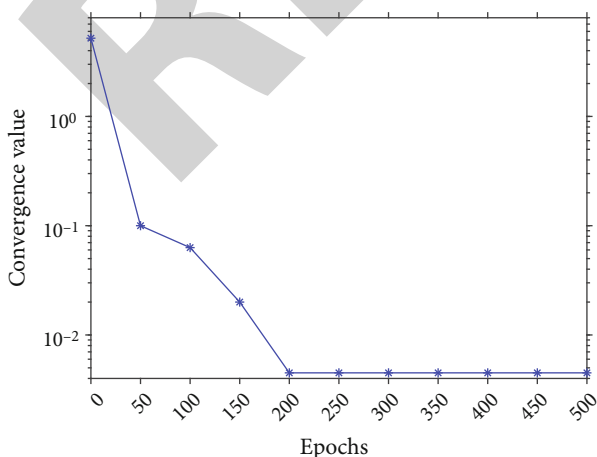


FIGURE 5: PSO-RBF neural network model training effect.

best possible location, known as gBest, is the other extreme value, which is referred to as the group extreme value or gBest. Set the search space to be D -dimensional and the number of particles to N for the conventional PSO algorithm's mathematical formulation. The position of the i th particle is expressed as $X_i = (x_{i1}, x_{i2}, \dots, x_{iD})$; the optimal solution searched by the i th particle in the iterative process is denoted as $p_i = (p_{i1}, p_{i2}, \dots, p_{iD})$, that is, individual extrema pBest. The optimal solution in the individual extreme value p_i searched by all particles is recorded as p_g , which is the group extreme value gBest. The flying speed of the i th particle is the vector $V_i = (v_{i1}, v_{i2}, \dots, v_{iD})$. Then, the D -dimensional flight speed of each particle is expressed as

$$v_{id}(t+1) = \omega v_{id}(t) + c_1 \text{rand}() (p_{id}(t) - x_{id}(t)) + c_2 \text{rand}() (p_{gd}(t) - x_{id}(t)), \quad (5)$$

$$x_{id}(t+1) = x_{id}(t) + v_{id}(t+1), \quad (6)$$

where $i = 1, 2, \dots, N$, $d = 1, 2, \dots, D$, acceleration factors c_1 and c_2 are normal numbers, $\text{rand}()$ is a random number of $[0, 1]$, ω is called inertia factor, $x_{id}(t)$ is the current position of the i th particle, $v_{id}(t)$ is the current velocity of the i th particle, $p_{id}(t)$ is the optimal solution in the historical solution of the i th particle, and $p_{gd}(t)$ is the entire particle swarm the optimal solution.

In the iterative process, the moving distance and moving speed of the ions need to be limited. The position change and speed change range of the d th dimension are $[-x_{d,\max}, x_{d,\max}]$ and $[-v_{d,\max}, v_{d,\max}]$, respectively. If the moving distance or moving speed of the particles exceeds the maximum variation range during the iteration, the boundary of the maximum variation range is taken. The main advantages of using PSO are its simplicity of use, robustness in controlling the parameters, and its ability to achieve optimal efficiency in comparison to other mathematical algorithms. PSO is a metaheuristic technique which does not make any assumptions about the problem which is being optimized, and it can be easily parallelized for the purpose of concurrent processing.

Various studies have been conducted using PSO in arts and related domain. As an example, the study in [35] analyzed the basic concepts of art therapy and children's painting using PSO technique. The study was conducted in preschool for art teaching among children. The study focused on finding the global optimal fitness function which reduced the computational complexity and also provided maximum coverage to the existing network. The study in [36] performed application analysis of fusion particle swarm optimization for the performance evaluation of the instructors in the academic domain. The PSO and fuzzy comprehensive evaluation was performed for evaluating the instructors' performance, and an index parameter was used between a scale of 2.5 and 3.0 which indicated that the performance was excellent.

3.5. IAD Evaluation Index System. According to the AI-based IAD framework proposed in this paper, an IAD evaluation index system is constructed, as shown in Table 1.

TABLE 2: Experimental comparison between model output and expert evaluation results.

Number	1	2	3	4	5	6	7	8
Model output	0.752	0.719	0.826	0.638	0.656	0.931	0.873	0.775
Expert results	0.753	0.720	0.826	0.638	0.657	0.930	0.870	0.774

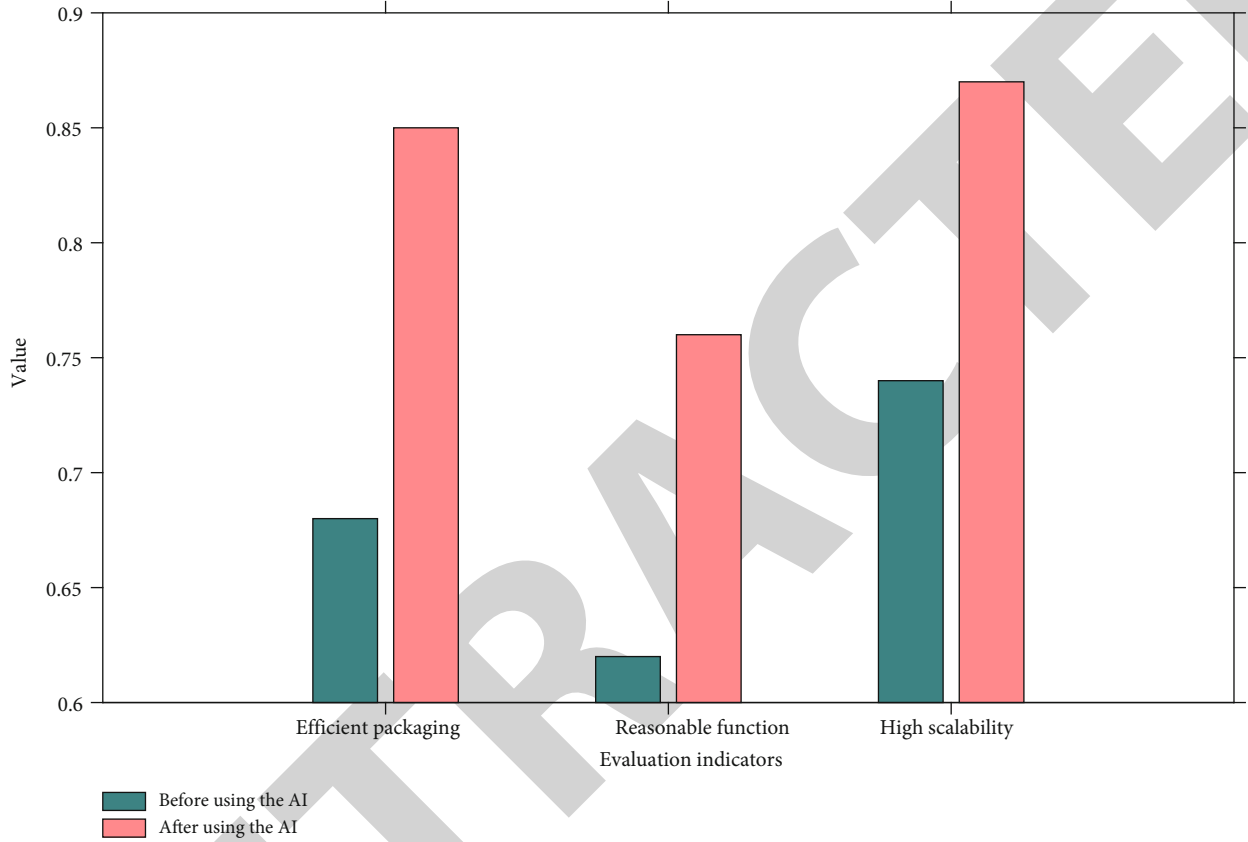


FIGURE 6: Comparison of IAD quality before and after the integration of AI.

4. Experiment and Analysis

4.1. Sample Data and Preprocessing. According to the IAD evaluation index system set in Chapter 3, this paper constructs a dataset for experimental testing, which includes 1600 sets of data. After selecting the experimental data, normalize the data, and normalize all the sample data to the interval [0,1], using the following formula:

$$x^* = \frac{x - x_{\min}}{x_{\max} - x_{\min}}. \quad (7)$$

4.2. Network Optimization Parameter Selection

4.2.1. RBF Neural Network Experiment Based on GA Optimization. In this paper, the crossover probability of the genetic algorithm is selected as 0.8, the mutation probability is 0.2, and the fitness value of the genetic algorithm when the number of neurons in the hidden layer of the neural network is 5-15 is shown in Figure 1.

It can be seen that when the number of neurons in the hidden layer is 10, the convergence is the best. At this time, the optimal individual fitness curve in the genetic algorithm group is shown in Figure 2.

4.2.2. RBF Neural Network Experiment Based on PSO. In the particle swarm optimization algorithm in this paper, the acceleration factor $c_1 = 2$ and $c_2 = 2$ and the inertia factor adopt a linear decreasing weight strategy and select $w_{\max} = 0.8$ and $w_{\min} = 0.4$. The fitness value of the particle swarm algorithm when the number of hidden layer neurons in the working day neural network is 5-15 is shown in Figure 3.

When the number of neurons in the hidden layer is 14, its convergence performance is the best. At this time, the fitness value of the optimal individual in the iterative process of the PSO algorithm is shown in Figure 4.

It can be seen from the above experiments that the PSO algorithm has the smallest number of iterations and the largest fitness value. Compared with the genetic algorithm, the number of iterations is reduced by 26%, and the fitness value

is increased by 16%. Therefore, from the overall performance point of view, the PSO algorithm has a faster convergence speed, and the searched optimal solution is more accurate.

4.3. Model Experiment Results. First, the PSO-RBF neural network model is trained, and the convergence of the model is obtained as shown in Figure 5. It can be seen that the model quickly reaches a very low convergence value.

The trained neural network is used to evaluate the non-training data in the sample data, and the prediction results of the PSO-RBF model are shown in Table 2. It can be seen that the output value of the model is very close to the evaluation results of experts, indicating that the model has superior performance in evaluating the quality of IAD.

4.4. The Effect of IAD Based on AI. In order to verify the effect of AI-based IAD proposed in this paper, the quality indicators of IAD before and after the integration of AI are compared, as shown in Figure 6.

5. Conclusion

The application of AI in IAD will not only generate new application paradigms but also make the two promote each other. When discussing AI and IAD, it becomes clear that AI has a significant place in the field. Designers' visual thinking is reconstructed and the audience's perspective and experience are profoundly altered as a result. Using IAD as a new art form, artists have sought to better serve their audiences' emotional and experiential needs while also enhancing their own spiritual selves. Therefore, this paper has completed the following work: (1) in-depth analysis mainly focuses on the research of AI in IAD at home and abroad and expounds the help and significance of AI in IAD in the current digital age. The following thesis lays the theoretical foundation. (2) The combination of AI and interaction design is proposed, and then, the basic principle of RBF neural network and intelligent optimization algorithm are introduced, and the evaluation index of interaction design art is constructed. (3) Using the constructed dataset to test two intelligent optimization algorithms, the results show that the PSO-RBF model is more excellent in evaluating the artistic quality of interaction design. The trained model is used for experiments, and the output of the model is compared with the expert evaluation results, and the error is very small. Comparing the quality indicators of IAD before and after the integration of AI, the results show that AI has an excellent improvement effect on IAD. The results generated by the PSO-RBF model are promising, but the metrics used for evaluation are confined to convergence value, fitness value, and no. of iterations at convergence. The superiority of the model could be further justified by including accuracy, specificity, sensitivity, precision, and recall. This could be considered as future scope of research and observe how the model functions when such metrics are used for evaluation.

Data Availability

The datasets used during the current study are available from the corresponding author on reasonable request.

Conflicts of Interest

The author declares that he has no conflict of interest.

References

- [1] S. Muggleton, "Alan Turing and the development of artificial intelligence," *AI Communications*, vol. 27, no. 1, pp. 3–10, 2014.
- [2] P. Van den Besselaar and L. Leydesdorff, "Mapping change in scientific specialties: a scientometric reconstruction of the development of artificial intelligence," *Journal of the American Society for Information Science*, vol. 47, no. 6, pp. 415–436, 1996.
- [3] S. K. Bhagat, T. M. Tung, and Z. M. Yaseen, "Development of artificial intelligence for modeling wastewater heavy metal removal: state of the art, application assessment and possible future research," *Journal of Cleaner Production*, vol. 250, article 119473, 2020.
- [4] F. Wu, C. Lu, M. Zhu et al., "Towards a new generation of artificial intelligence in China," *Nature Machine Intelligence*, vol. 2, no. 6, pp. 312–316, 2020.
- [5] J. Zhu, T. Huang, W. Chen, and W. Gao, "The future of artificial intelligence in China," *Communications of the ACM*, vol. 61, no. 11, pp. 44–45, 2018.
- [6] C. O. Wong, K. Jung, and J. Yoon, "Interactive art: the art that communicates," *Leonardo*, vol. 42, no. 2, pp. 180–181, 2009.
- [7] S. Carter and M. Nielsen, "Using artificial intelligence to augment human intelligence," *Distill*, vol. 2, no. 12, article e9, 2017.
- [8] J. Heer, "Agency plus automation: designing artificial intelligence into interactive systems," *Proceedings of the National Academy of Sciences of the United States of America*, vol. 116, no. 6, pp. 1844–1850, 2019.
- [9] L. Ma, "Realization of artificial intelligence interactive system for advertising education in the era of 5G integrated media," *Wireless Networks*, pp. 1–14, 2021.
- [10] M. Lewis, "Evolutionary visual art and design," in *The Art of Artificial Evolution*, Natural Computing Series, J. Romero and P. Machado, Eds., pp. 3–37, 2008.
- [11] S. A. Busari, K. M. S. Huq, S. Mumtaz et al., "Generalized hybrid beamforming for vehicular connectivity using THz massive MIMO," *IEEE Transactions on Vehicular Technology*, vol. 68, no. 9, pp. 8372–8383, 2019.
- [12] A. Stern, "Deeper conversations with interactive art: or why artists must program," *Convergence*, vol. 7, no. 1, pp. 17–24, 2001.
- [13] H. S. Kim and S. B. Cho, "Application of interactive genetic algorithm to fashion design," *Engineering Applications of Artificial Intelligence*, vol. 13, no. 6, pp. 635–644, 2000.
- [14] G. J. Hwang, H. Xie, B. W. Wah, and D. Gašević, "Vision, challenges, roles and research issues of artificial intelligence in education," *Computers and Education: Artificial Intelligence*, vol. 1, article 100001, 2020.
- [15] N. Singh, V. K. Gunjan, G. Chaudhary, R. Kaluri, N. Victor, and K. Lakshmana, "IoT enabled HELMET to safeguard the health of mine workers," *Computer Communications*, vol. 193, pp. 1–9, 2022.
- [16] Y. X. Cai, H. Dong, W. Wang, and H. Song, "Realization of interactive animation creation based on artificial intelligence technology," *Computational Intelligence*, vol. 38, no. 1, pp. 51–69, 2022.

Retraction

Retracted: The Application of Traditional Chinese Woodcut Printmaking Language in Digital Painting Based on Intelligent Computing

Journal of Sensors

Received 22 August 2023; Accepted 22 August 2023; Published 23 August 2023

Copyright © 2023 Journal of Sensors. This is an open access article distributed under the Creative Commons Attribution License, which permits unrestricted use, distribution, and reproduction in any medium, provided the original work is properly cited.

This article has been retracted by Hindawi following an investigation undertaken by the publisher [1]. This investigation has uncovered evidence of one or more of the following indicators of systematic manipulation of the publication process:

- (1) Discrepancies in scope
- (2) Discrepancies in the description of the research reported
- (3) Discrepancies between the availability of data and the research described
- (4) Inappropriate citations
- (5) Incoherent, meaningless and/or irrelevant content included in the article
- (6) Peer-review manipulation

The presence of these indicators undermines our confidence in the integrity of the article's content and we cannot, therefore, vouch for its reliability. Please note that this notice is intended solely to alert readers that the content of this article is unreliable. We have not investigated whether authors were aware of or involved in the systematic manipulation of the publication process.

Wiley and Hindawi regrets that the usual quality checks did not identify these issues before publication and have since put additional measures in place to safeguard research integrity.

We wish to credit our own Research Integrity and Research Publishing teams and anonymous and named external researchers and research integrity experts for contributing to this investigation.

The corresponding author, as the representative of all authors, has been given the opportunity to register their agreement or disagreement to this retraction. We have kept a record of any response received.

References

- [1] C. Chen, "The Application of Traditional Chinese Woodcut Printmaking Language in Digital Painting Based on Intelligent Computing," *Journal of Sensors*, vol. 2022, Article ID 2223868, 12 pages, 2022.

Research Article

The Application of Traditional Chinese Woodcut Printmaking Language in Digital Painting Based on Intelligent Computing

Changhuan Chen 

Guangzhou Academy of Fine Arts, Guangzhou 510006, China

Correspondence should be addressed to Changhuan Chen; anna6226@gzarts.edu.cn

Received 30 July 2022; Revised 12 August 2022; Accepted 16 August 2022; Published 25 September 2022

Academic Editor: Sweta Bhattacharya

Copyright © 2022 Changhuan Chen. This is an open access article distributed under the Creative Commons Attribution License, which permits unrestricted use, distribution, and reproduction in any medium, provided the original work is properly cited.

With the passage of time, information technology has been implicitly embedded in people's lives, bringing an important impact on artists' creations. Modern painting technology is advanced, using electronic products, digital devices, electronic hand-painting tools, and other equipment to simulate the real texture of brush strokes to paint the style and effect the artist seeks. The integration of woodcut prints into digital painting has enriched the form of digital painting, and one of the characteristics of digital illustration is its fast dissemination, which is more powerful to promote the charm of traditional art. In the new era, with new technology, we consider whether we can combine the digital painting style, expression, woodcut language, and cultural connotation of ancient Chinese woodcut prints with digital technology and use new methods and forms to speak about the unique and essential attributes of ancient Chinese woodcut prints to be innovated and continued. The emotional motivation and the implicit, obscure connotations of the art of painting are not as far apart as they seem, although they are more like logical computerized counterparts. The continued development of artificial intelligence has made it possible for computers to create paintings independently. This paper explores a process flow model for digital painting based on intelligent computing and effectively incorporates the language of traditional Chinese woodcut printmaking while looking at future trends in this field.

1. Introduction

Woodcut printmaking is the main form of traditional Chinese printmaking. The development of traditional Chinese woodblock printmaking has gone through four main periods and more than 1000 years. With such a long span of time, traditional Chinese woodblock prints, although basically existing as prints, provided relevant technical support in restoring the style of paintings. The first period was the Tang dynasty. The earliest woodblock print found is the woodblock print of the title page of the Vajra Sutra, "Sayings," carved in 868 AD, which predates Dürer's print by 700 years and can be considered the first surviving print in the world. Buddhism developed during this period, and Buddhist figures were largely personified by popular acceptance and the influence of indigenous philosophies. The characteristics of woodcut prints in the use of line modeling and the sun-engraving technique in figure engraving played an important role in the presentation of religious figures and the propaga-

tion of Buddhist ideology objectively. The second period is the Song and Yuan dynasties. The important feature of woodcut prints in this period was to get rid of the situation of serving and relying on religion and to move towards secularization and closer connection with the life of the people. In addition, the downward movement of woodblock prints made the source of subject matter more extensive, very diverse, and technically sophisticated, and the emergence of vermilion and ink two-color overprint woodblock prints objectively promotes the traditional woodblock art into a period of prosperous development. The third period is the Ming dynasty. This period of woodcut prints develops momentum; the reason, due to social stability, economic prosperity and scientific and technological progress and the refinement of engraving technology, brought about changes in the technical processing of woodcut prints. For example, in the past, woodcut prints used a single line engraving method, but in the Ming Dynasty, there was a black-and-white contrast, in which we are familiar with the illustrations

in “The West Wing” and “Water Margin,” representing the development of woodcut prints in this period. The fourth period was the Qing dynasty. Due to the book ban movement, the publishing industry was hit hard, and the publishing industry closely related to the woodcut prints was also affected. The more prominent phenomenon is the impact of woodblock prints; at the same time, the production of woodblock prints prevailed, not only the emergence of woodblock prints production centers, such as Weifang and Sichuan Mianzhu, but also a variety of print subject matter, which makes the traditional woodblock prints a stumble, until the modern era was replaced by the new prints.

Chinese prints have always been of great value, both in terms of content and expression, as well as in terms of technique and dissemination, and have subsequently expanded and developed in the field of art [1]. During the Ming and Qing dynasties, foreign missionaries came to China one after another, and when Matteo Ricci came to China, he used copperplate as a tool for spreading Christianity and employed a large number of Chinese to create prints, while in the Republic of China, woodblock prints continued to exist as a vehicle for spreading news [2]. In these times, the printmaking method was generally based on line engraving, combined with the perspective and chiaroscuro of western painting, which indirectly reflected the basic style of printmaking in these times [3]. In the new era, PS and digital prints have taken the development of printmaking to a new level in terms of creation and techniques, and digital printmaking has now become a part of contemporary painting expression [4].

Printmaking in China’s status is quite high; 1100 years ago, prints from the earliest works such as “Vajra Paramita Sutra” appeared; due to the origin of printing in China, the Han dynasty engraved topography and other methods of replication of efficiency appeared; for the late engraving and printing to provide the conditions and reference methods, China from replica topography to the original woodcut prints, the Chinese with their own wisdom and culture makes woodcut prints in the field of art radiant bloom [5] (see Figure 1).

The art of Chinese woodcarving has a long history of history, literature, folklore, and aesthetics into one, recording the long history, culture, and folklore of China and expressing the people’s strong desire for a better life [6]. In the development of Chinese civilization, China woodcut art itself has a popularity and reproducibility that no other art can replace. This paper summarizes and discusses the artistic language, culture, and aesthetic aspects of traditional China woodcarving art.

Facing today’s technologically advanced society, the survival of printmaking faces certain challenges, and the production of woodcuts requires materials, space, color, and manpower [7]. For modern people, there is often a reluctance to put in much effort to realize a woodcut print. At the same time, we also find that the number of people who are willing or know how to appreciate woodcuts is decreasing [8]. In the digital age, the circulation of paper books and newspapers is slowly decreasing (along with the advent of cell phones and electronic devices dedicated to reading



FIGURE 1: Woodcut on wood surface.

books), reducing the exposure of woodcuts even more. Publishers are gradually reducing the production of woodcut books because print is not popular and sales are not good. So woodblock prints are gradually fading out of the lime-light [9].

The main purpose of this paper is to analyze the development of digital printmaking in the new era and to show the openness and innovation of the vision of printmaking in the new era, as well as the innovation in the subject matter, content, ideas, and expression methods of printmaking [10]. At the end of the 20th century, computers entered everyone’s life and cameras changed from film to digital imaging, so digital image art has become one of the most important forms of artistic expression nowadays, and digital printmaking not only bridges the tradition in artistic creation but also can be expressed with the help of computer software technologies such as Photoshop, 3dsmax, and Corel Draw. In the 21st century, digital printmaking plays an important role in shaping new visual art forms and also makes the language of printmaking enter a new level of expression, and how to build “expressiveness” in the new digital printmaking is the question we need to think about now [11].

2. Related Work

Woodcut printmaking (Figure 2) refers to the use of tools to carve out reverse graphics on a wooden board and then the use of items with materials that can produce color such as ink and pigments, coated evenly printed on paper and finally presented to appreciate the art craft works. Prints mostly refer to woodblock prints; because of the scarcity of materials such as copper and iron types, there are also a few copper block prints with overlay color omission, and in modern times, screen printing has appeared [12]. But in times, due to the limitation of tools and materials, knife engraving and the combination of woodblock form a unique knife flavor and wood flavor.

In the information society, design has been integrated into all aspects of people’s life, and part of the design also has a strong commercial nature, so people will call it commercial digital painting, which is collectively known as “commercial art painting.” With the development of technology and the application of new technology, new methods,



FIGURE 2: Woodcut prints.

and new means, painting is gradually transformed from hand-drawn on paper to computerized drawing, synthesis, processing, and so on. Computer painting, also known as digital painting, is highly efficient, modifiable, and infectious and has various methods of realization, which is more in line with the commercial rhythm of today's society and conveys a commercial culture [13].

Printmaking differs from the form of drawing not only with a pen on paper or textile but also requires a variety of materials to produce different digital painting effects, such as wood, stone, and silk screen. At least three steps (drawing, engraving, and printing) can produce more than two works with the same image, which is called printmaking [14]. The art of printmaking is spreading with the momentum of a star fire, and the art of woodcut not only enriches the art form but also enriches the content of books and magazines, increasing the readability of books and enriching people's cultural life with artistic aesthetics [15]. Moreover, China has a long history as the birthplace of printmaking, with the advent of movable type printing providing technical support, coupled with the increased interest in woodcut printmaking by our literati painters, who also physically joined in the innovation of conservation production [16]. In Figure 3, the texture of the vase is depicted directly by inputting vectors to the texture effect and the cyan color among the vase, shaping the sense of brokenness to reexperience new feelings. A branch inserted into the vase adds color nicely, rearranging and reorganizing the pattern on top of the cyan porcelain, and then, it is well integrated into the work, and the smoke and clouds in the sky are well combined with the vase. By jerking, stretching, or deliberately blurring, the cyan strip gradually becomes blurred from clear in the changing shape, further creating a mysterious atmosphere [17].

In Figure 4, by depicting the scene of workers hard at work digging a cave and by shaping and accumulating this texture of stones in the material from time to time, especially the bumpiness of the rocks dug out, the author embodies the workers' hard work day and night and expresses his praise for the workers' tireless work.

In Figure 5, the picture feels distant and tranquil and certainly gives people a quiet feeling. In the midst of the dark



FIGURE 3: Misty rain, such as sky green.

green sky, a group of ducks with spots are walking leisurely forward, and they are lined up in turn, with their heads held high showing the forward pursuit of beauty, and this care-free state of mind also affects the mood of the viewer.

The art of computerized digital painting based on intelligent computation dates back to the time before computers became widespread, when there was no artificial intelligence to assist, but relied on pure ideas [18]. A typical representative is fractal art, which follows strict mathematical rules to recursively and cyclically replicate patterns, while the final presentation is stunning [19]. Traditional rule-based system art includes a human concept, which is then generated by algorithmic rules, either starting from scratch or based on some material to begin visualization [20]. As in the case of the revolutionary painting algorithm by researchers at Nagoya University [21], this algorithm, after being given a digital painting with a style, gradually evolves them by cutting, stitching, flipping, and discarding images that are not needed in each evolution and do not fit the initial style, to end up with a surprising image work. During the creation process, the creator strictly enforces the algorithmic rules. With the popularity of computers and the rapid development of artificial intelligence, algorithmic art is usually used more often in digitally painted images generated through computer code.

More than a dozen genres of algorithm-based digital painting have been developed, including fractal art, genetic art, cellular automata, proceduralism, and transhumanist art [22]. It can be said that it is algorithm-based digital painting that brings computers and art together autonomously. The further development for algorithm-based digital painting is an attempt to transform the identity of the computer in the creation of art [23]. However, the existing technology is unable to construct an artificial intelligence equivalent to a human being for painting from top down.



FIGURE 4: A sleepless night.



FIGURE 5: Free ducks.

Therefore, the existing attempts are based on bottom-up intelligent simulations of behavior. Algorithm-based digital painting is essentially the activity of using a computer as a tool to create art under the guidance of human intentions [24]. More ambitious attempts try to make the computer itself a painter, which requires the involvement of a higher level of intelligent computing, thus constituting a relatively independent computer-centered individual. There are two difficulties in the composition process: the first is how to achieve autonomous computer painting through intelligent computing; the second is the simulation of the painting intention.

3. Integration Application of Woodcut Printmaking and Digital Painting

3.1. A Framework for Digital Painting Based on Intelligent Computing. Leaving aside the level and intention of painting, the painting process is essentially an optimization process about how colors are manually assigned. Therefore, most of the digital painting features of smart painting programs are based on this principle. The difficulties in the implementation of this process lie in the image recognition capabilities of artificial intelligence, the construction of imagination, and the construction of the effects of uncertainty.

3.1.1. Imaginative Model Based on Intelligent Computing. Although the principle of imaginary model construction is simple, the difficulty lies in the algorithm design of image recognition and image reconstruction. Computer programs and the human brain are far apart in their ability to recognize images. The human brain can quickly recognize abstract shapes and symbols and generate images in a way

that computers still struggle to do. People provide the AI with image information to perform image recognition and reconstruct the recognized elements to produce paintings. The principle of this imagery model based on intelligent computing is shown in Figure 6. Google is one of the most advanced experimenters in this field, with its “initialist” AI creating a set of 29 digital paintings that were auctioned in Los Angeles in 2016. The program is essentially a simulation of a human neural network—an artificial neural network. Here, “Initiationism” is aimed at learning a series of case studies from which new works of art can be created. This is essentially a process based on learning rules and connecting patterns of guesswork.

3.1.2. Emotional Model Construction Based on Intelligent Computing. The intelligent computing-based emotional model construction attempts to make the process of computer painting more random and emotional and thus closer to the unpredictability of the artist’s painting creation. The approach used is based on an existing process with additional input of affective factors. Various forms of input can be used, such as for the capture of external signals or the generation of random influence signals through internal mechanisms. The principle is illustrated in Figure 7.

Examples of such are the interactive robotic drawing program published by Benjamin Grothe, which allows the ambient sounds around it (including dialogue sounds, background sounds) and its own mechanisms to have an effect on the drawing process. The real advantage of this approach is not as simple as just accepting random factors. When combined with big data mining techniques or the intentional input of information about a certain subject, it is able to complete paintings that humans cannot create. According to psychologist Carl Jung’s theory, the vast repository of human cultural and artistic information contains the patterns and information codes of the collective human unconscious. By allowing a computer program to mine the data and output it in the form of a painting, the final work created would be a digital painting with collective unconscious visual symbols that are not available to humans by virtue of their individuality.

3.2. Generation of Digital Painting Intent Based on Intelligent Computing. The main principles that allow programs to generate creative purposes and intentions alone, free from human input, are currently being attempted in this area as follows.

3.2.1. Imaginative Modeling to Generate Painting Themes and Motives. The most wonderful part of the painting process is the imagination. If a computer is given an imaginative model, then the computer is able to generate imaginative results from this model. In this process, the human only provides the input material for the computer’s imagination, the process of imagination is done by the computer, and the final output of the result is shown in the form of drawing. The process is shown in Figure 8.

The pioneer in this field was Harold Cohen, who started developing an intelligent computing-based digital painting

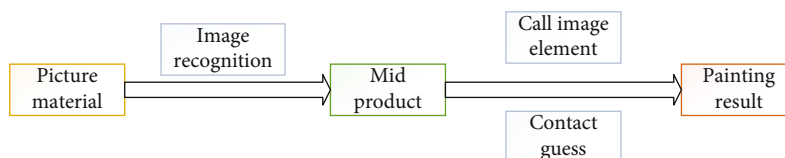


FIGURE 6: Digital painting model using intelligent computing.

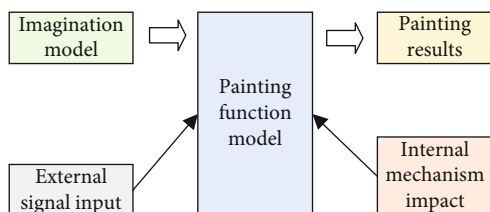


FIGURE 7: Painting function model for digital painting.

program called AARON in 1973. Through accumulated training, the AARON program's ability to paint digitally improved each year, and it began to simulate objects or people in the 1980s and to paint in color after the 1990s. At the same time, its paintings were exhibited and auctioned and collected by individuals and groups in various ways. AARON does not paint with pixels, but on a real canvas (AARON manages a physical painting machine through a painting function model, capable of mixing real paints and painting on real objects). During the development process, its imaginative model is constantly trained and reinforced. In this way, it can paint still life, portraits of people without receiving any reference image input, and has reached the level of children's painting. AARON's core design idea is to simulate the human brain's imagination, and its drawings are limited to its existing knowledge, driven by its limited imagination, without relying on any explicit artificial instructions.

3.2.2. Models That Enable Computers to Write Ideas and Thus Generate Creative Intent. This model is capable of collecting and discovering information autonomously to generate viewpoints and thus creative intent. Then based on the creative intention, and accompanied by the emotion model and imagination model, the painting is created. The principle is shown in Figure 9.

At the heart of this approach is the endowment of the ability to compose ideas, thus allowing the computer to generate painting themes and intentions on its own. A typical example of this type is *The Painting Fool*, an intelligent computational painting program created by Simon Colton, which is endowed with an imaginative power, an ability to articulate ideas, i.e., the ability to describe scenes and paint them with intent without any particular reference image. For example, the program downloads news about the war in Afghanistan, reads it, extracts keywords, finds images from the web on the subject, and then, in a painterly interpretation, makes an abstract collage of these images, presenting a fighter jet, an explosion, a family, an Afghan girl, and a war graveyard side by side. The designers opened an exhibition, "You Can't Know My Mind," in which "painting fools"

read the first 10 stories in the British newspaper *The Guardian* and then painted portraits for visitors. If the software reads very negative emotional articles, it may refuse to paint. For the rest of the time, its digital painting is guided by the customer's special expressions or appropriate emotional adjectives. And at the end of the painting, it self-evaluates the work.

3.3. Integration of Traditional Printmaking and Modern Digital Painting

3.3.1. The Visual Elements of Woodcut Printmaking Are Introduced into Digital Painting. Excellent woodcut works often contain the subtleties of plane composition and color composition, such as the relationship between black and white and gray and the relationship between real and imaginary, in the paintings. It is also because these relationships together constitute the plane language of woodcut prints and ultimately through these plane language build a harmonious work of art on paper.

(1) *Black and White Gray Relationship.* For woodcut prints, especially monochrome woodcut prints, the color elements in the whole picture creation should be harmonious enough, for example, the heaviness embodied in the large surface, combined with various forms of dotted line surface techniques for gouging, so that after inking, not stained with ink, so that after the topography of the picture presents a blank to show the white part, thus forming a strong contrast between black and white. The gray surface is between the black surface with a finer knife marks to distinguish between the light and dark parts.

(2) *The Relationship between Real and Imaginary.* Void is often a white space, while the positive form, which exists with a clear graphic sense, is real, for example, in Figure 10, the Chinese printmaker Wang Qi's 1953 print "Selling Surplus," the white space in the lower left corner and the representation of the figure from near to far make the picture full of tension. At the same time, the correct use of the relationship between reality and fiction can form a spatial relationship between the picture elements to guide the viewer visually. Like an invisible navigation, it leads the viewer to appreciate the whole picture in an orderly way.

(3) *Perspective Relationship.* In woodcut prints, perspective relationship is not as obvious as other painting categories, and woodcut prints emphasize more on flat language, but there is no lack of excellent works that use perspective relationship to express large scenes. For example, in the work shown in Figure 11, by enlarging the farmland in the near

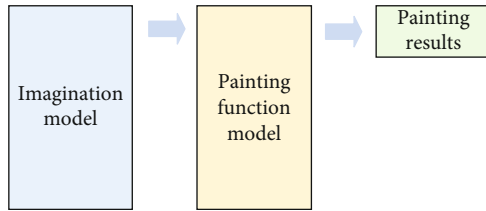


FIGURE 8: The process of digital painting with intelligent computing.

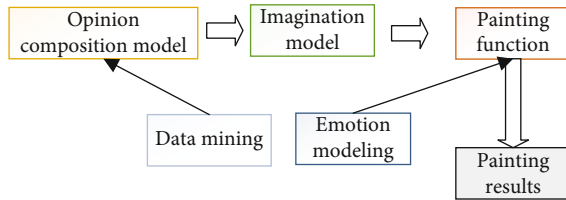


FIGURE 9: Creative painting model.



FIGURE 10: Selling the remaining food.

distance, regularizing it with lines, and then using the village under the mountain in the distance as the focus of perspective, the sense of space in the picture is satisfactorily expressed, and the whole work has a reasonable sense of order between feelings, making the woodcut quite interesting.

(4) *Brush and Ink.* In woodcut printmaking, brush and ink can also be understood as the artist's method of knife movement, that is, the angle and direction, force, and technique of knife movement. If we compare the techniques of Chinese painting, the inking of Chinese painters and the engraving of printmakers are in some ways compatible.

(5) *Formal Language of Point, Line, and Surface.* In the creation of wood carving, point, line, and surface are the picture of the painting language, which expresses the meridian relationship of the picture. The use of painting language is the skeleton of the artist's creation and the blood in the creation of engraving. The point, line, and surface of woodcut printmaking and their combination forms are mainly extracted from the point, line, and surface that constitute the constituent elements of woodcut works and decomposed into vari-



FIGURE 11: Raisen village.

ous forms to form unique visual effects with their own values and meanings, forming various combinations.

In woodcut printmaking, dots, as the smallest unit of existence in the picture, can be arranged in different combinations to produce refreshing stylistic features. By using dots of different sizes and densities for different subjects, the rhythm and atmosphere of the prints can also be enhanced. For example, in Figure 12, "Fox in the Snow," the woodcut prints show a series of footprints left by a small fox in the snow in the distance in the form of "dots," which enliven the atmosphere of the whole picture. Everything in the world has its shape and outline, so the use of lines in the creation of woodcut prints is particularly important, in addition to the outline of specific forms, but also through the different curvature of the lines to express the artist's creative mood. And the surface is a generalized and summarized shape. In the process of woodcut creation, there are two ways to shape the surface: one is to express the outline form concretely, and the other is to express the relationship of the picture abstractly, so as to balance the artistic expression of the picture. In terms of expression, there are also two ways of shaping the surface: one is to leave a large area white and show the bright part by hollowing it out; the other is also to leave a large surface blank, which means not to do any creation on this side in order to leave a black side after the inking.

(6) *Composition and Layout.* Layout is the domination and control of the picture, which is also called "management of position" in the theory of the six methods of Chinese painting. The highest standard of woodcut prints is the coexistence of diversity and uniformity. What is too neat or too messy does not appeal to the viewer, and the general personality of human beings always prefers change in order and



FIGURE 12: The Fox in the Snow.

unity in change. Therefore, the so-called “unity in diversity” layout of woodcut prints is not only a special product of woodcut but also a return to people’s nature.

The plane language of woodcut prints is reflected in different structures, showing different rhythms. The analysis of the graphic language of woodcut helps us understand the essence of art deeply and provides a methodological basis for the design practice of subsequent printmaking art.

3.3.2. The Possibility of Realizing Woodblock Print Elements in Digital Painting Creation. The development and progress of the times and the stability of social economy have ensured the colorful cultural life of people, and new artistic expressions are emerging, in terms of film and television (microfilm and small video) and photography (3D stereoscopic photography technology). In terms of fine arts (animation industry, 3D animation, and traditional Chinese art), digital painting has liberated the restraint of pen and paper for painting. Traditional art painting, or production, is done by repeatedly practicing works, drawing different artworks on paper or other bearers with the help of different digital painting materials, such as pencil, paint, water, brush, or the works printed by woodcut prints we are discussing today. All of them need the actual material to carry. The carrier of digital painting is the computer, which can realize different digital painting effects without the constraints and limitations of real materials; digital painting has created a new chapter of art. Nowadays, digital painting can not only simulate different brushstroke effects and painting styles but also achieve 3D effects that cannot be achieved by traditional painting, except for 2D effects, as long as the digital board is manipulated and practiced more, and the digital painting



FIGURE 13: Hand-drawn printmaking.

effects simulated by the computer can be mastered to the fullest.

Digital painting can produce works in a variety of fields, line, block, abstract, real, monochrome, and multicolor; digital painting can achieve the artistic effect that people want.

Although there are differences between digital painting and traditional art, there are many aspects of traditional art that can be learned from the creation process before and after, such as observing the surrounding area, selecting the subject and then deciding on the materials to be used, and then starting to conceptualize the composition. In the final art work, the traditional method requires the use of various materials, paper, gouache, watercolor, ink, etc., to complete the final work, while digital painting only requires the use of a computer and mouse; hand-drawn version can be drawn close to the real painting style than the light and translucent sense of ethereal, brushwork slim and simple, woodcut prints knife taste and sense of volume, airbrush sense of grain, and other works. Digital works are convenient, efficient, and reproducible, but there are two sides to everything; digital painting is not able to restore 100% of the real sense in the realization, but technology will continue to develop; I believe digital painting will continue to improve the function (see Figure 13).

4. Case Study

This section mainly explores the application process of printmaking language in digital painting through the complete creation process, taking the creation process of a work as an example.

4.1. Collection and Creation of Material. First, the creators conceived the idea of creating the relationship between human beings and nature, which is a very broad subject matter with various expressions. In particular, in today’s



FIGURE 14: Accumulation of creative materials.



FIGURE 15: Some ideas.

painting, artists are creating paintings that express the spirit of the times and the new customs and national spirit of the day. During creators' continuous study and practice, creators analyzed and deepened creators' understanding of "man and nature" several times and began to collect a series of materials, as shown in Figure 14.

In the formal law of woodcut printmaking, symmetry and balance are two ways to create a sense of picture.

Symmetry is balance in the strict sense, requiring a high degree of consistency in shape and volume, while equilib-

rium, as opposed to symmetry, refers to the universal balance of all asymmetries, which is not as strict as symmetry and can be different in volume and shape but needs to be balanced in visual psychology. Equilibrium is the grasp of the overall mood. While emphasizing the formal beauty and spatial picture effect, the language of woodcut printmaking also needs to take the overall tonality, color contrast, sparseness and rhythm, morphological changes, and texture direction into consideration. Thinking holistically is the key to creating a balanced picture, so that the picture presented

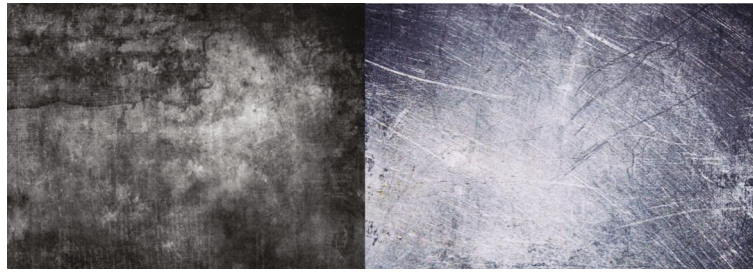


FIGURE 16: Photoshop under a special filter to create the texture effect try.



FIGURE 17: Copy of woodcut prints.

is rich in comprehensive beauty and has more personal characteristics. At the same time, the premise of equilibrium is the destruction of symmetry, and only when complete symmetry is destroyed can change be formed. In the composition of prints, symmetry and balance each have their own charm and can be used appropriately according to the needs of the picture.

4.2. Application and Experimentation of Printmaking Language: "Eternal Dreams" Digital Plate Making and Output. Based on the accumulation of creative materials in the early stage, creators started to select and organize the collected materials. Creator then tried to think about the composition in Photoshop and designed it repeatedly, with different compositions expressing different feelings, and the people, the natural environment, and even the animals themselves represent the main character and their relationship in the picture, as in Figure 15.

The works of Dali, Magritte, and other surrealist masters brought creators great inspiration, and after analyzing, studying, and learning from their works, creators' creative ideas were further inspired and expanded. Since digital painting is very convenient and easy to modify, after determining the size of the picture, the whole process of printmaking is drawn in computer software using a digital board, combining seemingly unrelated things, adding the

grotesqueness and absurdity of creators' inner world, and expressing some dreamy worlds in creators' subconscious.

So, in conclusion, only through a lot of creative experiments can creators find a digital painting language and method that matches the artistic effect and thoughts and feelings creators want to express. In addition to using digital media such as digital cameras and scanners to scan hand-painted watercolor textures and oil textures into the corresponding software for adjustment and testing, creators also used the brush and special filter functions in the software to conduct various experiments. In the process of these experiments, creators referred to and combined the artistic characteristics of traditional prints, such as the grainy effect of lithography, the delicate black tone of Melodyn, and the flying dust effect of copperplate, and applied the artistic language characteristics of traditional prints to digital prints, and finally found creators' own personal digital painting language and concluded a suitable plate making method, as in Figure 16.

After deciding what kind of digital painting to use, creators decided to mainly use Photoshop for digital painting. This layer is the key layer that determines the overall tone of the image. After rendering several times with special filters, a gray and black grainy effect is obtained, and in subsequent image input and editing programs, all kinds of image elements are processed according to this tone.



FIGURE 18: Digital painting inspired by Chinese print.

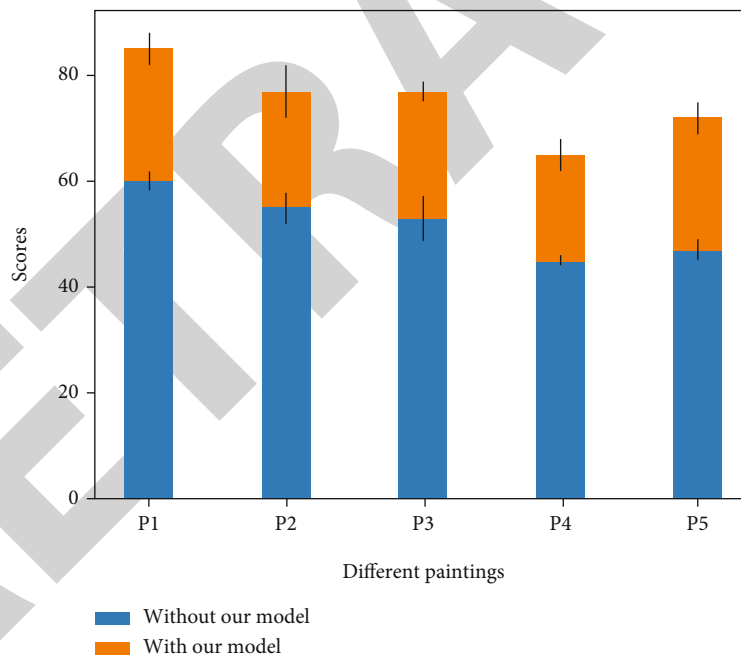


FIGURE 19: Quality comparison of digital paintings.

As mentioned above, image material can be obtained by digital camera, scanner, or 3dsmax software for 3D construction and rendering. In the creator’s creation, the creator mainly uses a Canon digital camera to capture image material and uses Sdsmax to create some special effects. After the images are imported, they are then edited to achieve certain artistic effects. Based on the design, the selected image elements are placed on different layers so that when we edit the elements in one layer, it will not affect other elements. Depending on the overall needs of

the image, different artistic treatments will be applied to different elements.

Finally, the content of all the layers will be integrated and adjusted to finalize the plate. The output of digital prints is usually made by professional digital printers or color inkjet printers, and creators chose raw rice paper as the substrate after experimentation. The images produced by computer printmaking are generally in RGB mode, but the printing mode is often in CMYK mode, so if the work is output directly, it will lead to serious distortion and major changes

in color tone. Therefore, before outputting the work, you need to make some adjustments to the master image, convert the RGB mode to CMYK mode, and then adjust the color tone to make sure there is no error.

4.3. Analysis. Chinese woodblock prints are not only a bright pearl in the history of Chinese art but also have an underestimated artistic and research value in the world. In this paper, we try to fuse digital painting with traditional Chinese prints and depict a set of handmade prints as well as digital prints with the small city of China as the big background. The traditional prints are made of linden wood, which is one of the common woodcut prints, using triangular knife, round knife, and flat knife, as shown in Figure 17.

Figure 18 mainly shows the customs of small towns in China. Because most of the production of Chinese prints is humanistic, people will add their yearning life content to the prints. In addition to the influence of Chinese Confucian culture, the works show "tranquility." Some works also express the beauty of inheritance of Chinese handicrafts and the beauty of family cultural system.

We evaluated the score of digital painting after our model drawing. The specific results are shown in Figure 19. A total of 5 works were compared, and the scores of the works with and without our model were compared. It can be seen that our model has obvious advantages.

5. Conclusion

With the rapid development of modern society and the rhythm of global cultural integration, art forms are diverse and the pace of innovation is accelerating. Both the development of woodcut printmaking and illustration design need to seek more diversified forms, and the mutual integration of the two is a good way to do so. In this paper, through an in-depth analysis of the language of woodcut printmaking, we break it down into basic language, formal laws, and aesthetic features and use theoretical research to guide design practice, which also makes printmaking design more inclusive and interdisciplinary. Computers are endowed with algorithm-based thinking patterns and image recognition functions that can be as diverse as painters and capable of creating digital paintings. There is still a lot of room for the language of woodcut printmaking in design, a kind of exploration based on practice to make a more cutting-edge style in the self-innovation of traditional art forms. We can only move forward in different attempts to make visual art design continue to create more value.

Data Availability

The experimental data used to support the findings of this study are available from the corresponding author upon request.

Conflicts of Interest

The author declared that there are no conflicts of interest regarding this work.

References

- [1] G. Yang, "The temporal spirit, expressiveness and nationality of contemporary Chinese painting," *Linguistics and Culture Review*, vol. 5, no. S2, pp. 472–486, 2021.
- [2] M. Skublewska-Paszowska, M. Milosz, P. Powroznik, and E. Lukasik, "3D technologies for intangible cultural heritage preservation—literature review for selected databases," *Heritage Science*, vol. 10, no. 1, pp. 1–24, 2022.
- [3] Y. Xu, Y. Tao, C. Zhang, M. Xie, W. Li, and J. Tai, "Review of digital economy research in China: a framework analysis based on bibliometrics," *Computational Intelligence and Neuroscience*, vol. 2022, Article ID 2427034, 11 pages, 2022.
- [4] H. Sun and W. Sun, "Research on Suzhou prints display based on VR technology," *Art and Design Review*, vol. 9, no. 3, pp. 233–241, 2021.
- [5] G. Cai, Y. Fang, J. Wen, S. Mumtaz, Y. Song, and V. Frascolla, "Multi-carrier M -ary DCSK system with code index modulation: an efficient solution for chaotic communications," *IEEE Journal of Selected Topics in Signal Processing*, vol. 13, no. 6, pp. 1375–1386, 2019.
- [6] R. Cho and C. Culver, "Supercut: printmaking for the present," *Griffith Review*, vol. 76, pp. 229–232, 2022.
- [7] K. Chandra, A. S. Marcano, S. Mumtaz, R. V. Prasad, and H. L. Christiansen, "Unveiling capacity gains in ultradense networks: using mm-wave NOMA," *IEEE Vehicular Technology Magazine*, vol. 13, no. 2, pp. 75–83, 2018.
- [8] X. Lu, "Benefiting new China art education industry-case study of Hu Yichuan," *Forest Chemicals Review*, pp. 1108–1128, 2021.
- [9] B. Wang, "On the expressive skills of enriching the artistic language of watermark woodcut," *International Journal of Social Science and Education Research*, vol. 4, no. 1, pp. 129–133, 2021.
- [10] F. B. Saghezchi, A. Radwan, J. Rodriguez, and T. Dagiuklas, "Coalition formation game toward green mobile terminals in heterogeneous wireless networks," *IEEE Wireless Communications*, vol. 20, no. 5, pp. 85–91, 2013.
- [11] C. C. J. Wang, "Art as a vehicle for social change: a biographical history of Xu Bing's Œuvre," in *Chinese Contemporary Art Series*, X. Bing, Ed., pp. 137–151, Springer, Singapore, 2020.
- [12] S. Palanisamy, B. Thangaraju, O. I. Khalaf, Y. Alotaibi, S. Alghamdi, and F. Alassery, "A novel approach of design and analysis of a hexagonal fractal antenna array (HFAA) for next-generation wireless communication," *Energies*, vol. 14, no. 19, p. 6204, 2021.
- [13] L. Chia, "Printing and publishing in East Asia through circa 1600: an extremely brief survey," *Media*, vol. 41, no. 1, pp. 129–162, 2020.
- [14] S. N. Alsubari, S. N. Deshmukh, A. A. Alqarni et al., "Data analytics for the identification of fake reviews using supervised learning," *Computers, Materials & Continua*, vol. 70, no. 2, pp. 3189–3204, 2022.
- [15] L. Qingfeng, L. Chenxuan, and W. Yanan, "Integrating external dictionary knowledge in conference scenarios the field of personalized machine translation method," *Journal of Chinese Informatics*, vol. 33, no. 10, pp. 31–37, 2019.
- [16] C. Hong and A. Sangiamvibool, "Traditional new year pictures of Tantou: re-invention of tradition in the process of commercialization," *Journal of Positive School Psychology*, vol. 6, no. 2, pp. 1945–1951, 2022.

Retraction

Retracted: Selection of Optimum Internal Control Genes for RT-qPCR Analysis of Schisandra chinensis under Four Hormone Treatments

Journal of Sensors

Received 19 December 2023; Accepted 19 December 2023; Published 20 December 2023

Copyright © 2023 Journal of Sensors. This is an open access article distributed under the Creative Commons Attribution License, which permits unrestricted use, distribution, and reproduction in any medium, provided the original work is properly cited.

This article has been retracted by Hindawi following an investigation undertaken by the publisher [1]. This investigation has uncovered evidence of one or more of the following indicators of systematic manipulation of the publication process:

- (1) Discrepancies in scope
- (2) Discrepancies in the description of the research reported
- (3) Discrepancies between the availability of data and the research described
- (4) Inappropriate citations
- (5) Incoherent, meaningless and/or irrelevant content included in the article
- (6) Manipulated or compromised peer review

The presence of these indicators undermines our confidence in the integrity of the article's content and we cannot, therefore, vouch for its reliability. Please note that this notice is intended solely to alert readers that the content of this article is unreliable. We have not investigated whether authors were aware of or involved in the systematic manipulation of the publication process.

Wiley and Hindawi regrets that the usual quality checks did not identify these issues before publication and have since put additional measures in place to safeguard research integrity.

We wish to credit our own Research Integrity and Research Publishing teams and anonymous and named external researchers and research integrity experts for contributing to this investigation.

The corresponding author, as the representative of all authors, has been given the opportunity to register their agreement or disagreement to this retraction. We have kept a record of any response received.

References

- [1] X. Liu, L. Zhang, and S. Yang, "Selection of Optimum Internal Control Genes for RT-qPCR Analysis of Schisandra chinensis under Four Hormone Treatments," *Journal of Sensors*, vol. 2022, Article ID 9299289, 10 pages, 2022.

Research Article

Selection of Optimum Internal Control Genes for RT-qPCR Analysis of *Schisandra chinensis* under Four Hormone Treatments

Xiuyan Liu ^{1,2,3}, Lifan Zhang ^{1,3} and Shihai Yang ²

¹Tong hua Normal University Key Laboratory of Evaluation and Application of Chang bai Mountain Biological Germplasm Resources of Jilin Province., China

²College of Chinese Medicine Materials, Jilin Agricultural University, Changchun 130118, China

³School of Life Sciences, Tong Hua Normal University, Tong Hua, 134000, China

Correspondence should be addressed to Shihai Yang; yangshihai@jlau.edu.cn

Received 2 August 2022; Revised 23 August 2022; Accepted 2 September 2022; Published 25 September 2022

Academic Editor: Sweta Bhattacharya

Copyright © 2022 Xiuyan Liu et al. This is an open access article distributed under the Creative Commons Attribution License, which permits unrestricted use, distribution, and reproduction in any medium, provided the original work is properly cited.

qRT-PCR technology is now one of the commonly used methods to study gene expression levels. The selection of accurate reference gene detection is an essential work before gene expressing analysis. In the current study, 8 candidate internal control genes (ACTIN, TUBA, GAPDH, UBC, MUB, TIP41, APX, and CAPA) were selected, and four statistical algorithms were used to evaluate their stability under different hormone treatments. The results confirmed that when using one internal control genes, TUBA emerged as the first ranking internal control gene in all experimental groups. When using two internal control genes, TUBA and MUB, were the most acceptable internal control genes for the GA3 treatment group; TUBA and GAPDH were identified as internal control genes in the IAA treatment group; TUBA and ACTIN were the most reliable combination in the ZT and ABA experimental groups; TUBA and TIP41 were recommended most suitable control genes in control group. Furthermore, the reliability of the internal control genes was further verified by the expression of GAG, a gene related to the development of *Schisandra chinensis*. The conclusion of this work will be helpful for the subsequent research on gene expression analysis of *Schisandra chinensis*.

1. Introduction

Quantitative real-time PCR (qRT-PCR) has become the most common assay for transcript and gene expressing levels due to its specificity, accuracy, efficiency, and high sensitivity [1, 2]. qRT-PCR results require data normalization by reliable internal control genes [3, 4]. As internal control genes, ideal ones are stably expressed in all tissues, and their expression is independent of environmental factors, experimental conditions, or other factors [5]. However, previous reports indicate that there were no such internal control genes, which can be applied to all plants and various experimental designs [6]. For example, different internal control genes were used under different experimental conditions in *Cocos nucifera* L. (Coconut) [7], *Momordica charantia* [8], *Bixa orellana* L. [9], *Salix matsudana* [10], and *Taihangia*

rupestris [11]. For reliable and precise qRT-PCR results, it is therefore important to evaluate and choice beneficiary internal control genes under different experimental conditions [12].

Schisandra chinensis (*S. chinensis*) is a monoecious liana of the family Magnoliaceae. It grows in the eastern most parts of Russia, the Kuril Islands, southern Sakhalin, Korea, Japan, and northeastern China [13]. The dried ripe fruit of *S. chinensis* is a Chinese traditional herbal medicine, used for tonifying qi, promoting the production of body fluid, nourishing kidneys, and its calming and astringent properties [14, 15]. Since male and female flowers of *S. chinensis* grow on the same plant, the quantity and quality of female flowers determine the yield of *S. chinensis*. Therefore, improving the differentiation rate of female flowers is of great significance to improve the yield of *S. chinensis*.

Many studies have shown that exogenous hormones have regulatory effects on plant flower development [16, 17]. However, the research on how phytohormones regulate flower development is not deep enough to fully explain its regulatory mechanism. In this study, the effects of exogenous hormones on the differentiation of female flowers of *S. chinensis* were investigated by spraying different concentrations of exogenous hormones. But it does not appear to be a universal internal control gene that would be suitable for *S. chinensis* to our knowledge. For this reason, it is important to choose correct internal control genes when interpreting RT-qPCR results. We selected eight candidate internal control genes (ACTIN, TUBA, MUB, UBC, GAPDH, GAPA, TIP41, and APX) from the transcriptome data, and their stability was evaluated. Furthermore, we used geNorm [18], NormFinder [19], BestKeeper [20], and the integrated sorting software RefFinder [21] to analyze the stability and variability of potential housekeeping gene for precise data normalization of qRT-PCR results [22].

2. Materials and Methods

2.1. *S. chinensis* Exogenous Hormone Treatment. The experimental materials came from the *S. chinensis* base of Jilin Agricultural University. Five-year-old *S. chinensis* plants ($n = 45$) with no diseases and insect pests were selected as the experimental material, each of which was a group of one, with three replicates. Water as the control group, four hormones (GA₃, IAA, ABA and ZT) were applied via spray bottle to *S. chinensis* plants on July 5 at specific concentrations shown in Table 1. In order to ensure adequate hormone absorption, spraying was then repeated on July 10 and samples were taken on July 20. Collected samples were immediately treated with liquid nitrogen and subsequently stored at -80°C to prevent mRNA degradation. mRNA degradation is an extremely important mechanism for controlling gene expressions in case of bacterial cells. The process includes structured and ordered action of a battery of endonucleases and exonucleases, and various other universal and ones existing are specific species alone.

2.2. Total RNA Isolation and cDNA Synthesis. According to the kit instructions, we extracted RNA from plants using the Spectrum Plant Total RNA Kit (Sigma). Qualified RNA quality was detected by a NanoDrop 2000C Spectrophotometer. Further verification of RNA integrity was conducted using a 1.5% (w/v) agarose gel electrophoresis. cDNA was synthesized by reverse transcription of RNA with an optical density (OD)₂₆₀/OD₂₈₀ ratio between 1.8 and 2.1. The DNA synthesis from an RNA template generates complementary DNA (cDNA). This can work as a template in various downstream applications for conducting RNA studies especially in case of gene expression. Thus, cDNA synthesis acts as the first step for various protocols in molecular biology. The reverse transcriptase (RT) uses the RNA template and complementaries of short primers to the 3' of RNA to guide the synthesis of the first-strand cDNA. The reverse transcription reaction was performed with $2\mu\text{L}$ of total

TABLE 1: The concentration of exogenous hormone spray on *S. chinensis*.

Exogenous hormones	GA ₃	IAA	ABA	ZT	H ₂ O (control group)
Concentration (mg/L)	500	500	500	300	/
	300	300	300	100	/
	100	100	100	50	/

RNA according to the procedure given in the Prime Script™ RT (Takara, Japan) kit. All cDNA samples used in subsequent experiments were stored in a -80°C freezer.

2.3. Candidate Internal Control Gene and Designing of Primers. The qRT-PCR primer pairs for eight reference gene candidates and target gene (GAG) were designed using the Primer 5 software with the following parameters: amplicon sizes were between 140 and 261 bp, primer lengths were between 18 and 22 bp, and amplification efficiencies (E%) between 91 and 109% ranged between linear correlation coefficients (R^2) of 0.982 to 0.998. Indicating that the efficiency of the reaction and degree of matching with the PCR standard curve were good [23, 24], ensuring the accuracy of the qRT-PCR data in subsequent experiments. Primer information is described in Table 2 and Figure 1.

2.4. qRT-PCR Analysis. qRT-PCR assays were performed using the qTOWER 3.0 Thermal Cycler (Analytik Jena, Germany) in 96-well plates. All cDNA samples were thawed and diluted four-fold. The total volume of each reaction was $20\mu\text{L}$, comprised of $10\mu\text{L}$ SYBR Premix ExTaq II kit (Takara, Japan), $2\mu\text{L}$ dilution cDNA, $1\mu\text{L}$ of each primer (forward and reverse), and $6\mu\text{L}$ RNase-free water. Following initial denaturation at 95°C for 30 s, 40 amplification cycles were conducted at 95°C for 5 seconds, 57°C for 30 seconds, and 72°C for 30 seconds, respectively. To exclude the formation of primer dimers, a melting curve analysis was performed at a temperature difference of 60°C and 95°C . Three technical replicates were used for each sample, and the same batch of cDNA was used throughout the experiment.

2.5. Data Analysis. Ct values were determined from qRT-PCR for each candidate internal control genes. In addition, the stability analysis of candidate internal control genes was assessed and ranked using four statistical packages: NormFinder, BestKeeper, geNorm, and RefFinder. The NormFinder is an algorithm that is used for identifying the optimal normalization gene from a set of candidate genes. The BestKeeper algorithm helps to identify the best standard genes for normalizing the data. The geNorm algorithm helps in identifying the most stable reference genes from a set of tested candidate reference genes. The RefFinder is a comprehensive tool that is used for evaluating and screening reference genes from large extensive datasets.

2.6. Normalization of GAG. AG belongs to the C functional gene in the ABCD model and plays a central regulatory role in the regulation of the termination of floral meristem development, as well as in the determination of floral organs between stamens and pistils [25, 26]. In the second half of

TABLE 2: Primer pairs of reference gene and target gene for qRT-PCR in *s. chinensis*.

No.	Genes	Functional description	Gene ID	Primer sequence forward/reverse (5-3)	Length (bp)	E%	R ²
1	ACTIN	Actin	TRINITY_DN37950_c0_g1_i1	A:CCATTCCGACCATACAC S:GATGCCGAGGACATTCAG	142	98	0.995
2	GAPA	Glyceraldehyde-3-phosphate dehydrogenase B	TRINITY_DN106361_c0_g1_i1	A:ATCCGTCCAAAAGCCGTTA S:CAAGACTCCTCACCCCTCA	228	105	0.996
3	TUBA	Tubulin alpha-3	TRINITY_DN112332_c0_g2_i1	A:CCGCTCGATGTCAAAGGGA S:GGTGGCACTGGGTCTGGTT	237	97	0.996
4	APX	Ascorbate peroxidase	TRINITY_DN110618_c1_g1_i1	A:AGCACAGCACCGAAACAT S:ATCTCTCTCTCGCAACC	170	93	0.995
5	MUB3	Membrane-anchored	TRINITY_DN98949_c1_g1_i1	A:GTCCCTGCTGTCTCCAAT S:CCCAGACAAGTATGCTCC	146	103	0.982
6	UBC4	Ubiquitin-conjugating enzyme 4	TRINITY_DN161958_c0_g1_i1	A:TGCTTCTATCCGTCCTGTA S:TTCTCCAGATTATCCATT	231	109	0.994
7	TIP41	TIP41-like protein	TRINITY_DN44616_c0_g1_i1	A:CAGCCAACTCGTCTTCATAC S:CAGCAGCCAAAGTGGAAAT	261	93	0.991
8	GAPDH	Glyceraldehyde-3-phosphate dehydrogenase	TRINITY_DN108444_c3_g8_i3	A:TTTGGCACCCCTTGAT S:TGTTGGATGGCTCTACTC	170	91	0.998
9	GAG	AG flower homologous gene	TRINITY_DN114911_c4_g2_i1	A:GTAATGCCCTCGTTCAAGC S:CCACCAAATACAAATCCT	114	92	0.995

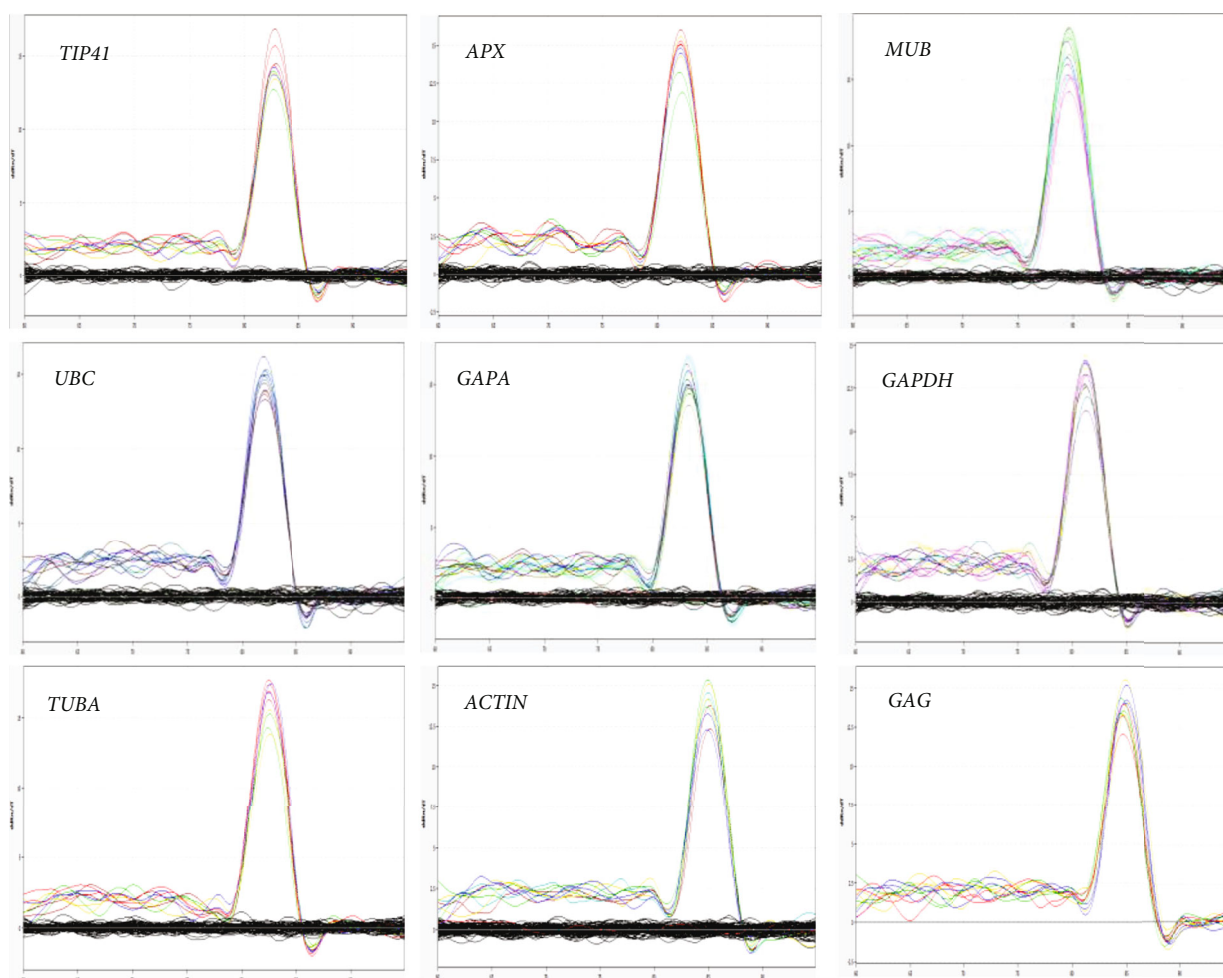


FIGURE 1: Melt curves generated from each reference gene and target gene (ACTIN, TUBA, MUB, UBC, GAPDH, GAPA, TIP41, APX, and GAG) showing a single peak.

flower ontogeny, it regulates the development of style and carpel and terminates flower development [27]. To further validate the credibility of the housekeeping genes recommended in this work, different combinations of internal control genes were used to detect the expression of GAG gene in female and male flowers.

3. Results

3.1. qRT-PCR Results. Generally, preliminary determination of the abundance of internal control genes can be made using the cycle threshold (Ct) values, in which genes with lower Ct values represent those with higher transcript abundance [28]. A qualified housekeeping gene should have moderate expression level and above, and its CT value should be $15 < CT < 30$ [29]. In this paper, the eight candidate genes had high or moderate expression levels, with Ct values in the range of 18.44 (ACTIN) to 27.9 (GAPA). Among them, the Ct values of ACTIN, which ranged from 18.44 to 21.44, had the least variation. Conversely, Ct values for GAPA were highly varied, ranging from 22.5 to 27.9 (Figure 2).

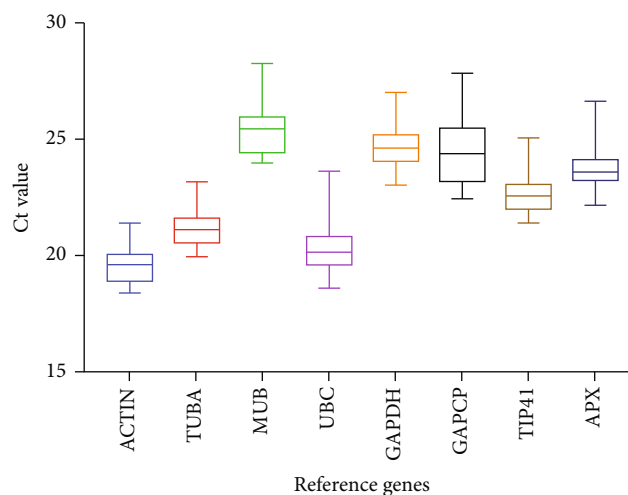


FIGURE 2: Distribution of crossing point (CT) values for eight internal control genes.

3.2. geNorm Analysis. The geNorm software evaluates the stability ranking and number of internal control genes by calculating the “M value” and the $(Vn/Vn + 1)$ value.

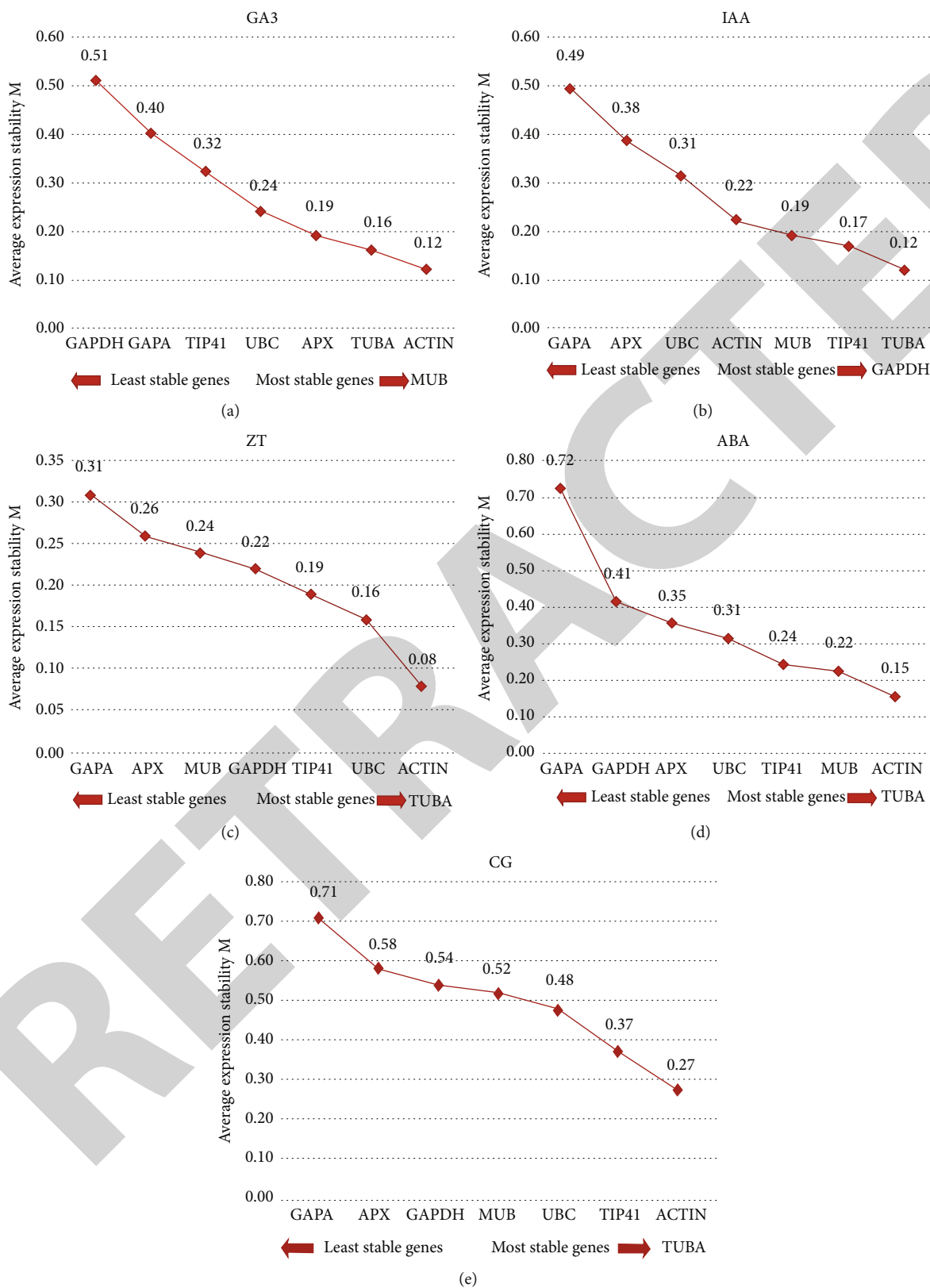


FIGURE 3: Eight candidate reference gene stability rankings are based on M-values calculated by geNorm. (a) GA3 treatment; (b) IAA treatment; (c) ZT treatment; (d) ABA treatment; (e) control group.

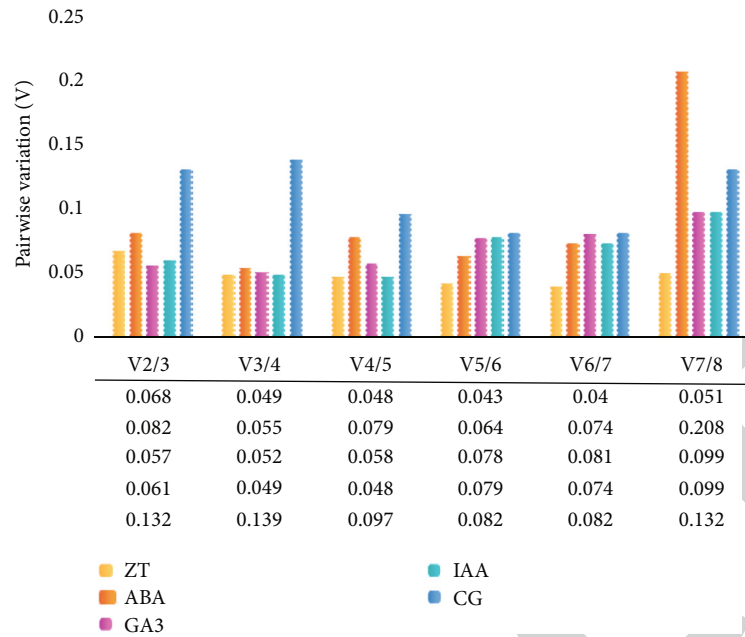


FIGURE 4: Selection of the optimal number of internal control genes based on the $(V_n/n+1)$ value of geNorm.

Among them, the greater the M value, the worse the stabilization. If the M value of a gene is greater than 1.5, the candidacy of the gene should be cancelled. After geNorm analysis, it was shown that the M values of the 8 candidate internal control genes in this paper were all less than 1.5; it was explained that their expression stability met the requirements of experimental analysis (Figure 3). The default threshold for pairwise changes (V_n/V_{n+1}) is 0.15. For calculating variants less than 0.15, select the number of internal control genes (N) suitable for analysis. For calculating pairwise variants greater than 0.15, $N + 1$ internal control genes are required. In this paper, the pairwise variation values of all candidate genes in all tissues for all hormone treatment were less than 0.15 (Figure 4), indicating that under all treatment conditions, two internal control genes were sufficient for normalization of gene expression data. The evaluation results of the geNorm software were as follows: The candidate genes ACTIN and MUB had the lowest stable values under GA3 treatment (Figure 3(a)). Under IAA treatment, GAPDH and TUBA were the best possible (Figure 3(b)). And under treatments with ZT or ABA, the optimum composition was ACTIN and TUBA (Figures 3(c) and 3(d)). The M value of ACTIN and TUBA was the smallest and the most stable in the control group (Figure 3(e)).

3.3. NormFinder Analysis. The NormFinder program is computationally similar to geNorm, ranking internal control genes by evaluating their stability values (M) across different experimental designs. The NormFinder tool is used to analyze and assess the stability of expression in case of reference genes involved in qRT-PCR data normalization. The algorithm identifies the optimal normalization gene from a set of candidates. The study in [30] examined six candidate reference genes in leaf, node, internode, root, cabbage, shoot primordial, and basal stem tissues in case of two-year-old

clonal oil palms. The NormFinder and BestKeeper algorithms verified the stability of the reference genes in the oil palm tissues being tested. A study used NormFinder and BestKeeper tools for the selection of reliable reference genes while conducting gene expression studies in peach using real-time PCR. The algorithms analyzed the stability of the genes, and it was found that TEF2, UBQ10, and RP II were the optimal reference with high statistical reliability [31]. The study in [11] highlighted the fact that the lowest stability value described genes with the best stability expression level. As shown in Table 3, according to the NormFinder sequence, four internal control genes TUBA (0.053), GAPDH (0.008), TIP41 (0.003), and TUBA (0.019) were calculated to have the lowest stability values under treatment with the four hormones (GA3, IAA, ZT, and ABA). TUBA (0.152) ranked the lowest in control group samples and was considered to be the optimum gene candidate.

3.4. BestKeeper Analysis. BestKeeper software ranks the stability of internal control genes mainly in the light of the standard deviation (SD) and coefficient of variation (CV) values of gene expression levels. The algorithm calculates the candidate gene stability considering the standard deviation of C_q values in addition to the coefficient of variance (CV), correlation coefficient and the p-value. It helps in identifying the best standard genes that contribute towards normalization of the data. The lower the two values, the more stable the reference gene. However, genes with a SD value greater than 1 should not be regarded as internal control genes [32]. The results of BestKeeper analysis are shown in Table 4. For hormone treatment (GA3, IAA, ZT, and ABA) and control group samples, the optimal internal control genes were GAPDH (0.22), APX (0.18), TUBA (0.53), ACTIN (0.03), and TIP41 (0.57), respectively, and GAPA was the most unstable gene in all sampling groups.

TABLE 3: The expression stability of 8 candidate internal control genes under different hormone treatments was evaluated by NormFinder.

No.	GA ₃ stress		IAA stress		ZT stress		ABA stress		CG	
	Gene name	M	Gene name	M	Gene name	M	Gene name	M	Gene name	M
1	<i>TUBA</i>	0.053	<i>GAPDH</i>	0.008	<i>TIP41</i>	0.003	<i>TUBA</i>	0.019	<i>TUBA</i>	0.152
2	<i>APX</i>	0.078	<i>TUBA</i>	0.032	<i>ACTIN</i>	0.107	<i>MUB</i>	0.075	<i>TIP41</i>	0.239
3	<i>MUB</i>	0.089	<i>MUB</i>	0.127	<i>MUB</i>	0.135	<i>GAPDH</i>	0.087	<i>ACTIN</i>	0.263
4	<i>ACTIN</i>	0.107	<i>TIP41</i>	0.129	<i>TUBA</i>	0.152	<i>TIP41</i>	0.110	<i>MUB</i>	0.294
5	<i>UBC</i>	0.144	<i>ACTIN</i>	0.167	<i>UBC</i>	0.154	<i>ACTIN</i>	0.194	<i>UBC</i>	0.317
6	<i>TIP41</i>	0.290	<i>UBC</i>	0.307	<i>GAPDH</i>	0.155	<i>UBC</i>	0.380	<i>GAPDH</i>	0.332
7	<i>GAPA</i>	0.446	<i>APX</i>	0.369	<i>APX</i>	0.166	<i>APX</i>	0.384	<i>APX</i>	0.374
8	<i>GAPDH</i>	0.544	<i>GAPA</i>	0.542	<i>GAPA</i>	0.280	<i>GAPA</i>	1.149	<i>GAPA</i>	0.721

TABLE 4: The expression stability of 8 candidate internal control genes under different hormone treatments was evaluated by BestKeeper.

No.	GA ₃ stress			IAA stress			ZT stress			ABA stress			CG		
	Gene name	SD	CV	Gene name	SD	CV	Gene name	SD	CV	Gene name	SD	CV	Gene name	SD	CV
1	<i>GAPDH</i>	0.22	0.87	<i>APX</i>	0.18	0.75	<i>TUBA</i>	0.53	2.50	<i>ACTIN</i>	0.03	0.14	<i>TIP41</i>	0.57	2.39
2	<i>APX</i>	0.40	1.71	<i>ACTIN</i>	0.32	1.63	<i>GAPDH</i>	0.56	2.24	<i>TUBA</i>	0.12	0.57	<i>ACTIN</i>	0.62	3.08
3	<i>TIP41</i>	0.54	2.39	<i>TIP41</i>	0.36	1.62	<i>UBC</i>	0.56	2.72	<i>TIP41</i>	0.16	0.73	<i>TUBA</i>	0.67	3.02
4	<i>TUBA</i>	0.55	2.65	<i>GAPDH</i>	0.45	1.85	<i>ACTIN</i>	0.58	3.00	<i>MUB</i>	0.26	1.02	<i>APX</i>	0.77	3.10
5	<i>MUB</i>	0.57	2.31	<i>TUBA</i>	0.48	2.30	<i>TIP41</i>	0.65	2.90	<i>UBC</i>	0.26	1.27	<i>UBC</i>	0.78	3.53
6	<i>ACTIN</i>	0.58	3.04	<i>MUB</i>	0.50	1.98	<i>MUB</i>	0.67	2.67	<i>APX</i>	0.30	1.29	<i>GAPDH</i>	0.81	3.14
7	<i>UBC</i>	0.60	3.04	<i>UBC</i>	0.71	3.56	<i>APX</i>	0.76	3.28	<i>GAPDH</i>	0.43	2.00	<i>MUB</i>	0.86	3.16
8	<i>GAPA</i>	0.98	4.04	<i>GAPA</i>	0.86	3.56	<i>GAPA</i>	0.96	4.06	<i>GAPA</i>	1.50	6.19	<i>GAPA</i>	1.02	3.97

TABLE 5: The expression stability of 8 candidate internal control genes under different hormone treatments was analyzed by RefFinder.

No.	GA ₃ stress		IAA stress		ZT stress		ABA stress		CG	
	Gene name	M	Gene name	M	Gene name	M	Gene name	M	Gene name	M
1	<i>TUBA</i>	1.86	<i>GAPDH</i>	1.41	<i>TUBA</i>	1.86	<i>TUBA</i>	1.41	<i>TUBA</i>	1.32
2	<i>MUB</i>	2.34	<i>TUBA</i>	2.11	<i>ACTIN</i>	2.00	<i>ACTIN</i>	2.11	<i>TIP41</i>	1.86
3	<i>APX</i>	2.63	<i>TIP41</i>	3.22	<i>TIP41</i>	2.11	<i>MUB</i>	2.34	<i>ACTIN</i>	2.06
4	<i>ACTIN</i>	3.13	<i>ACTIN</i>	3.98	<i>UBC</i>	3.50	<i>TIP41</i>	3.46	<i>UBC</i>	4.68
5	<i>GAPDH</i>	4.76	<i>MUB</i>	4.12	<i>MUB</i>	4.56	<i>UBC</i>	5.18	<i>MUB</i>	5.38
6	<i>TIP41</i>	5.05	<i>APX</i>	4.30	<i>GAPDH</i>	4.82	<i>GAPDH</i>	5.21	<i>GAPDH</i>	5.48
7	<i>UBC</i>	5.44	<i>UBC</i>	6.24	<i>APX</i>	7.00	<i>APX</i>	6.48	<i>APX</i>	6.09
8	<i>GAPA</i>	7.24	<i>GAPA</i>	8.00	<i>GAPA</i>	8.00	<i>GAPA</i>	8.00	<i>GAPA</i>	8.00

3.5. RefFinder Analysis. RefFinder is a web-based online tool that comprehensively ranks the results of geNorm, NormFinder, and BestKeeper assessments to obtain the best stability internal control genes for *S. chinensis* [20]. Based on the RefFinder ranking, *TUBA* was comprehensively ranked first in all test groups. *GAPA* was considered to have the worst stability among all candidate genes. Results from RefFinder analysis are provided in Table 5.

3.6. Validation of Reference Gene Selection. According to the RNA sequencing results of female and male flowers of *S. chinensis*, the AG homologous gene *GAG* was upregulated in female flowers and downregulated in male flowers. The results of the qRT-PCR show that when *TIP41*, *TUBA* or

TIP41, and *TUBA* were used as internal control genes, the relative expression of *GAG* gene in female flower buds was greater than 1, and the expression in male flower bud was less than 1, indicating that *GAG* gene was upregulated in female flower bud. This result was consistent with the result of RNA-sequencing. Using an inappropriate reference gene can lead to large errors in qRT-PCR results and even erroneous results. Further illustrate the importance of reference genes for RT-qPCR analysis of genes (Figure 5).

4. Discussion

Accurate qRT-PCR results are affected by many kinds of factors including RNA extraction efficiency, reverse

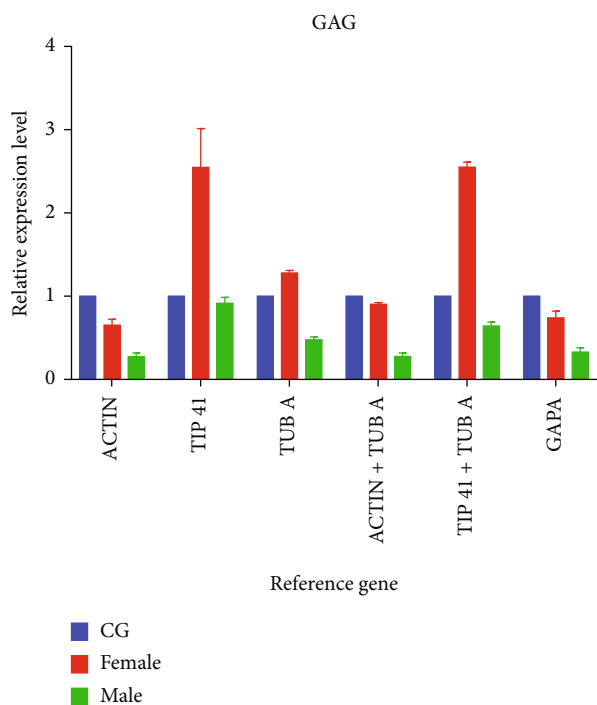


FIGURE 5: Relative expression of GAG genes when using different internal control genes.

transcriptional, and changes in amplification efficiency [28, 33]. The selection of reasonable internal control genes is the key to improving the accuracy of gene normalization during qRT-PCR detection [34, 35]. In this paper, eight candidate housekeeping genes (GAPDH, ACT, MUB, UBC, TIP41, APX, CPAP, and TUBA) were chosen based on the RNA-sequencing data of male and female flowers of *S. chinensis*. The stability of the genes was ranked by four (4) recognized reference gene evaluation statistical software. The result analysis displayed that the reference genes recommended by geNorm, NormFinder, and BestKeeper were not completely consistent. The appearance of such results may be due to their different calculation rules and analysis procedures [36]. To determine the final ranking of the stabilization of the internal control genes, the results of the algorithm were integrated using the online tool RefFinder, and a comprehensive ranking of the 8 candidate genes was performed. After comprehensive analysis, it was confirmed that TUBA was recommended as the most excellent reference gene for all experimental treatments, and CPAP was the most unstable. TUBA, as the best stability reference gene among *S. chinensis* candidates, was also used as an internal reference gene for celery studies at different developmental stages [23]. But when celery was subjected to four abiotic stresses (drought, cold, high temperature, and salinity) and four hormones (ABA, GA, MeJA, and SA), TUBA became the least stable reference gene [37]. This indicates that even the same internal control genes have different stability under different conditions. However, as qRT-PCR calibration and standardization by a single reference gene may lead to the deviation of the results, it is recommended to use two or more internal control genes to help the accuracy of the

results [38]. In all of the samples, the paired variation value (V_n/V_{n+1}) of the internal control gene standardization factor was less than 0.15, indicating that the two internal control genes could meet the relative quantitative requirements and that it is unnecessary to introduce the third reference gene for correction. Thus, according to the ranking results of RefFinder, in the GA3 treatment group, TUBA and MUB were the optimum combinations; The best partners of the internal control genes in the IAA experimental group were TUBA and GAPDH; TUBA and ACTIN were identified as the best possible housekeeping genes in the ZT and ABA experimental groups; the combination of TUBA and TIP41 exhibited the best stability in the control group. The research shows that the housekeeping genes MUB, ACTIN, TIP41, and GAPDH have different stabilities in different plants or under different experimental settings. For instance, TIP41 was the most reliable internal control gene for *Momordica charantia* under different stress treatments (H_2O_2 , NaCl, PEG6000, $CuSO_4$, MeJA, cold, and UV conditions) [8]. F-box and TIP41 were the best stability combination of internal control genes under drought stress in *Hedera helix* L. [39], but TIP41 was not the best reference gene in three tree peony cultivars [28]. Other housekeeping genes have similar conclusions. The stabilization of the same reference gene in different plants and different experimental treatments is also different [11, 32–42]. By using different internal control genes to detect the expression of GAG gene in male and female flowers, the reliability of the recommended internal control genes in this work was further verified. In summary, normalization of different internal control genes affects the accuracy of qRT-PCR data; that is, unstable internal control genes may lead to significant deviations from true expression levels and to a misunderstanding of data [3, 33]. Therefore, it is the key to evaluate the reliability and reproducibility of reference gene expression and a crucial choice for the appropriate internal control genes according to the research conditions.

5. Conclusions

To sum up, this work evaluated and ranked the stability of 8 candidate internal control genes in four hormones through four evaluation software and further verified the reliability of this study through GAG gene. The result proves that these housekeeping genes had different stability under different experimental conditions. When one reference gene was used, selecting TUBA satisfies all experimental groups. When two internal control genes are used, TUBA and MUB can be used in the GA3 group; the combination of TUBA and GAPDH can be selected in the IAA treatment group; TUBA and ACTIN are available for ZT and ABA experimental groups; TUBA and TIP41 are recommended as the most adaptive internal control genes for the control group; GAPA is the most unreliable as an internal reference gene for each experimental group of *S. chinensis*. This paper thus identifies suitable internal control genes for the expression study of *S. chinensis* under different hormone treatments.

Data Availability

The datasets used during the current study are available from the corresponding author on reasonable request.

Conflicts of Interest

The authors declare that they have no conflict of interest.

References

- [1] C. Li, H. Zhao, M. Li et al., "Validation of reference genes for gene expression studies in tartary buckwheat (*Fagopyrum tataricum* Gaertn.) using quantitative real-time PCR," *Peer J*, vol. 7, article e6522, 2019.
- [2] Q. Jiang, F. Wang, M. Y. Li, J. Ma, G. F. Tan, and A. S. Xiong, "Selection of suitable reference genes for qPCR normalization under abiotic stresses in *Oenanthe javanica* (BI.) DC," *PLoS ONE*, vol. 9, no. 3, article e92262, 2014.
- [3] X. Li, D. Tang, and Y. Shi, "Selection of reference genes for quantitative real-time PCR normalization in *Narcissus pseudonarcissus* in different cultivars and different organs," *Helvion*, vol. 4, no. 7, 2018.
- [4] F. Tang, L. Chu, W. Shu, X. He, L. Wang, and M. Lu, "Selection and validation of reference genes for quantitative expression analysis of miRNAs and mRNAs in poplar," *Plant Methods*, vol. 15, no. 1, pp. 1–15, 2019.
- [5] L. Cao, X. Li, D. Wang, H. Sun, and J. Gao, "Validation of reliable reference genes for accurate normalization in RT-qPCR analysis of *Codonopsis pilosula*," *Chinese Herbal Medicines*, vol. 9, no. 3, pp. 226–235, 2017.
- [6] H. Sun, X. Jiang, M. Sun, H. Cong, and F. Qiao, "Evaluation of reference genes for normalizing RT-qPCR in leaves and suspension cells of *Cephalotaxus hainanensis* under various stimuli," *Plant Methods*, vol. 15, no. 1, pp. 1–11, 2019.
- [7] K. E. Rachana and M. K. Rajesh, "Selection and validation of reference genes for gene expression normalization in coconut (*Cocos nucifera* L.) under biotic stress and hormone stimuli," *Plant Gene*, vol. 19, article 100184, 2019.
- [8] Z. Wang, J. Xu, Y. Liu et al., "Selection and validation of appropriate reference genes for real-time quantitative PCR analysis in *Momordica charantia*," *Phytochemistry*, vol. 164, pp. 1–11, 2019.
- [9] V. S. Moreira, V. L. F. Soares, R. J. S. Silva, A. O. Sousa, W. C. Otoni, and M. G. C. Costa, "Selection and validation of reference genes for quantitative gene expression analyses in various tissues and seeds at different developmental stages in *Bixa orellana* L.," *Physiology and Molecular Biology of Plants*, vol. 24, no. 3, pp. 369–378, 2018.
- [10] Y. Zhang, X. Han, S. Chen et al., "Selection of suitable reference genes for quantitative real-time PCR gene expression analysis in *Salix matsudana* under different abiotic stresses," *Scientific Reports*, vol. 7, no. 1, article 40290, 2017.
- [11] W. Li, L. Zhang, Y. Zhang, G. Wang, D. Song, and Y. Zhang, "Selection and validation of appropriate reference genes for quantitative real-time PCR normalization in staminate and perfect flowers of *Andromonoecious Taihangia rupestris*," *Frontiers in Plant Science*, vol. 8, p. 729, 2017.
- [12] Q. Nong, Y. Yang, M. Zhang et al., "RNA-seq-based selection of reference genes for RT-qPCR analysis of pitaya," *FEBS Open Bio*, vol. 9, no. 8, pp. 1403–1412, 2019.
- [13] J. L. Hancke, R. A. Burgos, and F. Ahumada, "*Schisandra chinensis* (Turcz.) Baill," *Fitoterapia*, vol. 70, no. 5, pp. 451–471, 1999.
- [14] Z. Peili, L. Junkui, F. Xiuqiong, and Y. Zhiling, "*Schisandra* fruits for the management of drug-induced liver injury in China: a review," *Phytomedicine*, vol. 59, article 152760, 2019.
- [15] V. V. K. Billa, K. Lakshmana, K. Rajesh, M. P. K. Reddy, G. Nagaraja, and K. Sudheer, "Efficient frequent pattern mining algorithm based on node sets in cloud computing environment," in *IOP conference series: materials science and engineering*, vol. 263, Atlanta, GA, 2017, November. 4, Article ID 042003.
- [16] A. Isam, H. Zain, A. Aziz, A. M. Zain, and A. Y. Wan, "The Influence of Exogenous Hormone on the Flowering and Fruiting of Strawberry (*Fragaria x ananassa* Duch)," *Journal of Biology, Agriculture and Healthcare*, vol. 2, no. 4, pp. 2224–3208, 2012.
- [17] W. Zhaolong, C. Weixing, D. Tingbo, and Z. Qin, "Effects of exogenous hormones on floret development and grain set in wheat," *Plant Growth Regulation*, vol. 35, no. 3, pp. 225–231, 2001.
- [18] B. Etschmann, B. Wilcken, K. Stoesesand, A. von der Schulenburg, and A. Sterner-Kock, "Selection of reference genes for quantitative real-time PCR analysis in canine mammary tumors using the GeNorm algorithm," *Veterinary Pathology*, vol. 43, no. 6, pp. 934–942, 2006.
- [19] C. L. Andersen, J. L. Jensen, and T. F. Ørntoft, "Normalization of real-time quantitative reverse transcription-PCR data: a model-based variance estimation approach to identify genes suited for normalization, applied to bladder and colon cancer data sets," *Cancer Research*, vol. 64, no. 15, pp. 5245–5250, 2004.
- [20] M. W. Pfaffl, A. Tichopad, C. Prgomet, and T. P. Neuvians, "Determination of stable housekeeping genes, differentially regulated target genes and sample integrity: BestKeeper – Excel-based tool using pair-wise correlations," *Biotechnology Letters*, vol. 26, no. 6, pp. 509–515, 2004.
- [21] F. Xie, P. Xiao, D. Chen, L. Xu, and B. Zhang, "miRDeepFinder: a miRNA analysis tool for deep sequencing of plant small RNAs," *Plant Molecular Biology*, vol. 80, no. 1, pp. 75–84, 2012.
- [22] H. Ren, X. Wu, Y. Lyu et al., "Selection of reliable reference genes for gene expression studies in *Botrytis cinerea*," *Journal of Microbiological Methods*, vol. 142, pp. 71–75, 2017.
- [23] M.-Y. Li, F. Wang, Q. Jiang, G.-L. Wang, C. Tian, and A.-S. Xiong, "Validation and Comparison of Reference Genes for qPCR Normalization of Celery (*Apium graveolens*) at Different Development Stages," *Frontiers in Plant Science*, vol. 7, p. 313, 2016.
- [24] Y. Yang, X. Zhang, Y. Chen et al., "Selection of reference genes for normalization of microRNA expression by RT-qPCR in sugarcane buds under cold stress," *Frontiers in Plant Science*, vol. 7, p. 86, 2016.
- [25] D. S. Ó'Maoiléidigh, S. E. Wuest, and L. Rae, "Control of reproductive floral organ identity specification in *Arabidopsis* by the C function regulator AGAMOUS," *Plant Cell*, vol. 25, no. 7, pp. 2482–2503, 2013.
- [26] Y. Liu, D. Zhang, J. Ping, S. Li, Z. Chen, and J. Ma, "Innovation of a regulatory mechanism modulating semi-determinate stem growth through artificial selection in soybean," *PLoS Genetics*, vol. 12, no. 1, 2016.

Retraction

Retracted: Consumption Behavior Prediction Based on Multiobjective Evolutionary Algorithm

Journal of Sensors

Received 22 August 2023; Accepted 22 August 2023; Published 23 August 2023

Copyright © 2023 Journal of Sensors. This is an open access article distributed under the Creative Commons Attribution License, which permits unrestricted use, distribution, and reproduction in any medium, provided the original work is properly cited.

This article has been retracted by Hindawi following an investigation undertaken by the publisher [1]. This investigation has uncovered evidence of one or more of the following indicators of systematic manipulation of the publication process:

- (1) Discrepancies in scope
- (2) Discrepancies in the description of the research reported
- (3) Discrepancies between the availability of data and the research described
- (4) Inappropriate citations
- (5) Incoherent, meaningless and/or irrelevant content included in the article
- (6) Peer-review manipulation

The presence of these indicators undermines our confidence in the integrity of the article's content and we cannot, therefore, vouch for its reliability. Please note that this notice is intended solely to alert readers that the content of this article is unreliable. We have not investigated whether authors were aware of or involved in the systematic manipulation of the publication process.

Wiley and Hindawi regrets that the usual quality checks did not identify these issues before publication and have since put additional measures in place to safeguard research integrity.

We wish to credit our own Research Integrity and Research Publishing teams and anonymous and named external researchers and research integrity experts for contributing to this investigation.

The corresponding author, as the representative of all authors, has been given the opportunity to register their agreement or disagreement to this retraction. We have kept a record of any response received.

References

- [1] J. Li, N. S. Jaharudin, and Y. Song, "Consumption Behavior Prediction Based on Multiobjective Evolutionary Algorithm," *Journal of Sensors*, vol. 2022, Article ID 2525740, 11 pages, 2022.

Research Article

Consumption Behavior Prediction Based on Multiobjective Evolutionary Algorithm

Jun Li,^{1,2} Nor Siahbinti Jaharudin ,² and Yu Song ³

¹School of Business, Guilin University of Technology, Guilin, China

²Department of Management and Marketing, School of Business and Economics, University of Putra, Malaysia

³College of Civil and Architecture Engineering, Guilin University of Technology, Guilin, China

Correspondence should be addressed to Yu Song; qjs@bbc.edu.cn

Received 27 July 2022; Revised 11 August 2022; Accepted 22 August 2022; Published 24 September 2022

Academic Editor: Sweta Bhattacharya

Copyright © 2022 Jun Li et al. This is an open access article distributed under the Creative Commons Attribution License, which permits unrestricted use, distribution, and reproduction in any medium, provided the original work is properly cited.

Consumption behavior prediction reveals customer attributes, personal preferences, and intrinsic laws. Organizations would benefit from knowing further about customer needs and business desires by monitoring client behavior to provide more precise recommendations and boost acquisition rates. The economics of the customer, buyer groupings, and product quality are only a few of the numerous variables that influence customer behavior. The key issue that has to be resolved at this time is how to filter out useful information from these vast amounts of data to forecast customer behavior. For customer consumption behavior prediction and analysis with an advanced quantitative research process, we proposed the multiobjective evolutionary algorithm, which significantly boosts the accuracy of consumption behavior predictions. The dataset is initially gathered based on consumer preferences and behaviors as the essential information for the entire prediction model. Min-max normalization is used as a component of the preprocessing of the data to get the elimination of redundant and superfluous data. The Word2vec model is utilized for feature extraction, and boosted ant colony optimization (BACO) is employed to choose the best features. Utilizing the suggested multiobjective evolutionary algorithm (MOEA), the predictions are made. The suggested system's performance is assessed, and the metrics are contrasted with more established methods. The findings demonstrate that the suggested MOEA technique performs well than the traditional ML, XGB, AI, and HNB algorithm methods in terms of accuracy (95 percent), quality of prediction (97 percent), precision (99 percent), recall (93 percent), *F1*-score (98 percent), and prediction time (50 seconds). Hence, the outcomes show that the regression model is sustainable. The suggested consumption behavior prediction system has demonstrated its efficiency in boosting profitability.

1. Introduction

Many business websites on the internet offer a wealth of data about occasions, connections, and attitudes. Understanding customer behavior may be useful in analyzing consumer traits, the interaction between products, and other topics. Therefore, building consumption structures based on data on distinct consumers' purchase behavior is a very useful study topic. To perform consumption behavior prediction, information extraction, and user influence analysis, a variety of technologies including text mining, statistical theory, association analysis, and visualization have to be employed. By evaluating the behavior data of e-commerce platforms, the behavior prediction extracts users' consuming preferences

and habits and calculates the complete likelihood to anticipate future payment behavior. Applications for forecast findings include product suggestions, placement of advertisements, and other things (Guo et al. [1]). Prediction of consumption behavior shows consumer characteristics, individual choices, and underlying constraints. By observing consumer behavior, businesses may gain greater insight into customer demands and company desires, which will help them, make more accurate suggestions, and increase the terms of the market. Only a handful of the many factors that affect consumer behavior include product quality, buyer groups, and customer economics. Well, how to extract relevant data from these massive volumes of data to predict client behavior is the main problem that has to be solved at the

moment. Consumption behavior prediction that successfully increases the prediction efficacy of consumer behavior is used for company growth prediction and analysis using sophisticated quantitative research methods. It is used to filter out useful information from this vast amount of data to anticipate (Tian et al. [2]).

In real-world applications, unbalanced data has made categorization issues much more difficult. Customers engage in online business by browsing and looking for similar items to carry out chores like purchasing or other connected activities in a computer-mediated environment. The unification and coherence of customer requirements, incentive, behavior, and recollection are the purchase choice. The probable links underlying several customer actions may be mined from the communication networks, and the prediction purpose can be achieved. The adoption of the consumer prediction strategy was rapid and efficient for identifying and segmenting consumer groups. It also made it easier to map the differences between these groups and to compare how customers behaved in other marketplaces (Li et al. [3]). Business has emerged as one of the primary means through which people are consuming in their daily lives, strictly monitoring the fast growth of computer Internet advances and the Internet service. Well, how value-extract from a big amount of user behavior consumption data, meanwhile, is a current issue (Mody and Bhoosreddy [4]). This is still a challenge for many businesses, especially when it comes to effectively analyzing and forecasting user behavior, creating customer information, classifying users based on similar actions, and providing individualized marketing and product recommendations.

Figure 1 depicts the application of consumption behavior prediction. In response to the aforementioned problems that e-commerce is experiencing, this performs a visual analysis of the many factors that influence customers' purchase decisions. Making tailored advice for pertinent firms and raising their operational profitability is important from a practical standpoint. It uses a logic model to forecast the user's buying behavior to fully understand the influence of the business (Xiao and Tong [5]). It is urgently necessary for individuals to adjust their consumption behavior to be more responsible to provide safe and wholesome living circumstances for both the coming generations due to the speeding up of biodiversity loss, economic reform, and related crises. Even though studies have demonstrated that individuals are buying goods and using service offerings that the surrounding habitat can renew, manage, or compost, most people still appear to think of the economy as largely being related to the creation and consumption of merchandise. To facilitate the transition to a circular economy, the present consuming culture must change with consumer prediction (Garg [6]).

The existing unprecedented growth structure will not be changed by the integrated resource action plan, which will remain purely theoretical instruments. Although ideas on sustainable consumption behavior have existed for some time, there is still a need for more study on the fundamental concepts because of the phenomenon's complexity and myriad justifications. For instance, there has been a request for a

study that investigates the relationships between combinations of factors rather than just one component to assess how well corporate concerns can anticipate consumer behavior (Saari et al. [7]). Consumers behave in groups or organizations while selecting and obtaining services, commodities, experiences, or innovations to meet their needs and to have an influence on the buyer and society. Entrepreneurial competitiveness is ensured by knowledge of the conditions, variables, and behavioral reasons of customers (Ahmed et al. [8]). An in-depth examination of market segmentation and customer needs is necessary to assess consumer behavior for the company's creation of new goods, new beliefs, and society's psychology. Companies must afterward adopt a dependable, efficient, and adaptable marketing plan that ensures earnings and sales based on an analysis of client behavior. By using strategic planning and an objective market segment objective based on a computational model, it has succeeded. This consumption durability component focuses on assessing how consumers' behavior is affected by promises and addressing obstacles to the transition of values into actions (Zhao et al. [9]). As a result, we suggested a multiobjective evolutionary algorithm, which much improves forecasts of consumer behavior and to lessen the inadequacies of existing technologies.

1.1. Contribution of the Study

- (i) This study offers a novel multiobjective evolutionary algorithm methodology for consumer forecasting to enhance business growth
- (ii) Min-max normalization is used for preprocessing to execute a sequence of procedures to modify or remove redundant data
- (iii) Using the Word2Vec model, the optimal data features may be extracted from unstructured data
- (iv) The metrics of the proposed model are examined and contrasted with conventional prediction techniques
- (v) This method corrects existing technology's inadequacies and significantly improves commercial forecasts of customer behavior

The remaining sections in the paper are structured as follows. The associated literature and the problem statement are presented in Section 2. The explanations of the proposed work are provided in Section 3. Section 4 has results and discussions. The proposed paper's conclusion is presented in Section 5.

2. Literature Survey

Shukla et al. [10] utilized supervised and unsupervised machine learning algorithms for investigation for correlation to the causality of consuming behavior prediction when integrating predictive ability with explanatory capacity and offer a more comprehensive understanding of proenvironmental business consuming behavior. It is unable to obtain

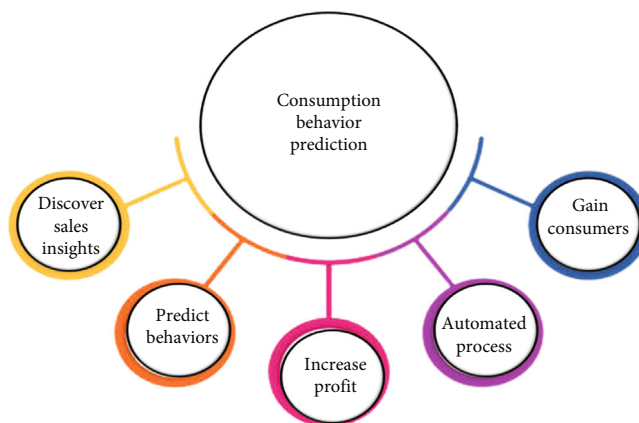


FIGURE 1: Application of consumption behavior prediction.

exact data filtering parameters. Chen et al. [11] employed the attitude-behavior-context (ABC) theory, which builds a methodological approach to discover whether a consumer's perception of a company's usefulness affects the acquisition of that product. It also looks at the partial mediator of an eco-friendly product's utilization mindset as well as the comment moderation impact of technology and communication implementations. Its incomplete consumer statistics data might affect the performance. Liu et al. [12] presented a bit-based latent spatiotemporal feature extraction approach for the optimum learning behavior. Organizations in a variety of industries continue to create new consumer consumption behavior value assessment algorithms owing to the advancement of big data and artificial intelligence to increase the likelihood of getting customer predictions. This modality performs poorly in terms of classification accuracy. Amasyali and El-Gohary [13] suggested the notion of big data technology based on machine learning to process data and analyze it to forecast customer behavior on social media. He stated that the social media is widely used in our community, currently. Social networking platforms are being used by people to consume a variety of goods. Data preprocessing in machine learning gives low enhancement of data and less accuracy in prediction.

VLN and Deeplakshmi [14] advocated the use of support vector machines based on machine learning to create effective systems for predicting consumer behavior. These systems may help businesses increase their revenue by attracting new clients, retaining existing ones, and improving customer loyalty. The targeted classifications might overlap occasionally (Shahabaz and Afzal [15]). Wang et al. [16] presented an adaptable deconstruction approach based on regression to break down the original measured values into a pattern sequence and a collection of variation posts and then create the matching prediction line regression model for the pattern sequence in consumption behavior prediction and to exhibit results in specific test situations in commercial users. If there are nonlinear correlations in the data, the linear regression model performs poorly. Revati et al. [17] suggested employing Gaussian process regression to anticipate consumer behavior to focus on a data-driven

approach to load profile prediction with the emphasized benefit of a model-free environment and useful for setting up a specific demand response plan to receive incentives like money. This modal cannot locate the grouped data. Malik et al. [18] promoted the use of machine learning techniques and functional link neural networks to build efficient systems for predicting customer multiresource cloud data centre consumption. To solve the under- and overprovisioning problems, overprovisioning of services results in higher expenses and increased energy use. The prediction of multi-variety cloud resource use is a difficult problem due to the potential for quick and disproportionate variations in resource utilization. It has very low accuracy.

Najman et al. [19] proposed using a GNG neural network to find and explore trends in customer purchasing behavior. This would help marketers fully appreciate customer behavior and create targeted tactics for international business. Predicting behavior requires more time. Chakladar et al. [20] employed robust long short-term memory-(LSTM-) based deep neural network model was constructed to categorize consumer preferences while visualizing advertising for consumers and seeks to provide a major contributor to the area of consumer behavior since it gives guidelines regarding the consumer preferences after viewing the internet commercials. LSTMs are susceptible to specific initializations of activation functions (Li [21]). Phyto et al. [22] suggested the utilization of machine learning algorithms with reduced error rates that are taught to create the planned voting regressor model, which is essential for energy producers in order to meet the needed quantity of energy between consumption and supply. The classification of data set is more complex by using this model.

Asiri et al. [23] employed multiclass random forest for predicting consumer behavior, which is a crucial sector in the industry for deciding how much to charge for each merchandise. The majority of a company's profit is directly related to the proportion of sales, which depends on a variety of client characteristics, including consumer behavior and market competition. The approach may be too sluggish and inefficient for authentic forecasts due to the enormous number of trees. Subroto and Christianis [24] suggested

utilizing a multilayer perceptron to forecast consumer behavior in categorizing reviews as highly or poorly rated using relevant business criteria. Having a better understanding of customer reviewing behavior can result in the adoption of effective strategy by the parties involved in this study, such as a policy to manage customer reviews by maintaining high levels of customer satisfaction. Tuning of features affects multilayer perceptrons (Salihu and Iyya [25]). Jupalle et al. [26] proposed the usage of machine learning algorithms to gather reviews from the internet and sort them into five categories highly positive, favourable, balanced, awful, and severely negative in attempt to forecast how people will behave while making purchases. Massive data sets are needed for machine learning in order to train the data set.

Chaubey et al. [27] recommended using k -nearest neighbors (KNN) to predict consumer behavior since many sales and service-providing businesses need to highlight connected clients while introducing new goods, services, and improved versions of old goods. They must focus on their current clients while doing this. These consumers' actions provide businesses with data on how to market their goods. It is rather inefficient in terms of computing. Sheoran and Kumar [28] investigated how the theory of planned behavior (TPB) has been used to comprehend the multifaceted character of sustainability consumer behavior using descriptive and analytical methodologies and to perform consumption behavior prediction, information extraction, and user influence analysis. It takes a lot of time and effort. Zhang and Wang [29] developed an enhanced deep forest strategy for predicting consumer behavior, which is crucial for growing a firm. It is among the most crucial element of corporate intelligence. Consumer predicting and estimation provide information on how a business should handle its labor, working capital, and revenue assets Maddikunta et al. [30]. When splitting the trees, it employs the complete feature memory space. Table 1 shows the list of existing methodologies.

The existing approaches have limitations with their inability to perform in nonlinear data correlations, inaccurate classification, inadequate data filtering, poor feature tuning, and more time consumption. Therefore, the procedures mentioned above are no longer able to satisfy the actual requirement of customer behavior. Therefore, this motivates to address the shortcomings of existing technology and greatly enhance predictions of consumer behavior; we presented a multiobjective evolutionary algorithm.

2.1. Problem Statement. The prediction of consumption behavior reveals consumer traits, personal preferences, and fundamental constraints. Businesses may better understand customer needs and corporate goals by monitoring consumer behavior. This will enable them to provide more informed suggestions and expand their market share. The development of several prediction models has several shortcomings in the categorization and prediction of consumer behavior. We thus introduced a multiobjective evolutionary algorithm to solve the limitations in existing technology and considerably improve predictions of customer behavior.

3. Proposed Methodology

Successful consumption behavior prediction improves the predictive value of consumer behavior and increases business profitability. Thus, we suggested a multiobjective evolutionary algorithm and for feature extraction, the Word2vec model is used, and boosted ant colony optimization (BACO) is used to choose the best features which improve the prediction of consumption behavior. Figure 2 depicts the flow of the proposed work, and this section gives a thorough description of it.

3.1. Data Collection. The data was gathered online utilizing QQ, e-mail, and WeChat from Chinese consumers who have participated in at most one online shopping carnival (OSC) in the preceding three years. As a result, a comfort survey method was used to gather information from consumers living in Changchun and Jilin City (N-E China), tier 2 and 3 cities in terms of social marketplace utilization (online networking) (DATA500). However, because the investigation was limited to four cities from the tier 1 bunch of social marketplace utilization, it was recommended that they also cover other geographic areas when examining OSC behavior. Initial data collection involved 357 questionnaires, however, after eliminating the invalid ones, 300 valid surveys (84.03 percent) were kept (Liu et al. [31]).

3.2. Data Preprocessing Using Min-Max Normalization. Data preprocessing is done as the first stage and is crucial to investigation since it assesses the data integrity for each prediction model's effectiveness in making predictions. Low information quality is the consequence, making it impossible to find quality findings and necessitating data changes for data analysis prediction. One of the most popular techniques for normalizing data is min-max normalization. Every feature's lowest and maximum values are each converted to a 0 and a 1, respectively, while all other values are converted to a decimal between 0 and 1. Each element in the complete data set y is represented by a value between 0 and 1.

It establishes a data range by designating the denominator as the difference between the greatest and lowest number. It is feasible to display each component as a value among 0 and 1 for the numerator by deducting the minimum value of each y component from each y component. It is feasible to establish a big value near to "1" and a lesser number close to "0" in respect of the numerator by deducting the maximum value of every y component from each y component, as shown in equation (2) shifting and inverted min-max normalization. It involves converting measured values from one scale to another, and it can get even more complicated to match the posterior distribution of the modified values. Min-max normalization splits the data values by the range, or the distance between the maximum and minimum, and deducts the data points with the minimum value.

$$Y^* = \frac{[Y - \min(Y)]}{\text{range}(Y)}, \quad (1)$$

where $\min(Y)$ represents the minimum, $\max(Y)$

TABLE 1: List of existing methodologies.

S. no	References	Techniques	Drawbacks
1.	Shukla et al. [10]	Supervised and unsupervised machine learning algorithms	It is unable to obtain exact data filtering parameters.
2.	Chen et al. [11]	Attitude-behavior-context (ABC) theory	Its incomplete consumer statistics data might affect the performance.
3.	Liu et al. [12]	Bit-based latent spatiotemporal approach	This modality performs poorly in terms of classification accuracy
4.	VLN and Deeplakshmi [14]	Support vector machines (SVM) based on machine learning	The targeted classifications might overlap occasionally
5.	Wang et al. [16]	Adaptable deconstruction approach	If there are nonlinear correlations in the data, the linear regression model performs poorly
6.	Revati et al. [17]	Gaussian process regression	This modal cannot locate the grouped data.
7.	Najman et al. [19]	Growing neural gas	Predicting behavior requires more time.
8.	Chakladar et al. [20]	Long short-term memory- (LSTM-) based deep neural network model	LSTMs are susceptible to specific initializations of activation functions
9.	Asiri et al. [23]	Multiclass random forest	It is sluggish and inefficient for prediction
10.	Subroto and Christianis [24]	Multilayer perceptron	Tuning of features affects multilayer perceptrons
11.	Chaubey et al. [27]	K -nearest neighbors (KNN)	Inefficient in terms of computing
12.	Sheoran and Kumar [28]	Theory of planned behavior (TPB)	It takes a lot of time and effort
13.	Zhang and Wang [29]	Enhanced deep forest strategy	When splitting the trees, it employs the complete feature memory space.
14.	Amasyali and El-Gohary [13]	Big data technology based on machine learning	Data preprocessing in machine learning gives low enhancement of data and less accuracy in prediction
15.	Malik et al. [18]	Machine learning techniques and functional link neural networks	Disproportionate precision variations in resource utilization
16.	Phyo et al. [22]	Machine learning algorithm and voting regressor model	The classification of data set is more complex by using this model
17.	Jupalle et al. [26]	Machine learning algorithm	Massive data sets are needed for machine learning in order to train the data set.

represents the maximum, and range (Y) represents the difference between maximum and minimum

$$Y^* = \frac{[Y - \min(Y)]}{[\max(Y) - \min(Y)]^a}, \quad (2)$$

where a is the constant of the denominator power.

3.3. Feature Extraction Using the Word2Vec Model. Feature extraction is the process of transforming unstructured data into numerical characteristics when the original data collection has the necessary information. In contrast to applying artificial intelligence to the raw data, computerized feature extraction uses specialized algorithms or neural networks to automatically extract features from data without requiring human input. This approach may be quite useful when trying to make a quick transition from creating raw data to artificial intelligence systems. To extract data features, we

employed the Word2Vec model. The Word2Vec model is created after the initial procedures.

Using this approach, Word2Vec is a two different layer, shallower neural network that has been trained to recreate data contexts in linguistic terms. A consumption data corpus serves as the input and a set of extracted vectors serves as the output of Word2vec. It features a huge corpus of texts as input and outputs a vector space, usually with several hundred dimensions, where each distinct word in the corpus is given a matching vector. The Word2vec approach maximizes the probability of guessing the word context or neighboring words by calculating each word's vector value and measuring the semantic distance between words. It uses a value of zero to identify characteristics in the data. The value will be changed to terms having semantically equivalent relationships.

Word2Vec determines the separations between the data in each text and the spam and ham keywords. Two more

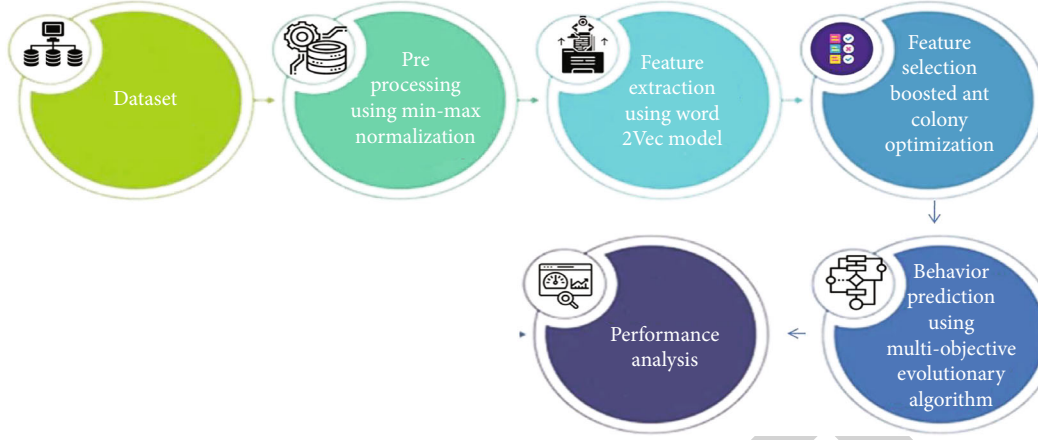


FIGURE 2: Flow of proposed work.

characteristics are created when the classes individually add these values. Organizational data is represented using the Word2vec-calculated distributed vector which is shown in equation (3). The fundamental benefit of distributed representations is the spatial proximity of related consumer data, which makes it easier to generalize observed patterns and produces a more accurate model estimate. Creating word vector representations that are exceptionally effective at predicting their context within the same material is the goal of Word2Vec training.

$$\frac{1}{S} \sum_{s=1}^S Q \sum_{i=-k}^{i=k} \log q(x_{s=i} | x_s). \quad (3)$$

3.4. Feature Selection Using Boosted Ant Colony Optimization (BACO). An algorithm inspired by nature called boosted ant colony optimization (BACO) imitates how ants look for feedstuffs. Since BACO offers parallelization while minimizing process dependence and provides feedback on the actions of ants in the search space, it is more rational than other algorithms. To make statistical judgments, BACO considers the pheromone trail and heuristic data. As they go along a path, the BACO updates the pheromone level at any feature. The more consumer data that pass over a feature, the more pheromones are deposited there, increasing the likelihood that the feature will be found along the short way.

$$Sq_i^j(G) = \begin{cases} \frac{[\tau_i(G)]^\alpha [\eta_i]^\beta}{\sum_{c \in c_i^j} [\tau_c(G)]^\alpha [\eta_c]^\beta}, & \text{if } c \in c_i^j, \\ 0, & \text{otherwise.} \end{cases} \quad (4)$$

The largest number of data points and the short way will both follow the way with the greatest pheromone value. Data are widely dispersed throughout a set of features with a predetermined largest amount of generations S , and the pheromone value $c = 1$ is initialized at each of the N features. The alternatives exist $Sq_i^j(G)$ of j th data at i th feature is displayed

below for each generation G which is shown in equation (4).

$$\tau_i(G+1) = (1-q)\tau_i(G) + \sum_{j=1}^N \Delta\tau_i^j(G), \quad (5)$$

where τ_i^j is a list of potential neighbors of the i th features that the j th data does not reach. Nonnegative variables, accordingly, provide the relevance of pheromone level i and heuristic information (c) for the motions of the data which shown in 5. A fitness function (FF) is used to evaluate the new set of selected features when the next feature in the data route has been picked. If the fitness value does not increase following the addition of any new feature, the j th ant's movement is stopped. The quantity of pheromone level at the following generation ($G+1$) at the i th feature is updated in followed equation (6) if the halting requirements are not met.

$$\Delta\tau_i^k(g) = \begin{cases} \frac{FF(S^j(G))}{|S^j(G)|}, & \text{if } i \in S^k(g), \\ 0, & \text{otherwise,} \end{cases} \quad (6)$$

where N is the number of data, $S^j(G)$ displays the number of features that were chosen, and ji indicates the pheromone that was deposited by j th ant if i th feature is on the shortest path of the data; otherwise, it is 0. As soon as G hits the predetermined maximum S , the halting requirements are satisfied. A group of characteristics will be chosen as a selected feature if it has the greatest pheromone level and lowest fitness value which is shown in equation (6). Figure 3 depicts the BACO's entire procedure.

3.5. Consumption Behavior Prediction Using Multiobjective Evolutionary Algorithm. Multiobjective evolutionary algorithm (MOEA) is the best method for predicting the consumption behavior of consumers, and it leads to an increase in sales and profitability of businesses. The two main categories of prediction algorithms are traditional gradient-based methods and gradient-free direct approaches. One of the traditional prediction techniques,

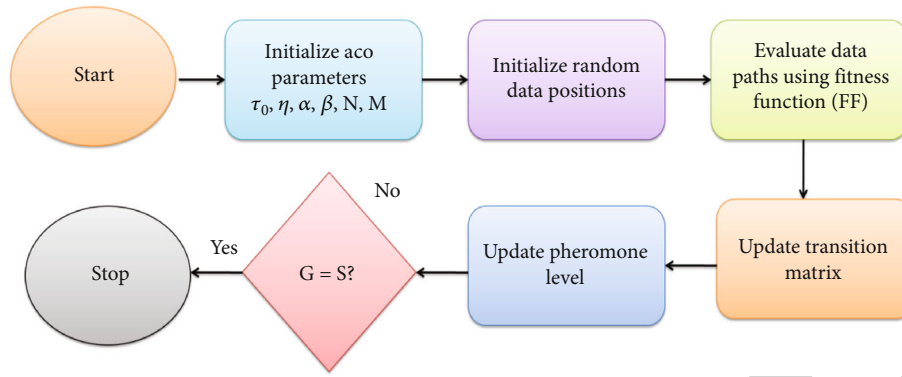


FIGURE 3: Flow of BACO.

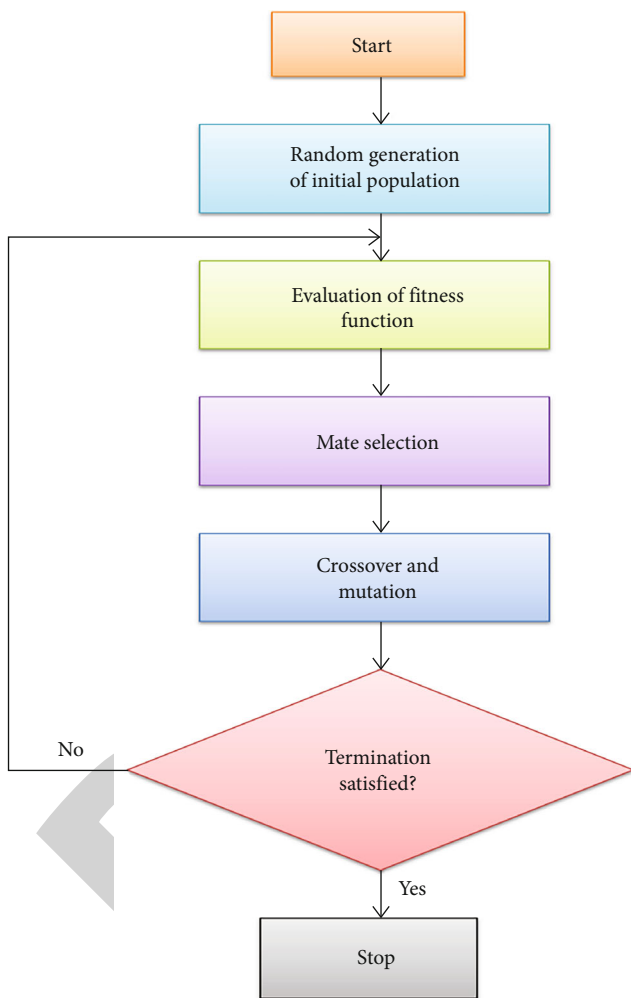


FIGURE 4: Steps of MOEA.

the multiobjective evolutionary algorithm predicts the best course of action by using variations of the nonlinear objective variable. The starting values are given greatly influence how well this algorithm performs. If the goal and constraint functions are differentiable, it converges to the best forecast.

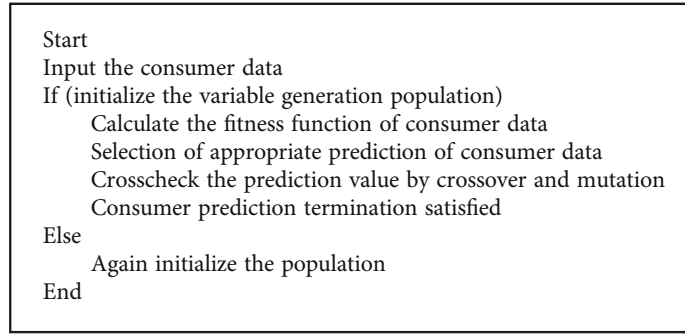
Discontinuous or nondifferentiable variables can be predicted efficiently by the multiobjective evolutionary algo-

rithm. This technique is appropriate for consumption prediction in the company since the link between the consumption characteristics and one another is nonlinear and produces a continuous function. This may be applied to resolve corporate concerns with consumption forecasting. To obtain the prediction answer, the MOEA algorithm is inspired by the evolutionary processes of replication and evolutionary theory. The replication, selection, crossover, and mutation processes in this algorithm are crucial ones. Figure 4 depicts the basic steps of the MOEA algorithm used for consumption prediction.

Algorithm 1 shows the working flow of the MOEA. To generate several viable solutions to the issue, population growth is the first step. The next step is to assess the prediction fitness function, which stands for the optimal prediction that has to be optimized. The most effective strategies are chosen to create the following population in this assessment. After a fitness assessment, mate selection is necessary so that the chosen prediction can go through a cross-over. Additionally, a new population is created to replace the existing one. Until the consumption prediction termination requirements are satisfied, this procedure continues constantly. The existing techniques exploit a collected data to construct an appropriate explanatory or predicting model. Multiobjective evolutionary algorithms improve their hyperparameters, frequently under competing performance objectives, and identify the optimal solution for a specific task. It correctly determines the inputs to the objective function in order to arrive at the best possible solution for the specified function and satisfy all necessary constraints. By avoiding the populations of data from evolving insanely identical to one another and so delaying or even blocking convergence to the global optimum, mutation operations are employed to try to avoid local minima. By switching some or all of the dataset's data, the crossover of two original datasets generates new solutions. It has higher probability.

4. Result

In this research, a multiobjective evolutionary algorithm is used to examine consumer consumption prediction (MOEA). Chinese consumer preferences data who have participated in at least one online shopping carnival (OSC) are used in this paper. The effectiveness of the consumer's



ALGORITHM 1: Multiobjective Evolutionary Algorithm.

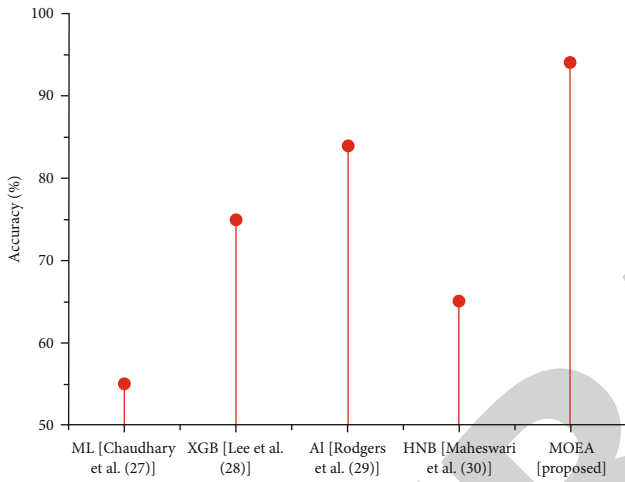


FIGURE 5: Comparison of accuracy.

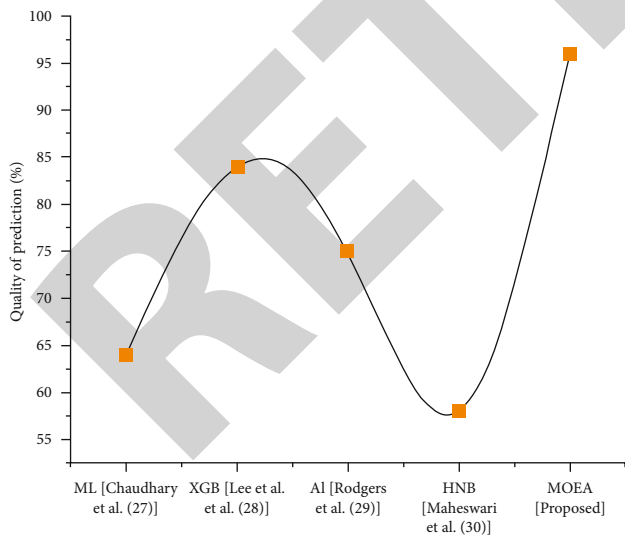


FIGURE 6: Comparison of quality of prediction.

consumption prediction is examined in this section. Accuracy, recall, precision, $f1$ -score, quality of prediction, and prediction time are the key parameters. These metrics are used to assess the efficacy of the proposed approach (MOEA). The results were contrasted with that of tradition-

ally used techniques including machine learning (ML), eXtreme Gradient Boosting (XGB), artificial learning (AL), and hybrid naive Bayes (HNB).

4.1. Accuracy. The accuracy of the model is the extent to which evaluations of a quantity are closer to that number's true value. Through using proposed methodology, it forecasts the essential information based on customer preferences from consumer data from several sources, identifies patterns, and envisions trends and future consequences. When compared to the existing method, the suggested method's consumer consumption predictions are shown to be more accurate. Figure 5 shows consumption prediction of accuracy in existing systems, and the proposed system is denoted. ML has attained 50%, XGB has acquired 75%, AI has reached 85%, and HNB attains 65% whereas the proposed system attains 95% of accuracy.

4.2. Quality of Prediction. In an effort to predict how individuals would respond whenever purchasing goods, the suggested technique effectively and accurately identifies customer preferences for their incredibly positive, overwhelmingly favourable, reasonable thoughts, dreadful, and significantly unfavorable items. The prediction quality metric will demonstrate the efficiency of the system when evaluated on historical data to estimate the performance of the measurements. The quality of prediction is interpreted in Figure 6. The quality of prediction of ML acquires 67%, XGB acquires 82%, AI has reached 75%, and HNB attains 58% whereas the proposed system attains 97%. Hence, the proposed system has higher efficiency.

4.3. Precision. The probability of pertaining recovery of consumer preference prediction on average is known as precision. When applying the recommended approach, precision characterizes how consumer data could be predicted with a high degree of authenticity for consumption preferences across a variety of purchases.

The proportion of appropriate concepts among the recovered occurrences is known as precision, also known as positive predictive value. It can define that precision is the measure of quality. Figure 7 represents the comparison of precision in existing and proposed methodologies. The precision of the proposed work is much greater than the existing methodologies. The consumption prediction of

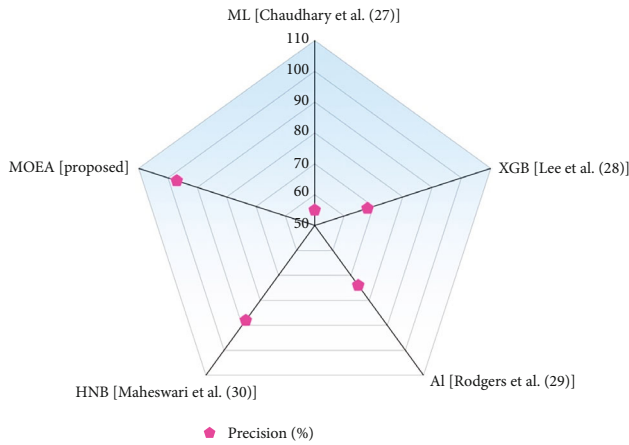


FIGURE 7: Comparison of precision.

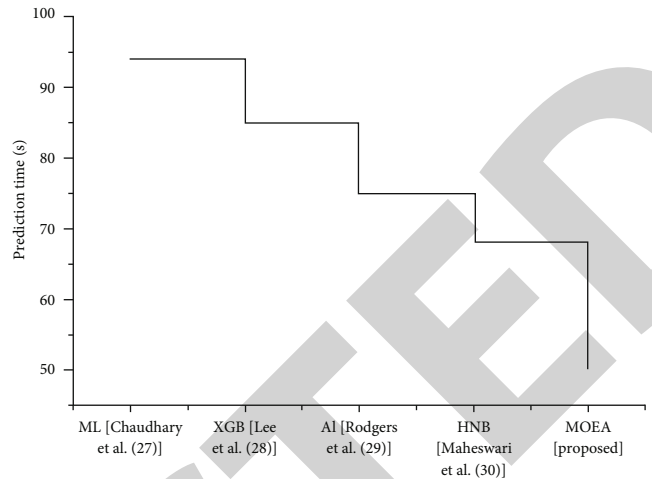


FIGURE 10: Comparison of prediction time.

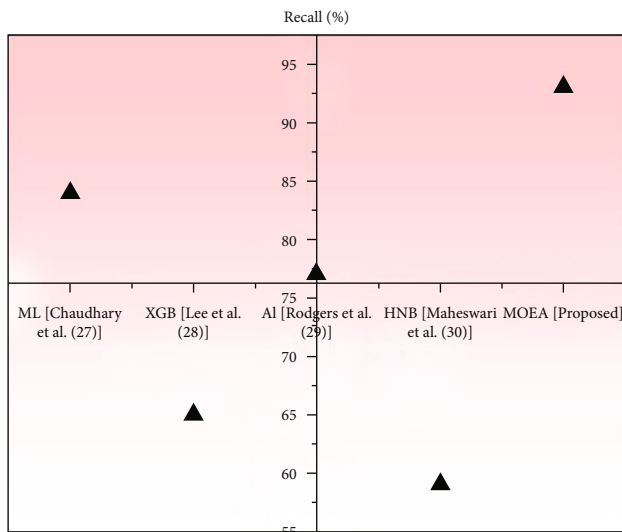


FIGURE 8: Comparison of recall.

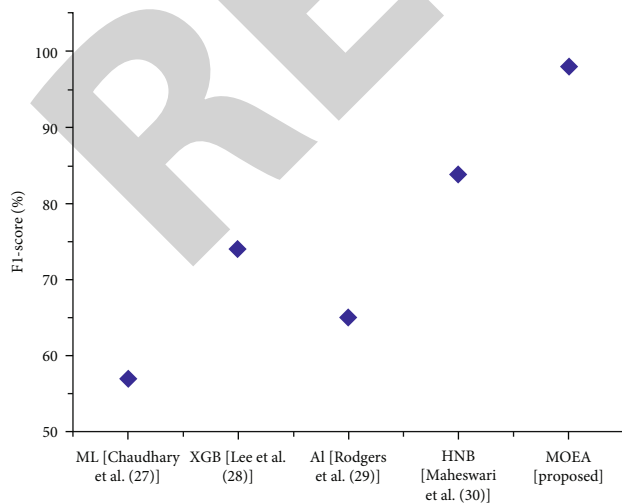


FIGURE 9: Comparison of F1-score.

precision in existing systems has the following level, therefore, ML has attained 55%, XGB has acquires 70%, AI has reached 75%, and HNB attains 90% whereas the proposed system attains 99% of precision. Hence, the proposed system has the greatest performance level.

4.4. *Recall.* Recall of proposed and existing methods is depicted in Figure 8. The percentage of pertinent occurrences that were recovered is known as a recall. The true positive rate or sensitivity is also referred to as the recall. Compared to the existing approaches, the proposed method has the highest level of recall. The behavior prediction of recall in existing systems has the following level of recall, therefore, ML has attained 84%, XGB has acquires 65%, AI has reached 76%, and HNB attains 58% whereas the proposed system attains 93% of recall. This denotes the efficiency of the proposed work is well-suited.

4.5. *F1-Score.* Figure 9 depicts the *F1*-score of existing and proposed techniques. A system’s clarity and recollection are combined into a single statistic known as the *F1*-score by determining their harmonic means. It mainly serves to contrast the effectiveness of the two systems. A higher *F1*-score is considered a better system performance. From Figure 8, ML acquires 68%, XGB acquires 75%, AI has reached 65%, and HNB attains 85% whereas the proposed system attains 98% of the *F1*-score. It denotes that the proposed system has higher performance.

4.6. *Prediction Time.* Figure 10 depicts the prediction time of existing and proposed approaches. When a system is anticipated to forecast something about what it is predicting is known as the prediction time. From Figure 10, the prediction time of ML acquires 93 (s), XGB acquires 85 (s), AI has reached 75 (s), and HNB attains 65 (s) whereas the proposed system attains 50 (s).

It is known that the proposed system has a low prediction time compared to the existing approaches. Hence, it indicates that the proposed system has well effective for

TABLE 2: Comparative analysis of various parameters for existing and proposed methods.

	ML	XGB	AI	HNB	MOEA (proposed)
Accuracy (%)	50	75	85	65	95
Quality of prediction (%)	67	82	75	58	97
Precision (%)	55	70	75	90	99
Recall (%)	84	65	76	58	93
F1-score (%)	68	75	65	85	98
Time (s)	93	85	75	65	50

implementation. The comparative analysis for existing and proposed methods is shown in Table 2.

5. Discussion

Chaudhary et al. [32] suggested using machine learning (ML) to analyze customer activity on social networking sites based on a few metrics, requirements, and user attitudes. Massive data sets are needed for machine learning to be trained on, and they should result in lower-level prediction. Lee et al. [33] developed the eXtreme Gradient Boosting (XGB) model to develop powerful tools for forecasting customer behavior and to assist companies in generating revenue and sales. On sparse and unstructured data, it does not execute well. Rodgers et al. [34] advocated the employment of artificial intelligence (AI), which develops a methodical technique to determine predicting customer behavior perception of a business and the usefulness effects the acquisition of that product. For prediction, a longer time is needed. Maheswari et al. [35] stated hybrid naive Bayes (HNB) was developed to classify consumer trends when they are making purchases of items and aims to be a significant addition to the study of consumer behavior. Assuming that each feature is isolated, naive Bayes is unable to learn how to anticipate patterns. Therefore, the proposed model MOEA overcomes these shortcomings in the prediction of consumption behavior.

6. Conclusion

In an era where consumer prediction is one of the innovative technical features, the integration of consumption prediction with business will result in substantial changes in growth and profit for business management. Due to the concept of predicting consumer behavior, all business categories may now be characterized as quantitative, which enhances the efficiency, accuracy, and competence of the business organization. For the betterment of business, this chapter advocated employing a multiobjective evolutionary algorithm (MOEA) to precisely estimate client consumption forecast. The results show that, in terms of accuracy (95%), quality of prediction (97%), precision (99%), recall (93%), F1-score (98%), and prediction time (50s), the proposed MOEA approach performs well than the conventional ML, XGB, AI, and HNB algorithm methods. For some ideas of

the process in the suggested method, it might be challenging to comprehend and interpret. Future research on the topic might focus on improving the ability to predict consumer behavior for successful business development. In the future, we may think about using evolutionary algorithm techniques to improve performance metrics and the application of consumption prediction in business economic domains.

Data Availability

The data used to support the findings of this study are available from the corresponding author upon request.

Conflicts of Interest

The authors declare that they have no known competing financial interests or personal relationships that could have appeared to influence the work reported in this paper.

Acknowledgments

This study was supported by (1) National Key Research and Development Program (2019YFC0507502), (2) National Foundation project “Research on collapse mechanism of karst water-soil coupling in Guilin under extreme climate conditions” (41967037), and (3) Guangxi Innovation-Driven Development Special Project “Research, Development and Experimental Demonstration of Key Technologies for Water Resources Utilization and Synergistic Development of Water Ecology Industry in Typical Karst Wetlands of Li River Basin” (Gui Ke AA20161004-1)

References

- [1] L. Guo, B. Zhang, and X. Zhao, “A consumer behavior prediction model based on multivariate real-time sequence analysis,” *Mathematical Problems in Engineering*, vol. 2021, Article ID 6688750, 5 pages, 2021.
- [2] Y. Tian, Y. Lai, and C. Yang, “Research of consumption behavior prediction based on improved DNN,” *Scientific Programming*, vol. 2022, Article ID 6819525, 9 pages, 2022.
- [3] Y. Li, X. Jia, R. Wang et al., “A new oversampling method and improved radial basis function classifier for customer consumption behavior prediction,” *Expert Systems with Applications*, vol. 199, article 116982, 2022.
- [4] R. N. Mody and A. R. Bhoosreddy, “Multiple odontogenic keratocysts: a case report,” *Annals of Dentistry*, vol. 54, no. 1-2, pp. 41–43, 1995.
- [5] S. Xiao and W. Tong, “Prediction of user consumption behavior data based on the combined model of TF-IDF and logistic regression,” *Journal of physics: conference series*, vol. 1757, no. 1, article 012089, 2021.
- [6] H. Garg, “Digital twin technology: revolutionary to improve personalized healthcare,” *Science Progress and Research (SPR)*, vol. 1, no. 1, p. 1.1, 2020.
- [7] U. A. Saari, S. Damberg, L. Frömbling, and C. M. Ringle, “Sustainable consumption behavior of Europeans: the influence of environmental knowledge and risk perception on environmental concern and behavioral intention,” *Ecological Economics*, vol. 189, article 107155, 2021.

Retraction

Retracted: Application and Analysis of RGB-D Salient Object Detection in Photographic Camera Vision Processing

Journal of Sensors

Received 23 January 2024; Accepted 23 January 2024; Published 24 January 2024

Copyright © 2024 Journal of Sensors. This is an open access article distributed under the Creative Commons Attribution License, which permits unrestricted use, distribution, and reproduction in any medium, provided the original work is properly cited.

This article has been retracted by Hindawi following an investigation undertaken by the publisher [1]. This investigation has uncovered evidence of one or more of the following indicators of systematic manipulation of the publication process:

- (1) Discrepancies in scope
- (2) Discrepancies in the description of the research reported
- (3) Discrepancies between the availability of data and the research described
- (4) Inappropriate citations
- (5) Incoherent, meaningless and/or irrelevant content included in the article
- (6) Manipulated or compromised peer review

The presence of these indicators undermines our confidence in the integrity of the article's content and we cannot, therefore, vouch for its reliability. Please note that this notice is intended solely to alert readers that the content of this article is unreliable. We have not investigated whether authors were aware of or involved in the systematic manipulation of the publication process.

Wiley and Hindawi regrets that the usual quality checks did not identify these issues before publication and have since put additional measures in place to safeguard research integrity.

We wish to credit our own Research Integrity and Research Publishing teams and anonymous and named external researchers and research integrity experts for contributing to this investigation.

The corresponding author, as the representative of all authors, has been given the opportunity to register their agreement or disagreement to this retraction. We have kept a record of any response received.

References

- [1] Q. Fu, "Application and Analysis of RGB-D Salient Object Detection in Photographic Camera Vision Processing," *Journal of Sensors*, vol. 2022, Article ID 5125346, 10 pages, 2022.

Research Article

Application and Analysis of RGB-D Salient Object Detection in Photographic Camera Vision Processing

Qiang Fu 

Qingdao Vocational and Technical College of Hotel Management, Qingdao, Shandong Province, 266100 Shandong, China

Correspondence should be addressed to Qiang Fu; fuqiang@qchm.edu.cn

Received 23 August 2022; Revised 5 September 2022; Accepted 11 September 2022; Published 24 September 2022

Academic Editor: Sweta Bhattacharya

Copyright © 2022 Qiang Fu. This is an open access article distributed under the Creative Commons Attribution License, which permits unrestricted use, distribution, and reproduction in any medium, provided the original work is properly cited.

To identify the most visually salient regions in a set of paired RGB and depth maps, in this paper, we propose a multimodal feature fusion supervised RGB-D image saliency detection network, which learns RGB and depth data by two independent streams separately, uses a dual-stream side-supervision module to obtain saliency maps based on RGB and depth features for each layer of the network separately, and then uses a multimodal feature fusion module to fuse the latter 3 layers of RGB and depth high-dimensional information to generate high-level significant prediction results. Experiments on three publicly available datasets show that the proposed network outperforms the current mainstream RGB-D saliency detection models with strong robustness due to the use of a dual-stream side-surveillance module and a multimodal feature fusion module. We use the proposed RGB-D SOD model for background defocusing in realistic scenes and achieve excellent visual results.

1. Introduction

The purpose of image saliency detection is to extract regions of an image that are of more interest to humans by simulating human visual characteristics through intelligent algorithms, and it is promising for a wide range of applications in various computer vision tasks, such as image retrieval, image compression, and visual tracking [1]. More and more saliency detection research works in recent years have designed a large number of deep Convolutional Nerve Networks (CNNs) for RGB saliency target detection and achieved better performance [2]. Compared with traditional methods, deep learning can automatically extract features from a large amount of data. However, these RGB saliency detection models may not be able to distinguish salient targets from the background when the salient targets and the background are similar.

In fact, depth data contains clear target shapes and rich spatial structures, which can provide many additional saliency cues compared to RGB data, which provides detailed appearance and texture information. In addition, the perceptual robustness of depth sensors (e.g., Microsoft Kinect or Intel RealSense) to illumination changes greatly

helps to extend the application scenarios of saliency detection. Therefore, for RGB-D saliency detection tasks, how to fully fuse RGB and depth information is the key issue. For how to clearly form the complementary information between the two modalities of RGB and depth and fully fuse them, most previous RGB-D fusion networks exploring the cross-modal complementarity of RGB and depth data are divided into two types of single-stream network architectures and dual-stream network architectures [3]. The single-stream network architecture considers that depth data can be used as an undifferentiated channel in tandem with RGB data to obtain salient maps by learning RGB and depth features together through the network. In the paper study [4], after superpixel segmentation of the input RGB data and depth data, the significant feature vector of each superpixel region is calculated, and then, the calculated significant value feature vector is used as the input of the network, which generates the significant graph by closely coupling the RGB information and depth information by combining the saliency features of the superpixels. The dual-stream network architecture learns RGB data and depth data separately through two independent streams and then learns the joint representation of RGB and depth features through a shared

network layer added at an early or late stage to obtain the final saliency map. The study [5] inputs RGB data and depth data as two small networks, trains them separately, and then forms a fusion network with the generated RGB and depth features through multipath and multimodal interactions to train them together. The study [6] proposed a CNN-based framework to automatically fuse RGB and depth data to obtain salient maps. A late fusion network model is proposed in study [7] to capture the higher-order features of both RGB and depth modalities to generate the saliency map. The study [8] argues that this deep CNN feature that only fuses RGB and depth modalities is unlikely to capture the complementary information of cross modalities well. Therefore, a progressive complementary-aware fusion network is proposed to effectively utilize the cross-modal complementary information at multiple levels. It is widely believed that features at different levels are complementary and they abstract the scene at different scales. However, not all levels of cross-modal information are complementary.

Therefore, for the problem of how to fuse different levels of cross-modal information, a dual-stream network structure is used in this paper. Firstly, RGB and depth maps are used as network inputs for two VGG16Nets [9]. Furthermore, a dual-stream side-supervision module is used to significantly predict the supervision of RGB and depth streams to speed up the network convergence and help the network learn the features of each layer better. In order to fully utilize and fuse the semantic information of RGB and depth at different layers of the network, the final significant prediction results are obtained by adopting a high-level guidance of the network to the lower layers, from global to local. Among them, a multimodal feature fusion module is constructed to generate multiscale multimodal fusion features for the high-dimensional multimodal information in the last three layers of the network, so as to obtain the network high-level significant prediction results, while the multimodal feature fusion module is not used for the fusion of the features in the first two layers of the network because the low-level features of the network contain the target detail information. Significant prediction results will appear noisy. In order to eliminate the negative effect brought by low-dimensional depth features, this paper chooses not to include low-dimensional depth features in the low-level feature fusion. Experiments on widely used datasets show that the model in this paper outperforms the current mainstream RGB-D saliency detection model and has strong robustness. It can accurately detect salient target regions.

2. Related Work

2.1. RGB Salient Object Detection. Early 2D saliency target detection methods typically rely on hand-crafted features and heuristic priors such as image contrast, color, texture, and other low-level visual cues. Obviously, hand-crafted features are insufficient to capture high-level semantic information, so approaches based on these features are not universally applicable and can only achieve salient target detection in limited scenes.

Recently, benefiting from the development of convolutional neural networks (CNNs), some work has made great progress in using CNNs to learn deep features. Some deep learning-based saliency methods divide images into small blocks or superpixels and extract single or multiple scale features from each block or superpixel to determine whether an image region is salient or not. Although better performance than traditional methods has been obtained, processing images in a block-by-block manner ignores the underlying spatial information of the entire image, which limits the accuracy of complete salient target detection. The study [10] used a fully connected CNN to extract features and combine global and local features to predict the saliency map. Reference [11] proposes a cyclic CNN with a prediction map guided by a previous cyclic step. Reference [12] used a dropout technique to learn deep uncertain convolutional features in the network to enhance its generalization ability. However, since these methods only employ features extracted at the deeper layers of the CNN, they tend to miss details in salient objects captured mainly at the shallow layers. Several recent works have improved the quality of saliency object detection by further aggregating features across multiple CNN layers to exploit more global and local contextual information simultaneously in the inference process. Among them, study [13] explored the semantic properties and visual contrast of salient objects. Reference [14] created short connections to aggregate features in different layers. Reference [15] derives a resolution-based feature combination module and a boundary-preserving optimization strategy. Reference [16] iteratively aggregated deep features to exploit the complementary saliency information between multilevel features and features in each individual layer. Later, [17] used residual learning to alternately define deep and shallow features. Reference [18] formulated a bidirectional message passing model to selectively aggregate features to improve saliency target detection accuracy. Reference [19] designed an attention-guided network to progressively select and integrate multiple levels of information to predict saliency targets. Reference [20] designed a symmetric CNN to learn complementary saliency information and proposed weighted structural loss to enhance the boundaries of salient objects. Reference [21] explored global and local spatial relationships in deep networks to locate salient objects and define object boundaries. Despite the increasing detection quality, the exploration of global spatial contexts (especially in shallow layers) is still strictly limited by the convolution operator in CNNs, which are essentially local spatial filters. In recent years, 2D-based saliency target detection algorithms have developed rapidly, and even some algorithms have been applied in industry, but there are still challenges to tackle, such as unclear edge prediction of salient objects, incomplete prediction of transparent and reflective objects, and missed detection of small objects. For specific tasks, we should design corresponding models according to the characteristics of the data.

2.2. RGB-D Salient Object Detection. In the past, most traditional saliency target detection methods relied on hand-extracted features to capture local details and global

contextual information separately or simultaneously. However, the lack of high-level semantic information limits their detection capability in complex scenes. Obviously, hand-crafted features are not sufficient to capture high-level semantics, so approaches based on these features are not universally applicable and can only achieve salient target detection in limited scenes. Recently, thanks to the ability of convolutional neural networks to extract high-level semantic features and low-level detail features in a multiscale space, salient target detection has been rapidly developed. These neural network-based methods have made a qualitative leap in experimental results compared to traditional manual feature-based methods. Massive RGB-based salient target detection has focused on using color RGB images to identify salient objects, with good results. Although many RGB-based saliency target detection methods have achieved attractive performance, these methods may still fail to accurately detect salient regions when dealing with complex scenes because of the poor predictive power of the appearance feature contributions in RGB data. Examples include low-contrast scenes, transparent objects, similar foreground and background, multiple objects, and complex backgrounds. In these environments, it is difficult to determine salient targets by referring to RGB color images alone. With the advent of consumer-grade depth cameras such as Kinect cameras, light field cameras, and LiDAR, depth cues with large amounts of geometric and structural information have been widely used for salient object detection (SOD). To better mine salient information in challenging scenes, several CNN-based methods combine depth information with RGB letters to obtain more accurate results. Long-standing research has produced the practice and theory of extracting RGB and depth representations equally for symmetric two-stream structures. Reference [22] designed a symmetric structure for automatically fusing the features of depth and RGB views to obtain the final salient map. Reference [23] used a two-stream CNN-based model to introduce crossmodel interactions in multiple layers by direct summation. Recently, several asymmetric structures have been proposed to handle different data types. Reference [24] used enhanced depth information as an auxiliary cue and a pyramid decoding structure to obtain more accurate salient regions. Reference [25] proposed a structure that consists of a backbone network for processing RGB values and a subnetwork that makes full use of depth cues, which fuses depth-based features into the backbone network by direct cascading. However, simple fusion strategies like direct cascading or summation are not well suited for locating salient objects due to the infinite possibilities of their locations in the real world. Taken together, these approaches ignore the fact that depth cues contribute differently to salient object prediction in various scenarios. In addition, existing RGB-D methods inevitably suffer from loss of detail information when employing convolution steps and pooling operations in RGB and depth streams. An intuitive solution is to use hopping connections or short connections to reconstruct the detail information. Although these strategies mentioned above bring satisfactory improvements, they still struggle to accurately predict the complete structure.

3. Methodology

The method in this paper uses two VGG16Nets as the backbone base network, as shown in Figure 1. RGB and depth maps are used as inputs to extract RGB and depth features to form RGB streams and depth streams, respectively. Since the high-level features of the network acquire the high-dimensional semantic information of the salient targets and ignore the boundary information of the targets, therefore, in this paper, we adopt the high-level guidance to the low level, from deep to shallow and from global to local, to obtain the saliency map and multimodal fusion saliency map of each layer based on RGB and Depth features, respectively; and optimize the network parameters under the supervision of the truth map; and finally take the output of the saliency map of RGB stream as the final prediction result. For the network layer, the RGB and depth features are concatenated, and the significant output of the truth map supervised by its side and the significant output of the upper layer are used as the guidance to obtain the high level significant prediction results using the multimodal feature fusion module. For the network layer, the high-level feature fusion method is not used in the first two layers of feature fusion because the low-level features are more concerned with local information. And the low-layer depth information is not good to affect the final prediction results, so the depth flow supervision of the lower two layers is removed, and the significant maps of each layer are guided by the upper layer.

3.1. Two-Stream Lateral Supervision. According to [10, 11], it can be concluded that network supervision can promote network convergence speed and generate better hierarchical representations to meet the feature requirements at each stage. Considering that single convolution will cause the number of channels to plummet and lose more information, the method of gradually reducing the number of feature channels by using three convolutions is used, while ref. [11, 12] fully consider that the deep high-dimensional feature output retains more target and location information and ignores the target detail information, while the low-dimensional features focus more on local and boundary information. Therefore, the number of channels is reduced to 64 for each layer of VGG16Net backbone base network after three convolution operations and then combined with the saliency map output of the higher layer and then through convolution, deconvolution, and convolution operations to produce the saliency map of this layer. The network learning process is supervised with the true value map, which can help the network to learn the features of each layer better. The above operations are processed separately for the RGB stream and depth stream, as shown in Figure 2, and are specifically expressed in the following equation:

$$\begin{aligned} P^{mr} &= \delta(\text{Conv}(\text{Dec}(\text{Conv}(3\text{Conv}(R^m) \cdot P^{m+1}))))), \\ P^{md} &= \delta(\text{Conv}(\text{Dec}(\text{Conv}(3\text{Conv}(D^m) \cdot P^{m+1}))))). \end{aligned} \quad (1)$$

Based on the literature [13, 14] and the experiments in this paper, it can be concluded that the depth features of

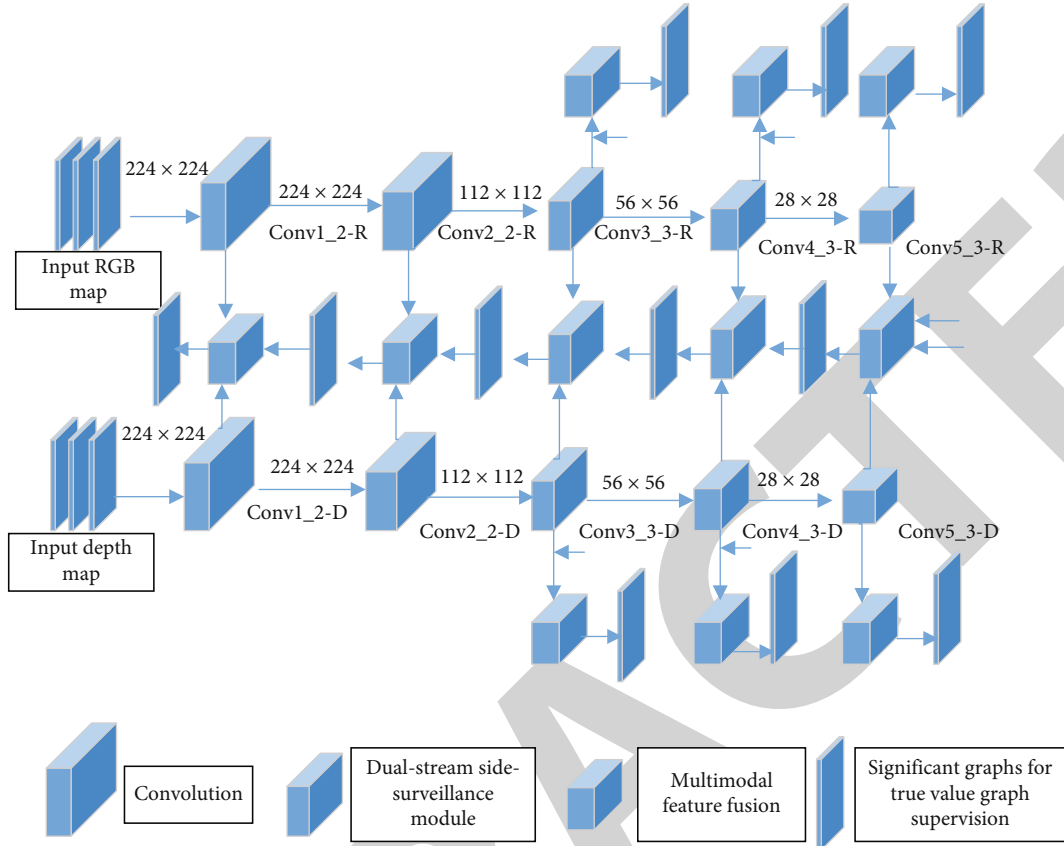


FIGURE 1: Flowchart of our method.

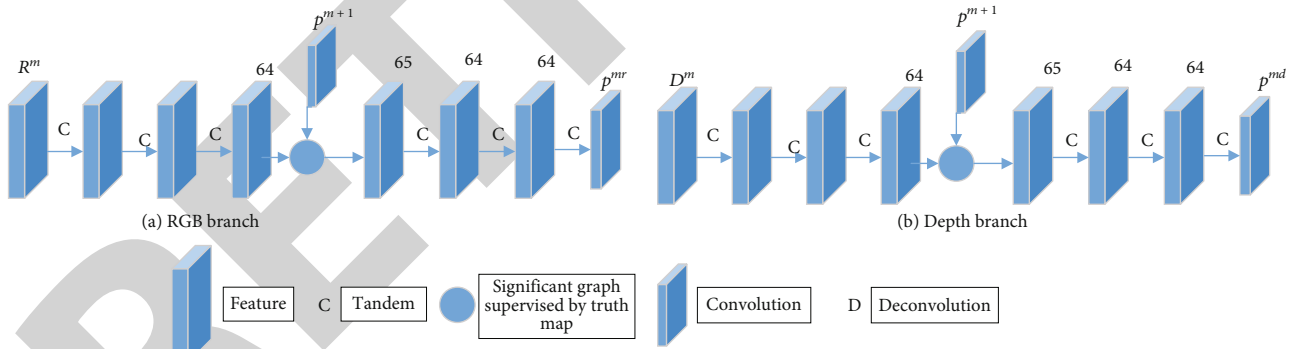


FIGURE 2: Dual-stream lateral supervision module.

the first two layers have low confidence; that is, the depth features containing more local information do not play a positive role in the detection of salient targets in the whole RGB-D image, and therefore, the extraction and supervision of the first two layers of features in the depth stream are eliminated. Also, it was found during the experiments that the indicated high-level saliency map works better when taking the saliency map of the fused high-level RGB stream and depth stream; therefore, the fused saliency map is used for the calculation of the side features of the high 3 layers of the dual streams in both the first and fifth rows on the right side of Figure 2.

3.2. Multimodal Feature Fusion. Considering that the features generated at the higher levels of the network have complete key information, simply generating the salient graph using one scale of convolution operation may pass the noise in some bad feature graphs to the salient prediction output without restriction. Therefore, in this paper, we propose a multimodal feature fusion method for RGB and depth features of layer 1 of the backbone network VGG16Net, as shown in Figure 3, where the two features are concatenated in series and the feature channels are reduced exponentially by the convolution operation, p^{m+1} , p^{mr} , p^{md} , and F^m . However, lacking the guidance of high-level information or

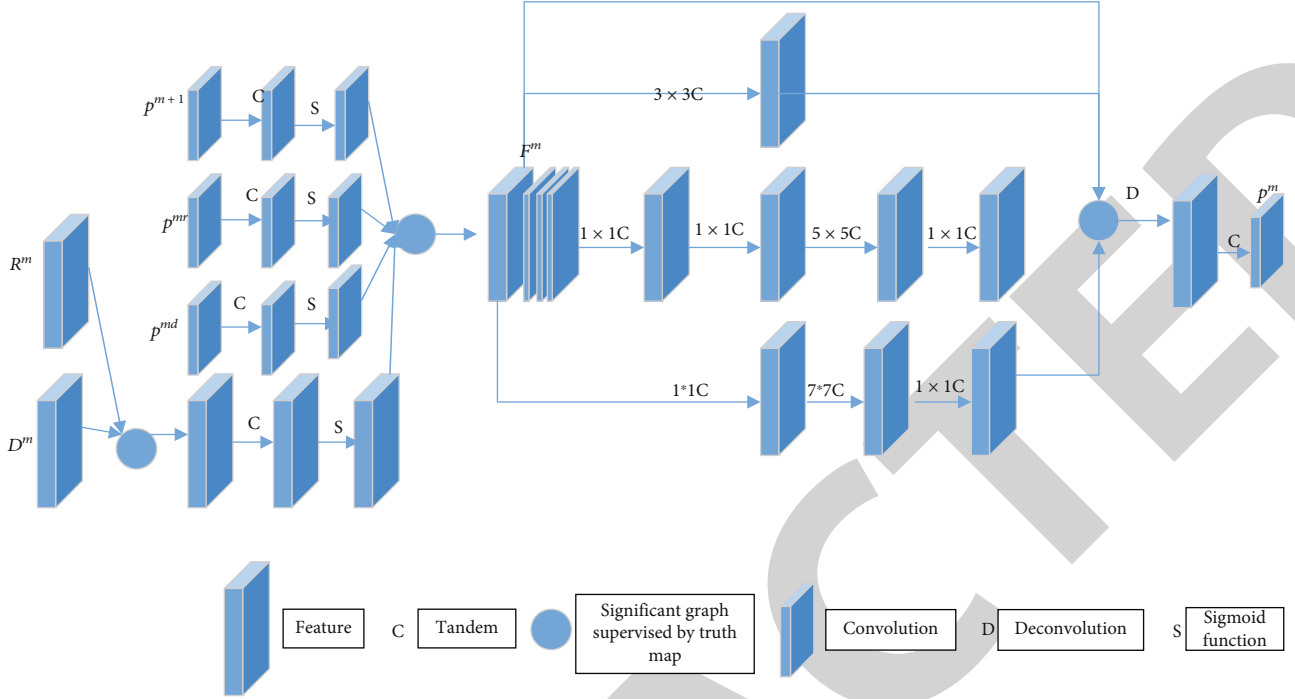


FIGURE 3: Multimodal feature fusion method.

output, the error between the side-by-side output and the true value map optimized directly by the supervised approach becomes larger and its effectiveness is also poor. Similar to the two-stream lateral supervision module, the high-level output and the supervised RGB stream output and depth stream output are used to provide semantic and positional information for the multimodal features to speed up the convergence of the network, optimize the target boundary, and obtain more suitable multimodal fusion features, which are calculated as follows (see Figure 3):

$$F^m = \delta(\text{Conv}(R^m \cdot D^m)) \cdot \delta(\text{Conv}(P^{m+1})) \cdot \delta(\text{Conv}(P^{mr})) \cdot \delta(\text{Conv}(P^{md})), \quad (2)$$

where F^m denotes the excitation function sigmoid, which normalizes feature values and significant values to the same interval to prevent significant output maps from being ignored.

RGB and depth multimodal feature fusion can complement and fuse the robust hierarchical feature representations across modal information and pave the way for generating hierarchical outputs based on multimodal features, compared with the way to process single RGB features and single depth features separately. After forming multimodal fusion features, this paper uses the multiscale convolution module to mine stronger fusion feature representations. The multiscale convolution module extracts multiscale contextual information, and its purpose is to obtain a spatial response mapping so as to adaptively weight the feature mapping at each location and to make each given input locate the most concerned part by learning weights for each pixel, thus mak-

ing it more applicable to scenes with complex backgrounds. The multiscale convolution module uses 4 scales of convolution kernels (1×1 , 3×3 , 5×5 , and 7×7), and the convolution layers with different kernel sizes have different sizes of perceptual fields to obtain feature information at different scales. At the same time, since larger convolution kernels correspond to more network parameters, this paper modifies the multiscale convolution module proposed in [16] by adding 1×1 convolution layer before and after the 5×5 convolution layer and 7×7 convolution layer to reduce the number of channels and then restore the number of channels to reduce the network parameters and then form multiscale multimodal fusion features by channel tandem.

$$f_{\text{Ini}}^m = \text{Conv}_{1 \times 1}(F^m),$$

$$f_{\text{cat}}^m = f_{\text{Ini}}^m \cdot \text{Conv}_{3 \times 3}(f_{\text{Ini}}^m) \cdot \text{Conv}_{1 \times 1}(\text{Conv}_{5 \times 5}(\text{Conv}_{1 \times 1}(f_{\text{Ini}}^m))) \cdot \text{Conv}_{1 \times 1}(\text{Conv}_{7 \times 7}(\text{Conv}_{1 \times 1}(f_{\text{Ini}}^m))). \quad (3)$$

Then, the significant output of the corresponding multiscale multimodal fusion feature is

$$P^m = \delta(\text{Conv}(\text{Dec}(f_{\text{cat}}^m))). \quad (4)$$

The multimodal fusion features of the backbone network VGG16Net better combine the high-dimensional features of RGB and depth and better characterize the salient object features after processing by multiscale convolution. Because multiscale convolution corresponds to different convolution kernels, the larger the convolution kernel is, the larger its corresponding perceptual field is, and the more global

information is seen. Low-dimensional features retain more information about target details, and a large convolution kernel may destroy its integrity. Therefore, this paper does not use the multiscale convolutional module in high-level fusion to process fused features in the first two layers of low-dimensional semantic information fusion part. The salient graph produced by the fusion network is similarly supervised by the truth graph to learn better multimodal fusion features. As mentioned in Section 2.1, the low-level depth information is not very reliable and will affect the final results, so in this paper, the depth stream supervision of the lower two layers is removed, and the saliency map of each layer is guided by the upper layer, and the final output of the saliency map of the RGB stream is taken as the final prediction.

4. Experimental Results

4.1. Dataset. This paper evaluates this model on three of the most widely used datasets. The NLPRI1000 dataset contains 1000 RGB images and depth maps and their corresponding truth maps, containing 11 indoor and outdoor scenes with over 400 objects. The NJU2000 dataset contains 2003 stereo RGB images and their corresponding hand-labeled truth maps, whose depth maps are generated by the optical flow method. The STEREO data contains 797 RGB images and corresponding truth maps (GT), which were collected mainly from the Internet and 3D movies, and their depth maps were generated by the optical flow method. For a fair comparison, similar to the literature [8], their same training and test sets are used for training and evaluation. To solve the problem of insufficient training set, in this paper, the training set is subjected to a data enhancement operation; i.e., the original image is flipped, and the boundary 1/10 cropping operation is performed to retain the main target information, and the training set is increased by a factor of 16.

4.2. Evaluation Criteria. Evaluation criteria are used to evaluate the performance of different significant target detection methods. In this paper, five assessment criteria are used to evaluate the goodness of the model and other models. PR curve is generated by binarizing the significance map through a series of thresholds and then comparing it with the true value map. In F -measure, for the precision rate (Pre) and the detection rate (Rec), they are negatively correlated, and in order to balance the effect between them, F -measure is used to evaluate the experimental effect. The formula is

$$F_{\beta} = \frac{(1 + \beta^2) \cdot \text{Pre} \cdot \text{Rec}}{\beta^2 \cdot \text{Pre} + \text{Rec}}. \quad (5)$$

MAE : mean absolute error (MAE) evaluates the mean value of the absolute error between the significant and true

value maps pixel by pixel. Its calculation formula is

$$MAE = \frac{\sum_{x=1}^W \sum_{y=1}^H |S(x, y) - G(x, y)|}{W \cdot H}, \quad (6)$$

where H and W are the length and width of the image, respectively, and $S(x, y), G(x, y)$ denote the significant and true values of the pixels, respectively.

S -measure: the structural similarity assessment criterion evaluates both the regional similarity and the target similarity between the salient and true value maps, which is defined as

$$S_{\lambda} = \lambda \cdot S_0 + (1 - \lambda) \cdot S_r. \quad (7)$$

E -measure: E -measure measures statistical information at the image level and local pixel matching information. In order to have a fair comparison with other methods, all evaluation criteria were tested using the code provided in the literature [23].

4.3. Experimental Details. In this paper, experiments were conducted using Python and Caffe toolbox with GTX Titan-x GPUs (12 GB) machine configuration. The experimental training impulse, learning rate, weight decay rate, and minimum batch size are set to 0.99, $1e-10$, 0.0005, and 1. The network structure of this paper is based on two pre-trained VGG16Net networks, and the final network model is obtained by using them as the initial weights and fine-tuning the model training iterations for 10 cycles, totaling 160,000 times, which takes about 8 h.

4.4. Experimental Comparison. This model is compared with other TAN, PCFN, MMCI, and DF models under the above evaluation criteria, and the significant graphs are provided by the corresponding papers or generated by their provided codes. The model in this paper is compared with four representative deep learning-based models on PR curves as shown in Figure 4. From the figure, it can be seen that the model in this paper has significantly improved relative to these four models and generally outperformed them on other evaluation criteria. Table 1 shows the experimental results of this model on three datasets based on four evaluation criteria, F -measure, MAE, S -measure, and E -measure; compared with other models, the higher the value of F , S , and E , the better, and the smaller the value of MAE, the better.

4.5. Experimental Comparison of the Lateral Supervision Module. The experimental comparison of the dual-stream lateral supervision module in Section 2.1 is shown in Table 2. NDS (No Deep Supervised) means that the above supervision module is not used for the lateral output supervision, and only one convolution is used to make the number of lateral feature channels to 1 for supervision. From the experimental results in Table 2, it can be seen that the supervision module in this paper can retain feature information better in the supervision process and generate better hierarchical feature representations to meet the feature requirements at each stage.

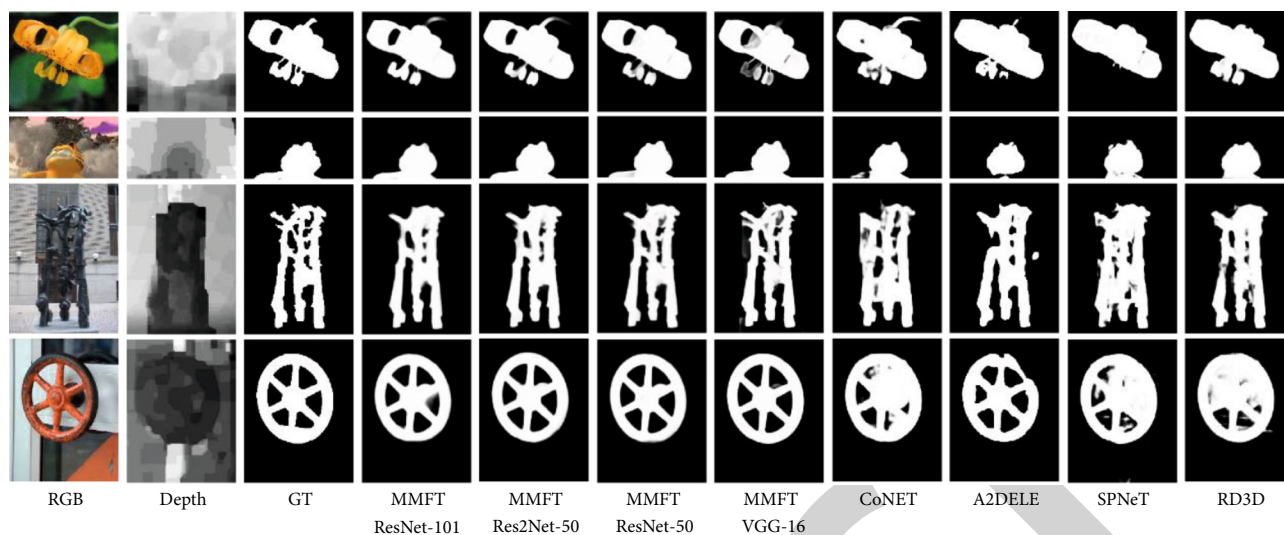


FIGURE 4: Visualization comparison of the model in this paper with the four models.

TABLE 1: Comparison with other models on F -measure, MAE, S -measure, and E -measure.

Algorithm	NLPR1000				NJU2000				STEREO			
	F	MAE	S	E	F	MAE	S	E	F	MAE	S	E
TAN	0.7955	0.0111	0.8862	0.9163	0.8440	0.0606	0.8786	0.8933	0.8488	0.0592	0.8774	0.9106
PCFN	0.7947	0.0436	0.8735	0.9162	0.8442	0.0592	0.8774	0.8967	0.8452	0.0608	0.8802	0.9055
MMCI	0.7398	0.0592	0.8556	0.8718	0.8123	0.0793	0.8586	0.8777	0.8122	0.0798	0.8558	0.8897
DF	0.7349	0.0892	0.7907	0.8600	0.7704	0.1405	0.7995	0.8384	0.7655	0.1396	0.7668	0.8425
Model of this paper	0.8628	0.0319	0.9116	0.9565	0.8589	0.0543	0.8856	0.8955	0.8623	0.0518	0.8896	0.9132

TABLE 2: Experimental comparison results of the effectiveness of the dual-stream lateral supervision module.

Algorithm	NLPR1000				NJU2000				STEREO			
	F	MAE	S	E	F	MAE	S	E	F	MAE	S	E
NDS	0.8356	0.0342	0.9081	0.9335	0.8501	0.0567	0.8847	0.8903	0.8525	0.0551	0.8877	0.9065
Model of this paper	0.8628	0.0319	0.9118	0.9465	0.8579	0.0542	0.8853	0.8955	0.8623	0.0518	0.8893	0.9132

TABLE 3: Experimental comparison results of multiscale module effectiveness.

Algorithm	NLPR1000				NJU2000				STEREO			
	F	MAE	S	E	F	MAE	S	E	F	MAE	S	E
BN	0.8487	0.0342	0.9058	0.9397	0.8505	0.0565	0.8812	0.8926	0.8571	0.0546	0.8849	0.9092
Model of this paper	0.8628	0.0317	0.9118	0.9465	0.8577	0.0542	0.8851	0.8955	0.8623	0.0518	0.8892	0.9132

4.6. Experimental Comparison of Multimodal Feature Fusion. The experimental comparison of multimodal feature fusion in Section 2.2 is shown in Table 3. BN indicates the results obtained by using only the normal convolution method without the improved multiscale convolution module. From the comparison results, it is found that multiscale convolution has an important role in significant computational results under the four evaluation criteria of F -measure, MAE, S -measure, and E -measure.

4.7. Experimental Comparison of Low-Dimensional Depth Features. In the experiments, it is found that depth features located in low dimensions are not good and affect the final results; as shown in Figures 5 and 6, depth 1 to depth 5 represent the significant maps corresponding to each stage of depth flow network, RGB1 to RGB5 represent the significant maps corresponding to each stage of RGB flow network, and Conv1 to Conv5 represent the significant maps generated by combining multimodal

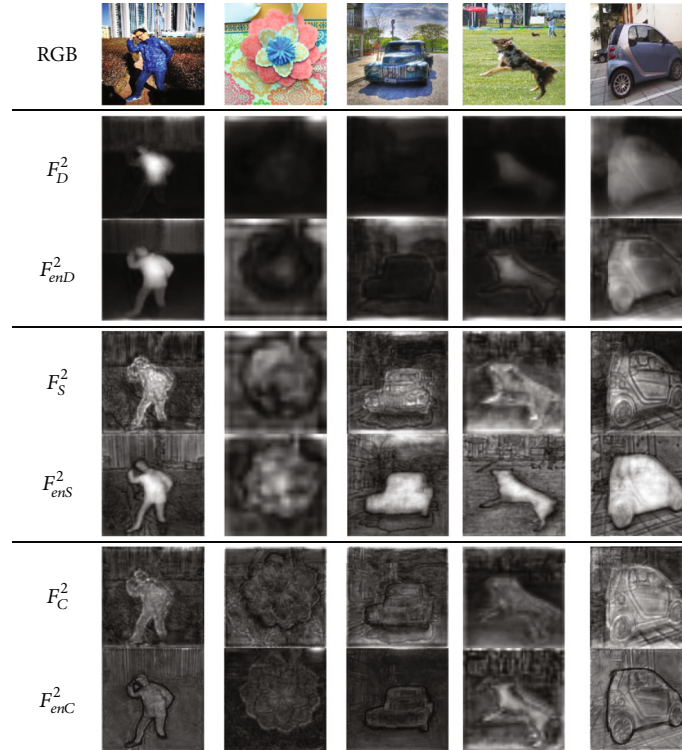


FIGURE 5: Visualization of the RGB-D fusion module.

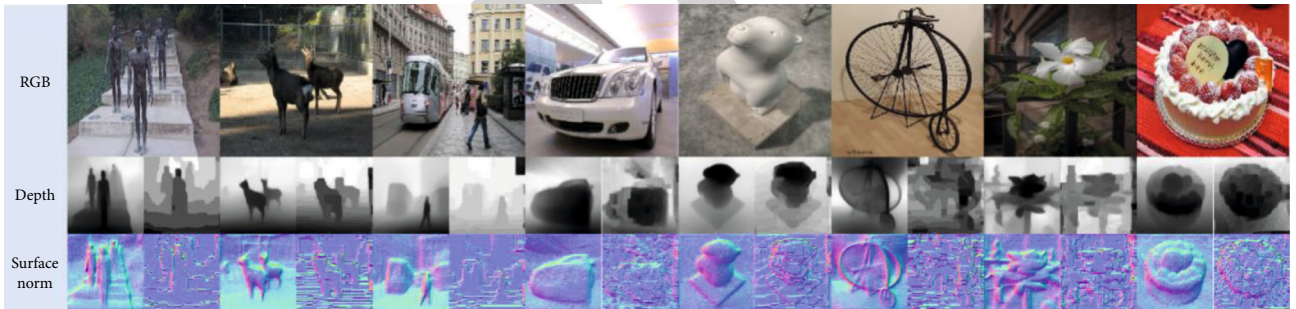


FIGURE 6: Visualization of the depth prediction.

TABLE 4: Experimental comparison results of low-dimensional depth features.

Algorithm	NLPR1000				NJU2000				STEREO			
	F	MAE	S	E	F	MAE	S	E	F	MAE	S	E
DY	0.8716	0.1088	0.8188	0.9477	0.8552	0.1312	0.8415	0.8786	0.8336	0.1278	0.8542	0.8985
Model of this paper	0.8628	0.0317	0.9118	0.9465	0.8577	0.0542	0.8851	0.8955	0.8621	0.0518	0.8895	0.9132

features. From Figure 5, it can be seen that due to the low-dimensional depth features of the depth flow network, the influence of depth 1 and depth 2 leads to noise in the low-level output, i.e., the final significant prediction results. Therefore, in order to eliminate the negative effect brought by low-dimensional depth features, this paper chooses not to include low-dimensional depth features in the low-level feature fusion, i.e., not to include depth 1 and depth 2. As shown in Figure 6, without the influence of low-dimensional depth features, this paper uses RGB1 as the

final result, and from the visualization comparison, it can be seen that the effect has been significantly improved and the noise of negative impact. Table 4 shows the specific data comparison.

5. Conclusion

In this paper, we propose a CNN-based RGB-D saliency detection network, which consists of two modules to assist the network in guiding the lower levels from global to

local and from deep to shallow, to obtain better saliency prediction results. The lateral supervision module facilitates the convergence speed of the network and generates better hierarchical representations to meet the requirements of each stage of features, while the multimodal feature fusion module obtains multiscale texture information of the high-level targets of the network and complements and fuses the robust high-level features with cross-modal information, proposing a different fusion method for the low-level features of the network than the high-level features. The proposed method can fuse the low-level features and high-level features extracted by the model. Information is not good leading to noise in the final prediction results, so the depth stream features of the lower two layers are removed from the final feature fusion. The experimental results on three widely used datasets show that the experimental results of this paper's method are generally better than the current mainstream algorithms and have stronger robustness. Future research can consider how to use depth information to make it more effective to assist RGB information to obtain better RGB-D saliency prediction results. The method in this paper can be applied to AI automatic bokeh of cameras in realistic scenes to speed up people's creative progress.

Data Availability

The experimental data used to support the findings of this study are available from the corresponding author upon request.

Conflicts of Interest

The author declared that there are no conflicts of interest regarding this work.

References

- [1] B. Charbuty and A. Abdulazeez, "Classification based on decision tree algorithm for machine learning," *Journal of Applied Science and Technology Trends*, vol. 2, no. 1, pp. 20–28, 2021.
- [2] M. Xin and Y. Wang, "Research on image classification model based on deep convolution neural network," *EURASIP Journal on Image and Video Processing*, vol. 2019, no. 1, p. 11, 2019.
- [3] X. Xie, X. Pan, W. Zhang, and J. An, "A context hierarchical integrated network for medical image segmentation," *Computers and Electrical Engineering*, vol. 101, article 108029, 2022.
- [4] E. Kremling and A. Subasi, "Performance of random forest and SVM in face recognition," *International Arab Journal of Information Technology*, vol. 13, no. 2, pp. 287–293, 2016.
- [5] J. Xia, N. Falco, J. A. Benediktsson, P. Du, and J. Chanussot, "Hyperspectral image classification with rotation random forest via KPCA," *IEEE Journal of Selected Topics in Applied Earth Observations and Remote Sensing*, vol. 10, no. 4, pp. 1601–1609, 2017.
- [6] D. R. Nayak, R. Dash, and B. Majhi, "Brain MR image classification using two-dimensional discrete wavelet transform and AdaBoost with random forests," *Neurocomputing*, vol. 177, pp. 188–197, 2016.
- [7] X. Xie, X. Pan, F. Shao, W. Zhang, and J. An, "MCI-Net: multiscale context integrated network for liver CT image segmentation," *Computers and Electrical Engineering*, vol. 101, article 108085, 2022.
- [8] Y. Zhang, G. Cao, X. Li, and B. Wang, "Cascaded random forest for hyperspectral image classification," *IEEE Journal of Selected Topics in Applied Earth Observations and Remote Sensing*, vol. 11, no. 4, pp. 1082–1094, 2018.
- [9] R. Chen, Z. Cai, and W. Cao, "MFFN: an underwater sensing scene image enhancement method based on multiscale feature fusion network," *IEEE Transactions on Geoscience and Remote Sensing*, vol. 60, pp. 1–12, 2021.
- [10] Y. Li and R. Chen, "SE-RWNN: a synergistic evolution and randomly wired neural network-based model for adaptive underwater image enhancement," *IET Image Processing*, vol. 14, no. 16, pp. 4349–4358, 2020.
- [11] M. Mathur and N. Goel, "Enhancement algorithm for high visibility of underwater images," *IET Image Processing*, vol. 16, no. 4, pp. 1067–1082, 2022.
- [12] S. Raveendran, M. D. Patil, and G. K. Birajdar, "Underwater image enhancement: a comprehensive review, recent trends, challenges and applications," *Artificial Intelligence Review*, vol. 54, no. 7, pp. 5413–5467, 2021.
- [13] X. Xie, W. Zhang, H. Wang et al., "Dynamic adaptive residual network for liver CT image segmentation," *Computers and Electrical Engineering*, vol. 91, article 107024, 2021.
- [14] T. Li, S. Rong, W. Zhao et al., "Underwater image enhancement using adaptive color restoration and dehazing," *Optics Express*, vol. 30, no. 4, pp. 6216–6235, 2022.
- [15] Y. Feng, J. Tang, B. Su, Q. Su, and Z. Zhou, "Point cloud registration algorithm based on the grey wolf optimizer," *Ieee Access*, vol. 8, pp. 143375–143382, 2020.
- [16] D. Wu, Y. Lei, M. He, C. Zhang, and L. Ji, "Deep reinforcement learning-based path control and optimization for unmanned ships," *Wireless Communications and Mobile Computing*, vol. 2022, Article ID 7135043, 8 pages, 2022.
- [17] F. Kulwa, C. Li, X. Zhao et al., "A state-of-the-art survey for microorganism image segmentation methods and future potential," *IEEE Access*, vol. 7, pp. 100243–100269, 2019.
- [18] N. Kleefeldt, K. Bermond, I. S. Tarau et al., "Quantitative fundus autofluorescence: advanced analysis tools," *Translational Vision Science & Technology*, vol. 9, no. 8, pp. 2–2, 2020.
- [19] L. Cheng, S. Chen, X. Liu et al., "Registration of laser scanning point clouds: a review," *Sensors*, vol. 18, no. 5, p. 1641, 2018.
- [20] S. Palanisamy, B. Thangaraju, O. I. Khalaf, Y. Alotaibi, S. Alghamdi, and F. Alassery, "A novel approach of design and analysis of a hexagonal fractal antenna array (HFAA) for next-generation wireless communication," *Energies*, vol. 14, no. 19, p. 6204, 2021.
- [21] Z. Dong, F. Liang, B. Yang et al., "Registration of large-scale terrestrial laser scanner point clouds: a review and benchmark," *ISPRS Journal of Photogrammetry and Remote Sensing*, vol. 163, pp. 327–342, 2020.
- [22] S. N. Alsubari, S. N. Deshmukh, A. A. Alqarni et al., "Data analytics for the identification of fake reviews using supervised learning," *CMC-Computers, Materials & Continua*, vol. 70, no. 2, pp. 3189–3204, 2022.

Retraction

Retracted: A Study of Language Use Impact in Radio Broadcasting: A Linguistic and Big Data Integration Approach

Journal of Sensors

Received 23 January 2024; Accepted 23 January 2024; Published 24 January 2024

Copyright © 2024 Journal of Sensors. This is an open access article distributed under the Creative Commons Attribution License, which permits unrestricted use, distribution, and reproduction in any medium, provided the original work is properly cited.

This article has been retracted by Hindawi following an investigation undertaken by the publisher [1]. This investigation has uncovered evidence of one or more of the following indicators of systematic manipulation of the publication process:

- (1) Discrepancies in scope
- (2) Discrepancies in the description of the research reported
- (3) Discrepancies between the availability of data and the research described
- (4) Inappropriate citations
- (5) Incoherent, meaningless and/or irrelevant content included in the article
- (6) Manipulated or compromised peer review

The presence of these indicators undermines our confidence in the integrity of the article's content and we cannot, therefore, vouch for its reliability. Please note that this notice is intended solely to alert readers that the content of this article is unreliable. We have not investigated whether authors were aware of or involved in the systematic manipulation of the publication process.

In addition, our investigation has also shown that one or more of the following human-subject reporting requirements has not been met in this article: ethical approval by an Institutional Review Board (IRB) committee or equivalent, patient/participant consent to participate, and/or agreement to publish patient/participant details (where relevant).

Wiley and Hindawi regrets that the usual quality checks did not identify these issues before publication and have since put additional measures in place to safeguard research integrity.

We wish to credit our own Research Integrity and Research Publishing teams and anonymous and named external researchers and research integrity experts for contributing to this investigation.

The corresponding author, as the representative of all authors, has been given the opportunity to register their agreement or disagreement to this retraction. We have kept a record of any response received.

References

- [1] Y. Praise Chukwunalu, A. U. N. Nwankwere, D. A. Orji, and M. Shah, "A Study of Language Use Impact in Radio Broadcasting: A Linguistic and Big Data Integration Approach," *Journal of Sensors*, vol. 2022, Article ID 1440935, 16 pages, 2022.

Research Article

A Study of Language Use Impact in Radio Broadcasting: A Linguistic and Big Data Integration Approach

Young Praise Chukwunalu ^{1,2}, Angela U. N. Nwankwere,¹ Dereck A. Orji,¹
and MohdAsif Shah ³

¹Department of Linguistics, Nnamdi Azikiwe University, Awka, Nigeria

²Department of Linguistic Data Sciences, University of Eastern Finland, Joensuu, Finland

³Kebri Dehar University, Ethiopia

Correspondence should be addressed to MohdAsif Shah; ohaasif@kdu.edu.et

Received 24 July 2022; Revised 19 August 2022; Accepted 5 September 2022; Published 24 September 2022

Academic Editor: Praveen Kumar Donta

Copyright © 2022 Young Praise Chukwunalu et al. This is an open access article distributed under the Creative Commons Attribution License, which permits unrestricted use, distribution, and reproduction in any medium, provided the original work is properly cited.

Broadcasting more culturally educating and language-reviving contents are ways radio stations can help revitalize indigenous languages in Delta North in Nigeria. The challenges faced in communicating through indigenous dialects on radio stations are majorly caused by the lack of indigenous language professionals and linguists in the broadcast stations. The absence of these professionals is a major constraint to the development of the community. The broadcast media can help manage multilingualism through the introduction of new words which would give little or no room for lexicon dearth but would expand the language lexicon. Using these dialects during broadcast gives relevance to all dialects, reduces language dearth, and keeps people connected to their culture. Programmes anchored in indigenous dialects enhance the vocabulary, comprehension, and language vitality of the language. The study examined the impact of local language used in radio broadcasting using a descriptive big data survey research design. The study's population comprises of all the inhabitants of Delta North from which a sample of 10 broadcast staff and 120 radio listeners in Delta North Senatorial District in Nigeria was drawn using a stratified random sampling technique. The instrument of data collection was a structured questionnaire with closed questions and a self-structured interview. The sample employed frequency distribution tables, percentages, and charts in the presentation and analysis of data. The results revealed that majority of the respondents in Delta North listened to radio broadcast indicating that the use of indigenous dialects/language can have massive impact on the people. The study also found that majority of the respondents use indigenous languages in their day-to-day activities, with English being used majorly only in schools. The study recommends, among others, that the National Broadcasting Commission review their policy on the allocated time of broadcast in indigenous languages and that more indigenous language experts and linguists should be incorporated into the broadcast system.

1. Introduction

Language is a form of communication which allows humans to share their thoughts, beliefs, ideas, experiences, etc. and is presumably known to the sender and receiver of such communication [1]. Language can determine and influence the thoughts of man and is needed for man's daily communication. It is used for domestic, religious, and commercial pur-

poses. Eka in [2] confirmed the usefulness of language, as it enables man to conceptualize, depict, and even portray the complexities and nature of his environment. The effectiveness of communication in a society is largely dependent on how well that society uses the language peculiar to their geographical area. Language serves as a major instrument of exchange through varied media such as electronic media, of which radio is one of the oldest electronic media of communication. The

need for community radio stations, especially in communicating their messages to the society via the use of indigenous languages, cannot be overemphasized.

Over the past decades, radio has played a significant role. It has helped maintain peace, unity, and harmony among people all over world. It has always been used during any matter of national security or emergency and has helped foster peace and unity among people. Radio as an electronic medium serves three major purposes—informing, educating, and entertaining. If some information is to be disseminated and the appropriate language is not used, the audience may not be able to comprehend such information. The language employed by a media-house goes a long way in determining the listenership strength and effectiveness of its services. Most of the electronic media operating in Nigeria are English-based. This is so because English language has grown all over the world as the predominant language at the expense of other languages. Using indigenous languages to interact with the masses through the media, especially the radio, enhances the effectiveness of mass communication. Studies have shown that indigenous language radio broadcasting is the most effective channel of mass communication because it reaches more peripheral areas than other media and is easily understood by the audience [3]. Many scholars argue that the global spread and acceptance of English as a world lingua franca poses a serious threat to the existence of most indigenous languages in Africa and the world in general [4, 5]. The authors in [6] argued that stronger indigenous languages like “Shona” and “Ndebele” also contribute to the killing of other smaller indigenous languages in Zimbabwe. They allege that due to their recognition as national languages, other languages are considered minor and remain on the fringes of the sociolinguistic milieu. The authors in [7] also argue that despite the multiplicity of dialects such as Mandarin dialect, the Cantonese dialect, the Kazakh dialect, and the Chinese Pidgin English in China and their use in the society, English language is still needed, used, and given a big platform. The same can be said for Nigeria, a multiethnic society, with English as the official language of the country and Hausa, Igbo, and Yoruba as the national languages. Despite the presence of national languages, English still enjoys high prestige to the detriment of the indigenous languages (both major and minor) as it remains the official language. Indigenous language in electronic media only carries about 5% of the whole period allotted to news, entertainment, and other programmes in the station.

Despite English being the official language of the country, the fact still remains that there are many out there who are yet to gain mastery of it. This is so because in a society, there exist the literate, semiliterate, and illiterate. People with different academic qualifications who have been privileged enough to be exposed to English language and culture would obviously be much better off than those who have not had such opportunity. In a multilingual society such as Delta North, Nigeria, we have the Enuani dialect, the Ika dialect, the Ukwuani dialect, and the Nigerian Pidgin English. Despite the widespread use of these dialects in the society in promoting their culture and tradition, a bigger platform

is still needed. The question is how well the radio media has contributed to the vitality of these dialects and how they can help improve the vocabulary of these dialects.

In light of the above, big data approach will be used to analyze the data obtained from the studies; this is because big data is data that contains large, hard-to-manage volumes of data, especially from new data sources, and since the research contains such data, a descriptive big data approach will be adopted for the studies. The big data approach is the process of extracting information from raw data through examination and analysis of patterns and behaviors with the use of quantitative and qualitative methods. Because large data cannot be evaluated with traditional tools, the advanced technique called the big data approach is used. They help enhance making of decisions, reduce risks, and discover important information from the data [8, 9]. The big data tool used in this study was Atlas.ti, particularly useful for real-time processing of large volumes of data [10]. This study as shown in Figure 1 examines that the communication breakdown of a society—Delta North Senatorial District—is bound to face when the language used for vital information dissemination by the broadcast media is not the language that is truly understood by all. It also examined the impact indigenous language used in radio broadcasting has on its listeners. The research contributions of this work include the following:

- (1) Determining whether the language used in broadcast stations has an impact on the local dialects in Delta North
- (2) Identifying the role of broadcast media in the management of multilingualism in Delta North
- (3) Examining the internal and external factors that influence the democratic distribution of languages in the radio stations in Delta North
- (4) Identifying the challenges faced in communicating through indigenous languages in the radio stations in Delta State
- (5) Determining how radio stations can revitalize the indigenous dialects through their broadcast in Delta North

The rest of this paper is organized as such: Section 2 gives an overview of related literature. Section 3 discusses the methodology of the research work. Section 4 discusses the results of the research. Finally, Section 5 concludes this paper.

2. Literature Review

The author in [11] affirmed radio as an important means of information dissemination and stated that its language should be the language popular to all. His theoretical framework was an eight-stage typology of language shifts and a set of priorities for reverse language shift programmes. According to his findings and suggestions, radio language is formal because most radio stations are operated by the government,

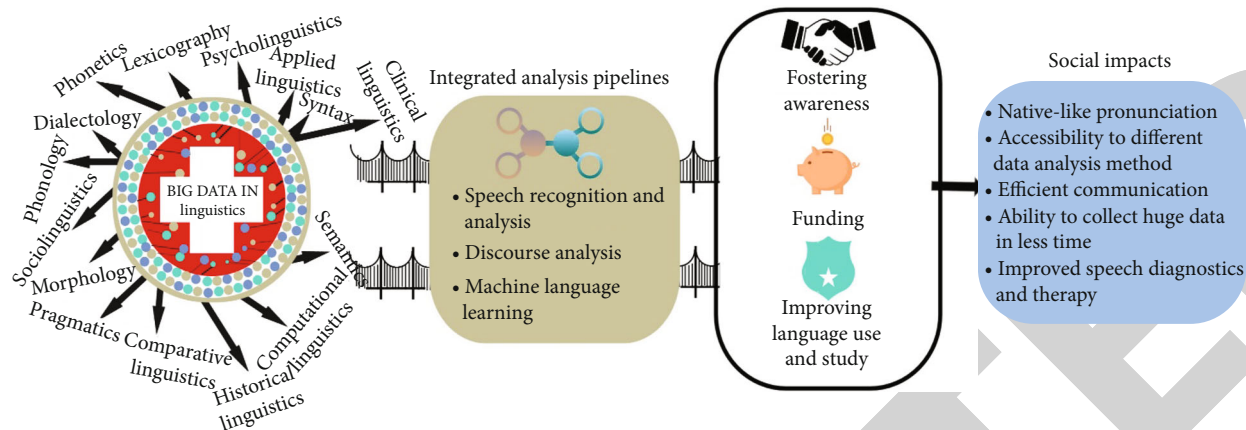


FIGURE 1: Application of big data in linguistics.

TABLE 1: Gender of the respondents.

Description	Frequency	Percent	Valid percent	Cumulative percent
Male	65	43.3	43.3	43.3
Female	85	56.7	56.7	100.0
Total	150	100.0	100.0	

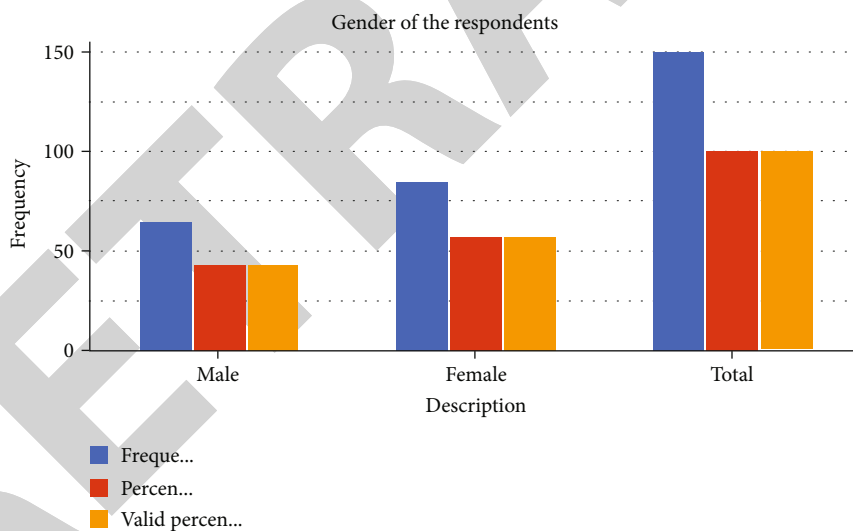


FIGURE 2: Gender of the respondents.

TABLE 2: Age distribution of the respondents.

Description	Frequency	Percent	Valid percent	Cumulative percent
18–30 years	41	27.3	27.3	27.3
31-40 years	66	44	44	71.3
41–50 years	28	18.7	18.7	90
51 years and above	15	10	10	100.0
Total	150	100.0	100.0	

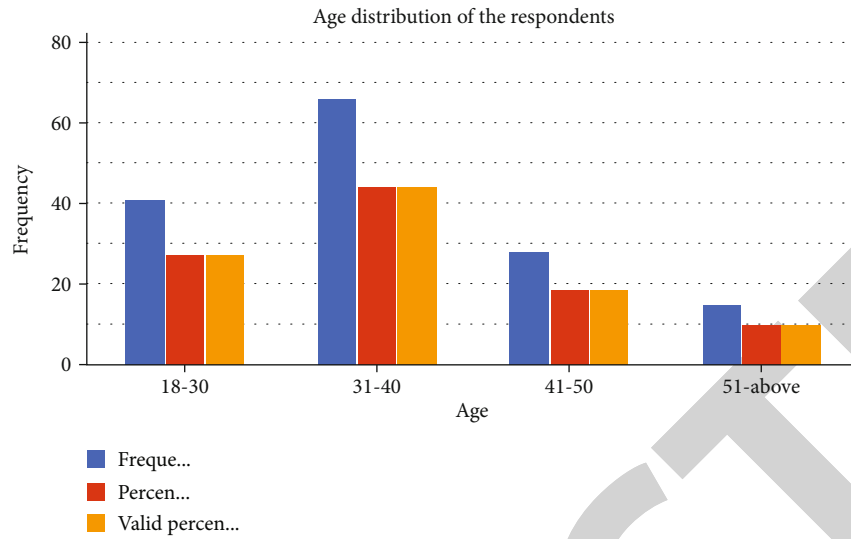


FIGURE 3: Age distribution of the respondents.

TABLE 3: Marital status of the respondents.

Description	Frequency	Percent	Valid percent	Cumulative percent
Single	69	46	46	46
Married	61	40.7	40.7	86.7
Divorced	11	7.3	7.3	94
Widowed	9	6	6	100.0
Total	150	100.0	100.0	

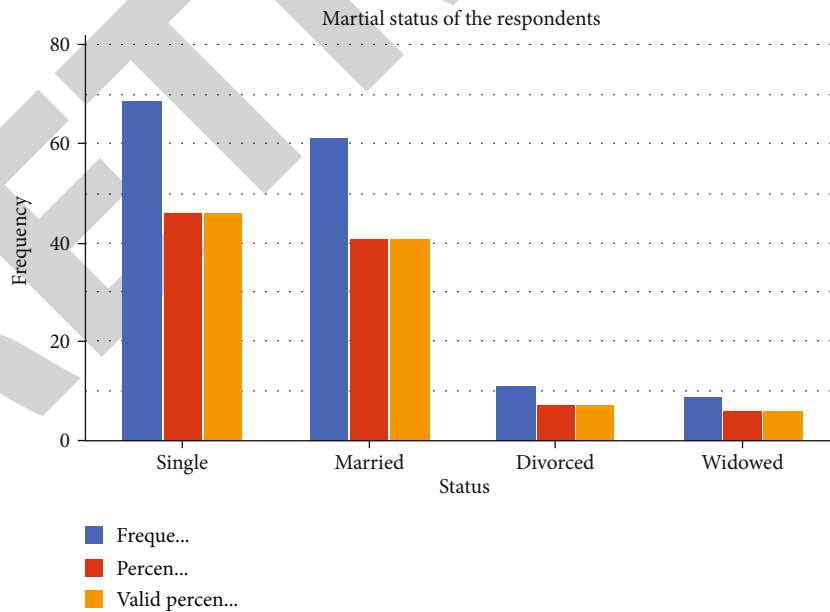


FIGURE 4: Marital status of the respondents.

but at the same time, it is also informal because it is spoken. He suggested here that it is not easy to determine whether radio language is formal or informal due to its two contrasting features: serious topics (governmental affairs) which are

formal and talk shows and programmes, which are informal. He tried to convey the idea of language shift; i.e., if the content on the radio becomes more governmental, then the indigenous language which is used in informal talk would

TABLE 4: Educational qualification of the respondents.

Description	Frequency	Percent	Valid percent	Cumulative percent
OND/NCE	48	32	32	32
HND/B.Sc/BA	62	41.3	41.3	73.3
PGD/M.Sc	40	26.7	26.7	100.0
Total	150	100.0	100.0	

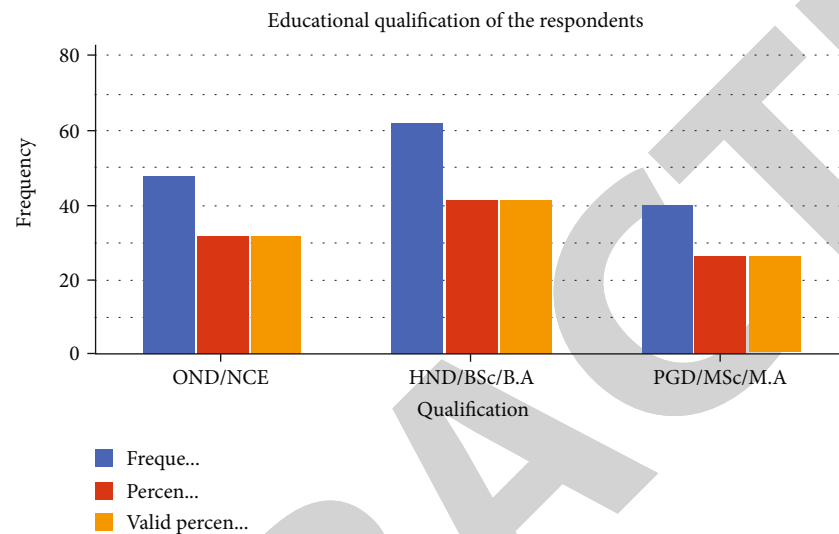


FIGURE 5: Educational qualification of respondents.

TABLE 5: Years of work experience of the respondents.

Description	Frequency	Percent	Valid percent	Cumulative percent
0-4 years	71	47.3	47.3	47.3
5-9 years	37	24.7	24.7	72
10-14 years	11	7.3	7.3	79.3
15-19 years	19	12.7	12.7	92
20 years and above	12	8	8	100.0
Total	150	100.0	100.0	

be replaced by English which is used for formal topics. The authors in [12] also examined the radio language. Using phenomenology as a theory, they researched on most radio stations in the United States and came up with the findings that language in radio is a mixture of spoken and written forms and that the social variables that determine the speech styles in radio situations are not the same as those in other situations. Going by this statement, it appears they are trying to say that language in radio is not fixed. In [13], the authors carried out a research on Yoruba language covering areas like technology, politics, football, economy, education, sports, and law. Orisun FM (89.5) located in Osun State was used as a case study. The paper zeroed in on the electronic media for its source of data and did not employ the use of any specified theoretical framework. At the end of the research, the researchers noted that the electronic media and its personnel have contributed in the development of

Yorùbá language and in the dissemination of information to the public. They concluded by opining that academia should endeavor to work hand-in-hand with the media in the formation of new words for the concepts being introduced to the society.

The authors in [14] researched and used Sinhala FM in Sri Lanka as their case study. The researchers used respondents which were drawn from among university undergraduates, language teachers, radio and television staff, and people randomly selected from the society (FM radio listeners). The results of the data proved that people are increasingly turning to radio, increasing radio listenership. The findings from the research further show that there is an increased level of competition between FM (frequency modulation) channels, now that increasingly listeners opt for radio. In [15], the authors proposed the agenda-setting theory in a study on the American presidential election in

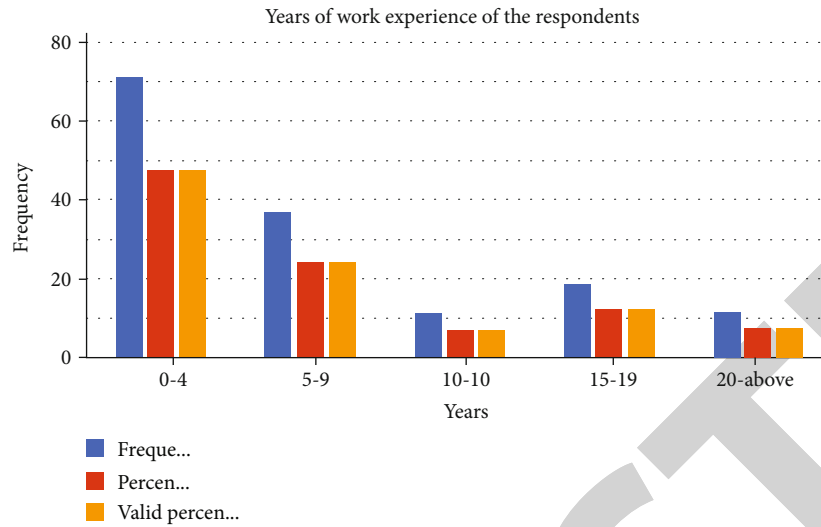


FIGURE 6: Years of work experience of the respondents.

TABLE 6: Nativity of the respondents.

Description	Frequency	Percent	Valid percent	Cumulative percent
Enuani	62	41.3	43.3	41.3
Ika	41	27.3	30.8	68.6
Ukwuani	47	31.3	25.8	100.0
Total	150	100.0	100.0	

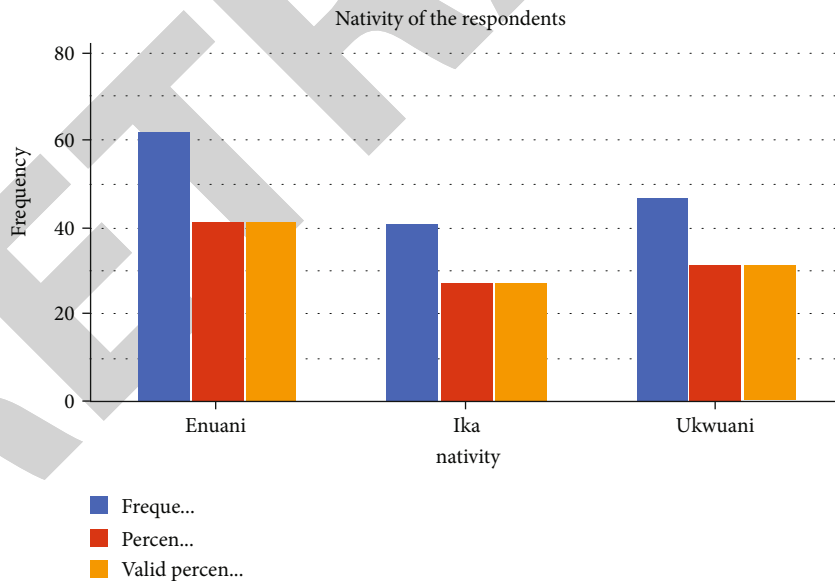


FIGURE 7: Nativity of the respondents.

1968, which states that the media are not always successful in telling us what to think, but they are quite successful in telling us what to think about. This means the media has a great influence on their audience. The authors in [16] believed that the notion of this theory can be traced to [17]. The authors were of the view that the media were responsible for the pictures in our head. According to the

authors in [18], the theory of agenda-setting by the media proposes that the public agenda or the things people discuss, think, and worry about is powerfully shaped and directed by what the media choose to publicize. In [19], the authors stated that the use of indigenous languages in the media can give rise to the revitalization of those indigenous languages that are endangered. This notion is reasonable as it

TABLE 7: How long the respondents have been in Delta North.

Description	Frequency	Percent	Valid percent	Cumulative percent
11 months and below	24	16	16	16
1-3 years	27	18	18	34
4-7 years	46	30.7	30.7	64.7
8 years and above	53	35.3	35.3	100.0
Total	150	100.0	100.0	

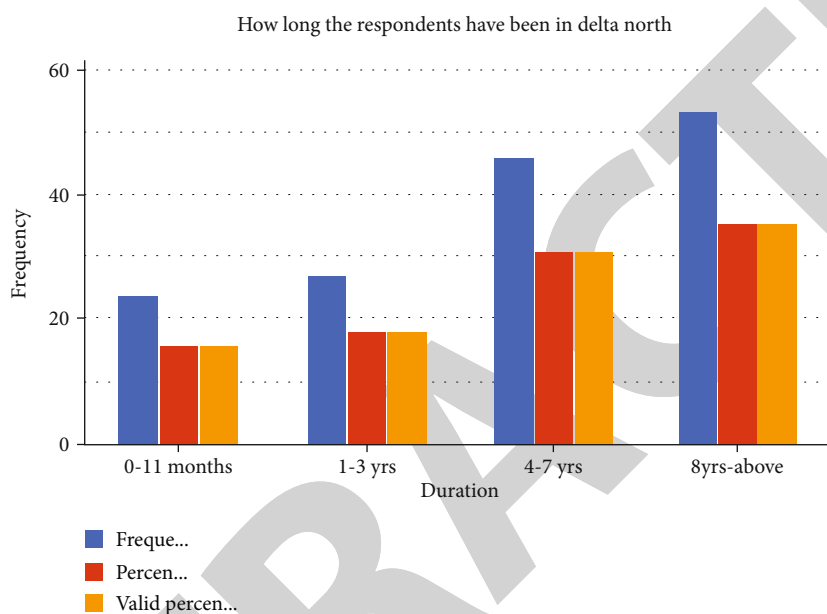


FIGURE 8: How long the respondents have been in Delta North.

TABLE 8: Frequency and percentage of statement of listenership strength of radio stations (audience response).

Do you listen to radio broadcasts?	Frequency	Percentage	Valid percentage	Cumulative percent
Yes	86	71.7%	71.7%	71.7%
No	34	28.3%	28.3%	100.0%
Total	120	100.0%	100.0%	

gives a voice to the neglected languages of the society by setting an agenda that would pave the way for the standardization and documentation of these languages.

The theory is relevant to the study because the media can be used to set the agenda for the use of indigenous languages in radio broadcasting. The use and gratification theory was propounded in [20]. The theory advocates that people use certain media based on the gratification derived from it. Specifically, the use and gratification theory directly places power in the hands of the users. The authors in [21] further described this theory as gratifications or benefits that attract and hold audiences to diverse types of media and the types of content that satisfy their social and psychological demands. The theory stresses how and why the audience uses the media. It also expatiates on the theory in [22]. The main point of the theory is the notion that there are dis-

tinct benefits consumers of social media messages need, get, or anticipate getting from the media; otherwise, they may desert the channel and look for alternative ones to satisfy their needs. However, the gratification theory holds that people are responsible for choosing a particular media to meet their needs in terms of the language they understand [20].

Large amounts of data have become accessible for decision-making in this digital era. Big data are datasets that have high velocity and variety, making them challenge to deal with making use of traditional techniques and methods. Big data has a wide range of applications including customer interactions, social network data, and daily transactions. In [21], the authors examined the various analytics tools and methods that can be applied to big data and how they are used in different decision domains. In [22], the authors

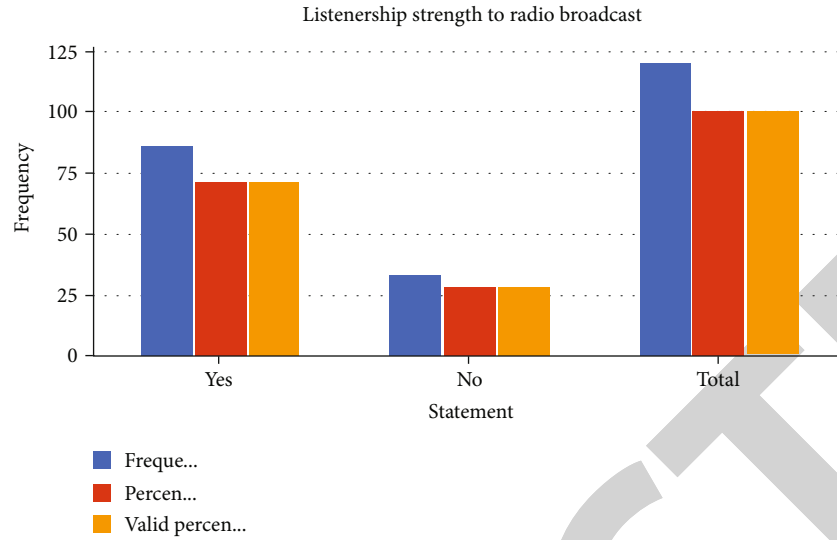


FIGURE 9: The listenership strength of radio broadcast.

TABLE 9: Frequency and percentage of statement of listenership strength of radio stations (audience response).

Do you listen to these radio stations?	Yes	No	Total
Voice of Delta (97.9)	80 (66.7%)	40 (33.3%)	120 (100.0%)
Trend FM (100.9)	70 (58.3%)	50 (41.7%)	120 (100.0%)
Crown FM (94.7)	65 (54.1%)	55 (45.9%)	120 (100.0%)

sought to develop a highly efficient platform to effectively examine big data and a suitable mining algorithm to pick out useful information from the data. In [23], the authors provided a comprehensive study of the concepts, applications, tools, techniques, and research challenges of big data. The use and gratification theory is also pertinent to this study as it will help explain the extent of impact the radio stations in Delta North can have on the listening audience through its use of indigenous languages. The proponents of the grounded theory method (GTM) [24] explained it as the “discovery of theory from data systematically obtained from social research,” and allow the researcher to explore and unfold the core issues of interest first from the perspective of the key participants involved. We believe the theoretical framework adopted for this study will help gather the required data and information necessary for a proper research.

3. Methodology

This section analyzes data collected from the sample population (30 broadcast staff and 120 radio listeners in Delta North Senatorial District) and makes an appropriate interpretation of the analysis using a big data approach with a view of ensuring that the objectives of this research work are achieved. The study adopted a descriptive big data survey

research design in analyzing the quantitative and qualitative data from the two questionnaire surveys and the interview conducted [7]. A total of 150 questionnaires were administered. To get a clearer picture of the classes of responses, the quantitative data were modeled on a four-point rating scale [25] with a response mode of strongly agree (SA) = 4, agree (A) = 3, disagree (D) = 2, and strongly disagree = 1. The interview responses were arranged to form themes around the research questions, and all results were discussed in line with the impact of language use in radio broadcasting in Delta North. All questionnaires and interviews served as a basis for the presentation for the analysis and interpretation of data.

3.1. Sociodemographic Data. Table 1 and Figure 2 reveal that 43.3% of the respondents are male, while 56.7% are female.

The results in Table 2 and Figure 3 show that 27.3% of the respondents interviewed are between the ages of 18 and 30 and 44% are between 31 and 40 years of age. 18.7% are in the age bracket of 41-50 years, while the remaining 10% are 51 years and above. Those that are within the ages of 31-40 years have the highest frequency of 66, which implies that majority of the employees in the radio broadcasting stations in Delta State North are within the productive years of their life.

Table 3 and Figure 4 show that 46% of the respondents are single, 40.7% are married, 7.3% are divorced, and 6% are widowed. This result shows that the majority of the respondents are single.

The information in Table 4 and Figure 5 shows that 32% have OND/NCE, 41.3% are HND/B.Sc/BA degree holders, and 26.7% are PGD/M.Sc degree holders. This result shows that the majority of the respondents are HND/B.Sc/BA degree holders.

Table 5 and Figure 6 show that 47.3% of the respondents have been working for 0-4 years, 24.7% of them have been working for 5-9 years, 7.3% have been working for 10-14

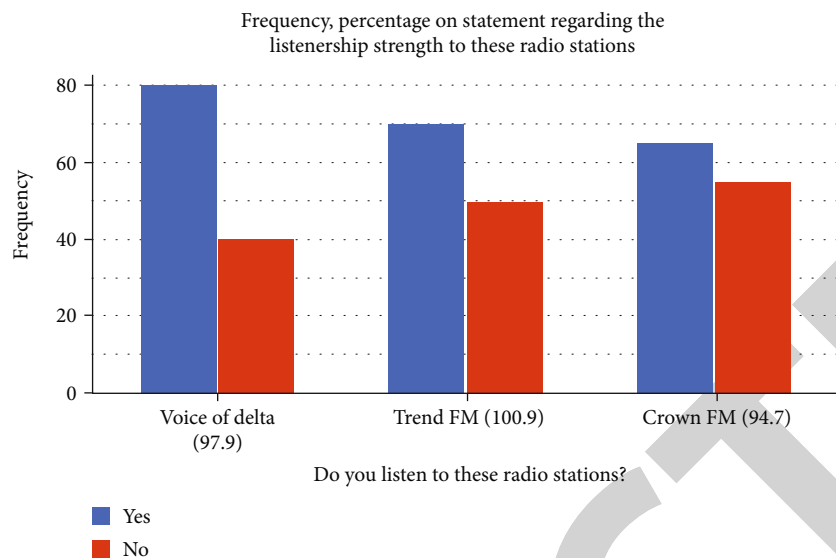


FIGURE 10: The listenership strength of these radio stations.

years, 12.7% have been working for 15-19 years, and 8% have been working for 20 years and above.

Table 6 and Figure 7 show that 41.3% of the respondents are Enuani natives, 27.3% are Ika natives, and 25.8% are Ukwuani natives. This result shows that the majority of the respondents are natives of Enuani speaking communities.

The result from Table 7 and Figure 8 shows that 16% of the respondents have been in Delta North for 11 months and below, 18% have been in Delta North for 1-3 years, 30.7% have been in Delta North for 4-7 years, and 35.3% have been in Delta North for 8 years and above.

3.2. Data Presentation and Analysis. This section analyzes the data obtained from the respondents according to the research questions for this study.

- (1) Research Q1. Do the indigenous dialects have any impact on the listening audience of radio stations in Delta North?

The results in Table 8 and Figure 9 show that 71.7% of the respondents listen to radio broadcast, while 28.3% do not.

Table 9 and Figure 10 show that 66.7% of the respondents listen to Voice of Delta (97.9), 58.3% listen to Trend FM (100.9), and 54.1% listen to Crown FM (94.7). The result revealed that majority of the respondents in Delta North listen to radio broadcast.

Table 10 and Figure 11 show that 33.3% of staff respondents which comprises of one broadcast station (Voice of Delta) broadcasts in English, Pidgin, Enuani, Ukwuani, and Ika dialects. The result also showed that the remaining 20 staff respondents which comprises of Trend FM and Crown FM broadcasts only in English and Pidgin.

The results from Table 11 and Figure 12 show that at home, majority of the respondents (44.7%) use Enuani,

10% use English, 5.3% use Pidgin, 14% use Ika, and 26% use Ukwuani. At work, 48% use English, 12% use Pidgin, 16% use Enuani, 10.7% use Ika, and 13.3% use Ukwuani. In school, 46.7% use Pidgin, 46% use English, 5.3% use Enuani, 2% use Ika, and none use Ukwuani. When interacting with friends, 14.7% use English, 32% use Pidgin, 22% use Enuani, 18% use Ika, and 13.3% use Ukwuani. In their place of worship, 40.7% use English, 27.3% use Enuani, 12.7% use Ika, 19.3% use Ukwuani, and none use Pidgin.

- (2) Research Q2. What are the roles of the broadcast media in the management of multilingualism in the radio stations in Delta North?

Table 12 and Figure 13 reveal that majority of the respondents (33.3%) and 37.5% are undecided and disagree that radio stations in Delta North help expand the language lexicon. 17.5% strongly agree, and 11.7% agree. It was affirmed by the supportive claim of 19.2% and 38.3% of the respondents who strongly agreed and agreed, respectively, that the use of indigenous dialect during radio broadcast gives relevance to all the dialects in Delta North. Although 21.7% were undecided, 15.8% and 5.0% disagreed and strongly disagreed with the statement, respectively. 64.2% strongly agreed and agreed that the use of indigenous dialect in radio broadcasts has helped improve their speaking and understanding of the dialect, 23.3% of them were undecided, and 12.3% disagreed with the statement.

68.3% of the respondents strongly agreed and agreed, respectively, that programmes anchored using indigenous dialects keeps people connected to culture and tradition, while 22.5% were undecided, and 9.2% disagreed with the statement. 66.7% agreed that programmes broadcasted in local dialects will help in the reduction in language dearth and increase in language vitality, 20.0% were undecided, and 13.3% disagreed with the statement. 64.2% of the

TABLE 10: Frequency and percentage on statement regarding the language of broadcast in your radio station (staff response).

Radio station	English	Pidgin	Enuani	Ukwuani	Ika
Voice of Delta (97.9)	10 (33.3%)	10 (33.3%)	10 (33.3%)	10 (33.3%)	10 (33.3%)
Trend FM (100.9)	10 (33.3%)	10 (33.3%)	—	—	—
Crown FM (94.7)	10 (33.3%)	10 (33.3%)	—	—	—
Total	30 (100%)	30 (100%)	10 (33.3%)	10 (33.3%)	10 (33.3%)

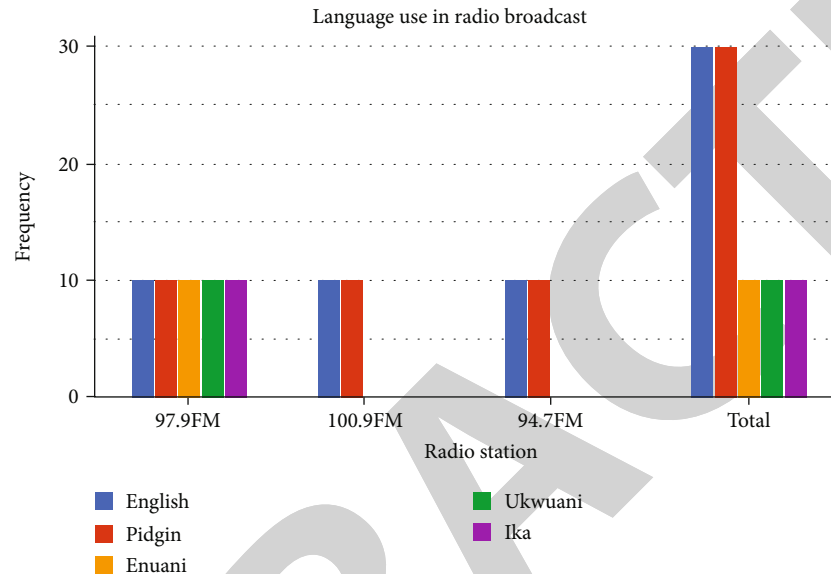


FIGURE 11: Language of broadcast in the radio stations.

TABLE 11: Frequency and percentage of language use in Delta North (staff/audience response).

Please tick the language you use in the following places	English	Nigerian Pidgin	Enuani	Ika	Ukwuani
At home	15 (10%)	08 (5.3%)	67 (44.7%)	21 (14%)	39 (26%)
At work	72 (48%)	18 (12%)	24 (16%)	16 (10.7%)	20 (13.3%)
In school	69 (46%)	70 (46.7%)	08 (5.3%)	03 (2%)	- (0%)
With friends	22 (14.7%)	48 (32%)	33 (22%)	27 (18%)	20 (13.3%)
In the place of worship	61 (40.7%)	- (0%)	41 (27.3%)	19 (12.7%)	29 (19.3%)

respondents agreed that use of indigenous dialect in radio broadcasts reduces the vocabulary dearth of the dialect, 16.7% were undecided, and 19.2% disagreed with the statement.

- (3) Research Q3. What are the factors that influence the democratic distribution of languages in the radio stations in Delta North?

Table 13 and Figure 14 show that the majority of the respondents (50%) agree with the claim that the NBC rules is an influencing factor to the distribution of language in radio broadcasting. This is followed by 23.3% who are undecided about the claim and 26.7% who disagree with the claim. It was affirmed by the supportive claim of 26.7% and 43.3% of the respondents who agreed and strongly

agreed, respectively, that the listenership strength of the audience is a factor that influences the democratic distribution of language. 6.7% were undecided about this claim, 20% disagreed, and 3.3% strongly disagreed with this claim. 16.7% and 40% of the respondents strongly agree and agree, respectively, that national language policy is an influencing factor of the democratic distribution of language in broadcast station in Delta North, while 43.3% disagreed with the statement. 23.3% and 36.7% strongly agreed and agreed, respectively, that sponsorship level is a factor that influences the democratic distribution of language in radio broadcast, while 26.7% and 13.3% disagreed and strongly disagreed to the claim.

10% and 50% strongly agreed and agreed that the location of the radio station is a big influence to the distribution of languages during broadcast in Delta North. According to

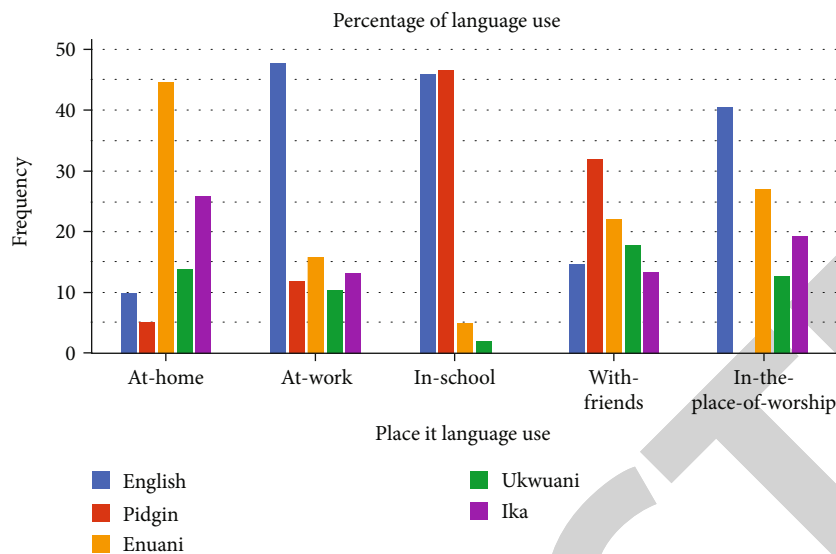


FIGURE 12: Percentages of languages in use.

TABLE 12: Frequency and percentage on statement regarding the roles of radio broadcast media in the management of multilingualism in Delta North (audience response).

S/N	Statements		Response					Total
			SA	A	U	D	SD	
1	Radio stations in Delta North has helped expand the language lexicon.	F	21	14	40	45	—	120
		%	17.5	11.7	33.3	37.5	—	100.0
2	The use of indigenous dialect during radio broadcast helps gives relevance to all the dialects in Delta North.	F	23	46	26	19	6	120
		%	19.2	38.3	21.7	15.8	5.0	100.0
3.	The use of indigenous dialect in radio broadcasts helps improve speaking and understanding of the dialect.	F	23	54	28	15	—	120
		%	19.2	45.0	23.3	12.3	—	100.0
4.	Programmes anchored using indigenous dialects keeps people connected to culture and tradition.	F	24	58	27	11	—	120
		%	20.0	48.3	22.5	9.2	—	100.0
5.	When programmes are broadcasted in the indigenous dialects, there will be reduction in language death and increase in language vitality.	F	26	54	24	16	—	120
		%	21.7	45.0	20.0	13.3	—	100.0
6.	The use of indigenous dialect in radio broadcasts reduces the vocabulary death of the dialect.	F	24	53	20	15	8	120
		%	20.0	44.2	16.7	12.5	6.7	100.0

an interview about this factor, these respondents said that the location of a radio station determines the language use. Citing an example, one of the respondents mentioned that a radio station situated in a multilingual environment like Delta North will end up broadcasting in the generally understandable language which in this case is Pidgin. 10% of the respondents were undecided, and 23.3% and 6.7% disagreed and strongly disagreed with the statement.

- (4) Research Q4. What are the challenges faced in communicating through the indigenous dialects in the radio stations in Delta North?

Table 14 and Figure 15 reveal that 63.3% of the respondents agreed that poor provision for indigenous language professionals in radio stations is also a challenge faced by broadcast stations in communicating through indigenous

dialects. 30% were undecided and 6.7% disagreed with the statement. 70% agreed that lack of linguists in radio broadcast stations is a challenge faced by broadcast stations. 10% were undecided, and 20% disagreed with the statement.

- (5) Research Q5. In what ways can radio stations revitalize the indigenous dialects in Delta North?

Table 15 and Figure 16 reveal that 69.2% of the respondents agreed that broadcasting more in indigenous dialects will help revitalize the indigenous dialects in Delta North. 7.5% were undecided, and 23.3% disagreed with the statement. 69.2% agreed that broadcasting more culturally educating and language-reviving contents by radio stations will help revitalize the indigenous dialects in Delta North. 11.7% were undecided, and 19.2% disagreed with the statement.

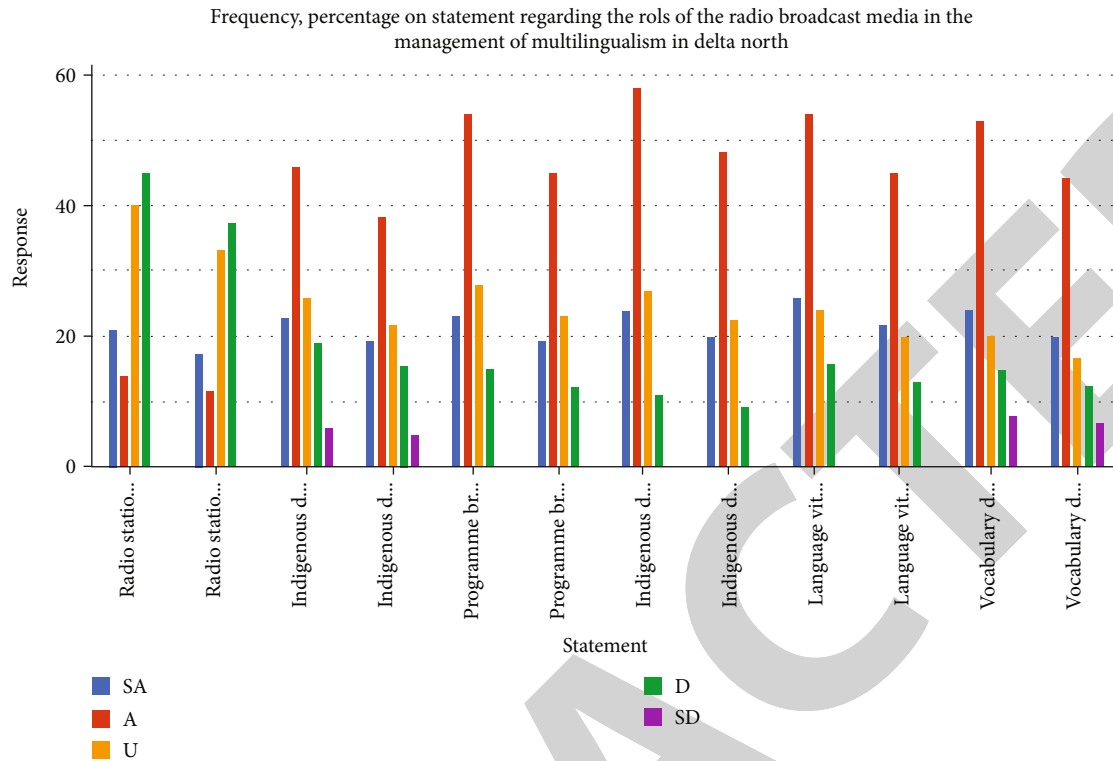


FIGURE 13: Roles of radio broadcast media in the management of multilingualism in Delta North (audience response).

TABLE 13: Factors that influence the democratic distribution of languages in the radio stations in Delta North (staff response).

S/N	Statement		Response					Total
			SA	A	U	D	SD	
1	Nigeria broadcasting commission rules	F	9	6	7	8	—	30
		%	30	20	23.3	26.7	—	100.0
2	Listenership strength	F	8	13	2	6	1	30
		%	26.7	43.3	6.7	20	3.3	100.0
3	National language policies	F	5	12	—	13	—	30
		%	16.7	40	—	43.3	—	100
4	Sponsorship level	F	7	11	—	8	4	30
		%	23.3	36.7	—	26.7	13.3	100
5	Location of radio station	F	3	15	3	7	2	30
		%	10	50	10	23.3	6.7	100

4. Results

The study was carried out to assess the impact of language use in radio broadcasting on local languages in Delta North senatorial zone. Based on the results of the data analysis, the following findings emerged:

- (1) Research Q1. Do the indigenous dialects have any impact on the listening audience in radio stations in Delta North?

The results from Research Q1 indicated that indigenous dialects have significant impact on the listening audience in radio stations in Delta North given that majority of the respondents agreed to the claim of using indigenous dialects in their day-to-day activities with English being used majorly in school. The result also revealed that the majority of the respondents listen to radio broadcast, and this indicates that the radio media could have a big impact on the audience through radio broadcast especially when using indigenous

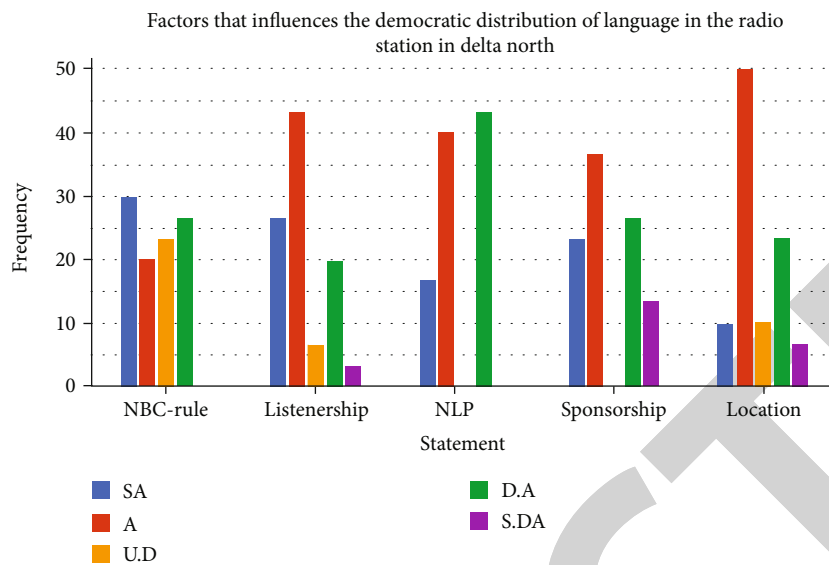


FIGURE 14: Factors that influence the democratic distribution of languages in the radio stations in Delta North.

TABLE 14: Challenges in communicating through the indigenous dialects in the radio stations in Delta North (staff response).

S/N	Statement		Response					Total
			SA	A	U	D	SD	
1	Poor provision for indigenous language professionals in the radio stations.	F	16	3	9	2	—	30
		%	53.3	10	30	6.7	—	100.0
2	Lack of linguists in radio broadcast stations.	F	8	13	3	6	—	30
		%	26.7	43.3	10	20	—	100.0

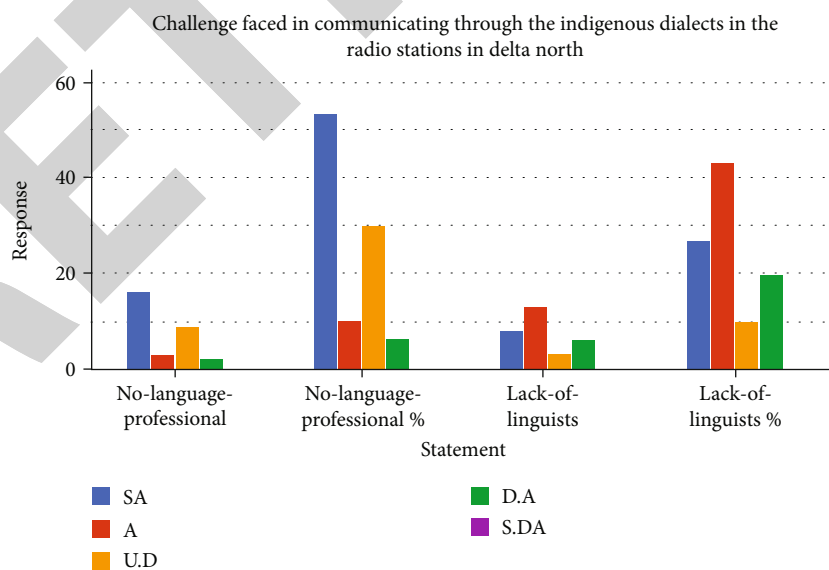


FIGURE 15: Challenges in communicating through the indigenous dialects in the radio stations in Delta North.

TABLE 15: Frequency and percentage on statement regarding the ways radio stations can revitalize the indigenous dialects in Delta North (audience response).

S/N	Questions	Response						Total
		SA	A	U	D	SD		
1	Broadcasting more in indigenous dialects	F	30	53	9	18	10	120
		%	25.0	44.2	7.5	15.0	8.3	100.0
2	Broadcasting more culturally educating and language reviving contents	F	42	41	14	11	12	120
		%	35.0	34.2	11.5	9.2	10.0	100.0

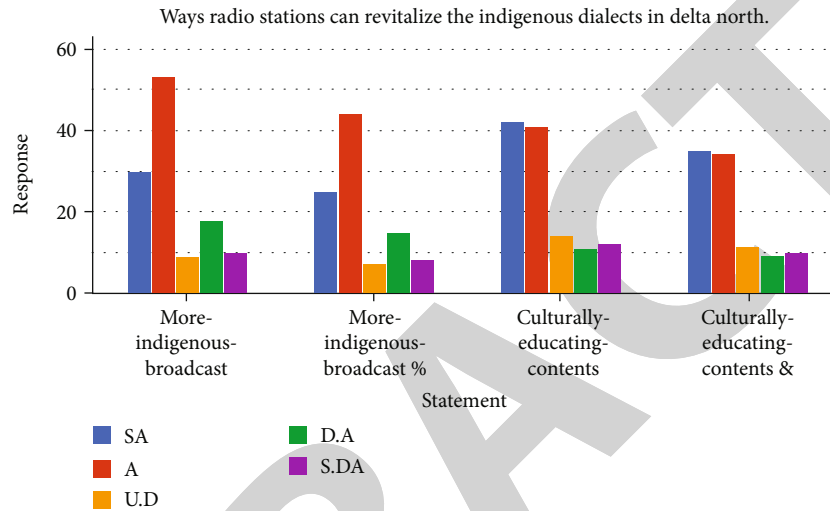


FIGURE 16: Frequency and percentage on statement regarding the ways radio stations can revitalize the indigenous dialects in Delta North.

dialects. This affirms the claim of [3, 26] that indigenous language radio broadcasting is the most effective channel of mass communication since it reaches more peripheral areas than other media and is easily understood by the audience.

- (2) Research Q2. What are the roles of the broadcast media in the management of multilingualism in the radio stations in Delta North?

The results from Research Q2 indicate that the roles of the broadcast media in the management of multilingualism are the expansion of language lexicon through introduction of new words and giving relevance to all the dialects through the use of these dialects during broadcast, which in turn helps in reduction of language dearth and keeps people connected to their culture. In the case of indigenous languages in Delta North, this is not so as English is the major language used in broadcast. This result agreed with the findings in [27] which rightly observed that using foreign languages in the media as the media language is indirectly setting an agenda on those languages at the expense of our indigenous languages.

- (3) Research Q3. What are the internal and external factors that influence the democratic distribution of languages in the radio stations in Delta North?

The results from Research Q3 explained that internal and external factors that influence the democratic distribution of languages in the radio stations in Delta North are National Broadcasting Commission rules, listenership strength, national language policies, sponsorship level, and location of the radio station. The analysis reveals that the majority of the respondents believe that the location of the radio station is a much bigger influence to the distribution of languages during broadcast in Delta North. This result agreed with the findings of [28] which states that the broadcast media in rural areas can hardly broadcast in indigenous dialects because there is lack of attention and allocation given to it. This is followed by the listenership strength with 40% and national language policy having the lowest agreement and highest disagreement of 34%. Proper planning and implementation of these policies (to suit both the urban and rural radio media stations) play vital roles in language use in broadcasting.

- (4) Research Q4. What are the challenges faced in communicating through the indigenous dialects in the radio stations in Delta North?

The results from Research Q4 revealed that lack of indigenous language professionals and linguists in the broadcast stations are the major challenges faced in communicating

through the indigenous dialects in the radio stations in Delta North. This response was supported by 70% and 63.3% of the respondents. The result agreed with [29] who argued that despite the fact that LPP is an academic discipline grounded in linguistics, it is controlled more by politicians, those with less experience of the discipline rather than the actual experts. It also corroborates the author's findings that the NBC's rule that allocates just twenty-five minutes to programmes or news in local languages is only relegating these languages to the background, making them almost ineffective in broadcast stations.

- (5) Research Q5. In what ways can radio stations revitalize the indigenous languages in Delta North?

The findings from Research Q5 revealed that the major ways radio stations can revitalize the indigenous dialects in Delta North are through broadcasting more culturally educating and language-reviving contents, as this aids promotion of culture and languages, and the use of indigenous languages in radio broadcasting which reduces marginalization of these languages. This affirms the argument in [6] that says the greater use of a language, the stronger the language becomes.

5. Conclusion

Radio is considered an effective tool in the dissemination of information quickly. Radio broadcast in Nigeria has been in existence from the colonial era and is still very important in disseminating information. This study examined the impact of language use in radio broadcasting in Delta North. It was aimed at discovering the extent to which the use of indigenous dialects in radio stations in Delta North can impact its listeners and help promote the dialect and culture of the study area. The indigenous language programmes play an important role in the life of the people living in a community as many depend on this radio for their various broadcast needs. The population of the study area makes it imperative for the use of indigenous language during radio broadcast to engender the desired development for the Delta North populace.

To verify the assumption that radio station has made no major impact in Delta North through its use of indigenous dialects, five research questions were raised in the study. This study adopted a big data survey method and made use of a self-constructed questionnaire for the collection of data. The questionnaire enabled the researcher to obtain first-hand information on the subject matter from respondents in some notable communities in the area of study. 150 respondents were randomly selected for the survey. The sample size was determined using stratified random sampling technique. Data was collected using the constructed questionnaire and was quantitatively analyzed using the Atlas.ti tool. The impact of language used in radio broadcasting in Enuani, Ika, and Ukwuani was studied using these selected stations (Voice of Delta 97.9, Trend FM 100.9, and Crown FM 94.7). The study concludes that the broadcasters in Delta North radio stations need to take the issue of indig-

enous language programmes more seriously, or the native languages will continue to suffer in the domineering hands of English language promoters. In the future, we shall apply other big data tools to these raw big, using a wider population and culture, and compare their different results.

Data Availability

The data used to support the findings of this study are available from the corresponding author upon request.

Conflicts of Interest

The authors declare that they have no conflicts of interests.

References

- [1] W. Odegbenle, "Enlightenment and attitudes of the Nigerian elite on the roles of languages in Nigeria," *Language Culture and Curriculum*, vol. 16, no. 2, pp. 185–196, 2013.
- [2] D. Eka, *Issues in Nigerian English Usage*, Scholars Press, Uyo, Nigeria, 2000.
- [3] S. Mufwene, "Colonization, globalization and the plight of 'weak' languages," *Journal of Linguistics*, vol. 38, pp. 375–395, 2002.
- [4] M. Ndhlovu, "Mainstreaming African indigenous knowledge systems in higher and tertiary education: the case of Zimbabwe," *South African journal of higher education*, vol. 18, no. 3, pp. 281–288, 2004.
- [5] A. Salawu, "Paradox of a milieu: communicating in African indigenous languages in the age of globalization," in *Indigenous Language Media in Africa*, pp. 1–20, CBAAC, Lagos, 2006.
- [6] B. Maseko and M. Moyo, "Minority language revitalization in Zimbabwe— fundamental considerations for Tonga language in the Zambezi Valley," *International Journal of Arts and Humanities*, vol. 2, no. 10, pp. 248–259, 2013.
- [7] R. Zhang, J. Zhou, T. Hai et al., "A big data study of language use and impact in radio broadcasting in China," *Journal of Cloud Computing*, vol. 1, 2015.
- [8] L. Rabhi, N. Falih, A. Afraites, and B. Bouikhalene, "Big data approach and its applications in various fields: review," *Procedia Computer Science*, vol. 155, pp. 599–605, 2019.
- [9] M. A. Memon, S. Soomio, A. K. Jumani, and M. A. Kartio, "Big data analytics and its applications," vol. 1, no. 1, 2017 <https://arxiv.org/abs/1710.04135>.
- [10] A. Morteza and G. Fatemeh, *Qualitative Data Analysis Using Atlas ti*, Sage, 2015.
- [11] E. D. Fishman, *Who are the Ebiras?*, A Division of Beth-Bekka Academic Publishers Ltd, Maiduguri, 1991.
- [12] K. D. Valentine, T. J. Kopcha, and M. D. Vagle, "Phenomenological methodologies in the field of educational communications and technology," *TechTrends*, vol. 62, no. 5, pp. 462–472, 2018.
- [13] T. Akanbi and O. Aladesanmi, "The use of indigenous language in radio broadcasting: a platform for language engineering," *Open Journal of Modern Linguistics*, vol. 4, no. 4, pp. 563–572, 2014.
- [14] D. Ranasuriya, "Effects of radio and television media on language," *Journal of Mass Communication and Journalism*, vol. 5, no. 6, pp. 1–6, 2015.

Research Article

Robot Obstacle Avoidance Controller Based on Deep Reinforcement Learning

Yaokun Tang ¹, Qingyu Chen,² and Yuxin Wei¹

¹Anhui Engineering Laboratory for Intelligent Applications and Security of Industrial Internet, Anhui University of Technology, Ma'anshan, Anhui 243032, China

²Institute of Intelligent Information Processing, School of Computer Science and Technology, Anhui University of Technology, Ma'anshan, Anhui 243032, China

Correspondence should be addressed to Yaokun Tang; youken@ahut.edu.cn

Received 11 August 2022; Revised 5 September 2022; Accepted 6 September 2022; Published 23 September 2022

Academic Editor: Sweta Bhattacharya

Copyright © 2022 Yaokun Tang et al. This is an open access article distributed under the Creative Commons Attribution License, which permits unrestricted use, distribution, and reproduction in any medium, provided the original work is properly cited.

As the core technology in the field of mobile robots, the development of robot obstacle avoidance technology substantially enhances the running stability of robots. Built on path planning or guidance, most existing obstacle avoidance methods underperform with low efficiency in complicated and unpredictable environments. In this paper, we propose an obstacle avoidance method with a hierarchical controller based on deep reinforcement learning, which can realize more efficient adaptive obstacle avoidance without path planning. The controller, with multiple neural networks, contains an action selector and an action runner consisting of two neural network strategies and two single actions. Action selectors and each neural network strategy are separately trained in a simulation environment before being deployed on a robot. We validated the method on wheeled robots. More than 200 tests yield a success rate of up to 90%.

1. Introduction

The robot obstacle avoidance method is a comprehensive approach integrating multiple submethods. Generally, the completion of robot obstacle avoidance is separated into three parts: the leading part, the core, and the back-end part. Among them, the algorithmic models such as robot obstacle avoidance and path planning, equivalent to the human brain for decision-making, serve as its core. The leading part is used to obtain obstacle information (by a camera or a radar) to simulate human vision. As in the human nervous system, the back-end part is used for automatic control, which receives signals from the brain to control the body for actions, as shown in Figure 1. Progress in any one of these three parts will advance the robot's obstacle avoidance technology, allowing faster and better obstacle avoidance and expanding in its obstacle avoidance adaptability in various environments.

From the perspective of navigation and path planning, most traditional obstacle avoidance methods plan one or

more paths or navigation paths based on the location of obstacles in the current spatial environment for avoidance. The artificial potential field method, which was proposed by Khatib [1], tended to reach perfection following numerous improvements and expansions under the efforts of many researchers, allowing a wide range of applications. Han introduced kinetic conditions [2], which were used to generate short and smooth routes under aerial conditions for unmanned aerial vehicle (UAV) obstacle avoidance.

Proposed as early as 1968 [3], the A* algorithm also shows extensive applications in the field of path planning with various improvements, such as a data-driven A* algorithm proposed by Ryo [4]. Recent years have also witnessed efforts on hybrid path planning algorithms such as [5] and various types of bionic path planning methods applied to different scenarios [6]. However, in the obstacle avoidance methods based on path planning, the lack of environmental information in the unfamiliar practical application environment is often ignored. That is also the case for people walking, in which decisions can only be

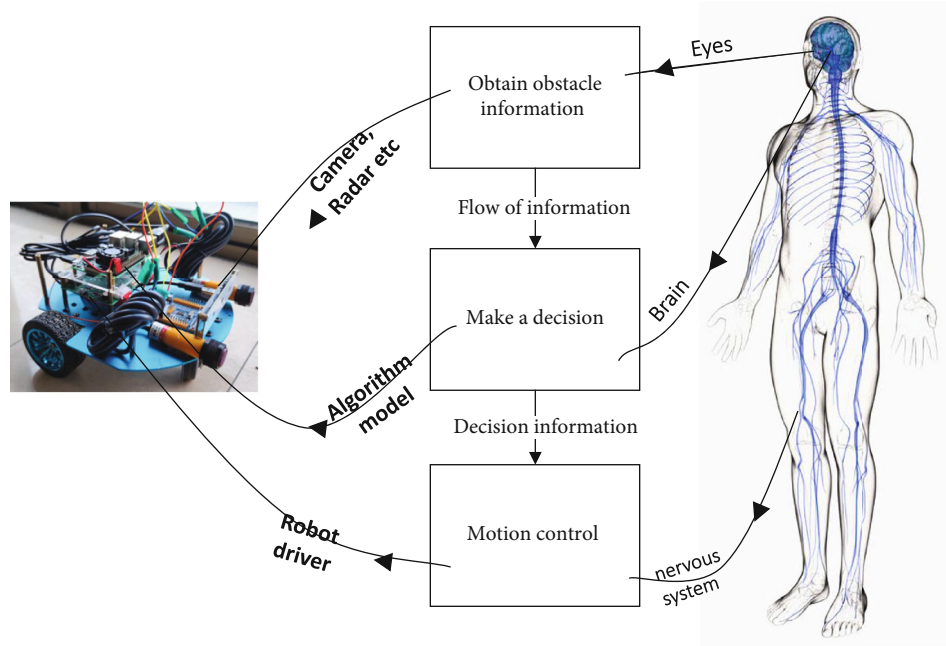


FIGURE 1: Three main components of robot obstacle avoidance technology and their corresponding robot components (our wheeled robot on the left).

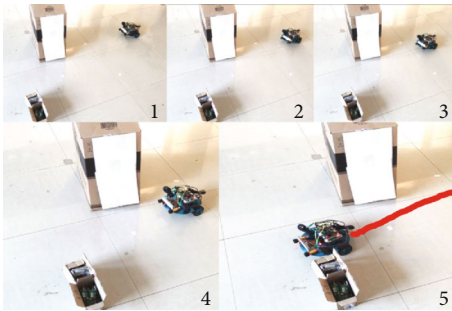


FIGURE 2: Robot completed obstacle avoidance task.

made according to current information acquired by vision. Therefore, we hereby consider building a controller specializing in dealing with obstacles without taking path planning into account.

2. Method

2.1. Deep Reinforcement Learning. Recent years have witnessed a widespread application of model-free deep reinforcement learning (DRL) in the field of robots, which can offer creative ideas and solutions for obstacle avoidance technology. The most distinguishing feature lies in that it enables the robot (program) to learn autonomously in the interaction with the environment, which is quite similar to the human growth and learning process. The concept “trial and error” functioned as the core mechanism of reinforcement learning, and “reward” and “penalty,” as the basic means of learning, were proposed by Waltz and Fu Jingsun in their control theory as early as 1965 [7]. Deep reinforcement learning has made tremendous progress in recent years. The DQN (Deep Q Network) algorithm proposed

and refined by Mnih et al. in 2013 and 2015 [8, 9] provided a powerful “weapon” for reinforcement learning. This deep reinforcement learning algorithm was employed in several components of our controller.

However, the “trial and error” learning approach requires a wealth of training for an effective model. Nonetheless, hardware systems such as robots cannot afford a mass of “trial and error” training for obstacle avoidance in terms of time and economy. As a result, training in a simulation environment emerges as a better option. Many recent studies have demonstrated that the experience gained from training in a simulation environment is also applicable to a real environment [10, 11]. It is critical to minimize the gap between the simulation environment and reality during training in a simulation environment. Neunert analyzed the potential causes of the gap in [12], Li solved some of them by system identification [13], and the DeepMind team enhanced fidelity by estimating model parameters [11]. Enlightened by these efforts, we rewrote the CarRacing-v0 environment based on the OpenAI Gym simulation environment [14] to enable the training of our selector.

Although training without any human guidance can yield a better model [15], training and learning with human guidance in their directions are more efficient. Furthermore, existing deep learning algorithms and neural networks are less effective when learning multiple strategies simultaneously [16]. The separate training of subaction strategies and selector strategies [17, 18] were a general approach in Behavior-Based Robotics [19], making the model training more efficient.

Based on the challenges discussed above and the efforts of previous researchers, an obstacle avoidance controller with a hierarchical structure was proposed in this paper.

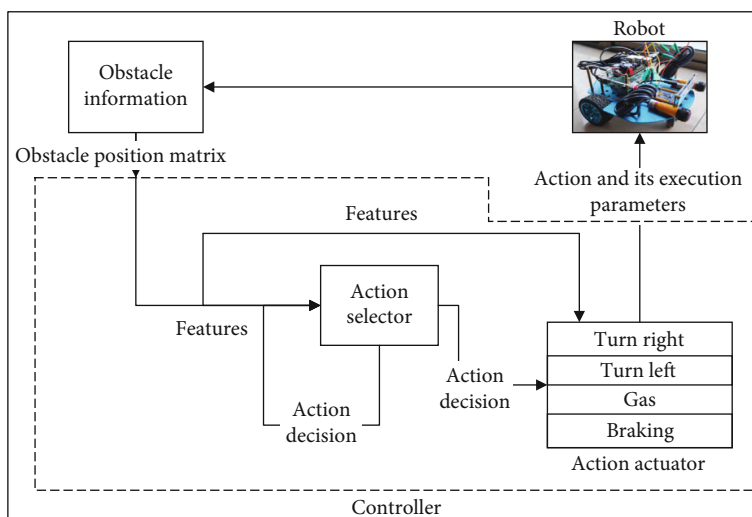


FIGURE 3: Framework of controller.

It only selected the information observable from the robot's current viewing angle as input, without considering path planning, allowing it to handle situations closer to people's progress in reality. To avoid obstacles, we decomposed an obstacle avoidance action into multiple subactions to train a DQN-based action selector to select and run appropriate actions, including Turn Left, Turn Right, Gas, and Stop. We deployed this method on a wheeled robot, as illustrated in Figure 2, and carried out more than 200 experiments in the real physical environment by arranging artificial obstacles, with the success rate of obstacle avoidance hitting 90%, demonstrating the effectiveness of the controller.

2.2. Overview. Unlike traditional path planning methods, we adopted a controller to avoid obstacles. Figure 3 presents the general framework of the controller. The action selector, along with the following four action runners, served as the core of the whole framework. Based on the DQN algorithm, the action selector made decisions based on the information in the environment and the ongoing actions in the current cycle. The action selector sent an action decision to the action runner for running in each running cycle.

We decomposed the obstacle avoidance action into four subactions: Turn Right, Turn Left, Gas and Braking. Among them, the subactions of Turn Right and Turn Left were also based on the DQN algorithm and determined the deflection angle in this direction based on the decision of the neural network. The subactions of Gas and Braking, as single actions, required no manipulation with the model and ran the selector's command directly upon receipt. The action selector and each action were separately trained in parallel in our rewritten simulation environment, making the design of complex loss functions unnecessary and parameter tuning and error finding more convenient.

2.3. Simulation Environment. In the CarRacing environment of OpenAI Gym [14] (Figure 4(a)), the designed task object

was for the racing car Agent to pass through the entire track as quickly as possible, without crossing the track or the boundary. In pursuit of perfection, the modeling for the simulation of the Gym involved the friction of the site, the wheels of the racing car, the ABS sensors, etc. On this basis, we improved the CarRacing simulation environment, which was called Car2D.

Inspired by [11–13], we readjusted the physical model of CarRacing (friction, mass of the wheeled robot, etc.) and added random noise to bring it closer to the actual conditions of our physical robot (Figure 4(b)) and the test site. The original road generation program is unsuitable for a single obstacle avoidance task training as it generates a complete circular road instead of obstacles. We also rewrote the part about road generation and added the obstacle generation function, with which the shape, number, and location of obstacles could be accompanied by random noise generation (Figures 4(c) and 4(d)). Randomization in Car2D could enhance the robustness of the training object, narrowing the gap between the simulation environment and the real environment, as has been demonstrated by studies [10, 20, 21].

For the performance of the four subactions of the robot in the simulation environment, we completed the design based on the physical model of the real environment. Each time running the Gas action command was run, the Agent would provide the robot with equal power to move forward, with the maximum speed reached when the action lasted for several consecutive cycles. The power would be gradually lost due to ground friction if the action stopped. The car would lose power due to running the Braking action command, with the braking distance determined by the car's mass and the elaboration of the physical model.

The task object for obstacle avoidance required no long runway or various curves; thus, only a limited straight runway was generated in Car2D. According to the set conditions, the environment sent a stop signal to stop this training and restart a new episode (Figure 5). Each cycle

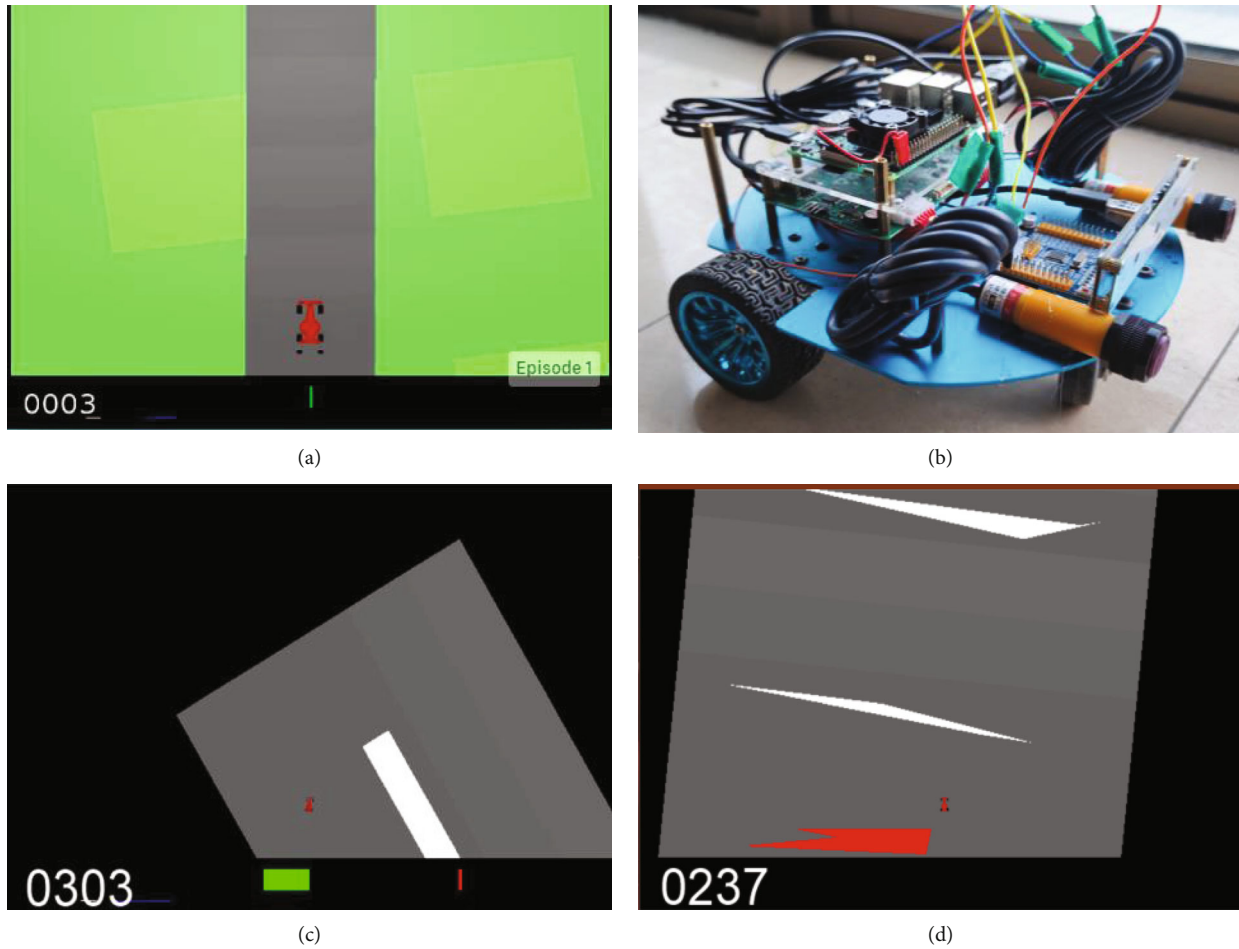


FIGURE 4: (a) OpenAI Gym CarRacing; (b) Our wheeled robots; and (c, d) Randomly generated obstacles on tracks.



FIGURE 5: An episode in training, with the obstacle in white, the end of the road in red, and the viewpoint following the Agent, where the car hit the obstacle, terminating this episode.

Car2D would present an RGB image generated according to the limited viewing angle in front of the Agent and add random noise before providing it to the controller.

2.4. Action Selector. As the core component of the controller, the action selector was implemented based on the DQN algorithm. Compared with the Q-Learning algorithm [22], this algorithm approximated the value function with a convolutional neural network and leveraged the experience replay mechanism to improve the efficiency of the neural network. In addition, a neural network called the Main Net was introduced to the DQN algorithm to generate the current Q value and a Target Net with the same structure as the Main Net was introduced to generate the

target Q value. The parameters of Main Net were copied to Target Net every certain number of iterations. By reducing the correlation between the current Q value and the target Q value, the stability of the algorithm has been improved. The pseudocode of the DQN algorithm is provided in Algorithm 1 [23]. For a detailed description of DQN, please refer to [8, 9, 24], as only the relevant details of this model are presented here.

In each running cycle, the action selector makes action decisions based on the environment observed by the Agent and the actions performed in the previous running cycle. The direct use of the RGB image in the simulation environment as the input of the selector would make it tough to apply the model to the real physical environment. For

Input: Pixels and reward
Output: Q action-value function
Initialization
Initialize replay memory space D
Initialize the Q network (action-value function) \mathcal{Q} with random weights θ
Initialize target network (action-value function) $\widehat{\mathcal{Q}}$ with weights $\theta^- = \theta$
1: Forepisode = 1 to M do
2: Initialize sequence $s_1 = \{x_1\}$ and preprocessed sequence $\phi_1 = \phi(s_1)$
3: For $t = 1$ to T do
4: Following ϵ -greedy policy, select
$a_t = \begin{cases} \text{a random action with probability } \epsilon \\ \arg \max_a \mathcal{Q}(\phi(s_t), a; \theta) \text{ otherwise} \end{cases}$
5: Run action a_t in an emulator and observe the reward r_t and image x_{t+1}
6: Set $s_{t+1} = s_t, a_t, x_{t+1}$ and preprocess $\phi_{t+1} = \phi(s_{t+1})$
7: Store transition $(\phi_t, a_t, r_t, \phi_{t+1})$ in D
8: Sample random minibatch of transitions $(\phi_j, a_j, r_j, \phi_{j+1})$ from D
9: Set $y_j = \begin{cases} r_j & \text{if episode terminates at step } j + 1 \\ r_j + \gamma \max_{a'} \widehat{\mathcal{Q}}(\phi_{j+1}, a'; \theta^-) & \text{otherwise} \end{cases}$
10: Calculate the loss (Perform a gradient descent step on)
$(y_j - \mathcal{Q}(\phi_j, a_j; \theta))^2$
11: Train and update weights θ of \mathcal{Q}
12: End
13: End

ALGORITHM 1: DQN.

TABLE 1: Symbols and rewards terms.

	Symbols
t	Running cycle
a_t	Set of actions at t th cycle
P	Position set of agent at t th cycle
x_t, y_t	Agent's central coordinates at t th cycle
r	Reward
O	Position set of the obstacle
T	Position set of the track
E	Position set of the end
K	Constant
\emptyset	Empty set
	Rewards terms
Distance reward	$r_d = K_d(y_t - y_{t-1})$
Obstacle collision penalty	$r_c = K_c$ if $P \cap O \neq \emptyset$, otherwise 0
Off the track penalty	$r_o = K_o$ if $P \cap T \neq \emptyset$, otherwise 0
Time penalty	$r_t = K_t t$
Obstacle avoidance reward	$r_a = K_a$ if $P \cap E \neq \emptyset$, otherwise 0
Speed reward	$r_s = K_s$ if $a_t = \text{gas}$, otherwise 0

the same input of the model in the real physical environment and the simulation environment, we processed the RGB image from the camera in front of the robot as a matrix describing the position of the obstacles, denoted as M . The subactions of Turn Left and Turn Right were mutually exclusive; thus, only 12 states were available for the action space of the action selector. We used a one-dimensional vector with a length of 3 to describe the actions run in the previous cycle, denoted as a . Therefore, the state space of the running cycle t was characterized as follows:

$$S_t = M_t a_{t-1}, \quad (1)$$

Table 1 presents the symbols and rewards terms. The reward function was denoted as R , indicating that the rewards obtained by $S_t \rightarrow S'_t$ through the action a_t , which was defined as follows:

$$R_t(S_t, a_t, S'_t) = r_d + r_c + r_o + r_t + r_a + r_s. \quad (2)$$

Distance reward encouraged the Agent to move forward as much as possible; the obstacle collision penalty was implemented for hitting an obstacle; the off-the-track penalty was implemented for crossing the boundary; the time penalty encouraged the Agent to avoid obstacles as quickly as possible to prevent them stopping in place; the obstacle avoidance reward was implemented for successful obstacle avoidance; and the speed reward was implemented for the throttle action under the premise of

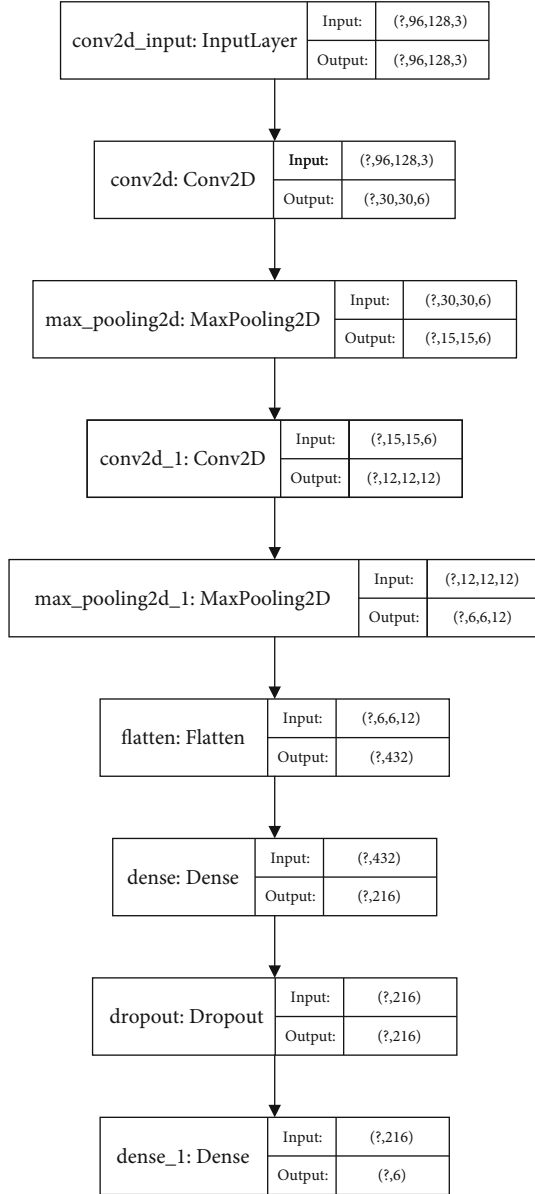


FIGURE 6: Network structure of selectors.

successful obstacle avoidance for another reward, encouraging the Agent to move as fast as possible. It is important to note that the multiple rewards and penalty mechanisms we designed were not superimposed on the Agent at the same time. We adopted the idea of curriculum learning (CL) [25], in which the training started with simple, single, and small obstacles, and the current episode was not stopped even after hitting an obstacle. After the Agent was capable of completing small task objects, the task difficulty would be increased, such as by increasing the area and number of obstacles or by randomizing the location of obstacles.

The score function of the current state was denoted as $Q(S, a)$, which evaluated the current action taking the future state into account, indicating the expectation of the sum of the rewards obtained by the Agent after running the action

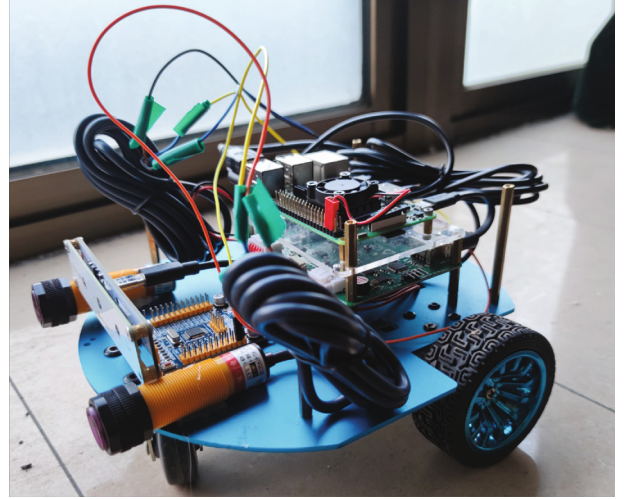


FIGURE 7: Self-built wheeled robot.

a in the state S until the end of the current episode. For the state S_t , and the action A_t run, there exists:

$$Q(s, a) = E[R_t + \gamma R_{t+1} + \gamma^2 R_{t+2} + \dots | A_t = a, S_t = s], \quad (3)$$

where E represents the expectation, γ , the discount factor ($\gamma \in (0, 1)$), which was used to measure the degree of influence of future rewards and current rewards on the Q value. The closer γ was to 1, the greater the influence of future rewards, and $\gamma = 0.85$ was taken for training. The optimal value action function of Q was denoted as Q^* , and there exists:

$$Q^*(s, a) = \max E[R_t + \gamma R_{t+1} + \gamma^2 R_{t+2} + \dots | A_t = a, S_t = s], \quad (4)$$

then the state transition equation can be obtained:

$$Q(s, a) \leftarrow Q(s, a) + \alpha [TargetQ - Q(s, a)], \quad (5)$$

where α is the decay learning rate of γ . Taking Q as a label, the loss function of network training can be obtained:

$$L(\theta) = E[(TargetQ(\theta) - Q(s, a, \theta))^2], \quad (6)$$

where $TargetQ$ can be expressed as follows:

$$TargetQ(\theta) = R(s, a, s') + \gamma \max Q(s', a', \theta). \quad (7)$$

Figure 6 provides the structure of the deep convolutional neural network used in our Main Net, and the Target Net had an identical structure and different parameters. Different from the structure of general DQN algorithms, we inserted a Dropout layer in the last fully connected layer, which was only enabled during training and not when the model was in use.

2.5. Action Runner. In the action runner, only two actions, “Turn Right” and “Turn Left,” which provided the deflection angle of the robot, required training. The two were also based

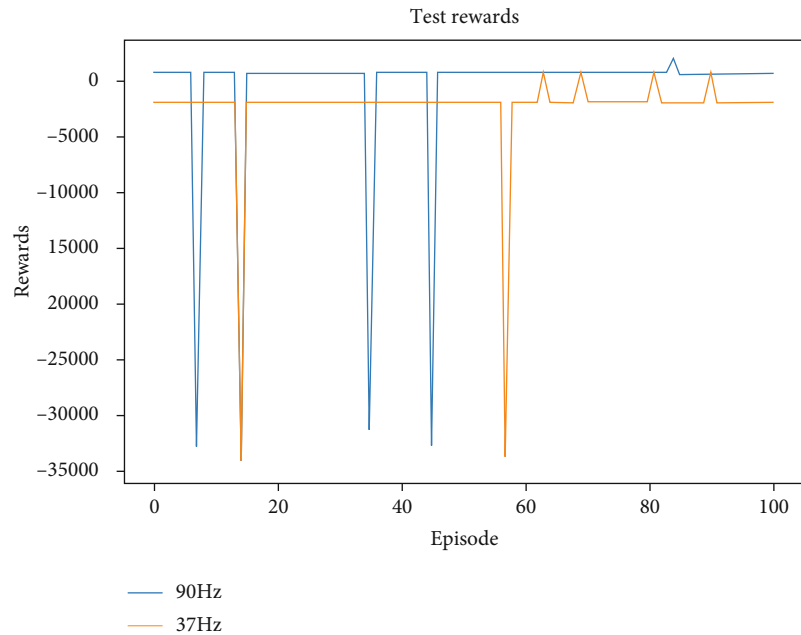


FIGURE 8: Rewards curve for a model trained at 37 Hz for 5,600 rounds and validated 100 times at 90 Hz and 37 Hz.

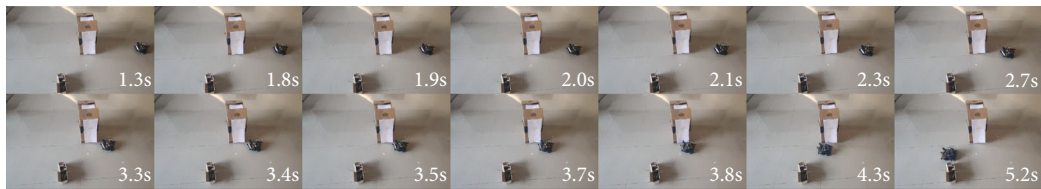


FIGURE 9: Wheeled robot avoiding irregular obstacles with the controller.

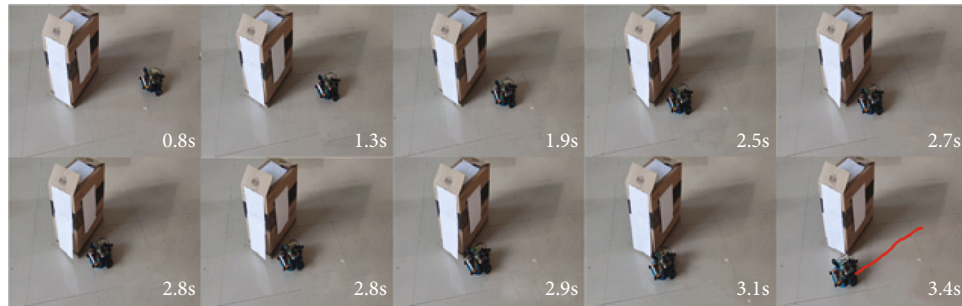


FIGURE 10: Wheeled robot avoiding multiple obstacles with the controller.

on the DQN algorithm, with the same characteristics of the space state of the input as the action selector, thus not elaborated here. However, the action space had a total of 36 states, which were categorized from 0° to 180° by a step length of 5° . Experimental experience showed that the deflection angle exceeding 180° would cause the robot to move in the opposite direction and eventually leave the runway.

3. Results and Discussion

This section presents the experimental results in the real environment and an analysis of the drawbacks of the model.

(a) Experiment Setting

We used a self-built wheeled robot, as shown in Figure 7, to validate the model. The model employed STM32F4 for the chip of the driver board, Raspberry Pi 4B for the upper computer, and ubuntu 18.04 for the system of the upper computer. An infrared camera and two independent infrared distance meters were applied to collect environmental characteristics. The matrix for the position description of the obstacle was constructed mainly through the identification and ranging of obstacles.

Tests showed that the configuration of the running frequency during training and verification in the simulation

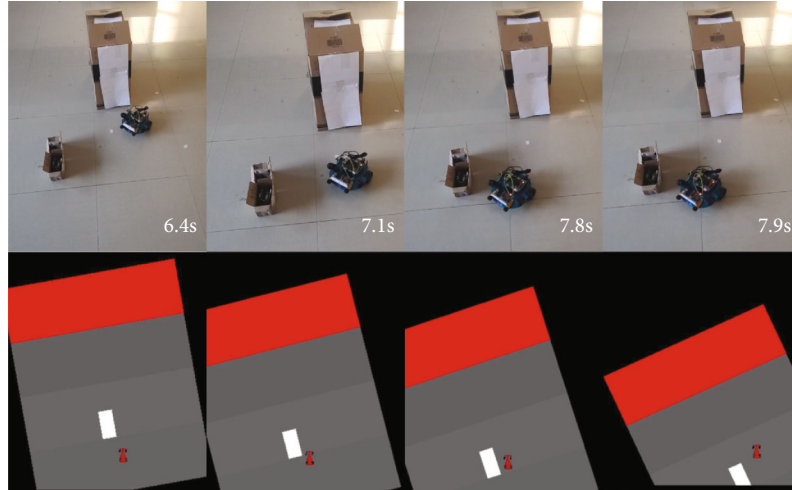


FIGURE 11: Large angular deviation for obstacle avoidance rather than crossing gaps. Agents run similar actions in the simulation environment.

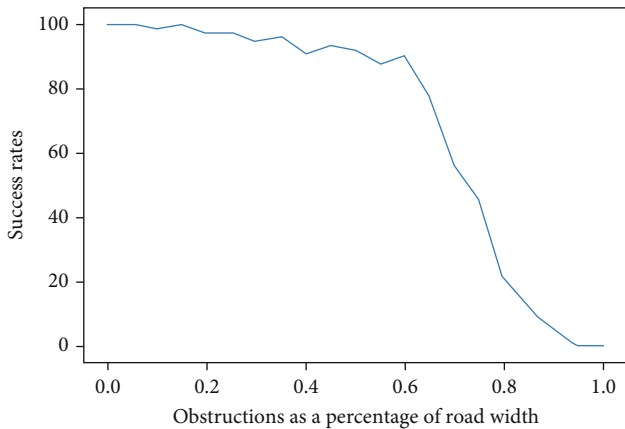


FIGURE 12: Poorer obstacle avoidance effect with bigger obstacle.

environment directly affected the success rate of obstacle avoidance. Figure 8 shows the rewards curve for a model validated 100 times at 90 Hz and 37 Hz, which was trained at 37 Hz for 5,600 rounds.

It can be seen from the curve that the same model accomplished the obstacle avoidance task in most cases when running at 90 Hz but failed at 37 Hz. This means that the model has to be run enough times in a second for the robot to have a coherent obstacle avoidance action. Finally, we set the training and testing frequency in the simulation environment to 90 Hz to ensure training efficiency while preventing the actions of the Agent from oscillating. When tested in a real environment, the controller would see its actions oscillate as it runs too fast. Therefore, we had the hard front-end hardware on the wheeled robot that provided environmental information run at a frequency of 55 Hz to monitor obstacles in real-time. The running frequency of the controller was set to 30 Hz to allow for a smoother running of the robot and avoid oscillations.

As the deployed model failed to play its full role due to the limitation of computing power, we quantified the

model to improve its running efficiency with reference to some methods introduced or mentioned in [26–28]. During the test, the robot was set with a fixed initial speed, and the obstacle avoidance controller was activated when an obstacle was identified to control the robot to avoid the obstacle.

Both the models used in the simulation environment and during the training were written in Python, but most of the programs for the robot were written in C++ and C languages to improve the efficiency of the model.

(b) Experimental Results

To validate the effectiveness of the controller, we conducted the test in three cases: a single obstacle, multiple obstacles (Figure 9), and irregular obstacles (Figure 10), with a total of 75 different obstacle positions. In more than 200 tests, successful obstacle avoidance was observed in most cases for multiple or irregular obstacles, with a success rate of up to 90%.

Unlike in our simulation environment, there existed no road limitations for some robot tasks in the real environment, such as in wild meadows and deserts. To test the generalization ability of the controller, we removed the road restrictions from the real environment and conducted the test 100 times, in which the controller also completed the obstacle avoidance task, with a success rate hitting 91%. However, there were several times when the obstacle avoidance effect failed to meet the expectations. In the case of a small gap between two obstacles, a farther path instead of passing through the gap would be the option (Figure 11 top half), similar to some performance in the simulation environment with small or few obstacles (Figure 11 bottom half). It seemed that when conditions permitted, the controller would leverage the drivable space furthest and stay away from obstacles as much as possible. We set 20 different ratios of obstacles to the width of the road in the simulation environment, each tested 100 times. Figure 12 shows the curve for the success rate of obstacle avoidance.

It can be seen that the success rate of obstacle avoidance became lower with the increase in the ratio of the obstacle to the road width. The obstacle avoidance failed when the Agent could not pass through the gap between obstacles, with a success rate of 90%. Our idea was validated.

4. Conclusion

This paper proposed a hierarchical controller for robot obstacle avoidance in progress, which enabled the robot to avoid obstacles without path planning flexibly. By decomposing the obstacle avoidance control task into multiple sub-actions of GAS, Turn Left, Turn Right, and Braking, an action strategy could be decomposed into multiple strategies for separate training. The idea of curriculum learning (CL) was used to improve training efficiency. With the limited information in front, our controller brought us a step closer to the real action of people dealing with unknown environments.

The controller was trained in a simulation environment before being deployed on a wheeled robot, producing satisfactory results with consistent performance compared with the simulation environment. Wheeled robots deployed with controllers yielded a success rate of up to 90% in more than 200 obstacle avoidance tests. It also applies to an environment similar to the wild without road restrictions, exhibiting good performance.

The controller was less effective in the case of dense obstacles with small gaps. More adjustments in running may be required for dynamic obstacles to yield better results. For these cases, traditional obstacle avoidance methods may outperform our controller when complete environmental information is available. We will make more efforts to solve problems and improve the controller.

Data Availability

All data, models, and code generated or used during the study appear in the submitted article.

Conflicts of Interest

The authors declare that they have no conflicts of interest.

Acknowledgments

The work described in this paper was fully supported by a grant from the Student's Platform for Innovation and Entrepreneurship Training Program of ANHUI UNIVERSITY OF TECHNOLOGY.

References

- [1] O. Khatib, "Real-time obstacle avoidance for manipulators and mobile robots," in *Autonomous Robot Vehicles*, pp. 396–404, Springer, New York, NY, 1986.
- [2] H. Zhijiu, W. Wenjiang, L. Xiaowei, Z. Dan, and L. Chunxin, "An improved artificial potential field method constrained by a dynamic model," *Journal of Shanghai University: Natural Science Edition*, vol. 6, pp. 879–887, 2019.
- [3] P. E. Hart, N. J. Nilsson, and B. Raphael, "A formal basis for the heuristic determination of minimum cost paths," *IEEE transactions on Systems Science and Cybernetics*, vol. 4, no. 2, pp. 100–107, 1968.
- [4] R. Yonetani, T. Taniai, M. Barekatin, M. Nishimura, and A. Kanazaki, "Path planning using neural a* search," in *International Conference on Machine Learning*, pp. 12029–12039, 2021.
- [5] H. Sang, Y. You, X. Sun, Y. Zhou, and F. Liu, "The hybrid path planning algorithm based on improved a* and artificial potential field for unmanned surface vehicle formations," *Ocean Engineering*, vol. 223, article 108709, 2021.
- [6] B. K. Patle, A. Pandey, D. R. K. Parhi, and A. Jagadeesh, "A review: on path planning strategies for navigation of mobile robot," *Defence Technology*, vol. 15, no. 4, pp. 582–606, 2019.
- [7] M. Waltz and K. S. Fu, "A heuristic approach to reinforcement learning control systems," *IEEE Transactions on Automatic Control*, vol. 10, no. 4, pp. 390–398, 1965.
- [8] V. Mnih, K. Kavukcuoglu, D. Silver et al., "Playing atari with deep reinforcement learning," 2013, <https://arxiv.org/abs/1312.5602>.
- [9] V. Mnih, K. Kavukcuoglu, D. Silver et al., "Human-level control through deep reinforcement learning," *Nature*, vol. 518, no. 7540, pp. 529–533, 2015.
- [10] J. Hwangbo, J. Lee, A. Dosovitskiy et al., "Learning agile and dynamic motor skills for legged robots," *Robotics*, vol. 4, no. 26, p. eaau5872, 2019.
- [11] J. Tan, T. Zhang, E. Coumans et al., "Sim-to-real: learning agile locomotion for quadruped robots," 2018, <https://arxiv.org/abs/1804.10332>.
- [12] M. Neunert, T. Boaventura, and J. Buchli, "Why off-the-shelf physics simulators fail in evaluating feedback controller performance—a case study for quadrupedal robots," *Advances in Cooperative Robotics*, pp. 464–472, 2017.
- [13] S. Zhu, A. Kimmel, K. E. Bekris, and A. Boularias, "Model identification via physics engines for improved policy search," 2017, <https://arxiv.org/abs/1710.08893>.
- [14] G. Brockman, V. Cheung, L. Pettersson et al., "Openai gym," 2016, <https://arxiv.org/abs/1606.01540>.
- [15] D. Silver, J. Schrittwieser, K. Simonyan et al., "Mastering the game of go without human knowledge," *Nature*, vol. 550, no. 7676, pp. 354–359, 2017.
- [16] G. Berseth, C. Xie, P. Cernek, and M. Van de Panne, "Progressive reinforcement learning with distillation for multi-skilled motion control," 2018, <https://arxiv.org/abs/1802.04765>.
- [17] P. Maes and R. A. Brooks, "Learning to coordinate behaviors," *AAAI*, vol. 90, pp. 796–802, 1990.
- [18] J. Merel, A. Ahuja, V. Pham et al., "Hierarchical visuomotor control of humanoids," 2018, <https://arxiv.org/abs/1811.09656>.
- [19] R. C. Arkin and R. C. Arkin, *Behavior-Based Robotics*, MIT press, 1998.
- [20] M. Hutter, C. Gehring, D. Jud et al., "Anymal—a highly mobile and dynamic quadrupedal robot," in *2016 IEEE/RSJ international conference on intelligent robots and systems (IROS)*, pp. 38–44, Daejeon, Korea (South), 2016.
- [21] J. Hwangbo, I. Sa, R. Siegwart, and M. Hutter, "Control of a quadrotor with reinforcement learning," *IEEE Robotics and Automation Letters*, vol. 2, no. 4, pp. 2096–2103, 2017.
- [22] C. J. Watkins and P. Dayan, "Q-learning," *Machine learning*, vol. 8, no. 3–4, pp. 279–292, 1992.

- [23] Y. Li, “Deep reinforcement learning: an overview,” 2017, <https://arxiv.org/abs/1701.07274>.
- [24] V. François-Lavet, P. Henderson, R. Islam, M. G. Bellemare, and J. Pineau, “An introduction to deep reinforcement learning,” 2018, <https://arxiv.org/abs/1811.12560>.
- [25] Y. Bengio, J. Louradour, R. Collobert, and J. Weston, “Curriculum learning,” in *Proceedings of the 26th annual international conference on machine learning*, pp. 41–48, Montreal, Quebec, Canada, 2009.
- [26] J. Wu, C. Leng, Y. Wang, Q. Hu, and J. Cheng, “Quantized convolutional neural networks for mobile devices,” in *Proceedings of the IEEE conference on computer vision and pattern recognition*, pp. 4820–4828, LasVegas,NV,USA, 2016.
- [27] A. Zhou, A. Yao, Y. Guo, L. Xu, and Y. Chen, “Incremental network quantization: towards lossless CNNs with low-precision weights,” 2017, <https://arxiv.org/abs/1702.03044>.
- [28] W. Fei, W. Dai, C. Li, J. Zou, and H. Xiong, “General bitwidth assignment for efficient deep convolutional neural network quantization,” *IEEE Transactions on Neural Networks and Learning Systems*, pp. 1–15, 2021.

Retraction

Retracted: A Smart Campus Implementation Architecture Based on Blockchain Technology

Journal of Sensors

Received 23 January 2024; Accepted 23 January 2024; Published 24 January 2024

Copyright © 2024 Journal of Sensors. This is an open access article distributed under the Creative Commons Attribution License, which permits unrestricted use, distribution, and reproduction in any medium, provided the original work is properly cited.

This article has been retracted by Hindawi following an investigation undertaken by the publisher [1]. This investigation has uncovered evidence of one or more of the following indicators of systematic manipulation of the publication process:

- (1) Discrepancies in scope
- (2) Discrepancies in the description of the research reported
- (3) Discrepancies between the availability of data and the research described
- (4) Inappropriate citations
- (5) Incoherent, meaningless and/or irrelevant content included in the article
- (6) Manipulated or compromised peer review

The presence of these indicators undermines our confidence in the integrity of the article's content and we cannot, therefore, vouch for its reliability. Please note that this notice is intended solely to alert readers that the content of this article is unreliable. We have not investigated whether authors were aware of or involved in the systematic manipulation of the publication process.

Wiley and Hindawi regrets that the usual quality checks did not identify these issues before publication and have since put additional measures in place to safeguard research integrity.

We wish to credit our own Research Integrity and Research Publishing teams and anonymous and named external researchers and research integrity experts for contributing to this investigation.

The corresponding author, as the representative of all authors, has been given the opportunity to register their agreement or disagreement to this retraction. We have kept a record of any response received.

References

- [1] J. Lu and B. Wu, "A Smart Campus Implementation Architecture Based on Blockchain Technology," *Journal of Sensors*, vol. 2022, Article ID 2434277, 14 pages, 2022.

Research Article

A Smart Campus Implementation Architecture Based on Blockchain Technology

Jin Lu ¹ and Bo Wu ²

¹Guangdong Key Laboratory of Big Data Intelligence for Vocational Education, Shenzhen Polytechnic, Shenzhen, China

²Guangdong Key Laboratory of Big Data Intelligence for Vocational Education, Shenzhen Pengcheng Technician College, Shenzhen, China

Correspondence should be addressed to Bo Wu; wubo@szpt.edu.cn

Received 22 July 2022; Accepted 5 September 2022; Published 22 September 2022

Academic Editor: Sweta Bhattacharya

Copyright © 2022 Jin Lu and Bo Wu. This is an open access article distributed under the Creative Commons Attribution License, which permits unrestricted use, distribution, and reproduction in any medium, provided the original work is properly cited.

With the application of 5G technology in the field of education, the construction of smart campus has set off a wave of digital transformation. At the same time, the traditional smart campus is also facing the exponential growth of the number of Internet of Things devices, servers, and application terminals, which makes it difficult to achieve flat management. In view of the current difficulties in the construction of smart campus, this paper proposes smart campus architecture based on blockchain technology. Unlike the traditional smart campus architecture, this paper combines the characteristics of decentralization, high confidentiality, and data sharing of block chain with the Internet of Things technology, which greatly reduces the demand for data storage and physical network equipment. The new smart campus architecture plans the application of smart education based on blockchain, and provides a new solution model and research ideas.

1. Introduction

The smart education environment builds an intelligent system by using Information and Communication Technology, including the IoT, cloud computing, and data mining, aimed at improving the quality of teaching courses, scientific research, student living, and campus management [1–3]. However, this environment faces numerous challenges under 5G, such as high management cost, high energy consumption, low data security, and low credit, due to the increase in the number of IoT terminal equipment under 5G [4, 5]. Further, 5G network will transfer a huge amount of personal data and consume energy deficiency [6]. Tracking these challenges become increasingly more difficult under the centralized framework of a smart environment. By some literature research and analysis, an emerging technology called blockchain is paid attention to this paper [7]. Bitcoin is a decentralized digital currency that is transferred using the peer-to-peer bitcoin network. The transactions in bitcoin are verified using encryption in the network nodes and also recorded in the public distributed ledger known

as Blockchain. As the underlying technology of Bitcoin, blockchain is considered the next revolutionary technology with the characteristics of decentralization, tractability, security, and nonavailability, which can be applied in almost every field, especially in the education [8, 9]. Due to these characteristics, applying blockchain to the IoT can be served as an effective solution to the above challenges of a smart education environment under 5G. Some inclusive researches of blockchain and smart education integration have been done, including education applications, data security, and intelligent operation.

Various studies have been done for the smart applications based on the blockchain. Jiang et al. designed a new industrial Internet of Things solution based on the smart contract-enabled blockchain technology, which can reduce data dependence on centralized systems [10]. By applying the MOSS smart contract, Zheng et al. proposed a permission blockchain trust framework for Multi-Operators Wireless Communication Networks. [11]. Sharples and Domingue proposed a distributed system for education records and integration through blockchain technology,

making full use of the functions of smart contracts in blockchain to achieve distributed management of smart education credit [12]. Skiba systematically analyzed the application of blockchain technology in education, and pointed out that blockchain would cater to the decentralized learning mode and spur new learning revolutions increasingly [13]. To solve the separation of IoT devices and the learning process in traditional smart classrooms, Mohamed and Lamia proposed an integration of blockchain technology into IoT devices and course resources, which can improve the learning efficiency substantially [14]. Different from the traditional teacher-centered education strategy, Kong et al. proposed the TELD learning method to build an education platform by adopting the blockchain into the IoT to improve the learner's participation [15]. In addition, since the strategy of traditional smart education cannot adapt to the requirement of education under 5G, Wang et al. proposed a new method that applied the decentralization function of blockchain to the management of physical network data layer, which can improve the flexibility of the smart education IoT [16]. In order to achieve data tractability and improve the stability of smart education management, Liu combined the Big Data application of the IoT and blockchain in the design of smart education, and the course information can be exchanged between IoT nodes [17].

IoT data security has been widely studied in the background of blockchain. Dorri et al. proposed a scheme using blockchain technology to solve the security and privacy problems of IoT devices in smart education [18]. Referring to the application of Bitcoin, Ouaddah et al. proposed a privacy protection access control model, which can replace traditional IoT encryption with the Hash algorithm in blockchain [19]. For improving data security of education IoT device, Huneini et al. proposed applying the distributed ledger function of blockchain to education data management, and any modifications must be agreed to by more than 51 percent of the users in the chain [20]. Similar to the related work above, Alam used the basic encryption algorithm of blockchain to enhance IoT data security, and the data were encrypted in a heterogeneous environment for different types of IoT nodes to ensure data reliability [21]. In view of the security loopholes in data processing of edge computing used in IoT terminal devices, Yang et al. proposed integrating blockchain technology into secure processing of edge computing to improve the security of terminal data [22]. For the similar application in the field of confronting Big Data Education Model, Zheng et al. developed a method of data storage using distributed blockchain management, which can resolve the mobile data security problem [23]. Moreover, because identity authentication is weak during the connection of IoT nodes, Christidis and Devetsikiotis proposed for the first time to apply the blockchain public chain algorithm to identity authentication in the IoT, and then the identities of registrants will be broadcast on the entire chain [24]. By studying the impact of blockchain on the development of the IoT, Rashid and Siddique pointed out that the traceability of blockchain can solve the data security problem of the IoT effectively and designed a preliminary architecture [25]. For data security

of the education IoT, Liang et al. proposed achieving the distributed management of core data by adopting the data management system using blockchain [26].

In recent years, several literatures have also been done in term of blockchain based intelligent operation. Samaniego and Deters applied blockchain as service in the IoT using the decentralized operation and the attribute of device sharing, which can effectively solve the aforementioned problems, including the wide variety of IoT devices and the high cost of centralized maintenance operations [27]. Vemuri built a TEduChain platform using the distributed ledger function of blockchain technology for school donation fund operation, and the funds were directly stored in the account books of students who received donations from [28]. In term of intelligent education operation theory research, Turcu et al. presented a literature review regarding the status of integrating the dynamic blockchain technology in the smart education [29]. Williams proposed a distributed degree evaluation system integrating blockchain, AI, and Big Data to focus on the overall development of students [30]. Chen et al. focused on discussing how to apply blockchain to solve the existing educational platform operational problems, including the innovative operation application of blockchain and education, and proposed a new framework of education operation [31]. Wang et al. provided a blockchain based solution for the operation of the IoT that has been applied in various aspects, such as medical care, education, and finance [32]. For the massive complex IoT devices in the current stage, Huh et al. developed a blockchain based unified management platform, and the device could be turned by the block nodes [33].

In addition to the above work of universities and research institutions, many companies had also carried out related research on the integration of blockchain and smart education IoT. Samsung, IBM, and other companies developed the ADEPT platform based on blockchain and the IoT, which had been initially applied to education, medicine, and other trade national IoT industries [34]. The ADEPT concept is abbreviated as Autonomous Decentralized Peer-to-Peer Telemetry. It enables blockchains to act as the backbone of the system using the concept of proof-of-work and proof-of-stake for ensuring secured transactions. EduChain proposed the concept of the education chain, which combines blockchain, smart contract, and Big Data to facilitate decentralized management and integrate platform applications, which can reduce cost and information redundancy [35]. The study in [36] focused on the aspect of privacy protection using occupant behavior data and relevant methods pertaining to Blockchain implementations. The data used was of temperature records which were sent as transactions between sensors and local building management systems. The study in [37] developed a blockchain based smart and secured scheme for question sharing in smart education system (BSSQ) using a two-phase encryption technique for the encryption of question papers. At the initial stage, the question papers are encrypted using timestamp and in the second phase, the previous QSPs are further encrypted using timestamp, salt hash, and previous hashes. The encrypted QSPs are stored in a blockchain in association with smart contract which enables the users to unlock the selected QSPs.

According to the above research on the integration of blockchain in the field of smart education IoT, most method focuses on the single point technology and aims to optimize the pain points at the software level. However, there is no end-to-end analysis from the perspective of system architecture regarding bottlenecks that blockchain can solve the education IoT, included hardware management, layout of the sensing layer, data security, and top-layer design. To optimize the responses to the above questions, we analyze the core features of blockchain, such as system decentralization, distributed management, and high security, and explore the integration of blockchain and the IoT in education. Thus, we propose a smart new education environment framework that can solve the problems of system centralization and large management dimensions in the construction of the traditional smart educational IoT. The new framework is a “4 + 2” architecture, including the blockchain sensing layer, block node communication layer, data processing layer, education application layer, credit systems, and encryption systems. The research for applications based on the new framework has been carried out.

This paper has designed as the following parts. Section 1 describes the background of the smart education environment and the current research status on the application of blockchain with education. In Section 2, the composition and pain points of the smart education environment are analyzed, explaining the bottlenecks encountered in the construction of the current trendy education environment. In Section 3 we systematically introduce the smart education environment framework based on the IoT and blockchain proposed in this study. In Section 4, we discuss some relevant education applications to evaluate the new smart framework of this study. Finally, in section 5, the development of our work is discussed, and the direction of future research is provided for as well.

2. Structure and Pain Points of Smart Education Environment

The advent of the IoT improves traditional education to smart education by allowing connection of devices to the cloud via the network. There are three key technologies from the perspective of bottom level smart education environment IoT: 1) acquisition and collection of smart information, i.e., perception of external information; 2) management and integration of core data, i.e., processing acquired data in the computing model of data center; and 3) smart display of education information, i.e., application of the whole smart education system [38–40]. External education information sensing comprises the foundation and nerve endings of the smart education environment, which is composed of sensors, cameras, terminals, and other intelligent devices. Then, the network communication layer transmits data to cloud computing centers for processing, which can provide support for the application of top-level stylish education. Based on the functions described above [41], the structure diagram of the IoT-based smart schooling environment is shown in Figure 1.

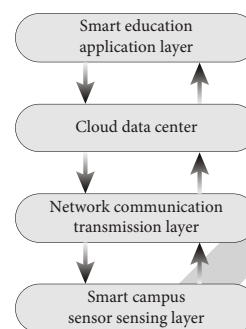


FIGURE 1: The campus environment detection system.

The above architecture been implemented in the field of smart education for many years. It has greatly improved the brisk level of teaching, research, and management. However, under 5G communication network, some associated problems have gradually become evident that will seriously affect its further development [42, 43]. Next, we analyze the pain points of the smart education environment, as shown in Figure 2.

Pain Point 1: The current solutions of the smart education IoT are expensive, because the infrastructure construction and maintenance of IoT devices have extremely high costs, such as IoT cloud servers and network equipment. Specifically, with the rapid increase of IoT node equipment under 5G more intermediate information must be stored, which will greatly increase the cost of construction, operation, and maintenance [44]. Even if these economic and engineering challenges are addressed, the management of cloud servers is another bottleneck. Once the cloud server of data center malfunctions, the data layer will be locked, which can eventually paralyze the entire smart education environment [45, 46].

Pain Point 2: The current smart education environment is controlled by a data center using a single centralized model based on the IoT, which makes the system architecture inflexible [47, 48]. Moreover, the smart education environment connects a large number of educational equipment through the IoT between the application layer and the acquisition layer, which could create great hidden danger in device management security [49, 50]. For example, there are a large number of LED screens for video display in the smart education environment, and its information source is transmitted to the terminal screen through the network by the remote management device. Once the remote host is attacked, the content on the screen cannot control.

Pain Point 3: Multiagent collaboration is adopted in the construction of the smart education environment through the joint construction of mobile operators and ICT enterprises in a “local area” network. Since there is no network standard, it will be difficult to achieve system integration of multiple ICT subjects when considering the establishment of the credit system in the later stage, thus will lead to several problems, such as high cost and a weak credit system [51].

Pain Point 4: Compared with the traditional digital education, the current educational IoT communication network is extremely complex under 5G. Particularly, there is not any

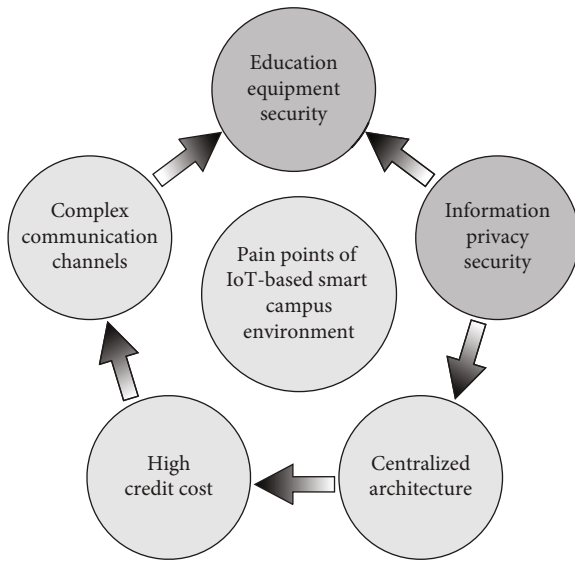


FIGURE 2: Pain points of existing IoT-based smart education environment.

unified communication protocol, which causes obstacles in the communication of equipment. On the other hand, the existence of multiple platforms would form the isolated island of information [52, 53].

Pain Point 5: Owing to the management strategy not being strict, there are high security risks towards basic educational IoT data. In addition, the sensing layer must collect and summarize user behaviors for the application layer, which leads to the frequent leakage of private information [54–57]. At some universities, due to student information always being leaked on the Internet, hackers pose as school staff to collect fee by sending zombie mail, which has caused much economic loss.

It is obvious from the above overview that the intrinsic design and logical structure of the smart education environment is studied to explore its internal working mechanism and root problems under 5G, which can provide the reference of framework optimization.

3. Methodology

3.1. Main Blockchain Algorithms in Education. As the underlying technology of Bitcoin, blockchain is a continuously growing distributed kind of database jointly maintained by multiple nodes which has the characteristic of decentralization, strong encryption, low application costs, high credit, and easy to trace back [58]. In terms of the data structure of the algorithm, blockchain is a data chain within the unit of blocks, and each block records all the data generated during the creation time [59].

The data structure of blockchain is shown in Figure 3, which consists of a block head and some blocks. The hash value of the block head is used as the unified identification of the block, and stored in the block head field of the next block. By recording the hash value of the block head, a data chain is formed to trace from the latest block to the first block, to ensure that the blockchain system can trace the

data at any time. In addition, the hash value of data in the block and the root node field of the Merkle tree in the chain will work together to assure the reliability of the system. To achieve the above function, some core algorithms will be transferred, such as the distributed ledger, asymmetric encryption algorithm, and smart contract [60]. The Merkle tree is also known as hash tree in which each leaf is labelled using a cryptographic hash of a data block and nodes that are not a leaf are labelled using a cryptographic hash of labels of its child nodes. The main algorithms are introduced as following.

- (i) Distributed ledger technology: distributed ledger technology uses the transaction ledger to summarize the subledgers distributed on different nodes, and each node maintains independent ledger data to ensure that it can conduct transactions under supervision [61]. The essence of the allocated ledger is a multinode database, and the access rights of the ledger are controlled by digital signature [62].
- (ii) Asymmetric encryption algorithms: different from the symmetric encryption algorithms, asymmetric encryption algorithms use public and private keys to implement data encryption and decryption, respectively, and the difficulty of cracking increases exponentially according to the length of the key [63, 64].
- (iii) Smart Contract: the smart contract is essentially a digital business contract which can build trust in the transaction process by matching the data structure of the blockchain. The smart contract adopts the programmable script mode, which can work automatically under the condition of meeting the rules to avoid the risks of external intervention, tampering, and malicious manipulation [65, 66].

The blockchain implements a multinode trust network through the above algorithms to achieve a decentralized trust system that cannot be achieved by traditional algorithms, and the features of blockchain include decentralization, difficulty of modification, data security, and collaborative maintenance, which makes it very suitable for multi agent management and dispersed individual collaboration scenarios, such as the smart education environment [67–69].

3.2. Integration Analysis of Blockchain and IOT Technology in Education. Based on the analysis of the smart education IoT and blockchain algorithm in the above sections, this paper intends to comprehensively optimize the pain points of the current smart education environment based on the integration IoT and blockchain, and the key technical points are shown in Table 1.

As being shown in Table 1, blockchain can solve the pain points of the smart education environment under the IoT architecture, and the details are shown below.

Autonomous backup and management of data between storage nodes can be achieved, which would improve user data safety [70, 71]. Moreover, the blockchain can ensure that the

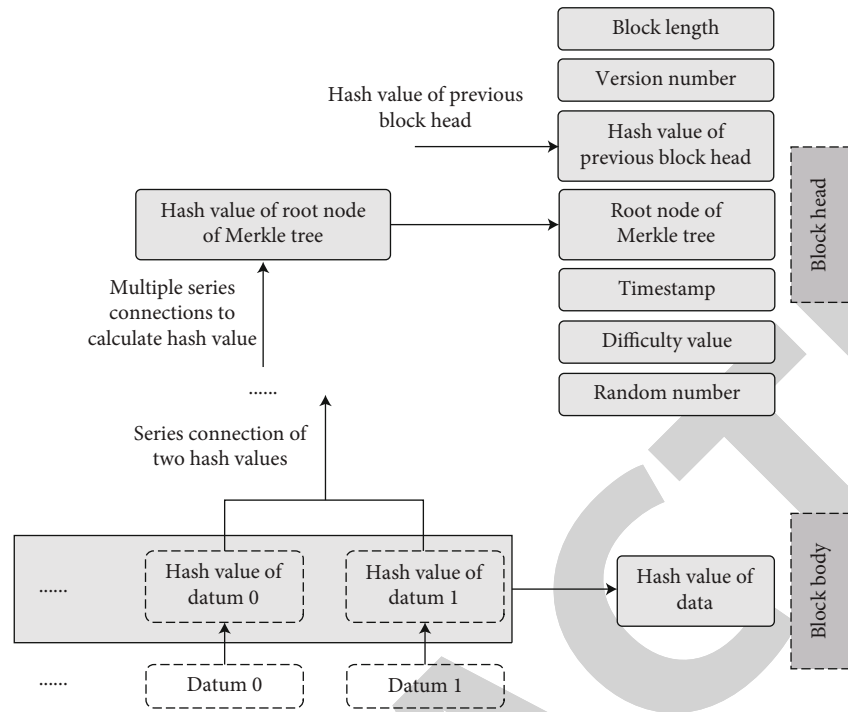


FIGURE 3: Data structure of blockchain.

TABLE 1: Integration of blockchain and IoT technology.

No.	Disadvantages of educational IoT	Advantages of blockchain technology	Functional requirements of smart education
1	Adopt centralized structure, high operation, and maintenance cost	Decentralized architecture, distributed operation	Low cost, decentralized, mobile, personalized, ubiquitous education network
2	No systematic credit system	Smart contract function	Sound credit system of smart education
3	Complex communication pipeline	Use block node as the unit for communication, low complexity	Use unified interface communication for smart education terminals, humanized human-machine interface, simple, and easy to operate
4	Poor information privacy security	Asymmetric digital encryption	Protect personal privacy information and eliminate user concerns
5	Low education equipment security	Powerful identity authentication function	Enhance equipment security and save terminal Maintenance

system adds node encryption functions on the basis of traditional asylum-metric encryption algorithms, and the data decryption can work normally even if the key is lost. With the above strategy, data security can be greatly improved.

For the traditional centralized management model, all data need to be aggregated and then dispersed. More-over, in the new solution, data of the sensing layer are stored in each distributed block unit to realize the distributed pipeline processing model [72, 73]. The above mode can break the centralized architecture of block is used to classify and manage sensors. A new sensing layer of block codes is proposed, which will simplify the communication network model of layer devices. Only the block interface is required for data communication, which greatly reduces the communication complexity between the sensing layer and data management layer.

To solve the problem of low security coefficient in the current IoT equipment, the identity authentication and traceability of blockchain are applied between the data layer and the application layer, which can check the identity of users accessing the IoT equipment in real time through time-series encryption. The traceability of the block authentication information enables consistent security levels in the management unit and device, thus improving the security of the IoT equipment.

3.3. *The Framework of Smart Education Environment Using Blockchain and IOT.* As shown in Figure 4, we propose a new framework using blockchain and IoT to optimize the smart education environment system. It is designed to optimize the smart education environment from multiple aspects such as data security, identity authentication, node

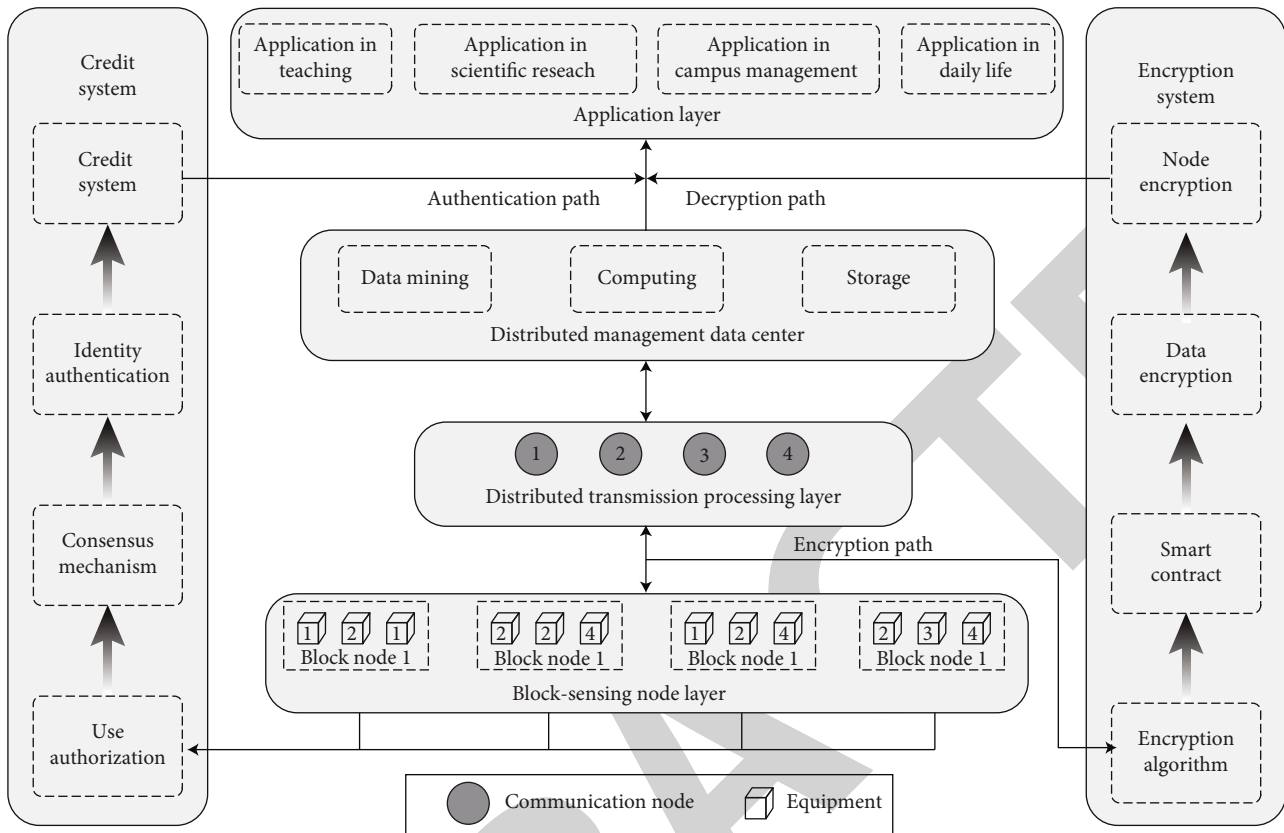


FIGURE 4: Smart education environment based on blockchain+IoT.

reconstruction, distributed sharing, and education applications; to solve the problems included rigid system architecture, weak credit system, and difficult network management.

The new framework has a four-layer data structure in contrast to the traditional smart education IoT. Then, both authentication and encryption systems are added to realize data processing at different levels, which consists of a four-layer system model and two management systems. The functions of the four layers are as following.

3.3.1. The First Layer: Block-sensing node layer. The IoT based smart education environment perception layer remains a major challenge, in that, e.g., the system layout is scattered and the number of sensor devices is large. Compared to the traditional design, this paper proposes a novel solution to perform device management at the perception layer through block nodes, and classifies different perception nodes according to its working mode. The design is illustrated in Figure 5.

In the traditional smart education environment, a single sensor only serves one education application. However, after the block node management is adopted, the device will be time-multiplex, which can support a variety of distinct upper-layer applications and improve the utilization of sensor devices. More broadly, one kind of device may be distributed in separate nodes to build a set of block awareness layers based on time-sharing multiplexing. The specific implementation is reproduced below.

- (1) The sensing layer equipment is set as nodes according to the region, and each application node is classified according to its purpose, including library, smart class-room, canteen, office building, and data center. Accounting layer node covers multiple sensing devices according to application scenarios, and can be shared according to the application.
- (2) The sensing layer is composed of several nodes with different purpose. The nodes communicate in UDP mode using the broadcast channel, and application data transmission can be greatly improved in this way.
- (3) The generic communication interface connects the sensing and network layers, through which all control signals and sensing data are transmitted. The blockchain API is an application programming interface that uses the Blockchain technology wherein the API provides set of guidelines to enable different applications to interact with each other seamlessly ensuring that the data is transmitted in the best possible way without any issues. The multiple applications gets connected with one another enabling them to access common information from a single source instead of acquiring data from multiple locations.

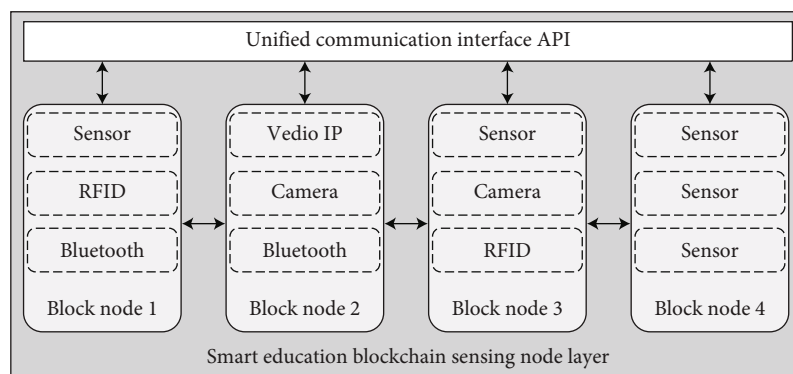


FIGURE 5: Sensing node layer of smart education blockchain.

- (4) Distributed management is adopted for the data of nodes in the sensing layer. Data are not stored in this layer alone, but are directly uploaded to the data layer for processing after collection by the sensing layer according to the strategy adopted by the application layer.
- (5) Distributed block nodes are used to realize the layout between sensing layers, and faulty equipment in a node can be maintained independently without affecting the function of other nodes, thus reducing maintenance costs.

3.3.2. The Second Layer: Block Node Communication Layer.

This layer adds a data encryption processing unit on the basis of the communication transmission layer of the smart education IoT which is performed at the data source. In addition, we propose the concept of blockchain node communication, and the complexity of the communication layer is reduced by unifying wireless AP, fixed equipment, and RFID in a communication node. The structure is illustrated in Figure 6.

With the concept of blockchain node communication, different communication network devices are integrated in one communication node according to application functions, which is less complicated and easier to manage. The traditional network layer binds all IoT devices in one layer to a bus, which is the same as to a serial structure, and this mode can improve management efficiency.

When a traditional network device requires maintenance, the devices of the whole communication layer cannot function normally. However, the distributed block nodes are used between the communication layers of block nodes to realize the layout of communication equipment, and the damaged equipment can be maintained independently without affecting the normal work of other nodes.

3.3.3. The Third Layer: Decentralized Data Processing Layer.

In the data processing layer, a novel distributed storage architecture is proposed that is based on the distributed decentralization of blockchain, as shown in Figure 7. This layer's distributed computing and data mining are basically the same as those in a traditional data center using the IoT, but the innovation mainly lies in distributed storage

and the AI deep learning module. Decentralized data processing layer has five parts.

- (1) Distributed storage: the distributed storage of blockchain is used to make data management easier, which can break the barriers on storage devices from different manufacturers. In detail, in distributed storage different storage modes are adopted for different types of data, including smart education activities, credit data, and core management data. Smart education activities are recorded through the node storage in the block, and the credit data are encrypted and stored in the node. However, core management data are directly transmitted to the system data center for processing
- (2) Data Center: the Big Data Computing center provides a platform for distributed storage and data analysis, including two computing modules: CPU and GPU. The CPU mainly performs large-scale data for calculations and the GPU performs blockchain class computing, including floating-point computation and model training. Through the hybrid operation of the above two units, the data computing center can meet the function requirements, including data operation, face recognition, speech recognition, and NLP
- (3) Data-mining platform: applying mainstream data-mining platforms such as Hadoop on mining data at the perception layer, especially intelligently classifying data in classrooms, libraries, bedrooms, canteens, and other places, and transforming the classified data to the Big Data analysis module
- (4) Analysis Unit: the Big Data analysis unit systematically processes the multimodel education data collected for the perception layer, including classification, labeling, and analysis. These preliminary data are transferred to the top-layer education application for further processing
- (5) AI Unit: in traditional solution, AI units work in the application layer. The innovation of this paper is

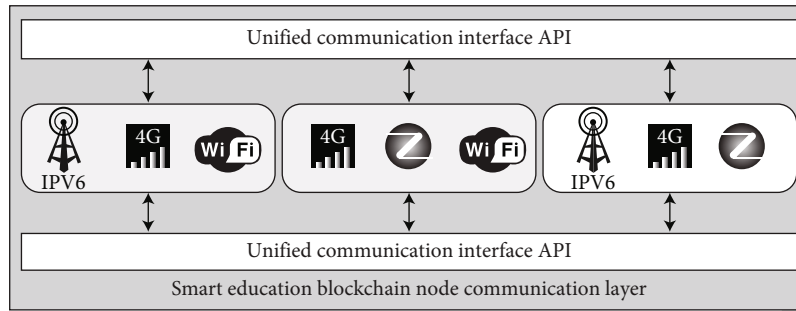


FIGURE 6: Node communication layer of smart education blockchain.

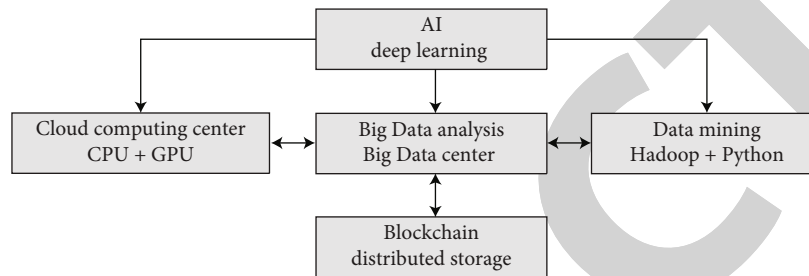


FIGURE 7: Data center layer of smart education blockchain.

tantamount to place. AI units in the data layer for data processing, thus avoiding secondary training of the model. In addition, cloud computing and deep learning integration can accelerate the computing operation

the core connection throughout the sensing, transmission, data, and application layers. The whole system has four parts: use authorization, consensus mechanism, identity authentication, and the credit system, as shown in Figure 8

3.3.4. The Fourth Layer: The Education Application Layer. This paper incorporates blockchain to further expand the application of existing education platforms. The detail is explained in the next chapter.

The above four-layer structure, including blockchain sensing layer, block node communication layer, data processing layer, and education application layer, constitutes the core structure of the entire intelligent education environment, and complete the entire smart education process through cooperation. Then, the smart educational environment using blockchain and IoT includes the following two extra management systems: credit system and encryption system.

- (1) Credit system: using the hierarchical identity authentication method of blockchain, a complete credit system of the sensing layer to the application layer is established for authorization, consensus mechanism establishment, and identity authentication. Through the application of the credit system in the smart education environment, it can provide identity authentication for the safe use of equipment; in addition, it can provide database resources for the later establishment of the whole society's academic degree credit authentication, record the students' information in a distributed way, and serve the wide education application. The credit system becomes

Use of accrediting connects the block sensing layer nodes to ensure that sensing layer devices can be used only with authorization. The consensus mechanism belongs to the interface unit between use accredit and identity authentication, which ensure that participants can perform verification through consensus. Identity authentication can authenticate a user's identity by calling the consensus mechanism module of the main process to performing full link authentication, and the main authentication method is the hash algorithm. As the core module, the credit system will serve educational applications and provide a credit database for later blockchain education trading platform and a blockchain online university.

- (2) Encryption system: the encryption system addresses the data security of the basic hardware through data encryption pipeline mechanism, which has four modules: algorithm module, smart contract, data encryption, and node encryption, as shown in Figure 9

The underlying layer integrates multiple encryption algorithms which are used in different scenarios, include AES, ECC, RSA, Hash, and DES. Smart contract is a specific transaction scenario of the blockchain, and different underlying transactions on the block are implemented by calling the underlying encryption algorithm. Data encryption refers to encrypt the transaction content of the contract on the

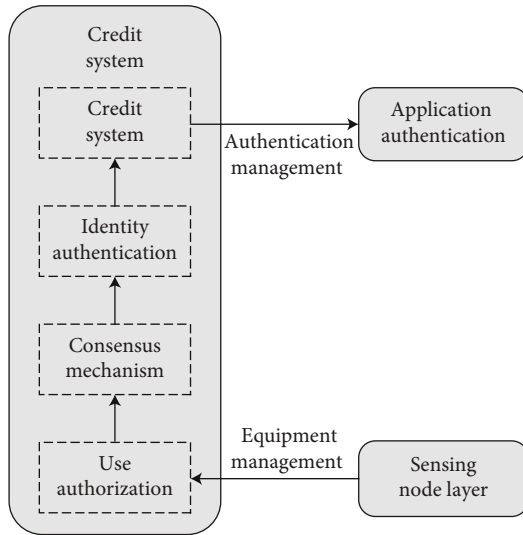


FIGURE 8: Credit system of smart education environment.

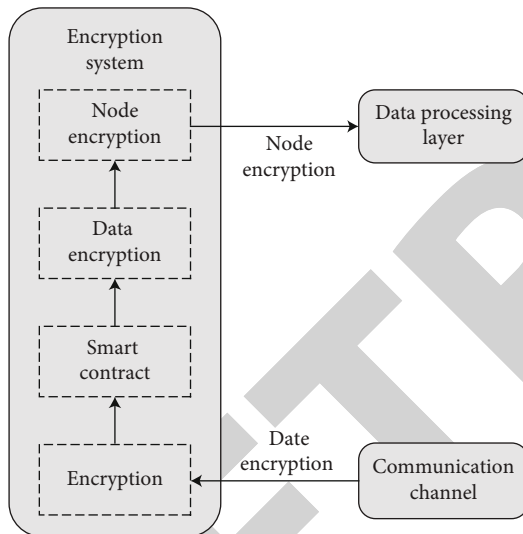


FIGURE 9: Encryption system of smart education environment.

basis of a smart contract, and outputting it in the form of block data, so as to facilitate the later block node encryption. As the top module of the system, node encryption is connected to the data processing layer to realize the ultimate output of the encryption system.

4. Main Application of Smart Education Environment Based on Blockchain and IOT

Four educational applications are proposed based on the new framework using blockchain and IoT in this study: blockchain education information authentication system, blockchain smart trading platform, blockchain online education platform, and blockchain smart open school. A complete smart education ecosystem based on these applications is presented in Figure 10.

4.1. Blockchain Education Information Authentication System. In recent years, education certification is increasingly attached, which can be applied in many educational fields, such as the protection of intellectual property rights of scientific research, academic degree verification, and professional title certification. The implementation architecture is illustrated in Figure 11. The whole authentication process has six steps, as the following:

- (i) User generated private key and corresponding public key in the student information authentication center for later identity authentication
- (ii) The authentication information of user transmitted through IoT communication unit, and transmitted data is encrypted using the public key
- (iii) The user-generated data, including public and private keys, are transmitted to the management center for backup
- (iv) The IoT communication unit uploads encrypted data to the smart contract module for processing
- (v) Encrypted chained data are managed in distributed storage for data query and table item generation
- (vi) After the third party passes the permission by the management center, application data are encrypted using the private key of the management center to complete the authentication

The blockchain education information certification system proposed in this paper is implemented through the above six steps which ensure that the relevant information of students from admission to graduation is uniformly managed. Different from the ordinary mode, the above certification system has three advantages.

- (1) Utilizing the traceability and the storage of nodes, the related rights of property owners are protected by recording information on the blockchain, such as property owner, grade time, and property limit
- (2) Through the application of smart property protection system, the illegal infringements will be screened in the whole network
- (3) The academic performance, physical fitness test results, activity performance, and scientific research achievements since enrollment of students can be stored in the distributed database of blockchain, which can be shared with universities, enterprises, and government institutions. As an essential standard of credit judgment, the end-to-end credit system is established in the students' further study, professional title recognition, work, and employment

4.2. Blockchain Smart Resource Trading Platform. Whether online education platform or traditional offline classroom teaching, learners must pay before learning in the process of acquiring educational resources, which would make learners

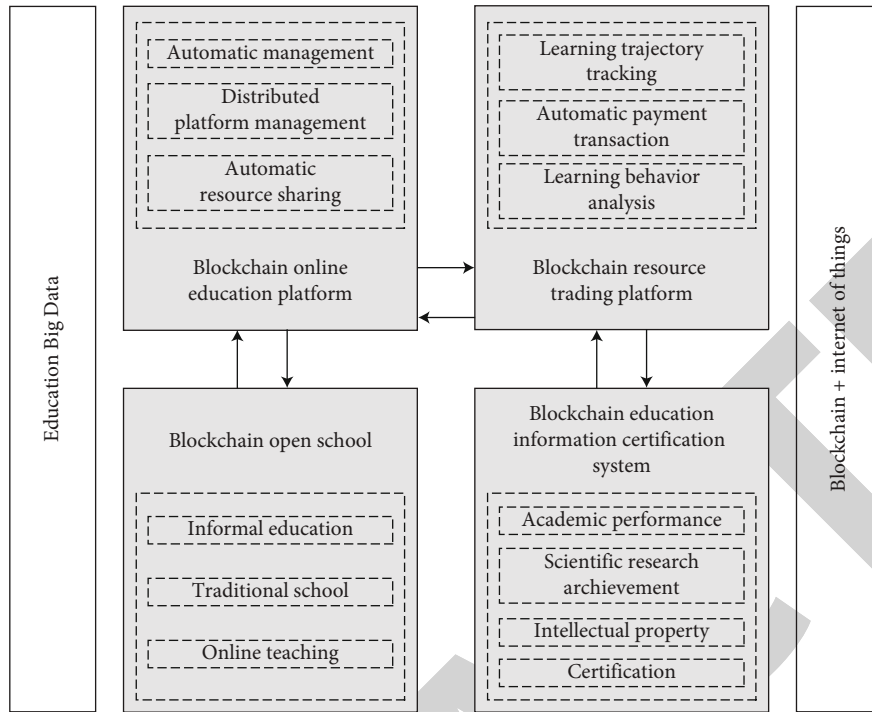


FIGURE 10: Smart education ecosystem based on blockchain + IoT.

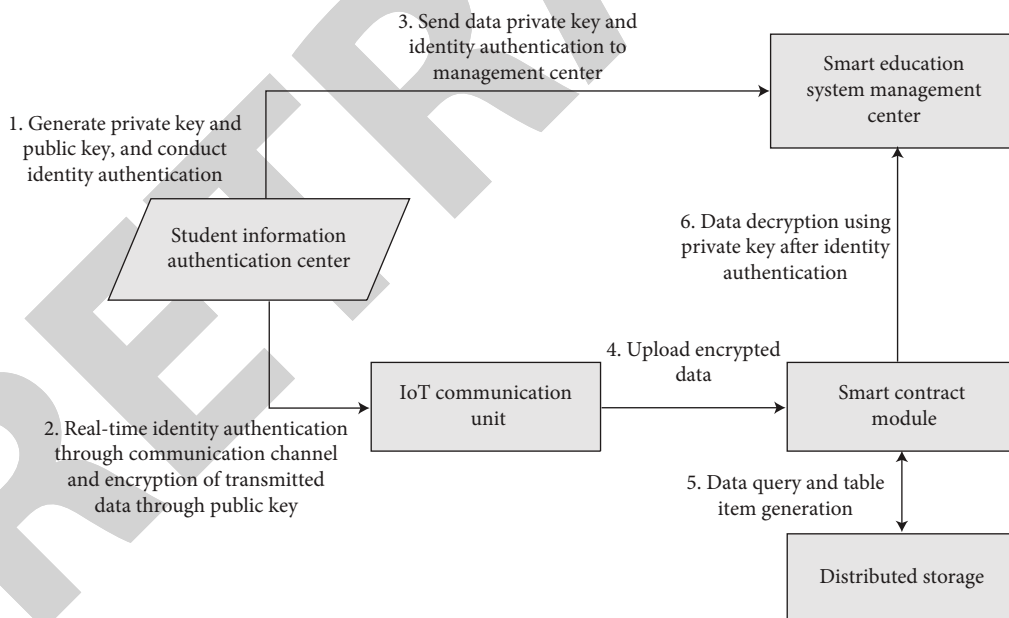


FIGURE 11: Blockchain education information certification system.

lose interest in course. Applying the distributed ledger and smart contract to resource trading, a modern platform is proposed. In the blockchain smart resource trading platform, people can learn first and the platform synchronously tracks learning records. When learners wish to acquire learning resources, the system can automatically pay according to previous learning records and there is no requirement for manual payment. The smart trading platform based on blockchain can

break the traditional mode of paying before learning, which improves the security of payment transactions, records the process and the transaction in real time, and automatically completes the transaction. This mode can realize peer-to-peer transactions between learners and educational institutions, learners and trainers, and education institutions and educational structures, reducing the intermediary costs of education platforms.

4.3. Blockchain Online Education Platform. Smart contracts have the characteristics of automatic execution, transparent management, and resource sharing, making them widely used in financial online transactions to achieve automated management, which can greatly improve the intelligence of the entire monetary system [73]. Reference to the above applications, smart contract technology can also improve the management efficiency of online education platform and automatically complete the uploading, dissemination, certification, and sharing of educational resources. In addition, uploading the IoT cloud database, allocated education resources are stored in different blocks to realize the real time sharing. Platform users can conduct online learning and communication in real time through smart terminals. It is helpful to improve the sharing Efficiency of education resource and solve the problems of resource isolated islands on the traditional education platform. In the future, the construction of the platform lays a solid foundation for the establishment of education Big Data.

4.4. Blockchain Smart Open School. The centralization feature of traditional smart education environment is not only reflected in the centralization of data management, but in the closeness of educational places [74, 75]. In the financial field, blockchain has broken the monopoly of the bank, which can be used for reference to create a new type of smart open school [76–78]. Based on the development of blockchain and the IoT, the smart decentralized education system can break the centralized situation in which traditional educational resources are monopolized by schools or other scientific research institutions. Accompanied by the building of blockchain credit certification systems and trading platforms, an institution with smart education qualifications can get qualified by obtaining certificates, so as to realize the integration of traditional school and other types of education to build smart open schools.

5. Conclusion

In this paper, an optimized framework for smart education environment using blockchain and IoT was proposed. We analyzed the work mechanism of the IoT-based smart education environment, and pointed out the principal problems in the functional structure of the existing framework using 5G. In view of the pain points of the existing framework, the second application and development were carried out by combining the smart IoT education with the blockchain, and optimization solutions were proposed. The design is implemented from the top layer to realize a smart education environment framework using blockchain and the IoT. The new framework is a 4+2 smart education environment mode, including blockchain sensing layer, block node communication layer, data processing layer, and education application layer, credit and encryption application systems. Blockchain optimization schemes were proposed for each module. The IoT and blockchain work together in the new framework to minimize the limitations of the traditional mode. A different way to perform device management was proposed at the perception layer through block nodes, which can improve the uti-

lization of sensor devices. In communication layer, different communication network devices were integrated in one communication node, and the complexity of communication layer was reduced by unifying wireless device. Moreover, the decentralized data center and smart application layer were aimed at improving the energy optimization and privacy protection.

Education applications were preliminaries studied based on the framework of the smart education environment. Four application scenarios were proposed, including blockchain education information authentication system, blockchain smart trading platform, blockchain online education platform, and blockchain smart open school. With the proposed new framework that integrates the smart IoT and blockchain technology, a complete ecology for the smart education environment is established, including the hardware layout, certification system, and new educational applications. These application cases can evaluate that the performance of blockchain solution is more promising than traditional solutions under 5G.

In the future, in-depth research on the internal working mechanism of the proposed blockchain-based smart education environment will be conducted, which can improve and optimize the system framework with 5G+AI+blockchain, and achieve further architectural upgrades with the new education application. There will be more fields in which blockchain technology can be applied, including academic certification, skill identification, learning records, identity management, infrastructure security, campus busing, data cloud storage, energy management, prepaid cards, learning markets, record managements, product retailing, human resource management, and library management. It can be said that the above covers most of the scenarios in the current education field, which will bring more changes to the construction of a smart education environment in the future, and will be of great significance for the development of the overall concept of smart education.

Data Availability

All data, models, and code generated or used during the study appear in the submitted article.

Conflicts of Interest

The authors declare that there are no conflicts of interest regarding the publication of this paper.

Acknowledgments

This work is partially supported by the Shenzhen Education Science “14th five-year plan”2021 Subject: Research on online learning emotion analysis and intelligent tutoring based on collaborative perception of multimodal education data (ybzz21015), the Key technology research and innovative application demonstration of intelligent education (2019KZDZX1048), the Guangdong Key Laboratory of Big Data Intelligence for Vocational Education (2019GKSYS001), and the Shenzhen Vocational Education Research Center Jointly Established by the Ministry and the Province (6022240004Q).

References

- [1] K. Valentin, B. M. Ț. Rocsana, B. M. Ț. Radu et al., "The potential of blockchain technology in higher education as perceived by students in Serbia, Romania, and Portugal," *Sustainability*, vol. 14, no. 2, p. 749, 2022.
- [2] I. Karamitsos, M. Papadaki, M. Themistocleous, and C. Ncube, "Blockchain as a service (BCaaS): a value modeling approach in the education business model," *Journal of Software Engineering and Applications*, vol. 15, no. 5, pp. 165–182, 2022.
- [3] Y. Lin, Z. Li, W. Yue, and J. Wen, "CrowdIoT: the crowdsourcing test system for IoT devices based on Blockchain," *Advances in Internet of Things*, vol. 12, no. 2, pp. 19–34, 2022.
- [4] S. Nurbayani and L. Utami, "Local wisdom education to develop geo-diversity understanding," *IOP Conference Series: Earth and Environmental Science*, 2018.
- [5] L. Yang, Y. Zou, M. Xu, Y. Xu, D. Yu, and X. Cheng, "Distributed consensus for blockchains in internet-of-things networks," *Tsinghua Science and Technology*, vol. 27, no. 5, pp. 817–831, 2022.
- [6] M. Humayun, N. Jhanjhi, M. Alruwaili, S. S. Amalathas, V. Balasubramanian, and B. Selvaraj, "Privacy protection and energy optimization for 5g-aided industrial internet of things," *Access*, vol. 8, pp. 183665–183677, 2020.
- [7] M. Pincheira, M. Antonini, and M. Vecchio, "Integrating the IoT and blockchain technology for the next generation of mining inspection systems," *Sensors*, vol. 22, no. 3, p. 899, 2022.
- [8] M. Hrouga, A. Sbihi, and M. Chavallard, "The potentials of combining blockchain technology and Internet of Things for digital reverse supply chain: a case study," *Journal of Cleaner Production*, vol. 337, p. 130609, 2022.
- [9] E. P. Maimon, "Information, knowledge, and wisdom: transforming education," *Procedia-Social and Behavioral Sciences*, vol. 55, pp. 94–99, 2012.
- [10] Y. Jiang, Y. Zhong, and X. Ge, "Smart contract-based data commodity transactions for industrial internet of things," *IEEE Access*, vol. 7, pp. 180856–180866, 2019.
- [11] S. Zheng, T. Han, Y. Jiang, and X. Ge, "Smart contract-based spectrum sharing transactions for multi-operators wireless communication networks," *IEEE Access*, vol. 8, pp. 88547–88557, 2020.
- [12] M. Sharples and J. Domingue, "The blockchain and kudos: a distributed system for educational record, reputation and reward," *European Conference on Technology Enhanced Learning*, 2016, pp. 490–496, Springer, 2016.
- [13] D. J. Skiba, "The potential of blockchain in education and health care," *Nursing Education Perspectives*, vol. 38, no. 4, pp. 220–221, 2017.
- [14] H. Mohamed and M. Lamia, "Implementing flipped classroom that used an intelligent tutoring system into learning process," *Computers in Education*, vol. 124, pp. 62–76, 2018.
- [15] X. T. R. Kong, G. W. Chen, G. Q. Huang, and H. Luo, "Ubiquitous auction learning system with TELD (Teaching by Examples and Learning by Doing) approach: A quasi-experimental study," *Computers in Education*, vol. 111, pp. 144–157, 2017.
- [16] X. Wang, P. Zeng, N. Patterson, F. Jiang, and R. Doss, "An improved authentication scheme for internet of vehicles based on blockchain technology," *IEEE Access*, vol. 7, pp. 45061–45072, 2019.
- [17] H. Liu, "The research of theoretical construction and effect of preschool wisdom education system in the background of big data," *Cluster Computing*, vol. 22, no. S6, pp. 13813–13819, 2019.
- [18] A. Dorri, S. S. Kanhere, R. Jurdak, and P. Gauravaram, "Blockchain for IoT security and privacy: the case study of a smart home," in *2017 IEEE International Conference on Pervasive Computing and Communications Workshops (PerCom Workshops)*, pp. 618–623, Kona, HI, USA, 2017.
- [19] A. Ouaddah, A. A. Elkalam, and A. A. Ouahman, "Towards a novel privacy-preserving access control model based blockchain technology in IoT," in *Europe and MENA Cooperation Advances in Information and Communication Technologies*, Advances in Intelligent Systems and Computing, pp. 523–533, Springer, 2017.
- [20] S. Hamood Al-Huneini, A. Walker, and R. Badger, "Introducing tablet computers to a rural primary school: an activity theory case study," *Computers & Education*, vol. 143, article 103648, 2020.
- [21] M. A. Ferrag, L. Maglaras, and H. Janicke, "Blockchain and Its Role in the Internet of Things," *International Conference on Strategic Innovative Marketing and Tourism*, 2018.
- [22] J. Yang, Z. Lu, and J. Wu, "Smart-toy-edge-computing-oriented data exchange based on blockchain," *Journal of Systems Architecture*, vol. 87, pp. 36–48, 2018.
- [23] R. Zheng, J. Jiang, X. Hao, W. Ren, F. Xiong, and Y. Ren, "bcBIM: a blockchain-based big data model for BIM modification audit and provenance in mobile cloud," *Mathematical Problems in Engineering*, vol. 2019, Article ID 5349538, 13 pages, 2019.
- [24] K. Christidis and M. Devetsikiotis, "Blockchains and smart contracts for the Internet of Things," *IEEE Access*, vol. 4, pp. 2292–2303, 2016.
- [25] A. Rashid and M. J. Siddique, "Smart contracts integration between blockchain and Internet of Things: opportunities and challenges," in *2019 2nd International Conference on Advancements in Computational Sciences (ICACS)*, Lahore, Pakistan, 2019.
- [26] W. Liang, M. Tang, J. Long, X. Peng, J. Xu, and K.-C. Li, "A secure fabric blockchain-based data transmission technique for industrial Internet-of-Things," *IEEE Transactions on Industrial Informatics*, vol. 15, no. 6, pp. 3582–3592, 2019.
- [27] M. Samaniego and R. Deters, "Blockchain as a service for IoT," in *2016 IEEE International Conference on Internet of Things (iThings) and IEEE Green Computing and Communications (GreenCom) and IEEE Cyber, Physical and Social Computing (CPSCom) and IEEE Smart Data (SmartData)*, pp. 433–436, Chengdu, China, 2016.
- [28] V. K. Vemuri, "Blockchain: a practical guide to developing business, law, and technology solutions," *Journal of Information Technology Case and Application Research*, vol. 20, no. 3–4, pp. 161–163, 2019.
- [29] C. Turcu, C. Turcu, and I. Chiuchisan, "Blockchain and its potential in education," 2019, <https://arxiv.org/abs/1903.09300>.
- [30] P. Williams, "Does competency-based education with blockchain signal a new mission for universities?," *Journal of higher education policy and management*, vol. 41, no. 1, pp. 104–117, 2019.
- [31] G. Chen, X. Bing, L. Manli, and N.-S. Chen, "Exploring blockchain technology and its potential applications for education," *Smart Learning Environments*, vol. 5, no. 1, p. 1, 2018.

- [32] Q. Wang, X. Zhu, Y. Ni, G. Li, and H. Zhu, "Blockchain for the IoT and industrial IoT: A review," *Internet of Things*, vol. 10, article 100081, 2020.
- [33] S. Huh, S. Cho, and S. Kim, "Managing IoT devices using blockchain platform," in *2017 19th International Conference on Advanced Communication Technology (ICACT)*, pp. 464–467, PyeongChang, Korea (South), 2017.
- [34] M. U. I. Hassan, M. H. Rehmani, and J. Chen, "Privacy preservation in blockchain based IoT systems: integration issues, prospects, challenges, and future research directions," *Future Generation Computer Systems*, vol. 97, pp. 512–529, 2019.
- [35] M. A. Rashid, K. Deo, D. Prasad, K. Singh, S. Chand, and M. Assaf, "TEduChain: A platform for crowd-sourcing tertiary education fund using blockchain technology," 2019, <https://arxiv.org/abs/1901.06327>.
- [36] J. Li, N. Li, J. Peng, Z. Wu, and H. Cui, *Privacy Protection of Occupant Behavior Data and Using Blockchain for Securely Transferring Temperature Records in HVAC Systems*, 2019.
- [37] A. Islam, M. Kader, and S. Y. Shin, "BSSQS: a blockchain based smart and secured scheme for question sharing in the smart education system," 2018, <https://arxiv.org/abs/1812.03917>.
- [38] N. Ashraf, M. Faizan, W. Asif, H. K. Qureshi, A. Iqbal, and M. Lestas, "Energy management in harvesting enabled sensing nodes: Prediction and control," *Journal of Network and Computer Applications*, vol. 132, pp. 104–117, 2019.
- [39] J. A. Muñoz-Cristóbal, V. Gallego-Lema, H. F. Arribas-Cubero, A. Martínez-Monés, and J. I. Asensio-Pérez, "Using virtual learning environments in *bricolage* mode for orchestrating learning situations across physical and virtual spaces," *Computers & Education*, vol. 109, pp. 233–252, 2017.
- [40] J. Hamilton and S. Tee, "Smart utilization of tertiary instructional modes," *Computers & Education*, vol. 54, no. 4, pp. 1036–1053, 2010.
- [41] S. Xiang, D.-D. Zhou, L.-D. Feng et al., "Influence of chain architectures on crystallization behaviors of PLLA block in PEG/PLLA block Copolymers," *Chinese Journal of Polymer Science*, vol. 37, no. 3, pp. 258–267, 2019.
- [42] Y.-T. Sung, K.-E. Chang, and T.-C. Liu, "The effects of integrating mobile devices with teaching and learning on students' learning performance: a meta-analysis and research synthesis," *Computers & Education*, vol. 94, pp. 252–275, 2016.
- [43] N. T. Butz and R. H. Stupnisky, "Improving student relatedness through an online discussion intervention: the application of self-determination theory in synchronous hybrid programs," *Computers in Education*, vol. 114, pp. 117–138, 2017.
- [44] R. K. Moloo, K. K. Khedo, and T. V. Prabhakar, "Critical evaluation of existing audio learning systems using a proposed TOL model," *Computers & Education*, vol. 117, pp. 102–115, 2018.
- [45] I. Miladinovic and S. Schefer-Wenzl, "NFV enabled IoT architecture for an operating room environment," in *2018 IEEE 4th World Forum on Internet of Things (WF-IoT)*, pp. 98–102, Singapore, 2018.
- [46] M. Hasan, M. M. Islam, M. I. Zarif, and M. M. Hashem, "Attack and anomaly detection in IoT sensors in IoT sites using machine learning approaches," *Internet Things*, vol. 7, article 100059, 2019.
- [47] L. Calderoni, A. Magnani, and D. Maio, "IoT manager: an open-source IoT framework for smart cities," *Journal of Systems Architecture*, vol. 98, pp. 413–423, 2019.
- [48] H. Aftab, K. Gilani, J. E. Lee, L. Nkenyereye, S. M. Jeong, and J. S. Song, "Analysis of identifiers in IoT platforms," *Digital Communications and Networks*, vol. 6, no. 3, pp. 333–340, 2020.
- [49] V. Casola, A. De Benedictis, M. Rak, and U.-b. Villano, "Toward the automation of threat modeling and risk assessment in IoT systems," *Internet Things*, vol. 7, article 100056, 2019.
- [50] M. Fahmideh and D. Zowghi, "An exploration of IoT platform development," *Information Systems*, vol. 87, article 101409, 2020.
- [51] D. Karimanzira and T. Rauschenbach, "Enhancing aquaponics management with IoT-based predictive analytics for efficient information utilization," *Information Processing in Agriculture*, vol. 6, no. 3, pp. 375–385, 2019.
- [52] Z. R. Hassenfeld and J. A. Levisohn, "The challenge of professional development in jewish studies: why the conventional wisdom may not be enough," *Journal of Jewish Education*, vol. 85, no. 1, pp. 53–75, 2019.
- [53] H. Jingzhao, "Research on the wisdom education platform of cloud computing architecture," in *2017 3rd International Conference on Computational Intelligence & Communication Technology (CICT)*, pp. 1–5, Ghaziabad, India, 2017.
- [54] K. Lakshmana, R. Kaluri, N. Gundluru et al., "A review on deep learning techniques for IoT data," *Electronics*, vol. 11, no. 10, p. 1604, 2022.
- [55] J. Fox, A. Donnellan, and L. Doumen, "The deployment of an IoT network infrastructure, as a localised regional service," in *2019 IEEE 5th World Forum on Internet of Things (WF-IoT)*, pp. 319–324, Limerick, Ireland, 2019.
- [56] F. Arici, P. Yildirim, Ş. Caliklar, and R. M. Yilmaz, "Research trends in the use of augmented reality in science education: content and bibliometric mapping analysis," *Computers & Education*, vol. 142, article 103647, 2019.
- [57] N. Dalal and D. J. Pauleen, "The wisdom nexus: Guiding information systems research, practice, and education," *Information Systems Journal*, vol. 29, no. 1, pp. 224–244, 2019.
- [58] Y. Li, W. Susilo, G. Yang, Y. Yu, D. Liu, and M. Guizani, "A blockchain-based self-tallying voting scheme in decentralized IoT," 2019, <https://arxiv.org/abs/1902.03710>.
- [59] K. R. Ozyilmaz and A. Yurdakul, "Designing a blockchain-based IoT with ethereum,swarm, and lora: the software solution to create high availability with minimal security risksEMC society history," *IEEE Consumer Electronics Magazine*, vol. 8, no. 3, pp. 28–34, 2019.
- [60] N. Fotiou, V. A. Siris, and G. C. Polyzos, "Interacting with the Internet of Things using smart contracts and blockchain technologies," *International Conference on Security, Privacy and Anonymity in Computation, Communication and Storage*, 2018, pp. 443–452, Springer, 2018.
- [61] J. Xiong and Q. Wang, "Anonymous auction protocol based on time-released encryption atop consortium blockchain," 2019, <https://arxiv.org/abs/1903.03285>.
- [62] W. She, Q. Liu, Z. Tian, J.-S. Chen, B. Wang, and W. Liu, "Blockchain trust model for malicious node detection in wireless sensor networks," *IEEE Access*, vol. 7, pp. 38947–38956, 2019.
- [63] C. I. Dick and A. Praktijnjo, "Blockchain technology and electricity wholesale markets: expert insights on potentials and challenges for OTC trading in Europe," *Energies*, vol. 12, no. 5, p. 832, 2019.

Retraction

Retracted: Improvement and Reduction of Self-Heating Effect in AlGaN/GaN HEMT Devices

Journal of Sensors

Received 23 January 2024; Accepted 23 January 2024; Published 24 January 2024

Copyright © 2024 Journal of Sensors. This is an open access article distributed under the Creative Commons Attribution License, which permits unrestricted use, distribution, and reproduction in any medium, provided the original work is properly cited.

This article has been retracted by Hindawi following an investigation undertaken by the publisher [1]. This investigation has uncovered evidence of one or more of the following indicators of systematic manipulation of the publication process:

- (1) Discrepancies in scope
- (2) Discrepancies in the description of the research reported
- (3) Discrepancies between the availability of data and the research described
- (4) Inappropriate citations
- (5) Incoherent, meaningless and/or irrelevant content included in the article
- (6) Manipulated or compromised peer review

The presence of these indicators undermines our confidence in the integrity of the article's content and we cannot, therefore, vouch for its reliability. Please note that this notice is intended solely to alert readers that the content of this article is unreliable. We have not investigated whether authors were aware of or involved in the systematic manipulation of the publication process.

Wiley and Hindawi regrets that the usual quality checks did not identify these issues before publication and have since put additional measures in place to safeguard research integrity.

We wish to credit our own Research Integrity and Research Publishing teams and anonymous and named external researchers and research integrity experts for contributing to this investigation.

The corresponding author, as the representative of all authors, has been given the opportunity to register their agreement or disagreement to this retraction. We have kept a record of any response received.

References

- [1] H. Chen, N. Tang, and Z. Zuo, "Improvement and Reduction of Self-Heating Effect in AlGaN/GaN HEMT Devices," *Journal of Sensors*, vol. 2022, Article ID 5378666, 10 pages, 2022.

Research Article

Improvement and Reduction of Self-Heating Effect in AlGa_N/Ga_N HEMT Devices

Hui Chen , Naiyun Tang, and Zhipeng Zuo

School of Electronics and Information Engineering, Shanghai University of Electric Power, 200000 Shanghai, China

Correspondence should be addressed to Hui Chen; 1209240372@mail.shiep.edu.cn

Received 2 August 2022; Revised 28 August 2022; Accepted 1 September 2022; Published 22 September 2022

Academic Editor: Sweta Bhattacharya

Copyright © 2022 Hui Chen et al. This is an open access article distributed under the Creative Commons Attribution License, which permits unrestricted use, distribution, and reproduction in any medium, provided the original work is properly cited.

GaN is one of the third-generation broadband semiconductor materials developed rapidly in recent years, and AlGa_N/Ga_N HEMT has a broad application prospect in the fields of high temperature, high power, high frequency and radiation resistance, etc. In recent years, gallium nitride based high electron mobility transistors have been widely used in emerging industries, such as 5G technology, new energy vehicles, unmanned aircraft and other fields, due to their high power and high voltage resistance. However, due to the high power density of HEMT devices, the self-heating effect will lead to a significant increase in the junction temperature of the device, which will seriously affect the performance, reliability, and lifetime of the device. In this paper, the temperature characteristics of Ga_N high electron mobility transistors (Ga_N HEMTs) are studied, and the effect of self-heating effect on Ga_N HEMT devices is analyzed. In order to reduce the device temperature and improve the reliability of the device, a new device structure is proposed in this paper. The new structure replaces the conventional silicon and Si₃N₄ with highly thermally conductive diamond and SiC as the substrate and passivation layer of the device, which facilitates the heat dissipation from the substrate and passivation layer. Also, the new structure employs a hybrid barrier layer and field plate. Simulation results show that the new structure has about 30% lower temperature peak, 47% higher output current, 28% higher transconductivity, and up to 18.22% higher current collapse rate compared to the conventional structure.

1. Introduction

Over the past decades, human society has entered the information age, and the semiconductor industry has stepped into the fast lane of development, gradually becoming an indispensable part of people's lives. With the continuous progress of science and technology, people have put forward higher requirements on the performance of semiconductor devices. Power devices based on gallium nitride (Ga_N) materials such as HEMT and MESFET have been widely used in 5G technology, new energy vehicles, unmanned aircraft, and other emerging industries with broad application prospects [1, 2]. Ga_N is a third-generation semiconductor material, which has the characteristics of wide forbidden band, high critical breakdown electric field, and high electron saturation rate compared with the first and second generation semiconductor materials. It can be seen that Ga_N materials have a forbidden band width of 3.39 eV and a critical breakdown

electric field of 3.3 mV/cm, which are well suited for making high-power, high-frequency devices [3, 4].

AlGa_N/Ga_N heterojunctions were first born in the 1990s and were successfully prepared on sapphire substrates by metal organic chemical vapor deposition (MOCVD) in a study by [5]. A year later, the first Ga_N-based HEMT device was developed by [6]. In recent years, Ga_N-based HEMT devices have become a research hotspot in the semiconductor industry due to the rise of 5G technology. The advantages of Ga_N HEMTs come from two main properties: a wide 3.39 eV forbidden band and a high concentration of two-dimensional electron gas (2DEG) accumulated at the heterojunction interface [7, 8]. 2DEG exhibits a very high electron mobility at room temperature (>2000 cm²/V · S) at room temperature, which gives HEMT devices superior power density and frequency.

When high currents flow through HEMT devices, the self-heating effect causes a significant increase in the junc-

tion temperature of the device and impairs the output characteristics of the device. It is known that the failure rate of electronic devices increases with temperature and is more significant at higher temperatures, which means that reducing the device junction temperature can significantly improve the device lifetime [9]. The traditional package level heat dissipation technology cannot effectively solve this problem, and the heat dissipation capability of GaN HEMTs must be improved from within the device. Nowadays, SiC materials with high thermal conductivity are usually used as the substrate for GaN HEMTs, but for higher power density HEMT devices, SiC substrates are difficult to meet the demand of fast heat dissipation; therefore, finding alternative substrate materials with better heat dissipation capability becomes one of the important ways to solve the self-heating problem of HEMT devices.

The thermal conductivity of diamond material is the highest among all known natural materials, up to 1000-2000 W/m-K, depending on the crystal structure, growth method, growth quality, and ambient temperature of diamond. Combining GaN epitaxial layers with diamond can significantly enhance the heat dissipation capability of HEMT devices. Natural diamond (SCD) is extremely expensive and difficult to fabricate large-size films, and GaN (GOD) HEMT devices on diamond substrates have been widely reported in recent years with the further development of synthetic polycrystalline diamond (PCD). PCD has the same structure as SCD, similar thermal conductivity, and substantially lower cost and is currently the most commonly used material for diamond substrates [10]. It has been shown that diamond substrates can increase RF power by a factor of 3.6, reach a power density of 56 W/mm (at DC), and significantly reduce the device junction temperature compared to HEMT devices on SiC substrates [11]. However, the conventional substrate materials have low thermal conductivity, and the devices do not dissipate heat significantly. In addition, it is a challenge to meet the demand for high-frequency and high-power devices, which severely limits GaN HEMT devices to unlock their original potential. Therefore, using a material with high thermal conductivity as a substrate or device heat sink layer can effectively improve the self-heating effect. Solutions that only change the material have limited thermal effect and must also change the device structure. Study [12] mitigated the self-heating effect of sapphire substrate devices by using a flip chip structure. Study [13] proposed the use of AlN and Si_3N_4 materials as double passivation layers for the devices and investigated the effect of their thickness on the electrical properties. The study [13] showed that the peak temperature of AlN decreased by 160 K at a thickness of 5 nm, and the most significant improvement in current and transconductivity was obtained.

To reduce the self-heating effect, the material and structure of the device are changed in this paper, and diamond and SiC with higher thermal conductivity are used as the substrate and passivation layer of the device, as well as the hybrid barrier layer and field plate to make the device suitable for operation at high power and high temperature.

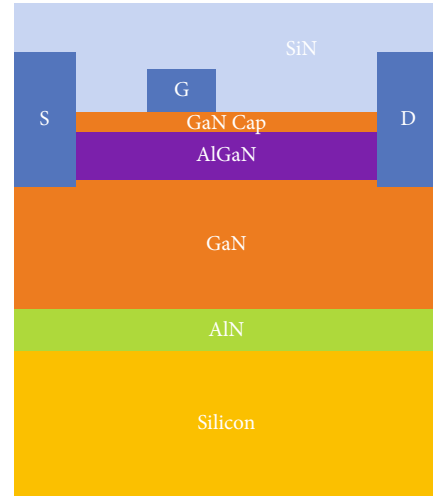


FIGURE 1: Traditional device structure.

2. Device Structures and Models

In this paper, AlGaIn/GaN device is simulated using the Silvaco TCAD software, and the referenced device structure is shown in Figure 1. The substrate material is Si with a thickness of $2.45\ \mu\text{m}$, the buffer layer GaN with a thickness of $2.25\ \mu\text{m}$, and the potential barrier layer $\text{Al}_{0.26}\text{Ga}_{0.74}\text{N}$ with a thickness of 23 nm. The thickness of the GaN bubble layer below the gate is 4 nm, where the doping type is n-type and the concentration is $1e20\ \text{cm}^{-3}$. The thickness of the passivation layer Si_3N_4 is $2.47\ \mu\text{m}$. The length of both source and drain is $0.5\ \mu\text{m}$, and the gate length is $0.25\ \mu\text{m}$. The gate-source spacing is $0.77\ \mu\text{m}$, and the gate-drain spacing is $1.32\ \mu\text{m}$. In 2019, the study [14] increased the power density of InGaIn HEMT to 22.3 W/mm by adding PCD film at the bottom of the HEMT device and reducing the thickness of the SiC substrate and improving the backside polishing process and significantly reduced the boundary thermal resistance of SiC/PCD, which is schematically shown in Figure 1. In addition, the gate is a Schottky contact, while the source and drain are ohmic contacts. To reduce the lattice mismatch between the buffer layer GaN and the substrate silicon, an AlN nucleation layer with a thickness of $0.05\ \mu\text{m}$ is grown between them [9].

This paper is mainly divided into two steps to reduce the device temperature. Firstly, the substrate material Si of the conventional GaN HEMT device is replaced with diamond, and Si_3N_4 is replaced with SiC as the passivation layer. The structure of the device is shown in Figure 2(a). Using materials with high thermal conductivity in the substrate and passivation layer enhances the device's ability to dissipate heat vertically, facilitating heat dissipation from the substrate and passivation layer. Secondly, a mixed barrier layer is used, and the structure of the device is shown in Figure 2(b). The barrier layer under the gate is divided into two layers: the upper layer is an $\text{In}_{0.15}\text{Ga}_{0.85}\text{N}$ thin layer with an optimal thickness of 0.5 nm, and the lower layer is AlGaIn. In addition, the device uses a field plate with an

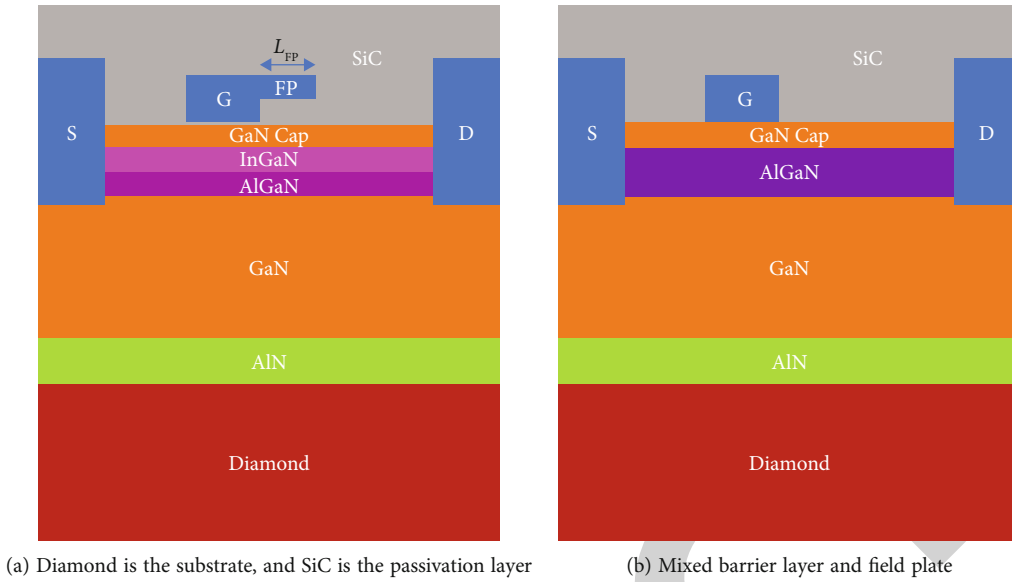


FIGURE 2: Structures of the device.

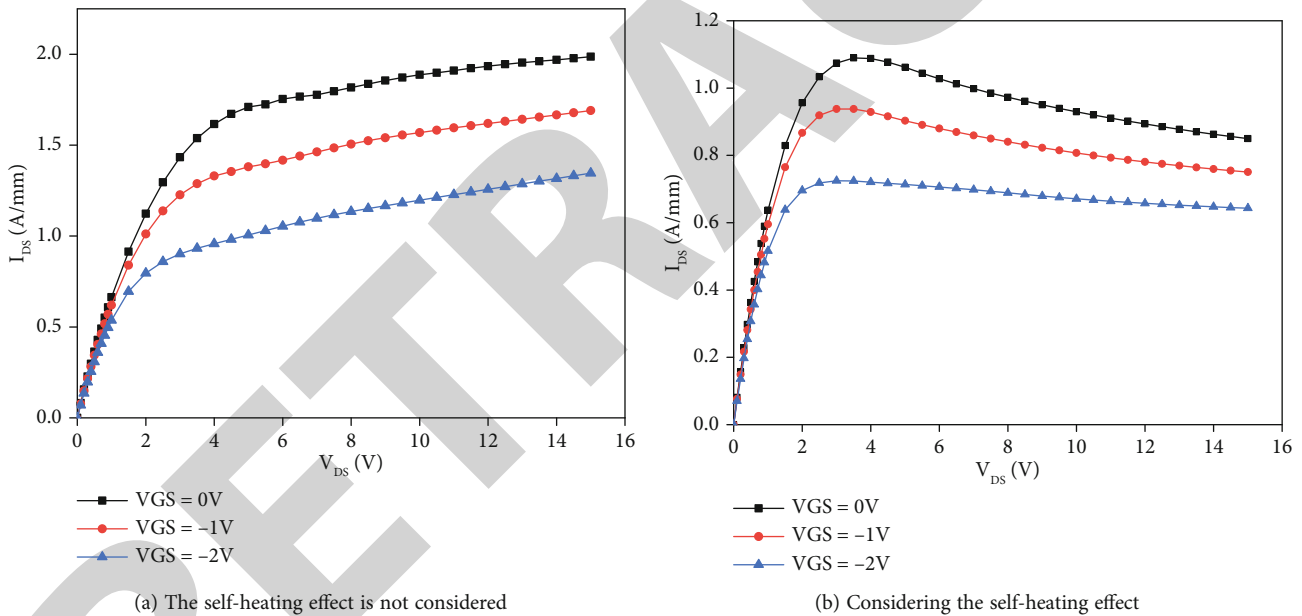


FIGURE 3: Comparison of output curves.

optimal field plate length of $0.3 \mu\text{m}$ and a field plate thickness of 35 nm .

In this paper, a variety of models are used for simulation. Due to the presence of two-dimensional electron gas, GaN HEMT devices have high electron mobility, so the simulation adopts the mobility model.

GaN HEMT devices will generate a lot of heat at the channel during operation, and this heat will diffuse to other locations through heat conduction. Therefore, a lattice heat transfer model and a heat generation model are used. The thermal conductivity of each layer material is different in GaN HEMT devices. In order to improve the accuracy of the simulation, the thermal conductivity model of the material is introduced. Considering that the generation and

recombination of carriers are related to temperature, the simulation also adds the SRH model. At the same time, the polarization model is also used in the simulation.

3. Simulation Results and Discussion

3.1. The Effects of Self-Heating Effect on Device Performance. In order to compare the effect of self-heating effect on the output curve of GaN HEMT devices, simulations were performed for conventional device structures. During the simulations, the gate-source voltage was varied from -2 to 0 V , and the drain voltage was varied from 0 V to 15 V . Figure 3(a) shows the output curve without considering the self-heating effect, which shows that the drain current does

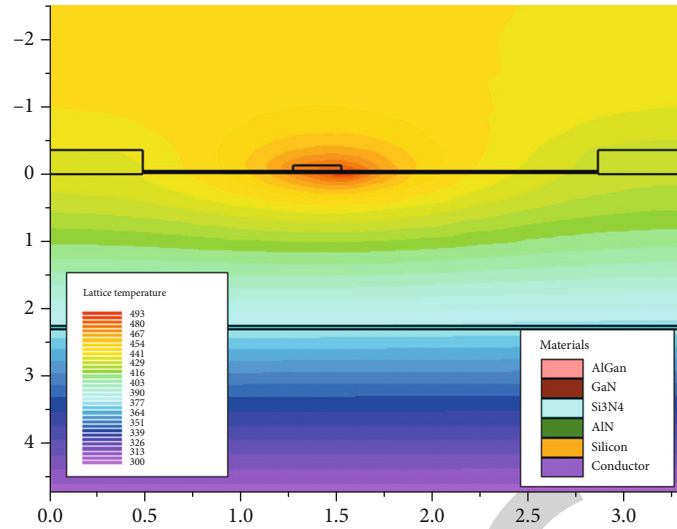


FIGURE 4: Temperature distribution of conventional device structure.

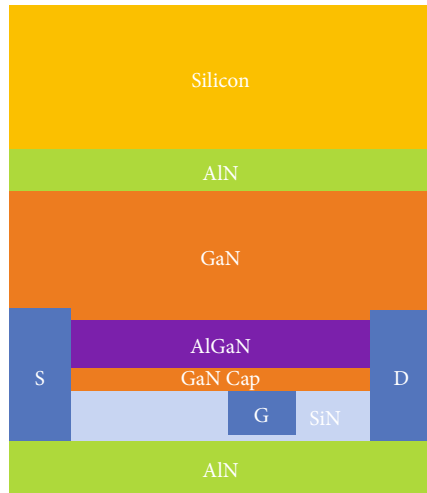


FIGURE 5: Flip-chip structure of the conventional device.

not drop rapidly when the drain voltage exceeds the knee point voltage. Figure 3(b) shows the output curve considering the self-heating effect, and it can be seen that the output current shows a significant drop at larger drain voltages, while at smaller gate voltages, the self-heating effect has less effect on the output current of the device.

Figure 4 shows the temperature distribution of the device at $V_{GS} = 0$ V. It can be seen that the temperature peak is 493 K when the substrate material of the device is Si and Si_3N_4 is the passivation layer. As shown in Figure 4, the temperature peak appears around the gate, and the maximum drain current is 1.08 A/mm. The simulation results show that the self-heating effect leads to the degradation of the device and reduces the performance of the device.

3.2. Effects of Diamond and SiC Materials on Device Temperature. The material's thermal conductivity coefficient limits the device's heat dissipation capability, and the higher the thermal conductivity, the better the heat dissipation. In

this paper, diamond material with high thermal conductivity is used as the substrate, and SiC material is used as the passivation layer. A flip-chip structure is also incorporated to highlight the contrast, as shown in Figure 5. The flip-chip structure is the original device structure upside down; the entire device buckled in the substrate. The dimensions of the flip-chip structure are the same as those of the referenced device structure.

Figures 6 and 7 show the channel temperature distribution curves and output curves for different device structures, respectively. It can be seen that the flip-chip structure with AlN substrate has a channel temperature peak of 424 K and a maximum output current of 1.35 A/ μm , while the device structure with diamond as the substrate and SiC as the passivation layer has a channel temperature peak as low as 360 K and a maximum output current of 1.65 A/ μm . Compared to the conventional device structure, the temperature peak of the device structure with diamond substrate and SiC passivation layer decreases by 133 K. In addition, the drain current increased by 0.57 A/ μm , and the current collapse was also significantly improved. Figure 8 shows the temperature distribution of the device structure with diamond substrate and SiC passivation layer. Due to the high thermal conductivity of diamond and SiC materials, the temperature is lowest in the substrate and passivation layer and highest near the channel. Therefore, the temperature difference allows the heat to be dissipated from both the substrate and the passivation layer. In addition, the temperature distribution near the channel is more uniform.

3.3. Effects of the Mixed Layer and Field Plate on Device Temperature. There is a limit to reducing the temperature of the device by changing the material. To further reduce the temperature of the device, the structure of the device must also be changed. Firstly, a new structure of the mixed potential layer is presented in this paper. The barrier layer under the gate is divided into two layers: the upper layer is an $\text{In}_{0.15}\text{Ga}_{0.85}\text{N}$, and the lower layer is AlGaN. Figure 9

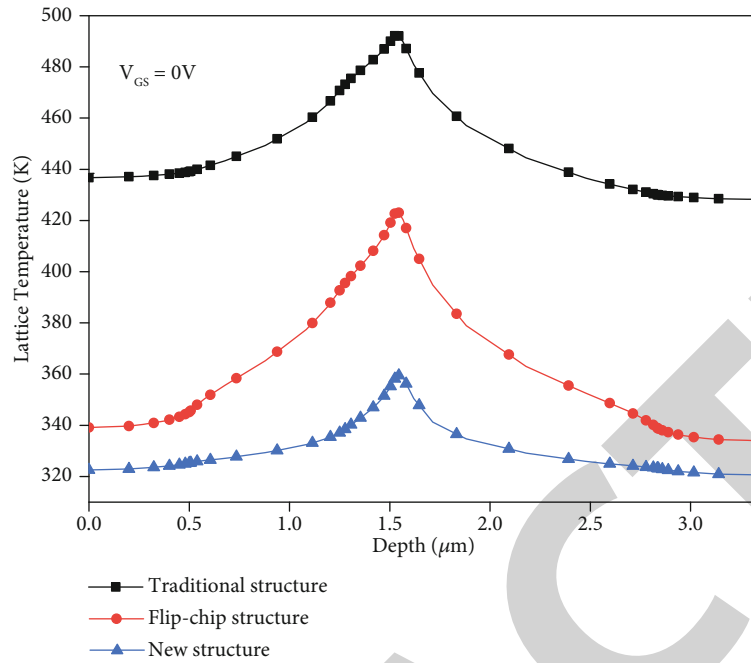


FIGURE 6: Comparison of channel temperature.

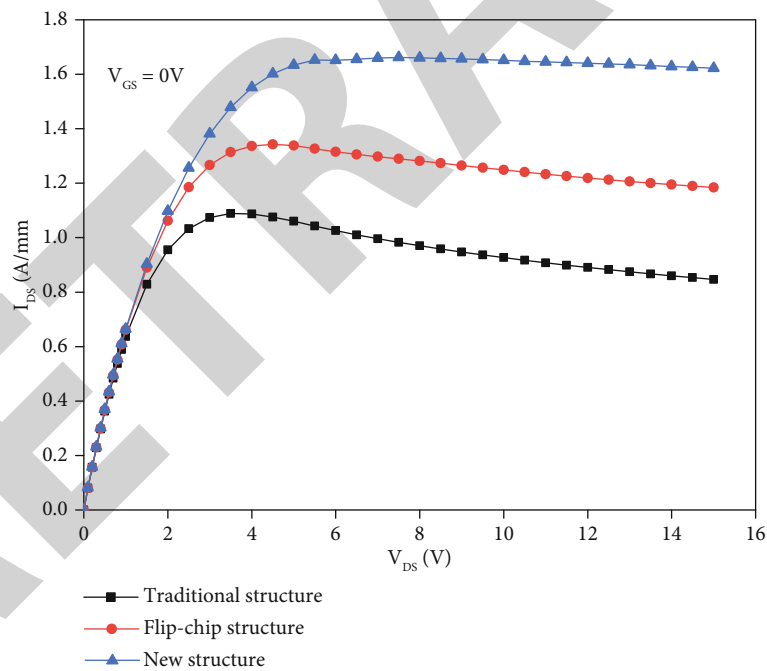


FIGURE 7: Comparison of output curves.

shows the effects of InGaN thickness in the potential barrier layer on the peak temperature and maximum output current. As can be seen from the figure, the temperature peak and maximum drain current decrease as the thickness of InGaN increases. When the thickness of InGaN is 5 nm, the channel temperature peak is 353 K, and the maximum drain current is 1.60 A/mm. This is when the peak channel temperature drops the most, and the current drops the least.

When the thickness of InGaN is greater than 5 nm, the temperature peak drops slowly while the maximum drain current drops sharply. The heterojunction formed by InGaN and AlGaIn induces a polarized negative charge, which decreases the electron concentration of the two-dimensional electron gas and leads to a decrease in the drain current. As a result, the temperature of the device can be reduced. In summary, the optimum thickness of InGaN is

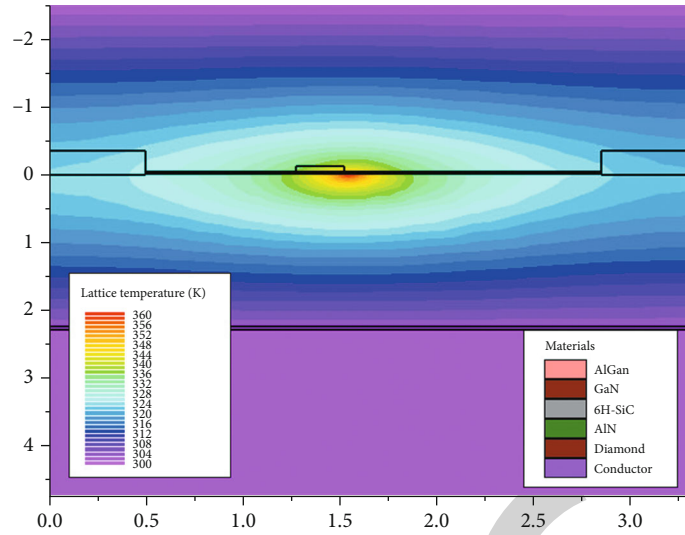


FIGURE 8: Temperature distribution of the device structure with diamond as the substrate and SiC as the passivation layer.

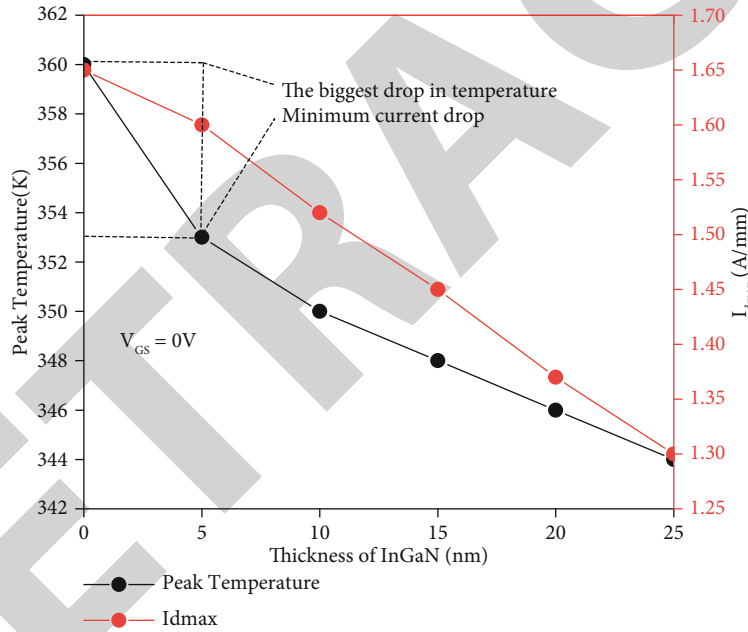


FIGURE 9: Effects of InGaN thickness on peak temperature and maximum drain current.

5 nm. Figure 10 shows a comparison of channel temperatures for InGaN thicknesses of 5 nm, with a 7 K drop in peak channel temperature and a more uniform channel temperature distribution for the structure with the hybrid barrier layer than for the structure without the hybrid barrier layer.

Secondly, the field plate is added at the gate near the drain, and the length of the field plate also impacts the device's performance. Figure 11(a) shows the effects of the length of the field plate on the channel temperature. As the length of the field plate increases, the channel temperature's peak gradually decreases, and the temperature spreads outward in a small way. Another peak in the channel temperature of the GaN HEMT device occurs when the length of the field plate is greater than $0.3 \mu\text{m}$. At the same time, it has been detrimental to reduce

the channel temperature of the device. Figure 11(b) shows the effects of field plate length on maximum output current and peak temperature. There is no new peak in channel temperature, and the output current is the nearby maximum when the channel length is $0.3 \mu\text{m}$. Although the use of field plates reduces the temperature, it also reduces the electron mobility and decreases the maximum output current of the GaN HEMT. As can be seen from the figure, the maximum output current decreases, then increases, and then decreases as the field plate length increases. Therefore, combined with Figure 11, it can be concluded that the optimal length of the field plate is $0.3 \mu\text{m}$ when temperature and output current are considered together. In addition, the thickness of the dielectric layer of the field plate is 35 nm. As shown in Figure 12, the final

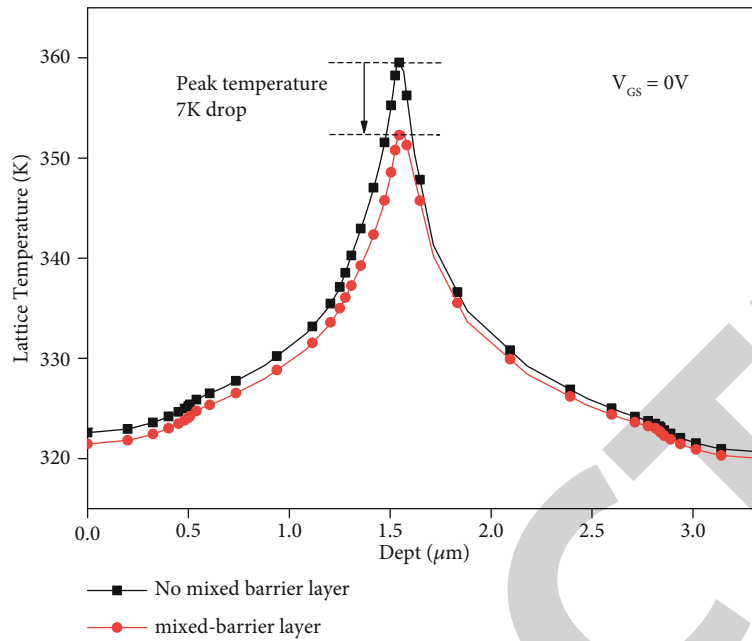


FIGURE 10: Comparison of channel temperature with and without a mixed barrier layer.

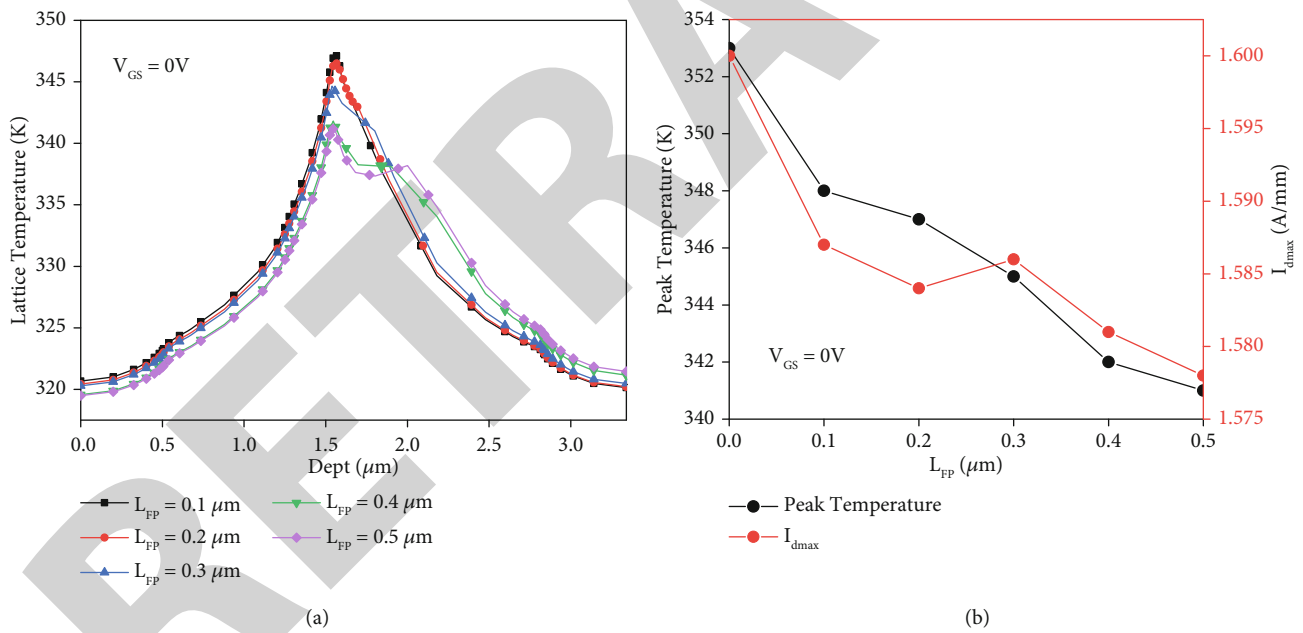


FIGURE 11: (a) Effects of field plate length on channel temperature. (b) Effects of field plate length on peak temperature and maximum output current.

temperature of the device is 345 K through material and structural changes, achieving a significant temperature reduction.

3.4. Analysis of Other Electrical Characteristics. GaN HEMT is a high-power device, and the magnitude of the saturation drain current has been an essential characteristic of the output characteristics. Figure 13 shows the comparison of the drain current between the conventional device structure and the new structure. The saturation drain current of the conventional device structure is 1.08 A/ μm , while the maxi-

imum saturation drain current of the new structure is 1.586 A/ μm , an improvement of about 47%. The current density increases due to its relationship to electron mobility and electric field. When the temperature of the device decreases, the lattice scattering effect decreases, and the electron mobility increases, which in turn increases the current density. The current collapse is also critical to the reliability of the device. Applying a linear approximation to the saturation region portion of the output characteristic curve, the current collapse rate of the conventional device is 22.5%.

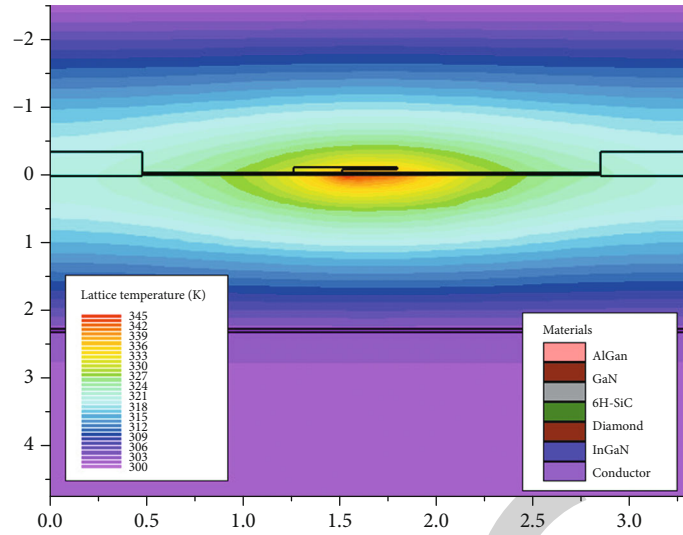


FIGURE 12: Temperature distribution of the final device structure.

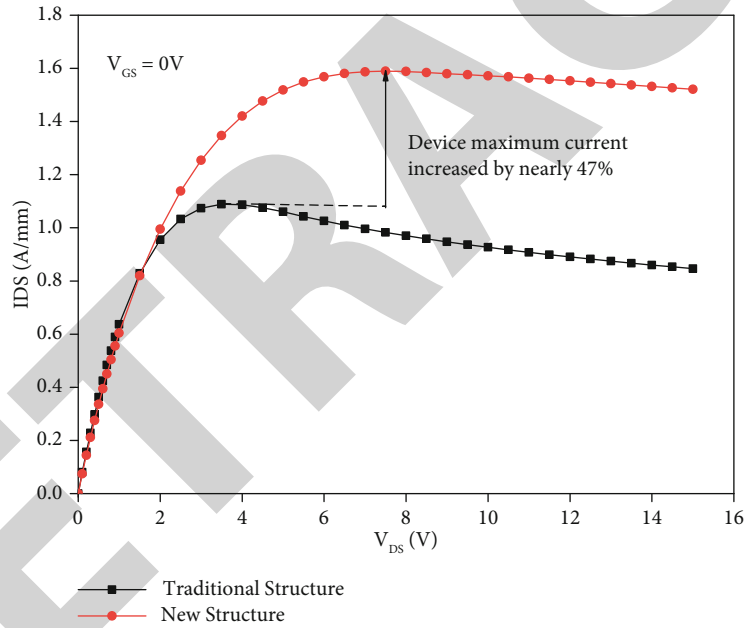


FIGURE 13: Comparison of the output curves of the conventional and new structures.

The new structure uses diamond and SiC materials, as well as a mixed barrier layer and field plate, to reduce device temperature, improve the electron mobility of the channel, and reduce the effect of temperature on device output characteristics. The current collapse rate is only 4.28%, and the improvement ratio is 18.22%, achieving significant improvement in the current collapse effect.

The transfer curves of the conventional and new structures are shown in Figure 14(a). As can be obtained from the figure, the threshold voltage of the conventional structure is -5.01 V, while the threshold voltage of the new structure is -5.56 V, which means that the device can be turned off at a lower voltage. Transconductance indicates the ability of

the gate voltage to control the drain current. The larger the transconductance, the stronger the gate voltage control to the channel. Figure 14(b) represents the transconductance curves of the conventional device structure and the new structure, which significantly improves transconductance compared to the conventional device structure. The peak transconductance of the conventional device structure is 282 mS/mA, while the peak transconductance of the new structure is 360 mS/mA. Compared with the peak transconductance of the traditional device structure, the peak transconductance of the new structure is increased by about 28%, indicating that the device's gate voltage has dramatically improved the control ability of the channel.

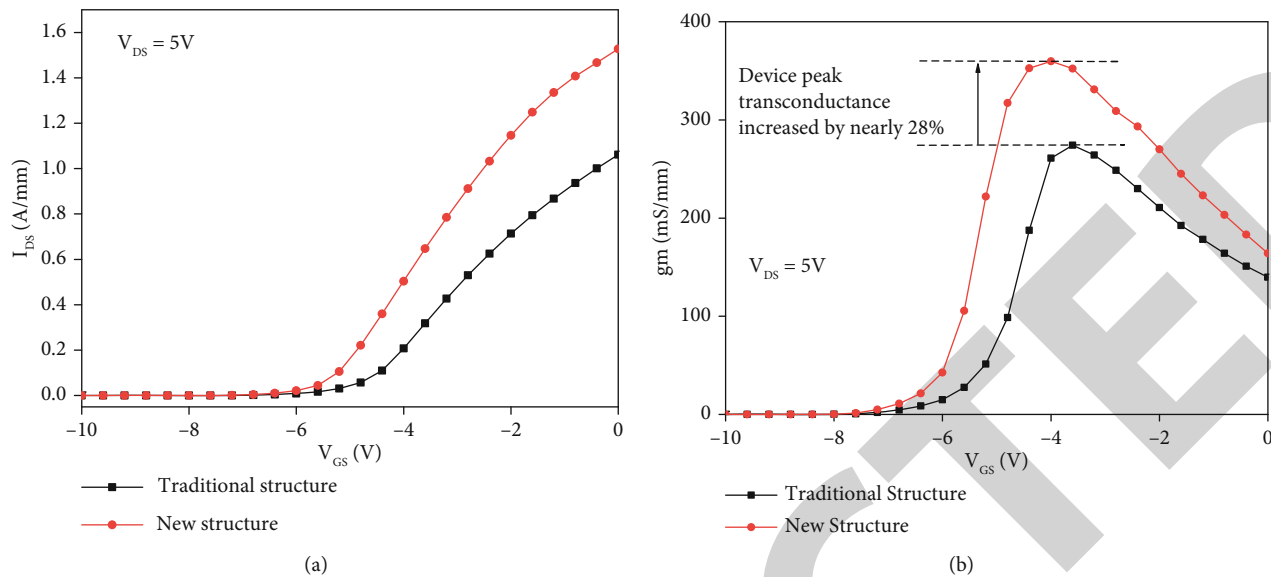


FIGURE 14: (a) Transfer curves of the traditional and new structures. (b) Transconductance curves of the traditional and new structures.

4. Conclusion

GaN HEMT devices have a wide range of applications in high-frequency and high-power fields. The research on GaN HEMT devices has made great progress so far, but with the high-power nonapplication, the increase of channel temperature caused by the self-heating effect of the device makes the thermal reliability problem become more and more serious. In this paper, the temperature of GaN HEMT devices at high bias voltage is reduced by changing the material and structure. The maximum temperature of the reference device structure is 493 K. The new structure uses diamond and SiC with high thermal conductivity as substrate and passivation layer to enhance the device heat dissipation in the vertical direction. Simulation results show that the new structure reduces the temperature by about 30%, increases the output current by 47%, and improves the transconductivity by 28% compared to the conventional structure. In addition, the current collapse improvement can reach 18.22%. Therefore, this new structure is suitable for operation at high temperature and high power, improving the reliability of GaN HEMT devices. The main goal for the future is to develop a multiphysics field 3D electric-thermal-force coupling model, which is expected to extract the device junction temperature and thermal stress more accurately. In this paper, specific experimental steps are lacking, and the relevant simulation data are obtained based on ideal cases, which need to be further verified in real situations. In the future, the process of GaN epitaxial layer preparation on diamond substrate can be improved to optimize the thermal characteristics of the device.

Data Availability

The experimental data used to support the findings of this study are available from the corresponding author upon request.

Conflicts of Interest

The authors declared that they have no conflicts of interest regarding this work.

References

- [1] P. Murugapandiyam, S. Ravimaran, J. William, J. Ajayan, and D. Nirmal, "DC and microwave characteristics of 20 nm T-gate InAlN/GaN high electron mobility transistor for high power RF applications," *Superlattices and Microstructures*, vol. 109, pp. 725–734, 2017.
- [2] F. Roccaforte, G. Greco, R. Lo Nigro, F. Giannazzo, F. Iucolano, and M. Saggio, "Emerging trends in wide band gap semiconductors (SiC and GaN) technology for power devices," *Microelectronic Engineering*, vol. 187, no. 5, pp. 66–77, 2018.
- [3] B. K. Jebalin, A. S. Rekh, P. Prajoun, D. Godwinraj, N. M. Kumar, and D. Nirmal, "Unique model of polarization engineered AlGaIn/GaN based HEMTs for high power applications," *Superlattices & Microstructures*, vol. 78, pp. 210–223, 2015.
- [4] X. Chen, S. Boumaiza, and L. Wei, "Self-heating and equivalent channel temperature in short gate length GaN HEMTs," *IEEE Transactions on Electron Devices*, vol. 66, no. 9, pp. 3748–3755, 2019.
- [5] N. V. Masalskii, "Influence of the self-heating effect on the I–V characteristics of field transistors on a silicon-on-insulator structure at high temperatures," *Journal of Communications Technology and Electronics*, vol. 65, no. 8, pp. 962–965, 2020.
- [6] S. J. Mukhopadhyay, M. Prajukta, A. Acharyya, and M. Mitra, "Influence of self-heating on the millimeter-wave and terahertz performance of MBE grown silicon IMPATT diodes," *Journal of Semiconductors*, vol. 41, no. 3, article 032103, 2020.
- [7] M. Werquin, C. Gaquiere, Y. Guhel et al., "High power and linearity performances of gallium nitride HEMT devices on sapphire substrate," *Electronics Letters*, vol. 41, no. 1, pp. 46–47, 2005.

Retraction

Retracted: Construction and Development of Modern Brand Marketing Management Mode Based on Artificial Intelligence

Journal of Sensors

Received 3 October 2023; Accepted 3 October 2023; Published 4 October 2023

Copyright © 2023 Journal of Sensors. This is an open access article distributed under the Creative Commons Attribution License, which permits unrestricted use, distribution, and reproduction in any medium, provided the original work is properly cited.

This article has been retracted by Hindawi following an investigation undertaken by the publisher [1]. This investigation has uncovered evidence of one or more of the following indicators of systematic manipulation of the publication process:

- (1) Discrepancies in scope
- (2) Discrepancies in the description of the research reported
- (3) Discrepancies between the availability of data and the research described
- (4) Inappropriate citations
- (5) Incoherent, meaningless and/or irrelevant content included in the article
- (6) Peer-review manipulation

The presence of these indicators undermines our confidence in the integrity of the article's content and we cannot, therefore, vouch for its reliability. Please note that this notice is intended solely to alert readers that the content of this article is unreliable. We have not investigated whether authors were aware of or involved in the systematic manipulation of the publication process.

In addition, our investigation has also shown that one or more of the following human-subject reporting requirements has not been met in this article: ethical approval by an Institutional Review Board (IRB) committee or equivalent, patient/participant consent to participate, and/or agreement to publish patient/participant details (where relevant).

Wiley and Hindawi regrets that the usual quality checks did not identify these issues before publication and have since put additional measures in place to safeguard research integrity.

We wish to credit our own Research Integrity and Research Publishing teams and anonymous and named external researchers and research integrity experts for contributing to this investigation.


The corresponding author, as the representative of all authors, has been given the opportunity to register their agreement or disagreement to this retraction. We have kept a record of any response received.

References

- [1] H. Cui, Y. Nie, Z. Li, and J. Zeng, "Construction and Development of Modern Brand Marketing Management Mode Based on Artificial Intelligence," *Journal of Sensors*, vol. 2022, Article ID 9246545, 11 pages, 2022.

Research Article

Construction and Development of Modern Brand Marketing Management Mode Based on Artificial Intelligence

Hailang Cui ¹, Yuankun Nie,¹ Zhanling Li,² and Jun Zeng³

¹Business School, Yunnan University of Finance and Economics, Kunming, Yunnan 650221, China

²Accounting School, Zhongnan University of Economics and Law, Wuhan Hubei 430073, China

³Accounting School, Yunnan University of Finance and Economics, Kunming, Yunnan 650221, China

Correspondence should be addressed to Hailang Cui; zz1771@ynufe.edu.cn

Received 29 July 2022; Accepted 25 August 2022; Published 20 September 2022

Academic Editor: Sweta Bhattacharya

Copyright © 2022 Hailang Cui et al. This is an open access article distributed under the Creative Commons Attribution License, which permits unrestricted use, distribution, and reproduction in any medium, provided the original work is properly cited.

The continuous development of the times and the application of artificial intelligence technology are more mature and common; as a new concept and way of thinking artificial intelligence technology plays an important role in brand marketing, brand marketing artificial intelligence era has truly arrived. Based on such a background, it is necessary to explore the value of artificial intelligence in brand marketing management and specific implementation strategies. With the help of artificial intelligence technology, we can realize the accurate capture of consumer demand, the accurate portrayal of consumer groups, and the high quality of brand marketing. The essence of strategic brand management is a brand management system based on brand value. With the help of the brand management system, all the company's contents are integrated and used to guide all the company's business actions. At the same time, the company's brand plan and framework are properly adjusted to constantly improve the brand's own value and promote the sustainable development of the brand and the company. In this paper, we briefly explain and analyze several brand marketing management modes and management countermeasures commonly used by modern enterprises and discuss the problems and optimization countermeasures in modern enterprise brand marketing management, hoping to enlighten the enhancement of enterprise brand marketing promotion effect and promote the sustainable development of enterprises.

1. Introduction

Artificial intelligence (AI) is a new technical science that simulates, extends, and extends the theories, methods, technologies, and application systems of human intelligence [1, 2]. In the past few years, innovative technologies represented by big data and artificial intelligence are reshaping the entire marketing industry, the application of AI to marketing can be seen as a disruption, and the introduction of AI allows brands to continuously adjust their marketing strategies through data to capture important business opportunities and value [3, 4]. The importance of "big data" in the field of artificial intelligence is very high, and data is considered to be the new energy in the information age. With the advent of the Internet era, the rapid development of information technology and big data has led to the rise of artificial intelligence (AI), which promotes the renewal of science and

technology in the industry and has profoundly affected the change of people's lifestyles and the innovation of business models [5, 6]. Artificial intelligence is a trendy term today, which covers a wide range of research on how to simulate human thinking and behavior to produce intelligent products that can respond with simulated human intelligence. Smartphones and intelligent robots are all products of artificial intelligence technology, bringing convenience and a new user experience to people's lives [7, 8]. The use of artificial intelligence in user data analysis and the experience of the value of user scenarios, as well as changes in human-computer interaction scenarios and behavioral habit insights can break the traditional marketing solidified thinking and can potentially change the marketing approach [9, 10]. Artificial intelligence and marketing from the media, brands to online operations at different stages, and from different types of analysis have different application scenarios. Combining

artificial intelligence and marketing, apply the analysis results of different data to different scenarios. At the same time, as artificial intelligence gradually deep into the marketing, the enterprise also faces three challenges, namely, the challenge of thinking, business challenges, and data challenges. For example, for business challenges, first, the use of IT technology to achieve the data of the enterprise's daily business is through the quantification and semantics of enterprise data management and user portrait depiction. Second, the marketing staff will promote the data business process, and the quantified user portrait will be directly used for customer analysis and positioning from the business perspective, so as to pave the way for the subsequent automated operation and continuously bring new value and business opportunities to the brand by combining technology and creativity around the pain points of the brand.

According to its internal conditions and external environment, the enterprise determines its mission and development goals. To ensure the realization of strategic planning and decision-making goals, the implementation of enterprise decisions relies on dynamic management in the implementation process [11, 12]. Enterprise strategy guides all enterprise activities, and the development and implementation of strategy are the focus of all management activities. The key to the development and implementation of strategy includes three aspects: first, analysis of changes in the external environment of the enterprise; second, review of internal conditions of the enterprise; and finally, the development of the strategic goals of the enterprise based on this and the dynamic balance of these three. Therefore, the task of strategic management is to achieve the strategic goals of the enterprise and maintain this dynamic balance by formulating strategy, implementing strategy and saying that management. The study [13, 14], on the other hand, studied the comprehensive competitiveness of corporate brands, and through this important indicator, fully recognized the opportunity brought by the rapid development of China's economy to enterprises, and that China has achieved a huge breakthrough in the cultivation of brand awareness and the creation of brand capability from scratch to excellence, which is unprecedented for China. Therefore, it is of great historical significance to improve the evaluation of brands for China's automobile enterprises. The study [15, 16] in "Strategic Brand Management and Control" starts from the development history of brands, explores and analyzes the measures and means for enterprises to strengthen their core competitiveness, and uses the extensive characteristics of brands to achieve a grasp of the connotation of brands. The elements of brand management such as how to establish a corporate brand management control system, scientifically manage each brand asset, optimize brand portfolio strategies, and innovate on mature brands are discussed, deepening the cohesion and understanding of deeper brand consciousness and enriching the essence of branding. Research [17, 18] in the article "Brand Management" based on the actual situation of enterprise development, from the enterprise practice to draw nutrients, came to the important conclusion that the development of enterprises cannot be separated from brand management. From the perspective

of enterprise brand management, the brand cultivation, brand management, and brand management of enterprises are introduced in detail. A sound management process—designing the brand, expanding the brand, perfecting the brand, and rebranding—is indispensable for a company to achieve long-term development. These basic brand development processes are the basic conditions for brand creation and are indispensable; therefore, companies should implement them without wavering in order to achieve true strategic brand management and operation.

In collecting domestic literature on brand strategy analysis, I found that although domestic scholars have rich research on brand strategy, it is not comprehensive, especially for domestic brand strategy research literature is not much, although there are also brand strategy research related articles, but brand management measures proposed on the lack of focus, and I hope the research in this paper can make up for the current lack of domestic research.

2. Modern Brand Marketing Management Mode

2.1. The Logical Model of Marketing Management Structure. The basis for the existence of modern marketing management ideas comes from the modern structure of market management. The framework has features related to existing elements of modern marketing management. This set of characteristics begins with human functional behaviors such as consumer behavior, organizational behavior, and adaptive behavior and creates stories based on the company's goal structure, business mechanisms, marketing relationships, and so on. Like resource allocation, supply, expenditure, etc., it reflects the essence of human production relations, exchange relations, consumption relations, and social relations. Modern market management is a comprehensive strategic socialization movement carried out in a broad social environment, its content is historical and practical, and there are many participants. Therefore, their governance structures cannot be analyzed and clarified from the perspective of traditional mechanisms, but can be explained with arguments based on the facts and reality of their existence in the sense of structural science and systems science. The content of the modern marketing management system clearly combines the three interdependent and interdependent components of marketing core elements, marketing organization core elements, and market environment computer peripherals. The market is based on consumer demographics. According to consumer demand, including potential demand determined by the nature of use and the scale of circulation, the logical structure corresponds to the potential market, efficient market, target market, and end consumer market for other goods or services. Marketing agencies often rely on their business and products or services to manage production and marketing to respond to the market and make a profit. The functional level of the organization is enterprise-level management, enterprise-level management, and product-level management. It is shown in Figure 1.

2.2. Current Situation of Enterprise Research

2.2.1. The Company's Market Competition Strategy. Now, private industrial enterprises understand the market, but not the market, to understand the market, product knowledge should be extended not only to commodities but also to quality issues, products, brands, services, etc. Enterprises as an effective complement to the national economy must have a deep understanding of the market, especially to survive and develop in the competition of large enterprises. Choosing the right sales and marketing staff is considered to solve the company's distribution problems, leading to a gap between marketing and production and purchasing and logistics. Private industrial companies no longer focus on business mechanisms, management, and mainstream competition, but on hype and packaging. At the same time, the means of market competition are unique, there is no market competition strategy, and price wars often focus on short-term rather than long-term interests.

2.2.2. The Construction of Marketing Channels of Enterprises. A marketing channel is a set of interrelated entities that facilitate the seamless transfer of products and services to consumers and users in market exchanges. Distribution channels create added value for end customers through the coordinated actions of their participants. In addition to horizontal channels, more and more multichannel marketing systems are making their voices heard, and channel members are also aware of the importance of channel resources and are trying to increase control over channel behavior through different strategies such as channel adjustment and channel smoothing. Participants are in the marketing channel "usually manufacturers, wholesalers, agents, retailers, subsidiaries and end users, consumers" and some distribution organizations. Each node in the channel system can be considered the next node provider and client of the previous node. The relationship between supply and demand runs through the entire channel process. Enterprises do not pay attention to channel creation, do not pay attention to the key links of the enterprise supply chain, and do not pay attention to the needs of market customers, which can easily lead to channel deadlock and serious channel conflicts.

2.2.3. Enterprise Sales Team Management and Talent Development. Currently, the management of the company is mainly controlled by the family, and the main investors are the main body. Currently, some private industrial companies have unclear stage skill requirements, unclear identification levels and professionals, insufficient attention to job structure, insufficient selection of appropriate tasks, lack of targeted identification strategies, and lack of initial identification. A major source of conflict between contractors and external talent is that many external talents suffer from overestimation of skills, unclear integration of business and personal goals, overlap or confusion between career plans and career goals, excessive demands on personal content, and lack of professional ethics. From a business perspective, we see no special requirements or business development stages for the above issues and implementation, and a thorough

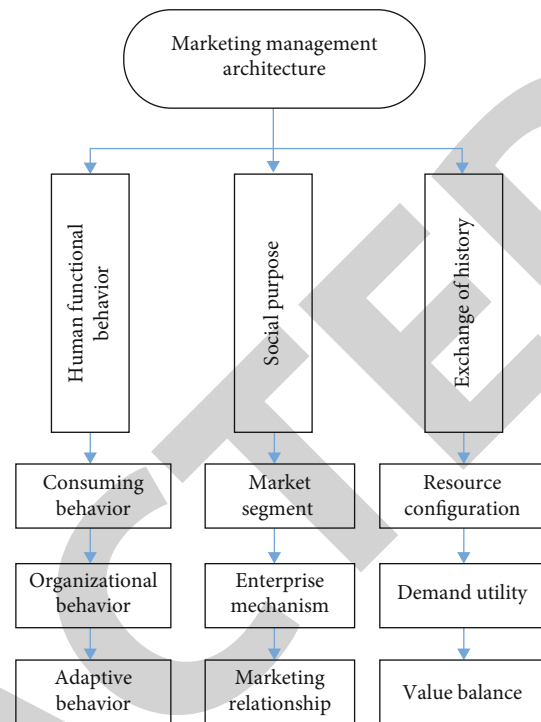


FIGURE 1: Logical model of marketing management architecture.

understanding of strategic options is essential. Gradually, based on the overall localization scheme, talents at different levels can be attracted to establish a management team with professional knowledge. For companies, it is important to move beyond family-based management in the start-up phase to accelerate the growth of the business.

2.3. Enterprise Marketing Cycle Theory

2.3.1. Characteristics of Product Introduction Period. When a new product just hits the market, this and the next generation of other branded products are not yet on the market. And the growing share continues to grow and even reaches replacement. We call this phase the initial phase of creating this product. The main feature of this stage is that the underlying demand in the initial market increases and the product becomes scarce. Although the volume on the market is small, sales are increasing. Second, other branded products of this generation have not yet entered the market. Products in this market occupy the entire market share, and there may be production products, but the cost of small units is high. Third, when there is competition, that is, the competition of this generation to replace the previous generation, the greater the comparative advantage of this generation in terms of price and quality, the longer the time of substitution.

2.3.2. Characteristics of Long-Term Growth of Enterprises. Due to the lack of products, knockoffs of other brands of this generation appeared and kept appearing on the market. Competition between different brands is getting fiercer. On the one hand, supply continues to increase, driving market growth and

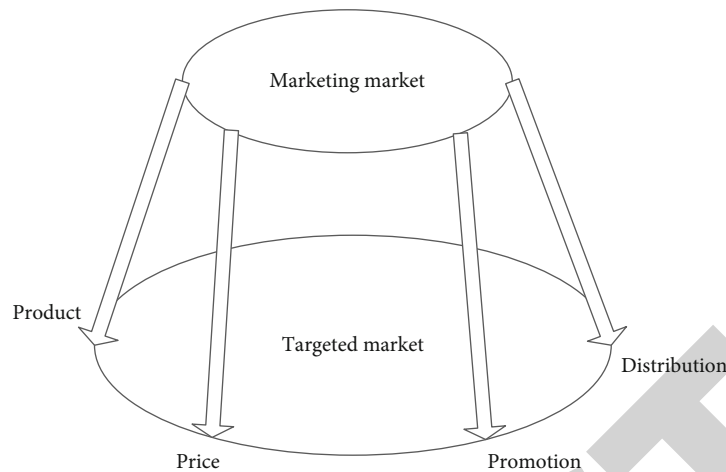


FIGURE 2: Marketing mix diagram.

sales, ultimately balancing supply and demand. On the other hand, different brands exchange information with each other and have their own market share, and social brands start reducing their share from the highest average price and finally reach the lowest price. The number of product brands in this stage increases rapidly, the market sales continue to increase, the absolute market turnover increases, the increase in the social supply capacity of the third product exceeds the increase in the social demand for this product, finally, the supply and demand balance is reached, and we call this stage the growth stage of the production of this product.

2.3.3. Characteristics of Enterprise Maturity. Due to the high switching cost of exiting the industry and the inertial products produced by the company reaching a balance between supply and demand, the competition between different brand products is further intensified. Prices of some products began to drop to stimulate sales growth. The market share is increasingly towards low cost prices, and the concentration of high-quality brands further promotes the scale expansion of these famous brands, which in turn drives the growth of social demand and sales. However, the products of other brands, under the background of market sales growth, have a backlog of products, their market share has declined, and finally, they must withdraw from the market. After a lot of scouring the sand, some famous brand products and leading companies finally appeared in the market. We call this stage the maturity of this generation of products. The main features of this stage are first, many well-known brands in the market are continuously optimized and concentrated in the process of elimination, forming some brand-name products; second, there is an oversupply of products, product prices fall, market sales increase, and absolute market profits may fall; third, the number of brands is decreasing, the average market share of brands rises from the lowest value and eventually reaches the highest value, and the profitability of brand-name products increases, as shown in Figure 2.

2.4. Strategic Management Process Theory. Strategic management process is a reasonable way for enterprises to gain stra-

tegic competitiveness and achieve excessive profits. It is a dynamic management process in which the three links of strategic analysis, strategic selection and evaluation, and strategic implementation and control are interrelated, repeated, and perfected.

The first step of the strategic management process is to analyze the internal and external environment where the enterprise is located. The external environment is analyzed to find the opportunities as well as threats to the development of the enterprise, to make use of the opportunities in the external conditions and to avoid the threats and other unfavorable factors in the strategy formulation and selection. The analysis of the internal environment is to develop the company's own strengths or weaknesses, so that it can make use of its own resources efficiently by avoiding its weaknesses when formulating and implementing strategies.

The second step of the strategic management process is the selection of strategy, and the essence of this process is to explore, develop, and select a strategy. With limited resources and capabilities, enterprises cannot choose all possible directions of development. Through strategic selection, enterprises can make use of their resources and capabilities to adapt to changes in the external environment, so as to achieve sustainable competitive advantages over competitors. The external opportunities and challenges are the external motivation for strategic choice, and the internal advantages and disadvantages are the constraints for strategic choice.

The third step of the strategic management process is the implementation and control of the strategy. After formulating the strategic plan, the enterprise needs to realize the strategic objectives through specific action plans. Generally, the implementation of the strategy can be promoted through the following aspects: developing functional strategies including specific production, R&D, and sales; constructing the organizational structure of the enterprise; and providing a favorable environment for the implementation of the enterprise strategy. In the specific implementation process to control the implementation, compare the feedback back to the actual results and the previously formulated strategic objectives, if there is a certain deviation, it is necessary to provide effective

measures to correct, if necessary need to reexamine the internal and external environment, develop and select a new strategic plan, and repeat the start of a new round of strategic management implementation process.

3. Artificial Intelligence Algorithms

3.1. GA Genetic Algorithm. Genetic algorithm (GA) is a computational model of biological evolution that simulates the natural selection and genetic mechanism of Darwinian biological evolution and is a method to search for the optimal solution by simulating the natural evolutionary process. Combining GA genetic intelligence algorithm with cognitive waveform technology, a GA genetic intelligence algorithm model based on adaptive waveform optimization is constructed. In this chapter, the theory of neural network and backpropagation algorithm is deeply analyzed and studied, GA genetic intelligence algorithm is applied to cognitive transmission system, and the adaptive parameter learning strategy of GA genetic intelligence algorithm is proposed. The sample data set is obtained through the adaptive waveform system constructed in Chapter 3, the pulse width T and the signal-to-noise ratio (SNR) are used as the input training data of the neural network, and the bit error rate is used as the output training data. The adaptive waveform parameter and environmental parameter learning model are used to verify the prediction performance of the constructed model by MATLAB code simulation. At the same time, the error analysis of the prediction model is carried out, and the influence of the number of samples on the prediction performance is studied. The simulation results show that the proposed GA genetic intelligence algorithm model has a good prediction effect. Compared with the adaptive waveform algorithm, the bit error rate prediction curve based on the GA genetic intelligence algorithm has a better convergence effect and effectively reduces the system code implementation. It can help the system achieve more efficient and intelligent cognitive communication.

$$P_G(z) = \frac{1}{\sigma\sqrt{2\pi}} \exp\left[-\frac{(z-\mu)^2}{2\sigma^2}\right], \quad (1)$$

$$R_G(t) = \frac{N_0}{2} \cdot \delta(t), \quad (2)$$

$$s_G(f) = \frac{N_0}{2}. \quad (3)$$

Lognormal noise refers to a noise signal whose logarithm of the probability density function follows a normal distribution. By consulting many literatures, it is found that in the measurement and control system, when the high-resolution radar observes the ground or the observation angle is small, the probability density curve of the ground clutter fits the logarithmic state distribution, so the ground clutter interference of the measurement and control communication system can be replaced with lognormal noise. The probability density function formula of lognormal noise

is expressed as

$$p_L(x, \mu, \sigma) = \left\{ \frac{1}{x\sigma\sqrt{2\pi}} \exp\left[-\frac{(\ln x - \mu)^2}{2\sigma^2}\right] \right\}, \quad (4)$$

$$E_n(x) = \exp\left(\frac{(\mu + \sigma^2)}{2}\right), \quad (5)$$

$$D_n(x) = [\exp(\sigma^2) - 1] \cdot \exp(2\mu + \sigma^2). \quad (6)$$

The probability density function distribution of the sea clutter noise obeys the distribution, so the sea clutter noise is also called Weber noise. The distribution of the probability density function of sea clutter noise obeys the distribution, so sea clutter noise is also called Weber noise. The expression of the probability density function of the noise distribution is equation (7). The measurement and control communication environment includes land, ocean, space, and other scenarios, among which, sea clutter is the main noise interference source of sea surface measurement and control communication.

$$f(x, \lambda, k) = \left\{ \frac{k}{\lambda} \left(\frac{x}{\lambda}\right)^2 \exp\left[-\left(\frac{x}{\lambda}\right)^k\right] \right\}, \quad (7)$$

$$J(t) = A_s \cos(2\pi f_s t + \varphi_s). \quad (8)$$

3.2. Minimum Mean Square Error Optimization Criterion. The minimum mean square error optimization criterion is a criterion function that minimizes the mean square error of unknown and known quantities. In the target detection of the measurement and control system, the smaller the MMSE value is, the better the target tracking effect is. At time $k+1$, the filtering state estimation error is expressed as

$$\mathcal{E}_{k+1|k+1}(\gamma_k) = x_{k+1} - x_{k+1|k+1}(\gamma_k). \quad (9)$$

The estimated state value is calculated from the waveform parameters at time $k+1$, and the mean square error function is expressed as

$$F[\mathcal{E}_{K+1|K+1}(\gamma_k)] = E\left[\left\|\mathcal{E}_{K+1|K+1}(\gamma_k)\right\|^2\right], \quad (10)$$

Then, the criterion function of the minimum mean square error criterion can be expressed as

$$\gamma_K^* = \arg \min \left\{ E\left[\left\|\mathcal{E}_{K+1|K+1}(\gamma_k)\right\|^2\right] \right\}. \quad (11)$$

The maximum signal-to-noise ratio optimization criterion is a criterion function that maximizes the ratio of signal strength to noise strength. During environmental detection, the transmitted signal will be interfered by various clutter and noise during the transmission process, and the noise intensity in the environment will change in real time with time, which will affect the real-time change of

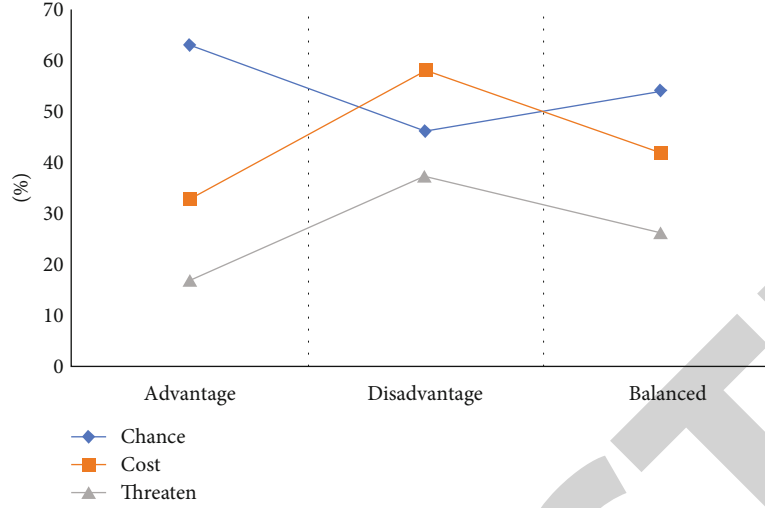


FIGURE 3: SWOT marketing matrix of enterprises.

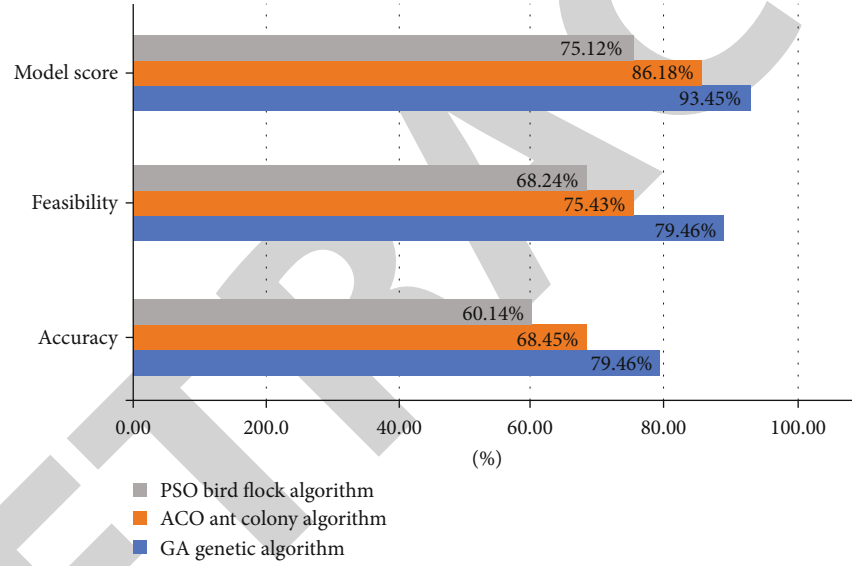


FIGURE 4: Performance comparison under different artificial intelligence algorithms.

the signal-to-noise ratio. Therefore, when the signal-to-noise ratio reaches the maximum value, the corresponding waveform parameters currently are most suitable for the current environment. The criterion function for the signal-to-interference-to-noise ratio is

$$\text{SINR} = \frac{|y_s^2(t)|}{E[|y_n^2(t)|]}, \quad (12)$$

$$a_k^* = \arg \max \left\{ \frac{|y_s^2(t)|}{E[|y_n^2(t)|]} \right\}. \quad (13)$$

The minimum mean square error criterion is not suitable for the measurement and control communication scenario because among the two criterion functions we have discussed above, the minimum mean square error criterion is mostly used in the tracking and detection system of cog-

nitive radar, which is more concerned with the accuracy of target state estimation, while the communication scenario in this paper is a measurement and control communication environment, which is more concerned with communication, quality optimization rather than target tracking and state estimation.

$$P_e = \frac{m_s}{n_s} \times 100\%, \quad (14)$$

$$\theta_k^* = \arg \min \left\{ \frac{m_s}{n_s} \times 100\% \right\}. \quad (15)$$

3.3. Quantized Convolution Calculation. The quantized convolution calculation is a convolution calculation using the quantized low-bit value, and the quantized convolution calculation that does not require an inverse quantization operation will be introduced. Different from the numerical

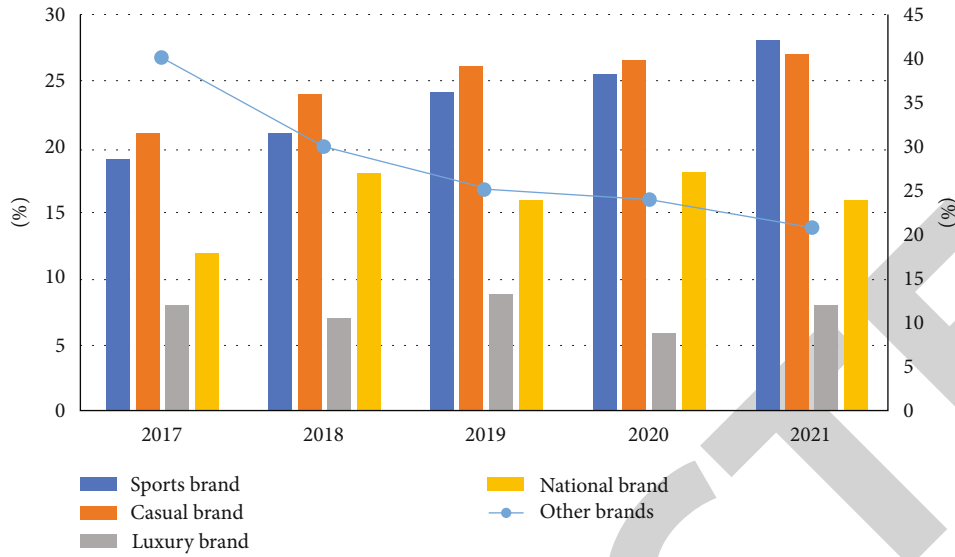


FIGURE 5: Marketing share of different brands.

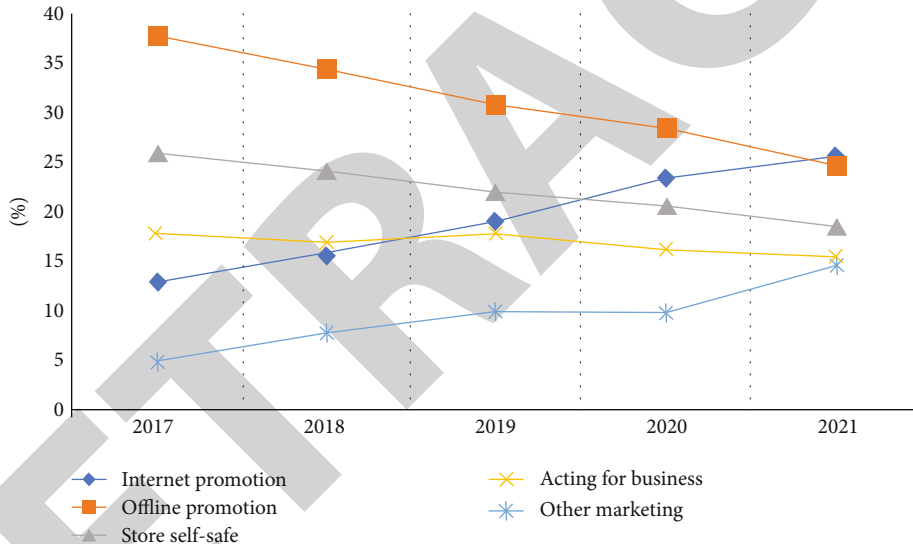


FIGURE 6: Proportion of different brand marketing strategies.

compression network that requires inverse quantization during model inference, the quantized convolution calculation only needs to perform sparse prediction (whether it is zero or not) and does not require inverse quantization to restore numerical accuracy, so less computation is required. The amount and less computational complexity, the operation is faster. Equation (16) shows a classical convolution calculation process:

$$Y = \sum_i^N w_i \otimes x_i, \quad (16)$$

where the multiplication sign represents the convolution operation. For simplicity of description, the bias is ignored here. For a given quantization function f , the correspond-

ing quantization convolution calculation process is shown in formula (17), where the plus sign represents the low-bit numerical quantization convolution operation.

$$f(Y) = f\left(\sum_i^N w_i \otimes x_i\right), \quad (17)$$

$$f(Y) = f\sum_i^N f(w_i \otimes x_i). \quad (18)$$

Since SeerNet only needs to predict the sparsity of the feature, that is, the spatial position of the zero value in the feature map after the ReLU layer and the max pooling layer, SeerNet does not need to perform inverse quantization. The calculation process of quantization convolution

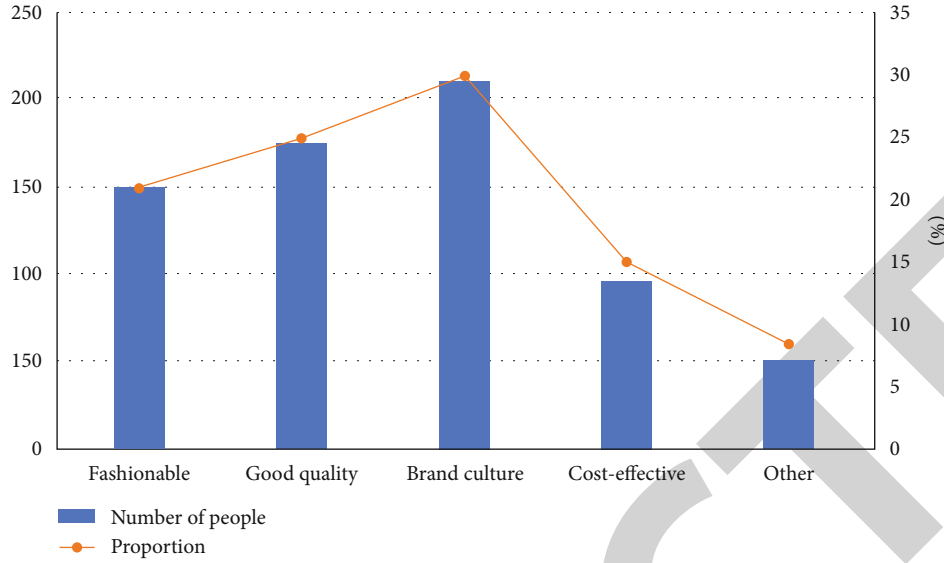


FIGURE 7: Marketing competitive advantages of different brands.

is shown in the following formula:

$$\text{sign}(f(Y)) = \text{sign} \left(\sum_i^N (f_w(w_i) \oplus f_x(X_i)) \right). \quad (19)$$

In many commonly used CNN models, Conv layers are usually followed by different combinations of batch normalization layers, ReLU layers, and max pooling layers. ReLU makes negative-valued features become zero-valued features, the max pooling layer makes only the value with the largest absolute value in a subregion to be retained, and other positions are discarded.

$$s(t) = A \cdot \text{rect} \left(\frac{t}{T} \right) \cdot \exp \left[j \left(2\pi fct + \frac{kt^2}{2} \right) \right]. \quad (20)$$

4. Construction and Development of Modern Brand Marketing Management Model under the Background of Artificial Intelligence

4.1. Modern Brand Marketing Management Mode under the Background of Artificial Intelligence. About the concept of brand strategy, commonly speaking, it is a corporate strategy implemented by enterprises to open up the market, increase the market share, and obtain a greater rate of return, through the improvement of product quality, considerate and meticulous service, and other means to increase the visibility of the enterprise in the industry and create a good brand image. Brand not only refers to the product's trademark, packaging, and other external signs but also the product quality, performance, quality, cost-effective, and other

aspects of the comprehensive performance. The brand strategy is a collection of enterprise reputation, production and operation, product development, human management, and other comprehensive work involving enterprise operation, which has a decisive role in the hierarchical position of the enterprise in the market body and needs to be raised to the core position of the top-level design of enterprise management. Therefore, the purpose of corporate brand strategy formulation is to maximize the brand influence in the industry and to be able to meet or even exceed customers' expectations of the company or its products.

Corporate brand strategy management is systematic, long-term, and comprehensive and is an effective way to cultivate corporate competitiveness, accumulate competitive advantages, and differentiate from competitors. However, within the enterprise, the implementation of brand strategy is related to all important departments such as technology, finance, personnel, and sales and is the result of mutual collaboration and cooperation; outside the enterprise, the brand strategy will involve the upstream and downstream industrial chain, sales, and circulation of all links, so it is necessary to systematically plan the brand strategy of the enterprise.

Under the market economy, in order to win in the extremely fierce interenterprise competition, as a business operator, we must put the brand strategy management in an important position, improve the ability of resource integration and management, give full play to the role of the top-level design of managers, establish a good enterprise target positioning and continuous reform and innovation, improve the quality and efficiency of enterprise development, establish positive corporate values, and promote the transformation of enterprises in the competition. In order to form a unique competitive advantage, the enterprise can develop steadily and healthily. Enterprises should first have a clear market positioning of their products, take targeted measures around the market positioning, and produce and operate products with their own characteristics and market

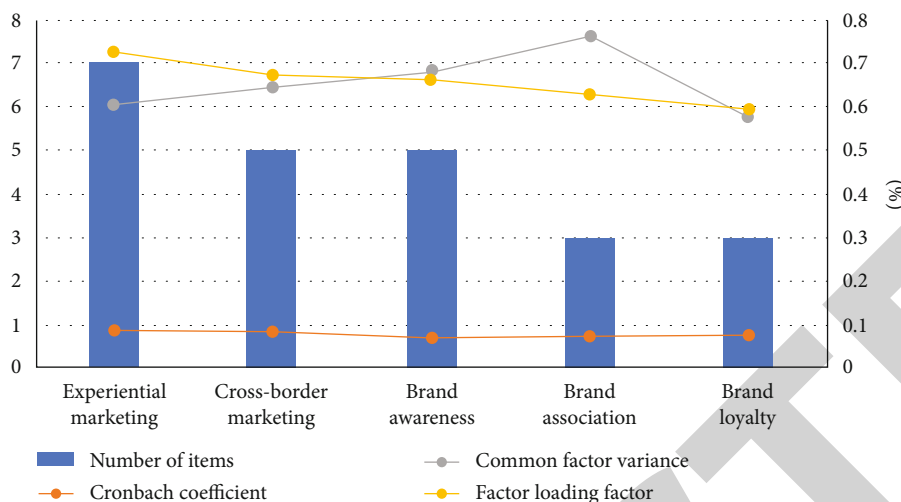


FIGURE 8: Reliability and validity test of different brands.

TABLE 1: Reliability and validity test of different brands.

	Experiential marketing	Cross-border marketing	Brand awareness	Brand association	Brand loyalty
Number of items	7	5	5	3	3
Cronbach coefficient	0.872	0.854	0.718	0.744	0.786
Common factor variance	0.605	0.645	0.681	0.759	0.576
Factor loading factor	0.726	0.673	0.66	0.628	0.594

needs, so as to stand out in the market competition for enterprises. “Know yourself and your enemy, a hundred battles will not be lost,” in the market competition, the enterprise only on the brand strategy for continuous self-analysis, the brand concept will be deeply implemented to each employee and enhance the cohesion of the enterprise staff, to be able to avoid deficiencies in the competition, strengths, and weaknesses and constantly improve business performance.

From the data in Figure 3, we can see that when an enterprise is in competitive competition, its opportunities account for 63%, costs account for 33%, and threats account for 17%. The proportion is 46%, the cost is 58%, and the threat is 37%; when the enterprise is in balanced competition, its opportunity is 54%, the cost is 42%, and the threat is 26%.

From the data in Figure 4, we can see that the accuracy of the GA genetic algorithm is 79.46%, the feasibility is 89.27%, and the average score of the model is 93.45%; the accuracy of the ACO ant colony algorithm is 68.45%, and the feasibility is 75.43%; the average score of the model is 86.18%; the accuracy of the PSO bird flock algorithm is 60.14%, the feasibility is 68.24%, and the average score of the model is 75.12%. The various performances of the GA genetic algorithm are the most accurate and reliable under the three still-intelligent algorithm models.

From the data in Figure 5, we can see that from 2017 to 2021, my country’s sports brands and leisure brands show a steady upward trend. In 2017, sports brands accounted for 19% of marketing, and in 2021, the proportion of marketing

rose to 28%; in 2017, leisure brands accounted for 21% of marketing, and by 2021, the proportion of marketing has risen to 27%, while luxury brands accounted for 8% of marketing in 2017 and 8% in 2021.

From the data in Figure 6, we can see that the current marketing methods of different brands mainly include Internet promotion, online promotion, self-selling in stores, and agency business. In 2017, Internet sales accounted for 13%, online sales accounted for 38%, store sales accounted for 26%, and agency business accounted for 18%; in 2018, Internet sales accounted for 16%, online promotion accounted for 34.5%, store sales accounted for 24.3%, and agent business accounted for 17.2%; in 2019, Internet sales accounted for 18.9%, online promotion accounted for 31%, and store sales accounted for 17.2%. 2.1% and 18% of the agents are engaged in business.

4.2. Construction and Development of Modern Brand Marketing Management Model. Under the increasingly fierce market competition of various brand products, the marketing of each brand not only actively improves the existing organizational structure to ensure a competitive advantage in development and operation but also pays special attention to the management of distribution channels, which greatly increases its profits. Improve marketing efficiency. In addition, in the process of operation, the company has also formulated a scientific strategic investment plan, sponsored large-scale events, and used the influence of celebrities to strengthen the brand, providing consumers with the possibility to enhance brand awareness. A rich

brand culture is the company's greatest competitiveness. But the company's current celebrity clout is difficult to replicate, especially for younger consumers in this day and age.

From the data in Figure 7, we can see that the main advantage of different brands in marketing competition is the degree of novelty of styles, with 150 people accounting for 21% and 175 people accounting for 25% of quality problems. The number of respondents is 210, accounting for 30%; the number of cost-effective people is 95, accounting for 15%.

From the data in Figure 8 and Table 1, we can see that the KMO value obtained by inspection is 0.946, which is close to 1, and the significance of 0.000 is greater than 0.05. In factor analysis, the cumulative variance of each item is 62.496%, which is greater than 50%. The common degree of each item is greater than 0.4, indicating that the information loss of each variable is less. The factor loading coefficients are all greater than 0.4, which proves that there is a correlation between variables and items.

5. Conclusion

The rapid development of the Internet era has led to the rapid development of artificial intelligence, which also has a profound impact on people's lifestyles. Companies have to develop unique intelligent products according to the rapidly changing market, timely adjustment of marketing strategies planned and organized marketing activities to provide consumers with satisfactory intelligent products and services, and marketing strategy is an important guarantee to achieve corporate value. However, any marketing strategy and means to bring consumers a sense of freshness is short-lived, especially for different consumer groups using the same marketing tools will certainly have limitations. At this point, enterprises must find a breakthrough, flexible response to market demand, the pursuit of more novel marketing strategies to attract consumers, and achieve sustainable development of enterprises. The core of strategic brand management is a brand management system based on brand values. With the help of brand management system, we can integrate the whole company's content and control the whole business of the company, while correctly matching the brand design and the company's reference structure with the company's own value, so that the brand can be continuously developed and strengthened, and the added value of the company can be continuously increased to achieve sustainable development.

Data Availability

The experimental data used to support the findings of this study are available from the corresponding author upon request.

Conflicts of Interest

The authors declared that they have no conflicts of interest regarding this work.

Acknowledgments

This study was funded by National Natural Science Foundation of China, The Effect of Negative Information on Brand Equity: The Moderating Role of Local vs. Foreign Brands (71662036) and 2021 Yunnan Provincial Department of Education Project Teacher Project, Research on brand marketing of Yunnan cities under the "One Belt, One Road" initiative (2021J0585).

References

- [1] A. Ligeza, "Artificial intelligence: a modern approach," *Applied Mechanics & Materials*, vol. 263, no. 2, pp. 2829–2833, 2009.
- [2] F. Glover, "Future paths for integer programming and links to artificial intelligence," *Computers & Operations Research*, vol. 13, no. 5, pp. 533–549, 1986.
- [3] P. Norvig and S. Russell, "Artificial intelligence: a modern approach (all inclusive), 3/E," *Applied Mechanics & Materials*, vol. 263, no. 5, pp. 2829–2833, 2005.
- [4] M. Negnevitsky, "Artificial intelligence: a guide to intelligent systems," *Information & Computing Sciences*, vol. 48, no. 48, pp. 284–300, 2005.
- [5] P. R. Cohen, "Empirical methods for artificial intelligence," *IEEE Intelligent Systems*, vol. 11, no. 6, p. 88, 2016.
- [6] I. A. Hardabkhadze, "Analysis of the key influence factors on brand of higher education organizations. Feature of the fashion industry," *Marketing, Menedment Innovacij*, vol. 4, no. 1, pp. 1–12, 2013.
- [7] F. Vlkner, H. Sattler, and T. Hennig-Thurau, "The role of parent brand quality for service brand extension success," *Social Science Electronic Publishing*, vol. 13, no. 4, pp. 379–396, 2010.
- [8] S. Lei, C. Ghosh, and S. Han, "Should they play? Market value of corporate partnerships with professional sport leagues," *Journal of Sport Management*, vol. 24, no. 6, pp. 702–743, 2010.
- [9] Y. Yang, "Research on the brand construction of agritourism enterprise in Chongqing," *Asian Agricultural Research*, vol. 8, no. 5, pp. 50–53, 2016.
- [10] T. Depoo and G. D. Shanmuganathan, "An empirical investigation on leadership styles applied for global brand management of multinational organizations in the United States," *Open Journal of Business & Management*, vol. 1, no. 2, pp. 11–17, 2013.
- [11] F. Glanert, "ss," *3R International*, vol. 40, no. 1, pp. 21–24, 2001.
- [12] Z. Zhu, T. Gao, and C. Shi, "Development and design of tourism destination marketing system," *Journal of Applied Sciences*, vol. 13, no. 23, pp. 5564–5567, 2013.
- [13] W. S. Siu and D. Kirby, "Small firm marketing: a comparison of Eastern and Western marketing practices," *Asia Pacific Journal of Management*, vol. 16, no. 2, pp. 259–274, 2000.
- [14] L. Sin, A. Tse, O. Yau, R. P. M. Chow, J. S. Y. Lee, and L. B. Y. Lau, "Relationship marketing orientation: scale development and cross-cultural validation," *Journal of Business Research*, vol. 58, no. 2, pp. 185–194, 2005.
- [15] M. H. Zhou, F. D. Wang, and H. H. Zhang, "Method of enterprise marketing risk early-warning and the index system construction," in *IEEE international conference on Management of Innovation & technology*, pp. 718–722, Singapore, 2006.
- [16] S. Bag, S. Gupta, A. Kumar, and U. Sivarajah, "An integrated artificial intelligence framework for knowledge creation and

Retraction

Retracted: A Machine Learning in Binary and Multiclassification Results on Imbalanced Heart Disease Data Stream

Journal of Sensors

Received 23 January 2024; Accepted 23 January 2024; Published 24 January 2024

Copyright © 2024 Journal of Sensors. This is an open access article distributed under the Creative Commons Attribution License, which permits unrestricted use, distribution, and reproduction in any medium, provided the original work is properly cited.

This article has been retracted by Hindawi following an investigation undertaken by the publisher [1]. This investigation has uncovered evidence of one or more of the following indicators of systematic manipulation of the publication process:

- (1) Discrepancies in scope
- (2) Discrepancies in the description of the research reported
- (3) Discrepancies between the availability of data and the research described
- (4) Inappropriate citations
- (5) Incoherent, meaningless and/or irrelevant content included in the article
- (6) Manipulated or compromised peer review

The presence of these indicators undermines our confidence in the integrity of the article's content and we cannot, therefore, vouch for its reliability. Please note that this notice is intended solely to alert readers that the content of this article is unreliable. We have not investigated whether authors were aware of or involved in the systematic manipulation of the publication process.

Wiley and Hindawi regrets that the usual quality checks did not identify these issues before publication and have since put additional measures in place to safeguard research integrity.

We wish to credit our own Research Integrity and Research Publishing teams and anonymous and named external researchers and research integrity experts for contributing to this investigation.

The corresponding author, as the representative of all authors, has been given the opportunity to register their agreement or disagreement to this retraction. We have kept a record of any response received.

References

- [1] D. Hamid, S. S. Ullah, J. Iqbal, S. Hussain, C. A. u. Hassan, and F. Umar, "A Machine Learning in Binary and Multiclassification Results on Imbalanced Heart Disease Data Stream," *Journal of Sensors*, vol. 2022, Article ID 8400622, 13 pages, 2022.

Research Article

A Machine Learning in Binary and Multiclassification Results on Imbalanced Heart Disease Data Stream

Danish Hamid,¹ Syed Sajid Ullah,^{2,3} Jawaid Iqbal,¹ Saddam Hussain ⁴,
Ch. Anwar ul Hassan ¹ and Fazlullah Umar ⁵

¹Capital University of Science & Technology, Islamabad 44000, Pakistan

²Department of Information and Communication Technology, University of Agder (UiA), N-4898 Grimstad, Norway

³Department of Electrical and Computer Engineering, Villanova University, Villanova, PA 19085, USA

⁴School of Digital Science, Universiti Brunei Darussalam, Jalan Tungku Link, Gadong,

Bandar Seri Begawan BE1410, Brunei Darussalam

⁵Khana-e-Noor University, Pol-e-Mahmood Khan, Shashdarak, 1001 Kabul, Afghanistan

Correspondence should be addressed to Saddam Hussain; saddam_1993@hotmail.com

Received 5 July 2022; Revised 5 August 2022; Accepted 10 August 2022; Published 20 September 2022

Academic Editor: Praveen Kumar Donta

Copyright © 2022 Danish Hamid et al. This is an open access article distributed under the Creative Commons Attribution License, which permits unrestricted use, distribution, and reproduction in any medium, provided the original work is properly cited.

In medical field, predicting the occurrence of heart diseases is a significant piece of work. Millions of healthcare-related complexities that have remained unsolved up until now can be greatly simplified with the help of machine learning. The proposed study is concerned with the cardiac disease diagnosis decision support system. An OpenML repository data stream with 1 million instances of heart disease and 14 features is used for this study. After applying to preprocess and feature engineering techniques, machine learning approaches like random forest, decision trees, gradient boosted trees, linear support vector classifier, logistic regression, one-vs-rest, and multilayer perceptron are used to perform binary and multiclassification on the data stream. When combined with the Max Abs Scaler technique, the multilayer perceptron performed satisfactorily in both binary (Accuracy 94.8%) and multiclassification (accuracy 88.2%). Compared to the other binary classification algorithms, the GBT delivered the right outcome (accuracy of 95.8%). Multilayer perceptrons, however, did well in multiple classifications. Techniques such as oversampling and undersampling have a negative impact on disease prediction. Machine learning methods like multilayer perceptrons and ensembles can be helpful for diagnosing cardiac conditions. For this kind of unbalanced data stream, sampling techniques like oversampling and undersampling are not practical.

1. Introduction

The healthcare industry generates a huge amount of data about patients, illnesses, and diagnosis, but because it has not been properly analyzed, it does not convey the significance that it should. The leading cause of death has been heart disease. In accordance with the World Health Organization, cardiovascular diseases (CVDs), which claim an approximate 17.9 million lives each year [1], are the leading cause of death worldwide.

Coronary heart disease, cerebrovascular disease, rheumatic heart disease, and some other conditions are among the group of heart and blood vessel disorders known as CVDs. Heart attacks and strokes account for four out of

every five CVD deaths, and one-third of these deaths happen before the age of 70 [2]. Sex, age, smoking, cholesterol, family history, high blood pressure, poor diet, obesity, inactivity, and alcohol consumption are the main risk factors for heart disease [3]. Hereditary risk factors like high blood pressure and diabetes also contribute to the disease. Obesity, poor eating habits, and physical inactivity are a few additional lifestyle factors that increase the risk.

The main signs and symptoms include palpitations, sweating, fatigue, shortness of breath, arm and shoulder pain, back pain, and chest pain. The most typical sign of poor heart blood flow or a heart attack is still chest pain. Angina is the name for this kind of chest pain [4]. There are various tests, including X-rays, MRI scans, and angiography, to diagnose the illness.

However, there are instances where there is a lack of resources in an emergency because medical equipment is available at crucial moments. Every second counts in the diagnosis and treatment of diseases like cardiovascular disease. The potential for big data analytics to enhance cardiovascular quality of care and patient outcomes is enormous [5] because the cardiac centers and OPDs generate enormous amounts of data related to the diagnosis of heart disease. However, because of noise, incomplete information, and inconsistency, it is difficult to make precise, accurate, and consistent decisions using that data. Artificial intelligence (AI) is now playing a significant role in cardiology thanks to enormous advancements in technology, storage, acquisition, and knowledge recovery [6–10]. Researchers have pre-processed data using a variety of data mining techniques in order to make decisions using various models of machine learning [11, 12].

The contents of this paper focus on the R&D of a decision support system to predict heart disease using 14 feature clinical data. Literature Review presents the related research up till now. The proposed research explains the loopholes in the previous research and discusses one of the right approaches to diagnose the disease accurately. Methodology and Results provides preprocessing techniques through data mining. It presents the analysis, precision, and accuracy of machine learning algorithms that can be effective to diagnose heart problems through clinical data. In the end, Conclusion describes the performance, analysis, and comparisons between different types of algorithms on the model.

1.1. Motivation and Contributions. Heart disease has historically been the main cause of death. The World Health Organization lists cardiovascular diseases (CVDs) as the number one killer in the world, claiming 17.9 million lives annually [1]. The group of heart and blood vessel disorders known as CVDs includes conditions like coronary heart disease, cerebrovascular disease, rheumatic heart disease, and others. Four out of every five CVD deaths result from heart attacks or strokes, and one-third of these deaths occur before the age of 70 [2].

Here are the following substantial contributions of the proposed work:

- (1) We start by addressing the problem of datasets, which we later refined and standardized. This is one of the proposed work's major contributions. Following that, the datasets are used to for training and testing the classifiers to see which ones offer the highest accuracy
- (2) We then use the correlation matrix to determine the best values or features
- (3) In the third step, we used the preprocessed dataset with the machine learning approaches to achieve the highest accuracy possible by fine-tuning the parameters
- (4) The accuracy, recall, precision, and F -measure of the proposed classifiers are assessed

- (5) In evaluation to the state-of-the-art accuracy listed in "Figures 1 and 2," the proposed classifiers provide better accuracy

The remainder of the document is structured as follows: Section 2 described the literature review. Section 3 provides the methodology while Section 4 presents the algorithms. Sections 5 discusses the results and discussion. Finally, Section 6 concludes the research.

2. Literature Review

The classification of heart disease using data mining and machine learning has been the subject of numerous studies and methodologies [13]. Al-Janabi provided a thorough analysis of the research on the use of machine learning in the field of heart disease. The author opined that a dataset with adequate samples and accurate data must be used to create an effective model for predicting heart disease. The dataset should be preprocessed appropriately, as this is the step that will have the biggest impact on how well the machine learning algorithm uses the dataset.

In the study, the author advocated for the use of a suitable algorithm, such as a decision tree (DT) or artificial neural network (ANN), when creating a prediction model. Decision tree and artificial neural network (ANN) both performed well in the majority of method for estimating heart disease (DT). Using data analytics tools and algorithms for machine learning like artificial neural networks (ANN), decision trees, fuzzy logic, K -nearest neighbors (KNN), Naive Bayes, and support vector machines, Marimuthu et al. [14] proposed a prediction of the heart disease model (SVM). The performance of the algorithm and an overview of previous work are also discussed in the paper. Yadav et al. [15] suggested an architecture that involves preprocessing of the input data before training and testing on various algorithms. Author emphasis using AdaBoost to increase the presentation of every ML algorithm. The author also supported the idea of parameter tuning to get good accuracies.

Sharma et al. [16] recommended a deep learning approach to diagnose heart disease using the UCI dataset of heart diseases. They suggested that heart disease diagnosing is one of the key zones where deep neural networks can be applied to improve the quality of classification. They presented that Talos hyperparameter optimization is more efficient than the other model optimization techniques. The prognosis of heart disease using machine learning models with high certitude, precision, and recall was discussed by Ramalingam et al. [17]. These models included KNN, SVM, DT, and RF algorithms. The support vector machine (SVM) classification in their prediction model had the highest accuracy of 86% for heart diseases in the UCI machine learning repository.

Ravindhar et al. [18] used four machine learning algorithms and one neural network to compare performance measurements to cardiac disease identification. To be able to predict cardiac attacks, the authors evaluated the algorithms' accuracy, precision, recall, and F1 settings. The deep

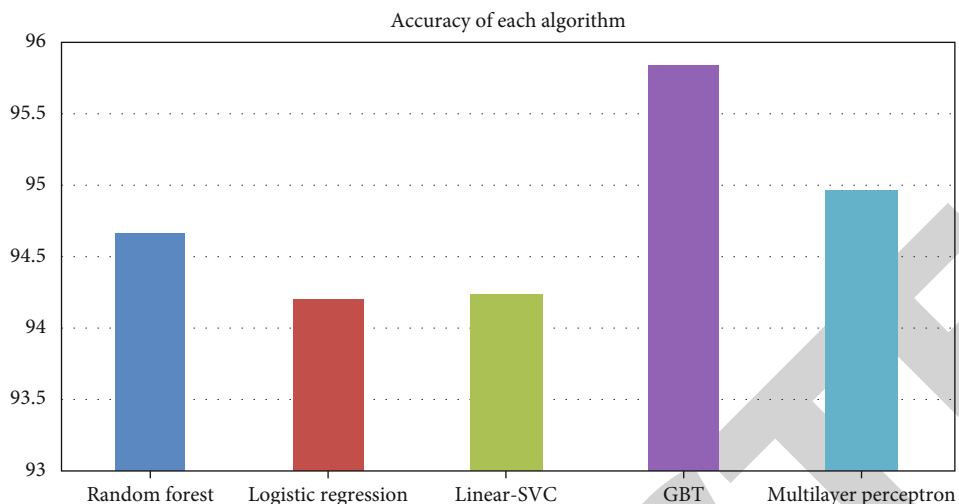


FIGURE 1: Binary classification algorithm accuracy.

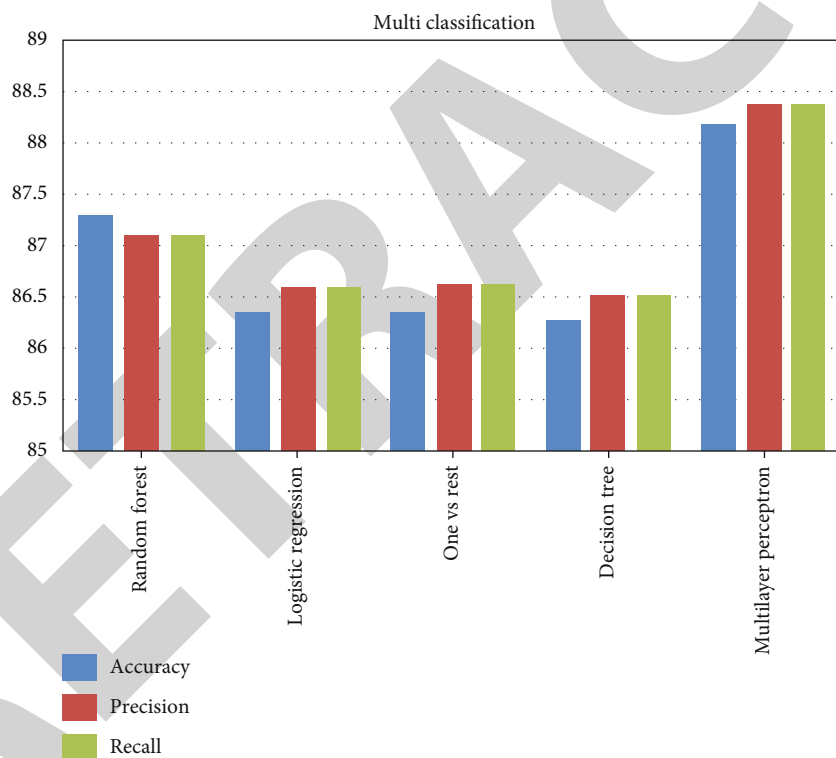


FIGURE 2: Multiclassification algorithm performance measures.

neural network algorithm achieved 98% accuracy in heart disease identification. In [19], Latha and Jeeva improves the prediction accuracy of heart disease using the ensemble classification models. In order to demonstrate the algorithm's value in early disease prediction, Latha and Jeeva [19] focuses on its application to a medical dataset. The study's findings show that ensemble techniques, like bagging and boosting, are useful for increasing the predictability of weak classifiers and perform admirably in calculating the risk of developing heart disease. Implementing feature selection improved the process' performance even further, and

the results revealed a notable rise in prediction accuracy. Ensemble classification helped weak classifiers achieve an accuracy improvement of up to 7%.

The author of [20] compared ML classifiers on various datasets such as heart and diabetes datasets. The authors of [21] examined ML classifiers on medical insurance cost datasets. [22] used six popular data mining tools to categorize heart disease: using LR, KNN, SVM, RF, and KNIME, these tools were compared to six commonly used machine learning techniques. The most frequently encountered effective learning issue researched in the literature is single-label

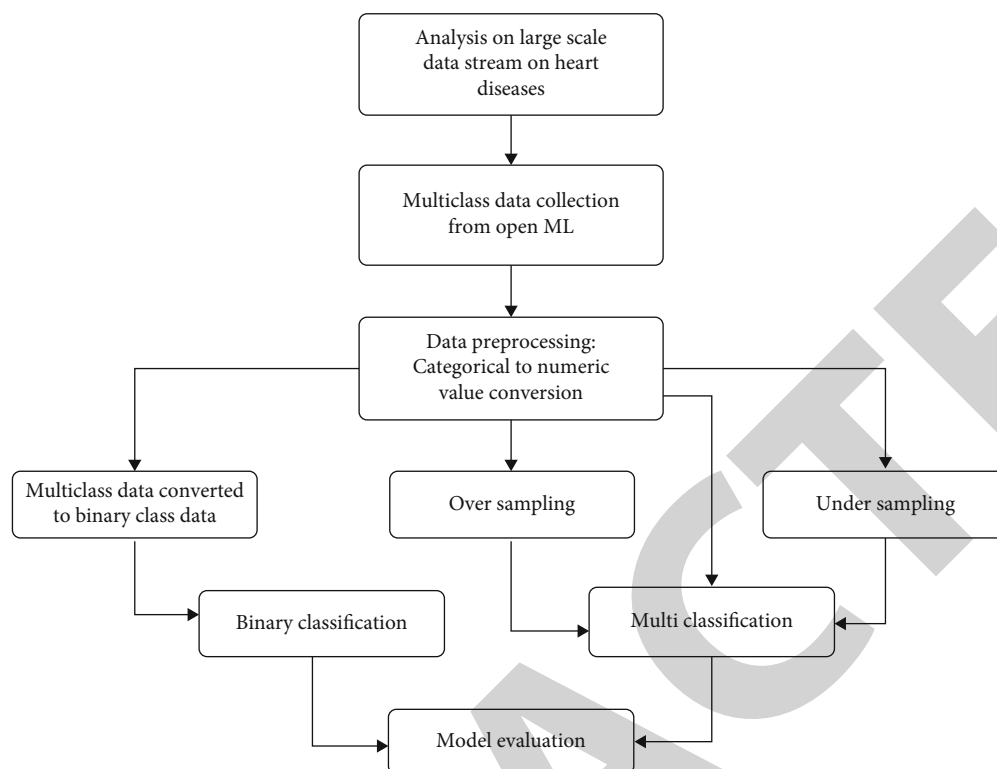


FIGURE 3: Working methodology.

classification. A training data classification algorithm is labeled for the instance that is the most ambiguous using the active learning strategy known as uncertainty sampling. Methods for sampling uncertainty are effective in terms of computation.

Despite the fact that they do not assess the candidate instance's future predictive informativeness on large amounts of unlabeled data, they have demonstrated good empirical performance [23]. A method for crystalline material prediction was proposed in [24] using the evolutionary optimization technique USPEX and machine-learning interatomic potentials consciously learning on the fly. [25] focused on the most effective methods to automatically represent configuration settings for the training set when developing moment tensor potentials, which were implemented in the MLIP package. [26] showed how to select automated hyperparameters solely through active learning. They enhanced the classification model hyperparameters that make up a super learner model using a Bayesian approach. To modify the solution close to the predicted optimum, they used simulations, deep learning training, and surrogate optimization.

They combined mixed data factor structure and RF-based MLA to create an autonomous systems framework in a paper [27]. RF was utilized to forecast disease by using the FAMD to find the relevant features. The proposed method had accuracy rates of 93.44 percent, sensitivity rates of 89.28 percent, and specificity rates of 96.96 percent. The same methodology was applied with a boosting hybrid model in [28], which resulted in accuracy of 75.9%. The boosting ensemble method was evaluated using the UCI lab-

oratory dataset, with an ANN model attaining an accuracy of 82.5 percent and a hybrid model attaining a performance of 78.88 percent [29]. The prediction of heart disease is a research area that involves numerous researchers. Numerous aspects of cardiac illness are covered in their study. [30] finds that SVM performs better, averaging 96 percent accuracy. The DT model, according to the author in [31], consistently outperforms the NB and SVM models. According to its findings, SVM achieves an accuracy of 87%, DT achieves an accuracy of 90%, and LR achieves the highest accuracy in heart disease prediction when compared to DT, NB, SVM, and KNN, as shown in [32]. For the assessment of congenital heart disease, the RF-based framework's prediction accuracy is 97 percent [33], with a specificity of 88 percent and a sensitivity of 85 percent. With a specificity of 95% and a sensitivity of 93.5 percent, we used LR, EVF, MARS, and CART ML models in [34] to detect the co-occurrence of CVD and 94 percent.

Researchers put forth a number of ensemble and hybrid models for predicting cardiovascular disease in an effort to reach a better conclusion. On CVD datasets taken from the Mendeley Data Center, IEEE Data Port, and Cleveland datasets, respectively, the proposed models in [35] achieve 96, 93, and 88.24 percent accuracy. The author of [36] successfully combined the RF and LR models to predict heart disease with 88.7% accuracy. These studies' objective is to examine correlations between carotid plaque and coronary artery calcium in asymptomatic individuals, as well as their relationships to predict CVD occurrence risk [37]. The Internet of Things (IoT) and ML and deep learning are now widely used for disease detection and prediction. In [38], the author used

TABLE 1: Dataset description.

No.	Feature name	Dataset description Description	Value
1.	Age	One of the most significant risk factors for heart disease is age. The likelihood of developing heart disease increases with age.	Integer value.
2.	Sex	Displays the gender of the individual having heart disease or not.	Male = 1 Female = 0
3.	Chest pain type	It shows how often the person experiences chest pain.	Standard angina = 1 Angina atypical = 2 3 for nonanginal pain Asymptotic = 4
4.	Resting blood pressure	Blood pressure is also one of the causes. Higher blood pressure occurs with other factors leads to the high risk.	It has whether integer or float value.
5.	Cholesterol	The serum cholesterol is shown in mg/dl (unit). Your danger of a heart attack is also increased by having high blood levels of triglycerides, a form of fat connected to your diet.	It has whether integer or float value.
6.	Fasting blood sugar	Compares a person's fasting blood sugar level to 120 mg/dl. A greater risk also results from an increase in blood sugar.	Value = 1 if fasting blood sugar > 120 (true) If not, value is 0 (false)
7.	Resting ECG	It displays resting electrocardiographic results.	Left ventricular hypertrophy = 2, ST – T wave abnormality = 1, and normal = 0
8.	Max heart rate achieved	This value is the highest heart rate achieved. It is linked with other factors such as blood pressure.	It has whether integer or float value.
9.	Exercise-induced angina	It is the chest pain induced during the exercise. Although it usually starts in the center of your chest, it can also affect one or both shoulders, as well as your back, chest, jaw, or arm.	Yes = 1 No = 0
10.	Exercise-induced ST depression compared to rest	Integer values or float value	It has whether integer or float value.
11.	Peak ST segment of exercise	When you see a horizontal or downward-sloping ST-segment depression of less than 1 mm 60–80 ms after the J point on a treadmill ECG stress test, it is deemed abnormal.	Upsloping = 1 Flat = 2 Downsloping = 3
12.	Major vessels colored by fluorescence in number	Integer values or float value	It has whether integer or float value.
13.	Thalassemia	It displays thalassemia.	Normal = 3 Fixed defect = 6 Reversible defect = 7
14.	Heart disease diagnosis	The fact that the person is either healthy or struggling from heart disease is indicated.	Absence = 0 Present = 1, 2, 3, 4

mobile technology and the deep learning approach to predict heart disease with an accuracy of 94%. The author combines IoT with ML classifiers for early heart infection prediction in [39]. The goal is to show how ML can be used to resolve the issue. By examining hundreds of healthcare data sets, we use machine learning to analyze cases that are related to diseases and other health issues [40].

3. Methodology

On data streams with multiple classifications as well as binary data, we have applied machine learning techniques. The steps of our process following are displayed in “Figure 3.”

3.1. Dataset. The large imbalanced heart disease data stream is gained from the OpenML repository. In the OpenML repository, various domain data streams are available. The

imbalanced data stream consists of 14 attributes, 100000 instances, and 5 target classes. The data stream is uploaded by Jan Van Rijn in 2014 in the OpenML repository. For binary classification, the multiclass data is converted into binary class by replacing target variable values 2, 3, and 4 with 1. The dataset description is in “Table 1.”

3.2. Data Descriptive Statistics. Data descriptive statistics is described in Table 2, such as Min., Max., mean, standard deviation, and variance.

3.3. Instance per Class. “Figure 4” is a graphical representation of data distribution, including the number of instances in each class of heart disease dataset.

3.4. Preprocessing. The data stream consists of nominal and numerical values feature sets. Many ML algorithms do not

TABLE 2: Dataset descriptive statistics.

Age	N	Minimum	Maximum	Mean	Std. deviation	Variance	Skewness
	1000000	27	82	54.38	9.082	82.475	-0.195 0.002
Sex	1000000	0	1	0.68	0.486	0.217	-0.775 0.002
cp	1000000	1	4	3.14	0.964	0.929	-0.919 0.002
trestps	1000000	94.03	210.08	131.6239	17.53299	307.406	0.626 0.002
chol	1000000	100.76	529.66	246.3325	51.80040	2683.282	0.766 0.002
rbs	1000000	0	1	0.15	0.360	0.129	1.932 0.002
Restecg	1000000	0	2	0.99	0.991	0.982	0.028 0.002
Thalach	1000000	62.09	211.39	149.6228	22.88460	523.705	-0.514 0.002
Exang	1000000	0	1	0.33	0.472	0.222	0.705 0.002
Oldpeak	1000000	.64	6.96	1.0431	1.16101	1.348	1.173 0.002
Slope	1000000	1	3	1.61	0.632	0.399	0.535 0.002
Ca	1000000	0	3	0.72	0.965	0.932	1.108 0.002
Thal	1000000	3	7	4.74	1.932	3.734	0.236 0.002
Valid N (listwise)	1000000						

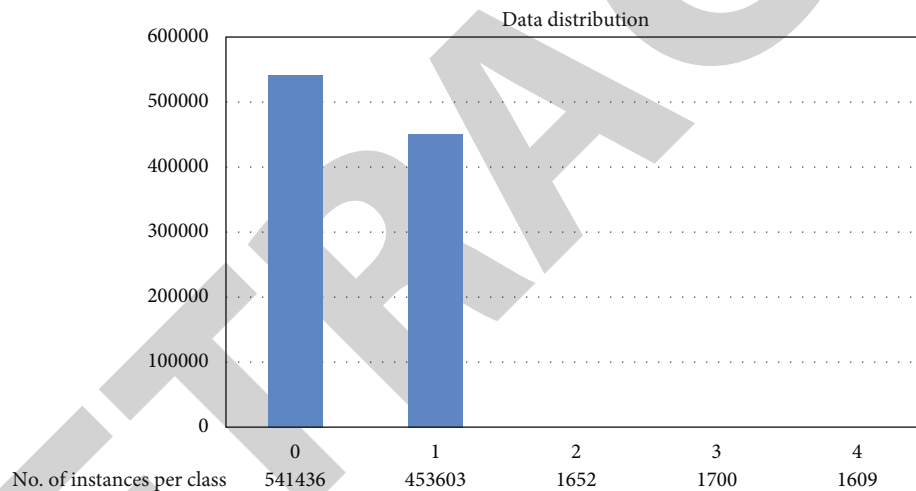


FIGURE 4: Dataset description.

process the nominal values; hence, these values need to be converted in numerical. In this approach, nominal values are replaced by the following table [1]. Also, some of the features in the dataset have relatively large values than the others which results in biased learning. In this approach, we have applied the Max Abs Scaler technique to the dataset [41].

3.5. Feature Engineering. Data mining techniques are used to create features from raw data using the process of feature engineering, which enhances the performance of ML algorithms. Feature importance provides the score for each feature of the dataset. The higher is the score, the more important feature is toward the target variable as shown in “Figure 5.”

3.6. Correlation Matrix with Heat Map. It is simple to see which functionalities are most related to other characteris-

tics or the target variable using a heat map [42]. Results are displayed in “Figure 6.”

3.7. Splitting. For the purpose of gathering training and test data for the analysis process, splitting is used. The entire data stream is split into train and test sets, with training data accounting for 70% of the data and testing data for the remaining 30%.

3.8. Classification. The training data is trained by using seven different ML algorithms for binary and multiclassification. The detail of models is shown in Table 3 [2].

4. Algorithms

In this paper, some ML algorithms are applied to the large imbalanced data stream of heart diseases to see them.

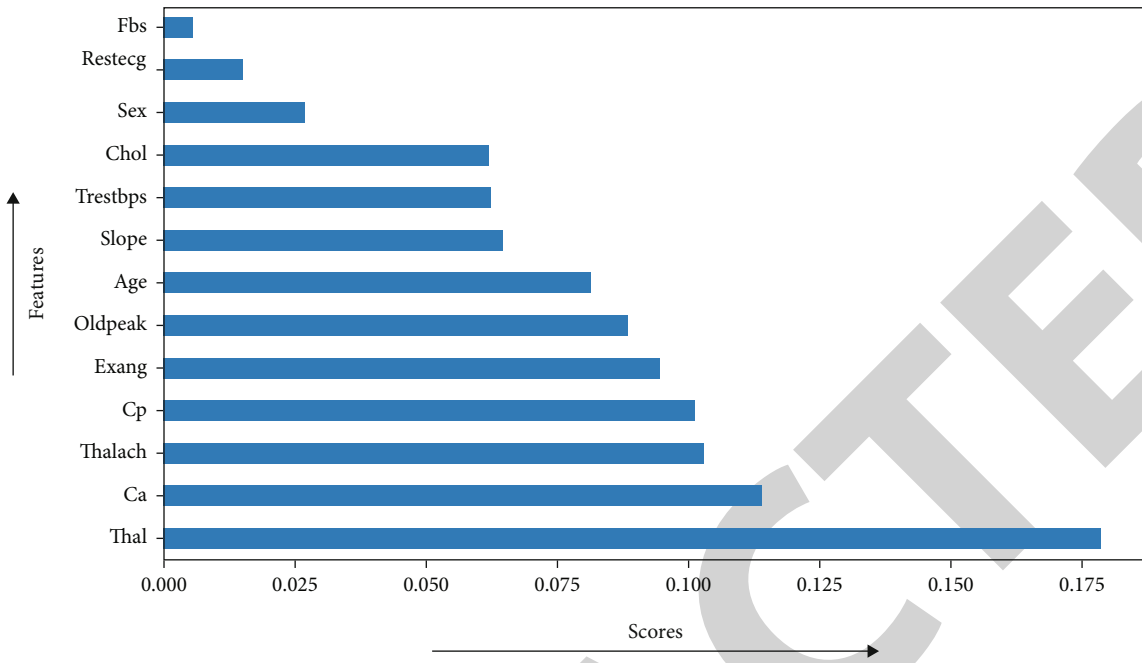


FIGURE 5: Feature importance.

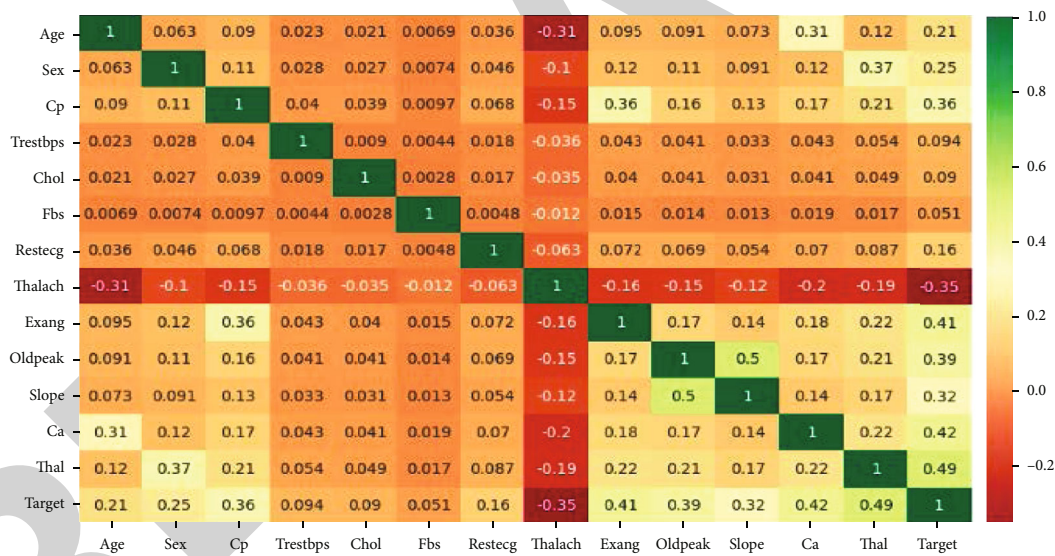


FIGURE 6: Heat map correlation matrix.

TABLE 3: Classification algorithms.

Classification techniques	DT	RF	GBT	LSVC	LR	One-vs-rest	MLP
Binary classification	✗	✓	✓	✓	✓	✗	✓
Multiclassification	✓	✓	✗	✗	✓	✓	✓

4.1. *Decision Tree.* The most effective and well-liked tool for prediction and classification is the decision tree. By learning straightforward decision rules implied from data features, the decision tree forecasts the value of the target variable. In most cases, the decision rules are made up of if-then-

else statements. The complexity of the rules as well as filter model increases with the depth of the tree [43].

4.2. *Random Forest.* One of the most well-liked and potent supervised machine learning algorithms, random forest or

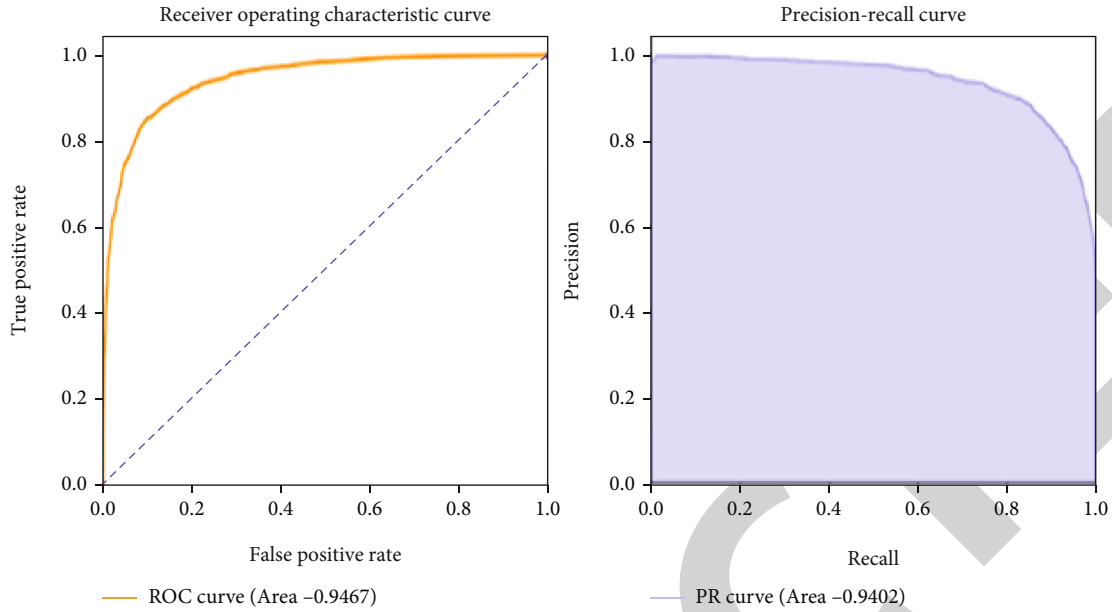


FIGURE 7: PR curve and ROC for random forest.

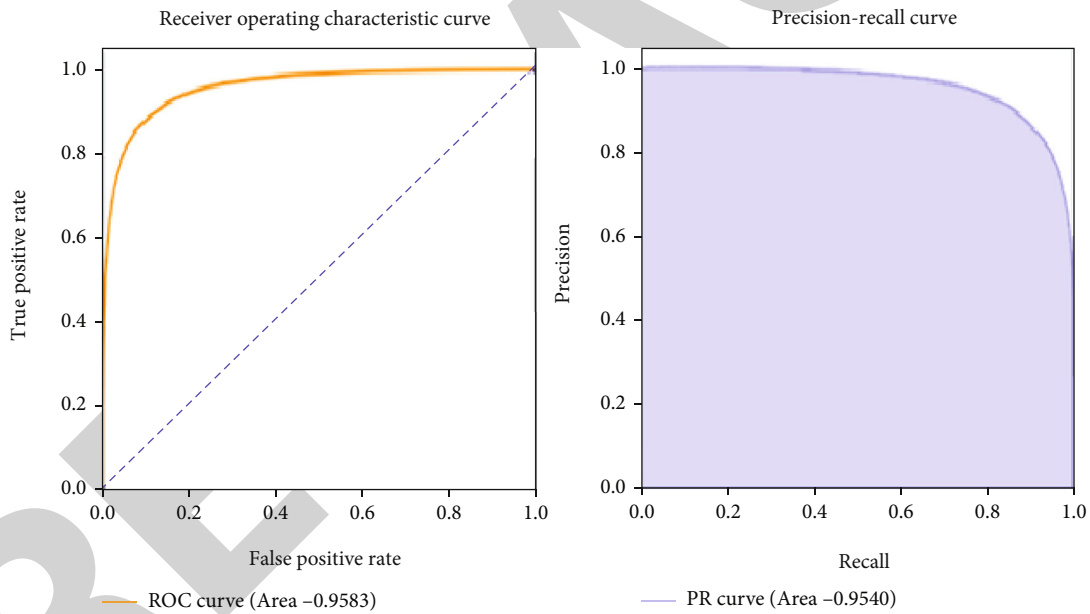


FIGURE 8: PR curve and ROC for GBTs.

extremely randomized forest can carry out both regression and classification tasks. It develops a decision-tree-filled forest. In general, a prediction is more accurate and robust the more trees there are in the forest. While regression takes the estimate of the outputs from various trees, classification uses a voting system to determine which class received the most votes from all the other trees within the forest. Additionally, it successfully manages higher dimensional large datasets. [44].

4.3. Gradient Boosting Tree. Gradient boosted tree learners are combined to form a strong learner, known as boosting. The GBT uses the same technique as AdaBoost in which

equal weights are assigned to each of the observations. It decreases the masses of those observations which are easy to classify as well as increases of those which are difficult to classify. The second tree is grown using new weights. New predictions are made, and the process repeats itself until several iterations [45]. The gradient is different in such a way that it uses gradient in the loss function as in “Eq. (1).”

$$y = ax + b + e. \quad (1)$$

Here “ e ” indicates the error that means how much algorithms are good at predicting than the actual class.

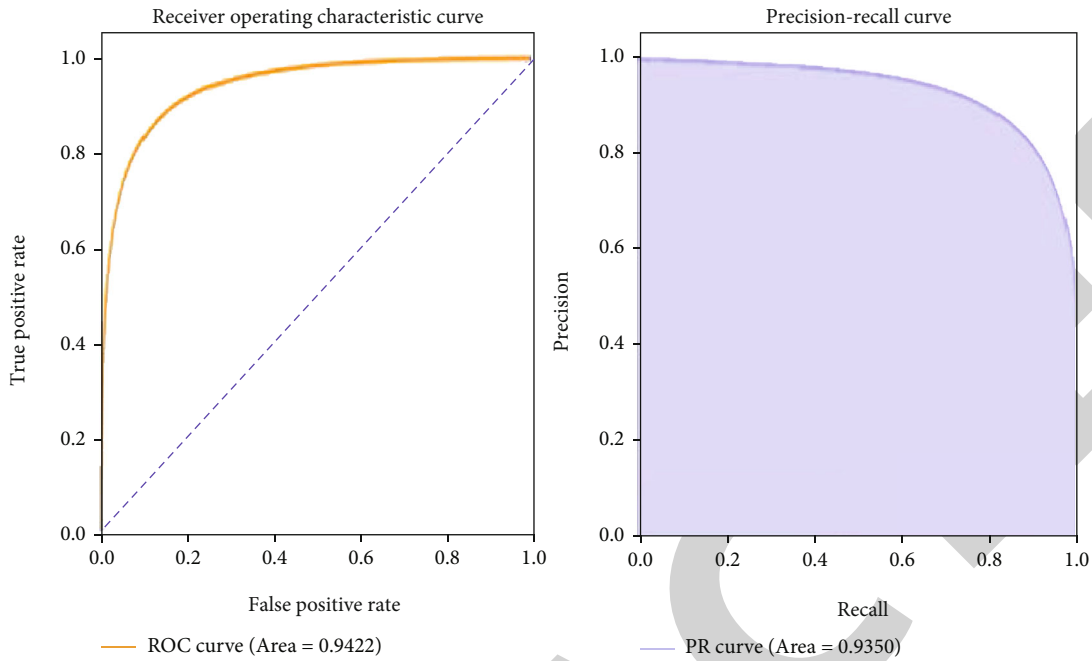


FIGURE 9: PR curve and ROC for linear support vector classifier.

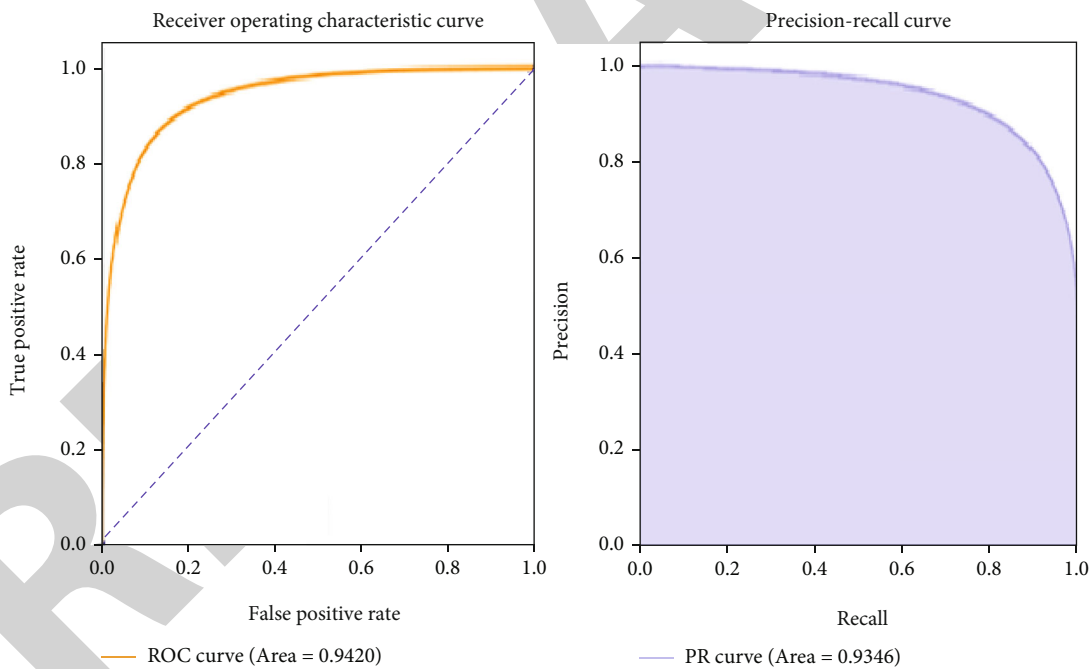


FIGURE 10: PR curve and ROC for logistic regression.

4.4. *Linear Support Vector Classifier.* The most effective technique which is used for binary classification is linear support vector classifier. Its objective is to learn from the data that is provided and returns the “best fit” hyperplane. The hyperplane is the decision boundary that helps classify the data points. The hyperplane dimension depends upon the features number. In this case, as the number of features is two, so hyperplane is just a straight separating line between the two classes. While building the SVC model, support vec-

tors help in maximizing the margin so that a perfect boundary should be created [46].

4.5. *One-vs-Rest.* The one-vs-rest algorithm uses the problem transformation technique, in which a multiclass problem is divided into multiple binary problems [47]. It makes use of binary different classifiers for multiclass classification using a heuristic approach. The multiclass dataset is divided into various binary classification issues. Since there are an equal

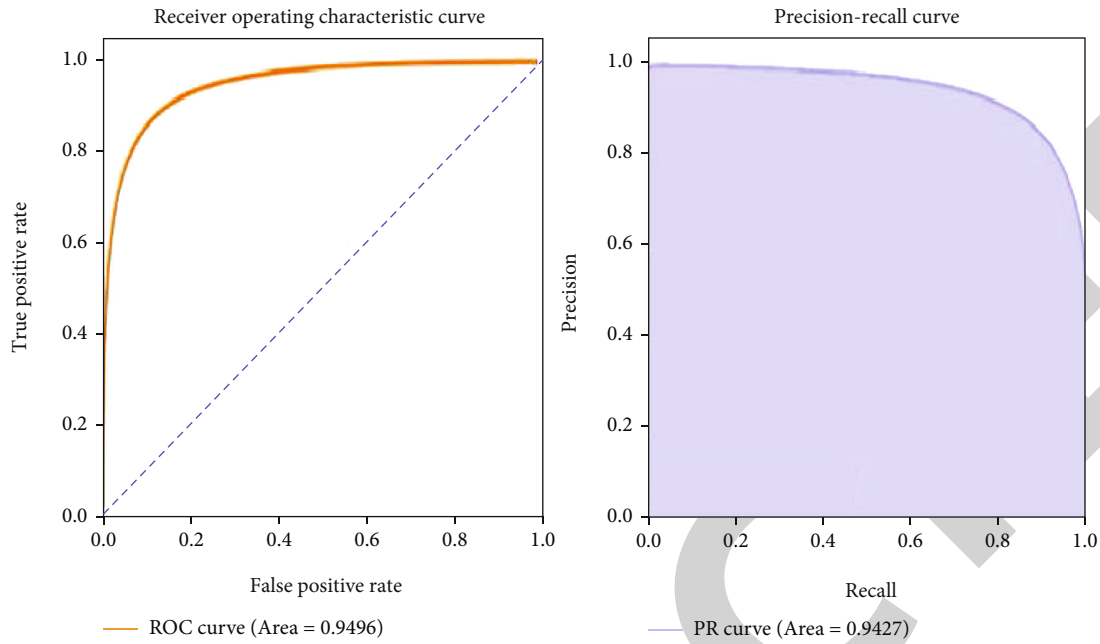


FIGURE 11: PR Curve and ROC for Multilayer Perceptron.

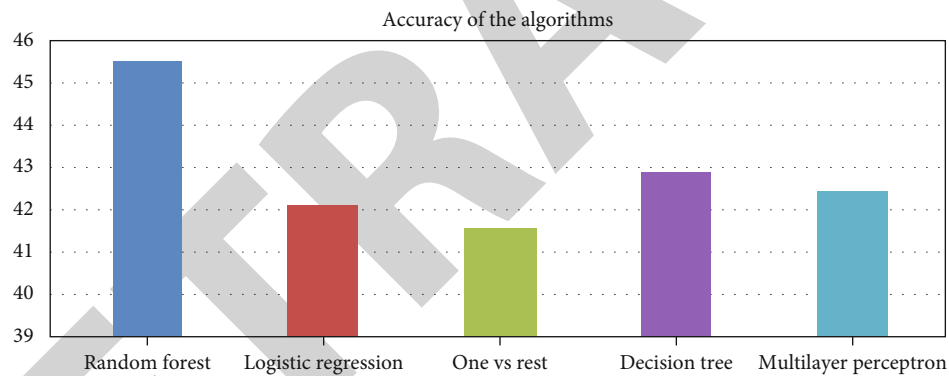


FIGURE 12: Oversampling algorithm accuracy.

variety of classes in the dataset, an equal number of models are created. The most certain model is then used to make predictions. Each model predicts response and membership probability. Class is chosen for which the respective model gave a positive response and the highest probability score [48].

4.6. Logistic Regression. Popular categorical response prediction techniques include logistic regression, which is a special case of generalized linear models that forecast the possibility of a target variable. It is the approach of choice for classification issues. A linear model or sigmoid function, which is a nonlinear function, is used to transform the output prediction. Logistic regression can be used for complex datasets where it can build more complex decision boundaries [49].

4.7. Multilayer Perceptron. A subclass of feedforward neural networks is the multilayer perceptron (ANN). It has several layers and produces a set of outputs from a set of inputs. It

typically has an input data, a hidden layer, and an output layer or at least three layers of nodes. The hidden layer uses a linear combination of data with the weights and bias of each node and appears to apply the activation function to map the inputs to outputs. The input layer represents the input data. Backpropagation is used to train the network [50].

5. Result and Analysis

Results of binary and multiclassification are discussed in this section.

5.1. Binary Classification Result. Several classification approaches are used for the classification, and their performance is measured. Accuracy alone is not enough for the evaluation. Binary classification algorithm accuracy is shown in Figure 1, and for that, the values of precision and recall are calculated, and ROC and PR curves are generated. Below

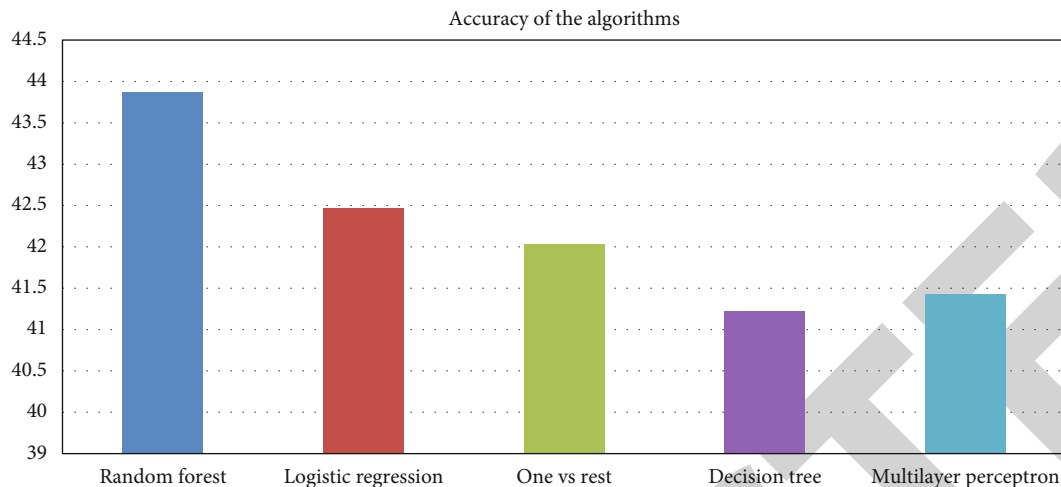


FIGURE 13: Undersampling algorithm accuracy.

diagrams illustrate the performance of our generated models (Figure 7–11) RF, GBT, LSV, LR, and MLP, respectively.

Following are the PR and ROC curves for applied models:

5.2. Multiclassification Result. Numerous machine learning algorithms are used in multiclassification to analyze the heart data stream, and their evaluated accuracies are shown in Figure 2.

6. Sampling

As the multiclassification provides biased or wrong results due to imbalanced data in the data stream, sometimes, all the data of classes 2, 3, and 4 splits either into training or testing data. To handle this, oversampling and undersampling balancing techniques are applied to the data stream using the abovementioned classification algorithm table [2] and measured the accuracies.

6.1. Oversampling. Oversampling involves the random selection of examples from the minority class, with replacement and adding them to the training data set [51]. Results are shown in “Figure 12.”

6.2. Undersampling. Undersampling involves the random selection of examples from the majority class and deleting them from the training dataset as in “Figure 13.”

7. Conclusion

In this paper, some ML algorithms are practical to the large imbalanced data stream of heart diseases to see their behavior. In this approach, the heart disease dataset from the OpenML repository utilized for training in addition testing purposes. Classification of heart diseases trailed the steps of preprocessing and features engineering and data splitting, then classification, and evaluation. In the case of both binary classification and multiclassification, only the accuracy of multilayer perceptron improved by 3% after applying Max Abs Scaler, whereas the rest of the algorithms does not have

such effect of Max Abs Scaler on their accuracies. Also, in both binary and multiclassification, the multilayer perceptron classifier performed adequately. For binary classification, the classification algorithms, random forest, logistic regression, GBT, linear SVC, and multilayer perceptron, provide high accuracy scores where the imbalance rate in the data stream is low, whereas in a multiclassification where imbalance rate in the data stream is high, the classification algorithms, random forest, logistic regression, decision tree, one vs rest and multilayer perceptron, provide fewer accuracy scores. Also, on this type of large imbalanced data stream, balancing techniques like oversampling and undersampling have an adverse effect on the accuracy of the data.

Data Availability

The data used in this research can be obtained from the corresponding authors upon request.

Conflicts of Interest

The authors declare that they have no conflicts of interest.

References

- [1] World Health Organization. *Cardiovascular Diseases (CVDs)*, 2022, https://www.who.int/health-topics/cardiovascular-diseases/#tab=tab_1.
- [2] World Health Organization. *Cardiovascular Diseases (CVDs)*, 2022, http://origin.who.int/cardiovascular_diseases/en/.
- [3] 2022, <https://www.heart.org/en/health-topics/high-blood-pressure/why-high-blood-pressure-is-a-silent-killer/known-your-risk-factors-for-high-blood-pressure>.
- [4] C. Balla, R. Pavasini, and R. Ferrari, “Treatment of angina: where are we?,” *Cardiology*, vol. 140, no. 1, pp. 52–67, 2018.
- [5] J. S. Rumsfeld, K. E. Joynt, and T. M. Maddox, “Big data analytics to improve cardiovascular care: promise and challenges,” *Nature Reviews Cardiology*, vol. 13, no. 6, pp. 350–359, 2016.
- [6] S. M. Arif, B. A. Bacha, S. S. Ullah, S. Hussain, and M. Haneef, “Tunable control of internet of things information hacking by

- application of the induced chiral atomic medium,” *Soft Computing*, vol. 4, pp. 1–8, 2022.
- [7] S. Hussain, I. Ullah, H. Khattak, M. A. Khan, C. M. Chen, and S. Kumari, “A lightweight and provable secure identity-based generalized proxy signcryption (IBGPS) scheme for Industrial Internet of Things (IIoT),” *Journal of Information Security and Applications*, vol. 58, no. 58, article 102625, 2021.
 - [8] S. S. Ullah, S. Hussain, A. Gumaedi, and H. AlSalman, “A secure NDN framework for Internet of Things enabled healthcare,” *Continua*, vol. 67, no. 1, pp. 223–240, 2021.
 - [9] S. Hussain, S. Sajid Ullah, M. Shorfuzzaman, M. Uddin, and M. Kaosar, “Cryptanalysis of an online/offline certificateless signature scheme for Internet of Health Things,” *Intelligent Automation & Soft Computing*, vol. 30, no. 3, pp. 983–993, 2021.
 - [10] T. Hussain, D. Hussain, I. Hussain et al., “Internet of Things with deep learning-based face recognition approach for authentication in control medical systems,” *Computational and Mathematical Methods in Medicine*, vol. 2022, article 5137513, pp. 1–17, 2022.
 - [11] K. W. Johnson, J. T. Soto, B. S. Glicksberg et al., “Artificial intelligence in cardiology,” *Journal of the American College of Cardiology*, vol. 71, no. 23, pp. 2668–2679, 2018.
 - [12] K. Gomathi and D. D. S. Priyaa, “Multi disease prediction using data mining techniques,” *International Journal of System and Software Engineering*, vol. 4, no. 2, pp. 12–14, 2016.
 - [13] M. Aljanabi, H. M. Qutqut, and M. Hijjawi, “Machine learning classification techniques for heart disease prediction: a review,” *International Journal of Engineering & Technology*, vol. 7, no. 4, pp. 5373–5379, 2018.
 - [14] M. Marimuthu, M. Abinaya, K. S. Hariesh, K. Madhankumar, and V. Pavithra, “A review on heart disease prediction using machine learning and data analytics approach,” *International Journal of Computer Applications*, vol. 181, no. 18, pp. 20–25, 2018.
 - [15] K. K. Yadav, A. Sharma, and A. Badholia, “Heart disease prediction using machine learning techniques,” *Information Technology In Industry*, vol. 9, no. 1, pp. 207–214, 2021.
 - [16] S. Sharma and M. Parmar, “Heart diseases prediction using deep learning neural network model,” *International Journal of Innovative Technology and Exploring Engineering (IJITEE)*, vol. 9, no. 3, pp. 2244–2248, 2020.
 - [17] V. V. Ramalingam, A. Dandapath, and M. K. Raja, “Heart disease prediction using machine learning techniques : a survey,” *Engineering & Technology*, vol. 7, no. 2.8, pp. 684–687, 2018.
 - [18] N. V. Ravindhar, H. S. Anand, and G. W. Ragavendran, “Intelligent diagnosis of cardiac disease prediction using machine learning,” *International Journal of Innovative Technology and Exploring Engineering*, vol. 8, no. 11, pp. 1417–1421, 2019.
 - [19] C. B. C. Latha and S. C. Jeeva, “Improving the accuracy of prediction of heart disease risk based on ensemble classification techniques,” *Informatics in Medicine Unlocked*, vol. 16, article 100203, 2019.
 - [20] C. A. U. Hassan, M. S. Khan, and M. A. Shah, “Comparison of machine learning algorithms in data classification,” in *2018 24th International Conference on Automation and Computing (ICAC)*, Newcastle Upon Tyne, UK, 2018.
 - [21] C. A. U. Hassan, J. Iqbal, S. Hussain, H. AlSalman, M. A. Mosleh, and S. Sajid Ullah, “A computational intelligence approach for predicting medical insurance cost,” *Mathematical Problems in Engineering*, vol. 2021, Article ID 1162553, 13 pages, 2021.
 - [22] I. Tougui, A. Jilbab, and J. El Mhamdi, “Heart disease classification using data mining tools and machine learning techniques,” *Health Technology*, vol. 10, no. 5, pp. 1137–1144, 2020.
 - [23] F. K. Nakano, R. Cerri, and C. Vens, “Active learning for hierarchical multi-label classification,” *Data Mining and Knowledge Discovery*, vol. 34, no. 5, pp. 1496–1530, 2020.
 - [24] E. V. Podryabinkin, E. V. Tikhonov, A. V. Shapeev, and A. R. Oganov, “Accelerating crystal structure prediction by machine-learning interatomic potentials with active learning,” *Physical Review B*, vol. 99, no. 6, p. 64114, 2019.
 - [25] I. S. Novikov, K. Gubaev, E. V. Podryabinkin, and A. V. Shapeev, “The MLIP package: moment tensor potentials with MPI and active learning,” *Machine Learning: Science and Technology*, vol. 2, no. 2, 2021.
 - [26] O. Owoyele, P. Pal, and A. V. Torreira, “An automated machine learning-genetic algorithm framework with active learning for design optimization,” *Journal of Energy Resources Technology*, vol. 143, no. 8, 2021.
 - [27] A. Gupta, R. Kumar, H. S. Arora, and B. Raman, “MIFH: a machine intelligence framework for heart disease diagnosis,” *IEEE Access*, vol. 8, pp. 14659–14674, 2020.
 - [28] I. D. Mienye, Y. Sun, and Z. Wang, “An improved ensemble learning approach for the prediction of heart disease risk,” *Informatics in Medicine Unlocked*, vol. 20, no. 1, p. 100402, 2020.
 - [29] S. Mohan, C. Thirumalai, and G. Srivastava, “Effective heart disease prediction using hybrid machine learning techniques,” *IEEE Access*, vol. 7, pp. 81542–81554, 2019.
 - [30] A. Saboor, M. Usman, S. Ali, A. Samad, M. F. Abrar, and N. Ullah, “A method for improving prediction of human heart disease using machine learning algorithms,” *Mobile Information Systems*, vol. 2022, Article ID 1410169, 9 pages, 2022.
 - [31] K. Arumugam, M. Naved, P. P. Shinde, O. Leiva-Chauca, A. Huaman-Osorio, and T. Gonzales-Yanac, “Multiple disease prediction using machine learning algorithms,” *Materials Today: Proceedings*, vol. 67, no. 6, 2021.
 - [32] C. Gupta, A. Saha, N. S. Reddy, and U. D. Acharya, “Cardiac disease prediction using supervised machine learning techniques,” *Journal of Physics: Conference Series*, vol. 2161, no. 1, p. 012013, 2022.
 - [33] V. T. Truong, B. P. Nguyen, T. H. Nguyen-Vo et al., “Application of machine learning in screening for congenital heart diseases using fetal echocardiography,” *The International Journal of Cardiovascular Imaging*, vol. 38, no. 5, pp. 1007–1015, 2022.
 - [34] A. S. Abdalrada, J. Abawajy, T. Al-Quraishi, and S. M. S. Islam, “Machine learning models for prediction of co-occurrence of diabetes and cardiovascular diseases: a retrospective cohort study,” *Journal of Diabetes & Metabolic Disorders*, vol. 21, no. 1, pp. 251–261, 2022.
 - [35] B. P. Doppala, D. Bhattacharyya, M. Janarthanan, and N. Baik, “A reliable machine intelligence model for accurate identification of cardiovascular diseases using ensemble techniques,” *Journal of Healthcare Engineering*, vol. 2022, Article ID 2585235, 13 pages, 2022.
 - [36] A. Kondababu, V. Siddhartha, B. B. Kumar, and B. Penumutchi, “A comparative study on machine learning based heart disease prediction,” *Materials Today: Proceedings*, vol. 67, no. 6, 2021.

Retraction

Retracted: GPS Receiver Position Estimation and DOP Analysis Using a New Form of the Observation Matrix Approximations

Journal of Sensors

Received 19 December 2023; Accepted 19 December 2023; Published 20 December 2023

Copyright © 2023 Journal of Sensors. This is an open access article distributed under the Creative Commons Attribution License, which permits unrestricted use, distribution, and reproduction in any medium, provided the original work is properly cited.

This article has been retracted by Hindawi following an investigation undertaken by the publisher [1]. This investigation has uncovered evidence of one or more of the following indicators of systematic manipulation of the publication process:

- (1) Discrepancies in scope
- (2) Discrepancies in the description of the research reported
- (3) Discrepancies between the availability of data and the research described
- (4) Inappropriate citations
- (5) Incoherent, meaningless and/or irrelevant content included in the article
- (6) Manipulated or compromised peer review

The presence of these indicators undermines our confidence in the integrity of the article's content and we cannot, therefore, vouch for its reliability. Please note that this notice is intended solely to alert readers that the content of this article is unreliable. We have not investigated whether authors were aware of or involved in the systematic manipulation of the publication process.

Wiley and Hindawi regrets that the usual quality checks did not identify these issues before publication and have since put additional measures in place to safeguard research integrity.

We wish to credit our own Research Integrity and Research Publishing teams and anonymous and named external researchers and research integrity experts for contributing to this investigation.

The corresponding author, as the representative of all authors, has been given the opportunity to register their agreement or disagreement to this retraction. We have kept a record of any response received.

References

- [1] A. K. N. P. S. Kumar, M. K. Mohiddin, M. T. Gameda, and A. Mishra, "GPS Receiver Position Estimation and DOP Analysis Using a New Form of the Observation Matrix Approximations," *Journal of Sensors*, vol. 2022, Article ID 6772077, 12 pages, 2022.

Research Article

GPS Receiver Position Estimation and DOP Analysis Using a New Form of the Observation Matrix Approximations

Ashok Kumar N ¹, P. Sirish Kumar ², Md. Khaja Mohiddin ³,
Mulugeta Tegegn Gemeda ⁴ and Anup Mishra ⁵

¹Department of Electronics and Communication Engineering, Anil Neerukonda Institute of Technology and Sciences (A), Visakhapatnam, India

²Department of Electronics and Communication Engineering, Aditya Institute of Technology and Management (A), Tekkali, India

³Department of Electronics and Telecommunication Engineering, Bhilai Institute of Technology, Raipur, Chhattisgarh, India

⁴Faculty of Electrical and Computer Engineering, Jimma University, Jimma Institute of Technology, Jimma, Ethiopia

⁵Department of Electrical and Electronics Engineering, Bhilai Institute of Technology, Durg, Chhattisgarh, India

Correspondence should be addressed to Ashok Kumar N; ashok0709@gmail.com, P. Sirish Kumar; sirishdg@gmail.com, and Mulugeta Tegegn Gemeda; mulugeta.geneda@ju.edu.et

Received 29 July 2022; Accepted 22 August 2022; Published 19 September 2022

Academic Editor: Sweta Bhattacharya

Copyright © 2022 Ashok Kumar N et al. This is an open access article distributed under the Creative Commons Attribution License, which permits unrestricted use, distribution, and reproduction in any medium, provided the original work is properly cited.

A location sensor is a feature that communicates with a Global Positioning System (GPS) receiver to learn about the status of the current location. This work presents the GPS receiver position estimation and Dilution of Precision (DOP) analysis using a new approximate form of observation matrix which can be used in place of the classic observation matrix that was derived from the Taylor's series. It has been realized that, the approximate observation matrix is numerically stable and provides greater precision in calculating DOP values and estimating the position of a GPS receiver. The experimental results show that the proposed observation matrix provides better precision in DOP analysis and GPS receiver position estimation with a fast convergence rate and improved algorithm stability. Therefore, it can be concluded that the proposed new observation matrix plays a significant role to estimate accurately the location of the GPS receiver position and to enhance all parameters of the DOP.

1. Introduction

The GPS sensors estimation process mathematically depends on the observation matrix which is formed by using the pseudo-range equations at a particular epoch. The observation matrix in use was derived from the first order Taylor's series. Thus, the classical observation matrix has a constant (unity) as the fourth parameter which affects the iteration process of position estimation and DOP computation in terms of precision. Therefore, a direct difference method is used in this paper to improve the order of the observation matrix. A direct difference method was used to the Extended Kalman Filter

(EKF) to modify its gain [1, 2]. Thus, EKF was modified and the developed new method was named as modified gain EKF (MGEKF). This method was used to obtain an approximate gain matrix " g " to replace the measurement matrix ($h(X)$) in the EKF covariance during the measurement update stage. The only distinction between EKF [3] and MGEKF is the covariance matrix in the measurement update stage. The new gain matrix " g " has proved to be effective in SONAR tracking applications [4, 5]. In this article, an attempt is made to obtain an approximate form of observation matrix (\tilde{H}) for GPS applications by using the *direct difference method*. Although classical observation matrix (H) is the standard

one, how can the *direct difference method* helps to obtain the approximate form of observation matrix \tilde{H} is presented in this article.

The performance of the approximation form of observation matrix is evaluated on analysis of dilution of precision (DOP) [6] and estimation of a GPS receiver position. Among DOP parameters, Geometric Dilution of Precision (GDOP) exhibits the geometric effect on the association of positioning determination error and measurement error. Errors in determining the GPS receiver positions are usually GDOP multiplied by measurement error; in other words, GDOP is the error gain, which means that a smaller GDOP usually results in a larger exact position. So, a smaller GDOP is better. It has been shown that more number of satellites make the GDOP value lesser for accurate position estimation, i.e., more satellites result in a lower GDOP, and fewer satellites generally result in poor GDOP [7] and lead to a corresponding reduction in the positioning error.

Many methods were developed to improve the position accuracy of the GPS based on GDOP [8–11]. One of the common methods is optimal satellite selection [12]. The easiest way is to choose a combination of all satellites, all of which must be taken into account to obtain optimum position accuracy with minimum GDP [13]. The other DOP parameters are Horizontal Dilution of Precision (HDOP), Position Dilution of Precision (PDOP), Time Dilution of Precision (TDOP), and Vertical Dilution of Precision (VDOP). The goal of any GPS algorithms for satellite selection is to reduce the GDOP to enhance positioning accuracy. A minimum GDOP can provide higher positioning accuracy by preventing the effects of poor geometry.

The GDOP computation using H is given by equation (1).

$$GDOP = \sqrt{\text{trace}(H^T H)^{-1}}. \quad (1)$$

Various research works has been presented in the literature which are dealing with the precise computation of the GDOP attempting to enhance the accuracy of the positioning [8, 10, 11]. It has been analyzed that selecting four satellites optimally from more satellites in the immediate vicinity is tedious, time-consuming, and power-consuming. Thus, a greater number of satellites in the immediate vicinity can decrease the GDOP. In case the number of visible satellites is small, then the above said choice is good for providing highly accurate positioning [11].

The GDOP computation formula includes receiver clock bias along with north, east, and up components. In [12–15], the direct difference method is used only for position estimation, but the *receiver clock bias* is not included either in the modified gain matrix ' g ' or in the observation matrix, without which it is impossible to obtain the GDOP and the accuracy enhancement in the GPS receiver position estimate. But the proposed \tilde{H} in this article includes the *receiver clock bias*. The *receiver clock bias* parameter is always equal to one for the H , while for the proposed \tilde{H} it is a function of the previous estimate and the current measurement.

To demonstrate the efficiency of the \tilde{H} over H , it is applied to compute GDOP and to estimate GPS receiver position [16–18]. Comparative results show a notable improvement due to the proposed observation matrix. The major contributions of this article are summarized as follows:

- (i) An approximate form of observation matrix (\tilde{H}) is derived using the *direct difference method*
- (ii) Experiments are being conducted with real-time GPS data to show significant performance improvements with the proposed \tilde{H} by analyzing GDOP and GPS receiver position estimates
- (iii) Position estimation analysis using EKF and MGEKF with the inclusion of the *receiver clock bias* parameter is also presented

The remaining part of this manuscript are ordered as follows. The derivation of the proposed observation matrix has been discussed in the second section [19–23]. The third section presents experimental results and applications [24–26]. Lastly the conclusion is given under section four.

2. Derivation for Proposed Observation Matrix

Let us consider the true GPS pseudo-range equation (13), for simplicity, by neglecting all other correctable error sources except *receiver clock bias* which is given by,

$$P_{sr}^i = \sqrt{(x_{sat}^i - x_r)^2 + (y_{sat}^i - y_r)^2 + (z_{sat}^i - z_r)^2} + Clk_r. \quad (2)$$

In the above equation, (x_r, y_r, z_r) and Clk_r are considered as true 3D position coordinates and the *receiver clock bias*, respectively, and $(x_{sat}^i, y_{sat}^i, z_{sat}^i)$ are i -th satellite coordinates. Now, consider the estimated pseudo-range equation as,

$$\tilde{P}_{sr}^i = \sqrt{(\hat{x}_{sat}^i - \hat{x}_r)^2 + (\hat{y}_{sat}^i - \hat{y}_r)^2 + (\hat{z}_{sat}^i - \hat{z}_r)^2} + Cl\hat{k}_r, \quad (3)$$

where $(\hat{x}_r, \hat{y}_r, \hat{z}_r)$ and $Cl\hat{k}_r$ are considered as estimated 3D position coordinates with receiver clock bias. To determine the proposed observation matrix (\tilde{H}) for GPS positioning application, it is given by the following format [13].

$$\begin{bmatrix} P_{sr}^i - \tilde{P}_{sr}^i \end{bmatrix} = \tilde{H} \begin{bmatrix} x_r - \hat{x}_r \\ y_r - \hat{y}_r \\ z_r - \hat{z}_r \\ Clk_r - Cl\hat{k}_r \end{bmatrix}. \quad (4)$$

Now, the proposed observation matrix (\tilde{H}) is obtained by simplifying the difference between equations (2) and (3), i.e., between true and estimated pseudo-ranges (using

the *direct difference method* in [1]). That is,

$$\left[P_{sr}^i - \hat{P}_{sr}^i \right] = \eta. \quad (5)$$

This approach is done differently, it starts by considering the difference between squares of true and estimated pseudo-range equations (2) and (3), respectively.

$$\begin{aligned} & (P_{sr}^i)^2 - (\hat{P}_{sr}^i)^2 \\ & \left(\sqrt{(x_{sat}^i - x_r)^2 + (y_{sat}^i - y_r)^2 + (z_{sat}^i - z_r)^2 + Clk_r} \right)^2 \\ & - \left(\sqrt{(x_{sat}^i - \hat{x}_r)^2 + (y_{sat}^i - \hat{y}_r)^2 + (z_{sat}^i - \hat{z}_r)^2 + Cl\hat{k}_r} \right)^2. \end{aligned} \quad (6)$$

This can be written as,

By considering the right-hand side of the equations (6),

$$\begin{aligned} \Delta\delta &= \left(\sqrt{(x_{sat}^i - x_r)^2 + (y_{sat}^i - y_r)^2 + (z_{sat}^i - z_r)^2 + Clk_r} \right)^2 \\ & - \left(\sqrt{(x_{sat}^i - \hat{x}_r)^2 + (y_{sat}^i - \hat{y}_r)^2 + (z_{sat}^i - \hat{z}_r)^2 + Cl\hat{k}_r} \right)^2. \end{aligned} \quad (7)$$

Now, equation (6) can be written as,

$$(P_{sr}^i)^2 - (\hat{P}_{sr}^i)^2 = \left[P_{sr}^i - \hat{P}_{sr}^i \right] \left[P_{sr}^i + \hat{P}_{sr}^i \right] = \Delta\delta, \quad (8)$$

$$\left[P_{sr}^i - \hat{P}_{sr}^i \right] = \frac{\Delta\delta}{\left[P_{sr}^i + \hat{P}_{sr}^i \right]}. \quad (9)$$

By solving $\Delta\delta$, the approximate form of equation (9) becomes, measurement vector, $[X - \hat{X}] = \Delta X$ is the differential state

$$\left[P_{sr}^i - \hat{P}_{sr}^i \right] \cong \begin{bmatrix} \frac{x_r + \hat{x}_r - 2x_{sat}^i}{P_{sr}^i + \hat{P}_{sr}^i} & \frac{y_r + \hat{y}_r - 2y_{sat}^i}{P_{sr}^i + \hat{P}_{sr}^i} & \frac{z_r + \hat{z}_r - 2z_{sat}^i}{P_{sr}^i + \hat{P}_{sr}^i} & \frac{2(Cl k_r Cl \hat{k}_r)(P_{sr}^i - \hat{P}_{sr}^i)}{(Cl k_r + Cl \hat{k}_r)(P_{sr}^i + \hat{P}_{sr}^i)} \end{bmatrix} \begin{bmatrix} x_r - \hat{x}_r \\ y_r - \hat{y}_r \\ z_r - \hat{z}_r \\ Cl k_r - Cl \hat{k}_r \end{bmatrix}. \quad (10)$$

$$\left[P_{sr}^i - \hat{P}_{sr}^i \right] \cong \tilde{H} [X - \hat{X}]. \quad (11)$$

Therefore, equation (11) can be written as,

$$\Delta Z = \tilde{H} \cdot \Delta X, \quad (12)$$

where $[P_{sr}^i - \hat{P}_{sr}^i] = \Delta Z$ is the differential pseudo-range

vector, and \tilde{H} is the proposed observation matrix.

The equation (12) is the same as the standard differential measurement equation $\Delta Z = H \cdot \Delta X$ as given in [13], where ΔZ is the differential pseudo-range measurement vector, ΔX denotes the differential state vector, and H is the classical observation matrix. Comparing both expressions \tilde{H} is similar to H of the standard differential measurement equation. Therefore, when comparing equations (10) and (12), the \tilde{H} is given by:

$$\tilde{H} \cong \begin{bmatrix} \frac{x_r + \hat{x}_r - 2x_{sat}^i}{P_{sr}^i + \hat{P}_{sr}^i} & \frac{y_r + \hat{y}_r - 2y_{sat}^i}{P_{sr}^i + \hat{P}_{sr}^i} & \frac{z_r + \hat{z}_r - 2z_{sat}^i}{P_{sr}^i + \hat{P}_{sr}^i} & \frac{2(Cl k_r Cl \hat{k}_r)(P_{sr}^i - \hat{P}_{sr}^i)}{(Cl k_r + Cl \hat{k}_r)(P_{sr}^i + \hat{P}_{sr}^i)} \end{bmatrix}. \quad (13)$$

For “i” the number of visible satellites, equation (13) can be written as,

$$\tilde{H} \cong \begin{bmatrix} \frac{x_r + \hat{x}_r - 2x_{sat}^1}{P_{sr}^1 + \hat{P}_{sr}^1} & \frac{y_r + \hat{y}_r - 2y_{sat}^1}{P_{sr}^1 + \hat{P}_{sr}^1} & \frac{z_r + \hat{z}_r - 2z_{sat}^1}{P_{sr}^1 + \hat{P}_{sr}^1} & \frac{2(Cl k_r Cl \hat{k}_r)(P_{sr}^1 - \hat{P}_{sr}^1)}{(Cl k_r + Cl \hat{k}_r)(P_{sr}^1 + \hat{P}_{sr}^1)} \\ \frac{x_r + \hat{x}_r - 2x_{sat}^2}{P_{sr}^2 + \hat{P}_{sr}^2} & \frac{y_r + \hat{y}_r - 2y_{sat}^2}{P_{sr}^2 + \hat{P}_{sr}^2} & \frac{z_r + \hat{z}_r - 2z_{sat}^2}{P_{sr}^2 + \hat{P}_{sr}^2} & \frac{2(Cl k_r Cl \hat{k}_r)(P_{sr}^2 - \hat{P}_{sr}^2)}{(Cl k_r + Cl \hat{k}_r)(P_{sr}^2 + \hat{P}_{sr}^2)} \\ \vdots & \vdots & \vdots & \vdots \\ \frac{x_r + \hat{x}_r - 2x_{sat}^i}{P_{sr}^i + \hat{P}_{sr}^i} & \frac{y_r + \hat{y}_r - 2y_{sat}^i}{P_{sr}^i + \hat{P}_{sr}^i} & \frac{z_r + \hat{z}_r - 2z_{sat}^i}{P_{sr}^i + \hat{P}_{sr}^i} & \frac{2(Cl k_r Cl \hat{k}_r)(P_{sr}^i - \hat{P}_{sr}^i)}{(Cl k_r + Cl \hat{k}_r)(P_{sr}^i + \hat{P}_{sr}^i)} \end{bmatrix} \cdot \quad (14)$$

In the above equation, (x_r, y_r, z_r) and $Cl k_r$ are considered as true 3D position coordinates and the receiver clock bias, respectively, which are practically unavailable. Hence, these are replaced with the estimated coordinates of the previous iteration in the Least Squares or any other optimization approach [1, 2, 4]. Then, the classical observation matrix H [13] is written as follows.

$$H = \begin{bmatrix} \frac{x_r - x_{sat}^1}{P_{sr}^1} & \frac{y_r - y_{sat}^1}{P_{sr}^1} & \frac{z_r - z_{sat}^1}{P_{sr}^1} & 1 \\ \frac{x_r - x_{sat}^2}{P_{sr}^2} & \frac{y_r - y_{sat}^2}{P_{sr}^2} & \frac{z_r - z_{sat}^2}{P_{sr}^2} & 1 \\ \vdots & \vdots & \vdots & \vdots \\ \frac{x_r - x_{sat}^i}{P_{sr}^i} & \frac{y_r - y_{sat}^i}{P_{sr}^i} & \frac{z_r - z_{sat}^i}{P_{sr}^i} & 1 \end{bmatrix} \cdot \quad (15)$$

Thus, the equation (14) shows that all parameters in \tilde{H} are a function of true and estimated values. If true and estimated values of all parameters are equal in equation (14), then the first three parameters of all rows \tilde{H} will be the same as the parameters H in equation (15). But the fourth parameter will be zero, and hence all values of the fourth column are zero, which not only contradicts H but also makes \tilde{H} a singular or degenerate matrix. Thus, \tilde{H} becomes a noninvertible matrix. Therefore, to eliminate \tilde{H} singularity, only the receiver clock bias terms are retained, and the $(P_{sr}^i - \hat{P}_{sr}^i)/(P_{sr}^i + \hat{P}_{sr}^i)$ term is excluded because its value is practically very low and affects the entire term to become zero. Thus, if the true and estimated values are equal, then the fourth term becomes $Cl k_r$, which is the receiver clock bias, and therefore \tilde{H} is not a singular matrix and can be the invertible matrix. Therefore, the final expression of the proposed approximate form of observation matrix is given by,

$$\tilde{H} \cong \begin{bmatrix} \frac{x_r + \hat{x}_r - 2x_{sat}^1}{P_{sr}^1 + \hat{P}_{sr}^1} & \frac{y_r + \hat{y}_r - 2y_{sat}^1}{P_{sr}^1 + \hat{P}_{sr}^1} & \frac{z_r + \hat{z}_r - 2z_{sat}^1}{P_{sr}^1 + \hat{P}_{sr}^1} & \frac{2(Cl k_r Cl \hat{k}_r)}{(Cl k_r + Cl \hat{k}_r)} \\ \frac{x_r + \hat{x}_r - 2x_{sat}^2}{P_{sr}^2 + \hat{P}_{sr}^2} & \frac{y_r + \hat{y}_r - 2y_{sat}^2}{P_{sr}^2 + \hat{P}_{sr}^2} & \frac{z_r + \hat{z}_r - 2z_{sat}^2}{P_{sr}^2 + \hat{P}_{sr}^2} & \frac{2(Cl k_r Cl \hat{k}_r)}{(Cl k_r + Cl \hat{k}_r)} \\ \vdots & \vdots & \vdots & \vdots \\ \frac{x_r + \hat{x}_r - 2x_{sat}^i}{P_{sr}^i + \hat{P}_{sr}^i} & \frac{y_r + \hat{y}_r - 2y_{sat}^i}{P_{sr}^i + \hat{P}_{sr}^i} & \frac{z_r + \hat{z}_r - 2z_{sat}^i}{P_{sr}^i + \hat{P}_{sr}^i} & \frac{2(Cl k_r Cl \hat{k}_r)}{(Cl k_r + Cl \hat{k}_r)} \end{bmatrix} \cdot \quad (16)$$

TABLE 1: Comparison of DOP values.

Type of DOP		Time of observation	Due to classical observation matrix H	Due to the proposed observation matrix \tilde{H}
GDOP	Maximum	05:39 Hrs.	2.281	1.882
	Minimum	15:42 Hrs.	1.244	1.146
PDOP	Maximum	05:39 Hrs.	1.976	1.882
	Minimum	15:42 Hrs.	1.146	1.146
HDOP	Maximum	05:39 Hrs.	1.812	1.715
	Minimum	15:42 Hrs.	1.054	1.054
VDOP	Maximum	05:56 Hrs.	0.797	0.780
	Minimum	00:69 Hrs.	0.416	0.416
TDOP	Maximum	05:39 Hrs.	1.139	0.032
	Minimum	15:42 Hrs.	0.484	0.017

Now, the fourth parameter (*receiver clock bias*) in the last column of the \tilde{H} is a variable unlike in H and its value changes for each iteration which impacts the GDOP calculation for each epoch and also on GPS receiver position estimation. Not only the fourth parameter but also the first three parameters in the \tilde{H} will have an impact on all DOP parameters and the position estimation process. Thus, the computation of all DOP parameters and estimation of GPS receiver/user position by using \tilde{H} leads to increased precision in the results when compared to that of H . The increased precision is due to the higher-order \tilde{H} approximation. This is proved by simulating on real-time GPS data which is presented in the next section. General range values of all DOP parameters are given in [27–29].

3. Experimental Results

The efficiency of the *proposed observation matrix* \tilde{H} is evaluated by computing the GDOP and estimating the position of a GPS receiver/user. The dual-frequency GPS receiver (NovAtel: DL-V3-L1L2) is used to collect real-time data which is installed at the Department of ECE, AUCE (A), Andhra University (Lat.17.73°N/Long.83.31°E), Visakhapatnam region, India.

The efficiency of \tilde{H} is presented in two stages. That is:

- DOP computational analysis is to prove there is an improved precision in the DOP parameters calculation
- In terms of Root Mean Square (RMS) position error to prove its fast convergence rate and improved precision in the estimated results

3.1. DOP Computation. In the proposed \tilde{H} , the fourth parameter is a variable for each iteration. The small change in the fourth parameter has high impact on the next iteration which improves the precision of the estimated parameters. Thus, at the end of final iteration the accuracy of the estimation improves. Table 1 presents the comparison of computed DOP values using H and \tilde{H} . Also, comparative results are shown in Figures 1–5. In the legend of the figures,

the notation “Existing observation matrix” means “classical observation matrix” (H). DOP parameters least value is generally unity (i.e., 1) if the best of 4 satellite vehicles data is considered. But DOP values are less than one (<1) when multiple satellite vehicle data is considered. In this article, GPS input data is taken from all satellite vehicles which are in view with respect to the GPS receiver. Due to page limitations, see [10, 13, 21–26], and [27] for a detailed explanation of all DOP parameters and their calculation formulas. But, the GDOP calculation formula is given in equation (1).

In Table 1, for the same satellite configuration and time, the obtained DOP values are more precise due to the application of the \tilde{H} . Some of these DOP values are less than one which is commonly obtained when a greater number of satellites are visible to a GPS receiver.

As shown in Figure 1, the minimum GDOP obtained using proposed observation matrix (\tilde{H}) is 0.831 at 23:36 Hrs. Whereas, the minimum GDOP obtained using classical observation matrix (H) is 1.244 at 15:42 Hrs. The proposed \tilde{H} calculated GDOP values with improved precision for the same number of considered satellites as the H . From the Figure 1, it is clearly observed that at each instant of the 24-hour duration the GDOP values are computed precisely by using \tilde{H} . Thus, in case of optimal satellite selection method, the proposed \tilde{H} is very significant for choosing optimal satellites among the available satellites in the vicinity.

As it can be seen from Figure 2, the minimum PDOP obtained using proposed observation matrix (\tilde{H}) is 0.832 at 23:39 Hrs. Whereas, the minimum PDOP obtained using classical observation matrix (H) is 1.146 at 15:42 Hrs. The proposed \tilde{H} calculated PDOP values with improved precision for the same number of considered satellites as the H . From the Figure 2, it is clearly observed that at each instant of the 24-hour duration the PDOP values computed precisely by using \tilde{H} . Thus, the proposed \tilde{H} is very significant to describe the error caused by the relative position of the GPS satellites.

The minimum HDOP obtained using proposed observation matrix (\tilde{H}) is 0.691 at 23:24 Hrs. While, the minimum HDOP obtained using classical observation matrix (H) is

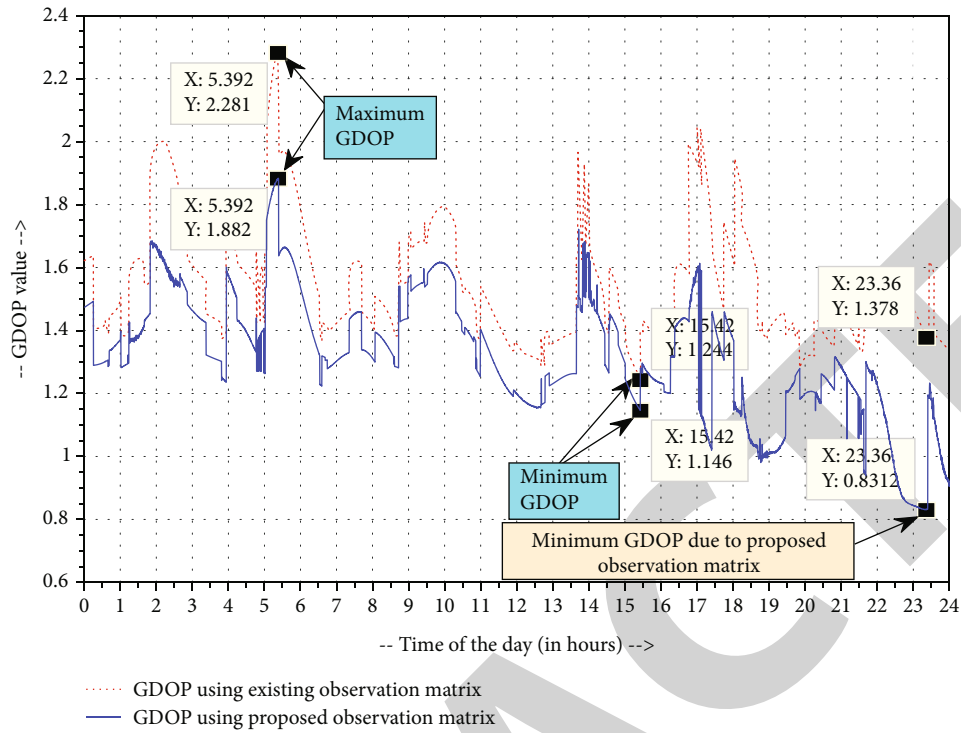


FIGURE 1: Comparisons of GDOP values.

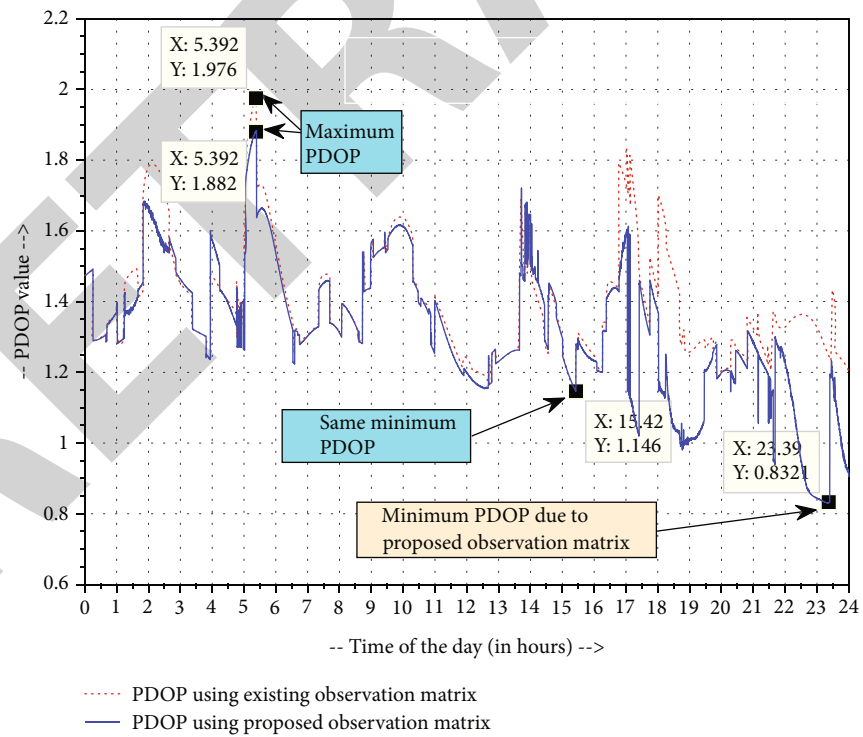


FIGURE 2: Comparisons of PDOP values.

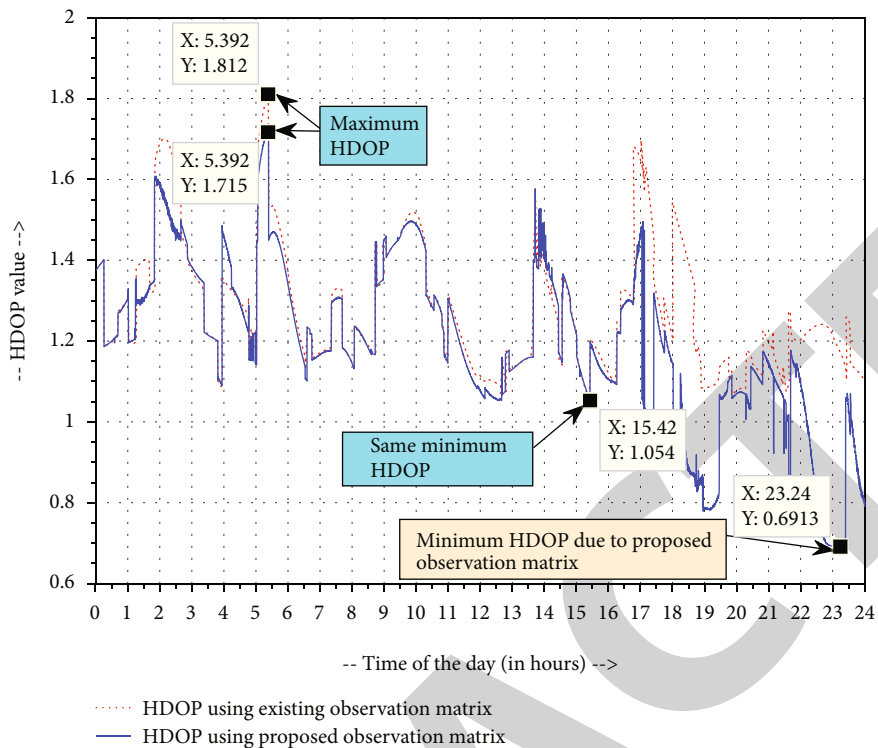


FIGURE 3: Comparisons of HDOP values.

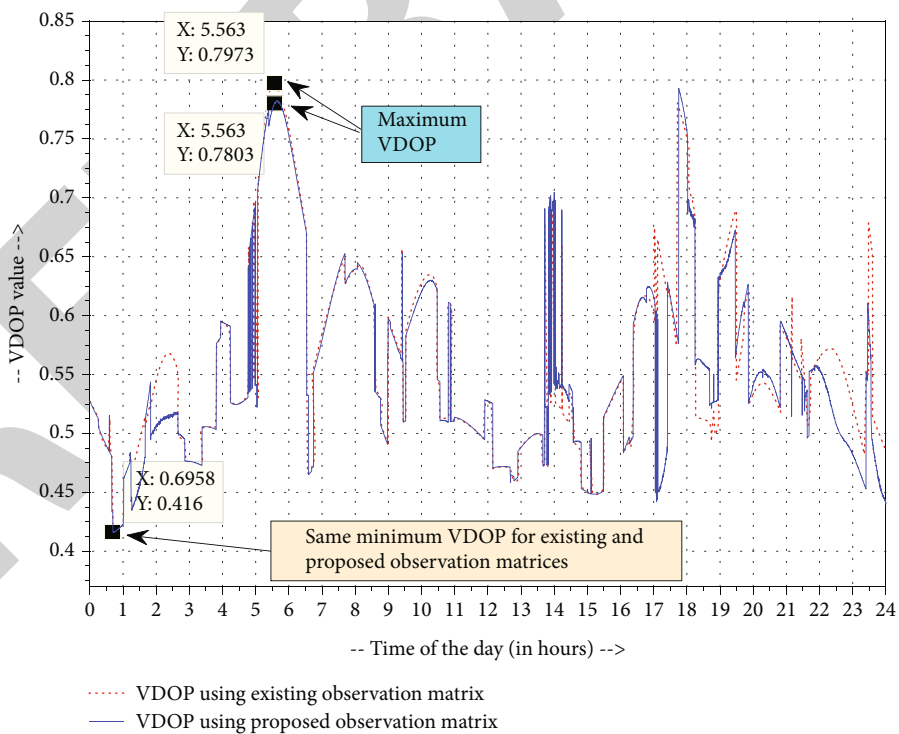


FIGURE 4: Comparisons of VDOP values.

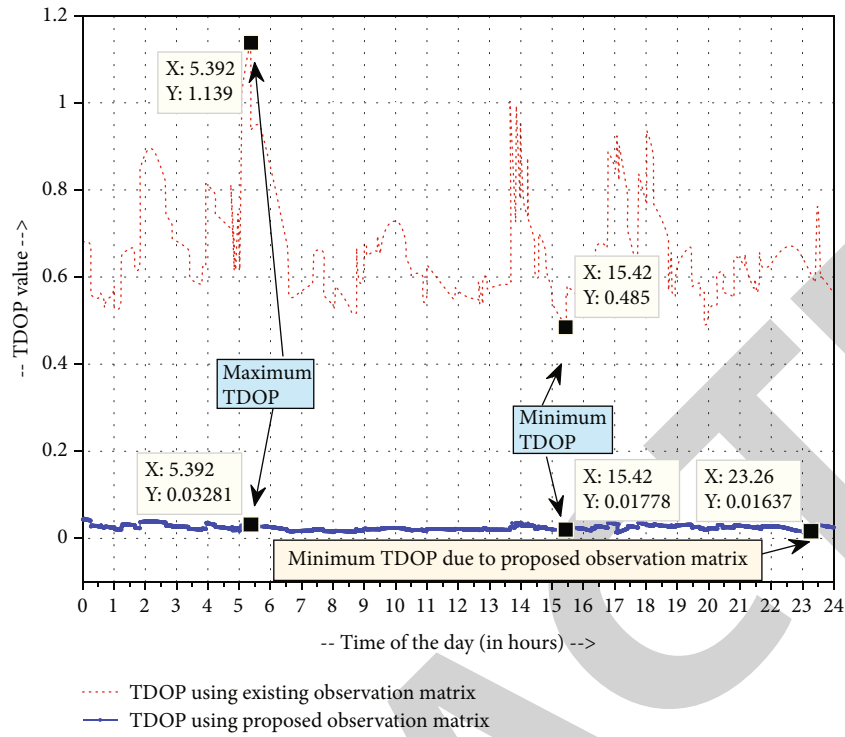


FIGURE 5: Comparisons of TDOP values.

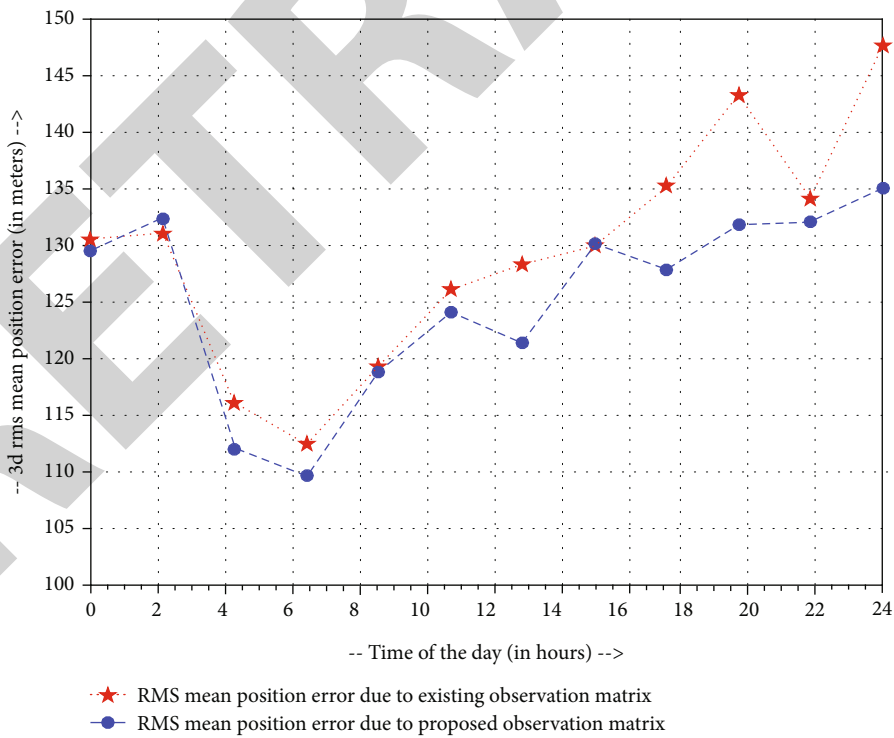


FIGURE 6: Comparisons of RMS mean position error due to LS algorithm.

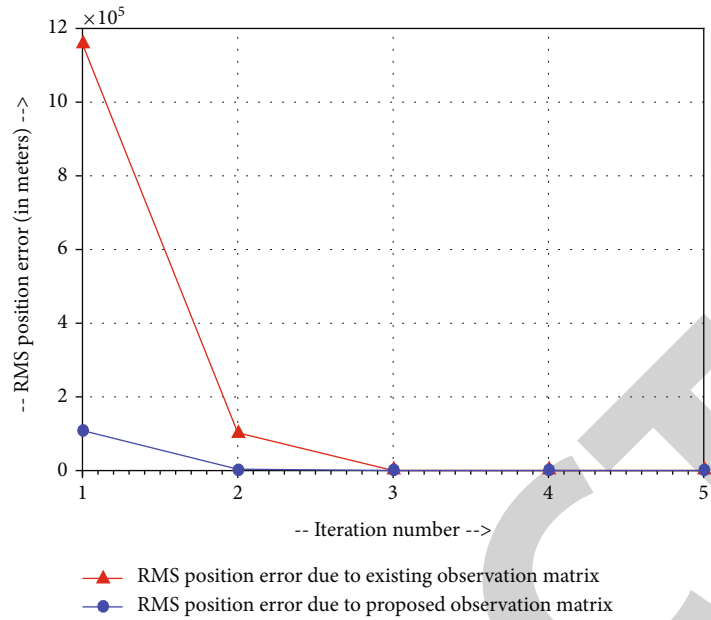


FIGURE 7: Comparisons of the iteration process.

1.054 at 15:42 Hrs (see Figure 3). The proposed \tilde{H} calculated HDOP values with improved precision for the same number of considered satellites as the H . From the Figure 3, it is clearly observed that at each instant of the 24-hour duration the HDOP values computed precisely by using \tilde{H} . Thus, the proposed \tilde{H} is very significant to more precisely estimate the accuracy of GPS horizontal (latitude/longitude) position fixes by adjusting the error estimates according to the geometry of the satellites used.

From Figure 4, it is evident that the obtained minimum VDOP using H and \tilde{H} is the same i.e., 0.416 at 00:69 Hrs, i.e., at 00:41 minutes.

The obtained minimum TDOP using proposed observation matrix (\tilde{H}) is 0.016 at 23:26 Hrs (see Figure 5). Whereas, the minimum TDOP obtained using classical observation matrix (H) is 0.485 at 15:42 Hrs. The TDOP precision is increased due to the variable expression introduced in the \tilde{H} unlike the constant in H . The variability will be effected for each iteration of each epoch, hence the precision changes which are improved here.

From Table 1 and the graphs (Figures 1–5), it is evident that DOP values due to \tilde{H} are more precise when compared to that of H for the same satellite configuration. Therefore, the \tilde{H} is much useful in the Visakhapatnam region for positioning, navigation, and timing applications.

3.2. GPS Receiver/User Position Estimation. The observation matrices H and \tilde{H} are applied in the least-squares (LS) algorithm to estimate the position of the GPS user/receiver. The comparative results reveal that, the RMS error in position due to the application of \tilde{H} is lesser than the RMS mean position error due H as shown in Figure 6. Thus, \tilde{H} improves the precision in the estimation of 3D position

[22, 25, 28–36]. The convergence rate of both proposed and existing observation matrices in terms of the number of iterations is given in Figure 7.

As it can be observed from Figure 7, \tilde{H} converge from the first iteration and converge completely on the second iteration. Whereas, H starts with a large error and converges on the third iteration, and offers a high RMS position error when compared to that of \tilde{H} , as shown in Figure 6. Consequently, \tilde{H} offers a fast convergence rate with less RMS position error, which is very useful in real-time applications.

Algorithms MGEKF [1] and EKF [3] are also implemented on the same GPS data, and the corresponding RMS position errors are compared, as shown in Figure 8. From the figure it can be depicted that the RMS error in position due to the EKF algorithm increasing from 08:00 hours onward, while MGEKF results continue to decrease from the start, which shows the stability of the MGEKF algorithm. Thus, the only distinction between EKF and MGEKF is the modified gain function “ g ”, which is the proposed observation matrix \tilde{H} in the MGEKF. Thus, the proposed observation matrix \tilde{H} provides not only fast convergence and stability to the MGEKF algorithm but also a precise result.

An analysis of the results presented in sections 3.1 and 3.2 shows that using \tilde{H} has two advantages. These are: (i) It provides fast convergence, (ii) It improves the precision of DOP calculations and estimation of receiver/user position by reducing the RMS position error. Due to the modified Taylor’s series first order parameters in the proposed \tilde{H} , the \tilde{H} is numerically stable than the H . Also described that how closely the both H and \tilde{H} are related at an ideal case. From the observation of MGEKF results, the state estimates are found to be much more consistent than from the EKF

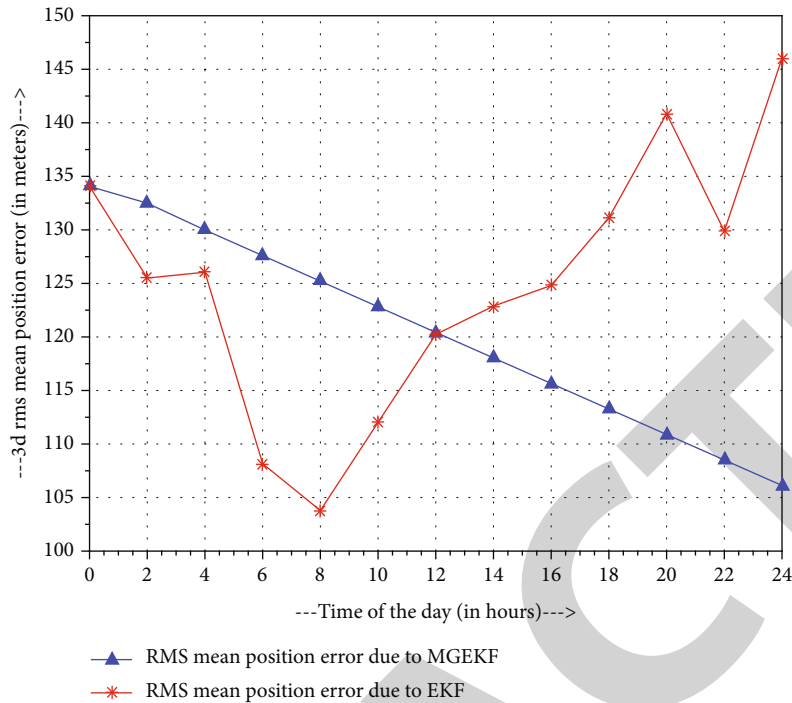


FIGURE 8: Comparisons of RMS position error due to MGEKF and EKF.

filter. Therefore, the *proposed observation matrix* \tilde{H} can be used in the place of the classical observation matrix H to obtain more precise DOP values which exhibits the geometric effect on the association of positioning determination error and measurement error and improved precision in the estimation of GPS receiver position coordinates. The *proposed observation matrix* \tilde{H} is useful for obtaining a more accurate body trajectory estimate in GNSS applications. It is also useful to identify the best GPS satellites with low DOP values in navigation evaluation applications where optimal satellites selection is applied. This can be useful for vertical guidance (APV) approaches at airports. It can also be used for advanced systems such as GPS Aided GEO Augmented Navigation (GAGAN).

4. Conclusion

A new observation matrix is derived based on the *direct difference method* presented in the works of Galkowski. The *proposed observation matrix* \tilde{H} is a higher-order approximate form which makes the fourth parameter as a variable unlike in the classical observation matrix. Thus, the precision of all DOP parameters improved and also provided a fast convergence rate, stability of the algorithm, and improved precision in GPS receiver position estimation. Hence, the proposed observation matrix is useful for GPS sensors in obtaining a precise location for location sensor-dependent applications, GNSS trajectory estimation, optimal satellites selection process, and also GPS depended augmentation systems. In future works, the present work can be tested for the suitability for Indian Regional Navigation Sat-

ellite System (IRNSS) and IRNSS based augmentation systems.

Acronyms

DOP:	Dilution of precision
GDOP:	Geometric dilution of precision
PDOP:	Position dilution of precision
HDOP:	Horizontal dilution of precision
VDOP:	Vertical dilution of precision
TDOP:	Time dilution of precision
GPS:	Global positioning system
EKF:	Extended Kalman filter
MGEKF:	Modified gain extended Kalman filter.

Data Availability

The GPS receiver data used to support the findings of this study are available from the authors upon request.

Conflicts of Interest

The authors declare that they have no conflicts of interest.

Acknowledgments

The experimented GPS receiver data, in this paper, has been collected from the Department of Electronics and Communication Engineering, AUCE (A), Andhra University, Visakhapatnam, India.

References

- [1] P. J. Galkowski and M. A. Islam, "An alternative derivation of the modified gain function of Song and Speyer," *IEEE Transactions on Automatic Control*, vol. 36, no. 11, pp. 1323–1326, 1991.
- [2] T. Song and J. Speyer, "A stochastic analysis of a modified gain extended Kalman filter with applications to estimation with bearings only measurements," *IEEE Transactions on Automatic Control*, vol. 30, no. 10, pp. 940–949, 1985.
- [3] N. Ashok Kumar, C. Suresh, and G. Sasibhushana Rao, "Extended Kalman filter for GPS receiver position estimation," *Intelligent Engineering Informatics*, vol. 695, pp. 481–488, 2018.
- [4] S. K. Rao, "Modified gain extended Kalman filter with application to bearings-only passive manoeuvring target tracking," *IEEE Proceedings-Radar, Sonar and Navigation*, vol. 152, no. 4, pp. 239–244, 2005.
- [5] P. Chen, H. Ma, S. Gao, and Y. Huang, "Modified extended Kalman filtering for tracking with insufficient and intermittent observations," *Mathematical Problems in Engineering*, vol. 2015, Article ID 981727, 9 pages, 2015.
- [6] R. Yarlagadda, I. Ali, N. Al-Dhahir, and J. Hershey, "GPS GDOP metric," *IEEE Proceedings Radar, Sonar and Navigation*, vol. 147, no. 5, pp. 259–264, 2000.
- [7] I. Prasad, "Smart grid technology: application and control," *International Journal of Advanced Research in Electrical, Electronics and Instrumentation Engineering*, vol. 3, no. 5, pp. 9533–9542, 2014.
- [8] Y. Yong and M. Lingjuan, "GDOP results in all-in-view positioning and in four optimum satellites positioning with GPS PRN codes ranging," in *Proceedings of the Position Location and Navigation Symposium*, pp. 723–727, Monterey, CA, USA, 2004.
- [9] D. Y. Hsu, "Relations between dilutions of precision and volume of the tetrahedron formed by four satellites," in *Proceedings of the IEEE Position Location and Navigation Symposium*, pp. 669–676, Las Vegas, NV, USA, 1994.
- [10] V. S. I. Dutt, G. S. B. Rao, S. S. Rani, S. R. Babu, R. Goswami, and C. U. Kumari, "Investigation of GDOP for precise user position computation with all satellites in view and optimum four satellite configurations," *The Journal of Indian Geophysical Union*, vol. 13, no. 3, pp. 139–148, 2009.
- [11] M. Zhang and J. Zhang, "A fast satellite selection algorithm: beyond four satellites," *IEEE Journal of Selected Topics in Signal Processing*, vol. 3, no. 5, pp. 740–747, 2009.
- [12] G. Ganesh Laveti, "Modified Kalman filter for GPS position estimation over the Indian sub continent," *Procedia Computer Science Journal*, vol. 87, pp. 198–203, 2016.
- [13] G. S. Rao, *Global navigation satellite systems - with essentials of satellite communication*, Tata McGraw-Hill, New Delhi, 2010.
- [14] D. J. Jwo and C. C. Lai, "Neural network-based GPS GDOP approximation and classification," *Gps Solutions*, vol. 11, no. 1, pp. 51–60, 2007.
- [15] S. K. Pagoti, B. S. S. I. D. Vemuri, and M. K. Mohiddin, "Enhanced Kalman filter navigation algorithm based on corentropy and fixed-point update," *International Journal of Engineering and Technology Innovation (IJETI)*, vol. 12, no. 2, pp. 1–20, 2021.
- [16] J. Song, G. Xue, and Y. Kang, "A novel method for optimum global positioning system satellite selection based on a modified genetic algorithm," *PLoS One*, vol. 11, no. 3, article e0150005, 2016.
- [17] M. Mohiddin, R. Kohli, V. B. S. Dutt, P. Dixit, and G. Michal, "Energy-efficient enhancement for the prediction-based scheduling algorithm for the improvement of network lifetime in WSNs," *Wireless Communications and Mobile Computing*, vol. 2021, Article ID 9601078, 12 pages, 2021.
- [18] M. Numan, F. Subhan, W. Z. Khan et al., "A systematic review on clone node detection in static wireless sensor networks," *IEEE Access*, vol. 8, pp. 65450–65461, 2020.
- [19] C. S. Chen, Y. J. Chiu, C. T. Lee, and J. M. Lin, "Calculation of weighted geometric dilution of precision," *Journal of Applied Mathematics*, vol. 2013, Article ID 953048, 10 pages, 2013.
- [20] M. Kihara, "Study of a GPS satellite selection policy to improve positioning accuracy," in *Proceedings of 1994 IEEE Position, Location and Navigation Symposium-PLANS'94*, pp. 267–273, Las Vegas, NV, USA, 1994.
- [21] J. Zhu, "Calculation of geometric dilution of precision," *IEEE Transactions on Aerospace and Electronic Systems*, vol. 28, no. 3, pp. 893–895, 1992.
- [22] K. Phasinam, T. Kassanuk, P. P. Shinde et al., "Application of IoT and cloud computing in automation of agriculture irrigation," *Journal of Food Quality*, vol. 2022, Article ID 8285969, 8 pages, 2022.
- [23] M. K. Mohiddin and V. B. S. S. Indira Dutt, "An optimum energy consumption hybrid algorithm for XLN strategic design in WSN'S," *International Journal of Computer Networks and Communications (IJCNC)*, vol. 11, no. 4, pp. 61–80, 2019.
- [24] M. K. Mohiddin and V. B. S. S. I. Dutt, "Minimization of energy consumption using X-Layer network transformation model for IEEE 802.15.4-based MWSNs," in *Proceedings of the 5th International Conference on Frontiers in Intelligent Computing: Theory and Applications*, vol. 515 of *Advances in Intelligent Systems and Computing*, pp. 741–751, Singapore, 2017.
- [25] M. Khaja and V. B. S. S. I. Dutt, "An efficient energy optimization XLN operation model for IEEE 802.15.4-based mobile WSNs," *International Journal of Control Theory and Applications (IJCTA)*, vol. 10, no. 9, pp. 255–264, 2017.
- [26] M. K. Mohiddin and S. I. Dutt, "Routing path estimation based on RWS method for competent energy dissipation employing X-layer network," *International Journal of Recent Technology and Engineering (IJRTE)*, vol. 8, no. 2, pp. 6296–6303, 2019.
- [27] R. B. Langley, "Dilution of precision," *GPS World*, vol. 10, no. 5, pp. 52–59, 1999.
- [28] R. Mishra, S. Ralhan, and M. K. Mohiddin, "A review on frequency stability enhancement and effective energy storage through various optimization techniques," *Mobile Information Systems*, vol. 2022, Article ID 4170938, 8 pages, 2022.
- [29] P. Agarwal, D. K. Sharma, V. L. Varun et al., "A survey on the scope of cloud computing," *Materials Today: Proceedings*, vol. 51, pp. 861–864, 2021.
- [30] E. D. Kaplan and J. H. Christopher, *Understanding GPS principles and applications*, Artech House Press, London, 2017.
- [31] G. Zhou, "Research on GPS user trajectory analysis and behavior prediction based on swarm intelligence algorithm," *Journal of Sensors*, vol. 2022, Article ID 7554560, 11 pages, 2022.
- [32] J. Machaj, P. Brida, N. Majer, and R. Ščehovič, "Impact of GPS interference on time synchronization of DVB-T transmitters,"

Retraction

Retracted: The Construction of Conceptual Framework of Enterprise Internal Control Evaluation Report

Journal of Sensors

Received 19 December 2023; Accepted 19 December 2023; Published 20 December 2023

Copyright © 2023 Journal of Sensors. This is an open access article distributed under the Creative Commons Attribution License, which permits unrestricted use, distribution, and reproduction in any medium, provided the original work is properly cited.

This article has been retracted by Hindawi following an investigation undertaken by the publisher [1]. This investigation has uncovered evidence of one or more of the following indicators of systematic manipulation of the publication process:

- (1) Discrepancies in scope
- (2) Discrepancies in the description of the research reported
- (3) Discrepancies between the availability of data and the research described
- (4) Inappropriate citations
- (5) Incoherent, meaningless and/or irrelevant content included in the article
- (6) Manipulated or compromised peer review

The presence of these indicators undermines our confidence in the integrity of the article's content and we cannot, therefore, vouch for its reliability. Please note that this notice is intended solely to alert readers that the content of this article is unreliable. We have not investigated whether authors were aware of or involved in the systematic manipulation of the publication process.

Wiley and Hindawi regrets that the usual quality checks did not identify these issues before publication and have since put additional measures in place to safeguard research integrity.

We wish to credit our own Research Integrity and Research Publishing teams and anonymous and named external researchers and research integrity experts for contributing to this investigation.

The corresponding author, as the representative of all authors, has been given the opportunity to register their agreement or disagreement to this retraction. We have kept a record of any response received.

References

- [1] Y. Kuang, Z. Li, and C. Pan, "The Construction of Conceptual Framework of Enterprise Internal Control Evaluation Report," *Journal of Sensors*, vol. 2022, Article ID 2753001, 11 pages, 2022.

Research Article

The Construction of Conceptual Framework of Enterprise Internal Control Evaluation Report

Yushu Kuang,¹ Zongkeng Li^{2,3} and Changliang Pan³

¹School of Accounting, Guangdong University of Finance and Economics, Guangzhou 510320, China

²Department of Management, Sumy National Agrarian University, Ukraine

³Hezhou University, Hezhou 542899, China

Correspondence should be addressed to Zongkeng Li; lizongkeng06@hzxy.edu.cn

Received 21 July 2022; Revised 15 August 2022; Accepted 20 August 2022; Published 19 September 2022

Academic Editor: Sweta Bhattacharya

Copyright © 2022 Yushu Kuang et al. This is an open access article distributed under the Creative Commons Attribution License, which permits unrestricted use, distribution, and reproduction in any medium, provided the original work is properly cited.

In practice, although there is no doubt about the role of enterprise internal control, how to evaluate the effect of enterprise internal control and the auditability of internal control has always been a difficult problem that plagues the theoretical and practical circles. The problems existing in the construction and development of enterprise internal control, such as the information content problem in the enterprise internal control evaluation report, are largely due to the lack of the conceptual framework of enterprise internal control to guide the internal control theory of enterprises. Therefore, the establishment of a set of conceptual framework for the evaluation report of internal control of enterprises and a full understanding of its importance play an important role in solving the practical problems faced in the practice of internal control of enterprises and promoting the construction and development of internal control of enterprises. The construction of the conceptual framework of the internal control evaluation report of an enterprise should adopt the viewpoint of the essential starting point theory, learn from the experience in the construction of relevant conceptual frameworks, start from the concept of the conceptual framework, clarify the main users of the report and their common needs, and combine the functions of the internal control evaluation report. Then, determine the objectives of the internal control evaluation report. This paper proposes that the introduction of information quality characteristics, elements of internal control evaluation reports, and cost-benefit measurement concepts can achieve the preset goals of enterprise internal control evaluation reports.

1. Introduction

In order to reduce the information asymmetry in the capital market, ensure that relevant stakeholders have better access to the internal control information of listed companies, and strengthen the supervision of the internal control of listed companies; the Chinese government has successively promulgated corresponding laws and regulations to regulate the disclosure of internal control information. With the change of the internal control information disclosure of Chinese-listed companies from “voluntary disclosure” to “mandatory disclosure”, the research focus of practical and theoretical circles has also shifted [1]. In the context of “voluntary disclosure”, the disclosure of internal control information is highly selective. Under normal circumstances, listed companies with sound internal control are more

inclined to disclose, while listed companies with imperfect internal control are more inclined to not disclose. Therefore, many scholars measure the quality of internal control information disclosure of listed companies through the signaling function of the disclosure behavior itself, which is based on whether to voluntarily disclose the internal control self-assessment report and the internal control audit report. In the context of “mandatory disclosure”, the content of internal control information disclosure, especially the disclosure of internal control defect information, can truly measure the quality of internal control information disclosure.

However, in the process of implementing the “mandatory disclosure” system, the study found that listed companies issued unreadable internal control self-assessment reports in order to cope with inspections, selectively disclosed internal control defects, or evaded actual performance

when disclosing internal control defects. False, unclear words, inconsistent opinions between the self-assessment report, and the audit report. According to the statistics on the overall effectiveness of the internal control evaluation of Chinese-listed companies released by DIB Company for 13 years (2007-2019) (as shown in Table 1), we found that the annual internal control evaluation of listed companies was identified as the proportions of overall effective and nonoverall effective were 98.87% (average) and 1.13% (average), respectively. Taking into account the mandatory disclosure of corporate internal control requirements in 2012 alone, the proportions of listed companies' annual internal control evaluations that were identified as overall effective and nonoverall effective were 98.28% (average) and 1.72% (average), respectively.

Statistics on the internal control audit data (as shown in Table 2) found that the standard opinions and nonstandard opinions in the internal control audit opinions of listed companies in 2013 accounted for an average of 97.26% and 2.74%, respectively. In the context of mandatory disclosure, standard opinions and nonstandard opinions account for an average of 95.94% and 4.06%, respectively. It can be seen that, after years of hard work, the internal control construction of Chinese-listed companies has achieved remarkable results, and has made positive contributions to improving operational efficiency and preventing various risks.

In recent years, there have been frequent cases of financial fraud in the capital market, such as Wanfu Biotechnology, Jinya Technology, Kangmei Pharmaceutical, and Kangdexin. What role can corporate internal control play in preventing, detecting, and correcting fraud and errors? Did it work? What is the benefit to the enterprise from the cost of investing in the construction, maintenance, and certification of internal control every year? Judging from the current disclosure of internal control, the internal control self-evaluation report of an enterprise is relatively random. What is the difference between this and "management discussion and analysis" (MD&A)? From the existing research, the research path of internal control is also very different from the research path of MD&A. So, can the future development and research of internal control learn from the research framework of financial reporting, starting with the conceptual framework of enterprise internal control evaluation report? Judging from the current laws and regulations, there is a certain discretionary control in the internal control evaluation report. Does this mean that the internal control evaluation report can be disclosed at will? The importance of internal control is self-evident, but the effect of internal control in actual work is sometimes unsatisfactory, and the disclosure of internal control evaluation reports is uniform, mere formality, and lacks substantive content. The auditability of enterprise internal control and its auditing standards have always been a difficult problem for practitioners and theoretical researchers. Since the "Basic Norms for Enterprise Internal Control" was released in 2008, the problems existing in the construction and development of enterprise internal control, to a large extent, are related to the lack of a conceptual framework similar to the conceptual framework of financial reporting to guide the theoretical research

and development of corporate internal control. Related to practical activities, with the increasing complexity of economic development and the increase of risks, the development of enterprise internal control theory is relatively lagging behind, and it is difficult to meet the urgent needs of the development of internal control practice. We should establish the conceptual framework of enterprise internal control evaluation report and fully understand its importance, in order to deal with the practical problems faced in the practice of enterprise internal control, and promote the construction and development of enterprise internal control. To this end, we should start to study and solve major theoretical issues such as the concept, objectives, and elements of the enterprise internal control evaluation report, clarify the thinking, solve the problems existing in the development of the enterprise internal control practice, and continuously optimize the construction of the enterprise internal control system. This paper summarizes the importance of the establishment of the conceptual framework for the internal control evaluation report of enterprises, and proposes how to construct the conceptual framework of the internal control evaluation report of the enterprise, which provides a theoretical basis for the construction of the conceptual framework of the internal control evaluation report of the enterprise.

2. The Necessity and Function of the Conceptual Framework of the Internal Control Evaluation Report of Enterprises

The internal control evaluation report mainly declares to the public that there are no major defects or major defects in the internal control of the enterprise, so that the public can understand the current situation of the internal control of the enterprise. It is the responsibility of management to establish an effective internal control system. It can better meet the information needs of investors; in addition, it can promote the management authorities to pay more attention to the internal control of enterprises; secondly, it can reduce the occurrence of corporate fraud to a certain extent [2].

The necessity of studying the conceptual framework of enterprise internal control evaluation reports should be recognized from the following aspects: first, the internal control of Chinese enterprises has not yet formed a complete theoretical system, and it is necessary to establish a set of a theoretical system based on basic internal control concepts that can guide the construction of an enterprise's internal control. Second, many concepts of China's current internal control obviously lag behind the needs of the economic and political environment, corporate governance and the development of internal control practices. Third, in the wave of economic globalization and integration, China cannot stay out of the way. It should integrate into the international community, and actively learn from relevant international advanced experience on the basis of fully considering China's national conditions. Fourth, the conceptual framework of corporate internal control evaluation report can draw lessons from the experience and lessons of the

TABLE 1: Statistical results of the effectiveness of annual internal control evaluation of Chinese-listed companies from 2007 to 2019.

Years	2007	2008	2009	2010	2011	2012	2013	2014	2015	2016	2017	2018	2019	Average	Average since 2012
Overall effective percentage	100.00%	99.72%	99.77%	99.69%	99.84%	99.82%	98.85%	98.57%	98.80%	98.95%	8.20%	96.62%	96.46%	98.87%	98.28%
Nonoverall effective percentage	0.00%	0.28%	0.23%	0.31%	0.16%	0.18%	1.15%	1.43%	1.20%	1.05%	1.80%	3.38%	3.54%	1.13%	1.72%

TABLE 2: Statistical results of annual internal control audit opinions of Chinese-listed companies from 2007 to 2019.

Years	2007	2008	2009	2010	2011	2012	2013	2014	2015	2016	2017	2018	2019	Average	Average since 2012
Standard opinion percentage	99.68%	98.67%	99.19%	99.86%	99.48%	98.36%	96.96%	95.92%	95.64%	95.61%	96.06%	94.29%	94.69%	97.26%	95.94%
Nonstandard opinions percentage	0.32%	1.33%	0.81%	0.14%	0.52%	1.64%	3.04%	4.08%	4.36%	4.39%	3.94%	5.71%	5.31%	2.74%	4.06%

construction of corporate financial reporting conceptual framework [2].

The research on the conceptual framework of enterprise internal control evaluation reports plays an important role in at least the following six aspects: (1) to provide guidelines for the formulation and evaluation of internal control rules, to ensure consistency, flexibility, and systematization, and to promote the development of internal control practices; (2) improve the information content of the internal control evaluation report, and provide useful internal control information for investors, lenders, and other stakeholders; (3) clarify the elements and content of the internal control report, improve the seriousness of the internal control report, and avoid the internal control report. It can improve the standardization of the internal control report; (4) it can help the users of the internal control evaluation report to better understand the purpose, content, and nature of the information provided in the internal control evaluation report, and improve the readability of the internal control report; (5) help internal control auditors form opinions on whether the internal control self-assessment report conforms to internal control norms, and improve the audit quality of financial reports; and (6) promote the development of internal control theory itself.

3. International Experience for Reference: The Development and Transformation of the Conceptual Framework for Financial Reporting

To construct the conceptual framework of enterprise internal control evaluation report, the first experience that can be thought of is the conceptual framework of financial reporting. The construction of financial reporting conceptual framework is one of the important accounting theoretical issues that have been discussed for a long time in domestic and foreign accounting circles. It is generally believed that a good financial reporting conceptual framework is the basis for the success of principle-oriented accounting standards. We can draw some useful inspirations from the construction of the conceptual framework of financial reporting.

3.1. Experience from the Private Sector. The Financial Accounting Standards Board (FASB) develops private sector accounting practices. The FASB began to formulate and publish the Statements of Financial Accounting Concepts (SFAC) in 1978. It studied the conceptual framework of financial reporting earlier and defined it as a charter, a set of objectives and basic principles. A system with internal logical relationships guides consistent accounting standards and identifies the nature, role, and limitations of financial accounting and financial reporting. The FASB believes that the conceptual framework for financial reporting is important because it has the following four functions: (1) it provides guidance for the formulation and evaluation of accounting standards, ensuring consistency, and systematization. (2) In the absence of authoritative documents, provide

a reference basis for analyzing new or emerging financial accounting and reporting issues. (3) Provide theoretical basis for accounting personnel to make professional judgments when compiling financial information. (4) Promote the consistency of accounting standards and the rationality of accounting practices, improve the comparability of statements, promote users' understanding of financial statements, and enhance users' confidence.

The International Accounting Standards Board (IASB) is also an important promoter of the conceptual framework for financial reporting [3]. The IASB issued the "Framework for Preparing Financial Statements" as early as 1989. Later, in 2004, it decided to jointly revise the conceptual framework of financial reporting with the FASB, and in September 2010 jointly issued Chapter 1 of the Financial Reporting Framework "General Purpose Finance". The Objectives of the Report" and Chapter 3 "Quality Characteristics of Useful Financial Information" replaced the corresponding content in the 1989 version of the conceptual framework, while other parts of the content were directly transferred into the 2010 version of the conceptual framework. In March 2018, it independently released a new conceptual framework for financial reporting (Conceptual Framework for Financial Reporting), measurement, presentation and disclosure, capital and capital preservation, and other basic concepts. The IASB also pointed out seven roles in its conceptual framework, including helping the IASB Board to formulate and review international accounting standards, coordinating regulations, standards and procedures related to the preparation of financial statements, and helping countries formulate their own accounting standards. Standards, which help preparers of financial statements to apply international accounting standards, help auditors to form opinions on whether financial statements comply with international accounting standards, and help users understand financial information, etc.

After comprehensively comparing the history of the development of conceptual framework projects in various countries and the role of conceptual frameworks in the development of these countries' accounting standards systems, Chinese scholars have concluded four major roles: (1) it can maintain the consistency of accounting standards-related documents and internal logic; reduce the inconsistency or conflict between different standards, limit the multiple processing methods and procedures of the same transaction in practice, and improve the standardization of accounting standards. (2) It can help users of accounting information to better understand the purpose, content, and nature of the information provided in financial reports, so as to make appropriate analysis and judgment and correct business decisions. (3) It can provide direction for the formulation of accounting standards and the solution of major accounting problems, and it can also reduce personal bias in the process of standard formulation and resist political pressure from different interest groups. (4) Conducive to the development of accounting theory and the renewal of concepts. The conceptual framework not only fully affirms the reasonable parts of the traditional framework theory that can continue to be applied but also strives to reflect the

corresponding accounting theory or basic concepts under the changing social and economic environment [4–7].

3.2. Experience from the Public Sector. In view of the trend of gradual convergence between the conceptual framework of government financial reporting and the conceptual framework of corporate financial reporting, we believe that the construction of a conceptual framework for corporate internal control evaluation reports should not only fully consider the experience of constructing a conceptual framework for corporate financial reporting but also actively learn from public sector financial reporting experience in conceptual framework building.

In the United States, public sector accounting standards are set by the Government Accounting Standards Board (GASB) and the Federal Accounting Standards Advisory Board (FASAB). GASB has issued four concept announcements, namely, “Objectives For Preparing Financial Reporting”, “Service Efforts And Achievements Report”, “Communication Methods For Common Reporting”, “Elements Of Financial Reporting”, and the basic concepts involved include financial reporting objectives and its information quality characteristics, performance reporting objectives, elements, information quality characteristics, disclosure of supplementary information, and financial reporting elements. FASAB’s Concept Bulletin “Objectives of Federal Government Financial Reporting”, “Subject and Presentation”, “Management Discussion and Analysis”, “Program Objectives and Quality Characteristics of U.S. Government Consolidated Financial Reporting”, “Definition of Accrual-Based Financial Statements” and “Confirmation” also involves basic concepts such as the objectives of financial reporting, the quality characteristics of financial reporting information, the measurement of costs and benefits, the main body of financial reporting, accounting elements and their confirmation measurement, management discussion and analysis, etc. The concept of operational performance reporting was put forward.

The basic concepts proposed by the International Public Sector Accounting Standards Board (IPSASB), Conceptual Framework for Public Sector Accounting Project launched in 2006 include the objectives of financial reporting, the scope of financial reporting, the information quality characteristics of general financial reporting, reporting entities, and financial statement elements. Definition and recognition are an effective measurement basis for identifying elements in financial statements, and the conceptual basis that underpins cash-based financial reporting.

4. The Logic of Constructing the Conceptual Framework of the Enterprise Internal Control Evaluation Report

What kind of logic to follow to construct the conceptual framework of enterprise internal control evaluation report is a key issue we face. In a general sense, the conceptual framework of any discipline should be composed of the most basic concepts and theoretical elements, which form a coherent and closely related framework system according to the

internal logic to clearly define the discipline’s tasks, research objects, and its nature and function play an important guiding role in practical activities.

When constructing a conceptual framework, where to start, or what starting point to choose is crucial. It determines the development of basic concepts or theoretical elements, and also affects the scientificity and practicability of the conceptual framework. Judging from the research results in the field of accounting, the induction of the starting point concept mainly includes the goal starting point theory, the environmental starting point theory, the essential starting point theory, and the hypothetical starting point theory.. For example, in reviewing the development and transformation process of the conceptual framework of financial reporting, we noticed that the goal starting point theory was generally adopted in the construction of the conceptual framework in the past; that is, the conceptual framework was deduced from the goal as the starting point. To provide information useful for decision-making; to be useful, information should meet specific quality requirements and future-proof, and the impact of transactions and other events on elements should be identified as promptly and fully as possible, and measured at current value in financial reporting as far as possible. These research results have merits, but we believe that in a general sense, it is unlikely to have the so-called “target” positioning before we “qualify” a thing. In other words, goal positioning is unlikely to appear before the characterization of things, or in other words, goal positioning should be after the characterization of things, otherwise it is water without a source, a tree without roots, and the second monk cannot figure it out. Therefore, as far as the construction of the conceptual framework of the enterprise internal control evaluation report is concerned, before determining the goal of the enterprise internal control evaluation report, the nature and function of the enterprise internal control evaluation report must be clarified. Therefore, we start from the connotation and essence of the enterprise internal control evaluation report to construct the conceptual framework of the enterprise internal control evaluation report: that is, adopt the point of view of the essential starting point.

The conceptual framework of the enterprise internal control evaluation report can be shown in Figure 1. Starting from the concept of the enterprise internal control evaluation report, the function of the enterprise internal control evaluation report can be positioned, that is, what the enterprise internal control evaluation report can do. In constructing the conceptual framework of the enterprise internal control evaluation report, it is necessary to clarify the main users of the report, that is, who the internal control evaluation report is mainly intended for, and to further clarify the main users’ common main needs for the enterprise’s internal control information. The common information needs of the main users put forward the goal of the internal control evaluation report from the perspective of demand, while the function of the internal control evaluation report is to clarify what the internal control evaluation report can and cannot do from the perspective of supply. Combining demand and supply is the realistic goal of the internal

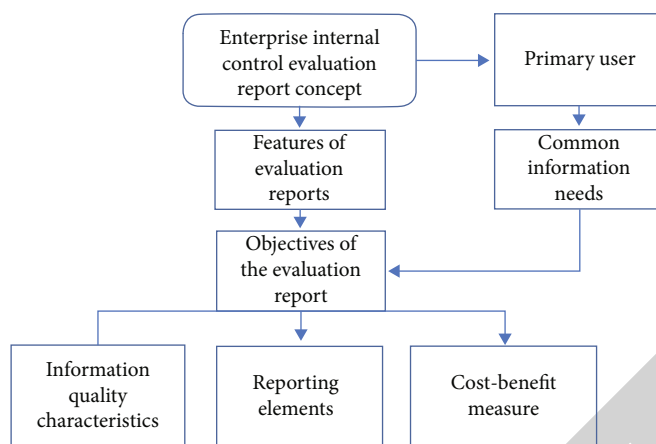


FIGURE 1: The framework of the conceptual framework of the enterprise internal control evaluation report.

control evaluation report. In order to achieve the preset goals of the enterprise internal control evaluation report, it is necessary to introduce other concepts, such as information quality characteristics, internal control evaluation report elements, and the measurement of costs and benefits.

5. Contents of the Conceptual Framework of Enterprise Internal Control Evaluation Report

We know that the conceptual framework of corporate financial reporting includes a series of basic concepts. Then, what basic concepts should be included in the conceptual framework of an enterprise internal control evaluation report? As with the financial reporting conceptual framework, this is a matter of opinion. We follow the experience and logic of constructing the conceptual framework. In general, we believe that the conceptual framework of the enterprise internal control evaluation report should include the following basic concepts: the concept of the conceptual framework, the main users of the general-purpose internal control evaluation report, and the main user's impact on the internal control of the enterprise. Common main requirements for information, functions, objectives, information quality characteristics, elements of internal control evaluation reports, and cost and benefit measurement of the general-purpose internal control evaluation report.

5.1. The Concept of the Conceptual Framework of the Enterprise Internal Control Evaluation Report. Drawing on the research results of the conceptual framework of financial reporting, we try to summarize the concept and important role of the conceptual framework of the internal control evaluation report of the enterprise.

The conceptual framework of enterprise internal control evaluation report is composed of a series of basic concepts that describe and apply to enterprise internal control, and is guided by the goal of enterprise internal control evaluation report. The theoretical system with the content of reports, etc., is used to guide the consistent internal control rules, and to point out the nature, function, and limitations of internal control, which is the theoretical basis for evaluating

the existing internal control system and guiding and developing the future internal control system. In essence, the conceptual framework of an enterprise internal control evaluation report is also a system of charters, a set of objectives and basic principles that are related to each other and have an inherent logical relationship.

5.2. Main Users of the General-Purpose Internal Control Evaluation Report. Internal control evaluation reports provided externally are for general purposes. This is because, no matter how the conceptual framework is built and modified, the complexity of the actual situation must be taken into account. For example, different types of users have different information needs, the same type of users have different needs in different institutional contexts, and so on. Another example is that the internal control of a modern enterprise involves all aspects of the enterprise and has many stakeholders. For these reasons, an internal control assessment report is not required to please everyone. As the saying goes: "It's hard to tell everyone." In fact, it is impossible to have such a perfect set of reports. Not only the internal control evaluation report but any report including financial report has its limitations. Therefore, to construct the conceptual framework of an enterprise internal control evaluation report, the main users of the report must first be identified; that is, the internal control evaluation report is mainly for certain people, as long as these people feel satisfied.

From the perspective of demand, the reason why people pay attention to the internal control evaluation report of the enterprise is that the internal control evaluation report should reflect some relevant information of the enterprise that they need to know, and their own interests are closely related to the internal control evaluation report of the enterprise from the supply side. See, corporate internal control information can only be reflected through corporate internal control evaluation reports, and subject to legal constraints, listed companies must provide external internal control evaluation reports.

Since the objective of financial reporting is one of the five objectives of an enterprise's internal control, the users of the financial report are the main users of the evaluation report of

the enterprise's internal control, mainly referring to "existing and potential investors and creditors".

The company's board of directors (audit committee), managers at all levels, and relevant regulatory agencies (industry regulators, China Securities Regulatory Commission, etc.), whose interests are more closely linked to the company, may need more and more targeted internal control information from the company. So, are they the main users? It should be admitted that these three types of users do have a demand for enterprise internal control information, and their decisions based on internal control information will have a greater impact on the enterprise. However, compared with other stakeholders, they have more power and convenience to ask enterprises for internal control information, and thus are more able to obtain additional financial information. Therefore, it is not necessary for enterprises to provide general-purpose internal control evaluation reports specifically for the needs of these three types of people. In addition, some regulatory agencies may choose the information disclosed in the internal control evaluation report for the realization of certain regulatory objectives, which will lead to the aforementioned general-purpose internal control evaluation report users unable to obtain the information they need. In short, the board of directors (audit committee), managers at all levels, and relevant regulatory agencies (industry regulatory agencies, China Securities Regulatory Commission, etc.) do not constitute the main users of the general-purpose internal control evaluation report (it should be noted that the information disclosed in the general-purpose internal control evaluation report can also be used by these three types of users.).

5.3. Major Users' Common Main Needs for Corporate Internal Control Information. Even major owners have difficulty meeting their internal control information needs. This is because, even if some nonmain users are excluded, there are still a large number of main users, and everyone has different ideas. Even everyone has many ideas at the same time, and the ideas at this time will overturn the ideas at that time, etc. Therefore, it is impossible to satisfy all the ideas of all major users, but to try to satisfy the ideas shared by most major users, and to find the "common divisor" rather than the "common multiple" of their requirements for the internal control evaluation report. This needs to consider two aspects: one is their common needs, and the other is what the internal control evaluation report can do. The former is the goal of the internal control evaluation report proposed from the perspective of needs, and the latter is the limitation of the internal control evaluation report, which is the goal of the internal control evaluation report proposed from the perspective of supply.

Consideration of limitations must be included when considering the target problem. We need to understand what the main users want the internal control evaluation report to achieve, what are the limitations of the internal control evaluation report, and further think about what the internal control evaluation report can do to achieve this goal under these limitations [8–11].

5.4. Functions of the General Purpose Internal Control Evaluation Report. What the enterprise provides is only the internal control evaluation report of the enterprise, and it is impossible to cover everything. Considering the limitations of the enterprise internal control evaluation report, it can be analyzed from two aspects of what the enterprise internal control evaluation report can do and what it cannot do.

- (i) What can be done by the enterprise internal control evaluation report? The internal control evaluation report of the enterprise can only provide information on the internal control evaluation of the enterprise, which mainly includes the statement of the board of directors on the authenticity of the internal control report, the overall situation of the internal control evaluation work, the basis, scope, procedures and methods of the internal control evaluation, internal control deficiencies and their identification, rectification of internal control deficiencies, proposed rectification measures for major deficiencies, and conclusions on the effectiveness of internal control
- (ii) What the enterprise internal control evaluation report cannot do? The internal control self-assessment report cannot replace the internal control audit report. The former belongs to internal supervision and process supervision, while the latter belongs to external supervision and result supervision. The two complement each other and are indispensable. Internal control evaluation is the self-evaluation of the company's board of directors on the effectiveness of the company's internal control, which is subject to a certain degree of subjectivity. Therefore, the internal control evaluation report formed on this basis can only be used as a way for relevant parties to understand the design and operation of the company's internal control. One, when using the internal control evaluation report, it should also be used in conjunction with the audit report of the internal control certified public accountant, internal control supervision information, financial report information, and other related information, so as to achieve the effect of comprehensive analysis, comprehensive judgment, and mutual verification

5.5. Objectives of the General Purpose Internal Control Evaluation Report. The reason why the main users read the internal control evaluation report is because they hope that the information provided by the report can meet their needs for internal control information; that is, the main users need to understand the level of corporate governance, management standardization, and the ability to resist various risks. Better to serve them in making investment and related decisions. After reading the report, the main users will get some information, their thoughts on certain things are likely to be different from before reading the report, and then they may

make different decisions than before. That is where the value of reports comes in because they provide incremental information. Therefore, the goal of the general-purpose internal control evaluation report is to meet the aforementioned needs of the main users. Otherwise, the main user will not be able to obtain the internal control information he needs by reading the report. In other words, it is the same whether reading the report or not, so there is no need to spend so much time and manpower to compile a set of useless reports.

5.6. Characteristics of Information Quality. The enterprise internal control evaluation report is the carrier of internal control information, and users care about the information, not the carrier itself. Therefore, what characteristics do these information need to have in order to achieve the preset goal; that is, to help the main users make investment decisions and related decisions. In fact, from the perspective of the development of the conceptual framework of financial reporting, changes in financial reporting objectives will inevitably bring about changes in the quality requirements of accounting information. Many scholars believe that it is very difficult to formulate optimal mandatory disclosure standards [1, 12], but once the information is disclosed, it must meet the required quality standards (Wu [13]). Combined with the characteristics of the enterprise's internal control system, we believe that the characteristics of the information quality of the enterprise's internal control evaluation report include at least the following aspects: comprehensiveness, importance, and objectivity.

- (i) *Comprehensiveness.* The requirement of comprehensive control necessarily requires that the scope of the internal control evaluation of the enterprise should be sufficiently broad, including the design and operation of internal control, covering various businesses and matters of the enterprise, and its affiliated units, including every level and link
- (ii) *Importance.* Enterprise internal control evaluation should be based on comprehensiveness, oriented to strategy and performance, focusing on risks, and highlighting key points. Specifically, one is to adhere to a risk-oriented approach, focusing on those high-risk areas, and risk points that affect the realization of internal control objectives; the other is to adhere to a focused approach, focusing on important business matters and key control links, and key business units
- (iii) *Objectivity.* The enterprise internal control evaluation report shall accurately reveal the risk status of operation and management, and truthfully reflect the effectiveness of internal control design and operation

5.7. Elements of Internal Control Evaluation Report. The elements of an enterprise internal control evaluation report refer to the content that constitutes the internal control evaluation report. In general, information quality characteristics,

reporting elements, etc. are all centered on objectives and are related to each other. Together, they constitute the conceptual framework of the enterprise internal control evaluation report, and together serve to achieve the goal. Article 22 of "Guidelines for Internal Control Evaluation of Enterprises" stipulates the elements of external evaluation reports, including as follows: (1) statement of the board of directors on the authenticity of the internal control report; (2) general situation of internal control evaluation; (3) internal control evaluation; (4) scope of internal control evaluation; (5) procedures and methods of internal control evaluation; (6) internal control deficiencies and their identification; (7) the rectification of internal control deficiencies and the rectification measures to be taken for major deficiencies; and (8) Conclusions on the effectiveness of internal control.

5.8. Measurement of Costs and Benefits. Everything has costs and benefits, and the acquisition and utilization of internal control information is no exception. Costs generally limit access and use of information. Access to information must have costs, and the benefits of using information must justify the associated costs. Things where the costs outweigh the benefits make us unprofitable, so this is generally avoided. The same is true in the process of obtaining, processing, and organizing the internal control information of the enterprise.

From a cost perspective, most of the effort associated with collecting, processing, validating, and disseminating internal control information is made by the provider of the internal control evaluation report (the preparer of the enterprise's internal control evaluation report). Users of internal control information will also incur expenses and costs when analyzing and understanding the information provided. If the required information is not provided, they may obtain it from other sources, or make estimates, all of which incur additional costs.

From a benefit perspective, reporting useful information can help users make decisions with more confidence. At the macrolevel, this will facilitate the functioning of capital markets more efficiently, which in turn will make the cost of capital lower for the entire socioeconomy. At the microlevel, key users can also benefit from making more informed decisions. Of course, because of the different preferences of key users and different decision-making patterns, general-purpose financial reporting cannot provide all the information that each of them finds relevant [14–16].

We look further at the cost-benefit issue from a standard-setting perspective. Given the cost constraints, standard-setters need to assess the benefits of reporting specific information to see if it is possible to justify the costs of providing and using the information. Of course, since each stakeholder evaluates the costs and benefits of specific items of reporting financial information differently, standard-setting bodies can only consider the costs and benefits of internal control evaluation reports in general, not just the costs and benefits associated with individual stakeholders' related costs and benefits.

It should be emphasized that it should be noted that for the acquisition, processing, and utilization of information,

cost is a limiting condition, a feature of the process of providing and utilizing information, not a quality feature of the information itself [17].

6. How to Construct the Conceptual Framework of Enterprise Internal Control Evaluation Report

Constructing the conceptual framework of enterprise internal control evaluation report is the need of enterprise internal control theory construction. We must not only recognize its importance but also fully recognize its urgency. We believe that the construction of the conceptual framework of an enterprise internal control evaluation report should follow the following principles:

- (1) For enterprise management, improve the theoretical research on internal control. The internal control of an enterprise is essentially a management activity of the enterprise, involving many aspects. In this regard, unlike the conceptual framework of financial reporting which focuses on accounting activities, the construction of the conceptual framework of the internal control evaluation report of an enterprise should be based on a broader perspective of enterprise management. The construction of the conceptual framework of enterprise internal control evaluation report should be regarded as an important part of the construction of enterprise internal control theory and enterprise internal control system, so as to strengthen its role in relevant management
- (2) Fully consider China's national conditions and actively learn from international experience. Internal control is closely related to politics, economy, culture, technology, etc., and is the most specific internal control connotation of each country. Therefore, the construction of the conceptual framework of the enterprise internal control evaluation report must fully consider the specific environment of China's internal control. It is necessary to highlight the characteristics of the conceptual framework of the internal control evaluation report of Chinese enterprises, and also strive to reflect the development law of internal control. For example, the impact of China's long-established culture on the internal control environment. At the same time, we must actively learn from the experience in the construction of relevant conceptual frameworks at home and abroad, but we must also proceed from China's actual national conditions. Learning from the useful experience of foreign countries is not simply to introduce the practice of a developed country or an international organization and recommend introducing it into China but to see whether the foreign laws, national conditions and practices match those of China

- (3) Scientific planning, continuous improvement, and due consideration of forward looking. The construction of the conceptual framework of the enterprise internal control evaluation report may be a relatively long-term project, which requires unremitting efforts to study and continuously improve, and cannot be accomplished overnight. Based on the needs of economic development and the actual situation of the enterprise, strive for theoretical breakthroughs and innovations, and take practical and effective measures to carry out research and implementation step by step, and finally realize the complete construction of the conceptual framework of the entire enterprise internal control evaluation report
- (4) Handle the relationship between the conceptual framework of the enterprise internal control evaluation report and the basic norms of enterprise internal control and its supporting guidelines. Judging from the current basic norms of enterprise internal control in China and its supporting guidelines, the conceptual framework of the enterprise internal control evaluation report belongs to the top-level design, and neither in terms of content nor requirements can replace the basic norms of enterprise internal control and its supporting guidelines. Moreover, the conceptual framework of the enterprise internal control evaluation report is out of sync with the revision of the basic norms of enterprise internal control and its supporting guidelines, and changes in the latter will not automatically change the former

In short, the construction of the conceptual framework of the enterprise internal control evaluation report can adopt the perspective of the basic starting point theory, learn from the experience of the construction of the relevant conceptual framework, start from the concept of the conceptual framework, clarify the main users of the report and their common needs, and combine the functions of the internal control evaluation report. The objectives of the internal control evaluation report are then determined. The introduction of information quality characteristics, internal control evaluation report elements, and cost-benefit measurement concepts can achieve the preset goals of enterprise internal control evaluation reports. Internal control evaluation report helps enterprises to find and overcome internal control deficiencies in order to better achieve the goals of the enterprise. With the improvement of the conceptual framework of the enterprise internal control evaluation report, the future internal control evaluation will be able to maintain the stability of the enterprise to a greater extent and contribute to the internal operation of the enterprise.

Data Availability

The experimental data used to support the findings of this study are available from the corresponding author upon request.

Retraction

Retracted: Logistics Supply Chain Management Mode of Chinese E-Commerce Enterprises under the Background of Big Data and Internet of Things

Journal of Sensors

Received 17 October 2023; Accepted 17 October 2023; Published 18 October 2023

Copyright © 2023 Journal of Sensors. This is an open access article distributed under the Creative Commons Attribution License, which permits unrestricted use, distribution, and reproduction in any medium, provided the original work is properly cited.

This article has been retracted by Hindawi following an investigation undertaken by the publisher [1]. This investigation has uncovered evidence of one or more of the following indicators of systematic manipulation of the publication process:

- (1) Discrepancies in scope
- (2) Discrepancies in the description of the research reported
- (3) Discrepancies between the availability of data and the research described
- (4) Inappropriate citations
- (5) Incoherent, meaningless and/or irrelevant content included in the article
- (6) Peer-review manipulation

The presence of these indicators undermines our confidence in the integrity of the article's content and we cannot, therefore, vouch for its reliability. Please note that this notice is intended solely to alert readers that the content of this article is unreliable. We have not investigated whether authors were aware of or involved in the systematic manipulation of the publication process.

In addition, our investigation has also shown that one or more of the following human-subject reporting requirements has not been met in this article: ethical approval by an Institutional Review Board (IRB) committee or equivalent, patient/participant consent to participate, and/or agreement to publish patient/participant details (where relevant).

Wiley and Hindawi regrets that the usual quality checks did not identify these issues before publication and have since put additional measures in place to safeguard research integrity.

We wish to credit our own Research Integrity and Research Publishing teams and anonymous and named external

researchers and research integrity experts for contributing to this investigation.

The corresponding author, as the representative of all authors, has been given the opportunity to register their agreement or disagreement to this retraction. We have kept a record of any response received.

References

- [1] X. Han and J. Wang, "Logistics Supply Chain Management Mode of Chinese E-Commerce Enterprises under the Background of Big Data and Internet of Things," *Journal of Sensors*, vol. 2022, Article ID 7818944, 7 pages, 2022.

Research Article

Logistics Supply Chain Management Mode of Chinese E-Commerce Enterprises under the Background of Big Data and Internet of Things

Xiao Han ¹ and Jingyi Wang²

¹Free Trade Office, Administrative Committee of Chongqing Liangjiang New Area, Chongqing, China 401122

²Economic Operation Bureau, Administrative Committee of Chongqing Liangjiang New Area, Chongqing, China 401122

Correspondence should be addressed to Xiao Han; 19403590@masu.edu.cn

Received 3 August 2022; Revised 18 August 2022; Accepted 24 August 2022; Published 19 September 2022

Academic Editor: Sweta Bhattacharya

Copyright © 2022 Xiao Han and Jingyi Wang. This is an open access article distributed under the Creative Commons Attribution License, which permits unrestricted use, distribution, and reproduction in any medium, provided the original work is properly cited.

With the development of information technology, the logistics supply chain of Chinese E-commerce enterprises still has the problem of backward industrial model and low product quality. It is necessary to deeply integrate the logistics supply chain with big data and Internet technology and develop a logistics intelligent supply chain management model in order to meet the needs of Chinese E-commerce enterprises for logistics supply chain. The management mode of the logistics supply chain of Chinese E-commerce enterprises will show the development trend of diversification and simplification, standardization and normalization, and intelligence and efficiency in the future.

1. Introduction

1.1. The Rise of Big Data and the Internet of Things. With the rapid development of information technology, big data and the Internet of Things came into being [5]. The two complement each other and promote the rapid development of information technology industry. E-commerce enterprises are also affected by the third industrial wave represented by big data and Internet of Things technology [1]. The rapid generation of big data can meet the needs of real-time data in all aspects of E-commerce logistics supply chain and increase the sustainability and efficiency of E-commerce enterprises. The electronic tracking system of Internet of Things can track the “order” status in real time and improve the control ability of E-commerce enterprises to the logistics supply chain cargo flow. The seamless connection between big data and the Internet of Things and the subsequent big data capture and analysis technology have promoted the reform of the supply chain management mode of E-commerce enterprises. More and more E-commerce enterprises [6], such as Dangdang and Suning Yibu, have aban-

doned the traditional “order” management mode, reformed the internal industrial structure of enterprises, and constructed the intelligent and efficient supply chain management mode of intelligent logistics.

1.2. E-Commerce Enterprise Logistics Supply Chain Management Model Drawbacks Appear. Electronic commerce enterprise logistics supply chain each link independence is strong, and information sharing is not high [7]. E-commerce enterprises have the problems of weak information sharing awareness and weak integration awareness in all aspects of logistics supply chain. Each link pays more attention to own benefit and neglects the overall benefit maximization [8]. Some high-value information cannot be timely dredged and fully utilized in all aspects, which often affects the implementation of the subsequent supply chain management mode, thus affecting the operation of the entire supply chain system. In order to solve this problem, Chinese E-commerce enterprises should vigorously promote the reform of intelligent logistics supply chain management

mode and establish information sharing and integrated logistics supply chain management mode [9].

2. Investigation on the Construction of Smart Supply Chain in Chinese E-Commerce Enterprises

2.1. Investigation Purpose. We investigate the major E-commerce enterprises in the Chinese market to understand their logistics supply chain management mode and their willingness to build smart logistics supply chain management mode based on big data and the Internet of Things.

2.2. Survey Object Design. Selection of survey objects: major E-commerce enterprises in the Chinese market control of the number of survey: since there are many E-commerce enterprises in China, 220 E-commerce enterprises are selected by filling out questionnaires, as shown in Table 1.

2.3. Survey Significance. Preliminary understand the logistics supply chain management model of major E-commerce enterprises in the Chinese market, clarify the advantages and disadvantages of the current logistics supply chain model of E-commerce enterprises, and understand the understanding and application willingness of E-commerce enterprises to big data and the Internet. Due to the large number of samples taken in the process of investigation, it has a certain guiding significance for the reform of China's E-commerce logistics supply chain management model. After fully understanding the problems of logistics supply chain management mode of Chinese E-commerce enterprises, this paper puts forward targeted solutions and predicts the development trend of logistics supply chain management mode of Chinese E-commerce enterprises [10].

2.4. Questionnaire Implementation of the Survey

2.4.1. Investigation on the Original Logistics Supply Chain Management Mode of E-Commerce Enterprises. At present, the common logistics supply chain of E-commerce enterprises is enterprise open logistics mode, joint distribution logistics mode, and third-party logistics mode, but these supply chain models have their own advantages and disadvantages. The current supply chain management model used by E-commerce enterprises in China market is shown in Table 2. Enterprise open logistics mode enterprises own warehouse, not only responsible for the parent company's logistics services but also to provide logistics services to the community. But its disadvantage is high cost and needs management personnel with high logistics supply chain management ability. The joint distribution logistics mode is excessively dependent on the distribution center. Once the distribution center is paralyzed, the entire logistics system will collapse. The third-party logistics mode outsources logistics services to logistics companies, which reduces the burden of E-commerce enterprises, but cannot directly contact users and cannot obtain feedback from users [11].

2.4.2. Survey of E-Commerce Enterprises' Understanding of Big Data and the Internet of Things. The rapid development

TABLE 1: Scale distribution and turnover of 220 E-commerce enterprises compared with 2020.

The turnover compared with 2020	Size of enterprise					Total
	0-99 people	More than 10000 people	1000-9999 people	100-499 people	500-999 people	
Rise	18	27	11	26	21	103
Decrease	18	22	33	22	22	117
Total	36	49	44	48	43	220

of big data and Internet of Things provides an opportunity for the change of the management mode of logistics supply chain in E-commerce enterprises. The sensor of Internet of Things technology can provide real-time data for the management of logistics supply chain. The analysis technology of big data technology can analyze massive data and facilitate real-time monitoring of all aspects of logistics supply chain. The Internet of Things is a network of people connected and things connected. Through the Internet of Things, things are connected to make all aspects of logistics supply chain management confidentially connected and integrated into an organic whole. The third industrial wave represented by big data and Internet of Things will promote the transformation of logistics supply chain management mode of E-commerce enterprises from traditional mode to intelligent supply chain management mode. Understanding the knowledge of E-commerce enterprise managers about big data technology and Internet technology helps to comprehensively grasp the logistics supply chain management mode in the Chinese market [12].

2.4.3. Survey of the Willingness of E-Commerce Enterprises to Establish a Smart Supply Chain. To promote the transformation of logistics supply chain management mode in E-commerce industry, we must start from a single E-commerce enterprise. Nowadays, some large E-commerce enterprises with their own logistics system have established intelligent logistics, but it is difficult for small E-commerce enterprises to establish intelligent logistics supply chain management model because of technology, manpower, capital, and other factors. In the investigation, investigating the reasons why it is difficult for small enterprises to establish logistics supply chain is of great help to promote the establishment of intelligent logistics supply chain management model.

2.5. Presentation of the Survey Results

2.5.1. Different Scale E-Commerce Enterprises Have Different Demands for Logistics Supply Chain Management Mode. In order to study the relationship between the scale of E-commerce enterprises and the satisfaction of E-commerce enterprises with their existing logistics supply chain management mode, variance analysis is conducted on the two, and the results are shown in the table. Table 3 shows that when P value > 0.05 is known by statistical knowledge, the original hypothesis should be rejected. That is, there is a correlation

TABLE 2: Logistics supply chain model and its proportion of Chinese E-commerce enterprises.

Type	Enterprise open logistics mode	JIT logistics mode	VMI logistics mode	Joint distribution logistics mode	Other
Number	48	39	49	42	42
Summary percentage	21.82%	17.73%	22.27%	19.09%	19.09%

TABLE 3: Analysis of variance of enterprise scale satisfaction with logistics supply chain management model.

(a)

Group	Number of observations	Sum	Average	Variance
0-99 people	2	36	18	18
More than 10000 people	2	49	24.5	4.5
1000-9999 people	2	44	22	50
100-499 people	2	48	24	8
500-999 people	2	43	21.5	60.5

(b)

Differential source	SS	df	MS	F	P value	F crit
Group room	53	4	13.25	0.4698582	0.7579227	5.19
Within the group	141	5	28.2			
Total	194	9				

between enterprise scale and logistics supply chain management mode. This survey results are echoing the abovementioned large E-commerce enterprises to establish intelligent logistics supply chain management system, but small E-commerce enterprises cannot establish [13].

This result tells us that different scale enterprises have different demands for logistics supply chain management mode. For small- and medium-sized enterprises, due to the limitation of capital and industrial scale, choosing third-party outsourcing companies to outsource their logistics business, or using the traditional “order” management mode, is sufficient to meet the logistics supply chain management of these enterprises; however, for large enterprises, it is necessary to establish a diversified streamlined, standardized, intelligent, and efficient intelligent logistics supply chain management model to meet the daily operation of the logistics needs of enterprises [14].

2.5.2. Strong Will of E-Commerce Enterprises to Develop Smart Logistics Supply Chain. It can be seen from Figure 1 that most E-commerce enterprises do not know about big data and the Internet of Things, but nearly 80% of E-commerce enterprises want to develop smart logistics supply chain management mode. It shows that E-commerce enterprises have realized their backward logistics supply chain management mode and want to use the Internet of Things and big data to realize intelligent logistics supply chain management and solve the dilemma faced by enterprises.

This survey also statistics the 220 E-commerce enterprises supply chain management model facing many problems, concentrated as shown in Figure 2.

As shown in Table 4, the logistics supply chain management of most E-commerce enterprises is faced with the problems of low product quality, high input cost, and low order processing efficiency [15]. Due to the fact that logistics supply chain of E-commerce enterprises is based on the “order” to deal with, in the process of goods transportation, the flow of goods and information flow is not synchronized, with a certain lag, and information sharing is low, which also leads to the low efficiency of order processing. The location information of goods cannot be updated in real time, resulting in the failure to track goods in real time in the process of goods circulation, which increases the possibility of goods being wrong in the transportation process, resulting in the problem of low product quality. These problems are in the final analysis because the traditional logistics supply chain management mode has certain disadvantages. To solve these problems, it is necessary to establish the intelligent logistics supply chain management mode.

According to the experimental results, the 220 enterprises surveyed have strong willingness to participate in the establishment of intelligent logistics supply chain management mode. Among them, small- and medium-sized enterprises have the strongest willingness to participate in improving their competitiveness, followed by large enterprises.

2.6. Reliability Analysis of the Survey Results. Reliability analysis is a common method to test the reliability of the survey results. Specifically, the questionnaire is used to repeatedly measure the subjects, and the consistency of the results is obtained.

Reliability analysis of Cronbach’s alpha in the experiment

$$\alpha = \frac{K}{K-1} \left(1 - \frac{\sum S_i^2}{S_x^2} \right). \quad (1)$$

In this survey, the value of α is 0.88, according to the provisions of the Cronbach’s alpha, when $\alpha > 0.7$ can be accepted, so the results of the survey have high credibility.

3. Current Situation of Logistics Supply Chain Management Mode in Chinese E-Commerce Enterprises

As shown in Figure 3, the four major factors that restrict the logistics supply chain management model of China’s E-commerce are talents, product quality, the effectiveness of

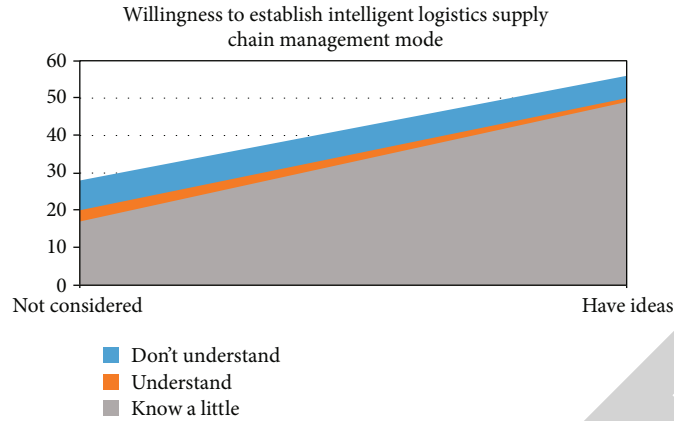


FIGURE 1: Willingness of E-commerce enterprises to establish a smart logistics supply chain management model and understanding of big data and the Internet of Things.

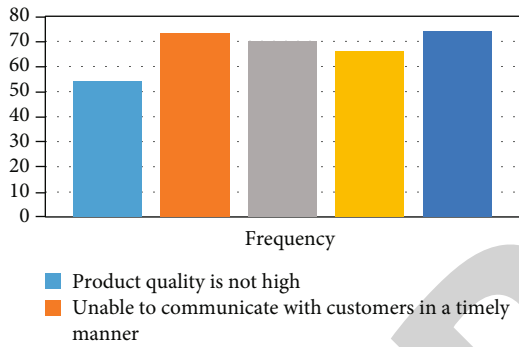


FIGURE 2: Problems of logistics supply chain management mode in 220 E-commerce enterprises.

TABLE 4: Ratio of logistics supply chain management cost to turnover in 220 E-commerce enterprises.

Cost share	10%-30%	30% above	5%-10%	5% below	Total
Number	61	48	50	61	220

data management, and the limitations of traditional methods.

3.1. Limitations of Traditional “Order” Supply Chain Management Model. Big data Internet of Things is developing rapidly, but the logistics supply management mode of small- and medium-sized E-commerce enterprises still stays in the traditional mode. “Order” is the core of this mode, the only recorder of goods information, and the only way to transfer information between E-commerce enterprises and node enterprises. In this mode, the market reflects the demand of customers on orders, and orders reflect it to each enterprise in the supply chain. This traditional logistics supply chain management mode can operate stably under the management of high-quality logistics personnel. However, due to the lack of human and material resources, small- and medium-sized enterprises cannot attract high-quality talents, leading to the use of traditional supply chain

management mode by small- and medium-sized enterprises not only has no advantages but also worsens. Big data and Internet of Things can provide technical support for the construction of new intelligent logistics supply chain management mode, which is of great significance in promoting E-commerce enterprises to abandon the original management mode and turn to new intelligent logistics management mode.

3.2. Limitations of Low Timeliness of Data Management [14]. The perfection of data management mode is an important factor restricting the development of logistics supply chain management mode, so the managers of E-commerce enterprises pay more attention to the logistics supply chain data management mode and strengthen the understanding of logistics supply chain data management. In the process of E-commerce enterprise operation, the amount of data generated by various activities is huge, such as supplier supply information, order processing, and customer demand information [15]. In the traditional order-order logistics supply chain management mode, the huge amount of data generated by each link will directly affect the turnover time of goods in each link, thus indirectly affecting the efficiency of logistics. The correctness of data processing is also a major factor hindering the development of logistics supply chain management mode. Correctness is the premise of efficient data processing, and correct data can ensure correct order processing. At present, the correctness and efficiency of data management mode in E-commerce enterprises are the two core of data processing mode reform. Big data and the Internet of Things play a very important role in improving the timeliness of data management and promoting the smart logistics supply chain management mode of E-commerce enterprises.

3.3. Product Quality Needs to Be Improved. E-commerce enterprises have developed rapidly in recent years, but due to the short development time, they still face many problems. Many E-commerce enterprise supply chain management level needs to be improved, management scope needs to be expanded, and product quality needs to be improved.

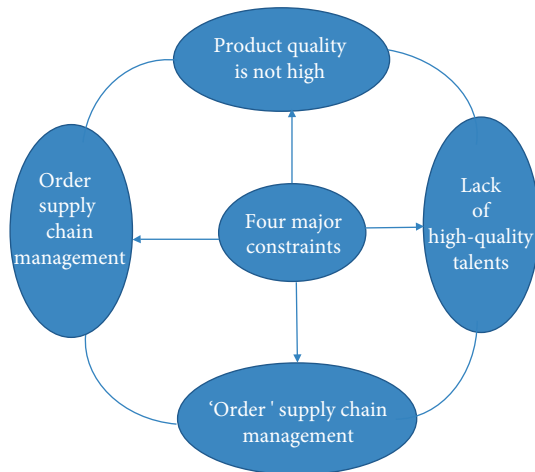


FIGURE 3: The restricting factors of E-commerce logistics supply chain management mode development.

Product direct contact with customers, product quality is an important problem that E-commerce enterprises must solve. The most important business of E-commerce enterprises is sales; many E-commerce enterprises focus on distribution, but do not care about the quality of products. Product quality plays a decisive role in the development of E-commerce enterprises, and the control of product quality must be strengthened.

3.4. Lack of High-Quality Talents in Logistics Supply Chain Management in E-Commerce Enterprises [16]. For E-commerce enterprises, the development of logistics supply chain management mode plays a decisive role in the overall development of enterprises. Science and technology are the first productivity; in order to promote the comprehensive development of E-commerce enterprises, we must introduce advanced science and technology. The vigorous development of big data and the Internet of Things in the third industrial revolution is of great significance for upgrading the enterprise logistics supply chain management mode and building a diversified and simplified, standardized and standardized, and intelligent and efficient logistics supply chain management mode [18].

4. Solutions to the Problems in Supply Chain Management of Chinese E-Commerce Enterprises

4.1. Integration of Logistics Big Data and Internet of Things. Big data and Internet of Things have great advantages in the realization of intelligent logistics supply chain management. Sensors based on Internet of Things can synchronize and share information and can realize positioning tracking and effective monitoring of products in the production and transportation process. The replacement of manual management with machine management saves a lot of manpower, material, and financial resources and reduces the loss caused by human subjective errors.

The visualization management of logistics supply chain can be realized through network. After locating the location information of an item through the network in the management process, the information of the item can be identified through the sensor of the Internet of Things and then transmitted to the general server, saving time for staff management [2]. At the same time, machine recognition is nondelay, which can timely and efficiently transfer information to the general server and improve the operation speed of the logistics supply chain [17].

Big data and the Internet can help optimize workflow. The two most important flows in logistics supply chain are goods flow and information flow. With the help of goods flow and information flow to monitor the flow of goods, the existing resources can be integrated efficiently. Build efficient intelligent logistics supply chain management mode.

4.2. Build Standardized Intelligent Logistics Supply Chain Management System

4.2.1. Real-Time Information Management System. "Order" is the cell of an E-commerce enterprise's running process. After the customer orders, the management personnel transfer goods from the warehouse, through many aspects of the logistics supply chain and finally reach the user. This process is very complex, and items need to go through a lot of circulation to enter the hands of users. Item information real-time management system, using big data and Internet of Things technology, through the noncontact information collection of moving objects, the location information and state information of objects in different links are collected to realize the automatic management of objects in different links, so as to realize the automatic management of objects. The system can be used to monitor the information of goods, prevent accidents, and ensure product quality.

4.2.2. Intelligent Storage System. The traditional mode of supply chain management warehouse adopts manual management; warehouse administrator is only responsible for guarding warehouse. However, the modern logistics supply chain management mode adopts the intelligent warehousing system and adheres to the important task of the warehouse. The warehouse administrator is responsible for integrating the process and coordinating the upstream and downstream of the supply chain. The intelligent storage system uses big data and Internet of Things technology to store the goods in the warehouse, which reduces the cost of manpower and material resources and improves the quality and efficiency of product supply [3].

4.2.3. Intelligent Storage and Automatic Sorting System. Two important factors restricting the development of logistics supply chain management mode are the timeliness of logistics and product quality, so it is necessary to set up an intelligent sorting system. The replacement of a large number of manual sorting with automated sorting technology not only reduces the cost but also greatly improves the efficiency and accuracy of sorting operations, making the traditional manual-based logistics business process gradually shift to intelligent and intelligent. The development of intelligent

logistics supply chain management mode is the common aspiration of E-commerce enterprises. It is bound to build a diversified and simplified, standardized and standardized, and intelligent and efficient intelligent logistics supply chain management mode.

4.2.4. Intelligent Decision System. Intelligent decision system is the brain of logistics, which is in charge of the context of the whole logistics supply chain system.

The logistics supply chain contains many links; if there is not a “commander” of many links of the logistics supply chain information flow, goods flow and many other flows will be chaotic. Internet of Things sensors get a lot of information in each link of the logistics supply chain, and the information accumulation of multiple links forms a super-large database. After analyzing a large amount of data produced by big data analysis, the intelligent decision-making system carries on machine learning according to the results of big data’s analysis, gradually constructs its own knowledge base, and finally develops to be able to make decisions according to different decision-making environments. The intelligent decision-making system can be the “head” of each subsystem and control the operation of other subsystems. Once the intelligent decision-making system collapses, the whole logistics system will collapse. In order to develop the logistics supply chain management model, E-commerce enterprises should take the construction of intelligent decision-making system as the first priority. Intelligent decision-making system deeply integrates the relevant technologies of big data and the Internet of Things and is the core system for E-commerce enterprises to develop logistics supply chain management model.

5. Conclusion

The development of intelligent logistics supply chain management model is the common aspiration of E-commerce enterprises. In the future, it will be established with diversification and simplification, standardization and normalization, and intelligence and efficiency as the main characteristics of intelligent logistics supply chain management model. Standardization and normalization are the foundation, diversification and simplification are the premise, and intelligence and efficiency are the purpose.

5.1. Diversification and Simplification of Management Mode. Diversification refers to diversified development, and simplification refers to streamline management. Diversification emphasizes all-round development, not single development, to go hand in hand, production, logistics, sales common development. Logistics supply chain plays a key role in the production and operation of enterprises. Simplification emphasizes the simplification of logistics supply chain management mode, improves the quality of core management personnel, and develops the management mode to intelligence. Replace human operation with machine operation. Man is only responsible for the management of core work and the development of core technology needed by the system [4].

5.2. Standardization and Normalization of Management Model. ISO is an internationally recognized standardization organization, and it has issued a number of international standards, among which there is no special logistics standard. Standardization in a narrow sense is the supply chain process standardization, in a broad sense is to establish a set of international logistics standards. Normalization refers to standardizing the behaviors of logistics supply chain management, clarifying the rights, responsibilities, and interests of each link, dividing the functions and responsibilities of each link, establishing the norms of information transmission in each link, and establishing a standardized logistics supply chain management model. Standardization and normalization of logistics supply chain management mode complement and promote each other and jointly promote the improvement of logistics supply chain management mode.

5.3. Intelligent and Efficient Management Mode. Intelligence refers to the combination of logistics supply chain management mode of E-commerce enterprises with big data technology and Internet of Things technology based on big data and Internet technology. Develop logistics information tracking system, intelligent storage system, real-time information monitoring system, and other intelligent management systems. In the process of building intelligent logistics supply chain management mode, synchronous information sharing is realized, the burden of management personnel is reduced, visual data management mode is realized, and the efficiency of logistics supply chain is improved. High efficiency refers to improving the operational efficiency of the supply chain without reducing product quality and ensuring the correctness of orders. Intelligence is the premise of efficiency, and the continuous pursuit of logistics supply chain management efficiency will promote the development of intelligent.

Data Availability

The datasets used and/or analyzed during the current study are available from the corresponding author on reasonable request.

Conflicts of Interest

It is declared by the authors that this article is free of conflict of interest.

References

- [1] P. Qian, “Discussion on the management mode and construction of international logistics supply chain from the perspective of cross-border e-commerce,” *Mall modernization*, vol. 17, pp. 46-47, 2018.
- [2] L. Rui, “Research on supply chain management of logistics enterprises in the era of big data,” *China market*, vol. 6, pp. 179-180, 2021.
- [3] H. Yue, “The impact of big data technology on supply chain management,” *Chinese business theory*, vol. 2, pp. 108-109, 2021.

Retraction

Retracted: Ethical Framework of Social Media Based on Text Analysis of Terms of Service of Six Major Platforms

Journal of Sensors

Received 19 December 2023; Accepted 19 December 2023; Published 20 December 2023

Copyright © 2023 Journal of Sensors. This is an open access article distributed under the Creative Commons Attribution License, which permits unrestricted use, distribution, and reproduction in any medium, provided the original work is properly cited.

This article has been retracted by Hindawi following an investigation undertaken by the publisher [1]. This investigation has uncovered evidence of one or more of the following indicators of systematic manipulation of the publication process:

- (1) Discrepancies in scope
- (2) Discrepancies in the description of the research reported
- (3) Discrepancies between the availability of data and the research described
- (4) Inappropriate citations
- (5) Incoherent, meaningless and/or irrelevant content included in the article
- (6) Manipulated or compromised peer review

The presence of these indicators undermines our confidence in the integrity of the article's content and we cannot, therefore, vouch for its reliability. Please note that this notice is intended solely to alert readers that the content of this article is unreliable. We have not investigated whether authors were aware of or involved in the systematic manipulation of the publication process.

Wiley and Hindawi regrets that the usual quality checks did not identify these issues before publication and have since put additional measures in place to safeguard research integrity.

We wish to credit our own Research Integrity and Research Publishing teams and anonymous and named external researchers and research integrity experts for contributing to this investigation.

The corresponding author, as the representative of all authors, has been given the opportunity to register their agreement or disagreement to this retraction. We have kept a record of any response received.

References

- [1] W. Mao and Z. Wang, "Ethical Framework of Social Media Based on Text Analysis of Terms of Service of Six Major Platforms," *Journal of Sensors*, vol. 2022, Article ID 1136017, 9 pages, 2022.

Research Article

Ethical Framework of Social Media Based on Text Analysis of Terms of Service of Six Major Platforms

Wanxi Mao ^{1,2} and Zhaoxin Wang ³

¹School of Journalism and Communication, Tsinghua University, China

²Department of Media and Culture Studies, Utrecht University, China

³Zhejiang Normal University, China

Correspondence should be addressed to Zhaoxin Wang; wangzhaoxin@zjnu.edu.cn

Received 19 July 2022; Revised 23 August 2022; Accepted 5 September 2022; Published 17 September 2022

Academic Editor: Sweta Bhattacharya

Copyright © 2022 Wanxi Mao and Zhaoxin Wang. This is an open access article distributed under the Creative Commons Attribution License, which permits unrestricted use, distribution, and reproduction in any medium, provided the original work is properly cited.

In the present digital world, people rely extensively on social media for networking and socializing. As a consequence, they face numerous ethical challenges which make it necessary to constantly reflect on new media ethics emerging from social media. The terms of service (ToS) of social media provide the opportunities for big tech companies' guidelines to design the ecology and the ethical environment of social media. The existing studies conducted in this domain emphasize on specific ethical issues pertaining to ToS such as privacy, freedom of speech, and copyright protection. But all of these studies lack the exploration of its general ethical framework. Considering the theoretical framework of the Potter Box Model of Reasoning, Schwartz's value scale, and Christians and Ess' ethical principles, this paper examines the ToS of social media run by six major platforms across the globe. The result reveals 15 values, which are summarized into three pairs of ethical principles: egoism and altruism, monism and pluralism, and utilitarianism and deontology. The paper further analyzes the hidden conflicts and reveals the emergence of "relational" ethical principle.

1. Preface

Media, central to the history of civilization, alter the social consciousness structure including the ethical structure with its formal changes [1]. The explosion of social media brought by the ubiquity of high-speed Internet in recent years has blurred the boundary between media texts and daily interactions and raised new ethical issues, making it imperative to deliberate on fast-evolving media ethics [2, 3]. In this context, social media ethics has been heatedly discussed in literature [4–8]. Terms of service (ToS), as the "scripts" of users' relationship and behavior written by the platforms, reflect the platforms' design ideas for the ecology of social media and, therefore, offer a crucial site for researchers to understand and examine the ethical environment of social media.

Previous literature has carried out exploratory studies on the ToS of social applications, with priority given to specific ethical issues such as privacy, freedom of speech, and copyright protection. However, it lacks a thorough and overall exploration of the ethical framework from the macro level, and most studies have dealt with the topic in the Western context rather than from a global perspective. Improvements are made to these two aspects in this paper. It selects ToS of social applications on a global scale, adopts the method of text analysis, and analyzes the implied ethical principles, based on the Potter Box Model of Reasoning, as well as the Schwartz value scale and Christians and Ess' ethical principle framework, based on which puts forward suggestions for future development of social media ethics.

The unique contribution of the paper includes the following:

- (i) Exploration of the theoretical framework of the Potter Box Model of Reasoning, Schwartz's value scale, and Christians and Ess' ethical principles
- (ii) Examination of the ToS of social media run by six major platforms across the globe
- (iii) Analysis of the hidden conflicts and reveals the emergence of "relational" ethical

2. Social Media Ethics and Terms of Service

Terms of service are service format contracts made by Internet service providers (ISPs) for users [9, 10], which were born as early as the rise of the Internet, and have come into the public view with the explosion and popularity of social applications in recent years. As the primary premise for users to get access to services from the platform and join the community of social media, ToS offer constraints and guidance for users' social behaviors and regulate the rights and obligations between users, network platform providers, and third parties, as well as the distribution of rights and responsibilities [9]. In other words, ToS can be regarded as the platform's design criteria for the environment of the social media, thus opening a window for researchers to understand the ethical ecology of social media.

In previous literature, some exploratory studies have been carried out on ToS of social applications, with priority given to such specific ethical issues as privacy, freedom of speech, and copyright protection. The balance of rights and responsibilities is the focus of most studies. Researchers have found that consensus between platforms and users is reached via the registration process with just a simple click [11], and the terms of the agreement are obviously serving the platforms' own interests in the distribution of rights and obligations [12]. According to user surveys, most people hold the view that the choice of "take-it-or-leave-it" in the face of privacy settings such as tracking walls is neither acceptable nor fair [13]. In this regard, we should promote the reasonable protection of users' rights and interests for the purpose of enhancing users' interests [14].

In some studies, emphasis has also been placed on whether the consensus-reaching process of the agreement of ToS is user-friendly. As demonstrated by experiments and surveys, the vast majority of users choose to skip the careful reading of ToS when registering for social networking services, with the information overload a significant negative predictor of reading time [15]. The empirical investigation of the ToS and privacy policies revealed poor readability and availability [16], insignificant update hints, and obvious errors in the texts [17]. Other studies focus on the specific ethical issues involved in the ToS of social applications, most of which from the perspective of user rights protection. Common topics include privacy [18, 19], freedom of speech and democracy [20], copyright [21], and account inheritance [22].

Previous literature has provided a general description of the contents of ToS and exploratory conclusions on specific ethical issues based on the analysis of empirical data. However, it omits the exploration of ethical frameworks from the macro level, as ToS are crucial in platforms' planning of the digital social ecology. Moreover, existing studies lack a global perspective due to data collection from within the same sociocultural background. In this paper, improvements will be made to those two aspects, so as to dig out the ethical framework contained in the text of the ToS of social media.

3. Choice of Social Platforms and Ethical Framework

The user registration agreements displayed on the user registration page of social applications are mostly ToS. Some ToS also include package agreements such as privacy agreements and copyright notices. These additional agreements are usually listed in the form of hyperlinks in ToS. As the main agreement, ToS also embody the ideas of the additional agreements, to which users can refer for details. Given that this paper is aimed at refining the ethical framework, only ToS are studied here. In addition, NVivo will be used as an auxiliary tool of text analysis to examine the user registration agreement of the social applications, so as to refine the ethical frameworks implied in it. NVivo is a software that helps in performing quantitative and mixed-method-based research work. The software is primarily used for performing analysis of unstructured text, audio, video, and image data which are collected from interviews, focus group meeting, surveys, social media, and journal articles.

Nonrandom purposive sampling was used to select key social media to conduct text analysis. Taking into account the popularity ranking and categories of social applications, as well as from a global perspective, ToS of six social applications, namely, WeChat, Weibo, TikTok, WhatsApp, Twitter, and YouTube, are selected as samples in this paper (Table 1). Among them, the popularity ranking is taken from the application ranking list provided by Mobile Observatory [23] and the global application popularity list provided by Qimai Data [24].

According to the Potter Box Model of Reasoning, a classic model of ethical reasoning, the code of conduct can be established in four dimensions: facts, values, principles, and loyalties [25]. To accurately refine the ethical principles adopted by the subject, the values should be deduced from the facts first, and then, the ethical principles can be deduced from the values. In this paper, the first three steps of this model will be employed to extract the overall ethical framework from the ToS text.

In the second step, the Schwartz value scale will be partially utilized [26], which summarizes the values that all people have through an extensive survey of the population in 20 countries. There are four high-order types of value: self-transcendence, self-enhancement, conservation, and openness to change, which are divided into 10 subtypes and 44 representative values (Table 2). Though thorough and comprehensive it is, the impact of changes in the media ecology in recent decades has not been embodied in the survey. To this

TABLE 1: Overview of six social applications and ToS.

Social application	Category	Country of service provider	Applicable areas	Length (words)	Number of clauses
WeChat	Instant messaging	China	China	9058	97
WhatsApp	Instant messaging	US	Global	3973	51
Sina Weibo	Microblog	China	China	7651	92
Twitter	Microblog	US	Europe/rest of world	2532/3127	10/11
TikTok	Video socialization	China	China	12947	74
YouTube	Video socialization	US	Global	4213	45

TABLE 2: Schwartz value scale (Schwartz [26]; redrawn by author).

Higher-value types	Value types	Representative values
Self-transcendence	Universalism	Being broadminded, wisdom, social justice, equality, a world at peace, a world of beauty, unity with nature, and protecting the environment
	Benevolence	Being helpful, honesty, forgiveness, loyalty, and responsibility
Self-enhancement	Power	Social power, authority, and wealth
	Achievement	Success, capability, ambition, and influence
Conservation	Conformity	Politeness, obedience, self-discipline, and honoring parents and elders
	Tradition	Humility, acceptance of my portion in life, devotion, respect for tradition, and being moderate
	Security	Family security, national security, social order, cleanliness, and reciprocation of favors
Openness to change	Self-direction	Creativity, freedom, independence, curiosity, and choosing one's own goals
	Stimulation	Daringness, a varied life, and an exciting life
	Hedonism	Pleasure, enjoyment in life

end, in cases that the scale fails to cover in the process of coding, the values will be summarized according to the actual situations reflected in the materials, so that an ethical framework that fits the actual situation will emerge.

Christians et al. [25] also put forward the five principles of metaethics, which have been frequently quoted by scholars for years as the criteria of media practice, namely, Aristotle's Doctrine of Mean/Confucius' Doctrine of Mean, Kant's Absolute Law/Islamic Sacred Precepts, Mill's Utility Principle, Rawls' Veil of Ignorance, Judeo-Christian Fraternity, and Nordin's/Feminist Care. With the development of digital media, Ess [27, 28] put forward seven ethical principles applicable to the digital era, namely, utilitarianism, deontology, ethical relativism/absolutism/pluralism, feminist ethics and caring ethics, virtue ethics, Confucian ethics, and African views, which can be regarded as the adaptation and development of mass media ethics theory proposed by Christians et al. Artificial intelligence has huge potential of identifying areas wherein digital vendors fail to adhere to legal obligations. Study has been conducted representing implementation of AI system for the automatic detection of unfair terms in business-to-consumer contracts as part of a project entitled as "CLAUDETTE." The contract terms that were used in various digital consumer markets emphasized on five categories of clauses, namely, the limitations in liability, unilateral changes to the contract or services, unilateral termination of the contract, removal of contract, and arbitration [29]. Statistical analysis is used as a major

criterion for classification considering the corporate analysis services, namely, economic, company, and investment aspects. The use of AI in developing statistical classification system has helped in the development of accurate and timely interactive statistical services [30, 31]. In this paper, the above-mentioned ethical principles are used as a toolbox to further analyze the value standards obtained in the second step.

To sum up, the research framework of this paper is as follows: by using the Potter Box Model of Reasoning, the first step is to collect the empirical data and analyze ToS text; the second step is to determine the values based on the Schwartz value scale; the third step is to analyze the ethics principles according to Christians and Ess' ethical principles; the fourth step is to further analyze and refine an ethical framework of ToS of social media. Figure 1 shows the research framework.

4. Ethical Principles in Terms of Service

According to the coding results of the TOS text via NVivo, a total of 25 nodes are defined and then integrated into 15 values, comprising the original values listed by Schwartz values scale (honesty, being helpful, power (combined by social power and authority), wealth, politeness, conformity, security, order, freedom, and independence) and newly added values (sharing, cooperation, self-protection, and result-orientation) (Table 3).

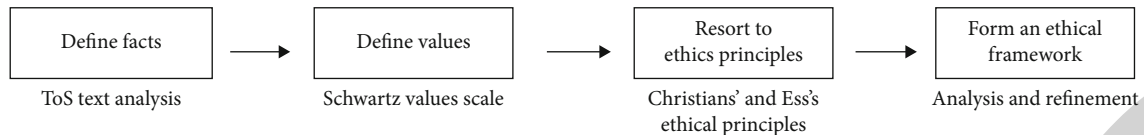


FIGURE 1: Research framework.

TABLE 3: Values reflected in ToS of social media.

High-value types	Specific value	Corresponding nodes	Node occurrences	
Self-transcendence	Honesty	Transparency	5	
	Being helpful	Readability	2	
	Sharing	Information sharing	2	
	Cooperation		Seek user cooperation	2
			Seek advice	3
Self-enhancement	Power	Nonacceptance means giving up	7	
		Consent by use	11	
		Unlimited right to change	7	
		Sent means delivered	2	
		Check the right of user information	3	
	Wealth	Autonomous adjudication right	10	
		Claim ownership and property rights	27	
		Suggest commercial use	6	
	Self-protection	Protect copyright of user-generated content	5	
		Exemption, limited liability	31	
Conservation	Politeness	Reserved unfinished rights	4	
		Politeness	2	
	Conformity	Abide by laws and observe discipline	18	
	Security	Security and privacy	12	
	Order	Order	10	
Openness to change	Freedom	Freedom and noninterference	3	
	Independence	Take one's own responsibility	19	
Other types	Result-oriented	Deal with things with result-oriented approaches	6	
	Respect for diversity	Respect for legal differences between countries	3	

Combining those values with their opposites (some of which are default values), the following 10 pairs of values are formed: power and participation, wealth and equality/universal benefit, openness and security, self-protection and responsibility, independence and cooperation, honesty and black box, order and freedom, unity and difference, result-orientation, and intention-orientation. With the help of metaethical principles put forward by Christians and Ess, these pairs are further integrated into three ethical principles: egoistic principle and altruistic principle, ethical monism and pluralism, and utilitarianism and categorical imperative.

5. Egoism and Altruism

5.1. Power and Participation. The node of power and participation appears in the ToS text most frequently among all the nodes. Social media seeks to dominate the digital community, including the power to set rules, review contents, and identify the treatment of violations.

In terms of the negotiation of the contents of ToS, all six social applications show the attitudes of “nonacceptance means giving up,” “consent by use,” “sent means delivered,” and “unlimited right to change” of the platforms, which have become the universal criterion for social applications worldwide. In ToS, all platforms have established a bundle of rights for themselves, including the right to limit or exempt liability, the right to adjudicate disputes, the right to make rules, the right to enforce rules (unilaterally), the right to punish the breach of contract, and the right to choose applicable laws. All these rights reflect the unidirectional domination of the platform, which easily leads to the imbalance of rights and responsibilities between the platforms and users, as well as the disequilibrium between obligations and duties of the platforms.

In spite of the prevalence of the so-called “participatory” culture in the era of social media, the platforms enjoy absolute power to formulate rules in ToS, while users have no say in the formulation. As long as users accept the services of the platforms, they can only choose to agree or accept those

terms in any case without making any change or consultations, let alone the formulation of the digital community rules through participation and autonomy of the user group.

5.2. Wealth and Inclusiveness. The occurrence of the node of wealth (ownership, property rights, etc.) ranks the second only to the node of power in the ToS text. All platforms attach great importance to the expression of interest demands.

Each platform has repeatedly declared the ownership of software and user-generated data, the right to profit from it, and the right to push business information. Platforms regard data as property and claim ownership and (exclusive) commercial benefits. Most platforms prohibit users and third parties from automatically crawling data on social media for whatever purpose, which also creates obstacles for academic research [32]. There is one exception, however, that Twitter allows crawlers “if done in accordance with the provisions of the robots.txt file.”

Meanwhile, values such as equality or universal benefit opposite to the accumulation of private wealth are missing in ToS text. Users, as owners of “small data,” have far less opportunity to profit than platforms which have access to “big data.” Despite acknowledging users’ ownership of self-generated information and promising to protect users’ copyright of self-made contents, platforms claim to have special permission to use personal information.

In the ToS text, platforms clearly define four roles of the users: digital workers who produce data for free or low pay, goods to be packaged and sold to advertisers, audience who receive advertising information, and customers who purchase platform services. These are also the relationship that the platforms presuppose to build with the users.

5.3. Self-Protection and Responsibility. Self-protection corresponds to the responsibility value in the Schwartz value scale. The Schwartz value scale uses an 8-point scale wherein 0 indicates that the value is against the selected principle, 1 indicates that the value is not of much importance, 4 indicates that the value is important, and 8 indicates that the value is of optimal importance. The Schwartz value scale is also known as short value scale which includes 57 items that represent ten distinct motivational values. The former emphasizes avoidance of responsibility, while the latter emphasizes taking responsibility. As a common core value of commercial enterprises, the value of “responsibility” is not highlighted in the ToS text. On the contrary, “taking no responsibility” and “disclaimer” are among the high-frequency words used by the platforms.

The cases of exemption that platforms assert include technical failures, data storage, user behaviors, security of accounts, disputes between the users and the third party, etc. Although it is difficult for users to determine whether that assertion is reasonable, platforms are in advantageous positions, and they choose to protect its own rights and interests first while failing to give priority to the rights and interests of users in the case of disputes.

5.4. Independence and Cooperation. “Independence” is a value especially emphasized in the Western society. As emphasized in the ToS text, whether it is the platform, the user, or the third party, the individual should bear the responsibility independently. For example, “the losses and consequences arising therefrom (including but not limited to missed promotion opportunities, loss of marketing revenue, etc.) shall be borne by the users themselves” (Sina Weibo ToS 8.4) and “Tencent and the third party shall be responsible for possible disputes within the scope stipulated and agreed by law” (WeChat ToS 11.2). Users should choose by and be responsible for themselves, such as “Your access to and use of the Services or any Content are at your own risk” (Twitter ToS).

Cooperative value, although also common across countries, is not included in the Schwartz value scale, which is added in this paper. This value appears sporadically in a few ToS. It should be noted that, on the surface, platforms are inviting the user for jointly improving products, building rules, and jointly maintaining the health and safety of the community environment, but “cooperation” in ToS still emphasizes that individuals are independent of each other (for example, Twitter thanks people for giving feedback or other suggestions on its services but emphasizes that users are not obliged to provide suggestions and the platform is not obliged to adopt suggestions), or for self-protection (for example, WhatsApp seeks protection and cooperation from users in legal disputes).

5.5. Openness and Security. Openness to third parties is repeatedly mentioned in the ToS. In fact, openness is one of the core values that platforms have always advertised. The security aspect in a platform is highly related to privacy and is considered as the most concerned ethical issue by the general public who use the respective platform.

The two values belong to the conservative/aggressive quadrant of the Schwartz value scale. The reason why security is placed under the principle of self-interest and altruism here is that from the text of ToS, it is altruistic for the platform to protect users’ privacy, while it is profitable for the platform to make private data open (at least in the short term). For one thing, privacy protection requires a lot of manpower and material resources; for another, it is also crucial that the platforms need to open or share user data with third parties from time to time for commercial profits or cost reduction, which is also a weak link with privacy risks.

For this reason, the platforms repeatedly commit to user privacy protection when sharing data with third parties in ToS. However, it is difficult for users to know whether their privacy has been violated by a third party, by whom, and to whom they claim their rights. There is no mention of the relevant supervision mechanism in ToS, and platforms usually assert exemptions in a case in which the third party infringes the user’s privacy.

5.6. Honesty and Blackbox. Regarding the value of honesty, the ToS text is self-contradictory. On the one hand, most platforms show frankness in the text. The first is transparency. “The operator will try its best to avoid the

inconvenience caused by the above entrustment or change to user's use of Weibo services, and the Weibo operator will try its best to make a timely notification by means of the website, platform, private message, mail, etc." (Weibo ToS). Secondly, platforms strengthen the readability of the ToS text. For example, they remind users of reading the key parts by using bold fonts, or specially mark the latest amendments to ToS "(We will provide you notice of amendments to our Terms, as appropriate, and update the "Last Modified" date at the top of our Terms)" (WhatsApp ToS).

At the same time, all platforms actually create obstacles for users to access and understand ToS, which makes honesty only a cosmetic rhetoric. All the ToS are accessible for the public, which, at first sight, is not the situation described by the term "black box," originally referring to the invisible state. However, as shown in Table 1, the length of these ToS generally takes a quarter of an hour to half an hour to browse according to the reading speed prescribed by the US Ministry of Education for middle school students and the Chinese Ministry of Education. Apart from ToS, there are several additional agreements that users need to agree to. Not only that, users are less likely to interpret and evaluate the real impact of ToS on their interests, due to their lack of technological knowledge and limited access to data compared to platforms.

5.7. Summary. The ToS text reflects a distinct tendency of the platforms to dominate in their relationship with the user and third parties. First of all, emphasis is placed on self-interest, the pursuit of power and wealth, but hardly involves the universal sharing of interests. Second, the rights and responsibilities of the platforms and the users are out of balance, and there is disequilibrium between the obligations and responsibilities of the platform. Third, the relationship between the platform itself and the user is defined as a contractual relationship rather than an intimate relationship or partnership, even when it involves seeking cooperation, coordination, advice, and help. Fourth, emphasis is placed on independency. The platform, the user, and the third party are independent of each other, each of whom takes its own responsibility and only takes its own responsibility, thereby downplaying the platforms' responsibility to society, and deny the rights and interests as a whole.

The above-mentioned values clearly highlight the principle of self-interest, as opposed to the ethical principle of altruism. The pair of ethical principles comes from the self-enhancement and self-transcendence of the high-value types of the Schwartz value scale. The conflict between the two principles corresponds to the debate between public and private, which has a long history in both Eastern and Western societies.

Neither the prevalence of the egoistic principle nor the decline of the altruistic principle can be simply attributed to the corruption of morality and the degeneration of human nature. Ratta [33] argues that this has to do with the control of production and distribution of communication by contemporary capitalism. Even the data protection regulations issued by the European Union, which are highly praised all over the world, are just minor repairs. They only protect

the small territory of individual freedom from the infringement of platform capitalism, which echoes the emphasis on the rights and responsibilities of individuals, rather than the users as a political collective. They do not challenge the whole system but only seek to alleviate the worst influence of capitalism.

Ratta suggested borrowing the concept of "care" from ethics as the core ethics of social media, emphasizing relationships rather than rights, sociality rather than individuality, interdependence rather than independence, and particularity, connection and context rather than universality and abstraction of legal contract thinking. This phenomenon is also related to the influence of Western individualistic values on global society. Modern Western thoughts tend to assume that human beings are atomic individuals, and as individuals, human beings are the basic elements of society, isolated from others. Cultural resources from other regions of the world should be introduced. For example, the Confucian ethics that defines people as the existence of relationship should be used to resolve conflicts on social media and build harmonious relationships with humans and things, so as to achieve the freedom and satisfaction of all parties [28].

6. Ethical Monism and Pluralism

6.1. Unity and Difference. As for the scope of application (see Table 1), although all three platforms from China require the user to grant permission to use personal information on a global scale in ToS, they all state that the terms are only applicable to Chinese laws, shunning the differences between countries and regions. Also, no specific provision for certain country or region has been formulated. Among the platforms from the United States, apart from that of YouTube, the other two ToS are widely applicable to countries all over the world and pay attention to the differences in laws and regulations of various countries in the terms.

WhatsApp makes it clear at the beginning of the terms that this application provides services to users all over the world, and that the laws, regulations, and standards of the country where information is stored or processed may be different from those of the country where users are located. Its ToS have some provisions for the United States and Canada that are different from other parts of the world, such as waiving the right of litigation.

Twitter has a special version of ToS for the European Union. The general version of the terms is similar to the European version in structure, but each clause is different in specific content. The requirements of the European version on platform rights and user responsibilities are significantly less than those of the general version. Compared with clause 5 of the two versions, the general version is 434 words long, which specifies the exemption and limitation of liability of the platform in detail. The EU version deleted the exemption part, only indicating that the platform's "responsibility is limited to the maximum scope allowed by the country where the user is located," with a length of only 38 words.

However, the introduction of those clauses or agreements does not mean that the platform's emphasis on differences in laws and regulations between countries is due to its genuine respect for social differences. In fact, Twitter has only issued a special agreement for the EU, and it has something to do with the EU's stricter data protection regulatory policy; WhatsApp has drawn up special clauses only for the United States and Canada, and most of the text related to national differences are related to exemption or reserved rights. Therefore, it is questionable about the value of difference embodied in the text on the surface.

6.2. Conformity and Challenges. Each platform shows adherence to the laws (of various countries) in ToS. For example, WhatsApp stipulates that if its services violate the local laws of any country or will make the platform bound by the laws and regulations of other countries, it will stop its services in that country. Besides, the platform also strictly restricts users and requires them to abide by local laws. For example, "country" and "law" appear 17 times and 36 times, respectively, in TikTok ToS.

Social applications are frequently used in various riot scenes, giving people the impression that social media are active participants in social movements. However, judging from the ToS text, platforms have not challenged mainstream authority, nor are they subversive of state power and laws. Instead, they are defenders and staunch executors and show obedience and cooperation to the current power order.

6.3. Order and Freedom. Platforms, especially those from China, emphasize the "conservation" values in the Schwartz value scale, such as "politeness" and "tradition." For example, "Users should speak politely in the process of using Weibo service ... to jointly establish a harmonious and polite online social environment (Weibo ToS 4.9)"; users should consciously abide by the requirements of "public order, social morality" (TikTok ToS 5.2.3); users are prohibited from posting information against "public order, good customs and social morality" (WeChat ToS 8.1.2.5).

The emphasis on these "conservation" values reflects the platforms' avoidance of uncertainties such as conflicts and chaos, affirmation of stability and order, and the pursuit of "normative and orderly network environment" (WeChat ToS 8.1.2).

Platforms declare that they do "not monitor the user or control the content the users publish through services of the application," which seems to be open to the value of diversity. However, ToS repeatedly emphasize the norms and order of maintaining the data environment and require the user to abide by the laws and social order. In essence, this kind of "freedom (or laissez-faire)" is only to exempt the platforms, which discourages the user group to make community rules through self-exploration.

6.4. Summary. On the whole, the ToS text shows that the platforms respect the political power of the host country, abide by the law, and maintain the social order and the stability of the social ecology, which indicates the platforms'

emphasis on the monistic value order and unwelcome of the pluralistic value order. On the one hand, this is to facilitate the management of the platform as a regional or even global organization; on the other hand, it also avoids the regulatory risks faced by the platform in different parts of the world.

This paper defines the ethical principle behind the values above as ethical monism, which is in contrast with pluralism. Ethical monism insists that there are universally valid norms, beliefs, practices, etc., in the world, which define truth, goodness, beauty, correctness, and goodness for all people at anytime and anywhere, while other norms, beliefs, and practices different from them are wrong. Ethical pluralism does not deny that there are some values, norms, practices, etc., that are valid for all human beings at any time and any place, but it is possible, inevitable, and desirable to explain, understand, and apply these norms in different ways in different environments. Based on this logic, on the one hand, the platform can abide by universal values, avoid slipping into relativism and thus tolerating all kinds of behaviors; on the other hand, it can simultaneously advocate tolerance of differences instead of directly rejecting them and truly respect the participatory culture, open culture, and multiculturalism in the era of social media.

7. Utilitarianism and Categorical Imperative

7.1. Result-Based and Intention-Based. In the TOS text, platforms declare to impose severe sanctions on some behaviors of the user mainly based on the results rather than the intention, which is different from the conventional practice of law or ethics. The latter usually considers first the motivation or intention of one's behavior when examining and evaluating one's behavior.

For example, "Any behavior that affects the operation of Weibo, damages Weibo's business model, or harms Weibo's ecology is prohibited" (Weibo ToS). Once the platform "discovers or receives reports or complaints from others about user violation", the platform "has the right to delete and block relevant content at any time without notice, and to impose penalties including but not limited to warning, restricting or prohibiting the use of some or all functions, account blocking and even account cancel according to the circumstances" (WeChat ToS 8.5.1).

In accordance with the result-based principle, users shall be fully responsible for their actions that cause a negative impact, whether on purpose or not. The reason why the platforms adopt this principle is easy to catch. Innovations of digital technologies in the IT field have brought about the fragmentation of media channels, which in turn entail the multiplier effect of social media, with greater impacts on the society. In that case, it is not surprising that platforms adopt this principle to be exempted from liability.

7.2. Summary. This moral philosophy of consequentialism and its opposite principle based on intention correspond to a pair of motifs, utilitarianism and deontology, which are repeatedly discussed in Western ethics.

According to the ethical principle of utilitarianism, one may be able to reason in complicated ways, determine the potential consequences, and bring greater benefits to the majority [34]. Following utilitarianism, the consequence principle that also puts forward higher requirements and greater moral responsibility for users accordingly, who shall be familiar with the traps and dangers on social applications, be able to make a comprehensive judgment on all the risks caused by their own behavior in the complex digital world, accurately predict future results, and bear all risks for them.

However, from the perspective of Kant's deontology, decision-makers cannot take actions based on potential consequences. Pure moral intentions are the basis of communication and the only motivation that is safe from corrosion [35]. According to deontology, the user should act based on rules, rather than focus on the consequence, and take moral responsibility to do the right thing according to Kant's absolute command without consideration of the specific situation on social media.

According to Bowen [4], the requirements for the user in the utilitarian media environment are beyond the capabilities of all humans. Apart from the most complicated "utilitarian calculus," he supports the ethical principles of Kant's deontology to guide media practice. This correspondingly raises a problem: the highly idealized deontology requires a high level of rationality of the actor, which makes it difficult for ordinary users in practice. In reality, what often happens to the user is that people have neither intention to harm nor adequately estimate the potential impact on others. James [36] also mentioned similar cases, suggesting to adopt "the ethics of roles"; that is, the responsibility related to the larger background in which one's role is located should be reflected, the influence of individual behavior on multiple and distant stakeholders should be considered, and decisions should be made in the interest of the larger community, the public, and the society, so as to build a better networked world of online communication.

8. Discussion and Conclusion

This paper analyzes with NVivo the ethical principle in the ToS from six major social applications across the globe, based on the theoretical framework of the Potter Box Model of Reasoning, Schwartz value scale, and Christians and Ess' ethical principles. We define 15 values and integrate them into ten pairs of values and further analyze the implied conflicts with three pairs of ethical principles. The ToS text reflects the values of honesty, being helpful, power, wealth, politeness, conformity, security, order, freedom, independence, sharing, cooperation, self-protection, and result-orientation, which embody ten pairs of values, namely, power and participation, wealth and equality/universal benefit, openness and security, self-protection and responsibility, independence and cooperation, honesty and black box, order and freedom, unity and difference, result-orientation, and intention-orientation. Those pairs of values can be three pairs of ethical principles: egoistic principle and altruistic principle, ethical monism and pluralism, and utilitarianism and categorical imperative.

In the summary of the research findings, we point out that the conflict between the principle of egoism and the principle of altruism requires one to pursue one's interests in the relationship with others; the conflict between ethical monism and pluralism requires one to understand values and norms in the context of others; the conflict between utilitarianism and categorical imperative requires one to consider the potential influence of one's own behavior in a larger public background. It can be seen that the conflicts between the three pairs of ethical principles all require that platforms and users define themselves in "relationship" and in a wider range of relationships.

Paying attention to the principle of "relationship" does not indicate the need to invent new ethics to cope with the social media environment. In fact, whether the value of relationship that Ratta [33] derived from care ethics, Ess [28] from Confucianism, or James [36] from role ethics theory, those theoretical resources they cited are nothing new. However, the reaffirmation of relationship ethics does remind us that some old principles need to be reexamined and reexplored. On the other hand, we should draw on theoretical nutrients on a global scale, from non-Western traditions and noncapitalist ideologies, reflect on the prevailing ethical principles, and move towards a more inclusive and imaginative social media ethics.

Data Availability

The datasets used during the current study are available from the corresponding author on reasonable request.

Conflicts of Interest

The authors declare that they have no conflict of interest.

Acknowledgments

This work was supported by the China Scholarship Council, Youth Foundation for Humanities and Social Science Research, China's Ministry of Education (21YJC860022), and Independent Research Project of Tsinghua University (2019THZWC57).

References

- [1] G. A. Gladney, "Technologizing of the word: toward a theoretical and ethical understanding," *Journal of Mass Media Ethics*, vol. 6, no. 2, pp. 93–105, 1991.
- [2] N. Couldry, M. Madianou, and A. Pinchevski, *Ethics of Media*, Springer, 2013.
- [3] J. H. Lipschultz, *Social Media Communication: Concepts, Practices, Data, Law and Ethics*, Taylor & Francis, 2017.
- [4] S. A. Bowen, "Using classic social media cases to distill ethical guidelines for digital engagement," *Journal of Mass Media Ethics*, vol. 28, no. 2, pp. 119–133, 2013.
- [5] B. Debatin, *Media Ethics in a Fast Changing Media Environment*, vol. 28, no. 1, 2013 Taylor & Francis, 2013.
- [6] K. Mukherjee, "Comparison between social communication ethics and social media communication ethics: a paradigm

Retraction

Retracted: A Mathematical Queuing Model Analysis Using Secure Data Authentication Framework for Modern Healthcare Applications

Journal of Sensors

Received 23 January 2024; Accepted 23 January 2024; Published 24 January 2024

Copyright © 2024 Journal of Sensors. This is an open access article distributed under the Creative Commons Attribution License, which permits unrestricted use, distribution, and reproduction in any medium, provided the original work is properly cited.

This article has been retracted by Hindawi following an investigation undertaken by the publisher [1]. This investigation has uncovered evidence of one or more of the following indicators of systematic manipulation of the publication process:

- (1) Discrepancies in scope
- (2) Discrepancies in the description of the research reported
- (3) Discrepancies between the availability of data and the research described
- (4) Inappropriate citations
- (5) Incoherent, meaningless and/or irrelevant content included in the article
- (6) Manipulated or compromised peer review

The presence of these indicators undermines our confidence in the integrity of the article's content and we cannot, therefore, vouch for its reliability. Please note that this notice is intended solely to alert readers that the content of this article is unreliable. We have not investigated whether authors were aware of or involved in the systematic manipulation of the publication process.

Wiley and Hindawi regrets that the usual quality checks did not identify these issues before publication and have since put additional measures in place to safeguard research integrity.

We wish to credit our own Research Integrity and Research Publishing teams and anonymous and named external researchers and research integrity experts for contributing to this investigation.



The corresponding author, as the representative of all authors, has been given the opportunity to register their agreement or disagreement to this retraction. We have kept a record of any response received.

References

- [1] A. S. A. Raj, R. Venkatesan, S. Malathi et al., "A Mathematical Queuing Model Analysis Using Secure Data Authentication Framework for Modern Healthcare Applications," *Journal of Sensors*, vol. 2022, Article ID 8397635, 15 pages, 2022.

Research Article

A Mathematical Queuing Model Analysis Using Secure Data Authentication Framework for Modern Healthcare Applications

A. Samson Arun Raj,¹ R. Venkatesan,¹ S. Malathi,² V. D. Ambeth Kumar ,³ E. Thenmozhi,⁴ Anbarasu Dhandapani ,⁵ M. Ashok Kumar,⁶ and B. Chitra³

¹Computer Science and Engineering, Karunya University, Coimbatore 641114, India

²Artificial Intelligence and Data Science, Panimalar Engineering College, Anna University, Chennai 600123, India

³Computer Science & Engineering, Panimalar Engineering College, Anna University, Chennai 600123, India

⁴Department of Information Technology, Panimalar Institute of Technology, Anna University, Chennai 600123, India

⁵Department of Electrical and Computer Engineering, Institute of Technology, Jigjiga University, 1020 Somali, Ethiopia

⁶Faculty of Computer Science and Software Engineering, Skyline University Nigeria (SUN), Kano, Nigeria

Correspondence should be addressed to Anbarasu Dhandapani; anbarasudhandapani@jju.edu.et

Received 28 July 2022; Accepted 24 August 2022; Published 16 September 2022

Academic Editor: Sweta Bhattacharya

Copyright © 2022 A. Samson Arun Raj et al. This is an open access article distributed under the Creative Commons Attribution License, which permits unrestricted use, distribution, and reproduction in any medium, provided the original work is properly cited.

Healthcare application is one of the most promising developments to provide on-time demand services to the end users, vehicles, and other Road Side Units (RSUs) in the urban environment. In recent years, several application interfaces have been developed to connect, communicate, and share the required services from one source to another. However, the urban environment holds a complex entity of both homogenous and heterogeneous devices to which the communication/sensing range between the devices leads to connectivity breakage, lack of needed service in time, and other environmental constraints. Also, security plays a vital role in allowing everyone in the urban area to access/request services according to their needs. Again, this leads to a massive breakthrough in providing reliable service to authentic users or a catastrophic failure of service denial involving unauthorized user access. This paper proposes a novel topological architecture, Secure Authentication Relay-based Urban Network (S-ARUN), designed for healthcare and other smart city applications for registered transportation stakeholders. The registered stakeholders hold a built-in data security framework with three subsystems connected to the S-ARUN topology: (1) authentication subsystem: the stakeholder must identify themselves to the source responder as part of the authentication subsystem before transmitting the actual data service request; (2) connectivity subsystem: to periodically check the connection state of stakeholders as they travel along with the road pattern; and (3) service subsystem: each source responder will keep a separate queue for collecting data service requests, processing them quickly, and sending the results to the appropriate stakeholder. The Kerberos authentication method is used in working with S-ARUN's model to connect the stakeholders securely and legitimately. The performance of the proposed S-ARUN is assessed, and the performance metric toward key generation and other data security-related metrics is tested with existing schemes.

1. Introduction

In networking, "data" refers to a collection of multimedia data streams. Data can be text, image, audio, video, or other document-type material ready for transmission with the appropriate stakeholders in the field. However, data transmission from one source to another is not easy but plays a vital role in various design applications [1]. The possible number of data

can be tapped, altered, or worse, rerouted by the third-party member. Researchers have introduced several algorithms and mathematical formulation ways of securing the wired and wireless communication channel from which the third party cannot alter the data shared among its stakeholders.

Recently, smart city application under various operational purposes has gotten the attention of constructing an effective topology by introducing a hybrid infrastructure in

the transportation environment. As a result, the stakeholders can easily interact with the nearest substation of RSUs anywhere and anytime. Jeong et al. [2] have addressed the standardization initiatives for smart transportation systems, protocols, applications, and security which have been thoroughly examined by researchers. However, this hybrid infrastructure faces certain topological flaws of its own such as lack of communication, mobility speed, network coverage, limited resources, data contention, and data congestion.

Since the transportation environment mode of communication and equipment changes, the stakeholder's evolution changes. However, the infrastructure from which the data is relayed is still conventional. The working mechanism of the existing transportation environment is like a flooding mechanism. If one RSU receives the service request to access the data, the source data of that particular is broadcasted to all its neighboring RSUs and finally reaches the appropriate stakeholder. Thus, it creates a huge security risk of revealing the service access throughout neighboring RSUs that find themselves unrelated to the store and unnecessary acceptance of information to relay the communication. The third party finds these weak RSUs node gains access and listens to all the surpassed information.

Moreover, most RSUs have limited and few operational resources to classify and process the needed information to be delivered in time. Hence, these RSUs undergo certain eco-friendly and communication difficulties as the on-road vehicles move quickly along the road. Furthermore, the potential increase/decrease in on-road vehicles entering and exiting the transportation environment makes maintaining the network topology and data flow critical. As a result, there are several technical challenges with RSUs providing dependable data service to on-road vehicles in the transportation environment. Surely, we can consider the end-user terminal for requesting the needed service. Since the topological design deals with vehicles and aerial nodes, the end user can also be considered a ground node depending on the configuration devices used in the application scenario.

1.1. Usage of UAVs. As intelligent transportation systems become more sophisticated with digital streams, each transport mode needs to cooperate under various application platforms to form a global network of hybrid-vehicular systems. Flying Ad-Hoc Networks (FANETs) have recently focused on civilian and military-based systems (<https://blog.rgbsi.com/what-is-v2i-technology>) [3]. FANET is a subclass of Vehicular Ad-Hoc Networks (VANETs) that use flying anchor nodes or small-scale Unmanned Aerial Vehicles (UAVs), as an intermediary agent in harsh locations where establishing infrastructure is nearly impossible. However, there are certain difficulties that the VANET system faces daily. For example, the transportation environment conditions and node behavior between ground vehicles and aerial vehicles change dynamically, leading to the isolation of stakeholders in the transportation environment. Therefore, an extensible wireless communication gateway must integrate existing technologies and make modern transportation systems more sustainable, ecofriendly, and safe for on-road vehicles to obtain the sought service promptly [1].

On the other hand, the height of RRSU nodes plays a vital role in providing network connectivity to vehicular nodes, which is one of the issues encountered in the contemporary application environment. Surely, deploying aerial nodes is quite challenging in the urban environment as the altitude against skyscrapers should be maintained with constant observation. Several mobility models with artificial intelligence are under development to address this issue. Few automobile nodes, for example, have poor network connectivity throughout their journey as they follow road patterns. Because the distance from the RRSU network in the transportation environment exceeds 300 meters, it is not considered to offer or receive the requested data service. Furthermore, the present ITS service system's incoming arrival rate indicates that the requested service lacks data priority due to significant data conflict from several vehicular nodes, resulting in a buffer overflow and packet loss.

1.2. Data Authentication in VANETs. In a vehicle ad hoc network, authentication is crucial. A VANET's basic structure comprises three primary elements: the Trusted Authority (TA), roadside units, and automobiles. The VANET's real-time, dynamic communication properties allow for efficient and continuous information sharing and attractive application services, which could significantly improve the driving experience of drivers. The TA is in charge of registering all RSUs and cars and assigning secret keys. To validate the participating automobiles, TA uses a twofold authentication process. Meanwhile, RSU serves as a communication hub. There are four rounds to the authentication process.

The connection between multiple vehicles is at the heart of VANETs, and the security of such communication is ensured via message authentication. Several approaches have been developed to improve message authentication efficiency. However, both techniques have the drawback of redundant authentication. The same message is authenticated several times, and they fail to identify erroneous messages in a batch of messages. Because VANETs are vulnerable to malicious assaults, the security of vehicular ad hoc networks has gotten much attention in wireless mobile networking. Several safe authentication systems based on asymmetric cryptography have been proposed to counter such attacks.

On the other hand, these techniques are not ideal for extremely dynamic environments such as VANETs since they cannot handle the authentication operation efficiently. As a result, an efficient authentication system for VANETs is still required. Furthermore, message authentication, a common mechanism for verifying information reliability, such as data integrity and authenticity, has a problem in VANETs.

When a vehicle receives many messages, typical exhaustive (or per message) authentication might cause unacceptably high processing overhead on the car, causing unacceptable delays in time-critical applications like accident warnings. For vehicular ad hoc networks, the trade-off between reliance on the tamper-proof device (TPD) and storage space in authentication schemes has recently become a hot topic [4]. Because the intelligent transportation systems of smart city technologies, vehicular ad hoc networks, and Internet of Vehicle (IoV) technologies are drawing special interest from industry communities [5], VANET's vehicle-to-vehicle (V2V) connectivity can help traffic

management and road safety. However, because V2V communication cannot handle many cars simultaneously, it must be split and communicated by region. As a result, essential agreements are created for V2V communication between the same or different regions, considering the locale. Furthermore, standard public key infrastructure and Kerberos systems incur computational costs to be used in a real setting.

Existing vehicular ad hoc network (VANET) authentication systems are not scalable to high-density and safety-critical VANETs. In their design, these methods overlook critical and unique VANET properties such as frequent path disconnections due to high mobility, bandwidth-limited channels, ultra-low latency applications, high channel-error rate, and much more. Furthermore, due to the usage of an open wireless communication medium where messages are transferred in plain text, which allows attackers to intercept, manipulate, replay, and delete them, VANET's security and privacy are of the utmost importance [6]. As a result, there is a good chance that the security of a VANET-based smart transportation system may be jeopardized.

1.3. Objectives of the Research Work. The primary objectives of the proposed topological design are listed as follows:

- (i) To introduce a secure authentication mechanism to all the registered stakeholders connected to the SARUN topology in the transportation environment
- (ii) To perform the data packet request by analyzing its parameters based upon the data security framework introduced in every RSU node
- (iii) The proposed work is compared with the existing schemes to verify the performance metric, and merits and demerits are notified in detail

2. Related Works

The deployment of vehicle networks in practice is still a work in progress. This study [7] presents a new self-organized authentication approach for VANETs that enables ubiquitous, quick, and safe deployment. Because the nodes themselves certify the authenticity of the public keys of the other nodes, there is no need for a central certification authority. On the one hand, researchers have devised a mechanism that each node must employ when selecting public key certificates for its local storage.

Because of the variety and severity of prospective assaults, communication security in VANETs is one of the essential concerns to enable their effective deployment. On the one hand, erroneous traffic warning messages can influence drivers' judgments, waste time and fuel, and even result in traffic accidents. As a result, VANETs must guard against attackers sending false information about road conditions, such as traffic jams, to deceive other vehicles. On the other hand, as a result, VANETs should not provide complete vehicle anonymity since the risk of sending misleading signals would jeopardize their practical implementation.

With promising technologies that provide rich multimedia data streams of information to all searching vehicular

nodes in the transportation environment, the need for intelligent transportation system services has grown dramatically worldwide [8, 9]. The existing intelligent transportation system has two application scenarios: pole infrastructure-based [8] and aerial mobility-based [7]. The data packets that convey the message flow from the source, i.e., the base control station (BCS), are sent through a sequence of communication RSU agents to reach and communicate with relevant vehicular traffic nodes in both application scenarios. In addition, the RSU agents have the authority to process data packets and alert the nearest subunits to monitor, track, and direct the vehicular nodes in the event of hazards, warnings, or event notifications.

In various intelligent transportation system applications, the roadside units are stationary constructed at the intersection points along with the road pattern. Over time, these stationary RSU agents lack the priority in establishing the desirable network connectivity and cannot provide the necessary reliable data service among the vehicular nodes. The RSU is a stationary unit normally permanently installed along the side of the road. Ad hoc domain is used for single/multihop communication between automobiles. A Dedicated Short-Range Communication (DSRC) technology is used to communicate between V2V and V2I. The DSRC is a short- to medium-range wireless communication system utilized in the VANET for data transfer. The DSRC system uses a spectrum of 75 MHz with a communication range of DSRC that is 100 to 1000 meters, and the data rate is 6 to 27 megabits per second [10]. Since the technological equipment and mode of communication changes, the existing RSU agents are packed with numerous amounts of information leading to a processing overload of limited resources and incapable of tracking high-speed vehicular nodes pursuing the transportation environment. Thus, replacing or reconstructing the entire ITS service system operating in the transportation environment over the years is impractical.

Fotohi et al. [11] talked about an agent-based self-protective technique for UAVNs called ASP-UAVN, based on the Human Immune System (HIS). In ASP-UAS, a self-protective system chooses the safest route from the source UAV to the destination UAV. Using an Artificial Immune System (AIS), a multiagent system identifies the attacking UAV and picks the safest approach. Furthermore, [3] covered the various sorts of attackers and security assaults in the VANET. The attackers are categorized based on their network activities. A node is considered adversarial if it injects or modifies any messages, causing the entire network to be disrupted. The attackers' primary goal is to cause network disruptions for personal gain. According to their actions and scope, the three types of attackers are insiders vs. outsiders, aggressive vs. passive, and malicious vs. reasonable attackers.

Authentication is a critical security issue for VANETs [12]. Over the last few years, many authentication systems based on public key infrastructure (PKI) or identification (ID) have been presented. The digital signature provides message authentication, integrity, and nonrepudiation. Knowing the signer's public key allows anyone to verify the signature's legitimacy. This property makes it possible to use the digital signature in one-to-one (unicast) and one-to-many (multicast) applications. In some multicast applications, the root node

may be required to gather messages from leaf nodes, resulting in many-to-one communication.

Lall et al. [8] concentrated on the many authentication techniques used in VANET because they are critical for safe communication. The three main authentication schemes are cryptography techniques, digital signatures, and message verification techniques. A taxonomy of authentication systems is also thoroughly examined. Also, authentication is necessary for accepting safety messages from legitimate VANET users. Authentication is divided into two parts: part 1 is the sender vehicle's signature, and part 2 is the receiver vehicle's signature verification of the message received. Authentication can be done at two levels in a VANET communication system: first at the node level, referred to as node authentication, and second at the message level, message authentication. Authentication of nodes and messages ensures a node's legitimacy and a message's integrity, respectively. Verifying the message's integrity and the node legitimacy check is critical to increasing VANET security. As a result, the most critical security aspect in VANET is message authentication.

Azees [13] and Tan et al. [14] have introduced a two-factor authentication and key management strategy for safe data transfer in vehicular ad hoc networks. According to the authors, the proposed approach is immune to replay and masquerade attacks. Chuang and Lee [15] have introduced a decentralized lightweight authentication technique for vehicle-to-vehicle communication networks dubbed trust-extended authentication mechanism (TEAM). To increase the efficiency of the authentication operation, TEAM uses the concept of transitive trust connections and only requires a few storage spaces. TEAM also meets the following security requirements: anonymity, location privacy, mutual authentication, forgery, modification, and replay attack resistance, no clock synchronization problem, no verification table, fast error detection, perfect forward secrecy, man-in-the-middle attack resistance, and session key agreement.

Lin and Li [16] have proposed an effective cooperative authentication strategy for VANETs that minimizes redundant authentication efforts on the same message by various vehicles while reducing the authentication overhead on individual cars and shortening the authentication delay. Because it simultaneously provides mutual authentication and privacy protection, the conditional privacy-preserving authentication (CPPA) technique [17] is appropriate for handling security and privacy-preserving challenges in VANETs. On the other hand, the bilinear pairing process is renowned as one of the most difficult operations in modern cryptography. Therefore, constructing a CPPA scheme for the VANET environment that does not require bilinear pairing becomes a challenge to improve performance and reduce the computational complexity of information processing in VANET.

Zhu et al. [18] discussed an efficient privacy-preserving authentication technique for automotive ad hoc networks based on group signature (VANETs). Although group signatures are commonly used in VANETs to achieve anonymous authentication, existing systems based on group signatures suffer from substantial calculation delays in the CRL checking and signature verification processes, resulting in high message loss. Liu et al. [4] talked about using identity-based encryption

and a short-lifetime region-based certificate to create a realistic distributed conditional privacy-preserving authentication mechanism for VANETs.

Lee et al. [5] presented a lightweight technique for managing regional segmentation and overhead resolution using dynamic features of vehicles. Furthermore, because vehicle data is sent through public networks, our protocol employs mutual authentication and honey list technology to protect against various threats. The concept of edge computing has been discussed in the message-authentication process of VANETs [19]. Even if the VANET is attacked, the suggested system can not only perform well in an ideal scenario where the attacker is not present but it can also swiftly distinguish valid and invalid messages.

Shao et al. [20] developed a new authentication protocol for VANETs in a decentralized group architecture that employs a novel group signature mechanism to address these difficult issues. VANET must have an authentication mechanism to protect against attacks and maintain privacy to enable safe communication. Azam et al. [21] examined security, privacy, and scalability requirements with a complete taxonomy for authentication systems in VANET. Shen et al. [22] has addressed the issues of high computing overhead caused by safety message authentication in the cooperative message authentication protocol (CMAP), which was developed to reduce the computational burden on automobiles.

Ying and Nayak [23] have developed a smart card (ASC) protocol-based anonymous and lightweight authentication system. ASC uses low-cost cryptographic operations to authenticate the legitimacy of users (vehicles) and validate data communications. ASC also has a way of changing passwords that do not rely on a trusted authority. As a result, it can withstand an offline password guessing attack. Finally, a formal security model is developed to demonstrate that our protocol is secure when the computational Diffie-Hellman problem is assumed. Asaar et al. [24] have proposed a new identity-based message authentication system based on proxy vehicles (ID-MAP) that satisfies the message authentication condition against adaptively chosen messages.

Al-Shareeda et al. [6] thoroughly examined the many authentications and privacy systems implemented over time. Vijayakumar et al. [25] have created a trusted authority to supply clients with various online premium services via VANETs. The security and authentication of messages exchanged between the TA and the VANET nodes are critical. As a result, we focus on the situation in which the TA divides users into primary, secondary, and unauthorized users to address the security issue. Lee et al. [5] stated that two public-key cryptosystems have developed a privacy-preserving localized hybrid authentication (PLHAS) mechanism for PKI and CL-PKC. Li et al. [26] have proposed a composite fault diagnosis methodology based on detecting and identifying the fault of the vehicle ad hoc network's onboard unit.

Certificateless public-key cryptography is used to tackle the complex certificate management problem in classical public-key cryptography and the key escrow problem in identity-based encryption [27]. The aggregate signature notion comes in handy when the signatures on various messages generated by various users must be compressed. Because it allows for

considerable bandwidth and calculation time reductions, this feature is highly appealing for authentication in a resource-constrained setting. A novel certificateless signature system is proposed in this paper. The new certificateless signature technique gives a novel certificate less aggregate signature scheme for vehicle-to-infrastructure communication in vehicular ad hoc networks.

Due to the high dynamics in topology, mobility, and link connectivity, data dissemination in VANET is a difficult issue. Due to the host/address-centric, connection-oriented communication mechanism primarily built for reliable wired networks, the Internet paradigm (i.e., TCP/IP) is inefficient for VANET data dissemination [28]. Arshad et al. [29] has developed a full block chain-based 5G vehicular network architecture that is cost-effective, scalable, and secure and addresses various vehicular network concerns in smart cities. All necessary components, such as a reputation system, an incentive mechanism, and priority-based strategies, are included in the proposed design. Soleymani et al. [30], as well as a trust model, have addressed a privacy-preserving node and message authentication approach. In addition, fog nodes were placed along the highway by the fog computing concept to reduce latency and enhance throughput.

The Password-Authenticated Key Exchange (PAKE) protocol is widely used to offer secrecy, data integrity, and authentication services in various settings. On the other hand, preshared passwords are insecure in a practical self-organized network because mass-produced devices frequently have similar default passwords, such as 0000 or 1234, which are seldom changed [31].

Eftekhari et al. [32], Ogundoyin and kamil [33], and Peixoto et al. [34] have developed a fog computing-based data clustering framework for traffic information reduction at the edge of vehicular networks. Rao and Ram [35] have improved the time synchronization and freshness plan for Kerberos 5 authentication using symmetric encryption keys in a client-server scenario. Also, [36] have proposed a secure protocol based on tickets for rigorous mutual authentication and session key establishment tokens that incorporate Kerberos' strong qualities. Based on their architecture and implementation specifics, [37] has comprehensively evaluated VANET, SDN, and SDN-based VANETs.

Section 3 describes the internal design and operation of the RSU agent's data security framework.

3. Data Security Framework and Their Working Process

The model for the data security framework we will use in our research effort is represented in Figure 1 in the application scenario [1]. Base control station, satellite relay station, aerial networks, and vehicular nodes (i.e., on-road vehicles) are the four primary components of the application scenario. However, these components are interrelated, each having a specific role in preserving data security and obtaining requested data packets in diverse mobility patterns.

- (i) Base control station: the transportation field station, also known as the base control station, organizes

and retains information concerning aerial nodes, vehicular nodes, situation awareness, and other relay subunits. In addition, the base control station monitors and guides the aerial network in a dedicated way-point lane in the transportation environment

- (ii) Satellite relay station: satellites provide a backbone relay communication across civilian platforms across the transportation environment in modern transportation applications. Depending on the necessity, the satellite can be utilized as a backbone transceiver, processing all microwave data into the proper data format between the source and destination platform communicators
- (iii) Aerial nodes: the aerial nodes, also referred to as Relay-Road Side Unit (RRSU) network, act as a buffer between the vehicle nodes. It improves network connectivity to all vehicular nodes and takes the initiative to process data packet requests and deliver road-assisted service messages on time. A single RSU network comprises many RSU nodes separated by a defined distance and travels at an ideal pace to avoid colliding with the RSU substation and each other
- (iv) Vehicular nodes: a vehicular node can be a commercial, semiautonomous, or fleet management vehicle that leads a group of subunits in the transportation environment. Autonomous vehicles have been created for various ITS service applications, including field support, exploration, search, and rescue

In this paper, we will be considering this application scenario for healthcare usage in which these aerial nodes have the following advantages as follows,

- (i) Aerial access points: unlike traditional networks, these aerial nodes are equipped with all communication functionalities to communicate to the nearest hospital if a vehicle or user requires an emergency service to the nearest hospital or doctors. Thus, it provides seamless and anytime connectivity who seek service
- (ii) Built-in data storage: since the urban environment is pouring with vehicles requesting service access, the aerial nodes are embedded with predefined information on how, when, where, and whom to process the request in time. Table 1 illustrates some of the information predefined in every aerial node to process
- (iii) Computation: once the connection establishment of the stakeholder is authentic, the request for the service is granted with priority. If the service is requested from an unauthorized user, the aerial nodes seek out other nodes for supporting service

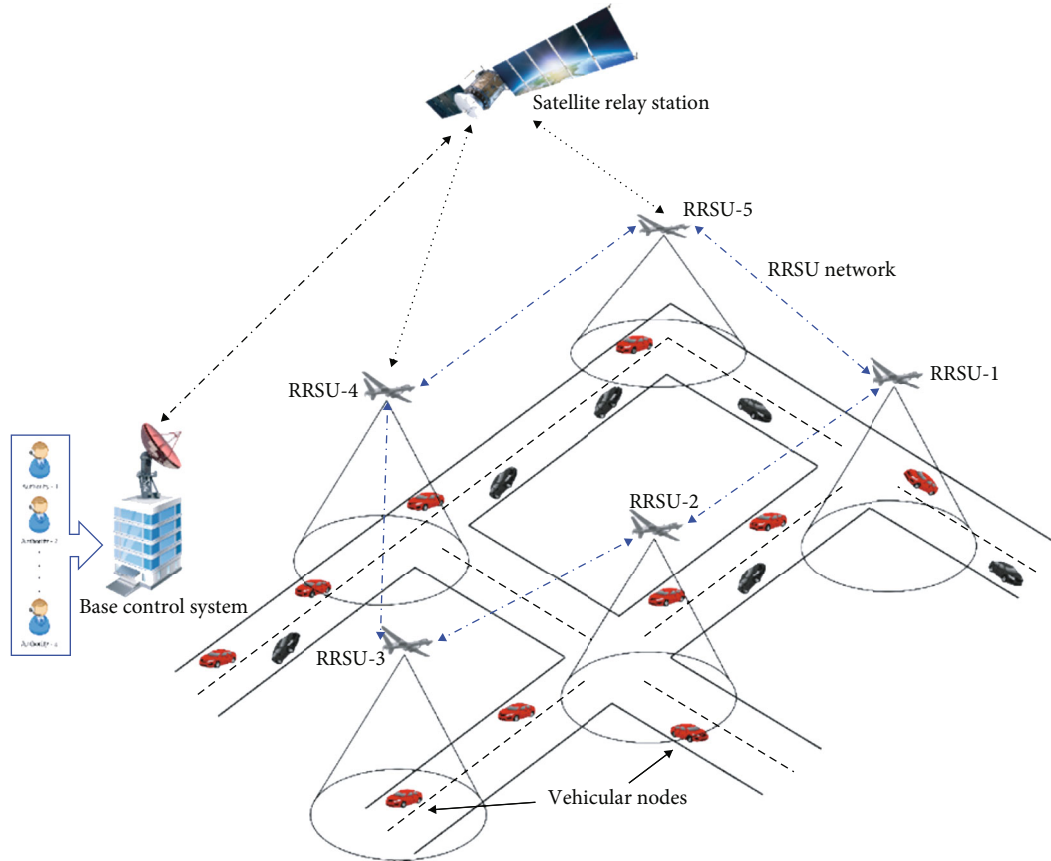


FIGURE 1: Application scenario [1].

- (iv) Service transmission: since the urban environment deals with moving vehicles, the requested service must be delivered in time. If the aerial node cannot transmit the service in time, the neighboring nodes will notify, providing service reliably

The working process of the data security framework in S-ARUN topology is of a three-stage level of subsystem process. At first, all the stakeholders must be connected to the nearest RSU agents for registration confirmation. The RSU agents first broadcast a series of control beacon messages (CBM) to all stakeholders by establishing unified network communication. The registered transportation stakeholders will quickly establish the connection apart from the non-registered stakeholders who seek data service must go through a secure authentication verification before offering the actual network connection, which will be explained in detail.

After connecting to their nearest RSU agent, vehicular nodes can request data service application information/messages, such as infotainment, location guidance, and safety awareness. The RSU agents process the data packet request according to their priority index of vehicle type and then respond to message/service to the appropriate vehicular node within the specified time frame. Figures 2 and 3 depict the information flow of data service packets and the internal subsystems of a data security framework inside a single RSU agent.

3.1. Authentication Subsystem. The authentication service provided in this subsystem follows the working principle concept of Kerberos. The Kerberos authentication scheme authenticates all the stakeholders who present an open distributed environment. In the case of nonregistered stakeholders seeking service, it is mandatory to prove that it has been identified for each service request to acquire the data service, or else their access request will be denied. Any stakeholder can request any RSU agent for data service if the topology is unprotected. Thus, the RSU agent cannot easily deny the data service requests without proper constraints. Every RSU agent is provided with an inbuilt Stakeholders Service Authentication (SSA) to ensure safety measures. This authentication server knows the true identity of the stakeholder and logs all the possible information maintained in a centralized database. In addition, every RSU agent provides a unique key in a ticket for granting access to the requested data service.

The following steps describe how the stakeholder's service authentication ticket is generated for stakeholders who seek service. This mechanism can be applied to registered and nonregistered stakeholders in the transportation environment. Table 2 illustrates the notations used for service access ticket generation under the authentication scheme, and Pseudocode 1 outlines the functional approach of the data security framework in a single RSU agent.

TABLE 1: Types of MPLS labels used in data security framework.

MPLS header label bits						
Emergency	Cater	Government	Private	Specific	Clinic	Shelter
	Bits	00001	00010	00011	00100	00101
Early warning	Cater	Accident zone	Intersections/roundabouts	Road bumps	Speed alerts	Collision alerts
	Bits	00110	00111	01000	01001	01010
Service application	Cater	Location of substations	Alternative routes	Navigation	Pedestrian crossing	Lane restrictions
	Bits	01011	01100	01101	01110	01111
On-the-Move (OTM)	Cater	Infotainment	Service access	Traffic status	Cruise control	Smart sensors
	Bits	10000	10001	10010	10011	10100

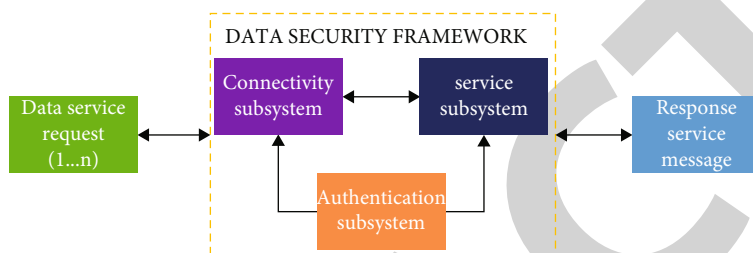


FIGURE 2: Overview of data security framework.

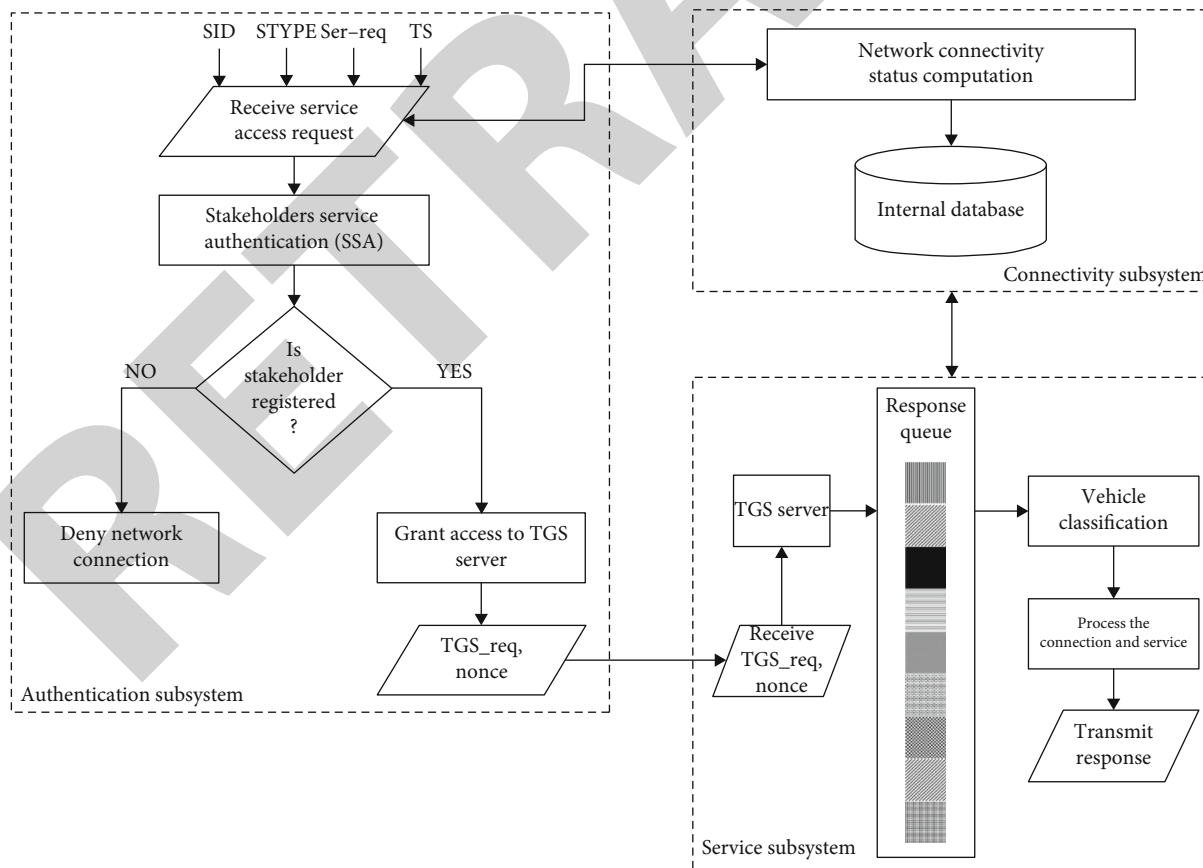


FIGURE 3: Internal architecture of the data security framework.

TABLE 2: List of notations used in authentication server.

S	Stakeholder
Kv	Secret encryption key shared by SSA
NDS	Network address of the stakeholder
Nonce	The lifetime of the TGS_Req
REG_DB	RSU registered database
REQ_Conn	Request connection
Req_Type	Service request type
RRSU _i	RSU agents
SA_Req _L	Service access request, $L = 1, 2, \dots$
SER	Service message
Ser_Auth	Service authentication
SID	Identifier of stakeholder
SSA	Stakeholder service authentication
TGS	Ticket granting server
TGS_Req	Ticket granting server request
TGSID	ID of ticket granting server
TS	Time stamp
V	Server
VID	Identifier of server
VTYPE	Type of stakeholder/vehicular node

Step 1. $S = > SSA:SID||STYPE||VID$.

Step 2. $SAA = > S:Ticket$.

Step 3. $S = > V :SID||Ticket$.

$$Ticket = E(K_v, [SID||NDS||VID]) \quad (1)$$

The above steps provide data service access to registered and nonregistered stakeholders in the transportation environment—the data security framework provides this simple authentication scheme. However, the problem encountered in this simple scheme is that the stakeholder would need a new ticket for every different data service. Therefore, the RSU agents hold a Ticket Granting Server (TGS) in the service subsystem to extend its authentication service needs to access different data services. However, its process of granting is quite similar to the previous simple authentication scheme.

Once per requesting data service access is as follows:

Step 1. $S = > SSA:SID||TGSID$.

Step 2. $SSA = > S:E(K_s, Ticket_{tgs})$.

Once per requesting the type of data service is as follows:

Step 3. $S = > TGS:SID||VID||Ticket_{tgs}$.

Step 4. $TGS = > S:Ticket_v//Ticket$ to access any RSU agent for service.

Once per requesting the type of data service is as follows:

Step 5. $S = > V:SID||Ticket_v$.

$$\begin{aligned} Ticket_{tgs} &= E(K_{tgs}, [SID||NDS||TGSID||Nonce]) \\ Ticket_v &= E(K_{tgs}, [SID||NDS||VID||Nonce]). \end{aligned} \quad (2)$$

The stakeholders can access the data service through a secure authentication scheme upon the application design and usage. The stakeholders can either go for one-time access to the server or access multiple servers for different types of data services by authenticating themselves and acquiring the $Ticket_{tgs}$.

At first, the authentication subsystem of every RSU agent obtains the service access request as a collective input from the stakeholders. On obtaining the service access request, the RSU agent crossverifies with the connectivity subsystem and notifies its connection status by updating its internal connectivity database. The service access requests are passed through the SSA for authentication verification. For example, suppose the requesting stakeholder is a registered member of the transportation environment or a regular authenticated user. In that case, the TGS_Req for the TGS server of every RSU agent is automatically granted full access. On the other hand, if the requesting stakeholder is not a member or unregistered, its network connectivity towards the RSU agents gets disconnected without any sign.

3.2. *Connectivity Subsystem.* In the application scenario, there are cases where vehicular nodes will be connected to their nearest RSU agents without requesting service. Thus, the network connectivity to such vehicular nodes leads to resource depletion. The proposed data security framework categorizes the incoming control beacon messages based on the vehicular node type and its service allocated upon the priority level to avoid such resource consumption. In this research work, we have not considered the authentication time limit for each packet to be served for accessing the data service. However, we have computed the connectivity time limit for each vehicular node connected with the aerial access points. Upon the connectivity time limit, the aerial nodes know where to process the request packet or not. The network connectivity status and vehicle types will prioritize data service for the vehicular nodes as they move along the road pattern. Table 3 illustrates various vehicular nodes that enter/exit the transportation environment.

3.3. *Service Subsystem.* The service subsystem is a functional module for processing and granting the service request to the TGS server. Every RSU agent holds a set of multimedia instructions and a limited number of services to be communicated with the appropriate stakeholders in the transportation environment. Once the authentication subsystem grants the TGS request for access, the TGS server classifies the service request based on their MPLS header labels, as shown in Table 1. The incoming service requests are discriminated with a 5-bit MPLS header label holding 20 possible data service messages that the stakeholders would need to access in time. For real-world applications, the MPLS header labels are defined as 6-bits, and some labels are reserved for research

Input: Transmission of Service Access Request
Output: Transmission of Service Grant TGS_Req or Connection Termination

1. **BEGIN**
2. Initialize SID, VTYPE, TS, Req_Type, SA_Req, SER, TGS_Req, Nonce, RRSUi
3. **Loop**
4. RRSUi \leftarrow **Process:** SA_Req_i (SER₁, SER₂, SER₃... SER_N)
5. Ser_Auth \leftarrow **Extract:** SER (SID, VTYPE, TS, Req_Type)
6. REQ_Conn \leftarrow Ser_Auth: **Compare** (SER, REG_DB)
7. **if** (REQ_Conn == Registered) **then**
8. RRSUi \leftarrow **Return** REQ_Conn (SER, TGS_Req, Nonce)
9. **else**
10. RRSUi \leftarrow **Return** REQ_Conn (SER, Terminate)
11. **end if**
12. **End Loop**
13. **END**

PSEUDOCODE 1: Authentication check for service request from stakeholders.

TABLE 3: Classification types of vehicular nodes.

Sl. No.	Vehicle types (VTYPE)	Vehicle names	Priority level
1	A	Ambulance	1
2	B	Government	2
3	C	Patrols	3
4	D	Subunits	4
5	E	Commercial	5
6	F	Logistics	6
7	G	Bicycles (optional)	7

TABLE 4: Simulation parameters.

Parameters	Value
Simulation environment	2000*2000*500
Number of RSU nodes	5, 10, 15, ...
Number of vehicular nodes	50, 100, 150, ...
Total number of packets	500, 1000, 1500, ...
The velocity of vehicular nodes	2 m/s
The velocity of RSU nodes	5 m/s
Time instant for every T second	60, 120, 180 s
Total simulation time	1000 s

and development. In our proposed idea, we have considered 5 bits of MPLS header label for our research idea. Table 1 illustrates the different MPLS labels used in the transportation environment.

Once the appropriate requested service is fetched from the TGS server, a response message is generated and arranged in the queue for transmission. The scheduling mechanism for the proposed scheme follows a non-preemptive methodology in which the priority packets trigger the queue for accessing the data service. The vehicle classification process crossverifies the connectivity subsystem of which type of stakeholder is requested and the current network status to communicate or relay the response message/service to the neighboring RSU agents in the transportation field. As shown in Table 3, it offers access to and obtains the most recent service updates for various types of requests represented by vehicular nodes.

4. Experimental Setup

A network simulator (NS-3) is used to test the viability of the data security framework. A 3D rectangular waypoint mobility model for RSU and vehicle nodes is used to assess the data security framework's performance. Auxiliary Network Animator (NetAnim) software with a third-party programming language is used to examine, classify, and compute the received data packet packets based on the queuing factors

toward the incoming arrival rates and simulation. Table 4 shows the simulation parameters employed in a three-dimensional transportation simulation.

The data security framework's performance is evaluated in two ways: (1) computation analysis and (2) performance comparison with competing methods. After experimenting with these two features, the data security architecture defines its best-case and worst-case scenarios for use over its vehicular nodes in the transportation environment. In our experiment, we have considered a storage file to which the requested data packets are received. We have used a readline () function to process and provide data service based on the network connectivity level. For example, if there are three vehicular nodes with a network connectivity level of high, then their corresponding node IDs and connectivity levels will be used as pointers to pinpoint the received data packets from the storage file for data service. The information exchanged among aerial and ground nodes are simple bit sequences; hence, the file size is a few kilobytes.

4.1. Computation Analysis. The MPLS label classification and queuing factors are computed to identify the demanding service from the vehicular nodes. Based on the data packet requests, the feasibility of the packet-label classifier subsystem is demonstrated under two test scenarios based on incoming arrival rates, namely, adaptive and static. The incoming request

TABLE 5: Usage of adaptive vs. static arrival rates.

Sl. No.	Arrival rates	Descriptions
1	Adaptive	(i) The arrival rate (λ) varies depending on the stakeholder's request and the network connections (ii) The service rate (μ) is set to a maximum threshold value X (urban or highway) depending on the service demand and environmental conditions (iii) Best-case scenario: RSU nodes can receive a range of 0 to N data packet requests from their stakeholders (iv) Worst-case scenario: a significant resource allocation is required to process the data packet request occasionally
2	Static	(i) The arrival rate (λ) collects a set number of data packet requests from stakeholders (ii) If the RSU node takes longer to process the data packet request, the service rate (μ) becomes dynamic (iii) Best case: to provide adequate data with its stakeholders in processing the request (iv) Worst case: lack of data priority and contention due to multiple stakeholders' requests sent over a fixed communication channel rate

TABLE 6: Queuing analysis of adaptive arrival rate under $\mu_1 = 1000/\text{sec}$.

Vehicular nodes	Queuing factors							Connectivity time (sec)	Vehicle priority
	(λ/sec)	(ρ) (%)	(P_0) (%)	(L_S)	(L_Q)	(W_S) (sec)	(W_Q) (sec)		
V-1	820	0.820	0.180	4.556	3.736	20.00	16.40	1.22	2
V-2	120	0.120	0.880	0.136	0.016	4.09	0.49	8.35	5
V-3	20	0.020	0.980	0.020	0.001	3.67	0.07	52.43	3
V-4	100	0.100	0.900	0.111	0.011	4.00	0.40	10.00	5
V-5	140	0.140	0.860	0.163	0.023	4.19	0.59	7.10	4
V-6	900	0.900	0.100	9.000	8.100	36.00	32.40	1.11	2
V-7	20	0.020	0.980	0.020	0.001	3.67	0.07	52.43	1
V-8	880	0.880	0.120	7.333	6.453	30.00	26.40	1.14	6
V-9	790	0.790	0.210	3.762	2.972	17.14	13.54	1.27	4
V-10	140	0.140	0.860	0.163	0.023	4.19	0.59	7.10	3
Average	393	0.393	0.607	2.5264	2.1334	12.695	9.095	14.21	

TABLE 7: Queuing analysis of adaptive arrival rate under $\mu_2 = 1000/\text{sec}$.

Vehicular nodes	Queuing factors							Connectivity time (sec)	Vehicle priority
	(λ/sec)	(ρ) (%)	(P_0) (%)	(L_S)	(L_Q)	(W_S) (sec)	(W_Q) (sec)		
V-1	800	0.800	0.200	4.000	3.200	18.00	14.40	1.25	6
V-2	450	0.450	0.550	0.818	0.368	6.55	2.95	2.22	5
V-3	200	0.200	0.800	0.250	0.050	4.50	0.90	5.00	3
V-4	110	0.110	0.890	0.124	0.014	4.04	0.44	9.18	4
V-5	440	0.440	0.560	0.786	0.346	6.43	2.83	2.27	2
V-6	850	0.850	0.150	5.667	4.817	24.00	20.40	1.18	1
V-7	110	0.110	0.890	0.124	0.014	4.04	0.44	9.18	6
V-8	900	0.900	0.100	9.000	8.100	36.00	32.40	1.11	1
V-9	700	0.700	0.300	2.333	1.633	12.00	8.40	1.43	5
V-10	440	0.440	0.560	0.786	0.346	6.43	2.83	2.27	4
Average	500	0.5	0.5	2.3888	1.8888	12.199	8.599	3.51	

packets follow the hybrid approach of dynamic and static arrival rates. To differentiate the arrival rates and their performance towards the queuing factors, we have separately measured them in two parts. The descriptive information about using these two test scenarios within the data security architecture is shown in Table 5.

The numerical dataset acquired in measuring the queuing factors from RSU agents under adaptive arrival rates with two different service rates, μ_1 , and μ_2 , is shown in Tables 6 and 7.

The service rate is set to a maximum threshold of μ_1 and μ_2 in the best-case scenario, allowing the RSU agents to receive a range of 0 to $N - 1$ data packet requests from its

TABLE 8: Queuing analysis of static arrival rate under $\lambda_1 = 100/\text{sec}$.

Vehicular nodes	Queuing factors							Connectivity time (sec)	Vehicle priority
	(λ/sec)	(ρ) (%)	(P_0) (%)	(L_S)	(L_Q)	(W_S) (sec)	(W_Q) (sec)		
V-1	100	0.100	0.900	0.111	0.011	4.00	0.40	10	2
V-2	100	0.100	0.900	0.111	0.011	4.00	0.40	10	5
V-3	100	0.100	0.900	0.111	0.011	4.00	0.40	10	3
V-4	100	0.100	0.900	0.111	0.011	4.00	0.40	10	5
V-5	100	0.100	0.900	0.111	0.011	4.00	0.40	10	4
V-6	100	0.100	0.900	0.111	0.011	4.00	0.40	10	2
V-7	100	0.100	0.900	0.111	0.011	4.00	0.40	10	1
V-8	100	0.100	0.900	0.111	0.011	4.00	0.40	10	6
V-9	100	0.100	0.900	0.111	0.011	4.00	0.40	10	4
V-10	100	0.100	0.900	0.111	0.011	4.00	0.40	10	3
Average	100	0.100	0.900	0.111	0.011	4.00	0.40	10	

TABLE 9: Queuing analysis of static arrival rate under $\lambda_2 = 200/\text{sec}$.

Vehicular nodes	Queuing factors							Connectivity time (sec)	Vehicle priority
	(λ/sec)	(ρ) (%)	(P_0) (%)	(L_S)	(L_Q)	(W_S) (sec)	(W_Q) (sec)		
V-1	200	0.100	0.900	0.111	0.011	2.00	0.20	10	2
V-2	200	0.100	0.900	0.111	0.011	2.00	0.20	10	5
V-3	200	0.100	0.900	0.111	0.011	2.00	0.20	10	3
V-4	200	0.100	0.900	0.111	0.011	2.00	0.20	10	5
V-5	200	0.100	0.900	0.111	0.011	2.00	0.20	10	4
V-6	200	0.100	0.900	0.111	0.011	2.00	0.20	10	2
V-7	200	0.100	0.900	0.111	0.011	2.00	0.20	10	1
V-8	200	0.100	0.900	0.111	0.011	2.00	0.20	10	6
V-9	200	0.100	0.900	0.111	0.011	2.00	0.20	10	4
V-10	200	0.100	0.900	0.111	0.011	2.00	0.20	10	3
Average	200	0.100	0.900	0.111	0.011	2.00	0.20	10	

TABLE 10: Comparative analysis techniques.

Sl. No.	Title	Descriptions
1	Misbehavior detection and efficient revocation within VANET [38]	A new framework for the certificate revocation process within VANET is introduced. This process can be activated by the misbehavior detection systems (MDSs) running within vehicles and the misbehavior authority (MA) within the infrastructure, which identifies and excludes misbehaving vehicles to guarantee the long-term functionality of the network.
2	A Certificate less Pairing-Free Authentication Scheme for Unmanned Aerial Vehicle Networks [27]	A pairing-free authentication scheme (CLAS) is proposed for Unmanned Aerial Vehicle Networks (UAVNs) based on the certificateless signature technology. It supports batch verification at both the data aggregator (AGT) and commands center (CMC) sides so that the verification efficiency can be improved greatly.

stakeholders every time interval T_i . When the RSU agents receive the data packet request, we also notice that they compute their vehicle priority checker's average server usage (ρ). Once checked, the associated RSU node can determine whether or not it can offer the desired service to the requested stakeholders on time.

Tables 8 and 9 show the numerical dataset gathered from a single RSU agent to measure the queuing factors of data packet requests under two different arrival rates, λ_1 , and λ_2 , respectively, in contrast to the adaptive arrival rate.

The best-case scenario for this strategy is that the data packet request at the arrival rate is set to a minimum threshold.

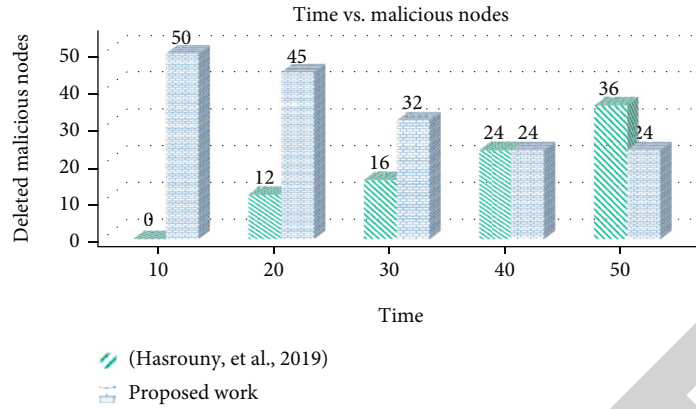


FIGURE 4: Time vs. detected malicious node.

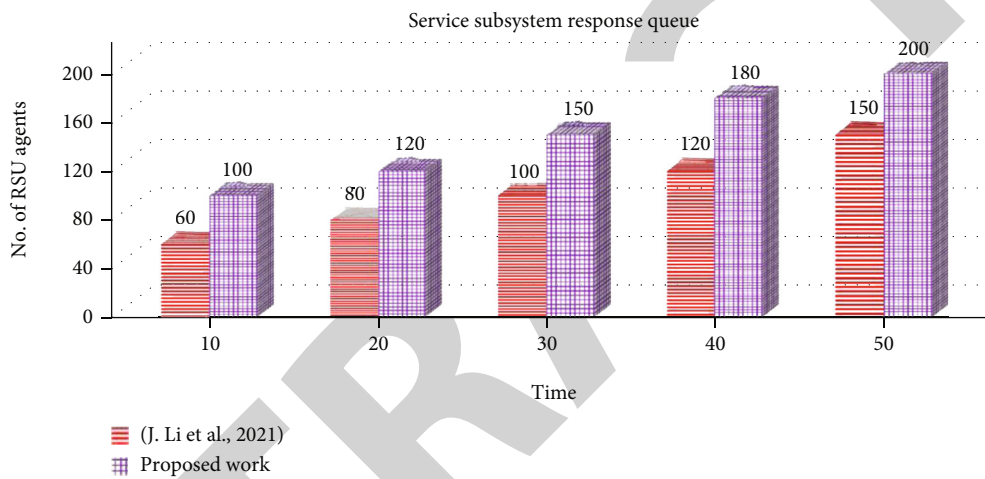


FIGURE 5: Time vs. response queue.

As a result, whether the RSU agent’s network connections are different in processing the desired service, the RSU agents can offer acceptable data to their stakeholders.

4.2. Comparative Analysis. The data security framework has been compared to existing methodologies for two performance indicators, key generation and malicious node detection, at various time instants and the rising number of data packet requests across vehicle nodes. Some of the comparison assessments performed against the proposed model are shown in Table 10.

Figure 4 shows the performance metrics for monitoring the misbehaving nodes in the environment. As time increases, the proposed work identifies the stakeholder behavior according to their idle state and requests unnecessary data queries to the RSU agents. The authentication right is revoked upon these constraints, and the service access link is disconnected.

Figure 5 depicts the service subsystem’s response queue of accepting data service requests from all the stakeholders in the environment. Several RSU agents must process and accumulate the data service requests as time increases. The proposed work requires more RSU agents since the idea of the work is

designed for smart city applications. However, in reality, the deployment of RSU agents in the field will be quite small.

The performance metric “network load” of each vehicular node is calculated against three existing schemes, (1) AIR-RSU framework [1], (2) load balanced routing (LBR), and (3) nearest neighbor routing (NNR) [39]. Each node periodically forwards controls beacon messages to its nearest node to communicate/reach aerial nodes. Figure 6 depicts the network load of individual vehicular nodes at time instants among the existing schemes. Also, it is observed that the network load in LDR and NNR gradually increases as the number of nodes in the transportation environment increases. However, for the AIR-RSU framework and proposed work, the network load in every individual node is equally shared between the vehicular nodes giving an equal chance to communicate and process the information with aerial nodes.

Finally, the level of network density is measured in terms of the percentage of actual connections of a single aerial node or the average of multiple aerial nodes. The network density is defined and given in (source: <https://www.the-vital-edge.com/what-is-network-density>) for the entire network. A single aerial node can establish one or more logical connections depending upon the number of vehicular nodes joining the

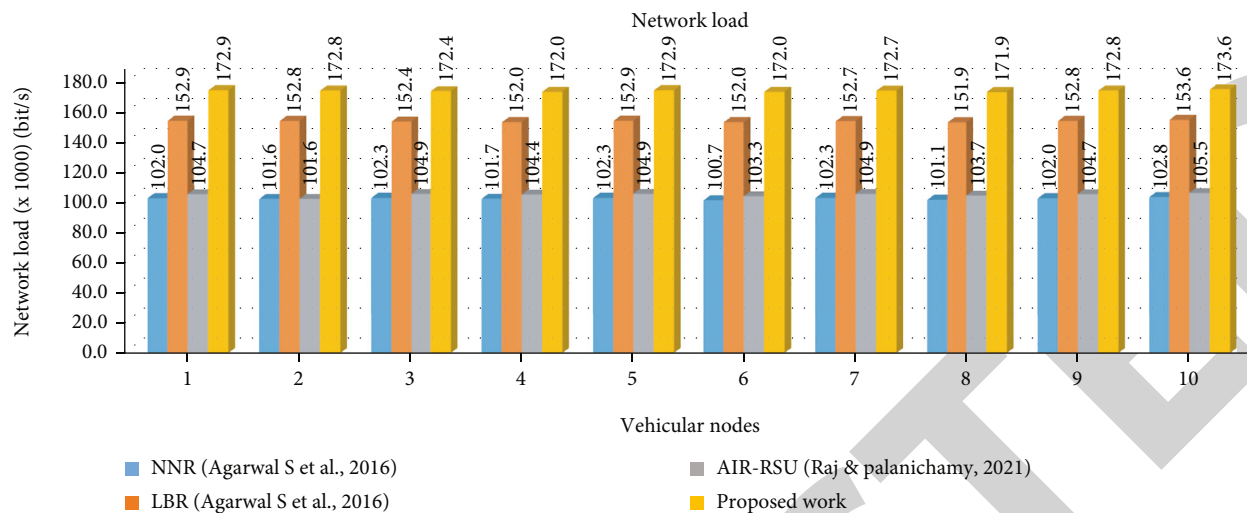


FIGURE 6: Network load of vehicular nodes.

TABLE 11: Network density for single aerial node with range of actual connections.

Nodes	Actual connections (10)	Actual connections (20)	Actual connections (30)	Actual connections (40)	Actual connections (50)
10	0.18	0.36	0.55	0.73	0.91
15	0.08	0.17	0.25	0.33	0.42
20	0.05	0.10	0.14	0.19	0.24
25	0.03	0.06	0.09	0.12	0.15
30	0.02	0.04	0.06	0.09	0.11
35	0.02	0.03	0.05	0.06	0.08
40	0.01	0.02	0.04	0.05	0.06

TABLE 12: Average network density for multiple aerial nodes with range of actual connections.

Nodes	Actual connections (10)	Actual connections (20)	Actual connections (30)	Actual connections (40)	Actual connections (50)
10	0.15	0.31	0.46	0.62	0.77
15	0.09	0.15	0.22	0.30	0.37
20	0.06	0.09	0.13	0.17	0.22
25	0.04	0.06	0.09	0.11	0.14
30	0.03	0.04	0.06	0.08	0.10
35	0.02	0.03	0.05	0.06	0.08
40	0.02	0.02	0.03	0.05	0.06

network within the range. The benefit of providing additional connections for a specific node has a backup connection, multiple hardware communications (i.e., sensors, GPS, tracking camera, and other secondary communications), and infotainment communication. Hence, the more the connection, the higher the network density. In other words, the higher the network density, the better the connectivity.

Tables 11 and 12 represent the network density measure under range of actual connections with a single aerial node and an average of multiple aerial nodes, respectively.

The best case of the proposed application scenario is that as the number of actual connections increases for aerial nodes, the network density among vehicular nodes is almost

entirely connected, and it approaches 1 in a normalized range. However, the worst case of this application scenario is that as the number of vehicular nodes joining the network increases, the network density tends to decrease to a minimum value of 0.01. The overhead of the entire network will increase concerning its bandwidth, latency, and network load as the number of mobile sink nodes and vehicular nodes joining the network increases.

5. Conclusion and Future Works

This paper proposes a new topological design for smart city applications, i.e., a Secure Authentication Relay-Based Urban

Network (S-ARUN) specially constructed for registered transportation stakeholders. These registered stakeholders were connected to the S-ARUN topology hold an in-built data security framework consisting of three subsystems: (1) self-authentication subsystem: the requesting stakeholder must authentic itself by sharing its identity to the source responder before transmitting its actual data service request, (2) vehicle classification subsystem: a priority for the data service request will be given based on the type of stakeholder and request needs, and (3) request accumulator subsystem: every source responder will be maintaining a separate queue to accumulate the data service requests to process and transmit the requested data service to the appropriate stakeholder in a short time. The working principle of S-ARUN follows the Kerberos authentication technique where the stakeholders are connected in a well-secured authentic manner.

Results indicate that the best and worst cases of the proposed work are tested under various queuing analysis arrival rates. On the other hand, the priority of the vehicle towards the vehicular nodes is allocated based on their query request type and physical parameters such as distance, signal strength, and velocity. Moreover, the comparison of the malicious node detection and request accumulator procedure with other schemes is analyzed in detail.

For future works, the data security framework will be tested in a real-time environment, where the benefits and drawbacks of the working process will be clearly defined. Also, we can compare the proposed idea with and without a security mechanism for future enhancement. Also, the idea of using without a security mechanism will show great performance value than working with a security mechanism. But the counterpart to using a security mechanism, the malicious nodes can be identified over time. In addition, the data security framework architecture will be evaluated in a heterogeneous vehicular network to experience the incoming arrival rate of data packets towards the RSU networks at the network layer, data-link layer, and physical layers.

Data Availability

The original data presented in the study are included in the article and queries can be directed to the all authors.

Conflicts of Interest

The authors declare that they have no conflicts of interest.

References

- [1] A. S. A. Raj and Y. Palanichamy, "Packet classification based aerial intelligent relay-road side unit (air-rsu) framework for vehicular ad-hoc networks," *Peer-to-Peer Networking and Applications*, vol. 14, no. 3, pp. 1132–1153, 2021.
- [2] H. H. Jeong, Y. C. Shen, J. P. Jeong, and T. T. Oh, "A comprehensive survey on vehicular networking for safe and efficient driving in smart transportation: a focus on systems, protocols, and applications," *Vehicular Communications*, vol. 31, article 100349, 2021.
- [3] R. S. Shukla, N. Tyagi, A. Gupta, and K. K. Dubey, "A new position based routing algorithm for vehicular ad hoc networks," *Telecommunication Systems*, vol. 75, no. 2, pp. 205–220, 2020.
- [4] Z. C. Liu, L. Xiong, T. Peng, D. Y. Peng, and H. Liang, "A realistic distributed conditional privacy-preserving authentication scheme for vehicular ad hoc networks," *IEEE Access*, vol. 6, pp. 26307–26317, 2018.
- [5] J. Lee, G. Kim, A. K. Das, and Y. Park, "Secure and efficient honey list-based authentication protocol for vehicular ad hoc networks," *IEEE Transactions on Network Science and Engineering*, vol. 8, no. 3, pp. 2412–2425, 2021.
- [6] M. A. Al-Shareeda, M. Anbar, I. H. Hasbullah, and S. Manickam, "Survey of authentication and privacy schemes in vehicular ad hoc networks," *IEEE Sensors Journal*, vol. 21, no. 2, pp. 2422–2433, 2021.
- [7] A. S. A. Raj and Y. Palanichamy, "An aerial intelligent relay-road side unit (AIR-RSU) framework for modern intelligent transportation system," *Peer-to-Peer Networking and Applications*, vol. 13, no. 3, pp. 965–986, 2020.
- [8] S. Lall, A. S. Alfa, and B. T. Maharaj, "The role of queueing theory in the design and analysis of wireless sensor networks: an insight," in *2016 IEEE 14th International Conference on Industrial Informatics (INDIN)*, pp. 1191–1194, Poitiers, France, 2016.
- [9] R. Zaghali, K. Thabatah, and S. Salah, "Towards a smart intersection using traffic load balancing algorithm," in *2017 Computing Conference*, pp. 485–491, London, UK, 2017.
- [10] S. S. Manvi and S. Tangade, "A survey on authentication schemes in VANETs for secured communication," *Vehicular Communications*, vol. 9, pp. 19–30, 2017.
- [11] R. Fotohi, E. Nazemi, and F. Shams Aliee, "An agent-based self-protective method to secure communication between UAVs in unmanned aerial vehicle networks," *Vehicular Communications*, vol. 26, article 100267, 2020.
- [12] S.-J. Horng, S.-F. Tzeng, P.-H. Huang, X. Wang, T. Li, and M. K. Khan, "An efficient certificateless aggregate signature with conditional privacy-preserving for vehicular sensor networks," *Information Sciences*, vol. 317, pp. 48–66, 2015.
- [13] M. Azees, "Reply to comments on dual authentication and key management techniques for secure data transmission in vehicular ad hoc networks," *IEEE Transactions on Intelligent Transportation Systems*, vol. 20, no. 9, pp. 3595–3595, 2019.
- [14] H. Tan, D. Choi, P. Kim, S. Pan, and I. Chung, "Comments on dual authentication and key management techniques for secure data transmission in vehicular ad hoc networks," in *IEEE Transactions on Intelligent Transportation Systems*, vol. 19, no. 7, pp. 2149–2151, 2018.
- [15] M. C. Chuang and J. F. Lee, "TEAM: trust-extended authentication mechanism for vehicular ad hoc networks," *IEEE Systems Journal*, vol. 8, no. 3, pp. 749–758, 2014.
- [16] X. Lin and X. Li, "Achieving efficient cooperative message authentication in vehicular ad hoc networks," *IEEE Transactions on Vehicular Technology*, vol. 62, no. 7, pp. 3339–3348, 2013.
- [17] D. He, S. Zeadally, B. Xu, and X. Huang, "An efficient identity-based conditional privacy-preserving authentication scheme for vehicular ad hoc networks," *IEEE Transactions on Information Forensics and Security*, vol. 10, no. 12, pp. 2681–2691, 2015.
- [18] X. Zhu, S. Jiang, L. Wang, and H. Li, "Efficient privacy-preserving authentication for vehicular ad hoc networks," *IEEE Transactions on Vehicular Technology*, vol. 63, no. 2, pp. 907–919, 2014.

Retraction

Retracted: A 516 μ W, 121.2 dB-SNDR, and 125.1 dB-DR Discrete-Time Sigma-Delta Modulator with a 20 kHz BW

Journal of Sensors

Received 23 January 2024; Accepted 23 January 2024; Published 24 January 2024

Copyright © 2024 Journal of Sensors. This is an open access article distributed under the Creative Commons Attribution License, which permits unrestricted use, distribution, and reproduction in any medium, provided the original work is properly cited.

This article has been retracted by Hindawi following an investigation undertaken by the publisher [1]. This investigation has uncovered evidence of one or more of the following indicators of systematic manipulation of the publication process:

- (1) Discrepancies in scope
- (2) Discrepancies in the description of the research reported
- (3) Discrepancies between the availability of data and the research described
- (4) Inappropriate citations
- (5) Incoherent, meaningless and/or irrelevant content included in the article
- (6) Manipulated or compromised peer review

The presence of these indicators undermines our confidence in the integrity of the article's content and we cannot, therefore, vouch for its reliability. Please note that this notice is intended solely to alert readers that the content of this article is unreliable. We have not investigated whether authors were aware of or involved in the systematic manipulation of the publication process.

Wiley and Hindawi regrets that the usual quality checks did not identify these issues before publication and have since put additional measures in place to safeguard research integrity.

We wish to credit our own Research Integrity and Research Publishing teams and anonymous and named external researchers and research integrity experts for contributing to this investigation.

The corresponding author, as the representative of all authors, has been given the opportunity to register their agreement or disagreement to this retraction. We have kept a record of any response received.

References

- [1] L. Kong, "A 516 μ W, 121.2 dB-SNDR, and 125.1 dB-DR Discrete-Time Sigma-Delta Modulator with a 20 kHz BW," *Journal of Sensors*, vol. 2022, Article ID 9047631, 9 pages, 2022.

Research Article

A 516 μ W, 121.2-dB-SNDR, and 125.1-dB-DR Discrete-Time Sigma-Delta Modulator with a 20kHz BW

Lingwei Kong 

School of Microelectronics, Tianjin University, China

Correspondence should be addressed to Lingwei Kong; konglingwei@tju.edu.cn

Received 1 August 2022; Revised 21 August 2022; Accepted 29 August 2022; Published 16 September 2022

Academic Editor: Sweta Bhattacharya

Copyright © 2022 Lingwei Kong. This is an open access article distributed under the Creative Commons Attribution License, which permits unrestricted use, distribution, and reproduction in any medium, provided the original work is properly cited.

This article proposed a discrete-time single-loop 3rd order 5-bit Sigma-Delta ($\Sigma\Delta$) modulator for the audio applications. In this modulator, a feed forward path is used to relax the design requirement of amplifier, which can reduce integrator's output swing. And a 5-bit asynchronous SAR ADC combined with analog summing is adopted to quantify the summation of feedforward signal and loop filter output, which can significantly reduce power consumption. In addition, chopper stabilization technique is used to alleviate the flicker noise introduced by the first integrator. To eliminate the nonlinearity introduced by multibit quantizer, an improved data weighted average algorithm calibration circuit is proposed. The proposed modulator is implemented in 130 nm technology with a 1.12 mm² core area. Operating at a 2.56MS/s sampling rate, post layout simulation results show that the modulator realizes 121.2-dB SNDR and 125.1-dB DR in a 20 kHz signal bandwidth, it dissipating 516 μ W from 1.5 V supply. It also achieves the energy efficiency, as demonstrated by a Schreier figure of merit (FoM_S) of 197 dB.

1. Introduction

High quality audio devices often require analog-to-digital converters (ADCs) with high resolution and energy efficiency [1]. Among different ADC topologies, $\Sigma\Delta$ ADCs can easily get high signal-to-noise-plus-distortion ratio (SNDR) above 90 dB by noise shaping and oversampling. So, they can avoid the need for complex calibration circuit or stringent matching between constituent elements [2]. Compared with other ADCs, $\Sigma\Delta$ ADCs are more energy-efficient and robust, and dominate the low-bandwidth high-precision signal processing applications. The $\Sigma\Delta$ ADC consists of an analog modulator and a digital filter, while analog modulator is the core circuit of the Sigma-Delta ADC. Among them, the continuous-time (CT) Sigma-Delta modulator (DSM) does not require high build-up speed of the integrator, which is beneficial for low-power design [3]. However, its signal path characteristics (e.g., noise shaping function) are closely related to the process-voltage-temperature (PVT) variation, the modulator has more stringent component matching requirements, and the SNDR is sensitive to clock jitter [4, 5]. The signal

path characteristics of the discrete-time (DT) Sigma-Delta modulator is determined by the capacitance ratio, which has better tolerances for PVT variations and clock jitter. Compared to CT DSM, DT DSM can achieve higher resolution and linearity [6].

In DT DSM design, to improve energy efficiency, the DSM topology by reducing the analog filter input signal amplitude has been proposed. These alleviate the performance demands of SC integrator. One architecture adopts a multi-bit quantizer and input feedforward path [7]. Another is the 0-L multistage noise shaping structure, for which the first stage uses a multi-bit Nyquist ADC and the second stage uses L-order DSM [8]. On the circuit level, using switched capacitors or dynamic amplifier to implement integrators can effectively reduce power consumption [9, 10]. However, the gain of passive integrator is very low and the normal operation of dynamic amplifier often requires strict control conditions. So, the robustness and resistance to process parameter drift of the modulator is weak, and ultimately achieve only moderate resolution [11].

In this paper, we proposed a 5-bit DT DSM with feed forward path. An improved current mirror structure

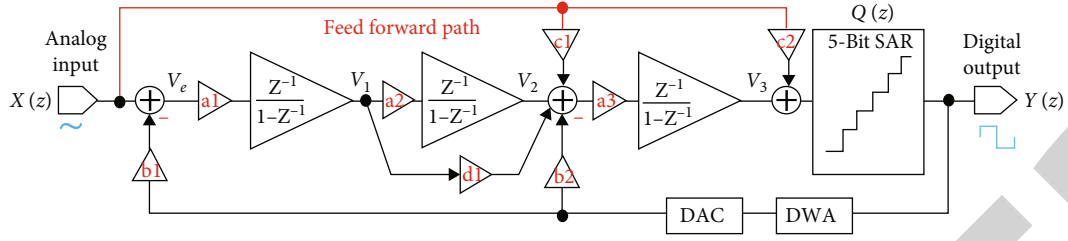


FIGURE 1: Sigma-Delta modulator architecture.

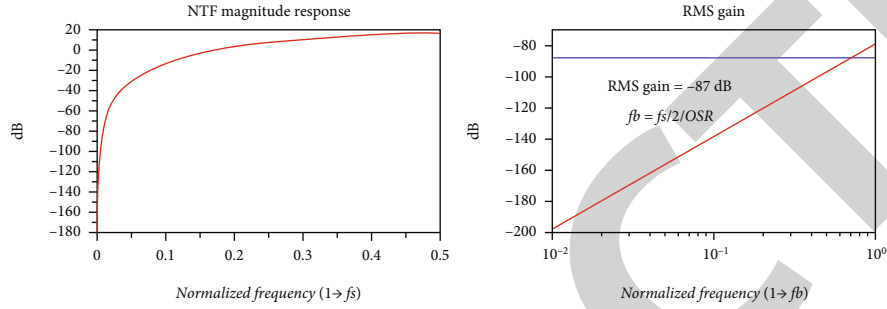


FIGURE 2: NTF spectrum and RMS gain.

amplifier is adopted to drive the large sampling capacitor, and a 5-bit asynchronous successive approximation-register (SAR) ADC combined with analog summing is employed to replace the traditional flash-type quantizer. Integrating the advantages of high accuracy DSM and low power SAR ADC, the proposed modulator achieves high accuracy and energy efficiency. In addition, a low temperature drift bandgap reference is integrated on-chip to further improve system's integration and reliability. The fabricated prototype achieves a dynamic range (DR) of 125.1 dB and a peak SNDR of 121.2 dB in 20-kHz bandwidth and dissipates 516 μ W from 1.5 V supply with core area of 1.12 mm².

This article is organized as follows: the architecture of proposed modulator is briefly described in Section II; the key circuit's implementation details of the DSM are provided in Section III; simulation results are given in Section IV; section V draws the conclusion.

2. Modulator Architecture

Figure 1 shows a block diagram of the proposed $\Sigma\Delta$ modulator. It is a third single-loop architecture with 5-bit SAR quantizer and feed forward path. The output expression of each integrator is calculated as:

$$V_1(z) = -\frac{(z-1)^2}{z^3} Q(z), \quad (1)$$

$$V_2(z) = -\frac{(z-1)}{z^3} Q(z), \quad (2)$$

$$V_3(z) = \left[\frac{(z-1)^3}{z^3} - 1 \right] Q(z). \quad (3)$$

Where $Q(z)$ is quantization error. The feed forward path is linked to multi-bit quantizer's input, causes the input signal to be bypassed. The output of each integrator only contains the quantization error after shaping, which can effectively reduce the integrator output swing. The design requirements of amplifier are relaxed. The modulator's z -domain transfer function is calculated as:

$$\begin{cases} Y(z) = \text{STF}(z) \bullet X(z) + \text{NTF}(z) \bullet Q(z), \\ \text{STF}(z) = 1, \text{NTF}(z) = (1 - z^{-1})^3. \end{cases} \quad (4)$$

Where $\text{NTF}(z)$ denotes noise transfer function and $\text{STF}(z)$ denotes signal transfer function. $\text{STF}(z)$ maintains unit gain within the bandwidth, and $\text{NTF}(z)$ can achieve third-order noise shaping. The magnitude-frequency response and root mean square (RMS) gain of the $\text{NTF}(z)$ within bandwidth is shown in Figure 2. $\text{NTF}(z)$ has an aggressive noise shaping ability. However, its gain factor in pass band is close to 20 dB which results in a smaller input range and poorer stability of the modulator. Therefore, this paper adopts a 5-bit quantizer to reduce quantization noise, and the finer quantization step reduces the voltage and current variations at each time-step [12]. So, the amplifier in modulator requires less energy to respond to signal changes, which can improve the modulator's stability and energy efficiency. To achieve 18-bit resolution, the oversampling ratio (OSR) of modulator is selected as 64.

The digital output is feedback to the analog loop via a 5-bit DAC and the data-weighted averaging (DWA) module is added to feedback loop to eliminate nonidealities from mismatch between the devices of DAC.

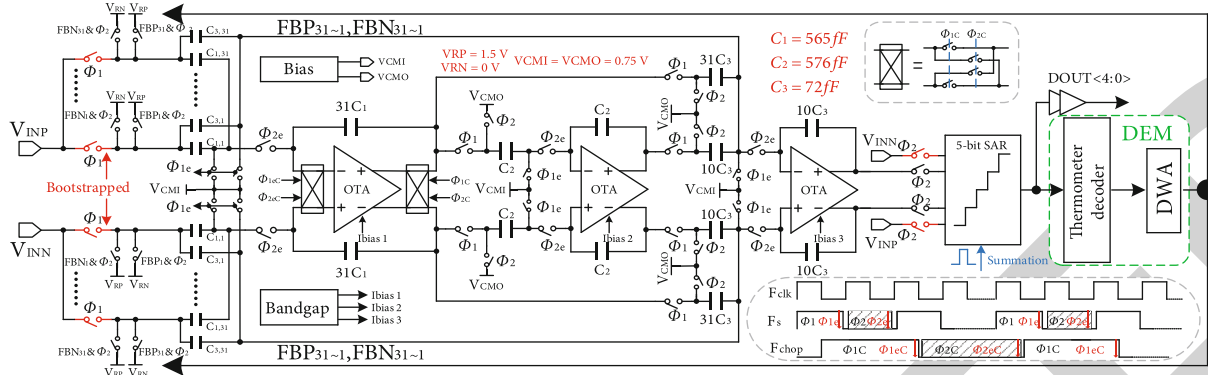


FIGURE 3: Modulator circuit.

3. Circuits Implementation

3.1. Switched Capacitor Scheme. Figure 3 presents the schematic of proposed DT DSM. It contains three integrators, a 5-bit asynchronous SAR incorporated with passive adder, dynamic element matching (DEM), and bandgap reference circuit, etc. The first-stage integrator uses gate voltage bootstrap switch to achieve high-precision signal sampling.

Besides, the 2nd and 3rd integrators employ CMOS switches to reduce the switch on-resistance [13]. At the same time, the 1st and 3rd integrators share a set of switch network, which can reduce circuit design complexity.

Actual switch exists on the on-resistance, and the thermal noise introduced by sampling switch network will severely limit the modulator's signal-to-noise ratio (SNR). Especially in 1st integrator, the thermal noise will be directly superimposed on the input signal, which has the greatest impact on modulator. Therefore, the total sampling capacitance value of 1st integrator is chosen as 17.5 pF for low thermal noise. The 2nd and 3rd integrators contributes less noise, their sampling capacitance is 576 fF and 720 fF, respectively.

To suppress low-frequency flicker noise, the 1st integrator adopts the chopper stabilization technique. As shown in Figure 3, the frequency of chopper is selected as half the sampling frequency, which contributes to achieve a better effect [14]. The feedforward input signal and 3rd integrator's output are added up in SAR quantizer and output a 5-bit digital code. Then, the digital output is decoded to thermometer and sent to DWA module for calibration. Finally, 5-bit DAC complete the loop feedback.

3.2. Bootstrapped Switch. Figure 4 shows the bootstrapped switch, it is critical to $\Sigma\Delta$ modulator's linearity. By adding a constant voltage across the gate-source of the M1, the on-resistance can be a constant while input varying. To eliminate the substrate effect, the sampling switch M1's bulk is often connected to its source. However, when M1 turns off, the input can be coupled to V_{out} through the parasitic capacitance C_{db} between the bulk and drain of M1, which brings errors to the sampling signal. Therefore, in this design, we selectively connect the bulk of M1 to its source and ground, which can solve this problem. The parasitic capacitance C_{ds} exists between the source and drain of M1,

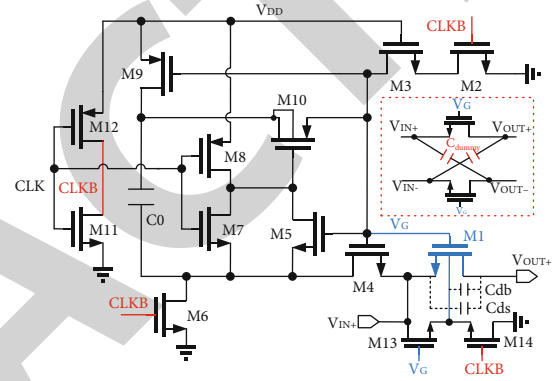


FIGURE 4: Bootstrap switch circuit.

it provides another coupling path. The effect of this path is mitigated by connecting a dummy capacitor between the drain of M1 and the other differential input.

3.3. Amplifier. Figure 5 shows the amplifier in 1st integrator. Since the nonlinearity and noise of later two integrators will be shaped by the 1st integrator, the requirements for gain and noise in 2nd and 3rd integrators can be relaxed appropriately. Thus, the design difficulty lies in the 1st integrator. The finite gain of amplifier will bring pole and gain errors into the integrator, resulting in quantization noise leaks. Therefore, high gain amplifier is necessary to alleviate this effect.

The gain of conventional current-mirror structure is low. In this paper, the current consumption technique is adopted. The cross-coupled $M_{3a,b}$ and $M_{4a,b}$ are connected in parallel to form a local positive feedback, which can improve the DC gain without increasing additional power consumption. Furthermore, we utilize a cascade structure in the output stage to increase the amplifier's output impedance and further boost the open-loop gain. The gain of amplifier can be calculated as:

$$A_V = \frac{B}{1-k} g_{m2a,b} [(r_{o5a,b} + r_{o6a,b}) // (r_{o7a,b} + r_{o8a,b} // r_{o9a,b})] \quad (5)$$

Where B is the current mirror ratio of $M_{4a,b}$ and $M_{5a,b}$, k is the scale factor of $M_{3a,b}$ drawing current from $M_{2a,b}$,

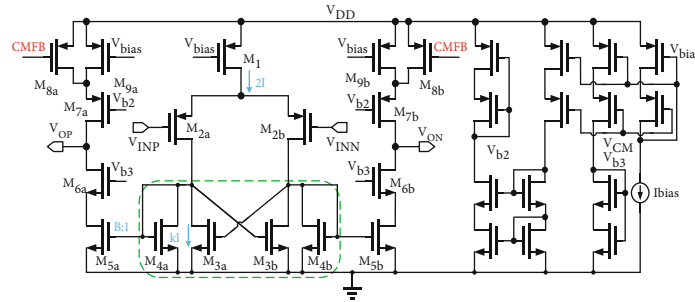
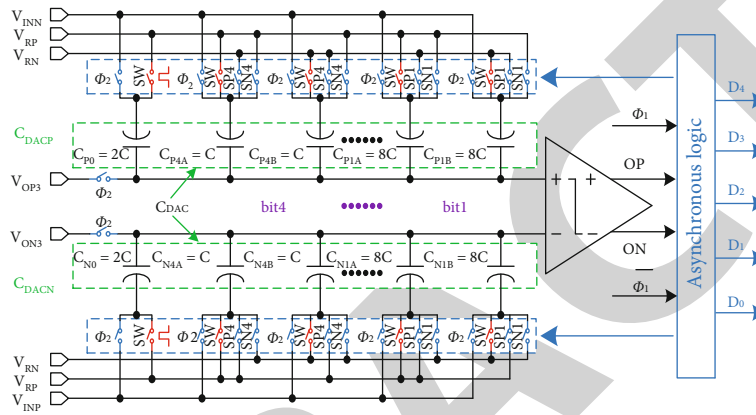
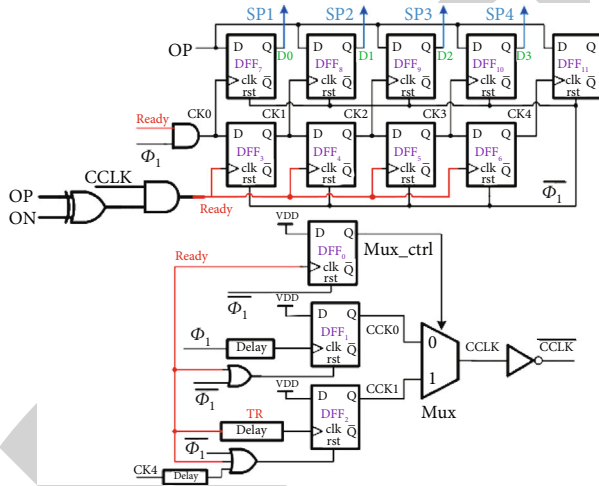


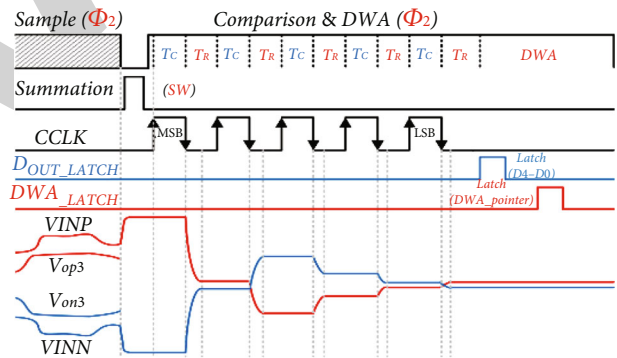
FIGURE 5: Schematic diagram of amplifier.



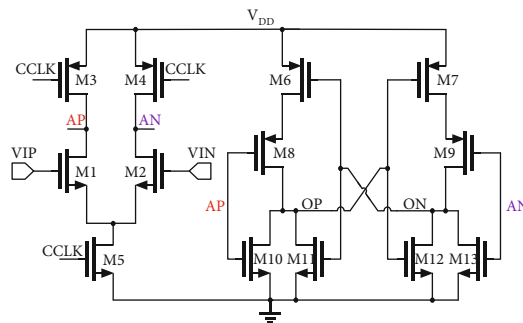
(a) Overall structure



(b) Asynchronous logic



(c) Working timing



(d) Dynamic comparator

FIGURE 6: Asynchronous SAR quantizer.

$g_{m2a,b}$ is the transconductance of $M_{2a,b}$, and $r_{o5a,b}$, $r_{o6a,b}$, $r_{o7a,b}$, $r_{o8a,b}$, and $r_{o9a,b}$ denotes the equivalent impedances of the corresponding transistors. From the above equation, it can be concluded that current consumption technique boosts the gain of amplifier by $1/(1k)$. In addition, the unit gain bandwidth product (GBW) of the amplifier is designed to $10F_S$ to avoid a poor modulator performance due to inadequate setting of integrator.

Most of noise is contributed by 1st integrator. So, it should be carefully designed. Since chopper technology can eliminate flicker noise, the main noise of 1st integrator will be thermal noise [15]. It can be expressed as

$$N_{tot} \approx \frac{2kT}{OSRC_S} \left(1 + \frac{2}{3}\gamma\right). \quad (6)$$

Where γ is the excess noise factor of amplifier. From the above equation, it can be observed that thermal noise can be effectively reduced by increasing C_S . For accuracy, power consumption, and area considerations, the value of C_S in 1st integrator is set to the first stage integrator sampling capacitance value is set to 17.5 pF.

Simulation results show that the amplifier achieves a 72 dB of DC gain, the GBW is 25 MHz and phase margin is 67° at the load capacitance is 18 pF. The amplifier in 2nd and 3rd integrators use the same topology. Since the load capacitance of second stage is small, the transistors' size is 1/5 of the first stage. The third stage needs to drive multi-bit quantizer, the transistors' size of amplifier is 1/3 of the first stage. The V_{bias} , V_{b2} , and V_{b3} is set by biasing circuit, and the current I_{bias} and common mode voltage V_{CM} are generated by bandgap reference circuit.

3.4. Asynchronous Successive Approximation Quantizer. Due to the introduction of feed forward path, an analog summing circuit is required to add the input signal to the 3rd integrator's output and send it to multi-bit quantizer completing the quantization. The asynchronous SAR quantizer proposed in this paper is shown in Figure 6(a). It consists of asynchronous logic, a dynamic comparator and a switch capacitors array. By designing appropriate operating timings and switching networks, the analog summing is embedded into the capacitor array to reduce the complexity and area of schematic. A common-mode voltage-stabilized capacitor switching strategy [16] is used by dividing the capacitance of bit 1-bit 4 into two equal parts and ensuring that the common-mode level at the comparator input is stable. Compared with conventional flash-type quantizers, asynchronous logic controlling the comparison process can avoid the use of high-frequency clocks, and single comparator operation can improve the modulator's tolerance to offset. Combining with the low-power advantage of SAR ADC, the resolution and energy efficiency of the modulator can be improved effectively.

During Φ_2 , the SAR quantizer is reset and the 3rd integrator outputs V_{OP3} , V_{ON3} , and the input signals V_{INN} and V_{INP} are sampled at the pole plates of C_{DACP} and C_{DACN} . At the end of Φ_2 , the charges stored at C_{DACP} and C_{DACN} are $(V_{OP3} - V_{INN}) C_{DACP}$ and $(V_{ON3} - V_{INP}) C_{DACN}$, respectively. During the time between Φ_1 and Φ_2 , the clock gener-

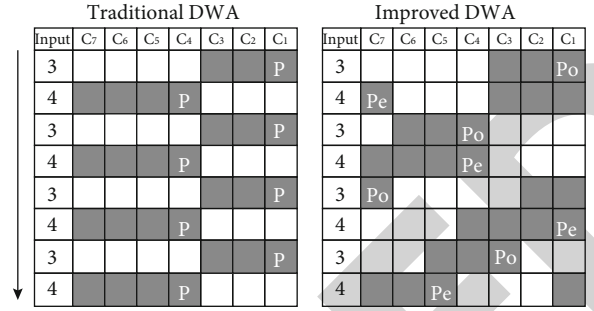


FIGURE 7: DWA algorithm diagram.

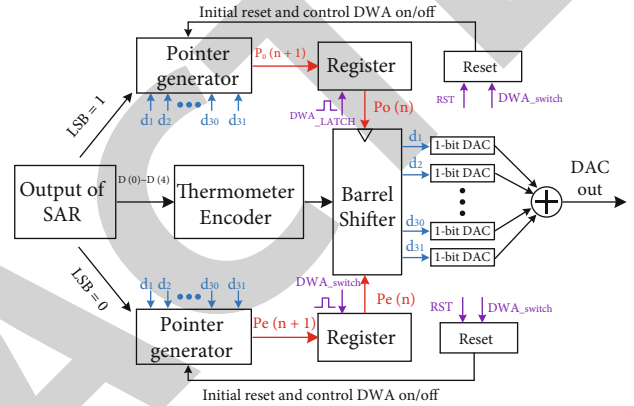


FIGURE 8: DEM module.

ation circuit generates a narrow pulse SW, as shown in Figure 6(c), forcing the bottom plate of capacitor to connect with V_{RP} and V_{RN} , and completes the summation process operation within the pulse duration. According to the charge conservation principle, the voltage difference between the upper half capacitors of the C_{DAC} can be calculated as:

$$\Delta V_{CDAC} = (V_{OP3} - V_{ON3}) + (V_{INP} - V_{INN}). \quad (7)$$

After completing the analog summation, the asynchronous logic controls the SAR to quantize and serially output the 5-bit digital code, the asynchronous logic circuit is shown in Figure 6(b). The comparator is triggered by the rising edge of Φ_1 , and generates comparison result during T_C time. Comparison completion signal ready is generated by XOR gate with comparison results as input. The comparator output result is stored in $DFF_7 \sim DFF_{11}$, which forces the corresponding capacitors' bottom plates connect to V_{RP} or V_{RN} . During T_R time, the charge redistribution of C_{DAC} is completed. Thus, the voltage of capacitor array's upper plate is changed. The comparator clock CCLK generated by asynchronous logic and the quantization procedure are shown in Figure 6(c). The voltage difference between the upper plates of C_{DAC} after each comparison is completed can be expressed as:

$$\Delta V_{CDAC} = (V_{OP3} - V_{ON3}) + (V_{INP} - V_{INN}) - \frac{1}{32} \left(\sum 2^j \times D_j \right) \times (V_{RP} - V_{RN}). \quad (8)$$

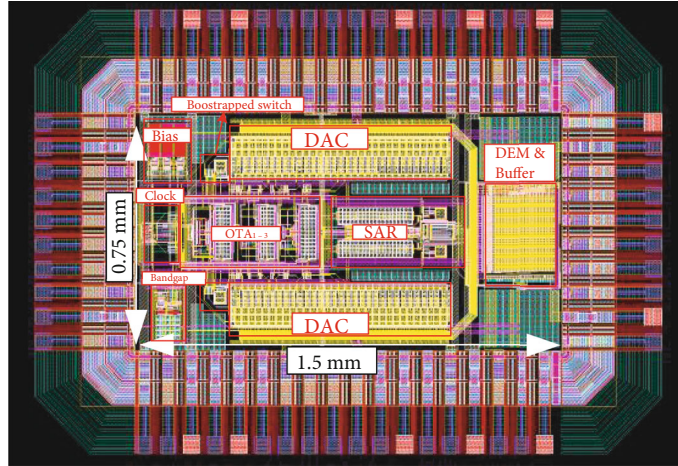


FIGURE 9: Modulator layout.

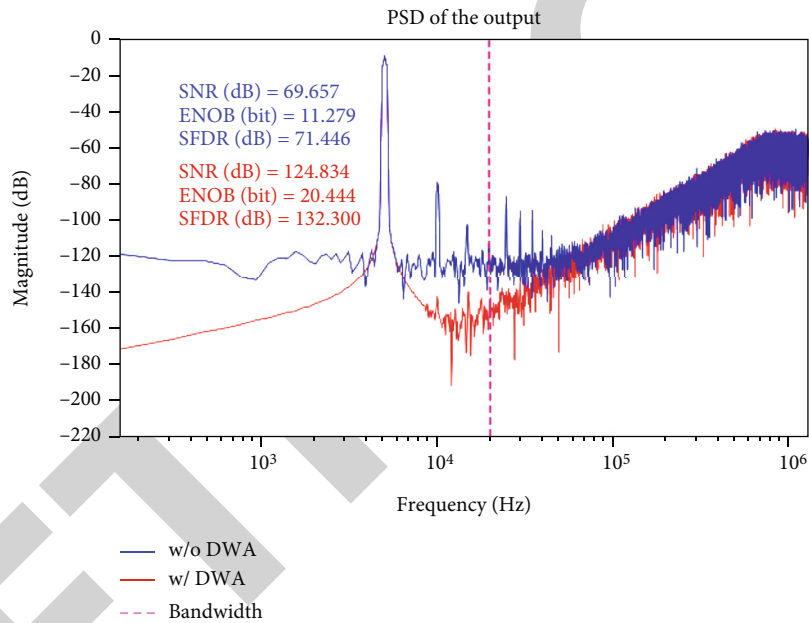


FIGURE 10: Output spectrum with DWA (red line) and without DWA (blue line).

In addition, the time of T_C and T_R can be adjusted by delay module. The comparator output result D_i ($i = 0, 1, 2, 3$, and 4) is latched into the post-stage register triggered by the D_{OUT_LATCH} signal.

Figure 6(d) shows the comparator schematic in proposed asynchronous SAR quantizer. It contains a preamplifier and a latch, and adopts double-tailed fully dynamic latching structure to avoid the existence of static current. When $CCLK$ is low, the comparator is stopped, A_p and A_n are charged to VDD , and O_p and O_n are reset to GND ; when $CCLK$ is high, the charge stored in the parasitic capacitors of $M1$ to $M4$ is leaked by $M5$, which generates different current determined by the input voltage. This results in different rates of voltage drop at AP and AN nodes, thus generating a voltage difference $\Delta V_{AP,AN}$ related to the input voltage. $\Delta V_{AP,AN}$ is amplified by a positive feedback loop formed by $M8 \sim M13$ and create a comparison result. In

addition, the interstage consisting of $M10/M13$ and $M8/M9$ provides an extra shield between the input and output to reduce kickback noise effectively.

3.5. Dem. The main weakness of the multi-bit quantization modulator is that it is sensitive to the nonlinear error of DAC, which comes from the mismatch among the internal capacitor arrays. Therefore, a dual-pointer DWA calibration circuit is proposed in this paper to eliminate mismatch error and improve the linearity of the DAC. Depending on the parity of quantization results, different independent pointers are used to control the barrel shifter operation.

Figure 7 represents the principle of the conventional DWA and the improved DWA algorithm in a 3-bit DAC; white cells denote unused and dark cells denote the DAC cells being selected for use. P is the pointer of conventional DWA, P_o is the pointer when the input value is odd and

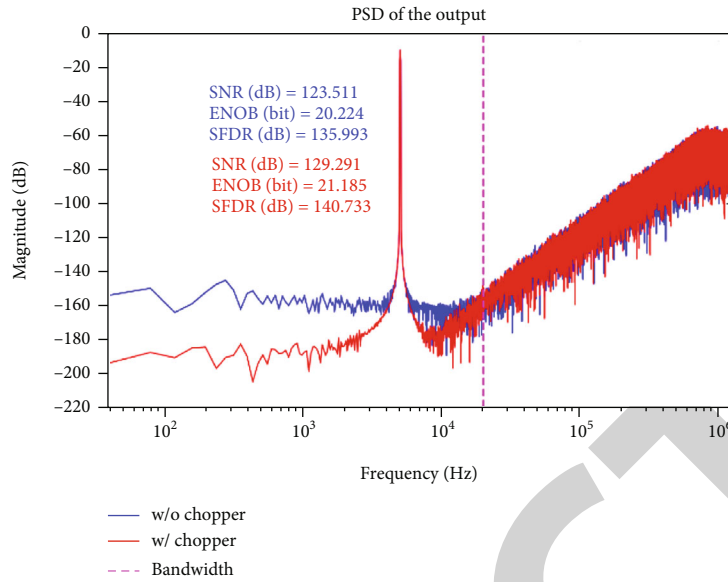


FIGURE 11: Output spectrum with chopper stabilization (red line) and without chopper stabilization (blue line).

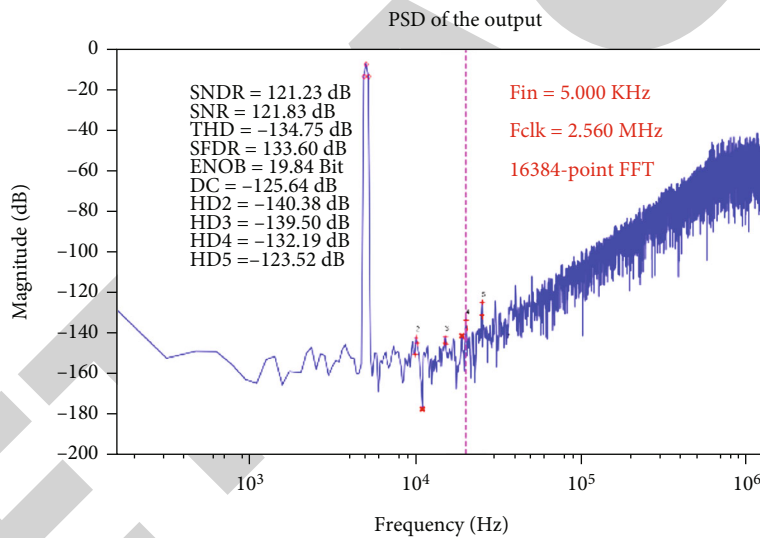


FIGURE 12: Post-layout simulated output spectrum.

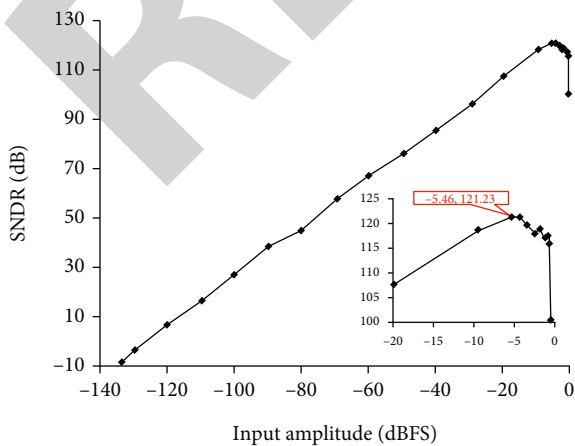


FIGURE 13: SNDR versus input amplitude.

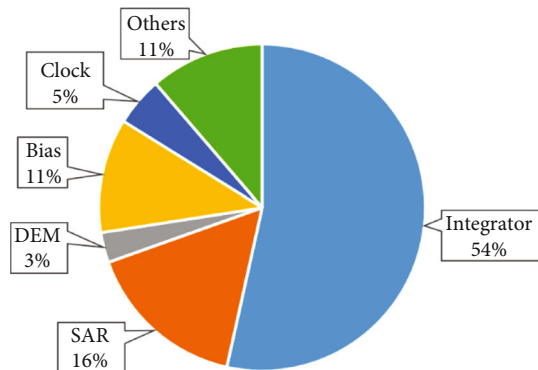


FIGURE 14: Power breakdown.

TABLE 1: Performance summary and comparison.

	Technology [nm]	Supply [V]	BW [kHz]	F_s [MHz]	SNDR _{Peak} [dB]	DR [dB]	Power [mW]	FoM _S ⁽³⁾ [dB]	Area _{Core} [mm ²]
[2]	180	1.8	24	6.144	98.5	103.6	0.28	177.8	1.33
[3]	180	1.8	10	6	105	106.5	1.17	174.3	1.81
[9] ⁽¹⁾	65	1.1	20	10	92.06	111.4	0.086	176	—
[12]	130	1.2	20	3.072	101.4	108.9	3.5	173.3	1.5
[15] ⁽²⁾	180	3.3	24	3.072	120	—	20	180.8	2.3
This work ⁽²⁾	130	1.5	20	2.56	121.2	125.1	0.516	197.1	1.12

⁽¹⁾ Schematic simulation results; ⁽²⁾ Post layout simulation results; Others are from measurements; ⁽³⁾ FoM_S = SNDR_{Peak} + 10 log(BW/power).

Pe is the pointer when the input value is even. It can be seen that although the input signal value appears regularly, the improved DWA algorithm does not cause the algorithm to fail due to regular selection of DAC units.

The DEM module is shown in Figure 8, including the thermometer decoder, pointer generator, barrel shifter, and reset circuit. The thermometer decoder converts the 5-bit binary code from SAR quantizer into 31-bit thermometer code; the pointer generator is the core logic circuit of the DWA algorithm, which generates the corresponding pointer according to the LSB value of digital output and determines the starting bit of the next barrel shifter operation. The reset module plays a protective role to avoid the pointer generator circuit being unable to recover itself due to interference. Besides, it performs initial reset of the pointer generator and controls DWA on and off. The barrel shifter is the execution circuit that cyclically shifts the input thermometer codes according to the starting bit determined by the pointer, and the shifted thermometer codes select the corresponding DAC units to complete feedback.

4. Simulation Results

The proposed modulator is fabricated in 130 nm 1P7M CMOS process. Figure 9 shows the modulator's layout. The core area is $1.5 \times 0.75 \text{ mm}^2$. Add 0.5% random mismatch to DAC capacitor array. Figure 10 shows the simulated output spectrum when the DWA is on and off. The mismatch among capacitors in the DAC causes serious harmonic distortion, which lowers modulator's SNDR, but alleviating its impact via turning on DWA. As illustrated in Figure 11, chopper stabilization technology can suppress flicker noise in low-frequency, which improves the SNR within the bandwidth. The post layout simulated output spectrum is presented in Figure 12. The peak SNDR and SNR are 121.2 dB and 121.8 dB, respectively, as the input is a 5 kHz, -5.5 dBFS sinusoidal signal. Figure 13 shows the post layout simulated SNDR versus input signal amplitude. The prototype modulator realizes a DR of 125.1 dB in 20 kHz bandwidth. Operating at a 2.56MS/s sampling rate, the modulator dissipates $516 \mu\text{W}$ under a 1.5 V supply. The breakdown of power consumption is presented in Figure 14.

The prototype modulator's performance is summarized and compared in Table 1. Although the performance parameters of the modulator acquired from the post-layout simu-

lation results, its Schreier figure of merits (FoM_S) is up to 197 dB with efficient power consumption. As can be seen from Table 1, the prototype modulator achieves higher SNDR in the same bandwidth compared with other modulators. With different signal bandwidths, the prototype modulator has obvious advantages in energy efficiency, achieving an excellent balance between cost and performance.

5. Conclusion

In this article, a high-SNDR low-power audio DT DSM fabricated in a 130 nm CMOS process is presented. The modulator employs third single loop with 5-bit SAR topology. Feed forward path is introduced to reducing integrator's swing. Adopting 5-bit asynchronous SAR ADC can avoid the use of high-frequency clocks, which can significantly reduce power and area consumption. Besides, an improved data weighted average algorithm calibration circuit is proposed to eliminate harmonic distortion. The post layout simulation results show that the proposed DT DSM achieves a peak SNDR of 121.2 dB with a 20 kHz bandwidth. It dissipates $516 \mu\text{W}$ under a 1.5 V supply.

Data Availability

The experimental data used to support the findings of this study are available from the corresponding author upon request.

Conflicts of Interest

The author declared that he has no conflicts of interest regarding this work.

References

- [1] J. H. Han, K. I. Cho, H. J. Kim, J. H. Boo, J. S. Kim, and G. C. Ahn, "A 96dB dynamic range 2kHz bandwidth 2nd order delta-sigma modulator using modified feed-forward architecture with delayed feedback," *IEEE Transactions on Circuits and Systems II: Express Briefs*, vol. 68, no. 5, pp. 1645–1649, 2021.
- [2] S. Billa, A. Sukumaran, and S. Pavan, "Analysis and design of continuous-time delta-sigma converters incorporating chopping," *IEEE Journal of Solid-State Circuits*, vol. 52, no. 9, pp. 2350–2361, 2017.

Retraction

Retracted: A 146-dB-Ohm Gain 14-pARMS Noise Patch-Clamp Amplifier for Whole-Cell Ion Current Detection

Journal of Sensors

Received 23 January 2024; Accepted 23 January 2024; Published 24 January 2024

Copyright © 2024 Journal of Sensors. This is an open access article distributed under the Creative Commons Attribution License, which permits unrestricted use, distribution, and reproduction in any medium, provided the original work is properly cited.

This article has been retracted by Hindawi following an investigation undertaken by the publisher [1]. This investigation has uncovered evidence of one or more of the following indicators of systematic manipulation of the publication process:

- (1) Discrepancies in scope
- (2) Discrepancies in the description of the research reported
- (3) Discrepancies between the availability of data and the research described
- (4) Inappropriate citations
- (5) Incoherent, meaningless and/or irrelevant content included in the article
- (6) Manipulated or compromised peer review

The presence of these indicators undermines our confidence in the integrity of the article's content and we cannot, therefore, vouch for its reliability. Please note that this notice is intended solely to alert readers that the content of this article is unreliable. We have not investigated whether authors were aware of or involved in the systematic manipulation of the publication process.

Wiley and Hindawi regrets that the usual quality checks did not identify these issues before publication and have since put additional measures in place to safeguard research integrity.

We wish to credit our own Research Integrity and Research Publishing teams and anonymous and named external researchers and research integrity experts for contributing to this investigation.

The corresponding author, as the representative of all authors, has been given the opportunity to register their agreement or disagreement to this retraction. We have kept a record of any response received.

References

- [1] W. Pan, "A 146-dB-Ohm Gain 14-pARMS Noise Patch-Clamp Amplifier for Whole-Cell Ion Current Detection." *Journal of Sensors*, vol. 2022, Article ID 8469476, 14 pages, 2022.

Research Article

A 146-dB-Ohm Gain 14-pARMS Noise Patch-Clamp Amplifier for Whole-Cell Ion Current Detection

Wenbin Pan 

School of Microelectronics, Tianjin University, Tianjin, China 300072

Correspondence should be addressed to Wenbin Pan; wb_pan@tju.edu.cn

Received 1 August 2022; Revised 21 August 2022; Accepted 25 August 2022; Published 9 September 2022

Academic Editor: Sweta Bhattacharya

Copyright © 2022 Wenbin Pan. This is an open access article distributed under the Creative Commons Attribution License, which permits unrestricted use, distribution, and reproduction in any medium, provided the original work is properly cited.

The membrane clamp technique is an important tool to reflect the electrophysiological characteristics of cells by recording the ionic currents of cellular channels. Embedded systems work in systems designed for specific user groups and are used to implement specific functions. The membrane clamp amplifier built with embedded technology has the advantages of miniaturization, specialization, low power consumption, high integration, high resource utilization, and a long life cycle, which can avoid the inconvenience to developers and experimenters due to the update of general-purpose computer software and hardware. In this paper, a patch-clamp amplifier (PCA) based on a transimpedance amplifier (TIA) is proposed, which includes a glass microelectrode series resistance/capacitance compensation circuit and feedback resistor parasitic capacitance compensation. The prototype is designed using 180 nm CMOS technology and occupies an area of $720 \mu\text{m} \times 630 \mu\text{m}$. The prototype achieves a transimpedance gain of 145.6 dB-Ohm, a -3 dB bandwidth greater than 15 kHz, and an input reference noise current of 13.98 pARMS. Experimental results show that the proposed PCA is capable of compensating up to 30 pF of electrode capacitance and up to 10 M Ω for 86% of the series resistance, respectively. In addition, when the feedback resistor parasitic capacitance compensation circuit is enabled, the overshoot phenomenon disappears, overcoming the shortcomings of the conventional diaphragm clamp amplifier current clamp and maintaining the original key performance.

1. Introduction

The diaphragm clamp amplifier design started in the late 1970s and gradually became a core instrument for electrophysiological measurements after the 1980s. It was originally designed to detect weak picoampere (10-12 A) currents in individual ion channels in conjunction with a high-resistance blocking technique [1], and thus, its core is a highly sensitive, ultralow noise I-V converter [2]. It was initially only suitable for voltage clamp experiments, and to be able to be used for current clamp experiments, a conventional diaphragm clamp amplifier A negative feedback method is used to make the cell membrane current track the current stimulus signal. Since it is not a direct current clamp and voltage measurement required for current clamp experiments, the negative feedback current clamp design shows inherent drawbacks, mainly in the form of current

clamp errors and distortion and aberration of the membrane potential measurement signal. In 1996 and 1998, Magistretti made a detailed analysis of this problem [3, 4] and proposed to consider the diaphragm clamp amplifier as a “black box” to estimate the system type and response of the diaphragm clamp amplifier through the control and response of the external circuit model. The system type and parameters of the diaphragm clamp amplifier are estimated by the control and response of the external circuit model. Based on this estimation, various types of errors generated by the current clamp of the conventional diaphragm clamp amplifier are derived. He proposed an improvement scheme [5], but no improvement results have been reported since then. The work done in this paper, on the other hand, analyzes the root causes of distortion in the current clamp and membrane potential measurement response of the conventional diaphragm clamp from the internal structure of the conven-

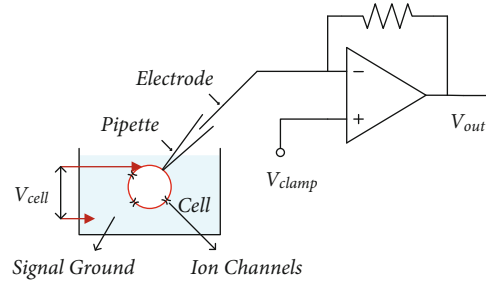


FIGURE 1: Conventional whole-cell recording system.

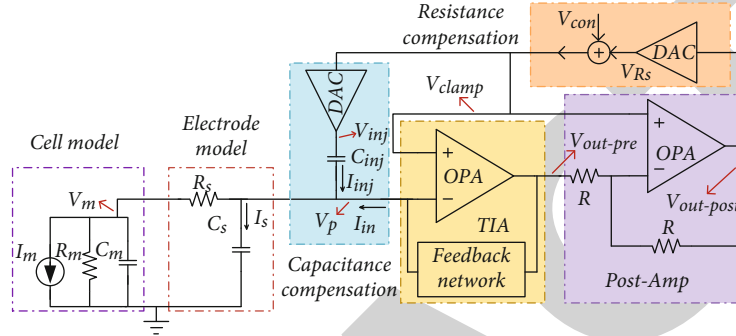


FIGURE 2: The top architecture of the proposed PCA.

tional diaphragm clamp amplifier, making the necessary additions and corrections to Magistretti's analysis.

Membrane clamp is an effective method for measuring cellular ionic currents [6]. This method is widely used in physiology to study the physiological functions of cells by recording the current changes of ion channels in the cell membrane [7]. The ion currents of single channels are typically on the order of pA; while in whole-cell recordings, the current is the sum of the currents of all ion channels on the cell membrane with an amplitude of several nA. [8]. This requires a low-noise amplifier to sense such weak ion currents, which can also be used for nanopore sensing applications [9]. As shown in Figure 1, in whole-cell recording, by clamping the potential difference between the cell membrane and the signal ground, ionic currents from the cellular ion channels in the bath flow through a glass microelectrode and then into the detection circuit. To convert the current into a voltage for further processing, the current-to-voltage conversion can usually be achieved with the help of a transimpedance amplifier (TIA) [10].

In whole-cell recording, the amplitude of the current is a few nanoamps over a bandwidth of 10 kHz, and the TIA enables continuous-time recording with a TIA resistance value in the range of a few M Ω s [11, 12]. In conventional CMOS processes, high resistances occupy a large area of the layout and generate significantly large parasitic capacitances, which affect the stability of the circuit [13]. Typical values of electrode resistance are in the range of 5-20 M Ω . During the measurement, the current flowing through the electrode causes a voltage drop across this resistance, which causes the intracellular voltage V_m to deviate from the ideal clamp voltage V_{clamp} [14, 15]. Also, the electrodes have a

TABLE 1: Parameters of whole-cell recording PCA.

Membrane resistance R_m (typical)	>G Ω
Membrane capacitance C_m (typical)	10-100 pF
Series resistance of electrode R_s (typical)	5-20 M Ω
Parasitic capacitance of electrode C_s (typical)	5-15 pF
Membrane current I_m	A few nA
Feedback resistance R_t	20 M Ω
Feedback capacitance C_f	500 fF

large parasitic capacitance, which will have a significant impact on the stability of the circuit.

This paper is organized as follows: Section 2 first briefly describes the overall structure of the proposed patch-clamp amplifier (PCA), then the circuit details of the developed feedback resistor parasitic capacitance compensation and glass microelectrode series resistor/capacitance compensation are presented, and this section also analyzes the noise model and operational amplifier of the PCA; section 3 shows the experimental results of the whole PCA, followed by a summary in Section 4. The conclusions are summarized in Section 4.

2. PCA

We propose a PCA with three compensation functions for whole-cell ion current detection. As shown in Figure 2, our PCA consists of four subblocks: (1) TIA; (2) postamplifier for converting ion currents to voltage; (3) capacitive compensation for feedback resistors; and (4) resistive/capacitive

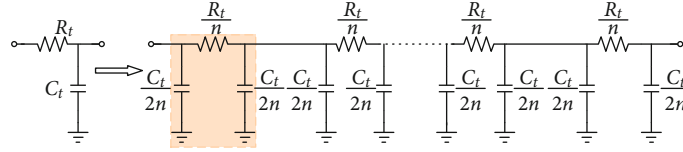


FIGURE 3: Distributed parasitic model.

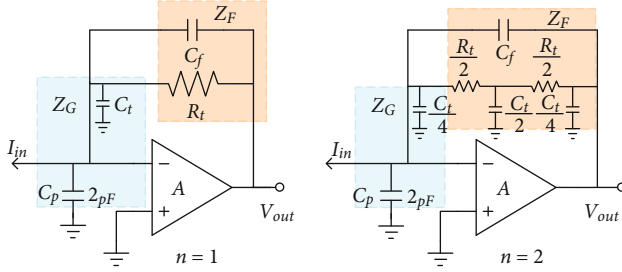


FIGURE 4: TIA with different parasitic models.

compensation circuit for electrodes. Table 1 shows the typical parameters of the whole-cell recording experiment and the design parameters of the PCA.

The TIA as the first stage performs voltage clamping to the commanded voltage (V_{clamp}) concerning the experimental ground. When a control voltage (V_{con}) is applied externally, the ionic current generated by the cell is converted to an output voltage by both the TIA and the postamplifier. The compensation circuits are used to compensate the parasitic resistor and capacitor of the microelectrode, and the DAC (digital-to-analog converter) in the compensation circuit is adopted to adjust the compensation ratio. The digital input of the DAC is provided by an external FPGA (field programmable gate array).

2.1. Parasitic Capacitance Compensation of the Feedback Resistor. As shown in Figures 3 and 4, the total feedback resistance (R_t) and parasitic capacitance (C_t) are divided into n segments, because this aggregation resistance will occupy a very large chip area for a CMOS process and will introduce large parasitic capacitance due to the presence of parasitic capacitance between the bottom aggregation layer and the substrate. The total parasitic capacitance (C_t) is estimated to reach ~ 8.24 pF. To convert the weak ion current to an output voltage in the mV scale, the resistor in the TIA is chosen to be 20 M Ω . In conventional schemes, a lumped capacitor is assumed to model the parasitic effect and is connected in parallel with the input of the TIA; however, when accurate frequency and transient simulation is required, using this simplified lumped model is not sufficient; therefore, we consider a distributed parasitic model.

To validate the necessity of the distributed parasitic model, the closed-loop transfer function of the TIA with the traditional parasitic model and the distributed parasitic model is analyzed and calculated with $n=1$ and $n=2$, respectively. The corresponding circuits are shown in Figure 4, C_p is the parasitic capacitance of the amplifier.

For simplicity, the gain (A) of the op-amp is regarded as a constant. The transfer function of the TIA is given by

$$\frac{V_{out}}{I_{in}} = \frac{-ZF}{1 + (1 + ZF/ZG)/A}, \quad (1)$$

With $n=1$, the transfer function can be expressed as

$$\frac{V_{out}}{I_{in}} (n=1) = \frac{-R_t \times A}{A + 1 + R_t [C_f + (C_t + C_p) + AC_f]s}. \quad (2)$$

With $n=2$, the transfer function can be expressed as

$$\frac{V_{out}}{I_{in}} (n=2) = \frac{-(R_t \times A + (1/8)R_t^2 C_t \times A \times s)}{(A + 1) + R_t \beta s + (1/8)R_t^2 C_t \beta s^2}, \quad (3)$$

$$\beta = (A + 1)C_f + \frac{C_t}{4} + C_p, \quad (4)$$

$$\zeta = \sqrt{\frac{2\beta}{(A + 1)C_t}} = \sqrt{\frac{2(A + 1)C_f + C_t/2 + 2C_p}{(A + 1)C_t}}. \quad (5)$$

When setting $n=2$, the damping factor ζ in (5) drops below unity; thus, the transfer curve has the potential to present overshoot which is not depicted by Equation (1). Figure 5 shows the closed-loop gain of the transfer function of the TIA with different values of n . Once n is 1, the amplitude is nearly flat within the interested frequency range. Upon setting $n=2$, the gain overshoot begins to appear. The value of C_f must be increased to stabilize the TIA. The influence of distributed parasitic model on the stability of the system will be aggravated. The larger the n value is, the worse the stability of the system will be. Therefore, a compensation method should be adopted to ensure circuit stability under the premise of maintaining bandwidth. For 20 M Ω polyresistors, when $n \geq 4$, the simulation results of the distributed parasitic model are relatively close. Therefore, $n=4$ is fixed in this work to represent the parasitic model with large resistance.

As shown in Figure 6, the large feedback resistor is divided into 4 segments, and in the layout stage, different N -well regions are drawn under these segments. A simple source follower (SF) circuit is used for the compensation of each segment, where the input and output of the SF are connected between the subresistor node and its N -well node [16, 17]. Since in the conventional circuit, the polysilicon resistor is placed directly on top of the p -substrate, and since the p -substrate must be connected at the lowest potential, the polysilicon resistor is placed on top of the N -well, which is

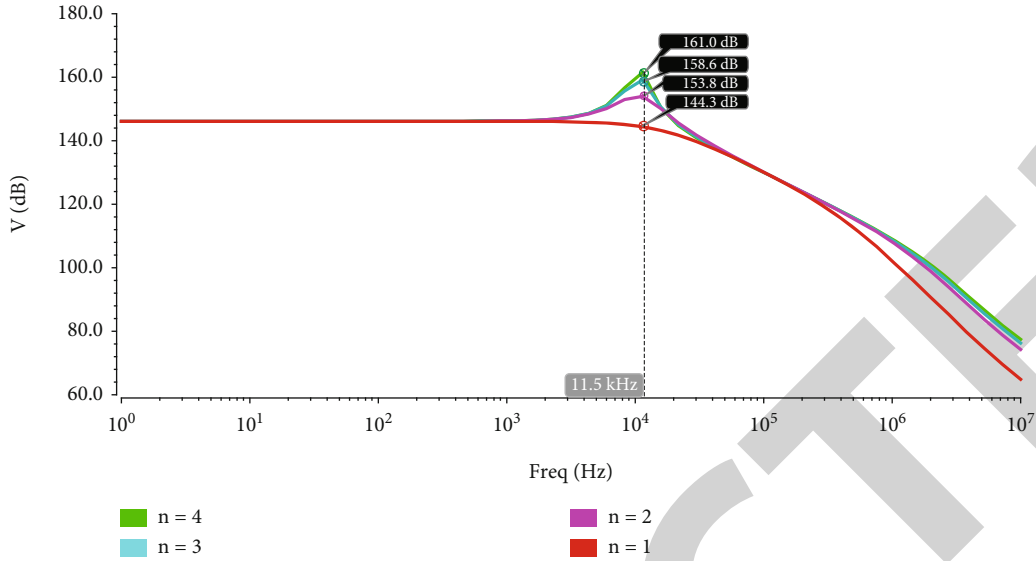


FIGURE 5: Simulation result of the TIA in the variation of the number of the n stages.

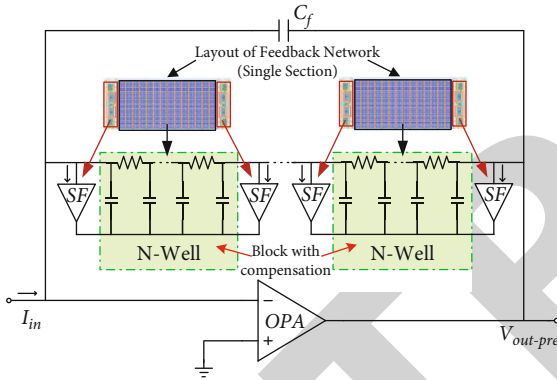


FIGURE 6: Distributed parasitic model of the TIA with compensation technique.

the bottom plate of the parasitic capacitor, to facilitate the voltage adjustment in this design. The poles generated by the feedback resistor and its parasitic capacitor will be shifted to a higher frequency, thus making the circuit more stable. Therefore, the voltage of the N -well can follow the voltage of the subresistor, the charging and discharging effect of the parasitic capacitor disappears, and the parasitic capacitance in the circuit can go to zero.

The source follower can be enabled or disabled to study the effect of the compensation circuit on the measurement, because the driving strength of the SF is designed to be sufficient to drive the induced parasitic capacitance between the N -well and the substrate, and the bandwidth of the SF is 48 MHz, which is sufficient to cover the bandwidth of the patch-clamp amplifier system.

2.2. Parasitic Capacitance Compensation. Considering the existence of the electrode parasitic capacitance (C_s can be estimated using a simple voltage clamp measurement), when the control voltage (V_{con}) is applied externally, the voltage

will charge/discharge C_s , resulting in a large transient current that will travel through the feedback network to disturb the output voltage. Meanwhile, the parasitic capacitance and the feedback resistor will form a low-frequency pole that affects the stability of the TIA. For these two reasons, compensation for C_s is very necessary. As shown in Figure 7, capacitance compensation is achieved by connecting the capacitor (C_{inj}) in parallel with C_s , and applying a voltage proportional to the V_{con} at the other port of C_{inj} , the currents of C_{inj} and C_s are equal in magnitude and opposite in polarity.

As shown in Figure 7, when the V_{con} is applied, V_{clamp} will follow the change of V_{con} . The 8-bit R-2R DAC is used to set V_{inj} proportional to V_{con} . The capacitance compensation capability can be adjusted through V_{inj} which is altered by S1-S8. According to the conservation of charge

$$(V_{inj} - V_{con})C_{inj} = V_{step} \times C_s. \quad (6)$$

When (6) is satisfied, the transient current of parasitic capacitance of the electrode is fully compensated.

2.3. Series Resistance Compensation. The series resistor (R_s can be estimated using a simple voltage clamp measurement) of the electrode has typical values in the range of 5-20 M Ω , when the current flows through the electrode, the voltage drop will be generated on the series resistor, and there is a voltage difference between the membrane potential V_m and external V_{con} . Because this voltage difference complicates the object of studying the voltage/current characteristics of the cell itself, to alleviate this problem, the series resistance of the microelectrodes is usually measured before the experiment, and its effects are eliminated by numerical data algorithms. However, we still need to consider another drawback posed by this series resistance. With the membrane capacitance (C_m) typically in the range of 10-100 pF, the RC network composed of C_m and R_s results in a time

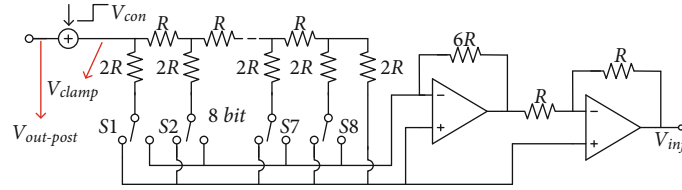


FIGURE 7: Schematic of the proposed electrode capacitance compensation.

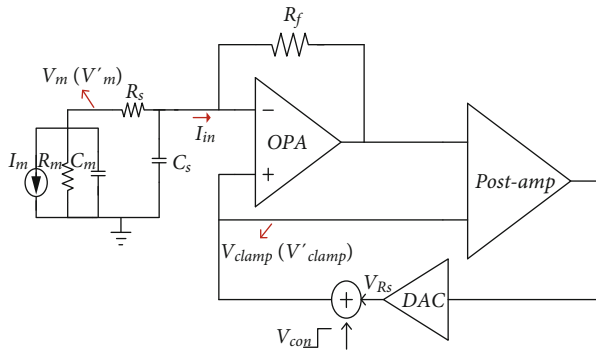


FIGURE 8: Schematic of the presented series resistance compensation.

constant of several mS, which slows down the establishment of the cell membrane potential and limits the bandwidth improvement of the PCA. Therefore, the series resistance compensation technique is proposed in the paper (see Figure 8).

The basic principle of series resistance compensation is relatively simple. As shown in Figure 8, when the V_{con} is intended to be increased/decreased, a higher/lower clamp voltage is needed to compensate for the voltage drop on the series resistor, ensuring that the membrane potential V_m approaches V_{con} as much as possible. Therefore, instead of directly applying the V_{con} to the noninvert input of the TIA, the new V_{clamp} is generated as the sum of V_{con} and the scaled output voltage (V_{Rs}). The scale factor of the output voltage is adjusted with an on-chip DAC. $\Delta V'$ and ΔV are the voltage difference between V_m and V_{con} before and after the resistance compensation, respectively.

$$\Delta V = V_{con} - V_m = V_{clamp} - V_m = I_{in}R_s,$$

$$\begin{aligned} \Delta V' &= V_{con} - V'_m = V_{con} - (V_m + V_{Rs}) \\ &= I_{in}R_s - V_{Rs} = I_{in}R_s - (V'_{clamp} - V_{con}), \end{aligned} \quad (7)$$

where V_m becomes V'_m and V_{clamp} becomes V'_{clamp} after the resistance compensation, respectively. To quantify the effectiveness of series resistance compensation, the compensation ratio a can be given as

$$a = \frac{\Delta V - \Delta V'}{\Delta V} = \frac{V'_{clamp} - V_{con}}{I_{in}R_s} = \frac{V_{Rs}}{I_{in}R_s}. \quad (8)$$

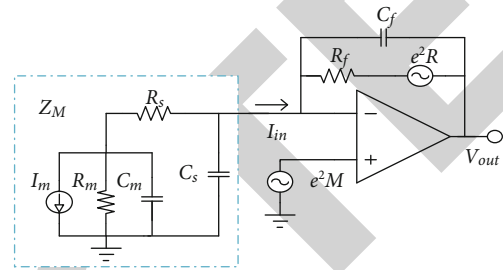


FIGURE 9: Noise model of the PCA.

2.4. Noise Analysis. Figure 9 shows the noise model of the TIA, as well as the input equivalent circuit. Although the noise of the PCA is mainly contributed by the TIA front-end and the battery electrode network, the noise of the post-amplifier can be neglected due to the high gain of the front TIA [18, 19].

The noise of the TIA consists of two main components, namely the current noise of the feedback resistor and the input noise of the op-amp itself, which are uncorrelated noise sources; the power spectral density of the equivalent output noise voltage of the TIA is written as

$$S_{OUT} = e^2_R + e^2_M + e^2_M \frac{R_f^2}{Z_M^2 (1 + sR_fC_f)^2}, \quad (9)$$

where e_M is the equivalent input noise voltage of the operational amplifier, which is mainly composed of flicker noise and thermal noise of input transistors, e_R is the thermal noise voltage of the feedback resistor R_f , and Z_M is the equivalent impedance of the electrical model of the cell and electrode. Z_M can be defined as

$$\begin{aligned} Z_M &= \frac{RM + RS + s \times RS \times RM \times CM}{a \times s^2 + b \times s + 1}, \\ a &= RS \times CS \times RM \times CM, \\ b &= RM \times CM + RM \times CS + RS \times CS, \end{aligned} \quad (10)$$

The cell-electrode network contributes considerable background noise in the whole-cell recording. The current noise power spectrum of the cell-electrode network can be expressed as

$$S_N = \frac{4kT}{\text{Re}\{Z_M\}}, \quad (11)$$

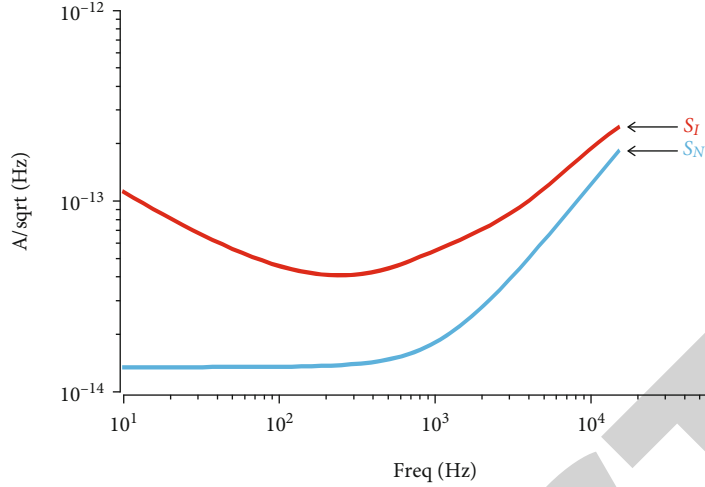


FIGURE 10: Simulated input current noise power spectrum of the cell-electrode network and the PCA.

TABLE 2: Performance of the operational amplifier.

Supply voltage	3.3 V
DC gain	127 dB
Gain-bandwidth product	9.5 MHz
Phase margin	60 dB
Equivalent input noise voltage (1-15 kHz)	$8.1 \mu\text{V}_{\text{RMS}}$

where k is the Boltzmann's constant and T is the absolute temperature. Therefore, the power spectral density of the equivalent input noise current of the PCA can be obtained as

$$S_I = \frac{S_{\text{out}}(1 + sR_f C_f)^2}{R_f^2} + S_N = \frac{e^2 R + e^2 M}{R_f^2 / (1 + sR_f C_f)^2} + \frac{e^2 M}{Z_M^2} + \frac{4KT}{\text{Re}\{Z_M\}} \quad (12)$$

Figure 10 shows the simulated current noise power spectrum of S_N compared with the total input current noise power spectrum. The flicker noise of the amplifier is the dominant noise source at low frequencies. At higher frequencies, S_N is the dominant component of S_I .

2.5. Operational Amplifier. At low frequencies, the noise consists mainly of the thermal noise of the transistor and $1/f$ noise, where the thermal noise is proportional to the temperature and the $1/f$ noise is opposite to the frequency [20, 21]. The cross-conductance of the input differential pair is increased while the cross-conductance of the current mirror transistor is reduced to reduce the thermal noise of the op-amp. To reduce the $1/f$ noise of the op-amp, the size of the transistor can be increased, especially the size of the input differential pair. In addition, the PMOS input pair is placed in a separate N -well to isolate the noise from the substrate. Table 2 summarizes the performance of this op-amp. Figure 11 shows a low-noise three-stage op-amp in a PCA.

3. Experimental Results

Figure 12 shows the chip photomicrograph of PCA, which has been fabricated in a 180 nm standard CMOS process and occupies the core area of $720 \mu\text{m} \times 630 \mu\text{m}$. Figure 13 shows the test fixture of the proposed PCA, and C_s , R_s , and C_m represent the electrode parasitic capacitance, electrode series resistance, and membrane capacitance, respectively. Cell membrane resistance (R_m) is too large which can reach $10 \text{ G}\Omega$; thus, it is ignored in the test. The output voltage ($V_{\text{out-post}}$) of the PCA and clamping voltage (V_{clamp}) is connected to the oscilloscope. Tektronix AFG31252 signal generator provides the voltage signal and converts it into current through the R .

Figure 14 depicts the measured frequency response of our PCA. It scores a 145.6 dB-Ohm gain, and the -3 dB bandwidth is 15.2 kHz. Figure 15 shows the measured pulse responses of the PCA without and with the parasitic capacitance compensation for the feedback resistor. As predicted, the parasitic capacitance compensation circuit greatly alleviates the problem of transient rings.

Due to the limited input resistance of the oscilloscope, it is inaccurate to measure the voltage V_m . Therefore, the Vc clamp is captured instead. With the test configuration, a current of 10 nA is injected, leading to a 100 mV voltage drop on R_s . To demonstrate the series resistance compensation, the control voltage (V_{con}) is changed to 50 mV (typical 0-100 mV). The intended change of V_{clamp} is the sum of Vc on and voltage drop of R_s ; thus, the change of the membrane potential V_m is the same as that of V_{con} . Figure 16 shows the impact of the series resistance compensation with different compensation ratios. The blue curve represents the voltage change at the V_{clamp} . Figure 16(a) represents the V_{clamp} without compensation. Figures 16(b)-16(d) show the compensation effect when the compensation ratio is 20%, 50%, and 86%, respectively.

Figure 17 outlines the measured responses of our PCA while using parasitic capacitance compensation. Figures 17(a)-17(d) exhibit the uncompensated, partially compensated, optimally compensated, and overcompensated, respectively. The

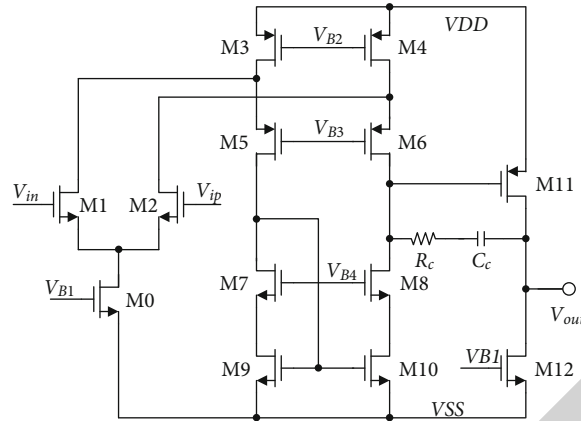


FIGURE 11: Schematic of operational amplifier.

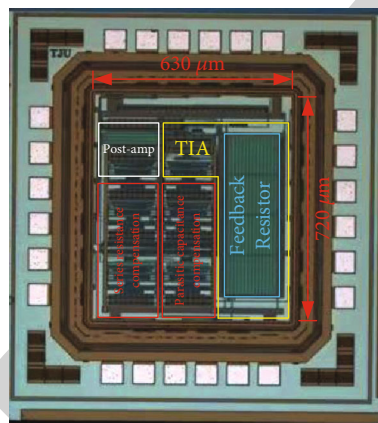


FIGURE 12: Chip photomicrograph of the proposed PCA prototype.

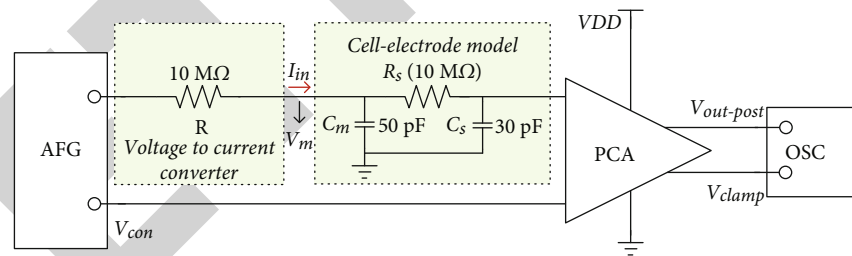


FIGURE 13: The test fixture of our PCA.

measurement results demonstrate that our design can compensate up to 30 pF electrode parasitic capacitance.

Figure 18 shows the measured integrated output noise of our PCA. The output equivalent noise voltage is $478.881 \mu\text{V}$. Note that the background RMS noise is $397.96 \mu\text{V}$ and needs to be subtracted. The equivalent input current noise can be expressed as

$$\overline{I_{in,rms}} = \frac{\sqrt{(478.881 \mu\text{V})^2 - (397.96 \mu\text{V})^2}}{145.6 \text{ dB}} = 13.98 \text{ pA}. \quad (13)$$

Table 3 summarizes the main performance of the proposed PCA compared to the prior art [22, 23] and commer-

cial devices (Axopatch 200B) [20, 24]. The proposed design shows a wider bandwidth and higher capacitance compensation and is the only design that integrates a glass microelectrode series resistance/capacitance compensation circuit and feedback resistor parasitic capacitance compensation.

4. Conclusion

This paper reports a PCA with series resistance compensation, microelectrode parasitic capacitance compensation, and feedback resistor parasitic capacitance compensation for whole-cell ion current detection. The PCA has a gain of 145.6 dB-Ohm, a -3 dB bandwidth over 15 kHz, and an RMS noise of 13.98 pA. It can compensate the capacitance

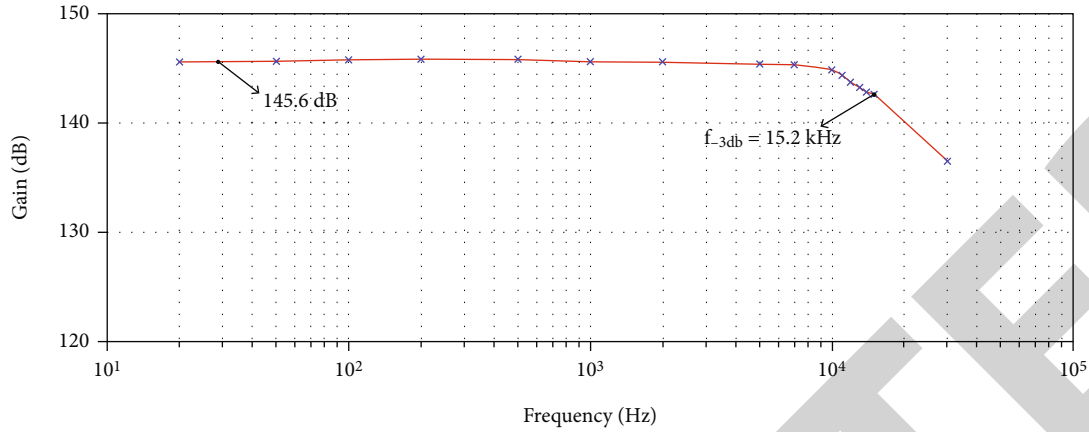
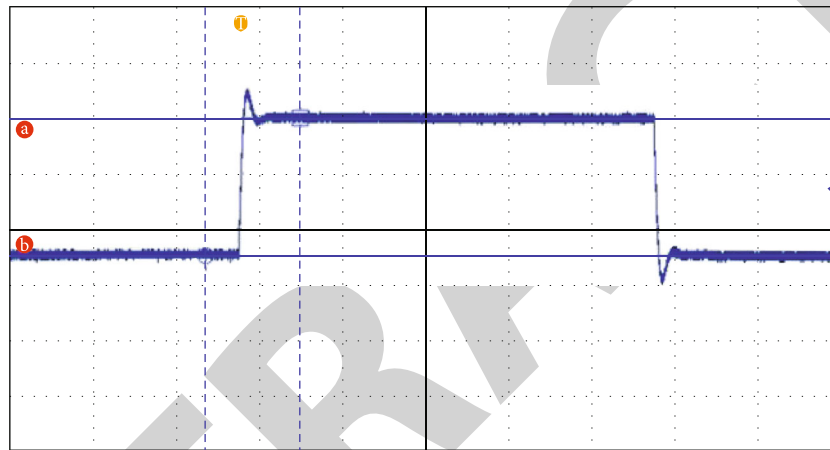


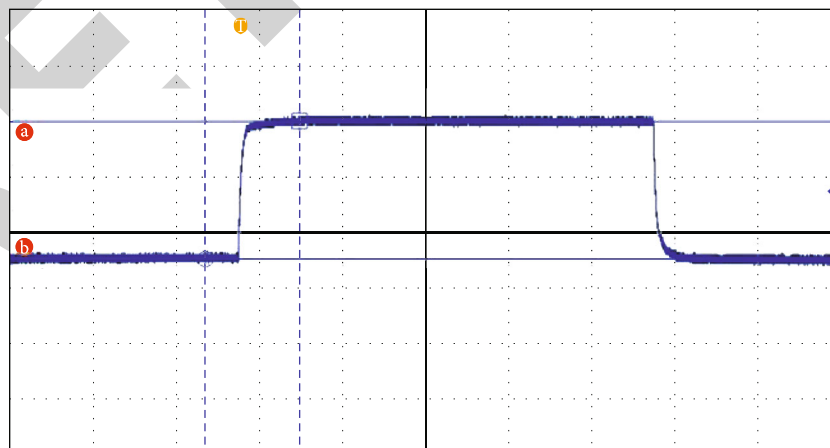
FIGURE 14: Frequency response of the PCA.



□ 706.8 μs
 ○ -433.2 μs
 Δ1.140 ms

ⓐ 1.932 V
 ⓑ 1.248 V
 Δ684.5 mV

(a)

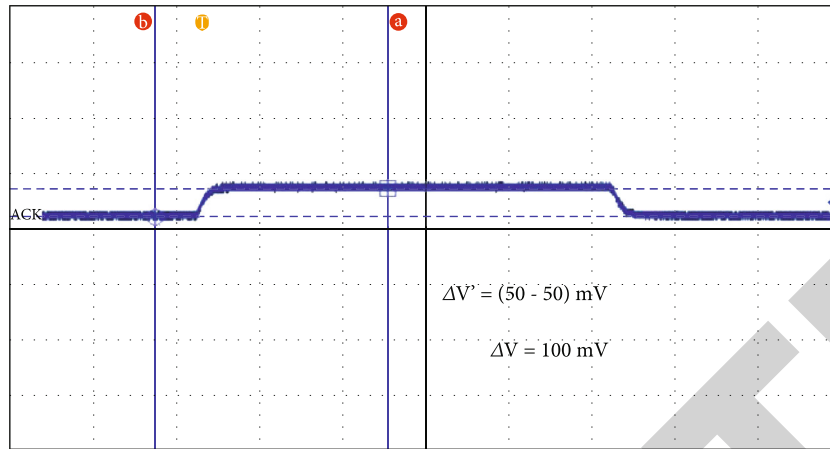


□ 706.8 μs
 ○ -433.2 μs
 Δ1.140 ms

ⓐ 1.932 V
 ⓑ 1.248 V
 Δ684.5 mV

(b)

FIGURE 15: Compensation effect of the presented feedback resistor parasitic capacitance compensation. (a) Uncompensated. (b) Compensated.

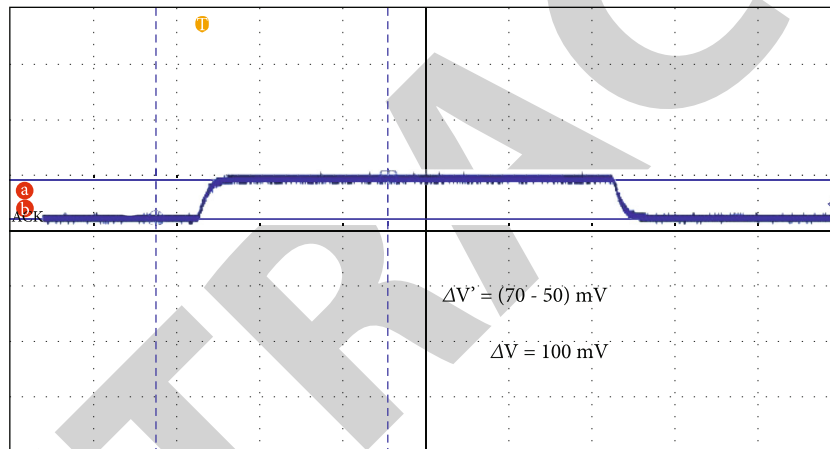


$\Delta V^* = (50 - 50) \text{ mV}$
 $\Delta V = 100 \text{ mV}$

□ 446.0 μs
 ○ -114.0 μs
 $\Delta 560.0 \mu\text{s}$

● a 1.650 V
 ● b 1.600 V
 Δ50.00 mV

(a)



$\Delta V^* = (70 - 50) \text{ mV}$
 $\Delta V = 100 \text{ mV}$

□ 446.0 μs
 ○ -114.0 μs
 $\Delta 560.0 \mu\text{s}$

● a 1.670 V
 ● b 1.600 V
 Δ70.00 mV

(b)

FIGURE 16: Continued.

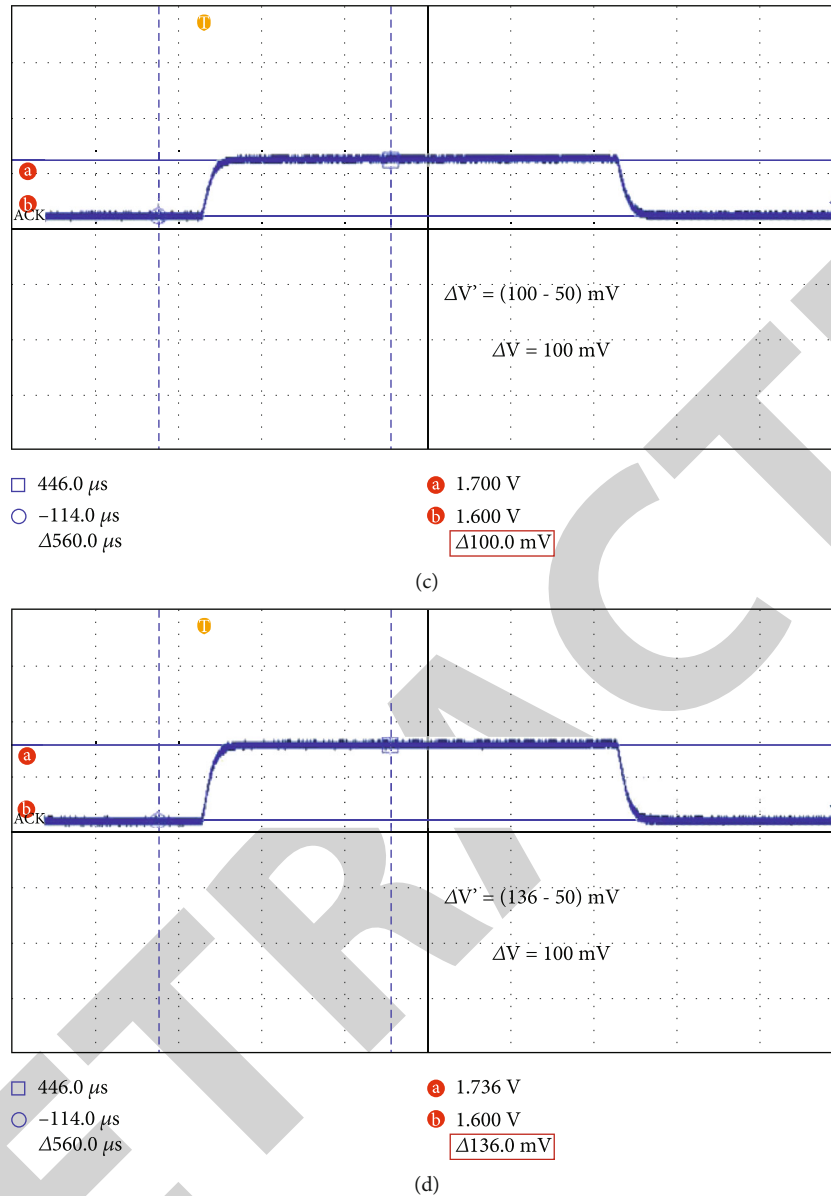


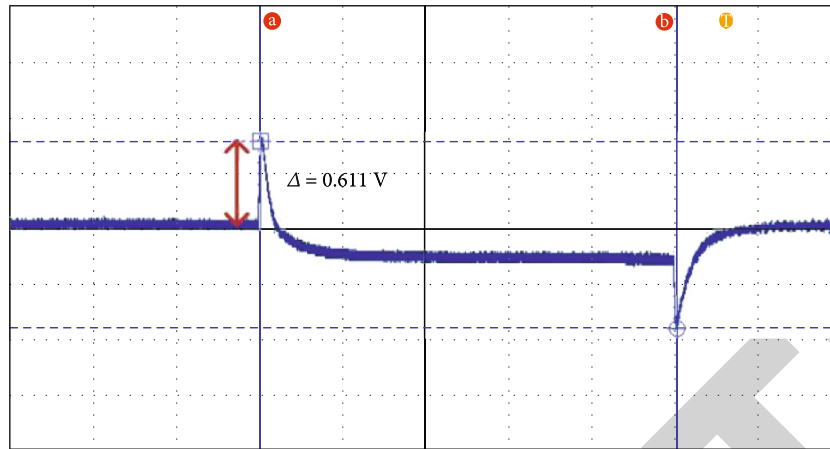
FIGURE 16: Compensation effect of the proposed series resistance compensation. (a) Uncompensated. (b) 20% compensation ratio. (c) 50% compensation ratio. (d) 86% compensation ratio.

and resistance of the electrodes up to 30 pF and 86% of the series resistance, respectively. Feedback resistance parasitic capacitance compensation can effectively improve the stability of the TIA and can eliminate output voltage overshoot.

Due to my limited research time and inexperience, the designed system has certain defects and needs further improvement. Further research by the next developers is needed. The following are the prospects for future work on the subject.

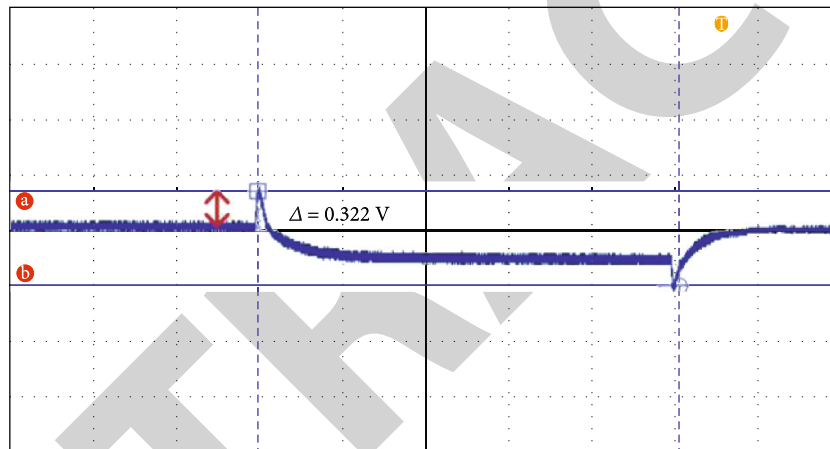
- (1) Further improvement of the application functionality. This application only has a simple display and zoom function in this aspect, and more functions can be considered to add to facilitate the experimenter to analyze the results

- (2) Data acquisition card sampling rate enhancement. The current data acquisition card can work at a sampling rate below 100k. When the sampling rate is higher than 100k, it will cause Linux scheduling problems and make data errors. The solution is to add RAM to the data acquisition card so that the data is first stored in RAM and then read into the application after the acquisition is completed by a Linux scheduling. The hardware part of this solution has been completed, and a new driver needs to be designed to solve the sampling rate problem
- (3) Noise reduction. At present, the noise of the test data acquisition card reaches about 20 mV, and after



- -5.640 ms
- -620.0 μ s
- Δ 5.020 ms
- a 2.211 V
- b 1.082 V
- Δ 1.129 V

(a)



- -5.590 ms
- -520.0 μ s
- Δ 5.070 ms
- a 1.922 V
- b 1.351 V
- Δ 571.2 mV

(b)

FIGURE 17: Continued.

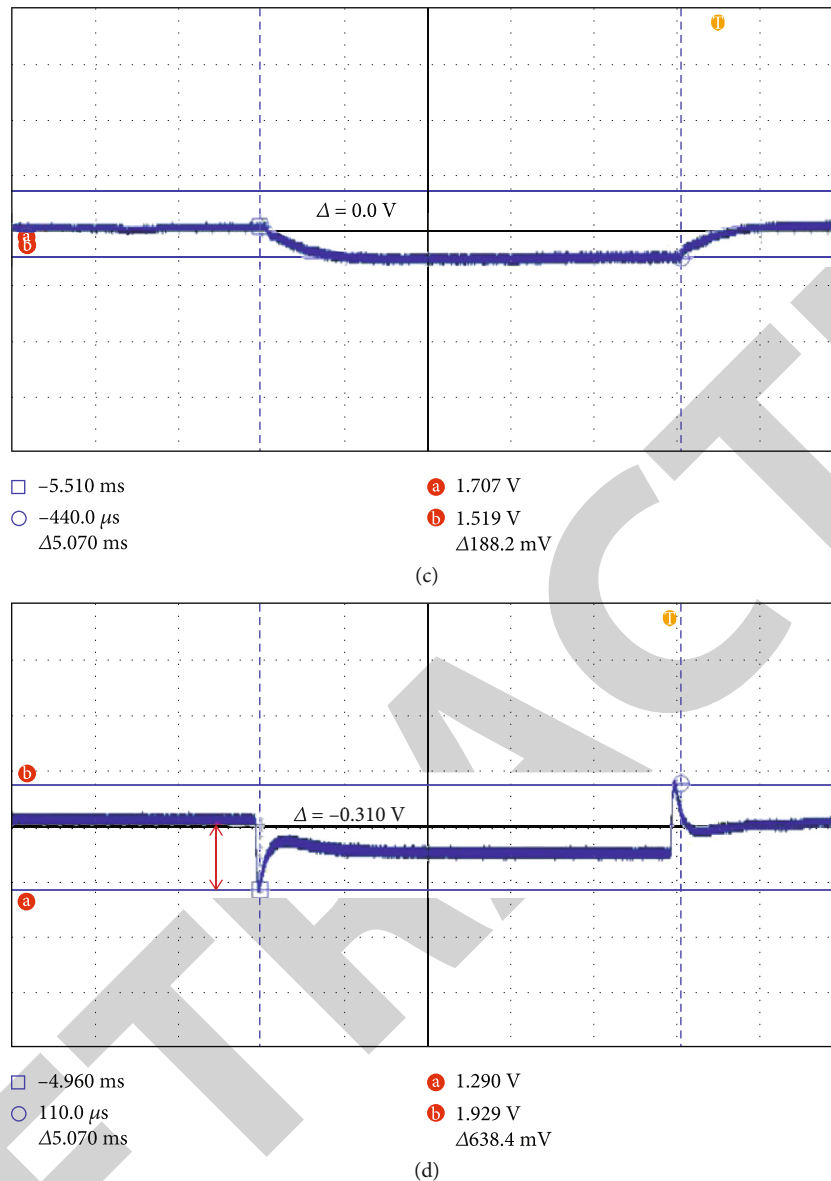


FIGURE 17: Compensation effect of the developed microelectrode parasitic. (a) Uncompensated. (b) Partially compensated. (c) Compensated. (d) Overcompensated.

using the regulated voltage to power the digital part of the system separately, the noise is also between 10 and 20 mV, so it is necessary to further reduce the noise

- (4) Increase the storage method. Diaphragm clamp experiments often take a long time and will produce a large amount of data, and the system Flash memory only has 64 M of space. The solution is to use a USB flash drive to store data, and the current system has been able to identify the USB flash drive, but the system does not automatically mount; you need to write a program to achieve automatic mounting of the USB flash drive. Hard

disk can also be used to store data, which not only requires hardware support but also requires the design of hard disk drivers

- (5) Network control. The system has a network interface and can access the network to transfer files. Further research can be done to achieve remote operation of the embedded system using the network. By establishing a server in the embedded system, the remote computer sends control commands, the server gives these commands to the application program to process, and the embedded system running the application program can also transmit the experimental information and experimental data to the computer client

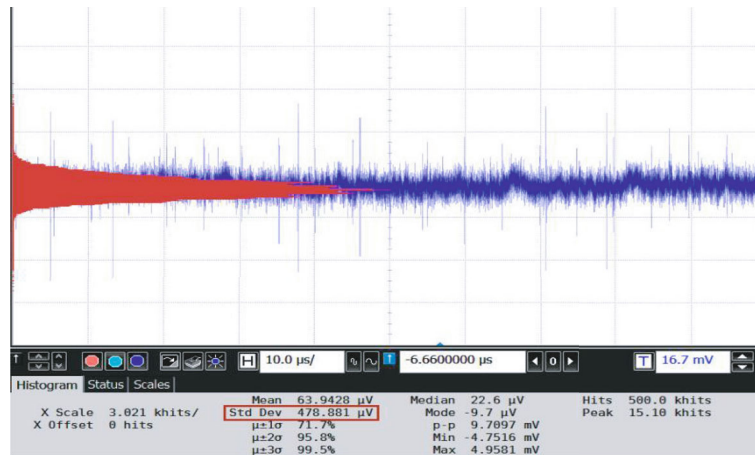


FIGURE 18: Measured integrated output noise of our PCA.

TABLE 3: Performance summary and comparison of the recent PCA.

Parameter	[13]	[16]	[17]	[18]	[19]	This work
Input-referred RMS noise (bandwidth)	2.09 pA (10-10 kHz)	5 pA (10 kHz)	1.1 pA (5 kHz)	3.3 pA (5 kHz)	1.65 pA (5 kHz)	13.98 pA (15 kHz)
Series resistance compensation	—	0-4 MΩ	0-32 MΩ	0-100 MΩ	0-100 MΩ	0-10 MΩ
Electrode capacitance compensation	—	0-20 pF	0-10 pF	0-10 pF	0-10 pF	0-30 pF
R_f parasitic capacitance compensation	Effective	—	—	—	—	Effective

(6) Improve the embedded diaphragm clamp amplifier system. At present, this system has preliminary results in both hardware module and software module, and the next step can be considered to combine these resources to conduct biological experiments. It is believed that with the continuous development of embedded technology and the increasingly widespread application of diaphragm clamp technology, the embedded diaphragm clamp amplifier system will have a broader prospect of use

Data Availability

The experimental data used to support the findings of this study are available from the corresponding author upon request.

Conflicts of Interest

The author declared no conflicts of interest regarding this work.

References

- [1] Y.-J. Nam, Y. J. Yoon, S.-K. Lee, M. Im, and J.-H. Park, "Fabrication of glass micropipette device using reflow processes and its integration with microfluidic channels for patch clamp recording of cell," *IEEE Sensors Journal*, vol. 20, no. 24, pp. 14694–14702, 2020.
- [2] D. C. Gadsby, "Ion channels versus ion pumps: the principal difference, in principle," *Nature Reviews. Molecular Cell Biology*, vol. 10, no. 5, pp. 344–352, 2009.
- [3] T. J. Jegla, C. M. Zmasek, S. Batalov, and S. K. Nayak, "Evolution of the human ion channel set," *Combinatorial Chemistry & High Throughput Screening*, vol. 12, no. 1, pp. 2–23, 2009.
- [4] M. Crescentini, F. Thei, M. Bennati et al., "A distributed amplifier system for bilayer lipid membrane (BLM) arrays with noise and individual offset cancellation," *IEEE Transactions on Biomedical Circuits and Systems*, vol. 9, no. 3, pp. 334–344, 2015.
- [5] Z. Gu, H. F. Wang, Y. L. Ying, and Y. T. Long, "Ultra-low noise measurements of nanopore-based single molecular detection," *Science Bulletin*, vol. 62, no. 18, pp. 1245–1250, 2017.
- [6] Y. Park, J.-D. Yun, and J. Kim, "Low-noise transimpedance amplifier design using chopper-stabilized technique for nanopore applications," in *2018 40th Annual International Conference of the IEEE Engineering in Medicine and Biology Society (EMBC)*, pp. 1–4, Honolulu, HI, USA, 2018.
- [7] M. Amayreh, G. Baaken, J. C. Behrends, and Y. Manoli, "A fully integrated current-mode continuous-time delta-sigma modulator for biological nanopore read out," *IEEE Transactions on Biomedical Circuits and Systems*, vol. 13, no. 1, pp. 225–236, 2019.
- [8] J. Kim, R. Maitra, K. D. Pedrotti, and W. B. Dunbar, "A patch-clamp ASIC for nanopore-based DNA analysis," *IEEE Transactions on Biomedical Circuits and Systems*, vol. 7, no. 3, pp. 285–295, 2013.
- [9] S. Dai, R. T. Perera, Z. Yang, and J. K. Rosenstein, "A 155-dB dynamic range current measurement front end for

Retraction

Retracted: Mixed Linear Programming for Charging Vehicle Scheduling in Large-Scale Rechargeable WSNs

Journal of Sensors

Received 23 January 2024; Accepted 23 January 2024; Published 24 January 2024

Copyright © 2024 Journal of Sensors. This is an open access article distributed under the Creative Commons Attribution License, which permits unrestricted use, distribution, and reproduction in any medium, provided the original work is properly cited.

This article has been retracted by Hindawi following an investigation undertaken by the publisher [1]. This investigation has uncovered evidence of one or more of the following indicators of systematic manipulation of the publication process:

- (1) Discrepancies in scope
- (2) Discrepancies in the description of the research reported
- (3) Discrepancies between the availability of data and the research described
- (4) Inappropriate citations
- (5) Incoherent, meaningless and/or irrelevant content included in the article
- (6) Manipulated or compromised peer review

The presence of these indicators undermines our confidence in the integrity of the article's content and we cannot, therefore, vouch for its reliability. Please note that this notice is intended solely to alert readers that the content of this article is unreliable. We have not investigated whether authors were aware of or involved in the systematic manipulation of the publication process.

Wiley and Hindawi regrets that the usual quality checks did not identify these issues before publication and have since put additional measures in place to safeguard research integrity.

We wish to credit our own Research Integrity and Research Publishing teams and anonymous and named external researchers and research integrity experts for contributing to this investigation.

The corresponding author, as the representative of all authors, has been given the opportunity to register their agreement or disagreement to this retraction. We have kept a record of any response received.

References

- [1] P. S. Prakash, M. Janardhan, K. Sreenivasulu, S. I. Saheb, S. Neeha, and M. Bhavsingh, "Mixed Linear Programming for Charging Vehicle Scheduling in Large-Scale Rechargeable WSNs," *Journal of Sensors*, vol. 2022, Article ID 8373343, 13 pages, 2022.

Research Article

Mixed Linear Programming for Charging Vehicle Scheduling in Large-Scale Rechargeable WSNs

P. Suman Prakash ¹, M. Janardhan ¹, K. Sreenivasulu ², Shaik Imam Saheb,³
Shaik Neeha ⁴, and M. Bhavsingh ²

¹Department of Internet of Things, G. Pullaiah College of Engineering and Technology, Kurnool, Andhra Pradesh, India

²Department of Computer Science & Engineering, G. Pullaiah College of Engineering and Technology, Kurnool, Andhra Pradesh, India

³Department of Computer Science & Engineering, Lords Institute of Engineering and Technology, Hyderabad, Telangana, India

⁴Department Computer Science Engineering (Artificial Intelligence and Machine Learning), Lords Institute of Engineering and Technology, Hyderabad, Telangana, India

Correspondence should be addressed to P. Suman Prakash; sumancse@gpcet.ac.in

Received 18 August 2022; Accepted 25 August 2022; Published 9 September 2022

Academic Editor: Praveen Kumar Donta

Copyright © 2022 P. Suman Prakash et al. This is an open access article distributed under the Creative Commons Attribution License, which permits unrestricted use, distribution, and reproduction in any medium, provided the original work is properly cited.

Because wireless sensor networks (WSNs) have low-constrained batteries, optimizing the network lifetime is a primary challenge. Rechargeable batteries are a solution to prolong the lifetime of a sensor node instead of restricting their functionalities to save energy. Wireless energy transmitters have the added benefit of providing a charger for the batteries of the sensor nodes in the WSN. However, scheduling one or more charging vehicles efficiently to recharge multiple sensor nodes is challenging. In this context, this paper provides a solution to recharge the sensor nodes using charging vehicle scheduling in WSNs through a mixed linear programming approach. Initially, we identify a heuristic value of each sensor node based on their residual energy, distance from a charging vehicle, available data packets, and other metrics. Further, a set of nodes is recharged by identifying the best charging vehicle to prolong their lifetimes, as well as the lifetime of the network as a whole. We simulated the proposed approach using a Python simulator, tested using different performance metrics, and compared using the recently published works. We notice the superior performance of the proposed work under various metrics in time and query-driven WSNs.

1. Introduction

The sensor nodes (SNs) of wireless rechargeable sensor networks (WRSNs) have rechargeable batteries, which can be charged to extend their lifespan [1]. There are several ways in the literature to recharge the sensor nodes, such as using energy harvesting techniques, battery-equipped unmanned aerial vehicles (UAVs) [2], solar panel-equipped SNs, and charging stations in between the network [3, 4]. Through recent advancements, one of the most promising approaches is wireless energy transmitters (WET). In general, a WET is equipped with a vehicle called a charging vehicle (CV), which is scheduled in the network to recharge the SNs without affecting their topological disorders [5]. A CV is

equipped with a battery of unlimited energy (due to energy harvesting), and it recharges the nodes while traveling in the network. Mainly, the CV visits a set of points called anchor points (APs) which is one hop distance from a group of nodes to recharge parallelly. There are several approaches in the literature to identify an optimal set of APs, with their benefits and limitations [6–8]. These approaches also specify a path for the CV to traverse in the network.

In large-scale WSNs, it is not easy to schedule a CV to recharge the whole network because recharging a node takes a long time than the data collection process [9]. So, it is required to introduce more than one CV to recharge a demanded or group of nodes in the network. Increasing

the number of charging will also increase the deployment cost, but a lower number of CVs cannot solve the issue [10, 11]. It is challenging to identify the best set of CVs, increasing the charger efficiency by prolonging the network lifetime. Hence, it is necessary to provide an efficient algorithm to choose the best quantity of CVs to recharge the energy demanded SNs because it is lacking in the literature. When more than one CV is in the network, scheduling them to solve the recharging purpose is difficult. So, it is further challenging to assign a group of charging requests to a specific CV. There are several approaches in the literature, but they are not dynamic, and many techniques use random or heuristic strategies [12, 13].

The scheduling problem of requests and CVs is solved using a mixed-integer programming (MIP) approach in this paper. Before that, we identify the weights of each SNs depending on various factors of an SN, including its residual energy, distance from the charger or base station, and available data packets. Using this weight, an MIP is applied to identify the best CV that can handle the charging request quickly and efficiently. With this motivation, we proposed a dynamic CV scheduling approach to prolong the lifetime through WET to recharge sensor nodes in WRSNs.

Overall, the contributions of the proposed MLPCV strategy are summarized as follows:

- (1) We propose a heuristic strategy to analyze the energy status and sustainability of each sensor node in the network and assigned a weight value to each node
- (2) A mixed linear programming strategy is used to identify the suitable charging vehicle, which can be scheduled to recharge a set of sensor nodes efficiently
- (3) The performance of the proposed work is evaluated under different scenarios and metrics using the existing charging vehicle scheduling approaches

This paper is organized as follows: The recently published charger scheduling algorithms are analyzed in Section 2. The system model along with the problem statement is defined in Section 3. The proposed MLPCV algorithm is presented in Section 4 along with illustrative examples. This section also analyzes the complexity of MLPCV. The simulation results are discussed and plotted in Section 5. Finally, Section 6 concluded the paper with future scope.

2. Related Work

We find several works in the literature using WET-based mobile vehicles to recharge the sensor nodes in the WSNs. This section categorizes the previous works into two types based on the number of CVs used in their works, such as one or more CVs. We summarize recent and related works in this section with their benefits and challenges.

2.1. Single Charging Vehicles. A CV can serve one or more recharge requests where coverage is the primary objective than the longest sustainability of sensor nodes [14]. This approach provides efficient charging scheduling and

increases connectivity, which further helps efficient data routing. Clustering is a common approach in WSNs, whereas this strategy is used to recharge the SNs in the WSNs using solar power. The efficiency and sustainability of the nodes are increased in this approach in terms of longer life. Similarly, Tomar et al. [15] use a clustering mechanism to identify the efficient AP to visit by the CV to recharge the needed nodes. The path of the CV is crucial in this approach, but this work is not for large-scale WSNs. The charger utility is maximized by Srinivas et al. in [16] using a heuristic strategy. This approach efficiently maximizes the CV utility while balancing the energy of the SNs among the network.

Identifying an efficient path for the CV is a challenging task in WSNs, whereas Jiang et al. [17] focused on this issue in their approach. Efficient anchor points are identified to recharge multiple nodes and serve the charging requests at a single instance. It takes time to restore an SN until the battery is full. Considering these challenges, a partial charging strategy is introduced in [18] with a genetic approach and multiattribute decision-making systems. This approach balances and simultaneously serve multiple requests to sustain the longer visibility of nodes. The charging scalability is optimized in [19] to maximize the CV's efficiency. Multiple SNs are recharged simultaneously in [20], where the scheduling is decided based on the residual energies of the SNs. In [21], a hierarchical clustering approach is used to identify the optimal clusters to schedule the CV to serve maximum requests in the WSNs. Since the computational complexity of this approach is high, it is not feasible for large-scale networks.

Depending on the need for charging, the on-demanded CV scheduling strategy is proposed in [22] for recharging more nodes to sustain the longer lifetime. In [23], multiple battery-filled sensor nodes are used to replace the SNs, which are critical with their battery. However, this is expensive to replace the number of SNs and not secure. It is also not feasible for all applications. Deep reinforcement learning is an efficient classification and learning method, and the benefits of this approach are used for WSNs to recharge the nodes in [24]. This approach is used a partial charging strategy, so the network lifetime is longer for small WSNs. This approach also takes high computational resources than other approaches. A collaborative charging strategy is presented in [25], in which the authors mainly focused on building an optimal tour for the CV. In this approach, the optimal charging points are decided to fit the large-scale WSNs.

From the above discussion, we identify several algorithms in the literature that use a single charging vehicle to recharge the sensor nodes in the network. However, these approaches are limited to small networks with limited SNs. The large-scale WSNs are deployed with unlimited SNs and receive multiple requests simultaneously. Handling such situations is not possible with a single charging vehicle.

2.2. Multiple Charging Vehicles. A new strategy for identifying the reason to charge a node along with the route from the current location of CVs to recharging nodes of WSNs

is presented in [21]. But identifying the best set of CVs required for the network to serve the requests efficiently is not determined in the paper. A traditional push-shuttle-back approach serves the charging requests in large-scale WSNs. This strategy is efficient and inexpensive but not optimal. Another charging request serving algorithm is presented in [26] using more CVs, and this approach achieves 1% efficiency over the traditional algorithms. However, this approach also failed to determine the optimal number of CVs that can serve the network requests. An electromagnetic radiation-based recharging algorithm is proposed for WSNs in [27]. In this, the TSP approach is used for the CV route to recharge the nodes, but this approach also failed to determine the optimal number of CVs that can solve the problem to minimize the CV cost. In [28], lifetime enhancement through CV is presented for large-scale WSNs. Unlike other traditional approaches, this approach determines the best number of CVs that can solve the charging requests in the network. However, this approach is computationally high and also not optimal.

With coverage intention, a CV scheduling approach is proposed for large-scale WSNs in [29]. In this strategy, identify the SNs with limited energy and give high priority to recharging them to maintain the connectivity and avoid sink-hole problems in the network. In [30], swarm intelligence is used to schedule multiple CVs in the network. In this, the APs are identified initially, and then, CVs are scheduled based on the APs to recharge the nodes in the network. However, this approach failed to decide the best number of CVs required to restore the requested network nodes. Control of the velocity of the CVs is a critical challenge, and it is addressed in [31] using approximation algorithms. Still, this approach is not efficient and optimal in terms of choosing the APs in the network. In [32], an integer programming approach is used to schedule the CVs in large-scale WSNs. Still, this approach failed to choose the best possible CVs to cover the entire network.

A ring-wandering approach used to schedule the multiple CVs to recharge the SNs deployed in large-scale WSNs is presented in [33]. This approach is efficient in balancing the energy of the SNs and prolonging their lifespan. However, the performance is improved but failed to identify the optimal number of CVs to control the cost. A clustering algorithm is also used in multiple CV scheduling in [34] using a statistical approach and heuristic formulae. This approach efficiently identifies the APs in the networks and controls the scheduling, but it does not provide the optimal number of CVs. In [35], an optimal number of CVs are determined to replenish the energy of the SNs in the network. However, this approach failed to produce the optimal route for the CVs and charging efficiency. In [36], a hybrid metaheuristic strategy is used to serve the charging requests by providing optimal scheduling. This approach efficiently finds the best set of APs and routes to recharge the nodes. Although this is efficient, it requires more computational resources to run the algorithm, whereas it is not feasible because of the constrained resources of WSNs.

As we noticed in this discussion, most of the works are using heuristic, clustering approaches to identify the APs and TSP for the traveling path for the CVs. While considering all these limitations, we proposed an efficient approach to schedule multiple CVs in the large-scale WSNs to recharge the nodes in the network. It can also decide the optimal visiting points.

3. Problem Formulation and Parameter Description

The representation of the WSNs is shown as a graph G with a set of nodes and edges. The n number of nodes are represented as $S^+ = S \cup S_0$, where S_0 is the BS and S means the set of nodes. The proposed algorithm is centralized, so it is executed in S_0 . So, the computational resources are unlimited for executing the code. The edges are identified using their communication range t_c and denoted using D . Each S is equipped with a battery of capacity E^0 and buffer of capacity B . The k number of CVs are denoted using $C = \{c_1, c_2, \dots, c_k\}$. The locations of the SNs are randomly decided using Sah et al. [37], and S_0 is located at $(0,0)$. Each node s_i drains some energy during operations like acquiring data from the environment or other SNs (s_j), or sometimes, the nodes are idle. So, at a particular time t , a node s_i have residual energy of E_i^t . Similarly, the buffer of each node is occupied with some data during the data transmissions, and at a time t , it is considered B_i^t for a node s_i . At time $t=0$, the energy of the battery is full capacity and the buffer is empty. E^{\min} is considered the threshold energy for any SN in G , and s_i sends energy request to S_0 when it meets the condition $E^{\min} \geq E_i^t$. All the charging and buffer capacities are updated through the control signal to S_0 . The charging requests are categorized and assigned to CVs by S_0 in the proposed work.

The CV can move quickly with v velocity, and the charging time is minimal. In the course of CV stay at the BS, it was recharged. The SN energy drain during the data transmission to the CVs is shown in

$$E_i^t = \text{⊙}_i^t \times \alpha_t + \text{⊙}_i^t \times \alpha_a \delta_i \forall i \in S^+, \quad (1)$$

where ⊙_i^t shows total packets transmitted by s_i ; Equation (2) computes δ_{ij} , where it is the distance from s_i to CV $_j$, he processing a bit need α_t energy, and amplification needs α_a energy:

$$\delta_i = \sqrt{(x_i - x_{cv_j})^2 + (y_i - y_{cv_j})^2}, \quad (2)$$

where (x_i, y_i) are the coordinates of the SN s_i and (x_{cv_j}, y_{cv_j}) is CV $_j$ location. The energy required to acquire sensed data from the field is

$$E_i^{rx} = \text{⊙}_i^t \times \alpha_r \forall i \in S^+, \quad (3)$$

where receiving a sensed packet from the field is required α , energy. The overall EC of SN s_i is considered

$$E_i^c = E_i^{rx} + E_i^t \forall i \in S^+. \quad (4)$$

The residual energy of SN at simulation time t is considered

$$E_i^r = E_i^r - E_i^c \forall i \in S^+. \quad (5)$$

The average residual energy of a cluster is computed as follows:

$$E_i = \sum_{j \in C_i} \frac{E_j^r}{|C_i|} \forall 1 \leq i \leq k. \quad (6)$$

In the recharging process, the energy harvest of SNs is calculated similarly to [38].

Through an optimal CV scheduling strategy with a low data loss rate, the proposed work is aimed at balancing the energy among the SNs.

4. Proposed MLPCV Algorithm

The proposed MLPCV primarily contains two modules. In the first module, different metrics are used to calculate the weight of each SN to determine the priority of charging. Based on these weights, the optimal CV is assigned to recharge the node. CVs are placed at a specific location in the network to get the highest variations in the weights of nodes instead of keeping them at BS. As a result, all the CVs are located at a particular distance from the SNs, and when they receive requests, it is easy to fulfill them quickly. The general model of the proposed work is summarized using Figure 1.

4.1. Finding CV's Initial Location and SN's Weight. In this section, we perform two operations including finding the initial deployment of the CVs and weight calculations.

4.1.1. CV Initial Locations. A new initial centroid selection approach is used in this phase based on enhanced k -means algorithms [39]. Aiming to select centroids that belong to different clusters, the farthest are chosen in such a way that they are different and vary from each other. As a result, more centroids will be likely to share the same cluster SNs. As a result, the chance of having data points from different centroids in the same cluster is maximized. This will result in a significant reduction in execution time. Algorithm 1 explains the detailed pseudocode of the proposed CV initial location (L) selection approaches.

Initially, we need to decide the number of CVs used in a particular environment. This is decided based on $k = \log_2(n)$. Once k is decided, it selects two locations (L_1 and L_2) based on the following:

$$\begin{aligned} L_1 &= (\max(x_i), \max(y_i)) \forall 1 \leq i \leq n, \\ L_2 &= (\min(x_i), \min(y_i)) \forall 1 \leq i \leq n. \end{aligned} \quad (7)$$

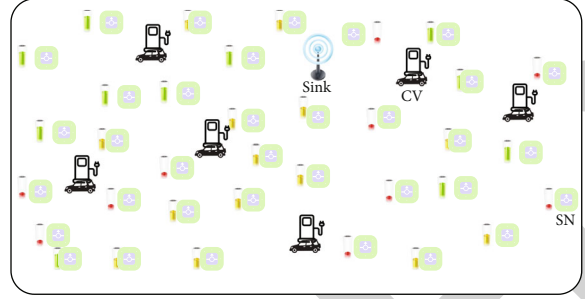


FIGURE 1: The general model of the proposed work with SNs of different residual batteries, charging vehicles, and a sink node in a WSN.

The remaining k locations for CVs are selected using

$$L_k = \max_{(1 \leq i \leq k), (1 \leq j \leq n)} d_{(L_i, S_j)} + d_{(L_{(i+1)/k}, S_j)}. \quad (8)$$

This process iterates until k locations are determined, and all the CVs are positioned in these locations initially. Further, we compute the weight of each SNs as known in the subsequent sections.

4.1.2. SN Weight Calculation. Weight calculation is an important metric and can be used to choose the charger that can recharge the node before it drains its entire power supply. In this context, we generate heuristic formulae to compute the weight of each SN. This uses different metrics such as distance from SNs to the CVs, heuristic information, and buffer capacity along with the energy information. Initially, we estimate a probability value as shown in

$$P_{ij} = \frac{\psi_j^{-\alpha} \times d_{ij}^{\beta}}{\sum_{i=1}^n (\psi_j^{-\alpha} \times d_{ij}^{\beta})} \times \left(\frac{\eta\omega}{4\pi}\right)^2 \forall j \in k, \quad (9)$$

where $\psi_j = r_j/x_j$ is the energy consumption rate of a CV. α and β are the heuristic information, and ω is the wavelength, and η is the efficiency of the rectifier. All these values are constants. The weight of SNs is shown in

$$\mathcal{W}_{ij} = \frac{E_i^{\max}}{E_i} \times P_{ij}. \quad (10)$$

As we know, most of the metrics used in Equations (9) and (10) are changed dynamically in the meantime. So, this process iterates after every unit time to notice the changes in the distance from nodes to CVs, residual energy, etc. So, the updated weight is supplied to the charging vehicle scheduling algorithm, to identify the best CV to recharge the SNs.

4.2. Charging Vehicle Scheduling. Once the weight calculation of all nodes ($\mathcal{W} = \{\mathcal{W}_i \forall i \in (1, n)\}$) is completed, we start assigning suitable CVs using the charger vehicle scheduling approach. This algorithm decides the suitable CV for each SN charging request according to their residual energy and distances, whereas a similar approach is implemented

```

Conditions:  $k \geq 2$  and  $n \neq \phi$ 
1:  $\mathcal{C} = \phi$ 
2:  $c_1 = \max \{D(n)\}$ 
3:  $c_2 = \min \{D(n)\}$ 
4:  $\mathcal{C} = \{\mathcal{C} \cup c_1\}$ 
5:  $\mathcal{C} = \{\mathcal{C} \cup c_2\}$ 
6: while(size( $C$ ) <  $k$ )
7:    $nC = DP(n, \mathcal{C})$ 
8:    $\mathcal{C} = \{\mathcal{C} \cup nC\}$ 
9: end while
10: return  $\mathcal{C}$ 

```

ALGORITHM 1: Initial CV location selection algorithm.

for the fog environment by Hazra et al. [40]. A weight matrix $E_{n \times k}$ is constructed for device allocation, of the size $n \times k$, in which the SNs are considered in rows and CVs considered in columns. The entry of E_{nk} is the \mathcal{W}_{nij} value, it is a nonnegative heuristic weight for a node $i (i \in (1, n))$ to consider a CV $j (j \in (1, k))$, and it is calculated as shown in equation (10). Using this information, we generate a scheduling matrix Ψ , where each entry of this matrix is either one or zero. The values associated with one mean an SN is assigned to a CV for recharging their battery. The primary object to generate Ψ is to minimize

$$\max_{\forall i \in (1, n)} \sum_{j=1}^k \Psi_{(i,j)} \times \mathcal{W}_{ij} \quad (11)$$

Subjected to $\Psi_{(i,j)} \in \{0, 1\}, \forall i \in (1, n) \wedge j \in (1, k)$.

The primary goal of this scheduling is to prolong the lifetime of the network while balancing the energy of the SNs choosing the best CV to recharge a node. The charger vehicle scheduling uses the following steps to assign a CV to a particular set or SNs or a single SN using the following steps.

Step 1. Arrange all the SN weights (\mathcal{W}_{nk}) in ascending (non-decreasing) order such as $\mathcal{W}_{nk(1)} \leq \mathcal{W}_{nk(2)} \leq \mathcal{W}_{nk(3)} \leq \dots \leq \mathcal{W}_{nk(\mathcal{R})}$, where \mathcal{R} indicates the rank of each element.

Step 2. Take the minimum \mathcal{R} as an element ($\mathcal{W}_{nk(\mathcal{R})}$) in the i^{th} row and j^{th} column E in ascending order while each row and column contain at least an entry.

Step 3. Change these entry \mathcal{R} with \mathcal{W}_{nk} of E according to equation (12) shown below:

$$E_{nk} = \begin{cases} 0, & \text{if } \mathcal{W}_{nk} \leq \mathcal{R}, \\ \mathcal{W}_{nk}, & \text{otherwise.} \end{cases} \quad (12)$$

Step 4. From a CV column (j) which had the least number of zeros, schedule all the SNs (i) which had value one.

Step 5. Repeat Step 4 until all the sensor nodes are assigned at least one CV.

This process is repeated to recharge all the SNs in the WSNs until the data aggregation process is interrupted.

4.3. Illustration. The charging vehicle scheduling approach is illustrated using a simple example by considering ten nodes and six charging vehicles as shown in Figure 2. In general, for ten sensor nodes, one CV is sufficient, but our intention here is to show how the proposed algorithm works. Initially, all the weighted information calculated using equation (10) is stored in E as shown in Figure 2(a). Next, we identify the ranks of each entry of E based on nondecreases and replace the entries in Ψ as shown in Figure 2(b). Our process consists of filling in rows and columns one by one until all rows and columns contain at least one entry, based on the rank of each entry. We start filling one by one rank in Ψ , and all the rows and columns contain at least an element after filling rank 22 as shown in Figure 2(c). Now, we use equation (12) and replace all the entries using zero for the no entries and replace the value associated with each ranking as shown in Figure 2(d). By giving high priority to Ψ with the fewest zeros in a column, we can now assign each task to a resource from Step 4 of the charger vehicle scheduling approach. We need to find the rows with the highest number of zeros. As we noticed from Figure 2(d), we need to find the rows with the highest number of zeros such as s_5 , s_8 , and s_{10} . So, we assign the appropriate CV for these two SNs such as $CV1 = \{s_{10}\}$, $CV4 = \{s_8\}$, and $CV2 = \{s_5\}$ as shown in Figure 2(e). Further, all zeros are replaced using ∞ , and assigned CVs are replaced as 1 as shown in Figure 2(f). The next highest zeros are found in s_3, s_4 , and s_9 , so we assign the appropriate CV for these nodes, and they are highlighted in Figure 2(g). If more than one charger is associated, we give high priority to the idle charger because the charging takes more time. As per this principle, s_9 can be assigned to CV1, and it can be represented as $CV1 = \{s_{10}, s_9\}$. Similarly, when checking s_3 , there are two possibilities, and we can consider any one. To break the tie, we can choose the ascending order, so s_3 is assigned to CV5, and it becomes $CV6 = \{s_4\}$. We repeat this process, until all the nodes are visited, and the final assignment is shown in Figure 2(h), i.e., $CV1 = \{s_{10}, s_9, s_7\}$, $CV2 = \{s_5, s_6\}$, $CV3 = \{s_2, s_1\}$, $CV4 = \{s_8\}$, $CV5 = \{s_3\}$, and $CV6 = \{s_4\}$.

4.4. Complexity Study. The proposed MLPCV approach's time complexity mainly works in two partitions: CV initial location selection along with the weight computation for each SN and the scheduling of the CVs to recharge the requested nodes. The time required to perform the initial CV locations using k -means required $O(n^3)$, and the weight calculation requires approximately $O(n \times k)$, where $k < n$. The time required to schedule is approximately $O(k \times n^2)$. The total complexity of MLPCV to recharge the requested nodes is $O(n^3) + O(n \times k) + O(k \times n^2)$. From this, the asymptotic complexity for MLPCV is $O(n^3)$, which is better than existing CV scheduling approaches. However, the proposed MLPCV is better than other existing approaches such as CSCT, M2C, and SPSS.

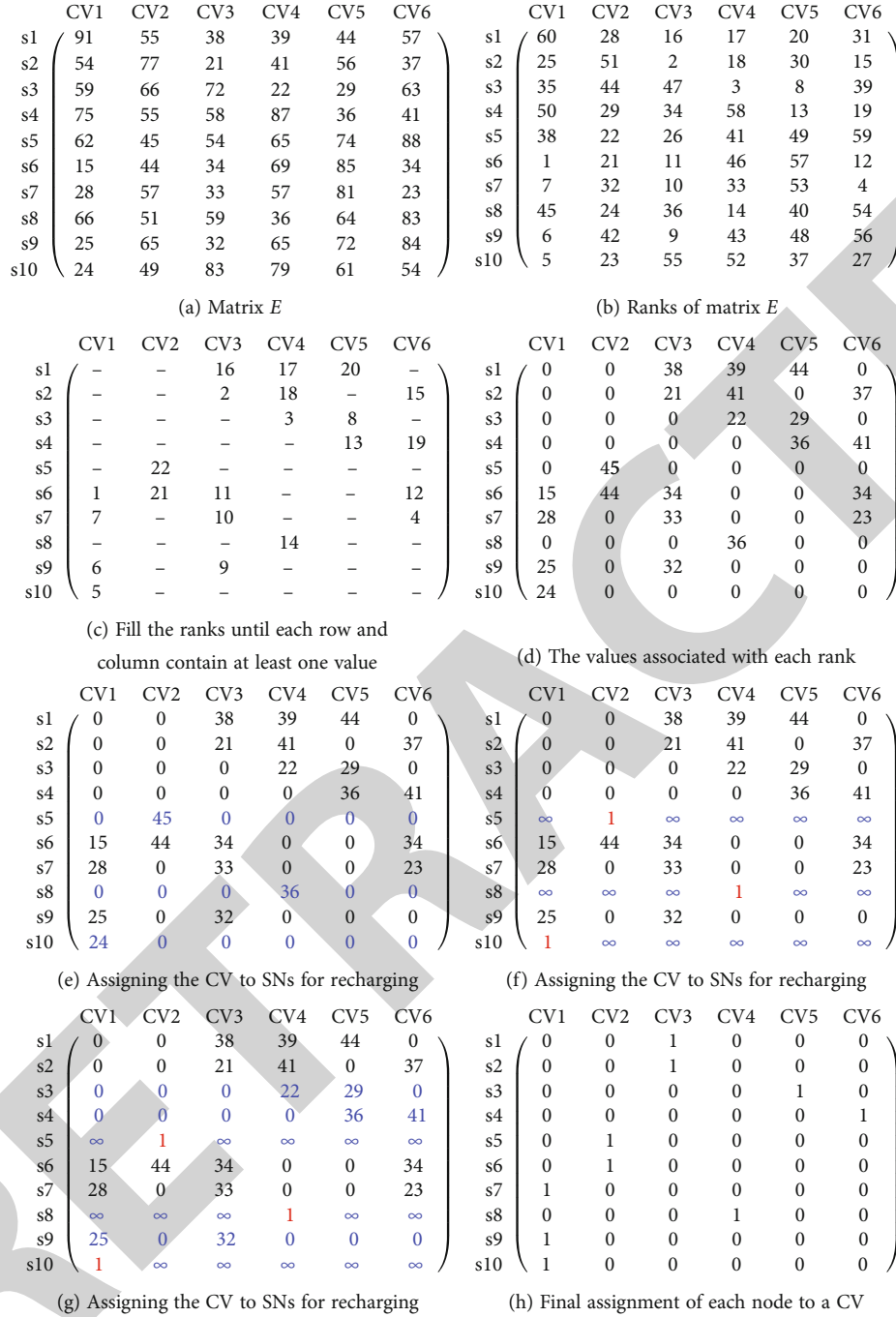


FIGURE 2: Illustration of charging vehicle scheduling through an example of 10 nodes and six chargers.

5. Simulation Studies

The simulator for experiments used Python (v3.11.0). A number of SNs are varied along with the size of the area to conduct experiments in two different scenarios. We consider 1000 to 1600 as the number of nodes, and they are deployed according to Sah et al. [37]. The CV battery capacity is 194.4 kJ, and its type is 12 V 4.5 Ah LiFePO₄ rechargeable battery. The total simulation time considered to run the experiments is 10 hours or 100 network cycles. Similarly,

the packet generation also followed from this approach. The area size during experiments are changes between 600 sq.m and 1000 sq.m. S_0 is located at (0,0) in all the experiments and two scenarios. The packet generation and receiving and transmissions require 0.05 mJ, 0.02 mJ, and 0.02 mJ energy, respectively. The communication and transmission proximity is considered 15 m and 12 m, respectively. The TDMA protocol is used as a MAC layer protocol, and MQTT is used as the application layer protocol [41]. Each unit of time generates approximately four packets during

experiments. All the SN's battery is full initially, and it is approximately 8 kJ. In case below 10% of the battery is available, it is assumed that it takes 50 min to recharge completely. The velocity of CV is 1 m/s, and approximately, it consumes 55 W/s during movement or standalone.

5.1. Average Charging Delay. An average charging delay (ACD) is the time it takes for all CVs in a WSN to charge a requested SN before it completely drains its energy. SNs are challenging to track because the CV does not reach them until they are completely drained. A travel time is included, as well as the charging of other requests waiting in line. Under two scenarios, including the size of the area and the number of SNs, we compute the average cost per node for a network. Traveling delay and queue size increase with area size and number of nodes. In order to simulate these two variables, we took into consideration both of them.

Figure 3(a) plots the results of SNs varying from 1000 to 1600 in 1000 sq.m area. We identify that the increasing number of SNs degrades the ACD, because more of the requested nodes are in queue. So, generally, it is difficult to serve all the nodes using available CVs. We notice that the ACD of the WSN is approximately 12 min after the end of the simulation time of 10 hours in the proposed MLPCV approach, which is the best compared with the existing techniques. Similarly, the existing CBCT results in a delay of approximately 18 min, M2C results in approximately 23 min, and the SPSS algorithm results in around 37 min delay on average. So, we can claim that the proposed work results in the least delay over the other techniques. In Figure 3(b), we consider the different area sizes such as 600 sq.m to 1000 sq.m while considering 1000 SNs which are deployed randomly in the network. With a constant number of sensors and a larger area, SNs have a lower communication burden than densely deployed sensor nodes. Therefore, it minimizes unnecessary data transmissions and reduces energy consumption. Consequently, there is a reduction in the number of requests for charging 1600 SNs in a 1000 sq.m area resulting in an average delay time of 12 minutes, and M2C results in a delay time of approximately 15 minutes. A delay of 18 seconds is used by the SPSS algorithm, and a delay of 21 seconds is used by the J-RCA algorithm.

5.2. Packet Reception Ratio. Based on the number of packets generated by each sensor node in a WSN, it is calculated. A total number of packets are received by the base station during the simulation time T [42]. As the WSNs transmit packets, packet reception rates (PRRs) are directly proportional to throughput. There is a direct correlation between the PRR means and the performance of the system.

Under two scenarios, including varying the number of SNs, the proposed MLPCV approach evaluates the PRR performance as shown in Figure 4(a) and PRR vs. the simulation time as shown in Figure 4(b). While varying the number of SNs between 1000 and 1600, the MLPCV always results in the highest performance compared to existing algorithms in Figure 4(a). Similar to the MLPCV algorithm, the PRR is detected when 1000 SNs are processed continu-

ously, and the results are plotted in Figure 4(b). It is evident from the plots that the MLPCV performs better than existing algorithms such as M2C, SPSS, and J-RCA. The proposed work should improve on the existing algorithms in terms of PRR, so we strongly agree with that assumption.

5.3. Residual Energy. For the data collection operations in the WSNs to be sustainable, any sensor node's remaining energy must be above zero. Increasing the RE results in a longer lifespan for the network as a result of a higher RE.

We compare the average RE between the proposed and existing works in Figures 5(a) and 5(b). Taking SNs from 1000 to 1600 in 1000 sq.m area and Figure 5(a), the average RE can be determined from the figure. Once the CV has been visited and recharged, the residual energy of any sensor node increases. Due to the fact that it can receive a much higher number of requests from a variety of sources in the network, in this scenario, the residual energy of the SNs is decreasing while increasing the number of SNs. A 100th cycle of the 1600 sensor nodes averages 4.7854 kJ for M2C and SPSS, but 2.3654 kJ for J-RCA. We propose an algorithm with an average RE of 5.96547 kJ, which is better than the existing algorithms.

Based on 1000 randomly deploying static SNs in the network, Figure 5(b) shows the average RE of the SNs. The large area and limited number of SNs result in a low data exchange rate. As a result, fewer requests are received by the CV, and delays are also reduced. As a bonus, the average RE of the sensor nodes will reduce congestion. According to the proposed work, the average RE is 7.1337 kJ for 1000 SNs in a 1000 sq.m area. There is an average RE of 5.3121 kJ for the existing M2C, SPSS, and J-RCA algorithms, respectively, 5.454 kJ, 4.5754 kJ, and 5.4454 kJ. In this case, there is a significant difference between the proposed algorithm and the three existing algorithms in terms of average RE.

5.4. Node Survival Rate. When the CV completes its cycle, the node survival rate indicates how many SNs survived. There are a large number of sensor nodes (SNs) in the network, and the area is extended, so it is not possible for all sensor nodes to be saved. As a result, we calculated the number of sustainable SNs after the mobile vehicle completed the threshold number of charging cycles and collected the data. As shown in Figure 6(a), we vary the number of SNs between 1000 and 1600 over a field of 1000 sq.m. By varying the field size between 600 sq.m and 1000 sq.m, we set the sensor nodes to 1000 in Figure 6(b).

Figure 6(a) shows the NSR of the proposed and existing algorithms by varying the 1000 to 1600 SNs in the area of 1000 sq.m. According to the proposed algorithm, the NSR is 96.79% at 1000 nodes and 90.12% at 1600 nodes after 100 cycles. As a result of the existing M2C algorithm, 95.99% of the network is deployed with 1000 SNs after 100 cycles, and 89.11% when 1600 SNs are deployed. When 1000 SNs are deployed in the network at the 100th cycle, SPSS and J-RCA result in 85.37 percent and 84.67 percent, respectively. A 100th round deployment of 1600 SNs results in 78.91% and 78.01%, respectively, for the SPSS and J-RCA algorithms. On the basis of these values, the proposed

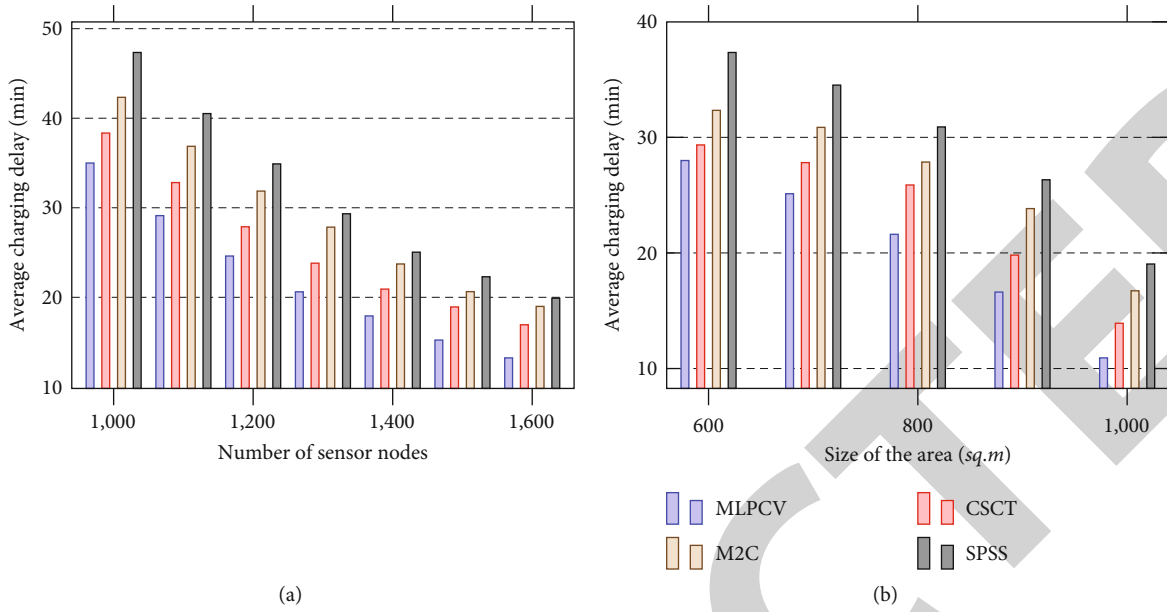


FIGURE 3: Average charging delay: (a) number of sensor nodes; (b) area size.

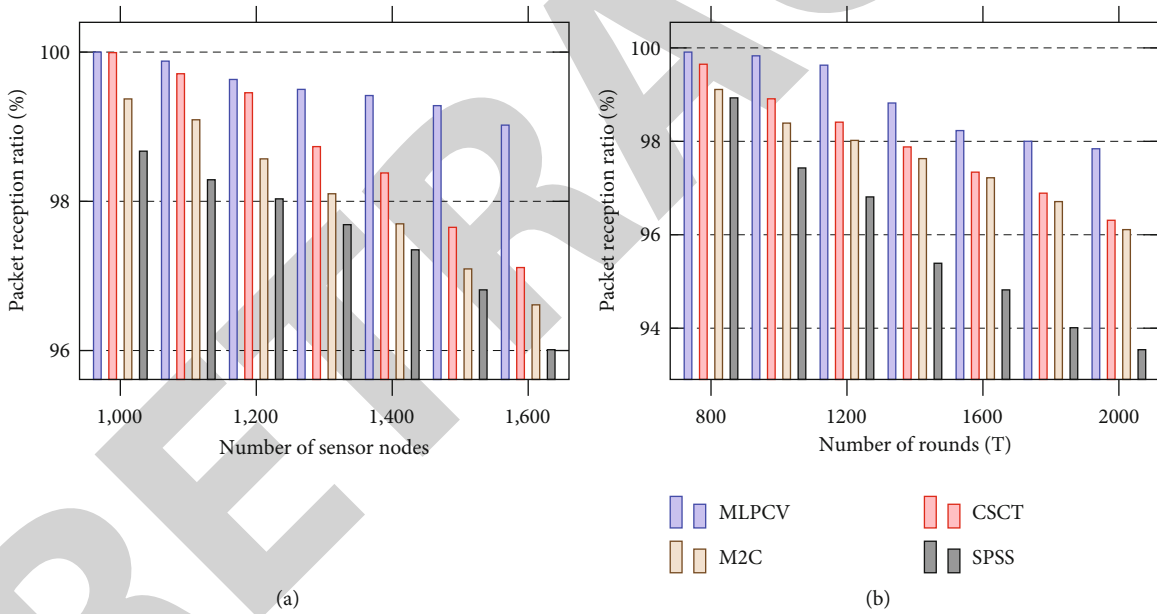


FIGURE 4: Packet reception rate: (a) number of sensor nodes; (b) simulation rounds.

algorithm appears to have a higher NSR than the existing algorithms. As a result of better scheduling by the network, this achievement has been achieved.

From Figure 6(b), we observe an NSR when the network size is expanded from 600 square meters to 1000 square meters with 1000 static SNs deployed randomly. The proposed algorithm also results in better NSR than existing algorithms, but the area size also decreases the NSR. After the 100th cycle of MLPCV, the NSR is changed from 97.85% to 91.12% in the small area when the area size is doubled. According to M2C, SPSS, and J-RCA algorithms, 80.61 percent, 84.85 percent, and 82.81 percent were obtained in the small area with 100 completed cycles, respec-

tively. M2C, SPSS, and J-RCA algorithms produce similar NSRs after 100 cycles in the 1000sq.m. size, as well as 82.82%, 80.872%, and 77.53%.

5.5. Charger Utility Efficiency. As a result of taking into account the CV's total energy usage during travel, data collection, and charging, the charger utility efficiency is calculated.

The CUE of the proposed and existing works is compared by varying the sensor node count and area size in Figures 7(a) and 7(b), respectively. We take the SNs in 1000 square meters based on Figure 7(a). A total of 100 cycles have been completed by both the CV and the

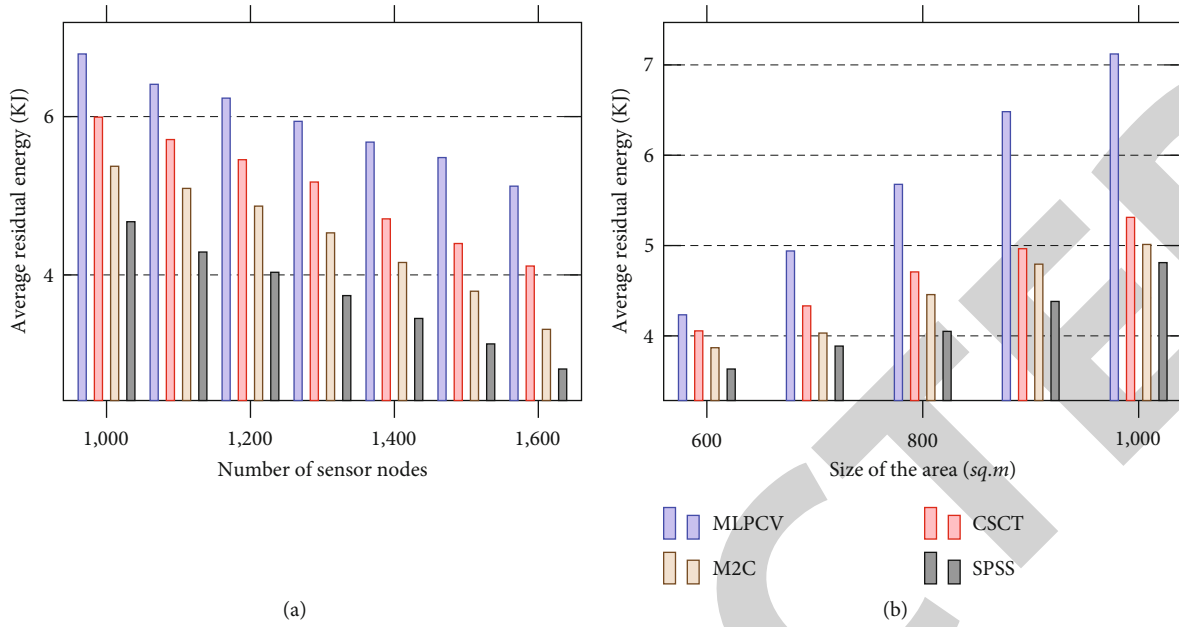


FIGURE 5: Average residual energy: (a) number of sensor nodes; (b) area size.

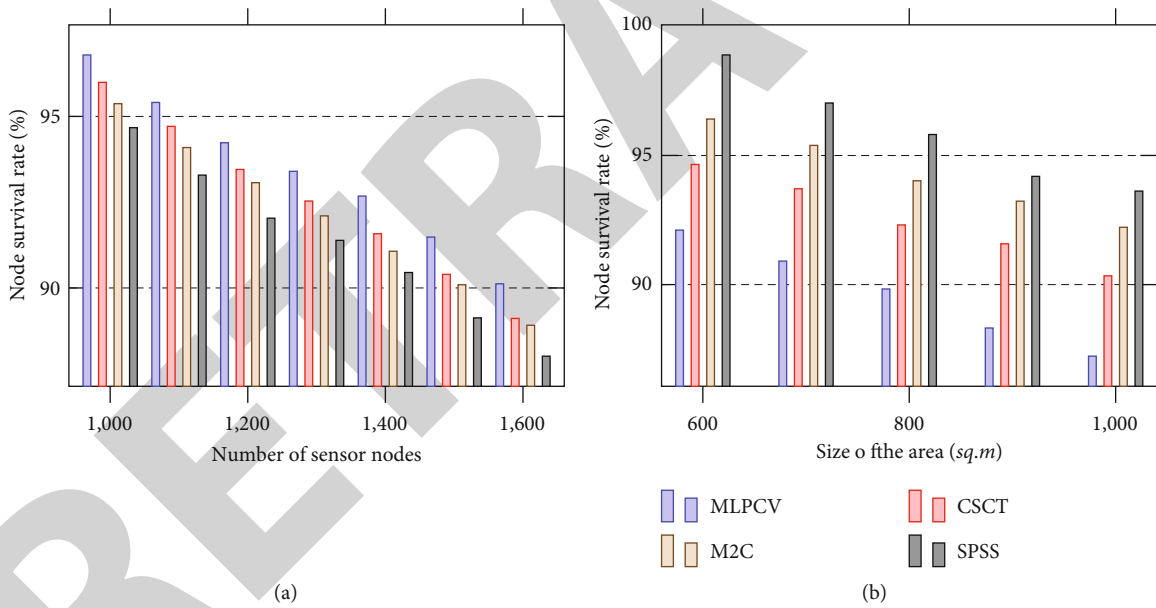


FIGURE 6: Node survival rate: (a) number of sensor nodes; (b) area size.

estimated CUE. Data and charging requests also increased as the number of nodes increased. Comparatively to the existing algorithms, the CV uses 186.23 kJ after the 100 cycles are completed for 1600 SNs. Unlike other existing algorithms, J-RCA drains completely before reaching the 100th cycle, whereas M2C uses 192.7 kJ, SPSS uses 199.31 kJ, etc. In order to recharge all the requests from SPSS and J-RCA algorithms, a large-capacity mobile charger was required. There is also the possibility of partitioning the network into multiple parts and scheduling more CVs to recharge and collect data. This task can be completed with a single CV and served in a timely manner with the proposed work.

We randomly deployed 1000 static SNs in a network with a network size varying from 600 square meters to 1000 square meters as shown in Figure 7(b). In this case, 100 cycles were completed by the CV. Figure 7(b) shows that with a larger area, the CUE is minimized as the network is extended to 1000 sq.m. As a result, the CV has to travel most of the time in order to charge. It is necessary for the CV to travel between various network parts to receive charging requests. In the existing algorithm, the 100th cycle of M2C consumes 196.16 kJ. Before assembling the 94th and 87th cycles, SPSS and J-RCA exhaust their energy completely. The proposed work consumes less energy than these

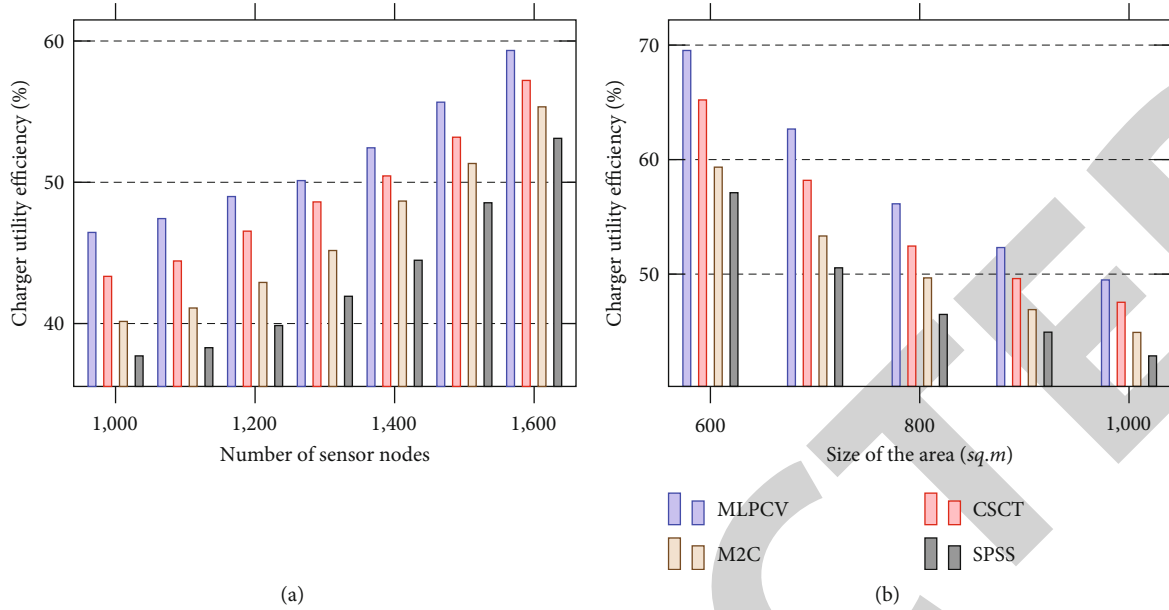


FIGURE 7: Charger utility efficiency: (a) number of sensor nodes; (b) area size.

algorithms, and when it reaches its 100th cycle, it consumes 192.22 kJ. However, it is much better than the existing algorithms but weaker than a small number of sensor nodes.

5.6. Average Service Time. In the process of charging and collecting data, the CV period from the base station is taken and returned to the station after the charging and data collection process is completed. Travel time, waiting time, and data collection time are all included in the service time. All nodes in a network are averaged to determine the AST. Indicators are more efficient when there are fewer of them, and vice versa.

In Figure 8, we compare the AST of the proposed MLPCV to the AST of existing algorithms by varying the number of sensors and the size of the field. Figure 8(a) shows the estimated AST for the proposed and existing works, ranging from 1000 to 1600 sensor nodes in 600 square meters. The proposed work involves ASTs during 1600 SNs in a 1000sq.m area noticed 49.68 minutes after the 100th occurrence. M2C, SPSS, and J-RCA receive 57.56 minutes, 66.74 minutes, and 72.47 minutes, respectively, in the existing algorithms. Comparing the proposed MLPCV to other algorithms, we can see that it serves very quickly. Optimizing the scheduling charger vehicles efficiently for data collection and recharge is the main reason for this improvement.

As shown in Figure 8(b), we notice the AST because we randomly deploy 1600 static SNs rather than 600 sq.m. With more sensor nodes that are randomly deployed, the communication burden is reduced on the SNs than with densely deployed sensors. So by doing this, there will be a reduction in the number of charging requests, and efficiency will be improved. There will not be much difference in AST between small and large fields throughout the system. Our AST changed from 600 square meters to 1000 square meters with 1000 sensor nodes. The ASTs in the proposed work

when the area is 600 square meters and 1000 square meters are 28.51 minutes and 23.43 minutes, respectively. Similarly, in 600 square meters, according to the existing algorithms M2C, SPSS, and J-RCA, 1000 SNs are processed in 28.75 minutes, 31.15 minutes, and 36.19 minutes, respectively. The M2C, SPSS, and J-RCA algorithms return AST when the area reaches 1000 square meters in 29.24, 36.54, and 39.142 minutes, respectively.

5.7. Impact on Link Failure. NSR shows that some SNs in the network are dying as a result of a lack of charging services. Additionally, some sensor nodes may be isolated as a result of the effect on the network link. To evaluate the performance of the existing and proposed work, it is necessary to evaluate this metric. For sensor nodes that fail existing links, the proposed work can identify another relay node. The reclustering mechanism is also present in M2C, which performs the mechanism by which relay nodes are assigned to sensor nodes whose links have failed due to a failure of the link.

Based on the link failure, Figure 9 shows the number of disconnected or isolated nodes as well as the number of partitions caused by the failure. When the partition number is greater than 1, it means that one network partition does not reach the base station, but another part of the network does. From Figure 9(a), we notice the minimum number of disconnected nodes in the network. The performance of the M2C algorithm is the most problematic until a few hours into the data collection, after which SPSS and J-RCA algorithms perform poorly. As a result, the J-RCA algorithm isolates more nodes, although it takes longer to simulate. As well as evaluating the partition count, we also estimate how many partitions are created when separate nodes are present. Yet, the proposed MLPCV does not divide the network into more parts, while isolated nodes form the same groups. By doing so, the base station is able to connect more

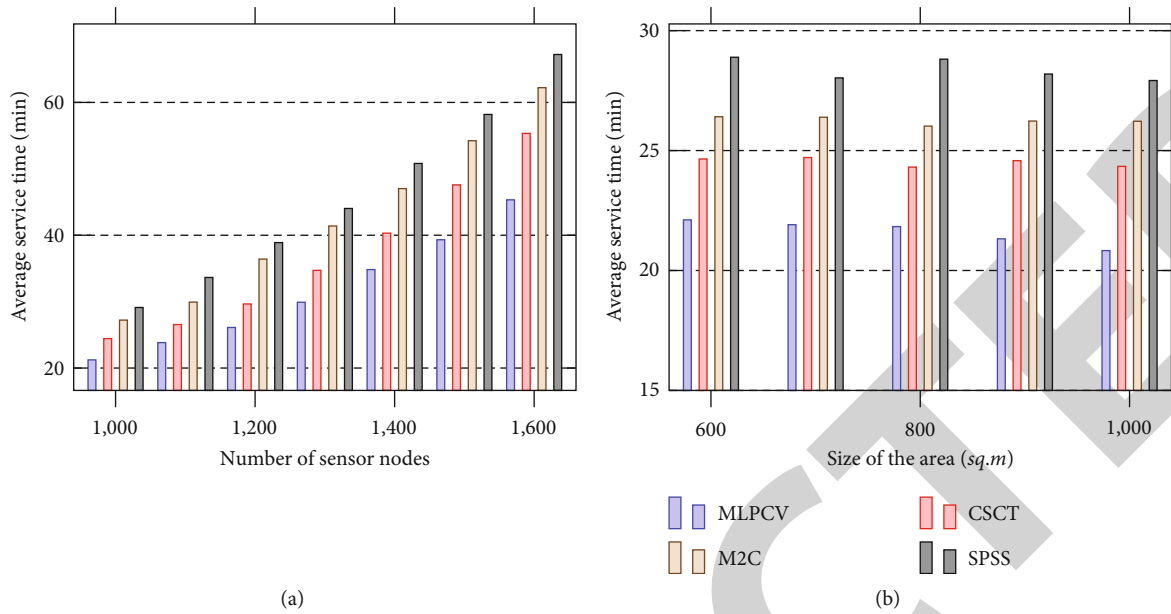


FIGURE 8: Average service time: (a) number of sensor nodes; (b) area size.

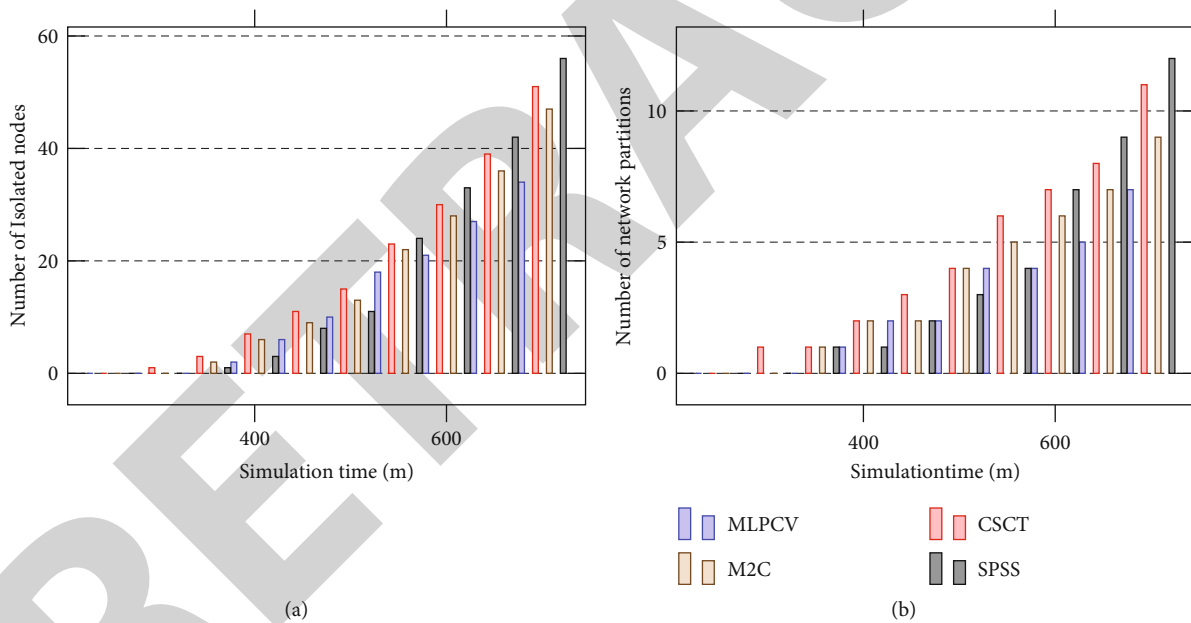


FIGURE 9: Impact on link failure: (a) simulation time vs. isolated nodes; (b) simulation time vs. number of partitions.

SNs. The most accurate results are often obtained through the J-RCA. The number of partitions also increases along with the simulation time, as shown in Figure 9(b). Therefore, compared with other mechanisms, the proposed work maintains a higher level of quality.

6. Conclusion

A mixed linear programming approach is proposed to schedule the charging vehicles in a large-scale WSN to recharge the sensor nodes. The approach is divided into two parts: weights for each SN to determine the charging

device and order and scheduling strategy for the order in which charging requests will be served. Initially, all the CVs are placed in a particular location in the network, which is decided using an intelligent centroid selection approach. Calculate the weight using heuristic formulas and select a schedule based on mixed linear programming. This approach is computationally efficient compared with the existing techniques. Regarding different metrics, the MLPCV approach is superior to the recently published CV scheduling approaches. However, this work achieved outstanding performance, but much more needs to be done in the near future. This is a challenging issue that can be

addressed in the future. Specifically, we can select the optimal number of charging vehicles for a given network according to the number of nodes, battery type, and data generated.

Data Availability

All data generated or analyzed during this study are generated randomly during the simulation. The details about data generation are included in this published article.

Conflicts of Interest

There are no potential conflicts of interest.

References

- [1] D. K. Sah and T. Amgoth, "Renewable energy harvesting schemes in wireless sensor networks: a survey," *Information Fusion*, vol. 63, pp. 223–247, 2020.
- [2] P. K. R. Maddikunta, S. Hakak, M. Alazab et al., "Unmanned aerial vehicles in smart agriculture: applications, requirements, and challenges," *IEEE Sensors Journal*, vol. 21, no. 16, pp. 17608–17619, 2021.
- [3] P. Joshi, A. S. Raghuvanshi, and S. Kumar, "An intelligent delay efficient data aggregation scheduling for distributed sensor networks," *Microprocessors and Microsystems*, vol. 93, p. 104608, 2022.
- [4] D. Praveen Kumar, A. Tarachand, and A. C. S. Rao, "Machine learning algorithms for wireless sensor networks: a survey," *Information Fusion*, vol. 49, pp. 1–25, 2019.
- [5] X. Lan, Y. Zhang, L. Cai, and Q. Chen, "Adaptive transmission design for rechargeable wireless sensor network with a mobile sink," *IEEE Internet of Things Journal*, vol. 7, no. 9, pp. 9011–9025, 2020.
- [6] E. Erdemir and T. E. Tuncer, "Path planning for mobile-anchor based wireless sensor network localization: static and dynamic schemes," *Ad Hoc Networks*, vol. 77, pp. 1–10, 2018.
- [7] C. Bala Subramanian, M. Maragatharajan, and S. P. Balakannan, "Retracted article: inventive approach of path planning mechanism for mobile anchors in wsn," *Journal of Ambient Intelligence and Humanized Computing*, vol. 12, no. 3, pp. 3959–3967, 2021.
- [8] P. Thilagavathi and J. Manickam, "Retracted article: Ertc: an enhanced rssi based tree climbing mechanism for well-planned path localization in wsn using the virtual force of mobile anchor node," *Journal of Ambient Intelligence and Humanized Computing*, vol. 12, no. 6, pp. 6665–6676, 2021.
- [9] H. Patel, D. Singh Rajput, G. Thippa Reddy, C. Iwendi, A. Kashif Bashir, and O. Jo, "A review on classification of imbalanced data for wireless sensor networks," *International Journal of Distributed Sensor Networks*, vol. 16, no. 4, Article ID 1550147720916404, 2020.
- [10] P. K. R. Maddikunta, Q.-V. Pham, D. C. Nguyen et al., "Incentive techniques for the internet of things: a survey," *Journal of Network and Computer Applications*, vol. 206, article 103464, 2022.
- [11] M. Zhang and W. Cai, "Data collecting and energy charging oriented mobile path design for rechargeable wireless sensor networks," *Journal of Sensors*, vol. 2022, Article ID 5004507, 14 pages, 2022.
- [12] M. Majid, S. Habib, A. R. Javed et al., "Applications of wireless sensor networks and internet of things frameworks in the industry revolution 4.0: a systematic literature review," *Sensors*, vol. 22, no. 6, p. 2087, 2022.
- [13] M. Numan, F. Subhan, W. Z. Khan et al., "A systematic review on clone node detection in static wireless sensor networks," *IEEE Access*, vol. 8, pp. 65450–65461, 2020.
- [14] H. Xue, H. Chen, Q. Dai, K. Lin, J. Li, and Z. Li, "CSCT: charging scheduling for maximizing coverage of targets in WRSNs," *IEEE Transactions on Computational Social Systems*, pp. 1–11, 2022.
- [15] A. Tomar, K. Nitesh, and P. K. Jana, "An efficient scheme for trajectory design of mobile chargers in wireless sensor networks," *Wireless Networks*, vol. 26, no. 2, pp. 897–912, 2020.
- [16] M. Srinivas, P. K. Donta, and T. Amgoth, "Mobile charger utility maximization through preemptive scheduling for rechargeable wsns," in *2021 19th OITS International Conference on Information Technology (OCIT)*, pp. 126–131, Bhubaneswar, India, December 2021.
- [17] G. Jiang, S.-K. Lam, Y. Sun, L. Tu, and J. Wu, "Joint charging tour planning and depot positioning for wireless sensor networks using mobile chargers," *IEEE/ACM Transactions on Networking*, vol. 25, no. 4, pp. 2250–2266, 2017.
- [18] S. Priyadarshani, A. Tomar, and P. K. Jana, "An efficient partial charging scheme using multiple mobile chargers in wireless rechargeable sensor networks," *Ad Hoc Networks*, vol. 113, article 102407, 2021.
- [19] W. Xu, W. Liang, X. Jia, H. Kan, Y. Xu, and X. Zhang, "Minimizing the maximum charging delay of multiple mobile chargers under the multi-node energy charging scheme," *IEEE Transactions on Mobile Computing*, vol. 20, no. 5, pp. 1846–1861, 2020.
- [20] C. Lee, W. Na, G. Jang, C. Lee, and S. Cho, "Energyefficient and delay-minimizing charging method with a multiple directional mobile charger," *IEEE Internet of Things Journal*, vol. 8, no. 10, pp. 8291–8303, 2020.
- [21] A. Madhja, S. Nikolettseas, and T. P. Raptis, "Hierarchical, collaborative wireless energy transfer in sensor networks with multiple mobile chargers," *Computer Networks*, vol. 97, pp. 98–112, 2016.
- [22] C. Moraes, S. Myung, S. Lee, and D. Har, "Distributed sensor nodes charged by mobile charger with directional antenna and by energy trading for balancing," *Sensors*, vol. 17, no. 12, p. 122, 2017.
- [23] Y.-C. Wang and J.-W. Huang, "Efficient dispatch of mobile sensors in a wsn with wireless chargers," *Pervasive and Mobile Computing*, vol. 51, pp. 104–120, 2018.
- [24] S. P. R. Banoth, P. K. Donta, and T. Amgoth, "Dynamic mobile charger scheduling with partial charging strategy for wsns using deep-q-networks," *Neural Computing and Applications*, vol. 33, no. 22, pp. 15267–15279, 2021.
- [25] W. Ouyang, X. Liu, M. S. Obaidat et al., "Utility-aware charging scheduling for multiple mobile chargers in large-scale wireless rechargeable sensor networks," *IEEE Transactions on Sustainable Computing*, vol. 6, no. 4, pp. 679–690, 2021.
- [26] W. Na, J. Park, C. Lee, K. Park, J. Kim, and S. Cho, "Energy-efficient mobile charging for wireless power transfer in internet of things networks," *IEEE Internet of Things Journal*, vol. 5, no. 1, pp. 79–92, 2017.
- [27] T. Rault, "Avoiding radiation of on-demand multi-node energy charging with multiple mobile chargers," *Computer Communications*, vol. 134, pp. 42–51, 2019.

Research Article

Fuzzy Data Mining and Bioinformatics Analysis in Methylation Analysis of M6A Gene Promoter Region in Esophageal Cancer

Shuoming Wu, Xiangbao Yang, Xie Qiu, and Yinpeng Pan 

The First People's Hospital of Lianyungang, 222000, China

Correspondence should be addressed to Yinpeng Pan; fengxiang@njmu.edu.cn

Received 28 July 2022; Accepted 18 August 2022; Published 7 September 2022

Academic Editor: Sweta Bhattacharya

Copyright © 2022 Shuoming Wu et al. This is an open access article distributed under the Creative Commons Attribution License, which permits unrestricted use, distribution, and reproduction in any medium, provided the original work is properly cited.

This work was aimed at analyzing the correlation between the methylation level of the M6A gene in esophageal cancer (EC) and the prognosis of patients based on bioinformatics technology and evaluating the prognostic predictive values of different data mining models. 80 EC patients and 80 healthy people were selected, and the serum of the patients was collected to detect the level of DNA methyltransferase. During the radical resection of EC, tumor tissues and adjacent normal tissues were collected from patients to detect the methylation level of the M6A gene. COX regression analysis was employed to analyze the independent risk factors (IRFs) of M6A gene methylation and other treatments affecting the prognosis of EC patients. The particle swarm optimization (PSO) algorithm was introduced to improve the fuzzy C-means clustering (FCM) algorithm. The differences in the prognostic prediction efficiency of logistic regression analysis (LRA), decision tree (DT) C5.0, artificial neural network (ANN), support vector machine (SVM), and improved FCM (IFCM) models were compared. The levels of DNA methyltransferase and human histone deacetylase 1 (HSD-1) in EC patients were increased greatly ($P < 0.05$). The methylation rates and methylation levels of M6A methylation regulators (*ALKBH5*, *HNRNPC*, *METTL3*, *WTAP*, *RBM15*, *YTHDC1*, *YTHDF1*, and *FTO*) in EC tissues were obviously higher ($P < 0.05$). The survival time of high-risk EC patients was much shorter than that of low-risk patients ($P < 0.05$). Univariate and multivariate COX regression analysis showed that gender, tumor grade, TNM grade, degree of infiltration, and methylation of *ALKBH5*, *HNRNPC*, and *METTL3* genes were IRFs for the prognosis of EC patients ($P < 0.05$). The areas under the ROC curve (AUCs) of LRA, DT C5.0, ANN, SVM, and IFCM algorithms for predicting the prognosis of patients were 0.813, 0.857, 0.895, 0.926, and 0.958, respectively, and the IFCM model had the best diagnostic effect. In conclusion, the detection of bioinformatics technology showed no obvious DNA methylation in EC patients, and the elevated levels of M6A methylation regulators in patients were an IRF affecting the prognosis of patients. In addition, the fuzzy data mining model can be undertaken as the preferred method for prognosis prediction of EC patients.

1. Introduction

Esophageal cancer (EC) is a malignant tumor of the upper gastrointestinal tract that occurs in the esophageal epithelial tissue. Histologically, it can be classified into esophageal squamous cell carcinoma and esophageal adenocarcinoma [1]. EC is one of the six most common malignant tumors, and its incidence and pathological types have obvious regional differences [2]. The EC morbidity and mortality of

residents in high-risk areas are 500 times higher than those in endemic areas. Moreover, the prognosis of EC patients is poor, and the 5-year survival rate is only about 10%, and there is no obvious improvement after the improvement of medical level [3]. Due to the high morbidity and mortality of EC, there is an urgent need to find better biomarkers, which can facilitate the early diagnosis of EC and improve the prognosis of patients. Current studies suggest that genetic changes and epigenetic changes are the main

mechanisms of tumor-induced tumor at the gene level [4]. Genetic changes refer to changes in the DNA base sequence, such as gene mutation, microsatellite instability, and deletion of heterozygosity. Epigenetic changes refer to the chemical modification of DNA itself and the regulation of DNA expression at the transcriptional level [5]. Epigenetics includes DNA methylation, genomic stress, and chromatin remodeling. Epigenetics is very common during the occurrence of malignant tumors, mainly the methylation of CpG islands in the promoter regions of tumor suppressor genes [6]. DNA methylation markers can be used in the classification and detection of diseases and can also reflect early changes in the occurrence and development of cancer. Therefore, exploring the DNA methylation of tumor suppressor genes is of great significance for the early diagnosis, risk assessment, prognosis prediction, and monitoring of EC.

RNA methylation modification accounts for 60% of all RNA modifications, and N6-methyladenosine (m⁶A) is the most common modification on mRNA and ncRNAs in higher organisms [7]. m⁶A is a methylation modification that occurs on RNA adenine (A). Current studies have found that miRNA, circRNA, tRNA, and snoRNA all have m⁶A modifications, which are mainly regulated by m⁶A methylation regulators [8]. Studies have confirmed that m⁶A methylation is closely related to the development and progression of tumors, and the expression level of m⁶A regulatory factors may directly determine the pathological process of malignant tumors [9]. Currently known m⁶A methyltransferase complexes include *METTL3* and *METTL14*, and *ALKBH5* and *FTO* can be considered as methylases to reverse methylation [10]. m⁶A-binding protein contains YTH domain proteins (YTHDF1, YTHDF2, YTHDC1, YTHDC2, etc.) and nuclear heterogeneity protein HNRNP family (HNRNPC, etc.) [11]. Abnormally expressed m⁶A methylation regulators can lead to abnormal m⁶A methylation modification, which in turn affects RNA processing, mRNA degradation, and translation and ultimately affects gene expression and promotes tumorigenesis and development [12]. Therefore, m⁶A methylation regulators can be used as potential prognostic biomarkers for the early diagnosis of EC and the prognosis prediction of patients.

In this work, bioinformatics methods and COX regression analysis were employed to find EC-related biomarkers, and a risk model for prognosis prediction of patients was constructed to explore the role of m⁶A methylation regulators in EC prognosis evaluation. Subsequently, an improved fuzzy data mining model was constructed, and the accuracy of different data mining models for prognosis prediction of EC patients was compared, aiming to provide a reference for improving the early diagnosis rate and prognosis prediction accuracy of EC.

2. Materials and Methods

2.1. Research Objects. 80 patients who were diagnosed with EC from March 2020 to January 2022 during clinicopathological examinations in The First People's Hospital of Lianyungang were selected, including 47 males and 33 females, with a median age of 63 years. The 80 normal controls were

from healthy people who underwent physical examination in the medical examination department of The First People's Hospital of Lianyungang during the same period, including 44 males and 36 females, with a median age of 60 years. The inclusion criteria were given as follows: those who met the clinical diagnostic criteria for esophageal cancer and were diagnosed by pathology, patients with complete clinical and follow-up data; and those who had not received chemotherapy or radiotherapy. The exclusion criteria were given as follows: patients with incomplete clinical and follow-up data and healthy people with no malignant tumors. This experiment had been approved by the Clinical Ethics Committee of the The First People's Hospital of Lianyungang, and all patients signed informed consent.

2.2. Determination of Serum Methylation-Related Protein Expression Levels by Enzyme-Linked Immunosorbent Assay (ELISA). 2 mL of fasting venous peripheral blood samples was taken from EC patients and healthy people to take the supernatant after centrifugation. Serum DNA methyltransferases (DNMTs) and human histone deacetylase 1 (HDAC1) were detected by ELISA. DNMTs include DNMT1, DNMT3a, and DNMT3b. The DNMTs and HDAC1 antibodies were coated with specific antibodies, respectively, and solid-phase antibodies were prepared. Then, the solid-phase carrier of the corresponding protein was added to the solid-phase antibody microwells and incubated. Then, horseradish peroxidase-labeled DNMTs and HDAC1 antibody were added to form antibody complexes and washed. 3,3',5,5'-Tetramethylbenzidine was added for color development, and the absorbance of each well was measured at a wavelength of 450 nm using a microplate reader to calculate the DNMTs and HDAC1 protein concentrations.

2.3. Surgical Treatment. All EC patients were treated with EC radical mastectomy. Routine skin preparation was performed before surgery, and artificial pneumothorax was established after tracheal anesthesia. A thoracoscopic observation hole was constructed in the seventh intercostal space of the patient's right axilla to determine the location of the lesion. Three operating holes were established in the third intercostal space of the anterior axillary line and the sixth intercostal space of the posterior axillary line, and surgical-related instruments were inserted into the thoracic tissue, and the mediastinal pleura was incised. The lymph nodes in the tracheoesophageal groove and the surrounding loose tissue were removed, and the esophagus was dissected, and then, lymph node dissection was performed. Subsequently, the surrounding involved tissues were excised, followed by hemostasis, indwelling drainage tube, sputum suction, and closure of pneumothorax. Finally, the patient's cancer tissue and adjacent normal tissue (normal esophageal epithelial tissue at 5 cm around the cancer tissue) were collected for follow-up experiments.

2.4. Determination of DNA Gene Methylation. The tissue DNA extraction kit was adopted to extract DNA from EC tissue, and a UV spectrophotometer was applied to detect

the concentration and purity of extracted DNA, and the DNA that met the requirements is stored in a -20°C refrigerator for later use. The DNA CpG Island Methylation Modification Kit was employed for bisulfite modification of the extracted DNA, and the bisulfite modified DNA was purified according to the instructions of the Promega Wizard Cleanup DNA Purification and Recovery Kit. Sequence numbers of 10 M6A genes including *ALKBH5*, *HNRNPC*, *METTL3*, *METTL14*, *WTAP*, *RBM15*, *YTHDC1*, *YTHDF1*, *YTHDF2*, and *FTO* were searched from the GenBank database (<https://www.ncbi.nlm.nih.gov/gene/>). The primers, including methylated and unmethylated primer sequences, were quantitatively detected by Shanghai Sangon Bioengineering Co., Ltd. The reaction system of PCR amplification was 1.5 mmol/L MgCl_2 , 0.2 mmol/L dNTPs, 200 nmol/L primer, and 2 μL bisulfite modified DNA template, and ddH₂O was used to make up to 25 μL . The degree of PCR reaction was set as 95°C for 10 min, adding 1.0 U hot-start polymerase; 95°C for 30 s, $58^{\circ}\text{C}/56^{\circ}\text{C}$ for 30 s, 72°C for 30 s (35 cycles); and 72°C for 5 min. In addition, it should prepare 2% agarose gel electrophoresis to detect the methylation level of each gene.

2.5. Data Mining Model. In this work, the input data including patient age, gender, tumor differentiation, TNM stage, tumor infiltration, M6A gene methylation, and other data were very neat, without missing values and in line with normal distribution, so no data transformation was required. For data mining, the sigmoid function in the model required the normalization of the original data to be in the range of [0,1]. Therefore, the maximum and minimum method was employed to normalize the data, and the processing equation was given as follows:

$$X = \frac{X - X_{\min}}{X_{\max} - X_{\min}}. \quad (1)$$

In the above equation (1), X_{\min} was the minimum value in the entire column of data, and X_{\max} referred to the maximum value in the entire column of data.

The sampling function of SPSS 19.0 was adopted, and the data were randomly divided into a training set and a test set with a ratio of 3 : 1. The training set included 59 normal controls and 61 EC patients, and the test set included 21 normal controls and 19 EC patients. Based on the sorted data, LRA, DT C5.0, ANN, SVM, and FCM algorithms were employed to construct the lung cancer-normal control prediction model.

- (1) The LRA model was a generalized linear regression analysis model. When it was used in this work, the main parameters in the model needed to be set as multinomial LRA, the modeling method was entered, the basic classification target was 1.0, and the model type was the main effect. The LRA model was trained by using the training set
- (2) The DT C5.0 algorithm was an improvement of the C4.5 model, which can be used for the analysis of

data sets containing large amounts of data [13]. Compared with the C4.5 model, the C5.0 model showed the advantages of fast speed, small scale of generating DT, high classification accuracy, and many options. The information gain of the model was given as follows:

$$\text{Gain ratio}(A) = \frac{\text{Gain}(A)}{-\sum_{i=1}^v (|S_i|/|S|) \log 2(|S_i|/|S|)} \quad (2)$$

In equation (2) above, A represented the data set, and S represented a certain value. The main parameters in the DT C5.0 model used in this work were set to partition selection and output DT. Accuracy was improved by bootstrapping with a pruning severity of 75 and a minimum number of records for subbranch 2. It should ensure global pruning, no discriminative attributes, and no error classification loss.

- (3) ANN is a group of connected units or nodes called artificial neurons, which is a loose modeling method of neurons in biological brains. Each link had a weight, which determined the strength of the node's influence on another node. At present, the most common ANN model is the back propagation (BP) network [14]. Therefore, the training parameters of the ANN model constructed in this work are set to be selected by the quick method. The number of random seeds was 10, the training setting was 50%, the cycle time was 1 min, the optimization condition was memory, the number of hidden layers was 1, and the number of hidden layer nodes was 15. The number of continuations was 200, the initial learning rate was 0.05, the minimum value was 0.01, the maximum value was 0.10, and the decay amount was 25
- (4) SVM is a two-class classification model, which is defined as a linear classifier with the largest interval in the feature space [15]. Because the interval was too large, the SVM model was different from the perceptron. The main parameters when constructing the SVM model in this work were set as nonlinear, stopping criteria = 0.0001, kernel type as polynomial, and gamma = 1
- (5) FCM algorithm is a widely used fuzzy data mining algorithm, but it is very easy to fall into the local extreme value, and the algorithm is sensitive to the setting of the initial value [16]. For this reason, the PSO algorithm was adopted in this work to improve and optimize the FCM algorithm into IFCM. The speed update equation of the standard PSO algorithm was as follows:

$$v_{ij}(t+1) = wv_{ij}(t) + c_1 \text{rand}_1(pbest_{ij}(t) - x_{ij}(t)) + c_2 \text{rand}_2(gbest_{ij}(t) - x_{ij}(t)) \quad (3)$$

In equation (3) above, w was the inertia weight value.

The larger the w was, the particles would perform a global search with a larger step size, and the local development would be finer. In the iterative process of the algorithm, w decreased linearly, which can be expressed as below equation:

$$w = w_{\max} - \frac{n(w_{\max} - w_{\min})}{N}. \quad (4)$$

In equation (4), N was the maximum number of iterations, n referred to the current number of iterations, w_{\max} was the maximum inertia weight, and w_{\min} represented the minimum inertia weight.

The PSO algorithm was adopted to improve the FCM algorithm, and the calculation steps of the algorithm are shown in Figure 1. Firstly, the PSO algorithm was used to solve the global optimal clustering center: (1) the initial setting of the clustering division of the FCM algorithm was carried out. It should set the initial position of the particle and the optimal position of the individual in the PSO algorithm and initialize the particle velocity to obtain the global optimal position and fitness. The initial number of iterations was $n = 1$. (2) The position and velocity of the individual in the particle swarm and the inertia weight w were updated. (3) It should set the cluster center according to the position of the particle and calculate the attribute value of the particle and the membership matrix of the FCM. (4) It should determine the individual optimal value of the particle and the overall optimal value. (5) Judgment of the termination condition was performed. If satisfied, it could output the global optimal solution and enter the next stage of calculation; if not, it should return to step (2). (6) It should take the global optimal solution as the initial clustering center, initialize the parameters of the FCM algorithm, and calculate the membership matrix. (7) It could calculate the cluster center Z in the FCM algorithm after iteration and calculate the membership function. (8) The condition for determining whether the threshold of iteration was full or not. If satisfied, the clustering had converged and the clustering result can be terminated; if not, it should return to step (7).

The data mining models LRA, DT C5.0, ANN, and SVM adopted in this work needed to be constructed by SPSS 19.0. The IFCM algorithm needed to be implemented using Matlab R2010a software. Before processing the experimental data, it was also necessary to use the data set in the UCI machine learning database to test the algorithm. The data set used in this work to test the clustering performance of the IFCM algorithm was Glass, which contained 214 research objects, the number of clusters was 6, and the attribute was 9.

2.6. Statistical Analysis. SPSS 19.0 was employed to organize and analyze the data. Enumeration data were expressed by n (%), and differences were compared using the chi-square test. Measurement data were expressed as mean \pm sd, and differences were compared using t test. Kaplan-Meier curves were drawn for EC patient survival analysis. The factors affecting the prognosis of EC patients were analyzed by Cox regression analysis model, the hypothesis test of regres-

sion coefficients was set as the likelihood ratio test, and variable screening was set as backward. The diagnostic tests were used to evaluate the prediction effects of various data mining models. Evaluation indicators included sensitivity (Se), specificity (Sp), accuracy (Acc), AUC, positive predictive value (PPV), and negative predictive value (NPV). AUC > 0.9 was the best. The test level was $\alpha = 0.05$ (two-tailed), and $P < 0.05$ was considered statistically significant.

3. Results

3.1. General Data. The differences between the general data of EC patients and normal controls were compared, as shown in Table 1. No obvious difference was found in the mean age, sex ratio, smoking history, diabetes history, and hypertension history between EC patients and normal controls ($P > 0.05$).

3.2. Detection of DNA Methylase Levels in EC Patients. The differences in the expression levels of DNA methylases DNMT1, DNMT3a, DNMT3b, and HDAC1 in the EC and healthy people were detected, as shown in Figure 2. Levels of DNMT1, DNMT3a, DNMT3b, and HDAC1 in healthy people were $21.55 \pm 1.24 \mu\text{g/L}$, $1123.67 \pm 128.65 \mu\text{g/L}$, $759.21 \pm 91.33 \mu\text{g/L}$, and $20.35 \pm 7.43 \mu\text{g/L}$, respectively, while those of EC patients were $49.51 \pm 1.62 \mu\text{g/L}$, $2985.42 \pm 130.12 \mu\text{g/L}$, $1120.99 \pm 118.62 \mu\text{g/L}$, and $69.03 \pm 11.87 \mu\text{g/L}$, respectively. The expression levels of DNMT1, DNMT3a, DNMT3b, and HDAC of EC patients were much higher ($P < 0.05$).

3.3. M6A Gene Methylation Analysis of EC Patients. The differences in methylation rates of *ALKBH5*, *HNRNPC*, *METTL3*, *METTL14*, *WTAP*, *RBM15*, *YTHDC1*, *YTHDF1*, *YTHDF2*, and *FTO* in EC cancer tissues and adjacent normal tissues were compared, as shown in Figure 3. It was found that the methylation rates of *ALKBH5*, *HNRNPC*, *METTL3*, *METTL14*, *WTAP*, *RBM15*, *YTHDC1*, *YTHDF1*, *YTHDF2*, and *FTO* in adjacent normal tissues were sharply lower ($P < 0.05$). The methylation rates of *ALKBH5*, *HNRNPC*, *METTL3*, *WTAP*, *RBM15*, *YTHDC1*, *YTHDF1*, and *FTO* in EC tissues were observably higher ($P < 0.05$). However, no great difference was observed between the methylation rate and unmethylation rate of *METTL14* and *YTHDF2* ($P > 0.05$).

The differences in *ALKBH5*, *HNRNPC*, *METTL3*, *METTL14*, *WTAP*, *RBM15*, *YTHDC1*, *YTHDF1*, *YTHDF2*, and *FTO* methylation levels in tumor tissues and adjacent normal tissues of EC patients were compared, as shown in Figure 4. The *ALKBH5*, *HNRNPC*, *METTL3*, *WTAP*, *RBM15*, *YTHDC1*, *YTHDF1*, and *FTO* methylation levels in EC tissues were higher ($P < 0.05$). However, no visible difference was observed in *METTL14* and *YTHDF2* methylation levels between EC tissues and adjacent normal tissues ($P > 0.05$).

3.4. IRF Analysis of EC Prognostic Impact. Univariate COX regression analysis of risk factors affecting the survival rate of EC patients is shown in Table 2. There were notable differences in gender, tumor grade, TNM stage, degree of

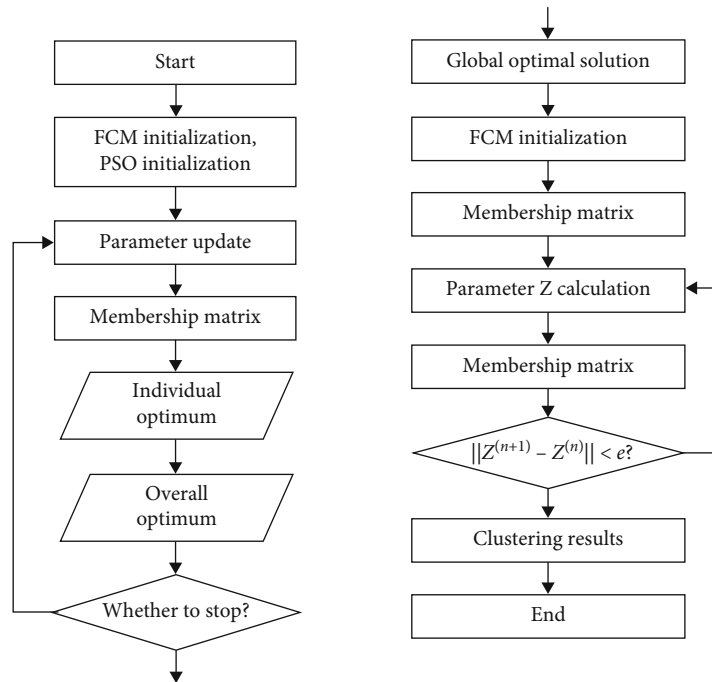


FIGURE 1: The process of improved fuzzy data mining algorithm.

TABLE 1: Comparison of general data of patients.

Item	EC	Controls	t/χ^2	P
n	80	80		
Age (years old)	63.59 ± 8.90	60.55 ± 10.42	1.298	0.513
Gender ($n/\%$)			-0.194	0.660
Male	47/58.8	44/55.0		
Female	33/41.2	36/45.0		
Smoking history ($n/\%$)			1.017	0.579
Yes	52/65.0	49/61.3		
No	28/35.0	31/38.7		
History of diabetes ($n/\%$)			1.598	0.434
Yes	60/75.0	58/72.5		
No	20/25.0	22/27.5		
History of hypertension ($n/\%$)			1.021	0.570
Yes	34/42.5	31/38.8		
No	46/57.5	49/61.2		

infiltration, and methylation of *ALKBH5*, *HNRNPC*, *METTL3*, and *YTHDC1* genes among EC patients with different survival rates ($P < 0.05$). The survival rate of EC patients with different ages and *METTL14*, *WTAP*, *RBM15*, *YTHDF1*, *YTHDF2*, and *FTO* methylation levels showed no obvious difference ($P > 0.05$).

According to the median risk assessment in TCGA database, EC patients were rolled into high-risk and low-risk groups, and Kaplan-Meier curves were used to analyze the differences in survival between EC patients with different risks, as shown in Figure 5. The overall survival of patients in the high-risk group of EC was shorter in contrast to that

in the low-risk group ($P < 0.05$). The AUC of the M6A gene methylation prediction model was 0.803, suggesting that the model had good sensitivity and specificity.

Multivariate COX regression analysis of IRF affecting the prognosis of EC patients is shown in Table 3. The results showed that gender, tumor grade, TNM grade, degree of infiltration, *ALKBH5*, *HNRNPC*, and *METTL3* were the IRFs that affected the prognosis of EC patients ($P < 0.05$), while *YTHDC1* was not ($P > 0.05$).

3.5. Validation of the Improved Fuzzy Data Mining Algorithm. Firstly, $f_1(x) = \sum_{i=1}^{D-1} [100(x_{i+1} - x_i)^2 + (x_i - 1)^2]$

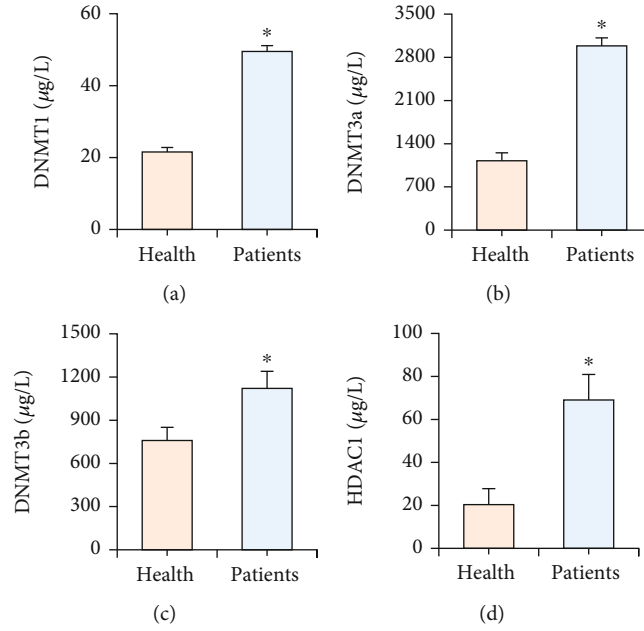


FIGURE 2: Detection of DNMT1, DNMT3a, DNMT3b, and HDAC1 of EC and healthy people. (a) DNMT1 level; (b) DNMT3a level; (c) DNMT3b level; (d) HDAC1 level; and * meant $P < 0.05$ compared with the health group.

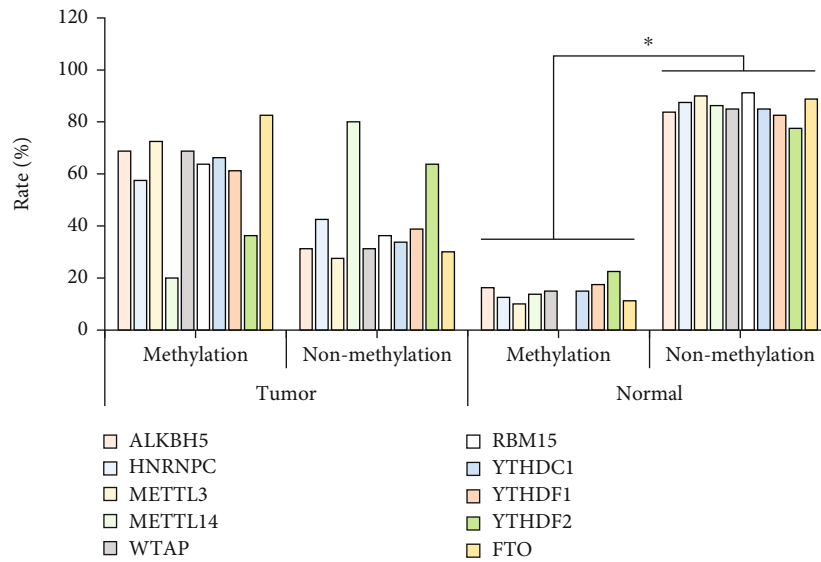


FIGURE 3: Detection of *ALKBH5*, *HNRNPC*, *METTL3*, *METTL14*, *WTAP*, *RBM15*, *YTHDC1*, *YTHDF1*, *YTHDF2*, and *FTO* methylation rates in EC and healthy people. * meant $P < 0.05$.

was adopted to verify the computational performance of the PSO algorithm used in this work. The maximum number of iterations in the PSO algorithm was set to 1000, the initial population size was 30, and the optimal solution of the algorithm was analyzed in 10, 30, 50, and 100 dimensions, as shown in Figure 6. It was found that with the increase of the algorithm dimension, the error of the PSO algorithm in searching for the optimal solution gradually increased, but the overall solution accuracy of the algorithm model was better. The PSO algorithm was employed to optimize the FCM

algorithm. It can be found that when the optimized IFCM algorithm was used for testing on the Glass data set, the error was 0.64 ± 0.08 , while it was 0.81 ± 0.05 before the optimization. It showed that using the PSO algorithm to optimize the FCM algorithm can obtain more accurate prediction results.

3.6. *EC Prognosis Prediction Evaluation Using the Data Mining Model.* The differences between the effects of different data mining models for the prognosis prediction and evaluation of EC patients were compared, as shown in Figure 7. The

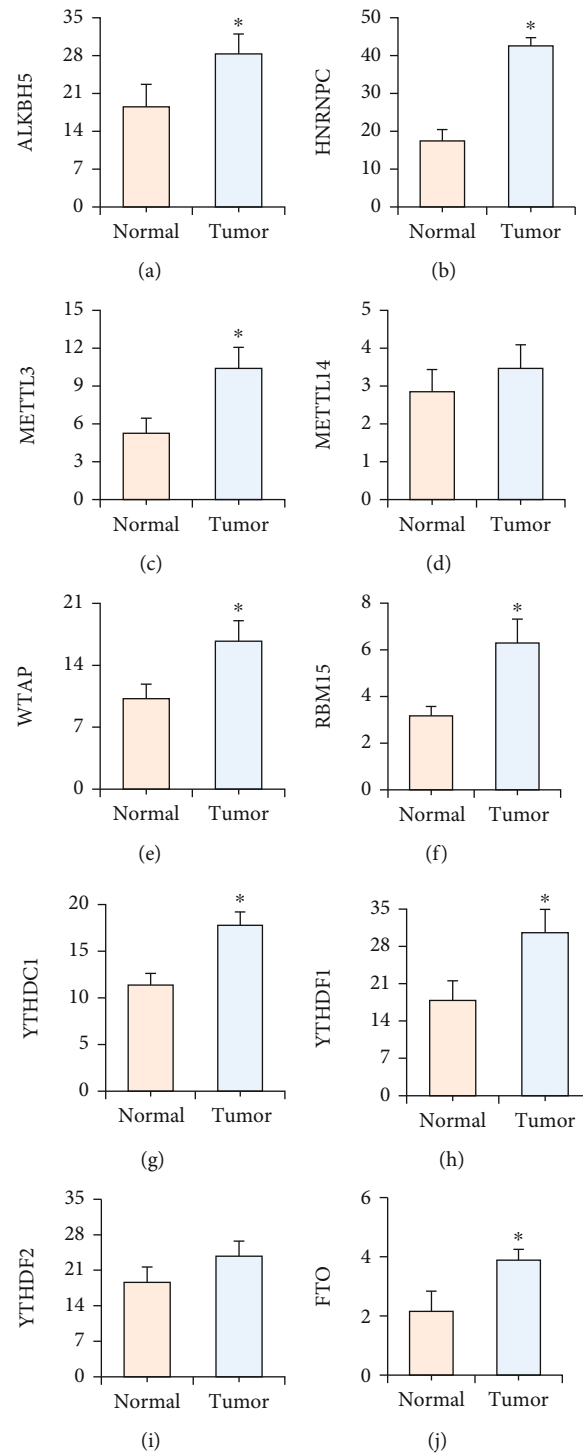


FIGURE 4: Detection of *ALKBH5*, *HNRNPC*, *METTL3*, *METTL14*, *WTAP*, *RBM15*, *YTHDC1*, *YTHDF1*, *YTHDF2*, and *FTO* methylation level in EC lesions and adjacent tissues. (a) *ALKBH5* methylation level; (b) *HNRNPC* methylation level; (c) *METTL3* methylation level; (d) *METTL14* methylation level; (e) *WTAP* methylation level; (f) *RBM15* methylation level; (g) *YTHDC1* methylation level; (h) *YTHDF1* methylation level; (i) *YTHDF2* methylation level; (j) *FTO* methylation level. * meant $P < 0.05$ compared with the normal group.

TABLE 2: Univariate analysis of prognosis in EC patients.

Indicators		<i>n</i>	Survival rate (%)			χ^2	<i>P</i>
			1 year	2 years	3 years		
Age (years old)	<65	54	75.9	51.9	38.9	0.213	0.098
	≥ 65	26	88.5	65.4	46.2		
Gender	Male	47	83.0	55.3	38.3	2.358	0.001
	Female	33	84.8	57.6	45.5		
Tumor grade	High	59	81.4	55.9	47.5	3.065	0.001
	Middle	16	87.5	56.3	43.8		
TNM staging	IIa/IIb	34	82.4	67.6	52.9	2.117	0.001
	III/IV	46	89.1	69.6	45.7		
Tumor infiltration	T1/T2	29	86.2	72.4	48.3	2.229	0.001
	T3	51	76.5	45.1	33.3		
<i>ALKBH5</i>	Yes	55	69.1	47.3	30.9	3.513	0.001
	No	25	88.0	64.0	40.0		
<i>HNRNPC</i>	Yes	46	60.9	37.0	32.6	3.370	0.001
	No	34	79.4	47.1	35.3		
<i>METTL3</i>	Yes	58	70.7	48.3	32.8	2.694	0.001
	No	22	86.4	59.1	36.4		
<i>METTL14</i>	Yes	16	87.5	68.8	37.5	0.513	0.067
	No	64	89.1	67.2	40.6		
<i>WTAP</i>	Yes	55	78.2	49.1	32.7	0.448	0.093
	No	25	80.0	56.0	36.0		
<i>RAM15</i>	Yes	51	76.5	47.1	35.3	0.550	0.088
	No	29	82.8	58.6	34.5		
<i>YTHDC1</i>	Yes	53	77.4	49.1	37.7	3.357	0.001
	No	27	85.2	66.7	33.3		
<i>YTHDF1</i>	Yes	49	83.7	51.0	32.7	0.215	0.102
	No	31	87.1	54.8	35.5		
<i>YTHDF2</i>	Yes	29	79.3	51.7	31.0	0.134	0.083
	No	51	76.5	54.9	33.3		
<i>FTO</i>	Yes	66	81.8	45.5	31.8	0.209	0.114
	No	24	83.3	54.2	33.3		

diagnostic Se, Sp, Acc, PPV, NPV, and AUC of LRA, DT C5.0, ANN, SVM, and IFCM algorithms were 68.8%, 83.8%, 76.3%, 80.9%, 72.8%, and 0.813; 63.8%, 91.3%, 77.5%, 87.9%, 71.6%, and 0.857; 86.3%, 65.0%, 75.6%, 71.1%, 82.5%, and 0.895; 88.8%, 85.0%, 86.9%, 85.5%, 88.3%, and 0.926; and 93.8%, 90.0%, 91.9%, 90.4%, 93.5%, and 0.958, respectively. It can be observed that the diagnostic effect of the IFCM model was the best.

4. Discussion

EC is a malignant tumor of the digestive tract due to esophageal epithelial cell lesions. Malnutrition, high eating temperature, smoking, and drinking are the main risk factors for EC, in addition to obesity, gastroesophageal reflux, advanced age, etc. [17]. A large amount of clinical evidence shows that the overall survival rate of EC patients is low, and the 5-year survival rate of patients is only 10% to 19% [18, 19]. In the pro-

cess of EC, epigenetic changes can lead to the activation of protooncogenes and the inactivation of tumor suppressor genes. DNA methylation is the main form of epigenetic modification, which is mainly the methylation of cytosine in the CpG sequence of gene promoter region to regulate gene expression level [20]. Therefore, DNA methylation is the main mechanism leading to the silencing/inactivation of tumor suppressor genes. The methylation process of DNA requires the catalysis of DNA methyltransferases (DNMT1, DNMT2, DNMT3a, and DNMT3b), transfers the methyl group from *s*-adenosylmethionine to the five carbon atoms of the cytosine ring, and finally forms DNA methylation [21]. HDACs also play an important role in tumor progression. When the expression of HDACs is upregulated, gene expression will be downregulated due to changes in chromatin structure, thereby affecting tumor progression [22]. In this work, the differences between the protein levels of DNMT1, DNMT3a, DNMT3b, and HDAC1 in peripheral

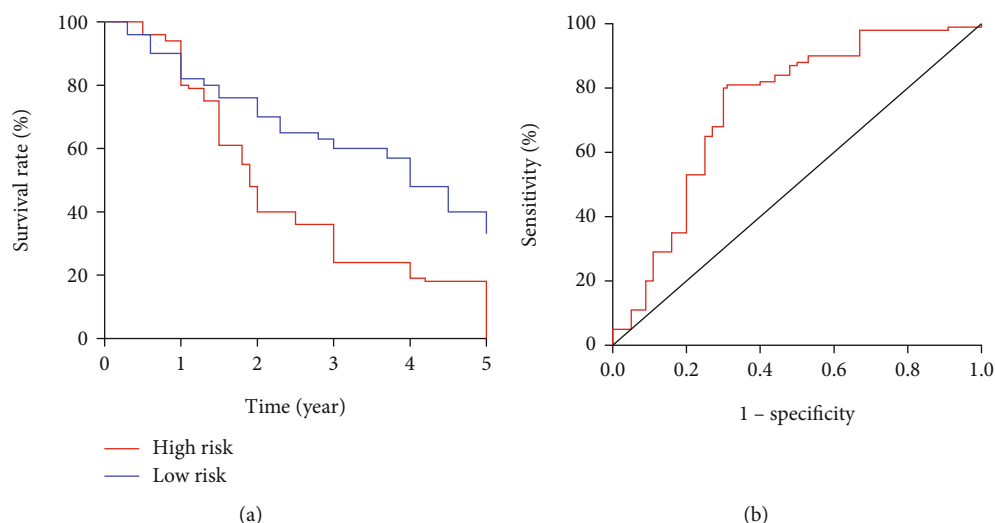


FIGURE 5: Prognostic analysis of EC patients with different risks. (a) Survival analysis; (b) ROC curve.

TABLE 3: Multivariate analysis of prognosis in EC patients.

Item	β	SE	Wald	df	P	HR	95% CI
Gender	-0.317	0.138	5.163	1	0.013	0.629	0.515~0.826
Tumor grade	0.508	0.154	4.891	1	0.010	1.083	0.667~3.015
TNM stage	0.411	0.247	6.558	1	0.005	1.597	0.753~2.729
Degree of infiltration	0.793	0.261	7.519	1	0.006	2.318	1.160~4.187
<i>ALKBH5</i>	0.188	0.114	6.783	1	0.003	1.936	0.614~3.151
<i>HNRNPC</i>	0.091	0.082	5.996	1	0.015	1.359	1.031~1.782
<i>METTL3</i>	0.085	0.195	6.605	1	0.039	0.958	0.513~1.575
<i>YTHDC1</i>	0.103	0.130	3.471	1	0.057	1.851	0.735~2.956

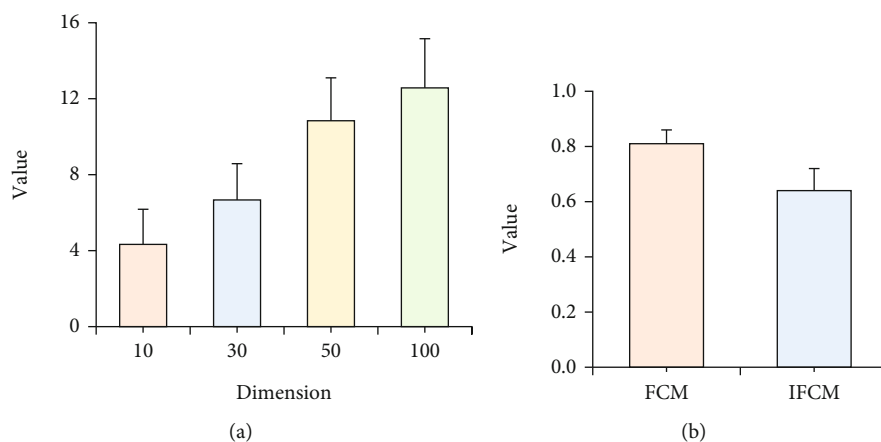


FIGURE 6: Verification of fuzzy data mining algorithm. (a) PSO algorithm solution results; (b) verification results of improved fuzzy data mining algorithm.

blood of EC patients and healthy people were detected, and it was found that the protein levels of DNMT1, DNMT3a, DNMT3b, and HDAC1 in peripheral blood of EC patients were significantly increased. It indicated that the high methylation level of related genes in the peripheral blood of EC patients may be involved in the disease process.

M6A is a very common methylation modification in eukaryotic mRNA. More and more studies have confirmed that M6A can regulate RNA stability, localization, splicing, and translation at the posttranscriptional level [23, 24]. M6A methylation is a dynamic and reversible process, which is regulated by three main types of methylation regulators,

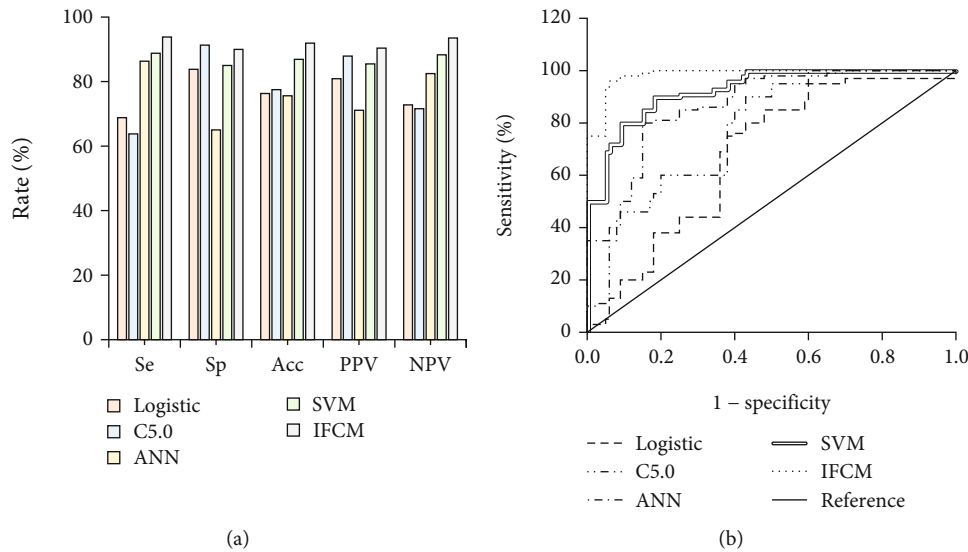


FIGURE 7: Analysis of the effect of different data mining models in predicting EC. (a) Evaluation of prediction efficiency; (b) ROC curve.

namely, methyltransferases, demethylases, and methylation-binding proteins. Methyltransferase can promote the methylation modification of RNA by M6A, and its encoding genes include *METTL3*, *METTL14*, *WTAP*, and *RBM15* [25]. Demethylase can remove the M6A group in RNA and maintain the M6A methylation in a dynamic and reversible transition, and its main encoding genes include *ALKBH5* and *FTO* [26]. Methylation-binding proteins can bind to and function at M6A methylation sites in RNA, and their main encoding genes include *YTHDC1*, *YTHDC2*, *YTHDF1*, and *HNRNPC* [27]. M6A methylation modification plays an important role in the regulation of gene expression, and the abnormality of its regulatory mechanism may be involved in the occurrence and development of disease or cancer. This work searched TCGA database to download and extract gene expression data for 13 EC-related M6A methylation regulators. Bioinformatics technology and analysis of test results showed that *ALKBH5*, *HNRNPC*, *METTL3*, *WTAP*, *RBM15*, *YTHDC1*, *YTHDF1*, and *FTO* methylation levels in EC patient tissues were significantly higher than those in adjacent normal tissues. It indicated that the level of M6A methylation regulators was closely related to the occurrence and development of EC. Then, univariate and multivariate COX regression analysis was performed to affect the prognosis of EC patients, and it was found that gender, tumor grade, TNM grade, degree of infiltration, *ALKBH5*, *HNRNPC*, and *METTL3* were the IRFs that affected the prognosis of EC patients. Tumor degree of infiltration is closely related to lymph node metastasis, which can be used in EC lymph node metastasis and prognosis evaluation [28]. The perioperative immune function of female EC patients is often better than that of males, and the postoperative quality of life of female EC patients is better, so gender is a protective factor for the prognosis of EC [29]. EC patients with high *ALKBH5* expression have a better prognosis because *ALKBH5* is able to inhibit the initiating ability of malignancy. *METTL3* can promote the growth, survival, and invasion of lung adenocarcinoma cells. *METTL3* deletion can

change the enrichment state of M6A and promote the growth, self-renewal, and tumor formation of glioma cells [30]. *HNRNPC* expression is upregulated in cancer cells, which can control endogenous dsRNA and lower-level interferon response in breast cancer cells and then participate in the disease process [31]. In this work, a prognostic model of EC patients was constructed and it was found that the level of M6A methylation regulators was closely related to the progression of the disease, so it can be undertaken as a molecular marker for the early diagnosis and prognosis prediction of EC for further research.

The combined detection of molecular markers can be used for early auxiliary diagnosis of EC, as well as for follow-up and recurrence detection after treatment. To find the deep relationship between variables, data mining technology can solve such multiparameter problems. Medical data has the characteristics of diversity, complexity, redundancy, irregularity, and timeliness. It is impossible to find the hidden laws of data only by relying on the clinical experience of doctors and traditional data statistics methods [32]. Data mining technology provides methodological support, which can combine computers, ANN, and cancer diagnosis to build an intelligent expert system, so it has become a research hotspot in the medical field. This work used logistic regression model, DT C5.0 model, ANN model, SVM model, and IFCM model to predict the prognosis of EC. The results showed that the predicted Se of the above model was 68.8%, 63.8%, 86.3%, 88.8%, and 93.5%, respectively; the Sp was 83.8%, 91.3%, 65.0%, 85.0%, and 90.0%, respectively; the Acc was 76.3%, 77.5%, 75.6%, 86.9%, and 91.9%, respectively; and the AUC was 0.813, 0.857, 0.895, 0.926, and 0.958, respectively. The logistic regression model needs to determine the effect of each variable based on the OR value of the independent variables in the multivariate analysis, so its prediction efficiency is relatively low [33]. ANN model has strong learning ability and fault tolerance ability, and its ability to identify and predict new samples is outstanding, and it is better than the logistic regression model [34]. Using

the PSO algorithm to improve FCM can improve the global search ability of the algorithm, reduce the scale difference between data objects, avoid the FCM algorithm falling into local extreme values, and reduce the sensitivity of the algorithm to the initial value setting [35]. In this work, the IFCM algorithm was employed to predict the prognosis of EC, which had stronger model division ability and better clustering effect.

5. Conclusions

The levels of DNA methyltransferase in peripheral blood of EC patients were significantly increased, and the levels of M6A methylation regulators *ALKBH5*, *HNRNPC*, *METTL3*, *WTAP*, *RBM15*, *YTHDC1*, *YTHDF1*, and *FTO* were increased in EC tissues. Tumor grade, TNM grade, degree of infiltration, and M6A methylation regulators *ALKBH5*, *HNRNPC*, and *METTL3* were IRFs for EC prognosis, and gender was a protective factor. The integration of M6A methylation regulators and clinical gender and other information combined with data mining technology for EC early diagnosis and prognosis prediction model showed good accuracy. This work only used the M6A methylation regulator data in TCGA database to construct and validate the EC patient prognosis evaluation model. Future research needed to further explore the CpG islands in the promoter regions of each factor to further improve the results of this work. This work can provide reference materials for the early diagnosis and prognosis evaluation of EC.

Data Availability

The data used to support the findings of this study are included within the article.

Conflicts of Interest

The authors declare that they have no conflicts of interest.

References

- [1] F. L. Huang and S. J. Yu, "Esophageal cancer: risk factors, genetic association, and treatment," *Asian Journal of Surgery*, vol. 41, no. 3, pp. 210–215, 2018.
- [2] D. J. Uhlenhopp, E. O. Then, T. Sunkara, and V. Gaduputi, "Epidemiology of esophageal cancer: update in global trends, etiology and risk factors," *Clinical Journal of Gastroenterology*, vol. 13, no. 6, pp. 1010–1021, 2020.
- [3] T. Jordan, D. M. Mastnak, N. Palamar, and N. R. Kozjek, "Nutritional therapy for patients with esophageal cancer," *Nutrition and Cancer*, vol. 70, no. 1, pp. 23–29, 2018.
- [4] L. Zhang, Q. Lu, and C. Chang, "Epigenetics in health and disease," *Advances in Experimental Medicine and Biology*, vol. 1253, pp. 3–55, 2020.
- [5] P. Kaliman, "Epigenetics and meditation," *Current Opinion in Psychology*, vol. 28, pp. 76–80, 2019.
- [6] L. Villanueva, D. Álvarez-Errico, and M. Esteller, "The contribution of epigenetics to cancer immunotherapy," *Trends in Immunology*, vol. 41, no. 8, pp. 676–691, 2020.
- [7] T. Sun, R. Wu, and L. Ming, "The role of m6A RNA methylation in cancer," *Biomedecine & Pharmacotherapie*, vol. 112, article 108613, 2019.
- [8] S. Ma, C. Chen, X. Ji et al., "The interplay between m6A RNA methylation and noncoding RNA in cancer," *Journal of Hematology & Oncology*, vol. 12, no. 1, p. 121, 2019.
- [9] X. Guo, K. Li, W. Jiang et al., "RNA demethylase ALKBH5 prevents pancreatic cancer progression by posttranscriptional activation of PER1 in an m6A-YTHDF2-dependent manner," *Molecular Cancer*, vol. 19, no. 1, p. 91, 2020.
- [10] J. Han, J. Z. Wang, X. Yang et al., "METTL3 promote tumor proliferation of bladder cancer by accelerating pri-miR221/222 maturation in m6A-dependent manner," *Molecular Cancer*, vol. 18, no. 1, p. 110, 2019.
- [11] T. Liu, Q. Wei, J. Jin et al., "The m6A reader YTHDF1 promotes ovarian cancer progression via augmenting EIF3C translation," *Nucleic Acids Research*, vol. 48, no. 7, pp. 3816–3831, 2020.
- [12] S. Müller, M. Glaß, A. K. Singh et al., "IGF2BP1 promotes SRF-dependent transcription in cancer in a m6A- and miRNA-dependent manner," *Nucleic Acids Research*, vol. 47, no. 1, pp. 375–390, 2019.
- [13] K. Makino, S. Lee, S. Bae et al., "Simplified decision-tree algorithm to predict falls for community-dwelling older adults," *Journal of Clinical Medicine*, vol. 10, no. 21, p. 5184, 2021.
- [14] X. Zhou, Y. Li, and W. Liang, "CNN-RNN based intelligent recommendation for online medical pre-diagnosis support," *IEEE/ACM Transactions on Computational Biology and Bioinformatics*, vol. 18, no. 3, pp. 912–921, 2021.
- [15] Z. Wan, Y. Dong, Z. Yu, H. Lv, and Z. Lv, "Semi-supervised support vector machine for digital twins based brain image fusion," *Frontiers in Neuroscience*, vol. 15, article 705323, 2021.
- [16] J. Yin, H. Chang, D. Wang, H. Li, and A. Yin, "Fuzzy C-means clustering algorithm-based magnetic resonance imaging image segmentation for analyzing the effect of edaravone on the vascular endothelial function in patients with acute cerebral infarction," *Contrast Media & Molecular Imaging*, vol. 2021, article 4080305, 2021.
- [17] A. Ashok, D. Niyogi, P. Ranganathan et al., "The enhanced recovery after surgery (ERAS) protocol to promote recovery following esophageal cancer resection," *Surgery Today*, vol. 50, no. 4, pp. 323–334, 2020.
- [18] H. He, N. Chen, Y. Hou et al., "Trends in the incidence and survival of patients with esophageal cancer: a SEER database analysis," *Thoracic Cancer*, vol. 11, no. 5, pp. 1121–1128, 2020.
- [19] G. I. Moral Moral, M. Viana Miguel, Ó. Vidal Doce et al., "Complicaciones postoperatorias y supervivencia del cancer de esofago: analisis de dos periodos distintos," *Cirugía Española (English Edition)*, vol. 96, no. 8, pp. 473–481, 2018.
- [20] S. Horvath and K. Raj, "DNA methylation-based biomarkers and the epigenetic clock theory of ageing," *Nature Reviews Genetics*, vol. 19, no. 6, pp. 371–384, 2018.
- [21] H. Takeshima, T. Niwa, S. Yamashita et al., "TET repression and increased DNMT activity synergistically induce aberrant DNA methylation," *The Journal of Clinical Investigation*, vol. 130, no. 10, pp. 5370–5379, 2020.
- [22] M. Edderkaoui, C. Chheda, B. Soufi et al., "An inhibitor of GSK3B and HDACs kills pancreatic cancer cells and slows pancreatic tumor growth and metastasis in mice," *Gastroenterology*, vol. 155, no. 6, pp. 1985–1998.e5, 2018.

- [23] H. Zhang, X. Shi, T. Huang et al., "Dynamic landscape and evolution of m6A methylation in human," *Nucleic Acids Research*, vol. 48, no. 11, pp. 6251–6264, 2020.
- [24] S. Oerum, V. Meynier, M. Catala, and C. Tisné, "A comprehensive review of m6A/m6Am RNA methyltransferase structures," *Nucleic Acids Research*, vol. 49, no. 13, pp. 7239–7255, 2021.
- [25] S. Oerum, M. Catala, C. Atdjian et al., "Bisubstrate analogues as structural tools to investigate m6A methyltransferase active sites," *RNA Biology*, vol. 16, no. 6, pp. 798–808, 2019.
- [26] S. Nie, L. Zhang, J. Liu et al., "ALKBH5-HOXA10 loop-mediated JAK2 m6A demethylation and cisplatin resistance in epithelial ovarian cancer," *Journal of Experimental & Clinical Cancer Research : CR*, vol. 40, no. 1, p. 284, 2021.
- [27] S. D. Kasowitz, J. Ma, S. J. Anderson et al., "Nuclear m6A reader YTHDC1 regulates alternative polyadenylation and splicing during mouse oocyte development," *PLOS Genetics*, vol. 14, no. 5, article e1007412, 2018.
- [28] Q. Y. Chen, Y. N. Li, X. Y. Wang et al., "Tumor fibroblast-derived FGF2 regulates expression of SPRY1 in esophageal tumor-infiltrating T cells and plays a role in T-cell exhaustion," *Cancer Research*, vol. 80, no. 24, pp. 5583–5596, 2020.
- [29] S. Li, H. Chen, J. Man et al., "Changing trends in the disease burden of esophageal cancer in China from 1990 to 2017 and its predicted level in 25 years," *Cancer Medicine*, vol. 10, no. 5, pp. 1889–1899, 2021.
- [30] A. Visvanathan, V. Patil, A. Arora et al., "Essential role of METTL3-mediated m⁶A modification in glioma stem-like cells maintenance and radioresistance," *Oncogene*, vol. 37, no. 4, pp. 522–533, 2018.
- [31] Y. Wu, W. Zhao, Y. Liu et al., "Function of HNRNPC in breast cancer cells by controlling the dsRNA-induced interferon response," *The EMBO Journal*, vol. 37, no. 23, article e99017, 2018.
- [32] S. Xie, Z. Yu, and Z. Lv, "Multi-disease prediction based on deep learning: a survey," *CMES-Computer Modeling in Engineering and Sciences*, vol. 128, no. 2, pp. 489–522, 2021.
- [33] W. Sun, Z. Cai, Y. Li, F. Liu, S. Fang, and G. Wang, "Data processing and text mining technologies on electronic medical records: a review," *Journal of Healthcare Engineering*, vol. 2018, Article ID 4302425, 9 pages, 2018.
- [34] A. Arefinia, O. Bozorg-Haddad, A. Oliazadeh, and H. A. Loáigiga, "Reservoir water quality simulation with data mining models," *Environmental Monitoring and Assessment*, vol. 192, no. 7, p. 482, 2020.
- [35] J. B. Raja and S. C. Pandian, "PSO-FCM based data mining model to predict diabetic disease," *Computer Methods and Programs in Biomedicine*, vol. 196, article 105659, 2020.

Retraction

Retracted: A Novel Multidose Dry Powder Inhaler and Its Application in Patients with Asthma and COPD

Journal of Sensors

Received 22 August 2023; Accepted 22 August 2023; Published 23 August 2023

Copyright © 2023 Journal of Sensors. This is an open access article distributed under the Creative Commons Attribution License, which permits unrestricted use, distribution, and reproduction in any medium, provided the original work is properly cited.

This article has been retracted by Hindawi following an investigation undertaken by the publisher [1]. This investigation has uncovered evidence of one or more of the following indicators of systematic manipulation of the publication process:

- (1) Discrepancies in scope
- (2) Discrepancies in the description of the research reported
- (3) Discrepancies between the availability of data and the research described
- (4) Inappropriate citations
- (5) Incoherent, meaningless and/or irrelevant content included in the article
- (6) Peer-review manipulation

The presence of these indicators undermines our confidence in the integrity of the article's content and we cannot, therefore, vouch for its reliability. Please note that this notice is intended solely to alert readers that the content of this article is unreliable. We have not investigated whether authors were aware of or involved in the systematic manipulation of the publication process.

In addition, our investigation has also shown that one or more of the following human-subject reporting requirements has not been met in this article: ethical approval by an Institutional Review Board (IRB) committee or equivalent, patient/participant consent to participate, and/or agreement to publish patient/participant details (where relevant).

Wiley and Hindawi regrets that the usual quality checks did not identify these issues before publication and have since put additional measures in place to safeguard research integrity.

We wish to credit our own Research Integrity and Research Publishing teams and anonymous and named external researchers and research integrity experts for contributing to this investigation.

The corresponding author, as the representative of all authors, has been given the opportunity to register their agreement or disagreement to this retraction. We have kept a record of any response received.

References

- [1] F. Shi, C. Zhu, T. Zhou, and J. Liu, "A Novel Multidose Dry Powder Inhaler and Its Application in Patients with Asthma and COPD," *Journal of Sensors*, vol. 2022, Article ID 3051484, 14 pages, 2022.

Research Article

A Novel Multidose Dry Powder Inhaler and Its Application in Patients with Asthma and COPD

Feng Shi ¹, Chaoting Zhu ¹, Tianqi Zhou ¹ and Jianhui Liu ²

¹School of Medical Devices, Zhejiang Pharmaceutical University, Ningbo 315000, China

²Ningbo Yihe Pharmaceutical Co., Ltd, Zhejiang 315000, China

Correspondence should be addressed to Feng Shi; masd@zjpu.edu.cn

Received 1 August 2022; Revised 12 August 2022; Accepted 22 August 2022; Published 7 September 2022

Academic Editor: Sweta Bhattacharya

Copyright © 2022 Feng Shi et al. This is an open access article distributed under the Creative Commons Attribution License, which permits unrestricted use, distribution, and reproduction in any medium, provided the original work is properly cited.

Patient and physician satisfaction with the maintenance inhaler device is an important factor in medication adherence and effectiveness in respiratory disorders. We look at inhaler preferences in asthma and chronic obstructive pulmonary disease (COPD) from both the patient's and physician's perspectives, emphasizing the relative importance of device features and patient considerations in inhaler selection. Teva Pharmaceuticals developed the multidose dry powder inhaler (M-DDPI) to treat chronic respiratory diseases. It is a metered-dose dry powder inhaler device intended to seem like a standard pressured metered-dose inhaler, but its internal geometry is somewhat distinctive. Inhalation treatment permits medication delivered directly to the airways. Inhalation devices serve a vital role in the therapy of obstructive lung illnesses such as asthma and COPD. The purpose of this research is to see how M-DDPI achieves maximum bronchial deposition of the medicine; the device must provide a high percentage of small particles, be simple to operate, and supply continuous and exact dosages of the active ingredient in COPD and asthma patients. Patients with COPD and asthma who had been diagnosed and treated at the hospital were first recruited as research participants and split into two groups. The control group got oxygen therapy as part of their standard treatment, whereas the experimental group received M-DDPI therapy. Statistical analysis techniques such as the Mann-Whitney *U* test and chi-squared test were used to examine the effects. The data show that the efficacies of M-DDPI therapy for COPD and asthma for obstructive lung illnesses seem to be promising right now.

1. Introduction

Asthma is a common chronic illness of the airways characterized by fluctuating airflow restriction as a result of constriction of the airways, thickening of the airway walls, and increased mucus. Consequences of persistent airway inflammation such as plasma extravasation and the influx of proinflammatory cells such as neutrophils and mast cells include airway constriction and airway narrowing syndrome. Asthma's airway hyperresponsiveness (AHR) is a crucial physiological trait. AHR is an excessive reaction of the airways to a nonspecific stimulus that would have little or no impact on healthy individuals. Asthma may progress from a temporary blockage of the airways to a permanent reduction of lung function, despite the term "reversible" being often used. The prolonged airflow restriction might be due to an increase in mucus production in the airway lumen

(Boonpiyathad et al. [1]). Childhood-onset asthma is the term used to describe the majority of cases of asthma; however, some people get the condition much later in life (late-onset asthma). Several distinctions between asthma begin in childhood and that which begins later in life. Figure 1 depicts the differentiation of normal lungs and asthmatic lungs.

Delayed asthma symptoms are now more severe and are less often brought on by antigen exposure. Asthma in adolescents may be caused by a variety of conditions, including poor respiratory symptoms and pharyngitis, particularly coronavirus infections. In asthmatic patients, it is not clear whether the preexisting irritation improves the toxicity of respiratory pathogens or if the frequent viral infections that children experience at a young age promote the growth of asthma. Asthma therapy's primary objective is to control symptoms and decrease inflammation to prevent future exacerbations

Asthma

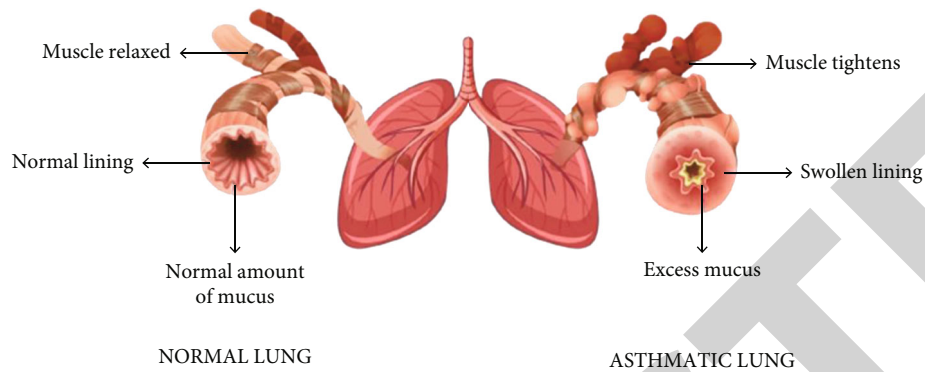


FIGURE 1: Differentiation of normal lung and asthmatic lung.

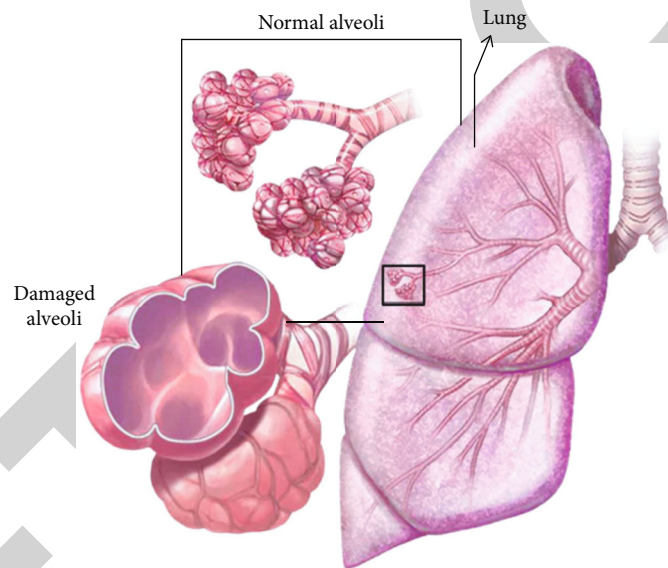


FIGURE 2: Lung is affected by COPD.

(Hammad and Lambrecht [2]). The mechanism by which TSLP produces its effects is by binding to a high-affinity heteromeric receptor complex consisting of “TSLPR” and “IL-7R.” It has been shown that polymorphisms in TSLP are linked to airway hyperresponsiveness, immunoglobulin E levels, eosinophilia, and asthma. There is evidence to suggest that TSLP has a role in the pathogenesis of asthma (Marone et al. [3]). When inhaled noxious particles and gases cause chronic obstructive lung disease (COPD), which is curable but avoidable, the inflammatory response increases. Even though emphysema and chronic bronchitis are often seen in people with COPD, many of these patients have exacerbations, which need hospitalization and other forms of treatment (Parris et al. [4]). Tobacco smoking was once assumed to be the primary cause of COPD. Nonsmoking risk factors for COPD have been increasing in relevance over the last decade, including research on the burden of the disease, risk variables, and

clinical presentations among never-smokers. Non-tobacco-related risk factors are responsible for around half of all COPD cases globally, which vary by area. Low socioeconomic levels and infectious illnesses are also on the list of contributing variables. Air pollution and occupational exposure are also on the list. Poor lung development in infancy is linked to an increased risk of chronic obstructive pulmonary disease (COPD). Figure 2 indicates the lung is affected by COPD.

Nonsmokers may develop COPD as a result of inflammation, oxygen depletion, airway remodeling, and premature aging of the lungs. However, exacerbations may still occur often in those who never smoked and who have moderate chronic respiratory symptoms and emphysema but little or no airflow obstruction. COPD in never-smokers is a major health problem that needs to be addressed via further research, including epidemiological, translational, clinical, and implementation studies (Yang et al. [5]). Asthma and COPD

symptoms may coexist in certain patients. Asthma-COPD overlap syndrome (ACO) is the name given to this illness by the Global Asthma/Global Chronic Obstructive Lung Disease (GINA/GOLD) statement [6] and other recommendations and publications. ACO's prevalence has ranged from 15% to 60%, depending on the demographic sample, age group, and criteria used. An ACO definition has yet to be agreed upon. ACO adopting alternative criteria has been associated with more frequent exacerbations, lower health-related quality of life, greater hospital admissions, and higher expenditures on healthcare when compared to asthma or COPD alone. There is currently no consensus on the diagnostic criteria for ACO, which is currently dependent on surveys and doctors' own opinions as well as the definition of certain minor and important criteria (Mostafavi-Pour-Manshadi et al. [7]). Such a form of long-term, continuous home monitoring of COPD patients may be made possible via a wearable sensor device. The majority of wearable sensor systems have severely constrained battery life, processing power, and storage capabilities. In a typical wearable sensor system, raw sensor data from sensor nodes are typically stored and sent to a nearby data aggregator (Moraveji et al. [8]).

With interconnected physical, social, behavioral, economic, and infrastructural concerns, a smart and connected community (SCC) intends to integrate embedded sensors and computers for better benefit to people, the community, and society. Utilizing physiological information from wearables, such as heart rate and SpO₂, to diagnose and track the course of COPD and asthma may enhance SSC self-management and general health (Siddiqui and Morshed [9]).

The objective of this study is to determine how M-DDPI promotes maximal bronchial deposition of the medication. The device must produce a high proportion of tiny particles, be easy to use, and provide continuous and accurate doses of the active component to COPD and asthma patients. Patients with COPD were given breathing methods as part of a rehabilitation program and motivated to use them often.

1.1. Contribution of This Study

- (i) We have collected data of patients with asthma and COPD
- (ii) The random number table method is used to randomly divide the control and experimental teams
- (iii) Several statistical analysis techniques including the chi-squared test and the Mann-Whitney *U* test were utilized to look into the effects
- (iv) Chi square is an effective tool for data analysis and for determining the kind of research data
- (v) Mann-Whitney test *U* tests are often used to determine if two autonomous groups' predictor factors vary

The remainder of the description is divided into five parts: part 2: related works and problem definition, part 3: the proposed methodology used, part 4: result and discussion, and part 5: conclusion.

2. Related Works

Li et al. [10] determine the cumulative bronchodilator dose of albuterol in a metered dose inhaler with a valved holding chamber (MDI+VHC) that allows patients with stable mild-to-moderate asthma and chronic obstructive pulmonary disease (COPD) to achieve comparable spirometry responses before and after bronchodilator tests. The spirometry necessary to verify bronchodilator reactions is difficult with individuals experiencing acute exacerbations and tricky enough with stable asymptomatic volunteers.

Broers et al. [6] offer a summary of the state-of-the-art research on the relationship between GERD and asthma and chronic obstructive pulmonary disease (COPD). With a disparity between the high frequency of GERD in asthma and the limited effectiveness of antireflux medication on asthma outcome, the relationship between GERD and asthma is complicated.

Dekhuijzen et al. [11] examine the causes and effects of poor adherence and provide summaries of significant research that show how increasing adherence might lower exacerbations, the need for inhaled corticosteroids (in situations when improved inhaler technique is used), hospitalizations, and treatment costs. Additionally, it is sometimes difficult for individuals with COPD to breathe in deeply enough to ensure sufficient delivery of medication from a dry-powder inhaler (DPI).

Katoh et al. [12] discuss making the distinction between COPD and asthma, which may sometimes be challenging in clinical practice and is crucial for implementing the proper medication. To differentiate between COPD and asthma, we analyzed biomarkers. The detection thresholds for IL-25, IL-33, TSLP, ST2, and 2 ng/mL were 1.9 pg/mL, 3.1 pg/mL, 3.4 pg/mL, and 32 pg/mL, respectively (periostin). For statistical analysis, concentrations below the detection limits were assumed to be zero.

Eryong and Li [13, 14] discuss that numerous odontogenic keratocysts are a common feature of several illnesses. On the face of a 12-year-old girl, odontogenic keratocysts were found. It was discovered that none of the further irregularities discovered throughout the testing involved a medical problem.

Garg [15] describes that customized medicine uses fine-grained data to identify issues. Engineers resorted to digital twins to comprehend these new data-driven healthcare practices better. By linking physical objects to a particular place, the condition of physical objects was digitally conveyed. Data structures and their interpretations imply moral disparities. In this article, digital twins are examined. Healthcare that is data-driven is becoming more popular. This technology may be used as a powerful social equalizer.

Ahmed and Ali [16] determine that a worldwide epidemic of allergic rhinitis would be devastating. The most often recommended therapies in Taiwanese hospitals are traditional Chinese or Chinese-Western drugs. When it came to outpatient Chinese medicine, allergy rhinitis was the most prevalent respiratory ailment to be treated. Asthma sufferers in Taiwan are treated with a combination of Eastern and Western therapy.

Shahabaz and Afzal [17] describe that HDR brachytherapy does not use a radioactive substance, allowing for outpatient treatment and quicker testing periods. Increased dose dispersion may result from changing a single-step source's dwell duration. Since there can be no mistake checks with HDR brachytherapy because of the shorter processing intervals, it must be done properly.

Li [18] provides a treatment technique and technology for domestic sewage to enhance rural life. Salihi and Iyya [19] explain that the samples taken from vegetable farms in Zamfara State, Nigeria, have been examined for thermodynamic and organophosphate agrochemicals. It was utilized to assess the testing method and the produced data using QuEChERS with GC-MS.

Lin et al. [20] explain that the systematic review's objective is to assess the effectiveness and security of sublingual immunotherapy (SLIT) for the management of allergic asthma. These problems made it difficult to ascertain whether the health state of the patient's asthma at the start of therapy had any impact on the results that were seen, which may restrict our capacity to generalize the findings to specific asthma patients.

Looijmans-van den Akker et al. [21] investigate the usage of asthma medications in primary care today and investigate if excessive SABA use is linked to exacerbations. One drawback of maintenance therapy is that some patients were given leukotriene antagonists or muscarinic antagonists rather than an ICS. The usage of maintenance therapy may be understated since these drugs were left out of the research.

Abrahamsen et al. [22] suggested that the patient's capacity to manage COPD during multidisciplinary in-hospital pulmonary rehabilitation programs is improved by these experiences. Priority is nonetheless given to patients who are anticipated to benefit most and who have the highest potential for rehabilitation owing to limited capacity and rationing of healthcare resources. The results show that the patients' knowledge and awareness of COPD were often restricted at first but that they increased with PR.

Song et al. [23] investigate the effects on illness manifestation and outcomes, as well as possible underlying processes, of COPD and asthma comorbidity in COVID-19 patients. Due to the small number of COPD and asthma patients getting mechanical ventilation, they were unable to compare the ratio of COPD and asthma patients who transitioned from noninvasive to invasive mechanical ventilation.

Gadekallu et al. [24] explain that in order to avoid eyesight loss, which is a result of diabetes mellitus being untreated among patients for an extended length of time, early diagnosis of the condition is crucial. For classification and disease prediction, a variety of machine learning and deep learning techniques have been used in the diabetic retinopathy dataset; however, the bulk of these techniques have overlooked the element of data preprocessing and dimensionality reduction, producing biased findings. Table 1 depicts the explanation of the current research in tabular format.

Pitta et al. [25] discuss evaluating and contrasting the two types of tools most often used to measure the amount of physical activity that COPD patients engage in on a daily basis: subjective techniques (questionnaires, diaries) and

motion sensors (electronic or mechanical methods). This implies that either daily physical activity in these groups is significantly different or the questionnaire's applicability to COPD patients is restricted.

2.1. Problem Statement. As the disease progresses, the lungs' airways narrow and thicken, causing damage to the tissue that transfers oxygen between the bloodstream and the lungs. The lungs' capacity to take in and expel air declines. Because of the reduced oxygen supply, your body has a harder time eliminating the waste gas carbon dioxide. When it comes to asthma, the airways are affected on a long-term basis and suffocate the lungs, resulting in wheezing and difficulty breathing. An allergen or irritant, infections, exercise, and mental stress are all examples of possible causes of hay fever symptoms. Swollen and inflamed bronchial tube walls are characteristic of asthmatic symptoms. Breathing becomes difficult in those with asthma and COPD, which includes emphysema and chronic bronchitis. They are, in reality, quite similar. They are, however, two distinct types of lung disorders. A condition known as Asthma-COPD overlap syndrome (ACOS) is characterized by the presence of both asthma and COPD symptoms. Activities of the upper extremities of the body are not monitored by motion sensors worn on the waist, hips, or ankles. Although evaluations only need little care from patients (e.g., remembering to put the device on, placing it appropriately, avoiding shocks, and checking battery level), a common problem with motion sensors is the subject's compliance with the measurement.

3. Methodology Used

The purpose of this research is to see how M-DDPI achieves maximum bronchial deposition of the medicine; the device must provide a high percentage of small particles, be simple to operate, and supply continuous and exact dosages of the active ingredient in COPD and asthma patients. Patients with COPD and asthma who had been diagnosed and treated at the hospital were first recruited as research participants and split into two groups. The control group got oxygen therapy as part of their standard treatment, whereas the experimental group received M-DDPI therapy. Statistical analysis techniques such as the Mann-Whitney *U* test and chi-squared test were used to examine the effects. Figure 3 represents the proposed methodology of this research.

3.1. Dataset Collection. Outpatients at the China-Japan Friendship Hospital served as the subjects of the study. This was accomplished by the use of longitudinal panel research including 37 patients with COPD and 45 patients with asthma from Beijing, China (Duan et al. [26]). Table 2 shows the dataset features.

3.2. Inclusion/Exclusion Criteria of Patients

3.2.1. Inclusion Criteria. The asthma patients had to be between the ages of 18 and 75, have physician-diagnosed asthma, and have FEV1 reversibility of >12% and 200 mL following postbronchodilator spirometry, according to the Global Asthma Prevention Initiative standards.

TABLE 1: Description of current research.

Sl. No.	References	Explanation	Drawbacks
(1)	Li et al. [10]	Determines the cumulative bronchodilator dose of albuterol in a metered dose inhaler with a valved holding chamber (MDI+VHC) that allows patients with stable mild-to-moderate asthma and chronic obstructive pulmonary disease (COPD) to achieve comparable spirometry responses before and after bronchodilator tests.	The spirometry necessary to verify bronchodilator reactions is difficult with individuals experiencing acute exacerbations and tricky enough with stable asymptomatic volunteers.
(2)	Broers et al. [6]	Offers a summary of the state-of-the-art research on the relationship between GERD and asthma and chronic obstructive pulmonary disease (COPD).	With a disparity between the high frequency of GERD in asthma and the limited effectiveness of antireflux medication on asthma outcome, the relationship between GERD and asthma is complicated.
(3)	Dekhuijzen et al. [11]	Examines the causes and effects of poor adherence and provides summaries of significant research that show how increasing adherence might lower exacerbations, the need for inhaled corticosteroids (in situations when improved inhaler technique is used), hospitalizations, and treatment costs.	Additionally, it is sometimes difficult for individuals with COPD to breathe in deeply enough to ensure sufficient delivery of medication from a dry-powder inhaler (DPI).
(4)	Katoh et al. [12]	Discuss making the distinction between COPD and asthma, which may sometimes be challenging in clinical practice and is crucial for implementing the proper medication. To differentiate between COPD and asthma, we analyzed biomarkers.	The detection thresholds for IL-25, IL-33, TSLP, ST2, and 2 ng/mL were 1.9 pg/mL, 3.1 pg/mL, 3.4 pg/mL, and 32 pg/mL, respectively (perioestin). For statistical analysis, concentrations below the detection limits were assumed to be zero.
(5)	Lin et al. [20]	Explains that the systematic review's objective is to assess the effectiveness and security of sublingual immunotherapy (SLIT) for the management of allergic asthma.	These problems made it difficult to ascertain whether the health state of the patient's asthma at the start of therapy had any impact on the results that were seen, which may restrict our capacity to generalize the findings to specific asthma patients.
(6)	Looijmans-van den Akker et al. [21]	Investigates the usage of asthma medications in primary care today and investigates if excessive SABA use is linked to exacerbations.	One drawback of maintenance therapy is that some patients were given leukotriene antagonists or muscarinic antagonists rather than an ICS. The usage of maintenance therapy may be understated since these drugs were left out of the research.
(7)	Abrahamsen et al. [22]	Suggested that the patient's capacity to manage COPD during multidisciplinary in-hospital pulmonary rehabilitation programs is improved by these experiences.	Priority is nonetheless given to patients who are anticipated to benefit most and who have the highest potential for rehabilitation owing to limited capacity and rationing of healthcare resources. The results show that the patients' knowledge and awareness of COPD were often restricted at first but that they increased with PR.
(8)	Song et al. [23]	Investigates the effects on illness manifestation and outcomes, as well as possible underlying processes, of COPD and asthma comorbidity in COVID-19 patients.	Due to the small number of COPD and asthma patients getting mechanical ventilation, they were unable to compare the ratio of COPD and asthma patients who transitioned from noninvasive to invasive mechanical ventilation.
(9)	Pitta et al. [25]	Discuss evaluating and contrasting the two types of tools most often used to measure the amount of physical activity that COPD patients engage in on a daily basis: subjective techniques (questionnaires, diaries) and motion sensors (electronic or mechanical methods).	This implies that either daily physical activity in these groups is significantly different or the questionnaire's applicability to COPD patients is restricted.

The COPD patients had to be 45–75 years old, have a physician-diagnosed COPD, and have an FEV1 to FVC ratio of less than 70% following postbronchodilator spirometry, according to the Global Initiatives for Chronic Obstructive Pulmonary Disease recommendations.

3.2.2. Exclusion Criteria. The exclusion criteria of a person's lifestyle or comorbidities may impair their lung function or their ability to finish all four sessions.

Both COPD and asthma patients have to meet the following exclusion criteria:

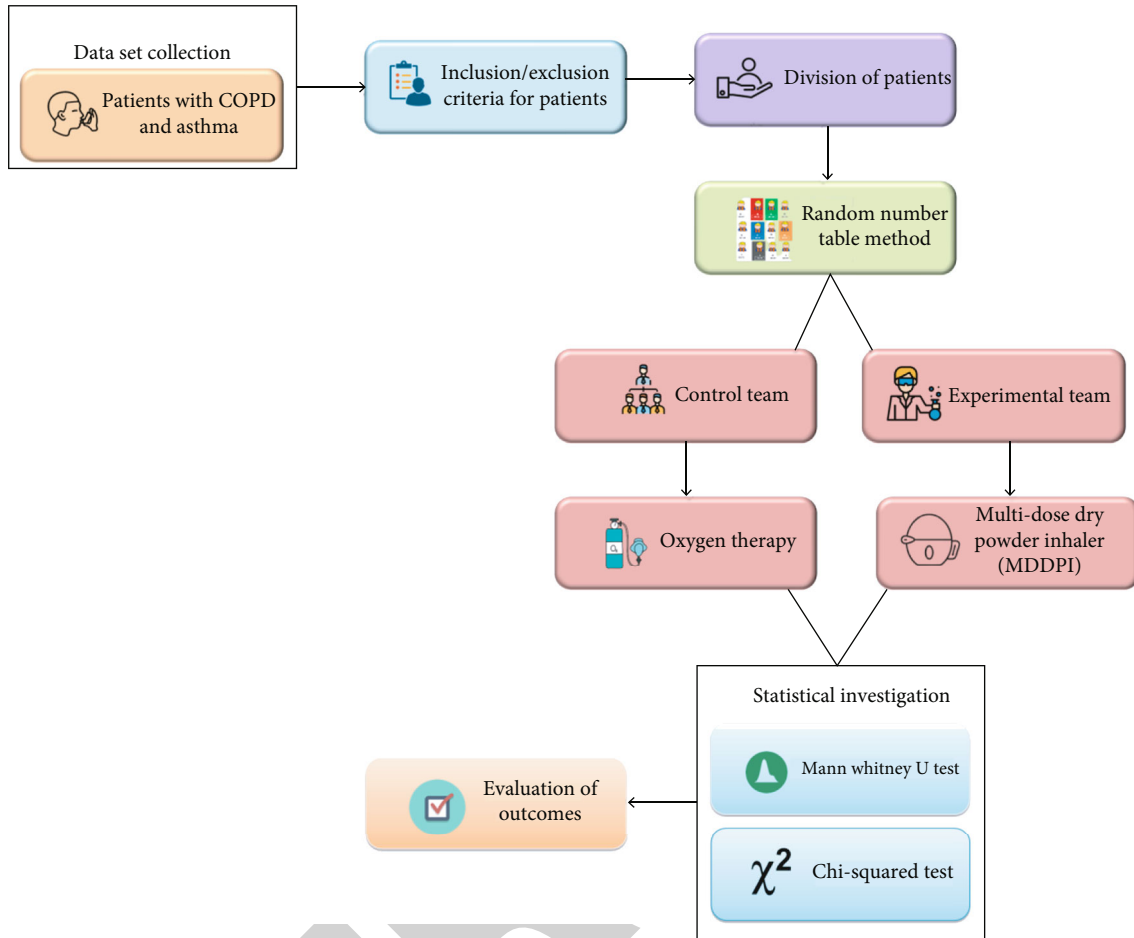


FIGURE 3: Flow of our proposed method.

- (i) Currently smoking or had not smoked for at least six months before the test date
- (ii) Severe cardiovascular and cerebrovascular illness, hepatic and renal failure, active TB, malignant tumors, complications, and comorbidity
- (iii) Evaluated the consequences of epilepsy or mental disorders
- (iv) Having just had surgery on their chest, abdomen, or eyes
- (v) Ladies who are pregnant or breastfeeding

3.3. Division of Patients. A control team and an experimental team are formed for each patient. Following oxygen therapy for the control team, the experimental group is administered M-DDPI.

3.4. Random Number Table Method. The control and experimental teams are randomly separated using the random number table approach. There are 12 sufferers with COPD and 23 individuals with asthma on the control team. There are 15 sufferers with COPD and 22 sufferers with asthma in the experimental group.

3.4.1. Control Team. On the control team, there are 12 patients with COPD and 23 patients with asthma. It is usual practice for that control team to undergo oxygen therapy.

(1) Oxygen Therapy. Oxygen therapy is a kind of treatment in which the patient's body is given more oxygen. The treatment of severe asthma attacks and patients with COPD is made possible by the use of oxygen therapy, which is prescribed by doctors. Approximately 21 percent of the air a person breathes is made up of oxygen. Oxygen is used by the body to generate energy for several different functions. Shortness of breath and confusion may occur if a person's blood oxygen levels are too low. The body may also be damaged by a lack of oxygen in the bloodstream.

People with low blood oxygen levels may get more oxygen via oxygen therapy. Certain medical problems may need the use of oxygen treatment, such as

- (i) COPD
- (ii) pulmonary fibrosis
- (iii) pneumonia
- (iv) asthma attack

TABLE 2: Dataset description.

Variable	COPD ($n = 37$)	Asthma ($n = 45$)
Gender (male)	23 (62.2%)	11 (24.4%)
Age (years)	63.0 \pm 9.0	55.7 \pm 12.3
BMI (kg/m ²)	26.3 \pm 4.9	25.2 \pm 3.9
Smoking		
Never-smoker	21 (56.8%)	35 (77.8%)
Former smoker	16 (43.2%)	10 (23.2%)
Pack-years	27.2 \pm 6.1	18.0 \pm 4.5
Disease duration (years)	5.1 \pm 6.2	11.7 \pm 9.8
Comorbidity		
Cerebrovascular disease	8 (21.6%)	8 (17.8%)
Connective tissue disease	0 (0.0%)	2 (4.4%)
Hypertension	6 (16.2%)	9 (20.0%)
Peptic ulcer	3 (8.1%)	6 (13.3%)
Diabetes	5 (13.5%)	5 (11.1%)
History of pollen or drug allergy	7 (18.9%)	13 (28.9%)
CAT/ACT score	13.8 \pm 8.6	21.7 \pm 3.3
Medication use ^a		
ICS	3 (8.1%)	3 (6.7%)
LAMA	15 (40.5%)	0 (0.0%)
ICS+LABA	32 (86.5%)	45 (100%)
SABA	2 (5.4%)	5 (11.1%)
SAMA	7 (5.4%)	1 (2.2%)
Oral glucocorticoids	1 (2.7%)	2 (4.4%)

(v) cystic fibrosis

During the time of an asthma attack, the muscles around the bronchial tubes contract, making breathing more difficult. In and out of the lungs, air travels via the bronchial tubes. Having bronchial tubes that are too small might make it difficult for a person to breathe and take in adequate oxygen. When the lungs' oxygen levels are low, oxygen treatment helps by supplementing the lungs' supply of oxygen. Oxygen therapy involves administering oxygen to a patient via the use of a face mask or nasal tubes.

(2) *Types of Oxygen Delivery System.* When administering oxygen treatment, clinicians have the option of using two different concentrations of oxygen source. Individuals may need varying amounts of oxygen depending on their medical state.

(2)1. *Oxygen Delivery Systems with Low Flow.* When a patient just requires a modest quantity of extra oxygen, treatment teams will turn to low-flow oxygen delivery devices. Air from the room is used to dilute a little quantity of additional oxygen in these systems. Oxygen levels are dependent on how much air a person takes in with each inhalation in low-flow systems. This means it is difficult to tell exactly how much oxygen a person is receiving.

Types of low-flow oxygen delivery systems include the following:

Nasal cannulas: to put it simply, nasal cannulas are two little tubes that go into the nostrils of a patient. At least 24–40 percent of the oxygen is delivered using a low-flow nasal cannula.

Simple face mask: face masks that fit over the nose and mouth are known as basic face masks. Air that is 35–55 percent oxygen may be supplied using these devices.

Nonrebreather mask: unlike a basic mask, a nonrebreather mask features a reservoir bag that prevents extra oxygen from being released into the atmosphere. Excess oxygen from the reservoir bag is inhaled when a diver wears a nonrebreather mask. There are nonrebreather masks that supply up to 95 percent oxygen and feature a valve that prevents the user from reinhaling their own exhaled air.

(2)2. *Oxygen Delivery Systems with High Flow.* Flow systems that give oxygen at a greater rate than a human can take in are known as high-flow oxygen delivery systems. A doctor can therefore precisely control the amount of oxygen a patient can inhale. Venturi masks, which cover the nose and mouth, and high-flow nasal cannulas, which can supply 100% oxygen, are two types of high-flow oxygen delivery devices. Additionally, high-flow nasal cannulas may heat the air, making it easier to inhale, as well. Asthma patients may benefit from using high-flow nasal cannulas. In an emergency department, high-flow nasal cannulas were studied to see how they affected patients with acute severe asthma. Study participants who had acute severe asthma had less shortness of breath using high-flow nasal cannulas than low-flow techniques.

3.4.2. *Experimental Team.* The experimental group includes 15 individuals with COPD and 22 patients with asthma. This group is treated with a multidose dry powder inhaler (M-DDPI) for asthma and COPD patients.

(1) *Multidose Dry Powder Inhaler (M-DDPI).* The proper and precise usage of the treatment equipment is a crucial factor in the effectiveness of inhaled therapy. There have been many complaints about the misuse of inhaler devices. As a result, every patient must learn how to properly use an inhaler. Having skilled personnel who can teach patients how to properly utilize the gadget is essential. Patients choose inhalers that are tiny, portable, easy to use, and handy. Dose counters on certain devices let patients keep track of how many doses they have taken and how many doses they have left, so they may avoid underdosing or overdosing. When patients adhere to recommended medication, it improves disease state management and lowers total healthcare expenditures as well as morbidity and mortality for patients. Inhalation aerosol treatment for patients may benefit from decreased dose frequency, inhaler technique, and patient satisfaction including the convenience of use. Figure 4 indicates the schematic representation of the inhaler.

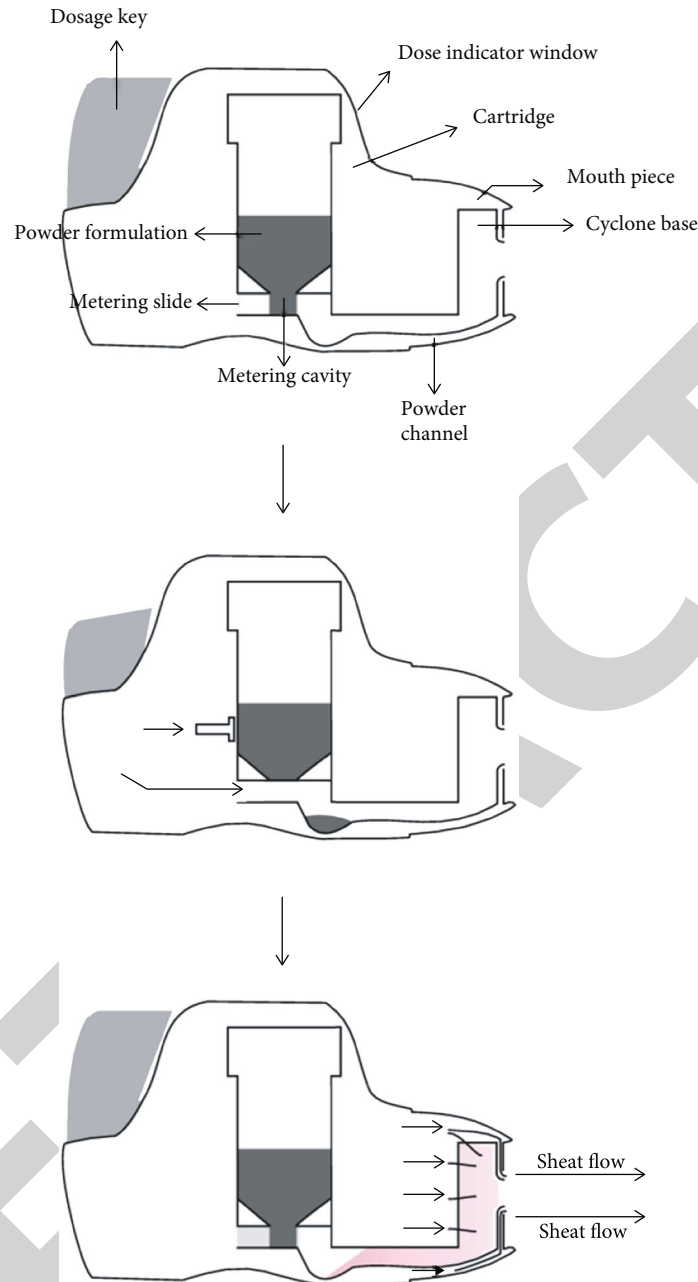


FIGURE 4: Schematic representation of inhaler.

(1)1. *The Most Effective M-DDPI for Asthma and COPD.* The inhaler Advair is one of the most often prescribed for the ongoing treatment of COPD. A corticosteroid and a long-acting bronchodilator, fluticasone, and salmeterol make up this medication. For the maintenance therapy of COPD, Advair is taken twice a day regularly. Asthma episodes may be prevented with the use of the combination medication Advair inhalation. Adults and children over the age of four may take Advair Diskus. Advair HFA may be used by both adults and children over the age of twelve. Asthma or bronchospasm episodes cannot be treated with Advair. For an attack, only use fast-acting

inhalation medications. Consult a doctor if patients breathing issues worsen or if patients suspect asthma treatments are not functioning as effectively as they should. The powdered version of fluticasone and salmeterol Advair Diskus has a unique inhaler device preloaded with blister packs carrying premeasured dosages. A canister of Advair HFA is used with an actuator inhaler device.

3.5. *Statistical Investigation.* To investigate the impacts, several statistical analysis methods including the chi-squared test and the Mann-Whitney U test were used.

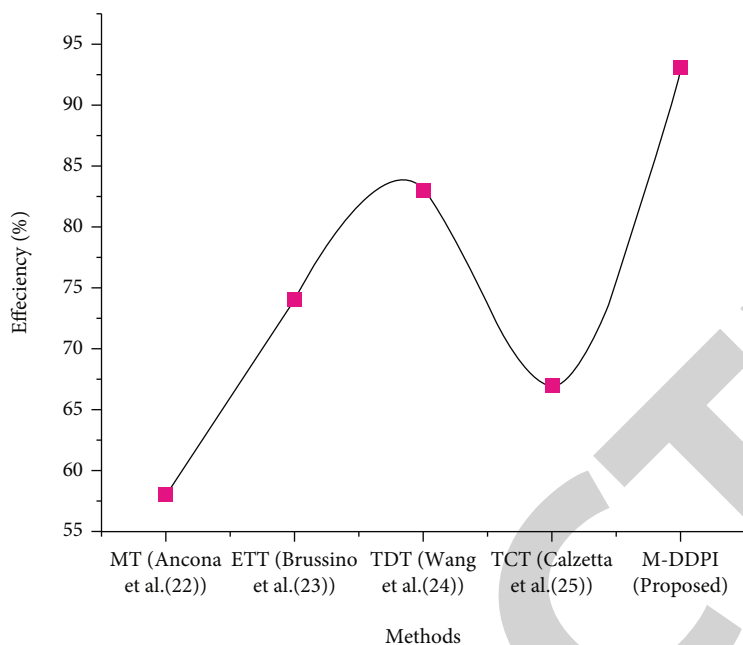


FIGURE 5: Efficiency of proposed and existing methods.

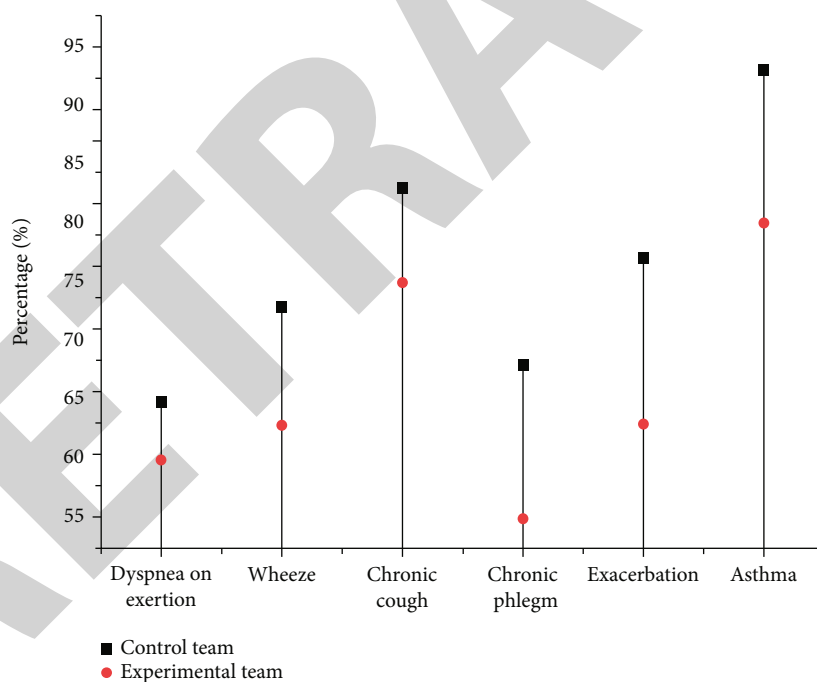


FIGURE 6: Percentage (%).

3.5.1. *Chi-Squared Test.* Pearson’s chi-squared test is a statistical process used to determine whether or not any measurable variance across collections of category data is random. This is a common circumstance where all of the episodes have a categorical data result. The idea that a standard six-sided die is “fair” is, in fact, a simplification.

In three sets of relationships, Pearson’s chi-squared assessment measures convenience, uniformity, and independence.

- (i) A convenient test estimates when a frequency distribution measured differs from the analytical distribution
- (ii) Using the same type parameter, a uniformity test evaluates the distribution of values among multiple groups
- (iii) Analysis of independence determines if findings comprised of 2 factors’ measurements, as

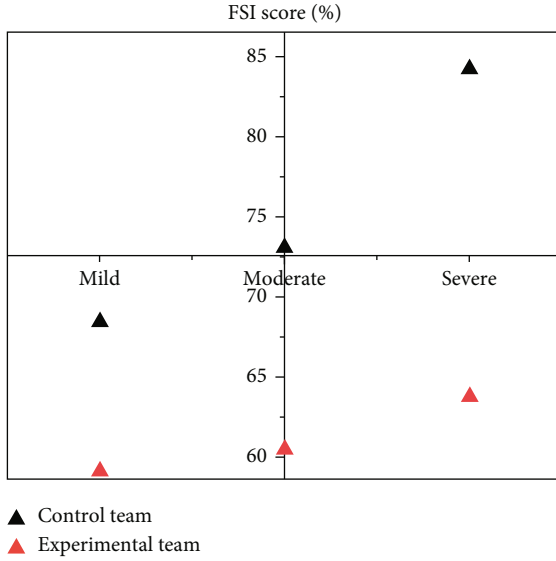


FIGURE 7: FSI score of patients.

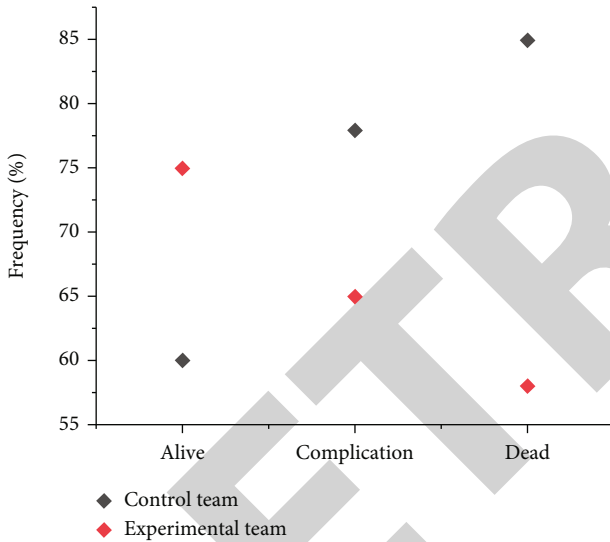


FIGURE 8: Frequency of control team and experimental team.

represented in a contingency table, were independent of one another:

$$\text{Pearson's chi-squared test} = \sum_{j=1}^n \frac{(N_j - F_j)^2}{F_j}. \quad (1)$$

Here, N_j are measurements of type j , N is the sum of measurements, F_j is the predicted count of type j , and N is the amount of cells.

Whether or not they had been treated, the expected chi-squared values are determined as follows:

$$E = \frac{N_V \times N_C}{o}, \quad (2)$$

where E reflects the work value of the unit, N_C denotes that cell nucleus row edge, N_V denotes that cell's row edge, and o reflects the sample group as a whole.

The sample size is split by the product of the row marginal and the column marginal for each cell:

$$y^2 = \frac{(Q - E)^2}{E}. \quad (3)$$

Correlation measures are statistical assessments of the strength of a relationship. Cramer's V test is the most often utilized chi-squared strength test. Using the formula below, it is easy to calculate:

$$\sqrt{\frac{y^2/o}{(l-1)}} = \sqrt{\frac{y^2}{o(l-1)}}. \quad (4)$$

Useful for analyzing data, the chi square is an excellent tool for discovering the nature of research data.

3.5.2. Mann-Whitney U test. The Mann-Whitney U test is often used for 2 autonomous groups having a difference in the predictor variables. It examines if the interdependent variable's dispersion is the same as the two groups, implying that they are from an identical community:

$$a = As(B_{11} > B_{21}) + \frac{1}{2}As(B_{11} = B_{21}) = - \int_0^{\infty} T_1^{\pm}(b) eT_2(b), \quad (5)$$

where $T_1^{\pm}(b) = \{T_1(b+) + T_1(b-)\}/2$ is the normalized version. The hypothesis $H_0 : T_1(b) = T_1(b) \forall b$ implies $q = 1 \setminus 2$:

$$S_0^q : a = 1 \setminus 2 \text{ vs. } S_1^q : a = 1 \setminus 2. \quad (6)$$

To test S_0^q , one can use Efron's estimator of q given by

$$W_o(a) = \sqrt{\frac{o_1 o_1}{o}} (\hat{a} - a) \xrightarrow{o \rightarrow \infty} O(0, \sigma^2) \text{ as } o \rightarrow \infty,$$

$$\sigma_{jl}^2 = \int_0^{\infty} \int_0^{\infty} T_j^{\pm\pm}(v, w) eT_l(v) eT_l(w), \quad (7)$$

$$DJ = \left[\hat{a} - c_{\alpha/2} \frac{\hat{\sigma}}{\sqrt{o_1 o_1 / o}}, \hat{a} + c_{\alpha/2} \frac{\hat{\sigma}}{\sqrt{o_1 o_1 / o}} \right],$$

where c_{α} is the upper percent point of $N(0, 1)$.

4. Result

The goal of this study is to examine how M-DDPI provides maximal bronchial deposition of medication. To do so, the device must have a high proportion of tiny particles, be easy to use, and offer continuous and precise doses of the active component in COPD and asthma patients. The impacts were investigated using statistical analysis approaches such as the Mann-Whitney test and the chi-squared test. The

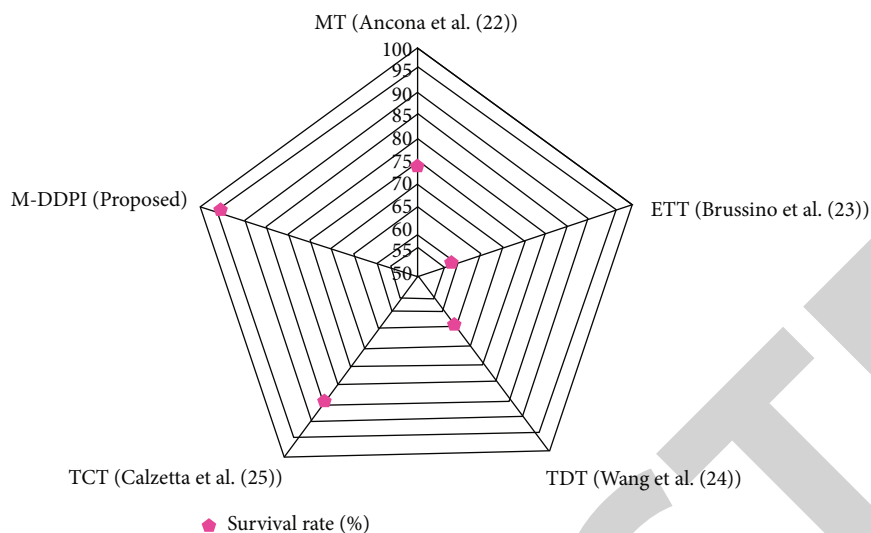


FIGURE 9: Survival rate of proposed and existing methods.

TABLE 3: Comparative analysis of existing and proposed methods.

	MT (Ancona et al. [27])	ETT (Brussino et al. [28])	TDT (Wang et al. [29])	TCT (Calzetta et al. [30])	M-DDI (proposed)
Efficiency (%)	58	74	83	67	93
Survival rate (%)	74	58	64	85	96

TABLE 4: Results of the chi-squared test.

Variable	COPD ($n = 37$)	Asthma ($n = 45$)
BMI (kg/m^2)	26.3 ± 4.9	25.2 ± 3.9
Duration of disease	5.1 ± 7.3	11.7 ± 7.8
Cerebral illness	8 (24.6%)	8 (17.8%)
Vascular dysfunction	0 (0.3%)	2 (4.5%)
Hypertensive	6 (17.3%)	9 (21.1%)
Esophageal ulcer	3 (8.3%)	6 (13.5%)
Oral glucocorticoids	1 (2.6%)	2 (4.6%)
Diabetes	5 (13.6%)	5 (11.4%)
ICS	3 (8.5%)	3 (6.5%)

TABLE 5: Results of the Mann-Whitney U test.

Variable	COPD ($n = 37$)	Asthma ($n = 45$)
BMI (kg/m^2)	27.3 ± 4.9	25.4 ± 3.9
Duration of disease	5.2 ± 7.2	11.7 ± 8.9
Cerebral illness	8 (23.6%)	8 (18.8%)
Vascular dysfunction	0 (0.3%)	2 (4.4%)
Hypertensive	8 (16.4%)	9 (21.1%)
Esophageal ulcer	5 (8.4%)	7 (13.4%)
Oral glucocorticoids	2 (2.9%)	2 (5.5%)
Diabetes	6 (13.7%)	5 (15.4%)
ICS	4 (8.6%)	3 (6.7%)

existing methods include Mepolizumab Therapy, Eosinophils Target Therapy, Targeted Drug Therapy, and Triple Combination Therapy. The parameters such as efficiency, overall percentage, Feeling of Satisfaction with Inhaler (FSI) score, frequency, and survival rate.

4.1. Efficiency. The use of available medical resources to get the greatest possible return on investment is what efficiency refers to. The provision of medical treatment may be seen as an intermediate good, in the sense that it is a means to the achievement of better health.

The effectiveness of proposed and existing works is shown in Figure 5. When compared to current approaches, the suggested methods (M-DDPI) are more efficient (Mepolizumab Therapy, Eosinophils Target Therapy, Targeted Drug Therapy, and Triple Combination Therapy).

4.2. Percentage. We calculated dyspnea on exertion, wheezing, chronic cough, chronic phlegm, exacerbation, and asthma in percentages for the patients.

The percentages for the control and experimental teams are shown in Figure 6. Exertion-induced dyspnea, wheezing, chronic cough, chronic phlegm, exacerbation, and asthma are all lower in the experimental group than in the control group.

4.3. FSI Score. Patient satisfaction with inhaler devices may be assessed using the Feeling of Satisfaction with Inhaler (FSI), which is a self-reported questionnaire that assesses

patient views on the simplicity of use, portability, and usefulness of inhaler devices.

The FSI score of patients is shown in Figure 7. The FSI score was determined using mild, moderate, and severe severity levels. Finally, the experimental team outperforms the control team in terms of FSI scores such as mild, moderate, and severe.

4.4. Frequency%. Using the control group and the experimental group, an analysis of the frequency of alive, complications, and death is carried out. In comparison to the control group, the experimental group had a much-increased risk of experiencing problems and passing away. Figure 8 is a representation of the frequency of both the control group and the experimental group.

4.5. Survival Rate. The survival rate is a component of the survival analysis. How many persons in a study or therapy group remain alive for a specific amount of time following diagnosis is known as the survival rate certain diseases have specific prognostic terms that may be used to describe the outlook for the patient. The rate of survival may be used as a measure for evaluating treatment standards.

The survival rate of both suggested and current approaches is shown in Figure 9. The survival rate of people with COPD and asthma is evaluated using the tools that are now available. When compared to the suggested approaches, the survival rate of the current methods is much greater. Table 3 represents a comparative analysis of existing and proposed methods.

When compared with other existing methods, our proposed method M-DDI (proposed) provides better performance for efficiency and survival rate.

4.6. Test Results for the Chi-Squared Test. Table 4 indicates the test results for the chi-squared test.

4.7. Test Results for the Mann-Whitney U Test. Table 5 indicates the test results for the Mann-Whitney U test.

5. Discussion

Mepolizumab Therapy (existing) is a therapy for asthma; it causes headaches, surgical site responses, itching, or burning sensations at the injection site which are the most frequent adverse effects of Mepolizumab. Back discomfort and weariness are other typical side effects (fatigue) (MT (Ancona et al. [27])). Eosinophils Targeted Therapy (existing) airway eosinophils are reduced, and the more airway eosinophils are main participants in airway inflammation, the less successful any asthma medication targeting eosinophils will be. Although eosinophil activation indicators are not presently accessible, this is likely to be a major barrier in identifying asthmatic patients who potentially benefit more from anti-IL5 therapy (ETT (Brussino et al. [28])). Targeted Drug Therapy (existing) is a treatment of COPD that can slow the progression of the illness' lung function decrease. These methods also cause side effects, and those methods are ineffective (TDT (Wang et al. [29])). Triple Combination Therapy (existing), a long-acting beta-agonist and a long-acting

muscarinic agonist, is used in conjunction with an inhaled corticosteroid as part of triple treatment for COPD. The side effects of this treatment include headaches, coughing, diarrhea, back and joint discomfort, and changes in taste (TCT (Calzetta et al. [30])). Hence, our proposed methods have better efficiency in COPD and asthma when compared to the other existing methods. The accuracy of a multisensor and a pedometer in patients with COPD while engaging in "real world" activities was also tested for the first time in this research.

6. Conclusion

Asthma and COPD patients' satisfaction with inhaler devices should be taken into account in clinical trials examining M-DDPI. Better adherence and improved clinical results may be linked to taking the preferences and happiness of patients into account when selecting an inhaler. COPD, lung inflammation, and pulmonary infections are among the conditions that DPIs are being utilized to treat in this research. The inhaler's performance may be affected by a variety of factors, including the design and formulation of the device. Drug physicochemical properties and the patient's ability to utilize the device appropriately all play a role in how well an M-DDPI pharmaceutical product will function in the end. The statistical analysis test was assessed using the chi-squared test, and the Mann-Whitney U test has become a greater outcome. Inhaled medicine is crucial for the treatment of asthma and COPD. However, it will not have any or very little advantage if you do not have a good inhalation technique. The lack of a correlation between prescription based on inhaler device usability and the severity of asthma may be a result of the medication's limited availability across a variety of delivery methods. Future studies must concentrate on patient-reported device preferences and efficiency, overall percentage, Feeling of Satisfaction with Inhaler (FSI) score, frequency, and survival rate. Future studies might look at the possibility of using inhalers to walk patients through the procedures necessary for effective medicine administration, according to scientists.

Data Availability

The data used to support the findings of this study are available from the corresponding author upon request.

Ethical Approval

All investigations were conducted under the ethical standards and procedures for research with human beings as approved by the institute's local ethics board Reg. No: (623121/2021/CPCSEA/24.04.2021).

Conflicts of Interest

The authors declare that they have no known competing financial interests or personal relationships that could have appeared to influence the work reported in this paper.

Acknowledgments

The research was funded by project No. LGF20E050002 entitled “Development of a new dry powder inhaler for asthma and COPD lung diseases” supported by the Zhejiang Province Public Welfare Technology Application Research Project of China.

References

- [1] T. Boonpiyathad, Z. C. Sözener, P. Satitsuksanoa, and C. A. Akdis, “Immunologic mechanisms in asthma,” in *Seminars in immunology*, p. 101333, Academic Press, 2019.
- [2] H. Hammad and B. N. Lambrecht, “The basic immunology of asthma,” *Cell*, vol. 184, no. 6, pp. 1469–1485, 2021.
- [3] G. Marone, G. Spadaro, M. Braile et al., “Tezepelumab: a novel biological therapy for the treatment of severe uncontrolled asthma,” *Expert Opinion on Investigational Drugs*, vol. 28, no. 11, pp. 931–940, 2019.
- [4] B. A. Parris, H. E. O’Farrell, K. M. Fong, and I. A. Yang, “Chronic obstructive pulmonary disease (COPD) and lung cancer: common pathways for pathogenesis,” *Journal of Thoracic Disease*, vol. 11, Supplement 17, pp. S2155–S2172, 2019.
- [5] I. A. Yang, C. R. Jenkins, and S. S. Salvi, “Chronic obstructive pulmonary disease in never-smokers: risk factors, pathogenesis, and implications for prevention and treatment,” *The Lancet Respiratory Medicine*, vol. 10, no. 5, pp. 497–511, 2022.
- [6] C. Broers, J. Tack, and A. Pauwels, “Review article: gastroesophageal reflux disease in asthma and chronic obstructive pulmonary disease,” *Alimentary Pharmacology & Therapeutics*, vol. 47, no. 2, pp. 176–191, 2018.
- [7] S. M. Y. Mostafavi-Pour-Manshadi, N. Naderi, M. Barrecheguren, A. Dehghan, and J. Bourbeau, “Investigating fractional exhaled nitric oxide in chronic obstructive pulmonary disease (COPD) and asthma-COPD overlap (ACO): a scoping review,” *COPD: Journal of Chronic Obstructive Pulmonary Disease*, vol. 15, no. 4, pp. 377–391, 2018.
- [8] N. Moraveji, P. Golz, J. Hollenbach, M. Holt, and R. Murray, “Long-term, ambulatory respiratory monitoring of COPD patients using garment-adhered sensors,” in *In 2019 IEEE International Symposium on Medical Measurements and Applications (MeMeA)*, pp. 1–6, Istanbul, Turkey, June 2019.
- [9] T. Siddiqui and B. I. Morshed, “Severity classification of chronic obstructive pulmonary disease and asthma with heart rate and SpO₂ sensors,” in *In 2018 40th Annual International Conference of the IEEE Engineering in Medicine and Biology Society (EMBC)*, pp. 2929–2932, Honolulu, HI, USA, July 2018.
- [10] J. Li, M. Zhao, M. Hadeer, J. Luo, and J. B. Fink, “Dose response to transnasal pulmonary administration of bronchodilator aerosols via nasal high-flow therapy in adults with stable chronic obstructive pulmonary disease and asthma,” *Respiration*, vol. 98, no. 5, pp. 401–409, 2019.
- [11] R. Dekhuijzen, F. Lavorini, O. S. Usmani, and J. F. van Boven, “Addressing the impact and unmet needs of nonadherence in asthma and chronic obstructive pulmonary disease: where do we go from here?,” *The Journal of Allergy and Clinical Immunology: In Practice*, vol. 6, no. 3, pp. 785–793, 2018.
- [12] S. Katoh, M. Ikeda, R. Shirai et al., “Biomarkers for differentiation of patients with asthma and chronic obstructive pulmonary disease,” *Journal of Asthma*, vol. 55, no. 10, pp. 1052–1058, 2018.
- [13] X. Eryong and J. Li, “What is the ultimate education task in China? Exploring strengthen moral education for cultivating people (Li De Shu Ren),” *Educational Philosophy and Theory*, vol. 53, no. 2, pp. 128–139, 2021.
- [14] R. N. Mody and A. R. Bhoosreddy, “Multiple odontogenic keratocyst: a case report,” *Annals of Dentistry*, vol. 54, no. 1-2, pp. 41–43, 2021.
- [15] H. Garg, *Digital Twin Technology: Revolutionary to Improve Personalized Healthcare*, vol. 1, no. 1, 2020 Science Progress and Research (SPR), 2020.
- [16] B. Ahmed and A. Ali, “Usage of traditional Chinese medicine, Western medicine and integrated Chinese Western medicine for the treatment of allergic rhinitis,” *Official Journal of the Zhende Research Group*, vol. 1, no. 1, pp. 1–9, 2020.
- [17] A. Shahabaz and M. Afzal, “Implementation of high dose rate brachytherapy in cancer treatment,” *Science Progress and Research*, vol. 1, no. 3, pp. 77–106, 2021.
- [18] Z. Li, “Treatment and technology of domestic sewage for improvement of rural environment in China-Jiangsu: a research,” *Science Progress and Research (SPR)*, vol. 2, no. 1, 2022.
- [19] S. O. Salihu and Z. Iyya, “Assessment of physicochemical parameters and organochlorine pesticide residues in selected vegetable farmlands soil in Zamfara State, Nigeria,” *Science Progress and Research (SPR)*, vol. 2, no. 2, 2022.
- [20] S. Y. Lin, A. Azar, C. Suarez-Cuervo et al., “Role of sublingual immunotherapy in the treatment of asthma: an updated systematic review,” in *International Forum of Allergy & Rhinology*, vol. 8, no. 9, pp. 982–992, 2018.
- [21] I. Looijmans-van den Akker, A. Werkhoven, and T. Verheij, “Over-prescription of short-acting beta agonists in the treatment of asthma,” *Family Practice*, vol. 38, no. 5, pp. 612–616, 2021.
- [22] C. S. Abrahamsen, H. M. Lang-Ree, K. Halvorsen, and C. M. Stenbakken, “Patients with COPD: exploring patients’ coping ability during an interdisciplinary pulmonary rehabilitation programme: a qualitative focus group study,” *Journal of Clinical Nursing*, vol. 30, no. 9-10, pp. 1479–1488, 2021.
- [23] J. Song, M. Zeng, H. Wang et al., “Distinct effects of asthma and COPD comorbidity on disease expression and outcome in patients with COVID-19,” *Allergy*, vol. 76, no. 2, pp. 483–496, 2021.
- [24] T. R. Gadekallu, N. Khare, S. Bhattacharya et al., “Early detection of diabetic retinopathy using PCA-firefly based deep learning model,” *Electronics*, vol. 9, no. 2, p. 274, 2020.
- [25] F. Pitta, T. Troosters, V. S. Probst, M. A. Spruit, M. Decramer, and R. Gosselink, “Quantifying physical activity in daily life with questionnaires and motion sensors in COPD,” *European Respiratory Journal*, vol. 27, no. 5, pp. 1040–1055, 2006.
- [26] R. Duan, H. Niu, Y. Tao et al., “Adverse effects of short-term personal exposure to fine particulate matter on the lung function of patients with chronic obstructive pulmonary disease and asthma: a longitudinal panel study in Beijing, China,” *Environmental Science and Pollution Research*, vol. 28, no. 34, pp. 47463–47473, 2021.

Research Article

FogDedupe: A Fog-Centric Deduplication Approach Using Multi-Key Homomorphic Encryption Technique

Mohamed Sirajudeen Yoosuf,¹ C. Muralidharan,² S. Shitharth ,³ Mohammed Alghamdi,^{4,5} Mohammed Maray ,⁴ and Osama Bassam J. Rabie ⁶

¹School of Computer Science and Engineering, VIT-AP University Amaravati, Andhra Pradesh, India

²School of Computing Technology, SRM University, Chennai, India

³Department of Computer Science and Engineering, Kebri Dehar, Kebri Debar University, Ethiopia

⁴Department of Information Systems, College of Computer Science, King Khalid University, Abha, Saudi Arabia

⁵Department of Information and Technology Systems, College of Computer Science and Engineering, University of Jeddah, Jeddah, Saudi Arabia

⁶Department of Information Systems, Faculty of Computing and Information Technology, King Abdulaziz University, Jeddah, Saudi Arabia

Correspondence should be addressed to S. Shitharth; shitharths@kdu.edu.et

Received 12 July 2022; Accepted 9 August 2022; Published 25 August 2022

Academic Editor: Sweta Bhattacharya

Copyright © 2022 Mohamed Sirajudeen Yoosuf et al. This is an open access article distributed under the Creative Commons Attribution License, which permits unrestricted use, distribution, and reproduction in any medium, provided the original work is properly cited.

The advancements in communication technologies and a rapid increase in the usage of IoT devices have resulted in an increased data generation rate. Storing, managing, and processing large quantities of unstructured data generated by IoT devices remain a huge challenge to cloud service providers (CSP). To reduce the storage overhead, CSPs implement deduplication algorithms on the cloud storage servers. It identifies and eliminates the redundant data blocks. However, implementing post-progress deduplication schemes does not address the bandwidth issues. Also, existing convergent key-based deduplication schemes are highly vulnerable to confirmation of file attacks (CFA) and can leak confidential information. To overcome these issues, FogDedupe, a fog-centric deduplication framework, is proposed. It performs source-level deduplication on the fog nodes to reduce the bandwidth usage and post-progress deduplication to improve the cloud storage efficiency. To perform source-level deduplication, a distributed index table is created and maintained in the fog nodes, and post-progress deduplication is performed using a multi-key homomorphic encryption technique. To evaluate the proposed FogDedupe framework, a testbed environment is created using the open-source Eucalyptus v.4.2.0 software and fog project v1.5.9 package. The proposed scheme tightens the security against CFA attacks and improves the storage overhead by 27% and reduces the deduplication latency by 12%.

1. Introduction

Cloud computing is a technological revolution that has enabled service providers to deliver computing resources to their users through the internet. It provides easy, scalable access to the applications installed and managed in the cloud servers. The usage of cloud computing services is increasing

exponentially [1]. According to the market research report from Cision 2020, the market size of cloud computing is expected to reach \$832.1 billion by 2025 with a CAGR of 17.5%. On the other hand, the advancements in communication technologies and the increase in the usage of IoT devices have resulted in increased data growth. On average, 2.5 quintillion bytes of data are generated every day. As per

the reports of International Data Corporation 2020, it is expected that in 2025, around 80 Zettabytes of data might be generated from IoT and smart devices [2].

Storing and managing a large quantity of data in the cloud storage servers degrades the performance of the applications that run on the cloud. It is important to address the performance degradation issues in cloud computing technology as the data are expected to grow exponentially in near future.

Storing multiple copies of the same data in the cloud storage servers is one of the reasons for performance degradation in cloud services. In 2017, Waterford Technologies, UK claimed that around 80% of data stored in the public cloud by corporate companies is redundant. Also, the MNC companies are incurring a 12% of revenue loss every year for storing redundant data in the cloud [3]. To address the performance degradation and to remove the redundant data from the cloud storage servers, deduplication schemes are executed. It identifies redundant data and eliminates it from cloud storage servers. Many cloud providers have implemented data deduplication algorithms in their cloud architecture to improve their performance. Data deduplication schemes ensure that only one copy of the data is stored in the cloud storage server. It identifies the redundant data and replaces them with a pointer to the original copy.

The deduplication techniques can be categorized into two types based on the location where the deduplication algorithm is executed. The first type is source-level deduplication where the redundancy check is performed before the data enters the cloud storage. It decreases the ingest rates of real-world data. The second type of deduplication is post-progress deduplication, in which the redundancy check is performed only after the data enters the cloud storage. To execute the post-progress deduplication algorithm, the cloud service provider must have enough space to store the full backup (unique as well as the duplicate copies) somewhere until the duplicate data is removed from the cloud storage servers.

Existing source-level deduplication schemes Hur et al. [4], Patgiri et al. [5], and Chhabraa et al. [6] use Bloom filter as an index table in the cloud servers to perform redundancy checks. Bloom filter is a space-efficient probabilistic data structure that helps in searching for a particular element from a large set. The applications of the Bloom filter in cloud computing are keyword search, retrieving the documents from cloud storage, and cache memory. However, the Bloom filter-based index tables cannot be implemented directly on the deduplication scheme as it has a high possibility of false-positive errors. Also, existing post-progress deduplication schemes Li et al. [7], Zhou et al. [8], Liu et al. [9], Liu et al. [10], and Shen et al. [11] use convergent key encryption methods to perform deduplication, in which the data blocks are hashed and the private keys for the encryption are derived from the message digest. However, the deterministic property of the hash function may produce the same private key and identical cipher text for the redundant data blocks. Later, by comparing the identical ciphertext, the redundant data are removed from the cloud storage servers. The convergent key-based encryption method is easy and efficient

to perform post-progress deduplication. However, the convergent key-based encryption methods are highly vulnerable to confirmation of file attacks (CFA) and increase privacy and security issues. Also, the convergent key-based deduplication schemes become inefficient when the number of data blocks is high.

To reduce the bandwidth wastage in the source-level deduplication, and CFA security issues in the post-progress deduplication, a FogDedupe framework is proposed. Instead of performing source-level deduplication in the cloud servers, the proposed framework introduces a concept of fog-centric deduplication, which effectively reduces bandwidth wastage. Also, to perform post-progress deduplication, additive homomorphic encryption is proposed. The data owners use a multi-key homomorphic encryption algorithm to secure their data and that allows the cloud administrator to perform operations on the corresponding ciphertexts without compromising the security. The proposed multi-key homomorphic deduplication technique allows the DOs to use different private keys to encrypt the data.

1.1. Drawbacks of Existing Deduplication Schemes. The following drawbacks in the existing deduplication schemes have to be addressed to improve the security and performance of cloud services.

- (i) The existing convergent key-based encryption model has a high probability of information leakage as it is vulnerable to confirmation of file attacks (CFA)
- (ii) High probability of false-positive issues in source-level deduplication when the incoming data increases
- (iii) Wastage of network bandwidth in source-level deduplication, i.e., the redundancy check is performed only at the premises of the CSP. So, the redundant data and its attributes are transferred to the cloud server and that increases the communication overhead

1.2. Contributions. Our research work proposes a FogDedupe framework that executes source-level deduplication on the fog layer and post-progress deduplication on the cloud storage server. The contributions of the proposed FogDedupe frameworks are as follows:

- (i) FogDedupe framework implements both source-level and post-progress deduplication simultaneously to increase the performance of the cloud services
- (ii) The source-level deduplication is performed on the fog nodes which are placed near the cloud customers. It efficiently reduces bandwidth wastages
- (iii) To perform source-level deduplication, a distributed index table (DIT) is created based on the Bloom filter and master-slave protocol

- (iv) To perform post-progress deduplication on the cloud storage server, a multi-key homomorphic encryption method-based scheme is proposed. It efficiently overcomes the vulnerabilities of CFA attacks

The remaining section of the paper is structured as follows: Section 2 summarizes the related works on source level and post-progress deduplication. Section 3 explains the preliminaries about homomorphic encryption and additive homomorphic operations. Section 4 provides the proposed FogDedupe framework and multi-key homomorphic encryption. The proposed work is evaluated with a testbed environment and the results are presented in Section 5, and Section 6 concludes the paper.

2. Related Works

For efficient storage utilization, many cloud service providers (CSP) such as IBM Cloud, Dropbox, Amazon Web Service, and Google Drive are using deduplication techniques in the cloud environment. This section explains the recent research works which are related to performing deduplication on cloud storage servers. There are two types of deduplication techniques as source-level and target-level deduplication.

2.1. Source Deduplication Technique. The source-level deduplication is mainly used to reduce the network traffic and bandwidth usage in large numbers. Only after performing a redundancy check using its hash values, the cloud users are allowed to transmit data blocks to cloud servers. Therefore, source deduplication has become very popular and unavoidable in cloud storage system management. To reduce network traffic, the popular cloud service providers (CSP) such as Wuala, Mozy, and Dropbox are using source-level deduplication. Some of the most popular source-level deduplication techniques are Veritas Symantec NetBackup and Amazon CommonVault.

Halevi et al. [12] have proposed source-level deduplication in the cloud storage system. Here, the data owner has to compute the hash value for each data block and sends it to the cloud server whenever the user wants to upload the data to the cloud storage. A hash table is maintained by the cloud server to store all the received data blocks and performs a redundancy check for the newly received data blocks. If there is no match found in the hash table, then the data blocks will be allowed to enter the cloud storage server. Else means that the data block is redundant. Here, the uses of hash values are as follows: (1) verify the redundancy of the data block by the cloud server and (2) act as a “proof of owner” (PoW) to the data owner. If the attacker intentionally or accidentally gains access to the hash value of the data blocks, then the attacker may claim ownership of the particular data. Internal adversarial attacks are possible as the cloud server maintains the hash value of all the user’s data blocks. The scalability feature is not used in a traditional hashing table method. The hash collision rate of the

hash table will be increased when the user/data block increases, and it will provide erroneous (false positive) redundant results.

To overcome the hash-based proof of ownership security threat in Halevi’s source-level deduplication, Pietro et al. [13], have proposed an s-PoW (secure PoW) method which is based on a challenge-response scheme. Here, to prove the ownership of the data, the server challenges the cloud users, and the data owner responds with some particular bits of the requested file. This method fails to address the security threats related to internal adversary attacks and to support scalability. Blasco et al. [14] have introduced a POW verification scheme based on the Bloom filter called “bf-PoW.” It is more efficient than Halevi’s method and Pietro’s method. But this method is not assuring scalability in handling a very large volume of user data.

Zhong et al. [15] have implemented a convergent key-based proof of ownership in the cloud storage system which follows Douceur et al. [16]. To verify the ownership the cloud server uses a convergent key instead of using hash values as PoW, which is created from the hash values of the data block, a master key is used to encrypt the actual data blocks. In this method, two keys were used to protect the user data a convergent key (to verify PoW), and the other is the master key to encrypt the data blocks. This method used both convergent keys and master keys which are created by the cloud server. Here, internal adversarial attacks are possible.

Agarwala et al. [17] have implemented source-level deduplication for images using the DICE (dual integrity convergent key) protocol. In this method, message locked encryption is used to encrypt the images. This method implemented the DICE protocol on each data block instead of encrypting the image (message) as a single file; it is decomposed into several data blocks. Here, the common blocks between two or more images are stored only once at the cloud storage. Youn et al. [18] have introduced a variant of source-deduplication using CP-ABE (Cipher policy attribute-based encryption) [13] where authorized convergent encryption is formed from attribute-based encryption (ABE). It allows only authorized users to access data stored in the cloud. Both use a third-party authorization server to generate keys for the cloud users. Yoosuf et al. [19] proposed a dual auditing scheme and an inline deduplication scheme using Bloom filters.

2.2. Post-Progress Deduplication. Post-progress deduplication is introduced to reduce the workload on cloud users because the source-level deduplication gives an extra workload (hashing data blocks, communicating hash values, and ownership tags to cloud server) to the cloud users. Here, a cloud user is unaware of the deduplication process which is performed to attain maximum storage efficiency. The workload on the client-side in performing target-level deduplication is nil. Here, the storage efficiency is improved by target deduplication.

Bellari et al. [20, 21] have introduced the first target deduplication method called DupLESS architecture using the message locked encryption (MLE) technique. The

private key is generated based on the data file (message) from the dedicated key-server which is received by the cloud users. A unique key is created by the MLE key generation algorithm for each message based on the content of the data. This key is used for data file encryption and mapping with a particular tag “T.” These tags are used for the file redundancy check, and the deduplication is performed on the storage server. The fixed and shorter keys are generated by the key server which avoids extra storage overhead. Bellari’s DupLESS architecture fails to address the solution for internal adversary attacks because the keys are generated by the key server (cloud key server or third party key server) from the content of data (message), which leads to the possibility of internal adversarial attacks. It also fails to support block-level deduplication and lacks security against brute force attacks.[22, 23].

Chen et al. [24] have modified the Bellari et al.’s [21] method and proposed a BL-MLE (block level-message locked encryption) to perform block-level deduplication for larger files in the cloud storage. This method addresses the issues which are block key management and proof of ownership in Bellari’s method. In the BL-MLE method, for any given input file, a master key, a single file tag, and a set of block-level keys are generated. These file tags and block tags are used to perform deduplication on the cloud storage system. Like the MLE method, BL-MLE also has a third-party key server, which creates a path to internal adversarial attacks.

Li et al. [7] have implemented a modified convergent key-based target deduplication, where the cloud user used a master key to encrypt the convergent key which is generated by the cloud server. The encrypted convergent keys are stored in the cloud storage. This modified technique uses a master-convergent key approach where an enormous number of keys are generated when the data blocks increase. The DeKey method is introduced to reduce the key size. It distributes the convergent key across multiple servers using the Ramp Secret Scheme (RSS) instead of the key managed by the user. It splits the secret key into “n” shares and distributes it to multiple servers, such that any “k” shares can recover the secret key. It is difficult to manage all the server’s keys. If a key of a data block is shared among “n” servers, then the complexity of handling and managing the key at those servers is increased. Communication between the servers on handling user keys is also increased, which leads to increased communication overhead [25–27]. The summary of the literature survey is presented in Table 1.

In all the previous deduplication methods, a dedicated key server is used to generate and manage keys for cloud users. Qi et al. [28] have implemented an encrypted deduplication scheme for multiple key servers. Liu et al. [10] have introduced the idea of target deduplication by performing an attribute-keyword search on the ciphertexts. The results are quite promising, but the computation overhead of searchable encryption is very high compared to the normal attribute-based encryption method. Here, outsourcing decryption is used to optimize the scheme. This searchable encryption-based deduplication scheme is implemented only for text documents.

2.2.1. Homomorphic Deduplication. Muguel et al. [29] have implemented the homomorphic operations on the encrypted ciphertext to identify the redundant data blocks in the cloud storage. This homomorphic-based deduplication is to overcome the convergent deduplication technique problems. This method deployed a dedicated key server at the premises of the cloud service provider called as HEDup (homomorphic encryption deduplication). The cloud user encrypts the data with the keys provided by the HEDup key server. Here, internal adversarial attacks are possible where the keys are generated by the key-server present on the CSP. It also has large storage and latency overhead in maintaining the ciphertext.

Liu et al. [30] have introduced searching on encrypted data. The traditional encryption method will not allow the user or CSP to perform any kind of operation on the ciphertext. But homomorphic encryption technique allows the CSP to search, add, and multiply (somewhat homomorphic encryption/partial homomorphic encryption) the ciphertext. It uses searchable homomorphic encryption with tags and matching keywords used to perform deduplication. Youn et al. [31] used a challenge-response protocol and a third-party auditor to ensure the security of the entire system. To perform challenge-response protocols, a homomorphic linear authenticator is created based on the BLS signature [17].

3. Preliminaries: Homomorphic Encryption

Homomorphic encryption (HE) is a technique, where computational operations are carried by cloud service providers on top of the ciphertext without modifying the data format or compromising the security of the user data. A function $f:G \rightarrow H$ between two groups is homomorphic when $fun(xy) = fun(x) \cdot fun(y) \forall x, y \in G$. Here, fun is a function, which takes the input from a group and performs an operation (addition and multiplication) to map with the other set.

Implementing homomorphic applications on cloud storage is a time-consuming process, but it ensures the security of the user data in the cloud environment. It also allows the cloud service provider to perform computations on the ciphertext. Rivest et al. (1976) and Rivest et al. (1978) implemented the first practical homomorphic encryption (RSA algorithm) in 1976 [32, 33]. But in the early 1980s, the computation power of the servers and systems was not capable of performing homomorphic encryption. The improvement in the computation power is achieved by homomorphic operations perform in cloud storage. In 2009, Gentry [34] has implemented fully homomorphic encryption on cloud storage based on ideal lattices. After the successful implementation of Craig Gentry’s (Stanford Ph.D. thesis 2009) work, homomorphic operations have become an important, futuristic technique in cloud computing. Some of the recent works on homomorphic encryptions are Cominetti et al. [35], Chou et al. [36], and Turan et al. [37].

3.1. Additive Homomorphic Encryption. An encryption scheme is called additive homomorphic encryption, if and only if, $(a + b) = E(a) + E(b) \forall a, b \in n$ where E is encryption

TABLE 1: Summarization of related works.

Author (s)	Technique used	Description	Findings
Halevi [13]	Verifying the proof of ownership (PoW) to overcome the security vulnerabilities	(i) Uses message digest to perform source-level deduplication and to verify the ownership of the data block	(i) Uses Merkle tree to verify the ownership (ii) Index table is not scalable
Blasco et al., [14]	Proof of ownership for deduplication using Bloom filter	(i) Cloud server maintains a Bloom filter to verify the ownership of the data by sending a challenge to the clients	(i) Traditional Bloom filter is not scalable (ii) The possibility of false-positive error is high
Agarwala et al. [17]	Client-side secure image deduplication using DICE protocol	(i) Data blocks of the images are encrypted using MLE and DICE protocol (ii) Redundant blocks in the image are removed	(i) Ensures security against poison attacks (ii) It fails to perform source-level deduplication when the same data block is received from different users
Youn et al. [18]	Authorized client-side deduplication using CP-ABE in cloud storage	(i) Provides authorized convergent encryption method using CP-ABE (ii) Allows only authorized users to access critical data	(i) A third-party server is introduced for generating convergent keys. It increases security vulnerabilities
Yoosuf et al. [19]	LDuAP: lightweight auditing with inline deduplication	(i) Two-dimensional Bloom filter is created and managed on the cloud servers to perform inline deduplication	(i) Bandwidth issues are not addressed as the inline deduplication is performed on the cloud servers
Bellari et al. [21]	DupLESS: server-ided encryption for deduplicated storage	(i) A separate key server is introduced to generate keys for the users	(i) If the authenticity of the key server is compromised, then the entire data present in the cloud may get leaked or misused
Chen et al. [24]	BL-MLE: block-level message-locked encryption for secure large file deduplication	(i) Reduces the metadata that is generated by the MLE method (ii) Allows to perform both file-level and block-level target deduplication	(i) Uses Bellaro et al.'s [21] method for POW

and n is set of all possible messages. To develop a practical additive homomorphic encryption (PHE), additive or multiplicative functions are the only options to perform a homomorphic operation on top of the encrypted data because any Boolean circuit can be designed only through the XOR and NAND gate, where XOR performs the addition and NAND performs the multiplication. Examples of additive homomorphic encryptions are Pallier's encryption [38] and Elgamal encryption [39] in which the plaintexts are encoded in the exponents.

4. Problem Statement

As discussed in the related works, the existing deduplication schemes have three major challenges, such as

- (i) Performing source-level deduplication on the cloud storage server results in increased network bandwidth wastage
- (ii) Due to the inability of scaling the index size, the false-positive errors are more in the source-level deduplication
- (iii) The convergent key-based deduplication models have a high probability of information leakage and are vulnerable to confirmation of file attacks (CFA)

To overcome these issues, the proposed FogDedupe framework implements source-level and post-progress deduplication simultaneously. To reduce bandwidth wast-

age, the source-level deduplication is performed on the fog nodes that are kept closer to the data owners. Also, a Bloom filter-based distributed index table (DIT) is created and managed in the fog layer to perform source-level deduplication. It uses the master-slave protocol to frequently update the index table. In addition, a multi-key homomorphic encryption method-based scheme is proposed to perform post-progress deduplication which efficiently overcomes the vulnerabilities against CFA attacks.

5. FogDedupe Framework

The proposed FogDedupe framework performs both source-level and post-progress deduplication. The entities that are involved in the proposed deduplication scheme are (i) data owners, (ii) fog layers and fog nodes, and (iii) cloud service providers (CSP). Figure 1 describes the overall design and the entities of the proposed FogDedupe deduplication framework.

Data owners (DO) are the one who creates the data and uploads it to the cloud storage. The data owners are accountable and eligible to decide who can access the information stored in the cloud within their functional limits. To retrieve the data faster and to perform source-level deduplication, the data owner hashes the data blocks with one-way hash functions and sends the message digest to the nearby fog nodes [40, 41]. Also, the data owner creates public and private keys and encrypts the data blocks using the homomorphic encryption technique. Later, it sends the cipher text to

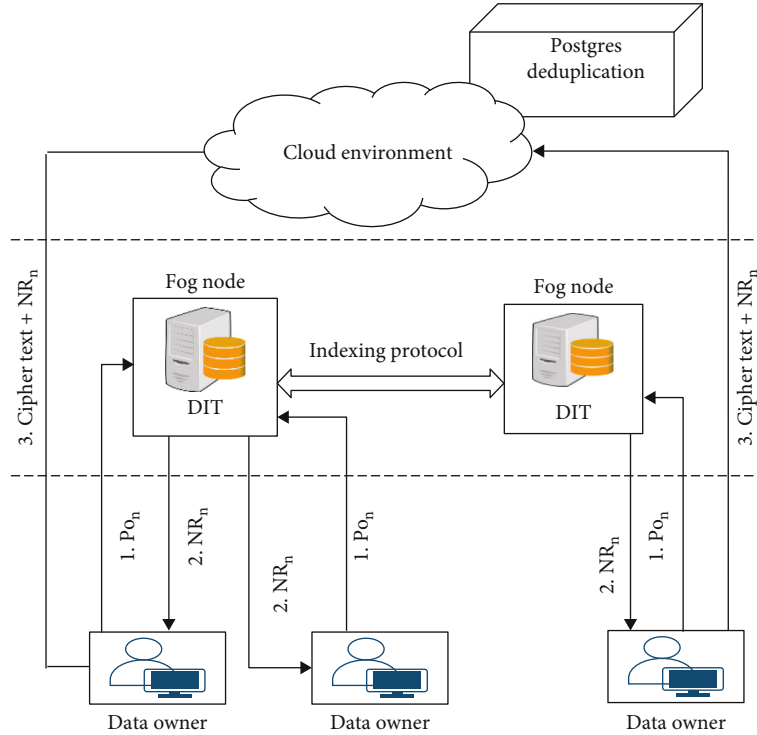


FIGURE 1: Overall architecture of proposed FogDedupe deduplication framework.

the cloud storage servers along with the non-redundant tag (NR_T) generated from source-level deduplication.

Fog layer is a cloud entity that acts as an intermediate layer between the DO and CSP. It consists of several fog nodes that are geographically dispersed and kept closer to the data owners. Also, a dynamically scalable distributed index table (DIT) is created and managed in the fog layer. Upon receiving a source-level deduplication request from the DO, the fog node verifies the index and creates tags. If the data block is unique, the fog node creates a nonredundant tag (NR_T) and sends it to the DO. If it is the redundant block, the fog node prohibits uploading the data block to the cloud storage server.

Cloud service provider (CSP) is the one who provides computing (hardware and software) services to cloud users. CSP has an unlimited resource capacity to store and process the uploaded data. It performs three major tasks:

- (i) Verifies whether the ciphertext has authentic tags or not
- (ii) Stores the ciphertext in the cloud storage server
- (iii) Frequently performs target-level deduplication on the cloud storage servers [23]

5.1. Generating Partial Hash Values ($p\alpha$) for Data Blocks. Initially, the data owner fragments the large size of data into several data chunks each with the size of 1024 KB. Later, for each data chunk, the data owner generates the partial hash $p\alpha$. The data owner hashes the data chunks using n number

of collision-resistant one-way hash functions (HF). As a result, each hash function generates a corresponding digest of size L bits. In the existing inline deduplication schemes, the data owner must share the entire L bit of message digests to the CSP to verify the non-redundancy in the index table. However, it increases the possibility of confirmation of file attacks. To overcome this issue, the proposed fog-centric inline deduplication scheme uses a partial hash value $p\alpha$ instead of the entire message digest. Algorithm 1 explains the process of generating partial hash values for the data chunks.

The data owner creates partial hash values for each data chunk and sends them to the nearby fog node. Sending redundant ciphertext directly to the cloud storage increases the communication overhead as well as the storage overhead. To reduce the wastage of bandwidth the proposed framework directs the data owners to send the computed partial hash values ($p\alpha$) to the nearby fog node. Using the distributed index table, the fog node verifies the incoming data chunk and generates a tag for each data chunk. If a data block is non-redundant, then the fog node creates a non-redundant tag (NR_T) and sends it to the corresponding data owner. If the data block is redundant, a redundant tag (R_T) is sent to the data owner. Upon uploading the ciphertext of the data block, the tags have to be sent along with it. Algorithm 2 explains the source-level deduplication on the fog layer.

After receiving the partial hash values, the fog node calculates its corresponding hash bits and stores it in the distributed index table (DIT). The values in the DIT will

Input: Data chunks $DC_{i=1, 2, \dots, m}$ (each with the size of 1024KB)
Output: Partial hash values ($p\alpha$)
Begin:

1. Data owner HASHES the data chunks ($DC_{i=1, 2, \dots, m}$) using ‘n’ number of hash functions.
2. Data owners stores resultant message digests (hash values) of the data chunks in their local storage.
3. Generate a partial hash value

Begin

 - a. Divide the hash values into ‘p’ partitions (i.e.) (L bits of message digest / ‘p’ partitions).
 - b. To derive the partial hash values ‘p α ’, choose odd partitions from the message digest and take the even bits from each partition.
 - c. Combines the even bits from each odd partition and create a partial hash value ‘p α ’ for each data chunk.
 - d. Creates chunk id (C_{id}), file id (F_{id}) for partial hash values.

End
4. Transfer the chunk id (C_{id}), file id (F_{id}), and its corresponding partial hash values ‘p α ’ to the nearby fog nodes.

ALGORITHM 1: Data owner—generating partial hash values.

Input: Partial hash values ($p\alpha$)
Output: Redundancy verification results.
Begin

1. Fog node receives the chunk id (C_{id}), file id (F_{id}), and hash values ($p\alpha$) from the data owners.
2. Fog node identifies the location of each data chunk and stored it in the DIT.
3. Redundancy verification (incoming data chunks)

If (all corresponding bit position of $p\alpha == 1$)

 - a. Data chunk \leftarrow Duplicate data chunk
 - b. Create a tag to represent that the corresponding ciphertext of the data chunk is duplicate and the fog node prohibits the data owner from uploading redundant data to the cloud servers.
 - c. Sends tag to the data owner.

Else (bit position (SIT) == 0 or bit position (SIT) == at least one 0)

 - a. Data chunk \leftarrow Non-duplicated data chunk
 - b. Calculate the percentage of non-zero hash bits in the index table.
 - c. Creates tag for the non-duplicated data chunk
 - d. Sends the non-duplicated tag to the data owner.
 - e. Sends the percentage of non-zero hash bits to the cloud admin.

End

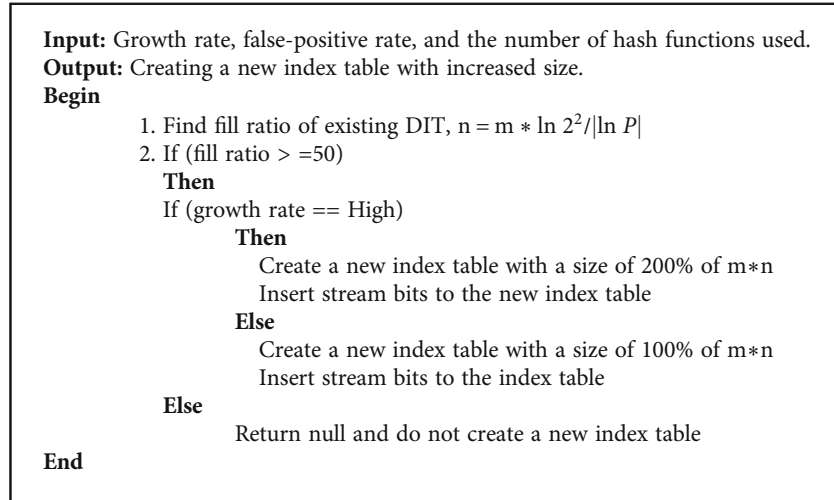
ALGORITHM 2: Fog node—identifying the redundant data chunks.

either be 0 or 1. Here, 0 represents that no data chunks have been accommodated in the particular location, and 1 represents that the location is already accommodated.

Consider that the data owner uses three hash functions and creates three partial hash values for a data chunk. If all the three corresponding bits of partial hash values ($p\alpha$) is 1, then it is determined as a replicated data chunk. If any two of three (2/3) corresponding hash bits in the index table are 1 and one of three (1/3) hash bits are 0, then also it will be considered as a non-duplicated data chunk. Though it is

considered a non-duplicated data chunk, there is a possibility for redundancy. To monitor these high-risk data chunks, the fog node calculates the percentage of corresponding non-zero hash bits in the index table and sends them to the cloud administrator very often.

5.2. *Distributed Index Table.* Managing a standard bloom filter in the fog nodes to perform source-level deduplication results in increased false-positive errors as it follows a one-dimensional data structure. Also, the standard bloom filters



ALGORITHM 3: Fog node—scalability in the proposed distributed index table.

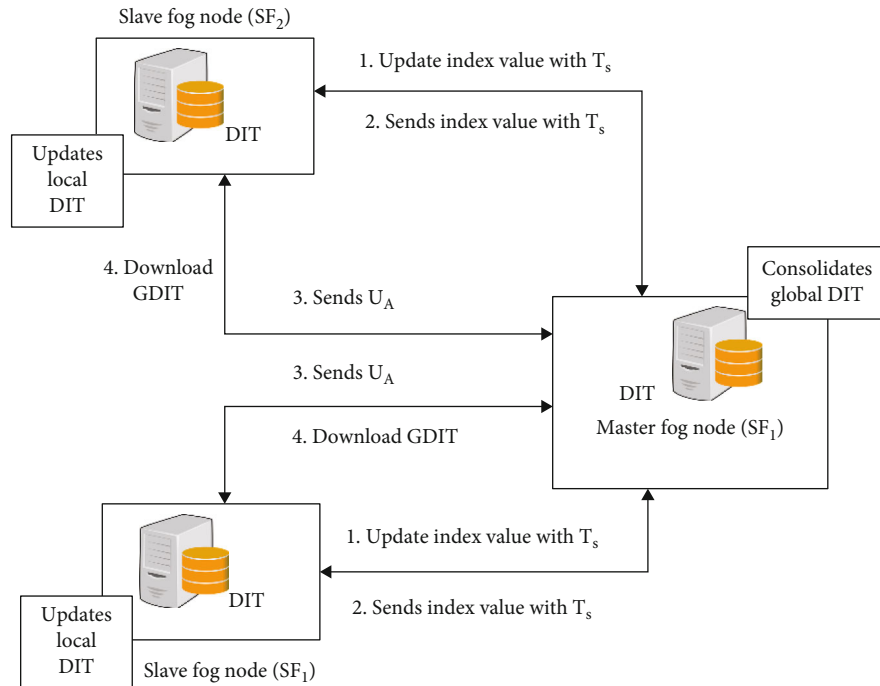


FIGURE 2: Updating the distributed index table.

do not support the scalability feature. However, the velocity of incoming data is very high in cloud services. So, managing a standard bloom filter in the fog nodes might result in a bottleneck situation.

To reduce the false-positive errors in identifying duplicate data chunks in the fog nodes, the proposed scheme creates a two-dimensional scalable index table that is distributed among all the fog nodes in the fog layer. When a request is received from the data owner to perform source-level deduplication, the fog node immediately accesses the distributed index table and sends the response as a tag to the DOs. Determining the initial size of the scal-

able index table in the fog node, the following formula is used:

$$m = \text{Sqrt} \left(\frac{-\text{Total number of data chunks} * \ln(\text{False positive rate})}{\ln(2)^2} \right). \quad (1)$$

The initial size of the index table is determined based on the data chunks received at a particular period. Later, based on the velocity of incoming data chunks, the size of the index table is increased.

<p>Input: Computation workload of each fog node Output: Synchronized Distributed Index Table Begin</p> <ol style="list-style-type: none"> 1. Compute the workload of each fog node. 2. Pick the fog node which has the least computation overload in the last few hours and make it a master fog node (MF). 3. The remaining nodes in the cluster are considered as slave nodes (SF) 3. MF node requests the SF nodes to send the current index table along with the time stamp (T_s). 4. MF node consolidates the values received from the SF nodes and updates the Global Distributed Index Table present in it. 5. After updating the Global DIT, MF sends an update alert (U_A) message to all the SF nodes present in the cluster. 6. The SF downloads the recent update in the Global DIT and synchronizes with the local DIT. <p>End</p>
--

ALGORITHM 4: Updating the distributed index table.

5.3. Scalability of the Index Table. The proposed distributed index table (DIT) is capable of scaling its size from m to $2 * m$ when the velocity of the data increases. The fog nodes continuously monitor the remaining available free slots in the index, i.e., the number of 0s in the index table is continuously monitored. If the non-accommodated slots in the index table go below a certain limit, then a large index table is generated on the same fog node. If the velocity of incoming data is less, then the newly generated index table is two times larger than the old index table and four times larger if the velocity is high. The false-positive rate of the newly created index table is always lesser than the old index table as it has a larger size. Algorithm 3 discusses the scalability of distributed index table in the fog nodes.

5.4. Updating Distributed Index Table Using Master-Slave Protocol. To perform source-level deduplication, a distributed index table is introduced in the FogDedupe architecture. Yoosuf et al. [42] suggested the source-level deduplication in the fog node. However, the index tables were managed in the fog nodes themselves, and it has a high risk of unavailability. To overcome this issue, the proposed FogDedupe framework introduces a distributed index table (DIT), where the same copy of the index table is present in all the fog nodes of the cluster. Using distributed index table (DIT) in the fog layers efficiently overcomes the unavailability issue. Figure 2 depicts the workflow of the proposed distributed index table, and Algorithm 4 explains the process of dynamically updating the records in the DIT.

5.5. Multi-Key Homomorphic Encryption-Based Target Deduplication. After receiving the non-redundant tag (NR_T) from fog nodes, the DO encrypts the data chunks using the additive homomorphic encryption method. Existing homomorphic encryption methods can perform computational operations on top of the ciphertext only if the data blocks are executed using the same public and private keys. It opens a path to information leakage and makes the cipher-

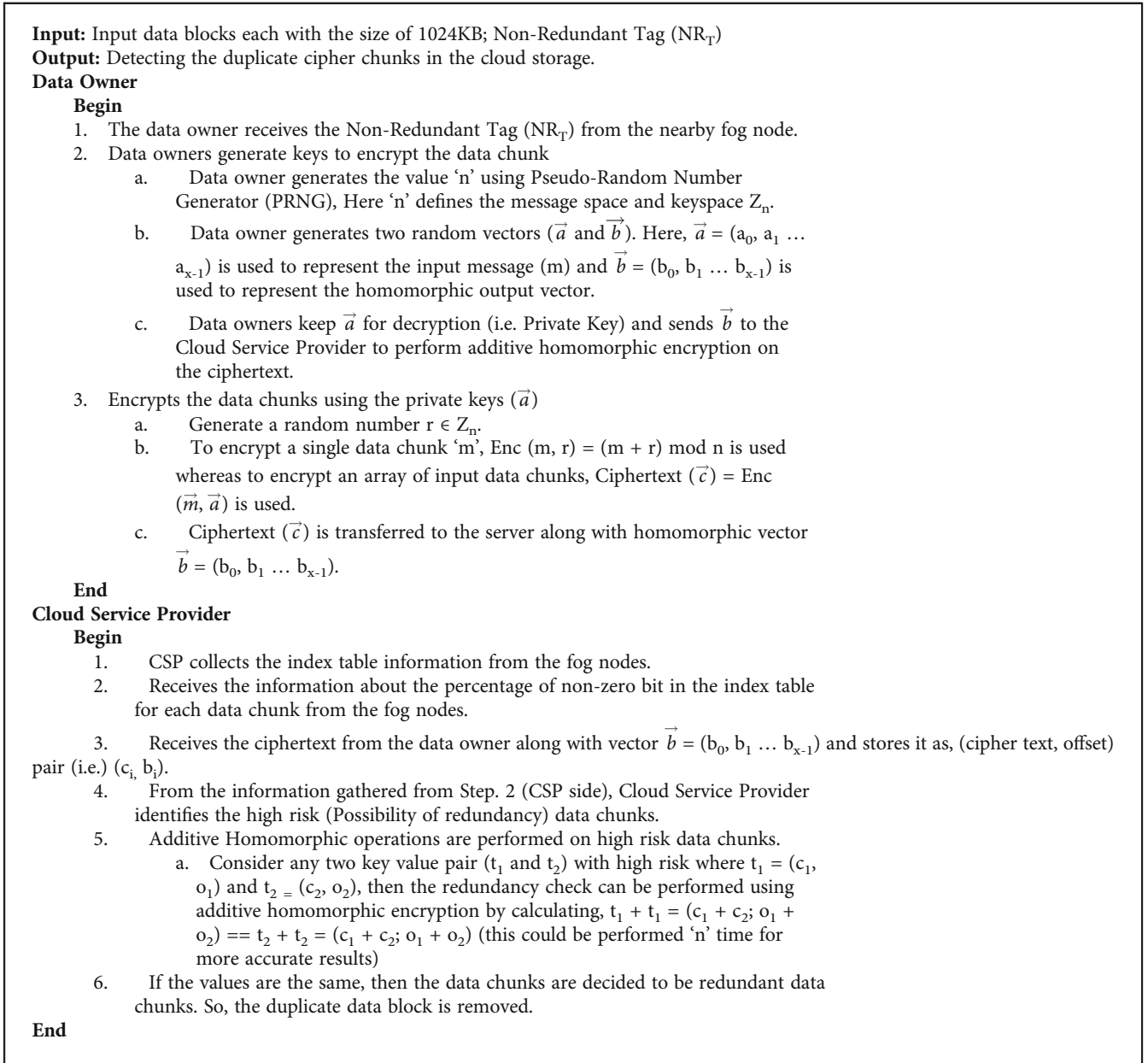
text vulnerable to confirmation of file attacks (CFA). To overcome this issue, the proposed deduplication scheme allows the data owners to encrypt the data blocks using different ciphertexts.

In the key generation model, the data owner creates two vector keys (\vec{a} and \vec{b}) in which \vec{a} is used as a private key and \vec{b} is used as an offset value to perform an additive homomorphic operation by the cloud service provider. After creating the keys, the data owner uses a one-time pad encryption method to encrypt the data blocks. To perform an additive operation on the ciphertext “modulo n ” operation is used. However, the computation overhead of executing homomorphic encryption-based deduplication remains high in the cloud environment. Continuously performing target deduplication in cloud storage servers is impractical and may lead to an extensive workload for the cloud service provider. So, in the proposed target deduplication method, the CSP calculates the high-risk data blocks, i.e., the data chunks that have a high possibility to be redundant are calculated, and only for those data chunks, the target deduplication is performed. The high-risk data blocks are identified from the information received from the fog nodes. Algorithm 5 explains the proposed multi-key homomorphic encryption algorithm to encrypt the non-redundant data block.

The proposed deduplication scheme uses an additive homomorphic encryption-based algorithm to perform deduplication. It effectively identifies the redundant block in the cloud storage servers by comparing the corresponding ciphertext. However, executing an additive homomorphic operation on the ciphertext stored in the cloud puts an extra workload on the CSP.

6. Performance Evaluation

The prime objectives of the proposed FogDedupe frameworks are (1) reducing false-positive errors in the index table



ALGORITHM 5: Multi-key homomorphic encryption-based target-level deduplication.

and (2) improving the security against confirmation of false Attacks (CFA).

6.1. False-Positive Error Rate. The false-positive error in the proposed fog-centric inline deduplication refers to a situation in which an element points to a particular location as that of another element in the index table. The probability of false-positive error in the proposed index table is

$$\text{Probability (false Positive)} = \left(1 - e^{-k*n/m}\right)^k, \quad (2)$$

$$\text{Expected (false positive)} = \sum_{i=0}^{n-1} Cf(i). \quad (3)$$

Here, Cf represents the collision in the index table and i is the factor of collision. The false-positive rate of the fog-centric inline deduplication highly depends on the number of collisions that happens in the index table. Since the proposed index table is capable of scaling its size, the probability of hash collision is always lesser than the standard Bloom filter-based index tables. Table 2 depicts the false-positive error rate in the distributed hash table.

The probability of false-positive errors ranges between 0.002 and 0.004. It is very low compared to the standard bloom filter. Table 3 shows the probability of the false-positive errors after scaling the size of the index table.

The probability of false-positive error after scaling the size of the index table is always lesser than the initial size of the index table. So, the proposed fog-centric inline

TABLE 2: False-positive errors in the distributed index table.

Number of data blocks	Number of the hash function used (k)	Total bits in index table	Prob. of false-positive error in the index table
1024	3	9801	0.003319
2048	3	19600	0.003319
3072	3	29241	0.002969
4096	3	39204	0.003319
5120	3	48841	0.003058
10240	3	97969	0.00319
102400	3	980100	0.00321
204800	3	1960000	0.00325
512000	3	4906225	0.00312
1024000	3	9809424	0.00317
2048000	3	19624900	0.00319

deduplication can effectively be performed even if the velocity of the data increases.

6.2. Security Analysis of the Proposed Scheme. The existing deduplication algorithm uses the entire message digest of the data block to generate the encryption keys. It makes the existing schemes vulnerable to the confirmation of file attacks (CFA). To overcome this issue, instead of using the message digest of the data blocks to generate keys, the proposed scheme derives the partial hash values, i.e., L bits of message digest/ p partitions from the message digest are sent to the fog nodes. Sharing the partial hash values to the fog node allows them to perform source deduplication using the scalable index table and tightens the security. Even if the partial hash values get leaked from the fog node, no intruder can match the remaining hash bits. Let us consider a data block of size 1024KB is hashed and produces 256 hash bits. Here, instead of sending the entire 256 bits to the fog node, the proposed deduplication method derives partial hash values ($p\alpha$) from 256 bits, i.e., $256 \text{ bits}/\text{No. of } p \text{ partitions}$ of bits are shared to the fog nodes. From these partial hash bits, it is impossible to perform confirmation of file attacks. Moreover, the proposed system uses k hash functions to derive the partial hash values. So it makes it more secured against hash collision attacks.

On the other hand, the proposed multi-key additive homomorphic encryption allows the CSP to execute computational functions on top of the ciphertext stored in the cloud storage servers. Though it increases the computational overhead, it also tightens the security of the data in the aspect of both internal and external attacks.

7. Implementation and Result Discussion

To assess the performance of the proposed FogDedupe framework, an open source Eucalyptus software is installed on an Intel Xeon E5 2620 server that has a processing speed of 2.1GHZ with 64GB RAM. Eucalyptus-based private cloud setup consists of cloud controller (CLC), cluster controller

(CC), and walrus (W). The cloud controller is responsible for performing administrative operations of the CSP. The cluster controller controls the cluster nodes connected to the main cloud server. Two personal computers with Intel i5 -7th gen processor and 8GB RAM are used to create the cluster nodes. The walrus represents the storage servers of the Eucalyptus private cloud. A total of 4TB storage space with RAID 5 configuration is used as a storage server. The Eucalyptus open-source software is compatible with Amazon AWS and well-suitable for evaluating fog-based source-level deduplication. Also, the fog nodes are created between cloud storage servers and the DOs by installing FOG project v1.5.9 Intel i5 -7th gen processor with 8GB RAM.

The data chunking process and the generation of partial hash values for the data chunks are carried out by the data owner. Operations like data chunking, key generation, encryption, and creation of partial hash values were written in the python programming language. An open-source mhealth (mobile health) dataset from UCI repository is used to assess the proposed fog-centric deduplication scheme. It comprises 172,824 IoT healthcare sensor values.

The prime objective of the proposed work is to reduce the communication overheads and improve storage efficiency. To assess the proposed scheme, the communication overhead and computation overhead on the fog nodes to perform inline deduplication and the computation overhead on the CSP to execute additive homomorphic operations on the ciphertext stored in the cloud are measured. Also, the redundancy elimination ratio of the proposed scheme is compared with BL-MLE, DupLESS, Youn et al. [18] deduplication schemes.

7.1. Communication Overhead. Two different scenarios are considered to measure the communication overhead for performing inline deduplication. (a) The data owner uploads the ciphertexts of the data chunks directly to the cloud, i.e., no fog layers are formed to perform inline deduplication. (b) The data owner verifies the redundancy of the data chunks in fog nodes first and then sends the ciphertext to the cloud.

Introducing a fog layer between DOs, the cloud effectively reduces the communication delay to a maximum of 60%, because the proposed FogDedupe source-level deduplication framework prohibits DOs to upload redundant ciphertext to the cloud storage servers directly.

The fog nodes are usually kept near to the DOs to quickly perform source-level deduplication, and the ciphertext of the DOs data is stored in the Amazon AWS-walrus storage. Table 4 shows the communication time required to access the fog node and the walrus storage. Results show that introducing fog nodes in the cloud services reduces the communication overhead by a maximum of 60%.

The communication overhead of the data owner transferring the $p\alpha$ to the fog nodes and uploading the ciphertext to the cloud storage is measured and shown in Figure 3.

7.2. Computation Overhead on the Fog Nodes. Fog nodes receive the hash value $p\alpha$ from the data owners and compute

TABLE 3: Probability of false-positive error after scaling the size of index table.

Data blocks	Total bits in index table (before scaling) (m_{prev})	Prob. of false-positive before scaling its size (fP_{prev})	Total bits in the index table after scaling its size (m_{new})		Prob. of false-positive fP_{new} (new matrix)	
			Min (GR)	Max (GR)	$fP_{new} = fP_{prev} * r$	
					Min ($r = 0.8$)	Max ($r = 0.9$)
1024	9801	0.003319	19602	39204	$2.6 * 10^{-3}$	$2.9 * 10^{-3}$
2048	19600	0.003319	39200	78400	$2.6 * 10^{-3}$	$2.9 * 10^{-3}$
3072	29241	0.002969	58482	116964	$2.3 * 10^{-3}$	$2.6 * 10^{-3}$
4096	39204	0.003319	78408	156816	$2.6 * 10^{-3}$	$2.9 * 10^{-3}$
5120	48841	0.003058	97682	195364	$2.4 * 10^{-3}$	$2.7 * 10^{-3}$
10240	97969	0.00319	195938	391876	$2.5 * 10^{-3}$	$2.8 * 10^{-3}$
102400	980100	0.00321	1960200	3920400	$2.5 * 10^{-3}$	$2.8 * 10^{-3}$
204800	1960000	0.00325	3920000	7840000	$2.6 * 10^{-3}$	$2.9 * 10^{-3}$
512000	4906225	0.00312	9812450	19624900	$2.5 * 10^{-3}$	$2.8 * 10^{-3}$
1024000	9809424	0.00317	19618848	39237693	$2.5 * 10^{-3}$	$2.8 * 10^{-3}$
2048000	19624900	0.00319	39249800	78499600	$2.5 * 10^{-3}$	$2.8 * 10^{-3}$

TABLE 4: Communication time required to access AWS storage.

Number of Data blocks	Data owner directly accessing AWS storage (without fog node)		Data owners accessing the AWS with fog nodes	
	Time in milliseconds	Standard deviation in milliseconds	Time in milliseconds	Standard deviation in milliseconds
5	320.26	136.26	66.51	15.02
25	1350.76	540.45	246.40	166.63
50	2750.50	994.21	1428.11	358.55
100	5556.93	1899.01	3112.98	767.92
200	11789.12	3444.56	6802.11	1480.92

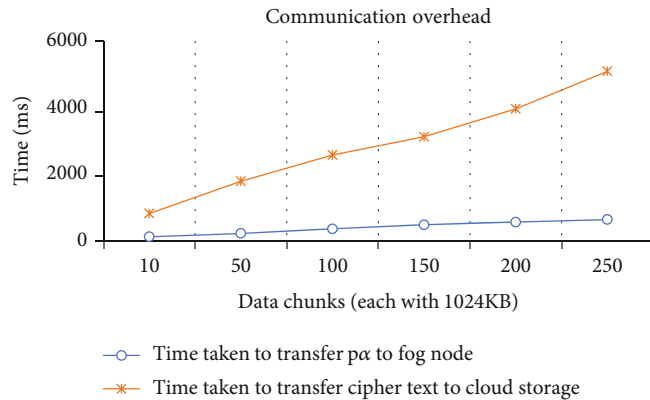


FIGURE 3: Communication overhead.

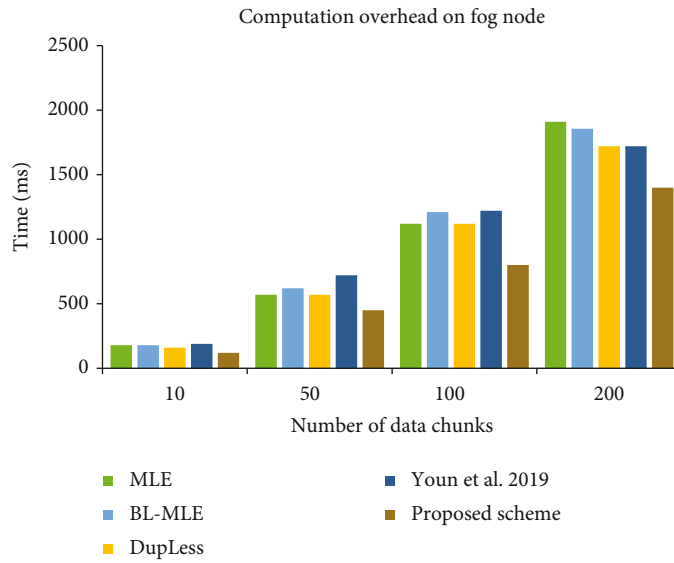


FIGURE 4: Comparison of computation overhead on fog node with existing additional key server schemes.

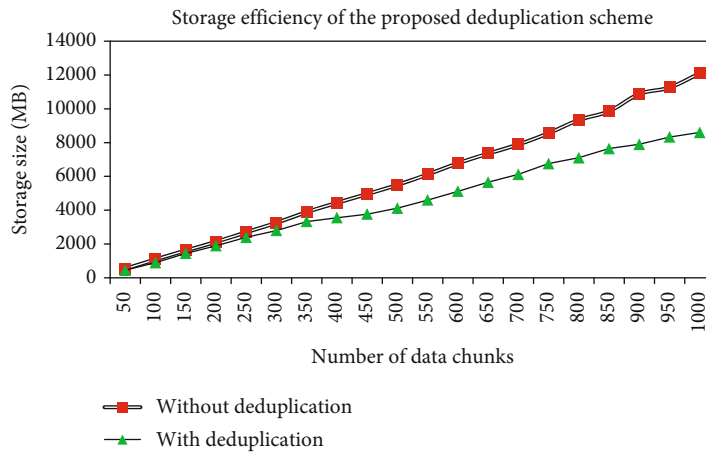


FIGURE 5: Storage efficiency of cloud storage servers.

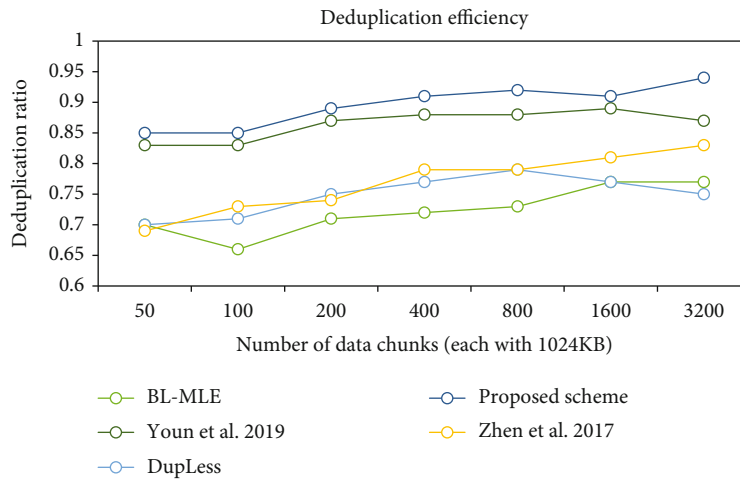


FIGURE 6: Comparison of deduplication ratio.

its corresponding locations in the distributed index table (DIT). In the proposed deduplication scheme, fog nodes do not generate any keys on behalf of the data owner; rather, it simply calculates the bit position from the partial hash values and changes the values from 0 to 1. However, the existing deduplication schemes use a separate key server on the third parties to create convergent keys to encrypt the chunks.

The computation overhead of the proposed deduplication scheme in the fog node is much lesser than the existing methods. Figure 4 compares the computation time required in the fog nodes to execute the proposed inline deduplication with existing key server deduplication schemes.

To evaluate the proposed scheme, 25,000 IoT healthcare IoT sensor values are randomly chosen. The data owner hashes each sensor value and creates $p\alpha$. Later, they are communicated to the nearby fog node. The $p\alpha$ is stored in the DIT, and the fog node dynamically performs source-level deduplication. The deduplication ratio of the proposed source-level deduplication is calculated using the following formula:

$$\text{Deduplication Ratio} = \frac{\text{Size of the input data} - \text{Storage utilized}}{\text{size of the input data}}. \quad (4)$$

To assess the performance of the proposed scheme, two different scenarios are considered. (i) The randomly selected 25,000 data chunks from the mhealth dataset are encrypted, and the ciphertext is uploaded to the walrus directly by the DO, i.e., no deduplication algorithm is executed. (ii) The randomly selected 25,000 sensor values are uploaded to the cloud storage after performing fog-centric source level deduplication.

The storage utilization of the cloud storage server is calculated for both scenarios. After implementing the fog-centric source-level deduplication, the storage efficiency is increased up to 30%. Figure 5 shows the improvements in the storage efficiency after implementing the deduplication scheme.

The redundancy elimination ratio is calculated using the following formula:

$$\text{Redundancy Elimination Ratio} = \frac{\text{Total number of correctly removed redundant sensor values}}{\text{Total number of Sensor values sent to fog nodes}}. \quad (5)$$

Figure 6, compares the ratio of duplicate data that are removed by BL-MLE, DupLESS, Zhen et al. 2017, Youn et al. 2019, and the proposed fog-centric inline deduplication. The redundancy elimination ratio of the proposed deduplication scheme ranges from 0.84 to 0.93. It reduces the storage overhead of the cloud by approximately 30% by maintaining the redundancy elimination ratio between 0.85 and 0.94.

8. Conclusion and Future Works

To reduce the network bandwidth wastage and to overcome the false-positive errors in the source-level deduplication, a FogDedupe framework is proposed. It performs both source-level deduplication and post-progress deduplication to improve the efficiency of the cloud service and storage servers. To perform source-level deduplication a fog layer, consisting of “n” number of fog nodes is introduced. Also, a distributed index table is created and managed on the fog layer. The fog nodes present on the same cluster use master-slave protocol to update the index values. The scalability feature in the proposed distributed index table effectively reduces the false positive errors in the source-level deduplication. Likewise, to perform target-level deduplication, a multi-key additive homomorphic method is introduced. Though the post-progress deduplication takes a slightly larger time to identify the duplicate blocks, it overcomes the security threats raised by the CFA attacks effectively. In the future, instead of using additive homomorphic operations, fully homomorphic operations are planned to be implemented on the cloud storage server to perform post-progress deduplication.

Data Availability

The data that support the findings of this study are available from the corresponding author, upon reasonable request.

Conflicts of Interest

The authors declare that they have no conflicts of interest.

References

- [1] B. Alouffi, M. Hasnain, A. Alharbi, W. Alosaimi, H. Alyami, and M. Ayaz, “A systematic literature review on cloud computing security: threats and mitigation strategies,” *IEEE Access*, vol. 9, pp. 57792–57807, 2021.
- [2] IDC Data Age, “Whitepaper,” 2025, Available from, Error! Hyperlink reference not valid [Accessed on July 2022].
- [3] “Newspaper Article,” Available from, <https://waterfordtechnologies.com/banish-your-redundant-data-like-st-patrick-banished-snakes-out-of-ireland/>, [Accessed on July 2022].
- [4] J. Hur, D. Koo, Y. Shin, and K. Kang, “Secure data deduplication with dynamic ownership management in cloud storage,” *IEEE Transactions on Knowledge and Data Engineering*, vol. 28, no. 11, pp. 3113–3125, 2016.
- [5] R. Patgiri, D. Dev, and A. Ahmed, “dMDS: uncover the hidden issues of metadata server design,” in *Progress in Intelligent Computing Techniques: Theory, Practice, and Applications*, pp. 531–541, Springer, Singapore, 2018.
- [6] N. Chhabra and M. Balab, “An optimized data duplication strategy for cloud computing: Dedup with ABE and bloom filters,” *International Journal of Future Generation Communication and Networking*, vol. 13, no. 1, pp. 824–834, 2020.
- [7] J. Li, X. Chen, M. Li, J. Li, P. P. C. Lee, and W. Lou, “Secure deduplication with efficient and reliable convergent key management,” *IEEE transactions on parallel and distributed systems*, vol. 25, no. 6, pp. 1615–1625, 2013.

- [8] Y. Zhou, D. Feng, W. Xia, F. Min, F. Huang, Y. Zhang, and C. Li, Eds., "SecDep: a user-aware efficient fine-grained secure deduplication scheme with multi-level key management," in *2015 31st Symposium on Mass Storage Systems and Technologies (MSST)*, pp. 1–14, Santa Clara, CA, USA, 2015.
- [9] M. Liu, C. Yang, Q. Jiang, X. Chen, J. Ma, and J. Ren, Eds., "Updatable block-level deduplication with dynamic ownership management on encrypted data," in *2018 IEEE International Conference on Communications (ICC)*, pp. 1–7, Kansas City, MO, USA, 2018.
- [10] X. Liu, L. Tingting, X. He, X. Yang, and S. Niu, "Verifiable attribute-based keyword search over encrypted cloud data supporting data deduplication," *IEEE Access*, vol. 8, pp. 52062–52074, 2020.
- [11] W. Shen, S. Ye, and R. Hao, "Lightweight cloud storage auditing with deduplication supporting strong privacy protection," *IEEE Access*, vol. 8, pp. 44359–44372, 2020.
- [12] S. Halevi, D. Harnik, B. Pinkas, and A. Shulman-Peleg, "Proofs of ownership in remote storage systems," in *In Proceedings of the 18th ACM conference on Computer and communications security*, pp. 491–500, Chicago, IL, USA, 2011.
- [13] R. Di Pietro and A. Sorniotti, "Boosting efficiency and security in proof of ownership for deduplication," in *In Proceedings of the 7th ACM symposium on information, computer and communications security*, pp. 81–82, Seoul, Korea, 2012.
- [14] J. Blasco, R. Di Pietro, A. Orfila, and A. Sorniotti, "A tunable proof of ownership scheme for deduplication using bloom filters," in *2014 IEEE Conference on Communications and Network Security*, pp. 481–489, San Francisco, CA, USA, 2014.
- [15] W. Zhong and Z. Liu, "Proof of cipher text ownership based on convergence encryption," in *In AIP Conference Proceedings*, vol. 1864, Melville, NY 1147-4300, USA, 2017no. 1, Article ID 20051.
- [16] J. R. Douceur, A. Adya, W. J. Bolosky, P. Simon, and M. Theimer, "Reclaiming space from duplicate files in a serverless distributed file system," in *Proceedings 22nd International Conference on Distributed Computing Systems*, pp. 617–624, Vienna, Austria, 2002.
- [17] A. Agarwala, P. Singh, and P. K. Atrey, "Client side secure image deduplication using DICE protocol," in *2018 IEEE Conference on Multimedia Information Processing and Retrieval (MIPR)*, pp. 412–417, Miami, FL, USA, 2018.
- [18] T.-Y. Youn, N.-S. Jho, K. H. Rhee, and S. U. Shin, "Authorized client-side deduplication using CP-ABE in cloud storage," *Wireless Communications and Mobile Computing*, vol. 2019, Article ID 7840917, 11 pages, 2019.
- [19] M. S. Yoosuf and R. Anitha, "LDuAP: lightweight dual auditing protocol to verify data integrity in cloud storage servers," *Computing*, vol. 13, no. 8, pp. 3787–3805, 2022.
- [20] M. Bellare, S. Keelveedhi, and T. Ristenpart, "Message-locked encryption and secure deduplication," in *Annual International Conference on the Theory and Applications of Cryptographic Techniques*, pp. 296–312, Berlin, Heidelberg, 2013.
- [21] S. Keelveedhi, M. Bellare, and T. Ristenpart, "DupLESS: Server-Aided Encryption for Deduplicated Storage," in *In 22nd USENIX security symposium (USENIX security 13)*, pp. 179–194, Washington DC, 2013.
- [22] K. K. Chennam, R. Aluvalu, and S. Shitharth, "An authentication model with high security for cloud database," in *Architectural Wireless Networks Solutions and Security Issues*, pp. 13–25, Springer, Singapore, 2021.
- [23] B. T. Devi, S. Shitharth, and M. A. Jabbar, "An appraisal over intrusion detection systems in cloud computing security attacks," in *2020 2nd International Conference on Innovative Mechanisms for Industry Applications (ICIMIA)*, pp. 722–727, Bangalore, India, 2020.
- [24] R. Chen, M. Yi, G. Yang, and F. Guo, "BL-MLE: block-level message-locked encryption for secure large file deduplication," *IEEE Transactions on Information Forensics and Security*, vol. 10, no. 12, pp. 2643–2652, 2015.
- [25] T. R. Gadekallu, Q. V. Pham, D. C. Nguyen et al., "Blockchain for edge of things: applications, opportunities, and challenges," *IEEE Internet of Things Journal*, vol. 9, no. 2, pp. 964–988, 2021.
- [26] B. Prabadevi, N. Deepa, Q.-V. Pham et al., "Toward blockchain for edge-of-things: a new paradigm, opportunities, and future directions," *IEEE Internet of Things Magazine*, vol. 4, no. 2, pp. 102–108, 2021.
- [27] M. Liyanage, Q. V. Pham, K. Dev et al., "A survey on Zero touch network and Service Management (ZSM) for 5G and beyond networks," *Journal of Network and Computer Applications*, vol. 203, article 103362, 2022.
- [28] H. Qi, Y. Han, X. Di, and F. Sun, "Secure data deduplication scheme based on distributed random key in integrated networks," in *In 2017 3rd IEEE International Conference on Computer and Communications (ICCC)*, pp. 1308–1312, Chengdu, China, 2017.
- [29] R. Miguel and K. M. M. Aung, "Hedup: secure deduplication with homomorphic encryption," in *2015 IEEE International Conference on Networking, Architecture and Storage (NAS)*, pp. 215–223, Boston, MA, USA, 2015.
- [30] L. Zhenhua, K. Yaqian, L. Chen, and F. Yaqing, "Hybrid cloud approach for block-level deduplication and searchable encryption in large universe," *The Journal of China Universities of Posts and Telecommunications*, vol. 24, no. 5, pp. 23–34, 2017.
- [31] T.-Y. Youn, K.-Y. Chang, K.-H. Rhee, and S. U. Shin, "Efficient client-side deduplication of encrypted data with public auditing in cloud storage," *Access*, vol. 6, pp. 26578–26587, 2018.
- [32] R. L. Rivest, L. Adleman, and M. L. Dertouzos, "On data banks and privacy homomorphisms," *Foundations of secure computation*, vol. 4, no. 11, pp. 169–180, 1978.
- [33] R. L. Rivest, A. Shamir, and L. Adleman, "A method for obtaining digital signatures and public-key cryptosystems," *Communications of the ACM*, vol. 21, no. 2, pp. 120–126, 1978.
- [34] C. Gentry, *A Fully Homomorphic Encryption Scheme*[Ph.D. thesis], Stanford University, California, USA, 2009.
- [35] E. L. Cominetti and M. A. Simplicio, "Fast additive partially homomorphic encryption from the approximate common divisor problem," *IEEE Transactions on Information Forensics and Security*, vol. 15, pp. 2988–2998, 2020.
- [36] E. J. Chou, A. Gururajan, K. Laine, N. K. Goel, A. Bertiger, and J. W. Stokes, "Privacy-preserving phishing web page classification via fully homomorphic encryption," in *ICASSP 2020 - 2020 IEEE International Conference on Acoustics, Speech and Signal Processing (ICASSP)*, pp. 2792–2796, Barcelona, Spain, 2020.
- [37] F. Turan, S. S. Roy, and I. Verbauwhe, "HEAWS: an accelerator for homomorphic encryption on the Amazon AWS FPGA," *IEEE Transactions on Computers*, vol. 69, no. 8, pp. 1–1196, 2020.
- [38] P. Paillier, "Public-key cryptosystems based on composite degree residuosity classes," in *In International conference on*

the theory and applications of cryptographic techniques, pp. 223–238, Berlin, Heidelberg, 1999.

- [39] T. ElGamal, “A public key cryptosystem and a signature scheme based on discrete logarithms,” *IEEE Transactions on Information Theory*, vol. 31, no. 4, pp. 469–472, 1985.
- [40] B. C. Gajarla, A. V. Rebba, K. S. Kakathota, M. Kummari, and S. Shitharth, “Handling tactful data in cloud using PKG encryption technique,” in *4th Smart Cities Symposium (SCS 2021)*, pp. 338–343, Barcelona, Spain, 2021.
- [41] R. Aluvalu, V. Uma Maheswari, K. K. Chennam, and S. Shitharth, “Data security in cloud computing using Abe-based access control,” in *Architectural Wireless Networks Solutions and Security Issues*, pp. 47–61, Springer, Singapore, 2021.
- [42] M. S. Yoosuf and R. Anitha, “Low latency fog-centric deduplication approach to reduce IoT healthcare data redundancy,” *Wireless Personal Communications*, vol. 122, pp. 1–23, 2022.

Retraction

Retracted: Data Acquisition through Mobile Sink for WSNs with Obstacles Using Support Vector Machine

Journal of Sensors

Received 23 January 2024; Accepted 23 January 2024; Published 24 January 2024

Copyright © 2024 Journal of Sensors. This is an open access article distributed under the Creative Commons Attribution License, which permits unrestricted use, distribution, and reproduction in any medium, provided the original work is properly cited.

This article has been retracted by Hindawi following an investigation undertaken by the publisher [1]. This investigation has uncovered evidence of one or more of the following indicators of systematic manipulation of the publication process:

- (1) Discrepancies in scope
- (2) Discrepancies in the description of the research reported
- (3) Discrepancies between the availability of data and the research described
- (4) Inappropriate citations
- (5) Incoherent, meaningless and/or irrelevant content included in the article
- (6) Manipulated or compromised peer review

The presence of these indicators undermines our confidence in the integrity of the article's content and we cannot, therefore, vouch for its reliability. Please note that this notice is intended solely to alert readers that the content of this article is unreliable. We have not investigated whether authors were aware of or involved in the systematic manipulation of the publication process.

Wiley and Hindawi regrets that the usual quality checks did not identify these issues before publication and have since put additional measures in place to safeguard research integrity.

We wish to credit our own Research Integrity and Research Publishing teams and anonymous and named external researchers and research integrity experts for contributing to this investigation.

The corresponding author, as the representative of all authors, has been given the opportunity to register their agreement or disagreement to this retraction. We have kept a record of any response received.

References

- [1] G. Sulakshana and G. R. Kamatam, "Data Acquisition through Mobile Sink for WSNs with Obstacles Using Support Vector Machine," *Journal of Sensors*, vol. 2022, Article ID 4242740, 20 pages, 2022.

Research Article

Data Acquisition through Mobile Sink for WSNs with Obstacles Using Support Vector Machine

Guduri Sulakshana ¹ and Govardhan Reddy Kamatam ²

¹Department of Computer Science and Engineering, G. Pulla Reddy Engineering College-Research Center, Kurnool, Jawaharlal Nehru Technological University-Ananthapuramu (JNTUA), Andhra Pradesh, India

²Department of Computer Science and Engineering, G. Pulla Reddy Engineering College, Kurnool, Andhra Pradesh, India

Correspondence should be addressed to Guduri Sulakshana; suhaasraj21@gmail.com

Received 28 July 2022; Accepted 11 August 2022; Published 25 August 2022

Academic Editor: Praveen Kumar Donta

Copyright © 2022 Guduri Sulakshana and Govardhan Reddy Kamatam. This is an open access article distributed under the Creative Commons Attribution License, which permits unrestricted use, distribution, and reproduction in any medium, provided the original work is properly cited.

Mobile sink-based data collection in wireless sensor networks has become an attractive research area to mitigate hotspot issues. It further increases the efficiency of the WSN, such as throughput, lifetime, and energy efficiency, while decreasing delay and packet losses. Mobile sink algorithms developed by many researchers in recent years have only contributed to obtain efficient path planning, and only a few researchers have focused on solving the problem of network environment with obstacles. Here, constructing an obstacle-aware path for the mobile sink to collect data in WSN is a challenging issue. In this context, we present the data acquisition through mobile sink for WSNs with obstacles using support vector machine (DAOSVM). The DAOSVM algorithm works in two phases: visiting point selection and path construction. The visiting point selection uses spanning tree approach, and the path selection uses SVM. The computational complexity of the proposed DAOSVM is estimated and compared using the existing techniques, and it is lower. The DAOSVM also outperforms traditional methods concerning multiple performance metrics under various scenarios.

1. Introduction

Wireless sensor networks (WSNs) are the finite set of sensor nodes (SNs) deployed randomly in a region of interest to monitor and collect the data [1]. There are several WSN applications, which are air-quality monitoring, climate analysis, industries, defense, smart cities, etc. [2]. The SNs transmit their data using multihop communication to the base station (BS) or sink using relay nodes (RNs). These nodes are operated with low-powered batteries, and to replace them is a costly and hectic task [3]. Instead, energy can be harvested by using rechargeable SNs [4]. But, even here, it is uneconomical as a massive number of SNs have to be used in WSNs. Due to the use of a vast number of SNs and substantial data transmissions through multihop communications, the RNs near the BS drain more energy and die soon. In this case, there is a probability of BS being separated, giving rise to the energy hole or hotspot problem [5–7].

Many of the researchers address the energy hole problem by introducing the mobile sink (MS). The MS is a vehicle that visits each SN in the network and receives data packets from them and reports the data to the BS. In this case, the SNs directly report their data to the MS, so there is no involvement of the RN, and hence, the energy consumption is minimized. However, visiting each SN is not the right approach because it takes a long time to reach the end node. Notably, delay-sensitive fields such as medical, industrial, and defense require data immediately. Furthermore, due to SN's limited buffer overflow, it causes packet loss. Even if they adopt the shortest traveling path to visit all the SNs, it does not address the issue. So, instead of visiting each node in the network, the MS visits a few SNs called rendezvous points (RPs), and other nodes transmit their packets to the nearest RP. Thus, identifying optimal RPs and determining the best path by avoiding the delay and data losses are again challenging issues. However, some of the researchers address these challenges [8–10].

Most of the researchers in the literature consider RP as a node or location and used traveling salesman problem (TSP) for MS path constructions. In [11–15], the authors adopted clustering algorithms to determine cluster heads (CHs) and they have considered CHs as RPs. Notably, these approaches have not considered the region of interest's obstacles in a real-time environment while constructing the MS traveling path. So, there is a chance of getting obstacles in real-time environments, and determining the MS path by considering those obstacles is a more challenging issue. Besides that, the WSNs are operated dynamically with limited human intervention, so self-operated algorithms are needed. This requirement can be fulfilled by machine learning algorithms [1, 16]. However, data transmissions between child nodes and the RP are very high during multihop transmission. Introducing virtual RPs [14] will try to minimize the retransmission overhead by transmitting their data directly to the MS if they are near the MS path.

This article is motivated by these observations and presents data acquisition with mobile sink for WSNs with obstacles using support vector machine (DAOSVM). The DAOSVM initially determines optimal RPs set from the deployed SNs using a minimum spanning tree- (MST-) based clustering mechanism. Once it finds the RPs, the obstacles are identified and use a support vector machine algorithm to construct the path [17] among the RPs and the BS. Further, to lower the packet exchanges between the SNs and RPs, a set of virtual RPs (VRPs), at one-hop distance from the MS path, can be identified. Further, we compare the DAOSVM algorithm with recent and relevant published works such as eACO-MSPD [18], CMS2TO [19], EARTH [6], and ETDC [20] through various simulations and different performance metrics. The primary contributions of this article are listed as follows:

- (i) The proposed DAOSVM identifies the best RPs set from the WSN's environment using the MST-based clustering mechanism
- (ii) The shortest MS tour is determined by using the SVM algorithm between the RPs and the sink
- (iii) We also determine the best VRPs set around the MS trajectory to minimize the unnecessary packet transmissions between SNs and the RPs
- (iv) Finally, the superiority of the DAOSVM is compared with recently published relevant existing algorithms such as eACO-MSPD [18], CMS2TO [19], EARTH [6], and ETDC [20] using different quality metrics

The remaining sections of this article are organized as follows. In Section 2, we study the recently published relevant articles. In Section 3, we discuss the proposed work along with the problem formulation and network model. In Section 4, we analyze the simulation test of existing and proposed works. In Section 5, we conclude the paper.

2. Related Work

Several works in the literature introduce path finding strategies for mobile sink while collecting the data for WSNs. This

section summarizes most promising works with its advantages and limitations.

2.1. Path Construction in Regular WSNs. A typical network in this subsection considers WSNs without any obstacles while constructing a path. From literature [21], we identified several works and they are summarized as follows.

Lin et al. [22] used to determine a static path between VPs in WSNs and perform the data fusion using MS. An ant colony optimization- (ACO-) based path construction algorithm is used for event-driven WSNs [8]. In this approach, ACO is used for both RP selection along with pathfinding. Further, the authors extended this work by adding virtual RPs with an improved probability metrics of the ACO in [18]. These approaches not only provide an optimal path but also improve efficiency in terms of energy, lifetime, throughput, delay, etc. Mehto et al. [23] used the PSO approach to construct an efficient path between RPs under the event-driven approach. Mehto et al. used a squirrel search algorithm to partition the WSNs into cluster and cluster heads.

In a grid-based sensor deployment with uniform data rate, WSNs are considered in [24] for data collection using a mobile sink. This work is considered a density-based network during the simulation, providing an efficient path along with the best network performance. In [25], multiple MSs are used to acquire the data within the WSN in which uniform data is generated by all the sensor nodes. The network is partitioned according to the multihop manner RPs in the network. A MS-based data collection is presented in [26] in which the delay minimization is considered the primary objective. In this, the sensitive data is performed dynamic routing, whereas the MS acquires the delay insensitive data. Further, they extended this work in [27] to mitigate the hotspot problem. However, this approach results in a longer path and leads to high computational complexity. Another delay-sensitive method using MS is presented in [28] to lower the delay and energy utilization using a spanning tree-based approach.

Gupta and Saha [29] proposed an artificial bee colony (ABC) approach for path construction and data collection for WSNs where the data rate is evenly distributed. An optimal set of RPs is identified in [30] using PSO which can provide a longer life to sensor nodes with efficient energy utilization in the network where the data is uniformly distributed. An adaptive data rate control is maintained while performing data collection using MS in [31]. This approach requires low computation and efficient in balancing the energy and network. But, this approach did not consider an obstacle-aware network. A method for MS-based data collection with MS using fuzzy logic for clustering the network to identify the RPs and strategies for path construction for efficient data collection. Using geometric techniques, an efficient path for the mobile sink is introduced in [32].

From the above literature, it can be concluded that none of the above works considered an obstacle-aware path for the MS required to acquire data from sensor nodes or RPs. There are few works in the literature which considers obstacle-aware path finding approaches which are discussed in the following subsection.

2.2. Path Construction in Obstacle WSNs. In this subsection, we discuss the approaches which are used to construct mobile sink path in an environment of WSNs with obstacles.

An artificial intelligence (AI) and ACO approach is used in [12] to construct a path in an obstacle WSN environment and gather data using a mobile sink. Initially, ACO can be used for creating the clusters and AI-enabled approach is meant to construct path for mobile sinks in WSNs to acquire data. In [9], the authors proposed an efficient algorithm for MS path construction and buffer management using the Q-learning approach for WSNs. In this approach, the Q-learning algorithm schedules the MS efficiently to minimize the packet loss rate in the network. This approach has not adopted the VRP selection strategy for improving the data gathering process. In [13], the PSO-based mechanism used to select CHs in WSNs is also useful in constructing a path to the MS. In [6], the authors have proposed a MS tour plan for WSNs with limited buffers and nonuniform constraints.

Xie and Pan [33] introduced a cluster-based grid partition in WSNs with obstacles and a determined path for the MS. In this work, a heuristic method is used to decide an efficient path for the mobile element to get the data packets from the SNs while avoiding obstacles during its travel. Obstacle-aware connection management is introduced in [34] using the Delaunay triangulation-based approach for the mobile elements. This approach efficiently manages the connections between the sensor nodes to help route their data efficiently to the base station. In [35], Park et al. invented an iterative clustering mechanism to optimize the route of the MS while acquiring the data packets from SNs. This approach is efficient and intelligent while acquiring and improving the data gathering efficiency. This approach works efficiently and intelligently in improving the data gathering process. An obstacle-aware path for MS is introduced using the cluster-based approach in [36] for WSNs. In [37], Yang et al. present a dynamic path for MS using virtual potential fields in WSNs.

From the above study, it is evident that most of the existing algorithms have considered the mobile sink path without considering the obstacles. Even though, in some works, obstacles are considered, they failed in incorporating the VRP selection process to reduce the unnecessary packet transmissions between the SNs and RPs. Furthermore, MS traveling distance can also be optimized and dynamically constructed. All these challenges are addressed in the proposed DAOSVM mechanism.

3. Proposed Work

In this section, we present the problem formulation, algorithm proposed, illustration, and complexity analysis. In Section 3.1, we also discuss the network model and the parameters that affect the WSNs. Section 3.2 describes the detailed data collection process using MS in the obstacle/barrier containing WSNs. Finally, the complexity of the DAOSVM is analyzed, and it is also compared with the existing methods. The notations used in this paper are summarized in Table 1.

TABLE 1: Frequently used notations and their meanings.

Notation	Meaning
\mathcal{G}	WSN
n	Number of SNs
i	Sensor node index
\mathcal{D}	Adjacency matrix of distances between nodes
\mathcal{S}	Set of nodes
\mathcal{S}_0	Base station
$\delta(\mathcal{S}_i, \mathcal{S}_j)$	Distance between two nodes
r	Transmission range
\mathcal{V}	VRP set
\mathcal{M}	RP set
\mathbb{R}	MS communication range
λ_k	The time taken to complete a tour k
u_k	Distance travelled by MS at tour k
\mathcal{B}	Buffer capacity
ψ_i	i^{th} vector in the dataset
\mathcal{T}	MST
N_l	Network lifetime
\mathcal{S}	Set of indices for SVs
F	Fairness index of EC
BU	Buffer utilization
Λ_i	Associated label to the ψ_i

3.1. Problem Formulation. The WSN is considered an undirected and connected graph $\mathcal{G}(\mathcal{S}, \mathcal{D})$, where $\mathcal{S} = \{\mathcal{S}_0, \mathcal{S}_1, \mathcal{S}_2, \dots, \mathcal{S}_n\}$. Here, \mathcal{S}_0 is treated as BS and the remaining are the SNs. All these $n = (|\mathcal{S}| - 1)$ SNs are randomly deployed at fixed locations (no mobility after the deployment) and has unique properties. The $\mathcal{D} = \{\delta(\mathcal{S}_i, \mathcal{S}_j) | \forall \mathcal{S}_i, \mathcal{S}_j \in \mathcal{S} \wedge \delta(\mathcal{S}_i, \mathcal{S}_j) \leq r\}$ is the distance adjacency matrix, which includes the \mathcal{S}_0 . Euclidean distance and transmission ranges between two SNs \mathcal{S}_i and \mathcal{S}_j are treated as $\delta(\mathcal{S}_i, \mathcal{S}_j)$ and r , respectively. We consider the distance between two SNs \mathcal{S}_i and \mathcal{S}_j as ∞ , if they are not in r . The set of RPs are denoted using \mathcal{M} , where the RP is supposed to acquire data packets from SNs and VRPs. The \mathcal{V} is treated as the set of VRPs, where the VRPs transmit their data directly to MS or the closest RP. The MS acquires the data from RPs or VRPs and submits it to the \mathcal{S}_0 . The MS starts from \mathcal{S}_0 by traveling around the network while crossing each \mathcal{M} and reaches again to \mathcal{S}_0 . This is called a tour. The time taken to complete a tour k is denoted as λ_k . The distance travelled by MS in a tour k is denoted as u_k . The velocity of the MS is constant during the data collection process, and it is denoted with v . The MS communication range is indicated as \mathbb{R} , and the minimum distance from \mathcal{V}_i to the MS must be less than \mathbb{R} . The obstacles in the WSN environment are considered \mathcal{O} . All the SNs in the network have uniform buffer availability, and it can store a maximum of b bits in its buffer. The buffer occupancy is indicated with p_i , where $\forall p_i \leq b$.

The \mathcal{E}_0 is considered the initial energy of SNs, and it is same to all \mathcal{S} initially, and it is utilized mainly during sensing phenomenon, data transmitting, and processing. The energy model for the DAOSVM follows the free-space energy model, according to [14]. The needed energy for the amplification is α_a , needed energy to process a bit of data is α_t , and the circuit needs α_r energy to receive a bit. The energy consumption (EC) of the node \mathcal{S}_i , while transferring \mathcal{B} bits to the node \mathcal{S}_j is in

$$\mathcal{E}_t(i, j) = (\alpha_t \times \mathcal{B}) + (\alpha_a \times \delta_{ij}^2 \times \mathcal{B}). \quad (1)$$

The node \mathcal{S}_i consumes energy as shown in Equation (2), while receiving \mathcal{B} bits from node j .

$$\mathcal{E}_r(i) = \alpha_r \times \mathcal{B}. \quad (2)$$

The EC of a node \mathcal{S}_i during data transmission to $\mathcal{S}_j \in \mathcal{S}$ and acquiring data from $\mathcal{S}_j \in \mathcal{S}$ in the tour k is calculated using

$$\mathcal{E}_{ik} = \mathcal{E}_t(i, j) + \mathcal{E}_r(j) + \Delta, \quad (3)$$

where Δ is the node \mathcal{S}_i 's energy variation for data processing. The RP set count is indicated using $\zeta = |\mathcal{M}|$, and it is decided using Equation (4), and it is derived based on [38].

$$\zeta = \sqrt{\frac{n}{2\pi}} \times \sqrt{\frac{\alpha_a}{\alpha_t}} \times \frac{A}{\delta(\mathcal{M}_i, \mathcal{S}_0)}, \quad (4)$$

where A is the area of the WSNs in sqm and $\delta(\mathcal{M}_i, \mathcal{S}_0)$ is the distance between \mathcal{M}_i RP to the BS (\mathcal{S}_0).

The lifetime of the WSN (\mathcal{N}) is the epoch time till the first SN drains its energy completely, and we consider the metric in terms of minutes [8]. It is measured similarly to

$$\mathcal{N} = \sum_{k=1}^{\lceil \delta \rceil} \lambda_k, \quad (5)$$

where λ_k is MS one tour time and $\lceil \delta \rceil$ indicates the # of trips completed by the MS. Therefore, the objective of the DAOSVM is summarized as it prolongs the \mathcal{N} and reduces the data acquisition delay by avoiding the obstacles. Finally, the problem statement is to choose the optimal RP set, i.e., \mathcal{M} , which maximizes \mathcal{N} for obstacle-aware data collection using MS.

3.2. Obstacle-Aware Path Determination. The proposed DAOSVM algorithm involves three phases. In the first phase, the algorithm applies the MST-based clustering mechanism (MST-CM). From the MST-CM, it determines the best RPs set for further data collection process. In the second phase, MS path is constructed by avoiding obstacles with the SVM algorithm's help. In the final stage, the algorithm finds a set of VRPs with the help of which the number of retransmissions between the RPs and SNs can be minimized. For a better understanding of the proposed MS path

construction, we provided preliminaries of the SVM in this section. The overview of the proposed work is shown in Figure 1.

3.2.1. Preliminaries of SVM. The SVM is a supervised ML algorithm, which can solve the regression or classification problems with better accuracy [1]. The proposed DAOSVM uses a margin maximization mechanism with the help of SVM to address the issue by constructing an optimal hyperplane.

Let us consider the dataset $\{\psi_i, \Lambda_i\}_{i=0}^n$, where ψ_i is the i^{th} vector in the dataset and Λ_i is the associated label to the ψ_i and $\Lambda_i \in \{-1, +1\}$. This sample is separated with the hyperplane $\omega^T \psi \pm h = 0$. In case, the training samples are to be linearly separable, and ω and h has to be satisfied which is shown in

$$\Lambda_i (\omega^T \psi \pm h) \geq 1 \forall (i = 0, 1, 2, \dots, n). \quad (6)$$

By using these parameters, the two classes of samples are separated by the two hyperplanes such as $H_1 : (\omega^T \psi \pm h) = +1$ and $H_2 : (\omega^T \psi \pm h) = -1$ and ensures that no other data exists between them. $2/||\omega||$ represents the objective functions for minimizing the parameters as shown in Equation (7) under the constraints of Equation (6).

$$\mathbf{L}(\omega) = \frac{1}{2} ||\omega||^2. \quad (7)$$

The margin maximization can be obtained by using the Lagrange multipliers, as shown below:

$$\max_{\alpha} \left(\sum_{i=1}^n \alpha_i - \frac{1}{2} \left(\sum_{i,j=1}^n \psi_i \psi_j \Lambda_i \Lambda_j \alpha_i \alpha_j \right) \right), \quad (8)$$

subjected to Equation (9) and $\alpha_i \geq 0 \forall i = (1, 2, \dots, n)$.

$$\sum_{i=1}^n \alpha_i \Lambda_i = 0. \quad (9)$$

The training dataset ψ_i with α_i (nonzero) are either of the hyperplanes H_1 or H_2 and are treated as the support vectors (SV), because these data can only be helpful to compute the parameters. From this, a discrimination function is constructed which is shown in

$$\Lambda = \text{sign} (\omega^T \psi \pm h) = \text{sign} \left(\sum_{i \in \mathbf{S}} \alpha_i \Lambda_i \psi_i^T \psi \right), \quad (10)$$

where \mathbf{S} represents the set of indices for SV. The kernel trick of SVM is used to classify points which are not linearly separable. Various kernels like polynomial and rbf can be used. But here, we have used a polynomial kernel.

3.2.2. RP Selection Strategy. In this phase, the graph \mathcal{G} is considered an input and determines the best RP set \mathcal{M} . We use

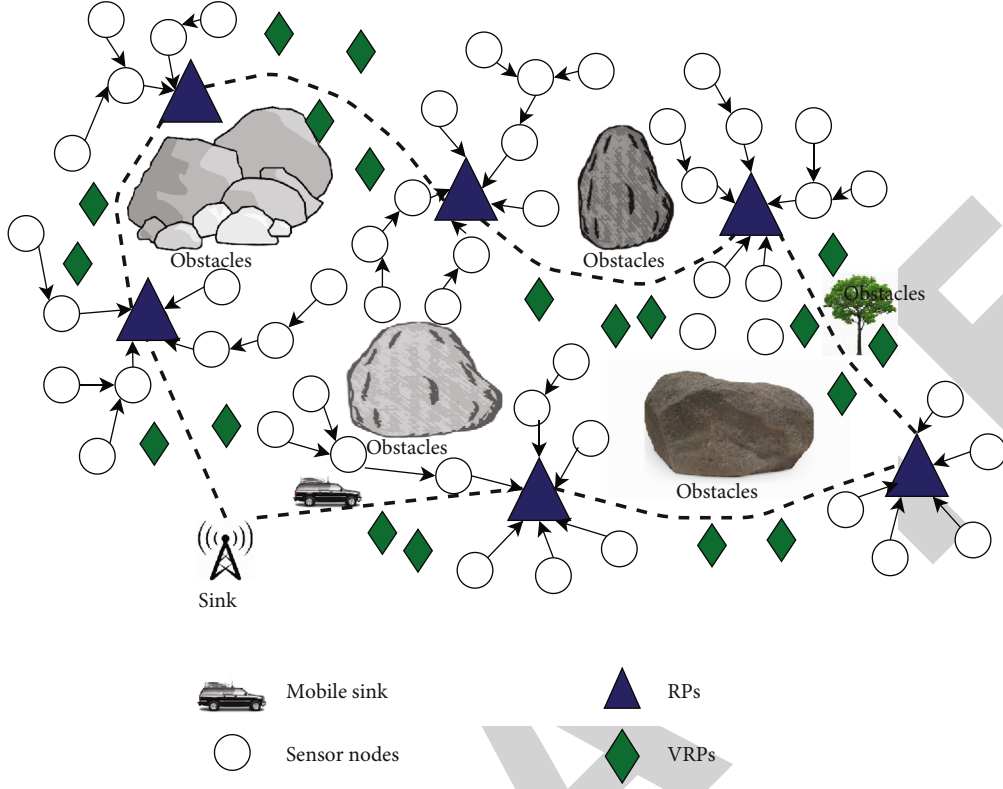


FIGURE 1: Overview of the proposed obstacle-aware path determination approach.

MST based clustering mechanism (MST-CM) to determine the best set of RPs, i.e., \mathcal{M} with low computational complexity. The initial SNs and base station deployment is illustrated in Figure 2(a). The graph \mathcal{G} is constructed by exchanging location information among SNs, and if the distance is less than r between SNs, they are connected with an edge. The \mathcal{G} construction is illustrated in Figure 2(b).

The MST-CM applies Prim's algorithm to construct the MST from the WSN graph \mathcal{G} . The resultant MST \mathcal{T} of the WSN \mathcal{G} is shown in Figure 2(c) (there is no difference between the edges with different colors). The MST-CM identifies the longest edges from T using Equation (11) by removing it temporarily and compute the next longest node until ζ times.

$$\text{long}_{ij}^{\zeta} = \arg \max_{i,j \in \mathcal{T}} \mathcal{D}. \quad (11)$$

This partition results in the best nearest neighbor set with limited cost. However, removing the most extended node always does not result in the best clustering strategy. So, before removing the node permanently, we use the coefficient of variation (CoV) to each node to decide the efficiency when an extended node is removed while forming the clusters. The CoV is used to measure the consistency, i.e., it can measure how the edge weight (distance between the two nodes) is uniform from one another. The CoV for MST-CM is the ratio of standard deviation (SD) and mean of the edge weights from the \mathcal{T} , as shown in

$$\text{CoV}_i = \frac{\sigma_i}{\chi}, \quad (12)$$

where σ_i is the i^{th} edge SD and χ is the arithmetic mean of the edges in the \mathcal{T} . The σ_i is computed using Equation (13), and χ is computed as shown in Equation (14).

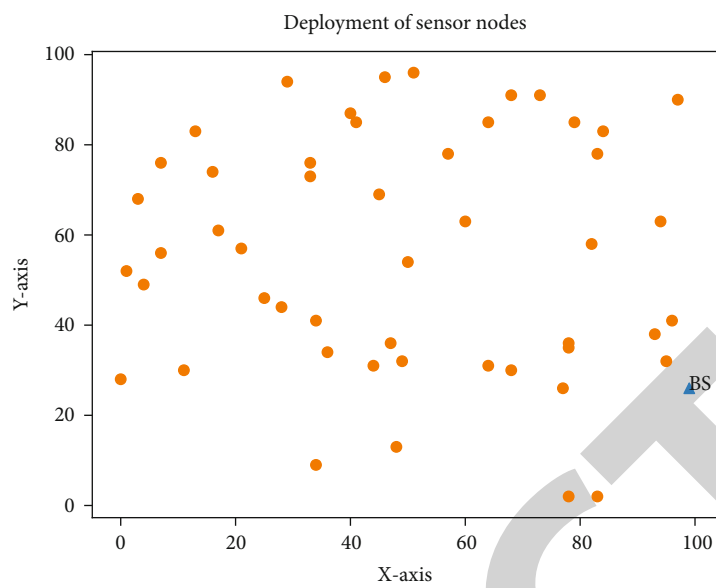
$$\sigma_i = \sqrt{\frac{1}{n} \sum_{i=0}^{n-1} (e_i - \chi)^2}, \quad (13)$$

where e_i is the edge weight of the SN i and χ is

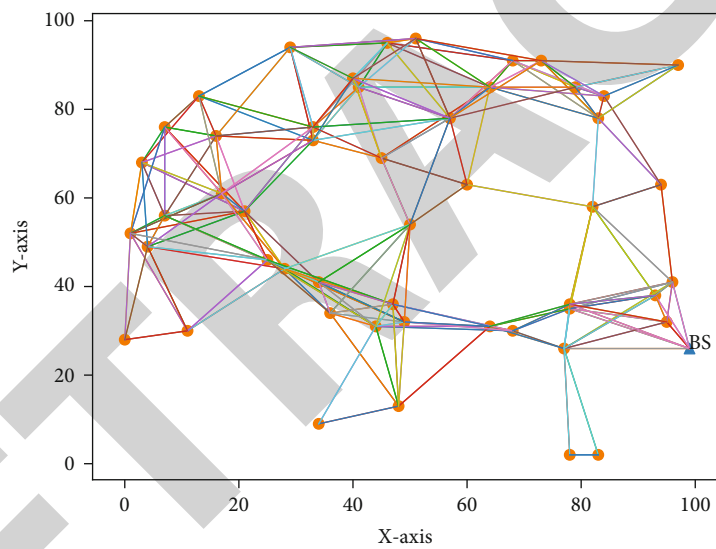
$$\chi = \frac{1}{n} \sum_{i=0}^{n-1} e_i. \quad (14)$$

From Equation (12), it can be seen that decreasing CoV means higher efficiency can be obtained. Before removing any node permanently from the \mathcal{T} , we test the CoV. This operation results in $\zeta + 1$ clusters from the \mathcal{T} . We use a threshold on the CoV to remove the inconsistent edges from the MST (\mathcal{T}) to generate the clusters. The cluster set after removing the longest edge depends on the CoV which is illustrated in Figure 2(d). From each cluster ζ , we find the RP using the Equation (15) and it is considered from [38].

$$T(n) = \frac{P}{1 - P(r \times \text{mod } P^{-1})} \times \frac{E_0 - E_{ik}}{E_0} \times \zeta, \quad (15)$$

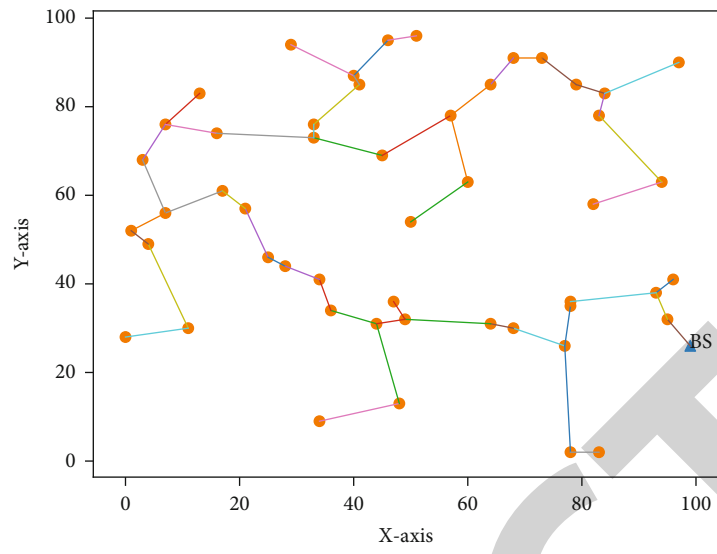


(a)

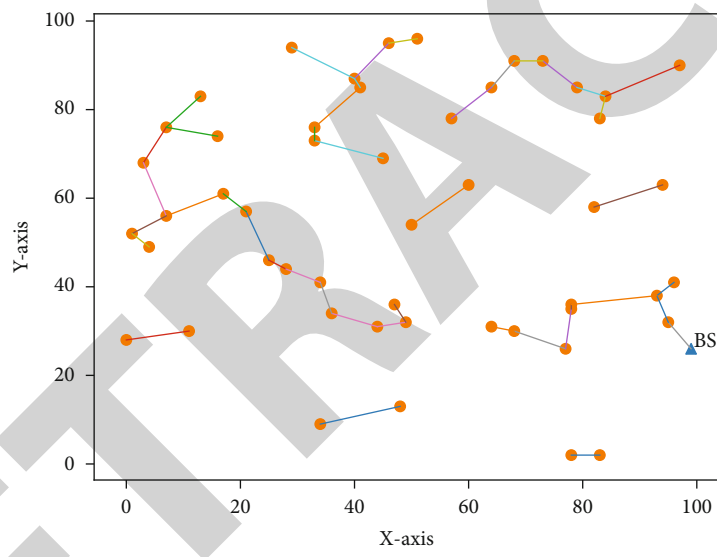


(b)

FIGURE 2: Continued.



(c)



(d)

FIGURE 2: Continued.

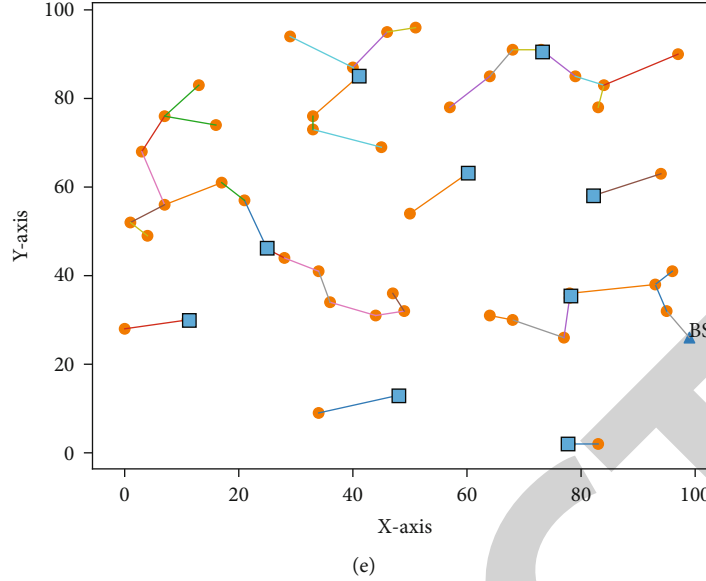


FIGURE 2: Steps involved in (a) SNs and BS deployment. (b) WSN graph $\mathcal{G}(\mathcal{S}, \mathcal{D})$. (c) MST using Prim's algorithms. (d) Clustering the MST. (e) Determine the RP from each cluster.

where P is the probability of choosing the node as RP, E_0 is the initial energy of the SN, and ζ is computed as shown in Equation (4). In each round, the SN generates a random threshold value between zero and one and compared it with the $T(n)$ to identify the RPs. In the first round of data collection, energy is not affected, but from the second round onwards, the selection of RPs considers energy. This process is illustrated in Figure 2(e).

The proposed DAOSVM also involves the reselection of RPs in each round using Equation (15) and energy models. The RP reselection also balances the energy among the SNs. Notably, the SNs near RPs face the same energy hole problem because of the relaying task, if no reselection is involved.

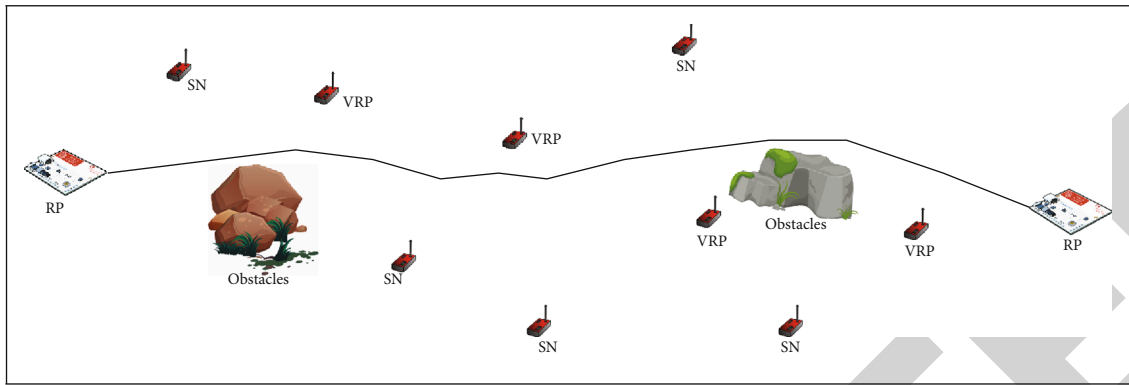
3.2.3. MS Path Determination. The MS path construction phase is a critical and challenging phase as it decides the efficiency of the data gathering process, and it is more complicated when the obstacles are considered. This phase is executed after the RPs set \mathcal{M} is decided. This algorithm is extended with two phases: (I) deciding the visiting order and (II) avoiding the obstacles in the path.

In phase I, visiting order of the RPs by the MS is decided. There are several algorithms in the literature which can choose the optimal and shortest path for the mobile sink using TSP, ACO, etc., but these require complex computations. Here, we plan to propose a lightweight path selection algorithm to fill the necessity of the shortest path using computational geometry methods [14]. This phase takes the \mathcal{M} as an input and produces the path as an output. We assume that all the \mathcal{M} are having coordinates X and Y in a plane \mathcal{A} . Initially, we determine the maximum and minimum X coordinates from the \mathcal{M} and assume a virtual line between these coordinates. So, the plane is split into two parts such as above the line and below the line. Then, all the \mathcal{M} 's are arranged below the line in ascending/descending order

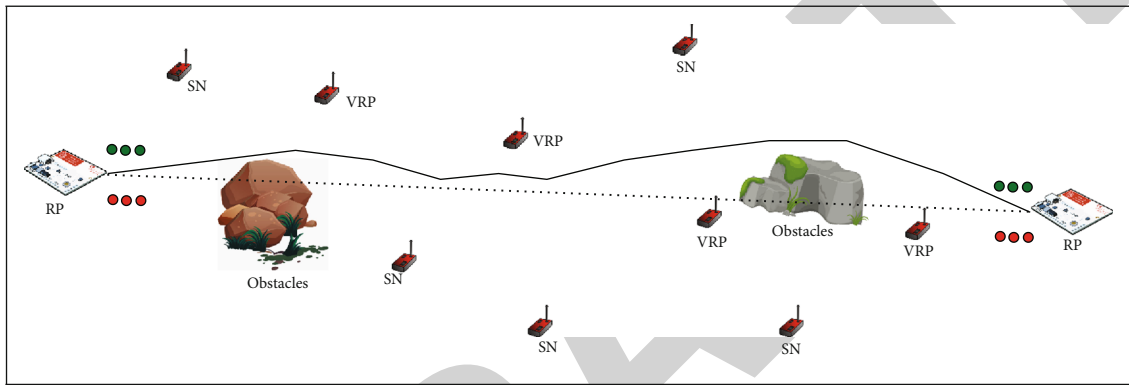
according to the X coordinates and descending/ascending (opposite to the above) order of \mathcal{M} 's according to the X coordinates. Then, concatenate both \mathcal{M} 's to get the visiting order of RPs. The algorithm detects the path by avoiding the obstacles in phase II.

In phase II, the support vector machine algorithm is applied to construct the path which can avoid the environment's obstacles. The step-by-step path determination algorithm explained through Figure 3. Before starting the algorithm, label the positive and negative obstacles. Note that the red dots indicate the negative obstacles, and green circles indicate the positive obstacles from Figure 3. Here, actual obstacles are highlighted, and the triangles indicate the RPs. Figure 3(a) is the primary example considered for illustration of path construction between two RPs by considering two obstacles of the WSN environment.

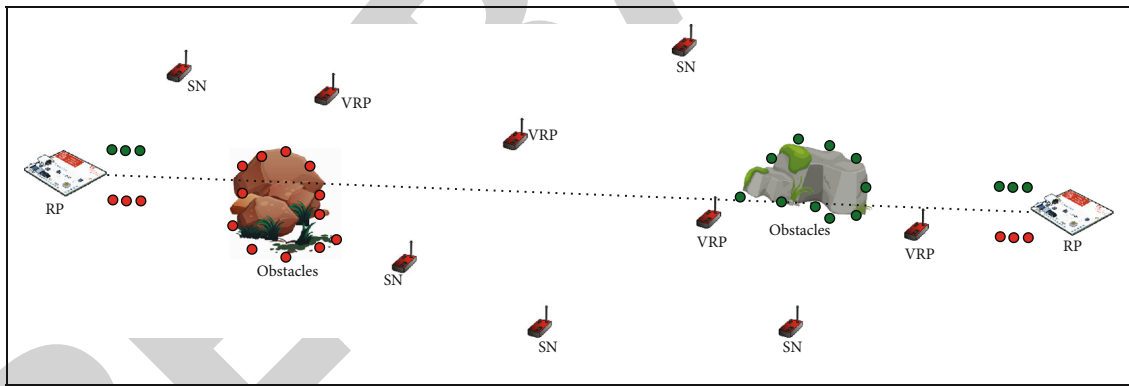
Initially, we construct a virtual path between the two RPs (\mathcal{M}_1 and \mathcal{M}_2), which is a regular straight line between them. Virtual obstacles are set around the RPs at a certain distance ($\delta \leq r$) from both the RPs and parallel to the straight path. These virtual obstacles are categorized into both positive (right side to the straight line) and negative (left side to the straight line), as shown in Figure 3(b). After that, we determine the pattern of the obstacles and identify the positive and negative obstacles depending on the obstacle centroid. If the centroid of the obstacle is right, then we highlight the obstacle as positive, and in case the centroid is in the left or on the line, we consider the negative obstacle sign as shown in Figure 3(c). The guided samples are arranged parallel to the sample line with a certain distance (δ_g) from the line, as shown in Figure 3(d). These lines are adjusted according to the negative virtual obstacles or the points. Depending on the obstacle, the line moves the opposite side, and the guided sample of that side near an obstacle also moves according to the distance of the obstacle to samples.



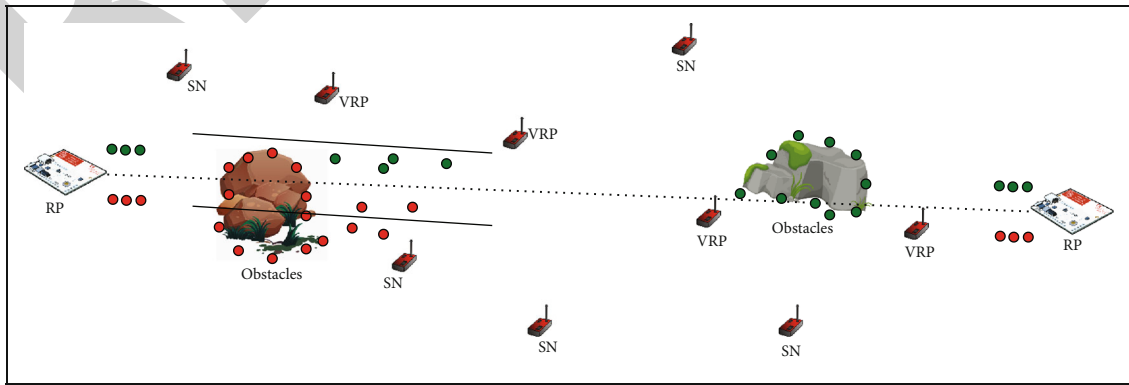
(a)



(b)



(c)



(d)

FIGURE 3: Continued.

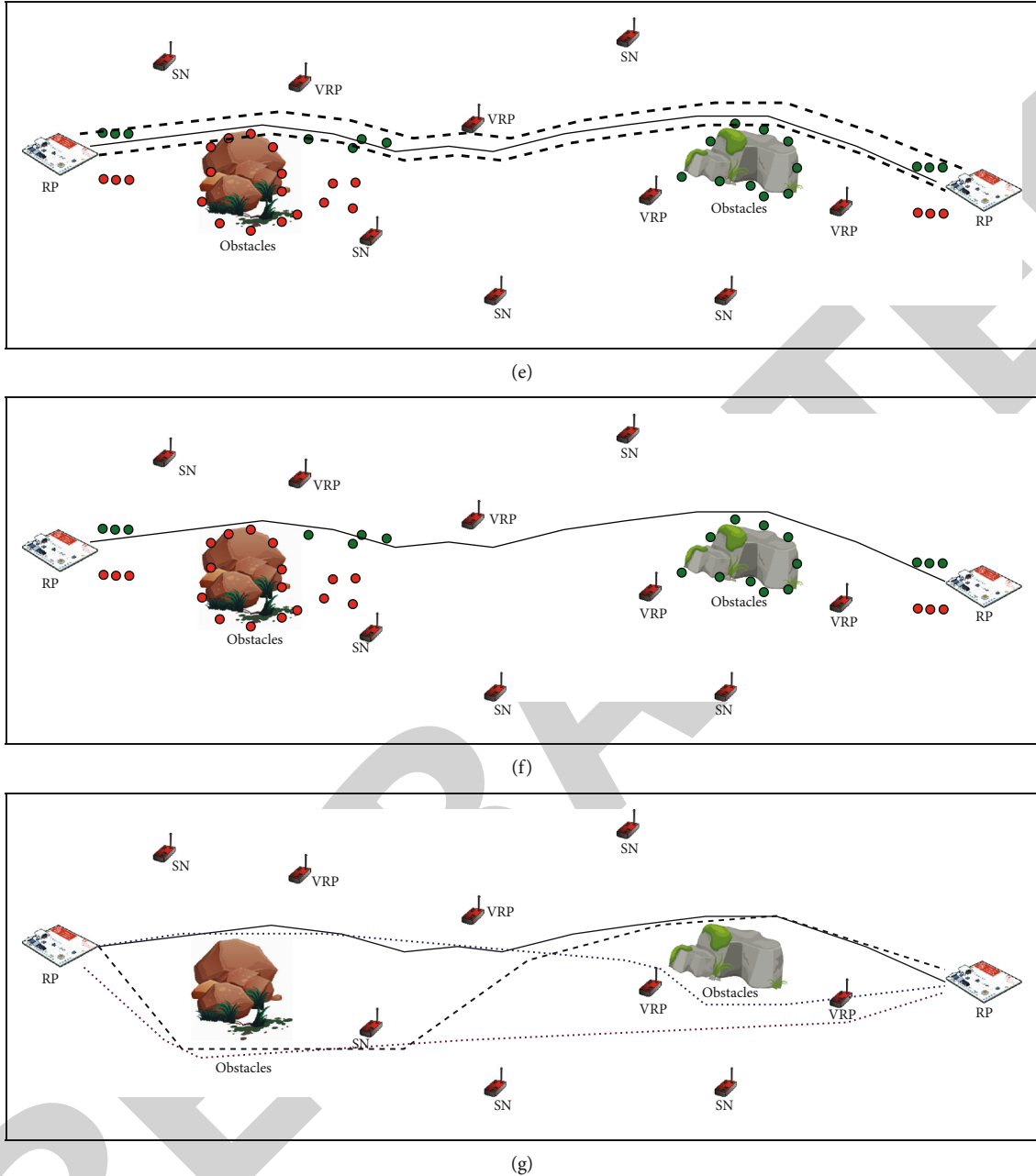


FIGURE 3: Mobile sink path construction using support vector machine technique. (a) Example of two RPs and two obstacles for path construction. (b) Deployment of virtual obstacles around the RPs. (c) Determine the patterns of the obstacles. (d) Construct guided sample lines parallel to sample lines. (e) Apply the SVM to determine the initial phase of path. (f) Best MS traveling path between two RPs. (g) Feasible paths between the two RPs by avoiding the obstacles.

We can now apply the SVM on the sample generated and analyze the results of the SVM learning process. By applying the learning process, the SVM results in support vector set and their weights can decide each point's region according to positive or negative obstacles. This region also constructs a collision-free separate line in a two-dimensional area, as shown in Figure 3(e). We try to determine the line separation from the obstacles by iteratively searching for the next point until Equation (16) results in value zero.

$$V = \sum_{i \in \mathcal{S}} \alpha_i \Lambda_i \psi_i^T \psi - h. \quad (16)$$

By repeating this, we get the MS path by avoiding the obstacles from \mathcal{M}_1 to \mathcal{M}_2 , as shown in Figure 3(f). However, this is a possible path and not the optimal path. We can also terminate the iteration when the $V < 1.0$, exceeding the number of iterations and then threshold values (this case may happen if the distance between the path and obstacles are minimal from both sides). We repeat the same process

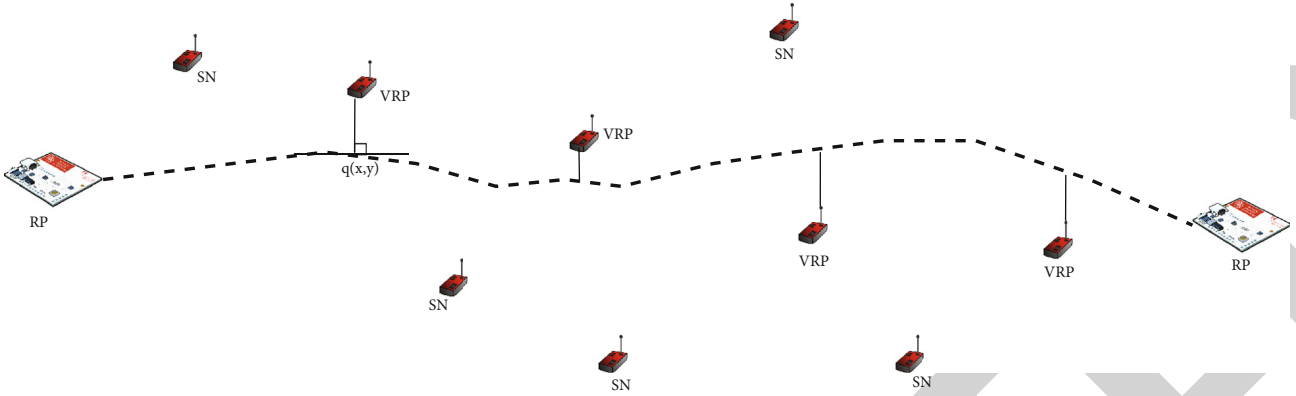


FIGURE 4: VRP selection strategies.

by adjusting the guided lines (Figure 3(d)) or flipping the positive or negative obstacles to make another pattern to construct several possible paths as shown in Figure 3(g) and choose the best one among them. This process is repeated until all the RPs are visited from \mathcal{M} which can complete the traveling tour from BS via RPs to the BS.

3.2.4. VRP Selection. The selection of VRPs of the proposed work improves the data acquisition process by minimizing the communications between the SNs and the RPs as shown in Figure 4. In this work, the VRPs are the SNs $((\mathcal{V} \in \mathcal{S}) \wedge (\mathcal{V} \in \mathcal{M}))$, which can directly communicate with the MS when it traverses in its range r . The VRPs in DAOSVM is determined based on the available time of MS on the trajectory within the range of the SNs.

Initially, we choose a line/curve $\mathcal{L}_p = y = \{f(x) \forall p \in 0 \leq p < |\mathcal{M}|\}$ between any two RPs from \mathcal{M} . The $f(x)$ is in the form of $ax^2 + bx + c$. We assume that $\mathcal{S}_i(x_i, y_i)$ be a VRP and we determine the distance to the \mathcal{L}_p with a particular point $q(x, y)$ on it which should be less than r . The shortest distance point on \mathcal{L}_p from each SN $\mathcal{S}_i(x_i, y_i)$ is computed as shown in

$$\begin{aligned} D &= \sqrt{(x_i - x)^2 + (y_i - y)^2} \\ &= \sqrt{(x_i - x)^2 + (y_i - (ax^2 + bx + c))^2}. \end{aligned} \quad (17)$$

From Equation (17), we can derive the x coordinate of q by applying the derivation of both sides, i.e., dD/dx to zero. Once we get x , we can easily determine the y coordinate of q . Similarly, this process is repeated with each SN to get all the possible paths between RPs. The following illustration gives a better understanding of the VRP selection process. We assume that $\mathcal{S}_i = (3, 8)$ and the equation of the curve as $y = x^2 + 8$; then, Equation (18) briefs the shortest point on the path \mathcal{L}_a .

$$\begin{aligned} D &= \sqrt{(3 - x)^2 + (8 - (x^2 + 2))^2} \\ &= \sqrt{9 - 6x + x^2 + (8 - x^2 - 9)^2} = \sqrt{x^4 + x^2 - 6x + 9}. \end{aligned} \quad (18)$$

Here, we set dD/dx to 0 and solve for x ; finally, it returns $x = 1$. We substitute the value of x in $y = x^2 + 8$, so that we get $y = 9$. So, the nearest point on the \mathcal{L}_p to the $\mathcal{S}_i = (3, 8)$ is $q = (1, 9)$. If the Euclidean distance between the $\delta(\mathcal{S}_i, q)$ is less than or equal to the r , then \mathcal{S}_i is included to \mathcal{V} .

3.3. Complexity Analysis. The complexity of the first stage is the RP selection which comprises of MST construction, identifying the edges to be removed and RP node selection. The complexity of the MST using Prim's algorithm is $O(E \log V)$, where E is the number of edges in the \mathcal{T} , and $V = n$ indicates the number of nodes. The complexity to identify the edges to be removed is $O(E^2)$. The complexity to identify the RPs is $O(n^2)$. Overall, the time complexity of final RP set selection is $O(E \log V) + O(E^2) + O(n^2)$, and the E in \mathcal{T} is $(n(n-1))/2$. After the E value is substituted, the asymptotic complexity of RP set selection is $O(n^2 \log n)$. The visiting order of \mathcal{M} requires $O(n \log n)$ computational time. The time complexity of path construction by avoiding the obstacles using SVM is $O(|SV|^3)$, where $|SV|$ indicates the number of support vectors, i.e., $|SV| \approx n$, so the complexity is treated as $O(n^3)$. The complexity to determine the VRPs set is $O(n^2)$. The overall computational complexity after evaluating all phases is $O(n^2 \log n) + O(n^3) + O(n^2)$, and the final asymptotic computational complexity of DAOSVM algorithm is $O(n^3)$.

4. Results and Discussion

In this section, we provide the theoretical and simulation results of the proposed model. The proposed DAOSVM and existing eACO-MSPD [18], CMS2TO [19], EARTH [6], and ETDC [20] methods are implemented using the Python simulator (v3.10.0). The packet size is considered 30 bytes, and data communication rate to be 80 kbps to 250 kbps [39]. We consider two scenarios of the network: (i) varying the area size and (ii) varying the number of SNs. In the first scenario (WSN#1), we considered 100×100 m with a maximum of 100 SNs deployed randomly and treated as a small network with few obstacles. In the second scenario (WSN#2), we increased the area size from

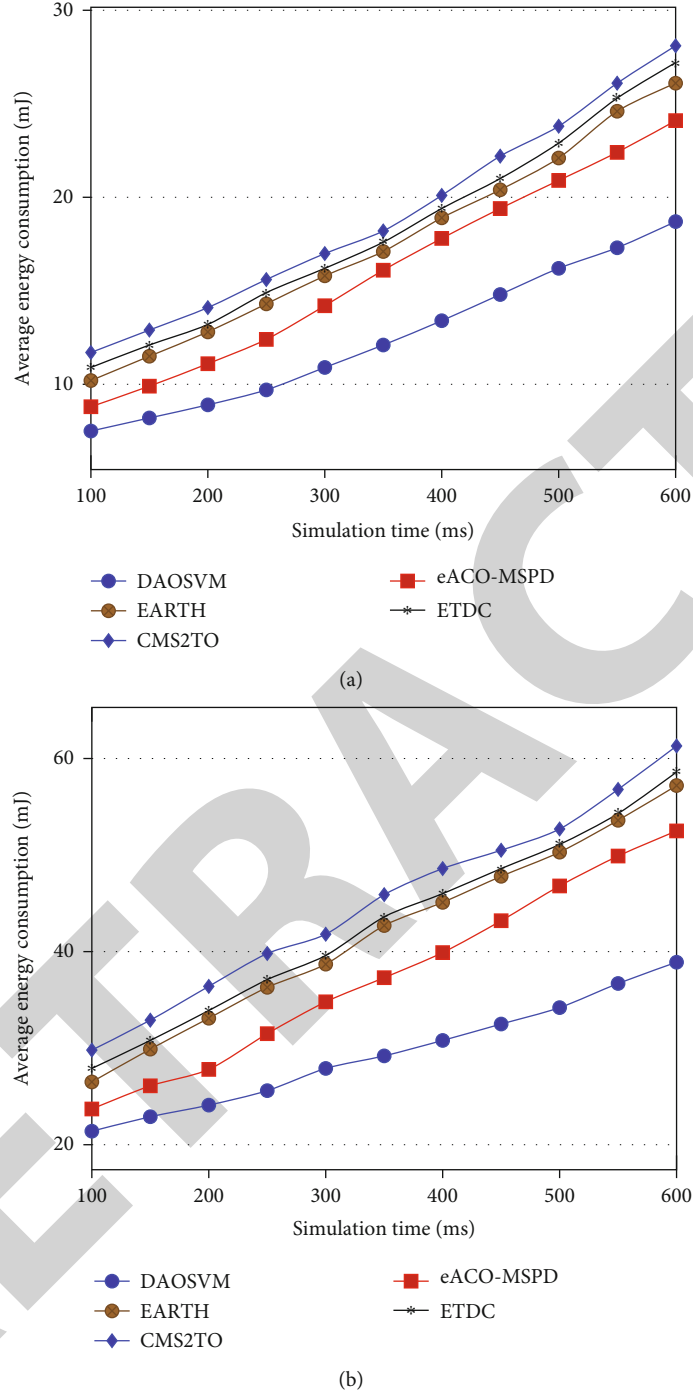


FIGURE 5: Average EC of (a) WSN#1 and (b) WSN#2.

100 m \times 100 m to 1000 m \times 1000 m, and the number of SNs increased up to 1000. The deployment and packet generations in the networks are considered according to Sah et al. [40], and MQTT application protocols considered. In WSN#2, we have increased the number of obstacles. The E_0 of all δ is equal, i.e., 100J. The EC of α_t and α_r are 42 mW (0.042J) and 29 mW (0.029J), respectively. We conduct the simulation by varying the communication range between 15 meters and 50 meters. The traveling speed of

the MS during the data collection is set to 1 Mbps. The proposed DAOSVM compared with eACO-MSPD, CMS2TO, EARTH, and ETDC algorithms with various performance metrics such as energy consumption (EC), fairness index (FI), network lifetime (NL), buffer utilization (BU), average path length (APL), and packet delivery ratio (PDR).

4.1. Average Energy Consumption. The network's AEC (μ_e^t) is calculated as the average energy dissipated from all the

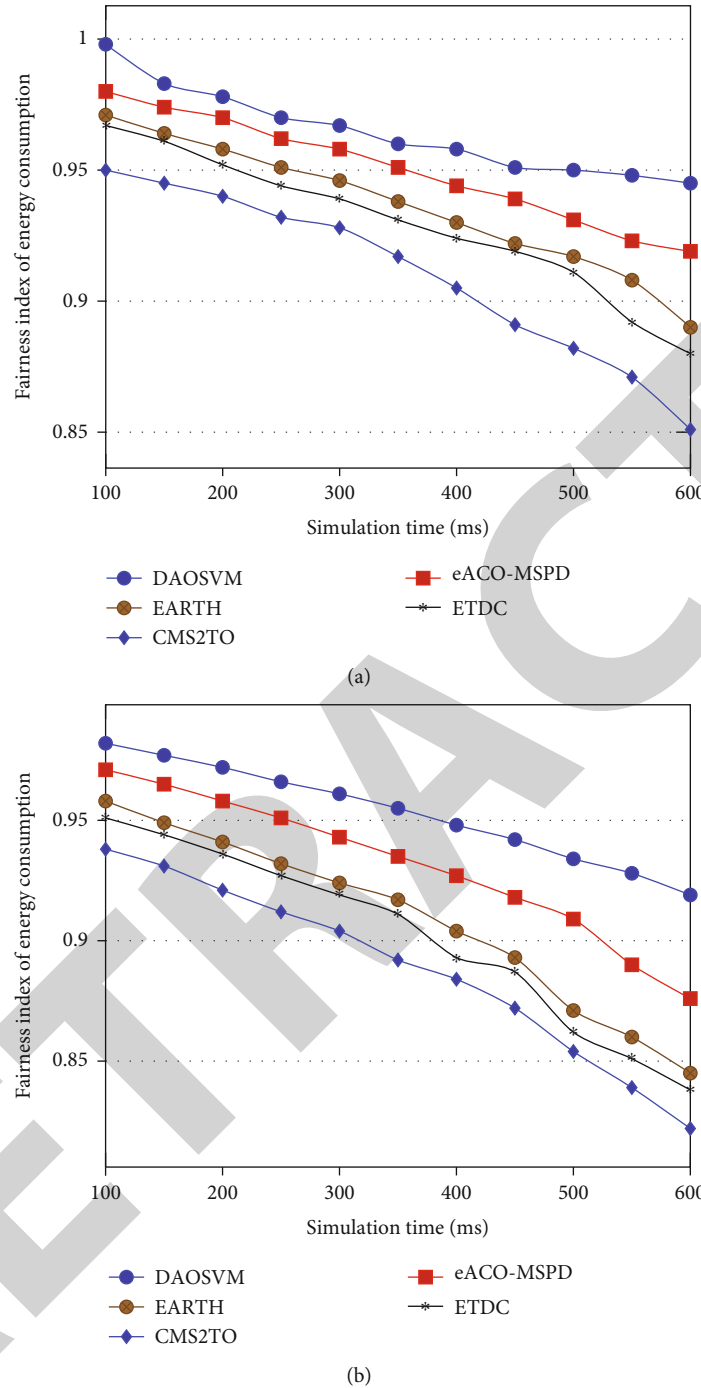


FIGURE 6: Fairness index of EC of (a) WSN#1 and (b) WSN#2.

SNs until a particular simulation time t is achieved, which is shown in Equation (19). The higher the μ_e^t will lower the N_t , and vice versa.

$$\mu_e^t = \frac{1}{n} \sum_{i=1}^n \mathcal{E}_i^t. \quad (19)$$

We examine the AEC of the proposed and existing algorithms in the two scenarios WSN#1 and WSN#2, as shown

in Figure 5. In Figure 5(a), the small network with 100 SNs average EC is examined by varying the simulation times between 100 ms and 600 ms. The μ_e of DAOSVM in WSN#1 is improved over the existing methods eACO-MSPD, EARTH, ETDC, and CMS2TO by 1.5-9 mJ, 2.7-19 mJ, 3.4-27 mJ, and 4.5-33 mJ, respectively, while changing the simulation times. From Figure 5(b), we noticed that the proposed DAOSVM improved the AEC by 2.3-24 mJ compared to eACO-MSPD, 5.1-29 mJ compared to EARTH, 6.5-32 mJ compared to ETDC and 8.4-36 mJ compared to

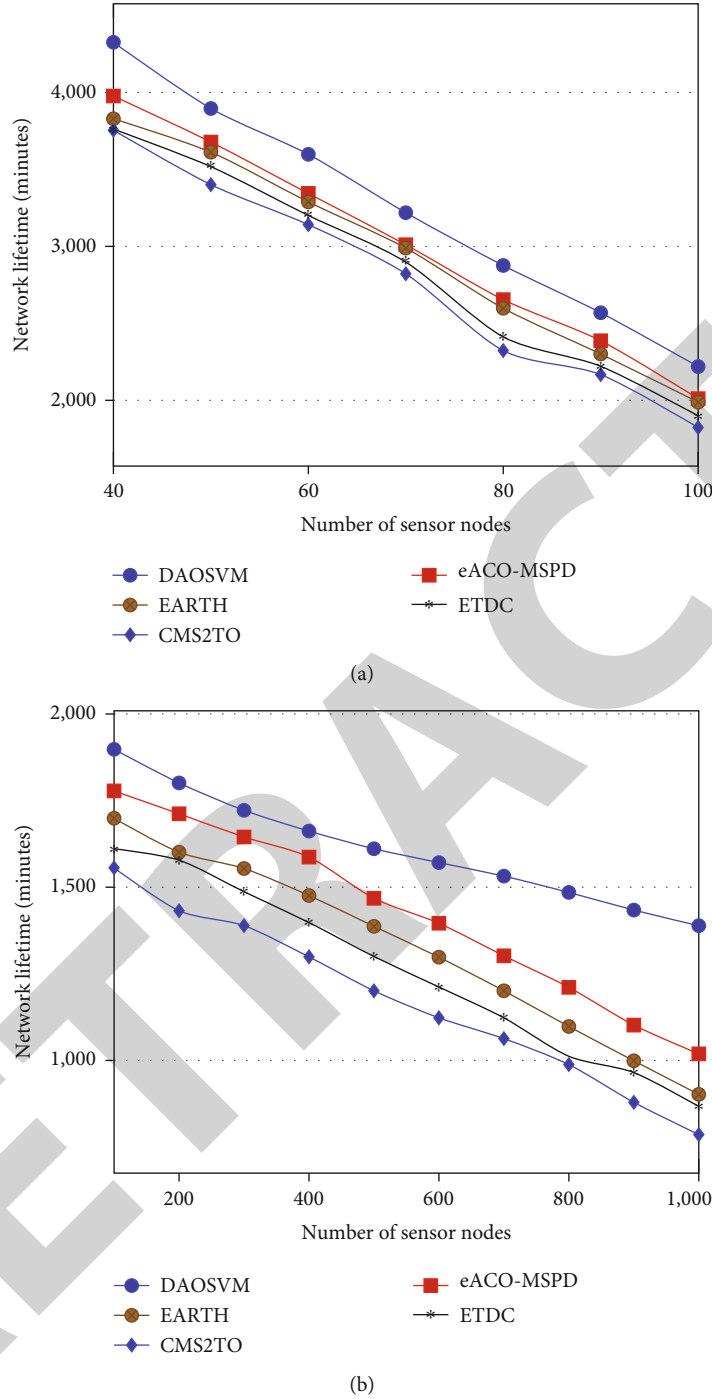


FIGURE 7: Network lifetime of (a) WSN#1 and (b) WSN#2.

CMS2TO algorithms. The best AEC is achieved in the DAOSVM due to an optimal selection of RPs and obtaining a best path. The VRP selection process also minimizes the energy consumption by avoiding packet transmissions to the RPs when MS is in its range.

4.2. *Fairness Index of AEC.* Achieving a best AEC of the WSN does not mean that energy is balanced among the SNs in a network. To determine the equal share of a bottleneck is represented the fairness index (FI) of the EC, and it is denoted as

F . The FI of any SN EC is in the range between zero and one. The F value nearer to one indicates the best FI, and near-zero means the lower FI. The FI of EC is computed as shown in

$$F = 1 - \left(\frac{2 \times \sigma_e}{H - L} \right), \quad (20)$$

where the standard deviation of EC denoted as σ_e , $H = \max \mathcal{E}_{ik}$, and $L = \min \mathcal{E}_{ik}$. The higher the SD, the lesser

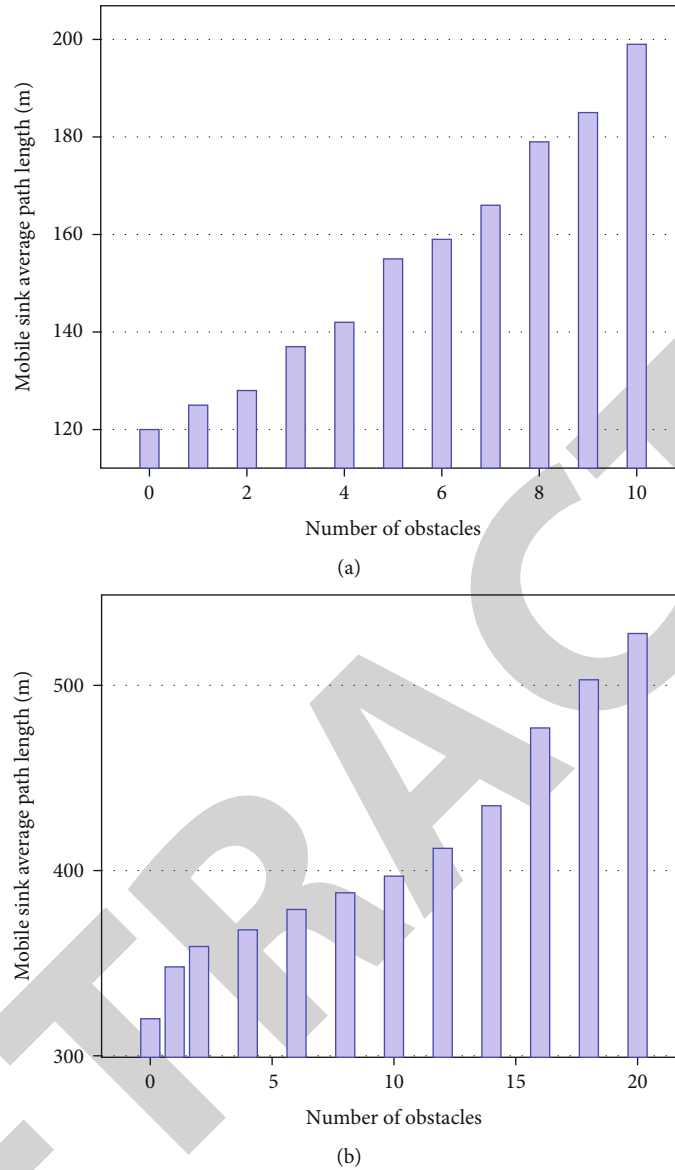


FIGURE 8: Average path length of (a) WSN#1 and (b) WSN#2.

the FI value and vice versa. The SD of the EC at tour k is computed using

$$\sigma_e = \sqrt{\frac{1}{n} \sum_{i=1}^n (\mathcal{E}_i - \mu_e)^2}. \quad (21)$$

The FI of the proposed and existing methods is evaluated for WSN#1 and WSN#2 in Figure 6. The FI of the first scenario with 100 SNs is compared by varying the simulation time which is shown in Figure 6(a). The FI of DAOSVM in WSN#1 is improved by 0.8-3% compared to eACO-MSPD, 1.6-5% compared to EARTH, 3.1-6.5% compared to ETDC, and 4-9% compared to CMS2TO algorithms. From Figure 6(b), we notice the improvement of the FI over the existing methods eACO-MSPD, EARTH, ETDC, and CMS2TO by 1-4%, 2.5-7%, 3.1-8.5%, and 4.5-

10%, respectively, for the WSN#2. The improved FI in the proposed work indicates balancing the energy among the SNs in the network. This improvement is also achieved by considering the best VRP set. This VRP set helps to minimize the data relay between the SNs and RP by transmitting it directly to the MS (in the communication range).

4.3. Network Lifetime. The network lifetime (NL) is an essential parameter to decide the performance of the WSNs [41]. The NL for the proposed DAOSVM algorithm is computed using Equation (5).

We test the N_l of DAOSVM, eACO-MSPD, CMS2TO, EARTH, and ETDC by varying SNs between 40 and 100 for WSN#1 and 100 and 1000 for WSN#2, as shown in Figure 7. After performing the various simulation tests, we confirm that the proposed work outperforms compared with the existing algorithms. Figure 7(a) compares the NL of the

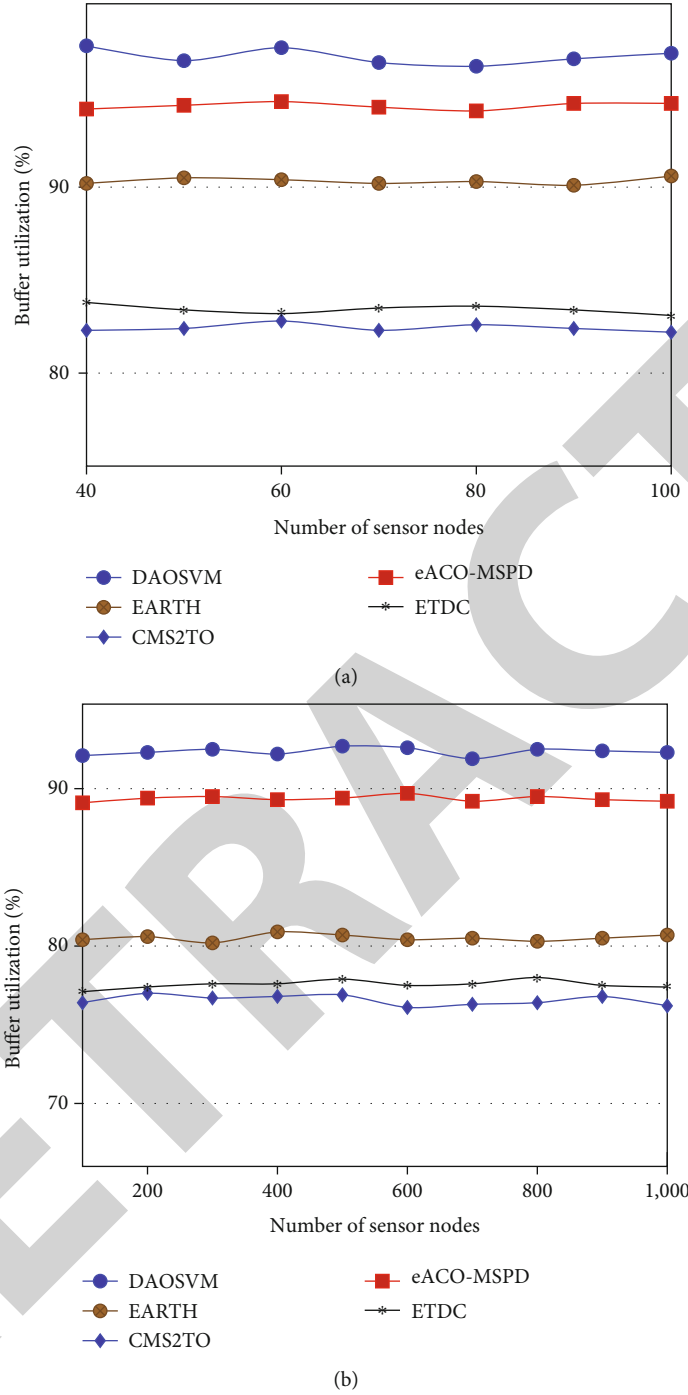


FIGURE 9: Buffer utilization of (a) WSN#1 and (b) WSN#2.

DAOSVM with eACO-MSPD, CMS2TO, EARTH, and ETDC. The N_l of the DAOSVM is longer by 208-349 minutes than eACO-MSPD, 231-497 minutes compared to EARTH, 320-564 minutes compared to ETDC, and 396-571 minutes compared to CMS2TO algorithms. Figure 7(b) shows the N_l of DAOSVM which is increased by 120-290 minutes than eACO-MSPD, 199-487 minutes than EARTH, 287-522 minutes than ETDC, and 342-603 minutes than CMS2TO algorithms.

4.4. Average Path Length. The average path length (APL) of the MS is calculated as the ratio of total distance traveled by the MS and the number of tours completed, as shown in

$$\mu_t = \frac{1}{|\varphi|} \sum_{k=1}^{|\varphi|} v_k. \quad (22)$$

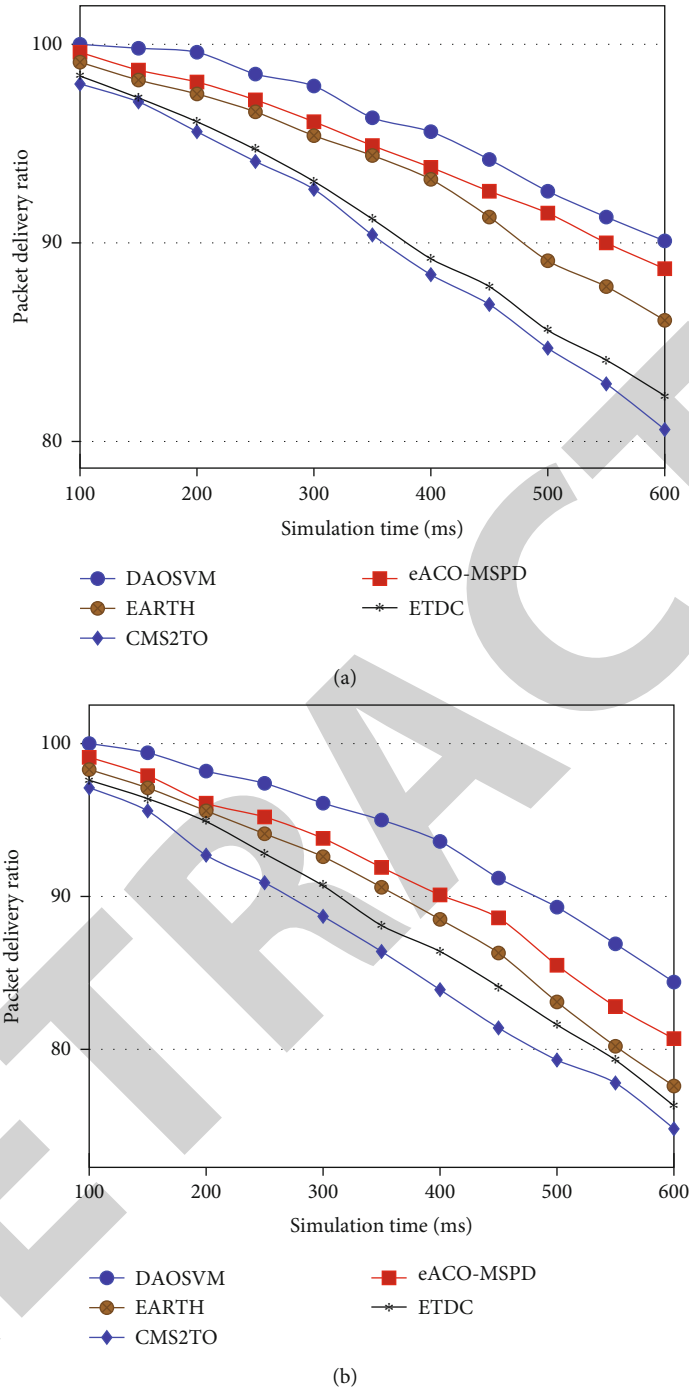


FIGURE 10: Packet delivery ratio of (a) WSN#1 and (b) WSN#2.

The OAPC performs the RP reselection, and path reconstruction can be done depending on the network condition changes. Unlike eACO-MSPD, CMS2TO, EARTH, and ETDC, the proposed DAOSVM algorithm varies the traveling distance based on the number of obstacles and also bring dynamic changes in the WSNs. The μ_t is computed in WSN#1 and WSN#2 by varying the number of obstacles in WSNs, as shown in Figure 8. In both scenarios, the path length increases because of avoiding the obstacles over the network. Here, while avoiding the obstacles, the path length increases

slightly compared to the Euclidean distance between two RPs. However, the μ_t with no obstacle is always less than or equal to the existing CMS2TO, eACO-MSPD, EARTH, and ETDC algorithms in both scenarios. In WSN#1, the μ_t is 120 m when 100 SNs without obstacles is considered. In WSN#2, the μ_t value is 320 m without obstacles.

4.5. Buffer Utilization. The amount of the buffer used in a unit time is treated as buffer utilization (BU). It is directly proportional to the PDR. The capacity of the buffer also

affects RP selection, because the best BU node may improve the data gathering process and reduce loss of data packets. The buffer capacity also affects the number of RPs. Increasing the buffer size will reduce the amount of RPs. Due to this, the tour length of the MS may also be reduced. The average BU of the proposed work and existing works computed at time T is depicted using

$$BU = \frac{\sum_{i=1}^n P_i}{b \times n}. \quad (23)$$

In both scenarios, if the $p_i > b$, the SN drops the packets. Figure 9 evaluates the BU of the DAOSVM, eACO-MSPD, CMS2TO, EARTH, and ETDC concerning two scenarios WSN#1 and WSN#2 by considering 100 and 1000 SNs, respectively. From Figure 9(a), we observe that the BU of proposed DAOSVM increased by 3-5% as compared to eACO-MSPD, 7-9% as compared to the EARTH, 13-15% as compared to ETDC, and 14-17% as compared to CMS2TO algorithms. Figure 9(b) shows that the DAOSVM algorithm BU increased by 2.5-3.5% than eACO-MSPD, 8.5-12% than EARTH, 14.5-16% than ETDC, and 16-18% than the CMS2TO algorithms. An improvement of BU in DAOSVM over the existing methods can be observed due to the efficient scheduling of the MS during the data collection process. Because of the efficient BU, the packet drop ratio is also reduced in the proposed DAOSVM algorithm.

4.6. Packet Delivery Ratio. It is the ratio of total # of packets received by the \mathcal{S}_0 which is denoted by (\mathcal{R}) , and the # of packets generated by \mathcal{S} (either through the nearest RP/directly to the MS) is indicated using (τ) during the time T . It is calculated using

$$PDR = \frac{\mathcal{R}}{\tau}, \quad (24)$$

where $\mathcal{R} \leq \tau$, and the computational strategy of τ is shown in

$$\tau = \sum_{i=1}^n P(\mathcal{S}_i), \quad (25)$$

where $P(\mathcal{S}_i)$ indicates the number of packets collected from the environment by a SN \mathcal{S}_i . The higher the PDR indicates the efficient data collection process and vice versa. It also shows the efficiency of MS scheduling over the network and reaches before the buffer overflows. The PDR of the proposed and existing algorithms are compared in Figure 10. This simulation considers the SN data generation similar to all the DAOSVM and existing algorithms. The PDR of the proposed and existing methods recorded during the simulation runs between 100 ms to 600 ms by varying 50 ms gap for both scenarios WSN#1 and WSN#2.

The amount of the buffer used in a unit time is treated as buffer utilization (BU).

From Figure 10(a), we noticed that the proposed DAOSVM increases the PDR by 10-12% than eACO-MSPD, 11-15% than EARTH, 12-17% than ETDC, and 12-19%

CMS2TO algorithms in the first scenario. Similarly, the performance improvements are also observed in WSN#2, as shown in Figure 10(b). Here, we find that the OAPC improves the PDR by 8-10% compared to the eACO-MSPD, 9-12% compared to EARTH, 10-14% compared to ETDC, and 11-16% as compared to CMS2TO algorithms.

5. Conclusion

Construction of the optimal MS traveling path and selecting the best RP set is a challenging task during the data collection in WSNs. It is more challenging in case of obstacles over the network in the traveling route. This paper uses the support vector machine to construct the obstacle-aware mobile sink path. In this, we also compute the best RPs and VRPs set and reselection, where VRPs are the nodes that can directly transmit their data to the MS. The RP set is selected and reselected using the minimum spanning tree-based clustering mechanism. The VRP selection mainly depends on the path between the RPs and the distance between the SNs, and the route should be within the communication range of MS. The proposed DAOSVM is compared with eACO-MSPD, CMS2TO, EARTH, and ETDC using a simulation run with various performance metrics such as AEC, FI, network lifetime, BU, average path length, and packet delivery ratio. These comparisons concluded that the proposed work outperforms the existing algorithms. In a future work, we consider the velocity control and waiting time at VPs are considered while scheduling the mobile sink.

Data Availability

All the data related to this research are embedded in the paper.

Conflicts of Interest

The authors declare that they have no conflicts of interest.

References

- [1] D. Praveen Kumar, A. Tarachand, and A. C. S. Rao, "Machine learning algorithms for wireless sensor networks: a survey," *Information Fusion*, vol. 49, pp. 1–25, 2019.
- [2] C. Tunca, S. Isik, M. Y. Donmez, and C. Ersoy, "Distributed mobile sink routing for wireless sensor networks: a survey," *IEEE communications surveys & tutorials*, vol. 16, no. 2, pp. 877–897, 2013.
- [3] Y. Sheng, B. Zhang, C. Li, and H. T. Mouftah, "Routing protocols for wireless sensor networks with mobile sinks: a survey," *IEEE Communications Magazine*, vol. 52, no. 7, pp. 150–157, 2014.
- [4] Dipak Kumar Sah and Tarachand Amgoth, "Renewable energy harvesting schemes in wireless sensor networks: a survey," *Information Fusion*, vol. 63, pp. 223–247, 2020.
- [5] P. K. R. Maddikunta, Q. V. Pham, D. C. Nguyen et al., "Incentive techniques for the internet of things: a survey," *Journal of Network and Computer Applications*, vol. 2022, article 103464, 2022.

- [6] Y. Wang and K. Chen, "Efficient path planning for a mobile sink to reliably gather data from sensors with diverse sensing rates and limited buffers," *IEEE Transactions on Mobile Computing*, vol. 18, no. 7, pp. 1527–1540, 2019.
- [7] P. K. Donta, T. Amgoth, and C. S. R. Annavarapu, "Delay-aware data fusion in duty-cycled wireless sensor networks: a q-learning approach," *Sustainable Computing: Informatics and Systems*, vol. 33, no. 1, article 100642, 2022.
- [8] K. D. Praveen, T. Amgoth, and C. S. R. Annavarapu, "CO-based mobile sink path determination for wireless sensor networks under non-uniform data constraints," *Applied Soft Computing*, vol. 69, pp. 528–540, 2018.
- [9] S. Redhu and R. M. Hegde, "Cooperative network model for joint mobile sink scheduling and dynamic buffer management using Q-learning," *IEEE Transactions on Network and Service Management*, vol. 17, no. 3, pp. 1853–1864, 2020.
- [10] M. Liyanage, Q. V. Pham, K. Dev et al., "A survey on zero touch network and service (ZSM) management for 5g and beyond networks," *Journal of Network and Computer Applications*, vol. 2022, article 103362, 2022.
- [11] A. S. Nandan, S. Singh, and L. K. Awasthi, "An efficient cluster head election based on optimized genetic algorithm for movable sinks in IoT enabled HWSNs," *Applied Soft Computing*, vol. 107, article 107318, 2021.
- [12] S. Najjar-Ghabel, L. Farzinvas, and S. N. Razavi, "Mobile sink-based data gathering in wireless sensor networks with obstacles using artificial intelligence algorithms," *Ad Hoc Networks*, vol. 106, article 102243, 2020.
- [13] J. Wang, Y. Cao, B. Li, H.-j. Kim, and S. Lee, "Particle swarm optimization based clustering algorithm with mobile sink for WSNs," *Future Generation Computer Systems*, vol. 76, pp. 452–457, 2017.
- [14] P. K. Donta, B. S. P. Rao, T. Amgoth, C. S. R. Annavarapu, and S. Swain, "Data collection and path determination strategies for mobile sink in 3D WSNs," *IEEE Sensors Journal*, vol. 20, no. 4, pp. 2224–2233, 2020.
- [15] A. Verma, S. Kumar, P. R. Gautam, T. Rashid, and A. Kumar, "Fuzzy logic based effective clustering of homogeneous wireless sensor networks for mobile sink," *IEEE Sensors Journal*, vol. 20, no. 10, pp. 5615–5623, 2020.
- [16] T. A. Al-Janabi and H. S. Al-Raweshidy, "A centralized routing protocol with a scheduled mobile sink-based AI for large scale I-IoT," *IEEE Sensors Journal*, vol. 18, no. 24, pp. 10248–10261, 2018.
- [17] J. Miura, "Support vector path planning," in *In 2006 IEEE/RSJ International Conference on Intelligent Robots and Systems*, pp. 2894–2899, Beijing, China, 2006.
- [18] P. K. Donta, T. Amgoth, and C. S. R. Annavarapu, "An extended ACO-based mobile sink path determination in wireless sensor networks," *Computing*, vol. 12, no. 10, pp. 8991–9006, 2021.
- [19] N. Gharaei, K. Abu Bakar, S. Z. Mohd Hashim, A. Hosseingholi Pourasl, and S. Ashfaq Butt, "Collaborative mobile sink sojourn time optimization scheme for cluster-based wireless sensor networks," *IEEE Sensors Journal*, vol. 18, no. 16, pp. 6669–6676, 2018.
- [20] C. Sha, D. Song, R. Yang, H. Gao, and H. Huang, "A type of energy-balanced tree based data collection strategy for sensor network with mobile sink," *IEEE Access*, vol. 7, pp. 85226–85240, 2019.
- [21] A. A. Kamble and B. M. Patil, "Systematic analysis and review of path optimization techniques in WSN with mobile sink," *Computer Science Review*, vol. 41, article 100412, 2021.
- [22] Z. Lin, H.-C. Keh, W. Ruikun, and D. S. Roy, "Joint data collection and fusion using mobile sink in heterogeneous wireless sensor networks," *IEEE Sensors Journal*, vol. 21, no. 2, pp. 2364–2376, 2020.
- [23] A. Mehto, S. Tapaswi, and K. K. Pattanaik, "PSO-based rendezvous point selection for delay efficient trajectory formation for mobile sink in wireless sensor networks," in *2020 International Conference on COMMunication Systems & NETWORKS (COMSNETS)*, pp. 252–258, Bengaluru, India, 2020.
- [24] "DED: joint density-aware and energy-limited path construction for data collection using mobile sink in WSNs," *Access*, vol. 8, pp. 78942–78955, 2020.
- [25] M. Naghibi and H. Barati, "EGRPM: energy efficient geographic routing protocol based on mobile sink in wireless sensor networks," *Sustainable Computing: Informatics and Systems*, vol. 25, article 100377, 2020.
- [26] K. K. Shubhra Jain, R. K. Pattanaik, S. B. Verma, and A. Shukla, "Delay-aware green routing for mobile-sink-based wireless sensor networks," *IEEE Internet of Things Journal*, vol. 8, no. 6, pp. 4882–4892, 2020.
- [27] S. Jain, K. K. Pattanaik, R. K. Verma, and A. Shukla, "EDVWDD: event-driven virtual wheel-based data dissemination for mobile sink-enabled wireless sensor networks," *The Journal of Supercomputing*, vol. 77, pp. 1432–11457, 2021.
- [28] L. Farzinvas, S. Najjar-Ghabel, and T. Javazadeh, "A distributed and energy-efficient approach for collecting emergency data in wireless sensor networks with mobile sinks," *AEU-International Journal of Electronics and Communications*, vol. 108, pp. 79–86, 2019.
- [29] G. P. Gupta and B. Saha, "Load balanced clustering scheme using hybrid metaheuristic technique for mobile sink based wireless sensor networks," *Journal of Ambient Intelligence and Humanized Computing*, pp. 1–12, 2020.
- [30] F. Xiuwen and X. He, "Energy-balanced data collection with path-constrained mobile sink in wireless sensor networks," *AEU-International Journal of Electronics and Communications*, vol. 127, article 153504, 2020.
- [31] C.-Y. Chang, S.-Y. Chen, I.-H. Chang, G.-J. Yu, and D. S. Roy, "Multirate data collection using mobile sink in wireless sensor networks," *IEEE Sensors Journal*, vol. 20, no. 14, pp. 8173–8185, 2020.
- [32] B. G. Gutam, P. K. Donta, C. S. R. Annavarapu, and Y. C. Hu, "Optimal rendezvous points selection and mobile sink trajectory construction for data collection in WSNs," *Journal of Ambient Intelligence and Humanized Computing*, pp. 1–12, 2021.
- [33] G. Xie and F. Pan, "Cluster-based routing for the mobile sink in wireless sensor networks with obstacles," *IEEE Access*, vol. 4, pp. 2019–2028, 2016.
- [34] R. Kumar, T. Amgoth, and D. Das, "Obstacle-aware connectivity establishment in wireless sensor networks," *IEEE Sensors Journal*, vol. 21, no. 4, pp. 5543–5552, 2021.
- [35] J. Park, S. Kim, J. Youn, S. Ahn, and S. Cho, "Iterative sensor clustering and mobile sink trajectory optimization for wireless sensor network with nonuniform density," *Wireless Communications and Mobile Computing*, vol. 2020, Article ID 8853662, 16 pages, 2020.

Retraction

Retracted: Next Generation IoT and Blockchain Integration

Journal of Sensors

Received 23 January 2024; Accepted 23 January 2024; Published 24 January 2024

Copyright © 2024 Journal of Sensors. This is an open access article distributed under the Creative Commons Attribution License, which permits unrestricted use, distribution, and reproduction in any medium, provided the original work is properly cited.

This article has been retracted by Hindawi following an investigation undertaken by the publisher [1]. This investigation has uncovered evidence of one or more of the following indicators of systematic manipulation of the publication process:

- (1) Discrepancies in scope
- (2) Discrepancies in the description of the research reported
- (3) Discrepancies between the availability of data and the research described
- (4) Inappropriate citations
- (5) Incoherent, meaningless and/or irrelevant content included in the article
- (6) Manipulated or compromised peer review

The presence of these indicators undermines our confidence in the integrity of the article's content and we cannot, therefore, vouch for its reliability. Please note that this notice is intended solely to alert readers that the content of this article is unreliable. We have not investigated whether authors were aware of or involved in the systematic manipulation of the publication process.

Wiley and Hindawi regrets that the usual quality checks did not identify these issues before publication and have since put additional measures in place to safeguard research integrity.

We wish to credit our own Research Integrity and Research Publishing teams and anonymous and named external researchers and research integrity experts for contributing to this investigation.

The corresponding author, as the representative of all authors, has been given the opportunity to register their agreement or disagreement to this retraction. We have kept a record of any response received.

References

- [1] S. Tanwar, N. Gupta, C. Iwendi, K. Kumar, and M. Alenezi, "Next Generation IoT and Blockchain Integration," *Journal of Sensors*, vol. 2022, Article ID 9077348, 14 pages, 2022.

Review Article

Next Generation IoT and Blockchain Integration

**Sarvesh Tanwar,¹ Neelam Gupta,¹ Celestine Iwendi ,² Karan Kumar ,³
and Mamdouh Alenezi ⁴**

¹Amity Institute of Information Technology, Amity University Uttar Pradesh, Noida, India

²School of Creative Technologies, University of Bolton, Bolton BL3 5AB, UK

³Electronics and Communication Engineering Department, Maharishi Markandeshwar Engineering College, Maharishi Markandeshwar (Deemed to Be University), Mullana, Ambala, 133207 Haryana, India

⁴College of Computer & Information Sciences, Prince Sultan University, Riyadh, Saudi Arabia

Correspondence should be addressed to Celestine Iwendi; celestine.iwendi@ieee.org, Karan Kumar; karan.170987@gmail.com, and Mamdouh Alenezi; malenezi@psu.edu.sa

Received 15 July 2022; Accepted 11 August 2022; Published 24 August 2022

Academic Editor: Sweta Bhattacharya

Copyright © 2022 Sarvesh Tanwar et al. This is an open access article distributed under the Creative Commons Attribution License, which permits unrestricted use, distribution, and reproduction in any medium, provided the original work is properly cited.

The Internet of Things (IoT) refers to the interconnection of smart devices to collect data and make intelligent decisions. However, a lack of intrinsic security measures makes next generation IoT more vulnerable to privacy and security threats. With its “security by design,” Blockchain (BC) can help in addressing major security requirements in IoT. Blockchain is an ever-growing list of records that are linked and protected using cryptographic methods. It offers its users the flexibility to conduct transactions with lower costs and faster speeds. Blockchain ledgers are also decentralized and a ledger is maintained at each node in the network. Blockchain’s security and adaptability help in making even entire systems on it a much easier task with the benefit of decentralization. BC capabilities like immutability, transparency, auditability, data encryption, and operational resilience can help solve most architectural shortcomings of IoT. In the vision of the Internet of Things, traditional devices are becoming smarter and more autonomous. This vision is becoming reality as technology advances but there are still challenges to be resolved. This is especially true in a security domain like data trust, and with the expected evolution of the IoT in the coming years, it is important to ensure that this great source of data arrives. This paper began with an overview of blockchain and IoT, as well as explore the IoT blockchain application challenges. This article also focuses to review the most relevant tasks to analyse how IoT blockchain can improve and examine current research concerns and developments in the use of blockchain-related techniques and technologies in the context of IoT security in depth. One of the best parts of working or learning about blockchain and its application is the curiosity about how it can impact the things that we have been accustomed to without trying to improve and make things more efficient and productive.

1. Introduction

Recently, the rapid advancement of blockchain technology and digital currencies has had an impact on the financial industry, resulting in the creation of a new crypto economy. These usages are growing with the number of areas such as Internet, banking sector, industry, and medical center security. In addition, IoT [1] has expanded its adoption by the development of urban development around the world. The IoT has evolved into a collection of technologies ranging from wireless sensor networks (WSN) to radio frequency

identification. (RFID) is used to identify, exploit, and communicate on the Internet. Today, IoT devices can range from wearables to hardware development platforms to electronic devices. IoT plays an important role in transforming today’s cities into smart cities with a wide range of applications that can be used in many sectors of society. Various research [2] reports predict that the number of connected devices will reach 20 to 50 billion by 2020, mainly due to the large number of devices that IoT can deploy.

The IoT envisions a fully connected world where measurable information can communicate and interact with

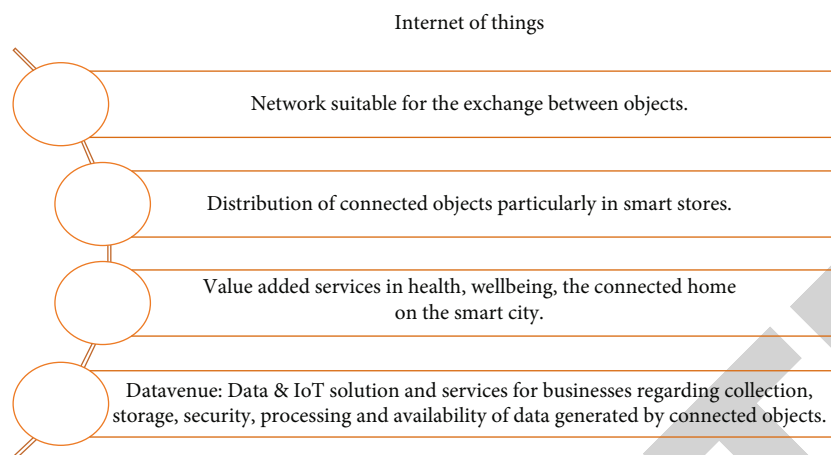


FIGURE 2: Internet of Things.

1.1. Authors' Contributions. Authors addressed major security requirements in IoT and provided solution by introducing BC capabilities to overcome IoT security issues. Searching relevant documents is an important component of performing a systematic review. This article focused on the review of the most relevant publications in the field of IoT and BC integration. The investigation is based on publications found in the Scopus electronic database to analyse how IoT BC can be improved and examined current research.

2. The Internet of Things

The way we interact with the environment and each other has changed dramatically. Internet of Things (IoT) technology is a very widespread technology. It should shape human life. Make big financial gains. IoT and blockchain technology can present a variety of challenges. Some IoT devices are sold with built-in functionality to connect to the embedded blockchain [8]. The company responsible for Ethereum allows the use of nodes on devices such as Odroid, Beaglebone, and Raspberry Pi. Similarly, EthRaspbian, and Raspnode have the ability to install Bitcoin, Litecoin, and Ethereum nodes on the Raspberry Pi. The Raspnode Wi-Fi Router Wallet also supports Litecoin and Bitcoin. Anrouter R-LTC also has this capability. Litecoin is mined, so this router can be easily installed on the IoT network as part of the Fog computing platform. It is still in its infancy and requires a lot of research for further integration. Some IoT devices also have a mining function. Not all IoT devices have this capability. Because it requires high-end hardware and invalidation on IoT devices, IoT mining is often not found to solve these challenges. The Internet of Things (IoT) offers a multitude of aspects of life. Our daily life is strongly influenced by the many applications in areas such as healthcare and manufacturing. IoT plays an important role in transforming homes into smart homes and cities. Blockchain has to deal with many inherent complexities of IoT [9] to become a smart city. Isolated integrating blockchain with IoT will build trust between customers and devices and reduce costs such as cutting out middlemen.

Transactions will be much faster, and for blockchain integration to work primarily for IoT purposes, it is necessary to connect some aspects like scalability. Collaboration security requires transcending blockchain into the IoT. Blockchain is for them to harness the power of each other. Blockchain and IoT are interdependent and evolving. Blockchain is an opportunity provided by IoT, and IoT is essential to the functions of blockchain exist. Blockchain provides a service layer for integration with standard IoT frameworks. In general, frameworks play three main roles: sensors, miners, and agents. IoT sensors receive data and interact with services using blockchain agents. The sensors are not integrated with the blockchain function [10]. Transactions in the form of sensory information can be interpreted and then transmitted over a network. These agents also provide security through the use of private keys. IoT devices do not have this security. Network miners use the main function of the blockchain to verify transactions and place them in blocks.

The Internet of Things, as shown in Figure 2, is made up of devices that generate, process, and share massive volumes of security and safety-critical data as well as privacy-sensitive data, making them attractive targets for cyberattacks [43]. Many of the new networkable devices that make up the Internet of Things [11] are low-power and lightweight. These devices must concentrate the majority of their available energy and processing to executing core application functions, making it difficult to enable security and privacy in a cost-effective manner. In terms of energy usage and processing overhead, traditional security methods are often too expensive for IoT. Furthermore, because of the difficulty of scale, the many-to-one nature of the traffic, and single point of failure, many state-of-the-art security frameworks are extremely centralized and hence are not necessarily well-suited for IoT.

2.1. IoT Security. Notwithstanding the benefits provided by IoT services, where IoT technology is successfully implemented on lamps, refrigerators, air conditioners, washing machines, wristwatches, mobile phones, etc., managing IoT [12] communications has become a challenge. A large number of IoT devices can be installed anywhere the end-user

TABLE 1: Entities and methods enforcing security and privacy properties in different tiers.

Properties	Smart home	Overlay network	Cloud storage
Identity and authentication	Ledger of transaction	Signatures	Block-number along with hash
Access control	Policy header and transactions in BC	Multiset transaction	Block-number with hash
Protocol and network	Encryption	Encryption	Encryption
Privacy	Not-private	PK or ID	Block-number along with hash
Trust	Predefined	Verification	Signed hash of data
Nonreputation	Encryption	Signatures	Signed hash of data
Policy enforcement	Policy header	PK lists	Accounting
Authorization	Policy header and transactions	List of keys	Accounting
Fault tolerance	Medium	High	Low

wants, leaving them unattended and being a desirable target for others to attack. In addition, manufacturers do not consider the security of these devices because of the large-scale deployment of IoT devices. For bulk-manufactured devices, default usernames and passwords are the same. Many IoT devices are shipped with a preprogrammed key that cannot be changed. In addition, IoT networks are heterogeneous and dynamic in nature, allowing various (untrusted) devices to indefinitely join the network. In the event of a hack, device intentions may differ during connection time, or malicious devices may masquerade as benign. Data integrity is another issue in IoT security. One of the most important IoT applications is the decision support system [3]. The information gathered by the sensors can be used to make timely decisions. As a result, the system must be protected from injection attacks, which attempt to inject false measures and thus influence decision-making.

2.2. IoT Security Using Blockchain. Moving towards decentralized architectures, blockchain technology has gained tremendous attention in terms of addressing security, anonymity, traceability, and centralization. Entities and methods are enforcing security and privacy properties in different tiers of IoT security using blockchain, as shown in Table 1. The security [13] of this technology stems from the use of hash functions to chain blocks to ensure immutability, as well as the use of encryption and digital signatures to secure data. The distributed nature of the blockchain ensures its availability. Enabling blockchain technology in IoT can help to achieve a properly distributed consensus based IoT system that overcomes security issues. Even if this is an ideal match, it is still a challenging endeavor. Most existing blockchain schemes do not work in the IoT ecosystem and cannot meet the specific needs of the IoT. IoT environments are resource-constrained, computationally, power-intensive, and storage-constrained, resulting in high computational complexity, limited scalability, high bandwidth overhead, and high latency blockchain. There are some devices that are not recommended to be use with IoT. This is due to how the Block name manages device identities [14]. The author uses an open source implementation of the Kademia Distributed Hash Table (DHT) which provides the secure encrypted communication, thus define how devices are used with smart contracts. Fakhri and Muti-

jarsa built IoT systems with and without blockchain and compared the two approaches. MQTT is a communication protocol used in IoT systems that do not use blockchain. Ethereum was used as a blockchain platform, along with a smart contract, in the other system. The security levels of both IoT systems were evaluated by simulating attacks and observing their security features. The results of the tests showed that the IoT system based on blockchain technology had a higher level of security than the IoT system that did not use blockchain technology. Mik presented a novel hybrid blockchain architecture for IoT, referred to as Hybrid IoT. In Hybrid IoT [15], subgroups of IoT devices, referred to as PoW (proof of work) subblockchains, were created. The connection between the PoW subblockchains was then made using a Byzantine Fault Tolerance (BFT) interconnector framework, such as Cosmos or Polkadot. The authors' work focused on the formation of PoW subblockchains that are guided by a set of metrics, dimensions, and bounds. The performance evaluation validated the PoW subblockchain design according to the guidelines of the sweet-spot. The results showed that the guidelines of sweet-spot help to prevent security vulnerabilities. To provide an IoT network with a scalable and dynamic communication architecture, a dynamic blockchain-based trust system was proposed in. The proposed architecture practically labelled all IoT devices and mapped them as full nodes and lightweight nodes. If the attacker pretends to be a full node, high-level security verification will either catch him or make the attack extremely costly [4]. It is also difficult if the attacker just wants to pretend to be a lightweight node because all history is recorded and the attacker must fake everything all over again each time they try to attack. However, IoT with blockchain topology should not only manage the ID but also protect the information exchanged in the IoT network.

3. Literature Review

Various problems in IoT despite authentication and best methods for incorporating security such as Zhen Ling, Junzhou Luo et al. (2017), Yiling Xu et al. (2017), Chao Gao et al. (2017), Kui Wu et al. (2017), and Xinwen Fu et al. (2017) found that there are numerous challenges that arise when there is an authentication method (2017). The lack of an authentication mechanism in the IoT is the fundamental

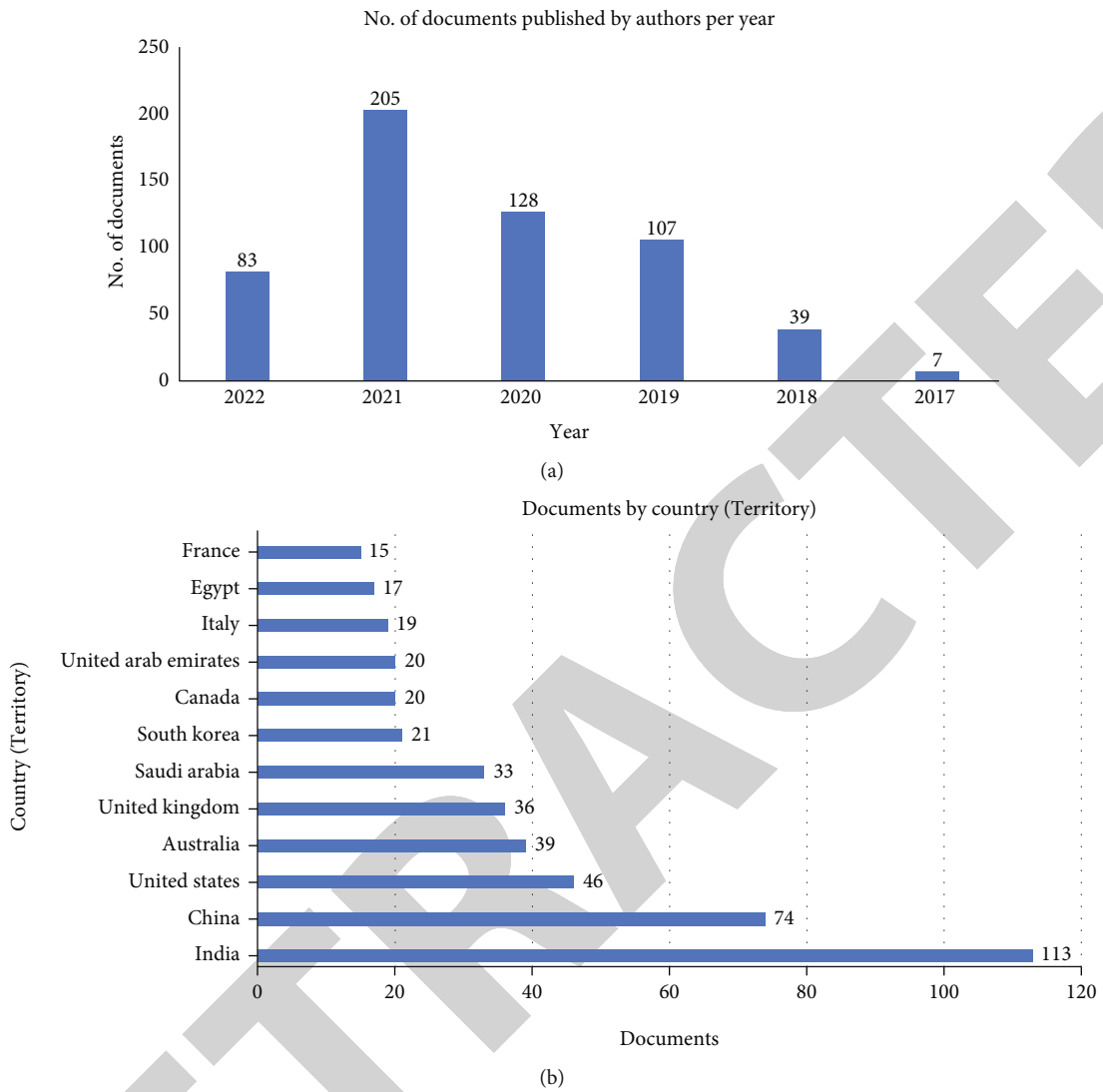


FIGURE 3: Continued.

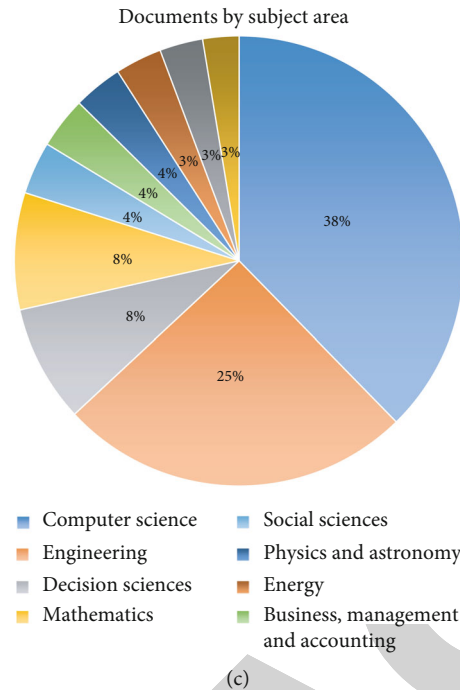


FIGURE 3: (a) The annual and cumulative numbers of research documents related to blockchain and IoT integration. (b) The country and cumulative numbers of research documents related to blockchain and IoT integration. (c) The subject area and cumulative numbers of research documents related to blockchain and IoT integration.

cause for this. Despite the fact that most IoT [16] apps have authentication enabled, there are security concerns that lead to data loss. Some of the difficulties are as follows. The authors offer a case study on a smart plug system in which they effectively exploit protocols and launch attacks such as brute force, device scanning, firmware assault, and spoofing attack. Their experiments reveal that they are capable of gaining the upper hand.

In the importance of authentication in IoT systems [40], authentication is the cornerstone of providing good security. In IoT systems and m2m applications, a variety of authentication mechanisms are used. These authentication procedures are simple and rely on XOR and hash operations to communicate inside the IoT technology ecosystem [17]. Leakage of critical data is a major concern in many IoT networks Munindar P. Singh et al. (2017) and Muhammad Shahzad et al (2017). The fundamental cause, according to the authors, is that IoT networks lack authentication procedures. The authors suggest alternative approaches for user identification and authorization for IoT networks that lack traditional user interfaces. The authors discuss why authentication is critical in an IoT network. They also [41] provide a solution for overcoming the lack of a traditional user interface for IOT networks.

The search approach should be thorough and objective, as well as simple and repeatable. The search is restricted from 2017 to 2022. The work done on blockchain and Internet of Things integration in the last six years is given below, as shown in Figures 3(a)–3(c).

This investigation is based on publications found in the Scopus electronic database. Searching is an important component of performing a systematic review. In our search,

we employed terms such as keywords, title, authors, abstract, references, and index/subject terms, as shown in Figures 4(a) and 4(b). And historiography and average citation per year are shown in Tables 2 and 3. Authors have worked on various next generation IoT and Blockchain Integration concepts for the last seven years, as shown in Table 4.

Table 2 presented historiography based on clustering in Figure 4(b).

Blockchain is an ever-growing list of records that are linked and protected using cryptographic methods. It also offers its users the flexibility to conduct transactions with lower costs and faster speeds. This is presented in Table 3 in the form of citations.

4. Blockchain and IoT Integration

IoT is transforming and optimizing manual workflows to become part of the digital age. By receiving a large amount of information that provides a level of knowledge that has never been heard before, this knowledge facilitates the development of intelligent applications, such as improving the management and quality of people's lives through the digitization of city services. In the past few years [2], Cloud computing technology has contributed to the IoT's essential functions for analysing and processing data and turn them into real-time actions and knowledge. Unprecedented growth in the IoT [18] has opened up new opportunities for communities, such as mechanisms for accessing and sharing information. The open data paradigm is the primary guide to these initiatives. However, one of the most important vulnerabilities of these initiatives which happened in many the situation is lack of confidence. A centralized

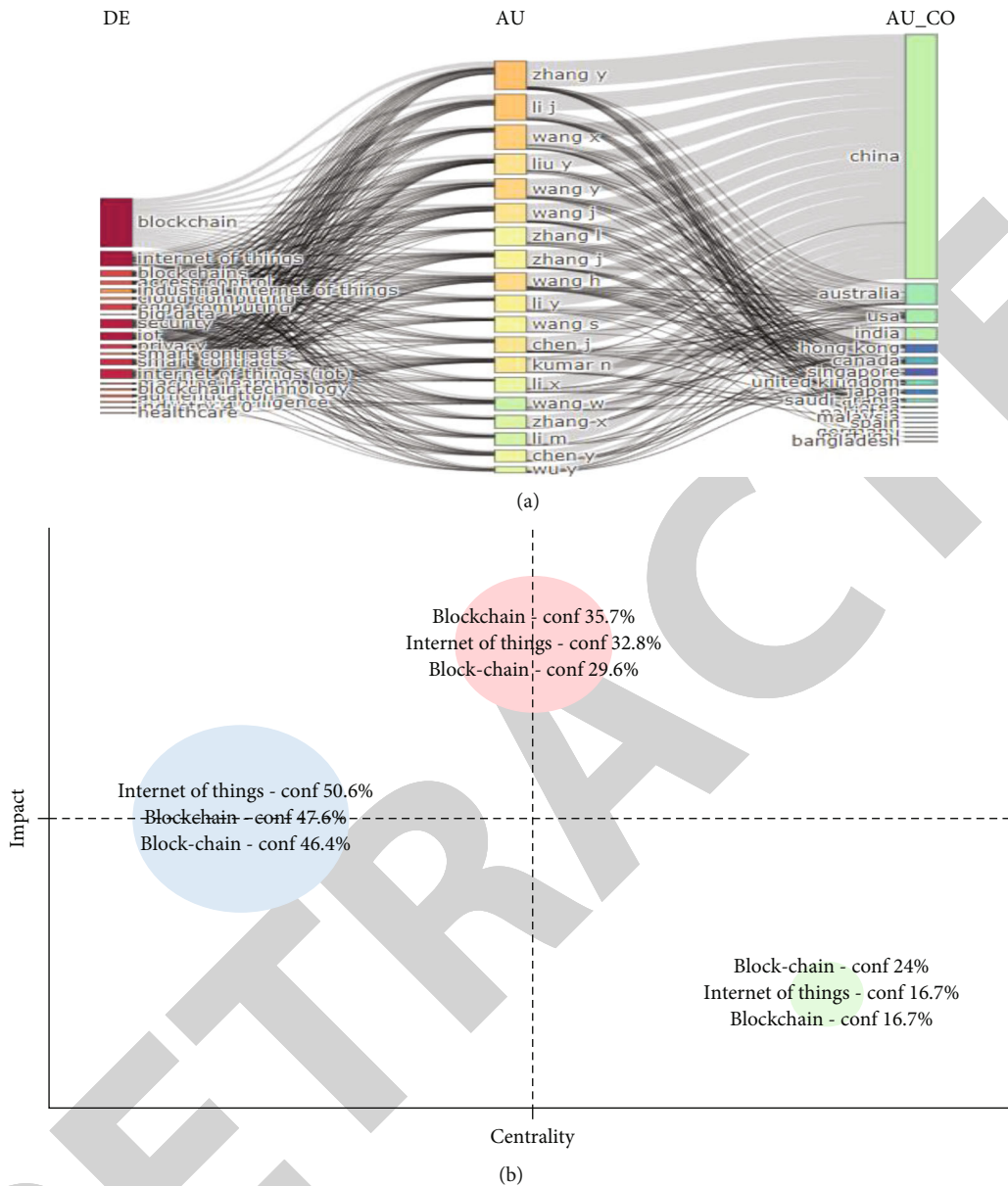


FIGURE 4: (a) A screenshot of the three fields plot in bibliometric analysis created based on keywords, authors with author's country. (b) Clustering by coupling map.

architecture like the one used in cloud computing is crucial to the development of IoT. They act as a black box, and network participants do not have a clear vision of where and how to use the information they provide.

The integration of promising technologies such as IoT and cloud computing has proven invaluable. In the same way, we recognize the enormous potential of blockchain in revolutionizing the IoT [19]. Blockchain can empower the IoT by providing reliable sharing services. The information is reliable and traceable. The source of information can be identified at any time. And the data will remain unchanged over time. Improve safety where IoT data should be shared securely between large numbers of participants. This integration represents a major revolution. For example, thorough traceability in many food products is a key factor in ensuring food safety. Food traceability may require the par-

ticipation of a large number of participants: production, feeding, treatment, distribution, etc. A leak in any part of the chain could lead to a breach and slows down the process of finding infections. This can have a devastating impact on citizens' lives and cause enormous economic costs to companies, sectors, and countries. In the event of a food-borne outbreak, better controls in these areas would increase food safety [6, 20], improved sharing of information between participants, reduce search time in case of foodborne outbreaks and saving human lives. In addition, in other areas such as smart cities and smart cars, trusted sharing of information can be beneficial to include new participants in the ecosystem and contribute to improving service and acceptance. Therefore, the use of blockchain can complement the IoT with reliable and secure data. This became known, as mentioned, where blockchain technology was identified as the

TABLE 2: Historiography.

Paper	Title	DOI	Year	Cluster
Bodkhe, 2020, Trans emerg telecommun technol	Blockchain for precision irrigation: opportunities and challenges	10.1002/ett.4059	2020	1
Li, 2022, Trans emerg telecommun technol	Blockchain as a service models in the internet of things management: systematic review	10.1002/ett.4139	2022	1
Khan, 2021, Electronics (Switzerland)	Reliable Internet of Things: challenges and future trends	10.3390/electronics10192377	2021	2
Guru, 2021, Electronics (Switzerland)	Approaches towards blockchain innovation: a survey and future directions	10.3390/electronics10101219	2021	2
Sadawi, 2021, IEEE access	A survey on the integration of blockchain with IoT to enhance performance and eliminate challenges	10.1109/ACCESS.2021.3070555	2021	2
Tran, 2021, J network comput appl	Integrating blockchain and Internet of Things systems: a systematic review on objectives and designs	10.1016/j.jnca.2020.102844	2021	3
Alkhateeb, 2022, Sensors	Hybrid blockchain platforms for the Internet of Things (IoT): a systematic literature review	10.3390/s22041304	2022	3

TABLE 3: Average citation per year.

Year	N	MeanTCperArt	MeanTCperYear	CitableYears
2018	18	35.78	8.94	4
2019	35	37.71	12.57	3
2020	40	18.07	9.04	2
2021	63	6.27	6.27	1
2022	42	0.74		0

key to solving scalability problems, privacy and reliability associated with the IoT paradigm, increased security, trust and lowering costs were all cited as top benefits of Blockchain/IoT, as shown in Table 5.

From our perspective, IoT can benefit greatly from blockchain functionality and will help to develop the current IoT technology in the future. It is worth noting that there are still a number of research challenges and open issues that need to be explored in order to seamlessly integrate these two technologies, and this research topic is still in its preliminary stages, especially improvements that this integration can bring (but not limited to):

Decentralization and scalability: the transition from a centralized architecture to a distributed P2P removes the center of failure and bottlenecks [21]. It also prevents situations where few powerful companies control the processing and storage of many people. Other benefits along with the decentralization of the architecture is to improve the system's fault tolerance and scalability, and it reduces IoT silos and contributes to further improvements in IoT scalability.

Identity: using common blockchain participants can identify every device. The data provided and entered into the system are immutable and uniquely identifies the actual data provided by the device. Additionally, the blockchain can provide distributed authentication and device authorization for IoT applications. It will represent improvements in IoT and participants.

Autonomy: Blockchain technology powers next-generation application features [22]. This makes it possible

to develop intelligent automated assets and hardware as a service. With blockchain, devices can interact without servers involved. IoT applications may benefit from this functionality in application procurement.

Reliability: IoT data remains immutable and distributed over time in the blockchain. System participants can verify the accuracy of the information and ensure that it has not been tampered with. In addition, this technology allows the collection and monitoring of sensor data. Trust is an important part of the blockchain brought by the IoT.

Security: data and communications can be secured by storing blockchain transactions. Blockchains can be used to translate device messages into transactions [23]. Validated by smart contract, in this way, communication between devices is secure. Today's secure standard protocols used in the IoT can be extended with blockchain applications.

Services market: Blockchain can accelerate the creation of the IoT ecosystem of services and data markets. There, transactions between colleagues can be done without employees, and microservices can easily implement and make micropayments. It can be done safely in an unreliable environment. This will improve IoT connectivity and access to IoT data on the blockchain.

Secure code alignment: uses secure, unmodified blockchain storage. The code can be secured and securely inserted into the device [24]. Manufacturers can track status and update with confidence. IoT middleware can take advantage of this capability to securely update their IoT devices.

4.1. Blockchain Technology Solution to IoT. The challenges that IoT systems confront might be solved more effectively with blockchain technology. The number of interacting items or devices in IoT systems is likely to expand in the future. As the number of gadgets increases, they will attempt to communicate with one another, resulting in the internet becoming a medium. Because most acquired data in IoT devices is stored on central servers, this would provide a number of challenges. If devices wish to access data, they must communicate via a centralized network, [8] with data flowing through a central server. Decentralized or dispersed networks with peer-to-

TABLE 4: Authors have worked on various IoT and Blockchain Integration concepts for the last seven years.

References	Year	Objectives	Future scope
[16]	2016	IoT middleware, cloud platforms, and cloud infrastructures are all surveyed as integration components. Additionally, certain integration ideas and data analytics methods are reviewed, along with various difficulties and unresolved research problems.	Users can choose the essential components depending on their own needs in order to achieve a smooth integration based on the comparisons performed and the aspects examined.
[29]	2017	A test bed is described to compare central and local data processing and highlight benefits of distributing data across multiple locations in a network.	Using test bed, this system offers network saving, real-time processing, intelligent local data processing, and potential local processing mechanisms within the smart grid.
[30]	2018	It discusses several application areas, groups the literature that is now available into these categories, introduces two usage patterns—device manipulation and data management, and provides information on the stage of development of some of the solutions currently available.	The machine economy was created as a result of attempts to commercialise data due to the prevalence of IoT devices and rising data creation. The use of BC to address the issue of data trading and interchange is an example of how this could be applied in the real world.
[34]	2019	Implementation of five privacy-preserving techniques, including privacy protection, encoding, private enterprises, combining, and discrepancy secrecy, in blockchain-based IoT systems.	Before being put into use, blockchain-based IoT devices need to be protected against a number of privacy issues.
[36]	2020	A case study is implemented in a smart IoT system utilizing the Ethereum-based Blockchain technology.	The IoT smart environment is created using sensor devices, and on the Ethereum platform, devices are authorised using the Dec AUTH protocol.
[40]	2021	The suggested BaaU-based framework for trustworthiness in the HIoT systems of the future.	Next-generation healthcare IoT (HIoT) applications may be one of the industries that the blockchain network will likely revolutionize as a technical improvement.
[41]	2022	A cooperative data sharing system where numerous data sources and consumers work together to complete data sharing tasks using cloud-edge computing and blockchain technology.	The outcomes demonstrated that it can be helpful in examining the effectiveness of any blockchain-enabled data sharing system. This will facilitate the successful implementation of efficient data exchange systems.

TABLE 5: Benefit of implementing integrated IoT with Blockchain networks.

Benefits	1 st choice	2 nd choice	Sum
Increased security and trust in shared multiparty transactions and data	33%	30%	63%
Increase in business efficiency and lowering costs	27%	29%	56%
Increase in revenue and business opportunities	21%	22%	43%
Improved constituent or participant experiences	19%	17%	37%

peer networking (PPN), distributed file sharing (DFS), and autonomous device coordination (ADC) capabilities are one of the best ways to tackle this [25]. These three roles may be carried out by blockchain, allowing IoT systems to track a large number of linked and networked devices. BC enables IoT systems to coordinate the processing of transactions between devices. BC will improve the security and dependability of IoT systems, making them more resilient. With the support of a distributed ledger, BC enables for speedier peer-to-peer communications.

4.2. Blockchain Scalability in IoT. Blockchain has gained popularity as a result of the use of Bitcoin for online transactions that do not require third-party security. However, the most difficult challenge for blockchain providers is the scalability. Scalability issues must be addressed to integrate IoT and blockchain. On the one hand, because of their sheer number, IoT devices will generate transactions at a rate that

current blockchain [10] solutions will not be able to handle. However, owing to resource constraints, it is impossible to implement blockchain peers on IoT devices. Both technologies cannot directly be integrated in their current state [26]. To address the issue of scalability, various techniques such as Segwit, Sharding, block size increase, POS, and off-chain state have been proposed. Segwit, or segregated witness, is a scalability solution that increases the number of transactions in a block while keeping the block size constant. By removing the signature data from the Bitcoin transaction, a segregated witness creates room for new transactions.

Biswas et al. proposed a framework that enables the blockchain ledger to scale across all peers by establishing a local peer network. It limited the number of transactions that enter the global blockchain by implementing a scalable local ledger while maintaining peer validation of transactions at both the local and global levels. The results of the implementation testbed showed that significant improvements in the

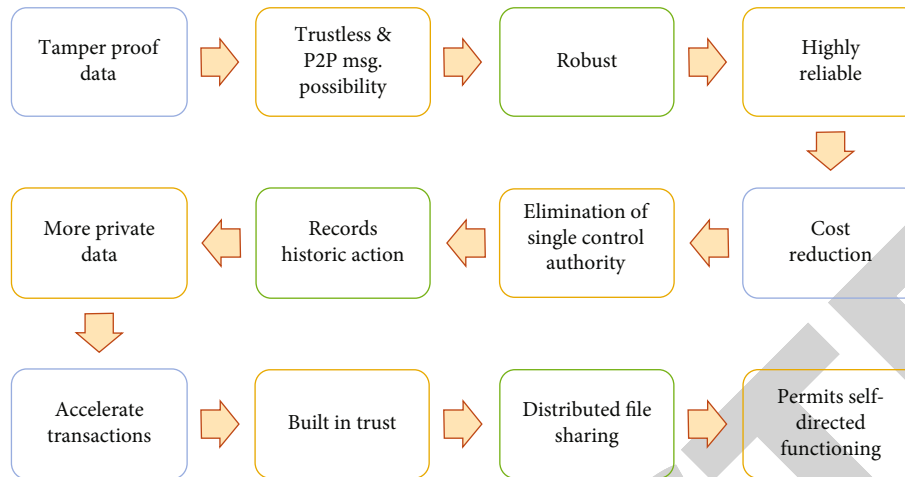


FIGURE 5: Blockchain technology have the following advantages for large scale IoT systems.

transaction rate and ledger weight were possible. This would improve the scalability of large-scale business transactions in IoT [27] and address the issue of memory requirements for storing blocks. However, the current implementation and evaluation have been carried out in part on virtual machines, with the application written in Node-red.

There are several fields that deploy IoT systems for all the advantage that it provides such as the ability to capture the data and communicate with its peer devices without any human or machine intervention. During these interactions, there is a high possibility of the data leakage. In order to overcome this, there are various methods that are employed to address this area of security.

4.3. Importance of Combining IoT with Blockchain. For industries, IIoT (Industrial Internet of Things) [14] [28] is an inseparable part. Here, people are made mandate for delivering IIoT systems that are secure, general, and scalable. Due to problems like malicious attacks and single point of failure, the existing IIoT systems are unstable in providing services. Although blockchain is a technology that has qualities like security promise and recovery combing IoT, and blockchain is interesting. Most of the IoT devices are power constrained and are not suitable for blockchain though it has low-throughput and less power-intensive. For the purpose of protecting the sensitive data confidentiality, authors came up with a method that regulates the access to sensor data.

In a centralized architecture, there are problems associated with obstacles and the center of failure. Moving to a peer-to-peer architecture solves this problem. Because the storage space is decentralized, small businesses can control and process the data, unlike a centralized architecture where large businesses can control the data [22]. This allows for better fault tolerance and system scalability. The identity of the connected device is important because it can lead to security and reliability issues. All connected devices can be uniquely identified through a single blockchain system. Credentials are also required to identify the data that devices receive. Blockchain also provides authentication for IoT devices.

Many standalone smart devices can be made using blockchain technology, which enables advanced functions to be integrated into smart hardware. Smart devices can also interact with each other without an IoT server. It can be used for modular applications. The system is also reliable as there is no risk of data loss from the blockchain. Users can verify data integrity, and data will remain intact. The system can track and account for data, so reliability is an important factor in integration considerations [15]. The system is also secure as the data is stored as blockchain transactions. This allows you to change the type of transactions monitored by smart contracts. A secure key can be provided to be securely embedded into IoT devices, allowing organizations to secretly track and update devices. It can also create an environment conducive to market exploitation [29]. Transactions between different actors can be done without an agency, and micropayments can be made instantly even if there is no trust between different people. It can improve IoT by providing more blockchain insights.

When integrating a blockchain, it is important to consider whether the devices in the system can interact with each other. A new layer known as fog computing has been added between IoT devices and cloud computing for better integration. Blockchain technology has the following advantages for large scale IoT systems, as shown in Figure 5.

Communication between two IoT devices is fast and secure. They can also work offline and have the ability to communicate with each other using routing techniques, so they do not need a blockchain to communicate. Only a small amount of data is stored in the blockchain. It is used in applications that require minimal delay [30], on the other hand, for communication between the IoT and the blockchain, all data recording all interactions that occur must pass through the blockchain. This ensures that all interactions can be tracked and recorded. In effect, this increases bandwidth usage. Therefore, this can be considered as a major limitation of blockchain. When communicating with hybrid technologies, small units of information are shared with the blockchain. Although the IoT [31] connection is direct, it is difficult to choose which interventions must be carried out during operation by the blockchain. Fog computing, which

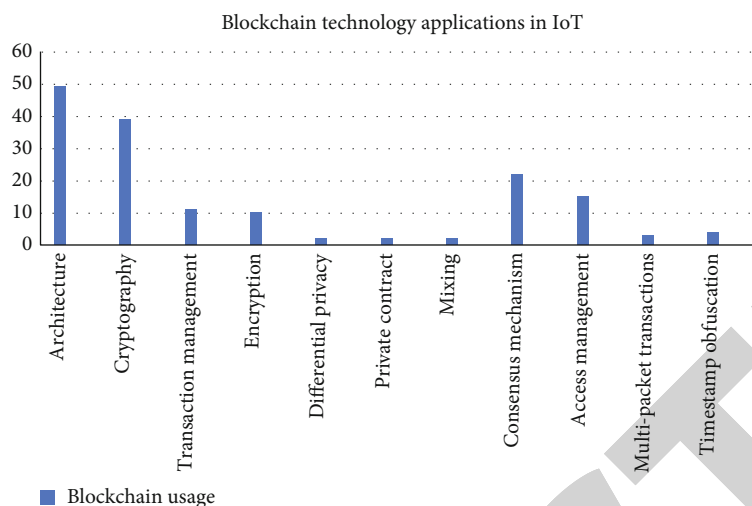


FIGURE 6: Application types.

uses gateways and other devices for mining, has overcome these limitations, but the use of this technology is growing rapidly. But it is not necessary to use it everywhere. It should only be used for required applications. In general, private use of blockchain may not be suitable for applications that require high performance. However, hybrid techniques may be required to increase efficiency. Wust and Gervais introduced a process that identifies blockchain requirements based on their application.

To facilitate the integration of IoT and blockchain, major companies are teaming up and selling off-the-shelf devices [32]. Some IoT devices are sold with built-in functionality to connect to the EthEmbeddedblockchain, and the company responsible for Ethereum allows nodes to be installed on devices such as Odroid, Beaglebone, and Raspberry Pi. Configure Bitcoins, Litecoins, and Ethereum nodes in the Raspberry PI a. The RaspnodeWiFi Router also supports wallet support for Litecoin and Bitcoin. The R-LTC Anrouter can also mine Litecoin, which makes this router easy to set up. It is still in its infancy and requires extensive research for further integration. Some IoT devices also have mining capabilities. Not all IoT devices have this capability. Since it requires high-quality hardware and is not valid on IoT devices, you will generally not find mining with IoT.

There are other ways to integrate blockchain with the IoT, including integration with cloud computing. Devices have been integrated in this way for many years to address IoT shortcomings such as storage, access, and compute, but cloud computing operates in a centralized framework. It is therefore unreliable and secure when information is shared with specific recipients. Therefore, blockchain is preferred over cloud computing to solve this problem.

4.4. Blockchain Used Because of Its Decentralized Nature in Various Applications. The scattered nature of IoT networks and their huge scale, according to several academics, is a big concern, as shown in Figure 6. Even though, the Decentralized nature of blockchain techniques provide privacy and security, they are not ideal for devices with limited resources

due to delays, considerable energy use, and computational overhead. These elements define the smart home tier's different key functions and components [33]. A component called miner is used to handle the home writers' internal and external communications. This component is a high-resource gadget that is always online. Auditing and managing communications are two more responsibilities of the miner. Blockchains retain security goals such as integrity, availability, and secrecy. Because of the different security threats that have been put on the global IoT network, the advantages that may be derived from IoT networks may exceed the risks. Data stored on the central server is subject to DDoS and Sybil attacks, as well as single point failure, which reduces the availability of services and exposes the sensor data stored in the data center.

4.4.1. Potential of Smart Contracts (SC) in Blockchain. SC are well suited for business activities that involve purchase or exchange of goods, services, and rights, especially when frequent transactions occur among a network of parties and manual tasks are performed by counterparties for each transaction [2]. This application is a match for many financial services transactions (e.g., simplifying automatic dividend payments, stock splits and cryptographic signatures on stock certificates, and streamlining over-the-counter agreements). It also [41] describes many supply chain, manufacturing, and retail transactions. However, the technology is still in its infancy, so most use cases of smart contracts today consist of the transfer of cryptocurrency [34] and recording/changing ownership of land or other assets.

4.4.2. Could Blockchain Technology Can Be a Remedy? Yes. The blockchain technology could be one of the remedies for addressing the security and privacy issues in IoT. This is because, the blockchain technology eliminates the central server concept of IoT and allows the data to flow through the blockchain distributed ledger for each transaction with appropriate authentication.

5. Challenges

Storage capacity and scalability—it is still debatable whether blockchain scalability and storage capacity issues are widespread. And in combination with IoT applications, it becomes even more difficult. However, for this reason, Blockchain technology may seem unsuitable for IoT, but the challenges involved can be avoided or completely minimized: some IoT devices can generate large amounts of data [18] [35]. This makes integration difficult. This is because the ubiquitous blockchain cannot handle such large transactions. Therefore, it is beneficial to address these issues before combining the two technologies. Today, only a small percentage of IoT big data is useful for knowledge extraction and production operations. Therefore, many researchers have proposed filtering methods. Normalize and compress IoT data to reduce it. IoT includes devices such as embedded devices and communication devices. This stores the amount of data that the IoT provides to the blockchain. Data compression can reduce the data we transmit, process, and store from the IoT. Finally, negotiated protocols can be used to increase allocated bandwidth and reduce contract latency. This improves the integration between IoT and blockchain.

Security by insufficient efficiency and a large number of uneven devices—security challenges in IoT applications need to be addressed at different levels. Moreover, IoT environments have various characteristics such as wireless communication, mobility, etc. that compound security challenges. A full security analysis has been performed. It is important to build a highly secure IoT. Due to the increasing number of attacks and their severe impact, blockchain is considered the crucial technology to support much-needed security advancements in IoT, but the integrity of data generated by IoT [9] remains a major challenge. By integrating the two technologies, blockchain can ensure that the data transmitted through the chain remains intact and changes can be detected. Therefore, when the data reaches its destination, the corrupted data stays that way. Apart from suspicious sources, corrupted data in IoT [36] can come from many other sources. Factors such as disturbance, device failure, environment, and type of participant play a role in the integrity of the IoT framework. Sometimes, IoT devices do not perform well and are difficult to detect until they are properly secured. Sometimes, it works fine at first and works due to hardware or software issues. Eavesdropping, throttling, or denial of service (DOS) is a major threat that can have a huge impact on the IoT and therefore needs to be addressed. Test it properly before combining it. They must be properly positioned and packaged to avoid physical damage and include an instant device error detection mechanism.

Cost and energy—Blockchain adoption is hampered by a lack of processing capacity. For example, Bitcoin mining necessitates a significant degree of energy to verify and validate exchanges.

Complexity and inactivity—due to the proprietary nature of blockchain-based trades, it may take several hours for all gatherings to update their corresponding records.

Adoption and mindfulness—the lack of attention and reception is one of the most fundamental challenges in blockchain innovation. Many people, for example, have a limited understanding of how it works.

Limitation of capacity and adaptation—as previously said, the storage limit and adaptability of blockchain are still being debated, however, when it comes to IoT applications, the inherent limit and versatility constraints exacerbate these issues. In this respect, blockchain may appear to be unsuitable for IoT applications [37]; however, there are ways to alleviate or avoid these limitations. This constraint addresses a significant barrier to blockchain integration in the IoT, where devices can continuously generate terabytes (GBs) of data. It has been discovered that several existing blockchain operations can only handle a few transactions per second, which could be a bottleneck for the IoT.

Confidentiality and information security—many IoT applications operate with private information, such as when a device is attached to an individual, as in the e-healthcare situation, thus, it is critical to solve the issue of data security and anonymity. Although Blockchain is touted as the greatest solution for addressing the personalities of IoT [38–41] leaders, there may be applications where anonymity is required, similar to Bitcoin. This is the case with a wearable that can hide an individual's identity when delivering personal information, or with clever cars that preserve the security of customers' schedules.

Brilliant agreements—although brilliant agreements have been identified as the ideal application of blockchain innovation, there are still a few issues to be resolved, as previously said. The use of clever contracts in IoT [42–44] might be beneficial, but the way they integrate into IoT applications is different [45, 46].

6. Conclusion and Future Scope

Blockchain aims to revolutionize the next generation IoT. This review has provided a comprehensive overview of the interaction between blockchain technology and the IoT model. Implementing restrictions is important for integrating blockchain and IoT into government infrastructure. This recognition will accelerate engagement between citizens, governments, and businesses. Consensus will play an important role in integrating IoT as part of the process of mining and distributing more blockchains. Research efforts should be made to ensure the security and privacy of key technologies such as IoT and blockchain. One of the biggest concerns about blockchain is that people are taking advantage of this situation, especially in the context of the instability of digital currency. The paper then also went on to explain and chronologically introduce articles on Internet of Things, IoT security using blockchain, Blockchain scalability in IoT, and new challenges and opportunities in IoT and defense mechanisms, as well as using blockchain to ensure confidentiality, authentication, access control, trust, and reputation. Although enabling IoT data security, blockchain has numerous significant problems. For a successful blockchain and IoT integration, an analysis of the key problems of blockchain and IoT integration should be investigated, considering the issues raised in this study. As future work, we

intend to investigate how blockchain, edge computing, and IoT can complement each other in their integration, as well as how edge computing's many security and data integrity issues may be handled by using blockchain technology. Finally, we intend to launch a variety of blockchain applications in the IoT because of blockchain's autonomy to foster the creation of next generation IoT markets. The whole prospect of working on blockchain to maybe one day create something that has never been done before is the motivation behind trying to make this decentralized app.

Data Availability

No data were used to support this study.

Conflicts of Interest

We declared no competing interest exists.

Acknowledgments

The authors would like to acknowledge the support of Prince Sultan University for paying the Article Processing Charges (APC) of this publication.

References

- [1] S. N. Khan, F. Loukil, C. Ghedira-Guegan, E. Benkhelifa, and A. Bani-Hani, "Blockchain smart contracts: applications, challenges, and future trends," *Peer-to-peer Networking and Applications*, vol. 14, no. 5, pp. 2901–2925, 2021.
- [2] C. McPhee and A. Ljutic, "Editorial: Blockchain," *Management Review*, vol. 7, no. 10, pp. 3–5, 2017.
- [3] A. Angrish, B. Craver, M. Hasan, and B. Starly, "A case study for Blockchain in manufacturing: "FabRec": a prototype for peer-to-peer network of manufacturing nodes," *Procedia Manufacturing*, vol. 26, pp. 1180–1192, 2018.
- [4] T. Justina, "Blockchain technologies: opportunities for solving real-world problems in healthcare and biomedical sciences," *Acta Informatica Medica*, vol. 27, no. 4, pp. 284–291, 2019.
- [5] M. Andoni, V. Robu, D. Flynn et al., "Blockchain technology in the energy sector: a systematic review of challenges and opportunities," *Renewable and Sustainable Energy Reviews*, vol. 100, pp. 143–174, 2019.
- [6] M. Alharby and A. Van Moorsel, "Blockchain-based smart contracts: a systematic mapping study," 2017, <http://arxiv.org/abs/1710.06372>.
- [7] M. Iansiti and K. R. Lakhani, "Harvard Business Review," *HBR, R1701J, Jan-Feb*, 2017.
- [8] I. Karamitsos, M. Papadaki, and N. B. Al Barghuthi, "Design of the blockchain smart contract: a use case for real estate," *Journal of Information Security*, vol. 9, no. 3, pp. 177–190, 2018.
- [9] S. Nakamoto, "Bitcoin whitepaper," vol. 9, no. 7, p. 2019, 2008, URL: <https://bitcoin.org/bitcoin.pdf>.
- [10] Z. Wang, H. Jin, W. Dai, K. K. R. Choo, and D. Zou, "Ethereum smart contract security research: survey and future research opportunities," *Frontiers of Computer Science*, vol. 15, no. 2, pp. 1–18, 2021.
- [11] A. H. Mohammed, A. A. Abdulateef, and I. A. Abdulateef, "Hyperledger, Ethereum and blockchain technology: a short overview," in *2021 3rd International Congress on Human-Computer Interaction, Optimization and Robotic Applications (HORA)*, pp. 1–6, Ankara, Turkey, 2021.
- [12] H. Xiaoting and N. Li, "Subject information integration of higher education institutions in the context of Web3. 0," in *2010 The 2nd International Conference on Industrial Mechatronics and Automation*, vol. 2, pp. 170–173, Wuhan, China, 2010.
- [13] M. Hamilton, "Blockchain distributed ledger technology: an introduction and focus on smart contracts," *Journal of Corporate Accounting & Finance*, vol. 31, no. 2, pp. 7–12, 2020.
- [14] W. Metcalfe, *Ethereum, Smart Contracts, DApps*, Blockchain and Crypt Currency, 2020.
- [15] E. Mik, "Smart contracts: terminology, technical limitations and real world complexity," *Law, Innovation and Technology*, vol. 9, no. 2, pp. 269–300, 2017.
- [16] M. Díaz, C. Martín, and B. Rubio, "State-of-the-art, challenges, and open issues in the integration of internet of things and cloud computing," *Journal of Network and Computer Applications*, vol. 67, pp. 99–117, 2016.
- [17] J. Rivera and R. Van Der Meulen, "Gartner," *Forecast Alert: Internet of Things—Endpoints and Associated Services*, Worldwide, Gartner, Ed., 2016.
- [18] K. Zile and R. Strazdiņa, "Blockchain use cases and their feasibility," *Applied Computer Systems*, vol. 23, no. 1, pp. 12–20, 2018.
- [19] M. A. Engelhardt, "Hitching healthcare to the chain: an introduction to blockchain technology in the healthcare sector," *Technology Innovation Management Review*, vol. 7, no. 10, pp. 22–34, 2017.
- [20] S. Nakamoto, "Bitcoin: a peer-to-peer electronic cash system," *Decentralized Business Review*, p. 21260, 2008.
- [21] A. M. Antonopoulos, *Mastering Bitcoin: Unlocking Digital Cryptocurrencies*, O'Reilly Media, Inc., 2014.
- [22] Z. Zheng, S. Xie, H. N. Dai, X. Chen, and H. Wang, "Blockchain challenges and opportunities: a survey," *International Journal of Web and Grid Services*, vol. 14, no. 4, pp. 352–375, 2018.
- [23] N. Radziwill, "Blockchain revolution: how the technology behind bitcoin is changing money, business, and the world," *The Quality Management Journal*, vol. 25, no. 1, pp. 64–65, 2018.
- [24] E. Androulaki, A. Barger, V. Bortnikov et al., "Hyperledger fabric: a distributed operating system for permissioned blockchains," in *Proceedings of the thirteenth EuroSys conference*, pp. 1–15, 2018.
- [25] J. Kennedy, "\$1.4 bn investment in blockchain start-ups in last 9 months, says PwC expert," *Silicon.com*, vol. 4, 2016.
- [26] I. Eyal, A. E. Gencer, E. G. Sirer, and R. Van Renesse, "{Bitcoin-NG}: a scalable blockchain protocol," in *13th USENIX symposium on networked systems design and implementation (NSDI 16)*, pp. 45–59, 2016.
- [27] N. M. Kumar and P. K. Mallick, "Blockchain technology for security issues and challenges in IoT," *Procedia Computer Science*, vol. 132, pp. 1815–1823, 2018.
- [28] J. Bhosale and S. Mavale, "Volatility of select crypto-currencies: a comparison of Bitcoin, Ethereum and Litecoin," *Annual Research Journal of SCMS Pune*, vol. 6, 2018.
- [29] U. Ahsan and A. Bais, "Distributed big data management in smart grid," in *2017 26th Wireless and Optical Communication Conference (WOCC)*, pp. 1–6, Newark, NJ, USA, 2017.
- [30] A. Panarello, N. Tapas, G. Merlino, F. Longo, and A. Puliafito, "Blockchain and iot integration: a systematic survey," *Sensors*, vol. 18, no. 8, p. 2575, 2018.

Retraction

Retracted: Construal Attacks on Wireless Data Storage Applications and Unraveling Using Machine Learning Algorithm

Journal of Sensors

Received 23 January 2024; Accepted 23 January 2024; Published 24 January 2024

Copyright © 2024 Journal of Sensors. This is an open access article distributed under the Creative Commons Attribution License, which permits unrestricted use, distribution, and reproduction in any medium, provided the original work is properly cited.

This article has been retracted by Hindawi following an investigation undertaken by the publisher [1]. This investigation has uncovered evidence of one or more of the following indicators of systematic manipulation of the publication process:

- (1) Discrepancies in scope
- (2) Discrepancies in the description of the research reported
- (3) Discrepancies between the availability of data and the research described
- (4) Inappropriate citations
- (5) Incoherent, meaningless and/or irrelevant content included in the article
- (6) Manipulated or compromised peer review

The presence of these indicators undermines our confidence in the integrity of the article's content and we cannot, therefore, vouch for its reliability. Please note that this notice is intended solely to alert readers that the content of this article is unreliable. We have not investigated whether authors were aware of or involved in the systematic manipulation of the publication process.

Wiley and Hindawi regrets that the usual quality checks did not identify these issues before publication and have since put additional measures in place to safeguard research integrity.

We wish to credit our own Research Integrity and Research Publishing teams and anonymous and named external researchers and research integrity experts for contributing to this investigation.

The corresponding author, as the representative of all authors, has been given the opportunity to register their agreement or disagreement to this retraction. We have kept a record of any response received.

References

- [1] P. R. Kshirsagar, H. Manoharan, H. A. Alterazi, N. Alhebaishi, O. B. J. Rabie, and S. Shitharth, "Construal Attacks on Wireless Data Storage Applications and Unraveling Using Machine Learning Algorithm," *Journal of Sensors*, vol. 2022, Article ID 9386989, 13 pages, 2022.

Research Article

Construal Attacks on Wireless Data Storage Applications and Unraveling Using Machine Learning Algorithm

Pravin R. Kshirsagar ¹, Hariprasath Manoharan ², Hassan A. Alterazi ³,
Nawaf Alhebaishi ⁴, Osama Bassam J. Rabie ⁴, and S. Shitharth ⁵

¹Department of Artificial Intelligence, G. H. Rasoni College of Engineering, Nagpur, India

²Department of Electronics and Communication Engineering, Panimalar Engineering College, Poonamallee, Chennai, India

³Department of Information Technology, Faculty of Computing and Information Technology,
King Abdulaziz University, Saudi Arabia

⁴Department of Information Systems, Faculty of Computing and Information Technology, King Abdulaziz University, Saudi Arabia

⁵Department of Computer Science & Engineering, Kebri Dehar University, Kebri Dehar, Ethiopia

Correspondence should be addressed to S. Shitharth; shitharths@kdu.edu.et

Received 8 July 2022; Accepted 3 August 2022; Published 16 August 2022

Academic Editor: Sweta Bhattacharya

Copyright © 2022 Pravin R. Kshirsagar et al. This is an open access article distributed under the Creative Commons Attribution License, which permits unrestricted use, distribution, and reproduction in any medium, provided the original work is properly cited.

Cloud services are a popular concept used to describe how internet-based services are delivered and maintained. The computer technology environment is being restructured with respect to information preservation. Data protection is of critical importance when storing huge volumes of information. In today's cyber world, an intrusion is a significant security problem. Services, information, and services are all vulnerable to attack in the cloud due to its distributed structure of the cloud. Inappropriate behavior in the connection and in the host is detected using intrusion detection systems (IDS) in the cloud. DDoS attacks are difficult to protect against since they produce massive volumes of harmful information on the network. This assault forces the cloud services to become unavailable to target consumers, which depletes computer resources and leaves the provider exposed to massive financial and reputational losses. Cyber-analyst data mining techniques may assist in intrusion detection. Machine learning techniques are used to create many strategies. Attribute selection techniques are also vital in keeping the dataset's dimensionality low. In this study, one method is provided, and the dataset is taken from the NSL-KDD dataset. In the first strategy, a filtering method called learning vector quantization (LVQ) is used, and in the second strategy, a dimensionality-simplifying method called PCA. The selected attributes from each technique are used for categorization before being tested against a DoS attack. This recent study shows that an LVQ-based SVM performs better than the competition in detecting threats.

1. Introduction

Cloud computing is the ecosystem in which individuals pool information, services, and knowledge using system resources offered through the internet. It creates a convenient and dynamic infrastructure for computing for business organisations. There are a variety of dangers and difficulties that have emerged with the increased use of the computing environment. One of the greatest difficulties to cloud computing environments is keeping consumer privacy, information leakage, and identification concerns under control [1]. As a

result of the unique cloud computing infrastructure, old problems have been successfully combated, but new issues with infrastructure distribution have emerged. When it comes to cloud computing security, a major concern is that networking and security systems information, cloud architecture, and individual security requirements all vary. App layer carries out responses implementing the interprocess communication. These patterns resemble genuine responses, thus conventional defenses do not apply. Transaction and demand floods assaults, delayed performance assaults, and asymmetrical assaults may all be referred to as DDoS attacks

in the cloud. A flood of these assaults not only creates traffic but also imitates that of a genuine user [2]. This makes it difficult for the target to tell the difference between such a flood of attacks and legal traffic, and therefore, they need to provide services to the genuine user. A denial-of-service assault on a commodity causes it to become unavailable or service to legitimate customers to degrade.

A physical device, a collection of machines, or a system of computers may constitute a source. An attacker may place authorized customers in a state of denial if they can successfully deny the access of the specific part [3]. The means by which this assault is conducted out varies based on how far into the OSI and TCP/IP models it is carried out. The implementation of any type of denial-of-service attack has a variety of variables at play, including the assault instrument that is used to create bandwidth, the protocol being targeted, the communications layer, and the kind of victim. Assailant motivation is to reduce the amount of resources available to the legitimate customers to the minimum needed to deny them. Although many protections may be used to shield vital resources from being attacked in this manner, the flaws that are present in the systems are a fact of computing. An assault against computation's confidentiality, trustworthiness, and authenticity is underway. Threats such as unauthorized users, asset theft, and doing beyond the permitted limits are all often used by attackers for information security purposes [4]. The abovementioned problems may be addressed by the use of IDS, which identifies and evaluates whether internet traffic is regular or unusual in order to find a solution. The emergence of many different intrusion detection systems is attributed to network setup variability. There are distinct benefits and drawbacks to every kind of IDS. IDS are disseminated IDS because it use hypervisors to identify network hosts and disseminate the results. To investigate DDoS attacks in the cloud, machine learning is used to the NSL-KDD dataset [5]. The attributes chosen by both LVQ and PCA attribute selection approaches are essential for a successful implementation of mining algorithms. Attribute selection is a classification algorithm.

1.1. Review of Literature. Dwivedi et al. (2020) [1], using a machine learning technique, make a proposal for a new grasshopper optimization algorithm (GOA) with a machine learning algorithm (GOIDS). The plan of action is implemented based on the implementation of an intrusion detection system (IDS) in order to fulfill the monitoring needs and allow for the differentiation between a regular traffic flow and an attack. GOIDS is finding out the specific characteristics in the initial IDS dataset that are best suited to identify DDoS assaults of this low pace. Once the attributes have been chosen, they become inputs to classifiers. These machine learning models, namely, the SVM, DT, NB, and MLP, is utilized to identify the assault that occurred in the system. According to Prathyusha et al. (2020) [2], in this article, a novel DDoS detection method has been proposed by using artificial immune systems. This suggested approach can identify dangers and modulate the biological resistance mechanism to react accordingly. Wang et al. (2019) [3], in order to pick the best possible attributes dur-

ing the training phase, offer a multilayer perceptions (MLP) coupled sequential attribute selection. Once it is determined that substantial identification mistakes have been made, the feedback mechanism is built to update the assault detectors to prevent future breaches. Rabbani et al. (2019) [4] proposed probabilistic-neural network (PSO-PNN) for developing a new attack detector. The first step is to organize the data such that it is easy to interpret. Then, the multilayer neural network was used to distinguish harmful activities. According to Punitha and Indumathi (2020) [5], entrusting our data security to a central cloud database, which uses an algorithm that generates the empire's own security keys, puts our data security at risk. The suggested system is also capable of detecting and monitoring how information is used. ICKGA and trapdoor creator are used to generate secret keys for every user, whereas CP-ABE and key creation use the ICKGA and trapdoor generator. Once the trapdoor generator has verified the integrity of the user data in the cloud as well as on the user level, the trapdoor generator kicks in. Using a dynamically weighted ensemble neural network (DWENN), a dynamic classifier that adjusts its sensitivity dynamically to identify DDoS attacks with more strength is finally used.

According to Wani et al. (2019) [7], in order to identify the DDoS assault in the cloud environment, they developed a novel detection technique using SVM. According to the plan, it is compared to NB and RF. According to Shitharth and Sangeetha (2020) [8], a number of distributed denial of service (DDoS) assaults has been identified using machine learning-based models. Attribute selection is utilized to come up with the optimum attributes. The characteristics chosen have been trained and evaluated using support vector machines (SVM), naive Bayes (NB), ANN, and KNN classifiers. Ghanbari et al. (2020) [9] presented a new DDoS attack detection system that was intended to increase the DDoS attack detection rate in a power system. The identification rate is increased utilizing CNNs which are trained and tested in stages known as the training and testing process. According to Shitharth et al. (2020) [11], a novel DDoS detection method that leverages machine learning-based classifiers is proposed in a cloud environment. As input to the classifier, people have gathered and categorized characteristics that they believe to be helpful. Kishirsagar et.al [6, 10] elaborate the use of different algorithms for classification and prediction of benchmark datasets and real time dataset which were useful in the emerging all fields and elaborate the use of hybrid artificial intelligence along with optimization techniques for classification and prediction of various datasets with high accuracy [12]. The algorithms used in various research worked were useful in cyber security, mobile computing, and cloud computing for more accurate results with different evaluation parameters.

Deepa et al. [13] have devised an ensemble approach to combat DDoS assaults. They used four distinct machine learning algorithms in the SDN environment to identify suspicious network traffic. SVM-SOM method obtained superior results, with 98.12% accuracy, than the other ML algorithms. A DDoS attack-detection system for SDN was presented by the authors. Two separate security steps were used. Signature-based attacks were detected by Snort, which

is a tool designed to spot them. Using the SVM classifier and the DNN machine learning method, they launched an attack classification scheme thereafter.

Mašetić et al. and Rao et al. [14, 15] and developed an automated DoS attack categorization method for cloud computing. This research is conducted in stages, such as conducting an assault simulation, collecting information, and choosing attributes, before applying categorization to the results. For this research, data is acquired via mimicking the cloud environment and DoS assault, together with Wire-shark's Tshark capability. One of the categorization models for DoS attacks and standard network activity is the support vector machine (SVM).

1.2. Research Gap and Motivation. In addition to different methods that are provided in earlier sections, some recent articles also focused on detecting DoS attacks using different data set where [18] used CAIDA for experimental verification cases. However, if CAIDA is used, large data set cannot be stored in the system thus high case external attacks is not prevented. In [19–23], data detection in industrial applications is analysed as data in entire segment inside the industry must be protected in reaching external users. Thus, the protection is provided using machine learning algorithm with two directional data flow procedures. Even though bi-directional flow is provided, the amount of data traffic in the system can be handled with single traffic flow itself, thus preventing less amount of users. There is clearly a need of a strategic plan to use machine learning methods in a methodical manner in order to make comprehensive evaluations possible, as otherwise built-in issues like collinearity, multicollinearity, and duplication would present in machine-mined data. Additionally, the use of machine learning methods in data science-driven ways requires integrating all of the key needs of data science-driven approaches. A modeling may not fulfill its goal, but if that is the case, the model will always incorporate aspects of classifier. Integrating machine learning and attribute engineering techniques in a single framework also has a significant impact on the current research. In other words, all inclusive experimentation and trustworthy results need joint consideration.

1.3. Proposed Methodology. Many existing methods [1–15] emphases only on basic attacks where data is processed with low security features. Even many methods does not incorporate learning techniques for avoiding attacks from external users. It is always necessary that a user must acquire knowledge from existing data and unnecessary data must be eliminated using attribute engineering procedures. The abovementioned technique is carried out in case of intrusion prevention systems where different machine learning techniques can be allocated. To overcome the gap that is present in existing methods, proposed method is incorporated by reducing dimensionality of entire data handling systems.

The proposed methodology is used for preventing denial of service attack using a quantization model which eliminates all attacks using step processing procedures. By incorporating the proposed method, unidentified attributes are

directly removed from the system, thus making all data to revolve in a hassle free environment. Moreover, the losses that are present in this type of system are reduced even if the data is stored in the cloud. Furthermore, volume of information in presence of large data set is prevented using machine learning algorithm where ten initial attributes are completely knowledgeable; thus, it is used as reference data for preventing external attacks in the system.

1.4. Objectives. The major objective of proposed work focuses on deciphering three objectives which is considered as minimization problem as follows:

- (i) To minimize the denial of service attack on data that is included within the systems and to provide potential defence for large data set
- (ii) To incorporate machine learning algorithms by rationalization process without describing any dimensions for entire data set
- (iii) To categorize and allocate resources based on target customers, thus increasing the security of data that is provided to all users

2. Distributed DoS

The malicious distributed-denial-of-service (DDoS) assaults that plague the internet these days are a major worldwide threat. These assaults are deftly executed and use the same methods of conventional denial of service (DoS) attacks, but they are implemented on a larger scale due to the usage of botnets. In order to spread quickly, a botnet may spread by taking use of malware that infects tens or even hundreds of computers which are then used to further spread the malware by being managed by an attacker that is targeting a victim [16]. Attacks on the internet provide an exciting potential for attackers to take control of users computers and generate zombies. By infecting people through worms, Trojan horses, or backdoors, the zombies use the tricks of their trade: compelling links, e-mail content, or trustworthy sender addresses. Computers linked to the Internet, such as Web servers, have vulnerabilities and flaws that may be exploited by attackers using a range of different hacker methods. This leads to malicious malware being placed on these systems, and subsequently to these computers being placed in a vulnerable position, giving malevolent programmes full control over them. These machines are often known as “handlers” and “zombies.” The attackers, under control of the controllers, have the command of the zombie army.

When an attack is first begun, the assailant controls as many computer systems as possible, enabling him to initiate the assault. An estimate for the number of zombies may be anything from a few hundred to a few thousand. In the figure below, Figure 1, you can see how a botnet of zombie-related attacks develops [17]. The size of the botnet impacts the amount of damage, the intensity, and the range of an attack. A botnet that may inflict debilitating and catastrophic attacks is a serious threat. For

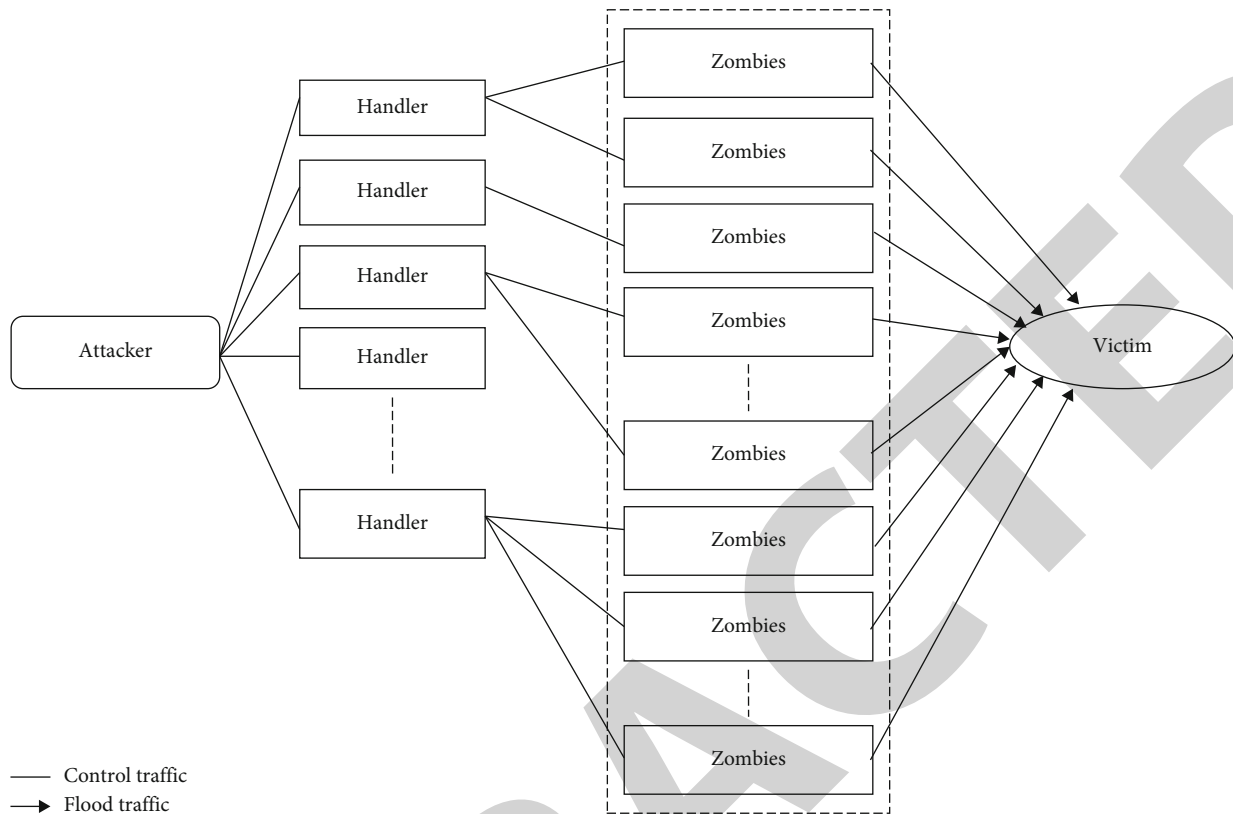


FIGURE 1: DDoS attack architecture.

example, just a little amount of information is given by one zombie. In contrast, on user devices, meanwhile, the huge amount of zombies that have risen depletes computer resources. When single connection speed traffic looks as normal, traffic floods using low packet rates that are part of a DDoS attack are especially difficult to detect. Attacks that inflict extreme damage may happen due to existing detection methods tending to increase the speed of DDoS attacks. At the present, DDoS assaults are done through link and packet flooding. This kind of attack has increased drastically on the Internet because hackers know where and how data is obtained [17]. This kind of assault may be carried out because weaknesses in the protocols, operating systems, and web applications constantly surface. In such attacks, the most common motives include money gain, blackmail, hacking, or personal problems. This usually happens when web-based media, such as internet poker, social media sites, or internet shopping, are attacked.

2.1. Detection Approach for DDoS Attack. ML techniques that include attribute engineering and data science procedures such as attribute extraction and information science best practices may be used to get the most optimal detection in a DDoS dataset. A conceptual plan, one that involves treatments of attributes in addition to machine learning advances, is presented in this study. In Figure 2, the fact that performance of the model may occur is emphasized. According to the nature and structure of data, characteristics

are always systematically treated. Extending this concept, any kind of cyber-intrusion such as a distributed denial of service (DDoS) assault may also be included in the suggested method to deal with all the inherent problems of data, including skewness, collinearity, and multicollinearity. Completing the attribute engineering process will also include attention to the missing values. This may be done by averaging, using the maximum and minimum values, or by replacing the missing data with the lowest, maximum, or average values. Attribute unusability is caused by high value for missing data vs. supplied values. Based on the proportion of missing values in the dataset, one may determine that the appropriate treatment should be done in an attribute elimination or attribute adjustment phase of the attribute engineering module. A collection of datasets are provided with a reduced range of attributes, enabling machine learning techniques to be used to analyse those attributes after the attribute selection stage is completed inside the new framework attribute engineering module.

These machine learning techniques may be seen in the research findings in Figure 2. The machine learning module of the proposed framework does not contain the full collection of algorithms (including AdaBoost and CART), but it is not limited to just those five algorithms. Regardless of whether it is supervised, unsupervised, or semisupervised, the machine learning algorithms may be used to any kind of study. The target classes are made available to supervised algorithms because of the nature of the supplied datasets.

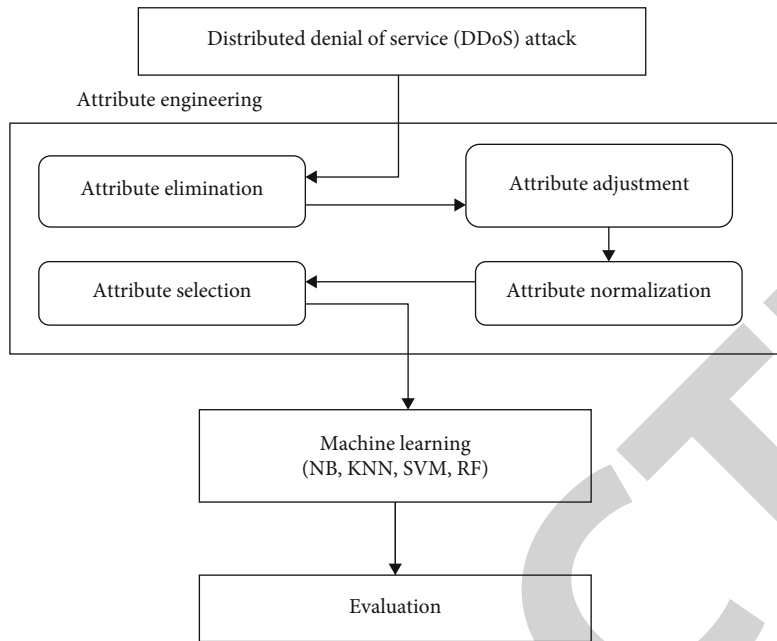


FIGURE 2: Strategic level framework for DDoS attack detection.

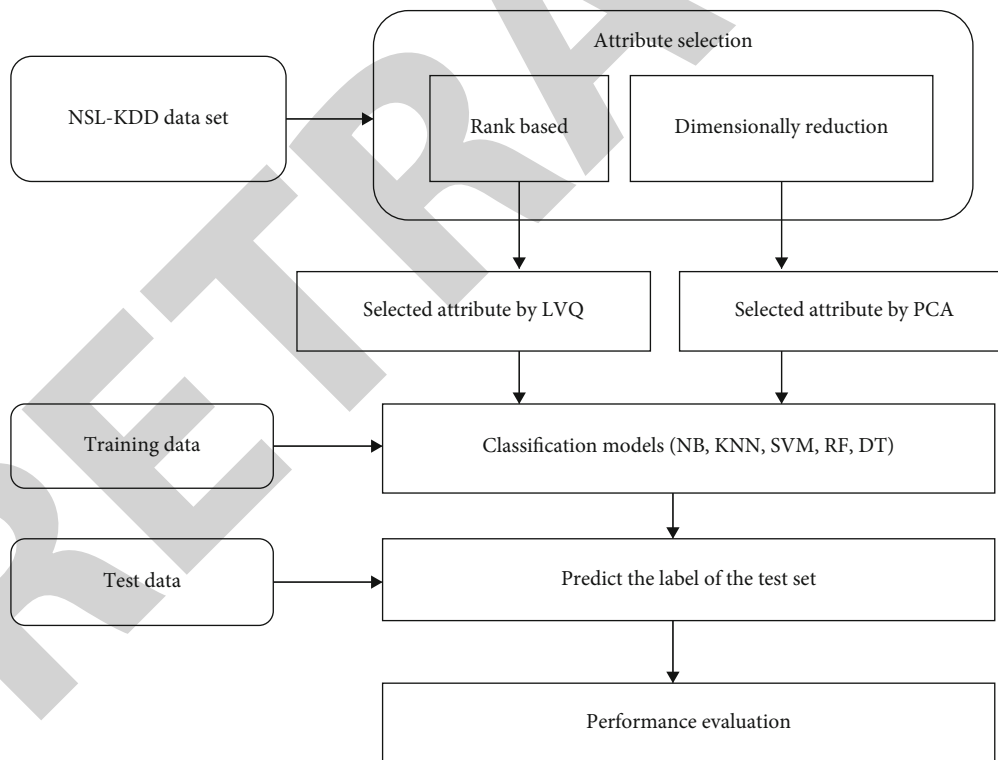


FIGURE 3: IDS in cloud environment.

3. Data Set Description and Attributes

In a dispersed test environment, wired network is extremely costly. Modeling is a widely-used technique in network research. It is useful for studying network issues that vary

depending on protocols, traffic, and topologies, as well as evaluating network protocol tests [14]. The sets of data that are accessible are those that are built from the ground up, like a direct data set, and those that have been obtained from public sources, like a public data set. When open source

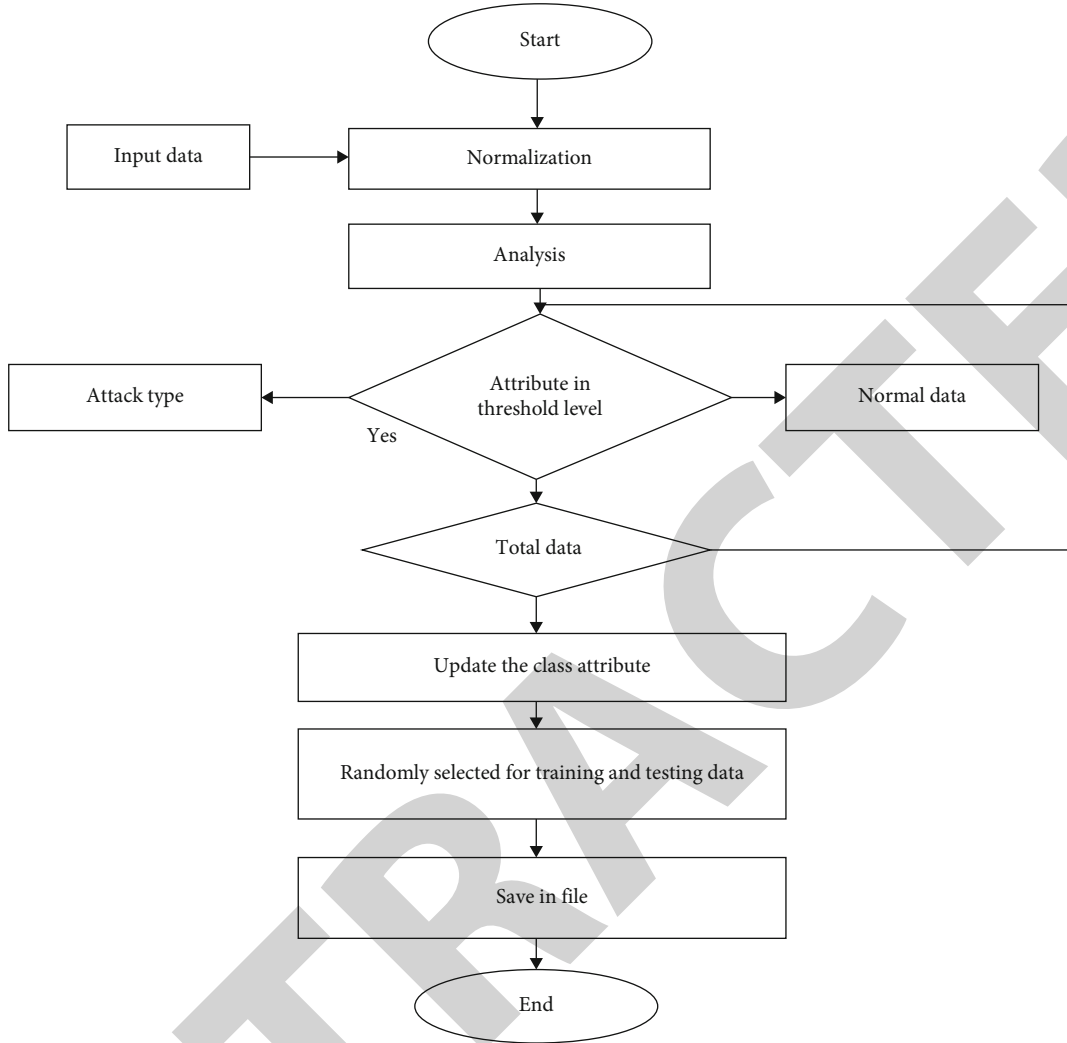


FIGURE 4: Flowchart of SVM algorithm for attack detection.

TABLE 1: Results of LVQ method.

Parameters	NB	DT	SVM
Accuracy	0.9286	0.9176	0.9985
Recall	0.9176	0.9142	0.9768
Precision	0.9814	0.9886	0.9928
<i>F</i> -measure	0.9486	0.9571	0.9940

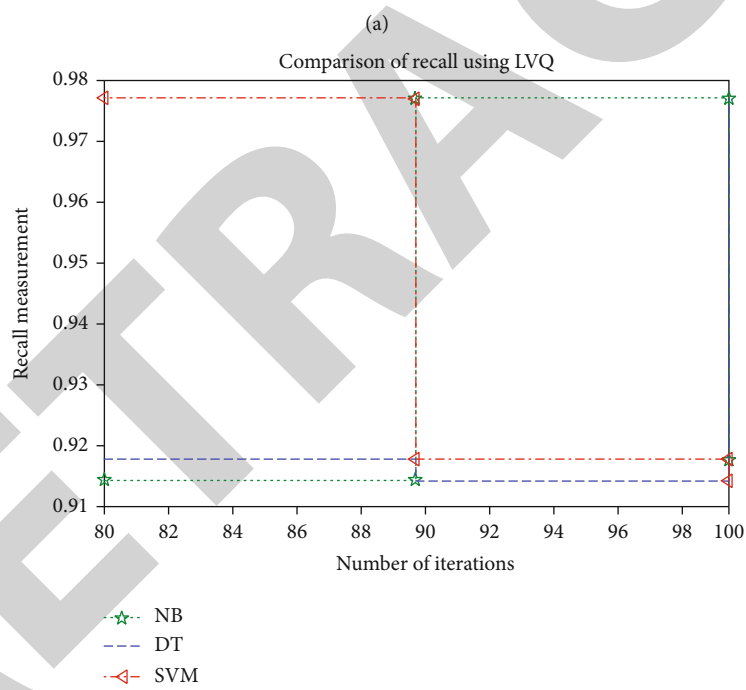
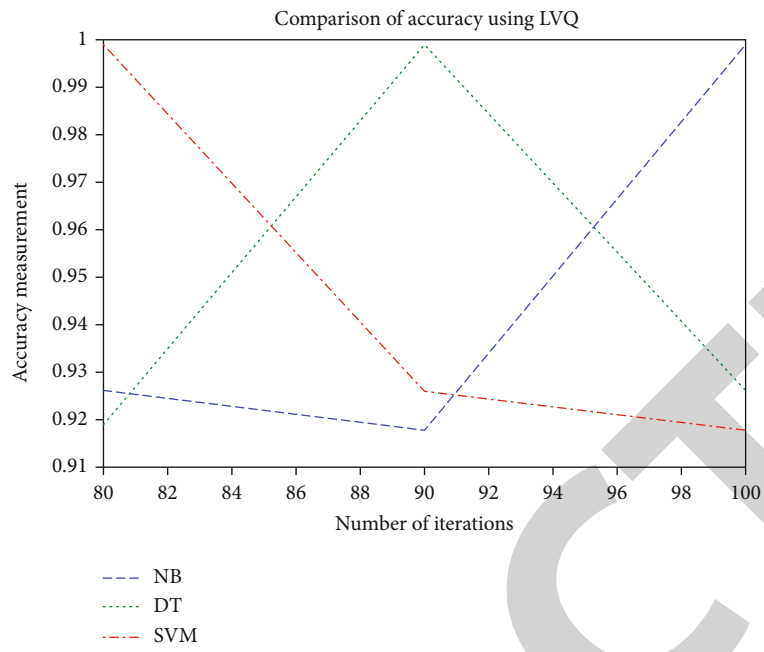
software is used to generate a direct dataset, the resulting dataset is termed direct data set. If the dataset is made available to the public, it is called public data set. This study makes use of a public dataset, NSL-KDD, which is deliberated in Figure 3.

Attribute selection method is a strategy that uses several parameters, selecting the ones that are the most significant and have the greatest effect on the anticipated variable. The data used in attribute selection is not the whole data set, with regard to attribute selections, the addition and deletion of information have no effect on the entire collection. Attribute

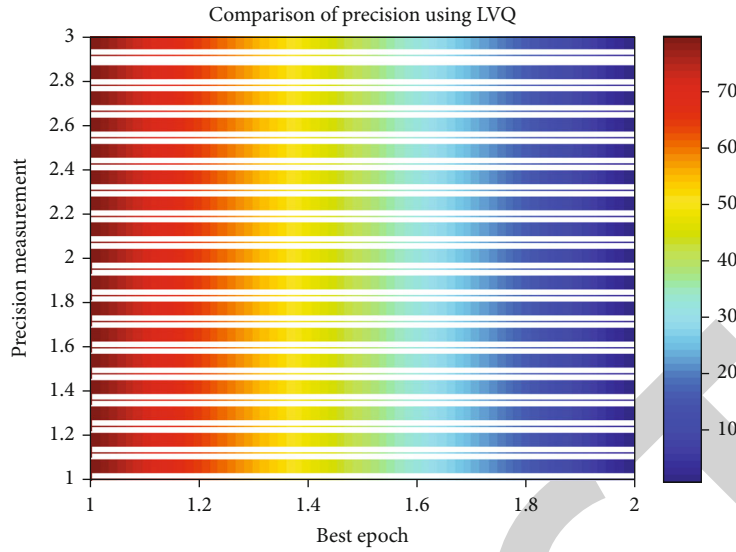
selection is done out in the proposed study using two different approaches. They are a technique of filtering and a means of reducing complexity.

3.1. Classification Technique. SVM is being used successfully for multiple-class classification, but researchers are still trying to figure out how to expand it. The two predominant kinds of multiclass SVM methods at this time are hypothesis-based and algorithm-based. The first method uses several binary classifiers to construct the overall classifier, whereas the second method directly incorporates all training examples to derive the classifier. By choosing examples at the edges of the class descriptors, the SVM may choose the optimal separating hyper plane for training inside the attribute space. The SVM model that we create has the number of classes equal to k . All of the positive instances are used in training an SVM with classifier set I, and all other examples are used in training an SVM with classifier set II.

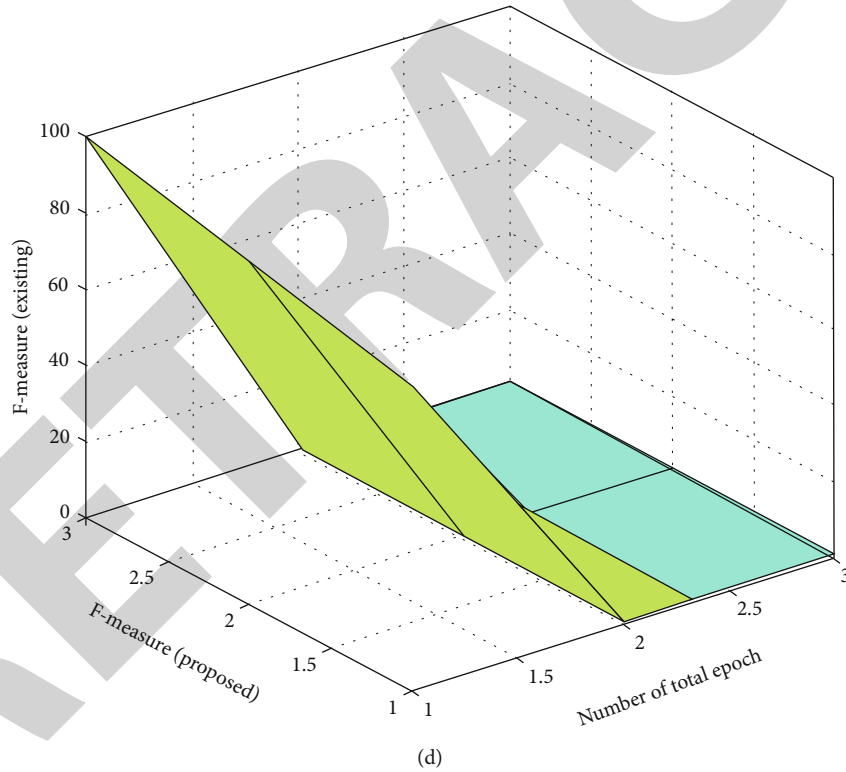
Thus, given l training data $(x_1, y_1), (x_2, y_2), \dots, (x_l, y_l)$, $i = 1, 2, 3, \dots, l$ where $x_i \in R^l$ and $y_i \in \{1, 2, \dots, k\}$ are the



(b)
FIGURE 5: Continued.



Comparison of F-measure using LVQ

FIGURE 5: Results of LVQ method. (a) Accuracy. (b) Recall. (c) Precision. (d) F -measure.

class of x_j the j^{th} SVM solves the following optimization problem

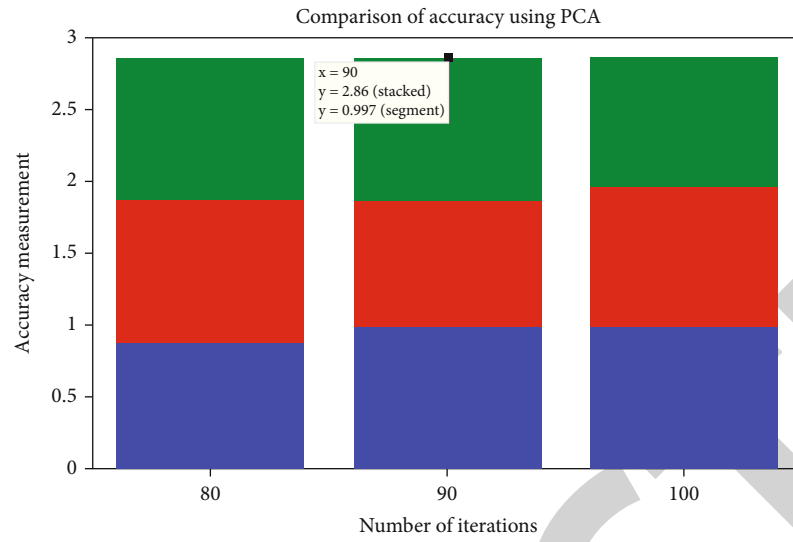
$$\min_{w^j, b^j, \xi_i^j} \left\{ \frac{1}{2} (w^j)^T w^j + c \left(\sum_{i=1}^l \xi_i^j \right) \right\}, \quad (1)$$

$$(w^j)^T \varnothing(x_i) + b^j \geq 1 - \xi_i^j \quad \text{if } y_i = j, \quad (2)$$

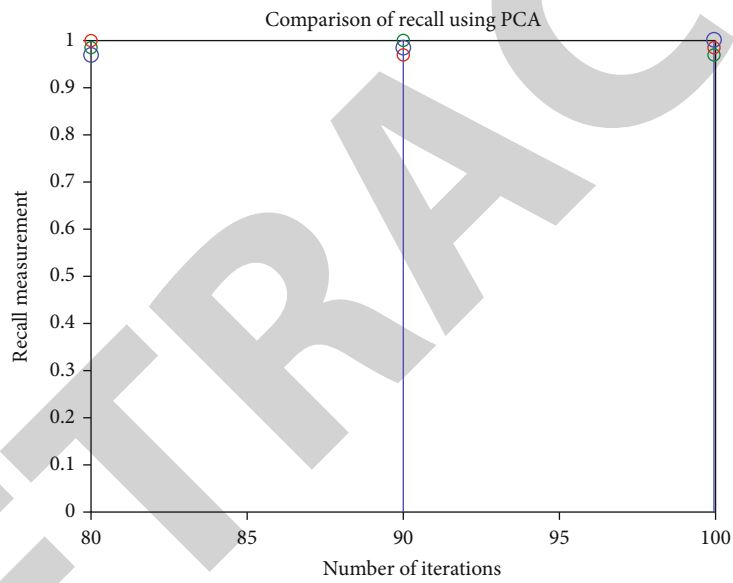
$$(w^j)^T \varnothing(x_i) + b^j \leq -1 + \xi_i^j \quad \text{if } y_i \neq j, \quad (3)$$

$$\xi_i^j \geq 0, i = 1, \dots, l. \quad (4)$$

Since the nonlinear function, w , b , and ξ have weight, bias, and slack variables, respectively, then $\varnothing(x_i)$ may be mapped into a higher dimensional space by the function. There is a constant, established a priori, which is C . Quadratic programming issue (shown as equation (1) in the



(a)



(b)

FIGURE 6: Continued.

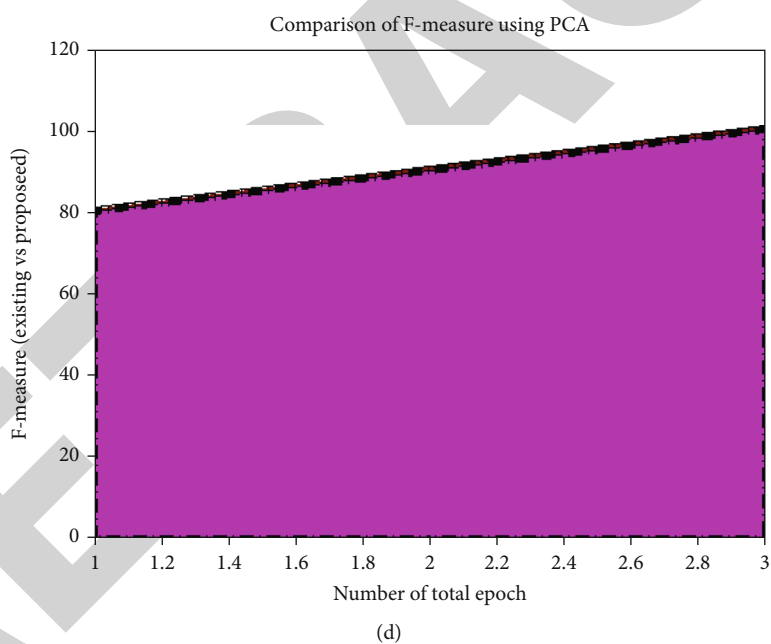
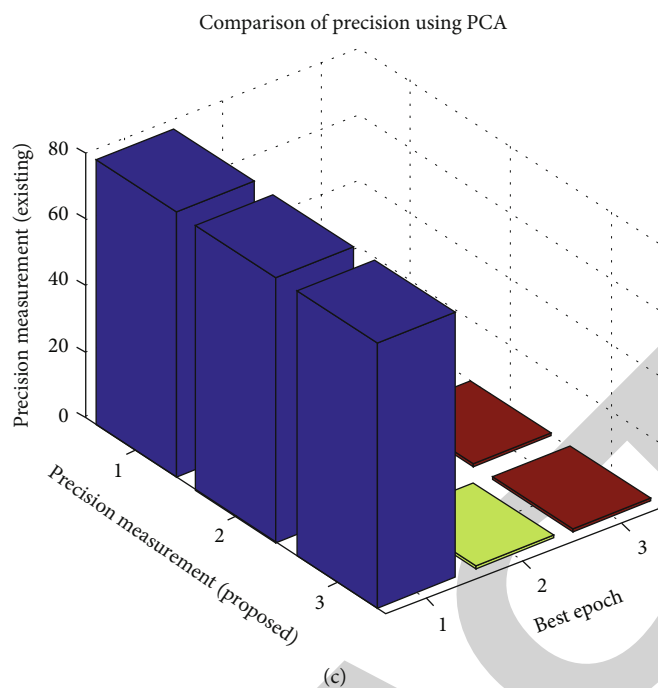


FIGURE 6: Results of PCA method. (a) Accuracy. (b) Recall. (c) Precision. (d) F -measure.

TABLE 2: PCA method results.

Parameters	NB	DT	SVM
Accuracy	0.8832	0.9758	0.9971
Recall	0.9673	0.9815	0.9975
Precision	0.8672	0.9753	0.9892
F -M	0.9143	0.9786	0.9975

TABLE 3: Comparable results of LVQ and PCA.

Classification algorithms	Detection accuracy	
	LVQ	PCA
NB	0.9289	0.8832
DT	0.9397	0.9756
SVM	0.9985	0.9951

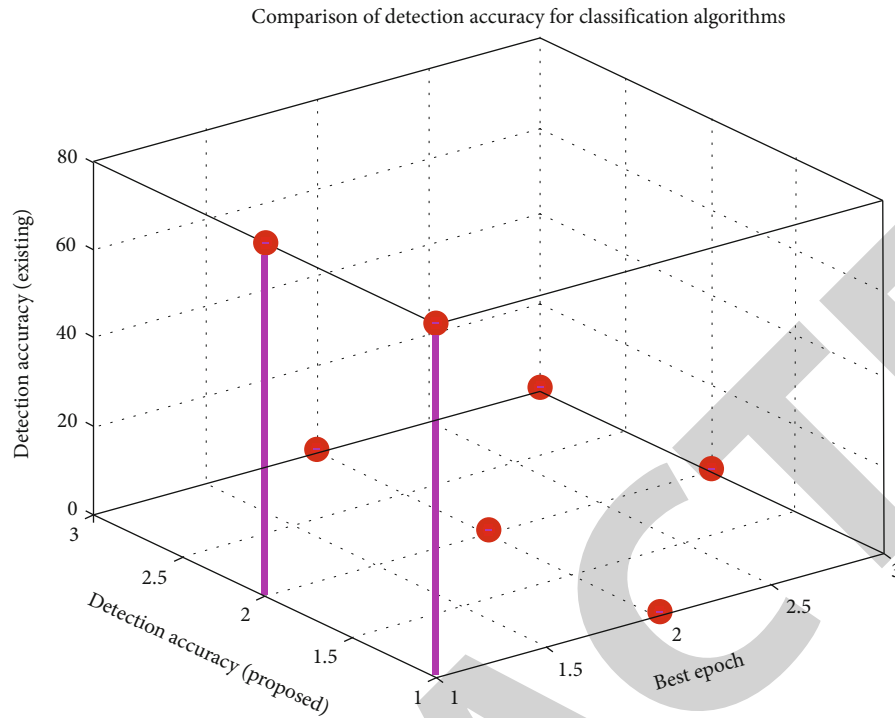


FIGURE 7: Comparative results of LVQ and PCA.

graphic below) involves searching for the best hyperplane in equation (1). Minimizing $1/2(w^j)^T w^j$, therefore, researchers want to increase $2/\|w^j\|$ the difference between assault categories. Data do not exist in a linear format, therefore, there is a cost. $c = (\sum_{i=1}^l \xi_i^j)$. SVM tries to find a compromise between the regularization term and training mistakes $1/2(w^j)^T w^j$ corrections and training mistakes. Once you have determined k decision functions from equation (1), you are finished solving for k .

$$\sum_{i=1}^l \alpha_i^j K(x, x_i) + b^1, \quad (5)$$

$$\sum_{i=1}^l \alpha_i^j K(x, x_i) + b^k. \quad (6)$$

We state that the value of the choice function for class x_i is in the class with the greatest value:

$$\text{class of } x = \operatorname{argmax}_{i=1 \dots k} \sum_{i=1}^l \alpha_i^j K(x, x_i) + b^j. \quad (7)$$

In this section, we will be using the Gaussian kernel $K(x, x_i)$ and the Lagrange multiplier. We will change the Gaussian kernel function $K(x, x_i)$ in a data-dependent manner to enhance SVM classifier classification accuracy. In SVM, the four common functions are linear, polynomial of degree d , RBF, and MLP. A flowchart depicting the algorithm's steps is given in Figure 4. The procedure

of a simulation method that uses support vector machines is shown using this flowchart. The origins from both equations (1) and (7) are provided in such a way it is integrated in a single equation for defining the objective functions as follows,

$$O_i = \min \sum_{i=1}^n \text{DoS}_i, A_i, \quad (8)$$

where DoS_i indicates various attack process. A_i describes different attribute in a system.

4. Outcomes

Attribute selection techniques are employed, and the attribute set that results from this is used for classification. Verification measurements are computed by using these theoretical method, which relate to accuracy, precision, recall, and f -measure.

4.1. Assessment of Characteristics: LVQ Process. These results in Table 1 and Figure 5 have been obtained from experiments that follow the research set of data. Applications of different classifiers like NB, SVM, and DT are made possible with the deployment of LVQ. With respect to malicious records, the SVM classifier has a higher performance level as compared to NB and DT.

4.2. PCA Strategy: Explore Various Qualities. PCA is used for dimensionality reduction. Figure 6 shows the findings. SVM method from Table 2 does better than NB and DT when it comes to detection accuracy (0.9971 vs. 0.9965). When using

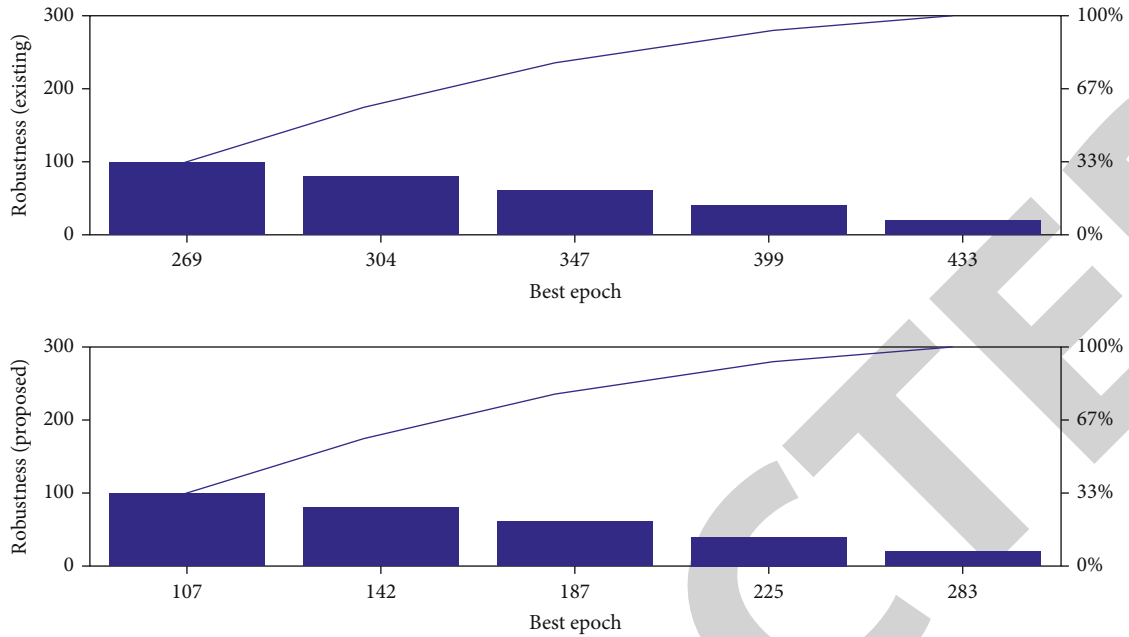


FIGURE 8: Comparison of robustness characteristics.

the attribute selection technique in this attribute-based selection process, 10 out of 21 attributes are used.

4.3. Comparative Results. Attribute selection techniques, such as SVM, were used to classifier performance, and the findings are summarized in Table 3. Table 3 and Figure 7 indicate that SVM performs better for both attribute selection methods. Classifying harmful records is best performed using an SVM-based approach.

4.4. Robustness Characteristics. In this comparative outcome section, the robustness characteristics with respect to LVQ and PCA are observed for different iteration periods, and their changes are simulated. Since more amount of data set is present in this process for preventing DoS, it is essential to find individual robustness for attributes. Further, the robustness of an algorithm determines the association between two distinct data set, thus solving the necessary properties for defining the learning rate. Figure 8 illustrates the simulation outcomes and comparison of robustness that is present in both LVQ and PCA.

From Figure 8, it is pragmatic that robustness of LVQ is much reduced as compared to PCA due to dimensionless characteristics. To validate the robustness of LVQ and PCA five best epoch is considered but original ranges are chosen from 10 to 100. Due to presence of vector quantization, the step size is chosen as 20, thus, the following best epoch such as 20, 40, 60, 80, and 100 is considered. During the abovementioned variations, it is much clear that robustness of LVQ reduces from 283 to 107 and further reduces for remaining periods. On the other hand, even though PCA reduces the amount of robustness, it is much higher for all epoch periods as dimension process for data is defined in existing method.

5. Conclusions

This page attempts to give a basic overview of the different DDoS attack methods in use, while also offering an in-depth look at potential defenses. An essential part in the overall data protection process is played by intrusion prevention. A benchmarking set of NSL-KDD standards is used to identify intruders for internet information. The study only uses information that pertain to DDoS attacks. Attributes such as LVQ and PCA were utilized to categories the attacks based on machine learning approaches such as SVM, NB, and DT. To verify whether the DDoS attack was occurring, the algorithms' performance was monitored. Ten attributes were selected using LVQ, and the remaining ten attributes were selected using PCA. Using an LVQ-based attribute selection in an SVM model was shown to be more successful in identifying attacks. When compared to other algorithms, it comes out to be more accuracy, has greater recall, is more precise, and has a higher F -score.

5.1. Policy Implications

- (i) The proposed DoS model can be incorporated in all industries even with large amount of data set where new security features are enabled
- (ii) By using the enhanced security features, more amount of data overflow can be prevented and even worst type of attacks can be prevented using loop formatting procedures
- (iii) All the target systems can process different type of packets inside a particular device where less resources are allocated in productions